Excerpta

99

A Rare Case of Chordoid Glioma

Jonathan W Nazha MD[1], Timothy Nguyen[2]
[1]Hartford Hospital, Hartford, CT, USA. [2]Touro University California, Vallejo, CA, USA

Abstract Category

Adult Brain

Clinical History

A 35 year old male with history of alcohol abuse, polysubstance abuse – including IV drug use and prior overdoses – , depression, GERD, IBD, obesity, anemia, and psychiatric history presented with complaints of depression, hopelessness, and headaches. The patient was alert and oriented to person and place, but not time. Patient was able to follow commands, had intact cranial nerves II-XII, full strength in extremities, intact sensation to light touch, and no abnormal reflexes. A noncontrast CT was ordered prior to MRI.

After discovery of a heterogeneous mass within the ventricular system causing obstructive hydrocephalus, surgical resection was performed. Postoperative course was then markedly complicated by seizures, panhypopituitarism, subdural hygromas, and a subdural empyema requiring surgical intervention with persistent ventriculomegaly and ventriculitis.

Imaging Findings

CT Head Without Contrast:

Heterogeneous mass centered on the hypothalamus and left thalamus with
moderate perilesional white matter changes. Associated effacement of the third ventricle with moderate expansion of the lateral ventricles.

MRI With and Without Contrast:

There is a large heterogeneously enhancing mass filling the third ventricle, the source of which appears to be the medial aspect of the left thalamus. Possible diagnostic considerations include an intraventricular meningioma, oligodendroglioma, glioblastoma, lymphoma, or metastasis. There is relatively extensive perilesional edema involving the basal ganglia, thalami, and midbrain. Mass effect results in obstructive hydrocephalus with transependymal flow of cerebrospinal fluid. No identifiable intrasellar mass.

Discussion

Chordoid gliomas are very rare low-grade tumors that typically arise from the anterior wall or roof of the third ventricle. Due to its rare nature, epidemiological data is quite scarce with less than 100 cases published ranging from small case series and case reports with subjects ranging between 30 and 60 years of age and a 2:1 female to male predominance. In this report we share a case of chordoid glioma presenting clinically with symptoms of hydrocephalus.

Teaching Point

Chordoid glioma is a very rare tumor for which understanding of etiology, typical features, and treatment is still developing. Readers should consider it on the long list of differential diagnoses for ventricular lesions, particularly in the case of a mass arising from the third ventricle.

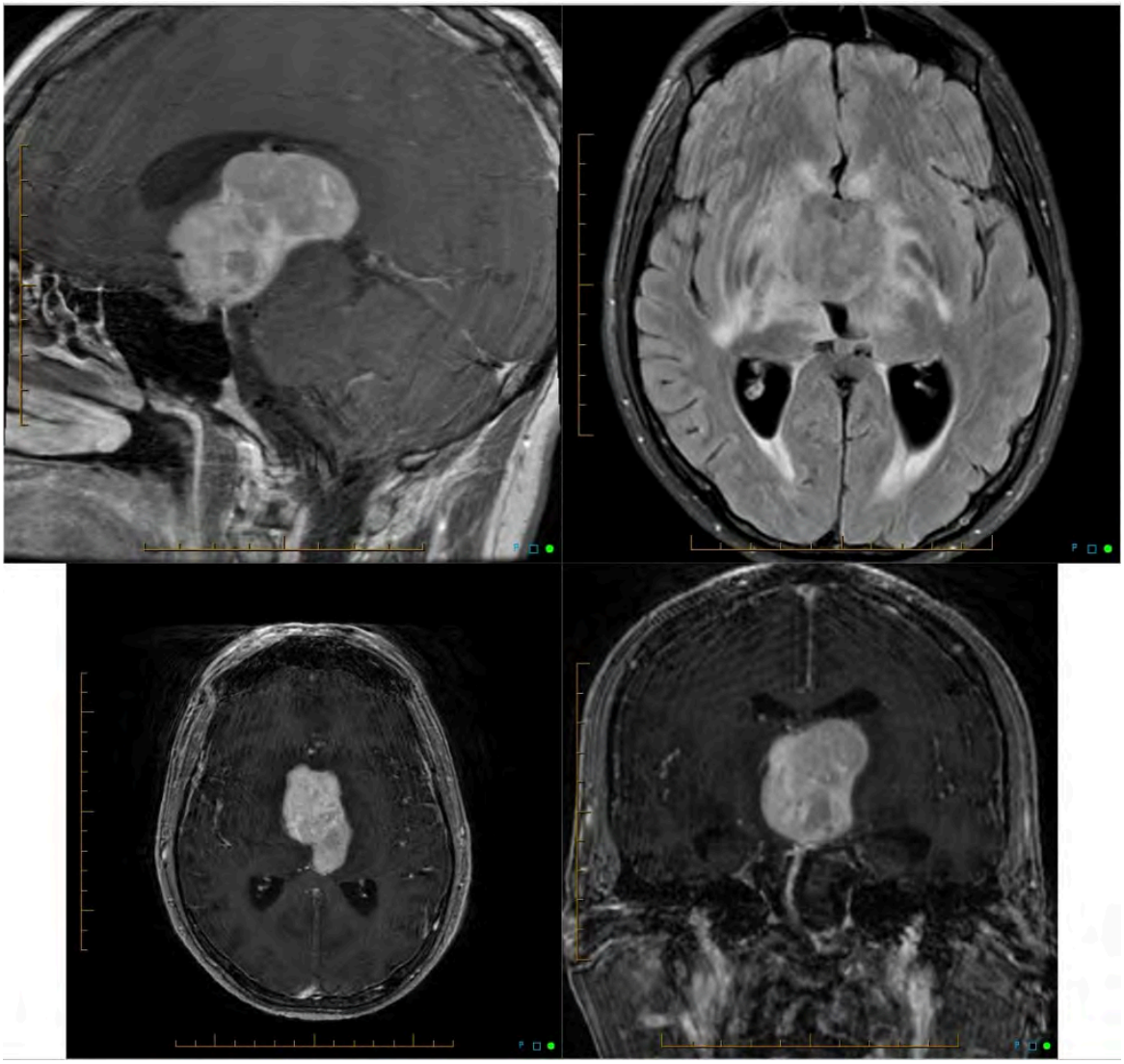
References

Journal Article
Liu, W., Cheng, J., Yi, X., Zhen, H., Fei, Z., Li, Q., & Zhang, X. (2011). Chordoid glioma. *The Neurologist*, 17(1), 52–56. https://doi.org/10.1097/nrl.0b013e3181e7db67

Journal Article
Morais, B. A., Menendez, D. F. S., Medeiros, R. S. S., Teixeira, M. J., & Lepski, G. A. (2015). Chordoid glioma: Case report and review of the literature. *International Journal of Surgery Case Reports*, *7*, 168–171. https://doi.org/10.1016/j.ijscr.2015.01.027

Journal Article
Yang, B., Yang, C., Du, J., Fang, J., Li, G., Wang, S., & Xu, Y. (2019). Chordoid glioma: An entity occurring not exclusively in the third ventricle. *Neurosurgical Review*, 43(5), 1315-1322. https://doi.org/10.1007/s10143-019-01161-w

Images/Tables



101

Malignant Melanotic Schwannoma and Carney Complex: A Case of Spinal Cord Compression and Multidisciplinary Management

Harjot Uppal MBA[1], Daniel Garcia BS[1], Peter Girgis BS[2], Nikhil Sahai MD[1], Kumar Sinha MD[1], Ki Hwang MD[1], Arash Emami MD[1]

[1]St. Joseph's University Medical Center, Paterson, New Jersey, USA. [2]SUNY Downstate Health Sciences University, Brooklyn, New York, USA

Abstract Category

Spine

Clinical History

A 41-year-old female with a history of papillary thyroid carcinoma, resected in 2012, presented with progressive lower back pain, bilateral lower extremity weakness, and difficulty walking. She reported numbness in her feet that gradually ascended to her waist, along with pelvic pressure. Her neurological symptoms worsened despite intact motor strength and reflexes during the initial examination. Further evaluation revealed a large epidural mass at the T10 level, compressing the spinal cord. The mass was confirmed to be malignant melanotic schwannoma (MMNST), and genetic testing identified mutations in the PRKAR1A gene, diagnosing her with Carney complex, a genetic syndrome linked to multiple neoplasms, including melanotic schwannomas and thyroid tumors.

Imaging Findings

Preoperative MRI showed a hypointense extradural, intramedullary mass on T2-weighted sequences at the T10 level, causing severe spinal cord compression. The tumor measured 5.2 x 3.7 cm and extended into the T10-T11 foramen. T1-

weighted images demonstrated the mass as hyperintense with heterogeneous contrast enhancement. Axial images confirmed circumferential involvement around the spinal cord, extending into the paraspinal tissues.
Postoperative imaging showed a significant reduction in mass effect at T10, with most of the tumor removed. A small residual tumor remained in the paraspinal region. A second surgery was performed to resect the remaining tumor. Follow-up imaging confirmed the complete mass removal, with axial and sagittal images demonstrating spinal cord decompression and no residual enhancing tissue.

Discussion

MMNST, a rare and aggressive schwannoma variant, presents substantial diagnostic and therapeutic challenges. This case highlights the importance of considering genetic syndromes in patients with malignancies like thyroid carcinoma. Genetic testing confirmed the diagnosis of Carney complex, identifying a PRKAR1A mutation. This finding was crucial for diagnosing the syndrome and guiding the screening for associated conditions, such as cardiac myxomas and endocrine tumors. Early identification and management of these complications were crucial for comprehensive patient care.
Imaging findings played a critical role in diagnosing MMNST and planning surgery. The mass's dumbbell appearance with intraspinal and paraspinal components and widening of the neural foramen suggest a nerve sheath tumor. The tumor's hyperintensity on T2-weighted MRI and heterogeneous enhancement on T1-weighted images indicated its malignant nature. In contrast, axial images revealed the extent of cord compression and paraspinal involvement, informing surgical approach and intraoperative strategy.

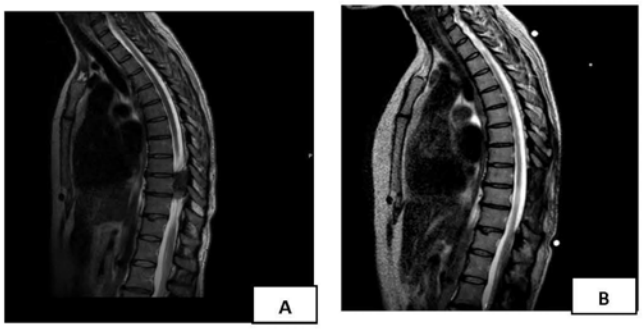
Teaching Point

Surgical resection is the primary treatment for MMNST, though achieving complete resection can be challenging when tumors invade paraspinal tissues. This patient required two surgeries to achieve near-total resection. The first surgery successfully decompressed the spinal cord, and the second resected the residual tumor. Intraoperative imaging was critical in guiding dissection and ensuring clean margins. Additionally, genetic testing is essential when the Carney complex is suspected. Identifying PRKAR1A mutations confirms the diagnosis and aids in screening for associated tumors and complications, enabling a comprehensive management plan. A multidisciplinary approach involving oncology, genetics, and surgery was crucial for optimal management and prognosis.

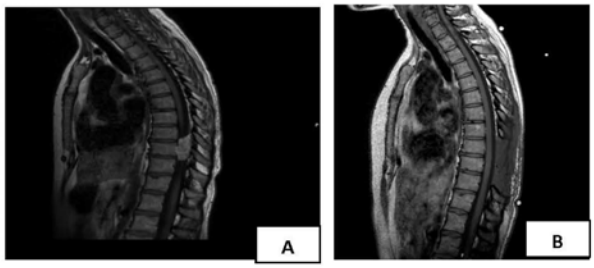
References

Chen, S., Wei, Y. Malignant melanotic schwannoma of the cervical spinal cord: a case report. *BMC Neurol* **24**, 181 (2024). https://doi.org/10.1186/s12883-024-03686-0

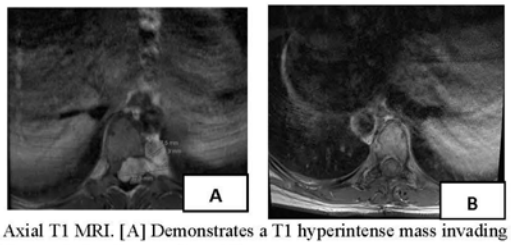
Images/Tables



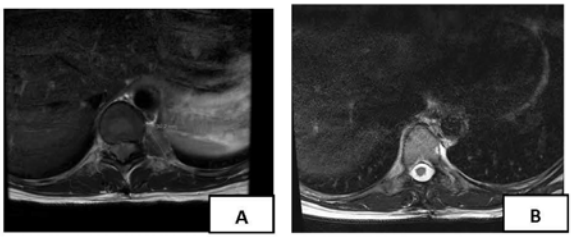
Sagittal T2 MRI. [A] Demonstrates a 5.2 x 3.7 cm T2 hypointense mass invading the spinal canal with severe cord compression at the level of T9 extending to the superior aspect of T11. [B] Demonstrates the resection of the mass.



Sagittal T1 MRI. [A] Demonstrates a 5.2 x 3.7 cm T1 hyperintense mass invading the spinal canal with severe cord compression at the level of T9 extending to the superior aspect of T11. [B] Demonstrates the resection of the mass.



Axial T1 MRI. [A] Demonstrates a T1 hyperintense mass invading the spinal canal with severe cord compression. [B] Demonstrates the resection of the mass.



Axial T2 MRI. [A] Demonstrates a T2 hypointense mass invading the spinal canal with severe cord compression. [B] Demonstrates the resection of the mass.

111

Basal ganglia stroke after minor head trauma in an infant- A case of lenticulostriate vasculopathy.

Kanza Noor Butt
Creighton University, omaha, NE, USA

Abstract Category

Pediatrics

Clinical History

A 16 month old female presented to an ER with reported right arm weakness and abnormal sucking following a witnessed ground level fall, and impact of the head with concrete 4 hours prior. She was discharged home due to low clinical suspicion for acute neurologic insult. She presented to the ER the following day with worsening right extremity weakness and facial asymmetry. Physical exam was positive for mild right facial droop, and right upper and lower extremity motor paresis. Brain imaging was performed and a diagnosis of acute left basal ganglia ischemic infarct, possibly associated with mineralizing lenticulostriate vasculopathy was made. She was admitted to the neonatal

intensive care unit for conservative management. Echocardiogram was normal. EEG showed asymmetric sleep spindles indicative of dysfunction of the left thalamocortical pathways. Extensive work up for underlying coagulopathy was negative. Her motor function significantly improved during hospitalization. She was discharged home and outpatient physical and speech therapy was recommended.

Imaging Findings

Non-enhanced head CT demonstrated branching hyperattenuation within bilateral basal ganglia predominantly the putamina. There was a 2 cm area of hypoattenuation in the left basal ganglia concerning for ischemic stroke. MRI of the head showed restricted diffusion and T2/FLAIR hyperintensity in the posterior head and body of the left caudate, globus pallidus, internal capsule and extending into left corona radiata consistent with an ischemic infarct. MRA of the head was negative.

Discussion

Mineralizing lenticulostriate vasculopathy (MLV) is a rare vascular condition seen in infants, characterized by calcification within the perforating lenticulostriate arteries that supply the basal ganglia. MLV is associated with a higher risk of ischemic stroke in infants, particularly those involving minor head trauma.

Basal ganglia strokes account for approximately 1 to 2 per 100,000 children annually. Strokes associated with MLV are even less common. Abnormal calcification creates fragile vasculature that is more susceptible to injury from even minor head trauma, leading to an increased risk of vascular compromise and ischemic stroke.

Clinical Presentation of MLV-associated basal ganglia stroke in infants depends on the extent and location of the ischemic injury. Common signs include hemiparesis or hemiplegia, seizures, developmental delays, behavioral changes and bulging fontanelle.

MLV manifests as branching echogenic stripes in basal ganglia on cranial ultrasound. MRI often shows arterial infarction in the basal ganglia, while head CT reveals typical bilateral, punctate, and asymmetric calcifications in the basal ganglia, indicating mineralization of the lenticulostriate arteries. Brain MRI with susceptibility-weighted sequences and brain MRA do not detect calcification or vascular abnormalities.

Iron deficiency is commonly associated with this condition, especially among Indian children. Most children recover from these strokes with no or minimal neurological deficits. However, there is a notable risk of recurrent stroke following subsequent minor head trauma, particularly in cases of untreated iron deficiency.

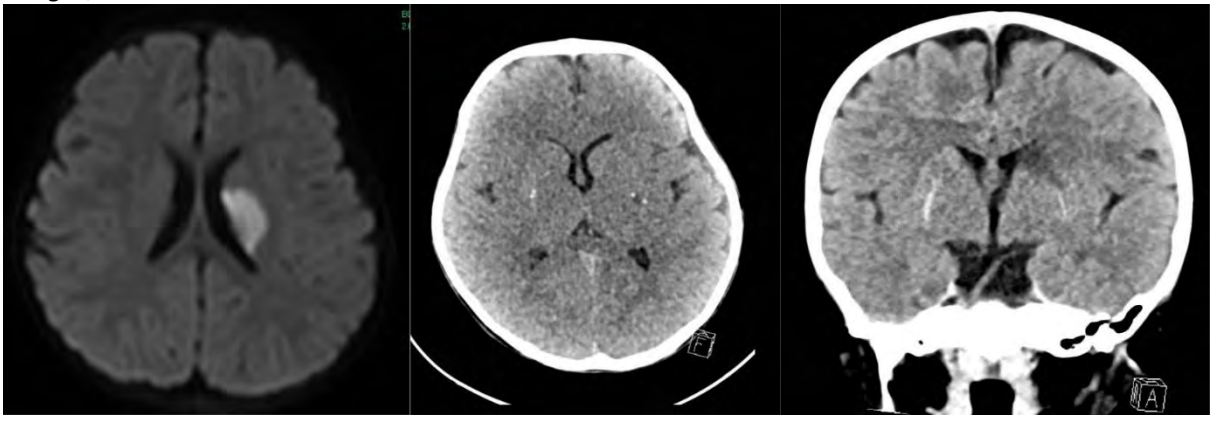
Teaching Point

While MLV itself is typically benign, it increases the risk of ischemic events in infants, even with minimal trauma. Understanding of the risk factors, clinical presentation, and imaging findings is essential for early diagnosis and intervention can significantly impact the infant's developmental trajectory and quality of life.

References

1. Jatinder Singh Goraya, Mineralizing Lenticulostriate Vasculopathy: An Emerging Risk Factor for Basal Ganglia Stroke After Minor Head Trauma in Young Children, Pediatric Neurology, Volume 145, 2023, Pages 22-27, ISSN 0887-8994,https://doi.org/10.1016/j.pediatrneurol.2023.04.024.
2. Gowda VK, Manjeri V, Srinivasan VM, Sajjan SV, Benakappa A. Mineralizing Angiopathy with Basal Ganglia Stroke after Minor Trauma: Case Series Including Two Familial Cases. J Pediatr Neurosci. 2018 Oct-Dec;13(4):448-454. doi: 10.4103/JPN.JPN_89_17. PMID: 30937087; PMCID: PMC6413602.
3. Lingappa, L., Varma, R.D., Siddaiahgari, S. and Konanki, R. (2014), Mineralizing angiopathy with infantile basal ganglia stroke after minor trauma. Dev Med Child Neurol, 56: 78-84. https://doi.org/10.1111/dmcn.12275

Images/Tables



142

Split Notochord Syndrome with Neuroenteric Fistula: An Exceedingly Rare Case Report

Michael A Negussie MD, Leul M Manyazewal MD, Fitsum A Gemechu MD, Samuel Mesfin MD
Addis Ababa University, Addis Ababa, Addis Ababa, Ethiopia

Abstract Category

Spine

Clinical History

A 7-day-old male neonate was admitted to our NICU for assessment and management of a lower back swelling accompanied by meconium extrusion. This followed an emergency cesarean section performed at 38 weeks and 3 days of gestation due to meconium-stained amniotic fluid. The mother had a normal antenatal care history with no reported fetal abnormalities. Upon examination, the patient presented with a significant lower back mass with active meconium leakage and flaccid paralysis in the lower extremities. Laboratory tests indicated elevated inflammatory markers while renal function remained normal. Diagnostic imaging revealed a complex spinal malformation consistent with a diagnosis of spinal dysraphism, characterized by a thoracolumbar cystic mass, spinal bifida, non-fusion of lumbar vertebral bodies, a neuroenteric fistula, and Chiari II malformation, as well as a right inguinal hernia and hydronephrosis. During laparotomy, intestinal malrotation and colonic duplication were also identified. The surgical interventions included neuroenteric fistula separation, a double barrel sigmoid colostomy, and a Ladd's procedure. By the 23rd day of life, the patient developed fever, tachypnea, and tachycardia, with purulent discharge from the surgical site. Despite antibiotic therapy, the patient's condition worsened, leading to death on day 28 of life from overwhelming sepsis.

Imaging Findings

Post-contrast abdominal CT scan revealed several key findings. A posterior lower back mass was identified, measuring 3.2cm by 5.4cm, which was found to be directly continuous with the central spinal canal. Notably, the posterior vertebral elements were absent in this area. Additionally, there was non-fusion of the lower lumbar vertebral bodies observed. A midline spinal osseous structure was also noted, suggesting the presence of bony diastematomyelia. The bowel loops appeared closely associated, with a tract-like continuity observed from the large bowel to the spinal canal through the bony defect. Furthermore, a right inguinal hernia was identified. On MRI, complete spina bifida and large thoracolumbar cystic mass with cord and nerve root within it (myelomeningocele) traversing both anteriorly and posteriorly were seen. Additionally, tubular structure (bowel loop) was noted protruding horizontally through the vertebral body. Tonsillar herniation with extensive hydrocephalus was also seen. Sacrum and coccyx were absent. So as a conclusion, split notochord syndrome with neuroenteric fistula and Chiari II malformation were diagnosed.

Discussion

Split notochord syndrome (SNS), as outlined by Bentley and Smith, is a multifaceted congenital anomaly characterized by various malformations. It predominantly impacts the spine, central nervous system, and gastrointestinal tract. The etiology of SNS lies in embryological development, particularly the atypical formation and division of the notochord. In approximately 50% of cases, SNS is associated with a neuroenteric fistula (NEF). To date, fewer than 30 cases of SNS with NEF have been documented.

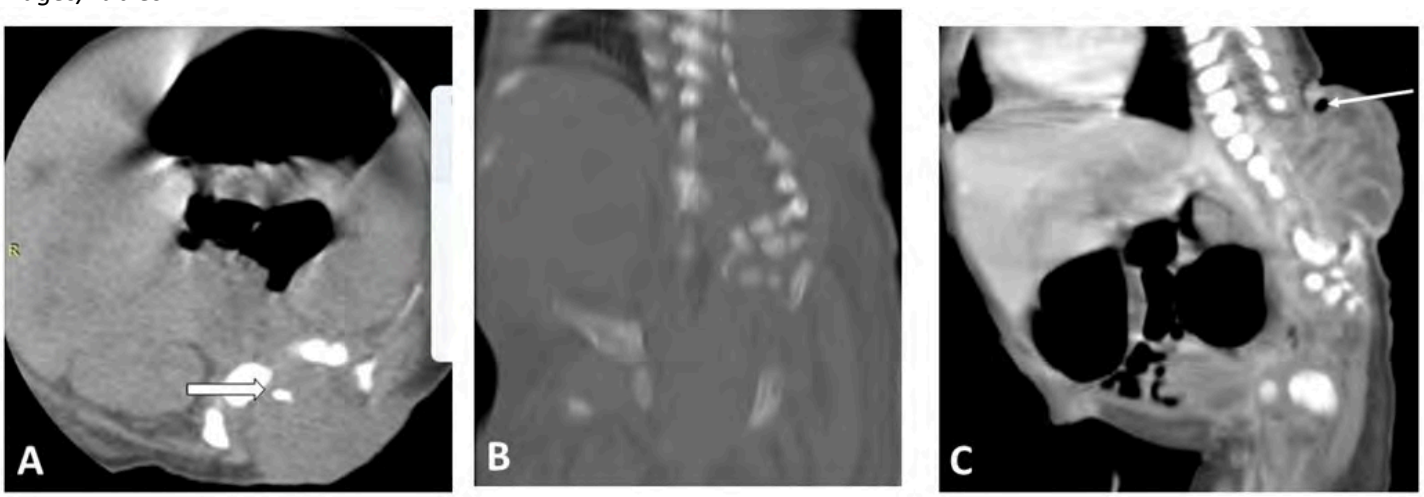
Teaching Point

This case highlights the intricate nature of patients with SNS and emphasizes the necessity for improved monitoring and swift interventions in individuals with this uncommon congenital malformation.

References

Journal article
Negussie MA, Manyazewal LM, Gemechu FA, Mesfin S, Mekonnen A, Negussie T. Split notochord syndrome with neuroenteric fistula: A case report. *J Pediatr Surg Case Rep.* 2024;103:102791. doi:10.1016/j.epsc.2024.102791.
Journal article
Bentley JF, Smith JR. Developmental posterior enteric remnants and spinal malformations: the split notochord syndrome. *Arch Dis Child*. 1960;35(179):76-86. doi:10.1136/adc.35.179.76.

Images/Tables



157

Classic CHANTER Syndrome

Jonathan W Nazha MD[1], Timothy Nguyen[2], Greg Wrubel MD[3]
[1]Hartford Hospital, Hartford, CT, USA. [2]Touro University, Vallejo, CA, USA. [3]Hartford, CT, USA

Abstract Category

Adult Brain

Clinical History

A 33-year-old male with history of multiple psychiatric disorders, polysubstance abuse, depression, anxiety, and prior suicide attempts presented with concerns of heroin overdose after his father found him unresponsive. Patient could not recall the events prior to LOC. An MRI was ordered.

Patient was diagnosed with anoxic brain injury and CHANTER syndrome related to heroin overdose and intubated. Complications included rhabdomyolysis and left compartment syndrome. He developed aspiration pneumonia, COVID-pneumonia, and a left leg abscess.

Imaging Findings

Restricted diffusion involving the globus pallidus, the hippocampal cortex, the basal ganglia, and the cerebellar hemispheres bilaterally as well as punctate foci of restricted diffusion involving the periphery of the cerebral hemispheres bilaterally in keeping with cytotoxic edema due to CHANTER syndrome in the setting of drug overdose, most likely opioid overdose.

Cytotoxic edema within the cerebellum results in significant effacement of the fourth ventricle inferiorly and there is new moderate to severe supratentorial hydrocephalus with transependymal CSF effusion.

There is mild cerebellar tonsillar herniation and there is ascending transtentorial herniation due to significant cerebellar edema.

Discussion

Cerebellar, Hippocampal, and Basal Nuclei Transient Edema with Restricted Diffusion (CHANTER) Syndrome is a rare and emerging condition typically seen in conjunction with opioid overdose[1]. It is usually linked to opiate-induced hypoxia with resulting mitochondrial injury. This condition affects neurons in the hippocampus, cerebellum, and basal ganglia – as can be seen in this patient's imaging findings.

Imaging is crucial in diagnosing CHANTER syndrome. MRI findings may show diffusion restriction in cerebellar cortices, hippocampus, and basal ganglia. Importantly, an appropriate clinical history must be considered, as other etiologies including, but not limited to, seizure-related signal changes, PRES, and ADEM can all exhibit similar appearance[2].

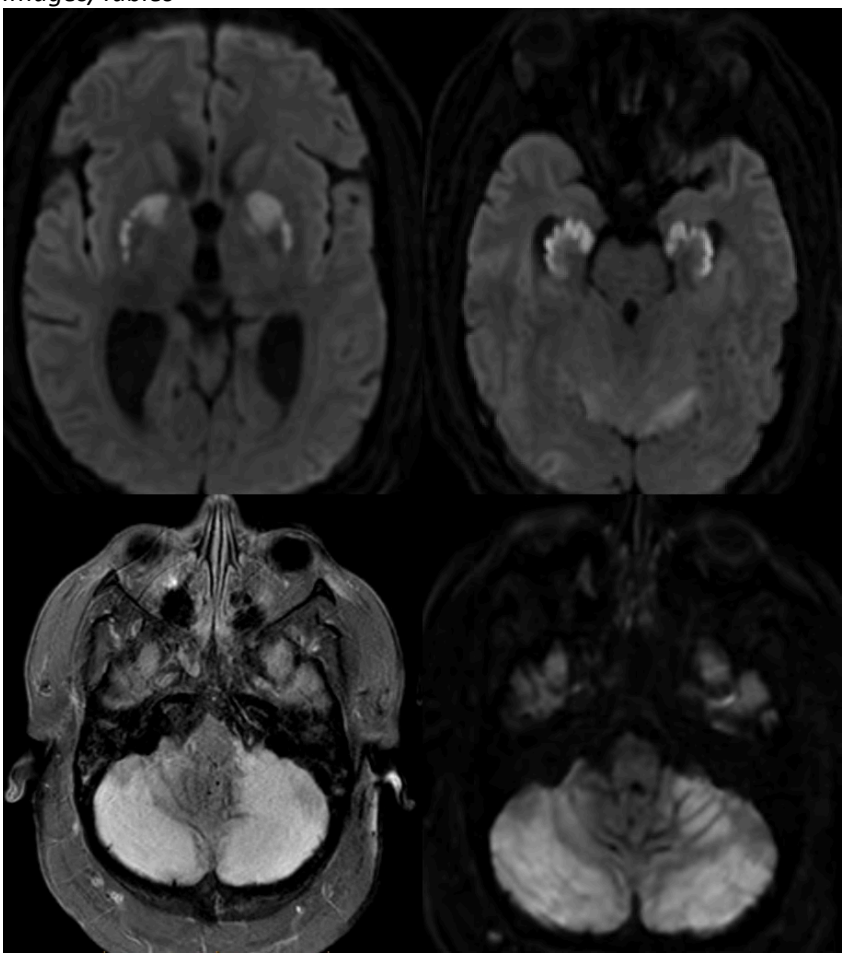
Teaching Point

CHANTER syndrome is a newly recognized, opioid-induced encephalopathy seen with distinct cerebellar and hippocampal MRI findings. Early identification and intervention, including opioid reversal with naloxone, are critical to reduce long-term neurological damage. This case highlights the importance of recognizing cytotoxic edema patterns on imaging in conjunction with adequate clinical history to promptly recognize the effects of opioid toxicity on the central nervous system.

References

1. Pandit R, Hamki O, Gaddamanugu S. Cerebellar, Hippocampal, and Basal Nuclei Transient Edema With Restricted Diffusion (CHANTER) Syndrome: Radiologic Features and Findings. Korean J Radiol. 2024 Mar;25(3):314-318. doi: 10.3348/kjr.2023.1142. PMID: 38413115; PMCID: PMC10912496.
2. Finsterer J, Mehri S. Before Diagnosing CHANTER Syndrome, All Possible Differential Diagnoses Must Be Carefully Excluded. Korean J Radiol. 2024 Jun;25(6):589-590. doi: 10.3348/kjr.2024.0244. PMID: 38807341; PMCID: PMC11136941.

Images/Tables



163

ICANS Believe It's Not Over: Unraveling the Brain Fog of CAR-T Therapy

Carlo Castro MD, Kassie McCullagh MD, David Bartlett MD

University of North Carolina Chapel Hill, Chapel Hill, North Carolina, USA

Abstract Category

Adult Brain

Clinical History

29-year-old man with DLBCL diagnosed 9 months ago whom failed initial chemotherapy regimen (R-CHOP), now with chemo-refractory DLBCL. Chimeric antigen receptor T-cell therapy (CAR-T) infusion was administered to the patient after lymphodepletion. The patient was counseled on the symptoms of cytokine release syndrome (CRS) and immune effector cell-associated neurotoxicity syndrome (ICANS) and presented to the hospital 1 day after infusion with fevers, chills, and body aches. The patient had sudden and progressive loss of neurological function on the 3rd hospital day. Initial Head CTs were negative for acute abnormalities. A Brain and C/T/L-spine MRI was ordered to further investigate neurologic changes.

Imaging Findings

Brain MRI:

On the FLAIR sequence, diffuse bilateral cortical, thalamic, and external capsule edema are present. Additionally, restricted diffusion and edema of the medulla oblongata and upper spinal cord are present.

C/T/L-spine MRI:

Extensive longitudinal central cord hyperintense signal on T2-weighted images (STIR) from the medulla oblongata to T12/L1, concerning for myelitis/edema.

Discussion

ICANS, formerly Cytokine Release Encephalopathy Syndrome, is a relatively new phenomenon associated with CAR-T infusions. CAR-T therapy was first approved by the FDA in 2017 and has increasing utility in diseases including lymphomas, acute lymphoblastic leukemia, and multiple myeloma. Increased use of CAR-T therapy with new clinical trials makes recognition of ICANS more important to the radiologist.

Imaging findings of ICANS are nonspecific. A history of recent CAR-T therapy, or a high suspicion, is very helpful in making the correct diagnosis or providing it within the differential of the case. Differential diagnoses include acute infarction, demyelinating disorders, and toxic leukoencephalopathy from etiologies including antineoplastic/immunosuppressive drugs, drugs of abuse, and metabolic abnormalities such as hyperammonemia. Most patients undergoing imaging for the evaluation of ICANS will have normal or unchanged findings from baseline imaging. Imaging findings of ICANS can be grouped into common and uncommon findings.

Common findings include:

- Periventricular or subcortical white matter FLAIR hyperintensities, new from baseline (the most common ICANS finding).
- The external and extreme capsules, brainstem, and thalami can also be affected.
- Focal or diffuse cerebral edema and its sequelae.
- Normal MRA.

Uncommon findings include:

- Intracranial hemorrhage/microhemorrhages.
- Findings similar to posterior reversible encephalopathy syndrome including bilateral occipital/parietal lobe or watershed cortical/subcortical edema,
- Cortical restricted diffusion.
- Leptomeningeal enhancement (although it may be due to underlying leptomeningeal disease).
- Myelitis of the spinal cord.

Teaching Point

1. ICANS is associated with exposure to CAR-T therapy which has increasing clinical utility in certain leukemias, lymphomas, and more recently multiple myeloma. Their expanding use makes recognition of ICANS imaging findings more important to the radiologist.
2. Most clinical cases of ICANS present with normal imaging findings on CT and MRI. When findings are present, they typically represent a worse prognosis.
3. Imaging findings of ICANS are nonspecific – clinical history of CAR-T therapy or a high suspicion is helpful. Findings can include periventricular or subcortical white matter FLAIR changes from baseline imaging, cerebral edema and its expected sequelae, intracranial hemorrhage/microhemorrhages, leptomeningeal enhancement, and areas of diffusion restriction from ischemia/cytotoxic edema.

References

1. de Groot PM, Arevalo O, Shah K, et al. Imaging Primer on Chimeric Antigen Receptor T-Cell Therapy for Radiologists. RadioGraphics 2022;42:176–94.
2. Grant SJ, Grimshaw AA, Silberstein J, et al. Clinical presentation, risk factors, and outcomes of immune effector cell-associated neurotoxicity syndrome following CAR-T cell therapy: A Systematic Review. *Transplant Cell Ther* 2022;28:294–302.
3. Lee DW, Santomasso BD, Locke FL, et al. ASTCT Consensus Grading for Cytokine Release Syndrome and Neurologic Toxicity Associated with Immune Effector Cells. *Biol Blood Marrow Transplant* 2019;25:625–38.

Images/Tables

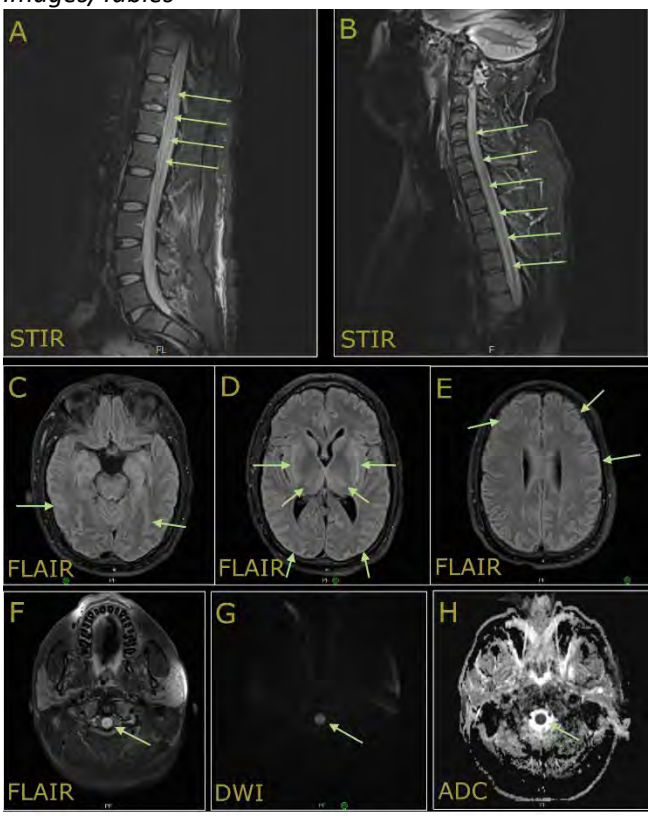


Figure 1. Sagittal images of the spine demonstrates extensive longitudinal central cord T2/STIR hyperintensities from the medulla oblongata to T12/L1 **(A, B)**. Axial images of the brain demonstrates diffuse bilateral cortical, thalamic, and external capsule T2/FLAIR hyperintensities **(C, D, E)**, as well as restricted diffusion and T2/FLAIR hyperintensity of the medulla oblongata and upper cervical spinal cord **(F, G, H)**.

184

Infantile Alexander Disease: A Case Report of a Rare Leukodystrophy

Matthew M Warrick MD, Mohammad Alberawi MD
University of Oklahoma Health Sciences Center, Oklahoma City, OK, USA

Abstract Category

Pediatrics

Clinical History

A 3-month-old female without significant past medical history presented with several weeks of vomiting, loss of control of head movements and increasing head circumference. Initial exam was notable for leukocytosis without fever.

Imaging Findings

Initial head CT demonstrated prominent, symmetric, bilateral frontal white matter hypodensities (Fig. 1a). Axial T2WI MR revealed extensive cystic hyperintensity within bilateral frontal white matter extending from the ventricular margins to the subcortical U-fibers; a hypointense, nodular, periventricular rim; and mild hyperintensity and swelling of bilateral striata, (Fig 1b). Axial T1WI MR revealed bilateral frontal white matter hypointensity with a hyperintense periventricular rim, (Fig. 1c). Axial and coronal T1 post-contrast MRI revealed thick enhancement along the margins of the cystic changes in the frontal lobes, along the periventricular rim and within the striata. There was leptomeningeal enhancement involving the oculomotor nerves, optic chiasm, interpeduncular cistern, and fourth ventricle, (Fig. 1d, 1e). Cystic T2 hyperintensity extending along the anterior aspect of bilateral middle cranial fossae was also noted. No distinct signal abnormalities were seen within the brainstem. Total spine MR was unrevealing.

Discussion

A leukodystrophy was suspected based on the initial CT. Subsequent MRI findings suggested a diagnosis of Alexander disease. Given the presence of leptomeningeal enhancement, lumbar puncture was recommended to evaluate for

infectious or inflammatory etiologies. LP revealed elevated opening pressures and protein but was negative for infection. No acute intervention was pursued by Neurosurgery and patient was discharged in stable condition. Epileptic seizures developed in the months after discharge and were managed medically and follow-up is ongoing. Genetic analysis later revealed a GFAP mutation confirming the diagnosis.

Alexander disease is a leukodystrophy caused by sporadic mutations in the gene encoding the glial fibrillary acidic protein, (GFAP), the major intermediate filament protein within astrocytes. The pathological hallmark of the disease, termed Rosenthal Fibers, are eosinophilic granular bodies which accumulate within the cytoplasm of fibrous astrocytes in the subependymal, subpial, and perivascular regions.

Four clinical subtypes have been described: neonatal, infantile, juvenile, and adult forms; and the severity of the disease is inversely proportional to the age of onset. The presently discussed infantile subtype is the most well described in literature. Patients with the infantile form present with macrocephaly, developmental delay and seizures and it is invariably fatal within a few years of diagnosis. The juvenile and adult forms tend to involve the brainstem and cerebellum and follow a more protracted course.

Diagnosis can be made with MRI if four out the five following imaging features are present in the appropriate clinical setting: frontal predominant white matter changes, periventricular rim of T1 hyperintensity and T2 hypointensity, involvement of the basal ganglia and thalamus, involvement of the brainstem, and enhancement of certain grey and white matter structures. Leptomeningeal enhancement, as seen in this case, is rare but has been reported in literature.

Teaching Point

This case highlights typical imaging features of a case of infantile Alexander disease. The frontal predominant distribution and associated enhancement can reliably distinguish it from other similar leukodystrophies.

References

1. Van der Knaap MS, Naidu S, Breiter SN, et al. Alexander Disease: Diagnosis with MR Imaging. *AJNR Am J Neuroradiol* 2001 Mar;22(3):541-52. PMID: 11237983; PMCID: PMC7976831
2. Cheon JE, Kim, IO, Hwang YS, et al. Leudkodystrophy in Children: A pictorial review of MR imaging features. *RadioGraphics* 2002 May; 22:3, 461-476. DOI: https://doi.org/10.1148/radiographics.22.3.g02ma01461
3. Shah M, Ross, JS. Infantile Alexander Disease, MR appearance of a biopsy proven case. *AJNR Am J Neuroradiol* 1990 Nov; 11(6):1105-1106 PMID: 2124037; PMCID: PMC8332150

Images/Tables

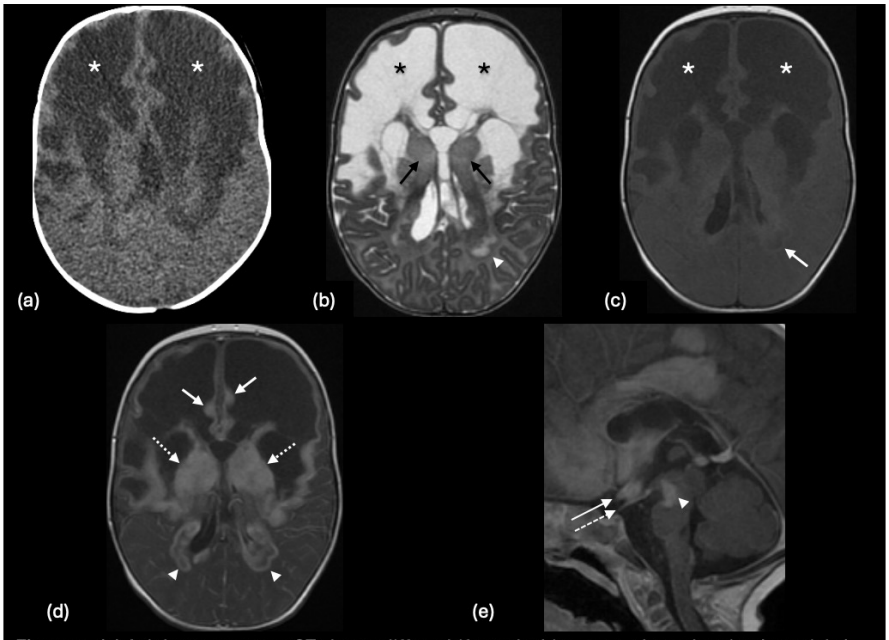


Figure 1. (a) Axial non-contrast CT shows diffuse bifrontal white matter hypodensity, (asterisks), extending into the bilateral basal ganglia. (b) Axial T2WI MR shows diffuse cystic hyperintensity within the bifrontal white matter extending from the ventricular margins to the subcortical U-fibers (asterisks); a hypointense periventricular rim, (arrowhead); and mild hyperintensity and swelling of bilateral striata, (arrows). (c) Axial T1WI MR shows diffuse bifrontal white matter hypointensity (asterisks), with a hyperintense periventricular rim, (arrow). (d) Axial post-contrast T1WI MR shows thick enhancement along the margins of the cystic changes in the frontal lobes, (solid arrows), along the periventricular rim, (arrowheads), and within the striata, (dashed arrows). (e) Sagittal post-contrast T1WI shows leptomeningeal enhancement involving the optic chiasm, (solid arrow), oculomotor nerves, (dashed arrow), and within the interpeduncular cistern, (arrowhead).

198

Spontaneous Mediastinal Hemorrhage Mimicking an Esophageal Mass: A Rare Presentation of Parathyroid Adenoma

Omar A Alharbi MD, Reese W Randle MD, Paul M Bunch MD
Wake Forest University School of Medicine, Winston Salem, NC, USA

Abstract Category

Head & Neck

Clinical History

A 60-year-old female presented to the emergency department with acute onset chest pain and dysphagia. Chest CT was performed to evaluate these symptoms.

Imaging Findings

Chest CT demonstrated ill-defined mediastinal soft tissue attenuation surrounding the esophagus, extending from the thoracic inlet to the diaphragm (arrows, Figure 1A and 1B).

Chest CT findings were interpreted as suspicious for esophageal neoplasm, prompting esophageal endoscopy with tissue sampling. Endoscopy revealed esophageal wall thickening without discrete mass. Histopathologic evaluation of the tissue samples demonstrated no evidence of malignancy. A follow-up MRI was planned to further characterize the mass and to guide repeat tissue sampling.

Neck MRI performed 1 month after the initial chest CT demonstrated marked improvement in the previous ill-defined mediastinal soft tissue. However, a focal right paraesophageal nodule was identified (circle, Figure 1C), which in retrospect corresponded to a hyperenhancing nodule on the original chest CT (circle, Figure 1A).

Parathyroid adenoma was raised as a diagnostic possibility, and biochemical evaluation confirmed the presence of primary hyperparathyroidism.

Following parathyroid CT (Figure 1D) for pre-operative localization, the patient underwent parathyroidectomy. Histopathological evaluation confirmed the right paraesophageal nodule to represent a parathyroid adenoma (circle, Figure 1D). The patient's calcium and parathyroid hormone levels normalized.

Discussion

Spontaneous hemorrhage of a parathyroid adenoma can be a life-threatening condition and was first reported in 1934 (1). Since then, more than 80 cases of hemorrhage linked to parathyroid adenoma have been reported in the literature (2). The pathophysiology behind such bleeding is not clearly understood, but possible predisposing factors include an imbalance between tumor growth and blood supply, the thin nature of the parathyroid gland's capsule, trauma, anticoagulant therapy, and use of non-steroidal anti-inflammatory drugs (3).

The clinical presentation is variable and may include neck swelling, dysphagia, and dyspnea. Hemorrhagic parathyroid adenoma warrants particular consideration in the setting of hypercalcemia and regional ecchymosis (4).

Initial treatment of ruptured parathyroid adenoma focuses on clinical assessment to determine the presence or absence of life-threatening airway compromise requiring immediate intubation, tracheostomy, or neck exploration. Once the patient has been stabilized, many surgeons prefer to postpone parathyroidectomy until the hematoma has resolved to decrease the risk of perioperative complications (5).

Teaching Point

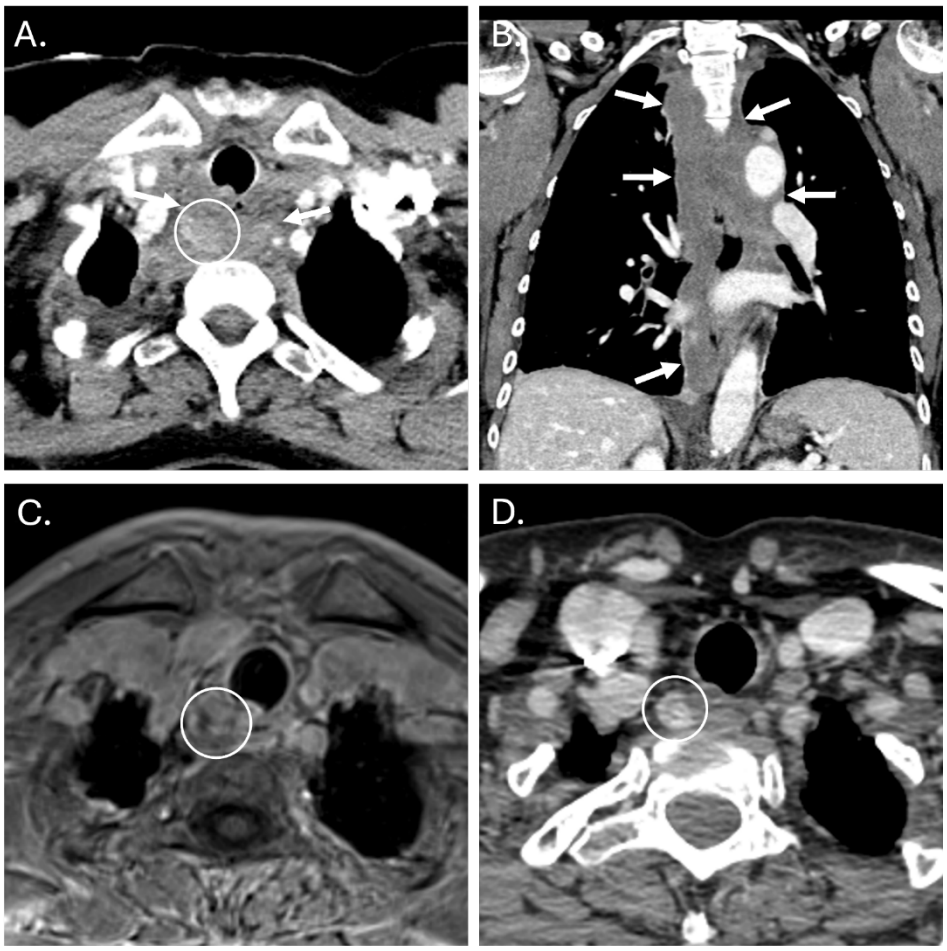
- Imaging findings of mediastinal hematoma can be confused for infiltrative neoplasm and lead to invasive additional testing.
- Although uncommon, spontaneous hemorrhage within the neck or mediastinum is an important presentation of parathyroid adenoma for the radiologist to consider and recognize.
- If no cause for hemorrhage is identified at the time of initial evaluation, a short-interval follow-up examination is prudent and may allow for identification of the parathyroid adenoma or other underlying lesion.
- When considering the possibility of parathyroid adenoma, correlation with serum calcium and parathyroid hormone levels is useful to determine the presence or absence of primary hyperparathyroidism.

References

1. Capps RB. Multiple parathyroid tumors with massive mediastinal and subcutaneous hemorrhage: A case report. *Am J Med Sci* 1934;188:800-805.
2. Han YZ, Zhou Y, Peng Y, et al. Difficult airway due to cervical haemorrhage caused by spontaneous rupture of a parathyroid adenoma: A case report. *World J Clin Cases*. 2023;11(5):1217-1223. doi:10.12998/wjcc.v11.i5.1217.

3. Huang J, Soskos A, Murad SM, et al. Spontaneous hemorrhage of a parathyroid adenoma into the mediastinum. *Endocr Pract*. 2012;18(4):e57-e60. doi:10.4158/EP11329.CR.
4. Merante-Boschin I, Fassan M, Pelizzo MR, et al. Neck emergency due to parathyroid adenoma bleeding: a case report. *J Med Case Rep*. 2009;3:7404. Published 2009 May 21. doi:10.1186/1752-1947-3-7404.
5. Familiari M, Di Santo D, Galli A, et al. Spontaneous extracapsular parathyroid adenoma hemorrhage: when surgery is required?. *Endocrine*. 2022;75(2):575-582. doi:10.1007/s12020-021-02876-x.

Images/Tables



200

Mitochondrial Complex I Deficiency Involving the Brainstem

Clara A Nemr BS[1], Justin D Chen BS[1], Talha Allam MD[2]
[1]Chicago College of Osteopathic Medicine, Downers Grove, IL, USA. [2]Advocate Health Care, Oak Park, IL, USA

Abstract Category

Pediatrics

Clinical History

A 10-year-old female presented with respiratory failure and pneumonia. The patient has a known past medical history of generalized hypotonia, developmental delay, respiratory failure, failure to thrive, seizure-like activity with abnormal EEG, nystagmus, and apnea requiring intubation. The patient had seizure-like activity in the hospital and underwent an MRI brain for further evaluation. The patient was admitted to the hospital for acute respiratory failure and intubated, unable to be weaned off. Whole exome sequencing showed a homozygous pathogenic variant in NDUFAF2, consistent with mitochondrial complex 1 deficiency. The patient expired a few weeks later due to respiratory failure.

Imaging Findings

MRI images of axial FLAIR show hyperintensity in substantia nigra, cerebral peduncles, medulla, and cervicomedullary junction

MRI images of axial DWI and ADC show symmetric hyperintensity in the hypothalamus, substantia nigra, cerebral peduncles, central tegmental tracts, restiform bodies, and cervicomedullary junction.

Discussion

Mitochondrial complex I deficiency is a rare genetic disorder that significantly impacts cellular energy production, leading to diverse clinical manifestations [1,2] It is characterized by predominant brainstem involvement with relative sparing of the basal ganglia. This atypical presentation poses unique diagnostic challenges and highlights the importance of recognizing varied clinical and radiological patterns in mitochondrial disorders.

The case presented here demonstrates several key features that distinguish it from classical Leigh syndrome which is associated with mutations of 16 mitochondrial genes and almost 100 nuclear genes [3]. The MRI findings in our patient differ from the bilateral, symmetrical basal ganglia, and thalamic lesions seen in Leigh Syndrome [4]. This relative sparing of the basal ganglia in the presence of extensive brainstem involvement represents a unique radiological pattern.

The patient's history of generalized hypotonia, developmental delay, respiratory failure, and seizure-like activity aligns with the complex clinical picture often seen in mitochondrial disorders and non-mitochondrial disorders. However, the prominence of respiratory issues and brainstem dysfunction, as evidenced by nystagmus and apnea, points towards a brainstem-predominant phenotype. Additionally, identifying a homozygous pathogenic variant in NDUFAF2 confirms the mitochondrial complex I deficiency diagnosis. NDUFAF2 is known to encode an assembly factor for complex I, and mutations in this gene have been associated with various presentations of complex I deficiency, including some cases with atypical features [5].

Teaching Point

This case emphasizes the importance of considering mitochondrial complex I deficiency in patients presenting with progressive brainstem dysfunction in the absence of basal ganglia involvement. The unique radiological pattern observed here can serve as a key distinguishing feature for clinicians and radiologists. Furthermore, this case emphasizes that although the more common Leigh disease usually features bilateral and symmetric lesions in the basal ganglia, other mitochondrial disorders can primarily present with lesions in the brainstem. This case also broadens our understanding of the clinical and radiological spectrum of mitochondrial complex I deficiency. It underscores the need for a high index of suspicion in infants presenting with progressive neurological symptoms, particularly those involving brainstem function. Early recognition of atypical presentations can facilitate timely diagnosis, appropriate genetic counseling, and optimal management strategies for these complex patients.

References

REFERENCES:

1. Mimaki M, Wang X, McKenzie M, Thorburn DR, Ryan MT (2012) Understanding mitochondrial complex I assembly in health and disease. Biochimica et Biophysica Acta (BBA) - Bioenergetics 1817:851–862. https://doi.org/10.1016/j.bbabio.2011.08.010

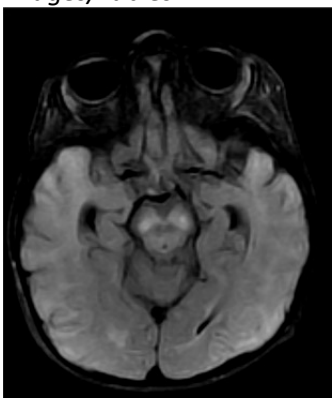
2. Lazarou M, Thorburn DR, Ryan MT, McKenzie M (2009) Assembly of mitochondrial complex I and defects in disease. Biochimica et Biophysica Acta (BBA) - Molecular Cell Research 1793:78–88. https://doi.org/10.1016/j.bbamcr.2008.04.015

3. Fassone E, Rahman S (2012) Complex I deficiency: clinical features, biochemistry and molecular genetics. J Med Genet 49:578–590. https://doi.org/10.1136/jmedgenet-2012-101159

4. Rahman S (2023) Leigh syndrome. In: Handbook of Clinical Neurology. Elsevier, pp 43–63

5. Abu Hanna F, Zehavi Y, Cohen-Barak E, Khayat M, Warwar N, Shreter R, Rodenburg RJ, Spiegel R (2024) Lack of mitochondrial complex I assembly factor NDUFAF2 results in a distinctive infantile-onset brainstem neurodegenerative disease with early lethality. Orphanet J Rare Dis 19:92. https://doi.org/10.1186/s13023-024-03094-0

Images/Tables



212

ALK-rearranged non-small cell lung cancer cystic brain metastases

Abdulrahman Al Halak DO[1], Francis Deng MD[2], Dhairya A Lakhani MD[1]
[1]West Virginia University, Morgantown, WV, USA. [2]Johns Hopkins University, Baltimore, MD, USA

Abstract Category

Head & Neck

Clinical History

A 53-year-old woman with anaplastic lymphoma kinase (ALK) rearranged non-small cell lung cancer (NSCLC) was referred to our institution due to an increase in the size and number of cystic brain lesions over 14-months, noted on staging brain MRI. She was asymptomatic and on alectinib (ALK inhibitor) therapy.

Imaging Findings

The MRI of the head revealed multiple cystic lesions in the brain, characterized by variable signal suppression on FLAIR and minimal to no contrast enhancement, except for a few areas of thin cyst wall enhancement (Figure 1). Over the 14-month period, there was an increase in both the size and number of lesions (Figure 2). These findings were consistent with cystic brain metastases, a rare manifestation of ALK-rearranged NSCLC.

Differential diagnoses based on the initial MRI included dilated perivascular spaces and neurocysticercosis. However, the lack of temporal evolution into different stages ruled out neurocysticercosis, while changes in size and number excluded the possibility of dilated perivascular spaces.

Discussion

Cystic brain metastases are rare but have been documented in patients with ALK-rearranged NSCLC, particularly in those receiving ALK inhibitors like crizotinib. These lesions differ from other causes of brain metastases, which typically present with significant surrounding edema and contrast enhancement.

Teaching Point

In patients with ALK-rearranged NSCLC undergoing ALK inhibitor therapy, cystic brain metastases should be considered when evaluating intracranial cystic lesions, despite their rarity. This case highlights the importance of recognizing this uncommon metastatic presentation for accurate diagnosis and management, as illustrated by Figures 1 and 2.

References

1. Hayashi H, Okamoto I, Tanizaki J, Tanaka K, Okuda T, Kato A, Nishimura Y, Nakagawa K. Cystic brain metastasis in non-small-cell lung cancer with ALK rearrangement. J Clin Oncol. 2014 Dec 20;32(36):e122-4. doi: 10.1200/JCO.2012.48.2141. Epub 2014 Feb 24. PMID: 24567432.
1. Lakhani DA, Joseph J. Giant Tumefactive Perivascular Spaces. Radiology. 2023 May;307(4):e222559. doi: 10.1148/radiol.222559. Epub 2023 Apr 4. PMID: 37014245.
1. Lakhani DA, Deng F, Lin DDM. Infectious Diseases of the Brain and Spine: Parasitic and Other Atypical Transmissible Diseases. Magn Reson Imaging Clin N Am. 2024 May;32(2):347-361. doi: 10.1016/j.mric.2024.02.002. PMID: 38555145.

Images/Tables

Figure 1: Axial T2-weighted (A), coronal T2-weighted (B), axial T2 fluid-attenuated inversion recovery (FLAIR) (C), axial diffusion weighted imaging (DWI) (D), axial apparent diffusion coefficient (ADC) map (E), and axial T1-weighted post contrast fat-suppressed images in a patient with ALK-positive non-small cell lung cancer. Images demonstrate numerous cystic lesions throughout the brain predominantly at gray-white matter interfaces. These lesions demonstrate internal T2 hyperintensity (A-B) that mostly suppressed on FLAIR (C); no perilesional edema; no diffusion restriction (D-E); and no or minimal rim enhancement (F, arrow).

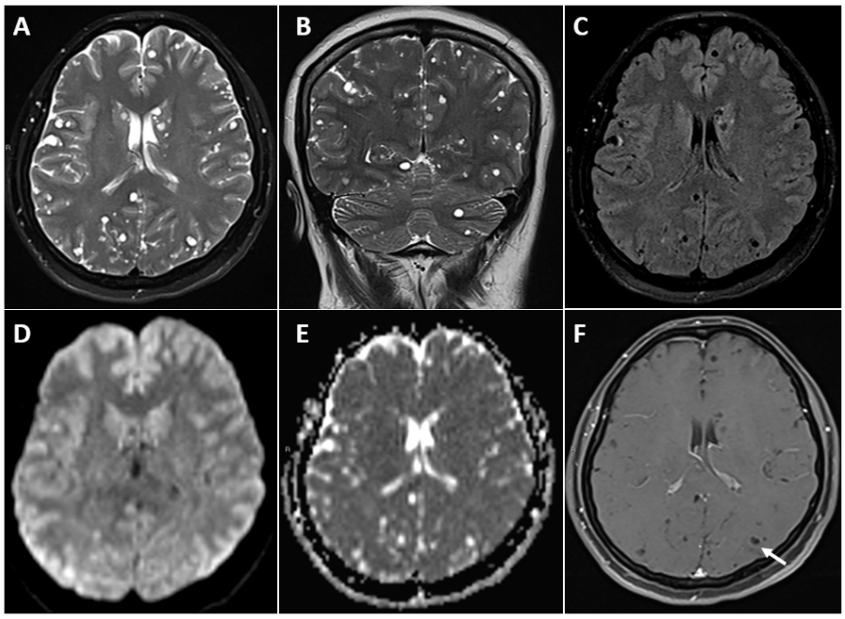
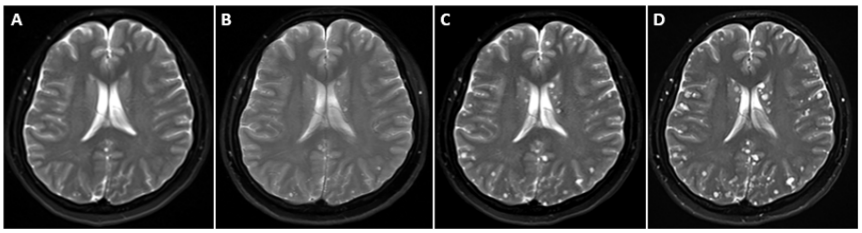


Figure 2: Axial T2-weighted images in a patient with ALK-positive non-small cell lung cancer, over a span of 14 months (A-D). At initial presentation (A), six-month following initial presentation (B), twelve-months following initial presentation (C), and fourteen-month following initial presentation (D), the lesions have shown progressive increase in size and number of numerous cystic brain lesions.



233

Granulomatous Blastomycosis Mimicking the Central Nervous System Neoplasms

Masoume Avateffazeli MD[1], Aparna Singhal MD[2], Siddhartha Gaddamanugu MD[2], Houman Sotoudeh MD[2], Dhanush Jayananda Amin MD[2]

[1]Shahid Beheshti University of Medical Sciences, Tehran, Tehran Province, Iran, Islamic Republic of. [2]University of Alabama at Birmingham (UAB), Birmingham, Alabama, USA

Abstract Category

Adult Brain

Clinical History

A 27-year-old male patient presented with vision alterations to an outside provider. He has a past history of bilateral functional endoscopic sinus surgery (FESS) about 9 years ago due to recurrent nasal polyposis with allergic fungal sinusitis. The patient complained of blurry vision, trouble reading with blind spots in the middle of his visual field bilaterally and mild headaches for a week. He denied any other accompanying symptoms including vertigo, focal weakness, sensory change, increased headache, seizure, nausea and vomiting.

The CT scan of the sinuses demonstrated a mass lesion in the anterior cranial fossa extending to the floor of the right frontal sinus, bilateral ethmoid air cells and medial right orbit. MRI of the paranasal sinuses revealed an enhancing mass lesion which is described in next section. In view of raised intracranial pressure (ICP) and visual disturbance, acetazolamide 750 mg a day was prescribed. A week later, a nasal endoscopy with biopsy was performed. Final pathology revealed granulomatous inflammation consistent with blastomycosis with lymphocytic infiltrate. Also, for further characterization, immunohistochemical staining was performed with the following results: Grocott methenamine silver stain (GMS) positive for fungi, Synaptophysin negative for neuroendocrine differentiation, CD3 and CD20: an appropriate mixture of T and B cells.

This was followed by skull base resection of the mass, septoplasty and skull base repair. Patient was discharged on Acetazolamide, Budesonide, Sulfamethoxazole-Trimethoprim and Voriconazole. He is being followed as an outpatient and has no recurring symptoms.

Imaging Findings

There is a well defined T1 isointense, Short tau inversion recovery (STIR) isointense mass lesion of anterior cranial fossa with extension to the location of ethmoidectomy. CSF cleft sign seen on axial STIR is in favor of extra-axial lesion. The lesion does not demonstrate diffusion restriction. There is avid homogenous post-contrast enhancement, with extension to right orbit mimicking a meningioma and esthesioneuroblastoma.

Discussion

Imaging may reveal similar features between neoplastic and non-neoplastic diseases of the central nervous system (CNS), including CNS blastomycosis. CNS blastomycosis is an uncommon condition, however it correlates with a significant fatality rate. Furthermore, it has a wide range of clinical symptoms. CNS blastomycosis has non-specific imaging findings like meningoencephalitis and intracranial abscesses. Focal dural based masses have been reported mimicking meningioma. However, we present a rare case of CNS blastomycosis presenting as an aggressive anterior cranial fossa lesion with osseous destruction and orbital involvement which has not been reported before.

Teaching Point

Granulomatous involvement of the skull base mimicking a skull base neoplasm is a rare manifestation of CNS Blastomycosis. While sinonasal malignancy and aggressive meningioma are the likely differential causes for destructive skull base lesions, fungal infections should be considered for patients who have had long standing sinonasal polyposis or in immunocompromised.

References

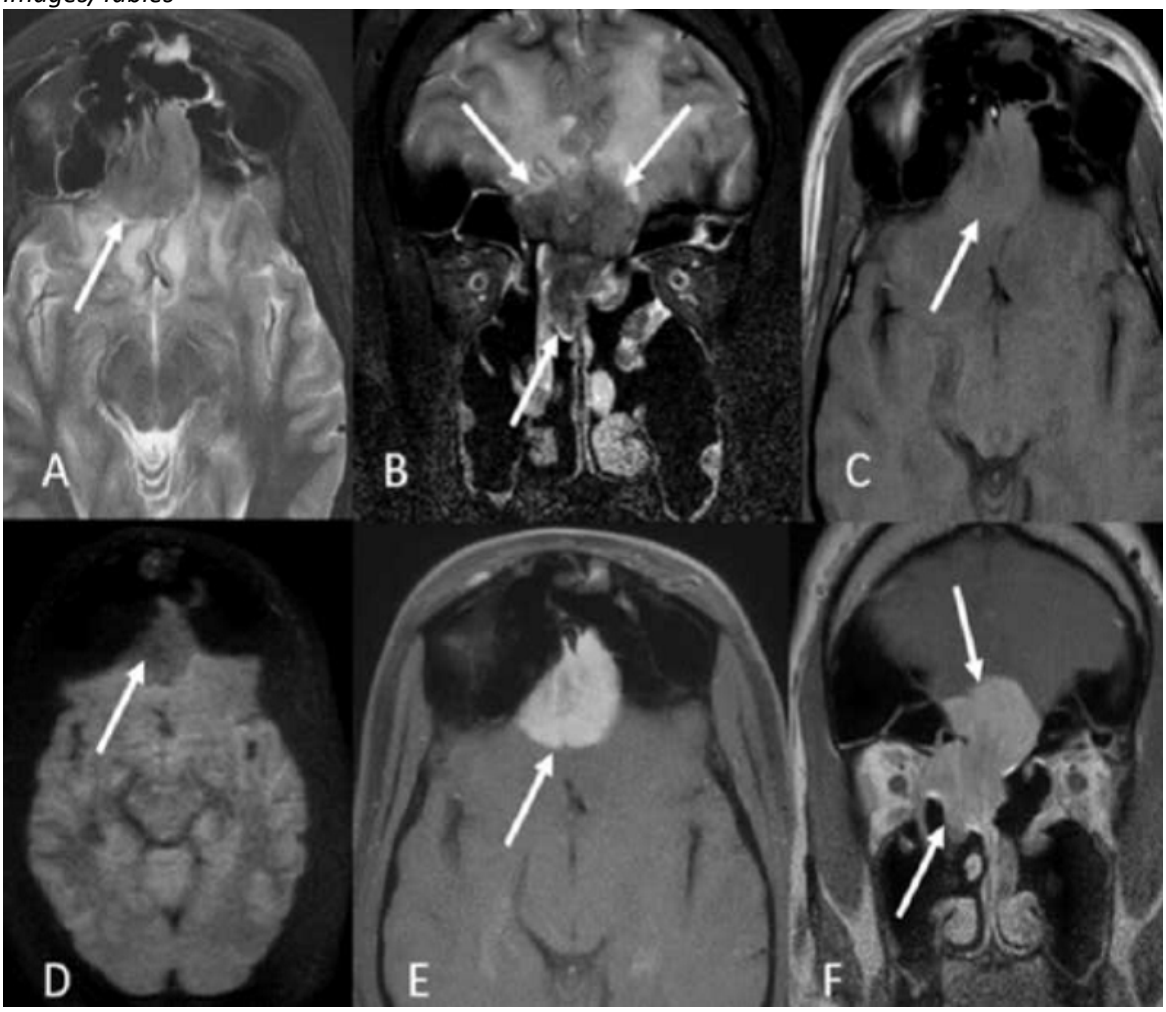
[1] V. Santosh, A. Mahadevan, Y.T. Chickabasaviah, R.D. Bharath, S.S. Krishna, Infectious lesions mimicking central nervous system neoplasms, Semin Diagn Pathol 27(2) (2010) 122-35.

[2] V.M. Godkhindi, V. Monappa, N.V. Kairanna, S. Sharma, G. Vasudevan, K.D. Hebbar, Brain infections that mimic malignancy, Diagnostic Histopathology 28(10) (2022) 456-466.

[3] M. Borni, H. Belmabrouk, B. Kammoun, M.Z. Boudawara, Gilchrist disease of the central nervous system mimicking malignant brain neoplasm: A rare and fatal complication of blastomyces dermatitidis: Diagnostic and therapeutic challenge, Interdisciplinary Neurosurgery 25 (2021) 101248.

[4] K. Majdick, K. Kaye, M.A. Shorman, Central nervous system blastomycosis clinical characteristics and outcomes, Medical Mycology 59(1) (2021) 87-92.

Images/Tables



245

Kimura Disease Presenting as a Right Neck Mass with Eosinophilia: A Case Report and Review of Imaging Findings

Patrick J Rock MD, Pattana Wangaryattawanich MD, Matt Xi Luo MD
University of Washington, Seattle, WA, USA

Abstract Category

Head & Neck

Clinical History

A 25-year-old male presented with a progressively enlarging right neck mass over the previous two weeks. The mass was painless and associated with a sensation of plugged ears, but there were no accompanying symptoms such as fever, chills, dysphagia, odynophagia, or hoarseness. The patient denied facial weakness, although there was concern about possible facial nerve involvement. His medical history included an episode of otitis externa, treated with ciprofloxacin-dexamethasone ear drops. A fine needle aspiration (FNA) yielded indeterminate results. Subsequent true cut biopsy was pursued. Laboratory results revealed marked eosinophilia. The patient was initially treated with reslizumab (Cinqair), an interleukin-5 (IL-5) inhibitor, for presumed eosinophilic involvement; however, there was minimal improvement. The patient underwent a right facial mass resection, superficial parotidectomy, right neck dissection, and abdominal fat graft. Surgical pathology showed eosinophil-predominant mixed inflammation and numerous lymph nodes with associated fibrosis and eosinophilic abscesses, most consistent with Kimura's disease.

Imaging Findings

MR imaging of the maxillofacial region with contrast, revealed a large, well-defined mass, located large in the right parotid space. The mass involved the right pinna and external auditory canal, and abutted the right mastoid bone without invasion. It extended into the subcutaneous soft tissues and dermis, protruding from the infra-auricular region. The lesions was T1 intermediate, hyperintense on STIR images, and demonstrated heterogeneous enhancement with internal vascularity. There were multiple enlarged right cervical lymph nodes involving levels II, III, and IV, as well as, in the right parotid gland. The imaging findings raised concerns for an aggressive dermal or parotid lesion, with differential diagnoses including desmoplastic tumor, or pleomorphic adenoma.

Discussion

Kimura disease is a rare, chronic, benign inflammatory disorder predominantly affecting young men of Asian descent. It is characterized by the presence of subcutaneous nodules, often in the head and neck, accompanied by eosinophilia and regional lymphadenopathy. The condition is thought to be immune-mediated, with a possible association to abnormal T-helper cell responses, though the exact etiology remains unclear. Histologically, Kimura disease is marked by dense eosinophilic infiltration, follicular hyperplasia, and vascular proliferation, which helps distinguish it from other neoplastic or infectious conditions.

In this case, the patient's clinical presentation of a painless neck mass, associated eosinophilia, and facial nerve involvement, along with imaging showing a large mass with regional adenopathy, was highly suggestive of Kimura disease. The histopathological findings from the biopsy confirmed the diagnosis of Kimura disease. Treatment typically involves corticosteroids to reduce inflammation, although some cases may require immunosuppressive therapy or surgical excision.

Teaching Point

When encountering a large subcutaneous mass in the head and neck region, it is crucial to consider eosinophilia as a diagnostic clue. If eosinophil levels are elevated, Kimura disease should be included in the differential diagnosis. Early recognition and appropriate biopsy are essential for distinguishing it from other benign and malignant lesions, which may require different management strategies.

References

1. S.-W. Park, H.-J. Kim, K.J. Sung, J.H. Lee, I.S. Park. Kimura Disease: CT and MR Imaging Findings. *American Journal of Neuroradiology*. Apr 2012, 33 (4) 784-788; DOI: 10.3174/ajnr.A2854
2. Chen H, Thompson LD, Aguilera NS, Abbondanzo SL. Kimura disease: a clinicopathologic study of 21 cases. Am J Surg Pathol. 2004;28(4):505-513. doi:10.1097/00000478-200404000-00010
3. Hiwatashi A, Hasuo K, Shiina T, et al. Kimura's disease with bilateral auricular masses. AJNR Am J Neuroradiol. 1999;20(10):1976-1978.

Images/Tables



258

Rare Case of Hypoglossal Nerve Palsy from an Atlanto-occipital Joint Synovial Cyst

Jawad Khan M.D.[1], Elleana Paradise[2], Steve Fung M.D.[1]
[1]Houston Methodist Hospital, Houston, Texas, USA. [2]Texas A&M University School Of Engineering Medicine, Houston, Texas, USA

Abstract Category

Head & Neck

Clinical History

An 80-year-old female presented with a 12-month history of progressive dysarthria, dysphagia, tongue weakness and right sided headaches. Physical exam revealed atrophy and fasciculations of the right side of the tongue, consistent with hypoglossal nerve dysfunction.

Imaging Findings

MRI demonstrated T1 hyperintense fatty replacement of the right tongue and relative posterior displacement (A). A T2 hyperintense cystic lesion was seen in direct communication with the atlanto-occipital joint and extended superiorly to the hypoglossal canal (B1 and B2). Axial post-contrast showed thin rim of peripheral enhancement of the lesion (C). Coronal post-contrast reformats showed a predominantly non-enhancing lesion occupying the right hypoglossal canal (D). There was no abnormal enhancement of the visualized hypoglossal nerve.

Discussion

Synovial cysts are fluid-filled para-articular outpouchings lined by synovial membrane. They are exceedingly rare in the cervical spine and even fewer cause cranial nerve compression, with only six observed cases reported in the literature[1-4]. In our case, a synovial cyst from the ipsilateral atlanto-occipital joint extended superiorly to occupy the right hypoglossal canal. The resulting mass effect led to chronic hypoglossal nerve palsy including atrophy and fatty replacement of the right tongue. Treatment is complex and evaluated on a case-by-case basis. Surgical resection may be considered, however neurological recovery is not guaranteed. Conservative treatment options are many including anti-inflammatory drugs, physical therapy, supportive braces, and steroid injections[2]. In our case, due to the patient's comorbidities and uncertainty of neurological recovery, conservative management was pursued. The patient's symptoms showed partial improvement with speech therapy and supportive care.

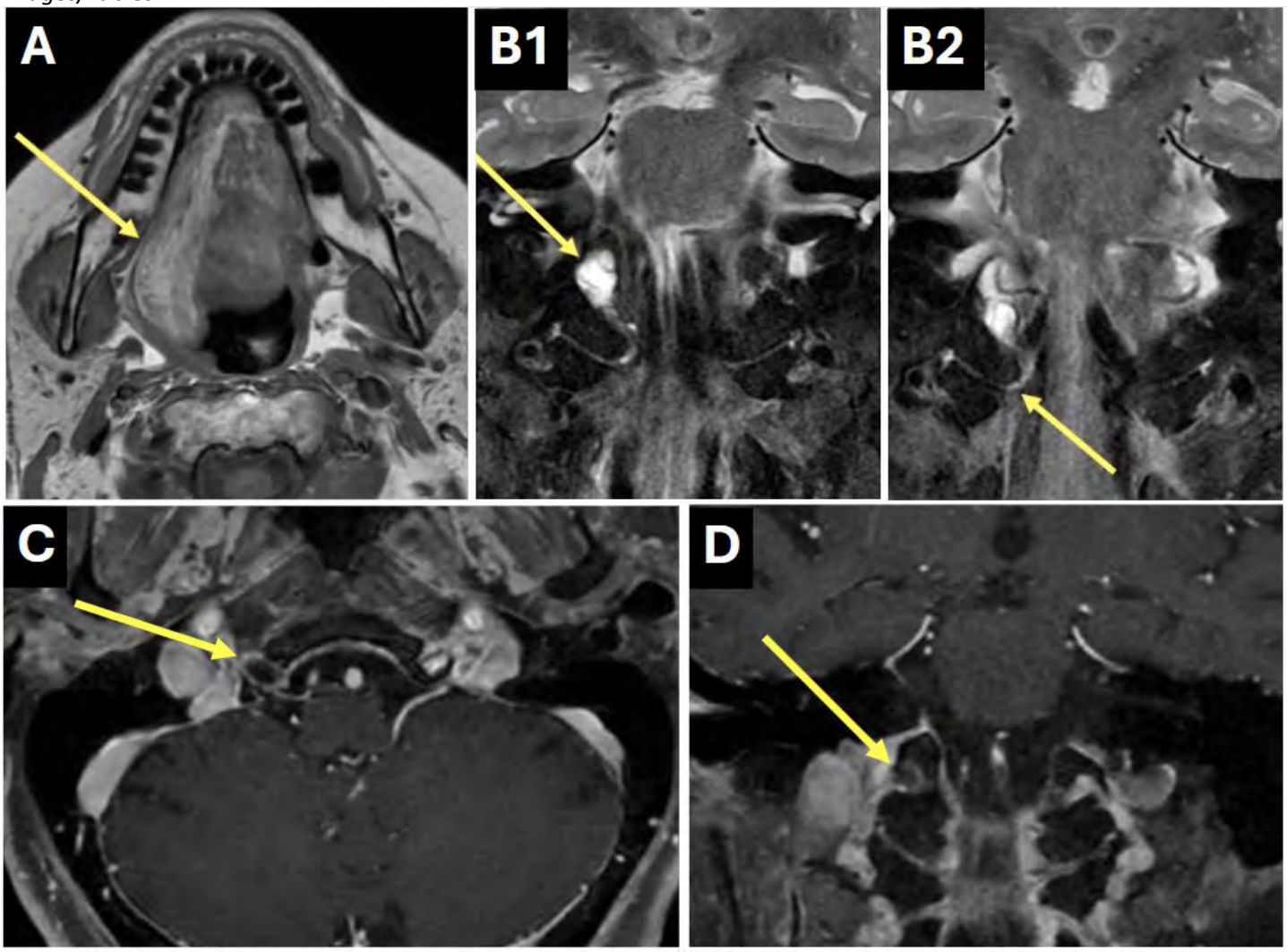
Teaching Point

It is important to consider synovial cysts as a potential etiology of cranial nerve palsies, particularly those localized to the skull base region. MRI is the modality of choice for diagnosing synovial cysts. Synovial cysts can be simple demonstrating CSF-like signal or have complex fluid signal depending on the degree of internal debris and hemorrhage. They can also enhance peripherally and communication with a joint is a key defining feature. Lastly, surgical resection does not guarantee restoration of neurological function.

References

1. De Biase G, Rivas GA, Domingo RA, Hurdle M, Chen S, Fox WC. Resolution of atlanto-occipital cyst with conservative management: A case report and review of the literature. Surg Neurol Int. 2022;13:478. Published 2022 Oct 21. doi:10.25259/SNI_841_2022
2. Gassie K, Grewal S, Chen SG. Atlantooccipital Synovial Cyst with Isolated Hypoglossal Nerve Palsy: Case Report of Nonfusion Surgical Approach and Review of Literature. World Neurosurg. 2019;126:434-438. doi:10.1016/j.wneu.2019.03.159
3. Mujic A, Hunn A, Liddell J, Taylor B, Havlat M, Beasley T. Isolated unilateral hypoglossal nerve paralysis caused by an atlanto-occipital joint synovial cyst. J Clin Neurosci. 2003;10(4):492-495. doi:10.1016/s0967-5868(03)00083-3
4. Yang DB, Harms J, Iyer RK, Arnold P. Synovial cysts at the cervicothoracic junction: Illustrative series of three cases. Surg Neurol Int. 2023;14:196. Published 2023 Jun 8. doi:10.25259/SNI_88_2023
5. Elhammady MS, Farhat H, Aziz-Sultan MA, Morcos JJ. Isolated unilateral hypoglossal nerve palsy secondary to an atlantooccipital joint juxtafacet synovial cyst. J Neurosurg Spine. 2009;10(3):234-239. doi:10.3171/2008.12.SPINE08158

Images/Tables



261

RANBP2-related Acute Necrotizing Encephalopathy Type 1

Gibson Klapthor MD, Paul M. Bunch MD
Wake Forest University School of Medicine, Winston Salem, NC, USA

Abstract Category

Pediatrics

Clinical History

A 13-month-old female with no past medical history presented to the emergency department for evaluation after multiple seizures. In the emergency department, she received lorazepam and midazolam and was loaded with levetiracetam. She also received empiric bacterial meningitis coverage with ceftriaxone and vancomycin. Her parents stated that the patient recently received a set of vaccinations and subsequently had low grade fevers and irritability that had been treated at home with acetaminophen and ibuprofen.

Imaging Findings

Initial axial head CT image (A) demonstrates symmetric abnormal hypoattenuation in the external capsules (arrows). Initial axial diffusion-weighted image (B) and corresponding ADC map (not shown) demonstrate restricted diffusion in the external capsules (arrows), hippocampi (arrows), and left greater than right temporal cortex. Follow-up axial diffusion-weighted images (C, D) and corresponding ADC map (not shown) obtained 8 months later demonstrate new areas of restricted diffusion in the thalami (circle, C), cerebral cortex (arrows, C), pons (circle, D), and cerebellar cortex (arrows, D).

Discussion

Given her seizures and abnormal imaging findings, the patient was admitted to the hospital for further work-up. Primary differential considerations included acute necrotizing encephalitis, hypoxic-ischemic encephalopathy in the setting of status epilepticus, viral encephalitis, and Leigh syndrome. Lumbar puncture was obtained and demonstrated no evidence of infection. Levetiracetam was continued for anti-epileptic treatment. Ultimately, genetic testing revealed a pathogenic variant in the *RANBP2* gene on chromosome 2.

The patient has had one additional episode of acute necrotizing encephalitis in the setting of a febrile illness since her initial presentation. She continues on levetiracetam and gabapentin for seizure control. Neurologically, she has diffuse appendicular hypertonia, hyper-reflexia, and a right cranial nerve VI palsy. Long term prognosis is poor with expectation for permanent neurological deficits.

RAN binding protein 2 (RANBP2) is a cytoplasmic nucleoporin that influences multiple cellular functions including mitochondrial function, immune regulation, and nuclear signaling. It is hypothesized that genetic mutations causing alterations to this protein can increase susceptibility to cytokine storm and alter neuron metabolism. After an inciting event, these patients can experience CNS inflammation with breakdown of the blood-brain barrier.

Teaching Point

Pathogenic variants of *RANBP2* can result in familial acute necrotizing encephalitis, a rare condition with an autosomal dominant inheritance pattern that is often incited by viral infections.

A characteristic imaging feature is restricted diffusion and T2 hyperintensity involving the thalami and brainstem.

The typical clinical presentation is rapid onset of neurologic deficits, seizures, and altered consciousness just after a prodromal illness. The timeline of presentation helps differentiate this entity from other differential considerations, such as acute disseminated encephalomyelitis (ADEM) (typically 1-2 weeks after a prodromal illness) and Leigh syndrome (gradual onset).

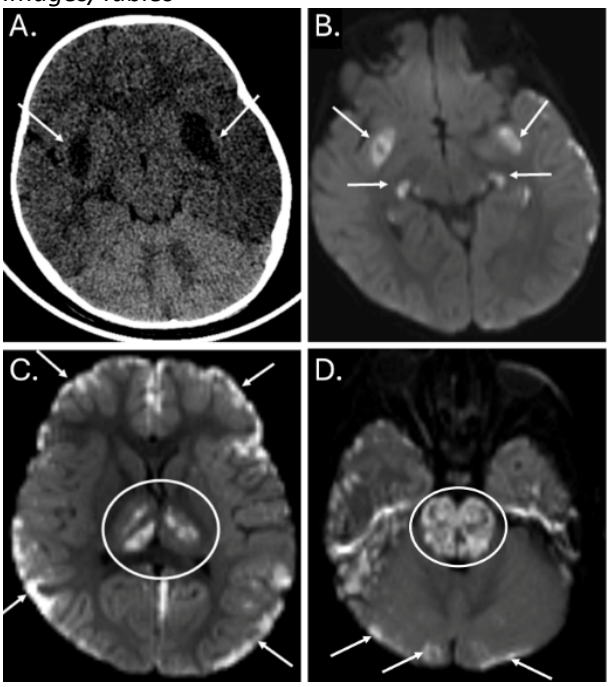
Acute necrotizing encephalitis is an important differential consideration as management relates to reducing the inflammatory response that is thought to be causal (corticosteroids, IL-6 blockade - tocilizumab, therapeutic hypothermia).

References

Levine JM, Ahsan N, Ho E, et al. Genetic Acute Necrotizing Encephalopathy Associated with RANBP2: Clinical and Therapeutic Implications in Pediatrics. *Mult Scler Relat Disord* 2020;43:102194 doi:10.1016/j.msard.2020.102194 pmid:32426208

Shukla P, Mandalla A, Elrick MJ, et al. Clinical Manifestations and Pathogenesis of Acute Necrotizing Encephalopathy: The Interface Between Systemic Infection and Neurologic Injury. *Front Neurol* 2022;12:628811 doi:10.3389/fneur.2021.628811 pmid:35058867

Images/Tables



285

Value of Flexion View in Cervical Spine MRI Protocol for Diagnosis of Hirayama Disease

Andrew S.C. Barty DO, Mattie Lewis MD, Michael J. Nisiewicz MD, Wilfred Furtado MD, Hossam Elbelasi M.B.B.Ch
University of Kentucky, Lexington, KY, USA

Abstract Category

Spine

Clinical History

A 17-year-old male presented with progressive weakness in his right upper extremity over the past two years, initially noticed during weightlifting, experiencing increasing weakness in his right arm and pectoral muscle. There was subsequent noticeable reduction in muscle mass in the chest, triceps and ulnar side of the hand. His condition worsened, accompanied by neck pain and intermittent paresthesia, aggravated by neck movements. Cold weather caused his ring and pinky fingers to curl inward, making it hard to straighten them.

Physical exam revealed asymmetric muscle wasting of the right pectoralis major, biceps, triceps and thenar muscles, along with decreased sensation in the fingers following an ulnar nerve distribution and reduced bilateral triceps reflexes. Radiographs of the right shoulder and neck were unrevealing but MRI cervical spine & EMG studies were ordered.

Imaging Findings

An initial routine non-contrast MRI of the cervical spine revealed a T2 hyperintense signal in the right aspect of the spinal cord from C5 to C7, accompanied by volume loss of the cord, but without clear evidence of compressive pathology. A subsequent cervical spine MRI with contrast, including neutral and flexion views, demonstrated similar signal abnormalities in the neutral position along. The flexion view revealed anterior displacement of the dura, more pronounced on the right side, and an enlarged posterior epidural space with multiple flow voids. Post-contrast images showed enhancement in the epidural space.

EMG results indicated evidence of damage to the cervical anterior horn cells at C7-T1, with greater involvement on the right side than the left, leading to amyotrophy.

Discussion

Hirayama disease (HD), also known as sporadic juvenile muscular atrophy of the unilateral upper extremity, is a rare neurological disorder that primarily affects adolescent and young adult males. First described in Japan in 1959 by Hirayama et al, HD typically involves the C5-C7 myotomes in Western patients and the C7-T1 segments in Asian populations. The disease manifests as asymmetric weakness and fatigue in the forearm and hand, sparing the brachioradialis muscle, and eventually leads to tremors and muscle atrophy. It can resemble conditions like syringomyelia, amyotrophic lateral sclerosis (ALS), and cervical spondylosis, making imaging crucial for diagnosis.

The etiopathogenesis is uncertain but two main theories propose that either a growth imbalance between the spine and its contents or repeated neck flexion causes damage to the spinal cord. MRI imaging, especially with flexion views, is essential for identifying key features such as anterior shifting of the dura and widening of the laminodural space (LDS), which compresses the spinal cord. Treatment focuses on preventing further neck flexion, typically with a cervical collar, which can halt disease progression. Surgical options like decompression and fusion are considered in more severe cases.

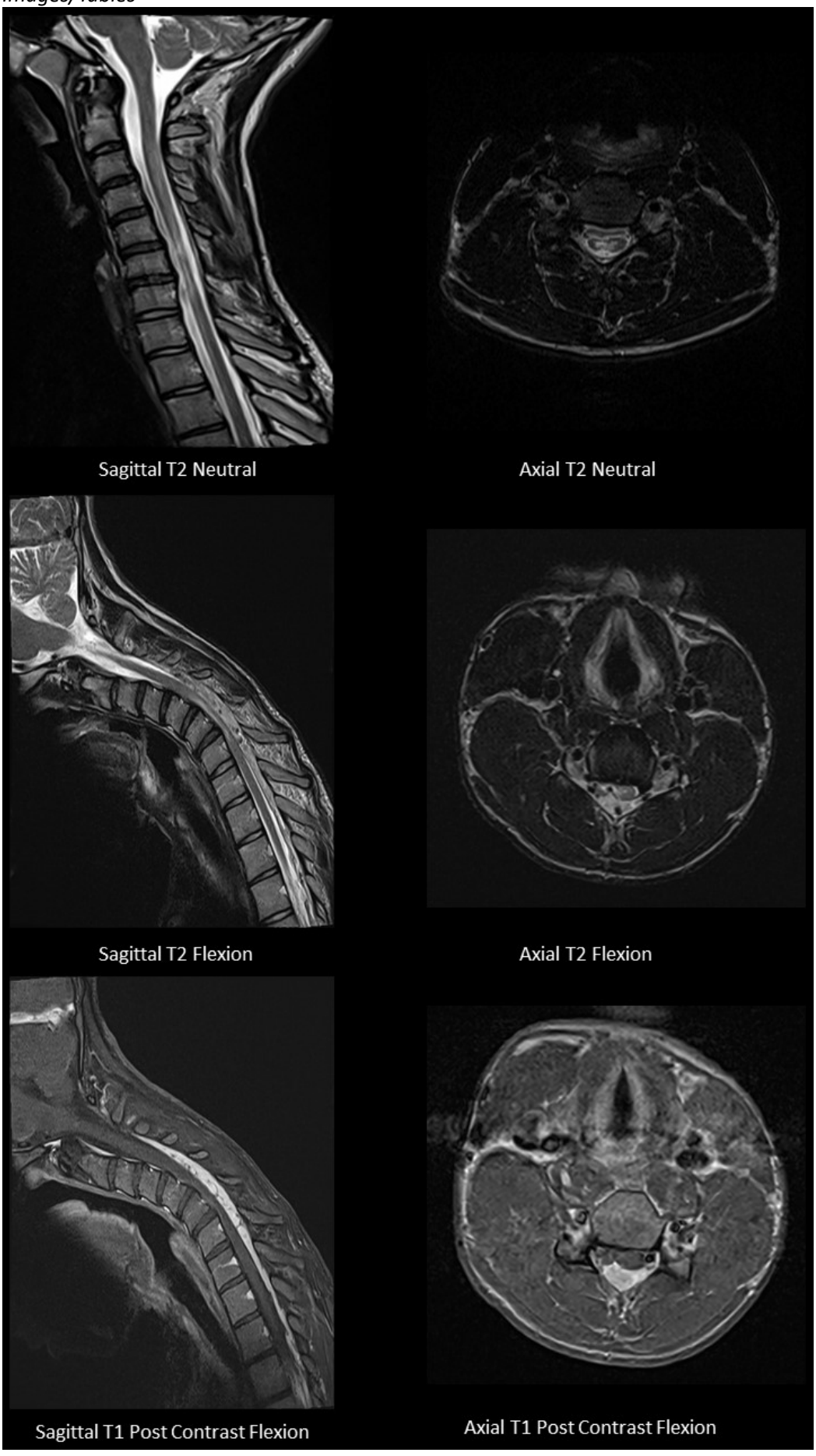
Teaching Point

Flexion MRI of the cervical spine is crucial for diagnosing Hirayama disease, as it highlights a defining feature: the widening of the laminodural space due to the anterior displacement of the posterior dura mater. This distinctive finding is key for diagnosing Hirayama disease and differentiating it from other causes of muscle atrophy and weakness.

References

1. Hirayama K, Toyokura Y, Tsubaki T. Juvenile muscular atrophy unilateral upper extremity a new clinical entity. *PsychiatrNeurol Jpn* 1959;61:2190–97.
2. Boruah DK, Prakash A, Gogoi BB, et al. The Importance of Flexion MRI in Hirayama Disease with Special Reference to Laminodural Space Measurements. Am J Neuroradiol 2018;39:974–80.
3. Raval M, Kumari R, Dung Dung AA, et al. MRI findings in Hirayama disease. Indian J Radiol Imaging 2010;20(4):245-9.
4. Vitale V, Caranci F, Pisciotta C, et al. Hirayama's disease: an Italian single center experience and review of the literature. Quant Imaging Med Surg 2016;6(4):364-73.

Images/Tables



313

Multifocal Intradural Cystic Ependymoma: Extremely Rare Presentation of a Common Spinal Neoplasm

Vivek P Patel MD, PhD
University of Pennsylvania, Philadelphia, PA, USA

Abstract Category

Spine

Clinical History

50-year-old male with 5-year history of progressive back pain, numbness in the extremities, and urinary and bowel urgency. Patient had a remote history of lumbar microdiscectomy.

Imaging Findings

MRI shows multifocal discrete intradural cystic lesions in the cervical and upper thoracic spinal canal, which are predominantly extramedullary although with suggestion of some intramedullary lesions. There was extensive cord deformation but without edema. There was no diffusion restriction or enhancement. No contrast filling was seen on delayed CT myelogram. MRI brain and lumbar spine were negative.

Discussion

Ependymomas are common neoplasms of the spinal cord, however primarily cystic and extramedullary presentation is extremely rare with only a few reported cases in the literature. The myxopapillary variant can have an extramedullary presentation although these are primarily seen along the conus medullaris and/or filum terminale. Absence of any convincing enhancement is an additional atypical feature of our case. This highly unusual presentation mimics other pathologies, most notably intradural cysts. Patient underwent biopsy with pathology consistent with an ependymoma, WHO grade 2. Intramedullary lesions were noted during the biopsy, suggesting that this was likely intramedullary in origin with extensive intradural dissemination throughout the cervical and upper thoracic spine rather than the very rare extramedullary origin. Patient was treated with spinal proton radiation with improvement of symptoms and without progression on follow-up imaging.

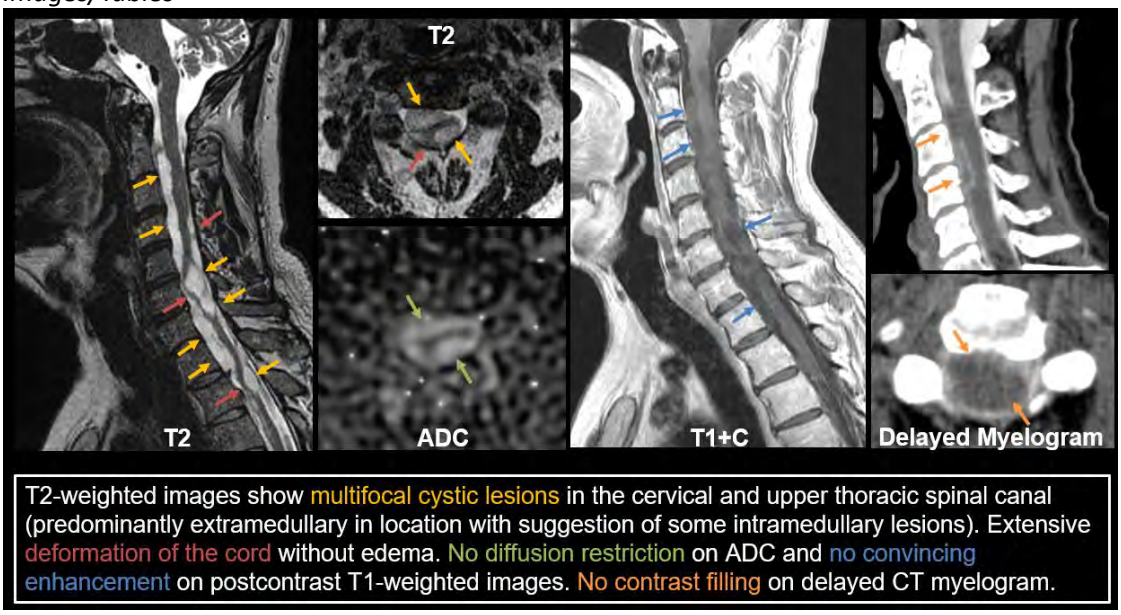
Teaching Point

Multifocal intradural cystic ependymoma is an extremely rare presentation that can mimic other pathologies and should be considered in the differential diagnosis of intradural cystic lesions of the spine.

References

1. Graca J, Gultasli N, D'Haene N, Brotchi J, Salmon I, Baleriaux D. Cystic Extramedullary Ependymoma. AJNR 2006; 27(4):818-821.
2. Koeller K, Shih R. Intradural Extramedullary Spinal Neoplasms: Radiologic-Pathologic Correlation. RadioGraphics 2019; 39:468-490.
3. Omerhodzic I, Pojskic M, Rotim K, Splavski B, Rasulic L, Arnautovic K. Myxopapillary Ependymoma of the Spinal Cord in Adults: A Report of Personal Series and Review of Literature. Acta Clin Croat 2020; 59(2):329–337.

Images/Tables



T2-weighted images show multifocal cystic lesions in the cervical and upper thoracic spinal canal (predominantly extramedullary in location with suggestion of some intramedullary lesions). Extensive deformation of the cord without edema. No diffusion restriction on ADC and no convincing enhancement on postcontrast T1-weighted images. No contrast filling on delayed CT myelogram.

323

Lost in the Lyme-Light: Garin-Bujadoux-Bannwarth Syndrome (or is it just Guillain-Barré?)

David E Bartlett MD, Carlo Castro MD, Matthew Gellatly MD, Sheng-Che Hung MD, PhD, Valerie Jewells DO
University of North Carolina, Chapel Hill, NC, USA

Abstract Category

Spine

Clinical History

26-year-old with recent travel to Connecticut, Wisconsin, and Antigua presented with progressive ascending weakness (from lower extremities to upper and facial muscles), numbness, and night sweats. Initially afebrile with mild transaminitis and thrombocytopenia, the patient was diagnosed with Guillain-Barré syndrome (GBS) but deteriorated despite IVIG treatment. Further evaluation with MRI and lumbar puncture revealed lymphocytic pleocytosis, elevated protein, and positive Lyme serology. Considering travel history and clinical progression, findings aligned with Garin-Bujadoux-Bannwarth syndrome (BWS), a neurological manifestation of Lyme disease, leading to treatment for disseminated Lyme with neurologic improvement.

Imaging Findings

MRI Brain with contrast was notable for increased enhancement in the fundus of bilateral internal auditory canals, the bilateral labyrinthine, tympanic, and extratemporal (descending) segments of the facial nerves, with right 6th cranial nerve involvement.

MRI C/T/L spine with contrast was notable for leptomeningeal enhancement in the L and T spine as well as subtle nerve root enhancement (though not in C-spine).

Discussion

Lyme borreliosis is a multisystem disease transmitted through the Ixodes tick, primarily affecting the skin, nervous system, or joints, with overlapping stages: early localized, early disseminated, and late disseminated stage.

BWS is a rare CNS manifestation in the disseminated stage. It is the most common manifestation of acute Lyme borreliosis in adults in Europe after erythema migrans, caused by Borrelia garinii. BWS is typically not encountered in the United States, although there are case reports.

BWS typically presents with a range of neurologic symptoms such as peripheral and radiculoneuropathy; including motor, sensory and autonomic symptoms. The hallmark triad includes painful radiculitis, lymphocytic meningitis, and cranial nerve involvement, often leading to facial palsy. Symptoms can occur weeks to months after tick bite/Lyme disease infection with a highly variable onset with both acute and chronic manifestations.

Imaging findings of BWS are nonspecific due in part to a relative paucity of cases and likely underdiagnosis. Select case reports demonstrate enhancement of spinal nerve roots on post-contrast T1 sequences. Notably, these findings are more commonly seen in the lumbar peripheral nerves and cauda equina rather than cervical nerve roots, although this is likely skewed secondary to limited variations in symptomatic presentation. Additional case reports have failed to identify an imaging correlation within the brain or spine.

Cases often require serological studies to aid in diagnosis. On imaging, the differential diagnoses include GBS, the Miller-Fisher variant of GBS, and other infectious/non-infectious polyradiculitis. In this patient with positive Lyme IgM. The constellation of findings should prompt the Radiologist to consider Lyme disease in the differential diagnosis.

Teaching Point

1. Approximately 60% of cases involve cranial nerve deficits, with up to 80% affecting the facial nerve and 1/3 being bilateral.
2. Neurologic symptoms following tick exposure in endemic regions should prompt Lyme neuroborreliosis evaluation, as BWS may be more prevalent in North America than previously thought. Radiologists' increased awareness can prevent diagnostic delays and reduce risks of Post-Treatment Lyme Disease Syndrome (PTLDS).
3. Imaging findings are non-specific and encompass a broad spectrum of infectious and non-infectious causes of polyradiculoneuritis, depending on clinical context

References

1. Rauer S, Kastenbauer S, Hofmann H, et al.; Consensus group. Guidelines for diagnosis and treatment in neurology - Lyme neuroborreliosis. Ger Med Sci 2020;18. DOI: https://doi.org/10.3205/000279. PMID: 32341686.
2. Shah A, O'Horo JC, Wilson JW, Granger D, Theel ES. An unusual cluster of neuroinvasive Lyme disease cases presenting with Bannwarth syndrome in the Midwest United States. Open Forum Infect Dis 2018;5. DOI: https://doi.org/10.1093/ofid/ofx276.

3. Agarwal R, Sze G. Neuro-Lyme disease: MR imaging findings. Radiology 2009;253:167-73. DOI: https://doi.org/10.1148/radiol.2531081103. PMID: 19587309.
4. Garkowski A, Łebkowska U, Kubas B, et al. Imaging of Lyme neuroborreliosis: a pictorial review. Open Forum Infect Dis 2020;7. DOI: https://doi.org/10.1093/ofid/ofaa370.
5. Marjelund S, Jaaskelainen A, Tikkakoski T, Tuisku S, Vapalahti O. Gadolinium enhancement of cauda equina: a new MR imaging finding in the radiculitic form of tick-borne encephalitis. AJNR Am J Neuroradiol 2006;27:995-7. PMID: 16687530.

Images/Tables

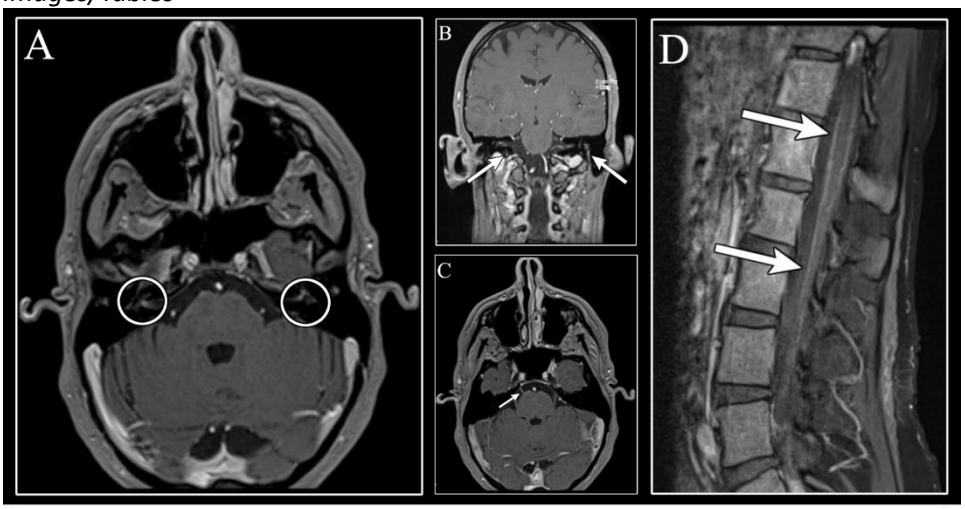


Figure 1. (A, B) MRI Brain with contrast axial and coronal images are notable for increased enhancement in the fundus of the bilateral internal auditory canals **(circles)** and the bilateral labyrinthine, tympanic, and extratemporal (descending) segments of the facial nerves **(arrows)**. Axial image **(C)** demonstrates 6th cranial nerve enhancement **(arrow)**. MRI Lumbar Spine with contrast **(D)** was notable for leptomeningeal enhancement **(arrows)** as well as subtle nerve root enhancement (not shown). Leptomeningeal and nerve root enhancement was also seen in the thoracic spine.

324

Barking up the Wrong Vasculopathic Tree: It's Varicella Zoster Virus Vasculitis, Not Moyamoya

Zahra Shokri Varniab MD, Nancy Fischbein MD
Stanford, Palo Alto, California, USA

Abstract Category

Head & Neck

Clinical History

A 35-year-old Asian female presented with one week of sharp, intermittent left headache and facial pain. Following chiropractic adjustment, she experienced a sensation of heat around her left ear and posterior neck. The next day, her left ear swelled, followed by numbness in her left tongue/face/lip. Emergent evaluation led to a CT angiogram to exclude dissection – no dissection was present, but CTA showed narrowing of the left M1 segment, concerning for moyamoya vasculopathy in a young patient of Asian descent. She was later diagnosed with herpes zoster oticus (a.k.a. Ramsay Hunt syndrome, RHS) after an ENT consultant noted conchal bowl vesicles. She also manifested left facial nerve enhancement on follow-up MRI, and CSF was positive for varicella zoster virus (VZV) DNA. Her final diagnosis was RHS complicated by VZV vasculitis.

Imaging Findings

- **Initial CT/CTA, Figure 1A-C:** No parenchymal abnormality, dissection or aneurysm was found. Segmental narrowing of the left M1 segment is seen (arrow, B/C).
- **Initial MRI, Figure 1D-F**: Moderate segmental narrowing of the left M1 (arrow, E), with concentric vessel wall enhancement on vessel wall imaging (VWI) (arrow, D). Additional abnormal enhancement involving the left facial nerve (arrows, F).

- **Follow-up MRI (+4 weeks), Figure 1G-I)**: Slight improvement in concentric vessel wall enhancement (arrow, G) and M1 segmental stenosis (arrow, H) after treatment with acyclovir and prednisone. Persistent enhancement of left facial nerve (arrows, I).

Discussion

Diagnosing uncommon neurological conditions with non-specific overlapping imaging findings is challenging. Moyamoya disease, characterized by progressive stenosis of cerebral arteries, is common in Asian patients and does not always demonstrate typical collateral vasculature [1]. RHS, characterized clinically by pain, viral vesicular eruptions and facial nerve dysfunction [2], classically shows contrast enhancement of cranial nerves seven and/or eight on MRI [3]. Had the presence of vesicles and the clinical suspicion of RHS been know at the time of CTA, findings would likely have been attributed to infectious vasculitis and not to moyamoya. On subsequent MRI with VWI, concentric enhancement was present, which can be seen with both moyamoya and RHS. Evolving clinical information, as well as enhancement of the facial nerve, shifted the diagnosis to RHS. This evolution underscores the necessity of accurate clinical correlation as well as serial imaging and clinical follow-up: when neuroimaging is ambiguous, specific symptoms help to guide differential diagnosis. Additionally, with the explosion of emergency CTA imaging [4], we must note that CT-based methods are often inadequate for complete patient evaluation and management – in this case, comprehensive neuroimaging, including T1-weighted post-contrast sequences, was essential to detecting the neural enhancement that supported the ultimate diagnosis [5]. Further imaging follow-up is planned to ensure return of the patient's L M1 segment to normal caliber and resolution of abnormal vessel wall enhancement.

Teaching Point

This case emphasizes the importance of a broad differential diagnosis in patients presenting with overlapping neurological symptoms and imaging findings. Though moyamoya is a relatively common diagnosis in young Asian patients presenting with vascular narrowing and abnormal VWI, evolving clinical information ultimately confirmed the diagnosis of RHS.

References

1. Li J, Jin M, Sun X, Li J, Liu Y, Xi Y, et al. Imaging of Moyamoya Disease and Moyamoya Syndrome: Current Status. J Comput Assist Tomogr. 2019; 43: 257-63.

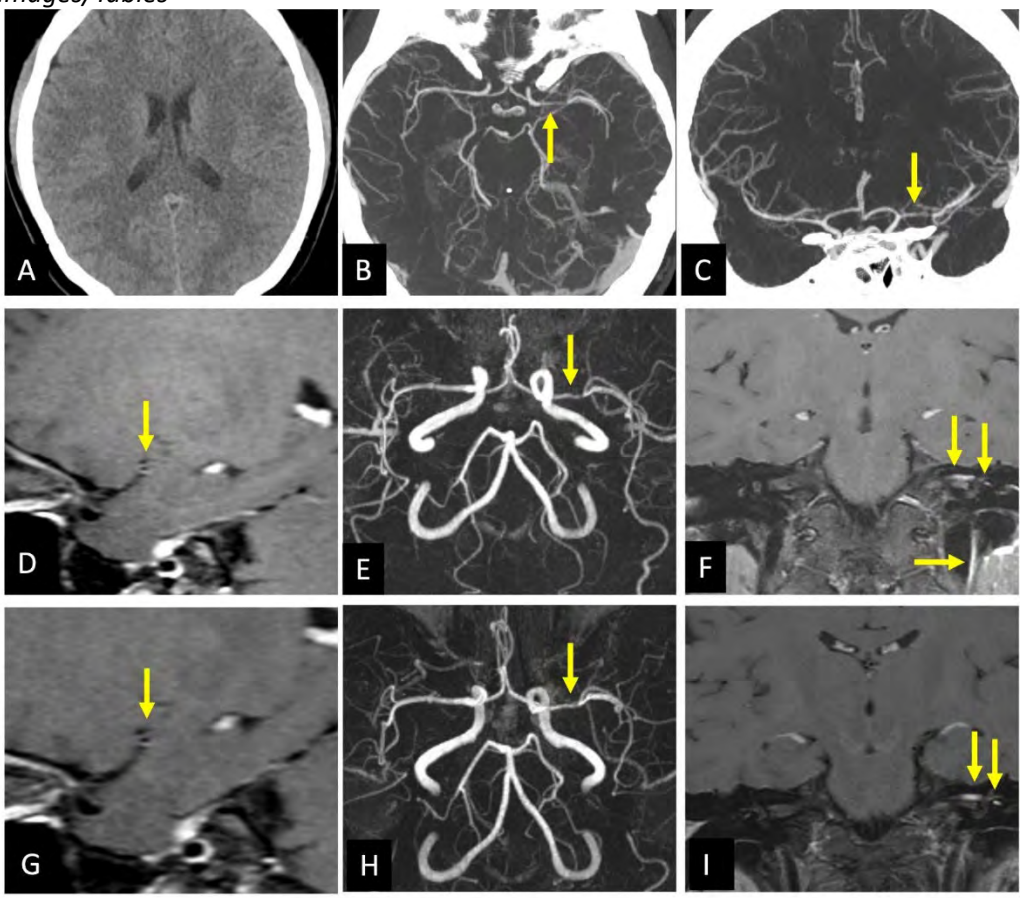
2. Gilden D, Cohrs RJ, Mahalingam R, Nagel MA. Varicella zoster virus vasculopathies: diverse clinical manifestations, laboratory features, pathogenesis, and treatment. Lancet Neurol. 2009; 8: 731-40.

3. Minakata T, Inagaki A, Sekiya S, Murakami S. Contrast-enhanced magnetic resonance imaging of facial nerve swelling in patients with severe Ramsay Hunt syndrome. Auris Nasus Larynx. 2019; 46: 687-95.

4. ElHabr A, Merdan S, Ayer T, Prater A, Hanna TN, Horny M, et al. Increasing Utilization of Emergency Department Neuroimaging From 2007 Through 2017. AJR Am J Roentgenol. 2022; 218: 165-73.

5. Kuya J, Kuya K, Shinohara Y, Kunimoto Y, Yazama H, Ogawa T, et al. Usefulness of High-Resolution 3D Multi-Sequences for Peripheral Facial Palsy: Differentiation Between Bell's Palsy and Ramsay Hunt Syndrome. Otol Neurotol. 2017; 38: 1523-7.

Images/Tables



328

Twig-like MCA: Don’t Let the Twigs Fool You

Christopher T Shin MD, Pamela Semaan MD, Mohamad Abdalkader MD
Boston University Medical Center, Boston, MA, USA

Abstract Category

Adult Brain

Clinical History

Case#1

27 year-old female with history of seizures presented with headaches and post-partum seizure 5 days after delivery

Initial diagnosis: Eclampsia

Patient had imaging and cerebral angiogram at an outside hospital where she was found to have M1 occlusion and severe M2 stenosis raising possibility of reversible vasoconstiction syndrome

Repeat MRA at our institution a few weeks after initial angiogram showed persistent M1 occlusion with collateral vessels, making reversible vasoconstriction syndrome unlikely

A repeat angiogram was performed to better characterize the anatomy

Patient was ultimately found to have a twig-like MCA which is a congenital anomaly of the M1 segment

Case#2

39 year-old female presenting with abrupt onset severe headache

Has a history of headaches which normally improve with medication, but did not on this occasion

CTA showed abnormal collateral vessels involving the right M1 segment and concern for right-sided moyamoya was raised

Case#3

45 year-old female with history of Moyamoya disease

Imaging Findings

Twig-Like MCA

Distal ICA is normal

M1 segment is replaced by a plexiform network of vessels.
Associated with microaneurysms which can rupture and cause subarachnoid hemorrhage, so may see hemosiderin deposition on SWI
Network of vessels is oriented horizontally
Usually unilateral
Moyamoya
Progressive stenosis involving the distal ICA
Classically has the "puff of smoke" appearance, which represents the collateral vessels
Network of vessels is oriented vertically
Usually bilateral

Discussion

Twig-like middle cerebral artery (MCA) is a rare vascular anomaly where the M1 segment is replaced by a plexiform network of vessels
Some authors have cited an incidence of 0.11%-1.17% in patients who undergo angiograms
Pathology thought to be related to abnormal embryogenesis (i.e. persistent primitive network of plexiform vessels)
Commonly mistaken for Moyamoya which is a disorder causing progressive stenosis of the ICA terminus and has a characteristic “puff of smoke” appearance
Cerebral angiogram helpful to confirm diagnosis

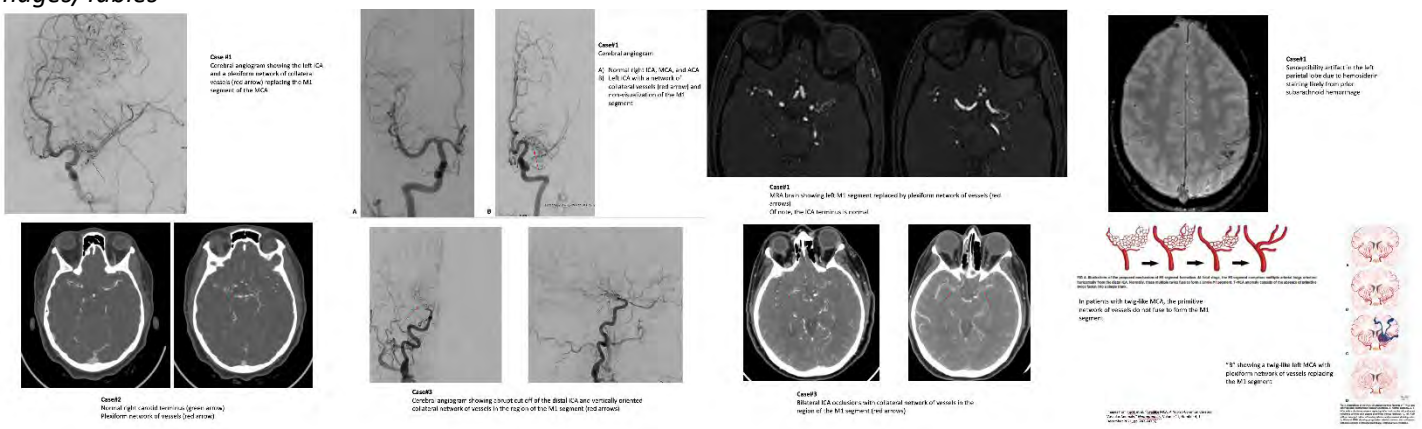
Teaching Point

Twig-like MCA is often mistaken for Moyamoya
Moyamoya becomes progressively stenotic starting at the ICA terminus whereas twig-like MCA does not involve the ICA terminus and is not thought to be progressive
Moyamoya is typically bilateral whereas twig-like MCA is thought to be almost exclusively unilateral
Moyamoya tends to have vertical collaterals, whereas the collaterals in twig-like MCA tend to be horizontal
More of a genetic predisposition for Moyamoya
Important to distinguish from Moyamoya due to differences in treatment
Surgery (bypass) for Moyamoya
Robust data for the management of twig-like MCA is not available but can range from conservative management (if asymptomatic), endovascular therapies to treat associated aneurysms, or surgery (bypass) if associated with ischemia
Patients with twig-like MCA should be kept well-hydrated and blood pressure under control
Twig-like MCA is known to be associated with microaneurysms and hemorrhage
Hemorrhage is thought to be related to microaneurysm rupture or due to weak twig vessel walls

References

Onoue K, Nguyen TN, Mian A, et al. Twig-like middle cerebral arteries: Clinical and radiological findings. Clin Imaging. 2021;73:31-37. doi:10.1016/j.clinimag.2020.11.049
Goto Y, Nanto M, Oka H, et al. Radiological and clinical features of twig-like middle cerebral artery in comparison with moyamoya angiopathy: a multicenter retrospective study. Journal of neurosurgery, 137(6), 1718–1726. https://doi.org/10.3171/2022.2.JNS212338
Ota T, Komiyama M. Twig-like middle cerebral artery: Embryological persistence or secondary consequences?. Interv Neuroradiol. 2021;27(4):584-587. doi:10.1177/15910199211024077
Chetoui A, Elkhamlichi A, Jiddane M, et al. Twig-like MCA: A rare cause of intracranial bleeding. Radiol Case Rep. 2024;19(11):4935-4939. 2024. doi:10.1016/j.radcr.2024.07.097
Tawk SY, Mourad CJ, Halut MB, et al. “Twiglike MCA: A Not-So-Common Cerebral Vascular Anomaly.” Neurographics. 2021;11:243-247. doi: https://doi.org/10.3174/ng.2100015

Images/Tables



329

False Alarm! Recognizing Granulation Reaction Related to Cotton-Assisted Aneurysm Clipping

Rishabh Agrawal MD, Allen Mao MD, Vikash N Sinha MD, Ibrahim S Tuna MD
University of Florida, Gainesville, FL, USA

Abstract Category

Adult Brain

Clinical History

Very small aneurysms (< 4 mm) are historically difficult to coil and clip effectively in neurosurgical practice. Especially when in conjunction with a small-based neck, they pose a higher risk of complications such as clip slippage, neck rupture, and parent artery occlusion. Cotton-assisted aneurysmal clipping was a technique popularized in 2004 that involves the addition of a cotton pad to bolster the aneurysmal neck and reduce risk of complications.

Our case series includes four patients who underwent cotton-assisted aneurysmal clipping between 2006 and 2016 with follow-up imaging changes worrisome for acute hemorrhage, intracranial mass, or other pathologies. There were varying radiologic findings and associated underlying inflammatory processes within the cases. In 3 of 4 cases, incidental findings were seen for diagnostic testing of unrelated neurological symptoms. However, in 1 case, findings were likely related to the clinical presentation of seizures.

Imaging Findings

Non-contrast head CTs in these patients demonstrate well-localized areas of varying hyperdensity in the region of the clipping, similar to the appearance of an intracranial hemorrhage. On CTA, these areas demonstrate preserved avid enhancement of the native arterial vasculature and, lesser nodular enhancement of the surrounding parenchyma, thought to be related to granulation tissue and inflammatory changes.

Correlation with follow-up MRI examinations shows expected susceptibility artifact at the site of the clip. Axial T2-weighted images demonstrate focal hypointensity immediately around the clip with surrounding T2/FLAIR hyperintense vasogenic edema and sometimes regional mass effect. Postcontrast T1 sequences demonstrate mild enhancement in the direct vicinity of the clip. In some cases, the enhancement pattern is well-circumscribed and could easily be mistaken for an intra-axial tumor.

Discussion

This constellation of imaging findings can be indistinguishable from other concerning pathologies, including intra-axial neoplasm, intracranial hemorrhage, and abscess, among others. Correlation with procedural history with attention to techniques and materials used could hint at the diagnosis of granulation tissue. In particular, the diagnosis should be considered in patients who underwent cotton-assisted wrapping approximately 7-12 years prior to presentation, as there is typically a delayed inflammatory response to the specific types of cottonoid material used. Fortunately, these patients typically get serial imaging after aneurysmal clipping, which could provide a more definitive differential diagnosis per the timeline of findings.

Similar findings have been scarcely reported in the literature with nickel-containing aneurysm clips, demonstrating cell-mediated Type IV hypersensitivity reactions with cerebral edema and intermittent mass effect. Additionally, there have been only a few reports of MR findings in postoperative foreign-body granulomas from synthetic materials left behind in craniotomies and embolization procedures, such as gelfoam and polyvinyl alcohol.

In past cases, such reactions have been misidentified as worrisome pathology including high-grade tumors. However, employing the use of MR spectroscopy and MR perfusion can assist in distinguishing overlapping features, with the limitation of being unable to exclude benign tumorous conditions.

Teaching Point

In summary, the neuroradiology and neuro-interventionalist communities should be aware of the potential sequelae of utilizing cotton-assisted aneurysmal clipping. We emphasize understanding potential imaging findings, differentiating findings from other pathology in the postoperative context, and correlating with procedural history and operative report.

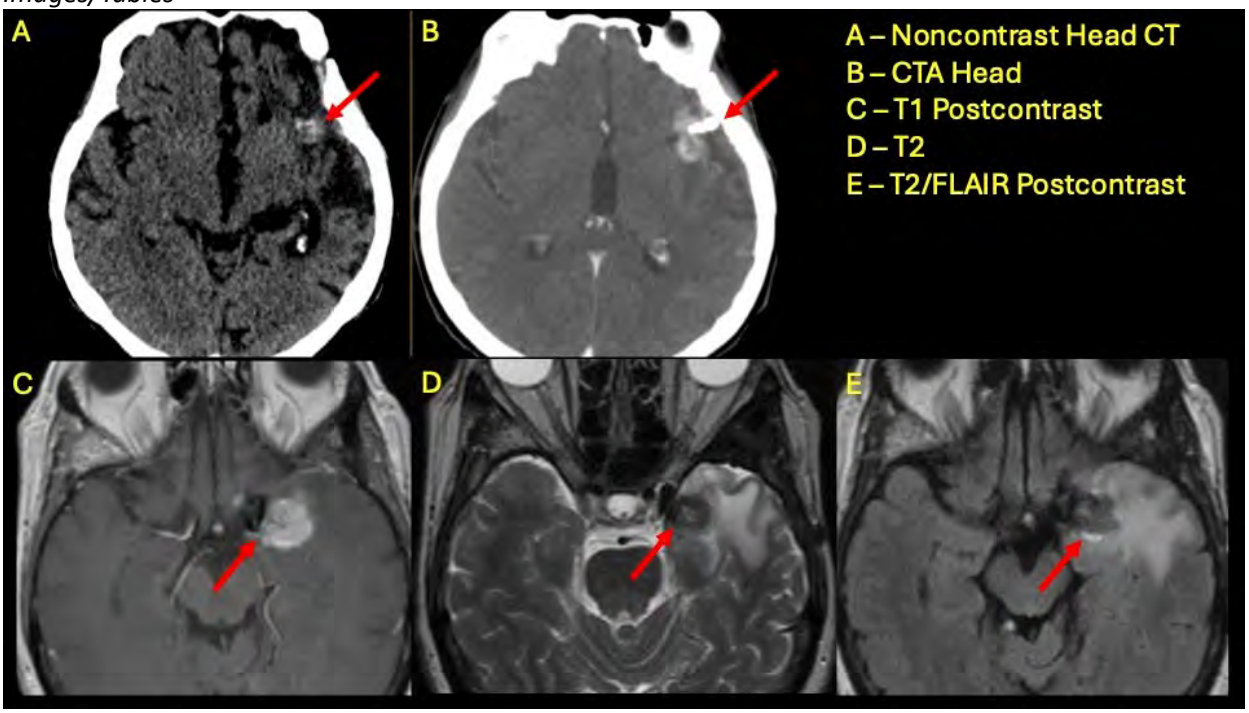
References

Huang Y, Gao G, Zhang S, et al. Surgical Treatment of Very Small Aneurysms: Cotton- Assisted Clipping. *Am J Otolaryngol Head Neck Surg*. 2023; 6(6): 1247.

Jang SW, Kim SJ, Kim SM, et al. MR Spectroscopy and Perfusion MR Imaging Findings of Intracranial Foreign Body Granuloma: a Case Report. *Korean J Radiol*. 2010; 11: 359-363. DOI:10.3348/kjr.2010.11.3.359

Tan T, Tee JW, Han TF. Cell-mediated allergy to cerebral aneurysm clip causing extensive cerebral edema. *J Neurosurg*. 2014; 121: 924-28. DOI:10.3171/2014.6.JNS132405

Images/Tables



334

Bilateral Medial Medullary Infarction: A Report of Two Cases with a Review of Unique MRI Signs

Abel T Abebe[1], Nihanth Palivela[1], Mohamed Tantawi[1], Azin Aein[1], John Heymann MD[2], Huda Al Jadiry[1]

[1]The University of Texas Medical Branch at Galveston, Galveston, TX, USA. [2]The university of Texas Medical Branch, Galveston, TX, USA

Abstract Category

Adult Brain

Clinical History

A 55-year-old male patient with a medical history of hypertension and diabetes presented with acute-onset bilateral lower extremity weakness and numbness, which progressively involved the upper extremities, accompanied by dysphagia and dysarthria.

Imaging Findings

A non-contrast CT scan of the head was unremarkable. However, an MRI of the brain performed two days later revealed diffusion restriction involving the bilateral medial medulla, displaying the classic "heart" sign pathognomonic for

bilateral medial medullary infarction, as seen on DWI (Fig. 3A) and ADC (Fig. 3B) MRI sequences. CT angiography demonstrated severe short-segment stenosis of the right intradural (V4) vertebral artery (Fig. 4).

Discussion

Medial medullary infarction is a rare form of stroke, accounting for only 0.5-1.5% of all stroke cases. Bilateral medial medullary infarction (BMMI) is exceptionally rare, as the medulla's paired arterial supply usually ensures adequate perfusion. The diagnosis of BMMI is clinically challenging and may not be evident on MRI during the early stages.

The anteromedial medulla can be anatomically divided into three segments: the ventral, middle, and dorsal portions (Fig. 1). Several signs have been described in the diagnosis of bilateral medial medullary infarcts on axial MRI, which can correlate with the specific anatomic territories involved. The "snake's eye" sign, mentioned in a single report, corresponds to infarcts affecting a smaller area of the ventral segments (Fig. 2A). Involvement of larger areas of the ventral portions results in an imaging feature known as the "fan" sign (Fig. 2B). When the ventral and middle portions are involved, the classic and pathognomonic "heart" sign is observed (Fig. 2C). Involvement of the ventral, middle, and dorsal medial medulla can produce the "letter Y" sign or the "air pod" sign (Fig. 2D). In our case, the MRI findings closely resemble the "heart " sign.

The extent of segmental involvement has a prognostic role, with single-segment involvement correlating with better outcomes, while multi-segment infarcts predict poorer prognosis.

The anteromedial portion of the superior medulla is primarily supplied by perforator branches from the vertebral arteries (VAs). Anatomical variants of these perforator branches can include supply from both VAs or from a single VA, which may provide blood to the medial medulla bilaterally. Common vascular etiologies described in BMMI include atherosclerotic vertebral artery stenosis (>50%) and small vessel (perforator branch) disease. Among these, unilateral intradural vertebral artery stenosis was the most commonly encountered, as noted by Hu et al., and this was also true in our case.

Teaching Point

The diagnosis of bilateral medial medullary syndrome presents a clinical challenge. Various signs on MRI, in addition to the classic "heart" sign, have been described and are essential for diagnosis, as they also reflect prognosis.

References

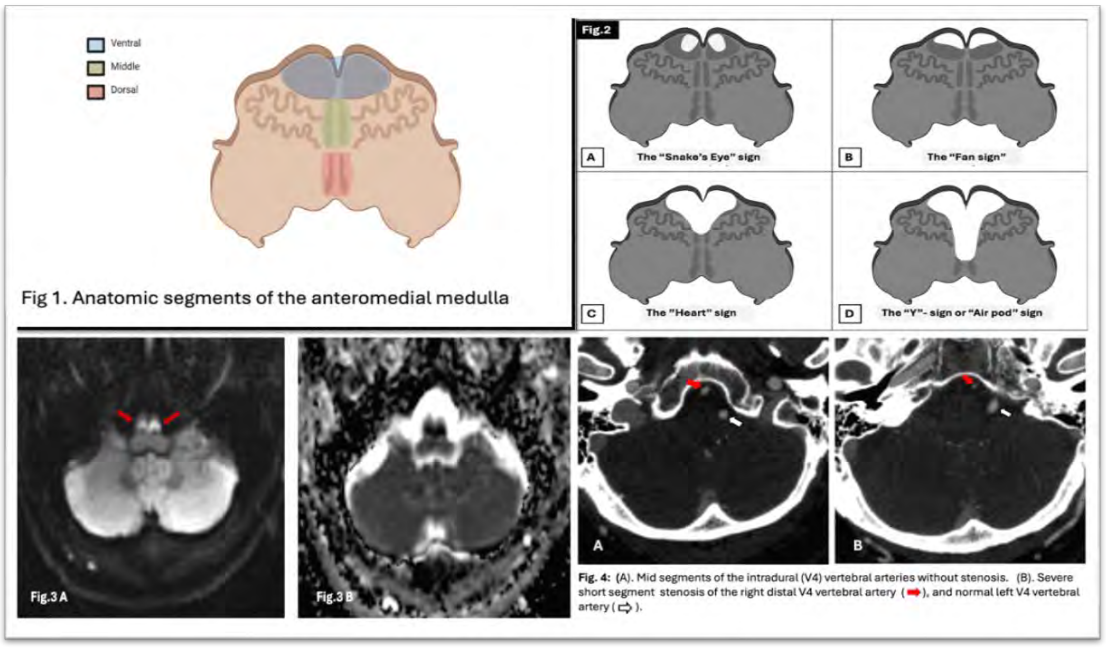
1. Hu F, Nie H, Bai Y, Liang X, Li L, Shen Y. The stroke mechanism, clinical presentation, and radiological feature of bilateral medial medullary infarction. *Neurol Sci*. 2022;43(12):6881-6888. doi:10.1007/s10072-022-06382-4

2. Kim JS, Han YS. Medial medullary infarction: clinical, imaging, and outcome study in 86 consecutive patients. *Stroke*. 2009;40(10):3221-3225. doi:10.1161/STROKEAHA.109.559864

3. Xu Y, Li K, Yao X, Yang Q, Wang P. Perioperative bilateral medial medullary infarction with "snake eyes appearance": A case report. *Front Med (Lausanne)*. 2021;8. doi:10.3389/fmed.2021.559381

4. Raj A, Alapatt PJ, R A, L K S, V V A. Airpod sign: A diagnostic radiological finding of a rare cerebrovascular accident. *Cureus*. December 2, 2022. doi:10.7759/cureus.32129

Images/Tables



342

An Atypical Presentation of Spontaneous Intracranial Hypotension

Devin Y Cao MD, Anil Vasireddi MD
Duke University Medical Center, Durham, NC, USA

Abstract Category

Adult Brain

Clinical History

67-year-old female was referred to Neurosurgery clinic for evaluation of left sided trigeminal neuralgia. She endorsed a prior history of positional headaches for which an MRI was obtained and she was initially diagnosed with a Chiari 1 malformation. In planning for microvascular decompression, the patient's outside hospital MRI from 2017 was obtained for re-interpretation and spontaneous intracranial hypotension was offered as an alternative diagnosis (SIH). A subsequent CT total spine myelogram was performed confirming low intracranial pressure and evidence of a cerebrospinal fluid (CSF)-venous fistula within the thoracic spine. A follow-up MRI brain was also performed. Patient subsequently underwent successful embolization of the fistula with subjective improvement in symptoms.

Imaging Findings

Review of the initial brain MRI demonstrated that in addition to low lying cerebellar tonsils, there were also findings of low intracranial volume as evidenced by diffuse pachymeningeal enhancement and suggestion of venous engorgement given distention of the torcula and transverse sinuses. A repeat exam without contrast redemonstrated the low lying cerebellar tonsils with effacement of the fourth ventricle. In addition, there was evidence of left uncal herniation with approximately 5 mm of downward transtentorial displacement. This resulted in partial effacement of the left ambient cistern and herniated temporal lobe abutting the left cisternal trigeminal nerve. CT myelogram identified the underlying etiology for low CSF pressure, revealing asymmetrically dense right paraspinal veins at the T10 and T11 levels compatible with a CSF-venous fistula.

Discussion

SIH is an important but often overlooked consideration in the patient with headache - classically described as an orthostatic headache secondary to low CSF volume. Less commonly, patients may also present with SIH related cranial neuropathies. This has typically manifested as an array of ocular manifestations related to cranial nerve (CN) III, IV, and VI or vestibular symptoms secondary to CN VIII. Abducens nerve palsy is the most common reported ophthalmoplegia among these and thought to be related to its long intracranial course along the clivus and through Dorello canal. However the underlying pathophysiology of cranial nerve injury remains unclear and is often presumed to be traction related due to decreases in intracranial pressure, mechanical irritation or adjacent venous engorgement.

In contrast, SIH related CN V palsy remains relatively uncommon. Sporadic case reports have identified neurovascular compression exacerbated by SIH related brain sag as a potential etiology. Here we present a unique case of trigeminal neuralgia in a patient with SIH secondary to direct mass effect from uncal herniation. Although more often associated with tonsillar descent, downward transtentorial herniations including uncal herniations can also be seen in patients with SIH. Secondarily, trigeminal nerve palsy may represent an early manifestation of SIH-related uncal herniation in addition to the above mentioned cranial neuropathies.

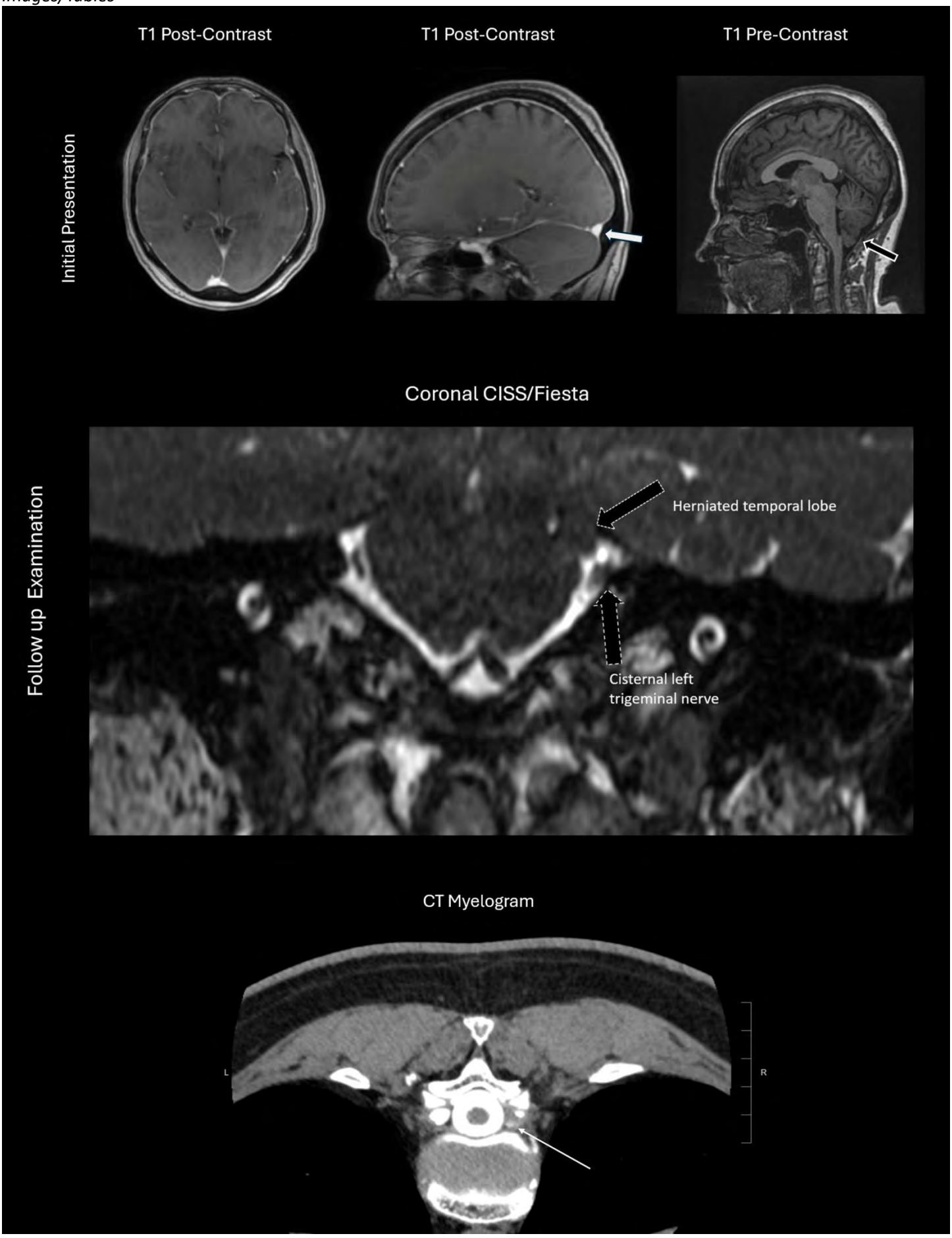
Teaching Point

SIH remains a poorly understood and often misdiagnosed condition with a wide array of clinical manifestations, including a variety of cranial neuropathies. Uncal herniation from low CSF pressure can act as a potential cause of trigeminal neuralgia in patients with SIH.

References

1. Amrhein TJ, Kranz PG. Spontaneous Intracranial Hypotension. Radiologic Clinics of North America. 2019;57(2):439-451. doi:https://doi.org/10.1016/j.rcl.2018.10.004
2. Cheshire WP, Wharen RE. Trigeminal neuralgia in a patient with spontaneous intracranial hypotension. Headache. 2009;49(5):770-773. doi:https://doi.org/10.1111/j.1526-4610.2009.01403.
3. Sajjadi A, Chang I, Djalilian M, Abouzari M, Djalilian AR, et al. Facial Nerve Paralysis Due to Spontaneous Intracranial Hypotension. Ear, Nose & Throat Journal. 2019;100(3):NP137-NP138. doi:https://doi.org/10.1177/0145561319864577
4. Zada G, Solomon TC, Giannotta SL. A review of ocular manifestations in intracranial hypotension. Neurosurgical Focus. 2007;23(5):E8. doi:https://doi.org/10.3171/foc-07/11/e8

Images/Tables



345

Laryngeal Mass with Dyspnea and Hemoptysis: Rare Extramedullary Manifestation of Multiple Myeloma

Anthony Santisi MD, Vivek P Patel MD, PhD
University of Pennsylvania, Philadelphia, PA, USA

Abstract Category

Head & Neck

Clinical History

58-year-old male with no past medical history presents to the emergency department with progressive dyspnea and hemoptysis over the past 5 months.

Imaging Findings

CT demonstrates enhancing soft tissue along the left thyroid cartilage and in the subglottic region along the cricoid cartilage. There was no associated expansion or erosion of the cartilages. MRI demonstrates enhancing submucosal laryngeal mass in these areas with marked diffusion restriction. Few enhancing osseous lesions are also detected on MRI. FDG PET/CT demonstrates diffusely increased metabolic activity in the bone marrow.

Discussion

Multiple myeloma is a plasma cell malignancy involving the bone marrow and less commonly extramedullary soft tissues, with a laryngeal manifestation being very rare. It accounts for less than 1% of all head/neck tumors. The most affected laryngeal sites include the epiglottis, glottis, false vocal folds, aryepiglottic folds, and even more rarely the thyroid cartilage. Our patient underwent bone marrow biopsy which demonstrated CD138+ plasma cells accounting for approximately 60% of overall cellularity and was diagnosed with multiple myeloma. Given the diffuse bone marrow involvement, this is consistent with extramedullary manifestation of multiple myeloma instead of an isolated extramedullary plasmacytoma. Imaging differential includes both neoplastic and non-neoplastic etiologies, which we further discuss in this excerpta.

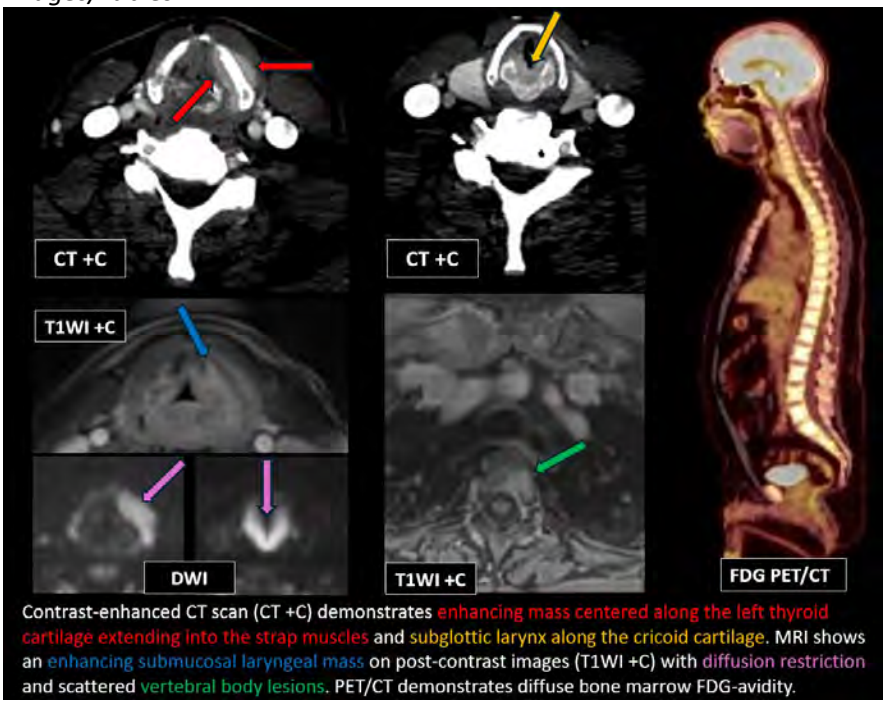
Teaching Point

Extramedullary laryngeal manifestation of multiple myeloma is extremely rare but should be considered in a patient presenting with a laryngeal mass.

References

1. Allegra E, Marino N, Modica D, Emmanuele C, Saita V. Primary laryngeal localization of multiple myeloma: A case report. Mol Clin Oncol. 2017; 6(2):154–156.
2. Kalina P, Rykken J. Multiple Myeloma of the Thyroid Cartilage. Case Reports in Hematology. 2012; Article ID 194797, 1-5.

Images/Tables



Contrast-enhanced CT scan (CT +C) demonstrates enhancing mass centered along the left thyroid cartilage extending into the strap muscles and subglottic larynx along the cricoid cartilage. MRI shows an enhancing submucosal laryngeal mass on post-contrast images (T1WI +C) with diffusion restriction and scattered vertebral body lesions. PET/CT demonstrates diffuse bone marrow FDG-avidity.

358

Anomalous Origin of the Right Vertebral Artery from the Right Common Carotid Artery, Associated with an Aberrant Right Subclavian Artery and a Diverticulum of Kommerell

Younus S Syed D.O.[1], Michael Corso D.O.[1], James Short MD[2]
[1]Aultman/Cleveland Clinic Foundation Mercy/NEOMED Program, Canton, Ohio, USA. [2]Aultman Hospital, Canton, Ohio, USA

Abstract Category

Head & Neck

Clinical History

A 32-year-old female presented with a three-day history of headache, vision changes, and left facial droop. She had a recent history of Bell's Palsy.

Imaging Findings

Computed tomographic angiography (CTA) of the neck showed no occlusion or hemodynamically significant stenosis in bilateral internal carotid and vertebral arteries. An incidental note was made of an aberrant right vertebral artery (VA) arising from the right common carotid artery (CCA), as well as an aberrant right subclavian artery (SCA) with a mild Kommerell diverticulum, originating as the last vessel from the aortic arch.

Discussion

The anomalous origins of the vertebral arteries (VAs) are rare and incidental findings. The left VA originating directly from the aortic arch is the most common of the anatomical variants, occurring in 2.4% to 5.8% of cases (1, 4). The right vertebral artery arising from the right common carotid artery (CCA) has an incidence of 0.18% and is often associated with an aberrant right subclavian artery (SCA). The combination of these two variants with the associated diverticulum of Kommerell is even less common (4).

The vertebral arteries (VAs) form from anastomosis of the first seven longitudinal segments, and obliteration of the first six horizontal parts of the cervical intersegmental arteries (CIAs). The seventh CIA gives rise to the subclavian artery (SCA). If longitudinal anastomosis of the right CIA stops between the 6th and 7th CIAs and the right side of the dorsal aorta is obliterated proximal to the 7th CIA, then the right SCA will originate from the left side of the aorta, distal to the left SCA. Additionally, the right VA will arise from the right common carotid artery (1-4).

Without prior knowledge of anatomical variants, there is a risk of inducing vertebrobasilar ischemia during endovascular and surgical procedures of the head and neck (3). The anomalous right VA arising from the right CCA carries a high risk of injury during thyroidectomy as it runs close to the inferior thyroid artery; variant right VA can be injured during the anterior cervical spine procedures during manipulation of the longus colli muscle (3); as well as during thyroid aspiration if the needle is placed posteriorly and injures the nearby aberrant right VA or CCA (2). Therefore, having prior information about the variant anatomy is important to prevent injury when performing these procedures (2).

The aberrant right subclavian artery with a diverticulum of Kommerell can cause complications such as dysphagia because of the retro esophageal course, as well as atherosclerosis, emboli, and dissection from the diverticulum (4). Most patients are asymptomatic, and treatment is aimed at managing complications associated with the variant right vertebral artery and aberrant right subclavian artery.

Teaching Point

Radiologists need to be aware of different vertebral artery variants as they can lead to complications during angiography and head and neck surgery if not identified beforehand.

References

1. Layton KF, Miller GM, Kalina P. Aberrant origin of the right vertebral artery from the right common carotid artery: depiction of a rare vascular anomaly on magnetic resonance angiography. *JVIR J Vasc Interv Radiol* 2006;17:1065–7. DOI: https:doi.org/0.1097/01.RVI.0000223709.35684.EC.
2. Park JK, Kim SH, Kim BS, et al. Two cases of aberrant right subclavian artery and right vertebral artery that originated from the right common carotid artery. *KJR Korean J Radiol* 2008;9(Suppl):S39–42. DOI: https://doi.org/10.3348/kjr.2008.9.s.s39.
3. Nalamada K, Chitravanshi N, Duffis EJ, et al. Anomalous origin of the right vertebral artery from the right common carotid artery associated with an aberrant right subclavian artery. *JNIS Journal of NeuroInterventional Surgery* 2011; 5(5): e34–e34. DOI: https://doi.org/10.1136/neurintsurg-2011-010229.

4. Goldbach A, Dass C, Surapaneni K. Aberrant Right Vertebral Artery with a Diverticulum of Kommerell: Review of a Rare Aortic Arch Anomaly. *JRCR J Radiol Case Rep*. 2018 May 31;12(5):19–26. DOI: https://doi.org/10.3941/jrcr.v12i5.3239.
5. Bonasia S, Di Caterino F, Robert T. Embryology of the vertebral artery and variants of the adult. *J.neuchi Neurochirurgie*, 2024;70:101517. DOI: https://doi.org/10.1016/j.neuchi.2023.101517.

Images/Tables

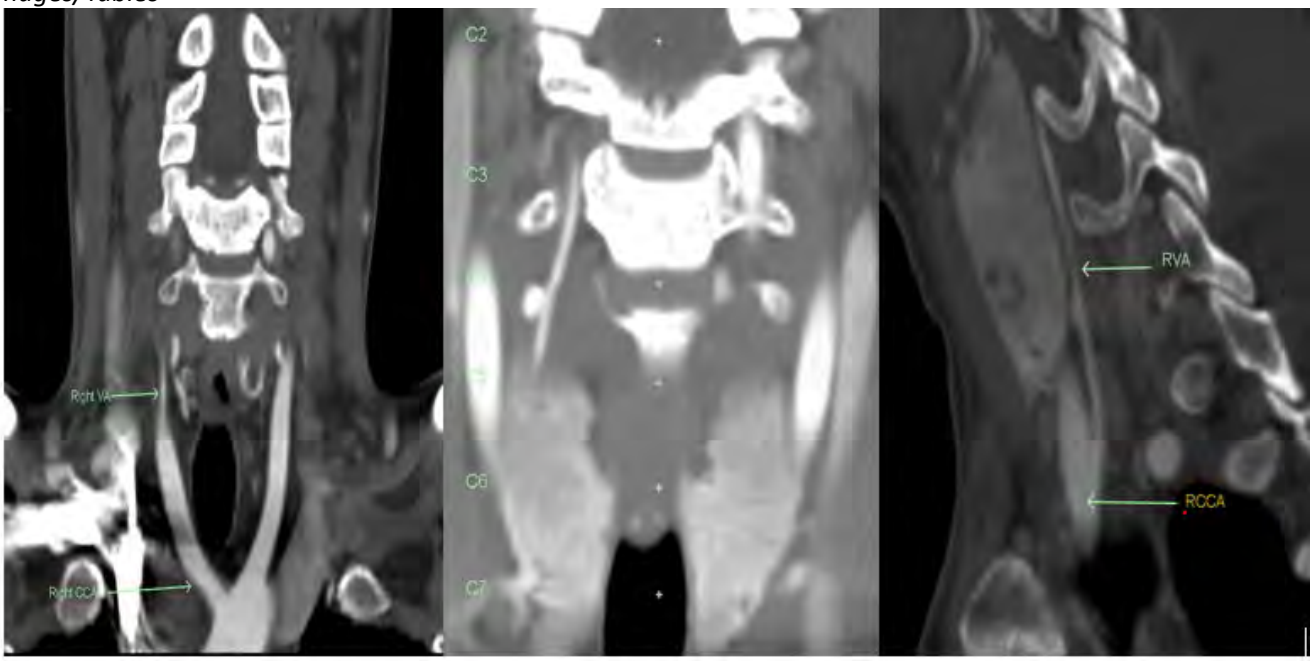


Figure 1: Coronal and sagittal CTA neck images show a hypoplastic right vertebral artery (VA) arising from the right common carotid artery (RCCA) with a retro thyroid course.



Figure 2: Axial and coronal CTA neck images show an aberrant right subclavian artery (RSCA) with a Kommerell diverticulum.

375

Invasive fungal sinusitis at the orbital apex

James P Newton MD, MS, Tabassum Kennedy MD
University of Wisconsin, Madison, Madison, WI, USA

Abstract Category

Head & Neck

Clinical History

68 year old female with h/o T2DM presents with progressive left monocular vision loss over the prior 2 days.

Imaging Findings

MRI demonstrates mass-like enhancement at the orbital apex extending into the sphenoid sinus and pneumatized optic strut, and along the intraconal optic nerve sheath. CT demonstrates bony erosion of the sphenoid sinus wall.

Discussion

Findings are most suggestive of invasive fungal sinusitis given involvement of the sphenoid sinus in a patient with poorly controlled T2DM and acute progressive ocular symptoms. Differential diagnosis could also include idiopathic orbital inflammatory disease, IgG4-related disease. Optic nerve sheath meningioma, lymphoma or other malignancy would be less likely given the time-course of the patient's presentation.

The patient underwent endoscopic biopsy and local debridement with pathology confirming invasive fungal sinusitis, followed by initiation of IV antifungal therapy. Orbital exenteration was avoided. The patient reported persistent left eye vision loss after the acute hospital course.

Teaching Point

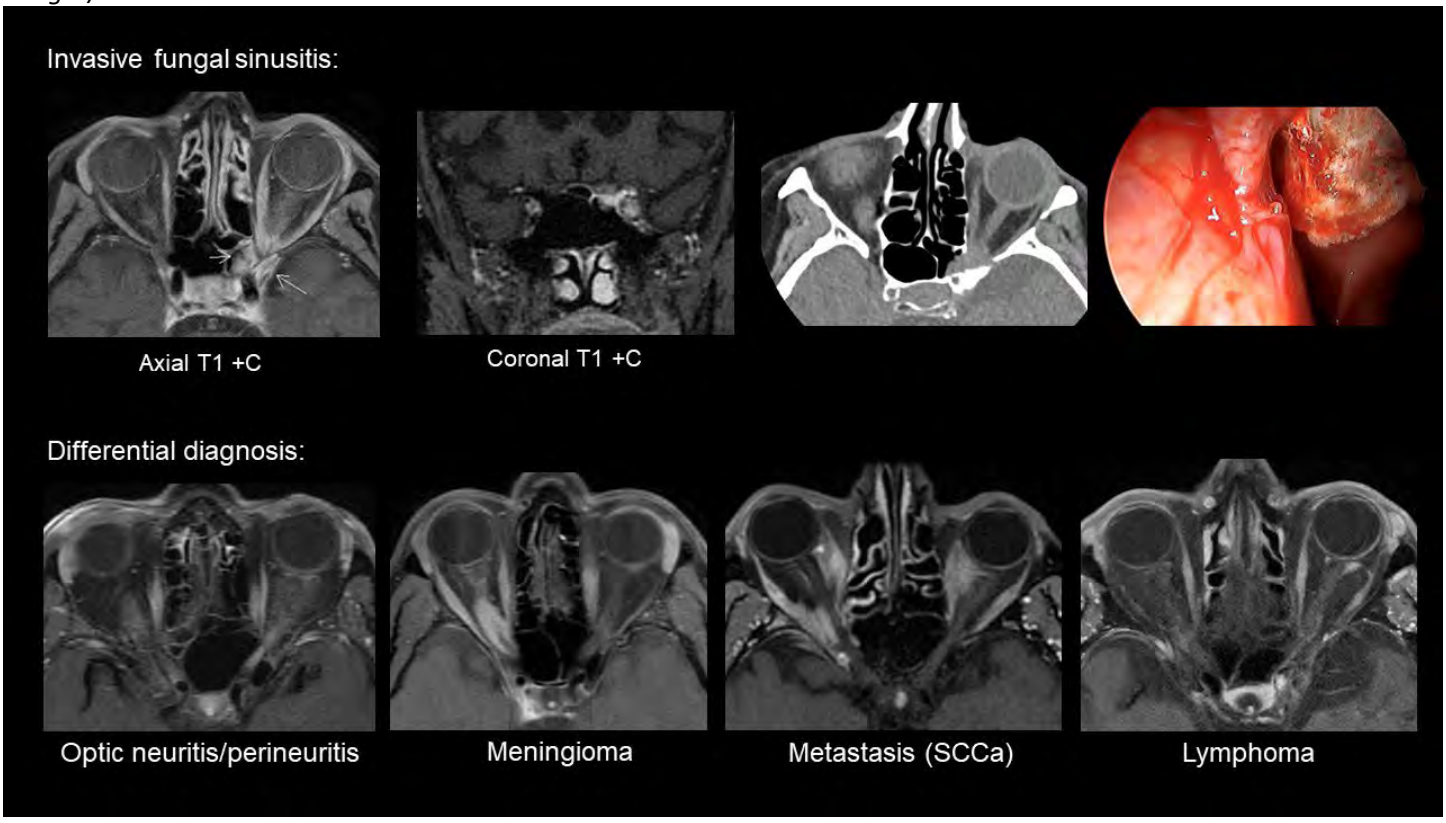
Invasive fungal sinusitis should be considered when there is an enhancing lesion at the orbital apex with sinus extension in an immunocompromised patient, especially given the potentially devastating consequences of delayed diagnosis.

References

Yuan M, Tandon A, Li A, Johnson E, et al. Orbital Apex Syndrome Secondary to Invasive Aspergillus Infection: A Case Series and Literature Review. *Journal of Neuro-Ophthalmology* 2020; 41(4):e631-e638. DOI:10.1097/WNO.0000000000001105

Kurokawa M, Kurokawa R, Baba A, et al. Deadly Fungi: Invasive Fungal Rhinosinusitis in the Head and Neck. *RadioGraphics* 2022; 42:7. DOI: https://doi.org/10.1148/rg.220059

Images/Tables



385

Initial Insights: Documenting the First Case of CHANTER in an Infant

Felipe Rosero Castro BS[1], Suyash Mohan MD[1], Arun Venkataraman MD PhD[1], Alex Z Copelan MD[2]
[1]University of Pennsylvania, Philadelphia, PA, USA. [2]Allina Health Neuroscience Institute, Minneapolis, Minnesota, USA

Abstract Category

Pediatrics

Clinical History

A 10-month-old female presented with severe respiratory compromise and abnormal coloration of her skin. In the ED, she was limp and had poor respiratory effort, which prompted the initiation of assisted ventilation and CPR lasting <60 seconds. On examination, she had bilateral pinpoint pupils, which led to administration of Narcan with marked improvement of respiratory effort. However, the patient remained obtunded and initial venous blood gas showed a combined metabolic and respiratory acidosis. She was subsequently intubated. A non-contrast head CT and was obtained, and she was admitted to the PICU, where she was found to have a UDSs positive for fentanyl.

She received continual respiratory support and supportive care. A cerebral angiogram was performed due to concern for vasculitis/ vasculopathy, which was normal. Her neurologic status gradually improved without any further intervention, and as of most recently, was noted to be awake, interactive, and moving all extremities equally.

Imaging Findings

Initial CT Head revealed areas of hypoattenuation in bilateral cerebellar hemispheres.

Subsequent MR brain was notable for near symmetric diffusion restriction within bilateral cerebellar hemispheres, right occipital lobe, as well as in the basal ganglia and bilateral hippocampi. On SWI, there were microhemorrhages in the right occipital lobe and in both cerebellar hemispheres. There was mass effect in the posterior fossa but with no overt herniation or hydrocephalus.

Cerebral DSA obtained by interventional neuroradiology was unremarkable with normal patency and flow in both anterior and posterior circulations. Based on clinico-radiological findings and a positive UDS for fentanyl, a diagnosis of CHANTER was established.

Discussion

CHANTER (Cerebellar Hippocampal and Basal Nuclei Transient Edema with Restricted Diffusion) is a clinical and radiologic syndrome that typically presents in adults with a history of polysubstance use and especially opioid use. Recent trends have been showing an increasing incidence of opioid intoxication in pediatric populations. Case reports of CHANTER in pediatric populations, though uncommon, have been documented.

Clinically, patients present with a depressed level of consciousness that persists beyond intoxication. On neuroimaging, the syndrome is characterized by cerebellar edema and diffusion restriction in cerebellar cortex, bilateral hippocampi and, variably, in the basal ganglia. Management consists of supportive care, osmotic therapy, and prevention of complications like herniation secondary to cerebellar edema, which has been a primary driver of mortality in case reports. Despite reported deaths, most patients made a partial or full neurological recovery within a few months of discharge.

Tho date, there are no existing reports of the syndrome being diagnosed in children under 12 months, making this the first report of CHANTER in an infant. There is existing literature of infants with findings that fall along the spectrum of opioid-induced encephalopathy however, such cases did not show diffusion restriction in bilateral hippocampi and tended to involve the white matter, features that are less consistent with CHANTER.

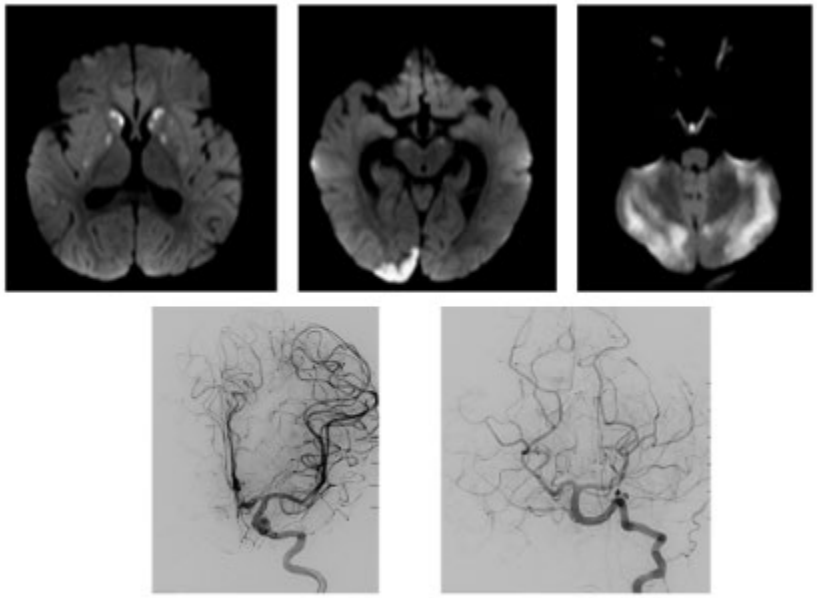
Teaching Point

CHANTER, a syndrome associated with opioid use and characterized by cerebellar edema and diffusion restriction in specific areas of cortex, is not limited to adult patients and can present in pediatric populations as young as 10 months old.

References

1. Jasne, AS, Alsherbini, KH, Smith, MS *et al.* Cerebellar Hippocampal and Basal Nuclei Transient Edema with Restricted diffusion (CHANTER) Syndrome. *Neurocrit Care* 2019;31:288–296. DOI: https://doi.org/10.1007/s12028-018-00666-4
2. Sharon L. Youth and the Opioid Epidemic. *Pediatrics* 2019;143(2): e20182752. DOI: https://doi.org/10.1542/peds.2018-2752
3. Koenigsberg RA, Ross L, Timmerman J, et al. Case of pediatric cerebellar, hippocampal, and basal nuclei transient edema with restricted diffusion (CHANTER) syndrome in a 2-year-old girl. *Pediatr Radiol* 2024;54:1220–1223. https://doi.org/10.1007/s00247-024-05928-2

4. Mallikarjun KS, Parsons MS, Nigogosyan Z, et al. Neuroimaging findings in CHANTER syndrome: a case series. *AJNR Am J Neuroradiol* 2022;43(8):1136-1141. DOI: https://doi.org/10.3174/ajnr.A7569
5. Villelli N, Hauser N, Gianaris T, et al. Severe bilateral cerebellar edema from ingestion of ketamine: case report. *J Neurosurg Pediatr* 2017;*20*(4):393-396. DOI: https://doi.org/10.3171/2017.5.PEDS16695
Images/Tables



387

Sometimes, It Takes Two: CNS Metastasis in Mycosis Fungoides Diagnosed by Repeat Brain Biopsy

Zahra Shokri Varniab MD, Nancy Fischbein MD
Stanford, Palo Alto, California, USA
Abstract Category
Adult Brain
Clinical History
A 75-year-old male with a history of cutaneous T-cell lymphoma (mycosis fungoides, MF) with CD30+ large cell transformation, on bexarotene and previously radiated to several sites of involvement, presented for a surveillance PET/CT that showed focal FDG uptake in the right frontal and left temporal lobes (Figure 1A, 1B). This prompted further evaluation with contrast-enhanced MRI, by which time the patient was experiencing dizziness, slurred speech, and facial droop. Initial imaging findings were concerning for brain parenchymal metastases (Figure 1C, 1D), a rare occurrence in MF. A biopsy of the right frontal lesion was therefore performed, revealing only inflammation and demyelination. Four weeks later, the patient's neurological status worsened. A follow-up MRI revealed both new (Figure 1E) and progressed (Figure 1F) lesions, and a repeat biopsy confirmed CNS involvement by MF.
Imaging Findings

- PET-CT (A/B): Focal FDG uptake in left temporal and right frontal lobes (black arrows).
- Initial MRI (C/D): Nodular and irregular enhancement in right frontal and left temporal lobes, with associated moderate edema (white arrows).
- Follow-up MRI (E/F): New nodular enhancing lesion in right parietooccipital region and progression of known left temporal lesion (white arrows), both with associated edema.

Discussion
This case highlights the challenge of diagnosing CNS involvement in MF. In our case, though concern for brain involvement by MF was high based on clinical history and imaging evaluation, the imaging findings were nonspecific, and the differential diagnosis included other conditions such as metastasis from an unknown tumor, or even multifocal glioma. When the initial biopsy suggested an inflammatory/demyelinating process, which seemed inconsistent with the imaging findings due to the solid nodular and homogeneous appearance of the lesions, a decision was made clinically to

initiate steroids to assess response of inflammation. The patient was monitored for response to steroids, but unfortunately his neurological condition deteriorated, leading to repeat MRI five weeks later. Emergence of new lesions on MRI ultimately necessitated a second biopsy, with CNS involvement by MF confirmed on neuropathological assessment of a stereotactic biopsy sample from the patient's right parietooccipital lesion.

The difficulty of distinguishing neoplastic from inflammatory CNS lesions has been reported in MF [1, 2]. Though CNS involvement in MF is rare before death, it is found in up to 14% of cases post-mortem [4, 5]. In our case, the emergence of new lesions on follow-up MRI and subsequent repeat biopsy allowed definitive diagnosis, emphasizing the importance of correlating evolving imaging findings with pathology, especially when clinical progression diverges from initial assessments. In situations of diagnostic uncertainty, repeat imaging and even repeat biopsy may be required to ensure appropriate diagnosis and management.

Teaching Point

CNS involvement in MF, though rare, does occur, and persistent imaging abnormalities warrant repeat investigation. Clinicians should be aware that both MRI and biopsy findings may be nonspecific and inconclusive initially, and a comprehensive, multidisciplinary approach is required for accurate diagnosis and optimal patient care. The use of serial imaging, vigilant monitoring of clinical symptoms, and readiness to re-image and re-biopsy are critical steps in managing such cases.

References

1. Tacconi L, Eccles S, Johnston FG, Symon L. Mycosis fungoides with central nervous system involvement--a case report: T-cell lymphoma of the brain. Surg Neurol. 1995; 43: 389-92.

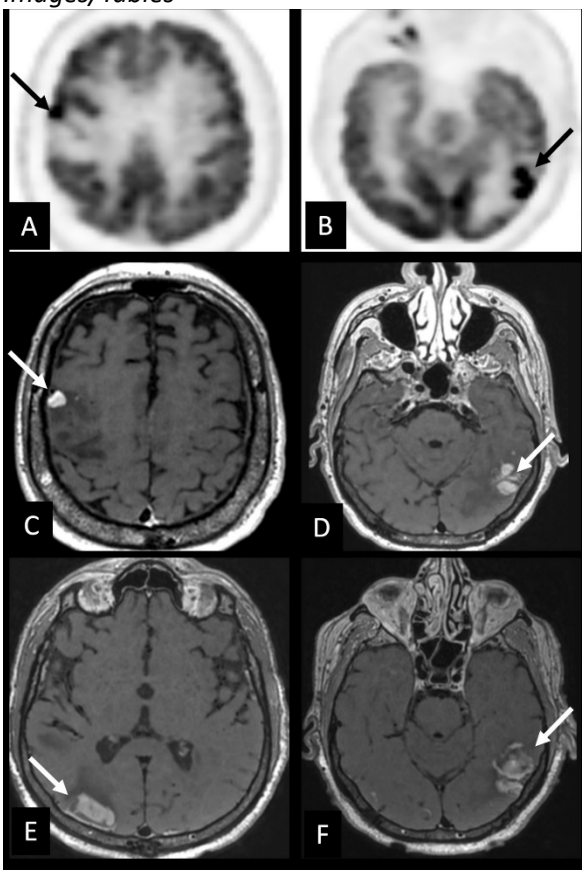
2. Zonenshayn M, Sharma S, Hymes K, Knopp EA, Golfinos JG, Zagzag D. Mycosis fungoides metastasizing to the brain parenchyma: case report. Neurosurgery. 1998; 42: 933-7.

3. Tien RD, Brown M, Massey EW. CNS mycosis fungoides: CT and MR findings. J Comput Assist Tomogr. 1992; 16: 529-33.

4. Zhao G, Chamberlain MC, Khot SP, Shustov A, Olerud JE, Shinohara MM. Central nervous system involvement in cutaneous T-cell lymphoma: 2 illustrative cases and a review of current literature. Clin Lymphoma Myeloma Leuk. 2014; 14: e25-30.

5. Zonenshayn M, Sharma, S. , Hymes, K. , Knopp, E. A. , Golfinos, J. G. & Zagzag, D. . Mycosis Fungoides Metastasizing to the Brain Parenchyma: Case Report. . Neurosurgery, 42 (4), 933-937. (1998).

Images/Tables



394

Facial Desmoplastic Cellular Neurothekeoma

Sanidhya S Karve MD[1], Suresh K Mukherji MD[2]
[1]Amrita Institute of Medical Sciences and Research Center, Kochi, Kerala, India. [2]University of Louisville, Louisville, Kentucky, USA

Abstract Category

Head & Neck

Clinical History

A 2-year-old child from Africa presents with a large right-sided facial swelling. Palpation revealed multiple nodular, non-tender, firm, non-mobile masses involving the right maxillo-facial region.

Imaging Findings

Contrast-enhanced axial CT scan, Axial T1-weighted, Axial T2-weighted, and Coronal T2-weighted MR images show asymmetric enlargement of the neck spaces on the right side by a large lobulated multicompartmental soft tissue. The mass is centered in the temporal and infratemporal fossa, replacing the temporalis, masseter, and pterygoid muscles. The medial extension is limited to masticator and parotid spaces with compression and displacement of parapharyngeal fat. The palatine tonsil and lateral pharyngeal wall are medially displaced, causing mild narrowing of the oropharyngeal airway. Supero-medially, it extends into and widens the pterygopalatine fossa (PPF). The mass extends into the nasopharynx through the sphenopalatine foramen, which is seen abutting the posterior bony nasal septum. Anteriorly, it extends to the orbital margin with the involvement of the orbital part of Orbicularis oculi. Posteriorly and inferiorly, it involves the parotid and submandibular spaces. Compared with the adjacent normal muscles on the left side, mass shows isointense signal intensity on T1Wt images and hyperintense signal intensity on T2Wt images. Post-contrast enhanced CT shows mild heterogeneous enhancement.

Differential diagnoses include Plexiform Neurofibromas in Neurofibromatosis type 1 and Dermal nerve sheath myxoma.

Discussion

Neurothekeoma, aka "benign cutaneous nerve sheath myxoma," is an uncommon benign soft-tissue tumor.[1] Harkin and Reed originally characterized it in 1969, and Gallager and Helwig came up with the name "neurothekeoma" in 1980[2]. It appears in three forms under a microscope: myxoid, cellular, and mixed. Low cellularity and significant myxoid tissue in the form of well-circumscribed lobules scattered with fibrous tissue and giant cells are characteristics of myxoid form. The cellular form consists of eosinophilic cytoplasm and epithelioid cells scattered among unencapsulated lobules[3].

Neurothekeomas are slow-growing, asymptomatic cutaneous tumors (female>male). They most commonly involve the upper limb, followed by head and neck, trunk, and lower limb[3]. Facial involvement predominantly occurs around the nose, cheek, and forehead region. Advanced disease can cause cosmetic distortion and mass effect on the orbit, airway, neck vessels, etc.

MRI is the most useful modality to help delineate its location and relationship with neurovascular structures, bones, etc. These lesions classically appear lobulated with T1 isointense and T2 hyperintense signal when compared to the muscle with heterogenous post-contrast enhancement. Ultrasound reveals heterogeneous hyperechoic lobulated lesions[4]. Neurothekeomas could be positive for immunohistochemistry stains like S-100, GFAP, etc. Thus, a comprehensive approach needs to be adopted for complete evaluation of Neurothekeoma.

The treatment of choice is complete surgical resection[5]. The recurrence rate is low, and malignant transformation is uncommon. Thus, they do not require chemotherapy or radiation.

Teaching Point

To highlight an atypical imaging presentation of a rare condition named Desmoplastic Cellular Neurothekeoma. Delineating the extent of this condition through MR/CT imaging guides the Surgeon in planning an approach and achieving complete resection. Learning about this condition and its imaging details will help Radiologists include it as a close differential to conditions like Plexiform neurofibromas in Neurofibromatosis type 1.

References

1. Stedman TL. Stedman’s Medical Dictionary. 26th ed. Baltimore, MD: Williams & Wilkins; 1995
2. Gallager RL, Helwig EB. Neurothekoma- a benign cutaneous tumor of neural origin. Am J Clin Pathol 1980; 74;759-64.
3. H.-J. Kim, C.H. Baek, Y.H. Ko, et al. Neurothekeoma of the Tongue: CT, MR, nad FDG PET Imaging Findings. AJNR Am J Neuroradiol 2006, 27 (9) 1823-1825.
4. Malkoc M, Ormeci T, Keskinbora M, et al. Nerve Sheath Myxoma of the Dorsal Paravertebral Space. Int J Surg Case Rep. 2014;5(11): 858-60. doi: 10.1016/j.ijscr.2014.10.003

5. Breuer T, Koester M, Weidenbecher M, et al. Neurothekeoma a rare tumour of the tongue. ORL J Otorhinolaryngol Relat Spec 1999;61: 161-4.

Images/Tables

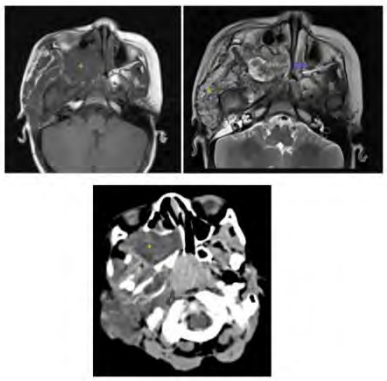


Figure 1: T1-weighted, T2-weighted MR axial and CT axial images at the level of Pterygopalatine fossa (PPF), respectively.

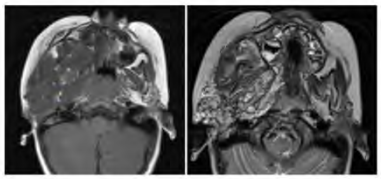


Figure 2: T1-weighted and T2-weighted MR axial images at the level of masticator space, respectively.

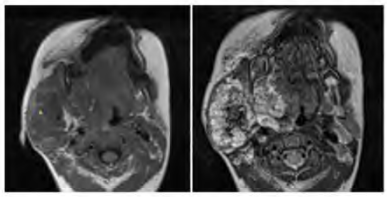


Figure 3: T1-weighted and T2-weighted MR axial images at the level of the tongue, respectively.

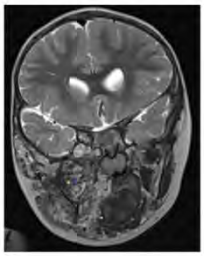


Figure 4: T2-weighted MR Coronal image at the level of infra-temporal fossa.

404

Fractional Tumor Burden (FTB) Mapping Helps to Monitor Glioblastoma Progression in the Clinical Trial of Gallium Maltolate: Case Report

Casey J Zoss, Melissa A Prah, Christopher R Chitambar MD, Jennifer M Connelly MD, Kathleen M Schmainda PhD
Medical College of Wisconsin, Milwaukee, WI, USA

Abstract Category

Functional/Advanced Imaging

Clinical History

A 38 year-old male presenting with a two-month history of headaches and new onset confusion and gait imbalance was found to have a diffusely infiltrative mass in the right frontal lobe extending into the parietal and temporal lobes. He underwent two craniotomies at an outside institution, achieving subtotal resection of the enhancing lesion. Histologic and molecular evaluation revealed WHO grade IV glioblastoma with giant cell and sarcomatous components, *IDH* wild type with *MGMT* promoter methylation. Molecular alterations included mutations in *TP53*, *NF1*, and *ATRX*, with homozygous copy number loss of *CDKN2A/2B* and copy-neutral loss of heterozygosity at 6q, 17q, 19q, and *TP53*. Following standard concurrent chemoradiotherapy, adjuvant temozolomide and tumor-treating fields were initiated. After one month of adjuvant treatment, MRI showed suspicious evolving enhancement with hyperperfusion. Another subtotal resection was performed, which pathologically confirmed progression of disease. A ventriculoperitoneal shunt was required post-resection. A shunt infection occurred and resolved with IV antibiotics without further complications. The patient was enrolled in the Phase I trial of oral gallium maltolate for the treatment of relapsed and refractory glioblastoma (NCT04319276). MRI with DSC perfusion imaging was used to monitor his progress at approximately eight-week intervals. The patient remains radiographically progression-free >17 months post-initiation of gallium maltolate, with no gallium maltolate-associated toxicities.

Imaging Findings

Delta T1 (dT1) mapping uses a calibrated difference algorithm to provide volumetric measurement of true contrast enhancement, free from blood products.[1] Within dT1 enhancement, fractional tumor burden (FTB) mapping assigns histologically validated classes of standardized relative cerebral blood volume: high (red), intermediate (yellow), low/no vascularity (blue).[2, 3] FTB is comprised of the red plus yellow regions. Blue regions are considered non-tumor. dT1 and FTB maps were created using Imaging Biometrics IB Delta Suite and IB Neuro plugins (version 21.12) in Osirix MD (version 14.0).

For this patient, FTB maps were created prior to redo-resection and at subsequent longitudinal imaging timepoints during gallium maltolate treatment (Figure 1). The pre-surgical maps showed substantial FTB with interval growth. Post-resection, volume across all FTB map classes decreased. Longitudinally, FTB volume remained stable, while fluctuations in total dT1 enhancement were driven by changes in FTB-blue (non-tumor) volume (Figure 2).

Discussion

FTB mapping is a tool used to aid in clinical discrimination of high-grade glioma (HGG) progression vs pseudoprogression. FTB mapping is becoming increasingly utilized among neuro-oncology clinicians and researchers. In this case, FTB mapping initially predicted tumor presence, which was pathologically confirmed, and subsequently showed minimal FTB over time despite fluctuations in dT1. These non-tumor volume changes likely reflect evolving post-surgical changes and/or treatment effect.

Ongoing and future analyses will apply longitudinal FTB mapping across all patients enrolled in the gallium maltolate clinical trial, with this case supporting the potential for FTB mapping as a valuable tool in clinical trial settings.

Teaching Point

FTB mapping enhances the interpretability of perfusion imaging in HGG, aiding in the differentiation between progression and pseudoprogression. Its capacity to monitor tumor burden longitudinally highlights its potential utility in HGG clinical trials.

References

1. Schmainda KM, Prah MA, Zhang Z, et al. Quantitative Delta T1 (dT1) as a Replacement for Adjudicated Central Reader Analysis of Contrast-Enhancing Tumor Burden: A Subanalysis of the American College of Radiology Imaging Network 6677/Radiation Therapy Oncology Group 0625 Multicenter Brain Tumor Trial. *AJNR Am J Neuroradiol* 2019;40:1132-1139

2. Prah MA, Al-Gizawiy MM, Mueller WM, et al. Spatial discrimination of glioblastoma and treatment effect with histologically-validated perfusion and diffusion magnetic resonance imaging metrics. *J Neurooncol* 2018;136:13-21
3. Connelly JM, Prah MA, Santos-Pinheiro F, et al. Magnetic Resonance Imaging Mapping of Brain Tumor Burden: Clinical Implications for Neurosurgical Management: Case Report. *Neurosurg Open* 2021;2:okab029
Images/Tables

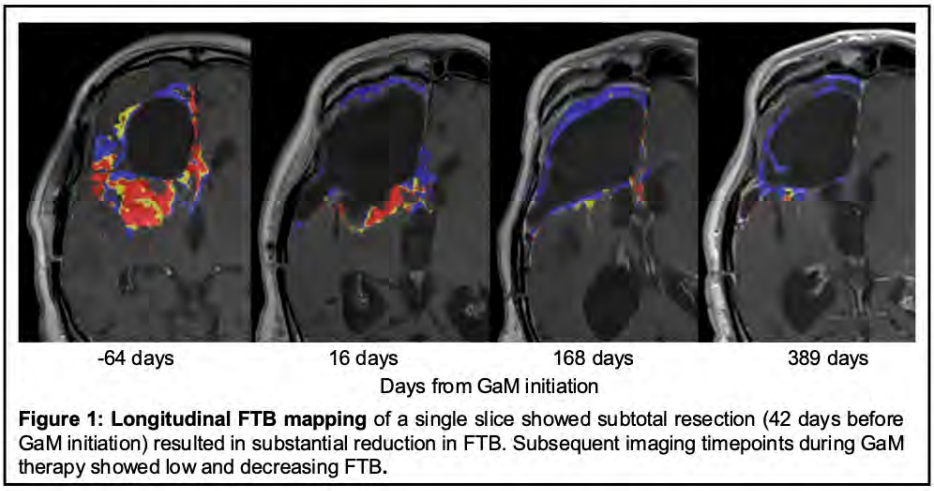


Figure 1: Longitudinal FTB mapping of a single slice showed subtotal resection (42 days before GaM initiation) resulted in substantial reduction in FTB. Subsequent imaging timepoints during GaM therapy showed low and decreasing FTB.

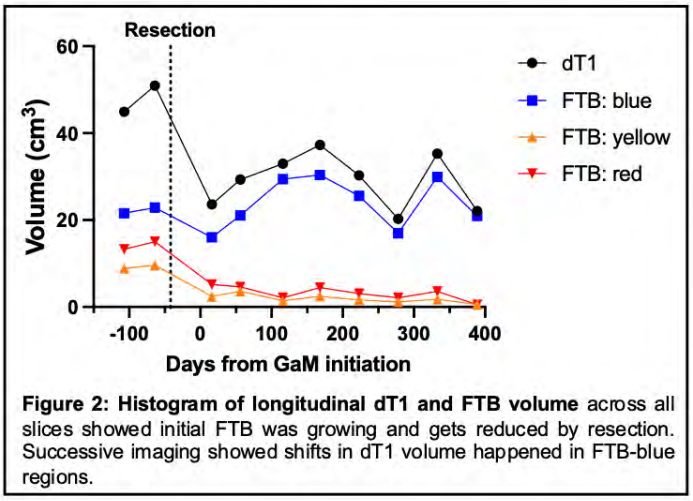


Figure 2: Histogram of longitudinal dT1 and FTB volume across all slices showed initial FTB was growing and gets reduced by resection. Successive imaging showed shifts in dT1 volume happened in FTB-blue regions.

409

Optic Nerve and Intraventricular Migration of Silicone Oil on Non-Contrast Head CT

Newton V Nagirimadugu MD[1], Matthew Conlan[2], Israel Saramago MD[1], Daniel Poliak MD[1], Pallav Shah MD[1], Andrew Shurman MD[1]
[1]St Luke's University Health Network, Bethlehem, PA, USA. [2]Temple St Luke's School of Medicine, Bethlehem, PA, USA
Abstract Category
Head & Neck
Clinical History
Case #1: 74 y/o female status post acute fall with remote history of right eye blindness and pars plana repair for retinal detachment.
Case #2: 68 y/o male initially presenting with stroke symptoms with a remote history of left eye blindness and intraocular silicone oil injection for retinal detachment. Subsequent imaging of the same patient presenting three years later with generalized weakness.

Imaging Findings

Case # 1 (figure 1): Non-contrast CT of the head demonstrates retrograde migration of the hyperattenuating intraocular postsurgical material into the ipsilateral optic nerve sheath, optic chiasm, optic tract, and lateral geniculate body.
Case # 2 (figure 2 and 3): Initial non-contrast CT of the head demonstrates hyperattenuating postsurgical material in the non-dependent portion of the frontal horn of the left lateral ventricle. (figure 3). Subsequent non-contrast CT head obtained three years later demonstrates intraventricular migration of silicone oil from the left frontal horn to the left temporal horn.

Discussion

The pathophysiology of silicone oil migration is unknown; however, one hypothesis proposes an association with increased intraocular pressure. Specifically, increased intraocular pressure facilitates migration of the oil through posterior retinal membranes into the optic nerve sheath and chiasm via retrolaminar diffusion. From there, the oil can seed the subarachnoid and intraventricular spaces, but the mechanism for this is unclear.
Interestingly, as silicone oil is less dense than CSF, when patients are supine migratory intraventricular silicone oil presents in the non-dependent portions of the ventricular system. Intraventricular hemorrhage, however, is denser than CSF and usually found in the dependent portions of the ventricular system

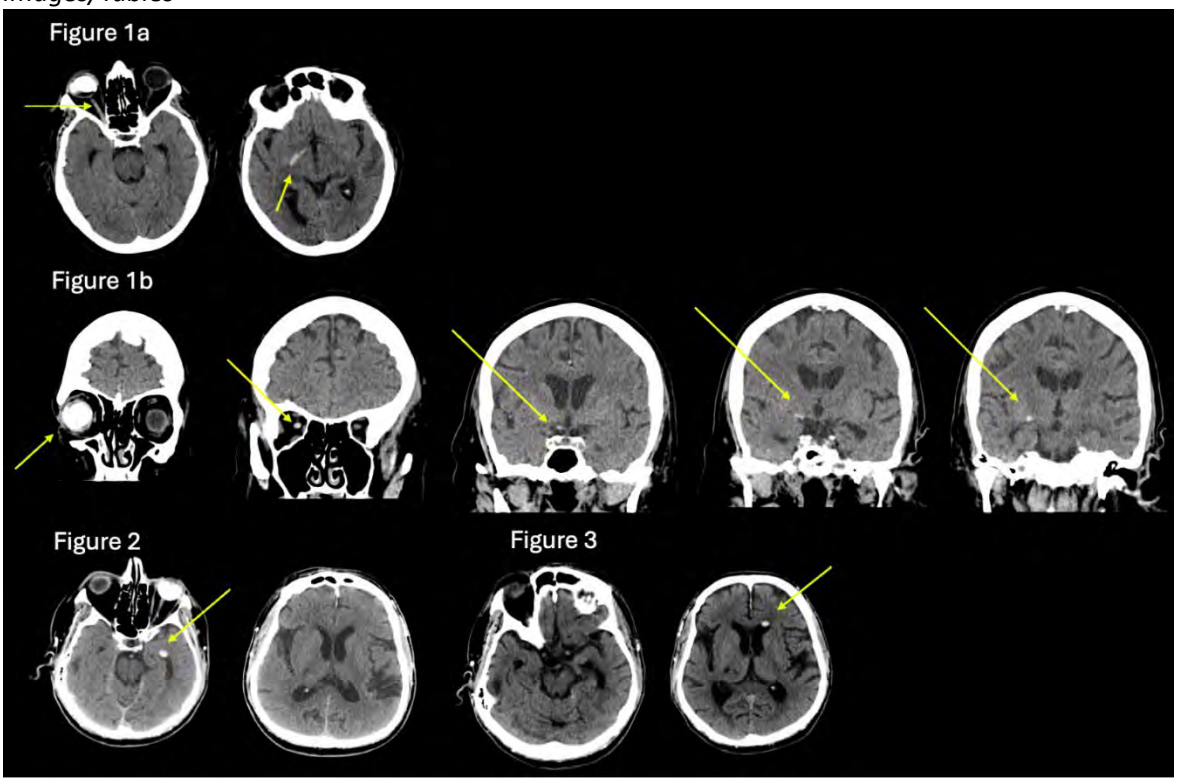
Teaching Point

The differential diagnosis for hyperattenuating intraventricular material on non-contrast CT imaging includes intraventricular hemorrhage, colloid cyst, hyperdense neoplasm, pyogenic debris, and intrathecal contrast. Migratory intraocular silicone is a rare but important diagnostic differential consideration in patients with a history of retinopexy. Careful evaluation of the orbital contents, comparison with prior imaging studies, and detailed review of patient history are key steps in the diagnosis of retrolaminar silicone migration.

References

1. Boren RA, Cloy CD, Gupta AS, et al. Retrolaminar Migration of Intraocular Silicone Oil. Journal of Neuro-Ophthalmology 2016;36:439.
2. Abdalkader M, Takumi K, Chapman MN, et al. Subretinal and Retrolaminar Migration of Intraocular Silicone Oil Detected on CT. AJNR: American Journal of Neuroradiology 2019;40:1557.
3. Zhong H, Bianchi CM, Patel SJ, et al. Intracranial migration of intraocular silicone oil following repetitive head trauma. Radiol Case Rep 2019;14:1163–6.
4. Mayl JJ, Flores MA, Stelzer JW, et al. Recognizing intraventricular silicone. Emerg Radiol 2018;25:215–8.

Images/Tables



410

Unique Case of Atrial-Esophageal Fistula Leading to Venous Air Embolic Infarct

Jonathan W Nazha MD[1], Steven Robinson DO[1], Timothy Nguyen[2], Ryan Babayev MD[1], Robert Hynecek MD[3]
[1]Hartford Hospital, Hartford, CT, USA. [2]Vallejo, CA, USA. [3]Denver, Colorado, USA

Abstract Category

Adult Brain

Clinical History

A 58-year-old male with past medical history of atrial fibrillation (on Eliquis), COPD, asthma, depression, migraines, and history of opioid use disorder (in remission) presented following a MAZE procedure on 2/5/24. One-month post-procedure, patient experienced acute neurological symptoms – left hemiparesis, dysarthria, and confusion. Initial head CT at an outside hospital revealed multiple air emboli in the right cerebrum, prompting transfer to the neuro ICU. Upon arrival to neuro ICU, patient remained drowsy and did not follow commands. Subsequent imaging demonstrated development of infarcts primarily throughout the right cerebral hemisphere.

Further imaging studies and consultations raised the suspicion of a possible atrial-esophageal fistula, a rare complication of the MAZE procedure, potentially allowing air to enter the venous system and embolize to the brain. Additional investigations included repeat imaging, showing edema and further ischemic injury.

Endoscopy performed demonstrated a fistula of 30 cm found in the Middle Third of the Esophagus. Upon surgical exploration, a 1x4 cm fibrinous growth was discovered emanating from the posterior left atrium, attached to a 1 cm defect consistent with a fistula. This was repaired surgically on the atrial side, while the esophageal side was closed endoscopically with a stent. Blood cultures from day 1 of admission revealed *S. salivarius* and S. vestibularis, and *S. mitis* bacteremia on blood cultures, all of which are found in the oral cavity.

Imaging Findings

First head CT:

Extensive linear areas of air along the sulci of the right cerebrum extending from the anterior frontal lobe posterosuperiorly through the prior no lobe. Findings are consistent with venous air emboli.

Follow up same day head CT revealed developing venous infarct throughout the right cerebrum.

Same day MRI showed multifocal areas of acute infarction in the bilateral cerebral and cerebellar hemispheres most prominent in the right frontal/parietal corona radiata.

Discussion

The MAZE procedure uses bipolar radiofrequency and cryoablation devices to create a “box lesion” that completely isolates the posterior left atrium.[1] This technique has proven to be effective in patients that suffer from various forms of atrial fibrillation.[2] Long term results showed high rates of restoration of sinus rhythm with concomitant cardiac procedures.[2]

This rare case illustrates a severe complication of the MAZE procedure for atrial fibrillation, in which an inadvertent perforation occurred between the left atrium and esophagus. This perforation, forming an atrial-esophageal fistula, allowed air and pathogens to enter the left atrium and subsequently travel to the venous system.

This case explores one cause of atria-esophageal fistulas, which are uncommon but can be a severe complication following cardiac procedures that involve atrial manipulation. The patient’s management included a multidisciplinary approach, incorporating neurocritical monitoring, imaging to assess air emboli resolution, and surgical and endoscopic repairs.

Teaching Point

Atrial-esophageal fistulas are rare but life-threatening complications from the MAZE procedure. They should be suspected in patients presenting with delayed neurological symptoms post-procedure, even in the absence of direct trauma. Early imaging (head CT and CTA chest) is crucial for diagnosis. Multidisciplinary management, including emergency surgical repair and infection control, is vital for a favorable outcome.

References

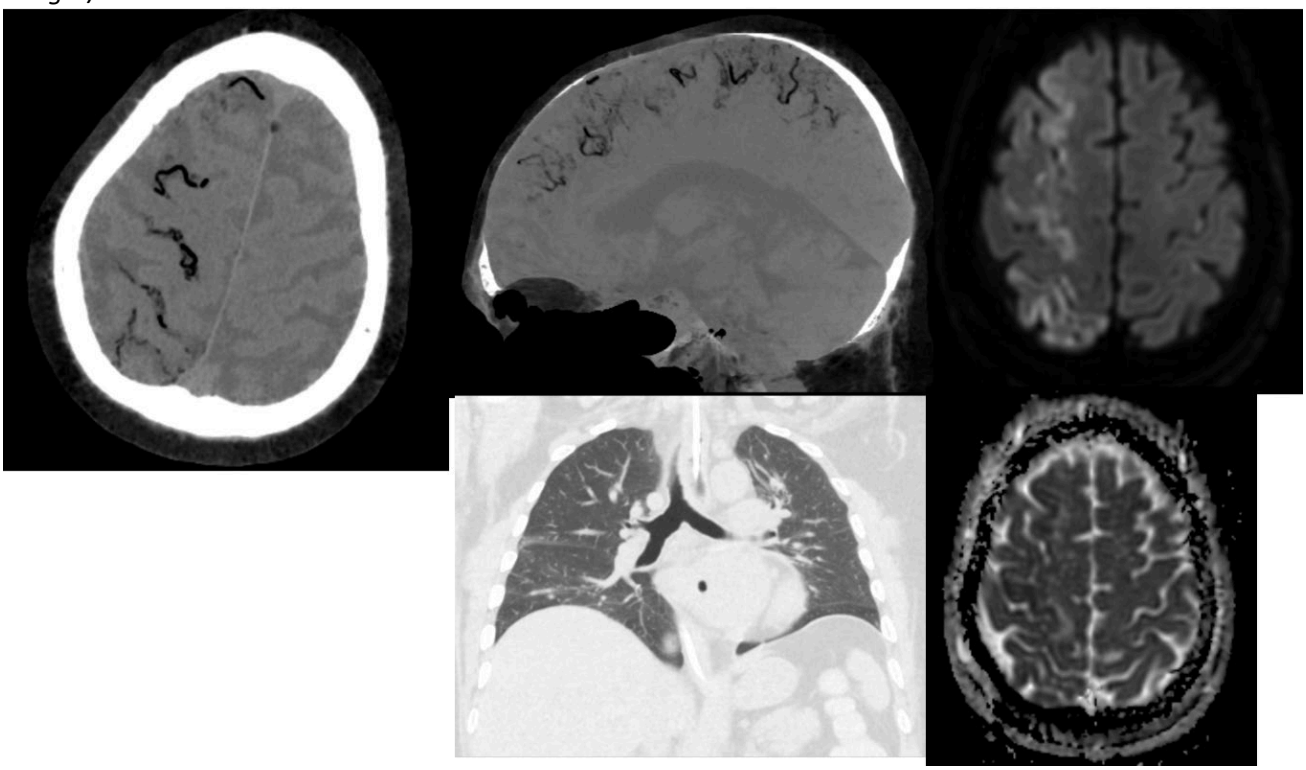
Journal Article

Ali J. Khiabani, Robert M. MacGregor, Nadia H. Bakir, et al. The long-term outcomes and durability of the Cox-Maze IV procedure for atrial fibrillation, The Journal of Thoracic and Cardiovascular Surgery, Volume 163, Issue 2, 2022, Pages 629-641.e7, ISSN 0022-5223, https://doi.org/10.1016/j.jtcvs.2020.04.100.

Journal Article

Matthew C. Henn, Timothy S. Lancaster, Jacob R. Miller, et al. Late outcomes after the Cox maze IV procedure for atrial fibrillation, The Journal of Thoracic and Cardiovascular Surgery, Volume 150, Issue 5, 2015, Pages 1168-1178.e2, ISSN 0022-5223, https://doi.org/10.1016/j.jtcvs.2015.07.102.

Images/Tables



430

Beyond the Brain: Rare Case of Extensive Systemic Metastasis of Glioblastoma

Elleana Paradise[1], Jawad Khan M.D.[2], Steve Fung M.D.[2]

[1]Texas A&M University School Of Engineering Medicine, Houston, Texas, USA. [2]Houston Methodist Hospital, Houston, Texas, USA

Abstract Category

Adult Brain

Clinical History

A 54-year-old male presented with large mass in his right frontal lobe. He underwent gross total resection with pathology showing glioblastoma, IDH wild-type, and unclear MGMT status. He received temozolomide, radiation, and adjuvant temozolomide and bevacizumab for radiation necrosis. Years later he developed extra-axial recurrence invading the right temporalis muscle. After subsequent resection, pathology showed IDH wild-type, negative MGMT, high proliferation (Ki-67 of 75%), TERT promotor mutation, PTEN mutation, and ST7-MET fusion. Chromosomal array identified loss of PTEN and amplification CDK4, MYC, MET, and MDM2. He was re-treated with temozolomide, radiation, and adjuvant temozolomide. Months later, he developed dural-based metastasis involving the right tentorium and parietal convexity and spinal metastases. FDG PET/CT confirmed widespread metastatic disease involving cervical and mediastinal lymph nodes, lungs, liver, and bone. Biopsy of an iliac bone lesion matched prior glioblastoma histomorphology, confirming metastasis. He received single-dose brain radiation but could not continue with palliative spine radiation and was discharged to home hospice.

Imaging Findings

Initial 2020 MRI demonstrated a large necrotic mass with peripheral enhancement (A). January 2024 MRI showed necrotic enhancing mass in the right temporal lobe invading the temporalis muscle (B). Post-resection MRI in July 2024, identified nodular dural-based enhancing metastases along the right tentorium and parietal convexity (C). Spinal MRIs showed extensive metastases (D). FDG PET/CT MIP image (E) highlighted hypermetabolic metastases throughout the body, including right parieto-occipital convexity, right parotid, supracervical, mediastinal and hilar lymphadenopathy, pulmonary metastases bilaterally, multiple hepatic metastases, and widespread osseous metastases.

Discussion

Extraneural metastasis from glioblastoma is extremely rare occurring in < 1% of patients[1]. While spinal drop metastasis and extracranial extension have been documented, widespread systemic metastasis involving lungs, liver, spine, or extremities is even rarer[2]. Several factors impede extraneural spread, including the lack of conventional brain lymphatic drainage, the physical impediment of the blood-brain barrier, and the unique requirements of glioblastoma cells for CNS-derived factors[1-3]. Literature on the pathogenesis of systemic spread is limited, but suggested mechanisms include surgical disruptions, mutations (e.g. MYC, PTEN, TERT, CDK4), sarcomatous de-differentiation, blood-brain barrier breakdown, CSF migration, and potential rare lymphatic/vascular pathways[1-4].

In our case, the presence of TERT and PTEN mutations along with amplification CDK4 and MYC may have contributed to the tumor's ability to metastasize. Such genes have been implicated in angiogenesis, epidermal-mesenchymal transition, and in maintaining the tumorigenic potential of glioblastoma stem-like cells[4]. Currently, no standardized treatment exists for extraneural metastasis although many patients are re-treated with gross total resection and chemoradiation[5]. Interestingly, immune checkpoint inhibitors for PD-L1 mutated glioblastoma and targeted molecular therapies are under investigation[5]. Therefore, early involvement of palliative care can be essential especially with extensive disease.

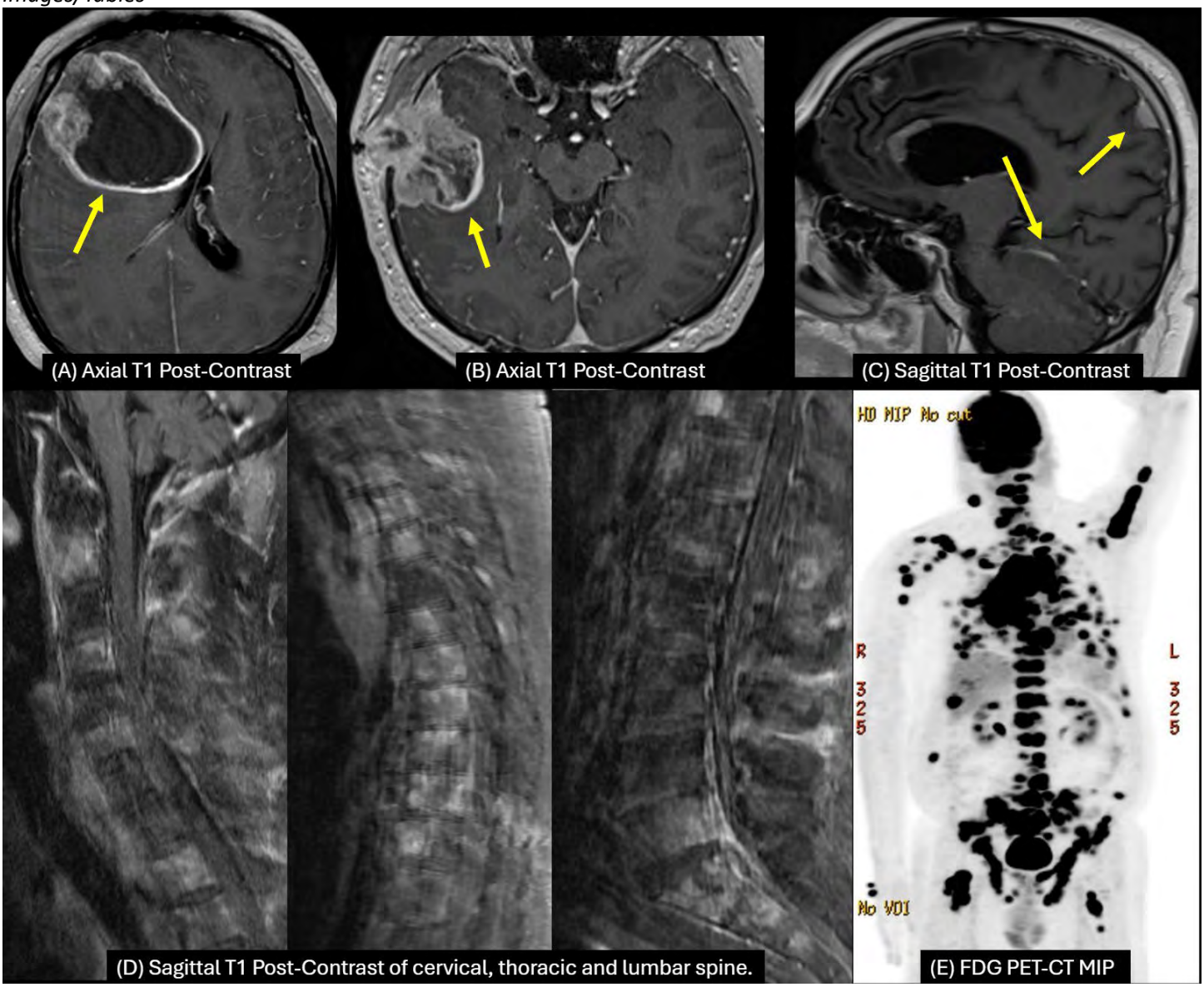
Teaching Point

Systemic metastasis of glioblastoma, though rare, is possible, likely influenced by iatrogenic, molecular, and genetic factors. Histopathological diagnosis of metastasis is challenging and can rely on molecular markers. However, in our case histomorphology was used to confirm metastasis. No standard treatment exists for extraneural metastasis, underscoring the need for further research into molecular mechanisms and potential therapies.

References

1. Kurdi M, Baeesa S, Okal F, et al. Extracranial metastasis of brain glioblastoma outside CNS: Pathogenesis revisited. Cancer Rep (Hoboken). 2023;6(12):e1905. doi:10.1002/cnr2.1905
2. Noch EK, Sait SF, Farooq S, Trippett TM, Miller AM. A case series of extraneural metastatic glioblastoma at Memorial Sloan Kettering Cancer Center. Neurooncol Pract. 2021;8(3):325-336. Published 2021 Feb 3. doi:10.1093/nop/npaa083
3. Taule EM, Brekke J, Miletic H, et al. Breaking boundaries: A rare case of glioblastoma with uncommon extraneural metastases: A case report and literature review. Brain and Spine. 2024;4:103927. doi:10.1016/j.bas.2024.103927
4. Majd NK, Vo HH, Moran CA, et al. Metastatic extraneural glioblastoma diagnosed with molecular testing. Oncologist. 2024;29(9):811-816. doi:10.1093/oncolo/oyae115
5. Gu P, Ding Y, Zheng G, Xu P, Xia X. Extracranial metastasis of glioblastoma: A case report and literature review. Int J Surg Case Rep. 2023;111:108895. doi:10.1016/j.ijscr.2023.108895

Images/Tables



440

Infantile Hemangiomas of the Upper Eyelid: A Case-Based Review of Imaging Findings

Joseph Kim MD, Matthew Hammer MD, Neal Shukla MD, Long Tu MD, PhD, Balaji Rao MBBCh
Yale New Haven Hospital, New Haven, CT, USA

Abstract Category

Pediatrics

Clinical History

We will show two cases of infantile hemangiomas (IH) of the upper eyelid in a 2-month-old girl and an 8-month-old boy, evaluated by ultrasound and MRI, respectively. The 2-month-old girl presented with a nontender, non-fluctuant bluish nodule on the right superior eyelid with associated restricted eyelid movement. The 8-month-old boy presented with worsening astigmatism.

Imaging Findings

In the 2-month-old girl, ultrasound revealed a 1.8 cm isoechoic to hyperechoic lesion in the superficial subcutaneous soft tissues of the right upper medial eyelid. There was extensive internal vascularity on color Doppler.

In the 8-month-old boy, MRI of the brain and orbits, performed with and without contrast, demonstrated a mass confined to the left upper eyelid measuring up to 1.9 cm. The mass was hypointense on T1-weighted images, isointense to white matter on T2-weighted images, and showed homogeneous enhancement.

Discussion

While IH are common benign vascular tumors, periocular IH has a birth prevalence of 1 in 1586 live births. Periocular IHs increase the risk of ocular complications, such as astigmatism and amblyopia, especially when they are larger than 1 cm, involve the upper eyelid, and have a deep component. While diagnosis is usually clinical, imaging modalities such as ultrasound or MRI can be used to assess the depth and extent of the lesion. Differential diagnoses include other vascular malformations and malignancies such as rhabdomyosarcoma.

Teaching Point

Early diagnosis and management of periocular IH are crucial in preventing ocular complications. Imaging modalities such as ultrasound or MRI can aid in the diagnosis and risk-stratification of these vascular lesions.

References

Alniemi ST, Griepentrog GJ, Diehl N, et al. Incidence and clinical characteristics of periocular infantile hemangiomas. Arch Ophthalmol. 2012 Jul;130(7):889-93. doi: 10.1001/archophthalmol.2012.213.

Dubois J, Milot J, Jaeger BI, et al. Orbit and eyelid hemangiomas: is there a relationship between location and ocular problems? J Am Acad Dermatol. 2006 Oct;55(4):614-9. doi: 10.1016/j.jaad.2006.05.042.

Images/Tables

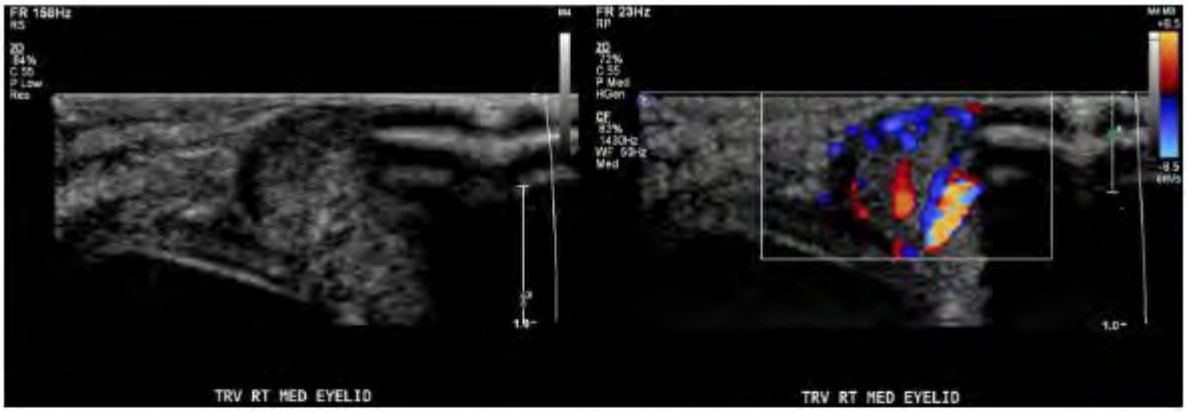


Figure 1. Transverse view of right upper eyelid. **(Left)** Gray-scale ultrasound. **(Right)** Color Doppler ultrasound.

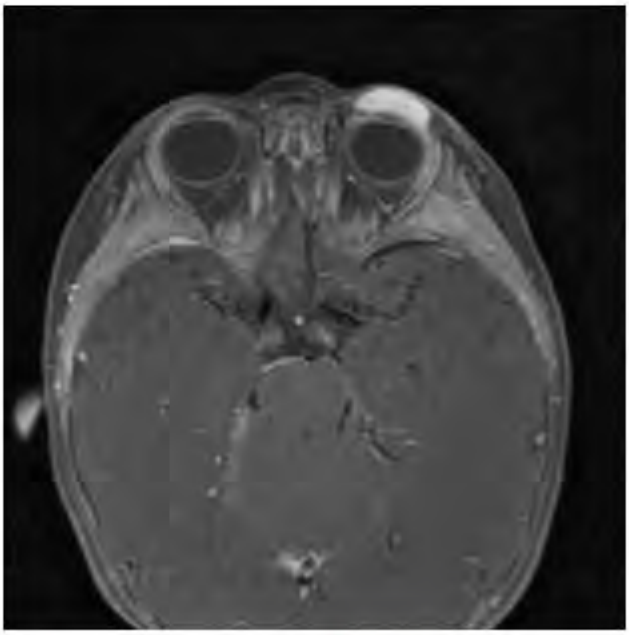


Figure 2. Axial T1-Weighted Post-Contrast MRI of the Brain and Orbits.

446

Imaging Features of Raccoon Roundworm (Baylisascaris procyonis) Encephalitis

Jeremy W Martin MD[1], Priya Rajagopalan MD[2], Reza Assadsangabi MD[2]
[1]University of Southern California, Los Angeles, CA, USA. [2]Los Angeles General Medical Center, Los Angeles, CA, USA

Abstract Category

Pediatrics

Clinical History

Herein, we describe two pediatric cases of raccoon roundworm (Baylisascaris procyonis) infection complicated by encephalomyelitis and neuroretinitis, presenting to our institution in recent months.

Case 1:

15 month old, previously healthy, who presented with encephalopathy, generalized weakness, gait instability, and progressively increasing muscle stiffness. Patient was found to have eosinophilia both in serum and in CSF. Subsequently, the patient developed visual impairment with CN3 and 6 palsies, and progressive neurological decline.

Case 2:

14 year old with autism and pica who presented with altered mental status, ataxia, and gaze preference. Patient was also found to have mild CSF pleocytosis with eosinophilia.

Imaging Findings

- MRI in both patients demonstrated extensive confluent white matter T2/FLAIR signal abnormality within the supratentorial and infratentorial brain with speckled periventricular enhancement in a perivascular distribution. No definite restricted diffusion.
- MRI of the spine demonstrated patchy non-enhancing T2/FLAIR hyperintensity within the cervical cord.
- MRI of the orbits were unremarkable.
- Subsequent examinations revealed significant interval brain parenchymal volume loss.

Discussion

- B. procyonis is endemic in raccoons in the United States, and infected eggs can be found concentrated in raccoon feces and latrines.
- If ingested, B. procyonis larvae can migrate into the CNS and orbits, causing encephalitis and/or neuroretinitis, with resultant severe morbidity and mortality.
- Diagnosis can be challenging; in both cases, eosinophilia was present and B. procyonis antibody testing was confirmatory.
- Imaging features can be nonspecific with diffuse white matter signal abnormality, and can appear similar to metabolic or other atypical infectious/inflammatory processes.
- Ophthalmologic exam identified retinal roundworms, which were ablated by laser photocoagulation in both patients.
- Though this is a rare entity (with approximately two dozen cases reported), young children or adults with pica are most frequently affected.

Teaching Point

- Although rare, zoonotic infection by the raccoon roundworm (Baylisascaris procyonis) can cause an eosinophilic encephalitis and/or neuroretinitis, particularly in young children and those with pica, with devastating neurologic outcome.

References

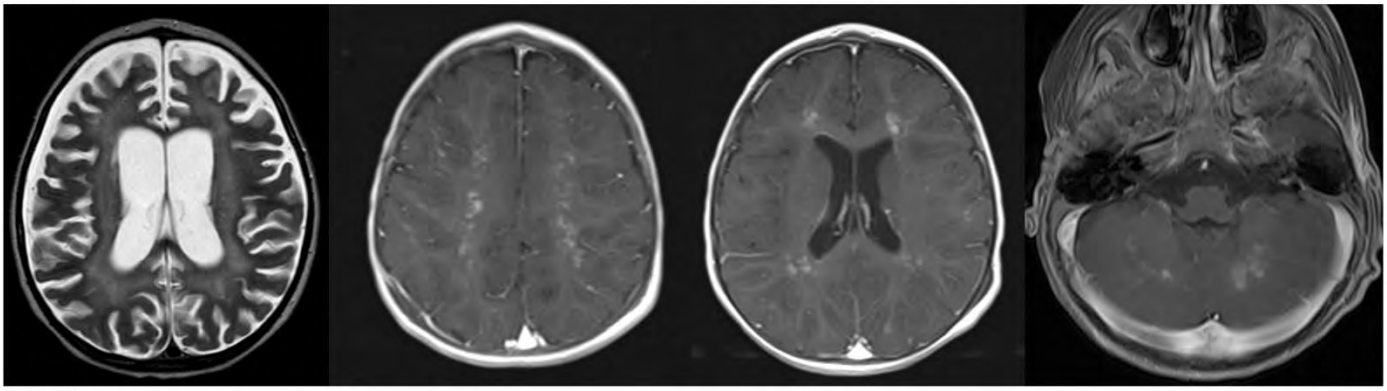
1. Strausbaugh LJ, Murray WJ, Kazacos KR. Raccoon Roundworm Encephalitis. *Clin Infect Dis*. 2004;39(10):1484-1492. doi:10.1086/425364

2. Rowley HA, Uht RM, Kazacos KR, et al. Radiologic-Pathologic Findings in Raccoon Roundworm (Baylisascaris procyonis) Encephalitis. *Am J Neuroradiol*. 2000;21(2):415-420.

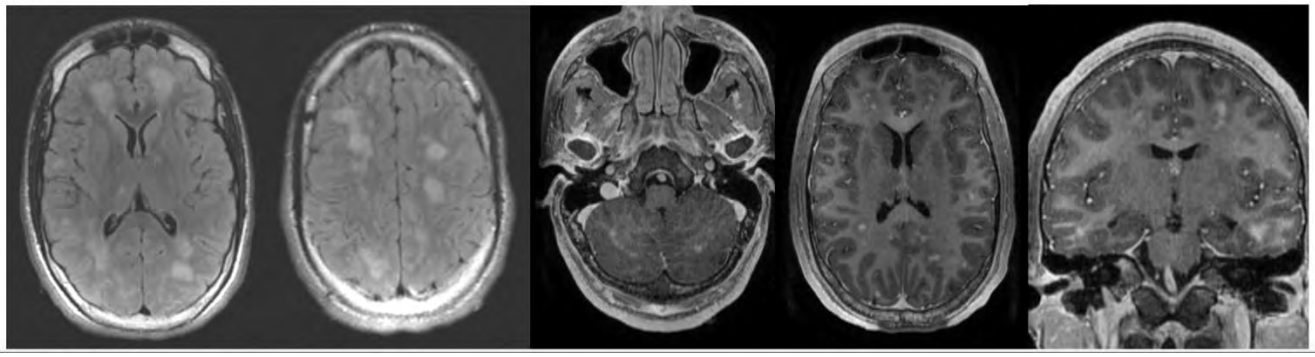
3. Goldman-Yassen AE, Derman A, Madan RP, Radmanesh A. A Worm's Tale or Why to Avoid the Raccoon Latrine: A Case of Baylisascaris procyonis Meningoencephalitis. *Case Rep Radiol*. 2022;2022(1):5199863. doi:10.1155/2022/5199863

Images/Tables

Case 1:



Case 2:



484

Adult-onset Leukoencephalopathy with brainstem and spinal cord involvement (LBSL): recognizing imaging features and clinical presentation

Mark Chen MD, Kathryn L Hughes MD, Akram Fadhl Mohammed Al-Warqi MD, Chanae Dixon MD
Rush University, Chicago, IL, USA

Abstract Category

Adult Brain

Clinical History

A 43-year-old woman without significant past medical history presented with several weeks of worsening bilateral lower extremity weakness, gait ataxia, and facial spasticity/paresthesia. Physical exam revealed nonspecific lower extremity hyperreflexia, upper motor neuron symptoms and mild proprioception loss. A brain MRI was obtained, revealing extensive cerebral white matter and spinal pathway abnormalities as described below. At this point, differential included broad toxic/metabolic, inflammatory, and genetic causes. Further history disclosed that the patient had siblings with more severe, childhood-onset learning and motor disabilities. Genetic workup demonstrated a mutation in the DARS2 gene, confirming a diagnosis of leukoencephalopathy with brainstem and spinal cord involvement and lactate elevation (LBSL).

Imaging Findings

MRI brain (Fig 1) showed patchy, non-enhancing T2/FLAIR hyperintensities throughout the periventricular and subcortical white matter with symmetric FLAIR hyperintensities through the anterolateral medulla (including pyramids) and cerebellar hemispheres extending to the middle peduncles. MRI cervical spine (Fig 2) showed long-segment T2 and STIR hyperintensities in the dorsal column and lateral corticospinal tracts.

Discussion

Our patient's imaging findings, genetic analysis, and clinical symptoms are consistent with LBSL. LBSL is an autosomal recessive disorder characterized by mutations in DARS2, a gene encoding the mitochondrial translation protein aspartyl-tRNA synthetase. This disorder predominantly presents in children with progressive ataxia, spasticity, proprioceptive dysfunction, and in severe cases, eventual wheelchair dependency[1]. Imaging criteria revised by Steenweg et al. in 2012 for diagnosis of LBSL's must fulfill three major criteria: involvement of the 1) cerebral white matter (with subcortical

sparing), 2) dorsal column and lateral corticospinal tract, and 3) medullary pyramids and/or medial lemniscus. At least one supportive minor criterion with involvement of the splenium, posterior limb of the internal capsule, cerebellum, and additional white matter tracts is also required[2].

Reports of adult-onset LBSL such as this case are rarer in literature. Our patient, like most published cases, shows MRI findings consistent with the accepted criteria[3]. However, clinical presentations of adult LBSL vary greatly, with some patients being asymptomatic while others progress gradually with less severe motor and cognitive decline compared with children[1,4]. To our knowledge, no adult-specific imaging features have been characterized. Furthermore, symptoms can vary greatly between siblings[5], like in our case with multiple siblings who experienced faster, more severe neurodegeneration during childhood. It has been suggested that subtle mutation variations affect LBSL phenotype[1,5], though their correlation with imaging findings is yet indeterminate.

Thus, our case adds to the growing pool of data on adult-onset LBSL and illustrates the importance of multidisciplinary workup in establishing a diagnosis.

Teaching Point

Our case emphasizes the multidisciplinary importance of imaging, clinical presentation, and genetic analysis/family history in recognizing LBSL. Though the diagnostic imaging criteria is well-established and specific to LBSL, other inherited leukodystrophies and metabolic disorders can overlap. Furthermore, while primarily described in children, adult-onset LBSL exists and can feature significant phenotypic variance, even within the same family. When radiologists recognize MRI findings suggestive of LBSL, family history and DARS2 mutation can help clinch the diagnosis. Ancillary tests such as lactate elevation in proton magnetic spectroscopy can complement diagnostic efforts[4].

References

1. Van Berge L, Hamilton EM, Linnankivi T, et al. Leukoencephalopathy with brainstem and spinal cord involvement and lactate elevation: clinical and genetic characterization and target for therapy. *Brain* 2014;137:1019–29.
2. Steenweg M, Van Berge L, Van Berkel C, et al. Early-Onset LBSL: How severe does it get? *Neuropediatrics* 2012;43:332–8.
3. Kassem H, Wafaie A, Abdelfattah S, et al. Leukoencephalopathy with brainstem and spinal cord involvement and lactate elevation (LBSL): Assessment of the involved white matter tracts by MRI. *European Journal of Radiology* 2013;83:191–6.
4. Labauge P, Dorboz I, Eymard-Pierre E, Dereeper O, Boespflug-Tanguy O. Clinically asymptomatic adult patient with extensive LBSL MRI pattern and DARS2 mutations. Journal of Neurology. 2011;258:335-337.
5. Li JL, Lee NC, Chen PS, et al. Leukoencephalopathy with Brainstem and Spinal Cord Involvement and Lactate Elevation: A Novel *DARS2* Mutation and Intra-Familial Heterogeneity. *Movement Disorders Clinical Practice*. 2021;8:1116-1122.

Images/Tables

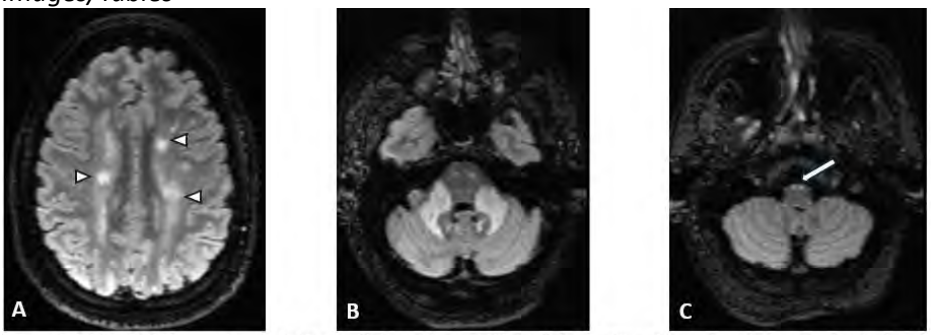


Figure 1. Axial T2 FLAIR images showing: *A,* Nonspecific hyperintense FLAIR signal abnormalities of the periventricular and subcortical cerebral white matter (arrowheads) with sparing of the U-fibers. *B,* Symmetric hyperintense FLAIR signal involving the bilateral cerebellar hemispheres with extension to the middle cerebellar peduncles. *C,* Extension of signal abnormalities to the medulla, specifically the pyramidal tracts (arrow).

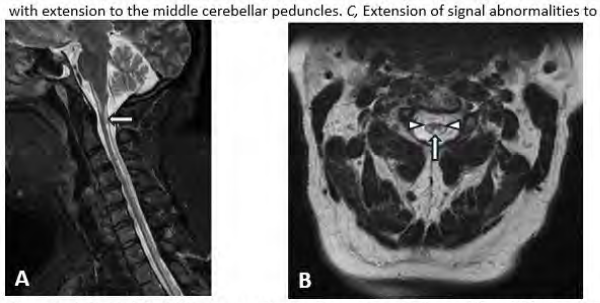


Figure 2. *A,* Sagittal T2 STIR sequence showing long-segment intramedullary T2 hyperintense signal throughout nearly the entire dorsal cervical spine. *B,* Axial T2 images showing specific involvement of the dorsal column (white arrow) and lateral corticospinal tracts (arrowheads).

488

Role of Neuroinflammation in Development/Progression of Demyelination in Multiple Sclerosis and its in-vivo visualization with C-11-PK11195 Positron Emission Tomography

Ajay Kumar, MD,PhD[1], Csaba Juhasz, MD,PhD[2], Otto Muzik, PhD[2], Harry T Chugani, MD[3]
[1]University of Pennsylvania Perelman School of Medicine, Philadelphia, PA, USA. [2]Wayne State University School of Medicine, Detroit, MI, USA. [3]NYU School of Medicine, New York, NY, USA

Abstract Category

Pediatrics

Clinical History

A 17-year-old female with relapsing remitting multiple sclerosis and multiple (>6) relapses within one year of diagnosis underwent C-11-PK11195 (PK) brain positron emission tomography (PET) to evaluate for pattern of neuroinflammation, about 4 weeks after her most recent relapse. She had weakness of the right arm, leg and face as well as diplopia and gait difficulties.

Imaging Findings

PK brain PET showed a focal area of increased radiotracer uptake and binding potential (a measure of radioligand-TSPO [translocator protein] receptor binding) in the left periventricular centrum semiovale and corona radiata (Image in center with black arrow), suggestive of neuroinflammation (see discussion below).

A brain MRI, performed two months before the PET scan, showed only subtle FLAIR changes in that corresponding focal area (image on left with red arrow). Multiple other scattered areas of periventricular and deep white matter T2/FLAIR hyperintensity were also noted on that scan and these showed various degrees of neuroinflammation ranging from mild binding to absent uptake on PET.

A repeat brain MRI, performed 15 days after the PET scan, showed interim development of a large area of lobular FLAIR changes in that focal area (image on right with red arrow) with corresponding enhancement. Other previously demonstrated scattered foci of FLAIR hyperintensity appeared stable.

Discussion

Multiple sclerosis and its progression are associated with underlying neuroinflammatory changes (1). However, direct in-vivo detection of neuroinflammation is not possible with routine imaging or biochemical techniques, except for histopathology, which is quite invasive or possible only post-mortem. Since neuroinflammation is mediated by activated microglia, which express TSPO receptors, neuroinflammation can be imaged in-vivo using PET and any radiotracer which selectively binds to these receptors (2). C-11 labeled PK-11195 is one of such radiotracers (2). Our case report suggests that the development of a new plaque in multiple sclerosis is associated with acute robust neuroinflammation which can be detected with PK-11195 PET. The focus of increased tracer uptake corresponds precisely to the area of MRI detectable white matter changes.

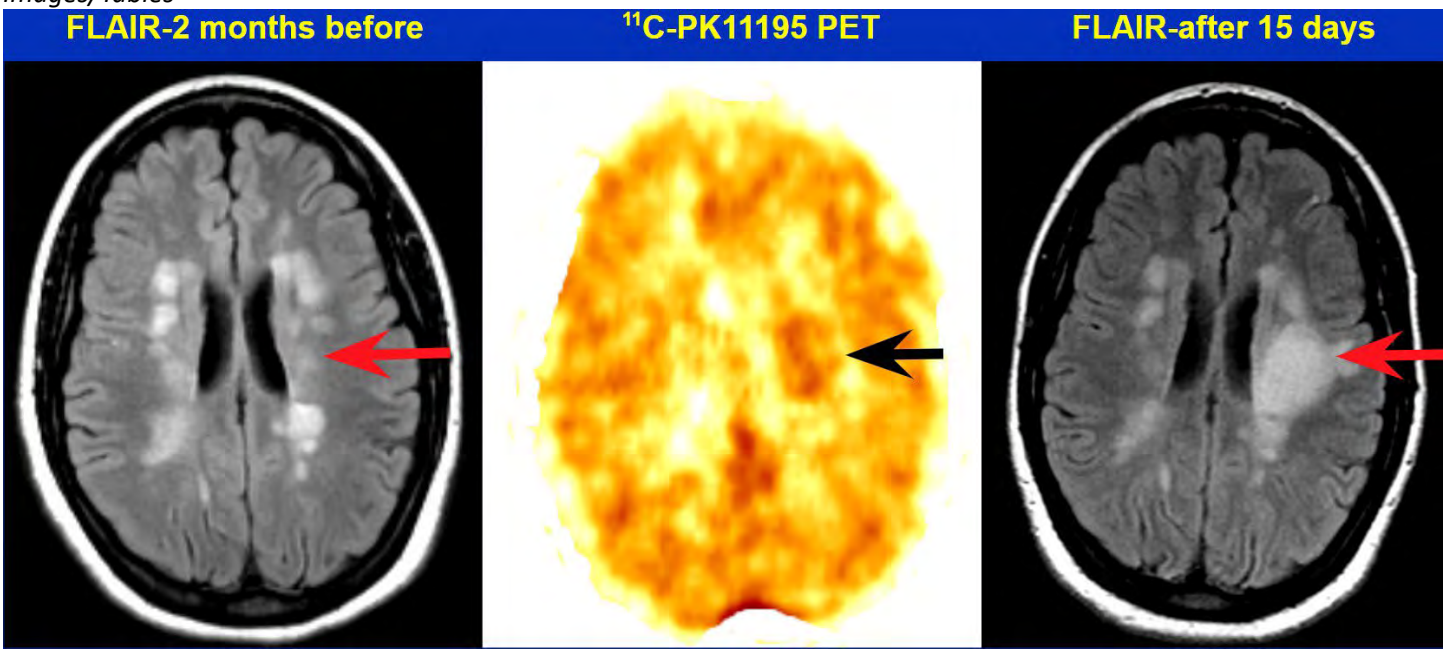
Teaching Point

Our case in-vivo demonstrates the role of neuroinflammation in the development/progression of demyelination in multiple sclerosis; these changes can be visualized using PET studies of neuroinflammation. Furthermore, careful MRI/PET comparison of each MS plaque allows dating of the lesion more obvious on PET than with MRI.

References

1. Reich DS, Lucchinetti CF, Calabresi PA. Multiple Sclerosis. N Engl J Med. 2018;378(2):169-180.
2. Cumbers GA, Harvey-Latham ED, Kassiou M, et al. Emerging TSPO-PET Radiotracers for Imaging Neuroinflammation: A Critical Analysis. Semin Nucl Med. 2024;29:S0001-2998(24)00082-5.

Images/Tables



492

Acute Pons Stroke with Narrowed Posterior Circulation in Young Healthy Adult - Narrowing the Differentials

Otavio Augusto Ferreira Dalla Pria MD[1], Nitesh Shekhrajka MD[1], Joan A Maley MD, FACR[1], Minako Hayakawa MD, Ph.D.[1], Leonardo Furtado Freitas MD[2]

[1]University of Iowa Health Care, Iowa City, IA, USA. [2]Baptist Health Quality Network, Miami, FL, USA

Abstract Category

Adult Brain

Clinical History

47-year-old healthy male presenting with slurred speech and left-sided weakness. 2 days before, while driving, he developed some burning in his face, which resolved. On the night before, he felt some burning in the right side of his nose, but otherwise, he felt fine and went to bed at 11 pm. He woke up at 345 am with left facial droop, slurred speech, and weakness.

Imaging Findings

Initial scan: CTP, CTA brain - On perfusion maps, there is a tiny area of core infarct surrounded by a large penumbra in the right hemi-pons. Delayed perfusion in the right-greater-than-left cerebellum. Occlusion of the right distal V4 (near the junction with the basilar artery) with severe narrowing into the left distal V4 and proximal basilar artery.

MRA head/neck: Irregular narrowing of the distal right greater than left vertebral arteries, as well as of the mid-proximal basilar artery, with areas of significant stenosis and focal wall enhancement in the vertebrobasilar junction.

MRI Brain: Known acute right hemi pons infarct along the ipsilateral perforating branches of the basilar artery. Subtle abnormal enhancement of the left facial nerve at the distal cisternal and labyrinthine segments.

Discussion

In an appropriate clinical context (severe headache, vigorous physical activity), the possibility of reversible cerebral vasoconstriction syndrome (RCVS) restricted to the posterior circulations should be considered.

The minimal focal wall enhancement in the vertebro-basilar junction could be secondary to walls apposition/collapse, unlike to be vasculitis.

Subtle abnormal enhancement of the left facial nerve at the distal cisternal and labyrinthine segments, suggestive of left facial neuritis, such as Bell's palsy.

Another differential that could explain left facial neuritis and acute vasculopathy in posterior circulation could be a virus SNC infection. The CSF analysis was recommended.

The final diagnosis was neurosyphilis in a non-HIV patient. Treatment was started, and posterior fossa circulation narrowing improved a few weeks later.

Teaching Point

Although meningovascular syphilis is a rare etiology of ischemic stroke, especially in the posterior circulation, this hypothesis should be included in the differential in appropriate clinical settings since it's treatable and an important cause of stroke. In this case, the radiologist played a pivotal role by suggesting CNS infection. However, in clinical practice, particularly during emergencies, any ischemic stroke should be screened for neurosyphilis.

References

1. Bäuerle, J., Zitzmann, A., Egger, K., Meckel, S., Weiller, C. and Harloff, A., 2015. The great imitator—still today! A case of meningovascular syphilis affecting the posterior circulation. *Journal of Stroke and Cerebrovascular Diseases*, *24*(1), pp.e1-e3.

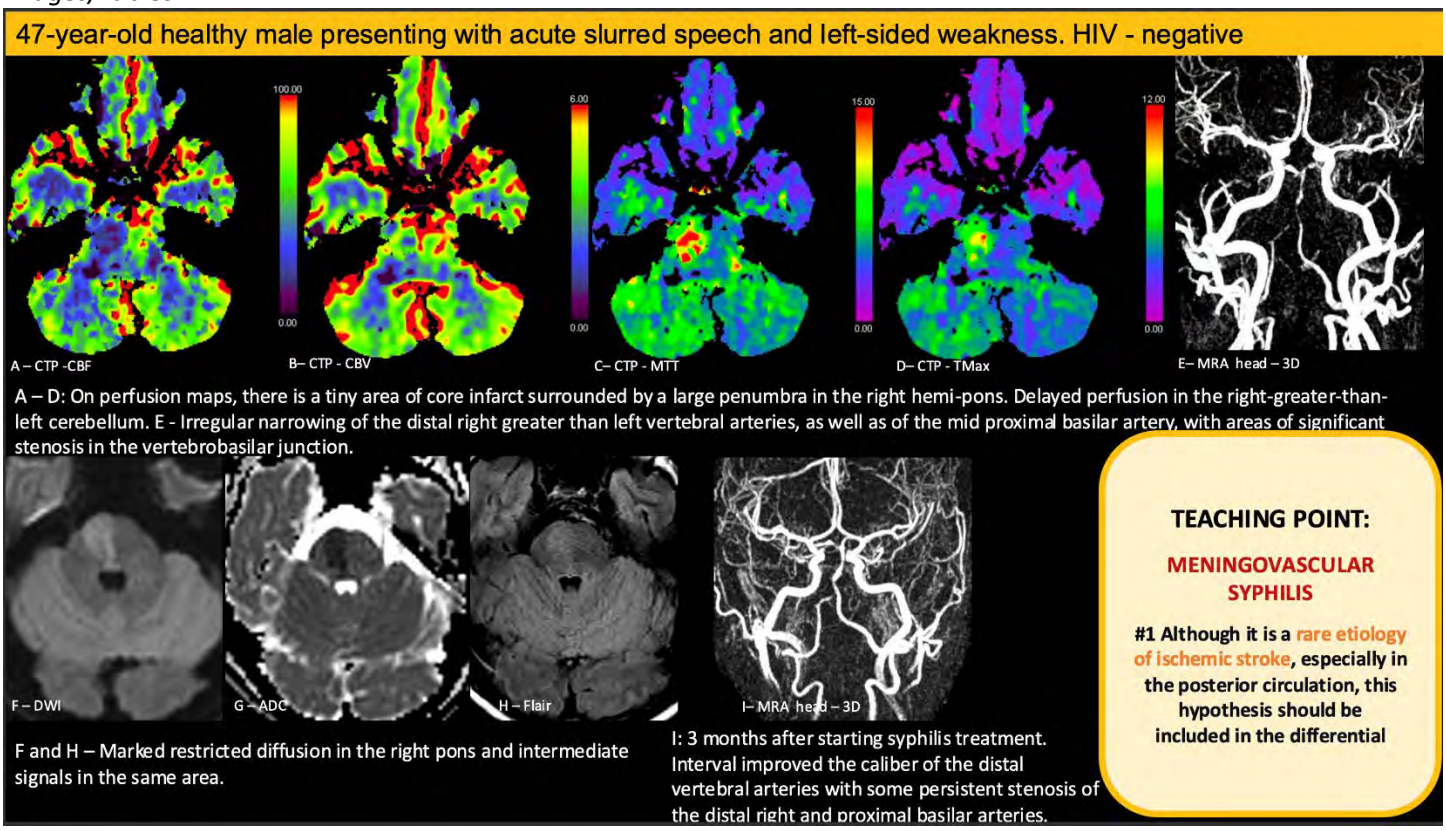
2. Liu, L.L., Zheng, W.H., Tong, M.L., Liu, G.L., Zhang, H.L., Fu, Z.G., Lin, L.R. and Yang, T.C., 2012. Ischemic stroke as a primary symptom of neurosyphilis among HIV-negative emergency patients. *Journal of the neurological sciences*, *317*(1-2), pp.35-39.

3. Currens, L., Sivakumar, S., Jun-O'Connell, A.H., Ionete, C. and Ghasemi, M., 2022. Neurosyphilis presenting with focal middle cerebral artery stenosis and acute ischemic stroke: A case report. *Radiology Case Reports*, *17*(5), pp.1620-1625.

4. Shaikh, J., Venkatesh, Y.S., Kothari, R., Singh, R., Moore, S., Peethambar, G.A., Haditaghi, M., Pradhan, S., Neighbors, A., Bhambri, A. and Arora, S., 2024. Neurosyphilis: A Great Masquerader of Acute Ischemic Stroke–A Case Report and Diagnostic Challenge. *Neurology*, *103*(7_Supplement_1), pp.S110-S110.

5. Corrêa, D.G., de Souza, S.R., Freddi, T.D.A.L., Fonseca, A.P.A., Dos Santos, R.Q. and da Cruz Jr, L.C.H., 2023. Imaging features of neurosyphilis. *Journal of Neuroradiology*, *50*(2), pp.241-252.

Images/Tables



497

Molecularly-defined Oligodendroglioma Presenting with Osseous Metastasis, 16 Years After Initial Diagnosis

Shweta Nelluri MD, Emily Ling-Lin Pai MD, MacLean Nasrallah MD, Suyash Mohan MD
Hospital of University of Pennsylvania, Philadelphia, PA, USA

Abstract Category

Adult Brain

Clinical History

22-year-old male presented with left frontal lobe mass after the first seizure of his life. Partial resection of neoplasm histologically demonstrated a grade 2 oligodendroglioma with 1p/19q co-deletion. Patient received radiation and remained stable for 9 years until follow up imaging revealed tumor progression. He underwent two more craniotomies for neoplastic recurrences. Imaging after the second craniotomy demonstrated new hemorrhage and involvement of right frontal lobe. Pathology confirmed recurrence of his known tumor with progression to CNS WHO grade 3, oligodendroglioma, IDH-mutant and 1p/19q co-deleted subclass confirmed by molecular studies. The patient received radiation but deferred adjuvant temozolomide treatment. 16 years after initial diagnosis, patient presented with left arm pain and imaging revealed an aggressive left proximal humerus lesion. Biopsy of the lesion confirmed metastatic oligodendroglioma. Further PET/CT imaging revealed additional left iliac bone metastasis. These osseous lesions were palliated with radiation.

Imaging Findings

Brain MRI demonstrated initial neoplastic recurrence as small foci of enhancement in the left frontal lobe with significant elevation of relative cerebral blood volume (Fig. 1A-D). Marked progression on brain MRI with new T2 hypointense fluid-fluid level (Fig. 1E) and hyperintensity on the axial pre-contrast T1-weighted (Fig. 1F), consistent with hemorrhage. When patient presented with left arm pain, plain radiograph of left humerus revealed lytic lesion with endosteal scalloping (Fig. 1H). MRI of the left humerus revealed an aggressive mass with associated cortical dehiscence and periosteal reaction (Fig. 1I). PET/CT showed significant uptake in the left proximal humerus and left iliac bone, consistent with metastases (Fig. 1J-K).

Discussion

It is rare for any primary brain tumor to metastasize to extracranial sites; exceedingly so for oligodendrogliomas. Literature review has identified fewer than 70 reports since the year 1951 of extracranial metastases from oligodendrogliomas and about 20 reported cases of bone and marrow involvement since 1970[1].

Our case is the first molecularly-confirmed case of metastatic oligodendroglioma that presented with osteolytic changes. The presence of neural cell adhesion molecule (NCAM), which is expressed by both gliomas and osteoblasts has been proposed to underlie the possible predilection of oligodendroglioma for bone marrow[2,3]. However, the specific mechanism responsible for osteoblastic or osteolytic lesions in the setting of metastases remains to be elucidated. The factors that precipitate oligodendroglioma metastases are not known. Previously proposed possible mechanisms include but are not limited to multiple craniectomies, metastasis through a VP shunt, chemotherapy effects, and long-term survival[4]. Indeed, in our case, the patient underwent multiple craniectomies and placement of a VP shunt both of which may have contributed to the distant metastases. It is also interesting that while the second resection was classified as oligodendroglioma, the third resection indicated a shift towards IDH-mutant high-grade glioma, which raises questions about epigenetic influences on tumor behavior.

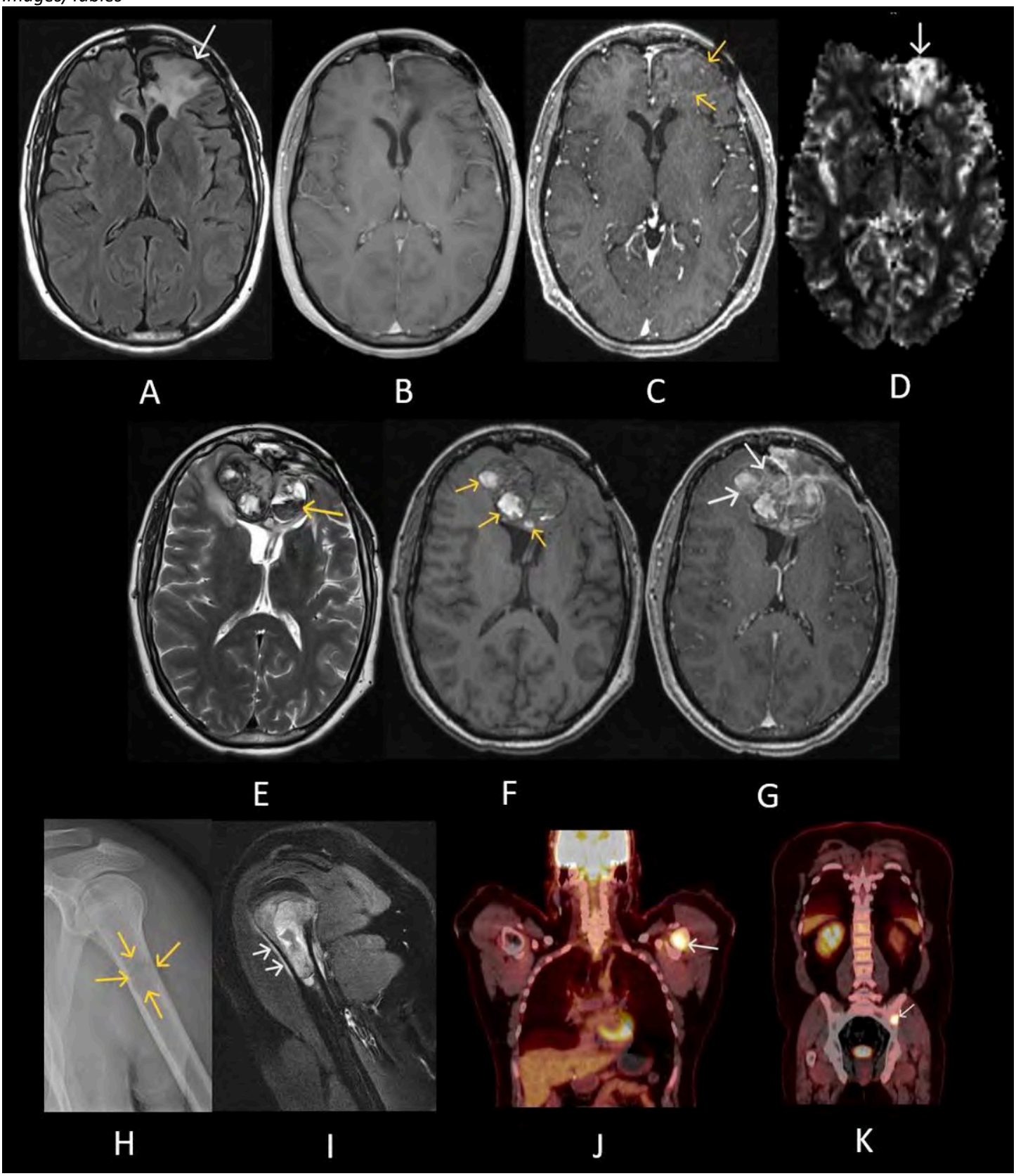
Teaching Point

This is an exceptional case of IDH-mutant 1p/19q co-deleted oligodendroglioma with multiple osseous metastases 16 years after initial diagnosis. Awareness of the metastatic potential of oligodendroglioma is crucial in managing the patient's care. This case also invites further investigation to understand the factors that make rare extracranial metastasis of this neoplasm possible.

References

1. Liwnicz BH, Rubinstein LJ. The pathways of extraneural spread in metastasizing gliomas: a report of three cases and critical review of the literature. *Hum Pathol* 1979;10(4):453-67. doi: 10.1016/s0046-8177(79)80051-9
2. Singh VK, Singh S, Bhupalam L. Anaplastic oligodendroglioma metastasizing to the bone marrow: a unique case report and literature review. *Int J Neurosci* 2019;129(7):722-28. doi: 10.1080/00207454.2018.1557165 [published Online First: 20190213]
3. Wang X, Hisha H, Taketani S, et al. Neural cell adhesion molecule contributes to hemopoiesis-supporting capacity of stromal cell lines. *Stem Cells* 2005;23(9):1389-99. doi: 10.1634/stemcells.2004-0343 [published Online First: 20050728]
4. Merrell R, Nabors LB, Perry A, et al. 1p/19q chromosome deletions in metastatic oligodendroglioma. *J Neurooncol* 2006;80(2):203-7. doi: 10.1007/s11060-006-9179-0 [published Online First: 20060519]

Images/Tables



503

The Rarely Described Association Between Pseudoaneurysm and Aberrant ICA: A Case Series

Paul Yousif M.D., Paul Farnsworth D.O., Julie Guerin M.D., Waleed Brinjikji M.D., Kirk Welker M.D., Jack Lane M.D.
Mayo Clinic, Rochester, MN, USA

Abstract Category

Head & Neck

Clinical History

We present three cases of patients who were incidentally diagnosed with aberrant ICA anatomy with pseudoaneurysms. Case 1 is a 73 year old female with a history of recurrent otitis media early in her life who presented with symptoms of right mixed hearing loss with pulsatile tinnitus. On otoscope exam, a vascular lesion was demonstrated on the lower portion of the right hypotympanum medial to the drum. Case 2 is a 49 year old female with worsening left hearing loss who had a reddish colored mass in the anterior-inferior quadrant extending over and touching the malleus and pressing on the medial aspect of the tympanic membrane on otoscope exam. Case 3 is a 14 year old female who had an incidental abnormality noted on her left tympanic membrane on a physical exam.

Imaging Findings

Case 1 had a CT without IV contrast which demonstrated an aberrant right ICA extending into the umbo of the right malleolus. The area that extends into the middle ear has focal dilatation consistent with a small pseudoaneurysm. Case 2 had a CT without contrast, and MR brain without and with IV contrast. Both demonstrated an aberrant left internal carotid artery extending into the tympanic cavity. This aberrant vessel did contact the umbo of the malleus and incus lenticular process which likely was contributing to the hearing loss. Some focal dilatation of the left ICA at its aberrant portion likely represents a pseudoaneurysm. Case 3 underwent a CT of the temporal bone which demonstrated an aberrant left ICA with lateral deviation along the lateral aspect of the cochlear promontory. Focal inferolateral outpouching of the left ICA which measured 2 mm and abuts the medial aspect of the malleolus manubrium with effacement of the lateral aspect of the vessel wall was suspicious for pseudoaneurysm with possible thin bony dehiscence along the lateral carotid wall. A subsequent CTA of the head and neck confirmed this pseudoaneurysm.

Discussion

While rare, aberrant left ICA vessels, and anomalies of these vessels such as pseudoaneurysms, are important to describe on imaging. In all three cases, CT of the temporal bone was adequate to diagnose the aberrant ICA and even raise suspicion for the pseudoaneurysm. Acquired pseudoaneurysms might have arisen due to prior trauma or surgical intervention, however could also be caused by atherosclerosis, or inflammatory conditions, or malignancy [1]. The location of the aberrant ICA vessel could put it at increased risk of pseudoaneurysm due to its course, it's association with the middle ear, and its proximity to the tympanic membrane Surgical intervention in the middle ear in the presence of an aberrant ICA in the middle ear can be catastrophic, and could even be the cause of pseudoaneurysm formation, as described elsewhere in the literature [2,3,4].

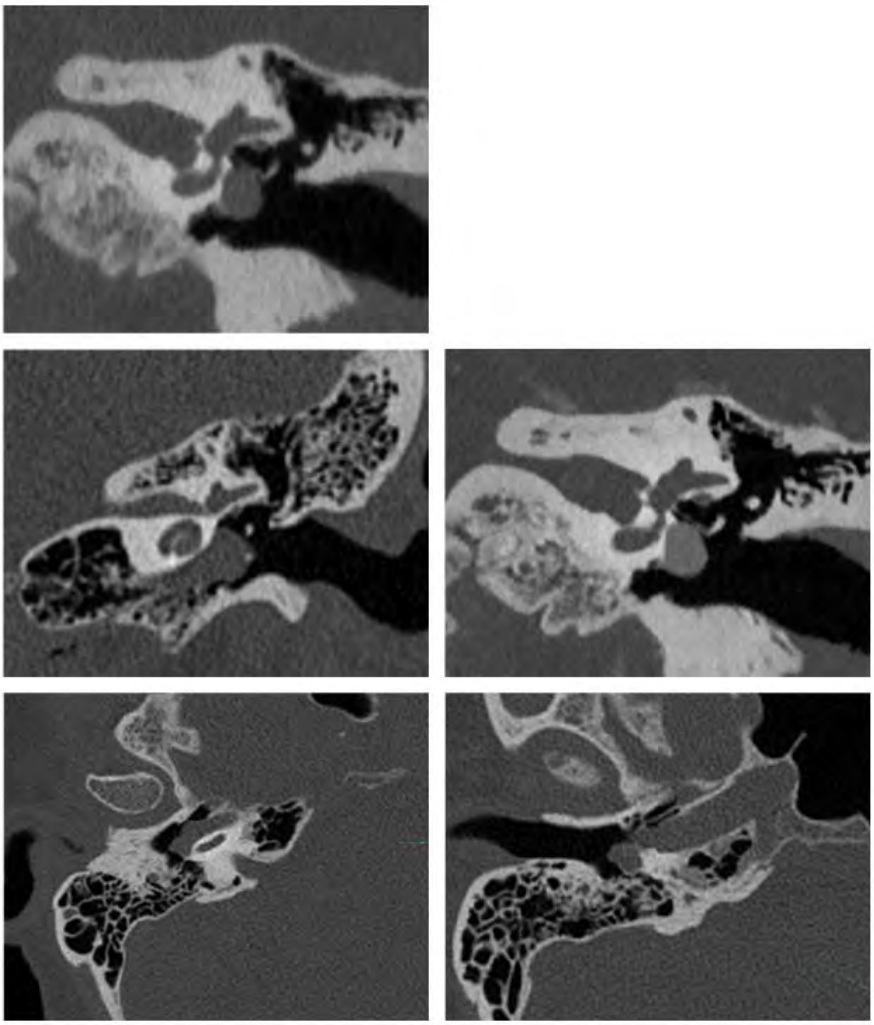
Teaching Point

This Electronic Excerpta will provide examples of the CT imaging features of aberrant ICA pseudoaneurysms, an association which is rarely described in radiological literature. This will provide neuroradiologists with the knowledge for diagnosis of these pseudoaneurysms, which could prove vital in patient care.

References

1. Zheng, Yongtao, Zheng Lu, et al. "Intracranial Pseudoaneurysms: Evaluation and Management." **Frontiers in Neurology** 11 (July 7, 2020).
2. Takano, Kenichi, Masahiko Wanibuchi, Fumie Ito, et al. "Pseudoaneurysm of an Aberrant Internal Carotid Artery in the Middle Ear Caused by Myringotomy." *Auris, Nasus, Larynx* 43, no. 6 (December 2016): 698–701.
3. Wadhavkar, Neha, David Y. Goldrich, et al. "Laceration of Aberrant Internal Carotid Artery Following Myringotomy: A Case Report and Review of Literature." *The Annals of Otology, Rhinology, and Laryngology* 131, no. 5 (May 2022): 555–61.
4. Muhayawi, Saad M., and Hisham A. Tawfik. "Unusual Presentation of Internal Carotid Artery Aneurysm in the Middle Ear." *Annals of Saudi Medicine* 27, no. 4 (August 2007): 293.

Images/Tables



519

Bilateral Orbital Meningoceles from the Oculomotor Cisterns Associated with Idiopathic Intracranial Hypertension

Justin D Chen MS[1], Clara Nemr BS[1], Talha Allam MD[2]
[1]Midwestern University, Downers Grove, IL, USA. [2]Advocate Christ Medical Center, Oak Lawn, IL, USA

Abstract Category

Head & Neck

Clinical History

A 63-year-old female presented with headaches and no other significant symptoms, such as orbital pain, vision, loss, diplopia, or proptosis.

Imaging Findings

A non-contrast CT scan of the head revealed hypodense tubular structures in the posterior orbits bilaterally. Further evaluation with MRI revealed hyperintense cystic tubular structures in the bilateral posterior orbits on T2-weighted images, which suppressed on FLAIR, and no enhancement on post-contrast T1-weighted images, suggesting simple cystic meningoceles. An MRI from seven years prior showed these cystic tubular lesions remained stable, supporting the diagnosis of simple fluid cysts. The patient was subsequently diagnosed with idiopathic intracranial hypertension (IIH) based on MRI findings.

MRI Coronal T2 images revealed cystic lesions extending from the oculomotor cisterns through the superior orbital fissures into the intraconal compartments, situated below the optic nerve sheaths. The pituitary gland was displaced downward in an enlarged sella.

SSFP axial and coronal MR images showed enlarged oculomotor cisterns communicating with the cystic lesions. Sagittal T1 and axial T2 images also displayed IIH-related features, including an enlarged empty sella, prominent Meckel's caves, arachnoid pits, and fluid distension of the distal optic nerve sheaths.

Discussion

Orbital meningoceles are characterized by the herniation of the meninges into the orbit through an osseous defect or normal anatomical foramen, often accompanied by CSF accumulation[1]. A key anatomical structure in this context is the oculomotor cistern (OMC), which typically tapers before reaching the anterior clinoid process, with the oculomotor nerve entering the orbit through the superior orbital fissure[3, 4]. Although OMCs generally do not extend into the orbital apices due to anatomical constraints, conditions such as idiopathic intracranial hypertension (IIH) can lead to their extension into these areas.

Elevated CSF and intracranial pressure associated with IIH play a significant role in OMC meningoceles development. Over time, this chronic elevation expands the subarachnoid space, causing the meninges to herniate through foramina and form cystic tubular lesions that can distend into the orbital apices. Though often asymptomatic, meningocele formation and rupture can cause CSF leaks or symptoms such as headaches, diplopia, and vision loss[2, 5.]

Our case reports the first known instance of bilateral orbital meningoceles originating from the OMCs. Increased CSF pressure in IIH contributed cystic tubular lesion formation, resulting in the distension of the OMCs and its subsequent protrusion into the superior orbital fissures. The sequelae of IIH prompted neuroimaging, which led to the incidental discovery of the meningoceles. The incidental nature of this finding highlights the importance of recognizing key imaging findings, even in the absence of overt clinical symptoms.

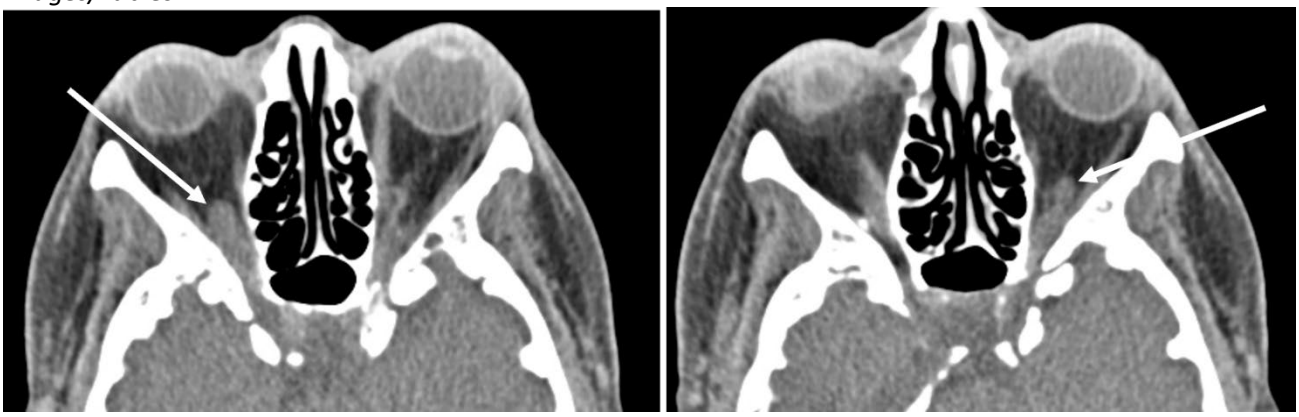
Teaching Point

Misidentifying benign cystic lesions as meningiomas or optic nerve gliomas may lead to unnecessary interventions and cause significant patient distress. Accurate differentiation depends on a thorough understanding of anatomical landmarks and the use of multiple imaging perspectives to distinguish among the optic nerve, the oculomotor nerve, and OMC. High-resolution MR techniques, such as SSFP, are particularly effective in identifying cranial nerve pathologies. Given these considerations, radiologists should remain attentive to how these findings may relate to bilateral orbital meningoceles and other related disorders.

References

1. Mbaye M, Thiam AB, Cissue MA, et al. Orbital meningocele in two case studies. Surg Neurol Int. 2020;11:119. Published 2020 May 23. doi:10.25259/SNI_148_2020
2. Wang MTM, Bhatti MT, Danesh-Meyer HV. Idiopathic intracranial hypertension: Pathophysiology, diagnosis and management. J Clin Neurosci. 2022;95:172-179. doi:10.1016/j.jocn.2021.11.029
3. Everton KL, Rassner UA, Osborn AG, et al. The oculomotor cistern: anatomy and high-resolution imaging. AJNR Am J Neuroradiol 2008;29:1344-1348
4. Martins C, Yasuda A, Campero A, et al. Microsurgical anatomy of the oculomotor cistern. Neurosurgery. 2006;58(4 Suppl 2):. doi:10.1227/01.NEU.0000204673.55834.BE
5. Truong M, Maclaurin W, Tan H, et al. A rare finding of bilateral facial canal meningoceles involving the tympanic segment in suspected idiopathic intracranial hypertension. *Radiol Case Rep*. 2023;18(9):3184-3187. Published 2023 Jun 28. doi:10.1016/j.radcr.2023.06.036

Images/Tables



534

Extraosseous Chordoma of the Nasopharynx Mimicking a Tornwaldt Cyst

Omnea Elgendy[1], Mark Gedrich DO[1], Ajit Karambelkar MD[2], William Coffey MD[1]
[1]Cooper Medical School of Rowan University, Camden, NJ, USA. [2]Thomas Jefferson University Hospital, Philadelphia, PA, USA

Abstract Category

Head & Neck

Clinical History

A 54-year-old female with no pertinent past medical history presented with chronic nasal stuffiness. Nasal endoscopy revealed a firm nasopharyngeal mass. Computed Tomography (CT) and Magnetic Resonance (MR) imaging was obtained, followed by a biopsy which showed pathologic features consistent with conventional chordoma. The mass was resected.

Imaging Findings

Axial CT with bone and soft tissue windows (Figures 1 & 2): An oval midline nasopharyngeal structure, 14.2 mm, measuring 27 Hounsfield units, associated with a foveola pharyngica, a common benign incidental finding, but no complete medial basal canal.

Axial T2-weighted MR (Figure 3): Axial image through the nasopharynx demonstrates the lesion to be heterogeneously hyperintense on T2-weighted imaging.

Axial T1-weighted MR before and after intravenous contrast (Figures 4 & 5): The nasopharyngeal structure shows no significant central enhancement, lesion-to-muscle ratio at pre-contrast imaging of 1.4 and at post-contrast imaging of 1.2.

Axial CT with bone window (Figure 6): Postsurgical changes of chordoma resection, including osseous component in the clivus.

Discussion

Chordomas are rare malignant bone tumors that arise from notochordal remnants, with a reported incidence ranging from 0.18 to 0.84 per million individuals per year worldwide.[1] Most are found in the sacrococcygeal region, skull base, and spine, which account for 50-65, 25-30, and 15-20% of chordoma localizations, respectively.[2] Extraosseous chordomas are postulated to occur when soft tissue harbors notochordal remnants, and their incidence is much lower than that of osseous chordomas. On CT, while the epicenter of the extraosseous chordoma is in the soft tissues, there is usually associated bony involvement in the form of lytic changes or a sinus tract.[3] On MR, these tumors are generally large, heterogeneous, and enhancing. We present a rare case of extraosseous chordoma of the nasopharynx with overall nonaggressive imaging features. This patient presented with a small, oval, midline mass with no significant central enhancement, osseous erosion, or associated sinus tract, making it difficult to distinguish from the much more common Tornwaldt cyst, a benign notochordal remnant. In this case, pathology was needed for definitive diagnosis, showing physaliphorous cells classic of chordoma and easily distinguishing it from the respiratory epithelium and proteinaceous contents found in Tornwaldt cysts. Treatment of nasopharyngeal chordomas consists of surgical resection, including any osseous component. Distant metastasis is very rare; the main complication is local recurrence, making post-treatment imaging surveillance vital.[4] This case draws into question the natural course of benign-appearing notochordal lesions commonly encountered on imaging and the potential role of imaging follow-up or biopsy to reduce misdiagnosis.

Teaching Point

Extraosseous chordoma of the nasopharynx is a rare but important tumor to include in the differential diagnosis of nasopharyngeal masses. This case emphasizes the importance of considering chordoma even in the absence of a sinus tract and other more typical aggressive features.

References

1. Bakker SH, Jacobs WCH, Pondaag W, Gelderblom H, Nout RA, Dijkstra PDS, Peul WC, Vleggeert-Lankamp CLA. Chordoma: a systematic review of the epidemiology and clinical prognostic factors predicting progression-free and overall survival. Eur Spine J. 2018 Dec;27(12):3043-3058. doi: 10.1007/s00586-018-5764-0. Epub 2018 Sep 15. PMID: 30220042.
2. Dwianingsih EK, Snak Y, Rinonce HT, Wasita B, Antoro EL, Amr SS. Primary Chordoma of the Nasopharynx: A Rare Case Report and Review of the Literatures. Case Rep Pathol. 2019 Sep 23;2019:3826521. doi: 10.1155/2019/3826521. PMID: 31662933; PMCID: PMC6778900.

3. Nguyen RP, Salzman KL, Stambuk HE, Ahuja AT, Harnsberger HR. Extraosseous chordoma of the nasopharynx. AJNR Am J Neuroradiol. 2009 Apr;30(4):803-7. doi: 10.3174/ajnr.A1446. Epub 2009 Feb 4. PMID: 19193749; PMCID: PMC7051767.
4. Yeh CY. Radiotherapy of extraosseous nasopharyngeal chordoma: A case report and literature review. Mol Clin Oncol. 2021 Apr;14(4):84. doi: 10.3892/mco.2021.2246. Epub 2021 Feb 26. PMID: 33758665; PMCID: PMC7947947.

Images/Tables



Figure 1: Pre-Op CT Bone Window



Figure 2: CT Soft Tissue Window



Figure 3: MR T2



Figure 4: MR Pre-Contrast T1



Figure 5: MR Post-Contrast T1

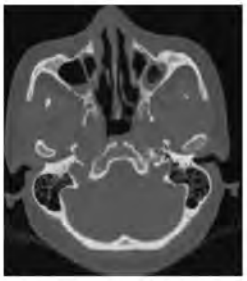


Figure 6: Post-operative CT Bone Window

541

Congenital Malformations of the Bilateral Trigeminal and Vestibulocochlear Nerves

Sarah N Navid BS[1], Efrain Segura MS[2], Adam M Basiago MD[3], Nourel H Tahon MD[3], Clark W Sitton MD[3]
[1]UTMB Health, Galveston, TX, USA. [2]Ponce Health Sciences University, Ponce, PR, Puerto Rico. [3]UTHealth Houston, Houston, TX, USA

Abstract Category

Head & Neck

Clinical History

An 8-year-old male presents with a history of developmental speech delay and previously diagnosed bilateral mixed conductive and sensorineural hearing loss.

Imaging Findings

There are significant bilateral congenital abnormalities in the trigeminal (CN5) and vestibulocochlear nerves (CN8). There is coalescence of the larger sensory fibers of the bilateral CN5 ($CN5_{sensory}$) with CN8 which arise from the pontomedullary junction as common nerve roots. These CN5 fibers then fan out and course to attenuated Meckel's caves which are contiguous with the internal auditory canals (IAC). The left CN5 ganglion is located in the prepontine cistern. The smaller motor fibers of CN5 ($CN5_{motor}$) have conventional pontine origins. The facial nerves (CN7) arise inferomedially to the common CN8/$CN5_{sensory}$ nerve roots from conventional locations. Once in the IACs, the right vestibular and cochlear nerves are distinct structures and the left CN8 branches are hypoplastic. Both vestibular apparatuses and cochlea are normally formed.

Discussion

The trigeminal nerve (CN V) supplies sensory innervation to the face and head and motor innervation to mastication muscles through its three branches—ophthalmic (V1), maxillary (V2), and mandibular (V3).[1,2] Sensory roots enter the anterolateral pons and motor roots emerge superomedially. The trigeminal nerves traverse the prepontine cistern,

through porus trigeminus, with the trigeminal ganglia located in Meckel's caves, where the nerves then divide.[1,3] Congenital abnormalities, such as the coalescence of CNV and CN VIII (vestibulocochlear nerve), arise from disrupted neural crest cell migration or hindbrain patterning during early embryological development, affecting sensory, motor, and auditory pathways.[3] Such anomalies can result in sensorineural hearing loss, altered facial sensation, and balance issues. High-resolution MRI, especially 3D FIESTA, helps visualize these nerve paths and structural deformities, and CT is useful for assessing bony anatomy. Differential diagnosis should include other congenital causes of sensorineural hearing loss. A multidisciplinary team is essential to manage hearing, sensory, and developmental impacts, with follow-up imaging guiding ongoing care.

Teaching Point

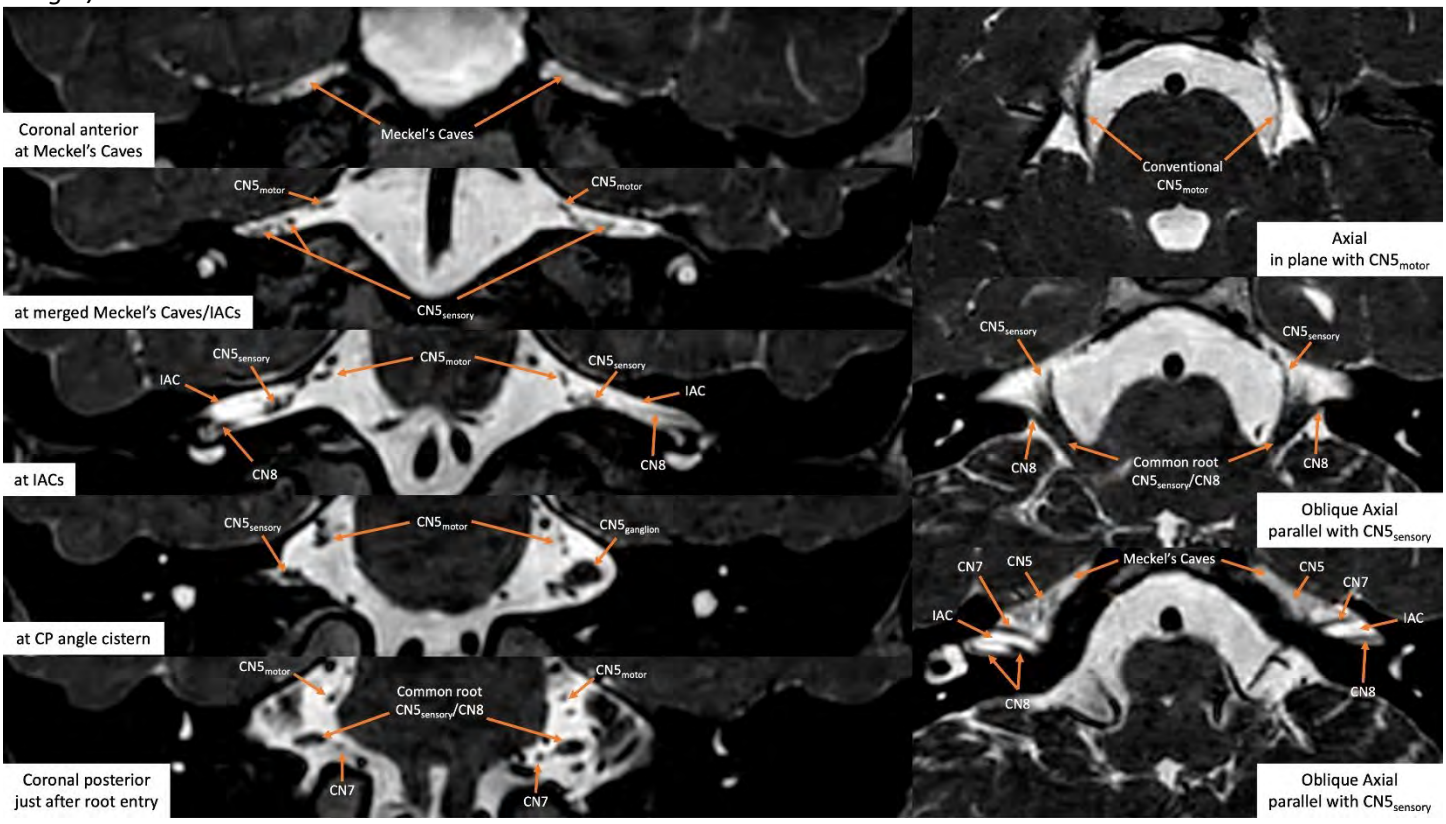
Abnormal coalescence of the trigeminal nerve with the vestibulocochlear nerve, as seen bilaterally in this case, is a rare congenital finding. These anomalies may lead to altered sensory and motor function of the trigeminal nerve, potentially impacting facial sensation and mastication. Recognizing this coalescence on imaging is crucial for differentiating from other cranial nerve pathologies or syndromic associations.

Congenital hearing loss can arise from a variety of causes, including structural abnormalities of the vestibulocochlear nerves (as is seen bilaterally in this case), congenital inner ear dysplasia, intrauterine infection, and teratogenic exposure. When assessing congenital hearing loss, it's important to evaluate for inner ear and cranial nerve anomalies, as these may impact prognosis and management, including the need for multidisciplinary care. Understanding the relationship between congenital nerve abnormalities and hearing loss is essential for accurate diagnosis and management.

References

1. Binder DK, Sonne DC, Fischbein NJ. *Cranial nerves : anatomy, pathology, imaging*. Thieme; 2010:xix, 228 p.
2. Hughes MA, Frederickson AM, Branstetter BF, Zhu X, Sekula RF. MRI of the Trigeminal Nerve in Patients With Trigeminal Neuralgia Secondary to Vascular Compression. *AJR Am J Roentgenol*. Mar 2016;206(3):595-600. doi:10.2214/AJR.14.14156
3. Romano N, Federici M, Castaldi A. Imaging of cranial nerves: a pictorial overview. *Insights Imaging*. Mar 15 2019;10(1):33. doi:10.1186/s13244-019-0719-5

Images/Tables



560

PTEN hamartoma tumor syndrome (PHTS) presenting as Hemimegalencephaly with cutaneous lesions in a neonate with intractable epilepsy

Sawsan Tabaza MD, Marcelle Mallery MD, Jessica Bolen MD, Eliana Bonfante-Mejia MD
UTHealth Houston, Houston, Texas, USA

Abstract Category

Pediatrics

Clinical History

3-day-old premature female patient born at 35 weeks. History of scant prenatal care and maternal gestational hypertension. Physical examination showed macrocephaly, dysmorphic features, a murmur, and skin/scalp plaque-like lesion. Brain MRI was obtained due to seizure-like activity and refractory status epilepticus on EEG.

Imaging Findings

Brain MRI showed morphologically abnormal cortex in the majority of the left cerebral hemisphere, with lack of sulcation and increased cortical thickness, as well as areas of polymicrogyria in the left occipital region. There is increased T1 signal in the left hemispheric white matter. Despite the left hemispheric enlargement, the left lateral ventricle is dilated. The cortical expansion results in medialization of the left uncus and effacement of the left crural cistern with mass effect on the left cerebral peduncle.

Discussion

Hemimegalencephaly, or unilateral megalencephaly is a rare congenital disorder of cortical formation characterized by hamartomatous overgrowth of all or parts of a cerebral hemisphere. Most patients with hemimegalencephaly present with focal or generalized infantile spasm. Hemimegalencephaly is a sporadic disorder. The prevalence is distributed equally by sex and is believed to be 1-3 per 1,000 epileptic children. It is an isolated finding in the majority of cases, but may also be associated with neurocutaneous syndromes, including epidermal nevus syndrome, neurofibromatosis type I, Klippel-Trenaunay syndrome, and tuberous sclerosis. It is believed to occur because of de novo mutations in somatic genes involved in the regulation of the mammalian target of rapamycin (mTOR)-signaling cascade. The most common gene mutation is PIK3CA. Our patient was found to have the PTEN mutation, which gives him the diagnosis of *PTEN* hamartoma tumor syndrome (PHTS). PHTS disorders are hereditary and include a group of clinical disorders caused by alterations in the PTEN gene. In the past, these clinical disorders were called by one of several names, including:

- Cowden syndrome (CS)
- Bannayan-Riley-Ruvalcaba syndrome (BRRS)
- Proteus and Proteus-like syndrome (PS)

Although CS, BRRS, and PS were once considered to be separate syndromes, any patient found to carry a *PTEN* mutation, regardless of their clinical features, should be classified as having PHTS. Patients with PHTS may develop cancers as well as benign hamartomas in different areas of the body. In addition, patients may have other clinical features, including:

- Macrocephaly
- Skin and oral mucosal lesions, such as: trichilemmomas, papillomatous papules and lipomas
- Learning disabilities, developmental delays, hyperactivity (ADHD) and/or autism spectrum disorders
- Development of specific cancers, most commonly breast, thyroid and endometrium; and less frequently, colorectal cancer, melanoma, and renal cell carcinoma.

Teaching Point

Hemimegalencephaly usually present with seizures. The diagnosis of sporadic versus syndromic entities depends on genetic testing. Genetic diagnosis is the first step in further surveillance, management and treatment of these patients depending on the associated clinical findings.

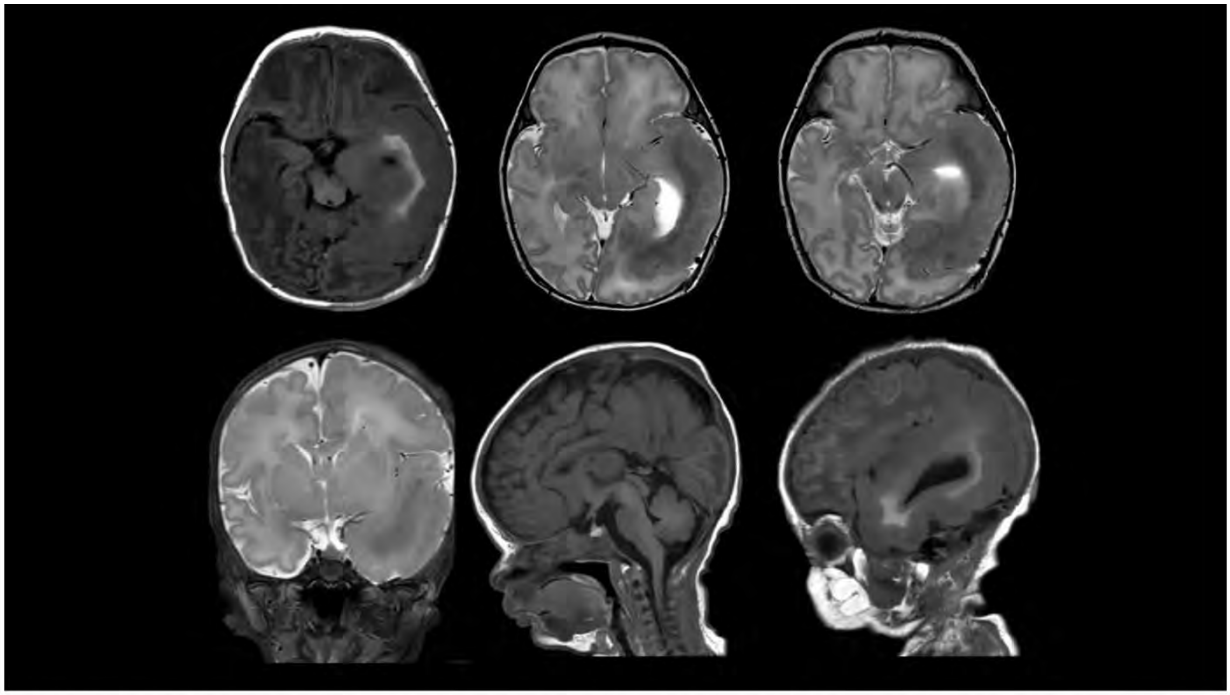
References

1- Kakish D, Tominna M, Krishnan A. Hemimegalencephaly: Evolution From an Atypical Focal Early Appearance on Fetal MRI to More Conventional MR Findings. Cureus. 2022 Aug 13;14(8):e27976. doi: 10.7759/cureus.27976. PMID: 36120272; PMCID: PMC9468183.

2- Yehia L, Eng C. PTEN Hamartoma Tumor Syndrome. 2001 Nov 29 [Updated 2021 Feb 11]. In: Adam MP, Feldman J, Mirzaa GM, et al., editors. GeneReviews® [Internet]. Seattle (WA): University of Washington, Seattle; 1993-2024.

3- Yehia L, Keel E, Eng C. Clinical spectrum of PTEN mutations. Annu Rev Med 2020; doi: 10.1146/annurev-med-052218-125823.
4- Mester J, Tilot AK, Rybicki LA, Frazier TW, Eng C. Analysis of prevalence and degree of macrocephaly in patients with germline PTEN mutations and of brain weight in Pten knock-in murine model. Eur J Hum Genet. 2011;19:763-8.
5- Fiala KH. Cowden Disease (Multiple Hamartoma Syndrome). Medscape. June 27, 2023. https://emedicine.medscape.com/article/1093383-overview Accessed Nov 6, 2023.

Images/Tables



Axial T1, Axial T2, Coronal T2 and Sagittal T1 Images showing left sided hemimegalencephaly with abnormal cortex, lack of sulcation, and polymicrogyria within the left occipital region. Deep white matter T1 hyperintense signal and dilated left lateral ventricle.



Skin lesion on the same side of the face and scalp. This lesion has direct supply from contralateral left ACA, MCA, PCA and dilated abnormal cortical veins with vascular channels through the left calvarium also visualized on Brain MRI.

566

Diffuse Susceptibility in the Subarachnoid Spaces and Vascular Structures After Ferumoxytol Injection

Garrick J Biddle MD, Tabassum A Kennedy MD, Kelly W Capel MD
University of Wisconsin, Madison, WI, USA

Abstract Category

Adult Brain

Clinical History

A 63-year-old female with a history of seronegative rheumatoid arthritis, currently managed with Humira and methotrexate, obstructive sleep apnea, paroxysmal supraventricular tachycardia, and microcytic anemia presents with generalized weakness, frequent falls, dizziness, and cognitive decline. The patient has been on immunosuppressive therapy with Humira, which carries a very low risk of demyelinating disease; therefore, an MRI was requested for further evaluation. Her microcytic anemia, previously managed with oral iron supplementation, was transitioned to intravenous Ferumoxytol as an inpatient due to concerns about constipation.

Imaging Findings

GRE T2* sequence (A) demonstrates signal loss in the subarachnoid spaces as well as within the intracranial arteries and veins due to T2* effects from intravascular ferumoxytol. FLAIR sequence (B) confirms absence of failure of CSF suppression in the sulci with normal appearance, and pre-contrast T1 weighted image (C) shows contrast within the intracranial vasculature. Axial noncontrast head CT (D) demonstrates no subarachnoid blood products or hyperdensity along the vasculature. T2 weighted image (E) demonstrates T2 hypointensity in the vasculature but not in the subarachnoid spaces. Diffusion weighted imaging (F) also shows subarachnoid signal loss and susceptibility artifact/ “blooming” related to recent ferumoxytol administration.

Discussion

Diffuse susceptibility in the subarachnoid spaces and vascular (venous and arterial) structures likely related to recent Ferumoxytol (Feraheme) injection administered approximately 6 hours prior to MRI with other less likely differential etiologies including cortical superficial siderosis from prior hemorrhage, trauma, vasculopathy, drug-induced vasculitis, amyloid-related process, or disseminated intravascular coagulation (DIC).

Teaching Point

Recognize that Ferumoxytol, an iron supplement used for treating anemia and off-label use as an MRI contrast agent, can produce diffuse susceptibility artifacts on MRI, especially within the subarachnoid and vascular structures. It is essential to consider recent Ferumoxytol administration in the differential diagnosis to avoid misinterpreting these artifacts as pathological findings.

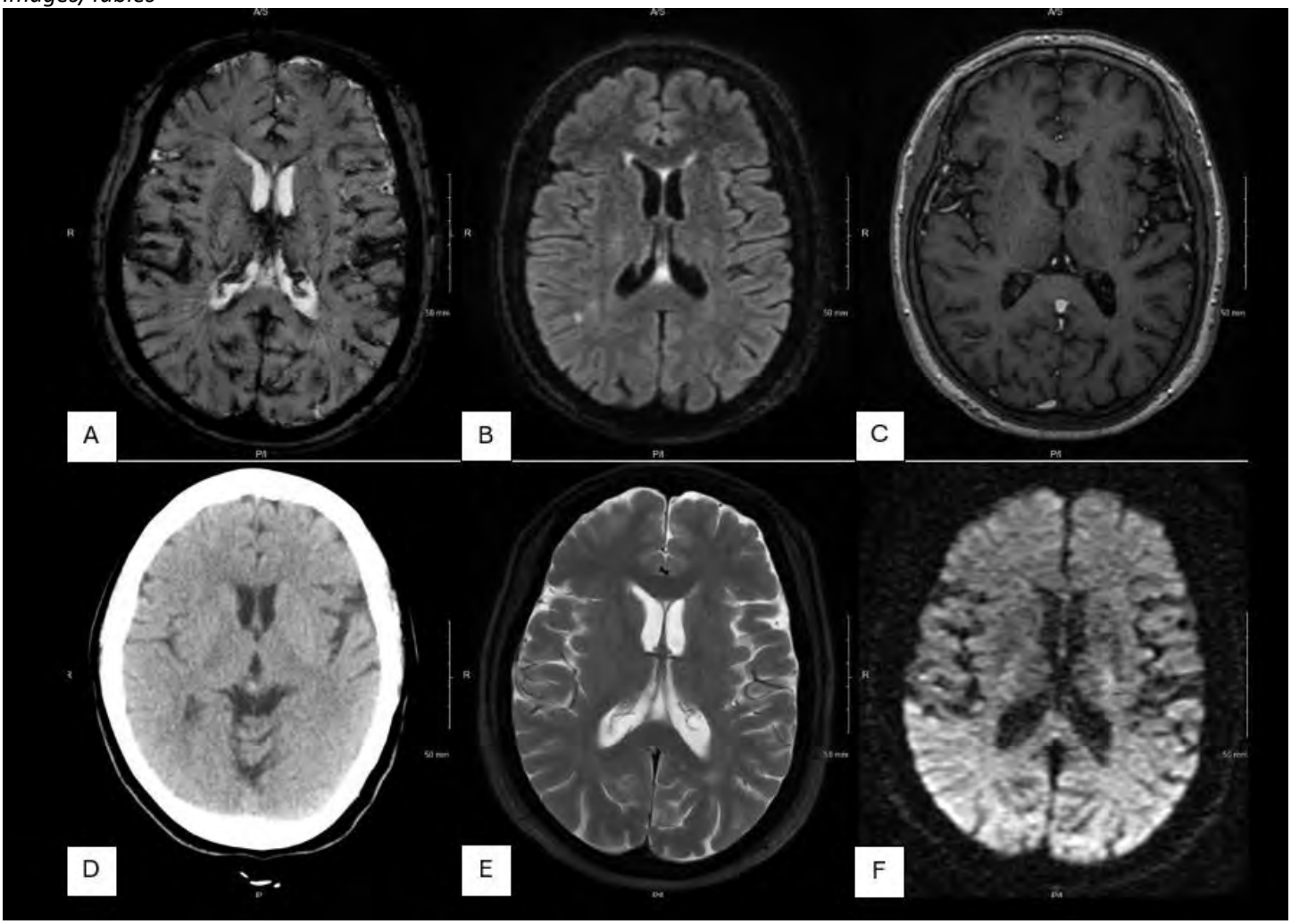
Unlike traditional gadolinium-based contrast agents, which enhance images by shortening the T1 relaxation time of tissues, Ferumoxytol shortens T2 and T2* relaxation times. This results in strong susceptibility effects that highlight vascular structures and areas with high iron concentration, making it particularly useful for vascular imaging and conditions where extended intravascular contrast is advantageous, as it remains in the blood pool for a prolonged duration. Ferumoxytol can affect diagnostic ability of MRI up to 3 months, but usually complicates interpretation within 3 days of administration. Recognition of these expected effects/artifacts is essential to avoid interpretation errors and avoid obtaining unindicated additional exams.

References

Toth GB, Varallyay CG, Horvath A, et al. Current and potential imaging applications of ferumoxytol for magnetic resonance imaging. *Kidney Int*. 2017;92(1):47-66. doi:10.1016/j.kint.2016.12.037

Bowser BA, Campeau NG, Carr CM, et al. Incidental ferumoxytol artifacts in clinical brain MR imaging. *Neuroradiology*. 2016;58(11):1087-1091. doi:10.1007/s00234-016-1747-1

Images/Tables



572

Congenital Cochlear Nerve Aplasia

Sammar Ghannam MD, MPH, Melissa Donate B.S., Achint Singh MD, Hasanagha Zalov MD
University of Texas Health at San Antonio Dept of Radiology, San Antonio, TX, USA

Abstract Category

Adult Brain

Clinical History

A 24-year-old female presents with right asymmetric sensorineural hearing loss (SNHL), 0% word recognition, and normal hearing sensitivity in the left ear. Normal external ear exam. Patient reports right-sided hearing loss since childhood.

Imaging Findings

Magnetic resonance (MR) imaging demonstrates an absent cochlear nerve on the right. Additionally, the right IAC is mildly asymmetrically small compared to the left. Otherwise, no other abnormalities are present. Findings represent Congenital Cochlear Nerve Aplasia.

Discussion

The cochlear nerve is a component of the vestibulocochlear nerve that is responsible for hearing by transmitting sensory information from the cochlea to the cochlear nuclei within the brainstem. SNHL can be acquired congenitally or secondarily following an insult such as trauma, meningitis, or bacterial labyrinthitis [1]. Acquired neural deficiency is not associated with a small internal auditory canal (IAC). A normal-sized IAC with a deficient (absent or hypoplastic) cochlear nerve favors acquired SNHL.

Complete absence of the cochlear nerve/cochlear nerve aplasia may be congenital. Findings that are suggestive of a congenitally acquired SNHL due to cochlear nerve aplasia include inner ear malformations, such as a stenotic cochlear aperture and decreased IAC diameter [2]. Cochlear nerve aplasia is typically unilateral and more commonly seen affecting the left side. An audiological evaluation must be performed to classify the type of hearing loss, with subsequent imaging using computed tomography (CT) of the temporal bone and MR imaging of the IAC to evaluate the middle ear and cochlear structures [3].

Imaging findings are best visualized on oblique-sagittal MR imaging of the IAC [2, 4]. Typically, four nerves traverse the IAC: the Superior Vestibular Nerve (SVN), the Inferior Vestibular Nerve (IVN), the cochlear nerve, and the facial nerve. The facial nerve is in the anterosuperior portion, the cochlear nerve in the anteroinferior portion, and the posterior portions contain the SVN (superiorly) and the IVN (inferiorly) [5]. The absence of the nerve in the anteroinferior position on MR imaging is diagnostic, although there are limitations in differentiating between hypoplasia and aplasia as it is often difficult to distinguish, especially in the setting of a narrowed IAC [3].

Cochlear implantation is rarely successful in cases where the nerve is completely absent. Treatment alternatives include auditory brainstem implantation where the cochlear nucleus is directly stimulated which can have greater surgical risks compared to cochlear implantation [1,3].

Teaching Point

1. Review the relevant anatomy of the inner ear.
2. Utilize a case-based approach to understand the underlying pathogenesis and treatment of cochlear nerve aplasia.
3. Identify key imaging findings with clinical findings for the diagnosis of cochlear nerve aplasia.

References

1. Glastonbury CM, Davidson HC, Harnsberger HR, Butler J, Kertesz TR, Shelton C. Imaging findings of cochlear nerve deficiency. *AJNR Am J Neuroradiol*. 2002;23(4):635-643.
2. Orzan E, Pizzamiglio G, Gregori M, et al. Correlation of cochlear aperture stenosis with cochlear nerve deficiency in congenital unilateral hearing loss and prognostic relevance for cochlear implantation. Sci Rep. 2021;11, 3338.
3. Freeman SR, Sennaroglu L. Management of Cochlear Nerve Hypoplasia and Aplasia. *Adv Otorhinolaryngol*. 2018;81:81-92. doi:10.1159/000485542
4. Casselman JW, Offeciers FE, Govaerts PJ, Kuhweide R, Geldof H, Somers T, D'Hont G. Aplasia and hypoplasia of the vestibulocochlear nerve: diagnosis with MR imaging. Radiology. 1997;202(3):773-781.
5. Kim HS, Kim DI, Chung IH, Lee WS, Kim KY. Topographical relationship of the facial and vestibulocochlear nerves in the subarachnoid space and internal auditory canal. AJNR Am J Neuroradiol. 1998;19(6):1155-1161.

Images/Tables



574

Skull Base Giant Cell Tumor: A Rare Pituitary Tumor Mimic

Lidia Guzhva MD, Miriam Peckham MD, Blair Winegar MD, Robert Rennert MD, Karen Salzman MD
University of Utah, Salt Lake City, Utah, USA

Abstract Category

Head & Neck

Clinical History

A 14-year-old female presented to the emergency room with jaw pain, left eye swelling, and blurry vision, after initially being seen by dentistry. Due to concern for a neurologic process, and symptom progression, it was recommended that the patient get further medical and imaging evaluation.

A large sellar and suprasellar mass was identified. The mass was surgically removed one month after initial symptom onset without adverse sequalae, where it was found to be entirely extradural. Pathology demonstrated a giant cell tumor.

Imaging Findings

Initial CT face exhibited a 3.1 cm well-circumscribed enhancing mass in the sellar and suprasellar region (A, B). The mass was solid, homogenous, and without internal calcifications (B). There was associated smooth osseous remodeling and erosion of the sella turcica (B, arrowheads) with extension into the sphenoid sinus (B, arrow). The mass extended toward the optic chiasm with partial encasement of the cavernous carotid arteries (A, arrows).

Subsequent pituitary MRI showed the mass as T2 hypointense with mild homogeneous enhancement (C, D). The mass elevated the pituitary gland, which appeared separate from the primary mass (C, arrow), and extended into the left cavernous sinus (D, arrow). There was no associated gradient susceptibility. Initial differential diagnosis was broad, including pituitary macroadenoma, Langerhans cell histiocytosis, or a primary osseous lesion.

Discussion

The sphenoid bone is unique because it is located at the intersection of the anterior, middle, and posterior cranial fossae (1). Additionally, there are multiple surrounding critical neurovascular structures, including the pituitary gland, internal carotid arteries, cavernous sinus, and multiple cranial nerves (1). Clinical manifestations of sphenoid central skull base tumors vary, including headache, visual disturbances, and cranial neuropathies (1). Pediatric sellar and suprasellar lesions have a broad differential, but lesions localized to the sphenoid bone include fibrous dysplasia, chordomas, chondrosarcomas, and giant cell tumor (2).

Giant cell tumors are benign osseous lesions characterized histologically by multinucleated giant cells that exhibit osteoclastic activity (3). These tumors usually occur in long bones near articular surfaces, though they can rarely occur in flat bones such as the calvarium (3). The typical appearance of a giant cell tumor is a well-defined lytic lesion with nonsclerotic margins and an eccentric location (3).

Giant cell tumors of the skull base are quite rare (4). Case reports and literature reviews reveal that they most often occur in the sphenoid and temporal bones, possibly because these bones develop through endochondral ossification (4). Per reports, sphenoid giant cell tumors tend to localize to the center of the sphenoid body with a symmetrical, expansile, and lobulated shape (4). These are often purely osteolytic on CT (4). On MRI, these appear T1 and T2 isointense to brain parenchyma with mild homogeneous enhancement (4).

Teaching Point

Although the most common sellar and suprasellar tumor in adults, pituitary macroadenomas are rare in pediatric patients.

Common lesions in uncommon locations can present as diagnostic dilemmas in radiology.

Giant cell tumors should be a differential consideration for osteolytic sellar and suprasellar lesions in pediatric patients.

References

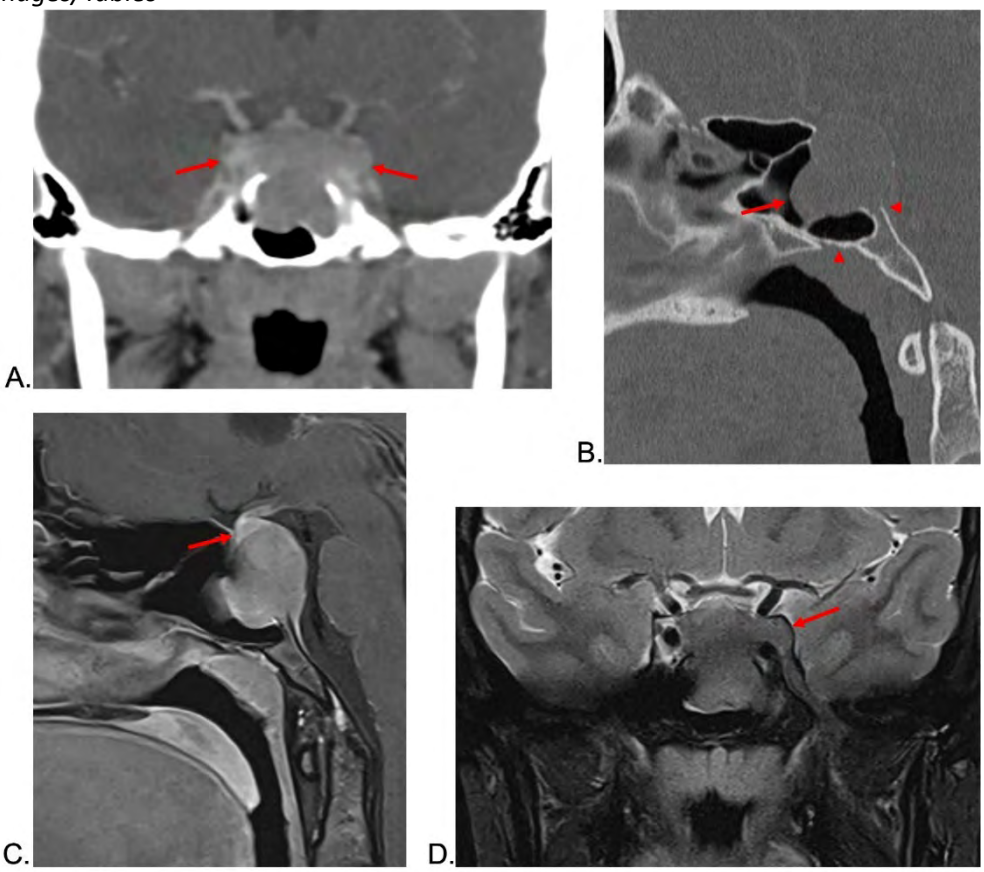
1. Nardi C, Davide Maraghelli, Pietragalla M, et al. A practical overview of CT and MRI features of developmental, inflammatory, and neoplastic lesions of the sphenoid body and clivus. Neuroradiology. 2022;64(8):1483-1509. doi:https://doi.org/10.1007/s00234-022-02986-x

2. Huang J, Sarma A, Harmsen H, Sumit Pruthi. Systematic Approach to Evaluating Sellar and Suprasellar Lesions in Pediatric Patients. Radiographics. 2022;42(7):E214-E215. doi:https://doi.org/10.1148/rg.210121

3. Chakarun CJ, Forrester DM, Gottsegen CJ, Patel DB, White EA, Matcuk GR. Giant Cell Tumor of Bone: Review, Mimics, and New Developments in Treatment. RadioGraphics. 2013;33(1):197-211. doi:https://doi.org/10.1148/rg.331125089

4. Kashiwagi N, Hirabuki N, Andou K, et al. MRI and CT findings of the giant cell tumors of the skull; five cases and a review of the literature. European Journal of Radiology. 2006;58(3):435-443. doi:https://doi.org/10.1016/j.ejrad.2005.11.045

Images/Tables



583

Intramuscular Rosai-Dorfman Disease (RDD) in the Masticator Space: A Rare and Extra-Protean Manifestation

Sherif S Helmey M.D., Siddhartha Gaddamanugu M.D.
University of Alabama Birmingham, Birmingham, AL, USA

Abstract Category

Head & Neck

Clinical History

A 61-year-old female with no pertinent past medical or surgical history presented with 1 year of left sided facial numbness localized to the inferior chin. MRI revealed a well-defined fat containing mass involving the left temporal muscle. CT and MRI performed 6 months after initial MRI demonstrated growth of the lesion which now demonstrated enhancement and loss of previous fatty signal. Notably, there was no significant adenopathy by imaging size criteria. Biopsy was non diagnostic and suggested benign fibroadipose tissue. The patient elected to proceed with total resection including left parotidectomy with cranial nerve VII preservation, mandibulotomy, open reduction and internal fixation of the mandible, teeth #21-32 extraction and dental implants. The patient tolerated the procedure well and was discharged on postoperative day 1. The final pathology revealed overall morphologic and immunophenotypic findings (CD68/CD163+, cyclinD1+, S100+, OCT2+) consistent with the diagnosis of Rosai-Dorfman Disease (RDD). Four months after resection the patient underwent adjuvant radiation therapy consisting of 30 Gy administered in 15 fractions over the course of three weeks.

Imaging Findings

CT images reveal an enhancing, ill-defined mass involving the left temporalis muscle. MR images of the face reveal a heterogeneously enhancing lesion with increased T2/STIR signal centered within the left temporalis muscle. Of note, there is remodeling of the posterolateral wall of the left maxilla.

Discussion

Rosai-Dorfman disease is a benign but progressive disease that belongs to the R group of sinus histiocytoses. This entity is also known as sinus histiocytosis with massive lymphadenopathy. There is a familial and sporadic subtype. The sporadic subtype is subcategorized into nodal, extra nodal, neoplasia-associated, and immune-associated. The most common presentation is nodal along the bilateral cervical chains. The most common extra nodal locations involved are within the soft tissues of the head, neck and sinonasal cavities. The most common age groups affected are children and adolescents. Imaging findings are nonspecific and overlap with other skull base and sinonasal tumors. Therefore, a high clinical index of suspicion is required when including Rosai-Dorfman disease in the differential of a skull base or sinonasal mass.

Teaching Point

Extra nodal sinus histiocytosis (RDD) is a poorly understood disease with protean imaging manifestations. We illustrate a case of RDD presenting as a slowly growing mass of the temporalis muscles in the masticator space causing facial numbness likely due to compression on the mandibular division of trigeminal nerve. While extra nodal RDD is common, isolated intramuscular RDD has not been described.

References

La Barge, III, Donald V., Salzman, Karen L., et al. Sinus Histiocytosis with Massive Lymphadenopathy (Rosai-Dorfman Disease): Imaging Manifestations in the Head and Neck. *American Journal of Roentgenology*: 2008; 191:W299–W306. DOI: https://doi.org/10.2214/AJR.08.1114

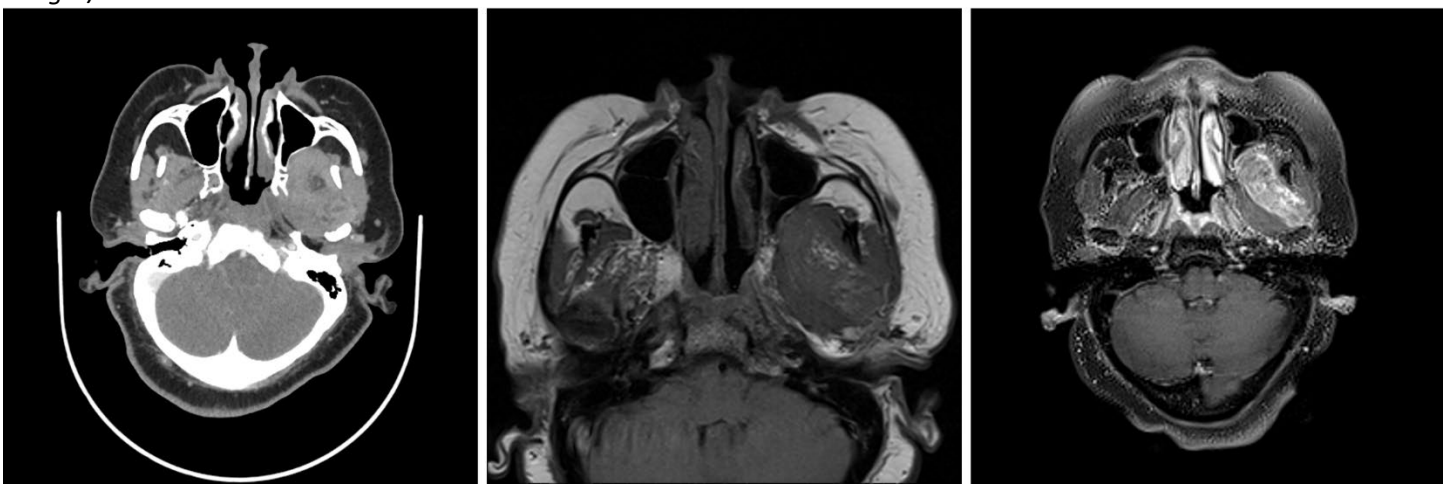
Carbone, Antonino, Devaney, Kenneth, et al. Review of Sinus Histiocytosis with Massive Lymphadenopathy (Rosai-Dorfman Disease) of Head and Neck. *Annals of Otology, Rhinology and Laryngology*: 1999;108(11 Pt 1):1095-104. DOI: https://doi.org/10.1177/000348949910801113

Raslan, Osama A., Schellingerhout, Dawid S., et al. Rosai-Dorfman Disease in Neuroradiology: Imaging Findings in a Series of 10 Patients. *American Journal of Roentgenology:* 2011;196(2):W187-93. DOI: https://doi.org/10.2214/AJR.10.4778

Bruce-Brand, Cassandra, Schneider, Johann W., et al. Rosai-Dorfman disease: An Overview. *Journal of clinical pathology*: 2020;73:697–705. DOI: https://doi.org/10.1136/jclinpath-2020-206733

Xu, Qinggang, Fu, Liping, et al. Multimodality Imaging-Based Evaluation of Rosai-Dorfman Disease in the Head And Neck . A Retrospective Observational Study. *Medicine* (2017) 96:51(e9372). DOI: http://dx.doi.org/10.1097/MD.0000000000009372

Images/Tables



593

A Case of Pediatric Hemorrhagic Transverse Myelitis

Joseph Kim MD, Neal Shukla MD, Matthew Hammer MD, Richard Lozano, Balaji Rao MBBCh, Long Tu MD, PhD
Yale New Haven Hospital, New Haven, CT, USA

Abstract Category

Pediatrics

Clinical History

A 16-year-old boy was transferred to our institution after experiencing a week of worsening numbness and weakness in his left lower extremity. Initially diagnosed with sciatica at an outside facility, he was treated with steroids. However, as his symptoms progressed, including difficulties with bowel movements, he returned for further evaluation.

Imaging Findings

Outside MRI studies of the lumbar spine and brain revealed hyperintensities and enhancement at T11-T12, raising concerns for transverse myelitis. Subsequent MRI of the cervical and thoracic spine and brain demonstrated extensive T2-weighted cord edema extending from C7 to the conus medullaris, along with a long segment of intramedullary hemorrhage, most pronounced from T8-T9.

Discussion

The differential diagnosis based on these findings included long-segment transverse myelitis complicated by cord hemorrhage or an intramedullary neoplasm, such as ependymoma or astrocytoma.

Comprehensive laboratory testing, including serologic and cerebrospinal fluid studies, ruled out infectious, autoimmune, metabolic, and demyelinating causes. Given the presence of intramedullary hemorrhage, a vascular etiology, such as an arteriovenous shunt, was considered; however, a diagnostic spinal angiogram showed no evidence of an aneurysm or vascular malformation.

Multi-specialty conferences involving radiology, infectious diseases, rheumatology, neuroimmunology, and neurosurgery were conducted, but no consensus was reached regarding the underlying etiology of the lesions. Ultimately, the patient was treated empirically for transverse myelitis with steroids, intravenous immunoglobulin (IVIG), and plasmapheresis.

Teaching Point

Hemorrhagic transverse myelitis can result from a variety of etiologies, including infectious, neoplastic, demyelinating, vascular, autoimmune, and idiopathic factors. Key MRI sequences for evaluation include T2-weighted and post-contrast images, which are essential for assessing spinal cord edema, inflammation, and hemorrhagic changes. Additionally, gradient echo (GRE) sequences are vital for detecting subtle blood products, as blood degradation products display increased hypointensity and blooming on GRE images compared to T2-weighted images. By understanding this rare condition and its potential underlying causes, as well as its mimics, radiologists can play a crucial role in guiding clinical teams toward accurate diagnosis and timely management of patients with hemorrhagic transverse myelitis.

References

Fukuoka M, Kuki I, Kawawaki H, et al. A pediatric patient of hemorrhagic acute transverse myelitis. Brain Dev. 2017 Mar;39(3):252-255. doi: 10.1016/j.braindev.2016.09.007.

Toljan K, Mahadeen A, Amin M, et al. Pearls & Oy-sters: Hemorrhagic Myelitis Following SARS-CoV-2 Infection. Neurology. 2023 Aug 8;101(6):e672-e676. doi: 10.1212/WNL.0000000000207213.

Images/Tables



Figure 1. Sagittal MRI sequences of the cervical and thoracic spine (A. STIR, B. T2, C. T1, D. T1 post-contrast) demonstrate blood degradation products of varying ages (brackets) in the visualized spinal cord.

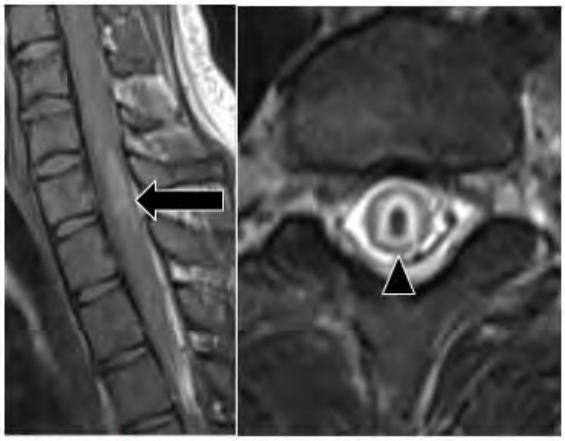


Figure 2. MRI of the cervical spine. Sagittal T1 on the left and axial T2 on the right. T1 intrinsic hyperintensity (arrow) and T2 dark signal (arrowhead) is consistent with spinal cord hemorrhage.

595

Posterior Reversible Encephalopathy Syndrome in a 20-Month-Old Boy with Denys-Drash Syndrome

Joseph Kim MD, Matthew Hammer MD, Neal Shukla MD, Richard Lozano, Long Tu MD, PhD, Balaji Rao MBBCh
Yale New Haven Hospital, New Haven, CT, USA

Abstract Category

Pediatrics

Clinical History

A 20-month-old boy with Denys-Drash syndrome, status post right nephrectomy for Wilms tumor and on peritoneal dialysis for end-stage renal disease, presented with altered mental status and seizures. Upon admission, the patient's blood pressure peaked at 230/140.

Imaging Findings

CT imaging of the head revealed confluent white matter hypodensities in the bilateral parietal and occipital regions, consistent with posterior reversible encephalopathy syndrome (PRES). Hyperdense foci were also noted in the bilateral posterior globes, suggestive of retinal hemorrhages. A subsequent MRI of the brain and orbits confirmed these findings, demonstrating confluent T2 FLAIR signal abnormalities in the bilateral parietal and occipital white matter. Additionally, bilateral subretinal exudate was observed, appearing slightly hyperintense on T2 FLAIR and T1-weighted images, without any associated restricted diffusion or loss of signal on susceptibility-weighted imaging.

Discussion

PRES is characterized by the acute onset of neurological symptoms, including headache, seizures, confusion, and visual disturbances, and is associated with vasogenic edema predominantly affecting the parieto-occipital lobes. In contrast to adults, pediatric PRES often presents with distinct imaging patterns. While parieto-occipital involvement is common in adults, children may exhibit more widespread and atypical distributions, affecting the frontal, temporal, and cerebellar regions. The incidence of PRES is estimated to be 0.04% in the general pediatric population and 0.7% in children with underlying malignancies. Children with PRES frequently have underlying renal disease, hematological malignancies, or a history of immunosuppressive therapy.

Teaching Point

In children presenting with new-onset neurological symptoms, especially those with underlying renal disease, PRES should be considered in the differential diagnosis of acute encephalopathy. The presentation of PRES in pediatric patients is associated with unique imaging findings, clinical manifestations, and risk factors that differ from those seen in adults. Early and accurate diagnosis is crucial, as it can significantly influence management strategies and improve the prognosis for affected children.

References

Halbach SM, Stein D. Posterior Reversible Encephalopathy Syndrome in Children and Adolescents. Curr Hypertens Rep. 2024 Aug;26(8):349-354. doi: 10.1007/s11906-024-01303-6.

Images/Tables

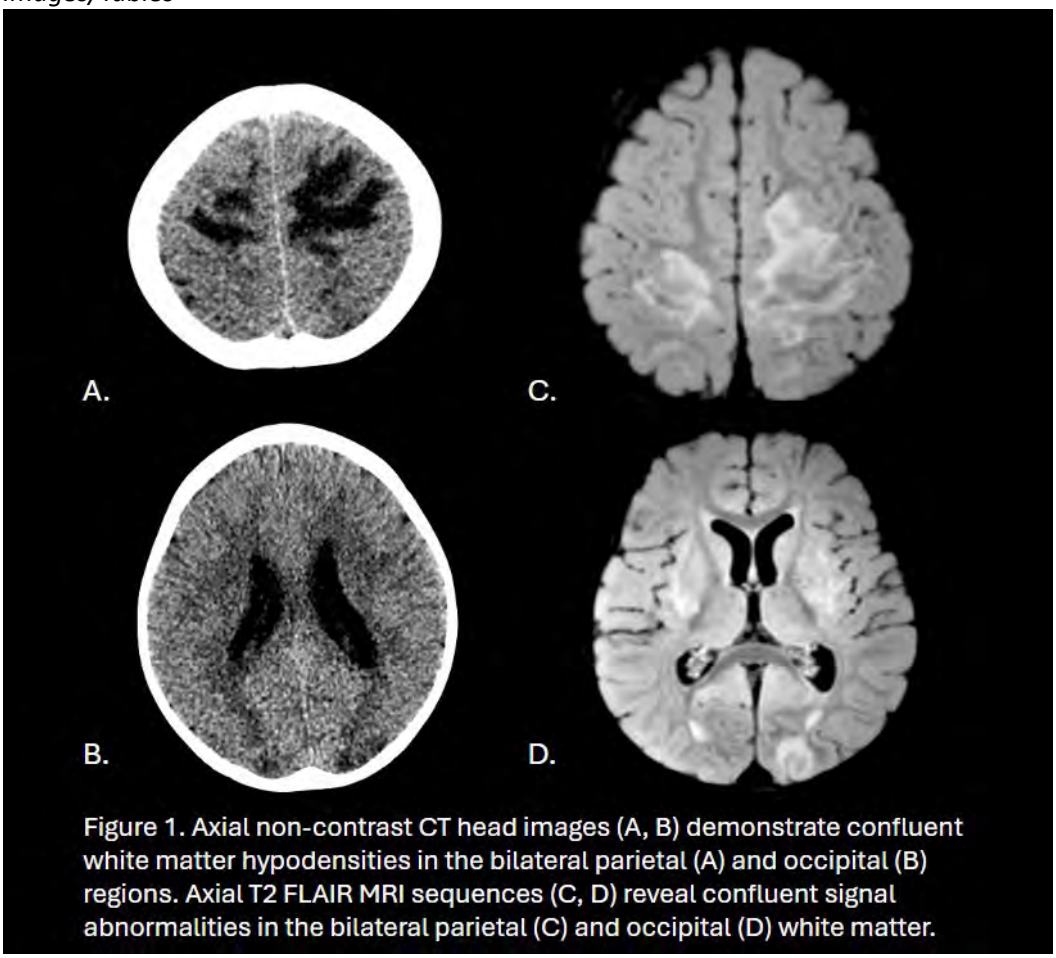


Figure 1. Axial non-contrast CT head images (A, B) demonstrate confluent white matter hypodensities in the bilateral parietal (A) and occipital (B) regions. Axial T2 FLAIR MRI sequences (C, D) reveal confluent signal abnormalities in the bilateral parietal (C) and occipital (D) white matter.

610

Diagnostic Challenges of Reversible Cerebral Vasoconstriction Syndrome in a Pediatric Patient with B-Cell Acute Lymphoblastic Lymphoma: A Case Report

Neal S Shukla MD, Joseph Kim MD, Matthew Hammer MD, Long Tu MD, Balaji Rao MD
Yale School of Medicine, New Haven, CT, USA

Abstract Category

Pediatrics

Clinical History

A 7-year-old male patient with a medical history of B-cell acute lymphoblastic lymphoma, currently undergoing treatment with intrathecal methotrexate, cytarabine, and IV vincristine was admitted to our institution for acute perforated appendicitis. On the second day of hospitalization, the patient developed left arm weakness which prompted evaluation with MRI/MRA brain.

Imaging Findings

Imaging revealed restricted diffusion in the left superior frontal gyrus with corresponding low ADC values and mild T2/FLAIR signal suggestive of an acute ischemic infarct. Vascular imaging showed a beaded appearance of the

supraclinoid ICA, ACA and MCA bilaterally. Transcranial doppler study of the arteries confirmed elevated velocities consistent with multifocal stenoses.

Discussion

Initial differential diagnoses included acute ischemic infarct secondary to vasculitis with infectious causes considered due to the patient's neutropenic state. Although, there was no evidence of vasculitis in other regions of the body and a primary CNS vasculitis typically presents with bilateral infarcts. Methotrexate leukoencephalopathy was also considered, although it typically affects white matter, primarily in the centrum semiovale. Posterior reversible encephalopathy syndrome was another possibility, but the absence of cerebral microhemorrhages argued against this. Given the vascular and ischemic findings, RCVS was ultimately suspected. A follow-up MRI performed several days later revealed a new infarct in the right frontal lobe. Notably, repeat CTA imaging showed complete resolution of the arterial stenoses, further supporting the diagnosis of RCVS.

Teaching Point

Reversible cerebral vasoconstriction syndrome (RCVS) is commonly seen in middle-aged patients. This syndrome is characterized by thunderclap headaches which may not be apparent or recognized in pediatric patients, posing a challenge in diagnosis. Several medications have been associated with the development of RCVS, though they are not reliably known to cause it: highlighting the potential influence of other underlying predisposing factors. RCVS is self-limiting with treatment focused on reducing the degree of vasoconstriction.

This case illustrates the diagnostic challenge of RCVS in a pediatric patient with comorbidities that initially pointed towards a neoplastic or infectious etiology. Although not performed in the presented case, vessel wall MRI may be a useful tool in differentiating between arterial narrowing from vasculitis versus RCVS or atherosclerosis.

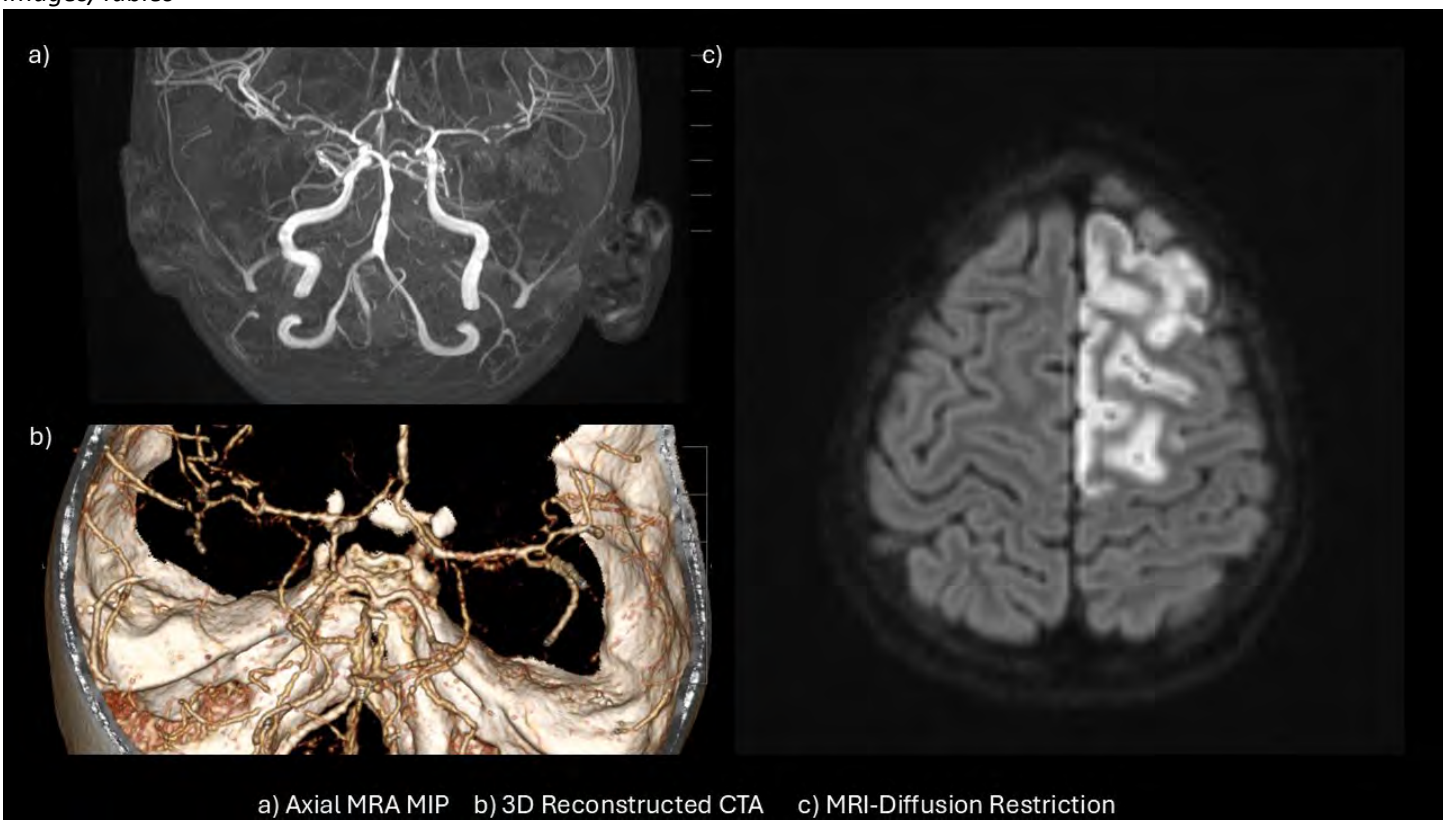
References

Gaillard F, Whitehead H, Sharma R, et al. Reversible cerebral vasoconstriction syndrome. Reference article, Radiopaedia.org (Accessed on 11 Nov 2024) https://doi.org/10.53347/rID-4426

Miller TR, Shivashankar R, Mossa-Basha M, Gandhi D. Reversible Cerebral Vasoconstriction Syndrome, Part 2: Diagnostic Work-Up, Imaging Evaluation, and Differential Diagnosis. AJNR Am J Neuroradiol. 2015 Sep;36(9):1580-8. doi: 10.3174/ajnr.A4215. Epub 2015 Jan 22. PMID: 25614476; PMCID: PMC7968777.

Anne Ducros, Monique Boukobza, Raphaël Porcher, Mariana Sarov, Dominique Valade, Marie-Germaine Bousser, The clinical and radiological spectrum of reversible cerebral vasoconstriction syndrome. A prospective series of 67 patients, *Brain*, Volume 130, Issue 12, December 2007, Pages 3091–3101, https://doi.org/10.1093/brain/awm256

Images/Tables



617

A Case of Septic-embolic Encephalitis Following Nasopharyngeal Abscess

Mona Gad

Radiology Department, Mansoura University Faculty of Medicine, Mansoura, Dakahlia, Egypt

Abstract Category

Adult Brain

Clinical History

50-year-old female patient with history of diabetes mellitus, presented with stroke-like symptoms, fever and leukocytosis.

Imaging Findings

- First row shows few left parietal lobe lesions in an embolic pattern displaying high T2 & FLAIR signal intensity with pseudonormalization of ADC in the form of high signal on DWI and isointensity on ADC map (denoting subacute embolic infarcts).
- Second row shows a well defined left parietal lobe periventricular lesion (red arrows) with related significant vasogenic edema (yellow arrows). The lesion has hypointense rim on T2WI and FLAIR with internal hypointense content as well as central restricted diffusion pattern and marginal enhancement on post-contrast T1WI.
-Third row demonstrates loss of the flow void signal of the left ICA (red circles) on T2WI and FLAIR image which is further confirmed by absent contrast filling (blue arrows) on CT angiography denoting thrombosed left ICA. Patent ICA is clearly noted on the right side.
- Fourth row demonstrates a nasopharyngeal abscess (orange arrows) with thick marginal enhancement depicted on contrast-enhanced T1WI and CT images.

Discussion

We present an interesting case of septic-embolic brain abscess. Constellation of imaging findings leads to a conclusion that nasopharyngeal abscess in an immunocompromised diabetic female patient resulted in thrombosed left internal carotid artery (ICA) with subsequent septic-embolic stroke evolving into abscess formation.

Septic-embolic encephalitis, also known as septic-embolic brain abscess, is defined as a focal or diffuse brain infection, ischemic or hemorrhagic changes following infective thromboembolism from any part of the body. It is usually caused by infective endocarditis in cardiac patients. Other possible risk factors include immunocompromised patients, intravenous drugs addicts and central venous catheters. In most cases, septic-embolic encephalitis favors the middle cerebral artery (MCA) territory, and rarely occurs in the posterior circulation. MRI has higher sensitivity than CT in depicting the different stages of evolution of septic-embolic encephalitis.

Teaching Point

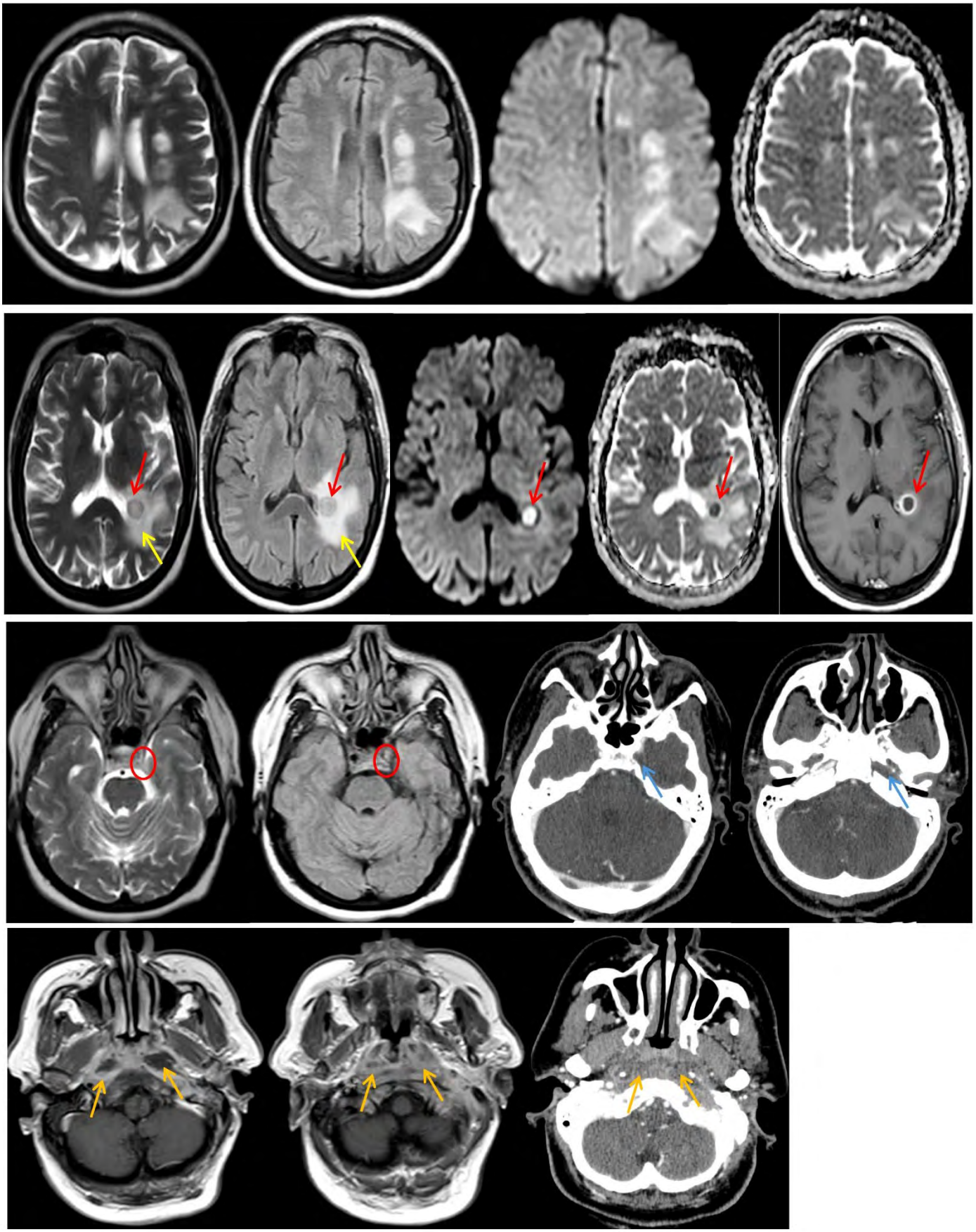
Marginally enhancing lesion showing central restricted diffusion in a patient with septic emboli should raise the suspicion for septic-embolic brain abscess. Radiologists should look carefully for the source of infection and the consequences of septic emboli in the brain, particularly in patients with risk factors.

References

1. Mohamud JA, Wu J, Jing Y, Wang Y. Septic Embolic Stroke Followed by Hemorrhage and Brain Abscess in a Patient with Systemic Infections: A Case Report and Literature Review. Case Rep Radiol.2018;2018:1-5. DOI:10.1155/2018/4602352

2. Judd D, Oldham J, Lish J. Septic Embolic Encephalitis Following Cardiac Valve Replacement. Cureus.2024. DOI:10.7759/cureus.51628

Images/Tables



620

A Rare Case of an Intracerebral Schwannoma in a Pediatric Patient

Carolina Soto MD, Tailong Xu MD, Prerana Ramesh BS, Dylan Scott BS, Joshua Strobel MD, Octavio Arevalo MD
LSU Health Shreveport, Shreveport, LA, USA

Abstract Category

Pediatrics

Clinical History

A previously healthy 15-year-old Caucasian male was referred to our neurosurgery department for complaints for progressively worsening headaches of fluctuating severity with associated intermittent episodes of pulsatile tinnitus, right-sided focal weakness and vision changes, and word-finding difficulties over a 3-month period.

Imaging Findings

An intra-axial solid and cystic mass arising from the left inferior frontal gyrus and causing significant mass effect, midline shift, and incipient left uncal herniation was identified. The nodular component of the mass demonstrated a homogeneous and avid contrast enhancement with internal areas of necrosis and measured approximately 33 x 35 x 24 mm (CCxAPxT). The cystic component of the lesion demonstrated a thin rim of enhancement and measured about 47 x 74 x 66 mm (CCxAPxT). No areas of restricted diffusion or hemorrhage were identified in the solid region of the tumor. No calcifications were identified on the non-contrast CT.

Discussion

The patient subsequently underwent craniotomy and resection of the mass, and his preoperative symptoms have since resolved with follow-up MRIs demonstrating no tumor recurrence. The pathology examination of the resected mass reported an intraparenchymal schwannoma with a Ki-67 labeling index of 10-15%. Intracranial schwannoma (IS) accounts for between 5 and 8% of intracranial tumors, whereas intracerebral schwannoma, a rare disease, accounts for <1% of intracranial schwannomas[1]. IS cannot be diagnosed from preoperative clinical manifestations or imaging appearance, and is definitively diagnosed based on postoperative pathology. Intracerebral schwannomas occur predominantly in children and young adults, consist of solid and cystic components, and are located primarily in the frontal, parietal, and temporal lobes[2]. There have also been reports of brainstem and cerebellar intracerebral schwannomas[3].

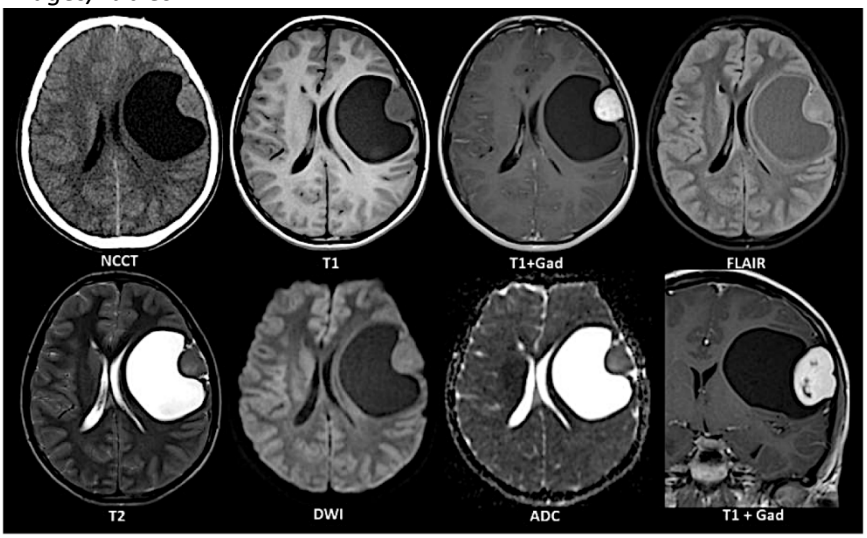
Teaching Point

Intracerebral schwannomas might be a reasonable differential diagnosis in cystic and solid intraparenchymal tumors in young patients alongside the more common oligodendroglioma, pleomorphic xanthoastrocytoma and ganglioglioma.

References

1. AlBatly AA, Zakzouk RS, Alhaidey AK. An atypical case of intracerebral schwannoma. *Pan Afr Med J*. 2014;18:342. Published 2014 Aug 27. DOI: https://doi.org/10.11604/pamj.2014.18.342.5075
2. Gao Y, Qin Z, Li D, et al. Intracerebral schwannoma: A case report and literature review. *Oncol Lett*. 2018;16(2):2501-2510. DOI: https://doi.org/10.3892/ol.2018.8949
3. Lin J, Feng H, Li F, Zhao B, Guo Q. Intraparenchymal schwannoma of the medulla oblongata. Case report. J Neurosurg. 2003;98(3):621-624. DOI: https://doi.org/10.3171/jns.2003.98.3.0621

Images/Tables



629

Tuberculous Meningitis Masquerading as Susac Syndrome

Anthony D. Yao MD, Jimmy S. Lee MD, PhD
Montefiore Medical Center, Bronx, NY, USA

Abstract Category

Adult Brain

Clinical History

31-year-old male recent immigration from Guinea otherwise no PMHx presents to the ED with headache and dizziness. MRI of the brain with imaging features as described in Figure 1 included Susac syndrome as a primary differential consideration.The patient was started on empiric steroid treatment. Diagnostic workup included a LP which was initially unrevealing, fundoscopic examination without evidence of retinal artery occlusion, and normal audiology evaluation. CT performed on hospital day 5 demonstrated pulmonary branching opacities and micronodules. The patient then developed status migrainosus and first lifetime seizure, with a subsequent MRI of the brain on hospital day 17 with imaging features as described in Figure 2 suspicious for meningitis. Thus, bronchoalveolar lavage was pursued which resulted in mycobacterium tuberculosis complex (MTBC). LP that was performed on initial presentation as well as a repeat LP were sent for further testing, and MTBC were confirmed on PCR analysis.

Imaging Findings

Initial CT of the head showed hypodensity in the corpus callosum. MRI was pursued for further evaluation, which demonstrated multiple regions of diffusion restriction (1A). In addition, there were spherical well-demarcated regions of FLAIR signal abnormality in the corpus callosum body (1B), which is a characteristic imaging feature of Susac syndrome. Furthermore, there was leptomeningeal enhancement most prominent along the interhemispheric fissure (1C) as well as cranial nerve enhancement at the skull base (1D). Differential diagnoses included Susac syndrome, demyelinating conditions, and less likely secondary disseminated disease.

Additional workup including MR of the spine and MR vessel wall imaging were unremarkable. Subsequent MRI on hospital day 17 demonstrated progression of communicating hydrocephalus (2A) and diffuse sulcal FLAIR hyperintensity (2B). There was persistent interhemispheric (2C) as well as posterior fossa (2D) leptomeningeal enhancement. These findings were suspicious for meningitis.

Discussion

Susac syndrome is a rare autoimmune endotheliopathy with a classic clinical triad of encephalopathy, branch retinal artery occlusions, and sensorineural hearing loss. However, there is no consensus diagnostic criteria for Susac syndrome[1-3], which presents a diagnostic challenge. Furthermore, only a minority of patients (13%) present with the full clinical triad at disease onset[4], as was the case for this patient. However, evolution of this patient's clinical and radiographic hospital course was atypical for Susac syndrome. The final diagnosis of tuberculous meningitis, which is the most lethal and disabling form of tuberculosis[5], was initially suggested on neuroimaging and later confirmed following further workup.

Teaching Point

- A small minority of patients with Susac syndrome present with the full classic clinical triad at disease onset.
- However, as one such proposed diagnostic criteria in 2016 suggests, neuroimaging findings alone is insufficient, and integration of the patient's other clinical findings is required.[1] In cases such as these where the clinical picture is incongruent, radiologists should consider other causes, such as infection, as other potential etiologies.
- There is a wide spectrum of radiological manifestations of CNS tuberculosis which can often mimic other infectious and noninfectious neurological conditions.
- Therefore, knowledge of the varied neuroimaging findings and correlation with patient's symptomology, laboratory findings, and CSF sampling is critical for timely diagnosis and initiation of appropriate treatment.

References

1. Kleffner I, Dorr J, Ringelstein M, et al. Diagnostic criteria for Susac syndrome. *J Neurol Neurosurg Psychiatry* 2016;87:1287-1295
2. Carruthers R, Paton G, Sheldon C, et al. Justification for New Diagnostic Criteria for Susac Syndrome: Evolving Beyond the Triad (S20.001). *Neurology* 2017;88:S20.001
3. Egan RA. Diagnostic Criteria and Treatment Algorithm for Susac Syndrome. *J Neuroophthalmol* 2019;39:60-67
4. Dorr J, Krautwald S, Wildemann B, et al. Characteristics of Susac syndrome: a review of all reported cases. *Nat Rev Neurol* 2013;9:307-316
5. Wilkinson RJ, Rohlwink U, Misra UK, et al. Tuberculous meningitis. *Nat Rev Neurol* 2017;13:581-598

Images/Tables

Figure 1.

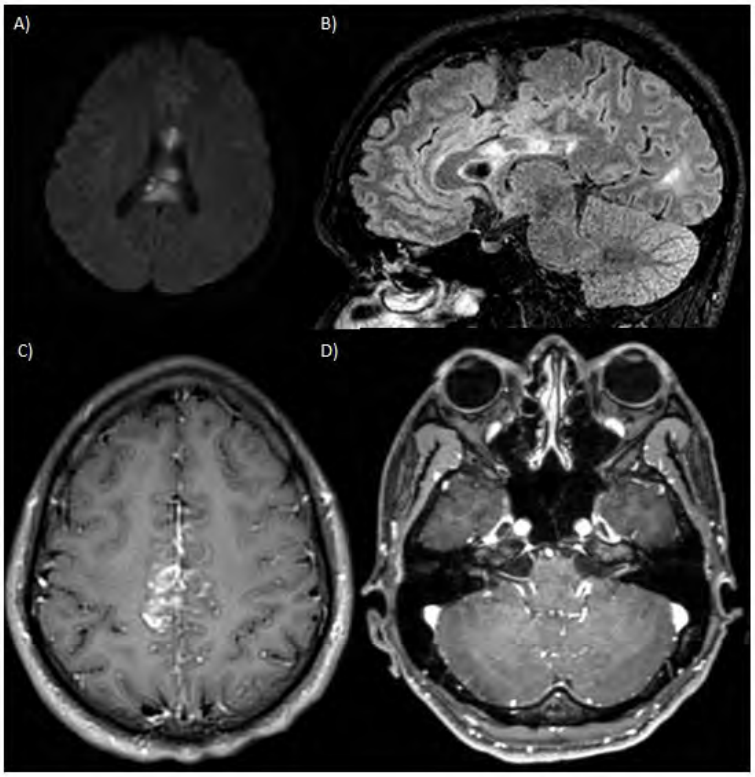
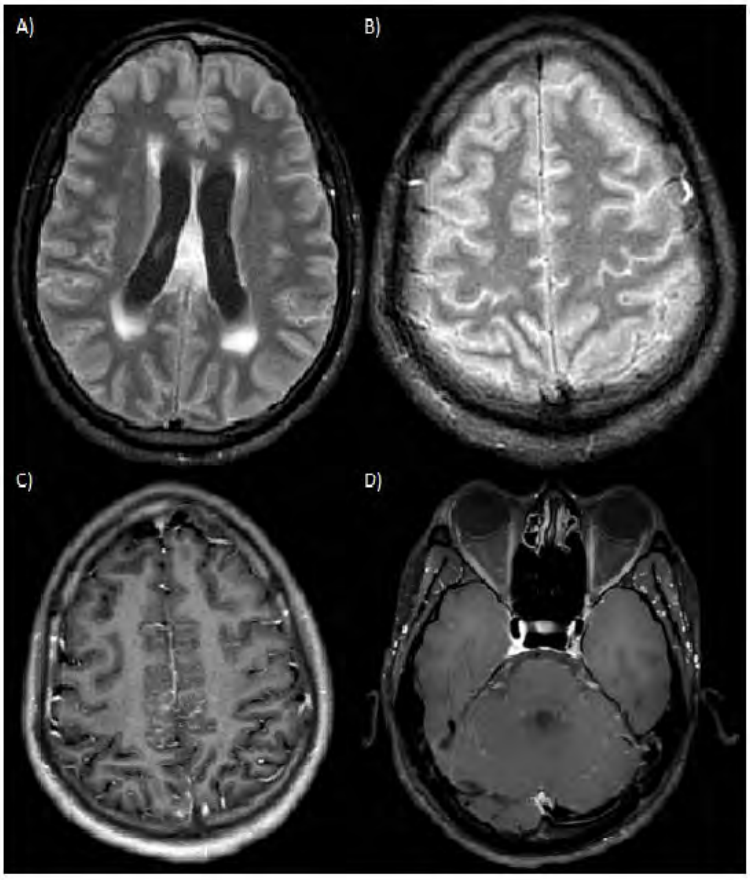


Figure 2.



641

What Are You Doing Here? Intradural Spinal Drop Metastasis from Clival Chordoma 20+ Years After Initial Diagnosis

Ivy Vo BS, Nancy Fischbein MD, Nancy Pham MD
Stanford Medicine, Stanford, CA, USA

Abstract Category

Head & Neck

Clinical History

A 49-year-old male was diagnosed with clival chordoma in 2002 following the onset of diplopia. He subsequently underwent extensive treatment, including endoscopic resection, four craniotomies (2002, 2013, 2017, and 2019), and proton beam therapy to treat initial and persistent/recurrent skull base disease. In 2021, he presented with lower extremity pain. Lumbar spine MRI revealed lobulated, T2 hyperintense, gadolinium-enhancing intradural extramedullary masses at L4-L5 and L5-S1 levels. Subsequent L5 hemilaminectomy and intradural resection confirmed drop metastasis from chordoma. In 2024, he reported worsening buttock pain radiating to the left hip and posterior thigh. Repeat lumbar spine MRI confirmed residual/recurrent spinal drop metastases.

Imaging Findings

The latest recurrence in 2023 presented as a large right clival mass, with multi-spatial extension into the middle cranial fossa, posterior fossa, and sellar/suprasellar region (A-B). Susceptibility artifact within the mass is related to prior carotid clipping due to intraoperative injury. Recent surveillance imaging showed no evidence of residual/recurrent clival chordoma at the primary site following the most recent resection. A recent lumbar spine MRI, however, revealed multiple intradural extramedullary masses involving cauda equina nerve roots (C-D), the largest measuring 8.0 x 13.2 mm at the L5-S1 level. These masses demonstrated heterogeneous, intermediate T2 signal and avid enhancement. The largest mass involved the exiting left S1 and descending S2 nerve roots (E-F), likely accounting for the patient's left lower extremity radiculopathy.

Discussion

Chordomas are rare neoplasms originating from notochord remnants, with an incidence of 0.08 per 100,000 individuals annually. These malignant lesions have variable metastatic behavior, with reported rates ranging from 10-43%, predominantly affecting the lungs, skin, bone, and lymph nodes. Intradural spinal drop metastases from skull base chordomas are exceptionally rare, with fewer than ten cases in the literature, generally discovered postmortem or concurrently with the initial tumor. Dissemination of tumor cells may occur during the natural course of the disease, particularly when there is dural transgression, or as a result of surgical intervention that disrupts the dura and seeds the cerebrospinal fluid. Symptoms may include back pain and neurological deficits, although many cases remain asymptomatic until autopsy.

Aggressive surgical resection with negative margins is the primary treatment, as chordomas are generally resistant to chemotherapy. Adjuvant radiotherapy can improve outcomes in cases of subtotal resection. Prognosis varies, with a median overall survival of approximately six years, influenced by tumor subtype and location. Our current patient is planned for surgery followed by radiation therapy.

Teaching Point

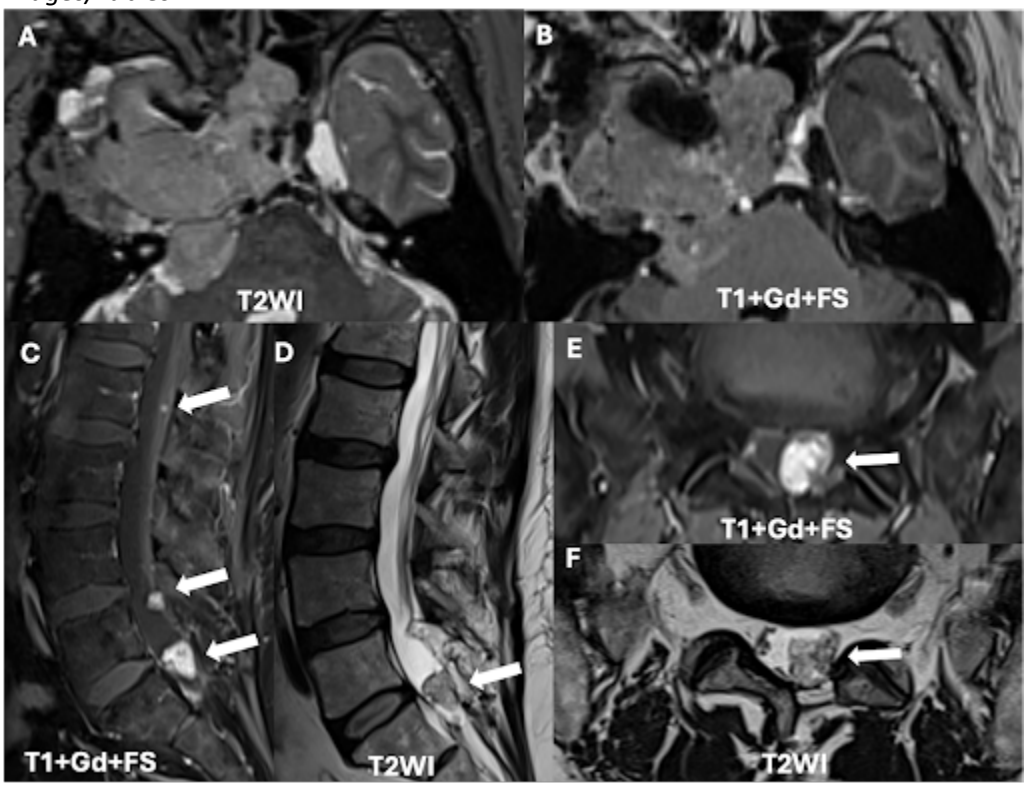
Intradural spinal drop metastases from clival chordomas are exceptionally rare, but their occurrence should be considered in patients with a history of clival chordoma presenting with new neurological symptoms referable to spinal cord or spinal nerves. MRI of the spine is crucial for examining the entire neuroaxis and identifying distant metastases.

References

1. Martin, M. P., & Olson, S. (2009). Intradural drop metastasis of a clival chordoma. *Journal of Clinical Neuroscience*, 16(8), 1105–1107.

2. Muhamat Nor, F. E., Desai, V., & Chew, L. L. (2018). Clival chordoma with drop metastases. *Journal of Radiology Case Reports*, *12*(3), 1–9.

Images/Tables



642

Pilomyxoid Astrocytoma Case Report

Efrain Segura M.S[1], Sarah Navid BS[2], Nourel Hoda M Tahon MD[3], Kamand Khalaj MD[3], Elham Tavakkol MD[3], Arash Kamali MD[3], Roy F Riascos-Castaneda[3]

[1]Ponce Health Sciences University, Ponce, PR, USA. [2]University of Texas medical branch Galveston, Galveston, tx, USA. [3]University of Texas Houston, Houston, tx, USA

Abstract Category

Adult Brain

Clinical History

A 27-year-old male patient presented with altered mental status and stroke-like symptoms. He was also diagnosed with COVID-19 at the same time. Multiple serology analyses were negative.

He was discharged after finishing his Paxlovid. Then, the patient returned back with altered mental status, headache, nausea, vomiting, and pain in the right eye. He was aphasic at the same time.

Imaging Findings

The patient is presented with a partially calcified, enhancing lesion in the right medial temporal lobe. The lesion is accompanied by diffuse leptomeningeal enhancement throughout the brain and spinal cord, with notable involvement of cranial nerves, including the trigeminal nerves. This pattern suggests extensive CNS involvement with potential leptomeningeal tumor spread.

Discussion

Pilomyxoid astrocytoma (PMA) is a distinct subtype of low-grade gliomas (WHO grade II), primarily affecting children but increasingly reported in adults. They differ histologically from PA (pilocytic astrocytoma), lacking Rosenthal fibers and eosinophilic bodies. Management remains challenging, with gross total resection offering the best outcomes, though recurrence is common. Studies show variability in presentation and prognosis, emphasizing the need for individualized treatment and close follow-up due to the risk of rapid growth and CSF dissemination.

PMA is generally T2 hyperintense and T1 hypointense and demonstrates avid enhancement in the post-contrast sequences. Usually large, well-circumscribed, and lobulated, PMA may have solid or cystic components with no or minimal surrounding edema. Typically described as H-shaped, it expands from the midline (hypothalamic and optic chiasm region) into both temporal lobes. Hemorrhagic components may be present. CSF dissemination can also be seen.

PMA presents with increased relative cerebral blood volume compared with PA (Pilocytic astrocytoma) in the infratentorial space, which may be displayed when differentiating PMA and PA.
A biopsy of the right temporal lobe revealed a diagnosis of pilomyxoid astrocytoma (WHO Grade 2) in suspicious tissue samples. The tumor exhibits a biphasic pattern with myxoid areas and moderately atypical glial cells. Immunohistochemical stains confirm positivity for GFAP, synaptophysin, and ATRX, with a Ki-67 index of 5%, indicating low to moderate proliferative activity. Our case demonstrates an unusual location of the tumor (medial temporal lobe) and a very rare representation of diffuse dissemination of the tumor along the neuroaxis.

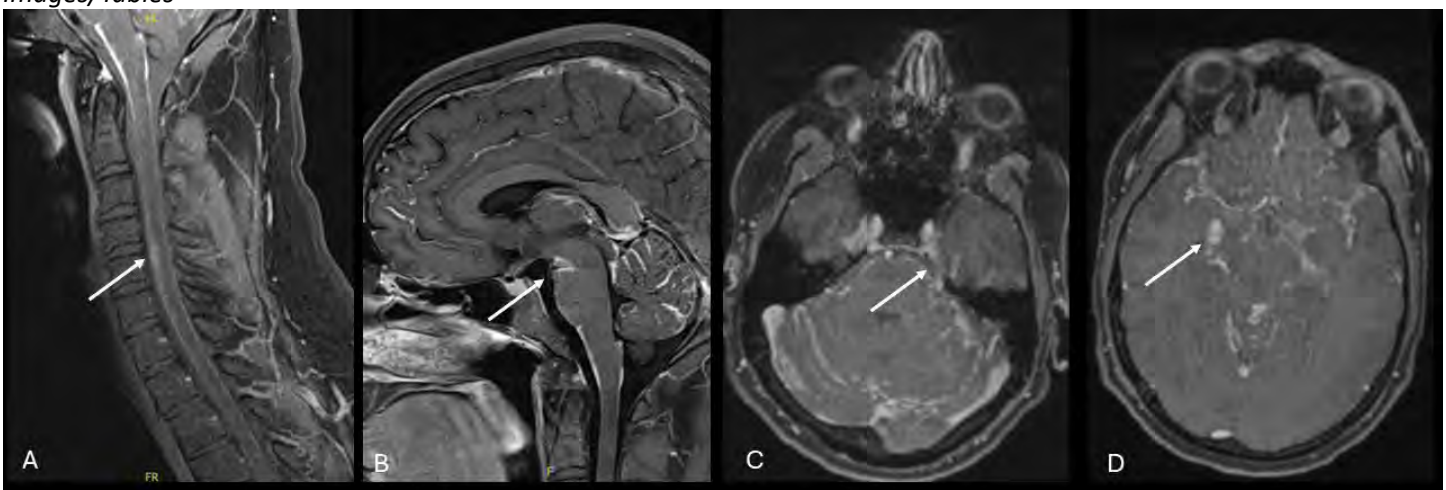
Teaching Point

PMA is a variant of PA that primarily affects the hypothalamic and chiasmatic regions of the brain. However, it can also develop in less typical areas, such as the brainstem and, as in our case, the temporal lobe.
PMA is characterized pathologically as monomorphous bipolar piloid cells with an angiocentric pattern in a myxoid pattern. Due to local recurrence and cerebrospinal fluid (CSF) dissemination, PMA is classically more aggressive than PA. Given the tumor's aggressive behavior, early initiation of adjuvant therapy is often recommended when complete surgical removal is not possible. Chemotherapy is typically preferred in younger patients to avoid early radiation. Establishing PMA registries would help clinicians gain insights and improve treatment strategies, ultimately leading to more standardized management guidelines as knowledge of the disease evolves.

References

Komotar RJ, Mocco J, Carson BS, Sughrue ME, Zacharia BE, Sisti AC, et al. Pilomyxoid astrocytoma: a review. **MedGenMed**. 2004 Dec 9;6(4):42. PMID: 15775869; PMCID: PMC1480592.
Linscott LL, Osborn AG, Blaser S, Castillo M, Hewlett RH, Wieselthaler N, et al. Pilomyxoid astrocytoma: expanding the imaging spectrum. **AJNR Am J Neuroradiol**. 2008 Nov;29(10):1861-1866. doi: 10.3174/ajnr.A1233. PMID: 18701580; PMCID: PMC8118951.
Pereira FO, Lombardi IA, Mello AY, Romero FR, Ducati LG, Gabarra RC, et al. Pilomyxoid astrocytoma of the brainstem. **Rare Tumors**. 2013 Apr 15;5(2):65-67. doi: 10.4081/rt.2013.e17. PMID: 23888217; PMCID: PMC3719112.
Pruthi SK, Chakraborti S, Naik R, Ballal CK. Pilomyxoid astrocytoma with high proliferation index. **J Pediatr Neurosci**. 2013 Sep;8(3):243-246. doi: 10.4103/1817-1745.123694. PMID: 24470824; PMCID: PMC3888047.
Azad S, Kudesia S, Chawla N, Azad R, Singhal M, Rai SM, et al. Pilomyxoid astrocytoma. **Indian J Pathol Microbiol**. 2010 Apr-Jun;53(2):294-296. doi: 10.4103/0377-4929.64283. PMID: 20551536.

Images/Tables



A)There is a diffuse contrast enhancement around the entire spinal cord with some focal thickening at C4-C5.
B)This contrast-enhancing leptomeninges extends up into the posterior fossa around the brainstem.
C) Diffuse leptomeningeal enhancement overlying the cerebral hemispheres, within the Sylvian fissures, MCA cisterns, basal cisterns, and overlying the cerebellar folia as well as along the left trigeminal nerve and likely within the Meckel's caves is present.
D) A 1 cm x 0 x 0.8 cm enhancing partially calcified lesion in the right medial temporal lobe.

661

Deep Learning–Based Reconstruction of 3D T1 SPACE Imaging for Detection of a Pituitary Microadenoma in Cushing Disease

Ian Mark[1], Marcel Dominik Nickel[2], Alto Stemmer[2], Pete Kollasch[3], Rachel Johnson[4], Arien North[1], Jodie Serum[1], Steve Messina[1]

[1]Mayo Clinic, Rochester, MN, USA. [2]Siemens, Erlangen, Germany, Germany. [3]Siemens, Minneapolis, MN, USA. [4]Mayo Clinc, Rochester, MN, USA

Abstract Category

Head & Neck

Clinical History

63-year-old female with an 8-year history of unintentional weight gain, hirsutism, and easy bruising. Endocrinological testing including inferior petrosal vein sampling was compatible with Cushing disease. She underwent a contrast enhanced MRI of the sella for identification of a causative pituitary adenoma.

Imaging Findings

3T pre-operative contrast enhanced MRI shows a normal pituitary. No findings for hypoenhancing lesion (left image), abnormal T2 signal, or mass effect. The imaging protocol included a contrast enhanced 3T T1-weighted sequence (SPACE, slice thickness 0.7 mm). During the same imaging session, an additional T1-weighted sequence (SPACE, slice thickness 0.55 mm) with a deep learning-based reconstruction, using a similar gradient time to the clinical protocol, was performed and found a discrete 5 mm hypoenhancing lesion in the inferior aspect of the gland. This lesion was resected a pathology confirmed corticotroph adenoma.

Discussion

Detecting adenomas in patients with Cushing disease is crucial, as surgery is the standard of care treatment. Accurate pre-operative lesion localization is directly associated with improved outcomes. Deep learning-based reconstruction imaging is used to decrease gradient time and increase patient throughput. We demonstrated using a deep learning-based construction utilizing a similar gradient time as the product sequence to improve image quality. Using this technique, we were able to identify a pathology confirmed pituitary adenoma in a patient with Cushing disease.

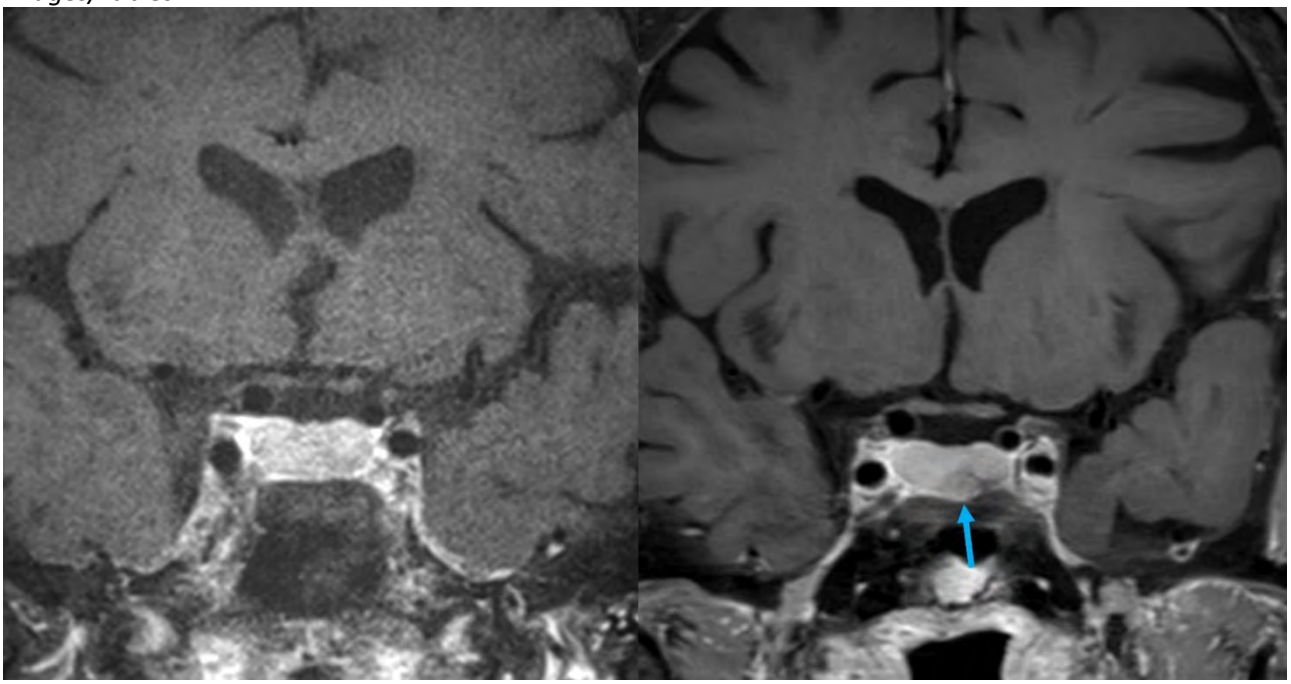
Teaching Point

We present the use of a deep learning-based reconstruction of a 3D T1 SPACE sequence for the identification of a pituitary adenoma in a patient with Cushing disease. Utilizing this technique for improved image quality may be helpful in the identification of pituitary microadenomas.

References

Shih RY, Schroeder JW, Koeller KK. Primary Tumors of the Pituitary Gland: Radiologic-Pathologic Correlation. *Radiographics*. Nov-Dec 2021;41(7):2029-2046. doi:10.1148/rg.2021200203

Images/Tables



666

Mandibular Ossifying Fibroma

Garret Miller, Jonathan Sanders, Joshua Strobel MD, Octavio Arevalo Espejo MD
LSU Health Shreveport, Shreveport, LA, USA

Abstract Category

Head & Neck

Clinical History

A 45-year-old female patient with prior medical history of iron deficiency presented with a fibro-osseous lesion of the anterior mandible after noticing gradual swelling of her mandible.

Imaging Findings

An expansile destructive mass located at the mandible apex was identified with numerous internal calcifications measuring 4.5 x 2.8 cm in axial dimensions and extending 3.2 cm cranial caudal. The mixed lucent/sclerotic lesions showed scalloped borders and adjacent cortical thinning within the posterior aspect of the left mandible body measuring about 2.6 x 1.8 cm. No pathologic appearing regional lymph nodes or other bone lesions are identified. Salivary and thyroid gland appear unremarkable.

Discussion

The patient underwent surgery to remove a mandibular mass and subsequent mandibular reconstruction. Pathologic examination showed a mass with irregular bone ossicles and cementum, a Ki-67 labeling index of 3-5%, and cortical thinning consistent with ossifying fibroma.

Ossifying fibromas (OFs) are benign neoplasms of bone or cementum surrounded by a fibrous capsule separating it from surrounding bone. Facial bone OFs are often solitary lesions with a slight female prevalence and a significant maxillary bone preference of 3:1 over the mandible. Swelling and jaw displacement are common presenting symptoms in facial OFs. Recurrence in OF is uncommon unless related to the juvenile type which is more aggressive and can present with multiple lesions. Diagnosis of OF requires coordination of patient history and imaging as other fibrous ossifying lesions such as cemento-ossifying fibroma, fibrous dysplasia, or florid osseous dysplasia can have similar pathological findings, but have different presentations and treatments. Through imaging, OFs can be distinguished from fibrous dysplasia: OFs have sharp, well-defined margins with peripheral radiolucency, whereas fibrous dysplasia has diffuse or poorly defined margins.

Teaching Point

Ossifying fibromas can lead to pathologic jaw fracturing and dental deformities due to root resorption. Differentiating ossifying fibromas from other fibro-osseous lesions with imaging guides different treatment of these lesions.

References

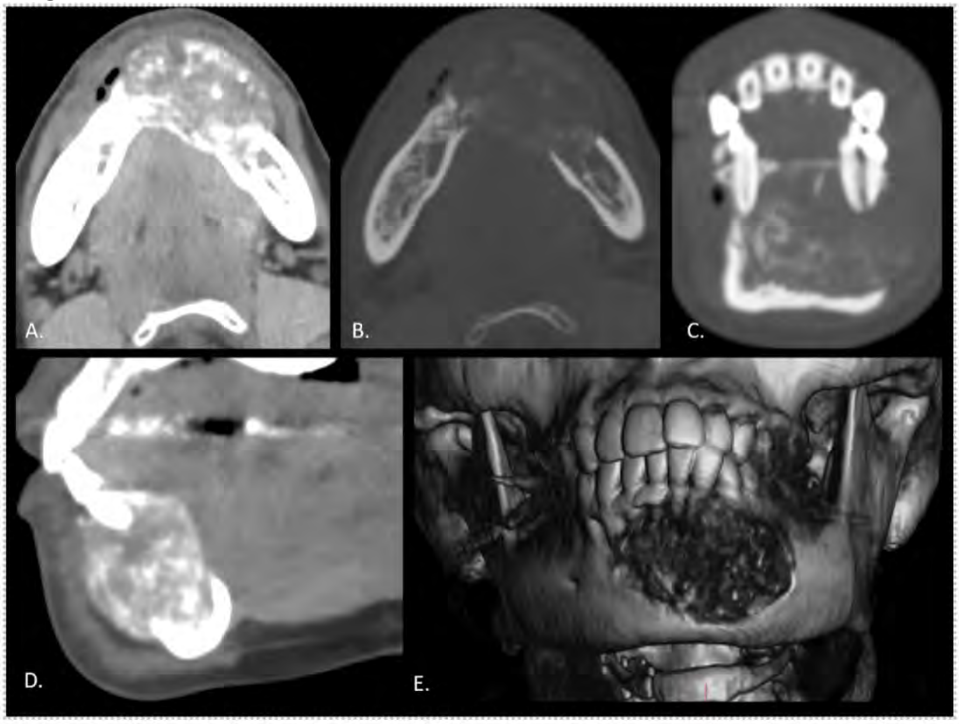
DS MacDonald-Jankowski, Ossifying fibroma: a systematic review, Dentomaxillofacial Radiology, Volume 38, Issue 8, 1 December 2009, Pages 495–513, https://doi.org/10.1259/dmfr/70933621

Sciubba, J.J. and Younai, F. (1989), Ossifying fibroma of the mandible and maxilla: review of 18 cases. Journal of Oral Pathology & Medicine, 18: 315-321. https://doi.org/10.1111/j.1600-0714.1989.tb01559.x

Ribeiro, Ana Carolina Prado, et al. "Bilateral central ossifying fibroma affecting the mandible: report of an uncommon case and critical review of the literature." Oral Surgery, Oral Medicine, Oral Pathology, Oral Radiology, and Endodontology 111.2 (2011): e21-e26.

Chidzonga, Midion, et al. "Ossifying fibroma in the maxilla and mandible: a case report with a brief literature review." Cureus 15.1 (2023).

Images/Tables



CT images of the maxillofacial region with IV contrast. Axial images through the mandibular symphysis in soft tissue (A) and bone window (B), coronal CT in bone window (C), and sagittal CT in soft tissue window (D). Three-dimensional volume rendering reconstruction (E). A heterogeneously enhancing mandibular mass is identified, with a partially calcified osseous matrix, narrow transition zone, and no periosteal reaction. The lesion expands the mandible and destroys its buccal and lingual cortices. No soft tissue component is seen. Of note, the mass surrounds the root of the mandibular incisors, without associated erosion.

675

The Sugar Spin! Unmasking Diabetic Striatopathy through Radiology.

Ayimen Khalid Khan MBBS, Tarek Daoud MBBCh, Mohiuddin Hadi MD
University of Louisville, Louisville, Kentucky, USA

Abstract Category

Adult Brain

Clinical History

An 81-year-old female with a history of Type 2 Diabetes Mellitus, Hypertension (HTN), Hyperlipidemia (HLD) and complications related to diabetic foot. She had undergone a distal Symes amputation due to wound dehiscence and recurrent bone infections, with cultures showing Enterococcus faecalis and Enterobacter cloacae. She was non-compliant with diet and insulin and following a carbohydrate-rich diet, presented with severe hyperglycemia (blood glucose >700 mg/dL), involuntary jerking movements in her right extremities and uncontrolled nonketotic hyperglycemia.

Labs showed hypoxia, hyperglycemia, acute kidney injury (AKI), and pseudohyponatremia. Her HbA1c was above 15, indicating chronic poor glycemic control. She received a single dose of insulin lispro (10 units) and was discharged with a new diabetes management regimen, though her blood sugars remained unstable.

Imaging Findings

T1 hyperintensity in basal ganglia on the left (contralateral to hemichorea-hemiballismus) with sparing of thalamus. T2-weighted and FLAIR images demonstrate isointense signal. No susceptibility on SWI images to suggest associated hemorrhage. No diffusion restriction.

Discussion

This educational exhibit aims to improve the understanding of diabetic striatopathy (DS), a rare but serious neurological complication related to poorly controlled diabetes. DS manifests predominantly in elderly diabetic population presenting with hemichorea-hemiballismus, a hyperkinetic movement disorder.

The exhibit's purpose is to educate not only neuroradiologists but also general radiologists about the imaging features of diabetic striatopathy. Since the condition may present with imaging characteristics that can resemble other pathologies, it poses diagnostic challenges. By highlighting the key radiological manifestations on CT and MRI, this exhibit aims to enhance diagnostic accuracy and increase awareness of this uncommon yet critical diabetes-related complication, facilitating timely and appropriate management.

Diabetic striatopathy is thought to result from metabolic disturbances caused by hyperglycemia, which disrupts cellular processes in the basal ganglia. It is believed that damage to striatum occurs due to a combination of ischemic injury and metabolic imbalances. Chronic hyperglycemia may induce cytotoxic edema and necrosis in the basal ganglia, particularly affecting the putamen and caudate nucleus.

Teaching Point

- Identify the radiological features of diabetic striatopathy (DS).
- Correlate clinical findings with imaging characteristics.
- Discuss the differential diagnosis for basal ganglia abnormalities in diabetic patients.
- Review the pathophysiology linking hyperglycemia to striatal damage.

References

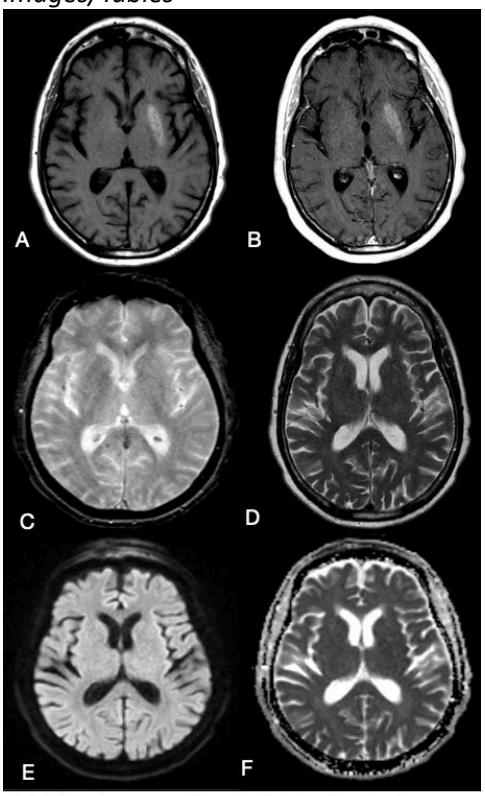
1. Yu F et al. T2*-based MR imaging of hyperglycemia-induced hemichorea-hemiballism. *J Neuroradiol*. 2017; 44(1): 24-30. doi: 10.1016/j.neurad.2016.09.005

2. Bizet J et al: Chorea, hyperglycemia, basal ganglia syndrome (C-H-BG) in an uncontrolled diabetic patient with normal glucose levels on presentation. *Am J Case Rep.* 2014; 15:143-6. doi: 10.12659/AJCR.890179

3. Zaitout Z: CT and MRI findings in the basal ganglia in non-ketotic hyperglycaemia associated hemichorea and hemi-ballismus (HC-HB). *Neuroradiology*. 2012; 54(10):1119-20. doi: 10.1007/s00234-012-1021-0

4. Cheema H et al: Hemichorea-hemiballismus in non-ketotic hyperglycaemia. *J Clin Neurosci*. 2011; 18(2):293-4. doi: 10.1016/j.jocn.2010.04.036

Images/Tables



Axial T1 pre-contrast image of the brain showing hyperintensity involving left lentiform nucleus with sparing of caudate head and thalamus (A).
No enhancement on axial T1 post contrast image (B). Axial SWI image (C) shows no susceptibility blooming to suggest associated hemorrhage. Axial T2 image (D) shows no corresponding signal abnormality. Axial DWI (E) and ADC (F) images show no evidence of diffusion restriction.

717

Cortical Vein Thrombosis as a Complication from Epidural Anesthesia: An Underrecognized Clinical Entity; Case Series and Literature Review

Warren Chang MD, MBA, Charles Li, Laura Eisenmenger MD, Michael Goldberg MD, MPH
Allegheny Health Network, Pittsburgh, PA, USA

Abstract Category

Adult Brain

Clinical History

Four recently postpartum patients (average age 29 years) without contributory medical histories that received epidural anesthesia for uncomplicated vaginal deliveries presented at network emergency departments between 2010 and 2024 within 5 days of delivery (average: 3.days) with stigmata of intracranial hypotension including postural headaches. Two of the patients also had seizures. Some of the patients had other concerning symptoms such as focal weakness or numbness.

Imaging Findings

CT imaging showed tubular hyperdensities along the vertex and MRI demonstrated susceptibility within parasagittal high cortical veins. CT and MRI venography revealed cortical vein thromboses. Two patients had restricted diffusion within the frontoparietal cortices compatible with cortical venous infarcts. All patients had findings of intracranial hypotension including cerebellar tonsillar ectopia, sagging of the brainstem, subdural collections, and dural thickening and enhancement. MRI of the spine in several patients found epidural CSF collections consistent with CSF leaks.

Discussion

Inadvertent dural puncture during epidural anesthesia resulting in CSF leak and intracranial hypotension can result in serious complications, including cortical venous sinus thrombosis. Several theories have been considered as the cause of the cortical vein thrombosis, including venous dilatation as a result of intracranial hypotension and increased traction of cortical veins as a result of brainstem/cerebellar tonsillar sagging/descent. Typically patients are treated with a combination of anticoagulation and blood patch to treat the CSF leak, and have typically done well. In our case series, all of the patients recovered without significant deficits.

Teaching Point

Cortical venous thrombosis in the setting of intracranial hypotension should be considered in recent postpartum patients who received epidural anesthesia presenting with postural headaches, especially in the setting of seizures or focal weakness/numbness. Imaging such as CT venography and MRI of the brain and spine could be considered if the diagnosis of cortical venous thrombosis is suspected to facilitate prompt treatment.

References

Yildiz O, Balaban H, Cil G et al. Isolated Cortical Vein Thrombosis After Epidural Anesthesia: Report of Three Cases. International Journal of Neuroscience (2010) 120:6

Bisinotto F, Dezena R, Abud T et al. Cerebral venous thrombosis after spinal anesthesia: case report. Brazilian Journal of Anesthesiology (2017) 67:3 305-310

Kabore R, Ouiminga H, Lompo L, et al. Cerebral Venous Thrombosis: A Rare Complication of Spinal Anesthesia. World Journal of Neuroscience > (2021) 11:11

Poteau S, Genis A, and Kumaraswami S. Postdural puncture headache and cerebral venous thrombosis in obstetric anaesthesia British Journal of Anesthesia (2023) 130:2

Coutinho J, Gerritsma J, Zuurbier S, et al. Isolated Cortical Vein Thrombosis: Systematic Review of Case Reports and Case Series Stroke (2014) 45:6

Images/Tables

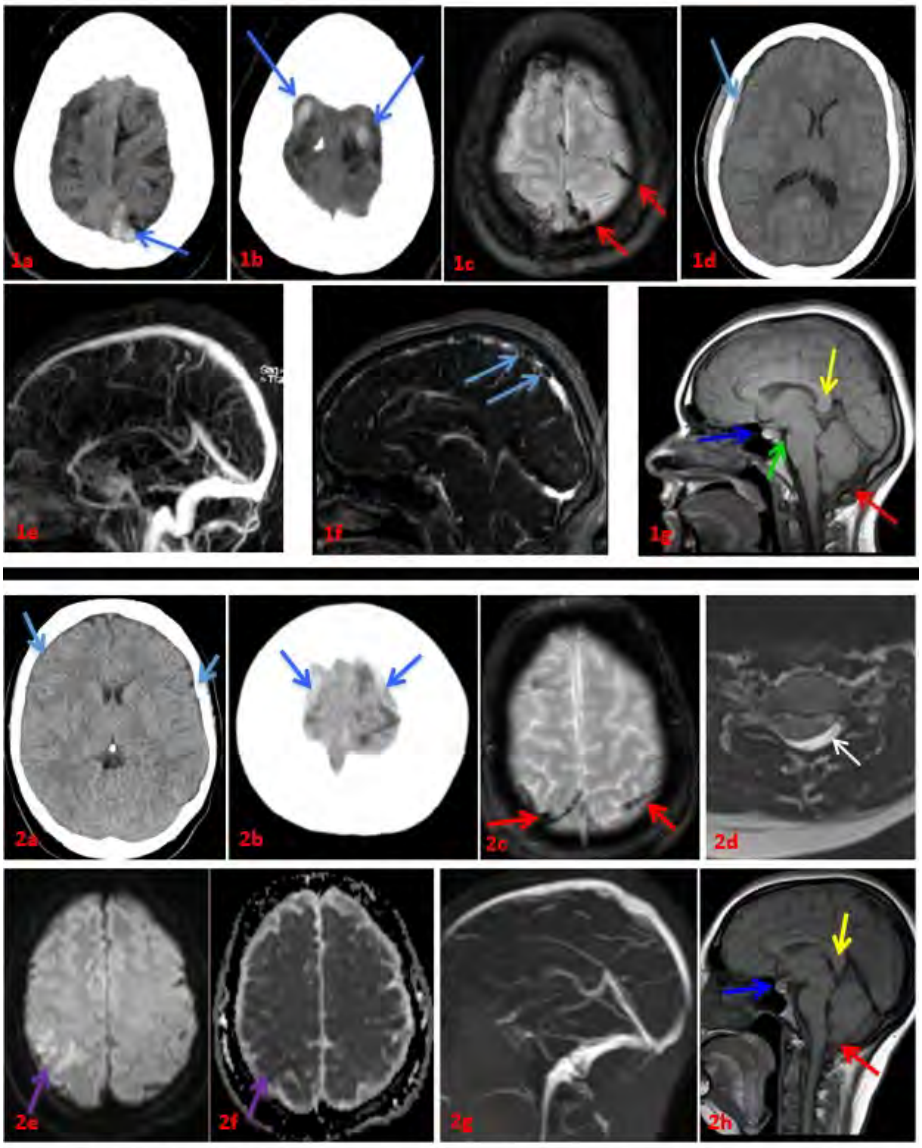


Figure 1 (from first postpartum patient): a-b: Small focal tubular hyperdensities (blue arrows) in the high parasagittal region likely represent thrombosed cortical veins. **c:** Increased susceptibility (red arrows) involving cortical veins in this region are also consistent with cortical venous thrombosis. **d:** Initial head CT demonstrated a right subdural collection of mixed density with acute subdural hematoma superficially and a low density collection deep likely reflecting a subdural hygroma (teal arrow) along the brain surface **e:** Reformatted MRV image demonstrates patency of dural venous sinuses. **f:** Parasagittal source image demonstrates thrombus in adjacent cortical veins (light blue arrows). **g:**T1 sagittal images demonstrate a relatively "closed" pons-midbrain angle (green arrow), splenium depressing the internal cerebral veins and vein of Galen junction (yellow arrow), and relative herniation of the cerebellar tonsils (red arrow), all of which are findings consistent with intracranial hypotension. Prominence of the pituitary (blue arrow) can be attributed to postpartum state and/or another finding of intracranial hypotension.

Figure 2 (from second postpartum patient: a: Initial head CT showed thin bilateral subdural collections (light blue arrows). **b:** Tubular hyperdensities (blue arrows) along the vertex bilaterally (blue arrows) and c: foci of increased susceptibility on gradient images (red arrows) involving cortical veins bilaterally, highly suspicious for thrombosed cortical veins. **d:** Small epidural collection along the dorsal epidural surface of the cervical spine (white arrow), shown here at the level of C6. **e-f:** Restricted diffusion in the right parietal lobe, near a thrombosed cortical vein, consistent with venous infarct. **g:** Reformatted MRV image demonstrates patency of dural venous sinuses. **h:** T1 sagittal images demonstrate splenium depressing the internal cerebral veins and vein of Galen junction (yellow arrow), relatively low-lying cerebellar tonsils (red arrow), and prominent pituitary (blue arrow).

718

The Cerebellum's Silent Rebellion: When Brain Injuries Trigger a Crossed Circuit!

Ayimen Khalid Khan MBBS, Tarek Daoud MBBCh, Ramin Hamidi DO, Mohiuddin Hadi MD
University of Louisville, Louisville, Kentucky, USA

Abstract Category

Adult Brain

Clinical History

A 90-year-old African-American male with a medical history of hypertension (HTN), prostate disease, and atrial flutter, previously not on anticoagulation, presented with acute stroke symptoms, including right gaze deviation, aphasia/dysarthria and hemiplegia. EKG showed atrial flutter with variable AV block,
left axis deviation, right bundle branch block and an old inferior wall infarct. Imaging confirmed an occlusion in the right middle cerebral artery (MCA). He underwent a mechanical thrombectomy with two passes, targeting the right MCA M1 segment.

Imaging Findings

Acute infarct involving right MCA distribution. On the perfusion images, there is diminished perfusion in the right MCA territory as well as the ACA territory in addition to diminished perfusion in the left lobe of the cerebellum consistent with crossed cerebellar diaschisis.

Discussion

This educational exhibit aims to enhance understanding of *crossed cerebellar diaschisis (CCD)*, a phenomenon characterized by reduced cerebellar activity secondary to a supratentorial lesion on the contralateral side. The exhibit highlights the pathophysiology and radiological imaging findings associated with CCD in patients with cerebral hemispheric damage. CCD is frequently observed in cases of ischemic stroke but can also be associated with tumors, traumatic brain injuries, and other focal brain lesions. CCD is believed to occur due to disruption in corticopontocerebellar pathways, leading to diminished input and subsequent metabolic depression in the contralateral cerebellum.

Teaching Point

1. Define and understand the concept of *crossed cerebellar diaschisis (CCD)*.
2. Review the pathophysiology of CCD in relation to cerebral infarcts and other supratentorial injuries.
3. Illustrate the radiological characteristics of CCD.

References

Strother MK et al. Crossed cerebellar diaschisis after stroke identified noninvasively with cerebral blood flow-weighted arterial spin labeling MRI. *Eur J Radiol*. 2016; 85(1):136-42. doi: 10.1016/j.ejrad.2015.11.003

Zhang M et al. Characteristics of cerebral perfusion and diffusion associated with crossed cerebellar diaschisis after acute ischemic stroke. *Jpn J Radiol*. 2020; 38(2):126-34. doi: 10.1007/s11604-019-00898-0

Chen S et al. Crossed cerebellar diaschisis detected by arterial spin-labeled perfusion magnetic resonance imaging in subacute ischemic stroke. *J Stroke Cerebrovasc Dis*. 2014; 23(9):2378-83. doi: 10.1016/j.jstrokecerebrovasdis.2014.05.009

Images/Tables

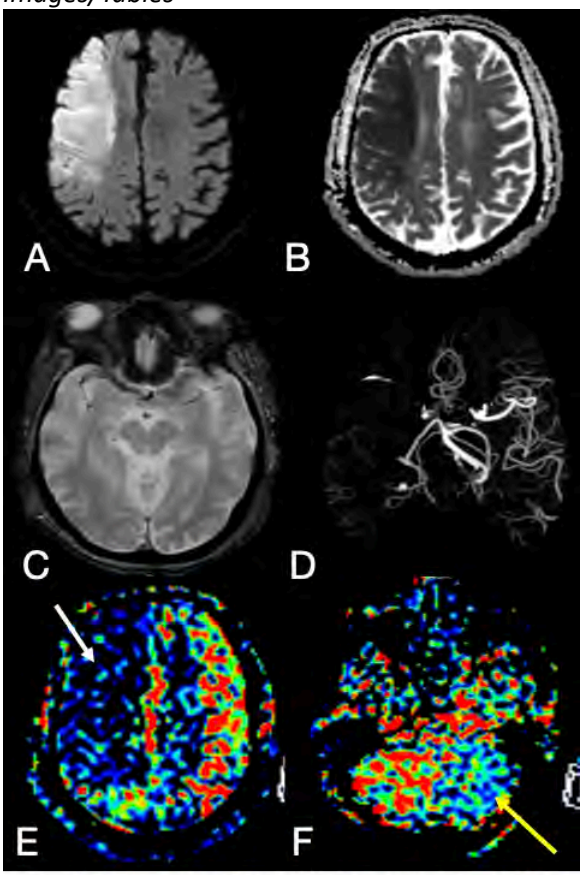


Figure 1: Diffusion images in (A) demonstrate right MCA distribution acute-subacute infarct which is confirmed on (B) ADC maps as dark signal. In (C), there is susceptibility blooming artifact along the expected course of the right MCA consistent with right MCA large vessel occlusion. The 3D reconstruction of the circle of Willis on the time of flight MRA confirms this as diminished flow related enhancement of the right MCA. Finally in (E) and (F), crossed cerebellar diaschesis is manifest as an area of relative diminished perfusion in the right MCA infarct bed (white arrow) as well as the left lobe of the cerebellum (yellow arrow).

737

Pituitary Abscess: a rare but life-threatening condition.

Jose Gavito Higuera MD
University of Texas Health Sciences Center Houston, Houston, Texas, USA, Houston, Tx, USA

Abstract Category

Adult Brain

Clinical History

43-year-old female presented to the ER with worsening headaches and nausea over the past week.

Past medical history of chronic rhinosinusitis, s/p bilateral functional endoscopic sinus surgery one year ago, also chronic lumbar pain syndrome with spinal stimulator that was complicated by infection and removed 6 months ago.

An MRI (Magnetic Resonance Imaging) showed a sellar/suprasellar ring enhancing lesion, suspicious for an abscess. Therefore, patient undergo an endoscopic hypophysectomy with the ENT and the Neurosurgery service, confirming diagnosis.

Imaging Findings

MRI is the modality of choice for evaluating a patient suspected of having a pituitary abscess. It typically involves the sella turcica and the pituitary gland, but may also extend beyond the pituitary fossa and adjacent structures.

It will demonstrate features of an abscess, with Hypointense signal on T1W-images, hyperintense on T2W- images, with peripheral (ring) enhancement, and internal restricted diffusion on DWI and low ADC values, reflecting the presence of purulent content, because it is a viscous fluid consisting of inflammatory cells, debris, and macromolecules such as fibrinogen.
The abscess can cause compression of adjacent structures, such as the optic chiasm, leading to symptoms like visual disturbances. It may also cause sellar expansion.

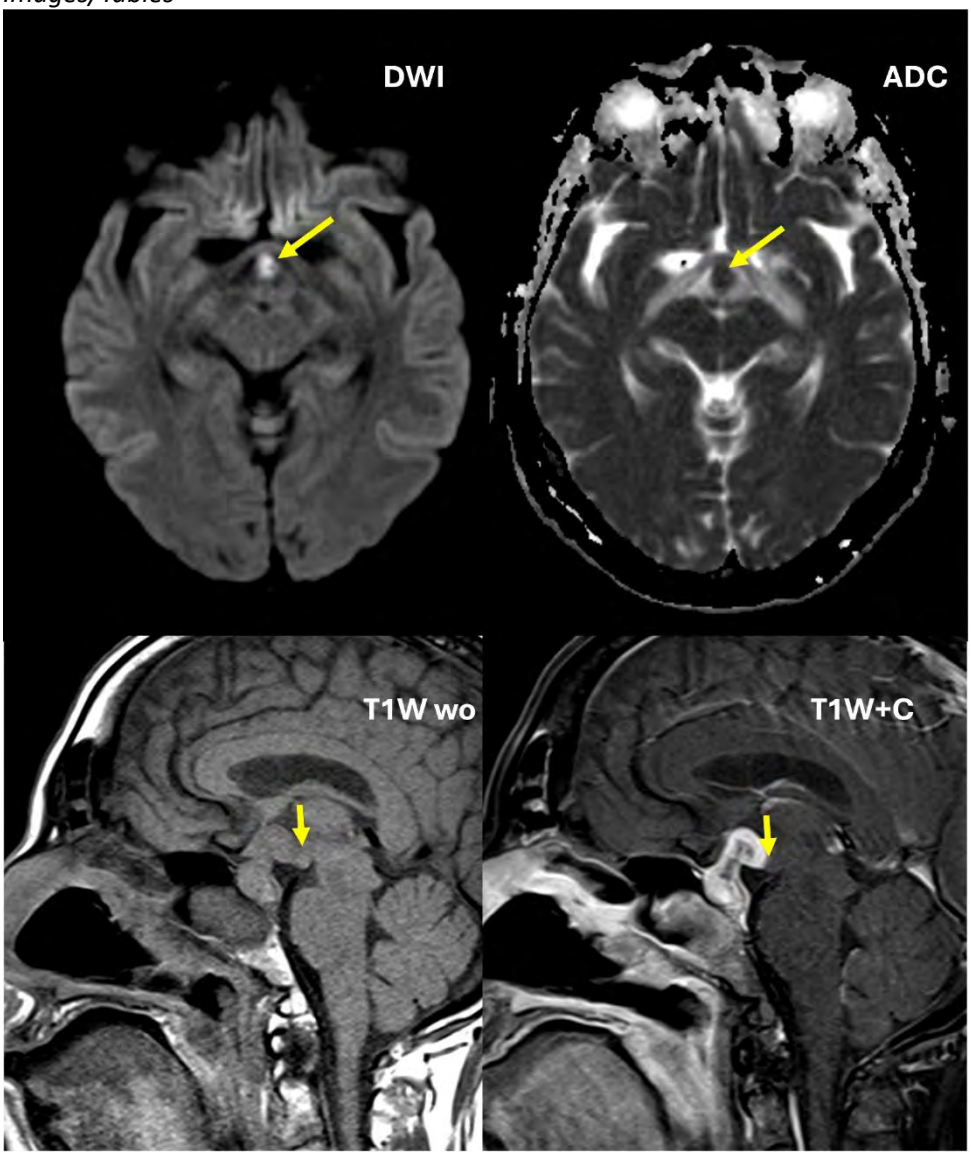
Discussion
Pituitary abscess (PA) is a rare but life-threatening condition, representing less than 1% of pituitary lesions [(1)], and is defined by the presence of an infected purulent collection within the sella turcica.
PA can be classified into 2 types: primary and secondary. The primary type develops in a previously normal pituitary gland (accounting for 70% of cases), and the secondary type when there is associated a pre-existing sellar pathology such as pituitary adenoma, Rathke's cleft cysts, or craniopharyngioma, with or without a recent history of surgery.
It can be observed because of the hematogenous spread of infection adjacent to the sellar region, such as sphenoid sinusitis or dental infection. In addition, there are possible risk factors, such as previous surgical or irradiation interventions, sepsis, local infection, or diabetes mellitus.
A preoperative diagnosis can be challenging, but these imaging characteristics, can lead to an efficient surgical and medical management that will result in a lower mortality.
When cultures are positive, the following micro-organisms can be seen: Gram-positive pathogens, including Staphylococcus Aureus (as in our case) or the Streptococcus species. However, almost half of the cultures can be negative [(3)].

Teaching Point
Pituitary abscess remains an uncommon clinical condition, and it should be considered in patients with rim-enhancing sellar cystic mass, with clinical manifestation of headaches, visual disturbances, and pituitary endocrine abnormalities, especially with a history of infectious disease of the sellar or an adjacent region, sinusitis, or transsphenoidal surgery. An efficient surgical and medical management will result in a lower mortality.
In more than half of the cases, the diagnosis is retrospective, since presurgery suspicion in some cases is extremely difficult due to overlapping clinical signs, variable symptoms, and imaging and laboratory findings related to other sellar lesions.

References

1. Chaichana K, Larman T, Salvatori. Pituitary abscess with unusual MRI appearance. Endocrine. 2016;54(3):837-8.
2. Gao L, Guo X, Tian R, *et al.* Pituitary abscess: clinical manifesta- tions, diagnosis and treatment of 66 cases from a large pituitary center over 23 years. *Pituitary*. 2017;20(2):189-194. Doi: 10. 1007/s11102-016-0757-7
3. Mallereau, C.-H.; Todeschi, J.; Ganau, M.; Cebula, H.; Bozzi, M.T.; Romano, A.; Le Van, T.; Ollivier, I.; Zaed, I.; Spatola, G.; et al. Pituitary Abscess: A Challenging Preoperative Diagnosis—A Multicenter Study. *Medicina*2023,*59*,565. https:// doi.org/10.3390/medicina59030565

Images/Tables



738

Cochlear-Carotid Interval Dehiscence - A Rare Cause of Third Mobile Window Syndrome

Christopher Trepanier[1], Nahill Matari[1], Ernst Garcon[1], Devin Feng[2], Gul Moonis[3], Anil Lalwani[1]
[1]Columbia University Irving Medical Center, New York, New York, USA. [2]McGill University, Montreal, Quebec, Canada. [3]New York University Langone Health, New York, New York, USA

Abstract Category

Head & Neck

Clinical History

A 39-year-old female presented to the otolaryngology office for right conductive hearing loss, bilateral pulsatile tinnitus and sound-induced vertigo. She had no relevant medical or surgical history and was not on ototoxic medications. Family history was negative for early hearing loss. On the physical exam, the Rinne test was normal, and the Weber test localized to the right ear, consistent with right conductive hearing loss. Binocular microscopy of the ears showed normal tympanic membranes and middle ear cavities on both sides. An audiogram demonstrated a small air-bone gap on the right consistent with mild conductive hearing loss. MRI of the internal auditory canals was performed to rule out retro-cochlear pathology and a CT temporal bone was obtained to evaluate for a potential cause of conductive hearing loss.

Imaging Findings

MRI of the internal auditory canals with and without intravenous contrast was initially performed. There was no evidence for labyrinthitis or vestibular schwannoma. A subsequent CT scan of the temporal bones demonstrated

bilateral cochlear-carotid interval (CCI) dehiscence dehiscence involving the apical turn of the cochlea. No other abnormalities were present.

Discussion

The CCI is described as the region of bone between the basal or apical turn of the cochlea and the petrous internal carotid artery [1].]. In this case, while there was CCI dehiscence present, it involved the apical rather than the more commonly affected basal turn. This is a notable and uncommon occurrence, as dehiscence in the apical turn of the cochlea is much rarer compared to the basal turn, which is likely more prone to dehiscence due to its proximity to the internal carotid artery. The discovery of CCI dehiscence in this patient serves as a potential explanation for her symptoms of conductive hearing loss, pulsatile tinnitus and noise-induced vertigo, which are classically seen with the "third mobile window" syndrome. Normally, sound waves travel through the oval window in the middle ear through the cochlea and out of the round window, where they stimulate hearing. However, with a dehiscence present, some of this energy is diverted to a "third window", leading to decreased vibratory transmission [2, 3]. The most common cause of this phenomenon is usually superior semicircular canal dehiscence, however, in this patient the absence of other imaging abnormalities favors her CCI dehiscence as the likely cause. Although assessment of the CCI may not be a routine part of temporal bone CT reporting, recognizing this finding is crucial for diagnosis and treatment. Further research on similar cases is needed to enhance our understanding of the impact of CCI dehiscence on auditory health.

Teaching Point

CCI dehiscence involving either the basal or apical turn of the cochlea may be a rare contributor to third mobile window symptoms, akin to superior semicircular canal dehiscence, and should be included in the CT temporal bone search pattern, particularly when other abnormalities are not present.

References

1. Young, R.J., et al., The cochlear-carotid interval: anatomic variation and potential clinical implications. *AJNR Am J Neuroradiol*, 2006. 27(7): p. 1486-90.
2. Shoman, N.M., R.N. Samy, and M.L. Pensak, Contemporary Neuroradiographic Assessment of the Cochleo-Carotid Partition. *ORL J Otorhinolaryngol Relat Spec*, 2016. 78(4): p. 193-8.
3. Ho, M.L., et al., Spectrum of Third Window Abnormalities: Semicircular Canal Dehiscence and Beyond. *AJNR Am J Neuroradiol*, 2017. 38(1): p. 2-9.

748

Uncommon Presentation: Mantle Cell Lymphoma with Pineal Mass and Leptomeningeal Spread

Donna Parizadeh MD MPH, Ahmed W Moawad MD, Christian Pedersen MD

Trinity Health Midatlantic/Mercy Catholic Medical Center, Darby, PA, USA

Abstract Category

Adult Brain

Clinical History

A 62-year-old male with a history of previously treated mantle cell lymphoma (MCL) presented with symptoms including headaches, disorientation, right-sided hearing loss, and tinnitus. His mantle cell lymphoma (MCL) was managed with initial chemotherapy regimens, followed by a BEAM autologous stem cell transplant, and Rituxan maintenance therapy completed 2 years prior to presentation. Upon admission, MRI revealed a pineal mass and leptomeningeal enhancement concerning for lymphoma. Stereotactic biopsy and cerebrospinal fluid (CSF) analysis confirmed central nervous system (CNS) involvement of MCL. Despite treatment with high-dose methotrexate, the patient experienced complications, including septic shock, and was transitioned to hospice care.

Imaging Findings

Initial CT imaging identified a high-density lesion in the pineal and tectal regions, with narrowing of the cerebral aqueduct and mild ventriculomegaly suggesting early hydrocephalus. MRI further characterized a well-circumscribed mass in the pineal region, showing isointense T1, hyperintense T2/FLAIR signals (Fig A, arrow), homogeneous enhancement (Fig B), and restricted diffusion (Fig C and D). The mass caused mass effect on the tectum and abutted the third ventricle, with peripheral calcifications noted on CT. MRI also highlighted confluent periventricular hyperintense signals on DWI (Fig C), faint enhancement, and mild enlargement of the pituitary gland (Fig E, arrow), suggestive of lymphomatous involvement. Leptomening

Discussion

Secondary CNS involvement occurs in about 10–15% of non-Hodgkin lymphoma (NHL) cases, primarily in relapsed patients. MCL, an aggressive NHL subtype, has a propensity for CNS involvement, although its clinical course is not well documented. MRI is essential for assessing parenchymal involvement, as CSF analysis is often insensitive without leptomeningeal disease. Conducting contrast enhanced MRI before CSF analysis helps avoid false-positive results due to lumbar puncture irritation. Leptomeningeal conditions typically present with symptoms across multiple sites, such as cranial nerve palsies and lumbosacral radiculopathies. CNS infiltration often occurs hematogenously, affecting areas like the pineal gland, which lacks a strong blood-brain barrier. Leptomeningeal spread is particularly concerning due to its poor prognosis and limited treatment options, manifesting as diffuse meningeal infiltration with characteristic MRI enhancements and indicating systemic involvement, which is linked to decreased survival rates.

Teaching Point

CNS involvement in MCL can present with headaches, neurological deficits, and altered mental status from CNS infiltration. Diagnosing leptomeningeal involvement is challenging and often requires CSF cytopathological evaluation, with flow cytometry enhancing detection sensitivity. When MCL presents as a pineal mass, primary CNS lymphomas, mainly diffuse large B-cell type, should be considered in differential diagnoses. Managing CNS involvement in MCL is complex, typically involving chemotherapy, targeted therapies, and sometimes radiation. Recent advancements, such as ibrutinib, show promise in improving patient outcomes. Prompt recognition and intervention are crucial for CNS involvement in MCL, emphasizing the need for ongoing research into effective treatments due to the unique pathophysiological challenges of MCL and leptomeningeal disease.

References

McLaughlin N, Wang Y, Witzig T, et al. Central nervous system involvement by mantle cell lymphoma. Leuk Lymphoma 2022;64:371-377. doi: 10.1080/10428194.2022.2148211.

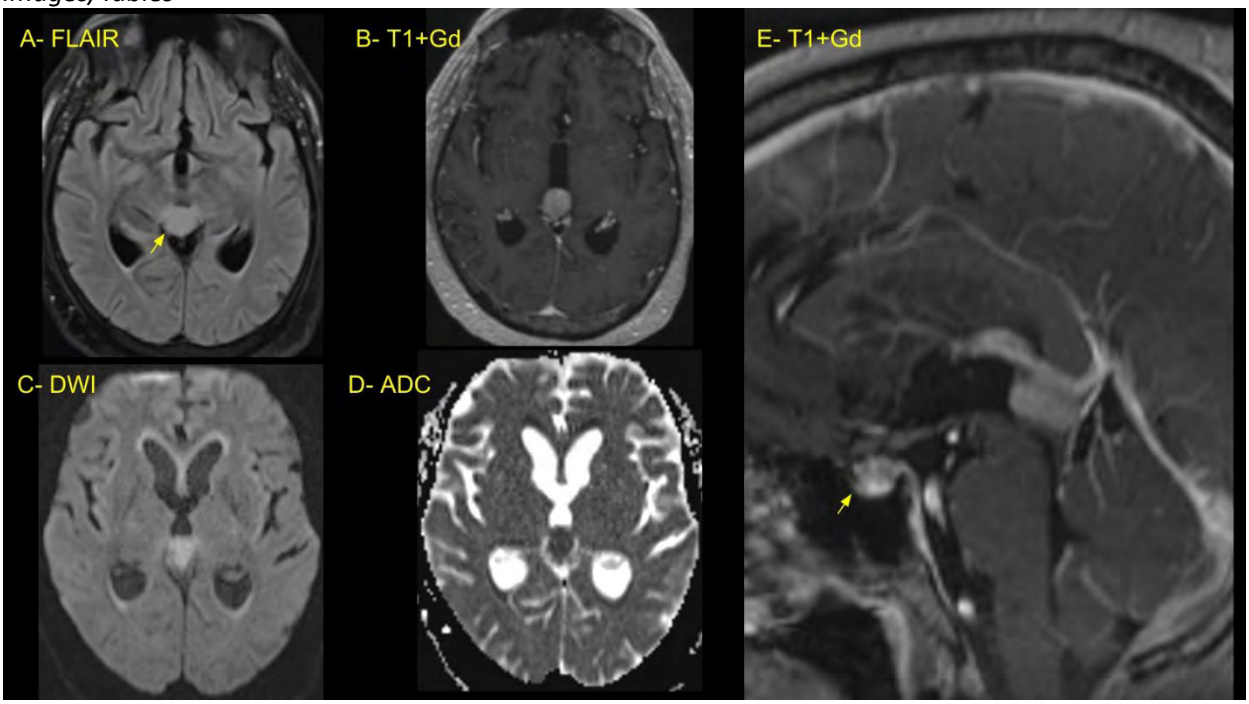
Cheah CY, George A, Giné E, et al. Central nervous system involvement in mantle cell lymphoma: clinical features, prognostic factors and outcomes from the European Mantle Cell Lymphoma Network. Ann Oncol 2013;24:2119-2123. doi: 10.1093/annonc/mdt139.

Keraliya AR, Krajewski KM, Giardino AA, et al. Imaging of nervous system involvement in hematologic malignancies: what radiologists need to know. AJR Am J Roentgenol 2015;205:604-617.

Rusconi C, Ferrero S, Croci GA, et al. Ibrutinib improves survival compared with chemotherapy in mantle cell lymphoma with central nervous system relapse. Blood 2022;140:1907-1916.

Hegde U, Filie AC, Little RF, et al. High incidence of occult leptomeningeal disease detected by flow cytometry in newly diagnosed aggressive B-cell lymphomas at risk for central nervous system involvement: the role of flow cytometry versus cytology. Blood 2005;105:496-502.

Images/Tables



769

MVNT Mimicker: Perivascular Spindle Cell Proliferation with PDGFRA mutation - Novel Entity

Sachin Gangele MD, Anousheh Sayah MD, Emily A Sloan MD, PhD
Medstar Georgetown University Hospital, Washington, DC, USA

Abstract Category

Adult Brain

Clinical History

28-year-old male with worsening headaches for 6 months and no neurological deficits, found to have a right frontal lobe lesion. Although this lesion was diagnosed as a benign multinodular and vacuolating neuronal tumor (MVNT) by imaging, the lesion was ultimately resected due to residual concern for low grade glioma. Final diagnosis was benign perivascular spindle cell proliferation with PDGFRA mutation.

Imaging Findings

Micronodular, bubbly lesion in the subcortical white matter of the right frontal lobe. This lesion demonstrates T2 hyperintensity/T1 hypointensity, lack of contrast enhancement, and completely suppresses on FLAIR sequences.

Discussion

Perivascular spindle cell proliferation with PDGFRA mutation is a recently described entity with a paucity of research. PDGFRA alterations have been described in other neoplasms including gastrointestinal stromal tumor (GIST) and sinonasal spindle cell neoplasm. On imaging, this entity demonstrates a micronodular bubbly area in the subcortical white matter with T2 hyperintensity/T1 hypointensity and lack of contrast enhancement. Since this simulates enlarged perivascular/CSF spaces, there is complete saturation on FLAIR sequences. Of note, this entity may be a correlate for cases diagnosed as giant tumefactive perivascular spaces.

Multinodular and vacuolating neuronal tumor (MVNT) is also a relatively new tumor type, first described in 2013 and included in the 2016 WHO Classification of Tumors of the CNS. This benign entity represents a unique CNS WHO grade 1 neuronal tumor with RAS/RAF/MAPK alterations. On imaging, MVNT has a predilection for the temporal lobes and presents as a micronodular, bubbly area in the subcortical white matter with T2 hyperintensity/T1 hypointensity and lack of contrast enhancement. However, MVNT demonstrates FLAIR hyperintensity, distinguishing it from perivascular spindle cell proliferation, which otherwise has very similar imaging characteristics. Clinically, MVNT can present as a seizure focus.

Both perivascular spindle cell proliferation and MVNT are benign "do not touch" lesions, highlighting the importance of recognizing their unique imaging characteristics.

Teaching Point

Perivascular spindle cell proliferation and MVNT have very similar imaging characteristics: a micronodular bubbly area of T2 hyperintensity/T1 hypointensity in the subcortical white matter without contrast enhancement. However, these entities can be distinguished on FLAIR sequences, with perivascular spindle cell proliferation demonstrating complete saturation on FLAIR and MVNT demonstrating FLAIR hyperintensity.

References

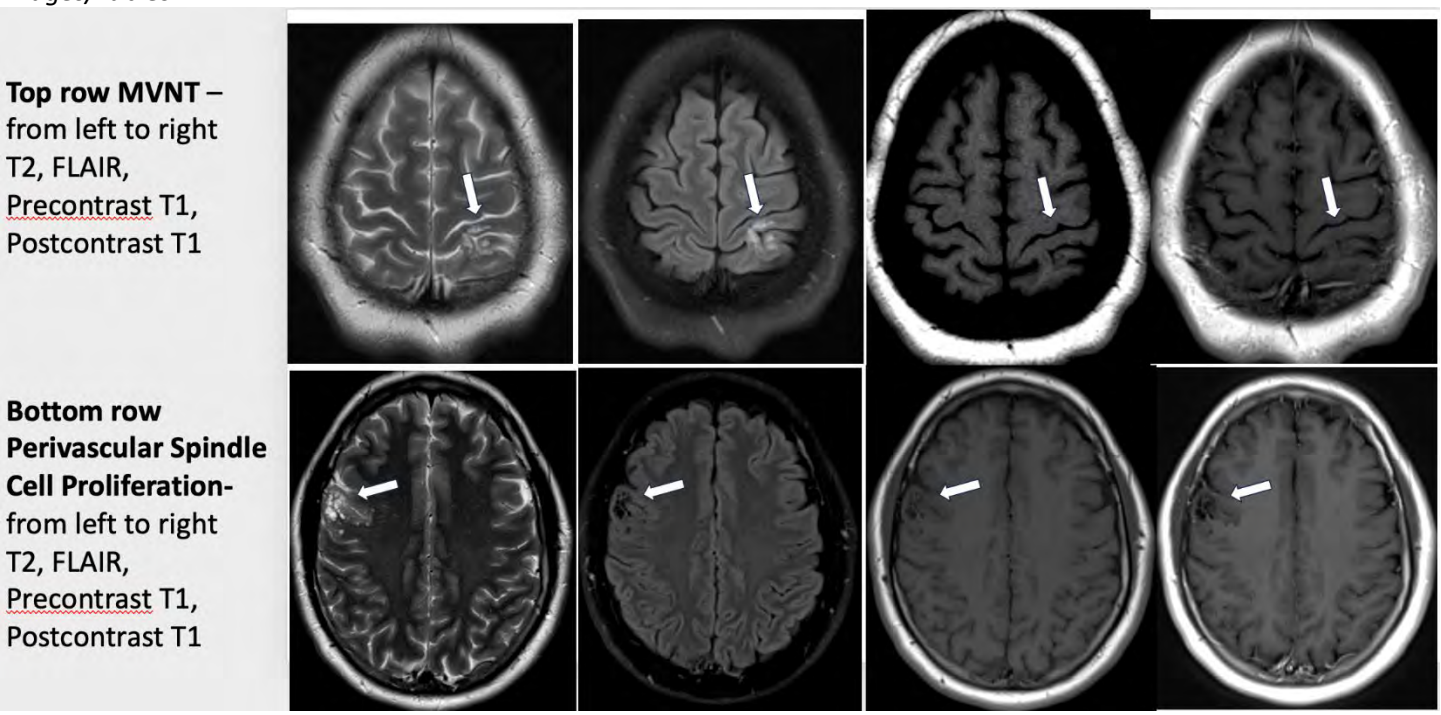
Nunes, R. H., Hsu, C. C., da Rocha, A. J et al. Multinodular and vacuolating neuronal tumor of the cerebrum: A new “leave me alone” lesion with a characteristic imaging pattern. *American Journal of Neuroradiology,* 38(10), 1899–1904. DOI: https://doi.org/10.3174/ajnr.a5281

Komori T. The 2016 WHO Classification of Tumours of the Central Nervous System: The Major Points of Revision. *Neurologia medico-chirurgica*, 57(7), 301–311. DOI: https://doi.org/10.2176/nmc.ra.2017-0010

Torp, S. H., Solheim, O., Skjulsvik, A.J. The WHO 2021 Classification of Central Nervous System Tumors: A practical update on what neurosurgeons need to know - a minireview. *Acta Neurochirurgica,* 164(9), 2453–2464. DOI: https://doi.org/10.1007/s00701-022-05301-y

Pekmezci, M., Stevers, M., Phillips, J. J. et al. Multinodular and vacuolating neuronal tumor of the cerebrum is a clonal neoplasm defined by genetic alterations that activate the MAP kinase signaling pathway. *Acta Neuropathologica*, 135(3), 485–488. DOI: https://doi.org/10.1007/s00401-018-1820-4

Images/Tables



770

Spinal Neurocysticercosis: A Case Series

Elaina T Van Patten MD, Sarah Ceglar MD, James Vu MD, Ricardo Paez MD
Harbor UCLA, Torrance, CA, USA

Abstract Category

Spine

Clinical History

This case series will present 3 cases of spinal neurocysticercosis (NCC) ranging in age from 20 to 68 years-old presenting with symptoms of low back pain and/or cauda equina syndrome. One patient had a history of remote CNS NCC, while the other two were diagnosed based on imaging combined with lumbar puncture or surgical biopsy.

Imaging Findings

A: Case 1: Sagittal FIESTA, Multiple intradural, extramedullary cysts within the lower lumbar spine.
B: Case 2: Axial T2WI, Clumped, peripherally displaced nerve roots creating an “empty thecal sac” sign.
C: Case3: Sagittal T1, Lumbar spinal lesions.
D: Case 3: Sagittal T1 Postcontrast, Lumbar spinal lesions with peripheral enhancement.

Discussion

Spinal NCC is rare, accounting for only 1.5% of NCC cases (1), and often seen in the setting of active intracranial neurocysticercosis. The MRI findings of spinal NCC can be non-specific, with a broad range of differential considerations including other infectious lesions (hydatid cysts, tuberculosis), congenital cysts, post-traumatic syrinx, leptomeningeal carcinomatosis, and other causes of arachnoiditis. This case series will review the typical imaging features and discuss the importance of a multidisciplinary approach to diagnosis and treatment of spinal NCC.

Teaching Point

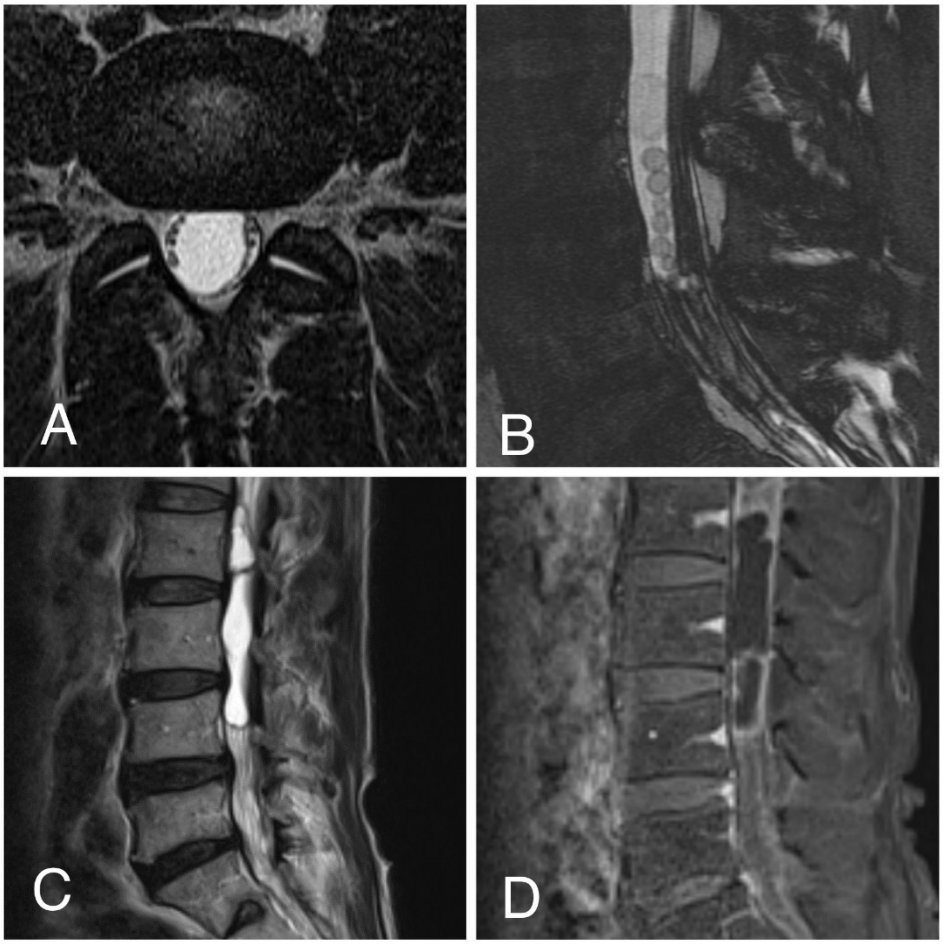
1. Review the epidemiology and clinical presentation of spinal NCC.
2. Present the imaging characteristics and differential considerations for spinal NCC.
3. Discuss the treatment, monitoring, and prognosis for spinal NCC.

References

- Eric T. Kimura-Hayama , Jesus A. Higuera , Roberto Corona-Cedillo , Laura Chavez-Macias , Anamari Perochena , Laura Yadira Quiroz-Rojas , Jesus Rodriguez-Carbajal , and Jose L. Criales. Neurocysticercosis: Radiologic-Pathologic Correlation. RadioGraphics 2010 30 : 6 , 1705-1719 DOI: https://doi.org/10.1148/rg.306105522

- C C Leite, J R Jinkins, B E Escobar, A C Magalhães, G C Gomes, G Dib, S A Vargas, C Zee, and A T Watanabe. MR imaging of intramedullary and intradural-extramedullary spinal cysticercosis. American Journal of Roentgenology 1997 169:6, 1713-1717 DOI: https://doi.org/10.2214/ajr.169.6.9393195
- White, A. C., Coyle, C. M., Rajshekhar, V., Singh, G., Hauser, W. A., Mohanty, A., Garcia, H. H., & Nash, T. E. (2018). Diagnosis and treatment of neurocysticercosis: 2017 clinical practice guidelines by the Infectious Diseases Society of America (IDSA) and the American Society of Tropical Medicine and Hygiene (ASTMH)1. Clinical Infectious Diseases, 66(8), 1159–1163. DOI: https://doi.org/10.1093/cid/ciy157

Images/Tables



779

Hiding in Plain Sight? Persistent IGF-1 Elevation in a Patient with Acromegaly and Transvenous Extension of PitNET

Charles Tandler MD, Scott Soltys MD, Juan Fernandez-Miranda MD, Nancy Fischbein MD
Stanford University, Palo Alto, CA, USA

Abstract Category

Adult Brain

Clinical History

A 48-year-old female had a one-year history of 40-pound weight gain, carpal tunnel syndrome, and hyperglycemia. MRI demonstrated a large sellar/suprasellar mass with bilateral cavernous sinuses and retroclival venous plexus/intercavernous sinus invasion (Figure A), consistent with a pituitary neuroendocrine tumor (PitNET). Insulin-like growth factor-1 (IGF-1) was 493 ng/ml (normal ≤227 ng/ml). Despite an initial subtotal endoscopic resection, a second endoscopic resection, and proton beam radiation (PBR), IGF-1 remained persistently elevated. MRI two years after the second resection demonstrated tumor filling/expanding the bilateral inferior petrosal sinuses (IPS) (confirmed on DOTATATE-PET/CT), and retrospective review of prior studies demonstrated tumor progressively involving the bilateral IPS and not included in the PBR treatment field. On the basis of the MRI findings, the patient completed a 2-plan

CyberKnife radiosurgical procedure, with a single 22 Gray fraction administered to each site of persistent/progressive disease in the IPS/jugular foramen.

Imaging Findings

A: Initial sagittal T1WI+C: homogeneously enhancing sellar/suprasellar mass with involvement of the intercavernous sinus/retroclival venous plexus (arrow)

B: Initial coronal T1WI+C: normal venous enhancement in the bilateral inferior petrosal sinuses (arrows)

C: Follow-up coronal T1WI+C, four years after A: persistent/progressive tumor now fills and expands the bilateral IPS (arrows), extending to the bilateral jugular bulb level (J)

D: Diagram of central skull base venous anatomy, with bilateral inferior petrosal sinuses indicated (arrows)

Discussion

Large PitNETs are not usually a diagnostic dilemma, as a lobulated sellar/suprasellar mass with cavernous sinus invasion, mass effect on the optic apparatus and pituitary stalk, and extension into the anterior, middle, and/or posterior fossa has a limited differential diagnosis. Though PitNETs are not typically diagnostically challenging, the cause of persistently elevated endocrine laboratory values in the post-operative setting can be difficult to determine. This warrants a thorough understanding of the potential patterns of spread of PitNETs in order to provide a checklist of sites to scrutinize for residual tumor, thereby improving surgical and radiation planning.

Classic pathways of PitNET extension include frontal, temporal, and posterior subtentorial extension, hypothalamic extension, cavernous sinus extension, and pharyngeal extension [2]. While direct osseous extension/erosion is often observed, with tumor extension into the clivus and paranasal sinuses for example, remote transvenous extension is not. The IPSs are paired dural venous channel that drain from the posteroinferior aspect of the cavernous sinus to the jugular foramen/jugular bulb [1]. Extension of PitNET in the IPS to the jugular foramen is a potential pattern of spread that can account for failure to control endocrinopathy in patients with PitNETs that have invaded the cavernous sinuses and retroclival venous plexus. In the literature, there is only one case report of unilateral invasion [2], however, and, to our knowledge, no report of bilateral inferior petrosal sinus invasion.

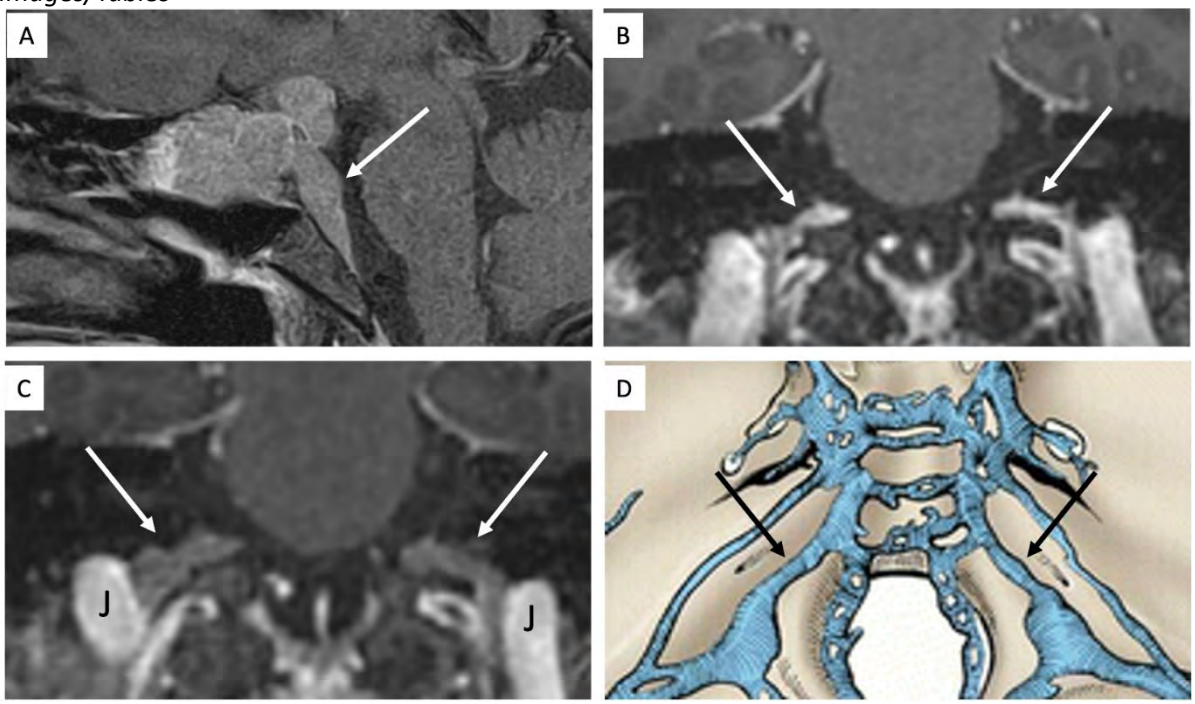
Teaching Point

We present a rare case of bilateral invasion of PitNET into the IPS with spread to the bilateral jugular foramina, highlighting the importance of understanding dural venous anatomy and scrutinizing venous pathways in the setting of persistent endocrinopathy following treatment of PitNET.

References

1. Mortazavi MM, Griessenauer CJ, Krishnamurthy S, et al. The inferior petrosal sinus: a comprehensive review with emphasis on clinical implications. Childs Nerv Syst 2014; 30:831-834.
2. Kuo AH, Nuñez DB. Giant Pituitary Adenoma With Inferior Petrosal Sinus, Jugular Foramen, and Hypoglossal Canal Extension. JAMA Otolaryngol Head Neck Surg 2020; 146:82-84.

Images/Tables



806

Post-Operative Recurrence of Spinal AVM

Matthew Hammer MD[1], Joseph Kim MD[1], Neal Shukla MD[1], Ramtin Hajibeygi MD[2], Richard Lozano BS[1], Long Tu MD, PhD[1]
[1]Yale New Haven Hospital, New Haven, CT, USA. [2]Tehran University of Medical Sciences, Tehran, Iran, Iran, Islamic Republic of

Abstract Category

Pediatrics

Clinical History

A 17-year-old male with a history of C4-C7 AVM status post embolization and partial resection, who was post-operatively asymptomatic for 10 years, initially presented to the emergency department with left upper extremity paresthesia after exercise. Over the course of his hospitalization, his symptoms progressed to bilateral lower extremity paresthesia and upper extremity hyperreflexia and clonus. Lab values and vitals were unremarkable. Neurosurgery was consulted and imaging was ordered to further evaluate symptoms. The patient was found to have recurrent cervical medullary AVM.

Imaging Findings

MRI and MRA cervical spine with and without contrast showed a C3-C4 left-sided intramedullary tangle of serpiginous vessels measuring 1.0 x 0.8 cm with adjacent dilated vascular channels along the dorsal and ventral aspects of the spinal cord. There was associated cord expansion at C3-C4 with associated T2 hyperintensity from C2-C4 reflecting cord edema. There was no evidence of intra-nidal aneurysm or hemorrhage within the limitations of non-gradient sequences. Feeding arteries were difficult to identify but likely originated from an adjacent left radicular or vertebral artery branch.

Discussion

Spinal AVMs are rare vascular lesions within the spinal cord with incidence rates as low as 300 total hospital admissions each year.[3] They are associated with significant neurologic morbidity, including diffuse pain, myelopathy, hemorrhage, and progressive neurologic deficits. They are characterized by abnormal connections between arteries and veins, either bypassing the capillary system or passing through a dysplastic capillary bed. Using the Takai classification system, spinal AVMs can be classified based on their shunt location into types 1-5: dural arteriovenous fistula (AVF), intradural intramedullary glomus AVM, intramedullary juvenile AVM, peri medullary AVF, extradural AVF.

Type 2 spinal AVM, the intradural intramedullary glomus AVM, is most commonly seen within the thoracolumbar spinal cord and is most commonly seen in young adults in their mid-20s.[1, 3] They are usually treated with resection and/or embolization, with recurrence rates reported as low as 2.3% and 27.7% for resection and embolization respectively.[2]

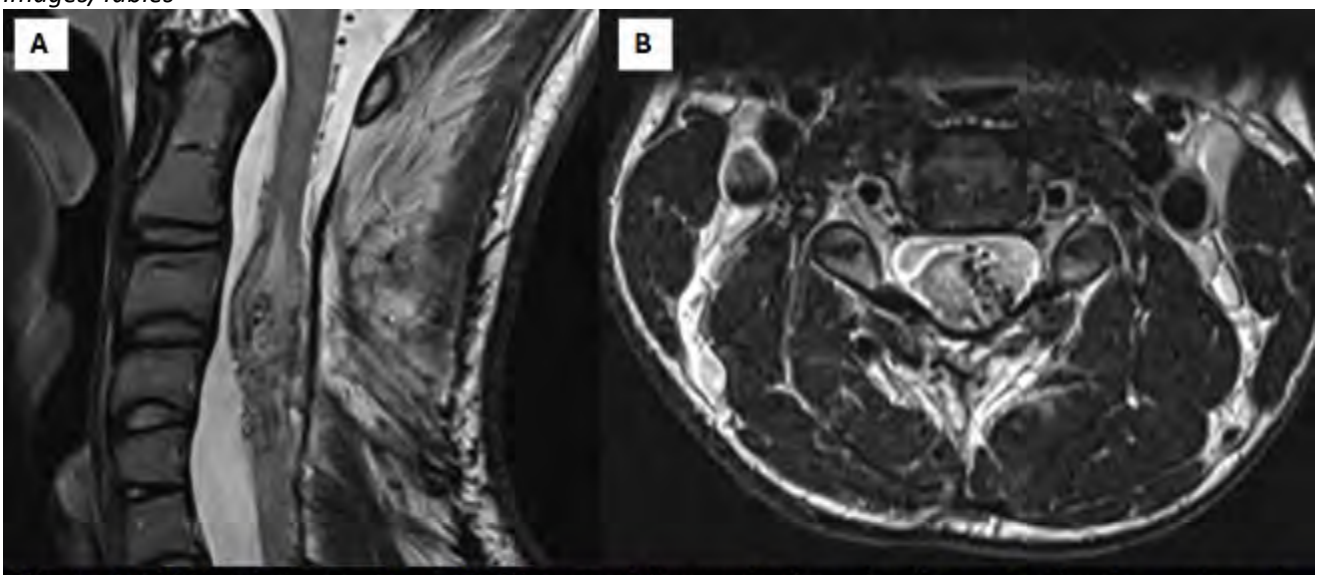
Teaching Point

Although spinal AVM recurrence is uncommon after treatment, especially after surgical resection, it remains an etiology to be wary of in a patient with a history of spinal AVM and new onset neurological symptoms. This case reminds us that type 2 spinal AVMs can occur anywhere throughout the spinal cord, and MRI/MRA sequences are best equipped to assess local spinal cord changes. Although most type 2 spinal AVMs are diagnosed in individuals within their mid-20s, it is important to note that most vascular malformations are present since birth and can manifest at any time during development, as in this patient who presented with initial symptoms at 3 years old.

References

1. Greenberg MS. Handbook of Neurosurgery. Thieme. (2010) ISBN:1604063262.
2. Mamaril-Davis J, Aguilar-Salinas P, Avila MJ, Dumont T, Avery MB. World Neurosurgery. 2023;173:e250-e297. doi:10.1016/j.wneu.2023.02.040.
3. Patchana T, Savla P, Taka TM, Ghanchi H, Wiginton J 4th, Schiraldi M, Cortez V. Spinal Arteriovenous Malformation: Case Report and Review of the Literature. Cureus. 2020 Nov 21;12(11):e11614. doi: 10.7759/cureus.11614. PMID: 33364131; PMCID: PMC7752798.

Images/Tables



A) Sagittal T2 MRI cervical spine shows a C3-C4 intramedullary tangle of vessels with associated cord expansion and C2-C4 cord edema. There is a prominent dilated vessel along the ventral surface of the cord. B) Axial T2 MRI cervical spine shows intramedullary AVM extension from the ventral to dorsal surface.

813

Longitudinally extensive spinal dural effusion reaction to Lutetium-177 PSMA therapy in a patient with metastatic prostate cancer

Cem Bilgin MD, Brian J. Burkett MD, MPH, Brendan W. Lunn MD, Greta B. Liebo MD, Derek R. Johnson MD, Karl N. Krecke MD

Department of Radiology, Rochester, Minnesota, USA

Abstract Category

Spine

Clinical History

A 66-year-old male with extensive lymph node and osseous metastases from prostate cancer presented with worsening right hip pain and right lower extremity weakness starting 2 days after his first cycle of lutetium-177 prostate-specific membrane antigen (Lu-177 PSMA) radiotherapy. He had a known epidural tumor in the lower thoracic vertebra without cord compression, previously treated with radiation. Despite prophylactic corticosteroid administration before the first cycle of Lu-177 PSMA treatment, he reported increasing difficulty with walking and gait instability but did not experience bladder or bowel incontinence or significant sensory deficit. He was admitted to hospital for pain control and evaluated by internal medicine and orthopedic surgery physicians, and his symptoms were initially managed with dexamethasone therapy.

Imaging Findings

The patient underwent MRI of the thoracic and lumbar spine during hospitalization, followed by MRI of the cervical spine the next day. MRI of the spine revealed longitudinally extensive circumferential fluid and gadolinium enhancement related to the dura and subarachnoid space, extending from the craniocervical junction to the L1 vertebral level. This process displaced the spinal cord toward the center of the canal without compression. Findings are most compatible with enhancing subdural effusion (1). Cauda equina roots were located centrally in the thecal sac and arrayed in horizontal orientation throughout the lumbar canal indicating extension of subdural effusion effacing the lumbar subarachnoid space. Extensive sacral and pre-sacral neoplasm, plus therapy effects, were the likely cause of leg pain and weakness.

A surveillance MRI exam five weeks later showed the subdural effusion was little changed, causing effacement of the subarachnoid space without cord compression. The effusion had extended across the craniocervical junction along the clivus and foramen magnum dura. The cauda equina remained centrally located and horizontally arrayed.

Discussion

Lu-177 PSMA therapy is increasingly used in clinical practice to deliver high doses of beta-particle radiation to tumors with PMSA affinity, most commonly prostate cancer. While its safety profile is well established, one can expect to identify uncommon side-effects as use expands. Our case is the first report of a longitudinally extensive dural effusion following Lu-177 PSMA therapy. We hypothesize that beta radiation concentrated in vertebral metastases can cause reactive inflammation in the dura, leading to elaboration of fluid into the intradural or subdural-extra arachnoid spaces. The effusion is under minimal pressure and spreads along the dura in the SI plane and circumferentially until it contacts solid tissue. Such effusions, while extensive, will tend to be minimally symptomatic as the transudate takes up space available.

Teaching Point

Our case shows that longitudinally extensive dural effusion reaction can occur following Lu-177 PSMA therapy to tumors with intimate association with the spinal canal dura. The passive accumulation of fluid, secondary to dural inflammation, is unlikely to cause cord compression. It is important to recognize this process as distinct from epidural tumor spread or metastases. Dural effusion should be considered a “don’t touch” benign manifestation, unless compelling clinical or imaging findings demonstrate otherwise. Successful lumbar puncture in the affected region may be difficult due to collapse of the subarachnoid space.

References

1) Sneyers, Bernard, and Kristof Ramboer. "Spinal subdural hygroma." *Acta Neurologica Belgica* 121.2 (2021): 311-319.

Images/Tables

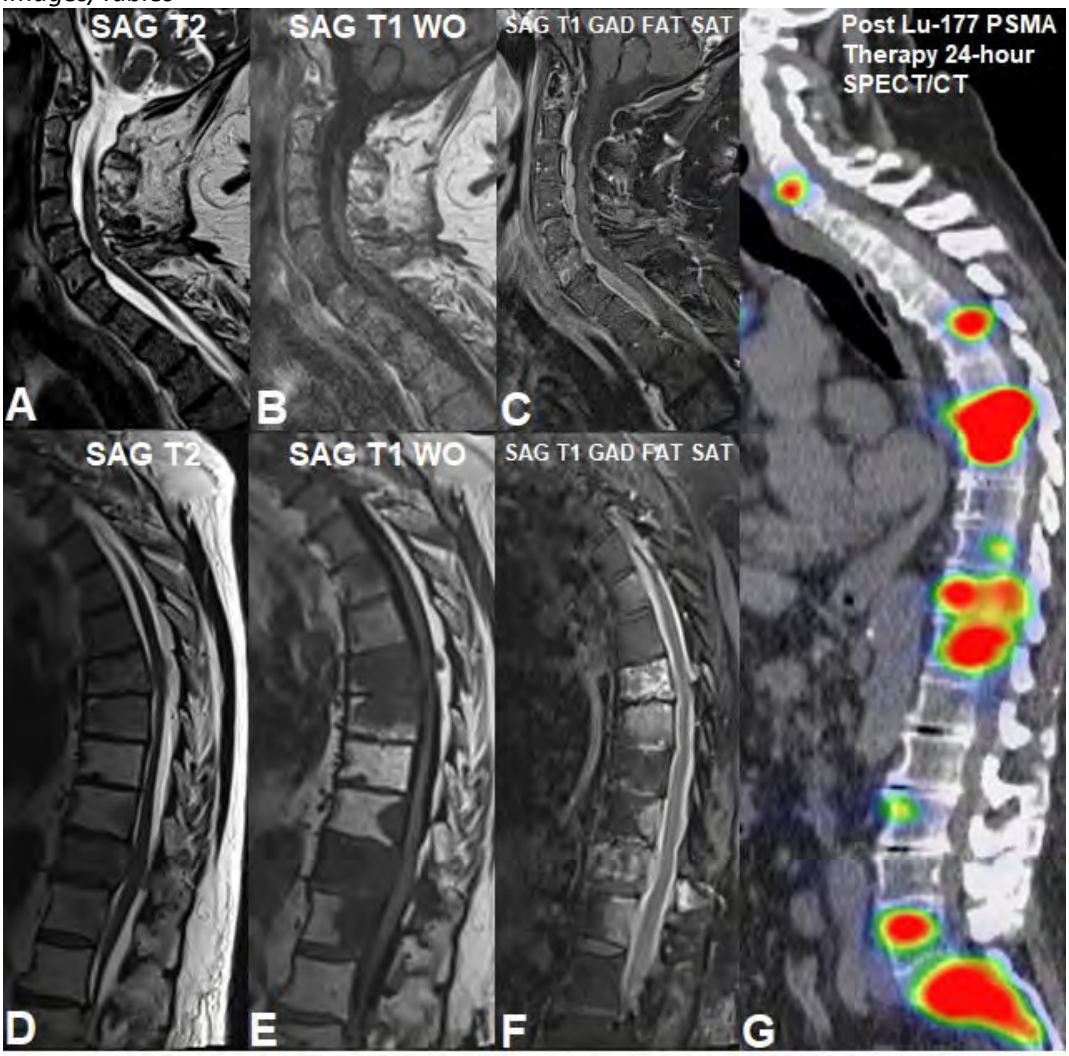


Figure: Sagittal T2-weighted images of the cervical (A) and thoracic (B) spine demonstrate a T2 hyperintense and T1 hypointense (C, D) dural effusion. Sagittal post-contrast fat-saturated T1-weighted images show enhancement of the effusion (E, F). Post Lu-177 PSMA therapy 24-hour SPECT/CT image demonstrates Lu-177 PSMA localization to known bone metastases, with no evident uptake in the dural effusion (G).

815

Primary Focal Intracranial Leptomeningeal Glioma: Two cases with pathology correlates and review of the literature

Lam H Tu DO[1], Sawan Patel MD[1], Ada Baisre de Leon MD[1], Pankaj Agarwalla MD[2], Pankaj Agarwalla MD[1], Hugo F Bueno MD[1], Esther A Nimchinsky MD PhD[1]
[1]Rutgers New Jersey Medical School, Newark, NJ, USA. [2]New Jersey Medical School, Newark, NJ, USA

Abstract Category

Adult Brain

Clinical History

Patient A:

65 year old male referred to ophthalmology for bilateral blurry vision. Ophthalmology then ordered an initial MRI orbits scan. The patient intermittently returned for follow-up imaging over the next 20 months. Patient finally underwent craniotomy and resection of the mass 20 months after initial MRI. Pathology returned as glioblastoma, IDH-wild type. Follow-up imaging 6 months after surgery demonstrated recurrent tumor, and the patient was lost to follow up.

Patient B:

37 year old male with a history of syphilis presented with headaches and left facial weakness, with right facial droop. Provisional working diagnoses included neurosyphilis, neurosarcoidosis and tuberculosis meningitis. Quantiferon, CSF studies returned negative. Initial biopsy was negative for neoplasm. Body and spinal imaging were negative for extracranial malignancy. Repeat biopsy returned as glioblastoma, IDH-wild type. The patient continued to worsen clinically and expired 2 weeks later.

Imaging Findings

Patient A:

Initial MRI orbits showed focal leptomeningeal enhancement in the left frontal lobe. For 9 months, over multiple scans, this enhancement remained leptomeningeal, with progression in extent and thickness. MRI at 20 months after presentation showed a new enhancing intraparenchymal mass surrounding the original leptomeningeal enhancement with markedly increased associated FLAIR signal.

Patient B:

Initial MRI showed leptomeningeal enhancement along the right midbrain and pons and in the left frontal operculum. Over the next 2.5 months, follow-up MRIs showed rapid progression of leptomeningeal enhancement, which progressed to parenchymal enhancement in the right midbrain and pons, as well as right gangliocapsular region and infundibulum. MRI one month later showed further progression of leptomeningeal and parenchymal enhancement.

Discussion

We will show 2 cases of pathology proven primary focal intracranial leptomeningeal glioblastoma. This entity is a very rare variant of glioblastoma that originally presents in the leptomeninges, without appreciable parenchymal mass. Our cases contain MRIs spanning the evolution from only leptomeningeal enhancement to parenchymal mass enhancement, rapid growth thereafter, and perioperative imaging.

Timely diagnosis remains challenging, as leptomeningeal enhancement can mimic meningitis, subarachnoid hemorrhage, metastasis, or other entities such as neurosarcoidosis and tuberculosis infection.

Histopathology remains essential for diagnosis. Timely surgical intervention is the mainstay of treatment. However, the prognosis remains very poor.

Teaching Point

To learn about cases of pathology proven primary focal intracranial leptomeningeal glioblastomas. This rare entity may be a differential consideration especially in an aggressive isolated leptomeningeal enhancing lesion. The aggressive nature of the tumor makes timely diagnosis both challenging and essential for appropriate intervention. Short interval imaging and close clinical follow-up are critical.

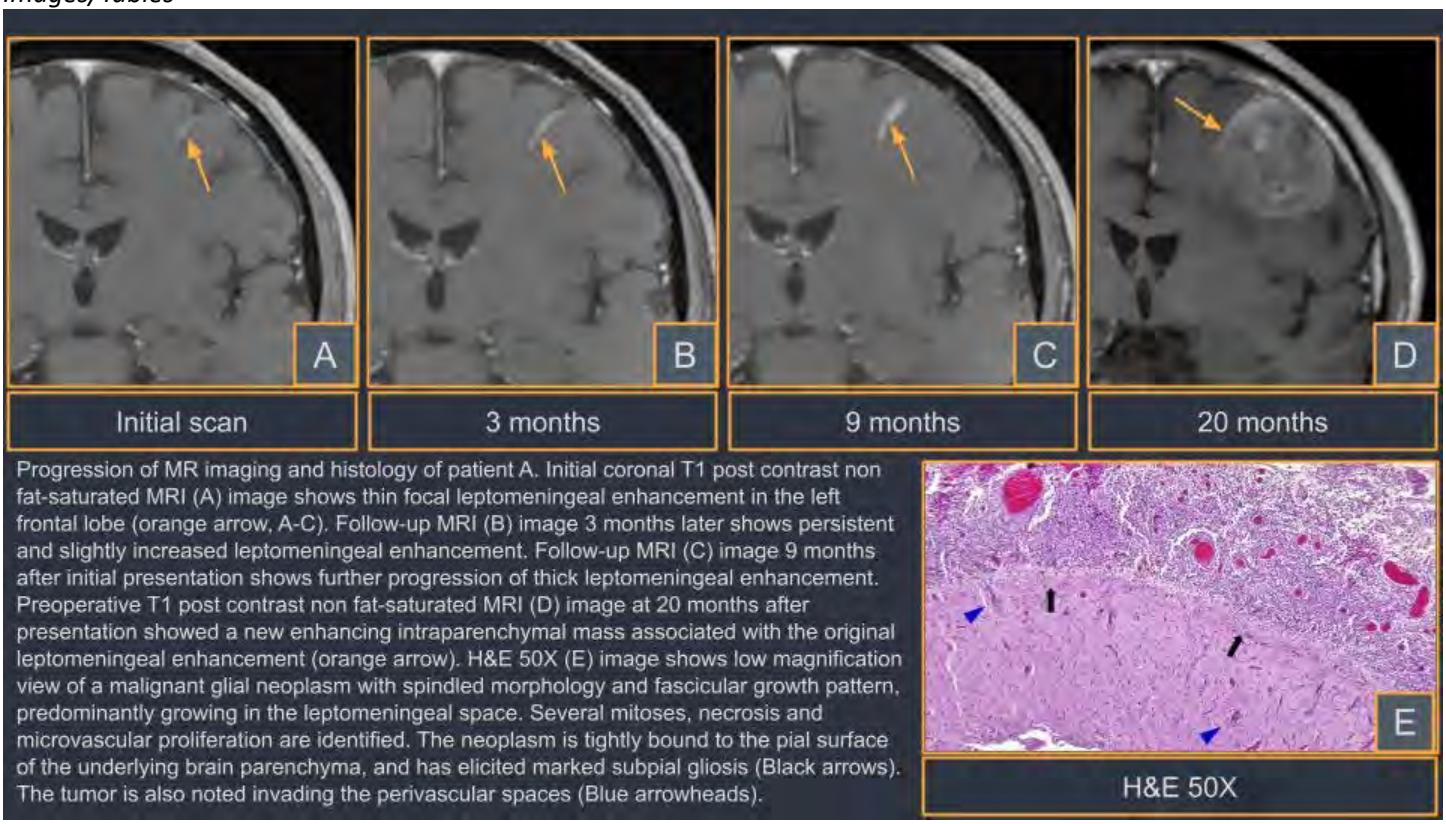
References

1. Jabeen SA, Chowdary AH, Kandadai RM, et al. Primary diffuse leptomeningeal gliomatosis: An autopsy case report. Ann Indian Acad Neurol. 2014 Apr;17(2):227-30. doi: 10.4103/0972-2327.132647.

2. Ahmad E, Mohamed M, Vrettos A. Primary Diffuse Leptomeningeal Gliomatosis: Radiological/Pathological Features. Case Rep Neurol Med. 2016;2016:5016840. doi: 10.1155/2016/5016840.

3. Narayan V, Savardekar A, Mohammed N, et al. Primary Focal Intracranial Leptomeningeal Glioma: Case Report and Review of the Literature. World Neurosurgery. 2018;116:163-168. doi:https://doi.org/10.1016/j.wneu.2018.04.080

Images/Tables



817

A Rare Presentation of Adulterated Cocaine-Induced Midline Destructive Lesion Mimicking Granulomatosis with Polyangiitis: Distinguishing Imaging Features

Abel T Abebe[1], Mohamed Tantawi[1], Azin Aein[1], Asif Jamal MD[2], Lawrence Ginsberg[1]
[1]The University of Texas Medical Branch, Galveston, Texas, USA. [2]The university of Texas Medical Branch, Galveston, TX, USA

Abstract Category

Head & Neck

Clinical History

A 46-year-old male with a history of chronic cocaine use presented with a chronic nasal wound and a gaping nasocutaneous fistula (Figure A). He had ceased cocaine use three months prior to the presentation. The patient had undergone multiple wound debridement sinus surgeries in the past. The work-up revealed anemia, thrombocytosis, and positive C-ANCA. Renal function had been impaired three months before presentation. Histopathology showed mixed inflammatory cells with focal abscess formation, with no evidence of malignancy. Tissue cultures were unremarkable.

Imaging Findings

CT imaging demonstrated extensive destruction of the nasal septum and turbinates (Figures B & C, white stars), with centrifugal progression leading to left-sided nasal wall destruction and a gaping nasocutaneous fistula (Figure B, white arrow). Thickening and stranding of the maxillary and nasal soft tissues were also observed (Figure B, red arrows). Post surgical changes from prior maxillary antrostomy, ethmoidectomy, sphenoidotomy, and frontal sinusotomy for chronic sinusitis were evident. The middle ear and mastoid air cells were clear (Figure D).

Discussion

CIMDL affects approximately 5% of chronic cocaine users. Cocaine is frequently adulterated with levamisole, an anthelmintic drug known to induce ANCA-positive small- and medium-vessel vasculitis, complicating its differentiation from idiopathic small vessel vasculitis, such as GPA. Septal perforation is a hallmark feature of CIMDL and is typically associated with turbinate destruction. CIMDL usually displays centrifugal progression from the septum to the nasal walls, and a nasocutaneous fistula develops in around 5% of cases. Levamisole-induced vasculitis frequently involves

cutaneous manifestations and may account for the nasocutaneous fistula in this case. Additionally, palatal perforation can occur in approximately 20% of CIMDL cases, providing a strong differentiating feature from GPA. In contrast, midline structure involvement in GPA is rare and, when present, typically remains confined to the nasal septum without centrifugal destruction. GPA also more commonly involves the middle ear, a finding less frequently seen in CIMDL. This case illustrates the classic centrifugal progression of CIMDL with positive C-ANCA serology, suggesting adulterated levamisole as a likely contributor. Furthermore, the presence of anemia, thrombocytosis, and prior renal function impairment supports levamisole exposure.

Teaching Point

The characteristic centrifugal progression observed in CIMDL is a key imaging feature that helps distinguish it from GPA, particularly in cases of ANCA positivity and levamisole adulteration.

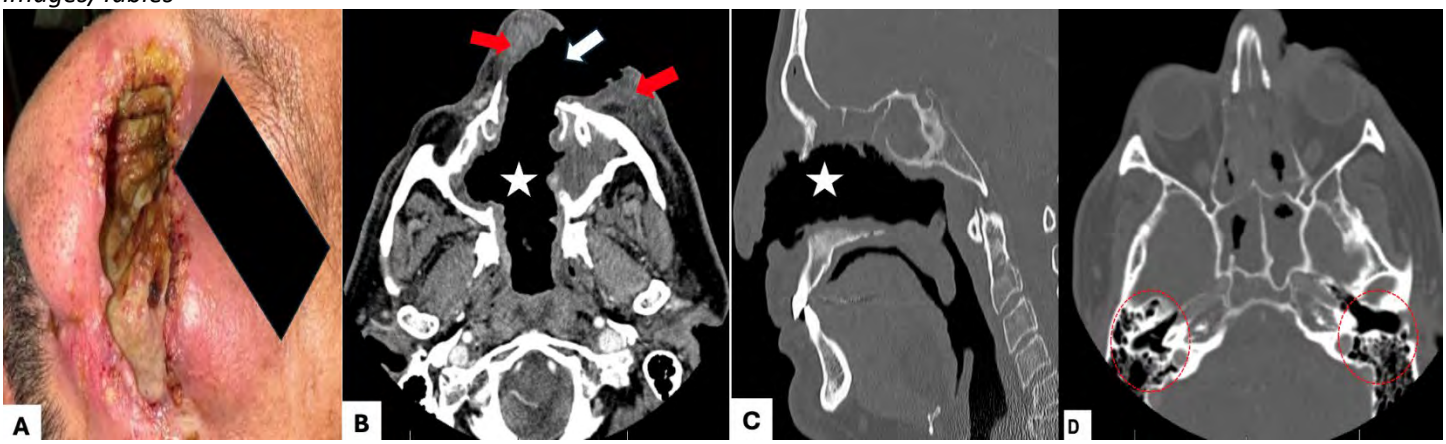
References

1.Muñoz-Vahos CH, Herrera-Uribe S, Arbeláez-Cortés Á, Jaramillo-Arroyave D, González-Naranjo LA, Vásquez-Duque G, Restrepo-Escobar M, Correa-Londoño LA, Arias-Restrepo LF, Vanegas-García AL. Clinical Profile of Levamisole-Adulterated Cocaine-Induced Vasculitis/Vasculopathy: A 30-Case Series. J Clin Rheumatol. 2019 Apr;25(3):e16-e26. doi: 10.1097/RHU.0000000000000813. PMID: 29782427.

2. Trimarchi M, Gregorini G, Facchetti F, Morassi ML, Manfredini C, Maroldi R, Nicolai P, Russell KA, McDonald TJ, Specks U. Cocaine-induced midline destructive lesions: clinical, radiographic, histopathologic, and serologic features and their differentiation from Wegener granulomatosis. Medicine (Baltimore). 2001 Nov;80(6):391-404. doi: 10.1097/00005792-200111000-00005. PMID: 11704715.

3.Mirzaei A, Zabihiyeganeh M, Haqiqi A. Differentiation of Cocaine-Induced Midline Destructive Lesions from ANCA-Associated Vasculitis. Iran J Otorhinolaryngol. 2018 Sep;30(100):309-313. PMID: 30245987; PMCID: PMC6147272.

Images/Tables



824

An interesting case of Glioblastoma arising from the areas of ischemic infarct.

Elham Tavakkol MD, Kamand Khalaj MD, David Timaran montenegro MD, Jose Gavito Higuera MD, Kamali Arash MD
University of Texas Health Sciences Center Houston, Houston, Texas, USA

Abstract Category

Adult Brain

Clinical History

A 67-year-old female with diabetes mellitus, end-stage renal disease on hemodialysis, and coronary artery disease initially presented to ER with weakness, visual disturbances, jaw pain, and gait instability. She was diagnosed with subacute right PCA infarction.

Two months later, she returned with headaches, unsteady gait, right facial droop, and transient left arm numbness. This time the non-contrast MRI supported a diagnosis of chronic infarction.

One year later, she presented with acute confusion, facial droop, and left-sided weakness. MRI showed an expansile enhancing mass in the right occipital lobe and right parahippocampal gyrus consistent with a diagnosis of glioblastoma.

Imaging Findings

Initial CT showed a low-density area in the right PCA territory, with MRI showing FLAIR hyperintensity, restricted diffusion, and scattered petechial hemorrhages compatible with a subacute ischemic infarct. Two months later non-contrast CT showed encephalomalacia in the right occipital lobe. MRI revealed gyriform susceptibility, T2 FLAIR hyperintensity, and ASL perfusion map supporting a diagnosis of chronic infarction. However, the subtle high-signal intensity in the right hippocampus and splenium of the corpus collosum was atypical for infarction. No contrast was used due to end stage renal disease.

Follow-up CT after one year showed gyriform calcification and encephalomalacia in the right occipital lobe and parahippocampal gyrus. MRI revealed a large, expansile infiltrative, enhancing mass in the right temporal, occipital, and parietal lobes, extending through the splenium into the left parahippocampal gyrus, suggestive of high-grade glioma. A biopsy confirmed Glioblastoma, IDH-wildtype, CNS WHO grade 4.

Discussion

Certain imaging features contribute to this diagnostic challenge. Diffusion-weighted imaging (DWI) hyperintensity, typically linked to acute ischemia, may also appear in glioblastomas due to high cellular density and restricted water movement. Here, subtle FLAIR hyperintensity in the hippocampus and splenium, noted in retrospect, was atypical for stroke. Generally, Gd enhancement is only seen in subacute ischemic infarcts. Persistent enhancement and expansile FLAIR hyperintensity should raise the possibility of a malignant neoplasm.

This case underscores the need for a high index of suspicion in patients with unusual imaging patterns and for follow-up imaging when clinical responses are inconsistent with ischemic infarct. Early identification of malignancies such as glioblastoma enables timely intervention and can significantly impact outcomes.

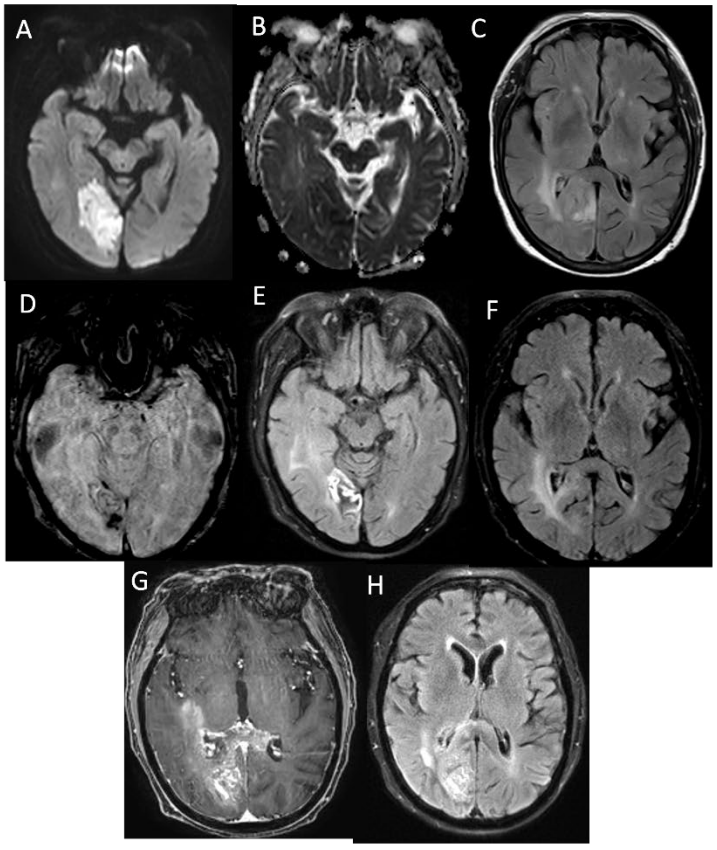
Teaching Point

In patients with atypical presentations for ischemic infarcts, particularly when clinical response is suboptimal, glioma should be considered as a differential diagnosis. Close follow-up imaging may reveal atypical findings, enabling prompt diagnosis of underlying malignancies, such as glioblastoma, which can lead to improved management and outcomes.

References

Sasagawa, Ayaka et al. “Stroke Mimics and Chameleons from the Radiological Viewpoint of Glioma Diagnosis.” Neurologia medico-chirurgica vol. 61,2 (2021): 134-143. doi:10.2176/nmc.oa.2020-0309

Images/Tables



The initial MRI, which included DWI (A), ADC (B), and FLAIR (C), revealed high signal intensity and diffusion restriction in the right occipital region, consistent with a subacute ischemic stroke. Two months later, SWI (D) and FLAIR (E&F) images demonstrated gyriform susceptibility areas along with associated T2 FLAIR hyperintensity. However, the FLAIR images (C&F) showed hyperintensity in the right hippocampus and splenium, which is not consistent with an ischemic stroke. After one year, MRI post-contrast T1 (G) and FLAIR (H) revealed a large expansile lesion that crossed the midline, suggesting glioblastoma.

852

Pop Goes the Cyst: A Case Series of Ruptured Intracranial Dermoid Cysts

Dr. Neelesh Jain MBBS
RNT Medical College, Udaipur, Udaipur, Rajasthan, India

Abstract Category

Adult Brain

Clinical History

A 25 year old female who presented with sudden loss of consciousness and history of mild headache for the past 2 months. No other history of trauma or any other relevant history. Patient had few episodes of vomiting. Routine investigations turn out to be normal. No history of fever.

Imaging Findings

CT Brain reveals a heterogeneously hypodense lesion with internal fat content and calcifications in right temporal lobe region with presence of few fat density globules in the ventricular system and sulcal spaces. MRI confirms the extra-axial location of the lesion with findings suggesting the diagnosis of Ruptured intracranial dermoid cyst.

Discussion

The rupture of an intracranial dermoid cyst is a rare but serious clinical event that can mimic other acute neurological conditions such as subarachnoid hemorrhage or meningitis. Imaging plays a crucial role in diagnosis, and early surgical intervention is often necessary to prevent further complications. Although the prognosis after surgery is generally favorable, the presence of chemical meningitis and associated neurological sequelae can complicate recovery.

Teaching Point

Its important to pick out these subtle important clues on a non-contrast CT brain like presence of fat density within the ventricles. Ruptured intracranial dermoid cysts present a challenging diagnostic and therapeutic dilemma. Timely recognition on imaging and prompt surgical intervention are essential to minimize morbidity. Clinicians should maintain a high index of suspicion for dermoid cyst rupture in patients presenting with acute neurological symptoms, especially in the context of prior known dermoid cysts.

References

Jacków J, Tse G, Martin A, Sąsiadek M, Romanowski C. Ruptured intracranial dermoid cysts: a pictorial review. *Neurosurg Rev*. 2019;42(4):947-957. doi:10.1007/s10143-019-01047-w. PMID: 30655926; PMCID: PMC6334092.

859

Duplication of the Pituitary Gland - Plus Syndrome in a Newborn

Lutof Zreik Dr., Mika Shapira Rootman Dr., Galia Ronen Dr., Ayelet Eran Dr.
Rambam Health Care Campus, Haifa, Haifa, Israel

Abstract Category

Pediatrics

Clinical History

We report the case of a newborn female, one of a set of twins, who was observed to be hyperventilating shortly after birth, with oxygen saturation of 80%, necessitating ventilatory support. A comprehensive physical examination revealed generalized hypotonia, facial dysmorphisms including hypertelorism, a broad nasal bridge, low-set ears, an isolated cleft palate without cleft lip, with a soft midline palatine mass. Initial cranial US findings were unremarkable.
Contrast enhanced brain CT and MRI scans were performed for further evaluation.

Imaging Findings

MRI revealed two pituitary infundibula, each connecting to a distinct pituitary gland located on either side of the sphenoid body (Figures 1–3). The sella turcica is absent, and there is incomplete ossification of the sphenoid body, as seen in the bone window of the CT image (Figure 4).
A midline soft tissue palatine mass is observed with signal characteristics consistent with fat on all sequences (Figures 5–7). This mass does not enhance following administration of contrast media.
Additional findings include thickening of the floor of the third ventricle with fusion of the tuber cinereum and mammillary bodies (Figure 8), signs of brainstem dysmorphism with bulky midbrain and indistinct differentiation between the midbrain and pons, mildly hypoplastic vermis, mild thickening of the optic chiasm, hypertelorism, relatively small upper cervical vertebrae, and an isolated cleft palate. A cavum septum pellucidum is also noted.

These findings of midline anomalies, along with the duplication of the pituitary glands, are consistent with duplication of the pituitary gland - plus syndrome.

Discussion

Duplication of the pituitary gland (DPG)-plus syndrome is an extremely rare developmental condition characterized by DPG along with other midline blastogenic defects. Limited information about this syndrome is found in literature, and according to the latest publications, fewer than 60 cases have been reported to date [1]. Most documented cases occur in females [2].

The cause of DPG, which is the hallmark of the syndrome, remains unclear as several theories have been proposed[3]. There are multiple other features associated with this syndrome. The most common of them, in order of decreasing frequency, include hypertelorism, cleft palate, hypothalamic enlargement or mass, broad or duplicated sella, oropharyngeal tumors (most commonly teratomas), vertebral anomalies, and agenesis or hypoplasia of the corpus callosum [3,4]. Less frequent findings include cleft basisphenoid bone, cerebellar hypoplasia, low-set ears, and several other anomalies [3]. Clinical manifestations may include hormonal imbalances with developmental delay and altered pubertal timing, with cases of delayed or precocious puberty reported [3,5].

In this case report, in addition to DPG, the patient presented with various findings consistent with DPG-plus syndrome, as outlined in the imaging findings section. The palatine mass was surgically removed, revealing a soft mass with hair. Histopathological analysis confirmed a mature teratoma.

Teaching Point

DPG - plus syndrome is a very rare entity, and awareness of its findings, varied presentation, and possible clinical implications allows neuroradiologists to contribute valuable insights for diagnosis and appropriate multidisciplinary care planning. This comes into play especially upon recognition of the duplicated gland, which should prompt searching for other associated features.

References

1. Serrallach BL, Rauch R, Lyons SK, et al. Duplication of the Pituitary Gland: CT, MRI and DTI Findings and Updated Review of the Literature. *Brain Sci* 2022;12. DOI: https://doi.org/10.3390/brainsci12050574
2. Sen D, Arora V. Duplication of the pituitary gland - plus syndrome. *Indian J Radiol Imaging* 2016;26:126–30. DOI: https://doi.org/10.4103/0971-3026.178361
3. Azurara L, Marçal M, Vieira F, et al. DPG-plus syndrome: new report of a rare entity. *BMJ Case Rep*https://doi.org/10.1136/bcr-2015-212416. DOI: https://doi.org/10.1136/bcr-2015-212416
4. Slavotinek A, Parisi M, Heike C, et al. Craniofacial defects of blastogenesis: Duplication of pituitary with cleft palate and orophgaryngeal tumors. *Am J Med Genet A* 2005;135A:13–20. DOI: https://doi.org/10.1002/ajmg.a.30694
5. Laurenson MWM. G180(P) Rare case of duplicate pituitary plus syndrome. *Arch Dis Child* 2017;102:A73–A73. DOI: https://doi.org/10.1136/archdischild-2017-313087.179

Images/Tables


Figure 1

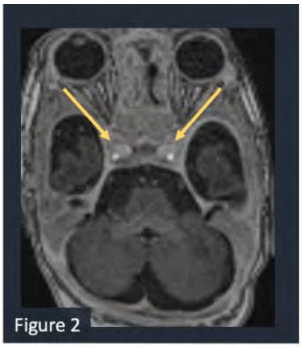

Figure 2


Figure 3


Figure 4


Figure 5

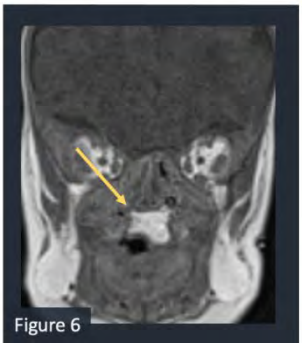
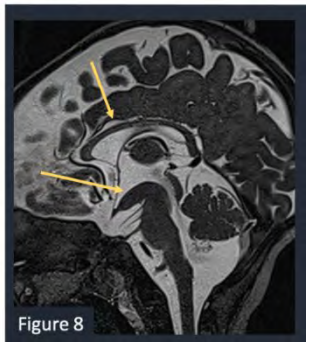

Figure 6


Figure 7


Figure 8

867

High Central Compartment Nodal Metastases from Papillary Thyroid Cancer: A Potential Surgical Blind Spot in Patients Undergoing Central Neck Dissection

Sahar Alizada, Anastasios Maniakas, Ahmad Abubaker, Salmaan Ahmed
MD Anderson Cancer Center, Houston, TX, USA

Abstract Category

Head & Neck

Clinical History

54-year-old male with history of acute promyelocytic leukemia in remission presented for evaluation of a thyroid nodule. Ultrasound revealed a stable right lobe 9 mm TR3 nodule in the right lobe and a suspicious 1.1 cm left neck lymph node (LN). Biopsy of the LN confirmed papillary thyroid cancer (PTC).

The patient subsequently had a total thyroidectomy with bilateral central neck dissection (CND), revealing a 1.2cm PTC in the right lobe. Cancer cells were absent in 3 right central neck LN but present in 4 of 6 left central neck LN (largest metastasis 4mm).

A follow-up ultrasound showed a persistent metastatic Left neck LN. An intraoperative guide wire was placed under ultrasound guidance to localize the metastasis. A repeat left CND was performed via a new, small, higher thyroidectomy incision, demonstrating a 9 mm LN positive for PTC.

Imaging Findings

Preoperative Ultrasound identified 8mm isoechoic solid nodule in the right thyroid lobe without calcification (Figure 1A, outlined arrow). A 1.4 cm LN with calcification was noted in the left neck (Figure 1B, filled arrows), medial to the common carotid artery (CCA) and extending above the thyroid cartilage (Figure 1B, outlined arrowhead). Biopsy confirmed PTC.

Preoperative Contrast-Enhanced CT Neck confirmed a metastatic LN in the left neck (Figure 1C, filled arrow), located slightly inferior to the hyoid bone and anteromedial to the CCA (Level III). However, correlating with the ultrasound, this node is medial to the CCA and can be approached via a CND, rather than a left lateral neck dissection.

Postoperative Ultrasound again showed 1.4cm LN in the left neck, medial to the CCA (Figure 1D and 1E, filled arrows). Guide wire tip was placed in the LN intraoperatively for surgical guidance (Figure 1E, filled arrowhead).

Discussion

Level VI and VII cervical nodes comprise the central compartment and are the first and most common site of metastasis from PTC. Preoperative ultrasound has a sensitivity of 35% in detecting central neck metastases. CND is performed prophylactically for larger PTC tumors (T3 and T4) and in cases of documented central or lateral neck nodal metastasis[1]. The central compartment boundaries are the hyoid bone superiorly, the CCA laterally, and the innominate artery inferiorly. The superior parathyroid glands in the upper central compartment are supplied by the inferior thyroid artery, and there is increased risk of hypocalcemia when CND is extended to the hyoid bone from vascular injury[2]. Since metastases to the upper central compartment are rare, CND is not routinely extended to the hyoid bone. American Head and Neck Society Consensus statement in 2017 describes a horizontal line at the inferior border of the cricoid and recurrent laryngeal nerve insertion as the superior landmark for CND, and central compartment metastasis located above this level may not get resected[3].

Teaching Point

The presence of high central compartment nodal metastases detected on preoperative imaging should be specifically communicated to the surgeon, thereby necessitating extension of CND to the hyoid bone for complete resection. Intraoperative confirmation may be necessary with frozen section to ensure the lymph node of concern is resected.

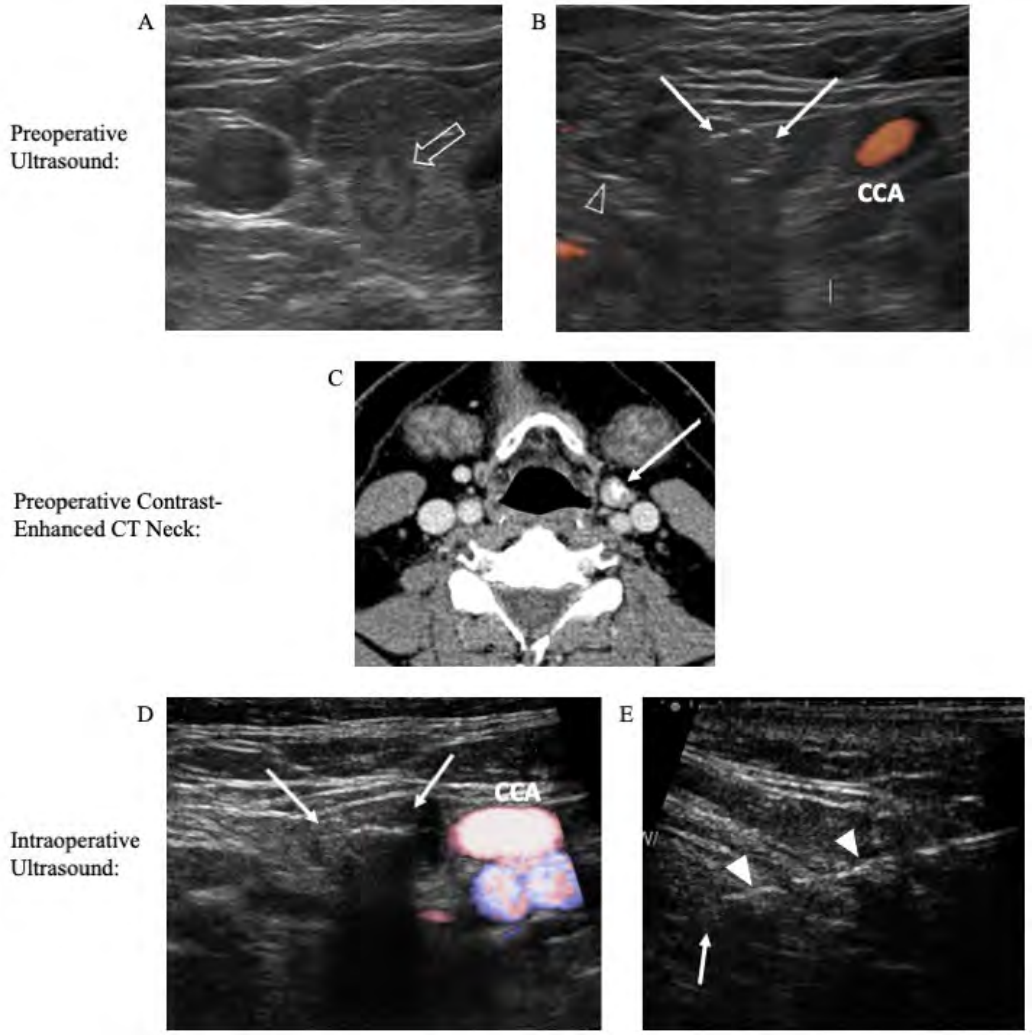
References

1. Khafif A, Yosef LM. Para-tracheal neck dissection – is dissection of the upper part of level Ⅵ necessary? *World j otorhinolaryngol-head neck surg* 2020;6:171–5. DOI: https://doi.org/10.1002/hed.24715

2. Holostenco V, Khafif A. The Upper Limits of Central Neck Dissection. *JAMA Otolaryngol Head Neck Surg*2014;140:731. DOI: https://doi.org/10.1001/jamaoto.2014.972

3. Agrawal N, Evasovich MR, Kandil E, et al. Indications and extent of central neck dissection for papillary thyroid cancer: An American Head and Neck Society Consensus Statement. *Head & Neck* 2017;39:1269–79. DOI: https://doi.org/10.1002/hed.24715

Images/Tables



876

Limitations of Perfusion Scans in Stroke Evaluation: Implications for Intervention

Saif Baig MD[1], Sadeem Hussain BS[2], Steven Lev MD[1], Saurabh Patel MD[1]

[1]Nassau University Medical Center, East Meadow, NY, USA. [2]NYIT College of Osteopathic Medicine, Old Westbury, NY, USA

Abstract Category

Adult Brain

Clinical History

1 - 68 year old female with history of hypertension and bradycardia presented with left facial droop, right gaze, left hemineglect, paralysis of the left upper and lower extremities with an otherwise normal exam, and NIH Stroke Scale score of 28.

2 - 89-year-old female with a history of hypertension presented with right-sided hemiplegia. Clinical findings included confusion, reduced level of consciousness, right-sided paralysis and sensory loss, and NIH Stroke Scale score of 23. Additionally, the patient exhibited global aphasia and inattention to bilateral simultaneous stimulation. The patient failed a dysphagia trial. Other physical exam findings were otherwise unremarkable.

3- 49 year old male was found unconscious and pulled out of a fire with burns to L face, L torso and upper extremity. Upon arrival, the patient was found to have new onset LUE & LLE weakness. Due to severity of burns, he was not given tPA despite NIH Stroke Scale of 13.

Imaging Findings

1 - CT perfusion overestimated CBF infarct volume of 98.3 ml, a larger volume then demonstrated with non-contrast CT Head demonstrating an ASPECTS score of 10, supported by CTA evidence of proximal right M1 occlusion.

2 - CT perfusion underestimated mismatch and core infarct volumes with an artifactually increased Tmax in an uninvolved area of the brain, due to regionally increased vascularity on CTA consistent with compensatory collaterals. However, the non-contrast CT head demonstrated an ASPECTS score of 5, supported by subsequent MRI which showed a moderately sized infarct of the left M2 region.
3- CT perfusion accurately showed 220.9 ml of mismatch volume and CTA evidence of proximal right M1 occlusion. Non-contrast CT head demonstrated an ASPECTS score of 2. Subsequent MRI demonstrated large right MCA territory infarct consistent with proximal occlusion.

Discussion

In acute ischemic stroke, perfusion imaging aims to identify the ischemic penumbra volumes - tissue that is hypoperfused but salvageable. However, perfusion scans are not infallible and can under or overestimate the penumbral region due to technical limitations or variable patient physiology. These imaging shortcomings can result in a misclassification of patients, potentially denying them life-saving interventions. Studies have shown that even in patients with low ASPECTS (≤5), who traditionally would be excluded from reperfusion therapies, mechanical thrombectomy can yield significant clinical benefits.

Given these findings, deferring treatment based mainly on perfusion imaging may not be justified if additional clinical or radiographic signs suggest there is viable tissue at risk, such as NIH Stroke Scale and ASPECTS score. Perfusion imaging should be interpreted with caution, and clinicians should not hesitate to proceed with reperfusion when other indicators point toward potential benefit [1, 3, 4]. The evolving evidence suggests that thrombectomy remains a viable treatment option even in the presence of imaging uncertainties.

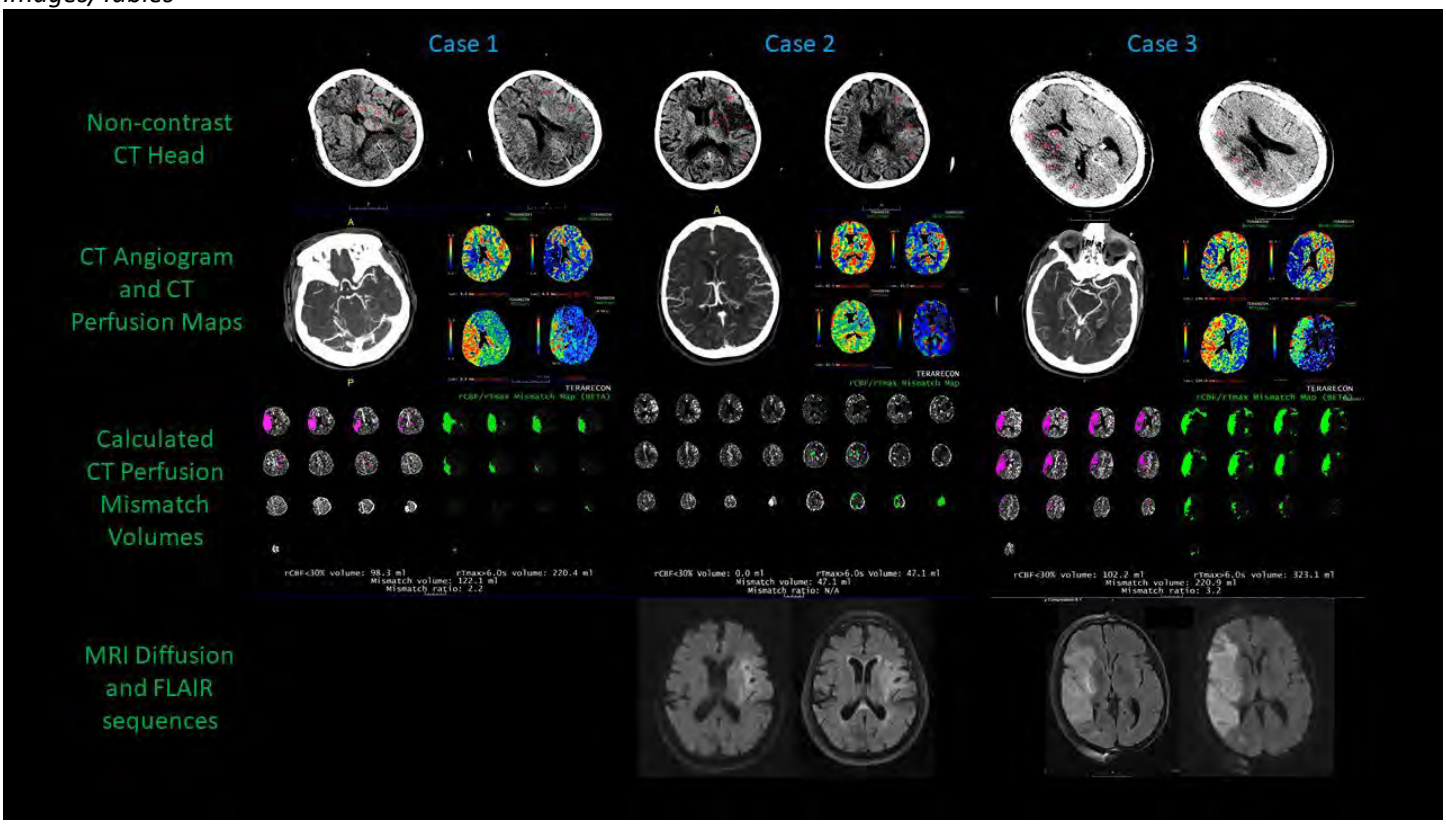
Teaching Point

The absence of standardized perfusion imaging protocols, combined with variability in patient presentation, warrants careful consideration of calculated ischemic area. Thrombectomy remains beneficial even in cases with apparent large matched perfusion deficits. Clinicians should assess other available imaging and clinical indicators to determine interventions, such as ASPECTS score, NIHSS score, CT or MR angiography and early diffusion sequences.

References

1. Baig AA, Bouslama M, Turner RC, et al. Mechanical thrombectomy in low Alberta stroke program early CT score (ASPECTS) in hyperacute stroke—a systematic review and meta-analysis. Br J Radiol. **2023**;96(1152):20230084.
2. Broocks G, Hanning U, Flottmann F, et al. Clinical benefit of thrombectomy in stroke patients with low ASPECTS is mediated by oedema reduction. *Brain*. **2019**;142(5):1399–1407.
3. Diestro JDB, Dmytriw AA, Broocks G, et al. Endovascular thrombectomy for low ASPECTS large vessel occlusion ischemic stroke: A systematic review and meta-analysis. *Can J Neurol Sci*. 2020;47(5):612-619.
4. Nicolas-Jilwan M, Wintermark M. Automated brain perfusion imaging in acute ischemic stroke: Interpretation pearls and pitfalls. *Stroke*. 2021;52(11):3728–3738.

Images/Tables



883

Ruptured Lumbar Dermoid Cyst With Intracranial Fat Dissemination: A Case Report

Zixin Yi BS[1], Manisha Koneru MD[2], Corey M Mossop MD[2], Todd Siegal MD[2]
[1]Cooper Medical School of Rowan University, Camden, NJ, USA. [2]Cooper University Healthcare, Camden, NJ, USA

Abstract Category

Spine

Clinical History

A 50-year-old man with a significant past medical history of intraspinal dermoid cyst who presented for acute onset of headache, aphasia, confusion, and vomiting. Patient's family denied any preceding trauma. Upon admission, the patient was afebrile and hemodynamically stable. He was intubated and sedated with a Glasgow Coma Scale score of 8.

Imaging Findings

The initial noncontrast head CT raised concerns for pneumocephalus, but subsequent imaging revealed acute obstructive hydrocephalus secondary to fat deposition in the intraventricular and subarachnoid spaces. Emergent external ventricular drainage was promptly initiated. Further T1-weighted MRI of the lumbar spine identified a ruptured dermoid cyst with cephalad migration of fat and an associated tethered spinal cord. Notably, an earlier MRI from 12 years prior had indicated the presence of an intraspinal dermoid cyst with evidence of a minor rupture. Patient subsequently underwent placement of a right frontal ventriculoperitoneal shunt and recovered without further medical or neurological complications.

Discussion

With a histologically benign nature, spinal dermoid cysts represent 0.6% of all dermoid cysts and 22.9% of CNS dermoid cysts. However, in exceedingly rare instances, the rupture of a spinal dermoid cyst can lead to dissemination of fat droplets into the cerebrospinal fluid, which then migrate caudally into the intraventricular and subarachnoid spaces. This migration can result in atypical neurological symptoms including headache, aseptic meningitis, and obstructive hydrocephalus, underscoring the clinical complexity and warranting emergent investigation.

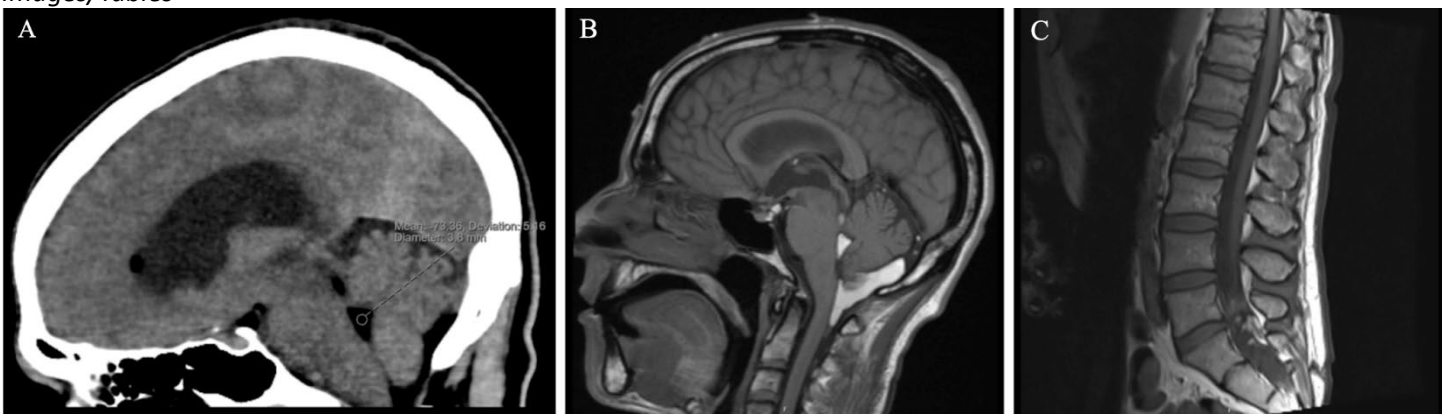
Teaching Point

This documented case of ruptured lumbar dermoid cyst with intracranial fat dissemination emphasizes the need for precise radiological imaging in acute obstructive hydrocephalus. Differentiating fat density from air density is crucial for accurately identifying the obstruction's source and guiding treatment.

References

1. Perdomo-Pantoja, A., Zakaria, H. M., Judy, B. F., et al. Traumatic sacral dermoid cyst rupture with intracranial subarachnoid seeding of lipid particles: illustrative case. *Journal of neurosurgery. Case lessons*, 2021,2(24), CASE21355. https://doi.org/10.3171/CASE21355
2. Bhatt, A. S., Mhatre, R., Nadeesh, B. N., et al. Nonneoplastic Cystic Lesions of the Central Nervous System-Histomorphological Spectrum: A Study of 538 Cases. Journal of neurosciences in rural practice, 2019,*10(*3), 494–501. https://doi.org/10.1055/s-0039-1698033

Images/Tables



915

Extra-articular Pigmented Villonodular Synovitis (PVNS) of a Spinal Facet Joint

Korrina Gidwani[1], Barton F. Branstetter IV[2]

[1]University of Pittsburgh School of Medicine, Pittsburgh, Pennsylvania, USA. [2]University of Pittsburgh Medical Center Department of Radiology, Pittsburgh, Pennsylvania, USA

Abstract Category

Spine

Clinical History

A 24-year-old female presents with a palpable mass in her posterior upper neck. The mass is tender and has been slowly enlarging over several months.

Imaging Findings

She undergoes CT of the neck with contrast and MR of the cervical spine, which are interpreted as concerning for soft tissue sarcoma. She undergoes CT-guided FNA and core biopsy. Preliminary cytopathology was interpreted as benign fibroxanthomatous lesion with differential including solitary xanthogranuloma, xanthoma, and lipidized fibrous histiocytoma. The final pathology was interpreted as extra-articular PVNS. The patient underwent complete surgical excision of the mass and displays no evidence of recurrence at one year follow-up.

Discussion

Extra-articular PVNS is a slowly progressive, benign tumor that typically targets the soft tissue lining of knee and hip joints [1]. Although the incidence of PVNS is around 1.8 cases per million in the United States, there is minimal data on spinal PVNS, with a total of 63 cases reported in the English literature [2,3]. PVNS can be described as either intra-articular, which is commonly observed in the synovium, or extra-articular, which involves the tendon sheath or bursa [2]. Extra-articular PVNS is mainly reported in the knee or shoulder as opposed to the spine [1,4]. Across these subtypes, PVNS typically presents with joint pain and is associated with joint effusion, presence of hemosiderin, and varied signal intensities on magnetic resonance imaging [5]. We report a case of extra-articular PVNS in the cervical spine.

Teaching Point

Extra-articular PVNS in the spine is a rare diagnosis, as previously reported cases have been predominantly observed in the knee or shoulder. Based on this example, it is important to consider that low T2 signal can be observed in a wider variety of tumors, in addition to its typical association with fibrous tumors or densely-packed cells. This case emphasizes the need for biopsy to exclude uncommon diagnoses when evaluating paraspinal masses. Lastly, neuroradiologists should be familiar with lesions that commonly affect the appendicular joints since similar findings may be observed in the spine and skull base in uncommon cases.

References

[1] Oe K, Kunihiko S, Yoshida Y, et al. Pigmented villonodular synovitis originating from the lumbar facet joint: a case report. *Eur Spine J 2007;16*(S3);301–305. DOI: https://doi.org/10.1007/s00586-007-0403-1.

[2] Teixeira R, Pimentel J, Norte S, et al. A rare case of extra-articular pigmented villonodular synovitis of the knee in a child. *J Case Rep Images Orthop Rheum 2021;5*:100023Z14RT2021.

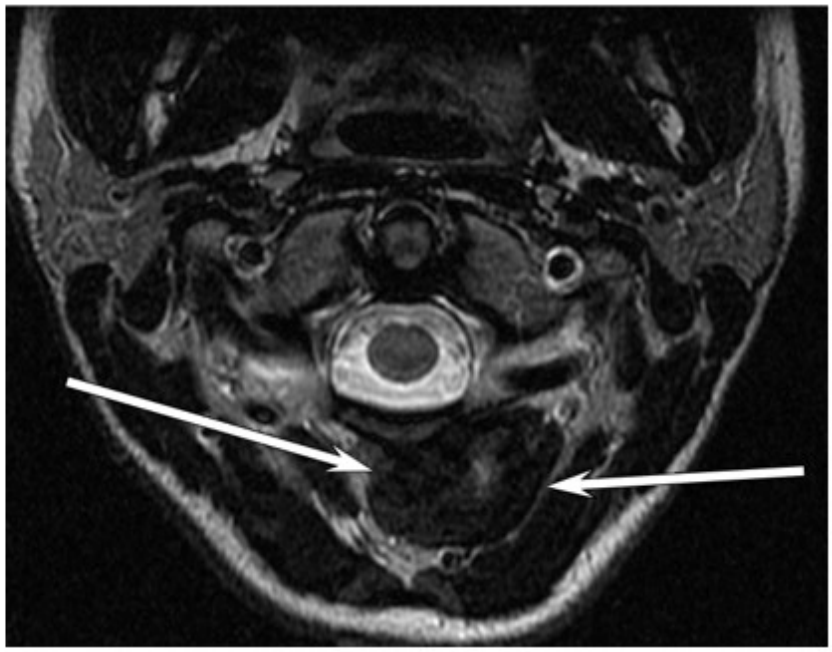
[3] Oh SW, Lee MH, Whan E. Pigmented Villonodular Synovitis on Lumbar Spine: A Case Report and Literature Review. *J Korean Neurosurg Soc 2014;56*(3);272–272. DOI: https://doi.org/10.3340/jkns.2014.56.3.272.

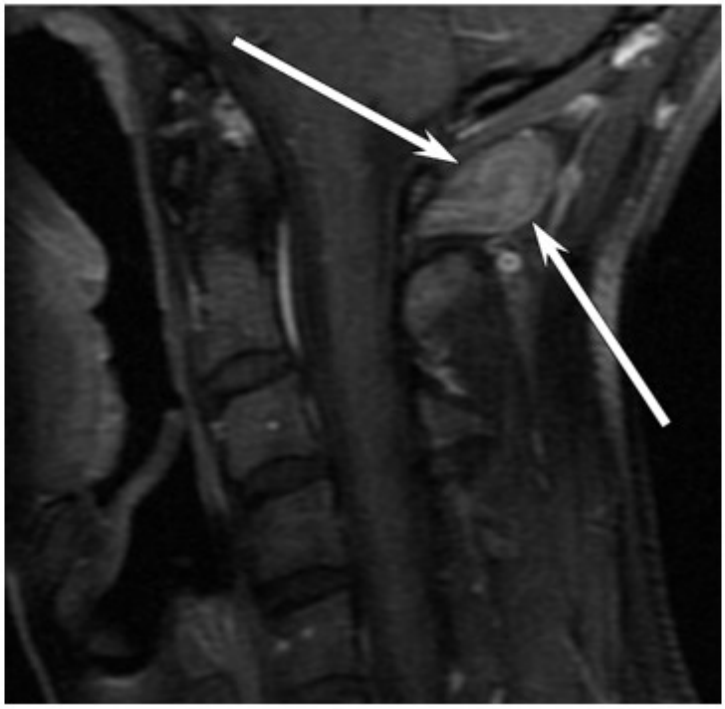
[4] Cho CH., Sohn SW, Song KS, et al. Extra-Articular Pigmented Villonodular Synovitis of the Subacromial Space. *Orthopedics 2008;31*(12);1–3. DOI: https://doi.org/10.3928/01477447-20081201-04.

[5] Cheng XG, You YH, Liu W, et al. MRI features of pigmented villonodular synovitis (PVNS). *Clin Rheumatol 2004*;*23*(1);31–34. DOI: https://doi.org/10.1007/s10067-003-0827-x.

Images/Tables







924

Glial Remnant within the Craniopharyngeal Canal

Korrina Gidwani[1], Gloria Joo[2], Barton F. Branstetter IV[2]
[1]University of Pittsburgh School of Medicine, Pittsburgh, Pennsylvania, USA. [2]University of Pittsburgh Medical Center Department of Radiology, Pittsburgh, Pennsylvania, USA

Abstract Category

Head & Neck

Clinical History

A 50-year-old man presents with intermittent vertigo that has persisted for months and is somewhat responsive to Epley exercises.

Imaging Findings

Brain MRI reveals a 23 mm pituitary mass in the sella turcica that extends into the right cavernous sinus. The mass demonstrates low signal on T1 imaging and hyperintensity on T2 imaging relative to the adjacent pituitary gland, with hypoenhancement relative to the normal glandular tissue. Based on these features, a pituitary macroadenoma was highly suspected with unlikely differential considerations of Rathke cleft cyst, craniopharyngioma, and meningioma. The patient underwent surgical resection and endoscopic endonasal biopsy of the mass. Pathology confirmed the presence of glial tissue with both reactive and degenerative features.

Discussion

Rathke's pouch forms during the 4th week of embryological development and gives rise to the anterior pituitary gland [1]. The lumen of the pouch develops into Rathke's cleft, which typically regresses during development but can lead to remnants such as Rathke cleft cysts or craniopharyngiomas [1,2]. Rathke cleft cysts are noted in 3-33% of autopsies; they appear radiologically as homogeneous non-enhancing rounded masses of varying density and signal intensity [3]. The incidence of craniopharyngiomas is only 0.18 per 100,000 people per year; these lesions are typically heterogeneous on all modalities and sequences with calcifications and mixed solid and cystic components [4]. Although these are the most common remnants of Rathke's cleft, other remnants such as patent craniopharyngeal canals have also been reported and can have well-described complications [5]. Despite this range of potential remnants, there are no previously reported cases of glial tissue within the path of the craniopharyngeal canal. We report a definitive case of glial tissue remnants in Rathke's cleft.

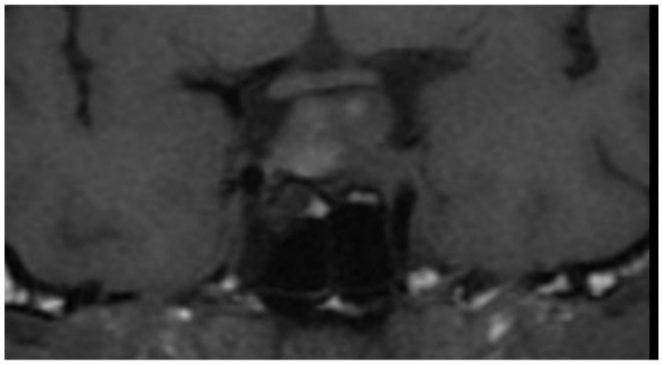
Teaching Point

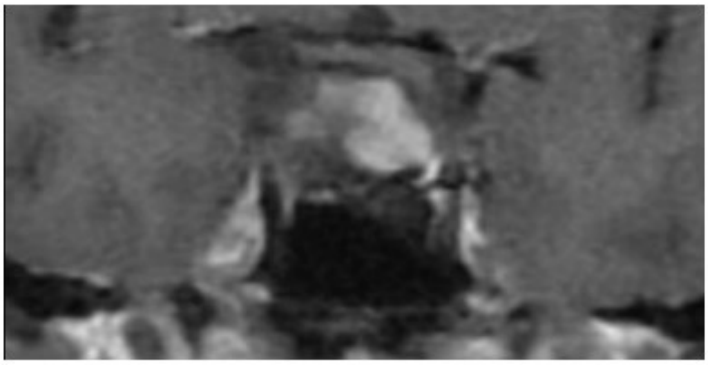
Persistence of Rathke's cleft can lead to various pathologies, but it is highly uncommon to observe glial tissue remnants in Rathke's cleft. This case emphasizes the need for biopsy of lesions along Rathke's cleft to exclude uncommon diagnoses.

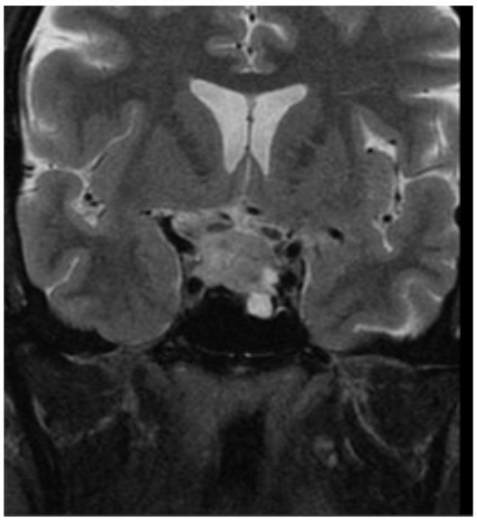
References

[1] Schmidt B, Cattin F, Aubry S. Prevalence of Rathke cleft cysts in children on magnetic resonance imaging. *Diagn Interv Imaging 2020*; 101(4), 209-215.
DOI: https://doi.org/10.1016/j.diii.2019.12.005
[2] Abele T, Salzman K, Harnsberger H, et al. Craniopharyngeal Canal and Its Spectrum of Pathology. *Am J Neuroradiol 2013;*35(4), 772–777. DOI: https://doi.org/10.3174/ajnr.a3745
[3] Higuchi Y, Hasegawa K, Kubo T, et al. The clinical course of Rathke's cleft cysts in pediatric patients: impact on growth and pubertal development. *Clin Pediatr Endrocrinol 2022*;31(1):38-43. DOI: https://doi.org/10.1297/cpe.2021-0034
[4] Lara-Velazquez M, Mehkri Y, Panther E, et al. Current Advances in the Management of Adult Craniopharyngiomas. *Curr Oncol 2022*;29(3), 1645-1671.
DOI: https://doi.org/10.3390/curroncol29030138
[5] Dougherty C, Branstetter B. Persistent Craniopharyngeal Canal with an Associated Sphenoid Sinus Fistula. *J of Radiol. Case Rep. 2023*;17(10), 14-20.
DOI: https://doi.org/10.3941/jrcr.v17i8.4707

Images/Tables







932

Chronic Alteration in Cerebral FDG Metabolism after MRI-guided HIFU for Essential Tremor – A case with PET and MRI correlation

Alexander R Asturias DO[1], Nghi Nguyen MD, PhD[2], Fabricio Feltrin MD[1], Orhan Oz MD, PhD[1], Bhavya Shah MD[1]
[1]UT Southwestern, Dallas, Texas, USA. [2]UT MD Anderson Cancer Center, Houston, Texas, USA

Abstract Category

Interventional

Clinical History

A 74-year-old man with a past medical history of monoclonal gammopathy of undetermined significance(MGUS) and essential tremor(ET) underwent routine surveillance FDG-PET(Figure 1 A/B). Less than 1 month later, the patient underwent MRI-guided High Intensity Focused Ultrasound(MRgHIFU) of the left dentato-rubro-thalamic tract(DRTT) for treatment of the patient's right-hand dominant debilitating ET. The patient was tremor free in his right-hand post procedure and remains tremor free in that hand on follow up examinations at approximately one year. Coincidentally, the patient underwent routine MGUS monitoring FDG-PET imaging approximately one year post MRgHIFU treatment.

Imaging Findings

The pre MRgHIFU FDG-PET imaging data did not show any abnormal intracranial glucose metabolism (Figure A/B). Immediate post-operative FGATIR MRI showed a 5.4x6.2 x 9.4 mm post MRgHIFU lesion in the posterior portion of the overlap between the decussating and non-decussating DRTT[1-3](Figure G/H/I). The post MRgHIFU FDG-PET showed a visible decrease in PET signal intensity(Figure C/D/E/F). However, normalized subtraction of the extracted cerebral FDG-PET images did not demonstrate statistically significant metabolic changes within the brain between baseline and 12-months post-MRgHIFU.

Discussion

Patients with medication refractory ET are candidates for procedural treatments such as radiofrequency thalamotomy, gamma-knife thalamotomy(GKT), deep brain stimulator implantation, and MRgHIFU. MRgHIFU is an incision-less image-guided procedure used to treat medically refractory ET[1-3]. Adverse effects of MRgHIFU to treat ET can include weakness, numbness, and paresthesia in up to a third of patients within one month following treatment[4]. Our site employs four-tract-tractography, a multi-parametric patient specific targeting method aimed at increasing treatment response and decreasing adverse effects[1-3].

Research on how thalamotomy-type procedures affect cerebral glucose metabolism in ET patients is limited. Most studies involve mixed movement-disorder cohorts and a variety of thalamotomy methods. A notable study examined 42 patients with right-sided ET treated with GKT targeting the ventral intermediate nucleus through a landmark-based approach[5]. This studies patient's experienced a statistically significant decrease in left thalamic metabolism as well as a significant decreases in FDG metabolism in the right cerebellum, left temporal gyri, and bilateral frontal gyri[5].

Teaching Point

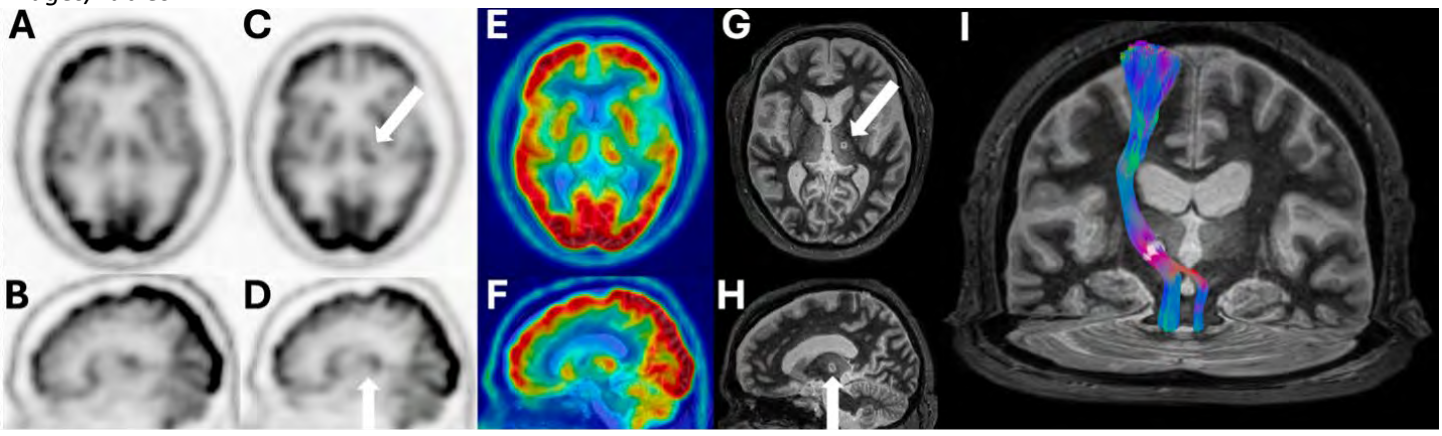
To our knowledge, this is the first case report documenting the FDG-PET effects of MRgHIFU on cerebral glucose metabolism in an ET patient. Although MRgHIFU might induce hypometabolism in the acute or subacute phases post-procedure, our findings cautiously suggest no significant long-term metabolic alterations. Notably, a persistent hypo-attenuated FDG-PET signal in the left dentato-rubro-thalamic tract(DRTT) was observed, even as the patient remained tremor-free at 12-months.

Several factors may explain the lack of significant post-procedural FDG-PET signal changes in this case, such as an anecdotal case report, which is underpowered relative to prior studies. However, the use of precision-targeted, patient-specific methods, absent in the gamma-knife cohort, may contribute to the observed metabolic differences. Additionally specific targeting methods may create smaller lesions in precise locations that may achieve superior tremor control without large metabolic changes. Further studies with larger MRgHIFU cohorts are necessary to understand its impact on cerebral glucose metabolism in ET.

References

1. Holcomb, J. M., Chopra, R., Feltrin, F. S., Elkurd, M., El-Nazer, R., McKenzie, L., ... & Shah, B. R. (2023). Improving tremor response to focused ultrasound thalamotomy. *Brain Communications*, *5*(4), fcad165.
2. Feltrin, F. S., Chopra, R., Pouratian, N., Elkurd, M., El-Nazer, R., Lanford, L., ... & Shah, B. R. (2022). Focused ultrasound using a novel targeting method four-tract tractography for magnetic resonance–guided high-intensity focused ultrasound targeting. *Brain Communications*, *4*(6), fcac273.
3. Seas, A., Hon, K., Chung, D., Todd, L., Shah, B. R., Lad, S. P., & Harward, S. (2024). Four-tract tractography: multiparametric direct targeting of the dentatorubrothalamic tract. *Neurosurgical Focus: Video*, *11*(2), V2.
4. Elias, W. J., Lipsman, N., Ondo, W. G., Ghanouni, P., Kim, Y. G., Lee, W., ... & Chang, J. W. (2016). A randomized trial of focused ultrasound thalamotomy for essential tremor. *New England Journal of Medicine*, *375*(8), 730-739.
5. Verger, A., Witjas, T., Carron, R., Eusebio, A., Boutin, E., Azulay, J. P., ... & Guedj, E. (2019). Metabolic positron emission tomography response to gamma knife of the ventral intermediate nucleus in essential tremor. *Neurosurgery*, *84*(6), E294-E303.

Images/Tables



955

MRI and CT Features of Notochord Remnant Tumors Causing CSF Leak

Emily Z Lin BA, Shanna Mayorov BS, MS, M. Beatriz Lopes MD, PhD, Michael P Catalino MD, Sohil H Patel MD
University of Virginia, Charlottesville, VA, USA

Abstract Category

Head & Neck

Clinical History

Case 1: A 58-year-old male presented after syncope leading to a motor vehicle collision. CT head without contrast showed an air-fluid level within the right sphenoid sinus, but without definite sinonasal fracture. Cardiac work up for syncope was negative. The patient was discharged to home but re-presented to the ED one month later due to cerebrospinal fluid (CSF) rhinorrhea and persistent headaches.

Case 2: A 65-year-old female with asthma presented with several months of shortness of breath and cough, treated with amoxicillin-clavulanate and prednisone without improvement. She then developed subacute nasal drainage and failed a course of cefdinir. She later re-presented to an outside hospital for a second opinion, where a CT head was performed, and the results prompted referral back to our institution.

For both cases, surgery was performed and a pathologic diagnosis of chordoma was confirmed.

Imaging Findings

Case 1: MRI of the skull base with non-contrast cisternographic imaging on re-presentation to the ED showed a 17 mm heterogeneous lobulated mass eroding the superior aspect of the clivus, with a dominant component extending into the posterior aspect of the sphenoid sinus directly inferior to the sella turcica, and a smaller thinner intradural component extending into the prepontine cistern, abutting the basilar artery. The mass displayed mild peripheral curvilinear enhancement. There was layering CSF intensity fluid in the sphenoid sinus consistent with CSF leak. CT of the skull base showed calcification associated with the mass, and a 4mm local clival defect. A notochord remnant tumor with associated CSF leak was suspected based on the neuroimaging, and neurosurgery was consulted.

Case 2: The outside hospital CT head revealed pneumocephalus centered on the suprasellar cistern. Subsequent high resolution skull base CT revealed an osseous defect in the clivus and posterior sphenoid sinus wall, and CSF density fluid filling the right sphenoid sinus. Dedicated skull base MRI with non-contrast cisternographic imaging at our institution demonstrated the clival defect and showed a small round mass in this location. The mass showed no contrast-enhancement. CSF intensity fluid filled the right sphenoid sinus. A band-like flow void within the CSF indicated a jet of CSF flowing into the sphenoid sinus. On the basis of the neuroimaging findings, a notochord remnant tumor with associated CSF leak was suspected and neurosurgery was consulted.

Discussion

Classically, symptomatic notochord remnant tumors of the skull base present with headache and progressive cranial nerve palsies. CSF leak resulting from clival tumors is rare and associated with delayed diagnosis. Previously reported imaging features include CSF accumulation in the sphenoid sinus, clival bony defect, pneumocephalus, and a clival/posterior sphenoid sinus mass that can appear lobulated with variable contrast enhancement, calcification, cystic appearance, and a stalk-like connection to the clivus.

Teaching Point

Notochord remnant tumor as a cause for CSF leak is rare and may not be suspected clinically. Furthermore, the imaging diagnosis can be difficult without a high index of suspicion. Our cases emphasize the importance of high-resolution skull base CT and MRI for optimal detection and characterization of these lesions.

References

S. H. Lee, K. Y. Kwok, S. M. Wong, C. X. J. Chan, Y. T. Wong, and M. L. Tsang, “Chordoma at the skull base, spine, and sacrum: A pictorial essay,” JCIS, vol. 12, p. 44, Aug. 2022, doi: 10.25259/JCIS_62_2022.

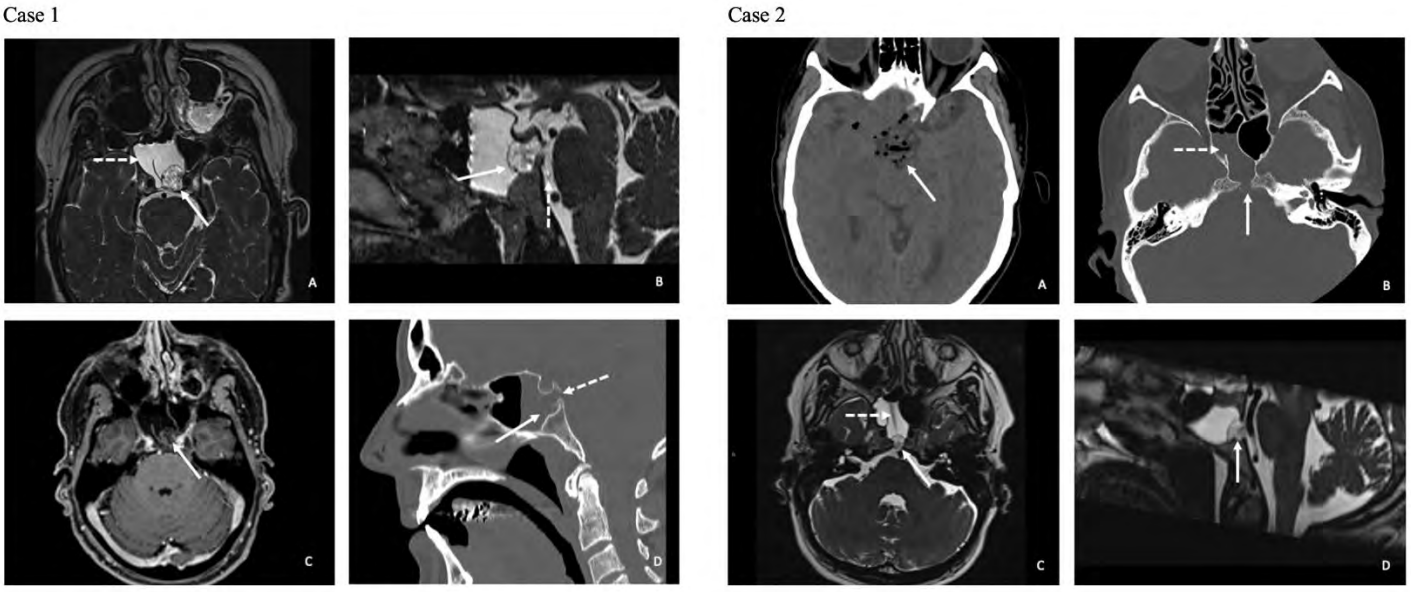
H. Hasegawa, J. J. Van Gompel, G. Choby, A. Raghunathan, J. T. Little, and J. L. Atkinson, “Unrecognized notochordal lesions as a likely cause of idiopathic clival cerebrospinal fluid leaks,” Clinical Neurology and Neurosurgery, vol. 224, p. 107562, Jan. 2023, doi: 10.1016/j.clineuro.2022.107562.

K. Y. Prather, H. H. Shi, K. A. McKinney, and I. F. Dunn, “Chronic cerebrospinal fluid rhinorrhea as an initial presentation of chordoma: illustrative case,” Journal of Neurosurgery: Case Lessons, vol. 5, no. 14, p. CASE2347, Apr. 2023, doi: 10.3171/CASE2347.

K. Feng, Z. Qiuhang, and Q. Qiuyi, “Transclival cerebrospinal fluid rhinorrhea as the initial presenting symptom of a tiny intradural chordoma,” Journal of Clinical Neuroscience, vol. 17, no. 8, pp. 1083–1085, Aug. 2010, doi: 10.1016/j.jocn.2009.12.012.

S. P. Meyers, W. L. Hirsch, H. D. Curtin, L. Barnes, L. N. Sekhar, and C. Sen, “Chordomas of the skull base: MR features,” AJNR Am J Neuroradiol, vol. 13, no. 6, pp. 1627–1636, 1992.

Images/Tables



961

28-year-old presenting with seizures related to MOGAD with FLAMES (FLAIR-hyperintense Lesion in Anti-MOG-associated Encephalitis with Seizure).

Nikhil R Kanthala DO, Elizabeth R Dutweiler MBBS
University of Pennsylvania, Philadelphia, PA, USA

Abstract Category

Adult Brain

Clinical History

28-year-old male presented to the emergency department following a seizure and three days of right sided headache. He was afebrile with normal CBC, and urine drug screen positive for cannabinoids. Initial brain MRI showed lack of FLAIR suppression of sulci in the right posterior temporal/occipital region with leptomeningeal enhancement. Lumbar puncture was performed with CSF showing neutrophilic pleocytosis but HSV and VZV PCR was negative. He was discharged with presumed viral meningitis, however he represented the following day with fever, vision changes and speech arrest concerning for seizure. A repeat lumbar puncture showed CSF bacterial and fungal cultures with no growth, flow cytometry with no evidence of hematolymphoid neoplasm, and autoimmune panel negative.

A repeat MRI one week after initial presentation was stable, and a CTA performed to rule out reversible cerebral vasoconstriction syndrome vs primary CNS vasculitis, considering history of marijuana use. CTA head was negative. A repeat Brain MRI, approximately one month after initial presentation, showed new leptomeningeal enhancement in the right frontal lobe sulci and undersurface of right temporal lobe.

A third lumbar puncture was low positive for MOG antibody (1:100). The patient went to brain biopsy of the right frontal lobe. Microscopic description from the biopsy included brain with acute and chronic inflammation, noting the inflammatory cells were seen in the vessels, in a perivascular distribution, focally involving the vessel walls and to a lesser extent the brain parenchyma, consistent with cortical encephalitis related to MOGAD. He was started on IVIG and IV methylprednisolone and transitioned to prednisone. A follow up MRI approximately 10 days following the biopsy showed improved sulcal signal abnormality.

Imaging Findings

Initial MRI showed lack of FLAIR suppression of sulci in the right posterior temporal/occipital region with leptomeningeal enhancement. MRI performed one month after initial presentation showed leptomeningeal enhancement in the right cerebral sulci mostly in right frontal lobe and undersurface of the right temporal lobe.

Discussion

Myelin oligodendrocyte glycoprotein (MOG) antibody associated disease is an inflammatory demyelinating disease characterized by the presence of IgG antibodies to myelin oligodendrocyte glycoprotein. It usually is encountered in children and young adults. It typically presents with optic neuritis, myelitis, or acute disseminated encephalomyelitis, but can rarely have focal cortical encephalitis type presentation with seizures. FLAMES stands for FLAIR hyperintense cortical lesions in MOG associated Encephalitis with Seizures. FLAMES can demonstrate unilateral or bilateral cortical encephalitis with possible meningeal inflammation. 60% of the cases occur in men and the mean presenting age is 29 years old. Clinical symptoms are seizures (85%), headache (70%), and fever (65%). Cortical symptoms can be referred to the location of FLAIR hyperintense signal abnormality. CSF studies show pleocytosis and anti-MOG seropositivity.

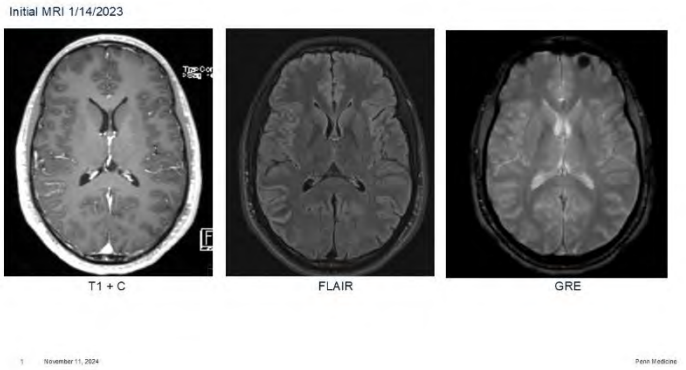
Teaching Point

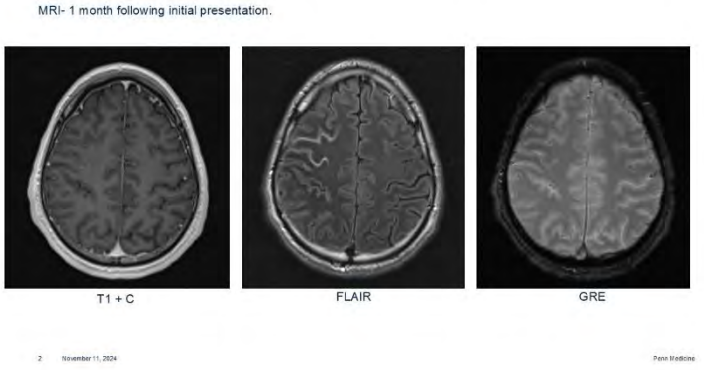
FLAMES is as subtype of the MOGAD spectrum that radiologists should be aware of. Although rare, with an estimated incidence of 1.6-3.4 per 1,000,000 person years, early recognition and diagnosis can help these patients as the condition is highly steroid responsive. It is also important to prevent misdiagnosis of MELAS (another entity with gyral signal in a nonvascular distribution).

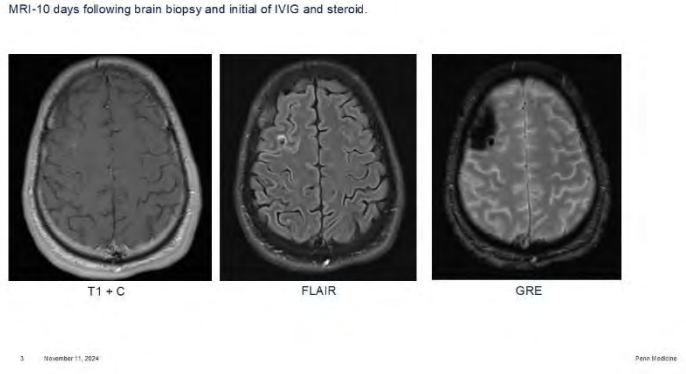
References

Reference: K. Jain et al. “FLAMES: A novel burning entity in MOG IgG associated disease”. Multiple Sclerosis and Related Disorders 49 (2021) 102759. “FLAMES: A novel burning entity in MOG IgG associated disease”

Images/Tables







964

"A Moth Eaten Sinus": A Rare Case of Sinonasal Ewing Sarcoma

Islam Ahmed Neuroradiology Fellow, MBBS, ABHS-R, FRCR, Faisal Alsugair Neuroradiology Fellow, MD, FRCPC, Santanu Chakraborty Professor Diagnostic Neuroradiologist.
University of Ottawa, The Ottawa Hospital, Ottawa, Ontario, Canada

Abstract Category

Head & Neck

Clinical History

A 69-year-old male patient presented with gradual-onset tearing and proptosis of the left eye over several months, along with numbness in the left cheek and upper lip.

On examination, there is no diplopia or vision changes, and no facial tenderness. Palpation of the bony skeleton reveals increased malar projection on the left side.

Imaging Findings

CT Findings: The CT scan of the sinuses reveals an expansile sclerotic lesion involving the left maxilla, the zygomatic process of the left maxilla, the left pterygoid plate, the left side of the hard palate, and the greater wing of the left sphenoid bone. Comparison with a CT scan from one-year prior shows progression of the lesion, with increased bone destruction and erosion.

MRI Findings: MRI with contrast reveals an enhancing soft tissue mass extending into the left masticator and buccal spaces, suggesting a malignant component. Associated inflammatory changes in the left maxillary sinus and proptosis of the left eye are also noted.

Interpretation: Initial differential diagnoses based on imaging included Fibrous dysplasia or Paget disease, with consideration of malignant transformation. However, histopathological analysis confirmed a diagnosis of a rare Ewing sarcoma with FUS-FEV fusion.

Discussion

Sinonasal Ewing sarcoma is a rare, aggressive tumor that usually originates in the bones and soft tissues of children and young adults. Primary Ewing sarcoma in the head and neck region is particularly uncommon, representing only 1–4% of all cases of Ewing sarcoma. Involvement of the sinonasal tract is extremely rare, with only a few cases reported in the literature worldwide.

Clinically, most patients present with an enlarging mass, nasal obstruction, rhinorrhea, and epistaxis. Other symptoms result from the tumor's mass effect. When the tumor extends into the periorbital area, patients may experience proptosis, periorbital swelling, and decreased visual acuity.

Diagnosing sinonasal Ewing sarcoma is challenging, as it requires ruling out other small round cell neoplasms. A definitive diagnosis is achieved through molecular analysis, specifically detecting the EWSR1/FLI-1 fusion, which results from a characteristic t(11;22) (q24;q12) chromosomal translocation.

The molecular hallmark of Ewing sarcoma (ES) is a fusion involving the EWSR1 gene and a member of the ETS family of transcription factors. EWSR1-FLI1 is the most common variant, present in 90% of cases, followed by EWSR1-ERG. In rare cases, the FUS gene can substitute for EWSR1 in these fusions. Reports of ES with FEV gene rearrangements are extremely rare.

In this case, a unique FUS-FEV fusion was identified. This fusion involves the FUS gene (on chromosome 16) and the FEV gene (on chromosome 2), producing a chimeric protein that contributes to tumor development.

The preferred treatment for Ewing sarcoma involves a multimodal approach, including surgery, radiotherapy, and chemotherapy. However, in this case, the patient declined surgical intervention and underwent both chemotherapy and radiotherapy.

Teaching Point

- Sinonasal Ewing sarcoma is an extremely rare diagnosis, especially in older individuals. The presence of a FUS-FEV fusion with FEV gene rearrangement is particularly uncommon.
- Clinical presentation depends on the involvement of nearby anatomical structures.
- Definitive diagnosis requires radiologic-pathologic correlation, which is essential for precise treatment planning.

References

Worthy, J., et al. “A Rare Case of Sinonasal Ewing Sarcoma With Radiologic-Pathologic Correlation.” *Cureus*, vol. 15, no. 8, 18 Aug. 2023, e43708, doi:10.7759/cureus.43708.

Al Hussain, O., Aldandan, A., Alkhatib, A., Alazzeh, G., Almomen, A. “Ewing’s Sarcoma of the Sinonasal Tract with Orbital Extension: A Rare Case Report and Literature Review.” *Journal of Surgical Case Reports*, vol. 2019, no. 3, March 2019, rjy362, doi:10.1093/jscr/rjy362.
Boone, M. A., Taslim, C., Crow, J. C., Selich-Anderson, J., Watson, M., Heppner, P., Hamill, J., Wood, A. C., Lessnick, S. L., & Winstanley, M. “Identification of a Novel FUS/ETV4 Fusion and Comparative Analysis With Other Ewing Sarcoma Fusion Proteins.” *Molecular Cancer Research*, Aug. 31, 2021, doi:10.1158/1541-7786.MCR-21-0354.
Tsuda, Y., Dickson, B., Swanson, D., Sung, Y.-S., Zhang, L., Meyers, P., Healey, J., & Antonescu, C. “Ewing Sarcoma with FEV Gene Rearrangements: A Rare Subset with Predilection for Extraskeletal Locations and Aggressive Behavior.” *Genes, Chromosomes and Cancer*, vol. 59, 2019, doi:10.1002/gcc.22828.
Images/Tables

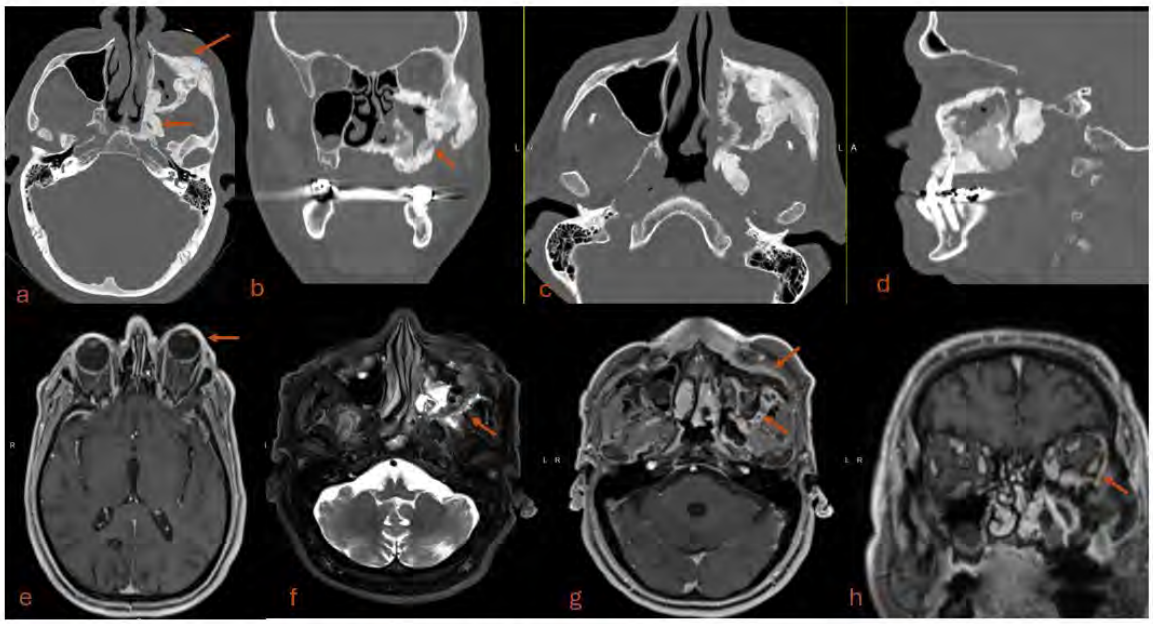


Figure: Axial CT scan of the nasal sinuses (a) shows an expansile sclerotic lesion involving the left maxillary sinus, hard palate, inferior wall of the left orbit, zygoma, pterygoid plate, and greater wing of the sphenoid bone. A follow-up CT scan taken one year later (b, c, and d) reveals further enlargement of the expansile lesion with increased bone destruction. MRI of the head with contrast (f, g, and h) demonstrates an enhancing soft tissue component with intra-orbital extension. Note the left eye proptosis (e).

974

Case of a Hypoplastic Left Meckel’s Cave with Trigeminal Neuralgia

Emilynn Cortese MD[1], Bethany Ho MD[1], Davishia Henderson BS[2], Valeria Potigailo MD[1], Abigail Anderson MD[1]
[1]University of Colorado Anschutz Medical Campus, Aurora, Colorado, USA. [2]University of New Mexico School of Medicine, Albuquerque, New Mexico, USA
Abstract Category
Adult Brain
Clinical History
A 29-year-old female with a medical history significant for traumatic brain injury, anemia, and depression presented to the neurology clinic with acute left-sided facial pain, characteristic of trigeminal neuralgia (TN), localized to the mandibular branch of the trigeminal nerve. The pain was paroxysmal, lancinating, and triggered by brushing teeth and talking. She had no additional sensory or motor deficits nor any preceding illness or identifiable precipitating event. Infectious and inflammatory laboratory findings were unremarkable, with brain imaging revealing the underlying pathology. Initially, the patient achieved symptomatic relief with medical management, but over time her symptoms became refractory to multiple medications. Subsequently, she was referred for neurosurgical evaluation.
Imaging Findings
Brain MRI with/without contrast revealed markedly asymmetric volume loss involving the left trigeminal nerve cisternal segment, including the root entry zone. Notably, the left Meckel’s cave also appeared diminutive, containing a small dysmorphic Gasserian ganglion without abnormal enhancement. Additionally, the left cavernous sinus and foramen

ovale were mildly diminished in size compared to the contralateral side. No evidence of a compressive lesion or neurovascular conflict was identified. These imaging features suggested a possible anatomic abnormality contributing to the trigeminal neuralgia.

Discussion

TN is characterized by recurrent, sudden-onset, electric shock-like pain along the trigeminal nerve branches. The pain is often triggered by innocuous stimuli, such as talking, eating, or brushing the teeth. TN is most often caused by vascular compression, commonly by the superior cerebellar artery at the root entry zone of the trigeminal nerve. However, any lesion along the trigeminal nerve course may contribute to the clinical syndrome.

One of the rarest causes of TN is the absence or hypoplasia of the Meckel's cave, a dural reflection housing the trigeminal nerve ganglion. Though extremely rare, several cases of hypoplastic or aplastic Meckel's cave have been reported, predominantly in females with a mean age of 44.6 years. Many of these cases involve the right side, though left-sided cases, such as the one described here, have also been documented.

The pathophysiology underlying the relationship between TN and Meckel's cave abnormalities, which can be congenital or acquired in nature, remains uncertain. These anatomical variations may disrupt the typical course of the trigeminal nerve, potentially contributing to nerve irritation or compression that may illicit the typical paroxysmal pain of TN.

Treatment of TN depends on the underlying cause and includes medical management (e.g., anticonvulsants such as carbamazepine, gabapentin, or pregabalin), surgical decompression, stereotactic radiosurgery, and percutaneous balloon compression. In this case, the patient experienced a gradual decline in pain control despite trying multiple medications and was referred for neurosurgical evaluation.

Teaching Point

Aplastic or hypoplastic Meckel's cave is an exceedingly rare cause of trigeminal neuralgia. When a patient presents with idiopathic TN, it is essential for radiologists to survey for structural abnormalities of Meckel's cave as part of their imaging evaluation, as such anomalies could contribute to nerve compression or dysfunction. This highlights the importance of a thorough radiologic evaluation in cases of TN, even when no vascular or obvious compressive lesion is apparent.

References

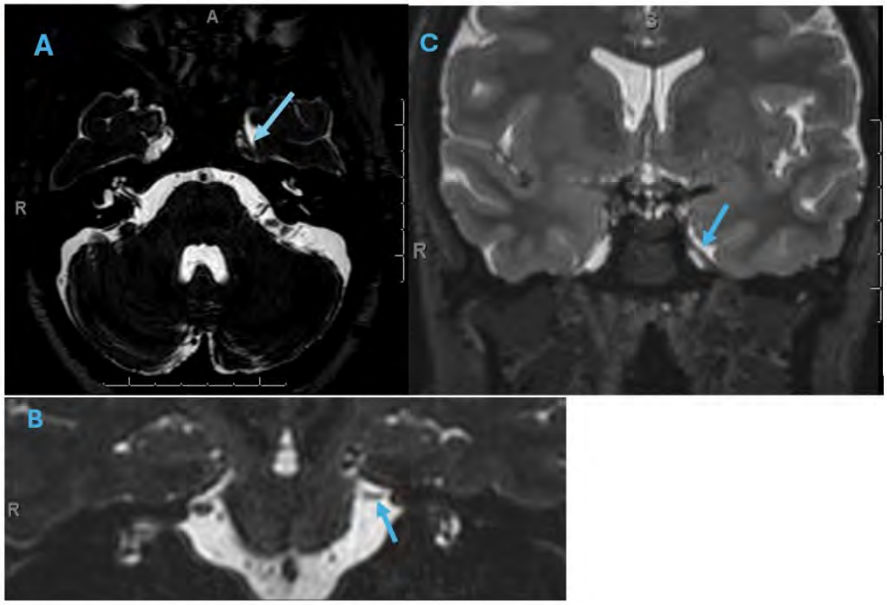
1. AlHatmi A, Al-Qassabi A, Raniga SB, et al. Absence of Meckel's Cave with Trigeminal Neuralgia: A Case Report. *Indian J Radiol Imaging*. 2022;33:124-128. DOI:10.1055/s-0042-1759638]

2. Jain A, Muneer MS, Okromelidze L, et al. Absence of Meckel Cave: A Rare Cause of Trigeminal Neuralgia. *AJNR Am J Neuroradiol*. 2021;42:1610-1614. DOI:10.3174/ajnr.A7205

3. Cleary D R, Handwerker J, Ansari H, Ben-Haim S. Three cases of trigeminal neuralgia with radiographic absence of Meckel's cave. *Stereotact Funct Neurosurg*. 2019;97:249–254. DOI: 10.1159/000502564.

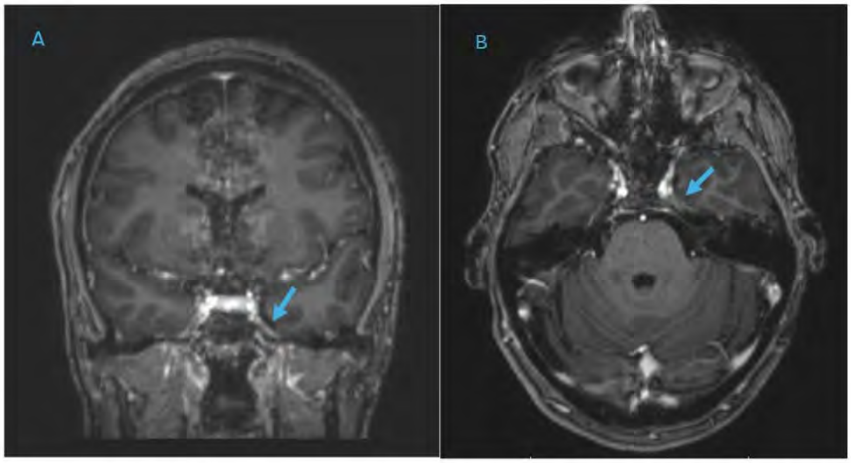
Images/Tables

Figure 1.



CISS images show the hypoplastic left Meckel's cave (arrow) in the axial plane (A). The Hypoplastic cisternal segment of the left trigeminal nerve is seen in the coronal plane (arrow) (B). A coronal T2 weighted image demonstrates hypoplasia of the Meckel's cave on the left (arrow) (C).

Figure 2.



Coronal (**A**) and axial (**B**) contrast enhanced T1 weighted images show the hypoplastic left Meckel's cave without an underlying lesion (arrow).

988

"Air in the brain?" : Dialysis related venous air embolism

Faisal Alsugair MD, FRCPC[1], Islam Ahmed ABHS-R, FRCR[1], Christine De Meulemeester MD, FRCPC[2], Mandeep Ghuman MD[3], Marlise P dos Santos MD, FRCPC[1], Paulo Puac Polanco MD[1]

[1]Department of Radiology, Radiation Oncology and Medical Physics, University of Ottawa, Ottawa, Ontario, Canada. [2]Department of Neurology , University of Ottawa, Ottawa, Ontario, Canada. [3]St. Joseph's Healthcare , McMaster University, Hamilton, Ontario, Canada

Abstract Category

Adult Brain

Clinical History

60-year-old man with end stage renal failure developed a thunderclap headache while on dialysis, together with speech difficulties and bilateral numbness of the hands. A non-contrast CT head and CT angiography were negative. An MRI revealed multiple T2/FLAIR hyperintensities at the convexities of the bilateral frontoparietal regions, suggestive of ischemia secondary to venous air embolism. Other considerations included septic emboli or infarcts from a cardiac cause.

75-year-old male with end-stage kidney disease. The venous line alarm went off during hemodialysis, and he immediately started with decreased LOC. An MRI showed gyriform areas of diffusion restriction in the frontal cortices. Air embolism was diagnosed, and he underwent hyperbaric oxygen therapy.

Imaging Findings

Multiple T2/flair hyperintensities within the cortical and subcortical region of the superior aspects of the bilateral frontoparietal regions at the convexity. These regions show high DWI signal with pseudonormalization of ADC in keeping with subacute ischemic lesions.

Multiple T2/flair gyrifrom hyperintensities within the cortical and subcortical regions of frontal lobes at the convexities. These regions show high DWI signal with low of ADC in keeping with acute ischemic lesions.

Discussion

Cerebral air embolism (CAE) is an uncommon yet devastating iatrogenic complication that can be a diagnostic dilemma. Symptoms include an altered level of consciousness, confusion, stroke-like manifestations, vision loss, and motor weakness. In addition, they may present with cardiopulmonary symptoms such as angina, cardiac arrhythmias, and respiratory distress or may remain clinically silent, making diagnosis difficult.

Most cases are iatrogenic, with common causes including central venous catheter placement or malfunction, hemodialysis lines, percutaneous lung biopsy, positive ventilation pressure, trauma, and mechanical thrombectomy. Obtaining a complete history can identify a potential culprit and narrow it down to an arterial or venous causes. The most likely cause in our two cases, given the exclusion of mimickers like encephalitis and cardioembolic stroke, was air. It is essential to obtain a CT brain immediately after CAE as air is absorbed quickly through the capillaries. MRI findings of CAE are diffusion restriction in a cortical and gyriform pattern. Blooming on SWI sequences has been reported in larger volumes of air.

Hyperbaric Oxygen Therapy (HBOT) is the mainstay of treatment. Patients with venous CAE are placed in left lateral decubitus (Durant's maneuver) or Trendelenburg position to prevent air from traveling to the right ventricular outflow tract. A right lateral decubitus position to prevent air from traveling to the left ventricular outflow tract is done in arterial CAE or kept supine to prevent cerebral embolisms. It is important to consider concurrent cerebral edema, as Trendelenburg may inadvertently raise intracranial pressure.

Teaching Point

- CAE remains a diagnostic dilemma and is usually iatrogenic from either venous or arterial causes.
- A detailed history and exclusion of other causes are crucial to establishing a diagnosis.
- An immediate CT may show air, but its absence does not exclude CAE.
- MRI demonstrates gyriform and cortical areas on DWI with blooming in larger volumes.
- Supportive treatment is provided while ensuring the patient's stability, resuscitation, and correct positioning so that further exacerbations are prevented.

References

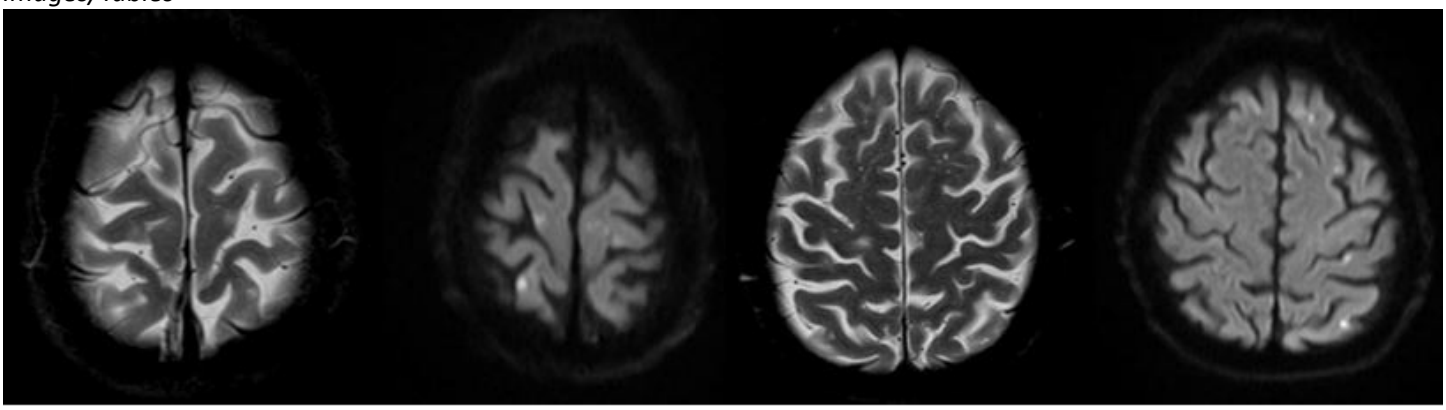
1-Characteristic MR Imaging Findings of Cerebral Air Embolism Infarcts: A Case Series
Vincent M. Timpone, Andrew L Callen
American Journal of Neuroradiology May 2024, ajnr.A8349; DOI: 10.3174/ajnr.A8349

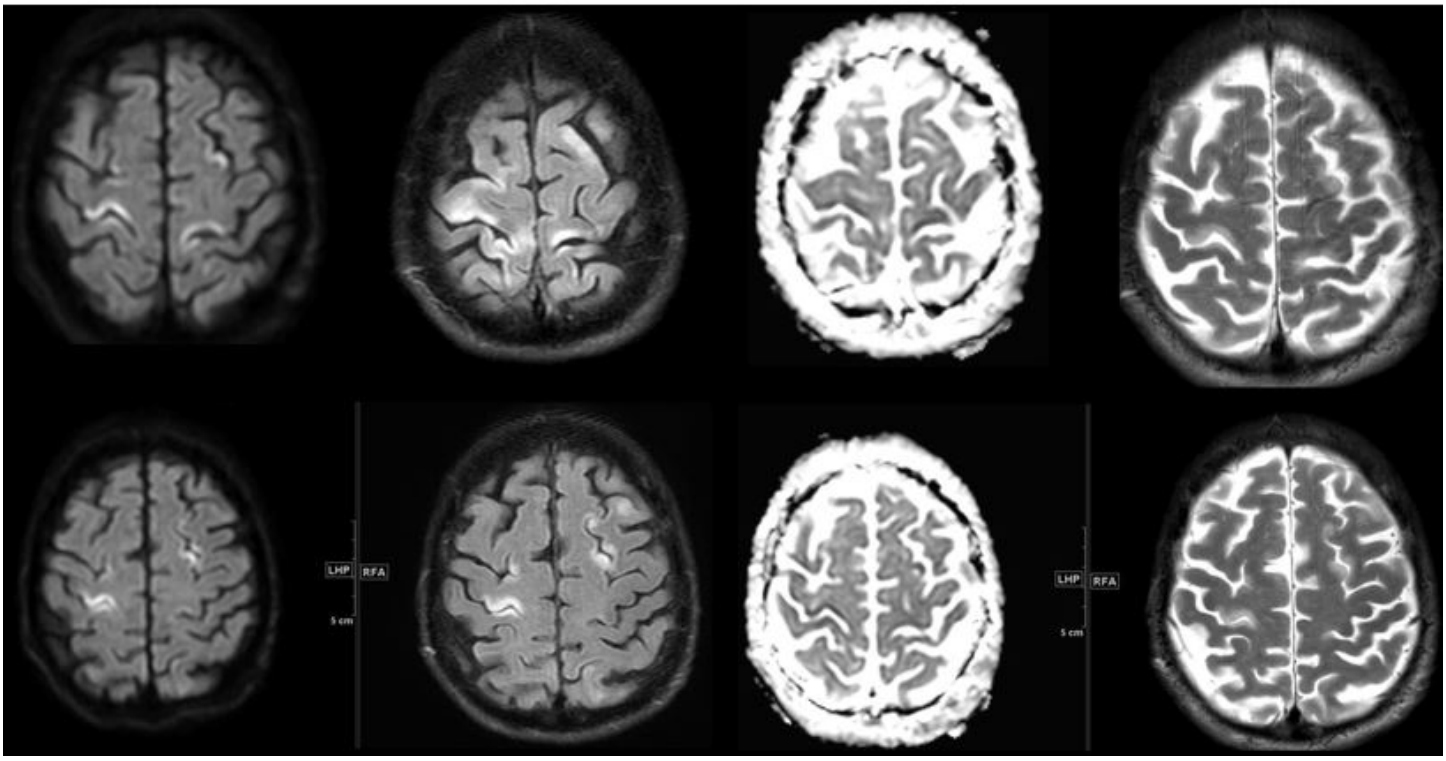
2-Cerebral air embolism: neurologic manifestations, prognosis, and outcome
Červeňák V, Všianský V, Cviková M, Brichta J, Vinklárek J, Štefela J, Haršány M, Hájek M, Herzig R, Kouřil D, Bárková V, Filip P, Aulický P, Weiss V. Cerebral air embolism: neurologic manifestations, prognosis, and outcome. Front Neurol. 2024 Jun 19;15:1417006. doi: 10.3389/fneur.2024.1417006. PMID: 38962484; PMCID: PMC11220112.

3- Cerebral Air Embolism: The Importance of Computed Tomography Evaluation
Brito C, Graca J, Vilela P. Cerebral Air Embolism: The Importance of Computed Tomography Evaluation. J Med Cases. 2020 Dec;11(12):394-399. doi: 10.14740/jmc3583. Epub 2020 Oct 21. PMID: 34434352; PMCID: PMC8383554.

4- MRI characteristics of cerebral air embolism from a venous source.
Caulfield AF, Lansberg MG, Marks MP, Albers GW, Wijman CA. MRI characteristics of cerebral air embolism from a venous source. Neurology. 2006 Mar 28;66(6):945-6. doi: 10.1212/01.wnl.0000203117.20406.eb. PMID: 16567722.

5- Kang SR, Choi SS, Jeon SJ. Cerebral Air Embolism: a Case Report with an Emphasis of its Pathophysiology and MRI Findings.
Investig Magn Reson Imaging. 2019 Mar;23(1):70-74.
Images/Tables





989

"Beyond the Adrenals, When Neuroblastoma Hits the Skull Base": A Pediatric Case with Multimodal Imaging.

Maria Laura Aragon Daza MD, Florencia Daniela Vespa MD, Agustina del Cerro MD, Manuel Sliman Perez Akly MD, Cristina Hilda Besada MD
Hospital Italiano de Buenos Aires, CABA, CABA, Argentina
Abstract Category
Pediatrics
Clinical History
24-month-old boy was admitted to the ER with one month of obtunded sensorium, headache, and sleepiness. The patient was first admitted to the pediatrics ER because of a medical history of multiple pulmonary vascular malformations, he was in critical condition for several days. During the hospitalization an adrenal gland mass was found.

This caused the patient to go through periodic ultrasound for months until an MRI was requested, but the parents refused. A Brain CT and MRI was performed.

Imaging Findings

Head and face contrast-enhanced CT

An expansive mass was observed at the sphenoethmoidal junction, extending into both the anterior and middle skull base, involving both orbits, as well as the brain parenchyma. Anteriorly, the mass extended into the posterior nasal cavity and roof of both orbits, engaging the extraconal fat and coming into contact with the superior and middle rectus muscles. It encased the optic nerves at the optic canal. The lesion displayed a permeative pattern in the adjacent osseous structures, resulting in alteration of their morphology, and some foci of "hair-on-end" periosteal reaction. The medial skull base involvement included the sella turcica, the anterior clinoid and clivus processes. The mass appeared faintly hyperdense, with post-contrast enhancement. It encased the intracavernous portions of the internal carotid arteries without caliber change.

Brain, face and orbits contrast-enhanced MRI

The expansive mass at the sphenoethmoidal junction and skull base had heterogeneous signal, hypointense in T1/T2, restricted diffusion and heterogeneous nodular postcontrast enhancement. The involvement of the posterior part of the nostrils, roof and medial wall of the orbits and the sphenoidal bone was better established with the MR. It was also evident the involvement of the sella turcica and intracranially, the right frontal orbital gyri. The lesion expanded to both cavernous sinuses and Meckel's cave. It surrounded the optic nerves, with high signal in T2/STIR. The mass also surrounds the internal carotid arteries at the intracavernous portion, without alterations in the caliber.

Discussion

Neuroblastoma, the third most common pediatric malignancy, represents 10–15% of childhood cancers. Osseous metastases typically originate from adrenal tumors or sympathetic chain involvement, though skull metastases are relatively rare. Improved systemic therapies that enhance survival rates may inadvertently create sanctuary sites in the CNS due to poor penetration of these drugs across the blood-brain barrier, resulting in delayed detection of CNS metastase, over 50% of which are diagnosed months or years post-treatment. Metastatic lesions can be classified by the site of manifestation:

1. Skull, can cause bone thickening, "hair-on-end" periosteal reactions, lytic defects, and suture separation.
2. Dural, often coincide with osseous metastasis.
3. Parenchymal, typically found supratentorially, appearing lobulated and well-defined, often showing cystic/hemorragic degeneration.
4. Intraventricular and leptomeningeal, may cause diffuse and focal nodular leptomeningeal enhancement.

Teaching Point

Although neuroblastoma is not the most common pediatric malignancy, recognizing its imaging features is crucial for guiding treatment and detecting secondary lesions.

The limited blood-brain barrier penetration of new chemotherapies, highlights the need for treatments addressing primary and metastatic tumors.

Metastases are classified by location: skull, dura, parenchyma, intraventricular, and leptomeningeal.

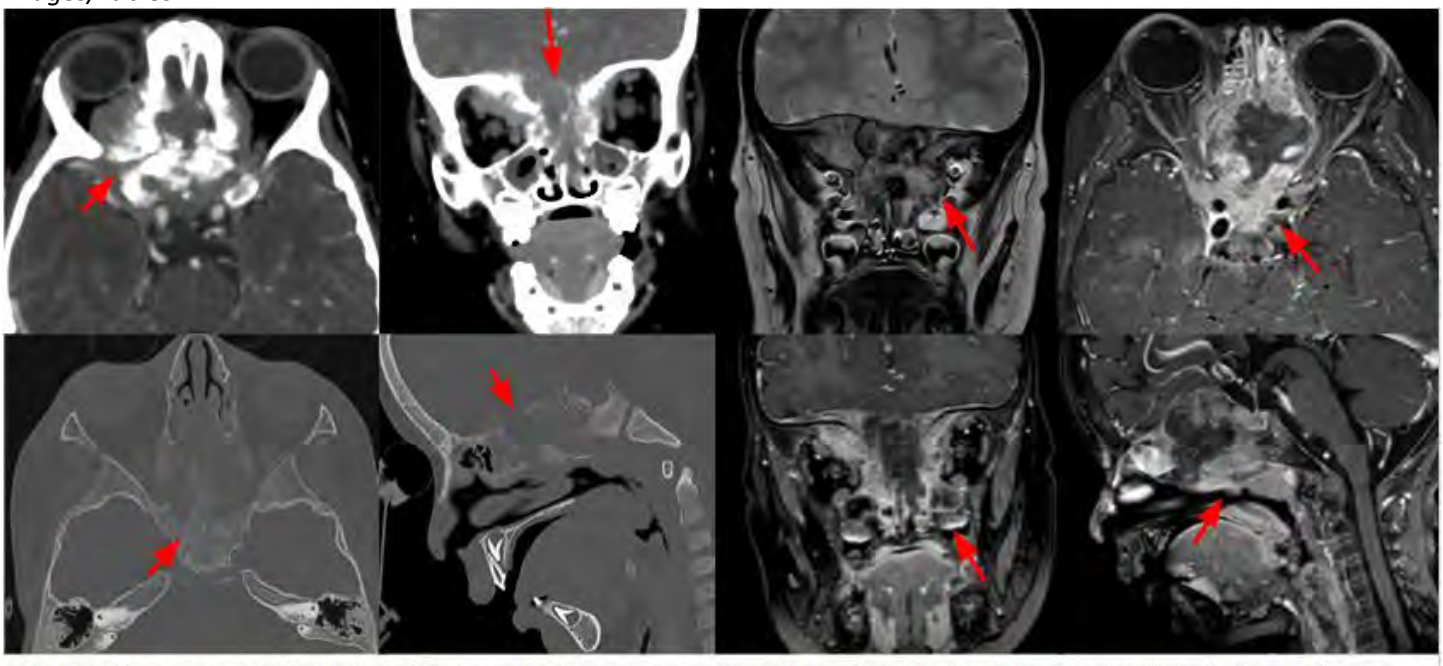
References

1. Nicholas D'Ambrosio, John K. Lyo, Robert J. Young, Sophia S. Haque, and Sasan Karimi; Imaging of Metastatic CNS Neuroblastoma; American Journal of Roentgenology 2010 194:5, 1223-1229.

2. Balaji, R., Ramachandran, K.N., & Kusumakumari, P. (2009). Neuroimaging Patterns of Central Nervous System Metastases in Neuroblastoma: Report of 2 Recent Cases and Literature Review. *Journal of Child Neurology, 24*, 1290 - 1293.

3. Mastronuzzi A, Colafati GS, Carai A, D'Egidio M, Fabozzi F, Del Bufalo F, Villani MF, Del Baldo G, Vennarini S, Canino C, Di Giannatale A, Tomà P, Garganese MC, De Ioris MA. Central Nervous System Metastasis in Neuroblastoma: From Three Decades Clinical Experience to New Considerations in the Immunotherapy Era. Cancers (Basel). 2022 Dec 19;14(24):6249. doi: 10.3390/cancers14246249. PMID: 36551734; PMCID: PMC9777007.

Images/Tables



Head and face non contrast enhanced CT, shows a expansive mass at the sphenoethmoidal junction, extending into both the anterior and middle skull base.
Brain, face and orbits contrast-enhanced MRI, mass at the sphenoethmoidal junction and skull base had heterogeneous signal, predominantly hypointense in T1 and T2, restricted diffusion and heterogeneous nodular postcontrast enhancement.

990

Cerebral Arterial Gas Embolism (CAGE) Following Bronchoscopic Biopsy: A Rare Complication of an Emerging Technique

Gautam Dua MD
Tulane University, New Orleans, LA, USA

Abstract Category

Interventional

Clinical History

A 70-year-old patient with bilateral upper lobe nodules underwent robotic transbronchial biopsy with cone beam CT guidance. The sampling device penetrated the full thickness of the bronchial wall to obtain needle aspiration samples from both right and left upper lobe nodules. In the PACU, the patient's mentation failed to improve. She exhibited pinpoint pupils, left gaze deviation, and posturing, prompting a code stroke.

Imaging Findings

Head CT showed multifocal gas within the bilateral subarachnoid space(Figure 1) and elevated Tmax in several areas(Figure 2). Intraoperative CT revealed pneumomediastinum with subcutaneous emphysema, as well as gas within the aorta, brachiocephalic, and jugular veins(Figure 3). Two days later, an MRI displayed diffuse bilateral gyriform T2/FLAIR cortical and subcortical hyperintensity with restricted diffusion(Figure 4). An echocardiogram showed no inter-atrial shunting.

Discussion

Cerebral air embolism (CAE) following transbronchial lung biopsy is a rare complication[1]. In this case, gas directly entered the aorta, leading to intracranial arterial gas and subsequent infarction. Transbronchial lung biopsy can disrupt vessel walls within the lung parenchyma. Elevated airway pressures, resulting from a patient exhaling against a bronchoscope wedged in a segmental bronchus, may then force air bubbles through these defects, potentially leading to air emboli[2]. However, given the extensive pneumomediastinum and gas within the aorta observed in this case, an intraprocedural complication likely contributed to the pneumomediastinum and subsequent air embolism.
Treatment for cerebral arterial gas embolism (CAGE) involves high-flow 100% oxygen, with the patient positioned supine[3]. The Trendelenburg position is contraindicated, as it may worsen cerebral edema and intracranial hypertension[4].

Teaching Point

Cerebral air embolism is a rare potential complication of transbronchial lung biopsy, a relatively new technique. Prompt recognition and management such as administering high-flow oxygen and ensuring proper patient positioning are crucial for optimizing patient outcomes.

References

1. Herout V, Brat K, Richter S, Cundrle I Jr. Cerebral air embolism complicating transbronchial lung biopsy: A case report. World J Clin Cases. 2021 Nov 16;9(32):9911-9916. doi: 10.12998/wjcc.v9.i32.9911.
2. Evison M, Crosbie PA, Bright-Thomas R, et al. Cerebral air embolism following transbronchial lung biopsy during flexible bronchoscopy. *Respir Med Case Rep*. 2014;12:39-40. Published 2014 Mar 28. doi:10.1016/j.rmcr.2013.10.005
3. Jorens PG, Van Marck E, Snoeckx A, Parizel PM. Nonthrombotic pulmonary embolism. Eur Respir J. (2009) 34:452–74. doi: 10.1183/09031936.00141708
4. Červeňák V, Všianský V, Cviková M et al. Cerebral air embolism: neurologic manifestations, prognosis, and outcome. Front Neurol. 2024 Jun 19;15:1417006. doi: 10.3389/fneur.2024.1417006.

Images/Tables

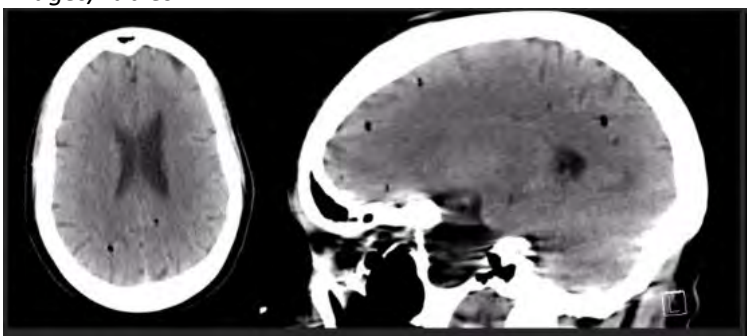


Figure 1. Non-contrast head CT showing multifocal gas within the bilateral subarachnoid space.

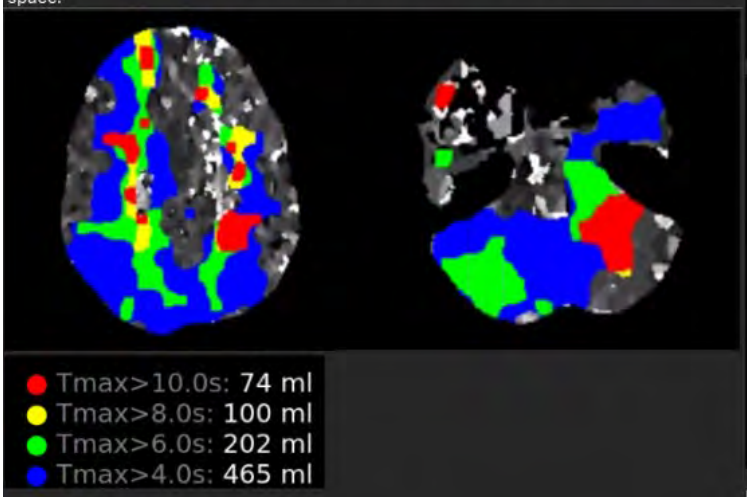


Figure 2. Multifocal elevated Tmax.

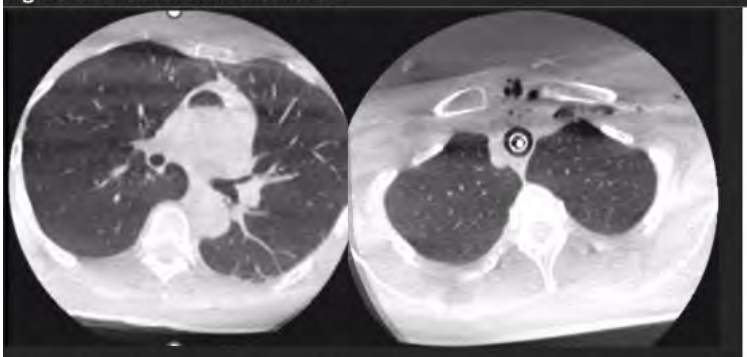


Figure 3. Intraoperative cone beam CT demonstrates extensive gas within the aorta(left) and subcutaneous and venous gas(right).

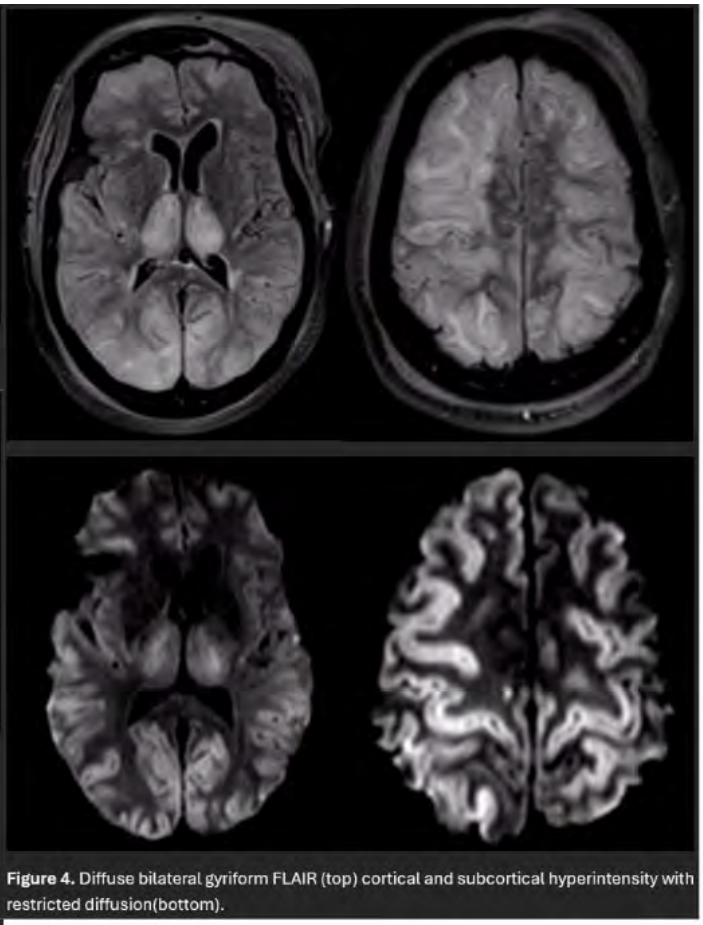


Figure 4. Diffuse bilateral gyriform FLAIR (top) cortical and subcortical hyperintensity with restricted diffusion(bottom).

992

Something in the air ? - Cerebral air embolism from a peculiar cause

Faisal Alsugair MD, FRCPC, Islam Ahmed MBBS, ABHS-R, FRCR, Abdullah Alqabbani MD, FRCPC , dABR, Paulo Puac Polanco MD, Marlise P dos Santos MD, FRCPC
Department of Radiology, Radiation Oncology and Medical Physics, University of Ottawa, Ottawa, Ontario, Canada

Abstract Category

Adult Brain

Clinical History

104-year-old woman who exhibited periumbilical that radiated to the right lower quadrant. Her prior history included a small bowel obstruction, a right femoral hernia, and an appendicitis (De Garengeot hernia). Shortly after assessing her, she became unresponsive with Glasgow Coma Scale (GCS) of 3.

A CT scan of the Head showed feature of air emolism. Further imaging of the chest, abdomen and pelvis showed a lower esophageal tear the level of gastric esophageal junction , emphysema in lower posterior mediastinal and extension of pneumomediastinum superiorly to lower left neck. In the abdomen and pelvis, a right inguinal hernia with proximal small bowel obstruction and features concerning for bowel ischemia. Both Thoracic surgery and General surgery were both consulted for these findings, however the patient passed away shortly after.

Imaging Findings

CT HEAD: Sizable diffuse intracranial arterial air embolism noted with subarachnoid air in multiple cerebral sulci, basal ganglia and deep cerebral white matter.

CT CHEST: Lower esophageal tear the level of gastric esophageal junction. Emphysema in lower posterior mediastinal and extension of pneumomediastinum superiorly to lower left neck.

CT ABDOMEN AND PELVIS: A right inguinal hernia with small bowel loops associated with proximal small bowel obstruction.A small amount of interloop free fluid was well as a segment of proximal small bowel with decreased mural enhancement, in keeping with bowel ischemia.

Discussion

Cerebral air embolism (CAE) is an uncommon yet devastating iatrogenic complication that can be a diagnostic dilemma. Symptoms include an altered level of consciousness, confusion, stroke-like manifestations, vision loss, and motor weakness. In addition, they may present with cardiopulmonary symptoms such as angina, cardiac arrhythmias, and respiratory distress or may remain clinically silent, making diagnosis difficult.

Most cases are iatrogenic, with common causes including central venous catheter placement or malfunction, hemodialysis lines, percutaneous lung biopsy, positive ventilation pressure, trauma, and mechanical thrombectomy. Obtaining a complete history can identify a potential culprit and narrow it down to an arterial or venous causes. It is essential to obtain a CT brain immediately after CAE as air is absorbed quickly through the capillaries. MRI findings of CAE are diffusion restriction in a cortical and gyriform pattern. Blooming on SWI sequences has been reported in larger volumes of air.

In our case, the patient had the unfortunate event of developing bowel obstruction complicated by bowel ischemia. Based on her severe pain and vomiting, it could be hypothesized that she had ruptured her esophagus (Boerhaave syndrome) and developed subcutaneous emphysema in the neck that extended into the intracranial space in combination with pneumatosis intestinalis resulting in fatal arterial air embolism.

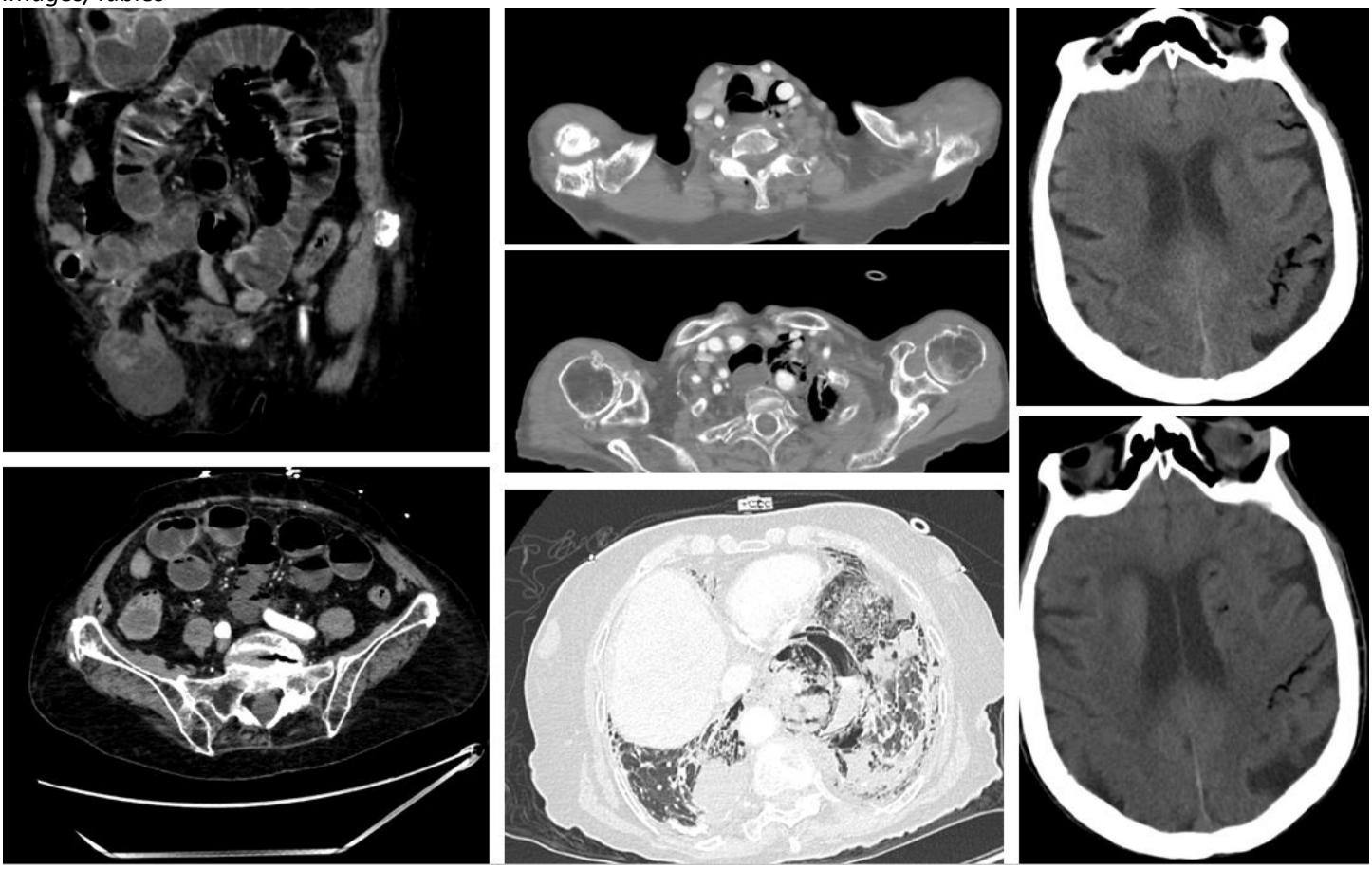
Teaching Point

- CAE remains a diagnostic dilemma and is usually iatrogenic from either venous or arterial causes.
- A detailed history and exclusion of other causes are crucial to establishing a diagnosis.
- An immediate CT may show air, but its absence does not exclude CAE.
- MRI demonstrates gyriform and cortical areas on DWI with blooming in larger volumes.
- Supportive treatment is provided while ensuring the patient's stability, resuscitation, and correct positioning so that further exacerbations are prevented.

References

1-Characteristic MR Imaging Findings of Cerebral Air Embolism Infarcts: A Case Series
Vincent M. Timpone, Andrew L Callen
American Journal of Neuroradiology May 2024, ajnr.A8349; DOI: 10.3174/ajnr.A8349
2-Cerebral air embolism: neurologic manifestations, prognosis, and outcome

Červeňák V, Všianský V, Cviková M, Brichta J, Vinklárek J, Štefela J, Haršány M, Hájek M, Herzig R, Kouřil D, Bárková V, Filip P, Aulický P, Weiss V. Cerebral air embolism: neurologic manifestations, prognosis, and outcome. Front Neurol. 2024 Jun 19;15:1417006. doi: 10.3389/fneur.2024.1417006. PMID: 38962484; PMCID: PMC11220112.
3- Cerebral Air Embolism: The Importance of Computed Tomography Evaluation
Brito C, Graca J, Vilela P. Cerebral Air Embolism: The Importance of Computed Tomography Evaluation. J Med Cases. 2020 Dec;11(12):394-399. doi: 10.14740/jmc3583. Epub 2020 Oct 21. PMID: 34434352; PMCID: PMC8383554.
4- MRI characteristics of cerebral air embolism from a venous source.
Caulfield AF, Lansberg MG, Marks MP, Albers GW, Wijman CA. MRI characteristics of cerebral air embolism from a venous source. Neurology. 2006 Mar 28;66(6):945-6. doi: 10.1212/01.wnl.0000203117.20406.eb. PMID: 16567722.
5- Kang SR, Choi SS, Jeon SJ. Cerebral Air Embolism: a Case Report with an Emphasis of its Pathophysiology and MRI Findings.
Investig Magn Reson Imaging. 2019 Mar;23(1):70-74.
Images/Tables



1001

CSF-Lymphatic Fistula and Cervico-Thoracic Syrinx with Intracranial Features of Intracranial Hypertension: Case Report and Discussion of CSF-Related Pathology

Thomas R Geisbush MD, Osama A Raslan MD, Arzu Ozturk MD, Connor Gemmell MD, Muhammad T Raj MD, Kader K Oguz MD, Lotfi Hacein-Bey MD
UC Davis Medical Center, Sacramento, CA, USA
Abstract Category
Spine
Clinical History
A 44-year-old female patient presented with a longstanding and progressively disabling pattern of left arm and leg numbness and burning sensation without motor weakness or ataxia. The patient denied headaches, orthostatic or other, and did not present with clinical signs of Chiari I malformation.

Imaging Findings

Cervical spine MRI demonstrated an extensive syringohydromyelia extending caudally to the thoracic spine, with relative preservation of bidirectional CSF flow about an enlarged cord. Associated tonsillar descent was present, not exceeding 5 mm. MRI of the brain not only did not demonstrate evidence of the usual signs of intracranial hypotension, but showed a partially empty sella without other imaging findings of intracranial hypertension. CT-myelography, obtained to assess the syringohydromyelia, demonstrated a subtle CSF-lymphatic fistula at the lower thoracic level draining into pleural lymphatics.

Discussion

Despite increasing characterization, spinal CSF leaks remain underdiagnosed, and their clinical manifestations incompletely understood. Known causes for spontaneous intracranial hypotension (SIH) will be reviewed in this presentation. Dural tears related to a bone spur, ruptured nerve root sleeve diverticulum, or (more recently defined) a CSF-venous fistula are the main currently recognized causes of spontaneous intracranial hypotension.[1] CSF-lymphatic fistulae remain poorly understood. The association between CSF leaks and a syrinx has been recognized and is thought to be promoted by partial obex obstruction.[2] However, the clinical presentation in those patients usually corresponds to the imaging features. Although the patient presented with central cord signs attributable to a large syrinx, they consistently denied headaches, whether orthostatic or not.

Teaching Point

The presence of a large syrinx, even when associated with tonsillar descent, should not be hastily diagnosed as Chiari I malformation in the absence of classic clinical signs. CSF leaks have been shown to cause a syringohydromyelia, especially when mild tonsillar descent is present to obstruct the obex. In our patient with evidence of a CSF-lymphatic fistula, a large syringohydromyelia, an empty sella, persistent bidirectional cervical CSF flow and absence of headaches, we speculate that imbalance of CSF flow dynamics between spinal and cranial compartments may have altered the clinical presentation, possibly in relation to a slower rate of CSF leakage into the lymphatic system compared to other known types of CSF leaks.

References

1. Farb RI, Nicholson PJ, Peng PW, et al. Spontaneous intracranial hypotension: A systematic imaging approach for CSF leak localization and management based on MRI and digital subtraction myelography. *American Journal of Neuroradiology* 2019;40:745–53.

2. Richard S, Humbertjean L, Mione G, et al. Syringomyelia Caused by Traumatic Intracranial Hypotension: Case Report and Literature Review. *World Neurosurg* 2016;91:674.e13-674.e18.

Images/Tables

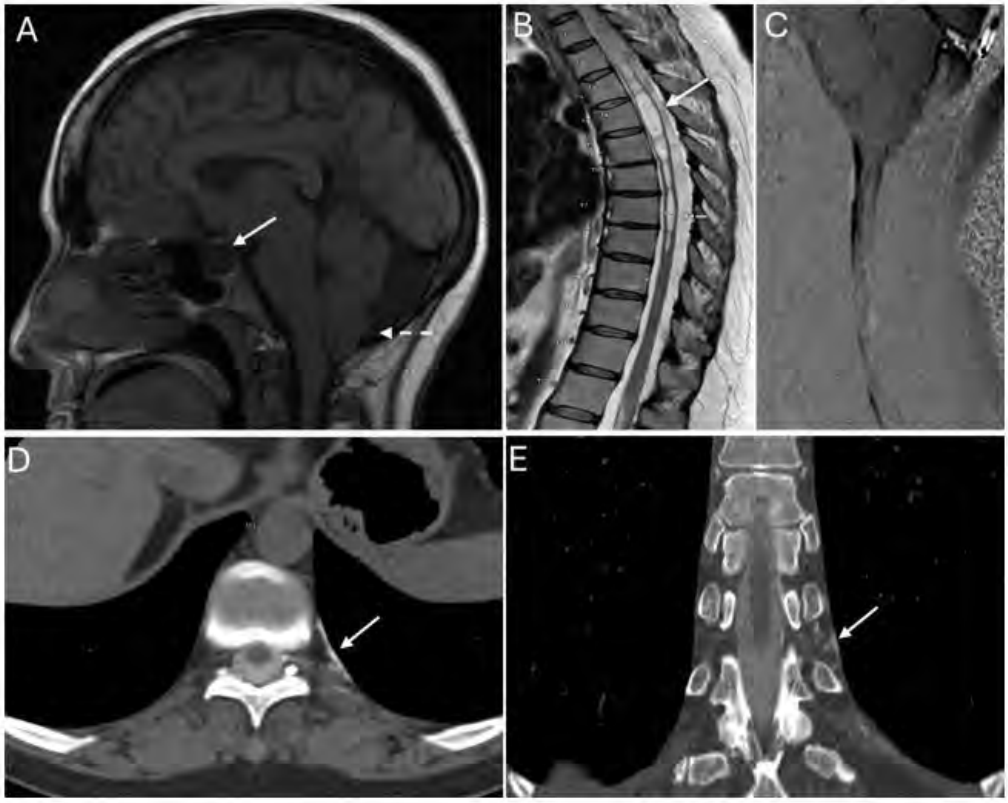


Fig 1.

A, Sagittal T1-weighted demonstrating cerebellar tonsillar descent < 5 mm (dashed white arrow) and partially empty sella (solid white arrow). *B*, Sagittal T2-weighted image demonstrating a multilocular syrinx extending from the cervical cord down to the level of T8. *C*, Sagittal phase contrast imaging demonstrating relatively preserved bidirectional CSF flow. *D and E* Axial and coronal images of a subsequent CT myelogram with intrathecal contrast flowing along the expected course of thoracic lymphatics at T10-T11 (white arrows).

1002

Giant Torcular Dural Sinus Ectasia without Arteriovenous Shunting and Delayed Ossification: Discussion of Venous System Embryology

Thomas R Geisbush MD, Arzu Ozturk MD, Connor Gemmell MD, Muhammad T Raj MD, Kader K Oguz MD, Osama A Raslan MD, Arthur B Dublin MD, Lotfi Hacein-Bey MD
UC Davis Medical Center, Sacramento, CA, USA

Abstract Category

Pediatrics

Clinical History

We describe a 17-year-old patient with developmental delay and septooptic dysplasia diagnosed at birth, with no evidence of hydrocephalus or significant cerebrovascular impairment. Imaging revealed a giant, thrombosed and ossified posterior sinus with an abnormal venous anatomical arrangement, but no evidence of arteriovenous shunting.

Imaging Findings

Prenatal ultrasonography demonstrated a large posterior sinus without evidence of arteriovenous shunting. MRI obtained at birth showed a large posterior sinus thrombus, absent torcular Herophili and straight sinus, and direct drainage of diencephalic veins within the anterior sinus wall. Although the jugular bulbs and veins were well formed, the cavernous sinuses were absent, with dilated temporosylvian veins bilaterally. Septooptic dysplasia was confirmed and diffuse dural ectasia was present. A cerebral angiogram obtained at age two confirmed the absence of arteriovenous

shunting, the absence of straight sinus and cavernous sinuses, and dilated temporosylvian veins draining both anterior hemispheric structures.

Discussion

Dural sinus malformations (DSM) are rare, poorly understood congenital vascular malformations which remain classified as dural arteriovenous shunts. Posterior fossa DSMs have been characterized as lateral (lateral sinus/jugular bulb) or posterior (torcular) types. Posterior DSMs are giant venous lakes that communicate with cerebral veins and are purported to include arteriovenous shunts within the dural wall, which can potentially lead to hydrocephalus and compressive cerebral infarction. Although various hypotheses have been proposed to explain the presence of shunting, spontaneous shunt closure and thrombosis of the enlarged venous sinus have been widely documented to commonly occur in infants and neonates. Furthermore, various anomalies of venous drainage have been described in these patients, which may further compromise clinical outcome. Embryological development of posterior fossa sinuses, well described by Okudera, takes place after the 15th week of intrauterine life when deep and superficial venous systems unite. The case presented herein suggests that in some patients, a failure of posterior dural sinus development may occur, resulting in a giant DSM without associated AV shunting.

Teaching Point

Dural sinus malformations are rare, poorly understood congenital vascular malformations which remain classified as dural arteriovenous shunts. The case presented herein supports the possibility of a wider spectrum of embryological anomalies contributing to posterior (torcular) DSM formation, highlighting the importance of adequate venous embryological development.

References

Lasjaunias P (1997) Vascular diseases in neonates, infants and children. Interventional neuroradiology management. Springer-Verlag, Berlin Heidelberg New York

Merzoug V, Flunker S, Drissi C, Eurin D, Grangé G, Garel C, Richter B, Geissler F, Couture A, Adamsbaum C; Multicentric study of the GRRIF (Groupe de Recherche Radiopédiatrique en Imagerie Foetale), part of SFIPP (Société Francophone d'Imagerie Pédiatrique et Prénatale). Dural sinus malformation (DSM) in fetuses. Diagnostic value of prenatal MRI and follow-up. Eur Radiol. 2008 Apr;18(4):692-9. doi: 10.1007/s00330-007-0783-y. Epub 2007 Oct 16. PMID: 17938934.

Barbosa M, Mahadevan J, Weon YC, Yoshida Y, Ozanne A, Rodesch G, Alvarez H, Lasjaunias P (2003) Dural sinus malformation (DSM) with giant lakes, in neonates and infants. Review of 30 consecutive cases. Interv Neuroradiol 9:407–424

Okudera T, Huang YP, Ohta T, et al (1994) Development of posterior fossa dural sinuses, emissary veins, and jugular bulb: morphological and radiologic study. AJNR 15:1871–1883

Images/Tables

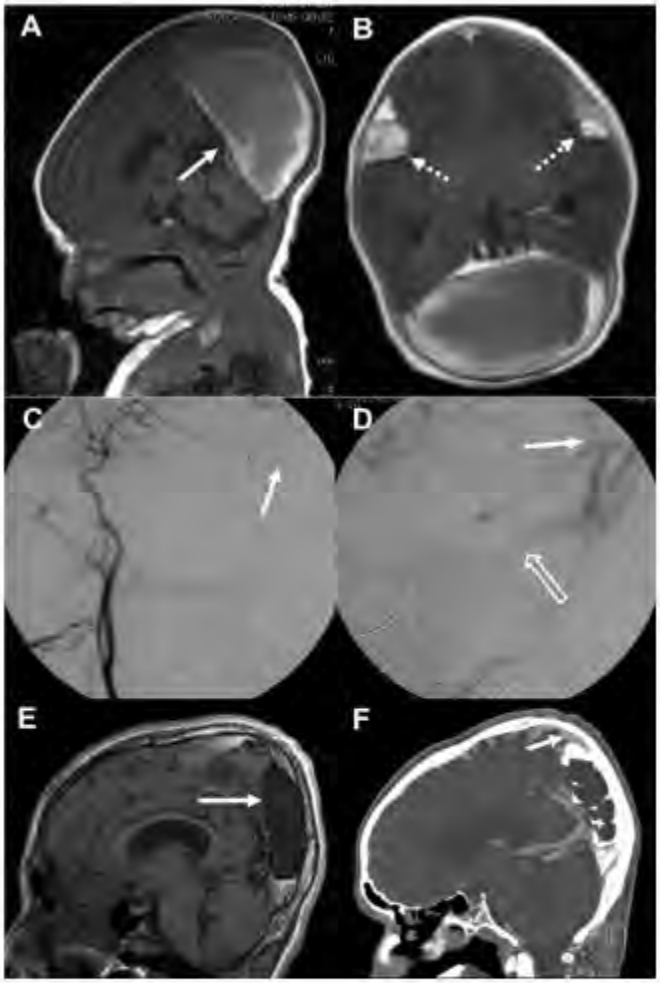


Fig 1.

A and B, Respective sagittal and axial views of a 3-day-old infant with prominent posterior dural ectasia, absence of the straight sinus, and absence of the torcular Herophili (solid white arrow). There is ectasia of the bilateral temporosylvian veins (dashed white arrows). *C and D*, Sagittal view of cerebral angiographic images of the common carotid artery demonstrating no appreciable arteriovenous shunting and absence of the flow through a straight sinus to the torcular Herophili (solid white arrows). Distal drainage through the transverse and sigmoid dural venous sinus is visualized (hollow white arrow). *E*, Sagittal T1-weighted image of the patient at 17 years old demonstrating now partially ossified thrombus in the posterior sinus (white arrow). *F*, Sagittal view of a CT angiogram demonstrating numerous deep cerebral veins draining into the distal superior sagittal sinus (white arrows).

1011

Erdheim Chester Disease Presenting as a Craniocervical Junction Mass Mimicking a Meningioma: The Importance of Multisite Imaging

Anant Krishnan MD[1], Ria Singh BS[2], Kunal Kedar MD[3]
[1]Troy, michigan, USA. [2]Kansas City, Missouri, USA. [3]Royal Oak, Mi, USA

Abstract Category

Adult Brain

Clinical History

A 39y.o. male with hypertension, diabetes, low testosterone presented to the emergency center (EC) with increasing difficulty in balance and coordination, headache, and blurry vision. Initial imaging of a round dural based enhancing mass at the craniocervical junction lead to the consideration of a meningioma. His symptoms progressed and eventually

he underwent surgical partial resection of a very hard mass. Post operatively his course was complicated by abdominal pain and distension for which he underwent a CT of the abdomen and pelvis that revealed hydronephrosis, perinephric stranding and lead to a suspicion of a systemic disorder and a perirenal biopsy. Both biopsies were similar, demonstrating foamy histiocytes, fibrosis with a final diagnosis of Erdheim Chester disease made. Molecular and genetic testing revealed a BRAF V600E mutation, and CHEK 2 mutation. The patient has been receiving targeted therapy.

Imaging Findings

CT of the head in the EC revealed an isodense mass at the craniocervical junction that in retrospect was present 2 years earlier but had grown. Brain MRI revealed a markedly T2 hypointense 3 cm round enhancing mass at the craniocervical junction encasing the left vertebral artery and compressing the medulla and upper cervical cord. Pituitary stalk thickening was seen but no additional dural or parenchymal mass was seen. Small (1 cm) orbital masses were identified. CT of the abdomen revealed splenomegaly, extensive perinephric soft tissue and bilateral hydronephrosis. Differential of renal lymphoma and Erdheim-Chester disease was raised given the multiplicity of findings. FDG-PET imaging performed 2 months after the surgery demonstrated focal uptake in the pituitary gland and residual craniocervical junction mass but with only mild uptake around the kidneys. Spine MRI did not reveal any spinal dural or leptomeningeal disease. Head MRI performed 4 months after surgery revealed improvement in the pituitary stalk, orbital masses but without a change in the residual craniocervical junction mass.

Discussion

Erdheim-Chester disease (ECD) is a rare multisystemic, non-Langerhans histiocytic neoplasm, that is most commonly characterized by multifocal osteosclerotic lesions of the long bones. Clinical manifestations are diverse due to organ of involvement. Ataxia is the most common neurologic symptom. CNS imaging findings include cranial bone or skull base involvement, orbital masses, cerebral and posterior fossa parenchymal masses, pituitary stalk and dural based lesions. The dural masses are T2 hypointense in most cases. There is currently no definite cure and prognosis is guarded. Treatment regimens range from steroids, interferon alpha, systemic chemotherapy and if an underlying mutation such as BRAF V600E is detected, directed targeted therapy.

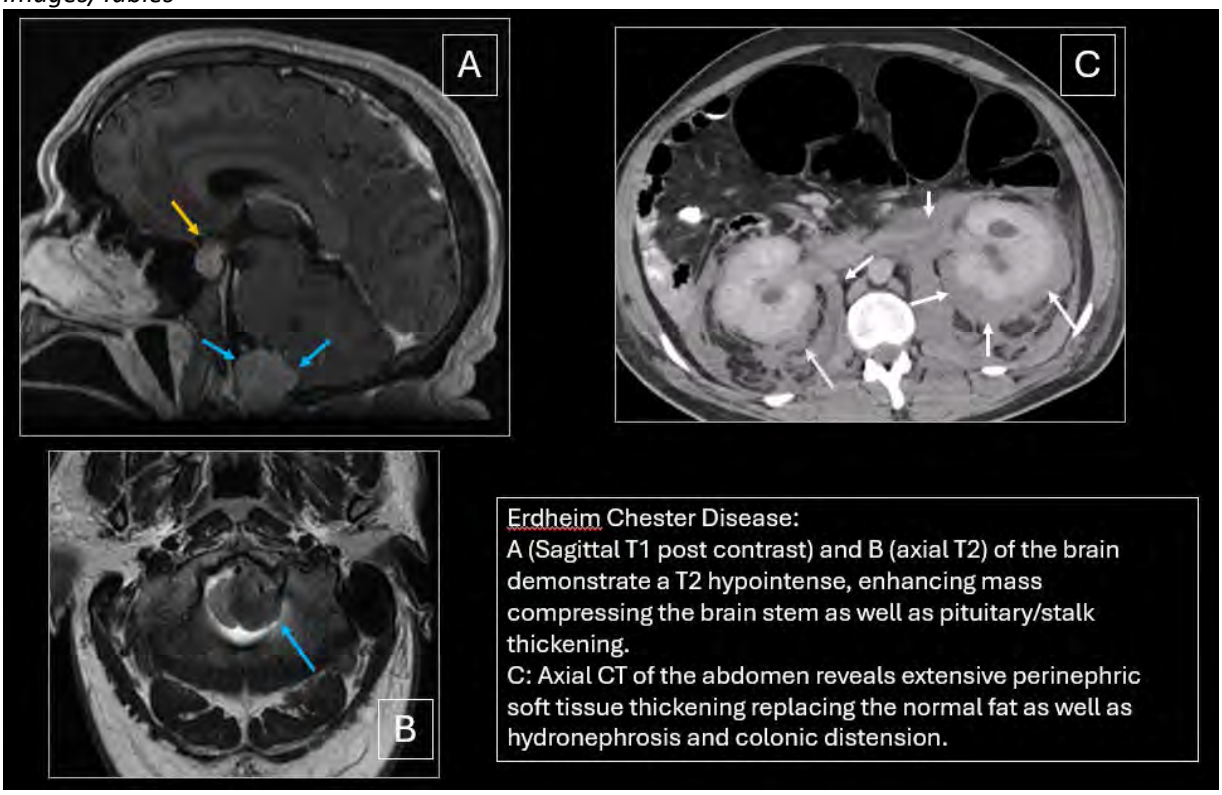
Teaching Point

Diagnosis of ECD is challenging. As clinical findings are diverse and non-specific at times, recognition of imaging findings can facilitate earlier diagnosis. Though the patient's manifestation of a solitary craniocervical junction slowly growing mass over at least 2 years lead to the initial consideration of a meningioma, the presence of pituitary stalk thickening, orbital abnormalities, and most importantly the subsequent detection of perirenal masses resulted in a suspicion of ECD and facilitated the pathological conclusion, highlighting the need for systemic multidisciplinary evaluation.

References

1. Bhatia A, Hatzoglou V, Ulaner G, Rampal R, Hyman DM, Abdel-Wahab O, Durham BH, Dogan A, Ozkaya N, Yabe M, Petrova-Drus K, Panageas KS, Reiner A, Rosenblum M, Diamond EL. Neurologic and oncologic features of Erdheim-Chester disease: a 30-patient series. Neuro Oncol. 2020 Jul 7;22(7):979-992. doi: 10.1093/neuonc/noaa008. PMID: 31950179; PMCID: PMC7339889.
2. Aswani Y, Patel A, Zhan X, Ansari S, Marcelino LG, Aswani N, Patel DD, Kandemirli S, Averill S, Bhatt S. Imaging in Erdheim-Chester Disease. Radiographics. 2024 Sep;44(9):e240011. doi: 10.1148/rg.240011. PMID: 39172709.
3. Haque A, Pérez CA, Reddy TA, Gupta RK. Erdheim-Chester Disease with Isolated CNS Involvement: A Systematic Review of the Literature. Neurol Int. 2022 Sep 5;14(3):716-726. doi: 10.3390/neurolint14030060. PMID: 36135995; PMCID: PMC9504932.

Images/Tables



1040

a rare case of intra-uterine sacro-coccygeal teratoma

vishva pravinchandra chauhan MD radiodiagnosis, jeet modi MBBS, shashi p verma mbbs
PDU government medical college, Rajkot, Gujarat, India

Abstract Category

Pediatrics

Clinical History

A two-day old male child was referred to radiology department for X-ray and local ultrasound examination of swelling over left gluteal region which was presented since birth. The child was delivered by spontaneous vaginal delivery at 39 weeks GA, weighing 2800 gram with spontaneous cry after birth. The mother had never undergone any antenatal visits throughout her pregnancy.

Ultrasound findings suggested a large solid cystic lesion at the left gluteal region with suspicious deeper communication with sacrum.

Laboratory investigations consisted of complete blood count, CRP and tumor markers (AFP, B-HCG and LDH), were perfomed and increased level of AFP and LDH were observed

At 15 days of life, he was referred for a Non-contrast CT scan and magnetic resonance imaging of pelvic region where the probable diagnosis of Type II Sacrococcygeal teratoma was made.

At 18 days of life, surgical excision of tumor mass was carried out whose histopathology confirmed the diagnosis as Benign mature teratoma.

The postoperative course was uneventful, and the baby was discharged after 10 days.

Imaging Findings

X-ray revealed a soft tissue mass protruding from the base of the coccyx.

NCCT pelvis suggested a soft tissue density predominantly solid lesion with fat component and few calcifications within from which coccyx cartilage was not seen separately.

MRI showed approx. 64 x 37 X 25 mm sized heterogenous altered signal intensity predominantly solid lesion in the coccygeal region with few focal areas of STIR hyperintensities and minimal focal post contrast enhancement, appearing to be invading the left gluteus maximus muscle with no communication with thecal sac or spinal cord.

Discussion

Sacrococcygeal teratomas is a rare type of tumour arising from the base of the coccyx (sacrococcygeal region), occurring in about 1 in 35,000 to 1 in 40,000 live births and most common in girls with girls to boys ratio of 3:1 to 4:1. It arises from all three germ cell layers of a trilaminar embryonic disc. They can be solid, cystic or a combination of the two, composing of mature, immature or malignant tissues.

Based on their anatomical location (Altman classification), Type I is predominantly external, type II is a dumb-bell shaped tumour with an almost equal size externally and internally, type III is mainly internal, and type IV is completely internal. In the case, pelvic MRI revealed a dumb-bell shaped mass with intrapelvic extension consistent with Altman type-II.

Teaching Point

Sacrococcygeal teratomas are rare congenital tumours that may threaten fetal survival. Diagnosis can be established in utero by obstetric ultrasound. MRI pre or postnatally is useful to assess intrapelvic extension of the tumour. Surgical excision provides a cure.

References

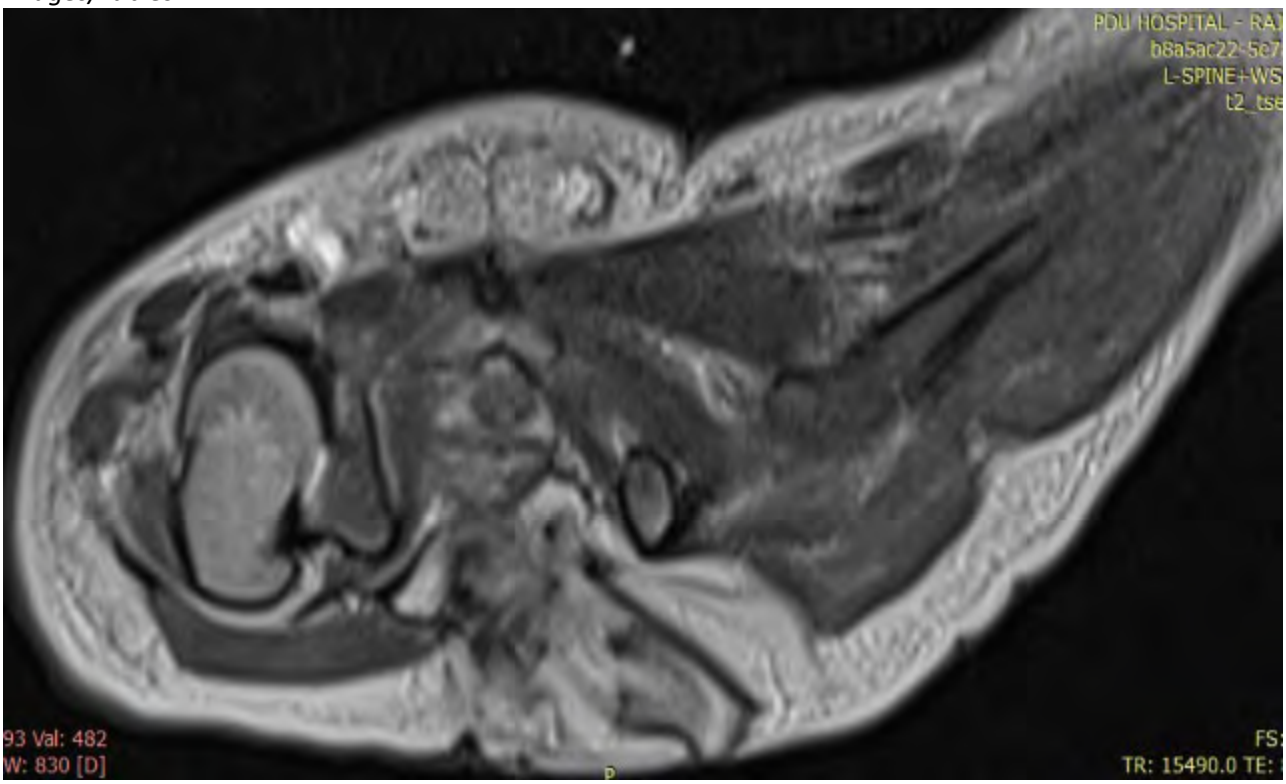
- Q. Savitri, S. Prihartano, A. Harahap;

Giant Sacrococcygeal teratoma in newborn: A rare case; Journal of pediatric surgery case reports, Vol 47, August 2019, 101223.

- M. Mondal, B. Biswas, A.Roy, et al.

A neglected case of Sacrococcygeal teratoma in a neonate; Asian J Med Sci, 6 (2) (2014), pp. 108-110.

Images/Tables



1041

A RARE CASE OF TYPE II ARNOLD CHIARI MALFORMATION WITH VANISHING CEREBELLUM

vishva pravinchandra chauhan MD radiodiagnosis, shashi p verma MBBS, jeet modi MBBS

pdu medical college, rajkot, gujarat, India

Abstract Category

Pediatrics

Clinical History

A 12-days old female child born to 23 years old $G_2P_1L_1A_0$; previous LSCS female; was referred to radiology department for the MRI evaluation the brain and spinal cord screening for the lower back , skin changes with tufts of hairs and discharge which was presented since birth. Delivered by emergency LSCS at 38 weeks GA, weighing 2800 grams with

spontaneous cry after birth. The mother visited to some private hospital during the 1st trimester and the repeated antenatal USG examination were done, however no detailed records were present.
During the pregnancy, the mother has taken 1 TT dose. No records of antenatal Folic acid consumption.

Imaging Findings

A small posterior fossa predominantly occupied by the occipital lobes and a profoundly small cerebellum. Small- sized pons with loss of normal pontine prominence, caudal elongation of medulla and tectal beaking. Herniation of the medulla and cerebellar tonsil through the foramen magnum**.** Low placed torcular heterophili is seen.
Discontinuity of skin and subcutaneous tissue in the lumbosacral region (extending from L3 to S1 vertebral body levels) with herniation of neural placode through a posterior element defect. The spinal cord is lying low and tethered cord is extending upto L4 – L5 IV-disc level and herniated through spinal defect with internal traversing linear hypointense neural elements and no overlying skin s/o myelocoele

Discussion

In myelocele, herniation of posterior fossa contents through the foramen magnum may result in the parenchymal damage. When tissue loss is severe, grossly reduced or virtually no cerebellum may be present.[1]
Reduced hindbrain herniation following the intrauterine myelomeningocele repair signify that the herniation is hereby resultant of the prolonged CSF leak.[2]
Mechanical compression and vascular compromise due to the impaction of the cerebellar tissue into the foramen magnum can obviously lead to the parenchymal loss.[1] The prevalence of vanishing cerebellum appears to be a rare phenomenon.[1] Vanishing cerebellum with its reduced volume may well have major implications for cognitive development which warrants intensive follow-ups. The cognitive impairments have been documented following cerebellar infarcts/ stroke[3] and cerebellar tumour resection[4] in adult as well children.
It may be worth correlating cognitive test scores with cerebellar volume and parameters of hindbrain herniation in cases of myelomeningocele.

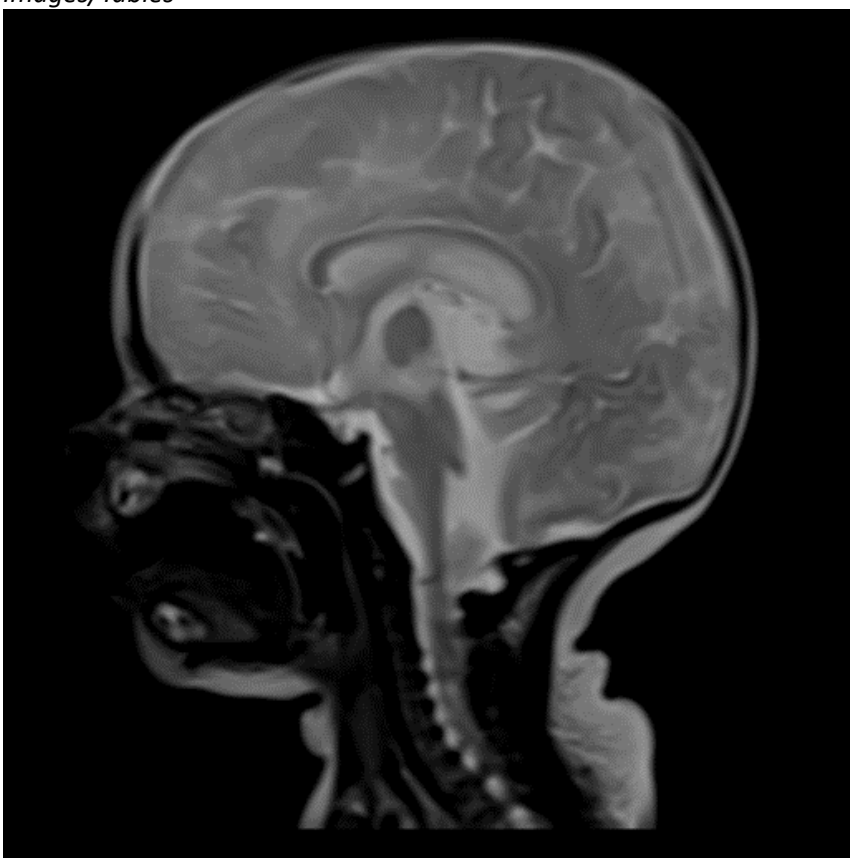
Teaching Point

Chiari malformations describe a group of deformities of the posterior fossa and hindbrain, involving the cerebellum, pons, and medulla oblongata, lead to problems ranging from tonsillar herniation through the foramen magnum to the absence of the cerebellum, with or without other associated intracranial or extracranial defects such as hydrocephalus, encephalocele, syrinx, or spinal dysraphism. MRI is a valuable complement to ultrasound to make the diagnosis. The main objective of surgery in Chiari malformation is to improve CSF flow across the foramen magnum and surrounding the brainstem, reduce the extent of the syrinx, and reduce pressure on the brainstem.

References

1. Bolthauser E, Schneider J, Kollias S, Waibel P, Weisser M. Vanishing cerebellum inmyelomeningocele. Eur J Pediatr Neurol 2002; 6: 109-113.
2. Tulipan N, Hernanz-Schulman M, Bruner JP. Reduced hindbrain herniation after intrauterine mye- lomeningocele repair. A report of four cases. Pediatr Neurosurg 1998; 29: 274-278.
3. Malm J, Kristensen B, Karlsson T et al. Cognitive impairment in young adults with infratentorial infarcts. Neurology 1998; 51: 433-440.
4. Schmahmann JD, Sherman JC. The cerebellar cogni- tive affective syndrome. Brain 1998; 121: 561-579.
5. Sener RN. Cerebellar agenesis versus vanishing cerebellum in Chiari II malformation.Comput Med Imaging Graphics 1995; 6: 491-494.

Images/Tables



1044

Polymorphous low-grade neuroepithelial tumor of the young (PLNTY): A Case Report

Matthew R. Bennett M.S., Coplen Johnson B.S., Joshua Strobel MD, Areli Cuevas-Ocampo MD, Octavio Arevalo-Espejo MD
LSUHS, Shreveport, LA, USA

Abstract Category

Adult Brain

Clinical History

Our patient is a 19-year-old male who presented with seizures characterized by bilateral shaking of both arms and legs, accompanied by tongue biting and foaming at the mouth. Each episode lasted approximately 3 minutes, followed by several hours of postictal confusion. An EEG conducted two months after his initial presentation showed a normal routine wake-and-sleep pattern. One month later, an MRI revealed a non-specific, heterogeneous lesion in the left middle temporal gyrus, likely representing the source of his seizures. Following a neurosurgical consultation, he underwent resection of the lesion 4 months later. Postoperatively, the patient experienced a reduction in seizure frequency.

Imaging Findings

Figure 1. Histological sections showed fragments of cortex infiltrated by mildly atypical oligodendroglioma-like cells with oval nuclei, accompanied by numerous microcalcifications. No mitotic figures
were observed (A). Immunohistochemically, the tumor cells were positive for GFAP (B), OLIG2 (E), and CD34 (C) and negative for IDH1 (R132H) (D).

Figure 2. Close-up axial images of the brain. Axial non-contrast CT of the head in bone window (A), pre and postcontrast T1 (B, C), FLAIR (D), T2 (E), DWI (F), gradient echo (G), and coronal FLAIR (H). A cortically-based non-enhancing T2/FLAIR hyperintense mass is identified at the left middle temporal gyrus (yellow arrows), associated with central coarse calcifications (red arrowheads). No restricted diffusion is noted. Please note the remodeling of the adjacent parietal bone, as an indicator of slow growth (blue arrows).

Discussion

The patient underwent a craniotomy for resection of the mass with pathological analysis positive for a low-grade glioma consistent with polymorphous low-grade neuroepithelial tumor of the young (PLNTY). Microscopic examination revealed leptomeningeal fragmentation, irregularly shaped blood vessels, and prominent diffuse calcifications. Immunohistochemistry demonstrated tumor cells positive for GFAP and CD34, with a low Ki-67 labeling index of approximately 1%. FISH analysis showed no detectable deletions or translocations.

Low-grade neuroepithelial tumors (LGNTs) are a group of relatively less aggressive tumors originating from neuroepithelial tissue. They vary in histological characteristics and degrees of glial differentiation. Common types include pilocytic astrocytomas, gangliogliomas, dysembryoplastic neuroepithelial tumors (DNETs), and pleomorphic xanthoastrocytomas. First identified in 2016, the polymorphous low-grade neuroepithelial tumor of the young (PLNTY) is a rare variant, now classified as an LGNT in the fifth edition of the WHO-2021 Classification of Brain Tumors. Accurate diagnosis of PLNTY requires detailed histological, immunohistochemical, and molecular analyses due to overlapping features with other LGNTs. PLNTY typically shows CD34 immunopositivity, an infiltrative growth pattern, and oligodendrocyte-like cells.

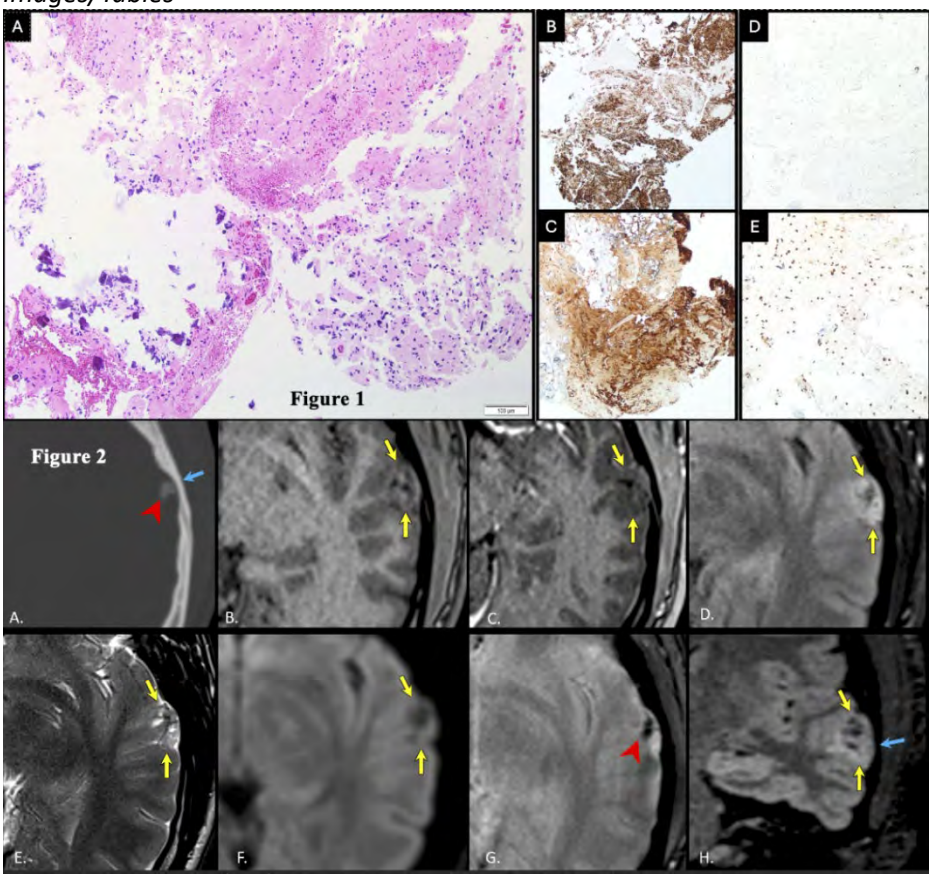
Teaching Point

PLNTY is an indolent tumor primarily affecting young individuals, often presenting with seizures that may be resistant to treatment. On MRI, it appears as a cortical-based lesion with high signal intensity on T2 and FLAIR sequences in cystic portions, frequently accompanied by calcifications that show as hypointense areas on T2 GRE imaging. Its radiographic features closely resemble those of DNETs and gangliogliomas, underscoring the importance of histological and molecular analysis for accurate diagnosis. Treatment generally involves surgical resection, with a favorable prognosis and low risk of recurrence.

References

1. Palejwala AH, O'Neal CM, Quinton MR, Battiste JD, Peterson JEG, Dunn IF. Polymorphous low-grade neuroepithelial tumor of the young: Rare tumor and review of the literature. *Rare Tumors*. 2022;14:20363613221083360. doi:10.1177/20363613221083360
2. Nair JN, Naidu B, Balasubramanian A, Krishnamurthy G. Polymorphous low-grade neuroepithelial tumour of young (PLNTY): the new kid on the block. Childs Nerv Syst. 2024;40(2):555-561. doi:10.1007/s00381-023-06162-1

Images/Tables



1057

Diffuse Metastatic CNS and Peripheral Nerve Involvement in a Patient with Relapse of T-Cell Acute Lymphoblastic Leukemia

Suryansh Bajaj MD, Divya Nayar MD
University of Arkansas for Medical Sciences, Little Rock, Arkansas, USA

Abstract Category

Adult Brain

Clinical History

32-year-old male patient initially presented with fever and weight loss was found to have a 13 cm mediastinal mass on imaging. The patient was diagnosed with T-cell ALL after biopsy of the mass and a bone marrow biopsy was performed. He was started on systemic chemotherapy and showed improvement. 3 years later, the patient presented with headaches and MRI demonstrated CNS new CNS involvement of disease. The patient was started on further treatment with intrathecal chemotherapy for relapse of ALL.

Imaging Findings

Initial MRI demonstrated thickening and enhancement of bilateral occulomotor nerves, asymmetric thickening of the right cisternal segment of the trigeminal nerve, and thickening and enhancement of the pituitary stalk.
MRI of the spine demonstrated diffuse thickening and enhancement of cauda equina nerve roots.
MR neurography demonstrated patchy STIR hyperintense signal involving the left C5, T1, and right C5 nerve roots.
Follow up MRI of the brain showed prominent thickening and enhancement of bilateral Meckel's cave extending into the maxillary and mandibular divisions of the nerve.

Discussion

CNS involvement is common in patients with ALL. Even in patients who do not initially present with CNS involvement, can later develop metastatic deposits in the brain, spine, and even the peripheral nerves.

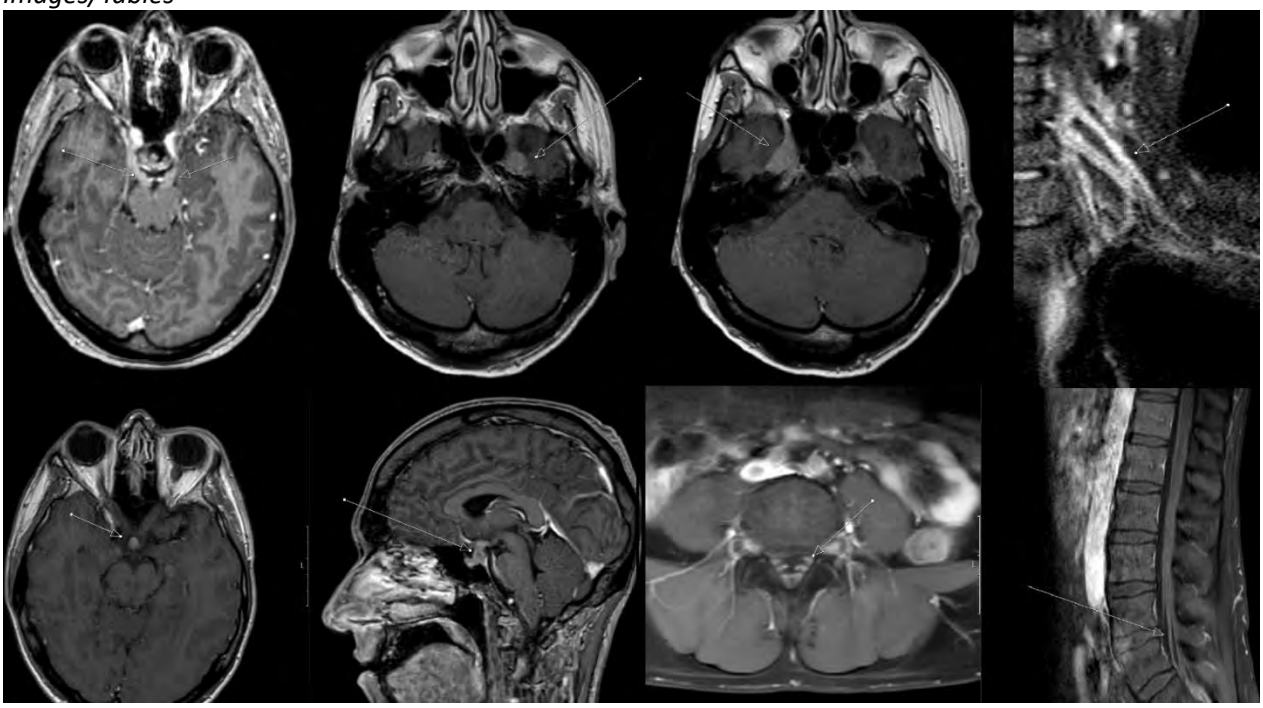
Teaching Point

This case highlights the importance of assessing cranial nerves in any patient with malignancy. Although the perineural spread of malignancy is a known pathway of CNS metastasis, it can often be missed if specific attention is not paid.

References

Deak D, Gorcea-Andronic N, Sas V, Teodorescu P, Constantinescu C, Iluta S, Pasca S, Hotea I, Turcas C, Moisoiu V, Zimta AA, Galdean S, Steinheber J, Rus I, Rauch S, Richlitzki C, Munteanu R, Jurj A, Petrushev B, Selicean C, Marian M, Soritau O, Andries A, Roman A, Dima D, Tanase A, Sigurjonsson O, Tomuleasa C. A narrative review of central nervous system involvement in acute leukemias. Ann Transl Med. 2021 Jan;9(1):68. doi: 10.21037/atm-20-3140. PMID: 33553361; PMCID: PMC7859772.

Images/Tables



1067

Valproate Toxicity on Imaging: A Case-Based Review of Radiological Findings

Suryansh Bajaj MD, Divya Nayar MD
University of Arkansas for Medical Sciences, Little Rock, Arkansas, USA

Abstract Category

Adult Brain

Clinical History

A 19-year-old male with history of schizoaffective disorder and catatonia presented to the ED due to lethargy and persistent nausea and vomiting. Patient had continued issues with vomiting. His medications included lorazepam, lithium, and valproate. Nausea/vomiting persisted for weeks despite use of anti-emetics and progressed to the point he had been unable to tolerate any PO intake or take medications. Patient had gotten progressively more lethargic and less responsive for past 2 days which prompted the visit to the ED. Following arrival to ED, he began having frequent episodes of coffee ground emesis. Due to lethargy and unresponsiveness CTH and LP performed.

Imaging Findings

CT head was negative for any acute findings.

MRI brain demonstrated diffusion restriction in bilateral cingulate gyri, insular cortex, and anterior temporal cortex without any FLAIR/T2 signal abnormalities. Bilateral basal ganglia and cerebellum appeared normal. Differentials of metabolic/toxic etiology were suggested including hyperammoninemia and possible medication overdose.

Discussion

Valproate-induced hyperammonemic encephalopathy (VHE), also known as valproic acid-induced hyperammonemic encephalopathy, is a rare form of non-cirrhotic hyperammonemic encephalopathy resulting from the use of sodium valproate, a drug commonly prescribed as an anticonvulsant and mood stabilizer.

Clinical presentation is non specific and may include altered mental status, focal neurological deficits, etc.

In the limited studies reporting MRI findings in VHE, the following features have been noted:

- **T2/FLAIR**: Bilateral symmetric areas of high signal in the cerebral cortex (especially frontal and insular regions), cerebellar white matter, and globus pallidi.
- **DWI**: Similar pattern of high diffusion signal as seen in T2/FLAIR.
- **MR spectroscopy**: Elevated glutamine/glutamate peaks, with reduced myoinositol and choline peaks on proton MR spectroscopy.

These signal changes typically resolve following treatment.

Although, no T2/FLAIR signal changes are noted in our case, given the history and abnormally elevated serum level of valproate were suggestive of the diagnosis.

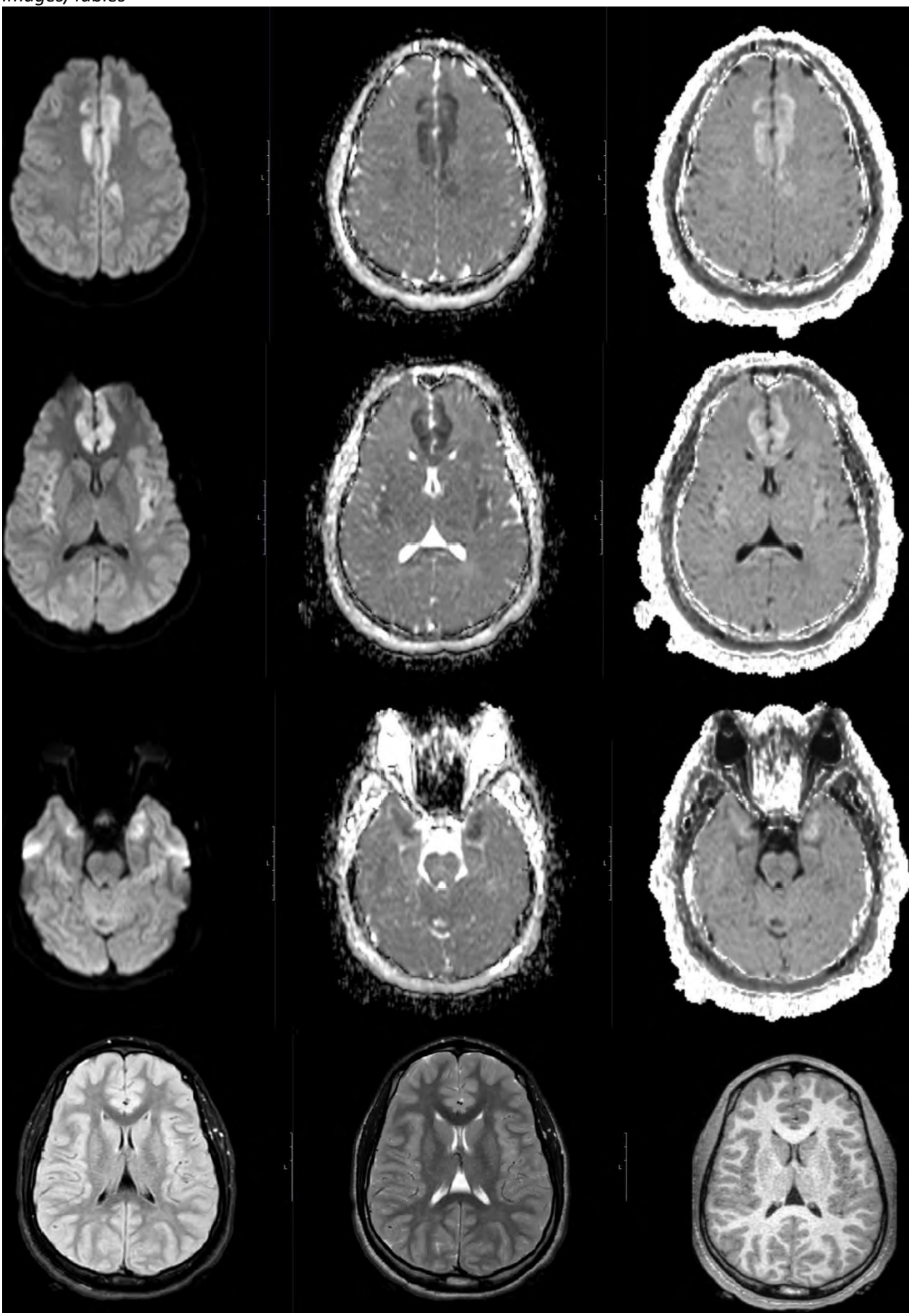
Teaching Point

This case highlights the importance of using clinical history while interpreting images and demonstrates classic imaging findings in toxic/metabolic derangements specifically in valproate toxicity.

References

https://radiopaedia.org/articles/valproate-induced-hyperammonaemic-encephalopathy?lang=us

Images/Tables



1081

Delayed contrast-induced encephalopathy following CT myelogram

Johnathan Vidovich MD, Denver Pinto MD, Valeria Potigailo MD
University of Colorado Department of Radiology, Aurora, CO, USA

Abstract Category

Adult Brain

Clinical History

A 72 year old male with type 2 diabetes, sleep apnea with an implanted INSPIRE device, and degenerative disc disease in the lumbar spine presented to the emergency room one day following a CT myelogram with Isovue M-200 performed for neurogenic claudication, complaining of back pain. He had tolerated the procedure well. The morning of presentation, he woke up feeling well but later developed worsening back pain, accompanied by subjective fever and chills. While in the ED, his mental status became acutely altered, and a stroke alert was called.

Following brain imaging, an external ventricular drain was placed. A CSF sample obtained during admission showed pleocytosis with elevated glucose and protein. CSF culture and gram stain were negative. Blood cultures were positive for streptococcus mitis. Patient was treated with methylprednisolone for possible iodine contrast neurotoxicity as well as IV Ceftriaxone followed by Linezolid. The drain was removed. At the time of discharge, patient had returned to near baseline level of function.

Imaging Findings

Non-contrast head CT ordered as a stroke alert revealed diffuse supratentorial and infratentorial white matter, basal ganglia, and dentate nucleus hypoattenuation with associated mass effect, including right uncal herniation and diffuse sulcal effacement. Sulcal hyperdensity was suspected to reflect contrast from the recent myelogram. CTA head and neck showed narrowing of the cortical branches of the right PCA, suspicious for vasospasm but was otherwise unremarkable. CT Perfusion was normal.

Discussion

While rare, contrast-induced encephalopathy is a known complication of imaging studies enhanced with iodinated contrast. It has been more commonly described in the setting of intravascular contrast injection for cerebral angiography and intravascular procedures. A few studies, however, have reported such a reaction in the setting of myelography with non-ionic contrast, including a recent case report describing acute onset encephalopathy immediately following intrathecal contrast injection. In the case of our patient, symptoms did not arise until over 24 hours after the procedure. Imaging findings of cerebral edema due to vasogenic edema with hyperdense CSF spaces are consistent with previously reported CT appearance in cases of contrast-induced encephalopathy following intravenous contrast injection.

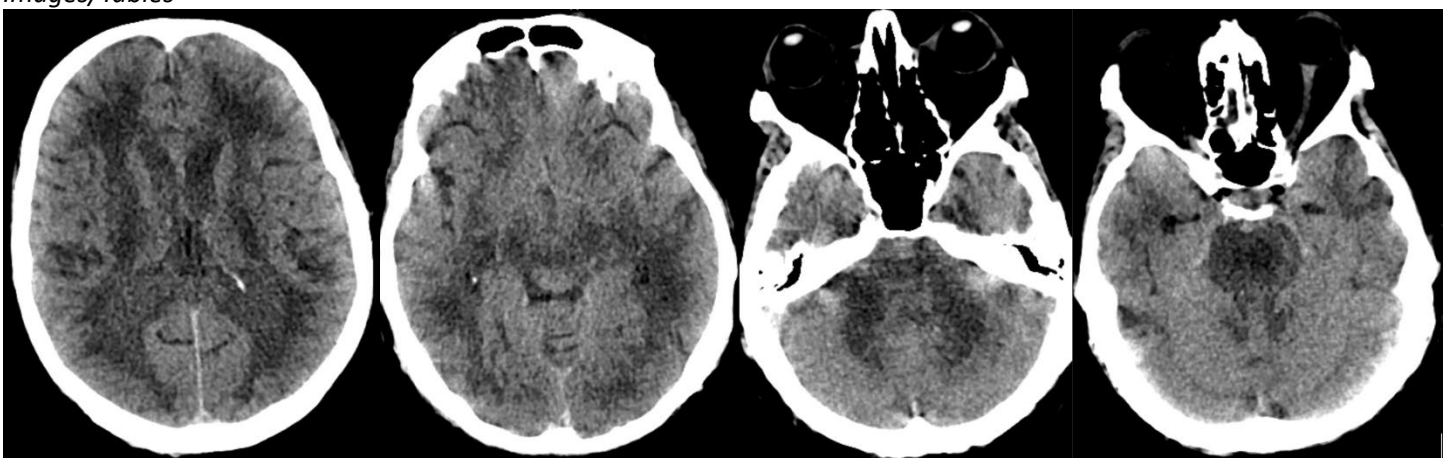
Teaching Point

Consider delayed contrast-induced encephalopathy in patients presenting with altered mental status and diffuse white matter edema on CT in the setting of recent myelography.

References

1. Hill KA, Brinjikji W, Darin Carabenciov I. Contrast-induced encephalopathy following CT myelogram with non-ionic contrast. *BMJ Case Reports CP* 2024;**17:**e259525.
2. Kawtharani S, Horanieh E, Ali B, et al. Contrast induced encephalopathy: Case report and review of the literature. *Journal of Neurology & Neuromedicine*, vol. 8, no. 1, 13 Feb. 2024, pp. 1–4, https://doi.org/10.29245/2572.942x/2024/1.1294.
3. Cecelia A, Sharma V, Park J, et al. “Contrast-induced encephalopathy after cerebral angiogram: A case series and review of literature.” *Case Reports in Neurology*, vol. 13, no. 2, 18 June 2021, pp. 405–413, https://doi.org/10.1159/000516062.

Images/Tables



1088

Photon Counting CT Demonstrating Ossicular Chain Anomalies in Mandibulofacial Dysostosis Patient without Congenital Aural Atresia.

Arka Dutta MD, John Lane MD
Mayo Clinic, Rochester, MN, USA

Abstract Category

Head & Neck

Clinical History

A 9-year-old female with a complex medical history, including mandibulofacial dysostosis Guion-Almeida Type and microcephaly syndrome, presents with predominantly left-sided hearing loss. Her birth was complicated by a tracheoesophageal fistula which required surgical repair within the first week of life. Afterwards the patient started wearing bilateral hearing aids at the age of 7 months. Now, at age 9, she presents with moderate to severe left-sided and mild to moderate right-sided conductive hearing loss, as noted on a recent audiogram.

Imaging Findings

Photon Counting Detector CT (PCD-CT) of the bilateral temporal bones with 0.2 mm slices demonstrates normal-appearing bilateral external auditory canals. In the right ear, a calcified bridge is noted between the malleus and the lateral wall of the middle ear cavity. Normally, the malleus is only connected by the thin anterior process, but here an additional calcified bridge is present which extends to the middle ear septation. Additionally, there is a dysmorphic appearance of the body of the incus, with partial ankylosis at the incudomallear joint. The stapes is hypoplastic and appears contiguous with a partially calcified oval window, which has an aperture measuring 1.4 mm. Contralaterally in the left ear similar findings including a mallear bar that appears contiguous with the anterior wall of the middle ear cavity is seen. The left ear also shows a dysmorphic incudomallear joint and a hypoplastic stapes with a partially calcified oval window. Bilateral imaging of the inner ear reveals moderately globular vestibules, with no other abnormalities in the internal auditory canals (IACs).

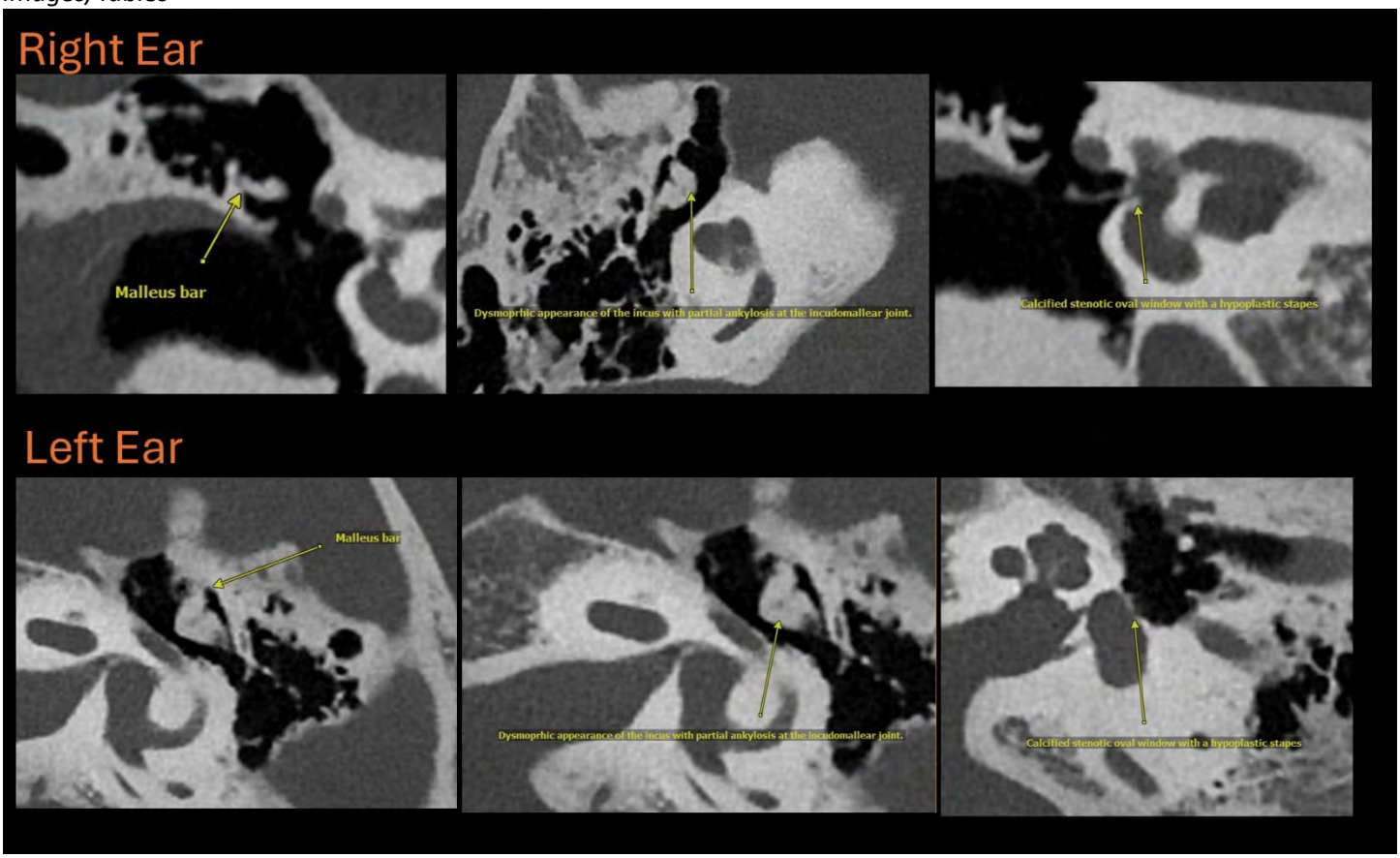
Discussion

Due to the rarity of high-resolution images depicting ossicular chain anomalies, these conditions are often underreported. This case report aims to improve the identification of such anomalies, particularly in pediatric patients with congenital head and neck malformations. Even in children with mandibulofacial dysostosis who do not have external auditory canal atresia, it is beneficial to evaluate for middle ear abnormalities using high-resolution CT or PCD-CT, especially if they present with conductive hearing loss. While ossicular chain anomalies can be challenging to visualize with conventional or cone beam CT, the recent use of PCD-CT has made it easier to detect these abnormalities.

Teaching Point

Any patient that may have malformation with the first and second branchial arch may also have ossicular malformations. When evaluating a pediatric patient with conductive hearing loss, it is beneficial to evaluate the morphology and articulation of the malleus, incus and the stapes. Additionally it is necessary to evaluate the footplate and the oval window for stenosis or closure. Furthermore, identifying specific congenital defects in this patient population is crucial for guiding ENT surgeons in their presurgical planning.

References
Teunissen EB, Cremers WR. Classification of congenital middle ear anomalies. Report on 144 ears. *Ann Otol Rhinol Laryngol.* 1993;102:606–12. DOI:10.1177/000348949310200807.
Swartz, J.D. and Loevner, L.A. *Imaging of the temporal bone*. 4th edn. New York: Thieme; 2009
Images/Tables



1122

Distinguishing myo-inositol from glycine in brain MRS: a pitfall using intermediate echo times

Peter B Barker D.Phil., Georg Oeltzschner PhD, Doris D.M. Lin MD, PhD
JHUSOM, Baltimore, MD, USA

Abstract Category
Functional/Advanced Imaging
Clinical History
A term male infant with suspected HIE after placental abruption and fetal anemia of unclear etiology was referred for evaluation with brain MRI and MRS after therapeutic hypothermia. There was significant acidosis on cord gas, and initial Sarnat exam revealed moderate encephalopathy at 3h of life. On exam he was very hypotonic with minimal reactivity. History and initial perinatal course were highly suspicious for HIE, but neurological exam and seizures on cranial EEG were out of proportion to imaging findings on ultrasound, on which there was no evidence of edema. There was acute hypoglycemia, which was corrected with glucose administration.
HIE mimics were considered, including epileptic encephalopathies such as nonketotic hyperglycinemia (NKH) or Ohtahara syndrome. The patient was referred for MRS for the evaluation of brain glycine (Gly) levels.
Imaging Findings
MRI showed multifocal cortical areas of restricted diffusion, as well as along the posterior limbs of the internal capsules. Single voxel (SV) brain MRS was performed at 3T using the PRESS sequence at both short and long TE (35 and 280ms) in the thalamus and right frontal white matter, and multi-voxel MRSI performed using the sLASER sequence at short and intermediate TE (40 and 135ms) in an axial plane at the level of the basal ganglia.

SV spectra at both short and long TE showed near normal levels of myo-inositol (mI), choline (Cho), creatine (Cr), glutamate plus glutamine (Glx), and NAA for a 6-day old neonate. There was a small elevation of lactate which was more pronounced in the frontal white matter than the thalamus.

Intermediate TE (135ms) MRSI spectra showed a well-defined, singlet peak at 3.56ppm throughout the sLASER volume, which was initially interpreted as being due to elevated Gly. However, there was no evidence of Gly on long TE (280 ms) spectra. It was therefore concluded that the peak at TE 140ms must be due to myo-inositol (mI) rather than Gly. Experiments in phantoms confirmed the presence of a mI peak using the MRSI-sLASER sequence at intermediate but not long TE.

Subsequent genetic testing was negative and final diagnosis based on MRI and clinical exam was mild HIE.

Discussion

Brain Gly has previously been reported to be elevated and detectable by MRS in NKH. Conventional wisdom is that mI and Gly, which both resonate at around 3.5-3.6 ppm in the proton spectrum, can be separated from each other by use of long TEs: the mI signal decays rapidly with TE due to its scalar couplings, whereas Gly is a singlet which decays more slowly.

This case study shows that at 3T in the neonatal brain, there can still be significant, singlet-like signal from mI even at TEs as long as 135-140 ms. While advanced MRS techniques are available for mI-Gly discrimination, in clinical practice using methodology available on standard MR scanners, the best way to evaluate the presence or absence of Gly is to use long TEs.

Teaching Point

Intermediate TE MRS at 3T may show similar signals for mI and Gly.

References

1. Choi C, Bhardwaj PP, Seres P, et al. Measurement of glycine in human brain by triple refocusing 1H-MRS in vivo at 3.0T. *Magn Reson Med* 2008;59:59-64

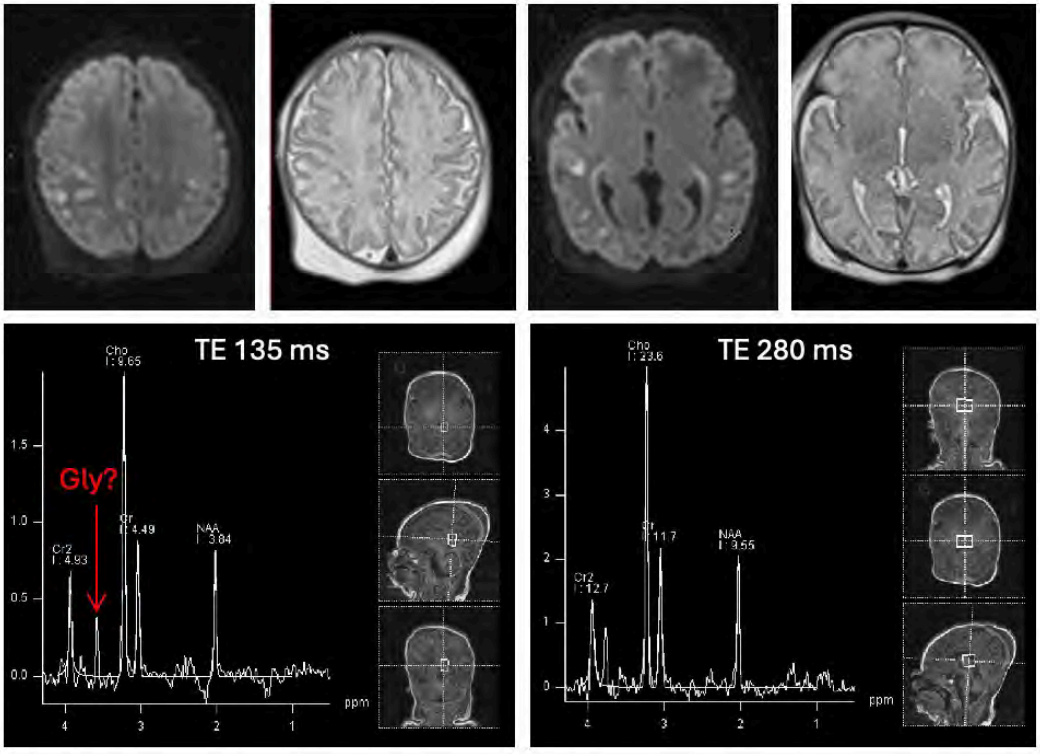
2. Gabis L, Parton P, Roche P, et al. In vivo 1H magnetic resonance spectroscopic measurement of brain glycine levels in nonketotic hyperglycinemia. *J Neuroimaging* 2001;11:209-211

3. Govindaraju V, Young K, Maudsley AA. Proton NMR chemical shifts and coupling constants for brain metabolites. *NMR Biomed* 2000;13:129-153

4. Heindel W, Kugel H, Roth B. Noninvasive detection of increased glycine content by proton MR spectroscopy in the brains of two infants with nonketotic hyperglycinemia. *AJNR Am J Neuroradiol* 1993;14:629-635

5. Shin JH, Ahn SY, Shin JH, et al. Sequential magnetic resonance spectroscopic changes in a patient with nonketotic hyperglycinemia. *Korean J Pediatr* 2012;55:301-305

Images/Tables



1141

Radiology Code Red: Brain on Fire! Multimodality Lessons for Early Detection of Anti-NMDA Receptor Encephalitis

Eunice Wu[1], Amy Condos MD[2]
[1]NMCSD, San Diego, CA, USA. [2]Naval Medical Center San Diego, San Diego, CA, USA

Abstract Category

Adult Brain

Clinical History

A 64-year-old female presented with 1 week of psychosis, preceded by new joint pains, but no viral prodrome. She became increasingly altered, developing predominantly left-sided motor abnormalities, with abnormal EEG. Workup ruled out infectious and neoplastic etiologies, eventually returning positive for CSF anti-NMDAR antibodies. She was started on steroids and intravenous immunoglobulin(IVIG), and full body neoplastic workup was initiated, however symptoms had progressed to periodic total catatonia with autonomic instability.

Imaging Findings

Four brain MRIs over one month showed consistent right-sided near-total hemispheric pachymeningeal enhancement with small areas diffusion restriction, sulcal effacement, sulcal /subarachnoid FLAIR hyperintensity, and subtle leptomeningeal enhancement. Nearly all findings improved with steroids/IVIG. Additional findings includes an enlarging right superior frontal gyrus white matter lesion with surrounding FLAIR hyperintensity.

18FDG-PET showed no associated tumor, but showed unilateral right frontotemporal and parietal hypermetabolism with perirolandic sparing, and bilateral occipital lobe hypometabolism, demonstrating an anterior-posterior gradient. There was corresponding crossed cerebellar hypermetabolism, with asymmetric left cerebellar and left skeletal muscle hypermetabolism.

Discussion

Anti-NMDA receptor encephalitis (ANMDARE) is rare, but is the most common autoimmune encephalitis (AE). Clinically our patient showed near-classic rapidly progressive multi-stage syndrome of ANMDARE. The exception is her preceding joint pains instead of the classic viral prodrome.1 Early recognition of ANMDARE requires awareness of classic presentations and progression. In fact, our patient met the Graus criteria for “probable” ANMDARE much earlier than her actual diagnosis, which would be enough for initiation of immunotherapy and neoplastic workup.[2]

Our case demonstrated primarily meningeal findings, which can present early and help raise suspicion for ANMDARE. Leptomeningeal enhancement is more specific in the acute setting (33% cases), possibly distinguishing it from hippocampal lesions more associated with the second most common anti-voltage-gated potassium channel(VGKC) encephalitis.[3] Pachymeningeal enhancement is much less common, only described by few case reports with no PET correlate, although a single retrospective study endorsed 7% prevalence.[4] Therefore, although atypical, pachymeningeal enhancement can also represent early ANMDARE.

Our patient’s PET/CT showed right hemispheric hypermetabolism with perirolandic sparing, anterior-posterior gradient, and bilateral occipital hypometabolism. These unusual, recognizable findings are consistent with existing literature, and provide functional data with greater sensitivity than MR.[5]

Teaching Point

- AE symptoms are often reversible when treated early, but complex clinical presentation and equivocal labs make diagnosis difficult. Therefore, radiologists have crucial roles in timely recognition, workup, and treatment.
- ANMDARE and other AEs should be on the differential whenever new-onset psychiatric symptoms and seizures are the predominant symptoms, especially with associated movement disorders and autonomic dysregulation.
- Awareness of clinical and radiologic Graus criteria for “definite” and “probable” autoimmune encephalitis is important for earliest recognition and treatment.
- Acute ANMDARE may present with only meningeal findings. Leptomeningeal abnormalities in particular may differentiate ANMDARE from Anti-VKGC encephalitis. Pachymeningeal enhancement is less common, but should still raise suspicions in the correct clinical setting.
- FDG PET provides functional data with characteristic findings and is more sensitive than MRI. Look at PET/CT as a valuable tool for earlier ANMDARE diagnosis, especially with high clinical suspicion and equivocal MRI/laboratory findings.

References
1. Dalmau J, Lancaster E, Martinez-Hernandez E, et al. Clinical experience and laboratory investigations in patients with anti-NMDAR encephalitis. The Lancet Neurology 2011;10:63–74.
2. Graus F, Titulaer MJ, Balu R, et al. A clinical approach to diagnosis of autoimmune encephalitis. The Lancet Neurology 2016;15:391–404.
3. Neo S, Yeo T, Chen Z, et al. Acute radiological features facilitate diagnosis and prognosis of anti-N-methyl-d-aspartate receptor (NMDAR) and anti-voltage-gated potassium channel (VGKC) encephalitis in adults. Journal of the Neurological Sciences 2020;419:117216.
4. Delgado-García G, Ramirez-Bermudez J, Flores-Rivera J, et al. Pachymeningeal Enhancement in Anti-NMDA Receptor Encephalitis (2567). Neurology 2020;94:2567.
5. Yuan L, Mao G, Zhang Y, et al. Typical metabolic pattern of 18F-FDG PET in Anti-NMDAR encephalitis in the acute and subacute phases and its correlation with T2 FLAIR-MRI features. BMC Neurosci 2023;24:51.
Images/Tables

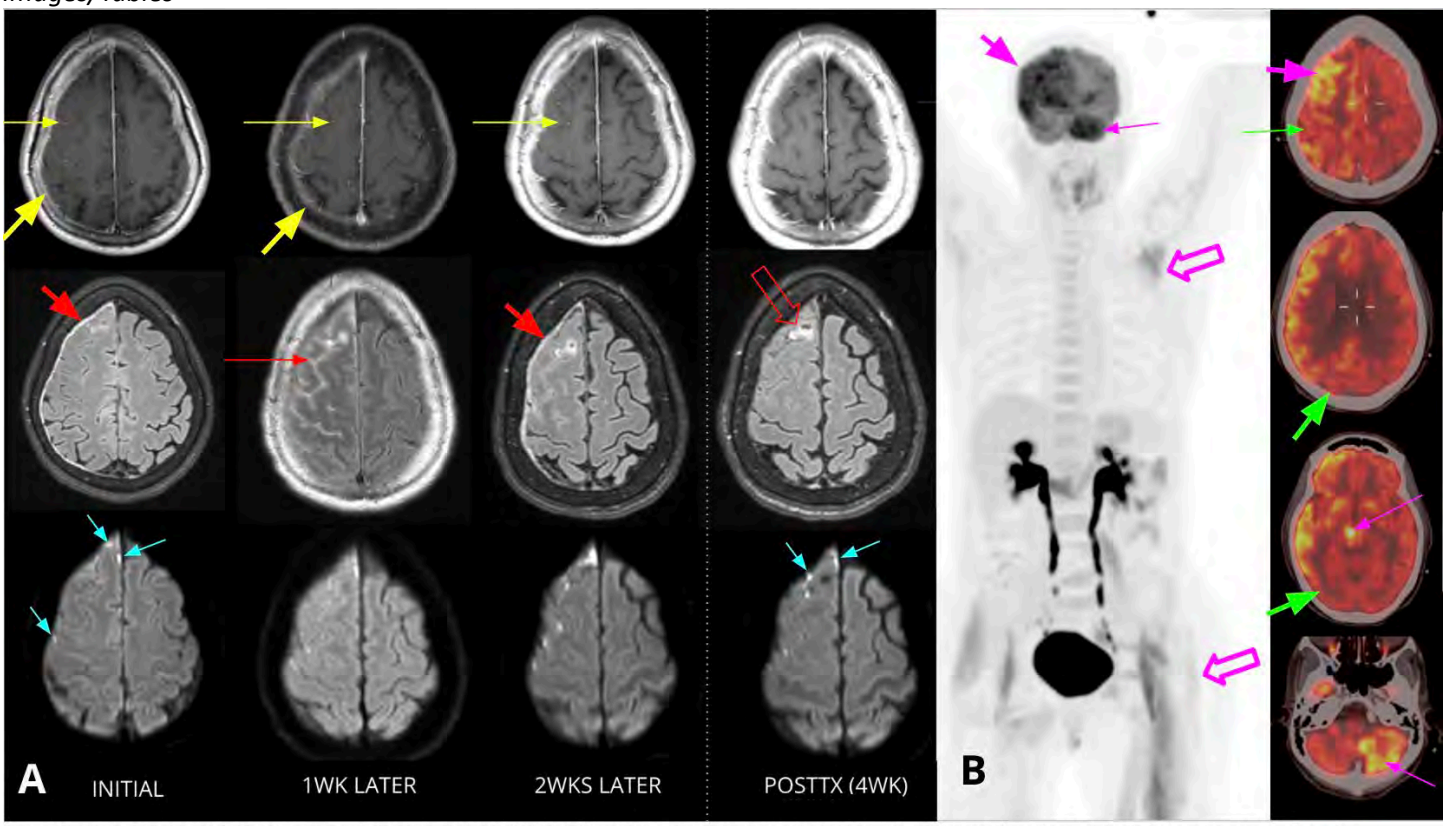


Image Group A: Four Brain MRs in the same Anti-NMDA Encephalitis(ANMDARE) patient, over the course of a month inpatient at two different hospitals. T1 Post-gadolinium: unilateral pachymeningeal enhancement best seen on the earlier images (large yellow arrows), and subtle ipsilateral leptomeningeal enhancement (small yellow arrows). FLAIR: Pachymeningeal thickening /hyperintensity (large red arrows) , and florid leptomeningeal hyperintensity / subarachnoid incomplete CSF suppression (small red arrow). Note the ipsilateral sulcal effacement. Additional right superior frontal gyrus CSF attenuation nonenhancing, non-restricting lesion with surrounding T2 hyperintensity. Its evolution over the disease course, and its location are consistent with ANMDARE encephalitis. DWI : areas of dural diffusion restriction (small blue arrows). Note that all findings improve on post treatment MRI except the superior frontal gyrus lesion.

Image Group B: FDG PET/CT shows unilateral right frontal, temporal and parietal increased uptake (large pink arrows) with perirolandic sparing (small green arrow) , demonstrating an anterior posterior gradient. There is corresponding crossed cerebellar hypermetabolism, with asymmetrically increased uptake at the right cerebral peduncle and left cerebellar hemisphere (small pink arrows), and predominantly left sided muscle glucose uptake (open pink arrows). Additional finding includes hypometabolism of bilateral occipital lobes (large green arrows).

1155

"Through the ophthalmic nerve and beyond ! " : A case of herpes zoster ophthalmicus with intracranial arteritis.

Faisal Alsugair MD, FRCPC[1], Islam Ahmed MBBS, ABHS-R, FRCR[1], Ammar Alam[1], Ahsas Nagee[2], Heather McDonald MD, FRCSC[3], Marlise P dos Santos MD, FRCPC[1]
[1]Department of Radiology, Radiation Oncology and Medical Physics, University of Ottawa, Ottawa, Ontario, Canada. [2]Faculty of Medicine, University of Ottawa, Ottawa, Ontario, Canada. [3]The Ottawa Hospital, Department of Ophthalmology, Ottawa, Ontario, Canada

Abstract Category

Head & Neck

Clinical History

62-year-old male presented with shingles around the left side of his face and eyes along with headaches and vision quality changes. His examination showed left eye scleral conjunctivitis and erythematous macules on left forehead toward left and left nose in V1 nerve distribution. He was diagnosed with herpes zoster ophthalmicus with optic neuropathy. Given the presentation, MRI orbits and brain was requested. This showed findings of subacute left herpes zoster ophthalmicus associated with an ipsilateral delayed subcortical hemorrhagic thalamic/midbrain infarction secondary to arteritis.

Imaging Findings

ill-defined, mildly expansile, T2/FLAIR hyperintense lesion with heterogeneous enhancement (g) and central hemorrhage (d and f) within the left thalamus and medial superior left midbrain. The lesion displays mild diffusion restriction (a and b).

There is minimal enhancement observed along the left optic nerve pathway (h, i, and j).

Incidental finding of a mildly expansile, avidly enhancing intraosseous lesion in the diploic region of the left frontal bone (j), likely representing an intraosseous hemangioma.

The constellation of orbital and intracranial findings suggests subacute left herpes zoster ophthalmicus associated with an ipsilateral delayed subcortical hemorrhagic thalamic/midbrain infarction secondary to arteritis.

Discussion

Herpes zoster ophthalmicus (HZO) originates from the reactivation of the varicella-zoster virus (VZV). After infection, VZV remains dormant in the nerve ganglia along the neuroaxis. In aging or declining immunity, the dormant virus can reactivate into HZO, affecting the ophthalmic branch of the trigeminal nerve. Varicella zoster is an alpha herpesvirus that only affects humans. Commonly referred to as shingles, an estimated 1 million new cases are diagnosed each year. Among those, 8% develop herpes zoster ophtalmicus.

The findings associated with VZV on neuroimaging include encephalitis, vasculitides, extraocular myositis, Ramsay Hunt syndrome (herpes zoster oticus), ischemic lesions of the grey-white matter junction, and less frequently, spinal cord and brachial plexus involvement.

HZO in our case induced a subacute hemorrhagic infarction of the left thalamus, reaching the midbrain. This indicates vascular compromise, likely secondary to arteritis. Initially presenting as HZO anterior uveitis in the left V1 area, further investigation showed that the patient had optic neuropathy (HZV showing altitudinal defect inferiorly) as well as hemorrhagic infarction secondary to arteritis upon MRI investigation.

An inflammatory response is triggered when reactivated VZV attacks the cerebral arteries, resulting in HZO-induced arteritis. VZV is very unique as it is the only known human virus to replicate inside artery walls and cause disease. This process involves the virus entering the artery directly, triggering an immune response, causing the arteritis. This facilitates the thickening of the artery walls, leading to stenosis or rupture, resulting in an ischemic or hemorrhagic stroke. To our knowledge, this is the first case with all three symptoms.

Teaching Point

- HZO is a manifestation of varicella-zoster virus reactivation.
- Neuroimaging findings of VZV, are nonspecific including encephalitis, arteritis, and ischemic or hemorrhagic lesions.
- HZO can present with anterior uveitis, optic neuropathy, and complications like hemorrhagic infarctions.
- MRI is vital in diagnosis and the management of the vascular effects, particularly in the context of potential strokes.

References

1- Nagel MA, Gilden D. Update on varicella zoster virus vasculopathy. Curr Infect Dis Rep. 2014 Jun;16(6):407. doi: 10.1007/s11908-014-0407-z. PMID: 24819870; PMCID: PMC4112991.

2- Nagel MA, Bubak AN. Varicella Zoster Virus Vasculopathy. J Infect Dis. 2018 Sep 22;218(suppl_2):S107-S112. doi: 10.1093/infdis/jiy425. PMID: 30247600; PMCID: PMC6151079. 3- Gilden D, White T, Khmeleva N, Heintzman A, Choe A, Boyer PJ, Grose C, Carpenter JE, Rempel A, Bos N, Kandasamy B, Lear-Kaul K, Holmes DB, Bennett JL, Cohrs RJ, Mahalingam R, Mandava N, Eberhart CG, Bockelman B, Poppiti RJ, Tamhankar MA, Fogt F, Amato M, Wood E, Durairaj V, Rasmussen S, Petursdottir V, Pollak L, Mendlovic S, Chatelain D, Keyvani K, Brueck W, Nagel MA.

3-Prevalence and distribution of VZV in temporal arteries of patients with giant cell arteritis. Neurology. 2015 May 12;84(19):1948-55. doi: 10.1212/WNL.0000000000001409. Epub 2015 Feb 18. PMID: 25695965; PMCID: PMC4433460.
4- Kim MJ, Lee KO, Lee KY, Oh SH, Na SJ, Yoon B, Kim YD. Hemichorea caused by intracranial hemorrhage following contralateral herpes zoster ophthalmicus. J Clin Neurosci. 2013 May;20(5):738-9. doi: 10.1016/j.jocn.2012.04.025. Epub 2013 Feb 26. PMID: 23453159.

Images/Tables

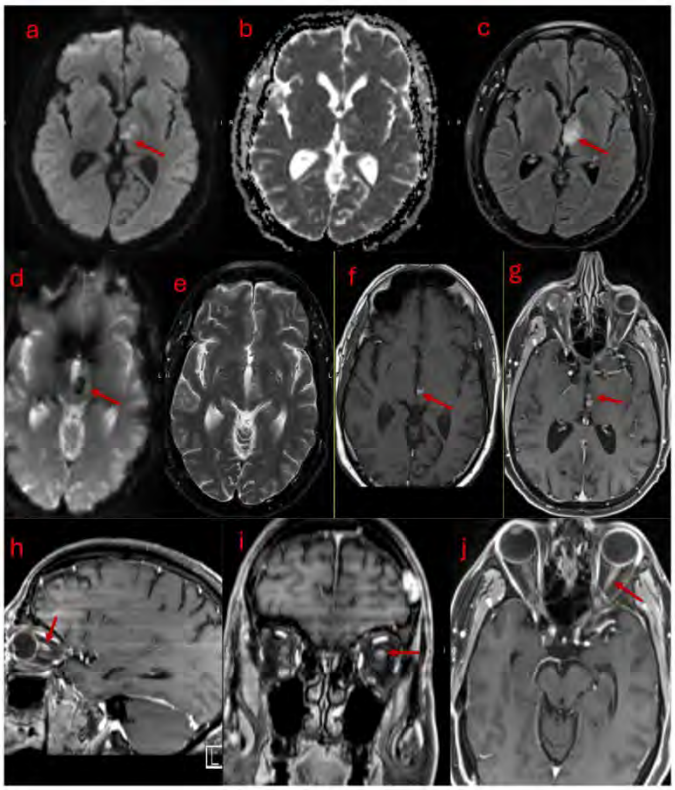


Figure: MRI with contrast shows an ill -defined, mildly expansile, T2/FLAIR hyperintense lesion with heterogeneous enhancement (g) and central hemorrhage (d and f) within the left thalamus and medial superior left midbrain. The lesion displays mild diffusion restriction (a and b).
There is minimal enhancement observed along the left optic nerve pathway (h, i, and j).
Incidental finding of a mildly expansile, avidly enhancing intraosseous lesion in the diploic region of the left frontal bone (j), likely representing an intraosseous hemangioma.

The constellation of orbital and intracranial findings suggests subacute left herpes zoster ophthalmicus associated with an ipsilateral delayed subcortical hemorrhagic thalamic/midbrain infarction secondary to arteritis.

1159

Subtle Glaucoma: MRI Imaging Findings

Nafisa Paruk MBChB[1], Richard H Wiggins MD[2]
[1]Ebrahim and partners, Pretoria, City of Tshwane Metropolitan Municipality, South Africa. [2]University of Utah, SAlt Lake City, UT, USA

Abstract Category

Head & Neck

Clinical History

A 14-year-old male patient presents with painful eyes, blurred vision, halos and colors in both eyes for approximately 7 months.

Imaging Findings

Thin section MRI images demonstrated bilateral small optic nerves, measuring 1.3mm in diameter. There was also decreased height of the optic chiasm, measuring 1.6mm. No proptosis, no myopic features, normal lens and globe shape. There were no features of obstructive or entrapment hydrocephalus.

Discussion

Glaucoma is one of the worldwide leading causes of irreversible blindness, however the etiology is still unclear and there is no cure. Approximately 6 million people are affected internationally each year with glaucoma. This has been predicted to increase from 76 million in 2022 to 112 million in 2040. It is the second commonest cause of blindness after cataracts. Early detection of glaucoma is very important since it's an irreversible cause of blindness, especially in advanced stages. Glaucoma is said to present insidiously like a "sneaky thief of sight". The neurodegenerative processes of glaucoma are nonspecific and are not just limited to optic nerve and chiasm but extends to the entire visual pathway and associated areas. Some studies indicate that non -visual areas are also involved. Hence, it is said to encompass neurodegenerative

process in the brain. The thought is that glaucoma not only heralds retrograde neurodegenerative pathology but may also result from primary neurodegenerative processes in the brain, anterogradely.

Teaching Point

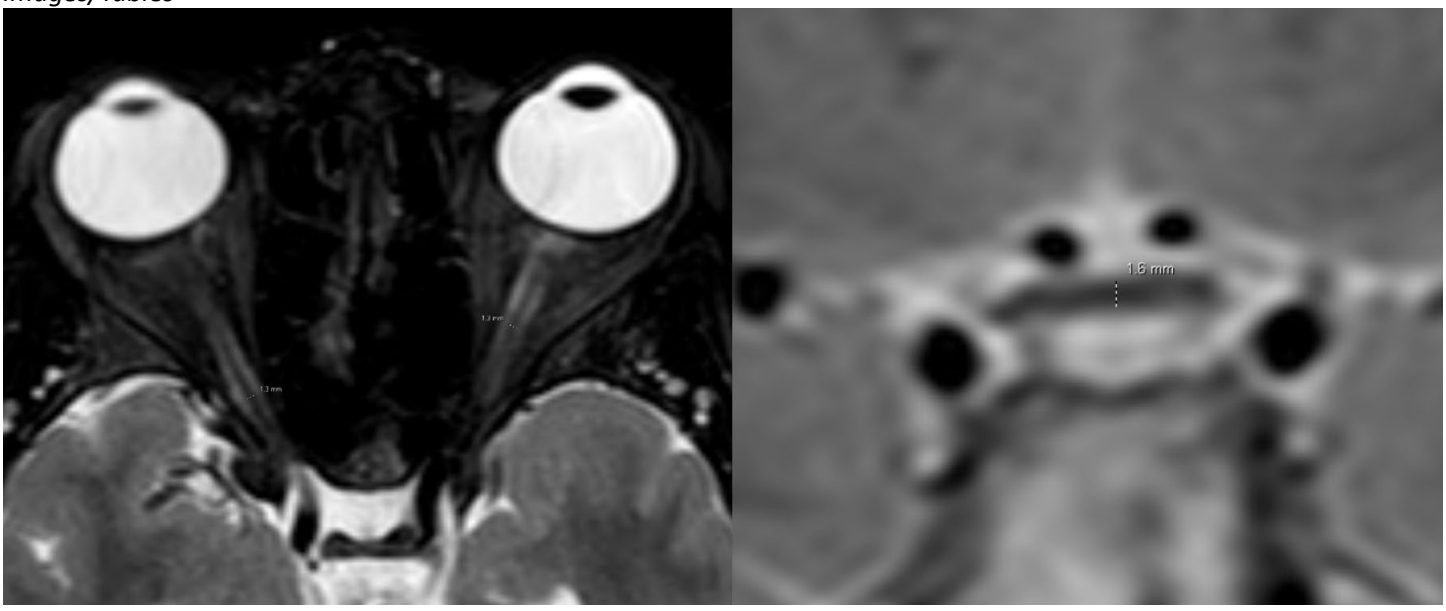
Teaching Points:

1. This is a rare and interesting case of primary open angle glaucoma in a young male patient where MRI findings may be correlated with findings on the ophthalmology examination.
2. Most radiologists think only about optic neuritis as being the cause of optic atrophy and attribute any high T2 signal similarly. Posteriorly, the extent of the atrophy needs to be evaluated not only at the optic chiasm, but throughout the visual pathway.
3. It provides the radiologist with important normal measurement parameters of the optic nerve and chiasm, which they may not be aware of.
4. When optic atrophy is present, an ophthalmology assessment is essential initially before extensive investigations for demyelinating diseases are undertaken.
5. Optic nerve enhancement is not present in glaucoma because there is no “blood-brain” barrier destruction.
6. Brain parenchymal changes may be present, since glaucoma is thought to be part of a larger complex of neurodegenerative disorders.
7. There has been research on the direct correlation of Glaucoma with Alzheimer’s disease. Hence, the entire brain requires assessment in Glaucoma.
8. Glaucoma may accompany comorbid features, like in this case, seizures.
9. Exclude space occupying lesion, pituitary macroadenoma and other causes of blindness due to mass effect.
10. Risk factors and complications of Glaucoma to be taken into consideration due to the irreversible sequelae of blindness that may occur. Hence, the importance of early detection, which MRI may contribute to.

References

1. Chan B, K Karuppannan J, McArdle D, et al. Glaucoma. Reference article, Radiopaedia.org (Accessed on 03 Nov 2024) https://doi.org/10.53347/rID-171323
2. Li M, He HG, Shi W, Li J, Lv B, Wang CH, et al. Quantification of the Human Lateral Geniculate Nucleus In Vivo Using MR Imaging Based on Morphometry: Volume Loss with Age.
3. AJNR Am J Neuroradiol. 2012 May;33(5):915-921.doi:10.3174/ajnr.A2884
4. Martucci A, Di Giuliano F, Minosse S, Pocobelli G, Nucci C, Garaci F. MRI and Clinical Biomarkers Overlap between Glaucoma and Alzheimer’s Disease. Int J Mol Sci. 2023 Oct 5;24(19):14932.doi:10.3390/ijms24191493
5. Ominde BS, Abadom GE, Ikubor JE, Achapu LC , Enakpoya PO, Igbigbi PS. Normal diameter of the optic nerve using magnetic resonance imaging : A retrospective Nigerian study.

Images/Tables



1169

Neuroimaging in 3rd Cranial Nerve Palsy: Recognizing Tolosa-Hunt Syndrome as a Diagnosis of Exclusion

Suryansh Bajaj MD
University of Arkansas for Medical Sciences, Little Rock, AR, USA

Abstract Category

Adult Brain

Clinical History

A 35-year-old female with past history of HFrEF , HTN, HLPD, polysubstance abuse (meth, tobacco, and cocaine) presented to the ED with headache and right eye vision issues for 1 week. Physical examination demonstrated complete pupil involving right CN 3 palsy. The patient was admitted for further work up of pupil involving right CN 3 complete palsy. Mass lesion, compression from aneurysm, and ischemic injury were the top differentials based on presentation.

Imaging Findings

Noncontrast head CT showed no mass lesion.

CT angiogram head and neck demonstrated no aneurysm.

MRI with and without contrast of head and orbits were performed and demonstrated asymmetric thickening and enhancement along its course from the cavernous sinus to the superior orbital fissure. No mass lesions were seen. Findings were concluded to be secondary to Tolosa Hunt syndrome.

Discussion

Cranial nerve (CN) 3 palsy can result from various etiologies, including **vascular** (e.g., **diabetic microangiopathy**, **hypertension**), **traumatic**, **neoplastic**, **infectious**, and **inflammatory** causes. **Aneurysms**, particularly at the **posterior communicating artery**, are a critical concern due to their potential for compressing the nerve. **Tolosa-Hunt syndrome** and **multiple sclerosis** can also affect the nerve, particularly in younger patients. **Clinical presentation** typically includes **ptosis**, **diplopia**, and **ocular motility deficits** (e.g., inability to elevate, depress, or adduct the eye). Incomplete palsy may preserve pupil function, while **pupil-involving palsy** raises suspicion for a compressive cause, such as an aneurysm. Prompt evaluation is essential.

The radiologic workup for **cranial nerve (CN) 3 palsy** typically begins with **MRI** of the brain, focusing on the brainstem and intracranial segment of the third nerve. **Contrast-enhanced imaging** is often employed to rule out **tumors**, **aneurysms**, or **vascular malformations** at the **posterior communicating artery** (a common site for aneurysms causing CN 3 palsy). **MRA** or **CT angiography** may be used to further assess for aneurysms. For cases where **Tolosa-Hunt syndrome** is suspected, **orbital MRI** can help identify inflammation of the cavernous sinus.

Imaging in Tolosa hunt syndrome may reveal signs of inflammation in the area of the anterior cavernous sinus, superior orbital fissure, and possibly the orbital apex. The signal characteristics are non-specific (with the clinical context being crucial for diagnosis) but may include:

- **T1**: The affected region appears isointense to hyperintense compared to muscle.
- **T2**: The involved area is hyperintense.
- **T1 C+ (Gd)**: Contrast enhancement may be visible during the active phase of inflammation, with a reduction in enhancement following treatment.

Treatment is with steroids. Differentials may include sarcoidosis, pituitary tumors, tuberculous meningitis, lymphoma, cavernous sinus thrombosis

Teaching Point

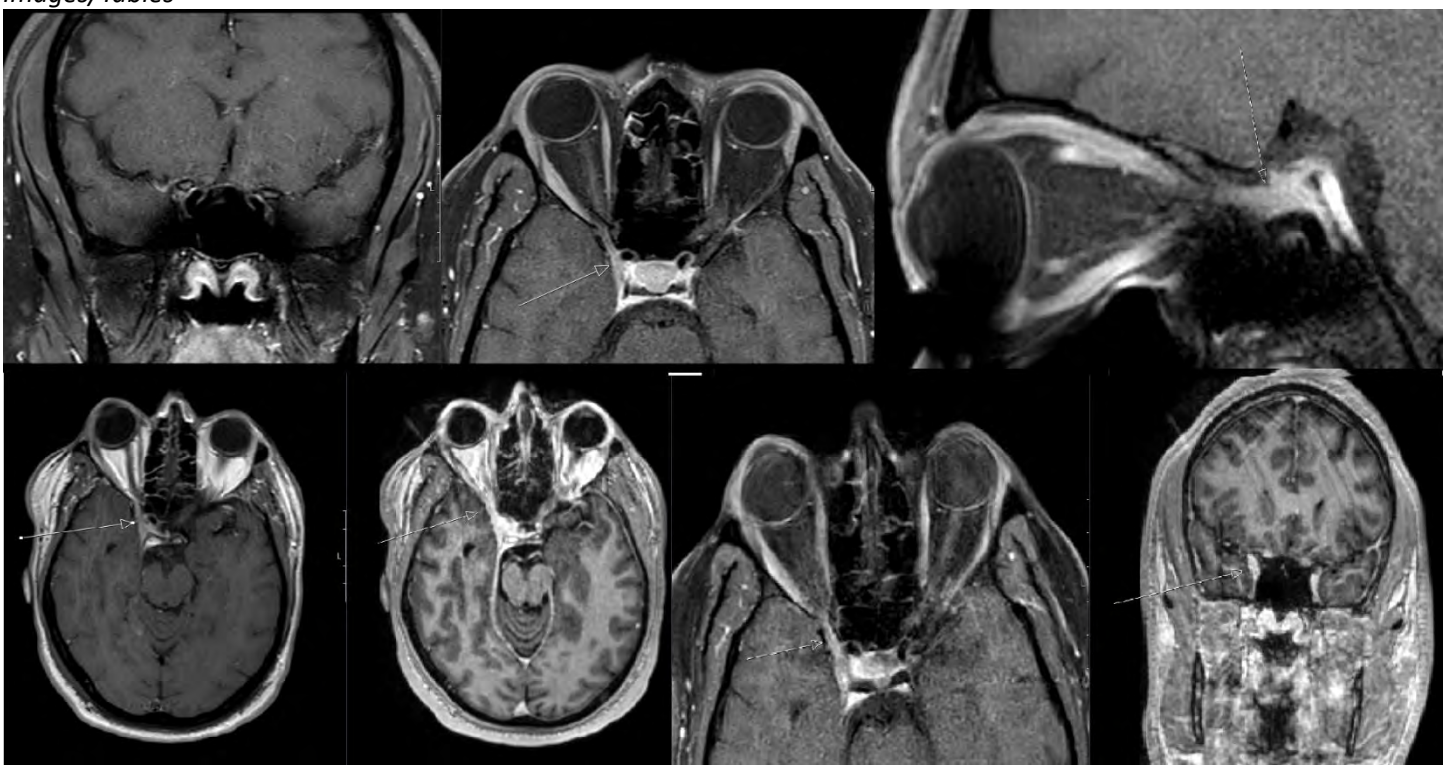
Tolosa Hunt syndrome is any idiopathic inflammation of the 3rd cranial nerve in around the cavernous sinus. It is a diagnosis of exclusion for cranial nerve 3 pathology. MRI is the imaging modality of choice that shows abnormal thickening and enhancement of the nerve along its course.

References

Kmeid M, Medrea I. Review of Tolosa-Hunt Syndrome, Recent Updates. Curr Pain Headache Rep. 2023 Dec;27(12):843-849. doi: 10.1007/s11916-023-01193-4. Epub 2023 Nov 30. PMID: 38032539.

Dutta P, Anand K. Tolosa-Hunt Syndrome: A Review of Diagnostic Criteria and Unresolved Issues. J Curr Ophthalmol. 2021 Jul 5;33(2):104-111. doi: 10.4103/joco.joco_134_20. PMID: 34409218; PMCID: PMC8365592.

Images/Tables



1179

Neuroimaging Insights in Zoster Neuritis: Correlating Radiological Findings with Painful Rash

Suryansh Bajaj MD
University of Arkansas for Medical Sciences, Little Rock, AR, USA

Abstract Category

Spine

Clinical History

A 60-year-old female presented to the ED with painful vesicular rash in the left lower extremity. The rash poss localized to a single dermatome. MRI of the lumbar spine was obtained to rule out epidural abscess due to complaints of back pain and signs of sepsis.

Imaging Findings

MRI of the lumbar spine demonstrated abnormal thickening and enhancement of the left L3 nerve starting at the neural foramina and extending till the visualized course of the left L3 nerve. Findings are suggestive of acute moderate neuritis of the left L3 nerve, which may be seen with Zoster neuritis.

Discussion

A single dermatomal painful rash is often suggestive of herpes zoster (shingles), caused by the reactivation of the varicella-zoster virus (VZV) in a specific sensory nerve root. The rash typically appears in one dermatome, which is an area of skin innervated by a single spinal nerve. The initial presentation is often characterized by unilateral pain, tingling, or burning sensation along the affected dermatome, followed by the development of a cluster of vesicular lesions on an erythematous base. The pain can precede the rash by 1-5 days. The most common sites for shingles are the thoracic, cervical, and trigeminal (face) dermatomes. A painful rash restricted to a single dermatome is a hallmark of zoster, though other conditions, such as contact dermatitis or bullous impetigo, can present similarly but typically involve more than one dermatome. Diagnosis is confirmed through clinical evaluation, and sometimes polymerase chain reaction (PCR) or direct fluorescent antibody tests for VZV. Treatment usually involves antiviral medications to reduce viral replication and prevent complications like postherpetic neuralgia.

The patient was treated with valacyclovir and showed improvement in 3 weeks.

Ramsay Hunt syndrome is the neuritis of the fusion secondary to postherpetic neuralgia. Similar to cranial nerve involvement, peripheral nerves can also be involved in these cases. Nonspecific findings of thickening and enhancement of the nerve is noted along with single dermatomal painful rash on physical examination.

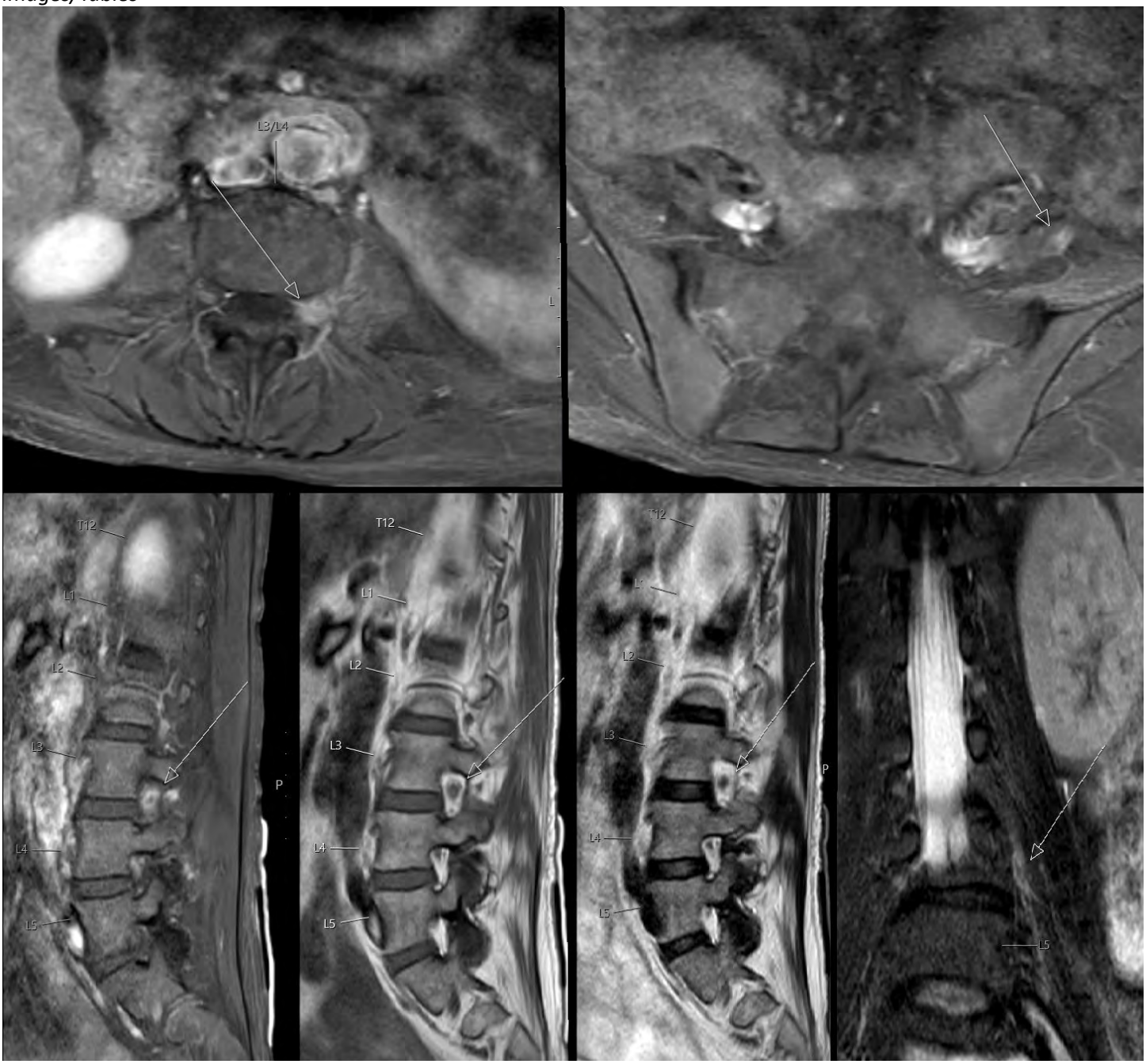
Teaching Point

Zoster neuritis is an important differential in patients with single dermatomal painful rash. Imaging findings of nerve thickening and enhancement can increase the diagnostic confidence.

References

Oak P, Modi T, Patkar D. Zoster neuritis of lumbar nerves: A clinical, magnetic resonance imaging, and electrodiagnostic evaluation. J Postgrad Med. 2022 Jan-Mar;68(1):48-50. doi: 10.4103/jpgm.JPGM_110_21. PMID: 34806655; PMCID: PMC8860118.d

Images/Tables



1220

Mastoid Bone Spindle Cell Carcinoma in a Patient with a Remote History of Breast Cancer: Diagnostic and Therapeutic Challenge.

Muhammad T Raj MD, Thomas R Geisbush MD, Connor Gemmell MD, Osama R Raslan MD, Lotfi Hacein-Bey MD
University of California - Davis, Sacramento, CA, USA

Abstract Category

Head & Neck

Clinical History

A 77-year old female with a remote history of breast cancer status post bilateral mastectomy and subsequent chemoradiation 18 years prior was considered in remission. CT obtained for right earache showed a rapidly expansile soft tissue mass within the right mastoid bone with air cell lytic changes and posterior fossa extension. A right mastoidectomy was performed with wide tumor resection including the posterior fossa component. Although pathology was initially equivocal, the diagnosis of spindle cell carcinoma was considered based on specific staining markers including AE1/AE3, PDL1 and CAM5.2.

Imaging Findings

Reported imaging features of spindle cell carcinoma are not specific. In this patient, CT and MRI (Fig 1. A-D) obtained following initial mastoidectomy demonstrated an avidly enhancing soft tissue mass with extensive locoregional spread into adjacent osseous structures, stylomastoid foramen and parotid gland with perineural facial nerve involvement, cerebellopontine angle, and right transverse/sigmoid sinus tumor thrombus.

Figure legend

1 A-D. 1A. Axial CT of the head showing a destructive lytic expansile mass in the right mastoid; 1B. Axial T1 fat-saturated post-contrast study demonstrating a large enhancing mass in mastoid air cells with tumor thrombus in the right sigmoid and jugular foramen; 1C. Right mastoid air cell mass demonstrating scattered diffusion restriction (ADC not shown); 1D. Subtle areas of scattered increased perfusion on arterial-spin-labelling (ASL) imaging.

Discussion

In adults, apart from metastases, the most common primary tumors of the mastoid bone are squamous and basal cell carcinoma. In children, one must consider rhabdomyosarcoma and acute myelogenous leukemia. These tumors have relatively distinctive imaging features, whether they arise from the external auditory canal, the mucosal space or surrounding tissues. In contrast, spindle cell carcinoma does not have specific imaging features. In addition, although encountered occasionally in head and neck imaging, this tumor type currently lacks clear management and treatment guidelines. Our patient was ultimately considered a nonsurgical candidate and by consensus of the multidisciplinary team was started on induction chemotherapy followed by radiotherapy.

Teaching Point

In patients with prior malignancy and presenting with tumor of the mastoid bone, typically metastatic disease is the first diagnostic consideration. Spindle cell carcinoma has been described in the neck with metastasis to the mastoids; however, we believe this is the first such case of primary spindle cell carcinoma arising from the mastoids. In this case, careful pathological evaluation including specific immunohistochemical staining helped establish the diagnosis. This bears significance as to management and prognostic implications of tumors in which treatment is established with clear guidelines. In contrast, spindle cell carcinoma of the mastoid bone lacks clear imaging criteria and treatment protocols. This highlights the importance of a multidisciplinary approach to such complex cases with an in-depth imaging and pathologic search.

References

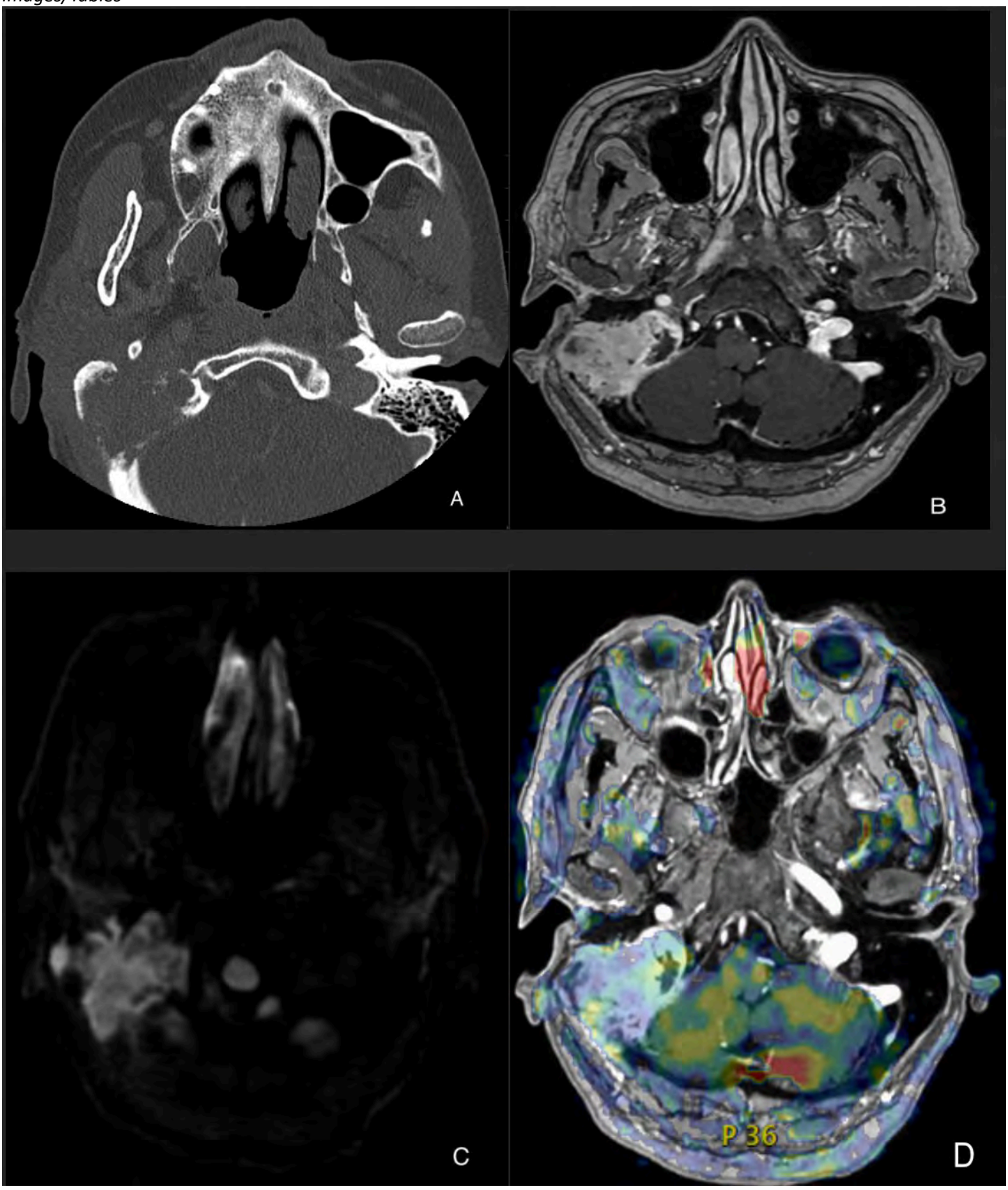
Jones AJ, Tucker BJ, Novinger LJ, et al. Metastatic Disease of the Temporal Bone: A Contemporary Review. *Laryngoscope*. 2021 May;131(5):1101-1109. doi: 10.1002/lary.29096.

Yoshihara, T., & Igarashi, M. (1986). Poorly differentiated fibrosarcoma (spindle cell sarcoma) involving the temporal bone. *ORL; journal for oto-rhino-laryngology and its related specialties*, 48(5), 249–255. https://doi.org/10.1159/000275877

Keidar E, Bowers I, Sargent E. Mastoiditis Masquerade. *Ear Nose Throat J*. 2022 May;101(4):221-223. doi: 10.1177/0145561320950493.

Ungar OJ, Santos F, Nadol JB, Horowitz G, Fliss DM, Faquin WC, Handzel O. Invasion Patterns of External Auditory Canal Squamous Cell Carcinoma: A Histopathology Study. *Laryngoscope*. 2021 Feb;131(2):E590-E597. doi: 10.1002/lary.28676.

Images/Tables



1225

Chiasm to Chasm: Unique Third Ventricular Herniations after Resection of Sellar and Suprasellar Masses

Kunal Kedar MD, Ay-Ming Wang MD
Corewell Health East William Beaumont University Hospital, Royal Oak, Michigan, USA

Abstract Category

Adult Brain

Clinical History

66-year-old male with hypothyroidism presented with weight loss and altered mental status. Imaging revealed a mass in the middle cranial fossa. He underwent craniotomy with suprasellar tumor resection and subsequently developed obstructive hydrocephalus and panhypopituitarism; pathology showed no evidence of malignancy. Twelve months later, the patient developed progressive visual field defects and worsening mental status. Follow-up imaging demonstrated recurrence of the suprasellar mass, measuring 2.9 x 3.4 x 3.6 cm in the craniocaudal, transverse and anteroposterior dimensions. Transsphenoidal resection revealed a retrochiasmatic tumor arising from the pituitary stalk with pathology showing cholesterol granuloma, without evidence of craniopharyngioma.

14-year-old female with no significant medical history presented with vision loss and endocrinopathy. MRI showed a cystic sellar mass measuring 5 x 4 x 2.8 cm in the craniocaudal, transverse and anteroposterior dimensions with expansion of the sella and a large suprasellar component, causing mass effect on the hypothalamus, optic chiasm, and prechiasmatic optic nerves. She underwent transsphenoidal resection, revealing attachment to the pituitary stalk and upward displacement of the diaphragma sella. Pathology confirmed adamantinomatous craniopharyngioma with cholesterol granulomas.

Imaging Findings

For the adult male, postoperative imaging obtained 4 weeks later showed removal of the suprasellar mass but new moderate dilation of the anteroinferior third ventricle, with herniation into a partially empty sella and anterior displacement of the optic chiasm. There was also development of third and lateral ventricular dilation, consistent with obstructive hydrocephalus. Follow-up CT after left frontal ventricular shunt placement demonstrated decompression of the lateral ventricles without significant change in third ventricular herniation.

For the adolescent female, follow-up MRI showed an enlarged empty sella with CSF signal and a dilated anteroinferior third ventricle, causing mass effect on the optic chiasm and leading to superior displacement.

Discussion

Third ventricular herniations are rare. Typically, they involve the suprasellar visual system (SVS), including the optic nerves, chiasm, tracts, and anteroinferior third ventricle. Third ventricular herniations into the sellae can occur with isolated anteroinferior herniation into the sellar space. SVS herniations can cause visual symptoms of varying degrees, which may not correlate with the degree of herniation. The large third ventricular herniations in this case, secondary to craniopharyngioma and recurrent cholesterol granuloma, are unique in their isolated herniation of the anteroinferior third ventricle, particularly the infundibular recess into the partially empty sella in the adult male and expanded empty sella in the adolescent female.

Teaching Point

The clinical significance of third ventricular herniations and of the degree of herniation are currently unknown. The adult male had a history of hydrocephalus after the initial procedure and underwent left frontal external ventricular shunt placement after second resection, with decompression of the lateral ventricles and minimal change in anteroinferior herniation of the third ventricle. This suggests that hydrocephalus and anteroinferior third ventricular herniation and dilation are unrelated to the obstructive hydrocephalus. The mechanism of third ventricular herniations is unclear but may involve adhesions or other postoperative changes. Further characterization and differentiation of third ventricular herniations could lead to better correlation with symptoms.

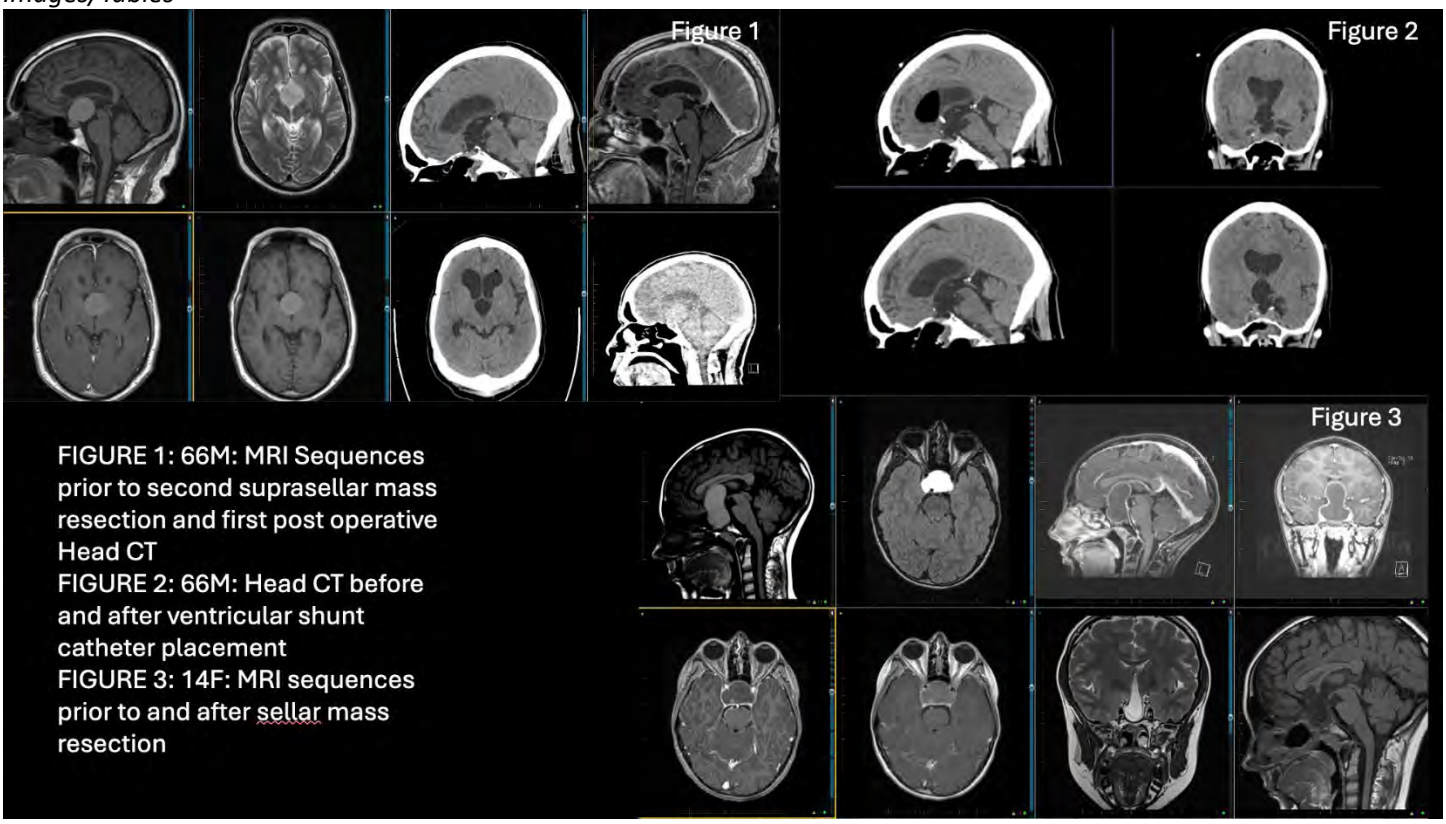
References

Jalessi M, Shariff G, Jahanbakhshi, et al. Third Ventricle herniation into the Sphenoid Sinus Following Endoscopic Transnasal transsphenoidal Fenestration of Rathke's Cleft Cyst. *Turkish Neurosurgery* 2014;24:63-66. DOI: 10.5137/1019-5149.JTN.5991-12.1

Kaufman B, Tomsak RL, et al. Herniation of the Suprasellar Visual System and Third Ventricle into Empty Sellae: Morphologic and Clinical Considerations. *AJR* 1989;152:597-608.

Kobayashi S, Otsuka A, Tsunoda T. Herniation of the third ventricle into empty sella caused by surgery for pituitary apoplexy--case report. *Neurol Med Chir* 1996;36:451-454. DOI: 10.2176/nmc.36.451.

Images/Tables



1230

Miyazaki Syndrome: Looking Beyond Slit-Ventricles in Overshunting

Amy C Yu DO, Charles Li MD, Edward Kuoy MD
University of California, Irvine, Orange, CA, USA

Abstract Category

Spine

Clinical History

84 years-old male with normal pressure hydrocephalus presented with upper extremity paresthesia, worsening ataxia, and mild cognitive impairment two months following ventriculoperitoneal shunt placement. After brain MR exam demonstrated findings concerning for overshunting-associated myelopathy, the patient underwent shunt revision with subsequent resolution of symptoms.

Imaging Findings

Figure 1. Pre-shunt brain MR sagittal (A) and axial (B) non-contrast T1 MP-RAGE imaging demonstrates normal caliber ventral venous plexus within the proximal cervical canal.

Figure 2. Post-shunt brain MR sagittal (A) and axial (B) non-contrast T1 MP-RAGE imaging demonstrates interval markedly engorged ventral venous plexus within the proximal cervical canal that severely narrows the thecal sac.

Figure 3. Post-shunt revision brain MR sagittal (A) and axial (B) non-contrast contrast T1 MP-RAGE imaging demonstrates normalized caliber of the ventral venous plexus within the proximal cervical canal.

Discussion

Miyazaki syndrome, or overshunting-associated myelopathy, is a potential complication of excessive CSF diversion where consequential cervical venous plexus engorgement may compress the cervical spinal cord or nerve roots. In this case report, the cervical venous plexus was followed by serial brain MR exams and no dedicated cervical spine MR exam was performed to examine for potential cord signal changes. While the exact mechanism for this entity is not known, one proposed hypothesis is that the Monro-Kellie doctrine plays a role with compensatory venous engorgement to compensate for CSF loss and likely superimposed venous congestion ultimately causing myelopathy symptoms.

Teaching Point

Potential imaging findings of CSF over-diversion include interval decreased, sometimes slit-like, ventricular calibers and subdural collections (hemorrhage and/or hygromas). It is important to recognize that cervical epidural venous engorgement may also be seen and cause related myelopathy symptoms. The proximal cervical spinal canal is included in most head CT and brain MR exams, and this may be sufficient to suggest this entity.

References

Várallyay P, Nagy Z, Szűcs A, et al. Miyazaki syndrome: Cervical myelo/radiculopathy caused by overshunting. A systematic review. *Clin Neurol Neurosurg* 2019 Nov;186:105531.

Images/Tables

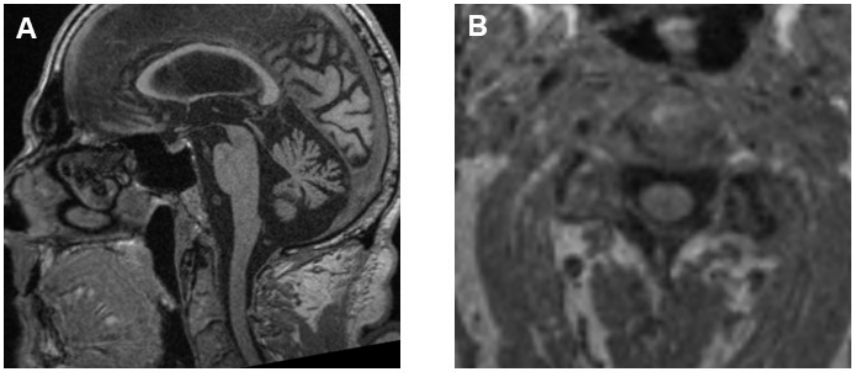


Figure 1. Pre-shunt brain MR sagittal (A) and axial (B) non-contrast T1 MP-RAGE imaging demonstrates normal caliber ventral venous plexus within the proximal cervical canal.

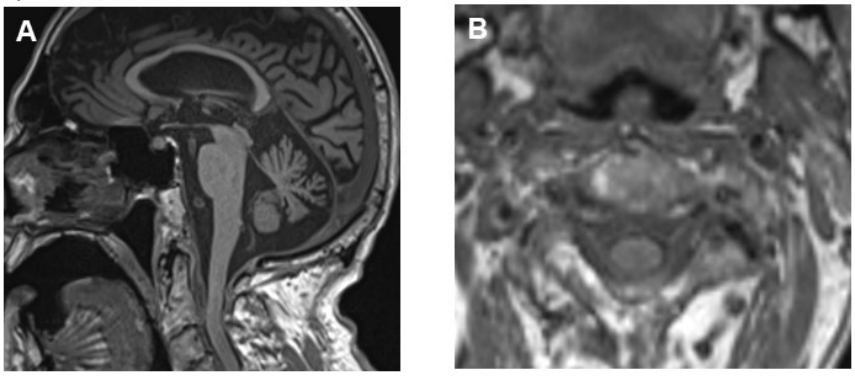


Figure 2. Post-shunt brain MR sagittal (A) and axial (B) non-contrast T1 MP-RAGE imaging demonstrates interval markedly engorged ventral venous plexus within the proximal cervical canal that severely narrows the thecal sac.

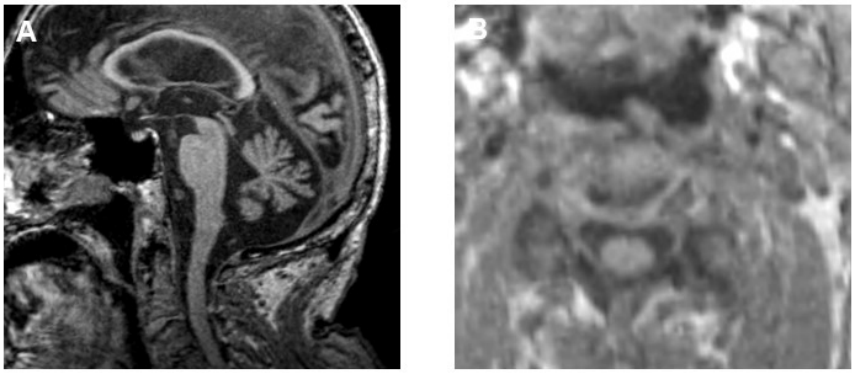


Figure 3. Post-shunt revision brain MR sagittal (A) and axial (B) non-contrast contrast T1 MP-RAGE imaging demonstrates normalized caliber of the ventral venous plexus within the proximal cervical canal.

1238

Hypoxia or Pseudo-Hypoxia: Post-operative Cerebral Venous Congestion

Joshua Wright MD, Edward Kuoy MD
University of California, Irvine, Orange, CA, USA

Abstract Category

Adult Brain

Clinical History

59 year-old male with atypical parasagittal meningioma status post resection with sacrifice of the involved superior sagittal sinus with poor post-operative neurological exam including inability to follow commands and spasticity on exam. Immediate postoperative brain MR was subsequently acquired showing changes predominantly involving the bilateral deep gray nuclei that essentially resolved on 2-month follow-up brain MR exam.

Imaging Findings

Figure 1. Immediate post-operative brain MR axial T2/FLAIR (A) and DWI (B) sequences demonstrate extensive T2/FLAIR hyperintense signal abnormality involving the bilateral basal ganglia, thalami, and occipital deep white matter with associated restricted diffusion in the bilateral basal ganglia. Additional bilateral frontal vasogenic edema was present on pre-operative brain MR exam related to patient's meningioma.

Figure 2. Head CTV sagittal demonstrates in-tact bilateral internal cerebral veins (arrow) (A) and axial demonstrates bilateral basal veins of Rosenthal (arrows) (B).

Figure 3. 2-month follow-up brain MR axial T2/FLAIR (A) and DWI (B) sequences demonstrate essential resolution of prior extensive signal changes without subsequent encephalomalacia.

Discussion

Postoperative intracranial hypotension-associated venous congestion, or pseudo-hypoxic brain swelling, is a potential postoperative complication that may occur after brain or spine surgeries. While prior case reports have attributed the venous congestion to rapid CSF drainage, this case may have occurred because of sinus sacrifice and subsequent drainage alterations. Venous infarction was a consideration, which may also demonstrate reversible imaging findings as in this case, but the lack of deep venous occlusion and atypical territory for superior sagittal sinus sacrifice made this a less likely cause. Central-variant posterior reversible encephalopathy syndrome was another consideration, but felt less likely due to lack of associated potential etiologies.

Teaching Point

When encountering post-operative brain MR findings with bilateral deep gray nuclei involvement, it is important to consider venous congestion as a potential etiology, which may be reversible.

References

Dickinson J, Kroll D, Bentley J, Gustin AJ. Pseudohypoxic Brain Swelling After Elective Lumbar Spinal Surgery: Case Report. Cureus. 2018 Apr 9;10(4):e2454. doi: 10.7759/cureus.2454.

Images/Tables

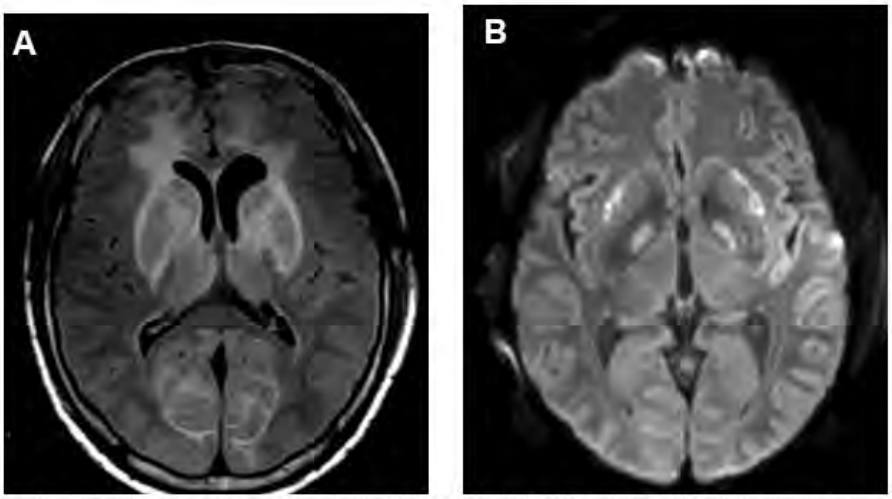


Figure 1. Immediate post-operative brain MR axial T2/FLAIR (A) and DWI (B) sequences demonstrate extensive T2/FLAIR hyperintense signal abnormality involving the bilateral basal ganglia, thalami, and occipital deep white matter with associated restricted diffusion in the bilateral basal ganglia. Additional bilateral frontal vasogenic edema was present on pre-operative brain MR exam related to patient's meningioma.

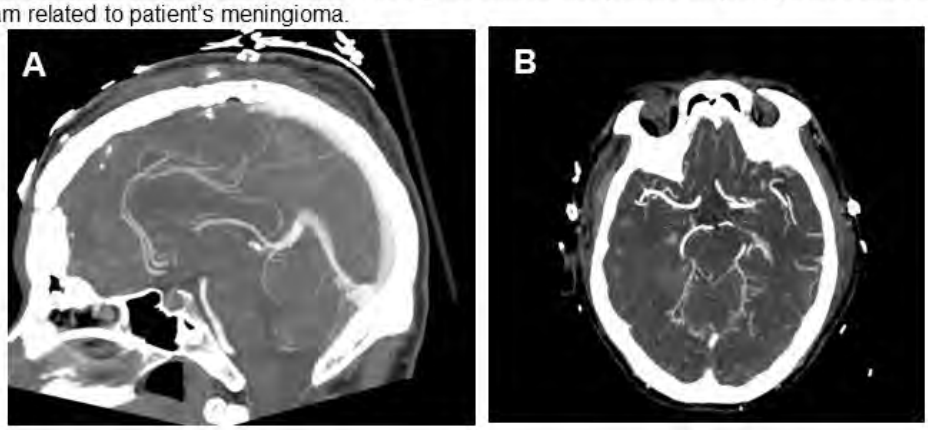


Figure 2. Head CTV sagittal demonstrates in-tact bilateral internal cerebral veins (arrow) (A) and axial demonstrates bilateral basal veins of Rosenthal (arrows) (B).

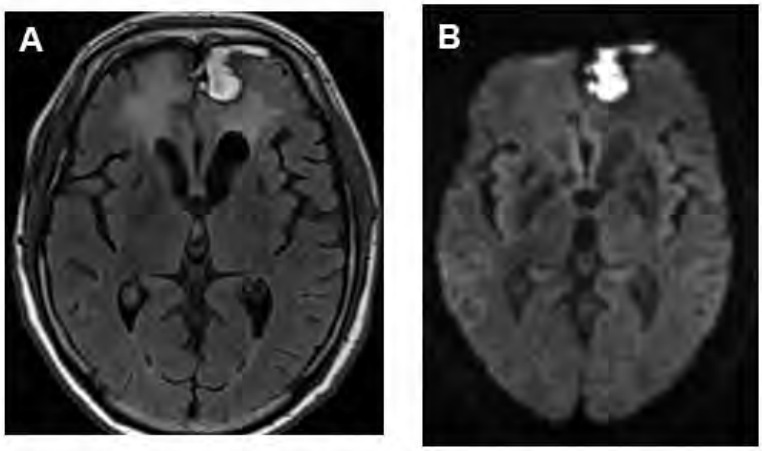


Figure 3. 2-month follow-up brain MR axial T2/FLAIR (A) and DWI (B) sequences demonstrate essential resolution of prior extensive signal changes without subsequent encephalomalacia.

Educational Exhibits

67

Navigating the Tracts: Advanced Diffusion Tensor Imaging in Traumatic Brain Injury Clinical Insights and Future Directions

Michael X Jin MD/MBA[1], Austin Young BS[2], Abhinav Mishra HBSc[2], Eric J Feldmann MD[2], Michael L Lipton MD/PhD[1]
[1]Columbia University Irving Medical Center, New York, NY, USA. [2]Renaissance School of Medicine at Stony Brook University, Stony Brook, NY, USA

Abstract Category

Adult Brain Inflammatory/Infectious Disease/Degenerative/Metabolic

Summary & Objectives

This educational exhibit will explore the latest advancements in Diffusion Tensor Imaging (DTI) with a focus on its application in traumatic brain injury (TBI). DTI, a powerful MRI-based imaging modality, is an essential tool for mapping and understanding white matter tracts in the brain. Attendees will gain insights into the fundamental biomechanics and technology underlying DTI, followed by a review of what DTI adds beyond conventional findings such as hemorrhage and white matter hyperintensities and associations of DTI microstructure and volumetric macrostructure changes. The session will present five case studies that highlight both common and complex DTI findings, demonstrating how cutting-edge methods are addressing current limitations. Finally, the session will discuss the future of DTI in neuroimaging, emphasizing its evolving role in understanding brain microstructure and improving patient outcomes.

Learning objectives include the following:

1. Describe fundamental biophysical and technological principles of Diffusion Tensor Imaging (DTI) and their application in neuroimaging.
2. Review approaches for the processing, analysis and visualization of DTI.
3. Evaluate the clinical findings of DTI in traumatic brain injury, expanding on what DTI adds beyond conventional findings such as hemorrhage and white matter hyperintensities through 5 clinical cases.
4. Explore cutting-edge DTI methods to overcome current imaging challenges can form the future of DTI in neuroimaging.

Purpose

N/A

Materials & Methods

N/A

Results & Conclusion

N/A

References

Hoogenboom, W. S., Rubin, T. G., Ye, K., Cui, M. H., Branch, K. C., Liu, J., Branch, C. A., & Lipton, M. L. (2019). Diffusion Tensor Imaging of the Evolving Response to Mild Traumatic Brain Injury in Rats. Journal of experimental neuroscience, 13, 1179069519858627. https://doi.org/10.1177/1179069519858627

110

Get Up to Snuff: Nasopharyngeal Carcinoma Overview with Pertinent Surgical Skull Base Anatomic Review

Michael J. Nisiewicz MD, Andrew S.C. Barty DO, Rony Aouad MD, Kwaku Obeng MD
University of Kentucky, Lexington, KY, USA

Abstract Category

Head and Neck

Summary & Objectives

- Review definition, risk factors, and epidemiology of nasopharyngeal carcinoma
- Review pathologic subtypes
- Identify key imaging modalities and their findings
- Summarize pertinent skull base anatomy critical for evaluation and reporting of nasopharyngeal carcinoma
- Review staging criteria

- Present case examples depicting patterns of disease progression/spread
- Review disease management and prognosis

Purpose

- To provide radiologists with a comprehensive overview of nasopharyneal carcinoma
- Improve imaging interpretation of disease
- Optimize disease reporting for clinicians and surgeons, with overall goal of improving patient management and outcome

Materials & Methods

- Contrast and non-contrast CT and MR images will be provided

Results & Conclusion

Nasopharyngeal carcinoma is one of the most aggressive malignancies of the head and neck. With high rates of metastatic disease, involvement of the skull base foramina and fissures is a typical occurrence. Fortunately this malignancy is susceptible to a variety of therapeutic options, allowing for local and regional disease control. Nonetheless, appropriate appreciation of anatomic involvement, staging, and thorough reporting is crucial for surgical and medical management

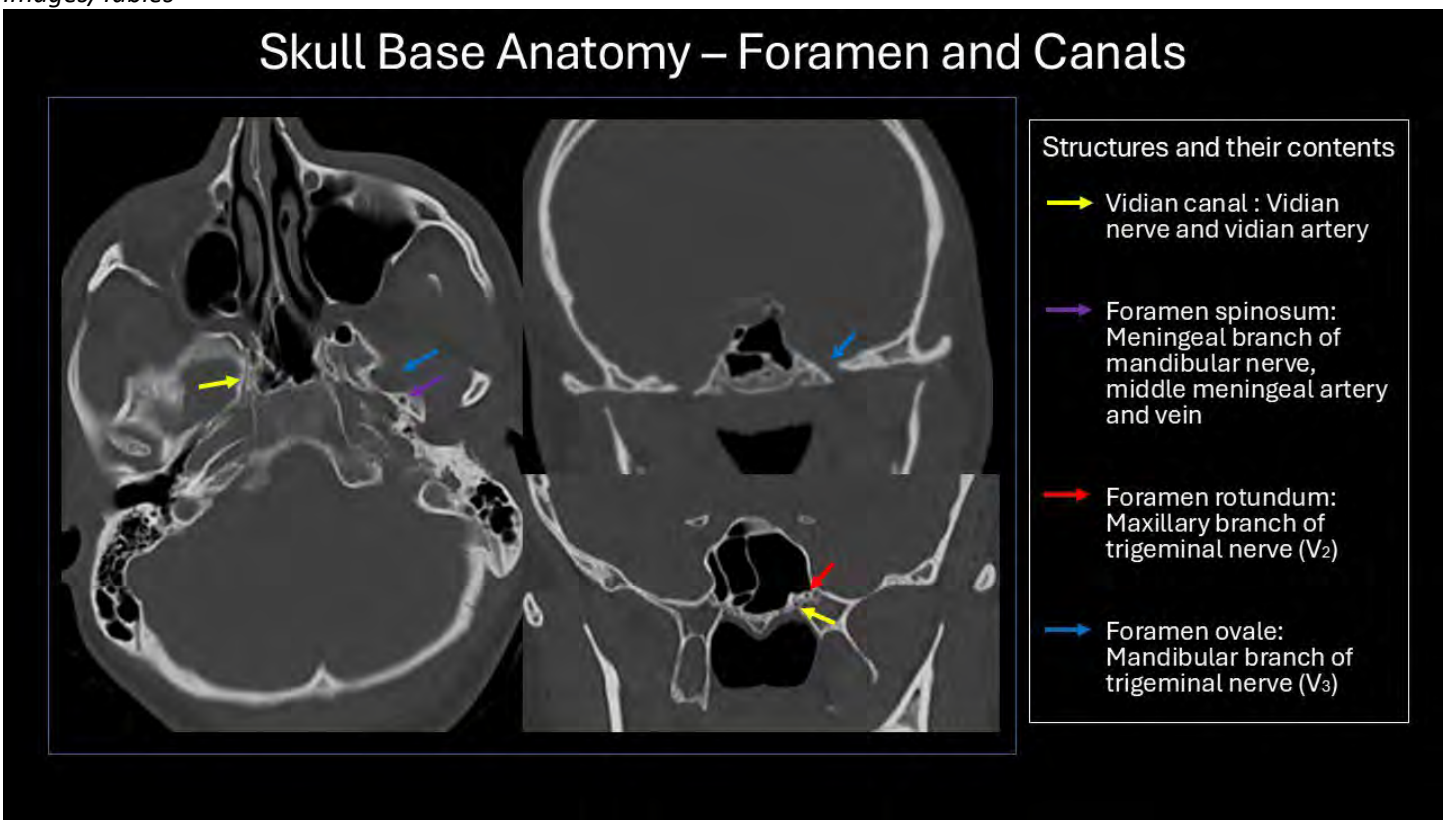
References

Razek A, King A. MRI and CT of Nasopharyngeal Carcinoma. AJR Am J Roentgenol *2021;198:*11–18.

Hsu C, Chang Y, Li H. Molecular diagnosis of nasopharyngeal carcinoma: past and future. *Biomed J 2024;*100748. https://doi.org/10.1016/j.bj.2024.100748

King A, Wong L, Law B, et al. MR Imaging Criteria for the Detection of Nasopharyngeal Carcinoma: Discrimination of Early-Stage Primary Tumors from Benign Hyperplasia. AJNR Am J Neuroradiol 2018;39:515-23.

Images/Tables



117

From a Tiny Calcification to a Cluster of Grapes – Imaging Spectrum of Neurocysticercosis

Ricardo Paez MD, Elaina Van Patten MD, James Vu MD, Ahmed Abdelhalim MD, David Sin MD, Min Tae Kim MD, Sarah Ceglar MD
Harbor UCLA, Torrance, CA, USA

Abstract Category

Adult Brain Inflammatory/Infectious Disease/Degenerative/Metabolic

Summary & Objectives

This educational exhibit is intended as an overarching review of the imaging manifestations of neurocysticercosis (NCC).
Learning objectives for education exhibit:
•Review life cycle of Taenia Solium
•Discuss clinical presentations of neurocysticercosis (NCC)
•Review imaging findings of 4 main stages of NCC
•Present rare extra-parenchymal manifestations
•Discuss treatment approaches by type of NCC
•Closing remarks

Purpose

Highlight key imaging findings to help radiologists differentiate between the stages of NCC and to identify rare complications in order to guide clinicians with treatment options.

Materials & Methods

Utilize unique cases from our home institution to demonstrate CT and MR imaging findings of:
1) Each stage of NCC, including the vesicular, colloidal vesicular, granular nodular, and granular calcified
2) Rare manifestations of NCC, including its racemose and spinal variants

Results & Conclusion

NCC is a common cause of seizure worldwide and is commonly encountered as an ordinary brain parenchymal calcification.
NCC however comes in various forms and it is important to identify the stage of NCC and its complications in order to determine between active and inactive disease which in turn guides clinical management.
Racemose and spinal NCC are rare and can result in additional complications that require keen attention on imaging.

References

Brutto D, H O. Human Neurocysticercosis: An Overview. Pathogens 2022;11:1212.
Prevention, (2021, January 7). CDC - Cysticercosis. https://www.cdc.gov/parasites/cysticercosis/index.html
Garcia HH, Nash T, Del Brutto O. Clinical symptoms, diagnosis, and treatment of neurocysticercosis. The Lancet Neurology 2014;13:1202–15.
Mahale, R. R., Mehta, A., & Rangasetty, S. (2015). Extraparenchymal (Racemose) Neurocysticercosis and Its Multitude Manifestations: A Comprehensive Review. Journal of Clinical Neurology, 11(3), 203.
Zhao, J.-L., Lerner, A., Shu, Z., Gao, X.-J., & Zee, C.-S. (2015). Imaging spectrum of neurocysticercosis. Radiology of Infectious Diseases, 1(2), 94–102.

Images/Tables

133

Missed Findings in Diagnostic Neuroradiology: Case Reports and Error Types Classification

Tatiana Mikhailova, Markus Lammle MD/PhD
SUNY Upstate Medical University, Syracuse, NY, USA

Abstract Category

New Techniques/Advanced Imaging/Informatics/AI/Professional Development/Misc

Summary & Objectives

The Renfrew Error Classification system serves as the leading framework for identifying diagnostic errors within the field of radiology. Through detailed case analyses, we highlight imaging findings and cognitive biases leading to diagnostic errors. Enhancing awareness of these biases is crucial for improving diagnostic accuracy and the overall skill set of radiologists.

Purpose

This educational exhibit delineates the diagnostic error classification system proposed by Renfrew. It features case reports that exemplify the types of diagnostic errors encountered in clinical practice. Each case is analyzed to highlight the differential diagnosis and clinical decision-making, underscoring the discrepancies that contributed to the initial diagnostic oversight.

Materials & Methods

We performed retrospective review of the clinical databases at our institution to search for cases in which crucial findings on MRI and CT images were initially missed by the attending radiologists. Discussed cases include diagnosis of spine fractures, arterial and venous obstructions on CT angiography, nerve lesions identification. We discuss the contribution of degraded imaging (motion or beam hardening artifacts, IV contrast timing, etc.), and other systemic factors such as early stage in training and high workload to diagnostic errors.

Results & Conclusion

Case review and error analysis are crucial for enhancing diagnostic accuracy. By integrating case studies with theoretical insights, this presentation aims to enhance diagnostic vigilance, and accuracy in radiological practice.

References

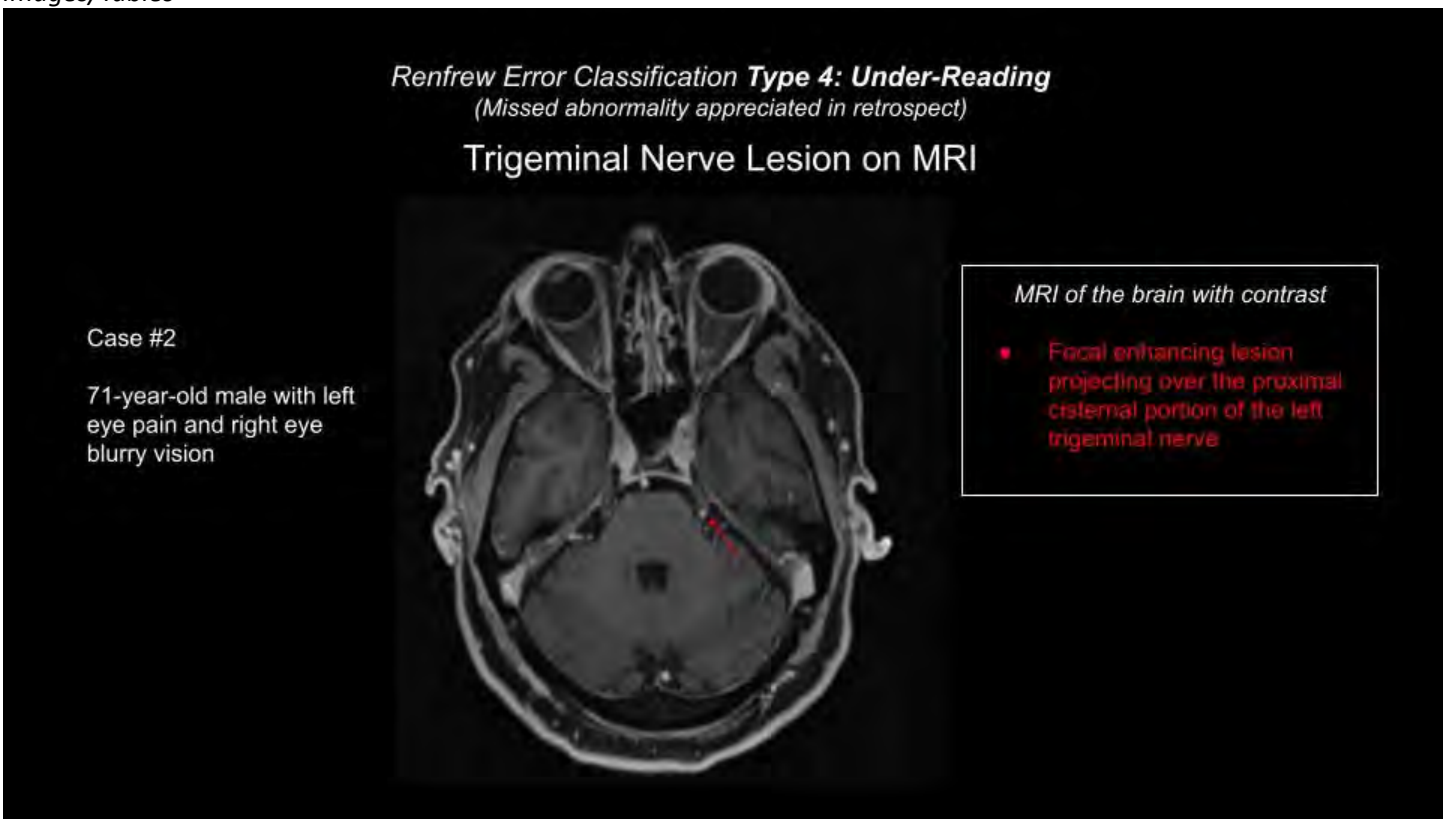
(1) Knipe H, Gaillard F, Murphy A, et al. Errors in diagnostic radiology. Reference article, *Radiopaedia.org* (Accessed on 29 Aug 2024). DOI: https://doi.org/10.53347/rID-31221

(2) Ivanovic V, Broadhead K, Beck R, et al. Factors Associated With Neuroradiology Diagnostic Errors at a Large Tertiary-Care Academic Medical Center: A Case-Control Study. Neuroradiology / Head and Neck Imaging 2023; 221. DOI: 10.2214/AJR.22.28925

(3) Huntley JH, Carone M, Yousem DM, et al. Opportunities for Targeted Education: Critical Neuroradiologic Findings Missed or Misinterpreted by Residents and Fellows. Special Articles 2015; 205. DOI: https://doi.org/10.2214/AJR.15.14905

(4) Biddle G, Assadsangabi R, Broadhead K, et al. Diagnostic Errors in Cerebrovascular Pathology: Retrospective Analysis of a Neuroradiology Database at a Large Tertiary Academic Medical Center. American Journal of Neuroradiology 2022; 43(9):1271-1278. DOI: 10.3174/ajnr.A7596

Images/Tables



137

PitNETs project: a visual guide approach.

Maria Tugores-Garcias MD[1], David Timaran-Montenegro MD[2], Elham Tavakkol MD[2], José Gavito-Higuera MD[2], Eliana Bonfante-Mejia MD[2], Rohan Samant MD[2], Roy Riascos-Castañeda MD[2]
[1]Son Espases University Hospital, Palma of Mallorca, Balearic Islands, Spain. [2]The University of Texas Health Science Center, Houston, Texas, USA

Abstract Category

Adult Neoplasms/Epilepsy/Trauma

Summary & Objectives

- To provide a comprehensive overview of imaging characteristics of pituitary neuroendocrine tumors (PitNETs), aiming to support a systematic approach in diagnosis and differentiation.
- To develop a visual guide that highlights key imaging features across PitNETs subtypes, enhancing diagnostic precision.

Purpose

PitNETs, previously known as pituitary adenomas, represent 10-15% of intracranial neoplasms, accounting for a significant portion of sellar and parasellar masses. Their classification has evolved, emphasizing histopathological, immunohistochemical, and molecular profiles, which now play a crucial role in diagnosis, management, and prognosis. This educational exhibit aims to synthesize the current scientific literature on PitNETs and provide a comprehensive, evidence-based visual guide for predicting PitNETs subtypes using imaging techniques. By correlating imaging findings with specific tumor subtypes, we aim to equip radiologists with practical tools to enhance diagnostic accuracy, anticipate tumor behavior, and support personalized treatment planning.

Materials & Methods

A literature review was conducted to collect and analyze imaging characteristics specific to PitNETs subtypes. Key sources included recent WHO classifications, studies on immunohistochemical markers, and published findings on advanced imaging techniques. Representative cases were selected to illustrate typical imaging patterns for each tumor subtype.

The proposed visual guide successfully consolidates distinctive imaging characteristics of PitNETs, including location, size, signal intensity, contrast enhancement patterns, and invasion tendencies. Imaging data were compiled into a visual guide with annotations to highlight distinctive features relevant to subtype identification.

The exhibit is organized to guide radiologists from general imaging features to specific diagnostic clues, using images, tables, and flowcharts.

Results & Conclusion

PitNETs represent a complex and evolving category of intracranial tumors, with distinct subtypes that exhibit varied clinical behaviors and treatment responses. Accurate clinical and neuroradiological diagnosis are crucial for identifying these subtypes, as imaging characteristics can provide valuable insights into tumor type, aggressiveness, and potential invasiveness.

This exhibit underscores the importance of a structured, evidence-based approach to PitNETs imaging. By equipping neuroradiologists with practical tools for subtype prediction, this guide aims to enhance diagnostic precision, facilitate targeted therapeutic strategies, and improve prognostic assessments, ultimately contributing to more personalized and effective care for these patients.

References

1. Asa SL, Mete O, Perry A, Osamura RY. Overview of the 2022 WHO classification of pituitary tumors. *Endocr Pathol*. 2022;33(1):6–26. DOI: 10.1007/s12022-022-09703-7
2. Tsukamoto T, Miki Y. Correction to: Imaging of pituitary tumors: an update with the 5th WHO Classifications-part 1. Pituitary neuroendocrine tumor (PitNET)/pituitary adenoma. *Jpn J Radiol*. 2023;41(8):807. DOI: 10.1007/s11604-023-01414-1
3. Bonneville J-F, Bonneville F, Cattin F, Nagi S. *MRI of the pituitary gland*. Cham, Suiza: Springer International Publishing; 2018.
4. Burlacu MC, Maiter D, Duprez T, Delgrange E. T2-weighted magnetic resonance imaging characterization of prolactinomas and association with their response to dopamine agonists. *Endocrine*. 2019;63(2):323–31. DOI: 10.1007/s12020-018-1765-3
5. Araujo-Castro M, Acitores Cancela A, Vior C, Pascual-Corrales E, Rodríguez Berrocal V. Radiological Knosp, revised-Knosp, and Hardy–Wilson classifications for the prediction of surgical outcomes in the endoscopic

endonasal surgery of pituitary adenomas: Study of 228 cases. *Front Oncol*. 2022;11. DOI: 10.3389/fonc.2021.807040

138

Lemierre Syndrome: A Link Between Anaerobic Oropharyngeal Infections and Septic Thrombophlebitis of the Internal Jugular Vein

Víctor L Guzmán Rivera MD, Claudia M Muns Aponte MD, Eduardo J Labat Álvarez MD, José A Lara Del Río MD
University of Puerto Rico School of Medicine, Diagnostic Radiology Residency Program, San Juan, Puerto Rico, USA

Abstract Category

Head and Neck

Summary & Objectives

Learning Objectives:

- Define Lemierre syndrome
- Discuss the most common organisms associated with Lemierre syndrome
- Describe the most common oropharyngeal infections seen in Lemierre syndrome
- Discuss unusual presentations of Lemierre syndrome
- Describe radiological findings seen in Lemiere syndrome
- Present cases of Lemiere syndrome
- Establish the importance of radiology in the assessment of Lemierre syndrome

Purpose

The main purpose of the exhibit is to provide an overview of the etiology, radiological findings, and clinical manifestations of Lemierre syndrome, in order to increase general interest and knowledge of this entity.

Materials & Methods

Lemierre syndrome, also known as necrobacillosis, is an uncommon, life-threatening infectious-thrombogenic disease which results in septic thrombophlebitis of the internal jugular vein, secondary to metastatic bacteremia from an underlying oropharyngeal infection, primarily from anaerobic organisms (1). The most common organisms associated with Lemierre syndrome are Fusobacterium necrophorum and Fusobacterium nucleatum, which are obligate anaerobic gram negative bacilli (2). Lemierre syndrome usually occurs in the clinical setting of acute bacterial pharyngitis or acute bacterial tonsillitis(2). Nevertheless, uncommon presentations of Lemierre syndrome have also been reported in patients with acute bacterial parotitis (3); which is one of the cases that will be presented in the educational exhibit. Clinical symptoms seen in Lemierre syndrome include fever, rigor, neck tenderness, neck swelling, and in severe cases due to septic emboli it can progress to lethargy, shock, and end-organ damage (2).

The diagnosis of Lemierre syndrome involves evaluation of clinical symptoms in combination with a multi-imaging modality assessment, which can include chest radiograph, ultrasound, computed tomography (CT), and magnetic resonance (MR) imaging (2). Typically, chest radiographs are introduced as a means of identifying pulmonary infiltrates and septic pulmonary emboli (4). Ultrasound allows for initial assessment of thrombosis of the internal jugular vein in patients with suspected Lemierre syndrome (4). Contrast enhanced CT (CECT) scan of the neck and chest is considered to be the most suitable imaging modality for diagnosing Lemierre syndrome, as it allows for the detection of septic thrombophlebitis of the internal jugular vein, including intraluminal filling defects and thickening and enhancement of the venous wall (4). Evaluation of abscesses, septic pulmonary emboli, and other complications that can be seen in patients with Lemierre syndrome may also be accomplished through CECT of the neck and chest (4). Although MR imaging provides illustrations of thrombus and emboli, it has a tendency to be less accessible due to its costly nature (4). Treatment for Lemierre syndrome typically consists of antibiotic therapy directed towards achieving penetration of fibrin clots (2). In some instances, radiologic or surgical interventions are necessary to treat abscesses and thrombotic complications (2). When thrombus extends into the dural venous sinuses, anticoagulation therapy may be pursued, although this is not fully supported by evidence (2).

Results & Conclusion

As an educational exhibit, multiple cases of Lemierre syndrome will be presented, portraying the most common radiological manifestations of this condition with the intention of providing general knowledge to the radiology community. In this exhibit common and uncommon manifestations of Lemierre syndrome will be presented.

References

1. Lee WS, Jean SS, Chen FL, Hsieh SM, Hsueh PR. Lemierre's syndrome: A forgotten and re-emerging infection. J Microbiol Immunol Infect. 2020 Aug;53(4):513-517. doi: 10.1016/j.jmii.2020.03.027. Epub 2020 Apr 4. PMID: 32303484.
2. Allen BW, Anjum F, Bentley TP. Lemierre Syndrome. 2023 Jul 31. In: StatPearls [Internet]. Treasure Island (FL): StatPearls Publishing; 2024 Jan–. PMID: 29763021.
3. Alabraba E, Manu N, Fairclough G, Sutton R. Acute parotitis due to MRSA causing Lemierre's syndrome. Oxf Med Case Reports. 2018 May 31;2018(5):omx056. doi: 10.1093/omcr/omx056. PMID: 29942528; PMCID: PMC6007696.
4. Harper LK, Pflug K, Raggio B, April D, Milburn JM. Clinical Images: Lemierre Syndrome: The Forgotten Disease? Ochsner J. 2016 Spring;16(1):7-9. PMID: 27026785; PMCID: PMC4795

Images/Tables

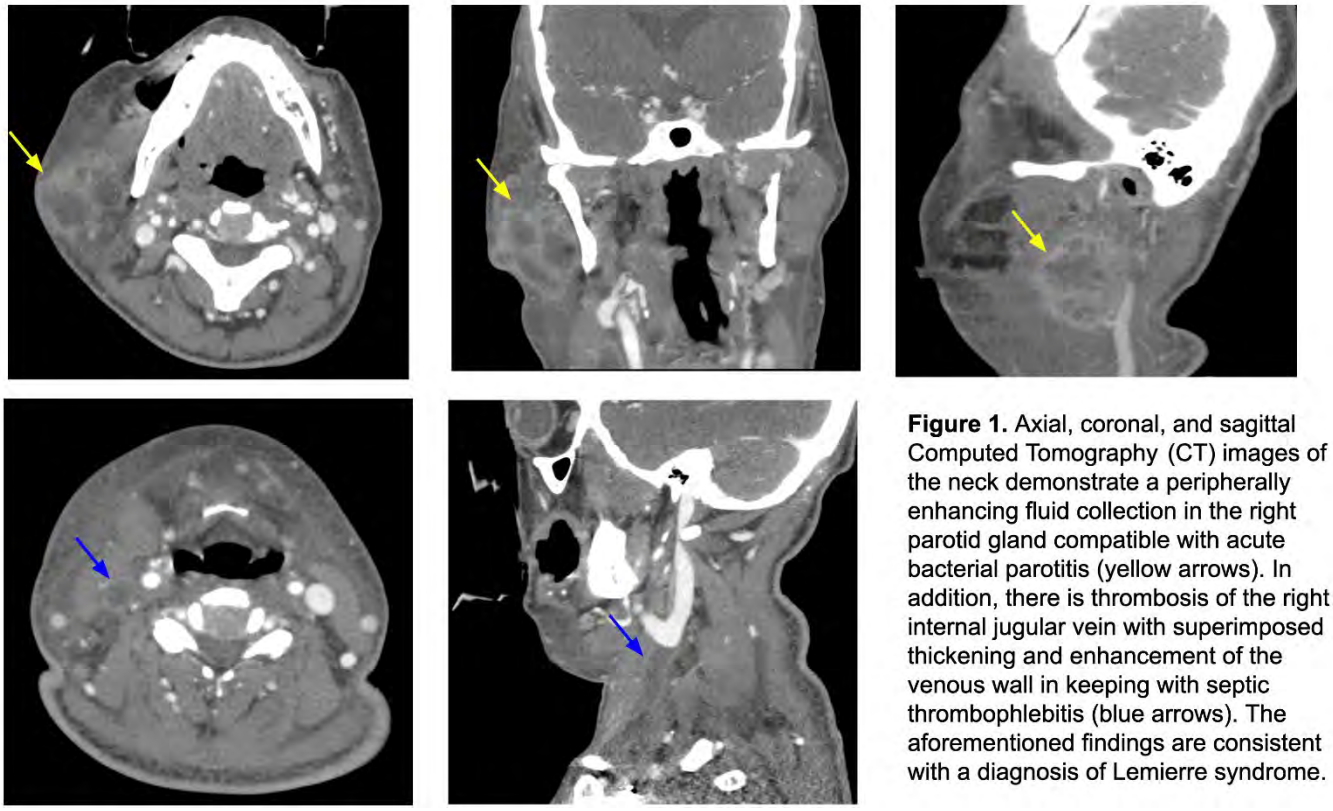


Figure 1. Axial, coronal, and sagittal Computed Tomography (CT) images of the neck demonstrate a peripherally enhancing fluid collection in the right parotid gland compatible with acute bacterial parotitis (yellow arrows). In addition, there is thrombosis of the right internal jugular vein with superimposed thickening and enhancement of the venous wall in keeping with septic thrombophlebitis (blue arrows). The aforementioned findings are consistent with a diagnosis of Lemierre syndrome.

152

Introduction to Perfusion MRI in Neuro-Oncology Applications: A Pictorial Review with Pathologic Correlation

Omar A Viqar MD[1], Julio Arevalo Perez MD[2], Karem Gharzeddine MD[2], John Kim MD[3], Gaurav Saigal MD[1], Ahmet T Ilica MD[1]

[1]University of Miami, Miami, Fl, USA. [2]Memorial Sloan Kettering Cancer Center, New York, NY, USA. [3]University of Michigan, Ann Arbor, MI, USA

Abstract Category

Adult Neoplasms/Epilepsy/Trauma

Summary & Objectives

Perfusion MRI is an advanced imaging technique that can be used for various neurological conditions including, stroke, neurodegenerative diseases, and assessment of brain tumors. This educational module provides an introduction to perfusion MRI with a particular focus on its application in evaluating brain tumors. The module will also explore the utility of perfusion MRI in clinical decision-making, particularly in differentiating tumor progression from pseudo-progression, as well as imaging findings that represent radiation necrosis in the post-treatment setting. Key imaging findings and concepts will be discussed that will aid in the proper reporting of the tumor evaluation. Additionally, special

attention will be given to addressing potential pitfalls in perfusion imaging to help the learner understand how to mitigate these challenges in their daily practice.The goal is, by the end of module for participants to gain a solid foundation in perfusion MRI techniques, their interpretation, as well as their clinical relevance in the management of brain tumors.

Purpose

The purpose of this educational module is to enhance trainees knowledge about the practical application in tumor assessment and its impact on patient management. The content that will be reviewed will highlight the fundamental techniques of perfusion imaging including dynamic susceptibility contrast (DSC), dynamic contrast enhanced (DCE), and arterial spin labeling (ASL). Our aim is to provide an overview of the common MR perfusion techniques, **the pros and cons of each technique as well as** demonstrate the utility and clinical applications of different MR perfusion findings in Neuro-oncology.

Materials & Methods

This exhibit is meant to be a pictorial review with examples of each key point with relevant imaging findings will be included with practical insights into the application of perfusion MRI in neuro-oncology.

Results & Conclusion

By completing this module, trainees will gain practical skills in interpreting perfusion MRI findings, recognize imaging patterns, and mitigate common pitfalls in neurooncologic imaging. The ultimate goal is for participants to develop a strong foundation for understanding perfusion MRI, and enable them to apply these techniques in their clinical practice.

References

1. Gharzeddine K, Hatzoglou V, Holodny AI, Young RJ. MR Perfusion and MR Spectroscopy of Brain Neoplasms. Radiol Clin North Am. 2019 Nov;57(6):1177-1188. doi: 10.1016/j.rcl.2019.07.008. PMID: 31582043.
2. Cha S. Perfusion MR imaging of brain tumors. Top Magn Reson Imaging. 2004 Oct;15(5):279-89. doi: 10.1097/00002142-200410000-00002. PMID: 15627003.

156

Imaging of Tongue Pathologies Other than Squamous Cell Carcinoma

Lutof Zreik M.D., Mika Shapira Rootman M.D.; PhD, Galia Ronen M.D., Goni Merhav M.D., Ayelet Eran M.D.

Rambam Health Care Campus, Haifa, Haifa, Israel

Abstract Category

Head and Neck

Summary & Objectives

Pathological findings in the tongue are diverse and can be categorized as congenital, vascular, infectious, neoplastic, and non-neoplastic masses. While the majority of lingual masses encountered in adults are squamous cell carcinomas (SCC)[1], making this the most common indication for imaging, other tongue pathologies are rare and are less frequently reviewed in scientific literature. However, it is crucial for radiologists to be familiar with these less common entities and to accurately recognize and characterize them on imaging.

Purpose

To present a series of cases involving tongue pathologies other than SCC to familiarize radiologists with their distinct imaging findings and characteristics.

Materials & Methods

Cases were collected retrospectively from the electronic medical records of Rambam Health Care Campus.

Results & Conclusion

6 cases of lingual pathologies are described herein and include –

- Figure 1: Anterior tongue microglossia - a 12-month-old baby presented with breathing and swallowing difficulties that had been present since birth, with a suspected diagnosis of Pierre Robin sequence. A sagittal T1-weighted MRI image shows microglossia (arrow). Additionally, micro-retrognathia with glossoptosis is noted. There is no evidence of cleft palate.
- Figure 2: Tongue ischemia - a 65-year-old woman was hospitalized with septic shock, requiring vasopressor therapy and an urgent laparotomy for ischemic colitis. Two weeks after surgery, she developed right-sided tongue swelling. Coronal and axial CT images revealed swelling and hypodensity of the right side of the tongue, consistent with ischemia secondary to shock and prolonged oral intubation. The lesion resolved, leaving residual scarring.

- Figure 3: Lingual thyroid – a 48-year-old woman underwent contrast-enhanced neck CT for the evaluation of a parapharyngeal lesion. Axial and sagittal images show a round, midline hyperdense lesion at the tongue base, consistent with a lingual thyroid (A, C). Note no visualization of entopic thyroid gland in the lower neck (B).
- Figure 4: Tongue hemangioma + DVA – a 31-year-old man with a known lingual vascular lesion. Axial T2- and T1-weighted images (A, B) demonstrate a dorsal tongue lesion that is hyperintense on T2, with enhancement and no mass effect (thick arrow), compatible with a hemangioma. Additionally, on a sagittal image (C), a small cerebellar DVA (developmental venous anomaly, thin arrow) is noted, which is associated with facial venous malformations [2].
- Figure 5: Tongue-base adenoid cystic carcinoma – a 78-year-old woman with a 4-year history of difficulty swallowing and neck pain, who developed tongue paresis. Direct inspection by an ENT revealed a bulge at the tongue base without ulceration. A sagittal reformatted contrast-enhanced neck CT (A) shows an enhancing tongue-base mass with heterogeneous enhancement. PET imaging demonstrates avid FDG uptake (B).
- Figure 6: Lingual leiomyoma – a 25-year-old woman presented with painless swelling on the right side of the dorsal tongue. Direct inspection and examination revealed a non-tender mass without ulceration. MRI shows a rounded, well-circumscribed lesion on the right side of the tongue, slightly crossing the midline, with mild T2 hyperintensity (A) and homogeneous enhancement (B). Note a prominent vessel on the upper border of the lesion (arrow). Biopsy revealed leiomyoma, which was completely excised.

References

1. Sigal R, Zagdanski AM, Schwaab G, et al. CT and MR imaging of squamous cell carcinoma of the tongue and floor of the mouth. *RadioGraphics* 1996;16:787–810. DOI: https://doi.org/10.1148/radiographics.16.4.8835972

2. Brinjikji W, Hilditch CA, Tsang AC, et al. Facial Venous Malformations Are Associated with Cerebral Developmental Venous Anomalies. *American Journal of Neuroradiology* 2018;39:2103–7. DOI: https://doi.org/10.3174/ajnr.A5811

Images/Tables

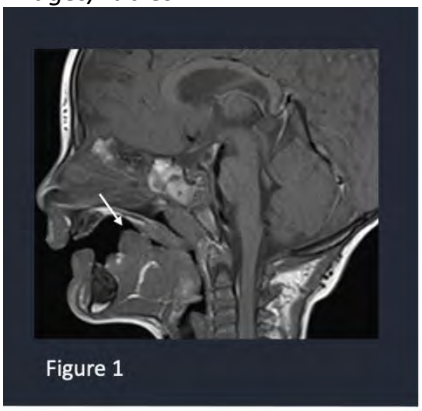


Figure 1

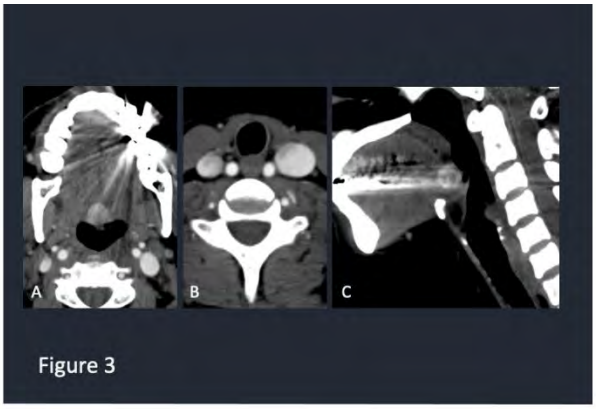


Figure 3

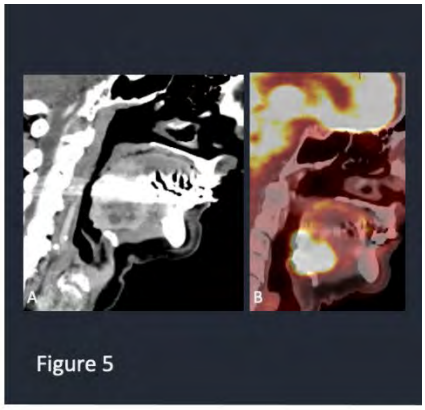


Figure 5

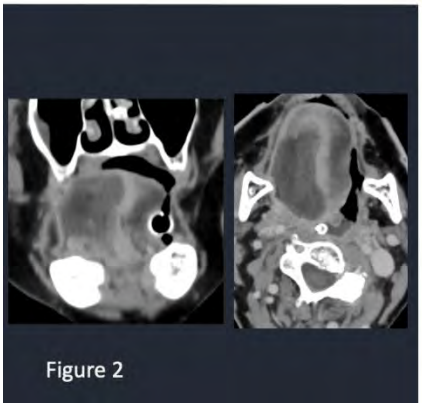


Figure 2

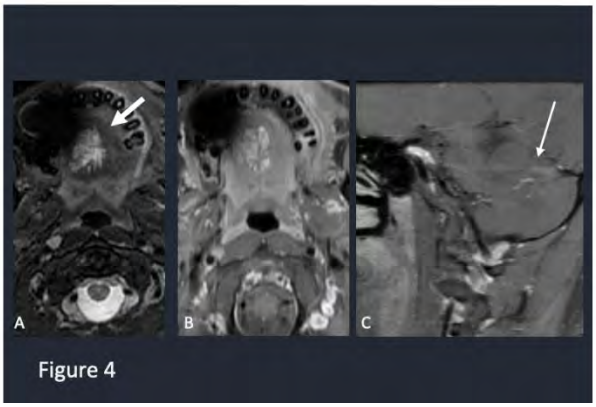


Figure 4

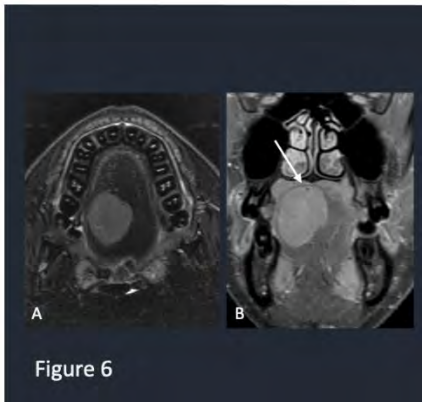


Figure 6

167

Bone Voyage: A Primer on Temporal Bone Imaging for Residents and Fellows

Brian Nguyen MD, Hunter Carlock MD, Steven Wheeler MD, Anthony Portanova MD
University of Rochester, Rochester, NY, USA

Abstract Category

Head and Neck

Summary & Objectives

To familiarize participants with the normal anatomy and important pathology of the temporal bone as seen on CT and MR imaging.

Purpose

The purpose of this talk is to equip radiology residents/fellows with essential knowledge and practical skills for interpreting temporal bone CT/MR. By understanding the complexities of this anatomical region, trainees will improve their diagnostic accuracy and confidence in clinical practice.

Materials & Methods

-Cover CT and MR imaging protocols specific to the temporal bone, including indications for each modality.
-Detailed overview of the anatomy of the temporal bone, partitioned into inner, middle, and outer ear structures. The goal is to allow for trainees to adopt a robust anatomy-based search pattern.
-Presentation of select cases illustrating common pathologies such as cholesteatoma, otosclerosis, temporal bone fractures etc. Key imaging findings associated with each pathology will be emphasized, particularly the important anatomical landmarks for each diagnosis.
-In addition to examples from multiplanar CT and MR, multimedia graphics/illustrations will be included to help better delineate the relatively complex 3-dimensional anatomy of the temporal bone
-Self-quizzing elements will be included throughout the presentation in order to deepen readers' knowledge of temporal bone anatomy, pathology, and imaging-based differential diagnosis.

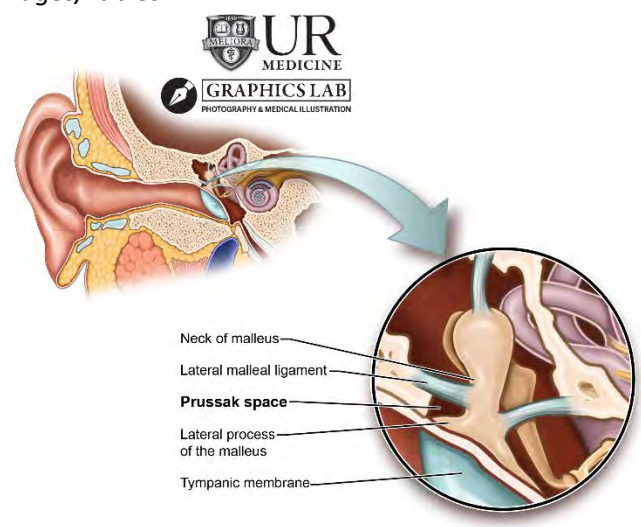
Results & Conclusion

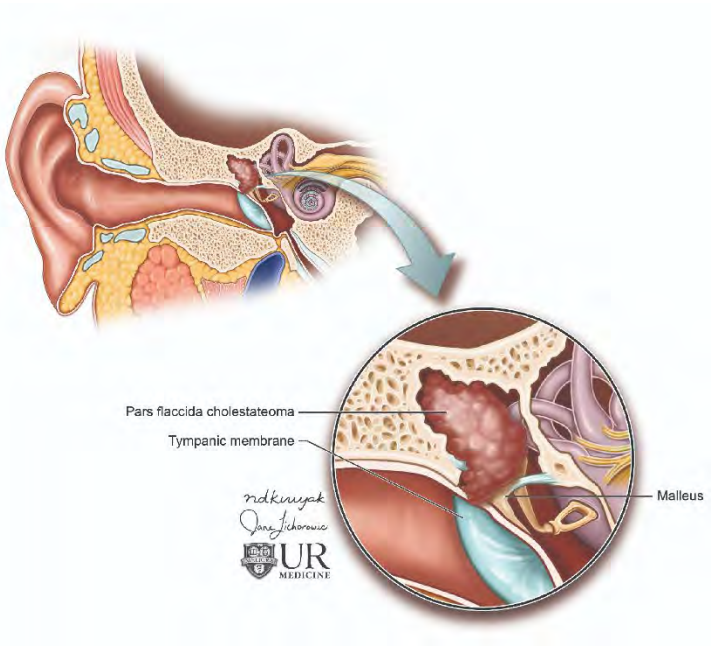
This project should provide educational benefit to trainees of all levels. Understanding fundamental concepts such as when to recommend dedicated temporal bone imaging or when to favor CT versus MR are crucial for junior residents who are still learning how to communicate with clinical teams. Meanwhile, senior residents and fellows will take interest in a detailed review of temporal bone anatomy and pathology they can expect to encounter both at the workstation and on board exams. While temporal bone imaging may initially seem daunting, it becomes much more manageable and rewarding after being equipped with the right tools to approach both simple and complex cases. Our project will hopefully add to that toolkit and encourage more learners to embark on their own temporal bone voyage.

References

Juliano, Amy F., Daniel T. Ginat, and Gul Moonis. "Imaging review of the temporal bone: part I. Anatomy and inflammatory and neoplastic processes." Radiology 269.1 (2013): 17-33.
Juliano, Amy F., Daniel T. Ginat, and Gul Moonis. "Imaging review of the temporal bone: part II. Traumatic, postoperative, and noninflammatory nonneoplastic conditions." Radiology 276.3 (2015): 655-672.
Kurihara, Yoshiko Y., et al. "Temporal bone trauma: Typical CT and MRI appearances and important points for evaluation." Radiographics 40.4 (2020): 1148-1162.
Phillips, Grace S., et al. "Interactive web-based learning module on CT of the temporal bone: anatomy and pathology." Radiographics 32.3 (2012): E85-E105.

Images/Tables





168

Shedding light on CHANTER syndrome

Mark J Greenhill DO, Nishtha Raval MD, Dan Cohen-Addad MD, Aline Camargo MD
Emory, Atlanta, GA, USA

Abstract Category

Adult Brain Inflammatory/Infectious Disease/Degenerative/Metabolic

Summary & Objectives

Patients presenting to the ED in an altered state will invariably receive neuroimaging studies. In the setting of an unconscious patient with limited provided clinical information, the neuroradiologist must consider ischemic, toxic, metabolic, hypoxic, and anoxic etiologies. This can result in a clouded clinical picture and nebulous radiology report. While vessel occlusion (VO) can be relatively straightforward to diagnose, the absence of VO on neuroimaging might provide minimal reassurance to the clinical team, particularly if the patient is clinically obtunded. Cerebellar, hippocampal, and basal nuclei transient edema with restricted diffusion (CHANTER) syndrome is a newly recognized disease process that is often associated with opioid abuse.[1,2] Significant clinicoradiologic overlap exists between this entity and the previously mentioned diagnoses. However, distinct and consistent imaging findings are usually present in CHANTER and are crucial to aid in diagnosis. Moreover, distinguishing CHANTER can have profound prognostic implications, as CHANTER has been associated with severe but potentially reversible deficits if treated early.[1] The objective of this educational exhibit is to improve awareness of CHANTER syndrome by familiarizing the radiologists and radiology trainees with the clinical and imaging manifestations of this entity, facilitating prompt diagnosis which has profound clinical implications.

Purpose

- Review the characteristic imaging findings of CHANTER on CT and MRI.
- Compare and contrast the imaging findings of CHANTER to other diagnostic considerations including ischemic stroke, anoxic injury, postictal changes, and other toxic etiologies.
- Discuss the clinical and laboratory findings associated with CHANTER.
- Discuss the course of disease and prognosis of CHANTER.

Materials & Methods

Retrospective chart review at a large university medical center and a large county hospital
Exclusion: <18 years of age,
Inclusion criteria: clinical history of substance abuse, restricted diffusion in the cerebellum and hippocampus not explained by other etiology such as stroke, acute toxic leukoencephalopathy, seizure, ischemia/hypoxia.
Searched via institutional EMR over a 5 year period from 1/1/2019-1/1/2024

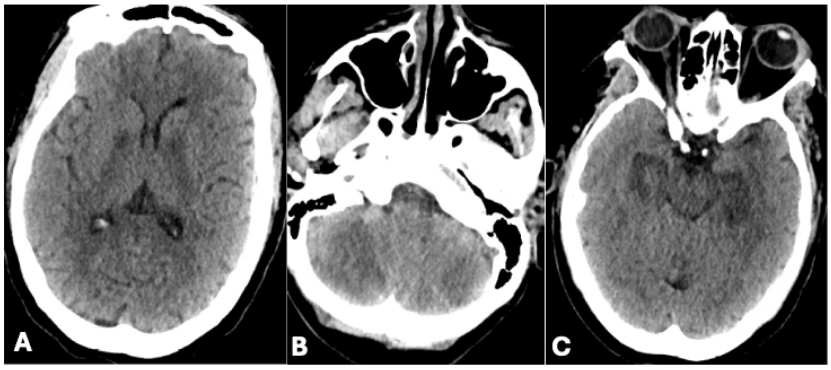
Results & Conclusion

CHANTER syndrome is a recently identified pathologic process with significant overlap to a myriad of closely related encephalopathies but does have distinct clinical and radiologic findings. It can be distinguished from ischemic stroke, hypoxic insult, postictal changes, and toxic injury based on location and distribution on cross-sectional imaging. Additionally, it can be suggested with the appropriate clinical presentation and laboratory markers. Together, these clinical and radiologic clues can guide the neuroradiologist towards shedding light on this unique diagnosis, resulting in significant positive prognostic ramifications if diagnosed early.

References

1. Mallikarjun KS, Parsons MS, Nigogosyan Z, Goyal MS, Eldaya RW. Neuroimaging Findings in CHANTER Syndrome: A Case Series. *AJNR Am J Neuroradiol*. 2022;43(8):1136-1141.
2. Jasne AS, Alsherbini KH, Smith MS, Pandhi A, Vagal A, Kanter D. Cerebellar Hippocampal and Basal Nuclei Transient Edema with Restricted diffusion (CHANTER) Syndrome. *Neurocrit Care*. 2019;31(2):288-296.

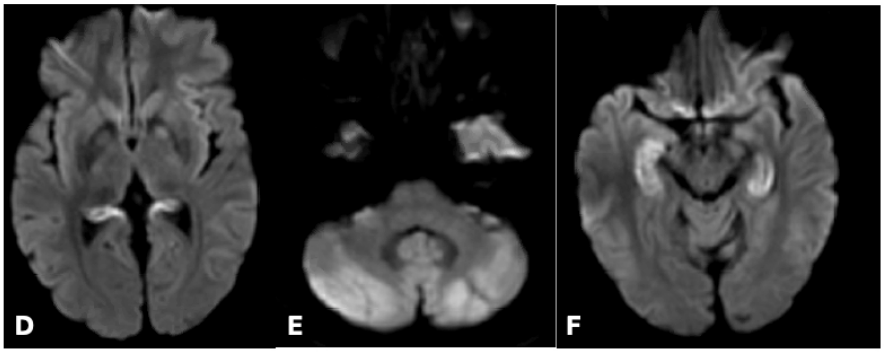
Images/Tables



45-year-old male presenting to the emergency department after being found down for an unknown length of time. Urine tox screen was positive for fentanyl.

Initial NCCT head was negative for large intracranial hemorrhage or territorial ischemia. Patchy regions of hypoattenuation were seen in the basal ganglia, cerebellum, and hippocampi bilaterally (A-C). Subsequent MRI demonstrated corresponding areas of restricted diffusion within these same areas (D-F).

The clinical and imaging findings were compatible with CHANTER syndrome.



173

Spectrum of skull base osteomyelitis- A Low middle income country perspective

fatima mubarak FCPS

Aga Khan university hospital, karachi, sind, Pakistan

Abstract Category

Adult Brain Inflammatory/Infectious Disease/Degenerative/Metabolic

Summary & Objectives

Skull base osteomyelitis is a dready clinical entity with diverse imaging manifestaions. We aim to present spectrum of CNS manifestations of Skull base osteomyelitis.

Purpose

To present spectrum of central nervous system manifestations of skull base osteomyelitis from a perspective of low middle incoming country with variable environmental and immuune status of patients

Materials & Methods

Imaging spectrum of skull base osteomyelitis spanning over 14 years was reviewed. After approval from the institutional ethics review board, data including demographic details, clinical characteristics, comorbidities, laboratory and

radiological investigations, treatment, complications and outcomes was retrieved from hospital records using a structured proforma.

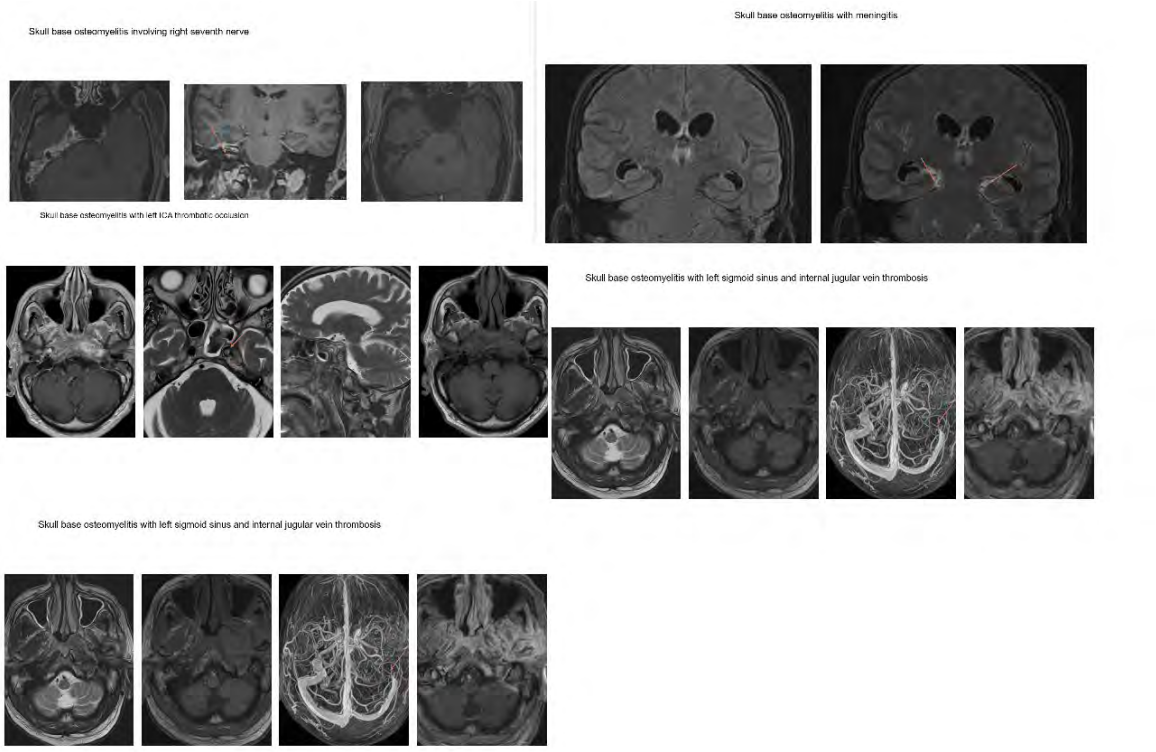
Results & Conclusion

The majority of the patients had cranial nerve and the most commonly affected was the 7th CN. Other manifestations were meningitis, ischemic stroke,
and cerebral venous sinuses thrombosis (CVST).

References

1.Khanum, I., Kanwar, D., Habib, K., & Mubarak, F. (2024). Skull base osteomyelitis (SBO): a dreaded clinical entity. *Journal of the Pakistan Medical Association*, *74*(10), 1767–1772. https://doi.org/10.47391/JPMA.9604
2.Seddon K, Low C. Osteomyelitis following an undisplaced basal skull fracture. N Z Med J. 2020; 133:73-3. Ulivi L, Squitieri M, Cohen H, Cowley P, Werring DJ. Cerebral venous thrombosis: a practical guide. Pract Neurol. 2020; 20:356-67. doi: 10.1136/practneurol-2019-002415.
4. Kaufmann MR, Camilon PR, Levi JR, Devaiah AK. Predicting Anticoagulation Need for Otogenic Intracranial Sinus Thrombosis: A Machine Learning Approach. J Neurol Surg B Skull Base. 2021; 82:233-43. doi: 10.1055/s-0040-1713105.
5. Furqana A, Jhanzeb I, Musa A, Aun R, Faisal S. Skull Base Osteomyelitis: A Single-Center Experience. Cureus. 2021; 13: e20162. doi: 10.7759/cureus.20162.

Images/Tables



174

Mycotic Aneurysms: Not Just a Fungal Affair

Gais Tarat MD, Megha Sanghvi MD, Erini Makariou MD, Earn Chun Christabel Lee MD
Medstar Georgetown University Hospital, Washington, DC, USA

Abstract Category

Adult Brain Inflammatory/Infectious Disease/Degenerative/Metabolic

Summary & Objectives

Infectious aneurysms, commonly referred to as mycotic aneurysms, are defined as breaks in the arterial wall secondary to infection, resulting in focal outpouching (1,2). The term “mycotic” was initially coined to describe fungal aneurysms, dating back to 1885 (3). Since then, many reported cases involved non-fungal microbes. Bacterial causes have since been accepted as the most common causes. Cerebral arteries are the third most commonly involved vessels, with aortic and

peripheral arteries being the most and second most common, respectively (2). Through six cases, this exhibit aims to showcase the clinical presentations and the radiological features of various etiologies of head and neck infectious aneurysms.

Purpose

The purpose of this exhibit is to showcase the radiologic appearance of cranial and extra-cranial infected aneurysms caused by a variety of different microbes including fungal, bacterial and viral agents. We aim to highlight the various underlying clinical risk factors, and present their course, imaging findings, and clinical outcome.

Materials & Methods

A retrospective analysis was performed using the PACS search engine with reports showing 'aneurysm' and 'infection' between February 2022-June 2024. We identified six representative cases of infectious aneurysms, including four bacterial, one viral, and one fungal aneurysm.

Each of these cases highlights a different clinical risk factor, including type 2 diabetes mellitus associated with a fungal aneurysm; bacterial aneurysms related to intravenous drug use, implantable devices, and sepsis in the setting of end-stage renal disease with dialysis; and a viral infectious aneurysm related to post-transplant status."

We present the clinical presentation, clinical course and the imaging findings of each of these cases.

Results & Conclusion

Infectious aneurysms are serious and potentially fatal conditions. Attention to a patient's clinical history and clinical course can heighten awareness to look for these often unsuspected aneurysms. We present a spectrum of various clinical case scenarios to highlight the importance of early detection and recognition of these conditions.

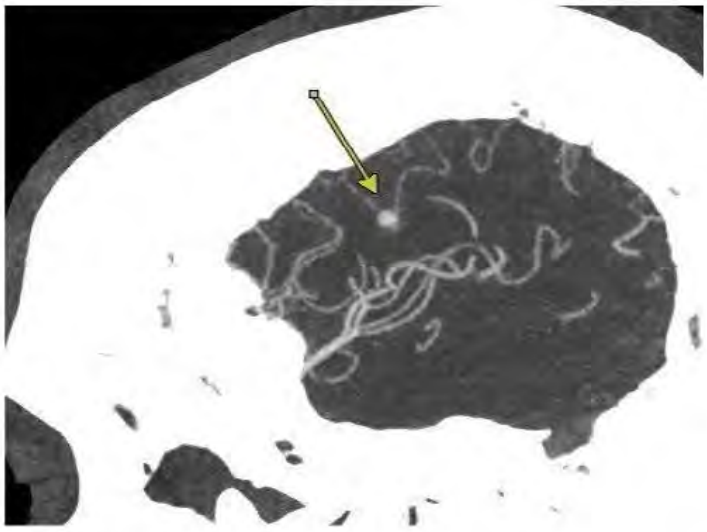
References

1. Kaufman SL, White RI Jr, Harrington DP, Barth KH, Siegelman SS. Protean manifestations of mycotic aneurysms. AJR Am J Roentgenol. 1978;131(6):1019–25. DOI: https://doi.org/10.2214/ajr.131.6.1019.

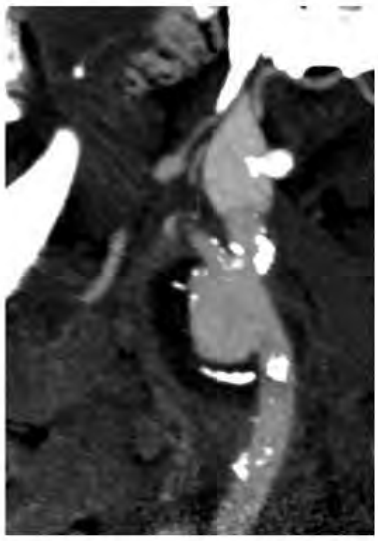
2. Lee WK, Mossop PJ, Little AF, Fitt GJ, Vrazas JI, Hoang JK, Hennessy OF. Infected (Mycotic) Aneurysms: Spectrum of Imaging Appearances and Management. Radiographics. 2007;27(5):1329-42. DOI: https://doi.org/10.1148/rg.287085054

3. Osler W. The Gulstonian Lectures, on Malignant Endocarditis. Br Med J. 1885;1(1263):522–6. DOI: https://doi.org/10.1136/bmj.1.1262.467

Images/Tables



Small mycotic aneurysm in distal M3 from enterococcal endocarditis



Left carotid pseudoaneurysm. Patient has MRSA septicemia related to pacemaker lead vegetation.

180

Central Variant of Posterior Reversible Encephalopathy Syndrome. Review from clinical cases.

Nicolás . Sánchez MD, Eduardo . Siña MD
Clinica Alemana, Santiago, RM, Chile

Abstract Category

Interventional/Vascular/Stroke

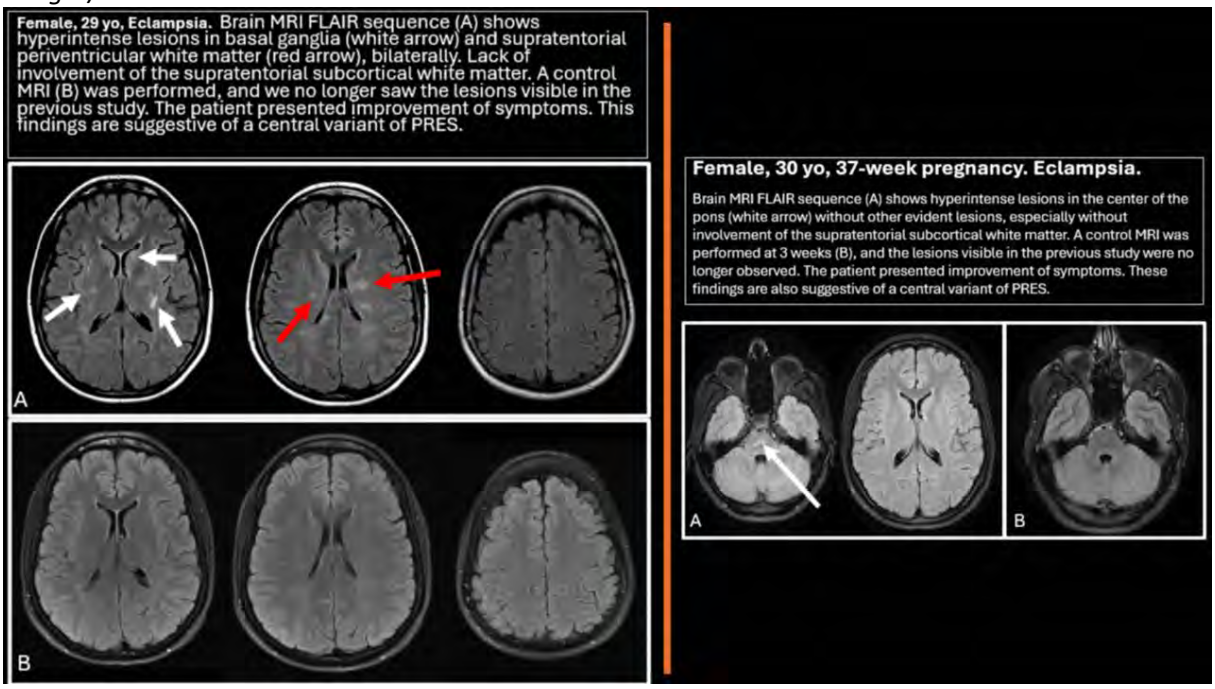
Summary & Objectives

Posterior reversible encephalopathy syndrome (PRES) is a clinic-radiological diagnosis that is based on a combination of typical clinical features and risk factors and supported by magnetic resonance (MR) brain scan findings, which usually resolve if promptly recognized and properly
treated.
Neuroradiologists are used to observe this syndrome and suspect it when clinical conditions and images are suggestive. This entity presents bilaterally in images and usually follows three classic and well known patterns of presentation, which are the parieto-occipital pattern, the superior frontal sulcus pattern and the holohemispheric pattern, which are characterized by involving borderline territories of the cerebral arterial circulation. Other sites that are often involved are the brainstem and cerebellum, but not in isolation, but accompanying the classic patterns.
An infrequent and little known form of presentation of PRES is the central variant, which consists of involvement of the basal ganglia, brainstem and/or periventricular white matter, without involvement of subcortical white matter. This variant corresponds to 4% of PRES.
In this poster we will present three cases of patients with central variant of PRES, we will review their images, the clinical presentation and the pathophysiology of this presentation with the aim of making known this unusual presentation of PRES and that neuroradiologists know when to suspect it.

References

1. Bartynski WS. Posterior reversible encephalopathy syndrome, part 1: fundamental imaging and clinical features. AJNR Am J Neuroradiol. 2008 Jun;29(6):1036-42. doi: 10.3174/ajnr.A0928. Epub 2008 Mar 20. PMID: 18356474; PMCID: PMC8118828.
2. Bartynski WS. Posterior reversible encephalopathy syndrome, part 2: controversies surrounding pathophysiology of vasogenic edema. AJNR Am J Neuroradiol. 2008 Jun;29(6):1043-9. doi: 10.3174/ajnr.A0929. Epub 2008 Apr 10. PMID: 18403560; PMCID: PMC8118813.
3. McKinney AM, Jagadeesan BD, Truwit CL. Central-variant posterior reversible encephalopathy syndrome: brainstem or basal ganglia involvement lacking cortical or subcortical cerebral edema. AJR Am J Roentgenol. 2013 Sep;201(3):631-8. doi: 10.2214/AJR.12.9677. PMID: 23971457.

Images/Tables



182

Never Too LATE to Learn a New Diagnosis: What Radiologists Should Know About Diagnosing LANS

Luke Miller MD
Johns Hopkins Hospital, Baltimore, MD, USA

Abstract Category

Adult Brain Inflammatory/Infectious Disease/Degenerative/Metabolic

Summary & Objectives

Purpose: This presentation aims to educate neuroradiologists about Limbic-predominant Age-related TDP-43 Encephalopathy Neuropathological Change (LATE-NC) and its newly proposed clinical correlate, Limbic-predominant Amnestic Neurodegenerative Syndrome (LANS). The focus is on improving diagnosis, understanding how this entity fits within the broader set of neurodegenerative diseases, and recognizing key imaging findings that distinguish LANS from Alzheimer's disease and other dementias.

Purpose

Methods: This presentation will summarize and illustrate new research on the definition, pathophysiology, and clinical presentation of LATE-NC and LANS. It will emphasize neuroimaging findings, particularly structural MRI and PET imaging characteristics. Diagnostic criteria and challenges will also be discussed, including the role of radiologists in the probabilistic diagnosis of LANS.

Materials & Methods

Findings: LATE-NC is a common pathological finding in older adults, present in 40% of individuals over 85, while LANS is estimated to affect about 10% of dementia clinic patients. Key imaging findings include disproportionate hippocampal atrophy relative to mild cognitive impairment, absence of neocortical atrophy, and negative tau pathology on PET or CSF testing. LANS diagnosis is important because it carries a better prognosis than Alzheimer's disease and patients do not qualify for anti-amyloid treatments, highlighting the importance of accurate diagnosis.

Results & Conclusion

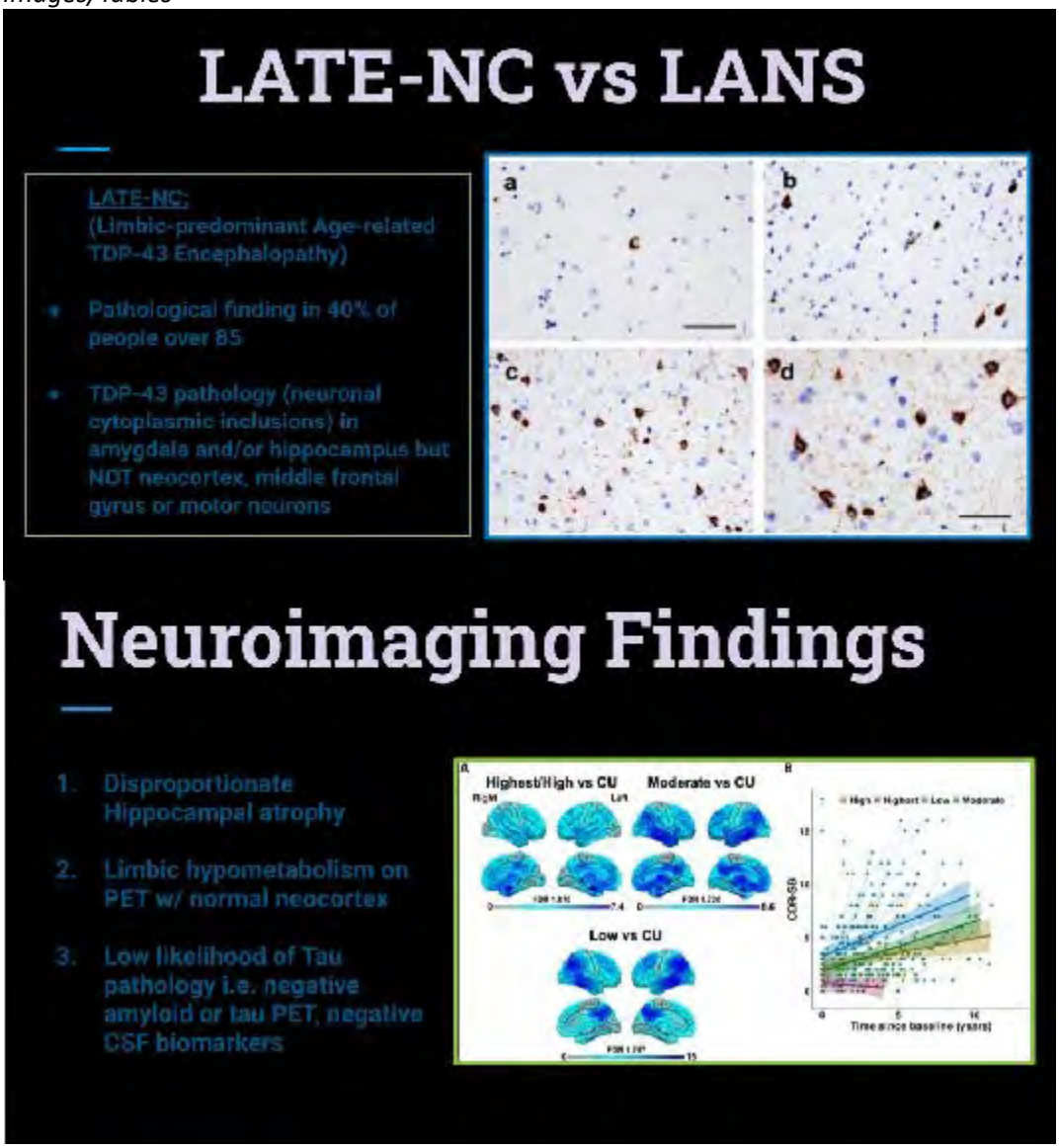
Summary/Teaching Points:

1. LATE-NC is a common pathological finding that can mimic and coexist with Alzheimer’s but can only be definitively diagnosed by biopsy. LANS is a correlated clinical syndrome with certain imaging and behavioral markers.
2. It is important to improve diagnosis of LANS since it carries a better prognosis than Alzheimer’s and these patients do not qualify for anti-amyloid treatment.
3. Key imaging findings are disproportionate hippocampal atrophy with relatively mild cognitive impairment and no neocortical atrophy or tau pathology on PET or CSF testing.
4. LANS is a proposed probabilistic diagnosis. Patients are placed in “high,” “moderate,” and “low” probability categories. Further research is needed for more definitive diagnosis and treatment, but raising awareness of this entity is the first step.

References

1. Corriveau-Lecavalier N, Botha H, Graff-Radford J, et al. Clinical criteria for a limbic-predominant amnestic neurodegenerative syndrome. Brain Communications. 2024;6(4):183. DOI: https://doi.org/10.1093/braincomms/fcae183
2. Meeter LH, Kaat LD, Rohrer JD, van Swieten JC. Imaging and fluid biomarkers in frontotemporal dementia. *Nature Reviews Neurology*. 2017;13(7):406-419. DOI: https://doi.org/10.1038/nrneurol.2017.75
3. Nag S, Yu L, Boyle PA, Leurgans SE, Bennett DA, Schneider JA. TDP-43 pathology in anterior temporal pole cortex in aging and alzheimer’s disease. Acta Neuropathological Communications. 2018;6. DOI: https://doi.org/10.1186/s40478-018-0531-3
4. Nag S, Schneider JA. Limbic-predominant age-related TDP43 encephalopathy (late) neuropathological change in neurodegenerative diseases. Nature Reviews Neurology. 2023;19:525–541. DOI: https://doi.org/10.1038/s41582-023-00846-7

Images/Tables



190

Salivary Gland Neoplasm: Imaging Features That Actually Matter for Diagnosis

Alexander D Pietroski MD[1], Carol Lima MD[1], Tannoz Norouzi BS[2], Samir Noujaim MD[1]
[1]Corewell Health William Beaumont University Hospital, Royal Oak, MI, USA. [2]Oakland University William Beaumont School of Medicine, Rochester, MI, USA

Abstract Category

Adult Neoplasms/Epilepsy/Trauma

Summary & Objectives

Salivary gland neoplasms are uncommon, comprising less than 3% of head and neck tumors and accounting for under 0.1% of cancer-related deaths. This exhibit offers a comprehensive overview of major salivary gland neoplasms in pediatric and adult age groups, focusing on imaging findings that actually matter for accurate diagnosis. Tumors of the major salivary glands (parotid, submandibular, and sublingual glands) present distinct imaging challenges due to similarities in clinical presentation, rarity, and the diversity of both neoplastic and non-neoplastic lesions. Identifying key imaging characteristics is crucial in the initial evaluation, as it helps delineate tumor location (intraglandular vs. extraglandular), differentiate between malignant and benign features, and assess local extension and regional spread, guiding treatment decisions and influencing prognosis and outcomes. Most tumors are benign, and the parotid gland is the most common site. The smaller the involved salivary gland, the higher the likelihood of the tumor being malignant.

Ultrasound serves as a valuable first-line tool, particularly for differentiating cystic from solid components. MRI, with its high soft tissue resolution and signal characteristics, provides a detailed assessment of tumor extent, helping to distinguish between benign and malignant features, with perineural spread suggesting malignancy, such as in adenoid cystic carcinoma. CT is especially effective in detecting calcifications and evaluating bone involvement, aiding in the distinction between benign and aggressive malignancies. Radionuclide imaging, when available, aids in diagnosis. Sodium pertechnetate (Tc99) is concentrated and secreted by salivary gland cells but appears as a cold spot in most neoplastic lesions, except Warthin's tumor and oncocytoma, which appear as hot spots. Gallium-67 detects diffuse inflammatory/neoplastic processes, such as sarcoidosis and lymphoma, by targeting actively dividing cells. PET imaging with FDG differentiates benign from malignant salivary gland tumors, with benign lesions appearing as cold spots, except for Warthin's tumor and oncocytoma.

Purpose

This educational exhibit provides a rapid-reference guide to key imaging characteristics of major salivary gland tumors. The guide aims to streamline the differential diagnosis, enhance diagnostic accuracy, and improve treatment planning, response, and outcomes.

Materials & Methods

A retrospective review was conducted on major salivary gland tumors at our institution, using imaging data from ultrasound, MRI, CT, and radionuclide scans to identify distinguishing features for each tumor type. Key imaging characteristics were grouped into diagnostic categories.

Results & Conclusion

Identifying key imaging characteristics is essential for the accurate diagnosis of major salivary gland tumors. The following features suggest that a salivary gland tumor may be malignant and warrant a biopsy: spiculated or irregular margins, T2 hypointensity on MRI, perineural spread, presence of necrosis, a pathologic lymph node, and a capsule that is thick, irregular, strongly enhancing, or does not completely surround the lesion.

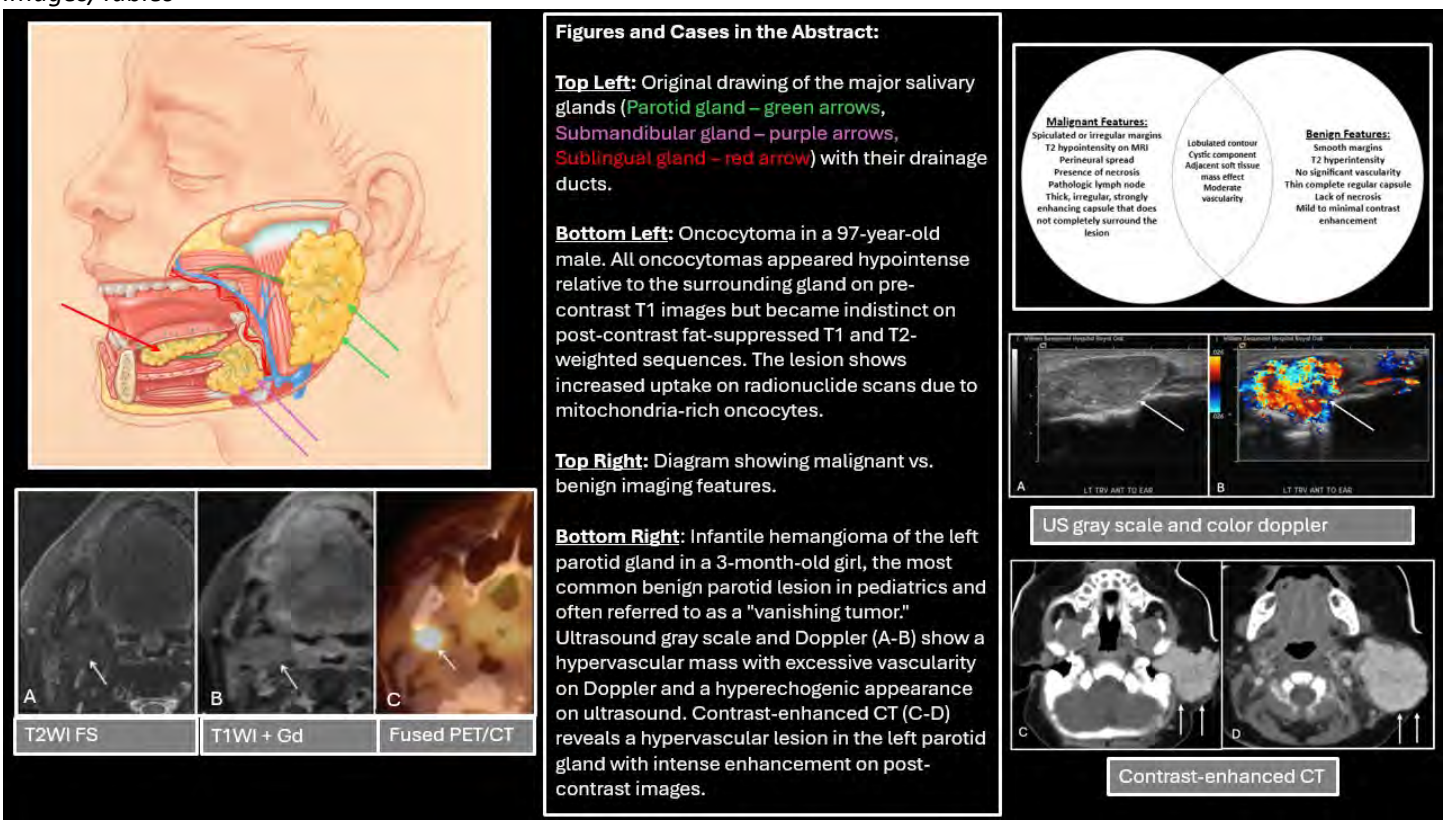
References

Meyers SP. *Differential Diagnosis in Neuroimaging: Head and Neck.* Thieme; 2016:384-403.

Lewis AG, Tong T, Maghami E. Diagnosis and Management of Malignant Salivary Gland Tumors of the Parotid Gland. *Otolaryngol Clin North Am*. 2016;49(2):343-380. doi:10.1016/j.otc.2015.11.001

Ginat DT. Imaging of Benign Neoplastic and Nonneoplastic Salivary Gland Tumors. *Neuroimaging Clin N Am.* 2018;28(2):159-169. doi:10.1016/j.nic.2018.01.002

Images/Tables



192

CT Angiography of the Head for the Initial Assessment of Giant Cell Arteritis: Presenting Symptoms, Biopsy Outcomes and Alternative diagnosis

Supriya Khatri MD Candidate[1], Arsalan Rizwan[2], Omar Islam[2], John Rossiter[2], Benjamin Kwan[2]
[1]Queen's University, Kingston, ON, Canada. [2]Queen's University, Kingston, Ontario, Canada

Abstract Category

Interventional/Vascular/Stroke

Summary & Objectives

Giant cell arteritis (GCA) is a form of large vessel vasculitis that poses a significant risk of vision loss if not diagnosed and treated promptly. Traditionally, the diagnosis is confirmed through a superficial temporal artery (STA) biopsy, an invasive and time-consuming procedure. This study aims to explore the potential of computed tomography angiography (CTA) as an initial, non-invasive diagnostic tool for patients suspected of having GCA. Specifically, we investigated the association between CTA findings—such as blurred STA wall and perivascular enhancement—and positive STA biopsy results, hypothesizing that certain imaging markers on CTA could predict positive biopsy outcomes. Additionally, we sought to identify alternative diagnoses in patients who displayed GCA-like symptoms but had negative biopsy results. Our objective is to provide insight into the utility of CTA as a supportive diagnostic modality in the early assessment of GCA, potentially reducing the need for invasive procedures and aiding in the differential diagnosis of GCA.

Purpose

The purpose of this study is to assess the diagnostic potential of CTA in GCA by examining the correlation between CTA imaging signs (e.g., blurred STA wall and perivascular enhancement) and positive STA biopsy outcomes. This study also seeks to provide alternative diagnoses for patients who presented with GCA-like symptoms but had negative biopsy results.

Materials & Methods

A retrospective review was conducted on 22 patients who underwent both CTA and STA biopsy at Kingston Health Sciences Center from 2010 to 2018. Baseline demographics, clinical presentations, laboratory markers (CRP, ESR), and CTA findings were collected. Key CTA signs (blurred STA wall, perivascular enhancement, stenosis/occlusion, calcification) were analyzed, and odds ratios were calculated to evaluate associations with biopsy outcomes. Alternative diagnoses were documented for patients with negative STA biopsies.

Results & Conclusion

The study included 22 patients, of which 8 had positive STA biopsies and 14 had negative results. Our findings demonstrated a strong association between specific CTA imaging signs—namely blurred STA wall and perivascular enhancement—and positive STA biopsy outcomes (OR: 29, 95% CI: 1.3 - 648, p=0.034). This suggests that these imaging features could serve as valuable non-invasive indicators for GCA. Other imaging markers, such as stenosis or occlusion of the STA, showed higher prevalence in positive biopsy cases but did not reach statistical significance. Importantly, none of the negative biopsy patients exhibited the blurred STA wall and perivascular enhancement, reinforcing the specificity of these signs for GCA. Among patients with negative STA biopsies, alternative diagnoses varied widely, with conditions like headache, temporomandibular joint disorder, glaucoma, and polymyalgia rheumatica noted, underscoring the challenges in differentiating GCA from other clinical entities.

In conclusion, this study highlights the potential role of CTA as a complementary diagnostic tool in the assessment of suspected GCA. The presence of blurred STA wall and perivascular enhancement on CTA may increase the likelihood of a positive GCA diagnosis, thereby assisting clinicians in making timely and accurate diagnoses. However, due to limitations such as small sample size and the retrospective design, further research with larger cohorts is needed to validate these findings.

References

1. Dejaco, C., Ramiro, S., Bond, M., Bosch, P., Ponte, C., Mackie, S. L., Bley, T. A., Blockmans, D., Brolin, S., Bolek, E. C., Cassie, R., Cid, M. C., Molina-Collada, J., Dasgupta, B., Nielsen, B. D., De Miguel, E., Direskeneli, H., Duftner, C., Hočevar, A., Molto, A., … Schmidt, W. A. (2024). EULAR recommendations for the use of imaging in large vessel vasculitis in clinical practice: 2023 update. *Annals of the rheumatic diseases*, *83*(6), 741–751. https://doi.org/10.1136/ard-2023-224543
2. Pradeep, S., & Smith, J. H. (2018). Giant Cell Arteritis: Practical Pearls and Updates. *Current pain and headache reports*, *22*(1), 2. https://doi.org/10.1007/s11916-018-0655-y

3. Luqmani, R., Lee, E., Singh, S., Gillett, M., Schmidt, W. A., Bradburn, M., Dasgupta, B., Diamantopoulos, A. P., Forrester-Barker, W., Hamilton, W., Masters, S., McDonald, B., McNally, E., Pease, C., Piper, J., Salmon, J., Wailoo, A., Wolfe, K., & Hutchings, A. (2016). The Role of Ultrasound Compared to Biopsy of Temporal Arteries in the Diagnosis and Treatment of Giant Cell Arteritis (TABUL): a diagnostic accuracy and cost-effectiveness study. *Health technology assessment (Winchester, England)*, *20*(90), 1–238. https://doi.org/10.3310/hta20900
4. Lariviere, D., Benali, K., Coustet, B., Pasi, N., Hyafil, F., Klein, I., Chauchard, M., Alexandra, J. F., Goulenok, T., Dossier, A., Dieude, P., Papo, T., & Sacre, K. (2016). Positron emission tomography and computed tomography angiography for the diagnosis of giant cell arteritis: A real-life prospective study. *Medicine*, *95*(30), e4146. https://doi.org/10.1097/MD.0000000000004146

195

A Primer to Deep Learning MRI Reconstructions and their Future in Neuroradiology

Felipe Rosero Castro BS[1], Shawn Lyo MD[1], Suyash Mohan MD[1], Sanjeev Chawla PhD, DABMP[2]
[1]University of Pennsylvania, Philadelphia, PA, USA. [2]Perelman School of Medicine at the University of Pennsylvania, Philadelphia, PA, USA

Abstract Category

New Techniques/Advanced Imaging/Informatics/AI/Professional Development/Misc

Summary & Objectives

Deep Learning (DL) is a subset of machine learning that has catapulted to the forefront of research as a tool for a multitude of applications in neuroradiology, including the reconstruction of MR images from under-sampled acquisitions (1). However, understanding the technical aspects of DL and DL reconstruction (DLR) as they are outlined in the literature often requires some background in mathematics, computer science, or image processing, making engaging with these concepts less accessible to many clinicians. Here, we outline conventional MRI reconstruction techniques and the advantages of DLR approaches. We then offer an accessible overview of the most common DL architectures used in MR reconstruction and their advantages and disadvantages. Next, we dive into the different methods that integrate DL in the reconstruction process including those involving the spatial domain, the k-space domain, and combined-domain approaches. We then outline recent clinical applications of this technology specific to the field of neuroradiology in reconstructing MRIs of the brain and spine. We end by outlining the current challenges and pitfalls facing the integration of DLR technologies into real clinical practice along with the proposal of possible solutions and future directions.

Educational Objectives:

1. To broadly increase learner comfort with the technical terms surrounding artificial intelligence, machine learning, deep learning, and image reconstruction.
2. To describe the clinical relevance and future potential of DL MRI reconstruction technology in neuroradiology
3. To explain accessibly the basics of deep learning, including the major components of a neural network and different training methods.
4. To describe the basics of conventional reconstruction techniques, including parallel imaging and compressed sensing, and their differences from DL approaches.
5. To accessibly outline the DL architectures most used in MR reconstruction and their comparative advantages and disadvantages, including:
    1. Convolutional neural networks (CNNs)
    2. Generative adversarial networks (GANs)
    3. Recurrent neural networks (RNNs)
6. To accessibly define the concepts of image space, k-space, and transformation.
7. To describe the different DL reconstruction and postprocessing methods within these “spaces”.
8. To report recent clinical applications and implications of DLR technologies in brain and spine imaging as seen in the literature, including:
    1. DWI reconstructions in patients with stroke-like symptoms
    2. Image enhancement in 1.5 T brain MR acquisitions
    3. Decreasing slice thickness in assessment of pituitary adenomas
    4. Impacts on workflow and the patient experience
9. To highlight the most salient artifacts and limitations of DLR technologies including those specific to neuroradiology.

10. To outline possible future directions of DLR technologies in neuroradiology.

Purpose

N/A

Materials & Methods

N/A

Results & Conclusion

N/A

References

1. Gassenmaier S, Küstner T, Nickel D, et al. Deep Learning Applications in Magnetic Resonance Imaging: Has the Future Become Present? *Diagnostics (Basel)* 2021;11(12):2181. DOI: 10.3390/diagnostics11122181.

201

Delayed Leukoencephalopathy following Endovascular Intervention

Jacob A Poliskey MD, PhD[1], Sreehari B Panicker MD[2], Leanne Y Lin MD, MPHS[3], Jeffrey M Wilseck DO[1], Zachary M Wilseck MD[3]

[1]Corewell Health East William Beaumont University Hospital, Royal Oak, MI, USA. [2]Henry Ford Health, Detroit, MI, USA. [3]University of Michigan, Ann Arbor, MI, USA

Abstract Category

Interventional/Vascular/Stroke

Summary & Objectives

Delayed leukoencephalopathy is a rare complication of endovascular intervention, presenting with non-ischemic cerebral inflammatory changes and varying degrees of neurologic sequelae. Although the exact cause is uncertain, the theory is that this is secondary to reactive inflammation to embolized hydrophilic polymer coating material and metals used in endovascular devices including microcatheters, wires, coils, and stents. These inflammatory reactions can lead to intracranial foreign body granuloma formation. Here we present cases of delayed leukoencephalopathy, with MRI findings revealing white matter lesions and symptoms appearing weeks to months following different types of endovascular intervention.

Purpose

Delayed leukoencephalopathy is a rare (<1%) complication of endovascular intervention that remains under-recognized. The purpose of this educational exhibit is to increase awareness of this unique diagnosis and its clinical implications for patients undergoing endovascular procedures, leading to earlier recognition and diagnosis which will impact patient outcomes. Potential treatment strategies are also discussed.

Materials & Methods

We intend to present a case series involving patients who underwent endovascular therapy who developed delayed leukoencephalopathy. Two examples include a 33-year-old male with a traumatic cervical internal carotid artery pseudoaneurysm and a 71-year-old female with a giant cavernous internal carotid artery aneurysm treated with flow diverting stents. MRI imaging was serially obtained and clinical data with treatment responses were evaluated.

Results & Conclusion

After flow diverting stent treatment, both patients presented with neurologic symptoms and enhancing white matter FLAIR hyperintensities occurring a few weeks to a few months following the initial treatment. The presence of the white matter lesions roughly correlated with each patient's symptomatology. The first case of a 33-year-old male improved without targeted intervention while the second case of a 71-year-old female improved with steroid use. The original aneurysm and pseudoaneurysm were resolving as intended. Ultimately, after excluding other etiologies, these imaging findings and symptoms were felt to represent delayed leukoencephalopathy following endovascular intervention, likely caused by embolized hydrophilic material during the treatment.

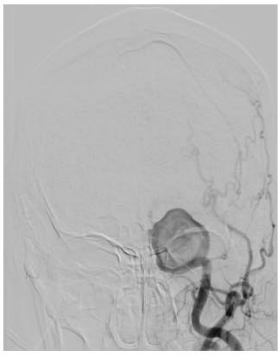
References

Skolarus LE, Gemmete JJ, Braley T, et al. Abnormal White Matter Changes After Cerebral Aneurysm Treatment with Polyglycolic-Polylactic Acid Coils. *World Neurosurg*. 2010;74(6):640-644. doi:10.1016/j.wneu.2010.03.026

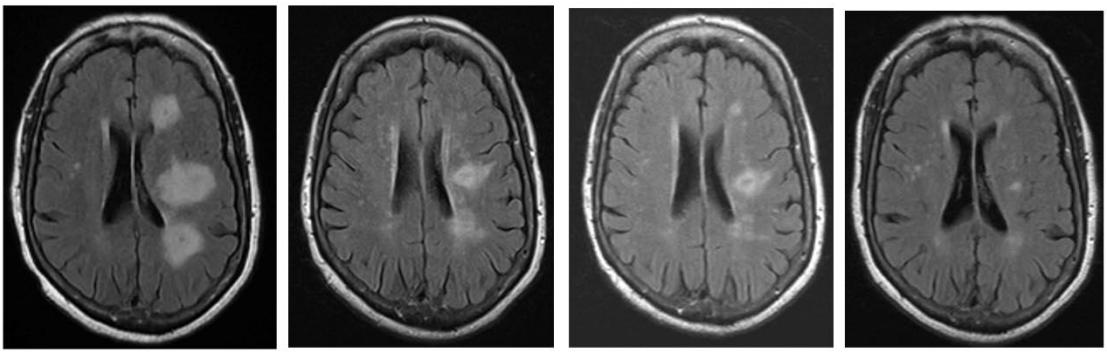
Ikemura A, Ishibashi T, Otani K, et al. Delayed Leukoencephalopathy: A Rare Complication after Coiling of Cerebral Aneurysms. *American Journal of Neuroradiology*. 2020;41(2):286-292. doi:10.3174/ajnr.A6386

Ridwan S, Kandyba JA, Schug A, et al. Delayed Leukoencephalopathy and Foreign Body Reaction After Endovascular Treatment in Patients with Intracranial Aneurysms and Aneurysmal Subarachnoid Hemorrhage—A Systematic Review of the Literature. *Front Surg*. 2021;8. doi:10.3389/fsurg.2021.732603

Images/Tables



Giant internal carotid artery aneurysm treated with flow diverting stent



One month later | Six weeks later | Two months later | One year later

Delayed leukoencephalopathy: The patient presented with headache, nausea, vomiting, and sixth nerve palsy. T2/FLAIR images show white matter lesions which demonstrate progressive improvement over time and with steroid use.

213

Anatomy and Pathology of the Trigeminal Nerve

Karam Musaitif DO, MS, Michael Markovic MD, Michael Bates DO, Kyle Hunter MD, Jeffrey Prescott MD, PhD, Vikas Jain MD

MetroHealth, Cleveland, Ohio, USA

Abstract Category

Head and Neck

Summary & Objectives

The trigeminal nerve (TGN) is the largest cranial nerve and contains both sensory and motor fibers. The nucleus originates within the brainstem and then the TGN divides into the cisternal segment, Meckel's cave, cavernous segment, and peripheral segment where it branches to form V1 (ophthalmic), V2 (maxillary), and V3 (mandibular) divisions. The anatomic segments should be understood to thoroughly evaluate the trigeminal nerve with neuroimaging, using MRI as the preferred modality. In some cases, standard MRI techniques may be supplemented with contrast administration, heavily T2-weighted sequences, or MR angiography. CT of the skull base may be beneficial in some cases to show the bony pathology. This educational exhibit aims to provide a review of the trigeminal nerve anatomy followed by discussion of various lesions that may cause trigeminal nerve disease.

Brainstem:

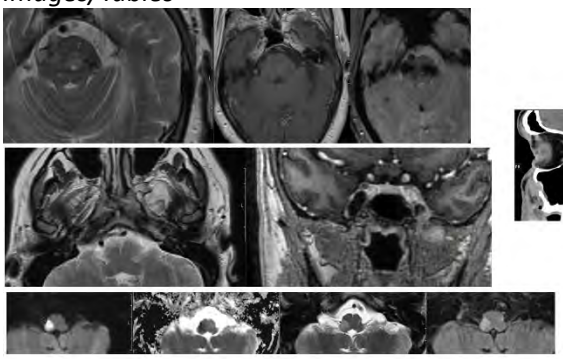
Multiple sclerosis is the most common cause of TGN disease in the brainstem. This is seen on imaging as T2 hyperintensity and may show contrast enhancement in the active stage of the disease.

Brainstem infarcts can cause Wallenberg syndrome and TGN symptoms such as ipsilateral facial pain and temperature loss.

Cisternal segment and Meckel's cave:

Trigeminal neuralgia is typically caused by lesions involving the cisternal segment at the root entry zone, where there is a transition between central and peripheral myelin. This region is susceptible to extrinsic compression due to the thinner myelin layer. Extrinsic compression is usually caused by a vascular loop, most commonly the superior cerebellar artery, crossing the nerve perpendicularly within the root entry zone and causing indentation or encasement of the TGN. The exact site of compression can be visualized with high-resolution MR angiography and 3D gradient echo steady-state free-procession (SSFP).

Schwannoma is the most common neoplasm to affect the TGN within the cisternal segment and trigeminal ganglion. Meningiomas and perineural tumor spread (PNTS) can also affect these segments.

Cavernous segment:
Tolosa-Hunt syndrome is one condition that specifically affects the cavernous sinus. It is characterized by lymphocytic dural infiltration and appears on MRI as a bulky cavernous sinus that is iso- to hypointense on T1 and T2-weighted images. Tolosa-Hunt also shows contrast enhancement and commonly shows narrowing of the internal carotid artery. Carotid aneurysms and caroticocavernous fistulas are vascular lesions affecting this segment. Neoplasms that could affect the cavernous segment include invasive pituitary adenomas, osseocartilaginous tumors, schwannomas, meningiomas, and PNTS.
Peripheral segments:
The supraorbital, infraorbital, and inferior alveolar nerves are the distal branches of V1, V2, and V3, respectively. Perineural spread of head and neck malignancies commonly follow these nerves, with the maxillary division being the most commonly affected. On imaging, metastatic spread along the TGN can be seen in both anterograde and retrograde directions and can also have skip lesions, necessitating the evaluation of the entire TGN in these cases. Features of metastatic spread along the TGN includes irregular thickening and enhancement of the nerve, obscuration of the juxta-foraminal fat pads, atrophy of the innervated muscles, and widening of the neural foramen.
Purpose
N/A
Materials & Methods
N/A
Results & Conclusion
N/A
References
Bathla G. and Hedge A.N. The trigeminal nerve: An illustrated review of tis imaging anatomy and pathology. Clinical Radiology, 2013-02-01, Volume 68, Issue 2, Pages 203-213, Copyright © 2012 The Royal College of Radiologists
Freddi TAL, Ottaiano AC, Lucio LL, Corrêa DG, Hygino da Cruz LC Jr. The Trigeminal Nerve: Anatomy and Pathology. Semin Ultrasound CT MR. 2022 Oct;43(5):403-413. doi: 10.1053/j.sult.2022.04.002. Epub 2022 Apr 6. PMID: 36116853.
Graff-Radford S, Gordon R, Ganal J, Tetradis S. Trigeminal neuralgia and facial pain imaging. Curr Pain Headache Rep. 2015 Jun;19(6):19. doi: 10.1007/s11916-015-0495-y. PMID: 26017711.
Images/Tables


221

A Radiologic Atlas of Suprasellar Masses and Mass-Like Lesions in Children and Adults

Caroline Rutten MD, Carlos Robles MD, Suzanne Laughlin MD, Elka Miller MD, Pradeep Krishnan MD, Manohar Shroff MD, Vivek Pai MD
The Hospital for Sick Children, Toronto, Ontario, Canada

Abstract Category

Pediatrics

Summary & Objectives

This educational exhibit explores the wide spectrum of pathologies affecting the sellar, suprasellar, and hypothalamic regions, as well as the optic chiasm and adjacent structures. The primary objective is to provide a comprehensive review of the diagnostic challenges posed by these complex and often overlapping conditions, offering insights into their key imaging features.

Purpose

The purpose of this educational exhibit is to:

1. Review the imaging characteristics of various sellar, suprasellar, hypothalamic, and optic chiasm lesions.
2. Highlight distinguishing radiologic features that aid in differentiating common, rare, and developmental pathologies.
3. Present a case-based approach to understanding these lesions, supported by a multimodality imaging review.
4. Provide radiologists with practical knowledge to improve diagnostic accuracy in pediatric and adult patients.

Materials & Methods

A broad range of pituitary, sellar, suprasellar, hypothalamic, and optic chiasm pathologies in both pediatric and adult patients were selected.

Results & Conclusion

1. Pituitary origin lesions: Rathke's cleft cyst, craniopharyngioma, macroadenoma
2. Bony sella / meninges lesions: , meningioma, solitary fibrous tumor
3. Pituitary stalk lesions: Ectopic posterior pituitary / stalk interruption syndrome, Langerhans cell histiocytosis (LCH), hypophysitis, sarcoidosis, quadrilateral retinoblastoma, germinoma, pituicytoma, metastasis
4. Hypothalamic lesions: Interhypothalamic adhesion, Tuberomamillary fusion, hamartomas, giant VR space, cavernoma, lymphoma, oligodendroglioma, inflammation (NMO, anti-Ma2 encephalitis)
5. Suprasellar developmental lesions: Arachnoid cyst, dermoid, epidermoid, lipoma, teratoma, diencephalic-mesencephalic junction dysplasia
6. Suprasellar masses: NGGCT, ganglioglioma, germ cell tumor
7. Optic chiasm lesions: Krabbe's disease related hyperplasia, cavernoma, NF1 and non-NF1 related gliomas, optic pathway GBM.
8. Miscellaneous: Aicardi syndrome related cysts, tuberculosis, suprasellar aneurysm, chordoid glioma

References

Huang J, Sarma A, Harmsen H, Pruthi S. Systematic Approach to Evaluating Sellar and Suprasellar Lesions in Pediatric Patients. *Radiographics*. 2022;42(7):E214-E215. doi:10.1148/rg.210121

234

Best Guess? Could Be RCVS! A Pictorial Review of RCVS with Emphasis on Vessel Wall Imaging

Catherine Song MD, Debayan Bhaumik MD, Gustavo Mendez MD
University of Colorado, Aurora, Colorado, USA

Abstract Category

Interventional/Vascular/Stroke

Summary & Objectives

Reversible cerebral vasoconstriction syndrome (RCVS) describes a set of clinical and radiologic findings which are the common manifestation of a variety of proposed mechanisms and precipitating factors. Clinical context is important for the diagnosis, given the female preponderance, self-limited course, and high prevalence of cases which are precipitated by specific triggers, though spontaneous cases occur as well.[1] Awareness of this syndrome has been gradually increasing, and it is estimated to have an incidence of approximately 3 per million per year.[2] While neurologic deficits can occur, the key presenting symptom is a thunderclap headache.[1] The key imaging feature is multifocal segmental vasoconstriction,

but this can also be seen with other conditions, most notably primary central nervous system (CNS) vasculitis, vasospasm after aneurysmal hemorrhage, or atherosclerosis.[3] The early distinction between primary CNS vasculitis and RCVS is clinically important as the steroids used to treat primary CNS vasculitis are not beneficial in treating RCVS, and may even lead to worse outcomes.[1]

Patterns more suggestive of RCVS are a beaded appearance involving multiple vascular territories, primarily affecting medium-to-large cerebral arteries, and rapid changes across examinations.[3] Imaging can also demonstrate sequelae of RCVS, such as convexal subarachnoid hemorrhage, intraparenchymal hemorrhage, or ischemic stroke, or demonstrate the frequently concomitant posterior reversible encephalopathy syndrome (PRES).[1]

The diagnosis of RCVS is confirmed retrospectively, after improvement and/or resolution is noted on follow-up imaging in about 1-3 months.[3] While RCVS has overlapping imaging features with other cerebrovascular pathologies, vessel wall imaging has emerged as a critical tool to help aid in the diagnosis. The pattern of wall thickening and enhancement is used to help differentiate it from other pathologies, most importantly primary CNS vasculitis. Generally, though both can demonstrate arterial wall thickening, RCVS has no significant wall enhancement while primary CNS vasculitis has intense circumferential wall enhancement.[4] At our institution, we most frequently see no abnormality or mild wall enhancement associated with RCVS. Whether or not this always holds true, however, is a subject of current inquiry as some cases of RCVS with more than minimal enhancement have been noted.[5] Overall, these findings can help make a presumptive diagnosis of RCVS to guide treatment, which includes withdrawing exogenous triggers and calcium channel blockers for symptom relief.[1]

We will present a series of RCVS cases to demonstrate the important clinical and imaging features to making the diagnosis, and which have been evaluated with vessel wall imaging to help differentiate them from other pathologies. These will be contrasted with typical vessel wall imaging findings of other pathologies. For example, we have a case of a female patient in her fourth decade who presented with weeks of recurrent thunderclap headache and transient focal neurologic deficits, seen on imaging to have multifocal cerebral arterial narrowing without evidence of wall enhancement (Figure 1).

Objectives:

1. Provide an up-to-date overview of important clinical and radiologic features of reversible cerebral vasoconstriction syndrome.
2. Illustrate the imaging features of RCVS, particularly its findings on vessel wall imaging, with a series of cases from our institution.

References

1. Miller TR, Shivashankar R, Mossa-Basha M, et al. Reversible Cerebral Vasoconstriction Syndrome, Part 1: Epidemiology, Pathogenesis, and Clinical Course. *AJNR Am J Neuroradiol* 2015;36(8):1392-1399. DOI: https://doi.org/10.3174/ajnr.A4214
2. Magid-Bernstein J, Omran SS, Parikh NS, et al. Reversible Cerebral Vasoconstriction Syndrome: Symptoms, Incidence, and Resource Utilization in a Population-Based US Cohort. *Neurology* 2021;97(3):e248-e253. DOI: https://doi.org/10.1212/WNL.0000000000012223
3. Miller TR, Shivashankar R, Mossa-Basha M, et al. Reversible Cerebral Vasoconstriction Syndrome, Part 2: Diagnostic Work-Up, Imaging Evaluation, and Differential Diagnosis. *AJNR Am J Neuroradiol* 2015;36(9):1580-1588. DOI: https://doi.org/10.3174/ajnr.A4215
4. Mossa-Basha M, Hwang WD, De Havenon, A, et al. Multicontrast High-Resolution Vessel Wall Magnetic Resonance Imaging and Its Value in Differentiating Intracranial Vasculopathic Processes. *Stroke* 2015;46(6):1567-1573. DOI: https://doi.org/10.1161/STROKEAHA.115.00903
5. Mandell DM, Mossa-Basha M, Qiao Y, et al. Intracranial Vessel Wall MRI: Principles and Expert Consensus Recommendations of the American Society of Neuroradiology. *ANJR Am J Neuroradiol* 2017;38(2):218-229. DOI: https://doi.org/10.3174/ajnr.A4893

Images/Tables

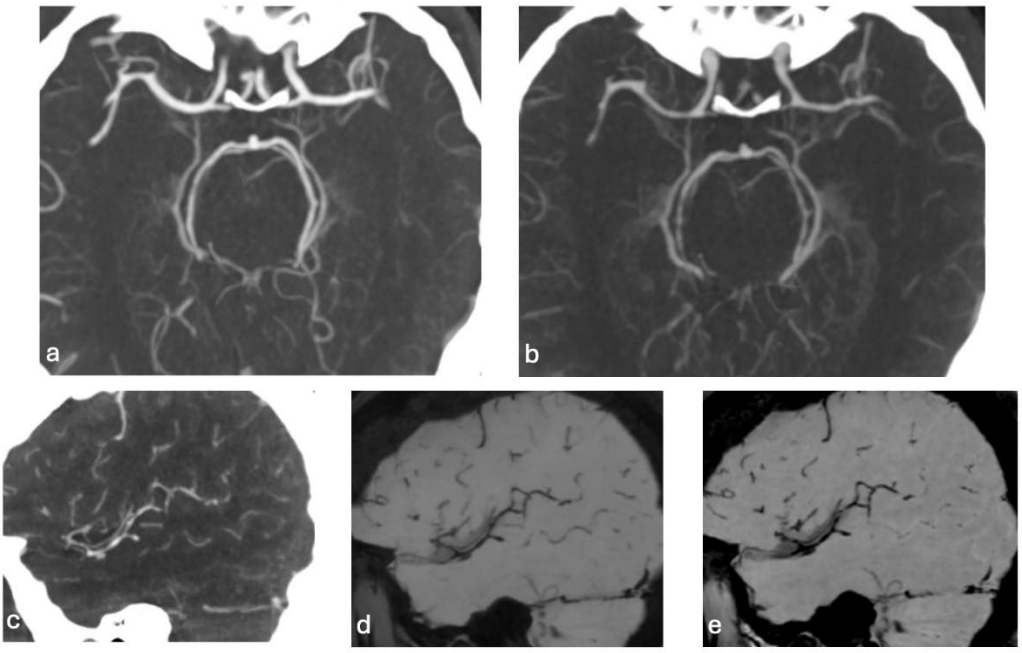


Figure 1: CTA brain (a, b (axial MIPs one day apart), c (sagittal MIP)) and MRA intracranial vessel wall imaging (d (pre-contrast MinIP), e (post-contrast MinIP)) were performed. The dynamic nature of the process is demonstrated by the rapid onset of multifocal stenoses in the anterior and posterior circulation after one day (a, b). In an area of multifocal left MCA narrowing (c), there was no associated abnormal enhancement (d, e).

254

Low-Flow Venous and Lymphatic Malformations: A Review of Diagnosis, Imaging, and Management

Jessica Vankawala BS[1], Hamza Shaikh MD[2]
[1]Cooper Medical School of Rowan University, Camden, NJ, USA. [2]Cooper Univeristy Health Care, Camden, NJ, USA

Abstract Category

Interventional/Vascular/Stroke

Summary & Objectives

Low-flow venous and lymphatic malformations are congenital vascular anomalies that arise during embryonic angiogenesis in about 1% of the population. About 40% of these venous malformations occur in the head and neck, 40% in the extremities, and the remaining 20% in the trunk. Clinical manifestations of superficial or deep vascular lesions include significant pain, musculoskeletal complications, intravascular coagulopathy, and disruption of local neurovasculature. While the diagnosis of VMs and LMs is largely clinical, specific radiographic findings may be used to differentiate and classify these lesions. The gold standard for diagnosis is MRI, which can be used to characterize the lesion's size, complexity, and relationship to anatomical structures and monitor its progress during serial treatments. Recent updates to the ISSVA classification system for vascular anomalies aimed to reduce the high rate of misdiagnosis in these patients and ultimately improve management. Recognizing syndromes that include these malformations is also important to guide treatment. Options for the treatment of VMs and LMs include percutaneous sclerotherapy, electroporation with chemotherapeutic drugs, and cryoablation for symptomatic control.

Educational objectives:

1. Review the pathophysiology and clinical manifestations of simple venous malformations.
2. Identify the characteristics of VMs/LMs on different imaging modalities, including their pathognomonic signs.
3. Review the ISSVA classification of vascular anomalies.
4. Understand the surgical and medical treatment modalities for VMs/LMs and their mechanisms of action.
5. Recognize patterns of VMs/LMs and related symptoms as they appear in certain syndromes.

Purpose

In this educational exhibit, we will review the clinical presentation and radiological appearance of low-flow venous and lymphatic malformations, as well as their systems of classification and new advances in treatment. We will also present a case of venous malformation from our institution to better exemplify these concepts.

Materials & Methods

A review of current literature focused on the prevalence, etiology, classification, diagnosis, and management of VMs and LMs was conducted to identify patterns in presentation. Images from a VM case were obtained to review in this exhibit.

Results & Conclusion

Venous and lymphatic low-flow malformations exhibit typical imaging characteristics and have useful classification systems to direct management and predict outcomes. New methods of treatment, including repurposed chemotherapeutics, are generally effective in reducing the size and symptoms of venous and lymphatic malformations.

References

1. Clapp A, Shawber CJ, Wu JK. Pathophysiology of Slow-Flow Vascular Malformations: Current Understanding and Unanswered Questions. *Journal of Vascular Anomalies*. 2023;4(3):e069. doi:10.1097/JOVA.0000000000000069
2. Legiehn GM, Heran MKS. Venous Malformations: Classification, Development, Diagnosis, and Interventional Radiologic Management. *Radiologic Clinics of North America*. 2008;46(3):545-597. doi:10.1016/J.RCL.2008.02.008
3. Horbach SER, Lokhorst MM, Saeed P, de Goüyon Matignon De Pontouraude CMF, Rothová A, van der Horst CMAM. Sclerotherapy for low-flow vascular malformations of the head and neck: A systematic review of sclerosing agents. *Journal of Plastic, Reconstructive & Aesthetic Surgery*. 2016;69(3):295-304. doi:10.1016/J.BJPS.2015.10.045
4. Cooke-Barber J, Kreimer S, Patel M, Dasgupta R, Jeng M. Venous malformations. *Seminars in Pediatric Surgery*. 2020;29(5):150976. doi:10.1016/J.SEMPEDSURG.2020.150976
5. van Es J, Kappelhof NA, Douma RA, Meijers JCM, Gerdes VEA, van der Horst CMAM. Venous thrombosis and coagulation parameters in patients with pure venous malformations. *The Netherlands Journal of Medicine*. 2017;75(8):328-334.

Images/Tables

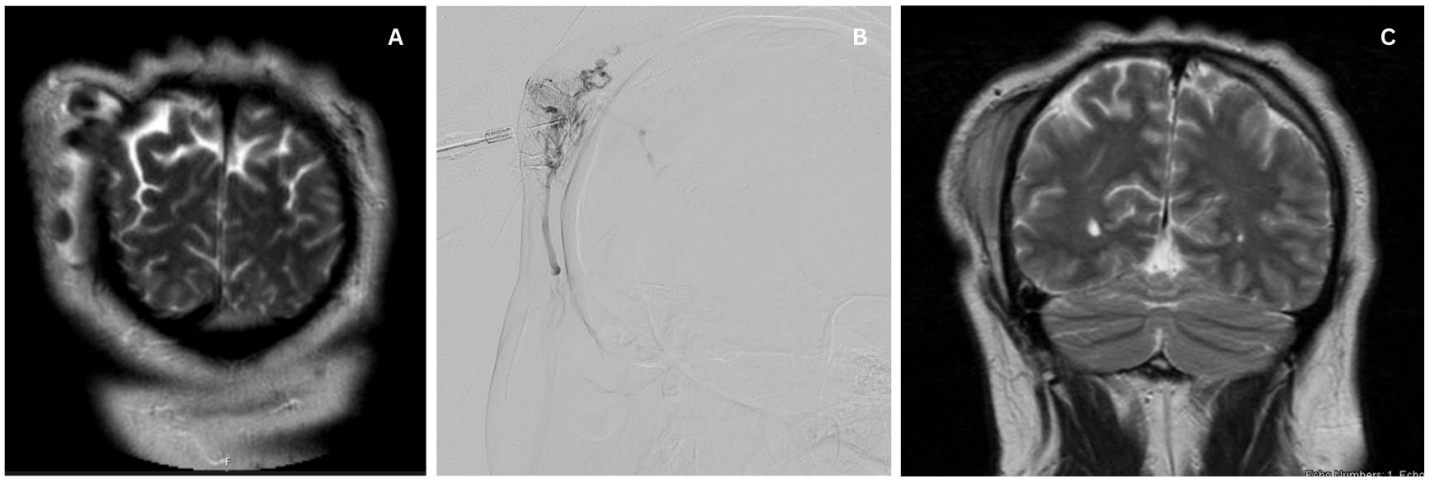


Fig. A: T2-weighted coronal MRI demonstrating a right parietal venous malformation. **Fig B:** Direct bleomycin embolization of venous lesion with angiography. **Fig C:** Post-embolization T2-weighted coronal MRI demonstrating a reduction in lesion size.

256

Intracranial Internal Carotid Artery Vasculopathies - Beyond Atherosclerosis

Matthew Liu MD, Erini V Makariou MD, Each Chun C Lee MD

Medstar Georgetown University Hospital, Washington, DC, USA

Abstract Category

Interventional/Vascular/Stroke

Summary & Objectives

Disease of the Intracranial internal carotid artery (ICA) is commonly related to atherosclerosis causing ICA stenosis. In this exhibit, we would like to showcase ICA disease from other pathologies. These pathologies can cause ICA stenosis, occlusion, dilatation or aneurysms. Patients typically present with acute neurological symptoms such as weakness, paresthesias, or headaches. We aim to correlate clinical presentations with imaging findings of various ICA conditions on MR and/ or CT.

Purpose

The purpose of this exhibit is to familiarize radiologists with intracranial ICA vasculopathies beyond atherosclerosis. We present cases of ICA disease from various pathologies.

Materials & Methods

We present MR and/or CT findings of about 10 cases of various causes of ICA disease. These include atherosclerosis, inflammatory vasculopathies (e.g., CNS angiitis, radiation induced vasculopathy, Takayasu arteritis, sickle cell vasculopathy), infectious vasculitis (e.g., cytomegalovirus), genetic disorders (e.g., fibromuscular dysplasia, tuberous sclerosis, glycogen storage disease), and idiopathic diseases (e.g. moyamoya disease). We highlight their clinical presentation, and discuss the imaging findings and characteristics.

Results & Conclusion

Acute neurological symptoms and headaches from ICA disease are common clinical presentations in our daily neuroradiology practice, and ICA atherosclerosis is by far the commonest cause. In this exhibit, we highlight other various causes of ICA disease, which can have similar clinical presentations, but require different patient management. Awareness of these etiologies will benefit patient management and patient outcomes.

References

Agarwal A, Bathla G, Kanekar S. Imaging of Non-atherosclerotic Vasculopathies. J Clin Imaging Sci. 2020 Oct 13;10:62. doi: 10.25259/JCIS_91_2020. PMID: 33194304; PMCID: PMC7656038.

Kang DW, Kim DY, Kim J, Baik SH, Jung C, Singh N, Song JW, Bae HJ, Kim BJ. Emerging Concept of Intracranial Arterial Diseases: The Role of High Resolution Vessel Wall MRI. J Stroke. 2024 Jan;26(1):26-40. doi: 10.5853/jos.2023.02481. Epub 2024 Jan 30. PMID: 38326705; PMCID: PMC10850450.

Images/Tables

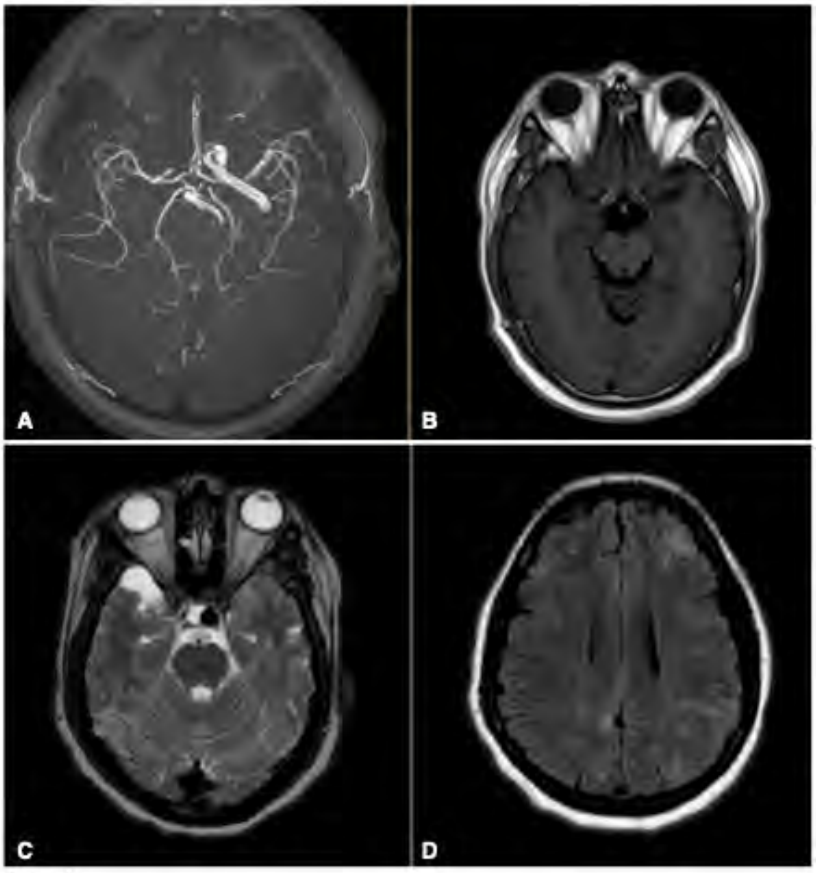


Figure 1:

CNS Angiitis:

(a) Time of Flight MR Angiography Maximum Intensity Projection showing bilateral distal ICA narrowing. (b) Axial Postcontrast T1W showing circumferential wall enhancement of the bilateral internal carotid arteries.

Tuberous Sclerosis: (c) Axial T2W showing 11 mm aneurysm of the distal left ICA. (d) Axial FLAIR showing multiple cortical signal abnormalities consistent with tubers of tuberous sclerosis.

259

Temporal Lobe Epilepsy: Not Just Mesial Temporal Sclerosis

Kathryn Hughes MD, Mark Chen MD, Sudeep Bhabad MD, Chanae Dixon MD
Rush University Medical Center, Chicago, IL, USA

Abstract Category

Adult Neoplasms/Epilepsy/Trauma

Summary & Objectives

- Briefly review anatomy of the amygdala and adjacent structures.
-Demonstrate cases of amygdala enlargement in patients with epilepsy; a nonspecific incidental finding or cause of temporal lobe epilepsy (TLE)?

Purpose

Imaging findings commonly reported in MRI evaluation of seizure include mesial temporal sclerosis (MTS), grey matter heterotopia, and focal cortical dysplasia. Though uncommonly described in neuroradiology literature, amygdala enlargement is an additional potential cause of epilepsy particularly in neurology and neurosurgery literature. It is unclear if amygdala enlargement is an incidental finding on imaging or serves as a true epileptogenic focus and distinct cause of TLE. Prior studies have described amygdala enlargement in patients with seizures but otherwise structurally negative MRI studies ("Imaging negative") but also in patients with hippocampal sclerosis and extratemporal or outside of the epileptogenic focus. Studies have also shown ipsilateral amygdala enlargement in normal control patients, bilateral amygdala enlargement or contralateral to proven epileptogenic foci on electroencephalogram (EEG) further confounding diagnostic utility. Furthermore, when undergoing surgery for temporal lobe epilepsy secondary to MTS, resection of the amygdala has been shown to be important for seizure control with similar outcomes between patients who underwent more extensive hippocampal resection in structurally negative TLE. We present a series of patients with amygdala enlargement and epilepsy.

Materials & Methods

This retrospective case series includes patients from our institution with amygdala enlargement on brain MRI. All patients in this series were undergoing seizure/epilepsy workup. Correlation was made between clinical history, follow-up imaging, EEG, and pathology, if available.

Results & Conclusion

Amygdala enlargement is a postulated cause of seizures in neurological and neurosurgical literature, but infrequently described in neuroradiology literature. Through this case series, we present several examples of amygdala enlargement on MRI highlighting the importance of thoroughly interrogating this region on imaging with consideration to AE as a cause of temporal lobe epilepsy.

References

Bower SP, Vogrin SJ, Morris K, et al. Amygdala volumetry in "imaging-negative" temporal lobe epilepsy. J Neurol Neurosurg Psychiatry 2003; 74(9):1245-9. doi: https://doi.org/10.1136/jnnp.74.9.1245.
Lv, RJ., Sun, ZR., Cui, T. et al. Temporal lobe epilepsy with amygdala enlargement: a subtype of temporal lobe epilepsy. BMC Neurol 2014; 14 (194). DOI: https://doi.org/10.1186/s12883-014-0194-z.
Peedicail JS, Sandy S, Singh S, et al. Long term sequelae of amygdala enlargement in temporal lobe epilepsy. Seizure 2020; 74: 33-40, DOI: https://doi.org/10.1016/j.seizure.2019.11.015.
Reyes A, Thesen T, Kuzniecky R, et al. Amygdala enlargement: Temporal lobe epilepsy subtype or nonspecific finding? Epilepsy Res. 2017;132: 34-40. DOI: https://doi.org/10.1016/j.eplepsyres.2017.02.019.

Images/Tables

Sample Case:

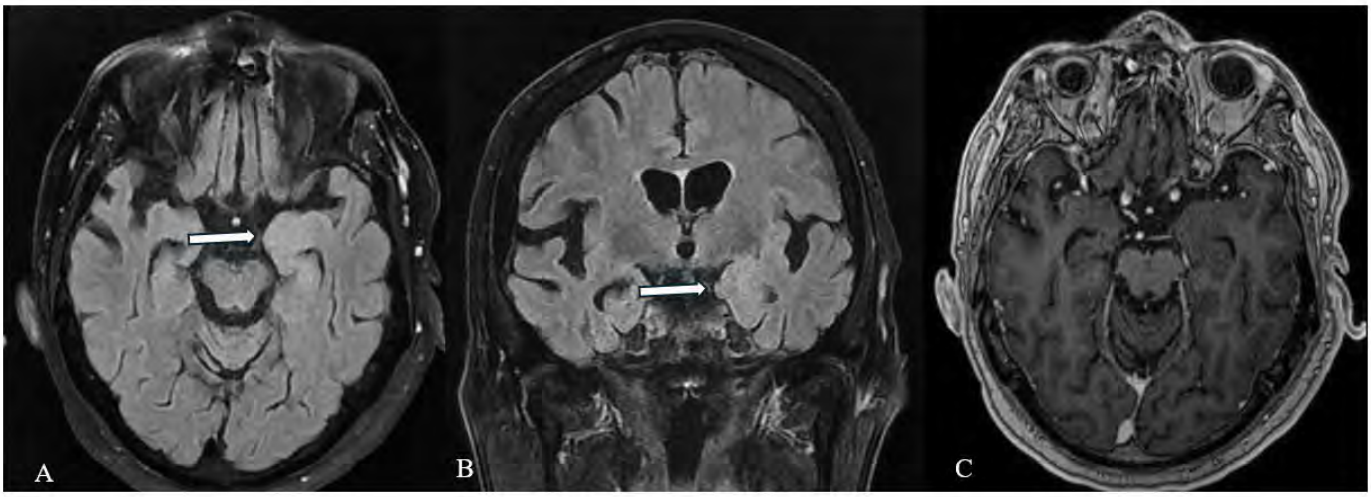


Fig 1: Axial T2 FLAIR (A), Coronal T2 FLAIR (B) and Axial T1 Post Contrast (C) images demonstrate a mildly expansile lesion centered in the left amygdala and extending into the left pyriform cortex without corresponding enhancement.

264

Understanding Head and Neck Vascular Malformations: A Multimodality Imaging Guide Through Diagnosis, Treatment, and Beyond

Diego A Mongui Moya Heah and Neck Fellow Ship, NICOLAS ROSSO Staff, Cecilia E. Marenco Staff, Manuel S Perez Akly Staff, Cristina H. Besada Section chief

Hospital Italiano de buenos Aires, Buenos Aires, Buenos Aires, Argentina

Abstract Category

Head and Neck

Summary & Objectives

This educational exhibit essay on head and neck vascular malformations will:

1. Provide a systematic approach to recognize imaging patterns across different modalities
2. Illustrate key diagnostic features that differentiate various types of vascular malformations
3. Demonstrate characteristic post-treatment changes and their clinical significance
4. Present a practical imaging-based approach to follow-up and recurrence detection

Purpose

To present a comprehensive pictorial review of the imaging characteristics of head and neck vascular malformations, highlighting diagnostic patterns, treatment response features, and follow-up findings that impact clinical management.

Materials & Methods

This educational exhibit presents selected cases from our institutional experience (2015-2023) demonstrating typical and atypical imaging features of head and neck vascular malformations. Cases were selected to illustrate: 1) Classic imaging patterns on ultrasound, MRI, CT, and Digital Subtraction Angiography (DSA) for each malformation type according to International Society for the Study of Vascular Anomalies (ISSVA) classification, 2) Key diagnostic features differentiating low-flow from high-flow lesions, 3) Spectrum of post-treatment changes, and 4) Imaging patterns of treatment success and failure. Each case includes correlative imaging across multiple modalities with emphasis on specific diagnostic features and follow-up findings.

Results & Conclusion

Results: The exhibit is organized by malformation type with comparison of imaging features:

- Venous malformations: Demonstration of characteristic serpentine morphology, phleboliths, and variable post-sclerotherapy patterns including successful volume reduction versus residual flow
- Lymphatic malformations: Illustration of macro versus microcystic components, fluid-fluid levels, and post-treatment septation changes
- Arteriovenous malformations: Showcase of flow void patterns, nidal architecture, and three distinct post-embolization outcomes (complete resolution, stable residual disease, and recurrence)
- Combined malformations: Complex imaging patterns requiring multimodality assessment

Key teaching points include:

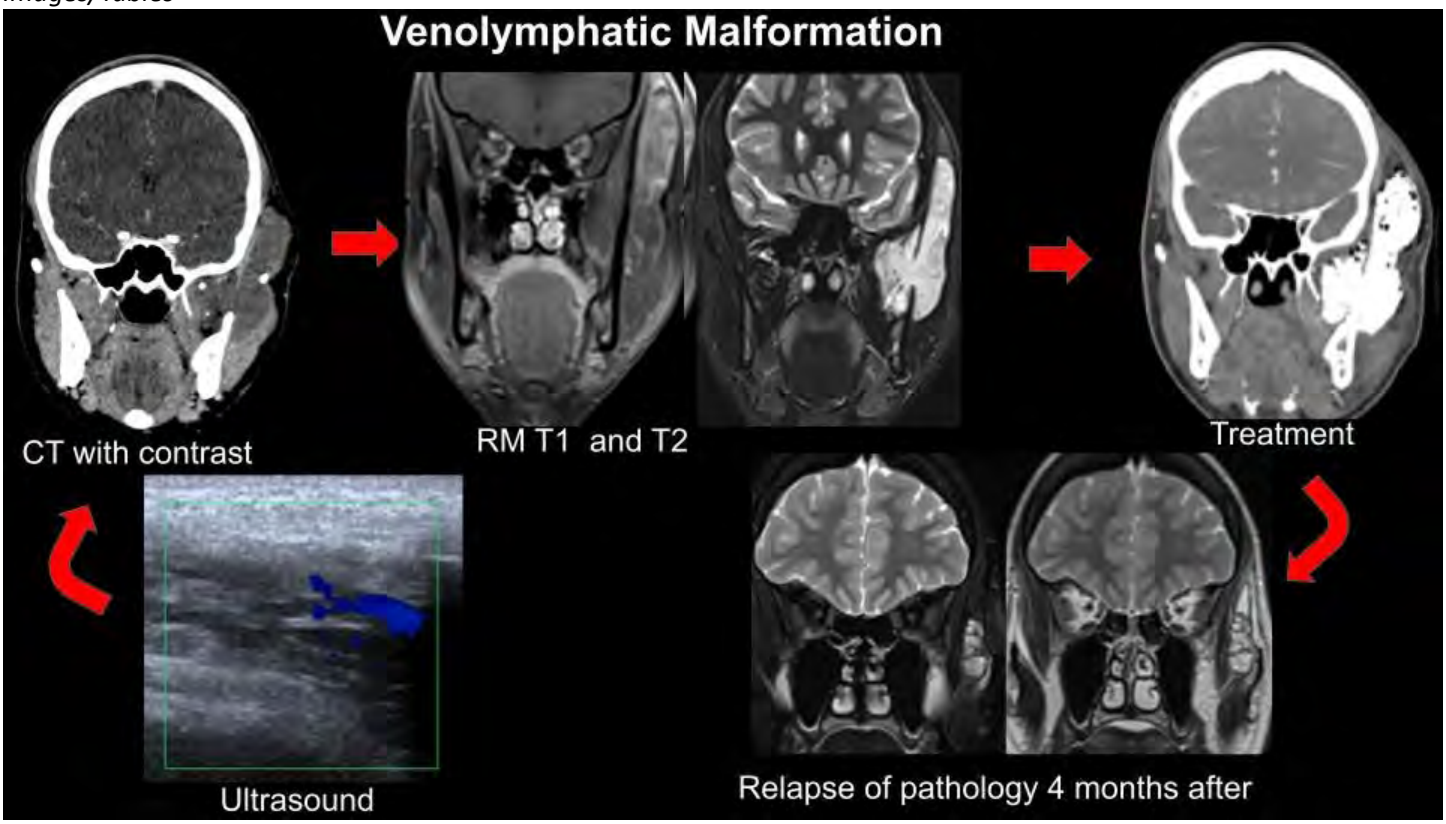
- Diagnostic criteria for each malformation type across imaging modalities
- Essential pre-treatment imaging features that guide therapeutic planning
- Standardized approach to post-treatment imaging assessment
- Critical imaging patterns that predict treatment success or failure
- Role of different imaging modalities in long-term surveillance

Conclusion: This educational iconographic exhibit provides a structured approach to the imaging evaluation of head and neck vascular malformations. Through carefully selected cases and side-by-side comparisons, we demonstrate key imaging features that facilitate accurate diagnosis, guide treatment planning, and enable effective post-treatment monitoring. Understanding these imaging patterns is crucial for optimal patient management and early detection of recurrence.

References

1. Brahmbhatt AN, Skalski KA, Bhatt AA. Vascular lesions of the head and neck: an update on classification and imaging review. Insights Imaging 2020;11:1-18
2. Bertino F, Trofimova AV, Gilyard SN, et al. Vascular anomalies of the head and neck: diagnosis and treatment. Pediatr Radiol 2021;51:1162-84
3. Sadick M, Wohlgemuth WA, Huelse R, et al. Interdisciplinary management of head and neck vascular anomalies: clinical presentation, diagnostic findings and minimally invasive therapies. Eur J Radiol Open 2017;4:63-8
4. Gallant SC, Chewning RH, Orbach DB, et al. Contemporary management of vascular anomalies of the head and neck-Part 1: vascular malformations: a review. JAMA Otolaryngol Head Neck Surg 2021;147:197-206
5. Lee JW, Chung HY. Vascular anomalies of the head and neck: current overview. Arch Craniofac Surg 2018;19:243-7

Images/Tables



268

Subarachnoid Contrast Staining – A Uncommon Entity

Joshua R Volin MD, Saumya Gurbani MD, Aline Camargo MD, Dan Cohen-Addad MD
Emory University, Atlanta, GA, USA

Abstract Category

Interventional/Vascular/Stroke

Summary & Objectives

SUMMARY

Contrast staining is commonly observed in subdural collections and infarcted brain tissues following diagnostic and interventional procedures like mechanical thrombectomy.[1,2] While subarachnoid contrast staining after interventions is well-documented, its occurrence in the absence of intervention is rarely discussed.[3] This exhibit presents two cases of subarachnoid hyperdensity initially misdiagnosed as subarachnoid hemorrhage (SAH) but later confirmed as benign contrast staining. Awareness of this rare phenomenon and the use of advanced imaging techniques, such as dual-energy CT (DECT) and MRI, are essential for differentiating contrast staining from true hemorrhage to prevent unnecessary treatment.[4]

OBJECTIVES

- Review common contrast staining patterns in subdural collections and parenchyma.
- Highlight the role of DECT and MRI in distinguishing contrast staining from hemorrhage.
- Present cases of subarachnoid contrast staining confirmed by imaging.

Purpose

PURPOSE

This exhibit aims to raise awareness of rare instances of subarachnoid contrast staining in cases without intracranial intervention but where contrast-enhanced imaging preceded the appearance of subarachnoid hyperdensity. It underscores the importance of advanced imaging techniques in distinguishing staining from hemorrhage, thereby reducing the risk of misdiagnosis and avoiding unnecessary interventions.

Materials & Methods

MATERIALS & METHODS

Materials:

- Two cases of patients who developed subarachnoid hyperdensity following diagnostic contrast administration, without a history of intracranial endovascular intervention.
- Imaging included multiple non-contrast head CTs, MRI, and Dual-Energy CT (DECT), all confirming contrast staining.

Methods:

- Case Selection: Identified patients with unexplained subarachnoid hyperdensity.
- Imaging and Diagnostic Confirmation: Subarachnoid contrast staining was confirmed through follow-up CT head scans showing rapid resolution of hyperdensity, no sulcal signal abnormality on MRI, and iodine subtraction on DECT.

Results & Conclusion

RESULTS

Both cases exhibited contrast staining in the subarachnoid space following contrast administration for diagnostic purposes. Neither case involved endovascular intervention. Imaging confirmation was provided by MRI, DECT, and follow-up CT head scans.

CONCLUSION

Contrast staining in the subdural space or parenchyma is common; however, contrast staining in the subarachnoid space without recent intracranial intervention is rare and may mimic SAH. While ruling out SAH is essential, awareness of possible subarachnoid contrast staining and the appropriate use of advanced imaging can prevent misdiagnosis and avoid unnecessary diagnostic tests.

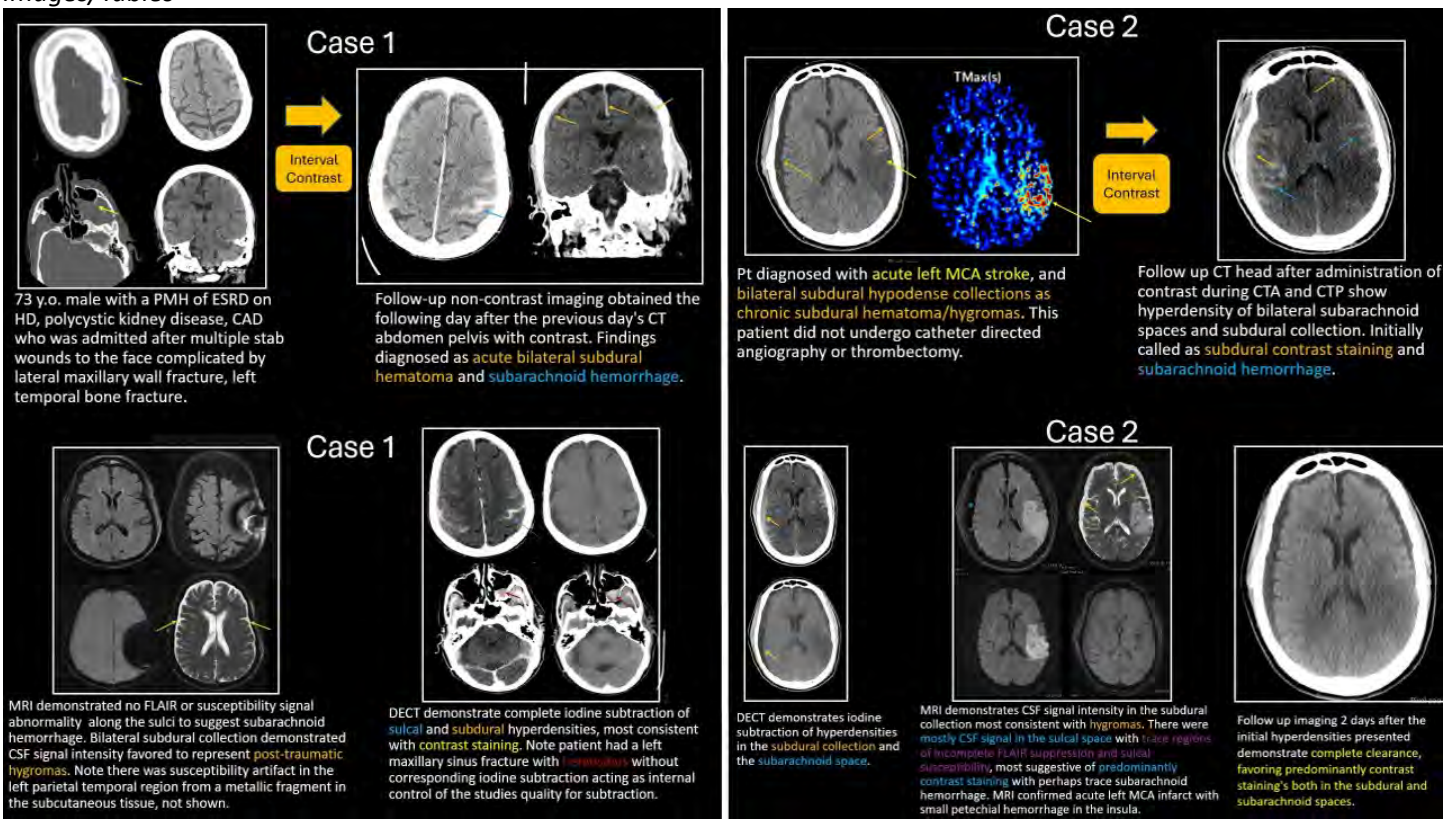
References

Rennert J, Hamer OW. Large subdural effusions after angiography mimicking acute subdural hematoma. J Comput Assist Tomogr 2010;34:249–50. DOI: https://10.1097/RCT.0b013e3181c6e704

Vangosa AB, Tortora D, Modestino F, et al. Reversible and Asymptomatic Gyral and Subarachnoid Contrast Enhancement after Carotid Stenting. Neuroradiol J 2015;28:184–6. DOI: https://10.1177/1971400915576630

Huda SA, Ahmed M, Sampat PJ, et al. Contrast extravasation mimicking subarachnoid hemorrhage after cardiac catheterization. Cureus 2020;12:e9212. DOI: https://10.7759/cureus.9212
Muhammad N, Ramayya AG, Srinivasan VM. Clinical Image: Contrast-Induced Encephalopathy Mimicking Subarachnoid Hemorrhage. World Neurosurg 2023;176:227–8. DOI: https://10.1016/j.wneu.2023.05.043

Images/Tables



271

Multimodal Imaging Approach to Primary Progressive Aphasia (PPA)

Michelle Chen MD[1], Faizullah Mashriqi MD[1], Marc L Gordon MD[1], Michelle Roytman MD[2], Ana M Franceschi MD, PhD[1]
[1]Donald and Barbara Zucker School of Medicine at Hofstra/Northwell, Manhasset, NY, USA. [2]Weill Cornell Medicine, New York, NY, USA

Abstract Category

Adult Brain Inflammatory/Infectious Disease/Degenerative/Metabolic

Summary & Objectives

Neurodegenerative disorders, such as primary progressive aphasia (PPA), are a clinically and histopathologically diverse group of conditions associated with progressive neurologic dysfunction. Specifically, PPA is characterized by language-predominant impairment associated with atrophy of the dominant language hemisphere. Notably, PPA can be classified into three subtypes: logopenic variant (lvPPA – AD pathology), semantic variant (svPPA – TDP-43 pathology), and nonfluent/agrammatic variant (nfvPPA – 4R TAU pathology) based on clinical features, pathologic evaluation, and radiologic findings. Each of the three PPA variants demonstrates characteristic features on multimodal structural, functional, and molecular neuroimaging, often identified as typical patterns of atrophy and/or hypometabolism. (Figure 1)

This educational exhibit aims to illustrate the structural, molecular, and functional imaging features of PPA and how it can support neuroradiologists in making a prompt diagnosis which confers significant implications for patient outcomes and therapeutic triaging.

Purpose

N/A

Materials & Methods

N/A

Results & Conclusion

PPA diagnosis relies on an interdisciplinary approach that combines findings from clinical presentation, neuropsychological assessment, histopathologic biomarkers, and imaging features. Recognizing characteristic features of PPA on multimodality imaging confers important prognostic implications, as early and accurate detection allows for improved outcomes through targeted therapeutic interventions.

References

Reference One:

Gorno-Tempini ML, Hillis AE, Weintraub S, et al. Classification of primary progressive aphasia and its variants. Neurology. 2011;76(11):1006-1014. doi:10.1212/WNL.0b013e31821103e6

Reference Two:

Jalilianhasanpour R, Beheshtian E, Sherbaf G, et al. Functional Connectivity in Neurodegenerative Disorders: Alzheimer's Disease and Frontotemporal Dementia. Top Magn Reson Imaging. 2019;28(6):317-324. doi:10.1097/RMR.0000000000000223

Reference Three:

Magnin E, Démonet JF, Wallon D, et al. Primary Progressive Aphasia in the Network of French Alzheimer Plan Memory Centers. J Alzheimers Dis. 2016;54(4):1459-1471. doi:10.3233/JAD-160536

Reference Four:

Montembeault M, Brambati SM, Gorno-Tempini ML, et al. Clinical, Anatomical, and Pathological Features in the Three Variants of Primary Progressive Aphasia: A Review. Front Neurol. 2018;9:692. Published 2018 Aug 21. doi:10.3389/fneur.2018.00692

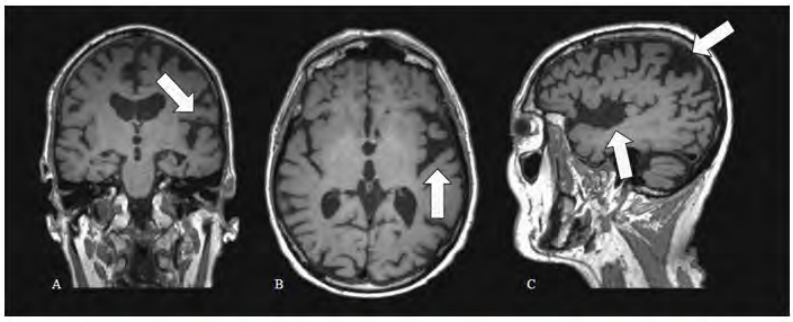
Reference Five:

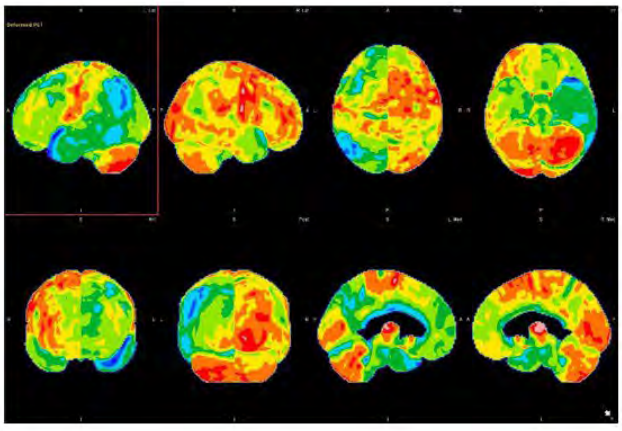
Roytman M, Chiang GC, Gordon ML, et al. Multimodality Imaging in Primary Progressive Aphasia. AJNR Am J Neuroradiol. 2022;43(9):1230-1243. doi:10.3174/ajnr.A7613

Images/Tables

lvPPA Imaging Findings

- Top: Structural Imaging
  - Coronal T1-weighted MRI (A), axial T1-weighted MRI (B) and sagittal T1-weighted MRI (C)
  - Asymmetric widening of the left sylvian fissure
  - Left posterior perisylvian and temporoparietal atrophy
- Bottom: Molecular Imaging
  - ^{18}F-FDG PET 3D-SSPs (stereotactic surface projections)
  - Moderate to severe hypometabolism in the left lateral temporo-parietal lobes including in the left precuneus and posterior cingulate gyrus





279

Sniffing Out the Source: Imaging Evaluation of Epistaxis

Ken Chang MD PhD, Shweta Kumar MD
Stanford University, Stanford, CA, USA

Abstract Category

Head and Neck

Summary & Objectives

Epistaxis is a common condition that radiologists encounter in clinical practice. The condition can range in severity from minor insults to life-threatening emergencies. Although many instances of epistaxis are self-limiting and do not necessitate medical intervention, there are cases that require a more comprehensive evaluation to identify the underlying cause, such as severe or recurrent bleeding. This evaluation often includes advanced imaging assessments to accurately diagnose and guide treatment. Accurate diagnosis of the underlying etiology can be helpful in preventing potential complications and ensuring effective treatment. This exhibit is designed to enhance radiologists' expertise through exploration of the nasal anatomy, imaging techniques, and the radiologic findings associated with various differential diagnoses. By broadening understanding within these areas, radiologists can improve their diagnostic accuracy and expedite workup of patients experiencing epistaxis.

The objectives are:

1) To review nasal vascular anatomy.

2) To understand the role of imaging in conjunction with clinical history, physical examination, and laboratory testing during evaluation.

3) To recognize the common and uncommon differential diagnoses, including neoplasms and vascular malformations, and their associated imaging findings.

Purpose

As above

Materials & Methods

This exhibit will integrate literature review, anatomical diagrams, and clinical case studies to provide comprehensive education on epistaxis. A general overview of the presentation, risk factors, and diagnostic workup of epistaxis will be presented. Anatomical diagrams and angiographic images will be used to illustrate the detailed vascular anatomy of the nasal cavity, highlighting relevant branches from the external and internal carotid arteries. A series of clinical cases will then be used to demonstrate various etiologies of epistaxis, including traumatic, neoplastic, vascular, and systemic causes, each accompanied by common imaging findings. Lastly, a diagnostic tree will be presented to show an algorithmic approach to narrowing the differential diagnosis.

Results & Conclusion

This exhibit will showcase the utility of radiological imaging in the evaluation and management of recurrent or severe epistaxis. A thorough understanding of nasal vascular anatomy is important, especially in differentiating between anterior and posterior nasal bleeding. Anterior bleeds can typically be managed conservatively while posterior bleeds often necessitate invasive interventions. Moreover, understanding the clinical context, such as age, sex, pregnancy status, behaviors, trauma, and family history, is key to narrowing the differential diagnosis. Knowledge of additional symptoms, imaging findings in other anatomic locations, and a detailed family history can help reveal systemic conditions such as hereditary hemorrhagic telangiectasia and coagulopathies. Imaging techniques like CT, MR, and diagnostic angiography can play a role in accurately identifying vascular malformations and mapping various sinonasal neoplasms. Earlier recognition through imaging may expedite further workup and tailored treatment, which may include a combination of radiation, embolization, and surgery.

References

Gifford TO, Orlandi RR. Epistaxis. Otolaryngol Clin North Am. 2008 Jun;41(3):525-36, viii. doi:10.1016/j.otc.2008.01.003.

Koh E, Frazzini VI, Kagetsu NJ. Epistaxis: vascular anatomy, origins, and endovascular treatment. AJR Am J Roentgenol. 2000 Mar;174(3):845-51. doi:10.2214/ajr.174.3.1740845.

Krajina A, Chrobok V. Radiological diagnosis and management of epistaxis. Cardiovasc Intervent Radiol. 2014 Feb;37(1):26-36. doi:10.1007/s00270-013-0776-y.

Willems PWA, Farb RI, Agid R. Endovascular treatment of epistaxis. AJNR Am J Neuroradiol. 2009 Oct;30(9):1637-45. doi:10.3174/ajnr.A1607.

282

Optimizing Imaging in the Diagnosis of Hearing Loss: The Role of Non-Contrast MRI in Initial Evaluation

Artineh Hayrapetian M.D., Ajay Malhotra MBBS, MD, MMM
Yale, New Haven, CT, USA

Abstract Category

Head and Neck

Summary & Objectives

Hearing impairment is a common complaint that leads patients to seek care from emergency rooms, primary care providers, and ENT specialists. The differential diagnosis of hearing loss is broad, ranging from benign causes like cerumen impaction to more serious conditions such as malignancies. In addition to physical examination and audiometric testing, imaging studies are essential for identifying the underlying etiology of hearing loss.

Purpose

The purpose of this presentation is to demonstrate the value of imaging in the differential diagnosis of hearing loss, with an emphasis on the fact that contrast-enhanced imaging is not always necessary in the initial evaluation.

Materials & Methods

A review of current literature on imaging techniques for the evaluation of hearing loss was conducted. The literature highlights that the need for contrast-enhanced imaging is often associated with cerebellopontine angle masses, such as acoustic neuromas or labyrinthitis. In rare instances of hearing loss, an MRI without contrast is recommended as the first imaging approach.

Results & Conclusion

Hearing loss can result from a variety of causes, most of which are benign. As an initial step, MRI without contrast is generally preferred over the use of contrast, as it minimizes the risks associated with contrast administration and reduces scan time. Contrast-enhanced imaging may be considered in rare cases involving cochlear or cerebellopontine angle tumors or labyrinthitis, where clinical symptoms suggest a more serious underlying cause and non-contrast imaging is inconclusive. Performing an initial non-contrast MRI helps eliminate potential risks related to contrast use and facilitates timely, appropriate diagnosis.

References

1. ACR Appropriateness Criteria Hearing Loss and/or Vertigo. Expert Panel on Neurologic Imaging. *J Am Coll Radiol*. 2018 Nov;15(11S)
2. Davies J, et al. Gadolinium: pharmacokinetics and toxicity in humans and laboratory animals. *Arch Toxicol*. 2022;96:403–429.
3. Shah LM, Wiggins RH III. Imaging of Hearing Loss. *Neuroimaging Clin N Am*. 2009 Aug;19(3):287-306. doi: 10.1016/j.nic.2009.06.010.
4. Annesley-Williams DJ, et al. Magnetic resonance imaging in the investigation of sensorineural hearing loss: is contrast enhancement still necessary? *J Laryngol Otol*. 2001;115:14–21.
5. Cho J, et al. Sudden sensorineural hearing loss associated with inner ear lesions detected by magnetic resonance imaging. *PLOS ONE*.

283

Review of Complex Maxillofacial Injuries, Postoperative Findings, and Complications

Kevin Jiang MD, Justin Tran MD, Achint Singh MD, Bundhit Tantiwongkosi MD
UT Health San Antonio, San Antonio, TX, USA

Abstract Category

Head and Neck

Summary & Objectives

Complex maxillofacial injuries are a common encounter in high impact traumatic clinical settings. CT is the first line modality for identifying clinically relevant facial fractures. These fractures patterns involve some subset of the eight different osseous buttresses that support the face. And surgical management is centered around reestablishing the integrity of these fractured buttresses. Follow up imaging is also helpful for recognizing possible postoperative complications.

- Understand the 8 osseous buttresses of the face.
- Identify common complex facial fracture patterns.
- Recognize common postsurgical hardware and possible complications.

Purpose

This educational exhibit will illustrate relevant information the radiologist can report in the setting of complex maxillofacial traumas by reviewing common facial fracture patterns, related postsurgical hardware, and possible complications.

Materials & Methods

We reviewed computed tomography and 3D reconstruction of high impact complex facial trauma patients at a level 1 trauma center in San Antonio, TX.

Results & Conclusion

Over 250 cases of complex facial fractures were identified at our institution. They could be categorized into discrete fracture patterns, including LeFort I/II/III, zygomaticomaxillary complex, naso-orbitoethmoid, and mandibular fractures. It's important for the radiologist to recognize and report these specific fracture patterns as they affect surgical management. In particular, 3D reconstruction can be helpful in identifying these fractures. On follow-up imaging, the radiologists can add value by evaluating postsurgical hardware for any possible associated complications such as hardware failure or infection.

References

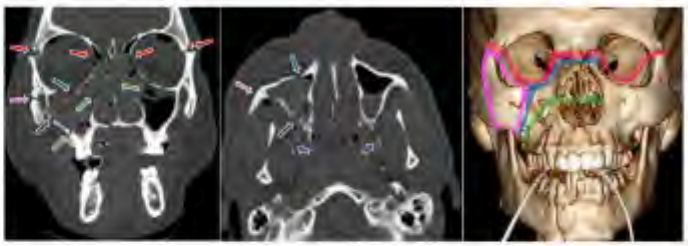
Dreizin D, Nam AJ, Diaconu SC, et al. Multidetector CT of Midfacial Fractures: Classification Systems, Principles of Reduction, and Common Complications. *Radiographics* 2018;38(1):248-274. DOI: https://doi.org/10.1148/rg.2018170074

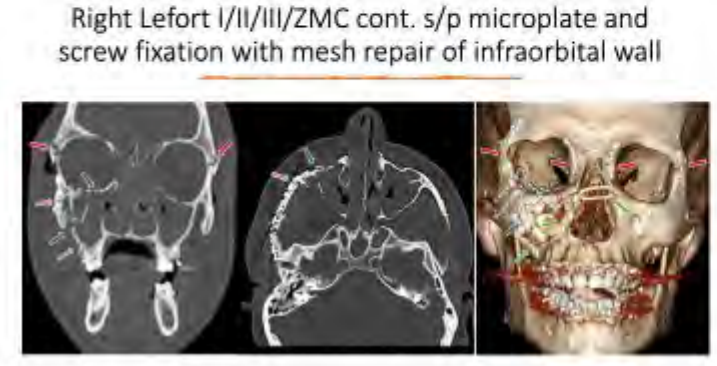
Smith EB, Patel LD, Dreizin D. Postoperative Computed Tomography for Facial Fractures. *Neuroimaging Clin N Am.* 2022;32(1):231-254. DOI: https://doi.org/10.1016/j.nic.2021.08.004

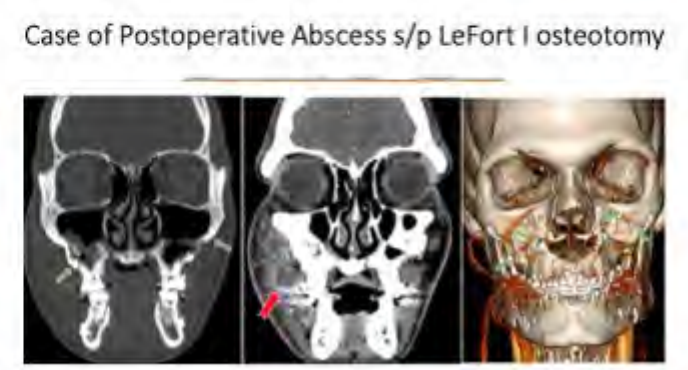
Winegar BA, Murillo H, Tantiwongkosi B. Spectrum of critical imaging findings in complex facial skeletal trauma. *Radiographics* 2013;33(1):3-19. DOI: https://doi.org/10.1148/rg.331125080

Images/Tables









292

Neck masses during the first year of life: Pearls and pitfalls for the neuroradiologist

Johna Joseph BA[1], Sarah J Moum MD[2]
[1]Northwestern University Feinberg SOM, Chicago, IL, USA. [2]Ann & Robert H. Lurie Children's Hospital of Chicago, Northwestern University Feinberg SOM, Chicago, IL, USA

Abstract Category

Pediatrics

Summary & Objectives

Summary

Neck masses presenting during early infancy pose a diagnostic challenge for neuroradiologists and clinicians alike due to the small size of these patients, rapidly changing anatomy, and potential for associated airway compromise. Prompt and accurate imaging of suspected lesions not only helps to differentiate benign and malignant pathologies but also guides acute and long-term patient management decisions. We aim to present a comprehensive review of the key clinical and imaging characteristics of neck masses presenting during the first year of life, including the common differential considerations categorized by neck space location. Technical imaging considerations will be discussed. Potential diagnostic pitfalls will also be reviewed.

Educational Objectives

- A comprehensive understanding of key imaging findings for neck lesions presenting during early infancy as well as practical imaging techniques for this patient population facilitates timely patient diagnosis and treatment as well as provides insights into patient prognosis.
- The spectrum of neck masses presenting during the first year of life will be presented categorized by neck space location, including:
    - Congenital (i.e. thyroglossal duct cyst, branchial cleft anomalies, foregut duplication cyst, lingual thyroid, thymic cyst, ectopic thymus)
    - Vascular malformations (i.e. venolymphatic malformation, infantile and congenital hemangioma, arteriovenous malformation)
    - Benign neoplastic or tumor-like lesions (i.e. fibromatosis colli, teratoma, aggressive fibromatosis and other fibrous lesions, plexiform neurofibroma)
    - Malignant neoplastic lesions (i.e. rhabdomyosarcoma and other soft tissue sarcomas, neuroblastoma, leukemia)
- For each differential consideration, the characteristic diagnostic features by ultrasound, MRI, and CT will be discussed. Clinical presentations, potential complications, and underlying pathogeneses will also be presented.
- Imaging plays a crucial role in monitoring treatment response for certain infantile neck masses, especially in cases where non-surgical treatment is pursued, such as lymphatic malformations.
- Common imaging pitfalls, clinical mimics, and important anatomical differences in this patient population will be highlighted, with a focus on strategies to improve diagnostic accuracy.
- Helpful imaging techniques tailored for this patient population, including feed and swaddle and motion correction techniques, will be discussed.

Purpose

N/A

Materials & Methods

N/A

Results & Conclusion

N/A

References

1. Meuwly JY, Lepori D, Theumann N, et al. Multimodality imaging evaluation of the pediatric neck: techniques and spectrum of findings. *Radiographics* 2005;25(4):931-48.
2. Mirsky DM, Shekdar KV, Bilaniuk LT. Fetal MRI: head and neck. *Magn Reson Imaging Clin N Am* 2012;20(3):605–18.
3. Ng TW, Xi Y, Schindel D, et al. Fetal head and neck masses: MRI prediction of significant morbidity. *AJR Am J Roentgenol* 2019;212(1):215–21.

4. Restrepo R, Francavilla ML, Mas R, Lee EY. Up-to-date practical imaging evaluation of neonatal soft-tissue tumors: what radiologists need to know. *AJR Am J Roentgenol* 2017;209(1):195-204.
5. Vazquez E, Enriquez G, Castellote A, et al. US, CT, and MR imaging of neck lesions in children. *Radiographics* 1995;15(1):105-22.

Images/Tables

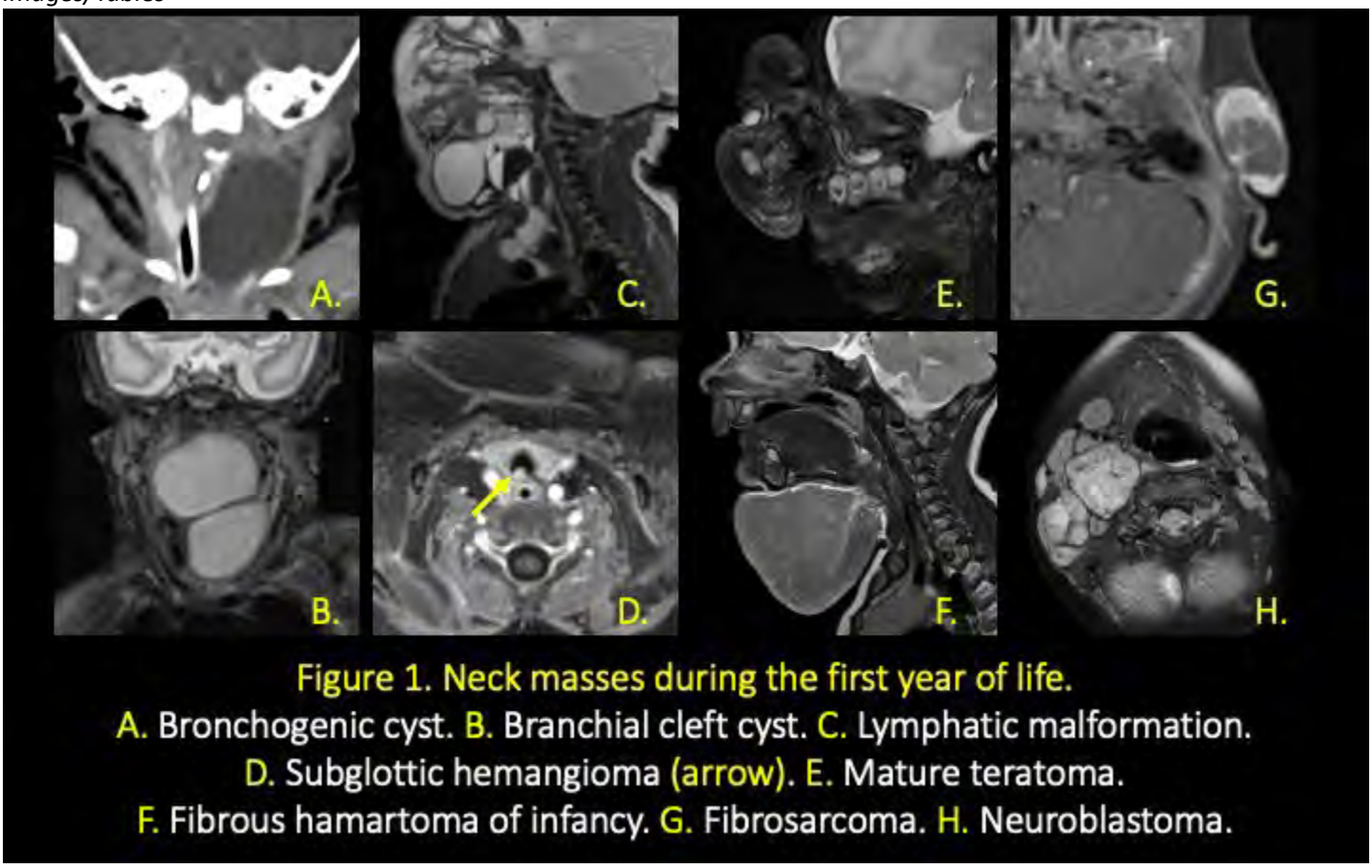


Figure 1. Neck masses during the first year of life.
A. Bronchogenic cyst. B. Branchial cleft cyst. C. Lymphatic malformation.
D. Subglottic hemangioma (arrow). E. Mature teratoma.
F. Fibrous hamartoma of infancy. G. Fibrosarcoma. H. Neuroblastoma.

301

Moyamoya Disease Revisited: Current State-of-the-Art MRI Insights and Predictors of Outcome After Revascularization

Mona Gad[1], Vivek Yedavalli[2]
[1]Department of Radiology, Mansoura University Faculty of Medicine, Mansoura, Dakahlia, Egypt. [2]Department of Radiology, Johns Hopkins University School of Medicine, Baltimore, MD, USA

Abstract Category

Interventional/Vascular/Stroke

Summary & Objectives

Educational Objectives:

1. Recognize the pathophysiology of Moyamoya disease.
2. Review the role of MRI in establishing the diagnosis and patient selection for revascularization.
3. Identify the treatment options for Moyamoya disease.
4. Elucidate the significance of advanced MRI sequences as imaging markers to predict the surgical outcome.

Purpose

The primary goal of this exhibit is to provide a brief overview on the role of advanced MRI techniques in diagnosis, presurgical mapping and therapeutic prognosis in the setting of Moyamoya vasculopathy.

Materials & Methods

In this exhibit, the following points will be discussed and illustrated with diagrams and cases.

A. Anatomy of the anterior circulation of the brain and Circle of Willis.
B. Definition and course of Moyamoya disease.

C. Diagnostic MRI features of Moyamoya disease which will include:
- State of cerebral vasculature in MRA and how to report MRA score.
- Significance of ivy sign (on FLAIR) and brush sign (on SWI.
- Pediatric Moyamoya MRI score.

D. Management options and postoperative complications.

E. Leveraging the state-of-the-art MRI techniques in determining the hemodynamic status and predictors of therapeutic outcomes which encompass the following:
- MR perfusion sequences including (DSC and ASL) and the importance of standardized MRI perfusion scoring system.
- Vessel wall imaging to identify patients at higher risk of future cerebrovascular events.
- Resting-state functional MRI for detecting the cerebrovascular reactivity changes.

Results & Conclusion

Moyamoya disease is an important cause of pediatric stroke. Neuroimaging plays a pivotal role in diagnosis and clinical decision making for such patients. Moreover, the use of current state-of-the-art MRI techniques can provide new insights for understanding the morphological changes of the cerebral vessels along with the hemodynamic compromise aiming at optimal patient selection for revascularization and better prediction of the therapeutic outcomes.

References

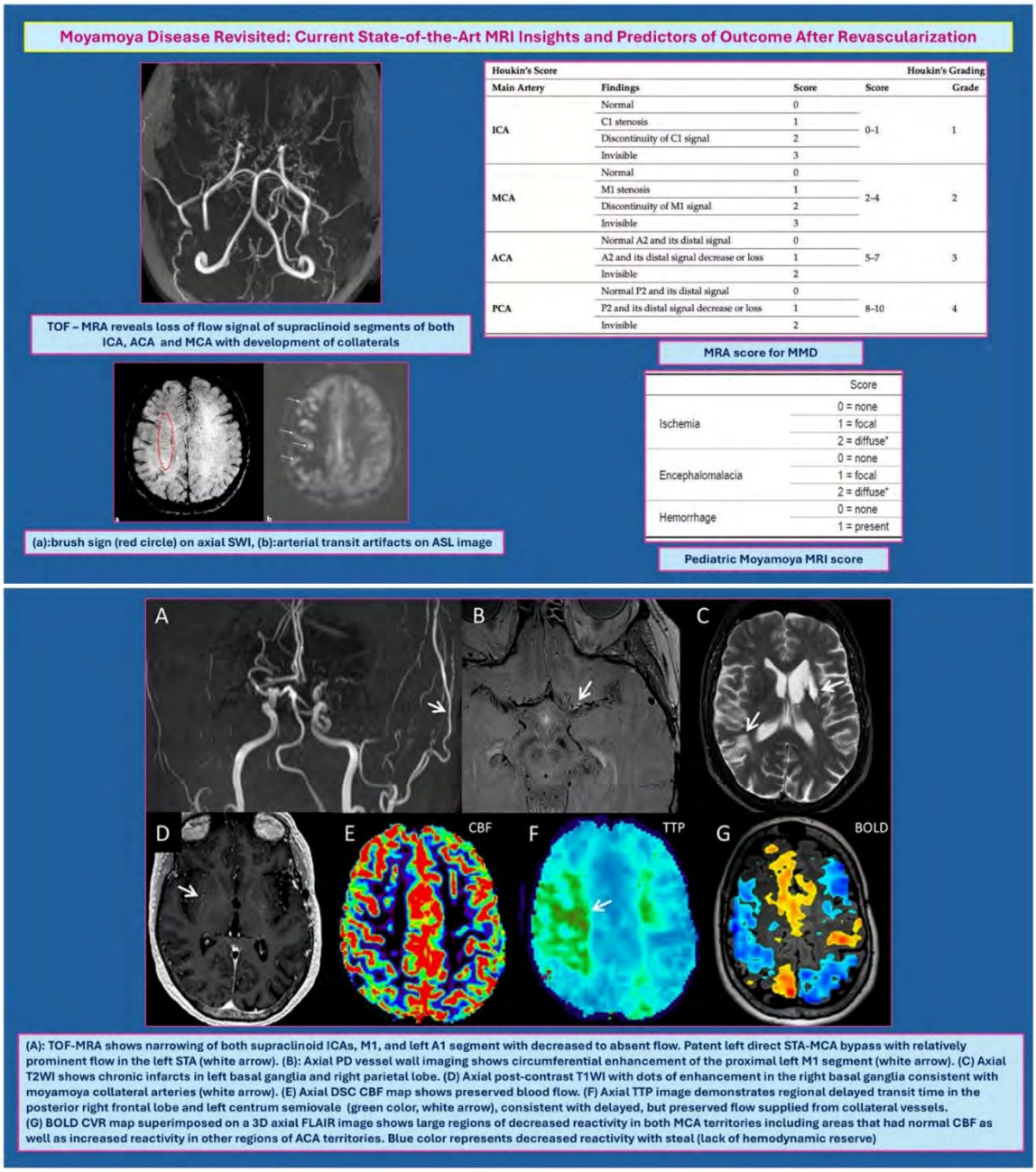
1. Li J, Jin M, Sun X, et al. Imaging of Moyamoya Disease and Moyamoya Syndrome: Current Status. J Comput Assist Tomogr. 2019;43(2):257-263. DOI:10.1097/RCT.0000000000000834

2. Lin YH, Kuo MF, Lu CJ, et al. Standardized MR perfusion scoring system for evaluation of sequential perfusion changes and surgical outcome of moyamoya disease. American Journal of Neuroradiology. 2019;40(2):260-266. DOI:10.3174/ajnr.A5945

3. Du L, Jiang H, Li J, Duan T, Zhou C, Yan F. Imaging methods for surgical revascularization in patients with moyamoya disease: an updated review. Neurosurg Rev. 2022;45(1):343-356. DOI:10.1007/s10143-021-01596-0

4. Filimonova E, Ovsiannikov K, Rzaev J. Neuroimaging in Moyamoya angiopathy: Updated review. Clin Neurol Neurosurg. 2022;222. DOI:10.1016/j.clineuro.2022.107471

Images/Tables



Houkin's Score				Houkin's Grading
Main Artery	Findings	Score	Score	Grade
ICA	Normal	0	0–1	1
	C1 stenosis	1		
	Discontinuity of C1 signal	2		
	Invisible	3		
MCA	Normal	0	2–4	2
	M1 stenosis	1		
	Discontinuity of M1 signal	2		
	Invisible	3		
ACA	Normal A2 and its distal signal	0	5–7	3
	A2 and its distal signal decrease or loss	1		
	Invisible	2		
PCA	Normal P2 and its distal signal	0	8–10	4
	P2 and its distal signal decrease or loss	1		
	Invisible	2		

	Score
Ischemia	0 = none
	1 = focal
	2 = diffuse*
Encephalomalacia	0 = none
	1 = focal
	2 = diffuse*
Hemorrhage	0 = none
	1 = present

306

Imaging Insights: A Practical Navigation Guide for Post-Treatment Evaluations of Head and Neck Tumors

Manuel S Perez Akly[1], Cecilia E. Marenco MD[2], Angeliet K. Carvajal S. MD[2], Diego A. Mongui M. Fellowship[2], Tatiana Gillanders MD[2], Manuel S. Perez A. MD.[2], Luis I. Belisle MD[2], Mauricio Valiere G. MD[2], Cristina H. Besada Section Chief[2]
[1]Hospital Italiano de buenos Aires, Buenos Aires, Buenos Aires, Argentina. [2]Hospital Italiano de Buenos Aires, Buenos Aires, CABA, Argentina

Abstract Category

Head and Neck

Summary & Objectives

1. Provide a general approach to the treatment methods available for head and neck cancer.
2. Identify the typical findings in CT and MRI images after treatment in patients with head and neck cancer.
3. Illustrate the key diagnostic features that differentiate post-treatment changes from tumor recurrence.

Purpose

To present a practical and comprehensive guide to analyze images in post-treatment controls of head and neck tumors, highlighting typical image patterns with regard to expected post-treatment findings and differentiating them from probable tumor recurrences/complications.

Materials & Methods

This educational exhibition presents selected cases from our institutional experience (2011-2024) in the follow-up and post-treatment control of head and neck tumors, where the radiological findings expected by the treatment are demonstrated.

Cases were selected to illustrate:

1) The spectrum of post-treatment changes to be expected on computed tomography (TC), magnetic resonance imaging (RM), or positron emission tomography (PET/TC). 2) key diagnostic characteristics to differentiate tumor recurrence. and 3) imaging patterns of post-treatment complications. Each case includes correlative imaging in multiple modalities with emphasis on specific diagnostic features for oncologic follow-up.

Results & Conclusion

Results: The exhibition is organized by type of treatment and its comparison of radiological findings in different imaging methodologies.

Post-surgical findings: morphological changes dependent on the size of the defect, with different materials used for tissue reconstruction.

Post-radiotherapy findings: early changes (mucosal and soft tissue edema, enlargement of the submandibular glands, etc.) and late changes (atrophy of the submandibular glands, soft tissue edema).

Post-chemotherapy - immunotherapy findings: no response, partial response or complete response.

Findings in tumor recurrence: hyperintense soft tissue lesion on T2, with diffusion restriction, infiltrated lymph nodes.

Key teaching points include:

- Standardized approach for post-treatment imaging evaluation of head and neck tumors.
- Patterns of radiological changes to be expected in post-treatment controls.
- Key points of imaging findings in tumor recurrence.

Conclusion: Understanding the expected imaging patterns in post-treatment follow-up of head and neck tumors and being able to differentiate them from findings suggestive of tumor recurrence is crucial for optimal patient management and early detection of recurrences.

References

1. Siegel RL, Miller KD, Fuchs HE, Jemal A. Cancer statistics, 2022. CA Cancer J Clin 2022;72(1):7–33.

2.Gonzalo Nazar M. - Gustavo Vial C. - Álvaro Ibarra V. - Lluis Cabezas l - Tumores de cabeza y cuello - REV. MED. CLIN. CONDES - 2007; 18(4) 360 - 335]

3.Saito N, Nadgir RN, Nakahira M, et al . Posttreatment CT and MR imaging in head and neck cancer: what the radiologist needs to know. RadioGraphics 2012;32(5):1261–1282; discussion 1282–1284. https://doi.org/10.1148/rg.325115160

4.Hiyama, T., Miyasaka, Y., Kuno, H., Sekiya, K., Sakashita, S., Shinozaki, T., & Kobayashi, T. (2024). Posttreatment head and neck cancer imaging: Anatomic considerations based on cancer subsites. RadioGraphics, 44(3). https://doi.org/10.1148/rg.230099

Images/Tables

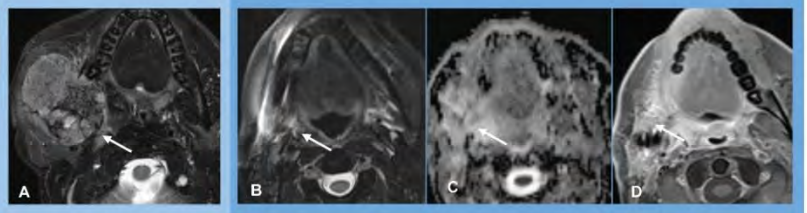
IMAGING INSIGHTS

A PRACTICAL NAVIGATION GUIDE FOR POST-TREATMENT EVALUATIONS OF HEAD AND NECK TUMORS

EXPECTED POST-TREATMENT FINDINGS

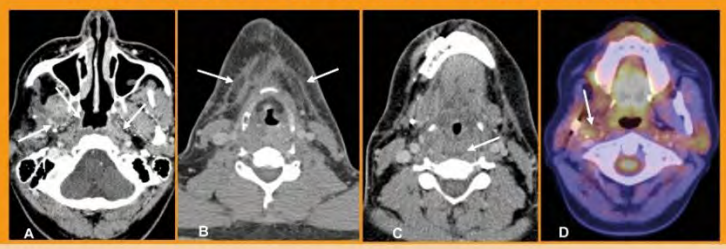
PREOPERATIVE

POSTOPERATIVE



Patient with Clear Cell Odontogenic Carcinoma of the right mandible. Post-treatment imaging shows expected findings: intermediate/low T2 signal (B), high ADC signal (C), and minimal post-contrast enhancement (D), with no evidence of residual tumor

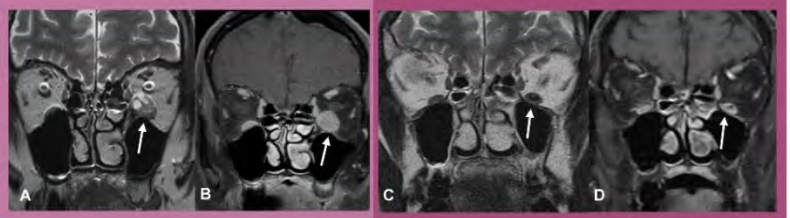
RADIOTHERAPY TREATMENT - EARLY FINDINGS



Follow-up with PET-CT 12 weeks post-radiotherapy shows soft tissue reticulation and mucosal enhancement post-contrast (A), thickening of the platysma muscle (B), fluid in the retropharyngeal space (C). A lymph node shows FDG uptake, with biopsy results negative for tumor infiltration (D).

PRE-IMMUNOTHERAPY

POST-IMMUNOTHERAPY



Melanoma metastasis in the left inferior rectus muscle (A-B), treated with Trametinib and Dabrafenib, showing complete response (C-D).

310

Comprehensive Imaging Review of Retroclival Hematomas: Implications for Diagnosis and Management

Dhanush Jayananda Amin MD, Ali Rezaei MD, Zahra Saadatpour MD, Manoj Tanwar MD
University of Alabama at Birmingham, Birmingham, AL, USA

Abstract Category

Adult Neoplasms/Epilepsy/Trauma

Summary & Objectives

Retroclival hematomas (RCHs) are a rare but critical condition characterized by haemorrhage along the posterior aspect of the clivus, with distinct etiologies and clinical manifestations across pediatric and adult populations. Due to its proximity to vital neurovascular structures, such as the brainstem and cranial nerves, RCH necessitates prompt and precise imaging for effective diagnosis and management. Most reported cases focus on pediatric presentations, creating a need for comprehensive understanding and imaging-focused analysis of RCHs in adults. This exhibit aims to address this gap by reviewing CT and MRI characteristics of RCH in adults, exploring their role in guiding clinical decisions.

Purpose

This educational exhibit aims to emphasize the critical role of CT and MRI imaging in the accurate diagnosis, characterizing RCHs, distinguishing them from other skull base pathologies, and evaluating the implications for treatment.

Materials & Methods

In this exhibit, we would be discussing the anatomy of the retroclival region, pathophysiology of bleed, causes and imaging manifestation of RCH. RCH can either be traumatic or spontaneous. Anticoagulation therapy, vascular anomalies, hypertension, connective tissue disorders are few of the risk factors for spontaneous RCH. The review produces data from a comprehensive literature search of case reports concerning adult RCHs. Imaging features are analysed using computed tomography (CT) and magnetic resonance imaging (MRI) findings, with a focus on CT for initial haemorrhage assessment and MRI for detailed anatomical evaluation, hematoma staging, and detecting smaller lesions. Digital Subtraction Angiography (DSA) offers a highly detailed visualization of the vertebral and basilar arteries, which is essential for identifying vascular pathologies like dissection, pseudoaneurysms, or arterial stenosis. Imaging differentials are also reviewed to illustrate key distinctions from tumors (schwannoma, meningioma, craniopharyngioma, chordoma), abscesses, and cysts.

We would be presenting a variety of imaging examples (10), including cases of spontaneous subdural (Figure 1) and extradural RCH, traumatic RCH associated with fractures, extradural RCH mimicking meningioma, IgG4-related disease mimicking RCH. Additionally, MRI images demonstrating ligamentous injuries in these contexts will be shown.

Results & Conclusion

This exhibit concludes that early, accurate imaging is important for adult RCH diagnosis and management, which helps in timely and targeted treatments that can prevent severe complications and improve patient outcomes. Imaging provides critical information on the size, location, and potential impact of hematomas, helping clinicians determine the need for surgical intervention versus conservative management.

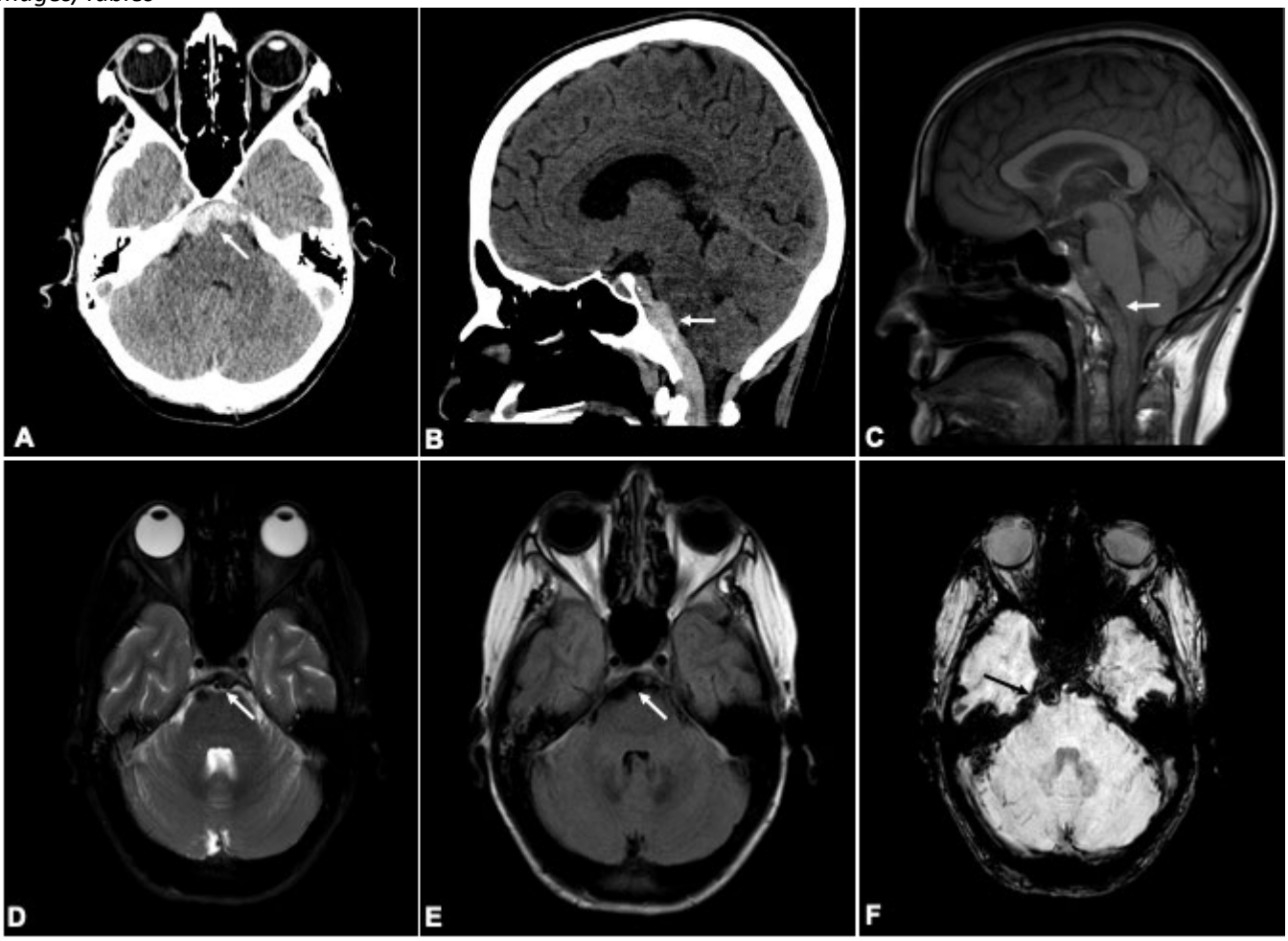
This review highlights key gaps in current research on imaging for adult retroclival hematomas (RCH), emphasizing the need for more studies to improve imaging-based diagnostic methods.

References

1. YusufSukru Caglar, K. Erdogan, CemilMustafa Kilinc, O. Mammadkhanli, O. Ozgural, U. Eroglu, Retroclival epidural hematoma: A rare location of epidural hematoma, case report, and review of literature, J Craniovertebr Junction Spine. 11 (4) (2020) 342.
2. P. Krishnan, R. Kartikueyan, S.R. Chowdhury, et al., Retroclival subdural hematoma: an uncommon site of a common pathology, Neurol India. 61 (5) (2013) 550–552, https://doi.org/10.4103/0028-3886.121951.
3. Medeiros, P. M., et al. (2014). Spontaneous spinal subdural hematoma associated with anticoagulant therapy. Arquivos de Neuro-Psiquiatria, 72(7), 539-540.

4. Tawk, R. G., et al. (2020). Nontraumatic retroclival hematoma: Case report and review of the literature. World Neurosurgery, 137, 138-141.
5. Saliou, G., Sacho, R. H., Power, S., & Tymianski, M. (2015). Clival hematomas: A case series and literature review of traumatic clival epidural and subdural hematomas. *Journal of Neurosurgery*, 122(6), 1408-1414. doi:10.3171/2014.10.JNS14393

Images/Tables



312

Image-Based Review of Common Deep Brain Stimulation Targets on CT and 7T MRI.

Mathew Smith M.D.[1], Sahith Mukku[2], Nathan Beckett[2], Jonathon Parker M.D. Ph.D.[2], Erik Middlebrooks MD[3], Ichiro Ikuta M.D.[4], Justin Cramer M.D.[4]

[1]Barrow Neurological Institute, Phoenix, AZ, USA. [2]Mayo Clinic Arizona, Phoenix, AZ, USA. [3]Mayo Clinic Florida, Jacksonville, FL, USA. [4]Mayo Clinic Arizona, Scottsdale, AZ, USA

Abstract Category

Adult Brain Inflammatory/Infectious Disease/Degenerative/Metabolic

Summary & Objectives

Deep brain stimulation (DBS) targets have traditionally been identified using coordinate-based atlases. Tractography now allows for improved visualization of these regions via the connections that define them.

Both CT and MRI play crucial roles in preoperative planning and postoperative assessment. For radiologists to contribute to these studies, they need to identify targets on both CT and MRI as well as complications from DBS. Often the targets are poorly delineated on imaging, and radiologists may be uncertain whether the leads are correctly placed; though 7T MRI is increasing conspicuity of anatomic landmarks. Existing atlases, while available, are not quickly referenced.

During this session we plan to review common targets for deep brain stimulation focusing on how to identify their location on both CT and MRI based anatomic landmarks and defining pathways. Each target review will include scrollable DICOM images with probabilistic tractography overlays to aid in the discussion, taking time to review the relevant

pathways and conditions treated with stimulation. To aid radiologist understanding, and for easy reference, we are creating a public website which reviews the targets alongside an interactive DICOM viewer with labeled stereotactic and probabilistic tractography overlays on CT and 7T-MRI images.

Purpose

- Provide a relevant and concise, image-based review of common DBS targets.
- Outline associated circuitopathies and relevant pathways manipulated.
- Review common complications encountered in DBS cases.
- Develop an accessible on-line guide to support radiologists reporting on pre- and post-procedural DBS cases. (Example showing the VIM (yellow) and traversing DRTT (Red))

Materials & Methods

After a brief introduction, we will review the common DBS targets listed below alongside scrollable, labeled DICOM images highlighting the target location based on identifiable landmarks and probabilistic tractography. Each target slide will include brief points on the disease treated with stimulation and the relevant pathways.

Results & Conclusion

This exhibit offers a structured, interactive approach to identifying common DBS targets by highlighting key anatomic landmarks and pathways on CT and 7T MRI. By reviewing each target with scrollable DICOM images and tractography overlays, participants will gain practical skills in locating DBS targets and understanding associated pathways and conditions treated with stimulation.

Our online resource—featuring labeled, interactive DICOM images and tractography—serves as a quick-reference tool designed to reinforce learning and build confidence in recognizing correct lead placement and identifying potential complications.

In conclusion, this exhibit equips radiologists with essential skills for DBS target identification, supporting accurate reporting and enhancing patient care in DBS cases.

References

Dormont D, Seidenwurm D, Galanaud D, Cornu P, Yelnik J, Bardinet E. Neuroimaging and deep brain stimulation. AJNR Am J Neuroradiol. 2010 Jan;31(1):15-23. doi: 10.3174/ajnr.A1644. Epub 2009 Sep 12. PMID: 19749225; PMCID: PMC7964047.

Middlebrooks EH, Domingo RA, Vivas-Buitrago T, Okromelidze L, Tsuboi T, Wong JK, Eisinger RS, Almeida L, Burns MR, Horn A, Uitti RJ, Wharen RE Jr, Holanda VM, Grewal SS. Neuroimaging Advances in Deep Brain Stimulation: Review of Indications, Anatomy, and Brain Connectomics. AJNR Am J Neuroradiol. 2020 Sep;41(9):1558-1568. doi: 10.3174/ajnr.A6693. Epub 2020 Aug 13. PMID: 32816768; PMCID: PMC7583111.

Abosch A, Yacoub E, Ugurbil K, Harel N. An assessment of current brain targets for deep brain stimulation surgery with susceptibility-weighted imaging at 7 tesla. Neurosurgery. 2010 Dec;67(6):1745-56; discussion 1756. doi: 10.1227/NEU.0b013e3181f74105. PMID: 21107206; PMCID: PMC3124849.

Fenoy AJ, Simpson RK Jr. Risks of common complications in deep brain stimulation surgery: management and avoidance. J Neurosurg. 2014 Jan;120(1):132-9. doi: 10.3171/2013.10.JNS131225. Epub 2013 Nov 15. PMID: 24236657.

Said N, Elias WJ, Raghavan P, Cupino A, Tustison N, Frysinger R, Patrie J, Xin W, Wintermark M. Correlation of diffusion tensor tractography and intraoperative macrostimulation during deep brain stimulation for Parkinson disease. J Neurosurg. 2014 Oct;121(4):929-35. doi: 10.3171/2014.6.JNS131673. Epub 2014 Jul 25. PMID: 25061862.

315

Insights into Abnormal Cortical Enhancement: A Diagnostic Perspective.

David J Wessling MD, Devin DeLuna MD, Jason T Helvey MD

University of Nebraska Medical Center, Omaha, NE, USA

Abstract Category

Adult Neoplasms/Epilepsy/Trauma

Summary & Objectives

Abnormal cortical enhancement can manifest from a range of potential etiologies and represents a diagnostic challenge with varying implications for patient management and prognosis.

This educational exhibit will present a series of various pathologies resulting in abnormal cortical enhancement. Our aim is to:

1). Provide a review of abnormal cortical enhancement including common and uncommon differential diagnoses.

2) Describe the clinical presentation, imaging characteristics, imaging interpretation as well as discuss clinical implications.
3) Provide a practical framework to improve recognition and interpretation of abnormal cortical enhancement for training neuroradiologists.
4) Entice the viewers curiosity and enhance diagnostic accuracy and confidence amongst neuroradiologists in clinical practice and improve clinical decision making.

Purpose

We hope to broaden the viewers differential diagnosis when presented with a case of abnormal cortical enhancement, provide helpful information for narrowing the differential and minimize adverse patient harm from unnecessary intervention or delayed diagnosis.

Materials & Methods

This exhibit is intended to serve as a collection of interesting pathologies with abnormal cortical enhancement.
Cases were selected from neuroradiology studies conducted at the University of Nebraska Medical Center PACS database. Inclusion criteria focused on patients with documented abnormal cortical enhancement on 1.5 and 3T MRI and, where applicable, CT imaging encompassing infectious, inflammatory, vascular and neoplastic etiologies. Advanced techniques such as MR Spectroscopy, perfusion imaging and functional MRI were utilized in specific cases in order to further characterize lesions of interest.
Cases are categorized based on the underlying etiology.
Where applicable, cases with annotated figures and diagnostic flowcharts will be provided.

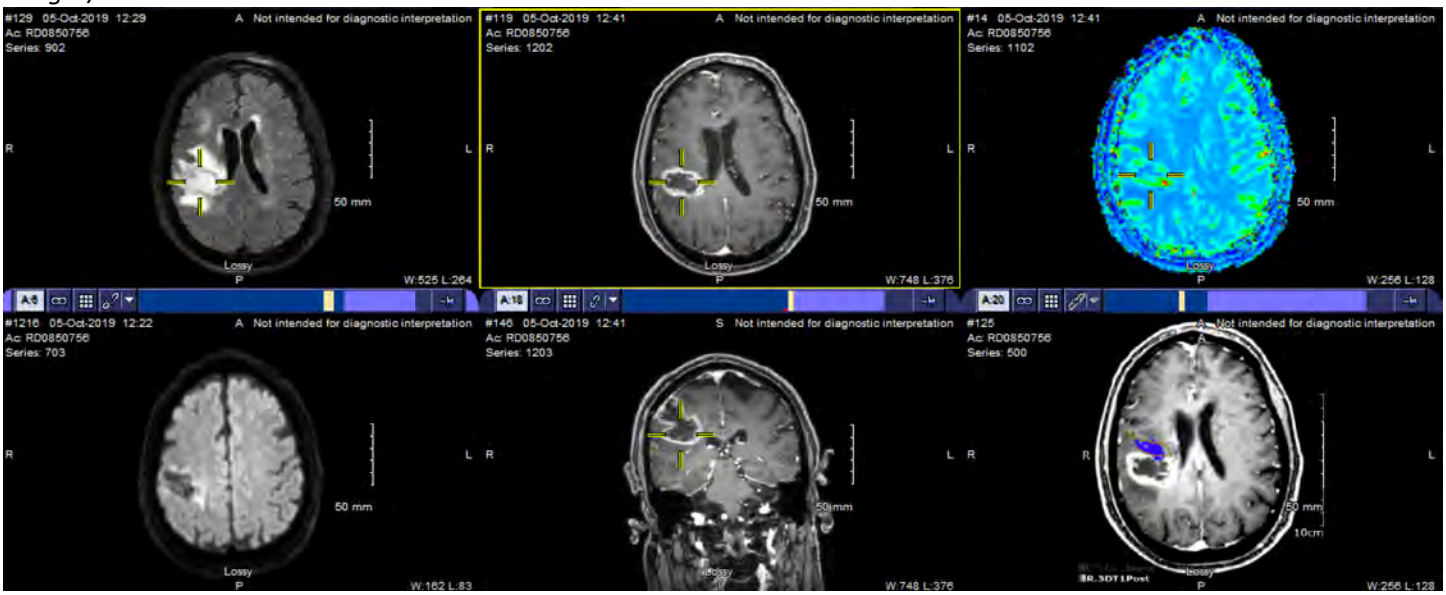
Results & Conclusion

Analysis of imaging characteristics in cases of abnormal cortical enhancement revealed differentiating features across various etiologies.
Familiarity with characteristic imaging patterns of abnormal enhancement allows neuroradiologists to more confidently narrow the differential diagnosis and suggest specific etiologies particularly in complex or ambiguous cases (ie SMART syndrome).
Improved diagnostic accuracy in assessing cortical enhancement abnormalities positively influences patient outcomes by guided treatment strategies.

References

Y. Ota, E. Liao, G. Shah, A. Srinivasan and A.A. Capizzano
American Journal of Neuroradiology May 2023, DOI: https://doi.org/10.3174/ajnr.A7859

Images/Tables



321

Apexology: A Practical Guide to Thoracic Pathology for the Neuroradiologist

Wasif Bala MD[1], Wen Wang MD[2], Muhammad Naeem MD[3], Benjamin Elstrott MD[4], Andrew Callen MD[4], Brent Weinberg MD, PhD[1]

[1]Emory University School of Medicine, Atlanta, Georgia, USA. [2]University of Florida College of Medicine, Jacksonville, Florida, USA. [3]Emory University, Atlanta, Georgia, USA. [4]University of Colorado School of Medicine, Aurora, Colorado, USA

Abstract Category

Head and Neck

Summary & Objectives

Cross sectional imaging of the head and neck routinely captures the superior thorax, presenting neuroradiologists with diagnostic obligations beyond traditional neurological pathology. This educational exhibit aims to provide a targeted overview of thoracic apex pathology captured on routine neuroimaging, with emphasis on conditions that may mimic or coincide with neurological disease. The exhibit will both highlight critical findings requiring urgent attention and explore the intersection of thoracic and neurological manifestations in this anatomically complex region.

Purpose

To establish a structured framework for thoracic apex evaluation during routine neuroimaging interpretation, focusing on three key areas: urgent findings requiring immediate action, apically predominant thoracic diseases, and thoracic diseases with neurological overlap. This knowledge is essential for neuroradiologists who serve as primary interpreters of head and neck imaging and may be the first to identify significant thoracic pathology.

Materials & Methods

This exhibit synthesizes imaging findings from multiple tertiary care centers' teaching files, incorporating cross sectional imaging examples of thoracic apex pathology identified on neuroimaging studies. Cases were selected based on clinical significance, diagnostic challenge, and relevance to neuroimaging practice. The material is organized into three main categories: vascular emergencies (including aortic dissection and pulmonary embolism), lung parenchymal disease (with emphasis on apically predominant conditions such as tuberculosis, sarcoidosis, and hypersensitivity pneumonitis), and processes that may present with overlapping neurological features (such as Pancoast tumors[1]).

Results & Conclusion

After reviewing this exhibit, attendees will be equipped to evaluate the thoracic apex during routine neuroimaging interpretation. They will be able to identify critical findings requiring urgent communication, recognize patterns of apically predominant disease that may mimic intracranial pathology, and confidently recommend evidence-based follow-up imaging recommendations. This knowledge will enhance their ability to serve as comprehensive interpreters of neuroimaging studies, bridging the traditional boundary between thoracic and neurological imaging.

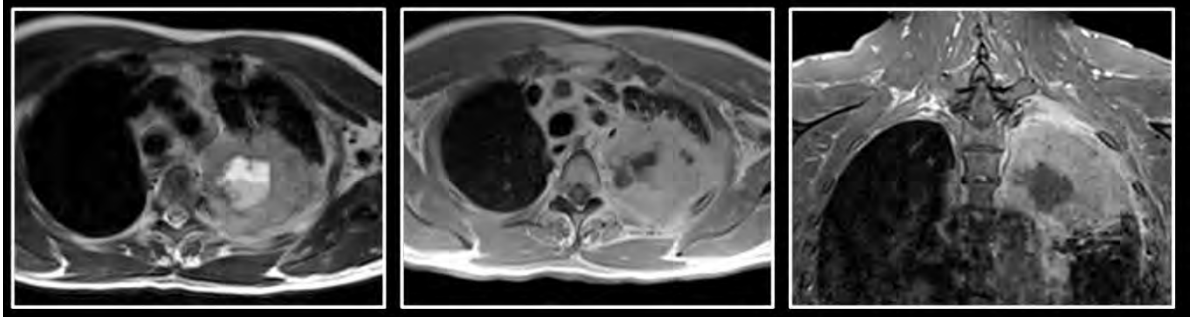
References

1. Gundepalli SG, Tadi P. Lung Pancoast Tumor. [Updated 2023 Jul 17]. In: StatPearls [Internet]. Treasure Island (FL): StatPearls Publishing; 2024 Jan-. Available from: https://www.ncbi.nlm.nih.gov/books/NBK556109/

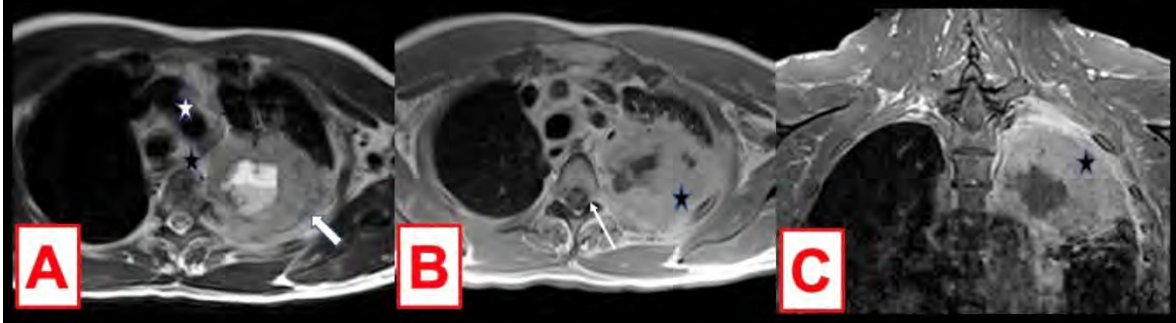
Images/Tables

Case 1

59 year old male presents with lower neck pain and left arm weakness.



Key Imaging Findings



- Axial T2 sequence demonstrates a **centrally necrotic cavitary mass** (thick arrow) in the left lung apex abutting the aortic arch (white star) and superior mediastinum (black star).
- Axial (B) and coronal (C) T1 post contrast sequence demonstrates thick-rind peripheral **enhancement** (black star) of the apical mass in close proximity to the upper thoracic neural foramen (white arrow). No gross invasion outside the chest wall.

Superior Sulcus (Pancoast) Tumor

Clinical features	Imaging evaluation	Differential	Recommendations
• Cough and hemoptysis • Upper extremity pain and weakness • Horner syndrome • Weight loss and fatigue	• Size and location • Invasion into chest wall? • Associated pleural thickening? • Relationship with neural foramen and brachial plexus	• Pulmonary malignancy • Metastatic disease • Infection such as TB or inflammatory process • Neurogenic tumor	• Oncology referral • Tissue biopsy • Complete staging with CT chest/ abdomen and pelvis and PET/CT

330

Pre and Post-Therapy Evaluation of Meningiomas Using Novel Imaging Techniques

Neil K Bhatia MD, Jeffrey P Guenette MD MPH, Elmira Hassanzadeh MD, Raymond Huang MD PhD
Brigham & Women's Hospital/Harvard Medical School, Boston, MA, USA

Abstract Category

Adult Neoplasms/Epilepsy/Trauma

Summary & Objectives

Multiple new and emerging imaging techniques are now available to evaluate meningiomas in both the pre-therapy and post-therapy settings. Utilization of these techniques can help guide appropriate management and assessment of post-treatment response.

Objectives:

1. Describe the imaging characteristics of meningiomas that may impact surgical approach including brain invasion, venous sinus involvement, and tumor consistency assessment.
2. Highlight novel imaging techniques that can be used to guide management of meningiomas such as magnetic resonance elastography (MRE), diffusion tensor MRI, and somatostatin-analog PET-CT.
3. Discuss how to differentiate tumor from scar tissue using MRI and somatostatin-analog PET-CT and compare the two methods for pre-radiotherapy planning.
4. Present evidence about the advantages of using tumor volume growth rate and somatostatin-analog PET-CT to assess post-treatment response assessment.

Purpose

The purpose of this educational exhibit is to highlight how various imaging techniques including conventional MRI, MR elastography, diffusion tensor MRI, and somatostatin-analog PET-CT can be utilized to assess meningiomas in both the pre- and post-therapy settings to guide management. This exhibit especially focuses on the promising role of somatostatin-analog PET in the diagnosis, pre-treatment planning, and response assessment of meningiomas. Using clinical examples, the exhibit will illustrate the unique application of each imaging technique and describe relevant imaging findings to show how they can contribute to patient care.

Materials & Methods

Not applicable.

Results & Conclusion

Not applicable.

References

Bashir A, Larsen VA, Ziebell M, Fugleholm K, Law I. Improved detection of postoperative residual meningioma with [^68Ga]Ga-DOTA-TOC PET imaging using a high-resolution research tomograph PET scanner. *Clin Cancer Res* 2021;27:2216–25.

Joo L, Park JE, Park SY, et al. Extensive peritumoral edema and brain-to-tumor interface MRI features enable prediction of brain invasion in meningioma: Development and validation. *OUP Academic* 2020 Aug 13. [Epub ahead of print].

Ong T, Bharatha A, Alsufayan R, Das S, Lin AW. MRI predictors for brain invasion in meningiomas. Neuroradiol J. 2021 Feb;34(1):3-7. doi: 10.1177/1971400920953417. Epub 2020 Sep 14. PMID: 32924772; PMCID: PMC7868592.

Streitberger KJ, Reiss-Zimmermann M, Freimann FB, et al. Higher resolution magnetic resonance elastography reveals early mechanical signatures of neuroinflammation in patients with clinically isolated syndrome. *Neurosurgery* 2015;77(4):748–55.

Graillon T, Ferrer L, Siffre J, et al. Role of 3D volume growth rate for drug activity evaluation in meningioma clinical trials: the example of the CEVOREM study. *Neuro Oncol* 2021;23:1139–47.

331

Imaging Features of Common and Uncommon Postsurgical Complications following Vestibular Schwannoma Resection

Emily W Avery MD, Nikdokht Farid MD
UC San Diego, Department of Radiology, San Diego, CA, USA

Abstract Category

Adult Neoplasms/Epilepsy/Trauma

Summary & Objectives

Vestibular schwannomas (VS) are Schwann cell proliferations arising from the vestibulocochlear nerve. Though benign, VS may be associated with sensorineural hearing loss, disequilibrium, or with sequela of mass effect on the cerebellum and brainstem. Given these implications, the primary therapeutic approaches for VS include: 1) watchful waiting ('wait and scan'), 2) radiotherapy/radiosurgery, and/or 3) resection. This educational exhibit focuses on resection, which is highly effective in reducing symptoms and has generally low morbidity and mortality.[1] Resection generally follows a translabyrinthine, retrosigmoid, or middle cranial fossa approach, and there are specific risks and benefits associated with each approach. Our exhibit highlights the imaging findings of common and uncommon postoperative complications associated with VS resection.

Purpose

This exhibit aims to highlight the imaging findings of common and uncommon postoperative complications following VS resection, including rare but critical complications which should not be missed.

Materials & Methods

We retrospectively reviewed postoperative VS resection CT and MRI studies stored on our institution's picture archiving system from January 2019 through October 2024. We searched reports for keywords related to specific complications known or suspected to have occurred. We evaluated the imaging studies from which those reports were created to compile our list of representative cases.

Results & Conclusion

We identified eight representative cases illustrating postoperative complications that were either commonly seen, or particularly clinically relevant. These cases include: postoperative hemorrhage, acute infarct, extra axial empyema, dural venous sinus thrombosis, facial nerve disruption, cerebral spinal fluid (CSF) leak, arachnoid adhesions, and fat migration into the CSF space (key images highlighted in Figure 1). Our eight patients range from age 26 to 50, three of eight are female, and all three standard approaches to VS resection are represented.

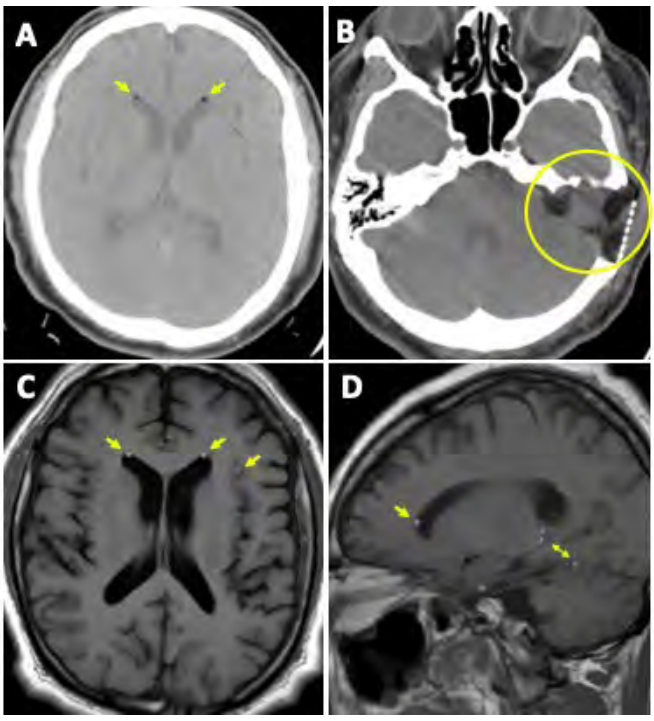
Our diverse compilation of cases provides an illustrative guide to both common postoperative complications and uncommon but clinically significant postoperative complications following VS resection.

Figure 1 legend: Migration of mastoidectomy fat graft material throughout the cerebral spinal fluid (CSF) space in a 63-year-old male following translabyrinthine approach resection of left vestibular schwannoma. Yellow arrows denote foci of fat. Anti-dependent foci of fat are noted on postoperative CT (A) and MRI T1 sequences (C and D) throughout the ventricles and sulci. The fat graft is seen in the expected location underlying the mastoidectomy defect (B, yellow circle).

References

1. Goldbrunner R, Weller M, Regis J, et al. EANO guideline on the diagnosis and treatment of vestibular schwannoma. *Neuro Oncol* 2020;22:31-45

Images/Tables



346

JAW-DROPPING LESIONS: ALL YOU NEED TO KNOW ABOUT PEDIATRIC MANDIBLE LESIONS

Taisa Guarilha MD[1], Marcus Otavio S. C. Meneses MD[1], Santiago Martinez-Correa[1], Patricia Rafful[1], Stephanie El Omeiri[1], Rodrigo Murakoshi[2], Sergio F Alves Junior[3], Lorenna Vidal[1], Karuna Shekdar[1], Sara Teixeira[1]
[1]Children's Hospital of Philadelphia, Philadelphia, PA, USA. [2]Universidade de Sao Paulo, Sao Paulo, SP, Brazil. [3]Universidade Federal do Rio de Janeiro, Rio de Janeiro, RJ, Brazil

Abstract Category

Pediatrics

Summary & Objectives

Mandibular tumors are uncommon in the pediatric population, and the majority are benign. Due to their low incidence and the wide spectrum of lesions that can occur in this area, this topic is often overlooked. However, early recognition and identification of these lesions are crucial. Benign lesions are often treated with curettage or surgery, while malignant lesions are more complex and may require the removal of part of the mandible. Early recognition aids in prompt treatment, which often leads to better clinical and aesthetic outcomes.

Purpose

Discuss relevant imaging anatomy and embryology of the mandible
Demonstrate imaging findings of benign and malignant tumors occurring in the pediatric age group
Create a flowchart to suggest each diagnosis using imaging findings
Summarize in an article what to look for in pediatric lesions

Materials & Methods

- Present cases and imaging findings:
- Benign:
- Bone related: infectious lesion, simple bone cyst, giant cell lesion of the bone, osteochondroma, benign fibro-osseous lesion of the bone, osteoblastoma, Langerhans cell histiocytosis, fibrous dysplasia
- Odontogenic: dentigerous cyst, odontoma, odontogenic keratocyst, ameloblastoma, fibro-odontoma, ameloblastic fibroma
- Soft tissue related: fibroma, vascular malformation, myofibroma, desmoid tumor, fibrous neuroma, mucosal histiocytoma, benign myofibroblastic tumor
- Malignant:
- Ewing sarcoma, osteosarcoma, rhabdomyosarcoma, leiomyiosarcoma, B-cell lymphoma, squamous cell carcinoma, malignant spindle cell tumor, yolc sac tumor, teratoma

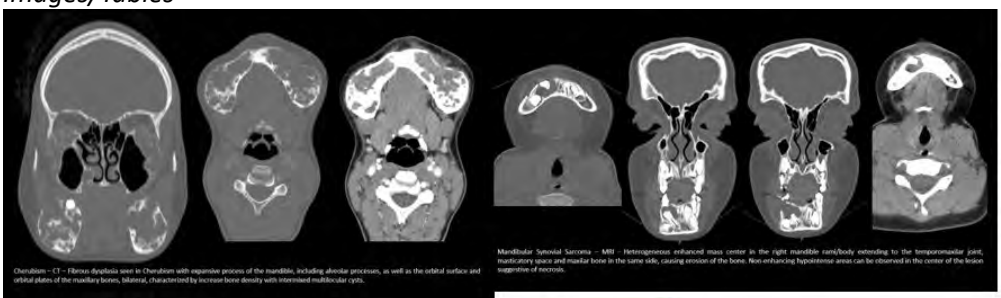
Results & Conclusion

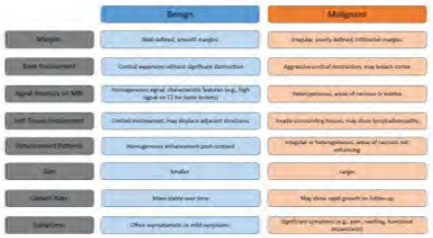
The mandible is the only movable bone in the skull and plays a crucial role in mastication and facial aesthetics. It has two main parts: the body, the horizontal portion supporting the teeth, and the rami, vertical structures extending upward that connect to the skull at the temporomandibular joint (TMJ). Features include the mental symphysis, where the two sides of the mandible fuse at the midline; the alveolar processes, which support the teeth; the coronoid process, a site of insertion for the temporalis muscle; and the condyle, which forms the articulation with the temporal bone.
Embryologically, the mandible primarily develops from the first pharyngeal arch, also known as the mandibular arch, which is composed of mesoderm and neural crest cells. The key developmental events include chondrogenesis, the formation of the cartilage that precedes bone development; osteogenesis, which is the replacement of cartilage with bone that occurs between the 6th and 8th weeks of gestation; and the development of the alveolar processes, which happens as the permanent teeth begin to form.
We will describe the lesions that can occur, focusing on imaging findings to distinguish malignant from benign lesions, thereby improving diagnostic accuracy.

References

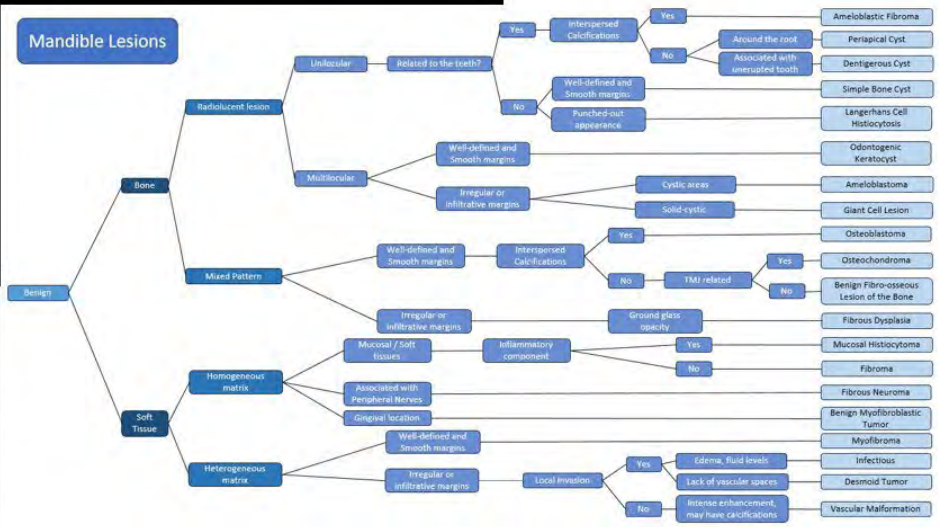
Benoit MM, Vargas SO, Bhattacharyya N, et al. The presentation and management of mandibular tumors in the pediatric population. Laryngoscope 2013;123:2035–42. DOI: https://10.1002/lary.24020
Hintze JM, Afshar S, Taghinia A, et al. A multi-disciplinary team approach to pediatric malignant mandibular tumors. Int J Pediatr Otorhinolaryngol 2023;168:111547. DOI: https://10.1016/j.ijporl.2023.111547
Lipski M, Tomaszewska IM, Lipska W, et al. The mandible and its foramen: anatomy, anthropology, embryology and resulting clinical implications. Folia Morphol (Warsz) 2013;72:285–92. DOI: https://10.5603/fm.2013.0048

Images/Tables









351

MR Imaging of High-grade Gliomas on Bevacizumab Therapy

Varun Rohatgi[1], Muhammad Atif Naveed MBBS[2], Rajiv Mangla MD[3], Robert Young MD[2]
[1]Weill Cornell School of Medicine, New York, NY, USA. [2]Memorial Sloan Kettering Cancer Center, New York, NY, USA. [3]SUNY Upstate Medical University, Syracuse, NY, USA

Abstract Category

Adult Neoplasms/Epilepsy/Trauma

Summary & Objectives

High grade gliomas include glioblastoma, IDH mutated grade WHO 4 gliomas, WHO grade 3 anaplastic astrocytoma, or WHO grade 3 anaplastic oligodendroglioma. Bevacizumab (Avastin) is an anti-angiogenic drug which decrease the neovascularity, or number of small leaky vessels in the brain tumors and normalize the remaining vessels. It has shown to the decrease the enhancing size and enhancing intensity of high-grade gliomas, although with little or no actual anti-tumor effect. This decrease in the enhancement represents a change in the permeability properties of the blood brain barrier.

Purpose

Advanced MR imaging for the evaluation of cellularity, perfusion, and internal tumoral microenvironment have emerged to differentiate pseudo-response from actual disease response in patients on bevacizumab; however, to date it is a challenge to accurately differentiate these two entities on MR imaging only.

Patients on bevacizumab treatment for high grade gliomas tends to demonstrate peculiar and characteristic MR imaging appearance.

Materials & Methods

We plan to describe 10-20 cases of patients with high grade gliomas on bevacizumab therapy. These cases will illustrate typical changes postbevacizumab, as well as progression, pseudoprogression, response, pseudoresponse, recurrence, and complications of therapy such as intracerebral hemorrhage or intratumoral bleed. We will explain the peculiar MR features of bevacizumab treatment on conventional T1 and FLAIR sequences as well as with advanced imaging techniques such as diffusion and susceptibility weighted imaging, MR perfusion, and MR spectroscopy.

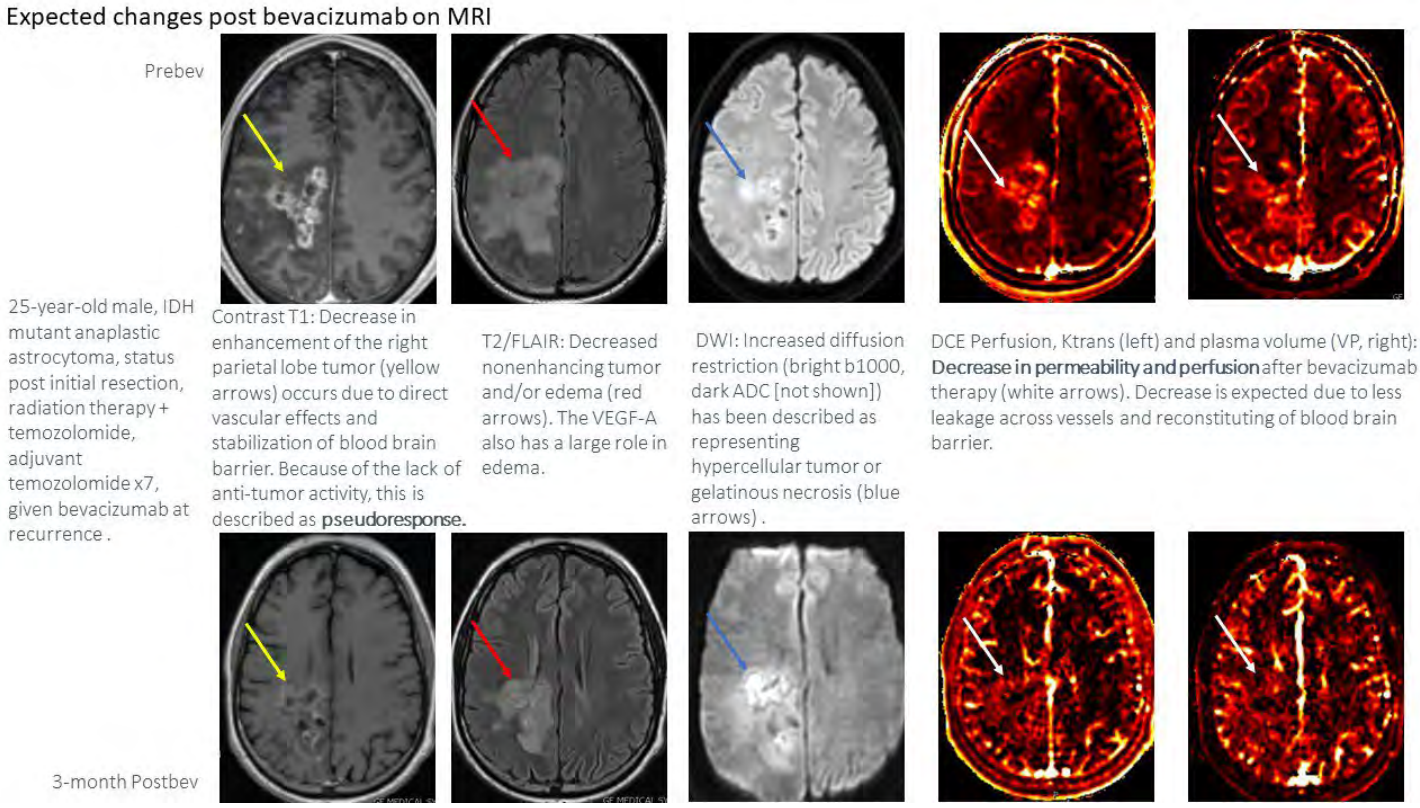
Results & Conclusion

Our educational exhibit will elaborate and illustrate the various MR imaging appearances of antiangiogenic therapy induced changes in the high-grade gliomas of the brain.

References

Arevalo OD, Soto C, Rabiei P, et al. Assessment of Glioblastoma Response in the Era of Bevacizumab: Longstanding and Emergent Challenges in the Imaging Evaluation of Pseudoresponse. Front Neurol. 2019 May 7;10:460. doi: 10.3389/fneur.2019.00460.

Images/Tables



357

Sellar/Suprasellar Pathology: What a Resident Should Know

Braeden Estes MD, Jay Voter MD, Jeremy Ross MD

Corewell Health East William Beaumont University Hospital, Royal Oak, Michigan, USA

Abstract Category

Adult Brain Inflammatory/Infectious Disease/Degenerative/Metabolic

Summary & Objectives

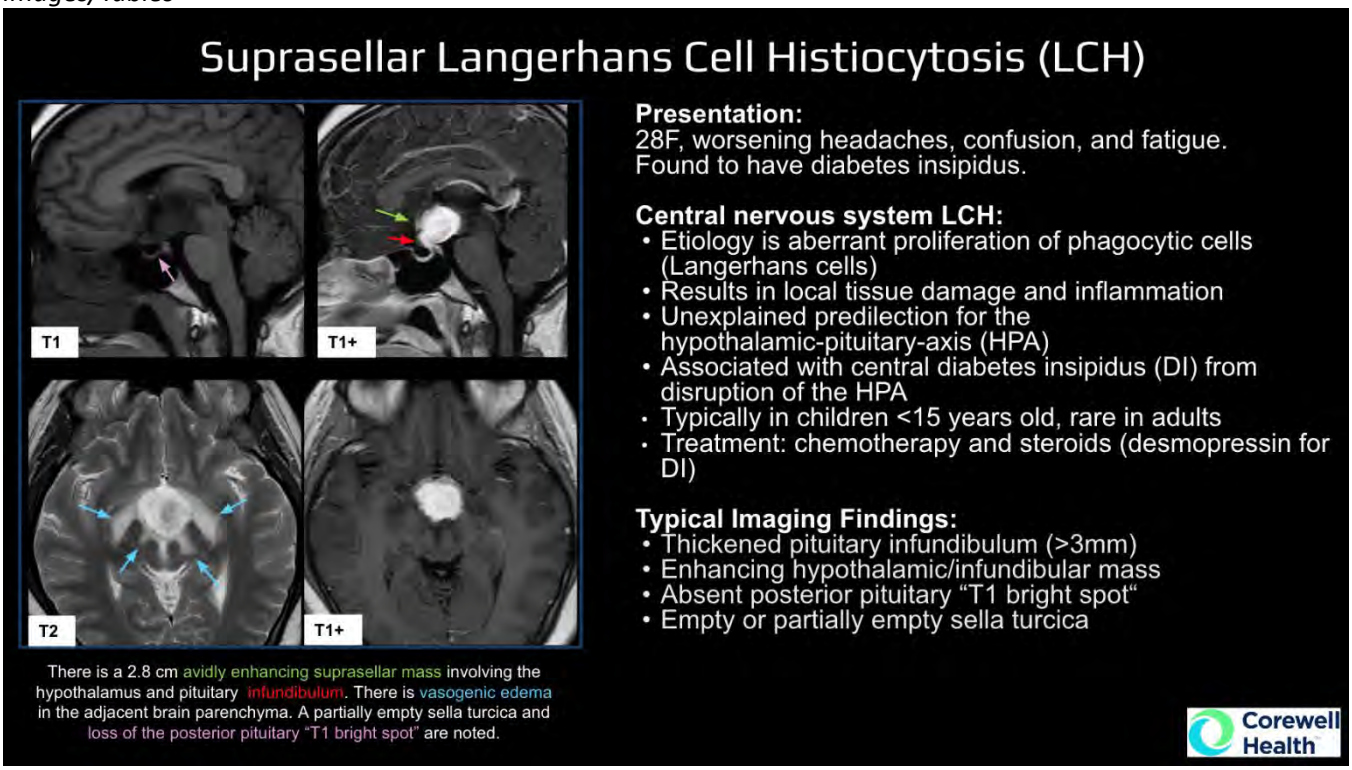
The sellar/suprasellar region is intricate and contains several crucial structures, including the hypothalamus, pituitary gland, optic nerves, and skull base. As a result, pathology in this region may result in significant symptomatology. A variety of mass lesions can arise in the sella/suprasella including but not limited to, neoplastic, inflammatory, and congenital etiologies.

The objective of this educational exhibit is to provide a case-based review of common and uncommon sellar/suprasellar masses, their typical imaging features, and key facts about each diagnosis. Understanding distinguishing imaging features of these pathologies allows the neuroradiologist to provide a concise differential diagnosis. Imaging findings must be correlated with the patient's clinical history and laboratory values to facilitate accurate diagnosis and to guide appropriate management.

Purpose

The exhibit will provide a multi-modality case-based review of sellar/suprasellar lesions, including craniopharyngioma, Rathke cleft cyst, pituitary langerhans cell histiocytosis, neurosarcoidosis, meningioma, pituitary macroadenoma, lipoma, metastases, arachnoid cyst, pituitary apoplexy, germinoma, and others. Pertinent clinical history, typical imaging features, and key facts about each lesion will be reviewed.

Materials & Methods
Cases were retrieved using the Corewell Health mPower search database.
Results & Conclusion
When evaluating sellar/suprasellar lesions, understanding the clinical presentation and key imaging features allows the neuroradiologist to provide a concise differential diagnosis.
References
1. Doerfler A, Rennert J. Imaging of sellar and parasellar lesions. *Clinical Neurology and Neurosurgery* 2007;109(2);111-124. https://doi.org/10.1016/j.clineuro.2006.11.001.
2. Durham B. Molecular characterization of the histiocytoses: neoplasia of dendritic cells and macrophages. *Semin Cell Dev Biol* 2019;86:62-76.
3. Grois N, Prayer D, Prosch H, Lassmann H. CNS LCH Cooperative Group. Neuropathology of CNS disease in Langerhans cell histiocytosis. *Brain* 2005; 128(4): 829–838.
4. Prayer D, Grois N, Prosch H, Gadner H, Barkovich AJ. MR imaging presentation of intracranial disease associated with Langerhans cell histiocytosis. *AJNR Am J Neuroradiol* 2004;25(5): 880–891.
5. Ugga L, Franca RA, Scaravilli A, et al. Neoplasms and tumor-like lesions of the sellar region: imaging findings with correlation to pathology and 2021 WHO classification. *Neuroradiology* 2023;65;675–699. https://doi.org/10.1007/s00234-023-03120-1
Images/Tables



391

Imaging of Pott's Puffy Tumor: A Review on its Different Imaging Presentations and Complications

Brian Won, Jo Ann Sun, Hunter Carlock, Jason Paek, Stephen Smith, Sankarsh Jetty
University of Rochester Medical Center, Rochester, New York, USA
Abstract Category
Pediatrics
Summary & Objectives
Educational Objectives:
1. Recognize and review the clinical presentation and course of Pott's puffy tumor (PPT).
2. Describe the common imaging characteristics of PPT and its complications through multiple cases.

3. Emphasize the importance of accurate and timely diagnosis in ensuring the best clinical outcomes for patients presenting with PPT.

Pott's puffy tumor (PPT) is a rare but significant clinical entity characterized by subperiosteal abscess formation and osteomyelitis of the frontal bone, typically arising as a complication of acute frontal sinusitis. Clinically, PPT manifests as soft tissue swelling in the frontal scalp and periorbital regions. The primary etiology is often infectious with spread from acute sinusitis, which is predominantly attributed to Streptococcus species [1]. This condition primarily affects adolescents and young adults, likely due to the increased vascularity of the diploic vascular system, which predisposes these structures to bacterial invasion and bony erosion [2].

Imaging plays a crucial role in the assessment of PPT, with computed tomography (CT), ultrasound, and magnetic resonance imaging (MRI) providing valuable insights into sinus anatomy and potential complications that significantly impact patient outcomes. CT is particularly effective for evaluating bony involvement and detecting osteomyelitis, a defining feature of PPT, and is often the first imaging modality utilized in these patients [3]. However, CT is less effective in assessing intracranial extension [3]. Ultrasound can also be beneficial for evaluating the soft tissues of the scalp without exposing the patient to radiation; however, it has limited capability in assessing the underlying osseous structures. Contrast-enhanced MRI excels in visualizing both bony and soft tissue structures, allowing for a comprehensive assessment of inflammation, subperiosteal fluid collections, and potential intracranial complications [3].

Intracranial extension is a serious and unfortunately common complication, occurring in approximately 60-85% of cases [4]. Intracranial spread of infection can range from meningitis and extra-axial empyemas to cerebritis and parenchymal abscesses. Timely recognition of the varying imaging appearances of these entities will ensure prompt treatment and better patient outcomes.

Given its potential for rapid progression, radiologists must maintain a high degree of clinical suspicion when evaluating patients presenting with forehead swelling, headache, and other sinus-related symptoms. A comprehensive imaging approach that incorporates both CT for bony detail and MRI for soft tissue and intracranial assessment is recommended. The synergistic use of these modalities facilitates timely and accurate identification of the primary infection site and potential complications, guiding necessary medical and surgical treatments.

Purpose

A clinical review of Pott's puffy tumor along with its imaging findings and complications

Materials & Methods

Case images are provided by authors' institutional imaging archives. Patient history was de-identified and obtained from the authors' institutional medical records.

Results & Conclusion

Pott's puffy tumor (PPT) is a clinical condition with significant implications that neuroradiologists are uniquely equipped to address. Advanced imaging techniques have enhanced the ability to diagnose this condition early, enabling timely interventions and mitigating the risk of severe complications. A thorough understanding of the varying imaging appearances of PPT across multiple modalities is essential in ensuring prompt treatment to prevent potentially life-threatening outcomes.

References

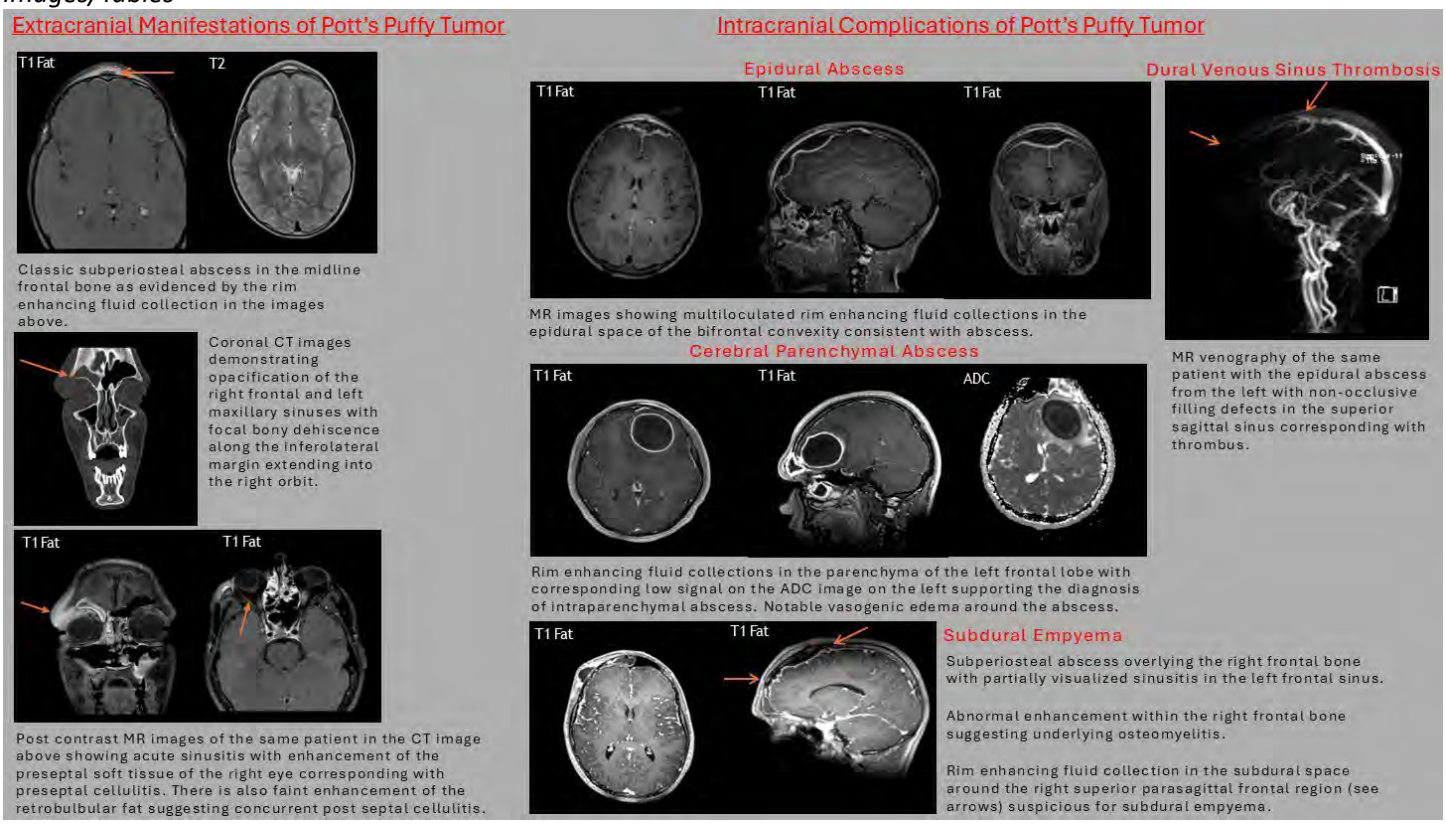
1. Apostolakos D, Tang I. Image Diagnosis: Pott Puffy Tumor. *Perm J*. 2016;20(3):15-157. doi:10.7812/TPP/15-157

2. Parida PK, Surianarayanan G, Ganeshan S, et al. Pott's puffy tumor in pediatric age group: a retrospective study. *Int J Pediatr Otorhinolaryngol*. 2012;76(9):1274-1277. doi:10.1016/j.ijporl.2012.05.018

3. Mafee MF, Tran BH, Chapa AR. Imaging of rhinosinusitis and its complications: plain film, CT, and MRI. *Clin Rev Allergy Immunol*. 2006;30(3):165-186. doi:10.1385/CRIAI:30:3:165

4. Rohde RL, North LM, Murray M, et al. Pott's puffy tumor: A comprehensive review of the literature. *Am J Otolaryngol*. 2022;43(5):103529. doi:10.1016/j.amjoto.2022.103529

Images/Tables



395

Imaging of Post-operative Decompression of Neurovascular Conflict in Trigeminal Neuralgia

Sanidhya S Karve MD[1], Suresh K Mukherji MD[2], Hemal M Manjrekar MBBS[3]

[1]Amrita Institute of Medical Sciences and Research Center, Kochi, Kerala, India. [2]University of Louisville, Louisville, Kentucky, USA. [3]TNMC and BYL Nair Charitable Hospital, Mumbai, Maharashtra, India

Abstract Category

Interventional/Vascular/Stroke

Summary & Objectives

Trigeminal neuralgia, aka tic douloureux, is characterized by sudden episodes of shooting, shock-like pain in the sensory distribution of cranial nerve V, often aggravated by activities such as shaving, chewing, brushing teeth, etc. It is most commonly caused by an artery (rarely a vein) compressing the cisternal portion of the nerve. Less often, it could be caused by pathologies like cavernoma, multiple sclerosis demyelination, trigeminal zoster, etc [1]. A commonly used treatment option in patients with identified neurovascular conflict is a surgical procedure called Microvascular Decompression (MVD). A retro-sigmoid craniotomy approach is preferred, and careful arachnoid dissection is performed. Correct identification of the offending artery and cranial nerve V is of paramount importance. A piece of shredded Teflon is placed between the offending artery and the nerve to relieve compression [2,3,4]. On postoperative imaging, these Teflon pledgets may appear as rectangular hyperdensity on CT and of hypointense signal intensity on T2-weighted MR images [3,4]. Teflon pledget should not show any enhancement in post-contrast T1 sequence in asymptomatic patients. Post-operative MR imaging can be used to assess for post-operative complications like hemorrhage, inflammation, etc. It can also help determine the proper placement of the pledget to ensure post-operative resolution of neurovascular conflict.

Objective:

Provide a post-operative imaging guide for patients who underwent MVD (Microvascular Decompression) through case-based MR images.

Purpose

Numerous papers have described pre-operative imaging in trigeminal neuralgia. However, the post-operative appearance following surgery is seldom discussed. This exhibit aims to familiarize readers with normal post-operative MR imaging findings and provide radiologists with a brief overview of the basics of microvascular decompression

surgery. Another important purpose is to educate trainees about the fundamentals of trigeminal neuralgia and develop an insight into it.

Materials & Methods

Apart from routine T1, T2, FLAIR, and post-contrast T1 MRI sequences, a specialized high-resolution heavily T2-weighted 3D sequence [CISS] was performed. Heavily weighted T2 sequence was the main sequence. Imaging in different orthogonal planes was performed to further improve our chances of appreciating finer details.

Results & Conclusion

This educational exhibit provides a comprehensive visual guide about the possible post-MVD MR imaging appearance. It aids Radiologists/Neurosurgeons in recognizing and interpreting these critical imaging findings. It addresses the relatively unexplored role of post-operative MR imaging in trigeminal neuralgia.

References

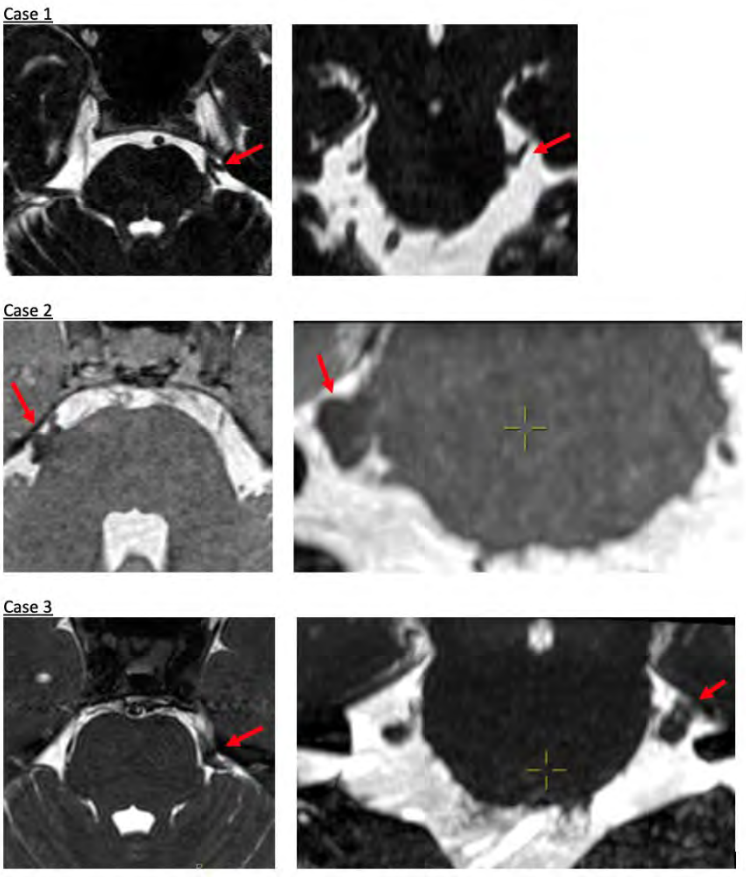
1] Kontzialis, M., & Kocak, M. (2017). Imaging evaluation of trigeminal neuralgia. *Journal of Istanbul University Faculty of Dentistry*, *51*(3 Suppl 1), S62–S68. https://doi.org/10.17096/jiufd.27242

2] Andersen, A.S.S., Heinskou, T.B., Rochat, P. *et al.* Microvascular decompression in trigeminal neuralgia - a prospective study of 115 patients. *J Headache Pain* **23**, 145 (2022). https://doi.org/10.1186/s10194-022-01520-x

3] Wenchao Lu, Hui Wang, Zhongnan Yan, Yuangang Wang, Hongmin Che. Microvascular decompression for the treatment of neurogenic hypertension with trigeminal neuralgia. (2019) BMC Neurology. 19 (1): 1. doi:10.1186/s12883-019-1569-y - Pubmed

4] Lee S, Lee PS, Lee JB, Lee J, Lee PK, Lee. Vascular Complications in Microvascular Decompression: A Survey of 4000 Operations. (2019) World neurosurgery. doi:10.1016/j.wneu.2019.06.155 - Pubmed

Images/Tables



Case 1: MR images show the normal appearance of a Teflon sling with a linear T2 hypointense signal placed between the trigeminal nerve root and the superior cerebellar artery loop on the left side.

Case 2 and 3: MR images show the normal appearance of a Teflon pledget with a T2 hypointense signal placed between the trigeminal nerve root and the superior cerebellar artery loop on the right and left side, respectively.

397

Eagle Syndrome: Flying under the Radar.

Stephen Hightower MD, Adam Robinson MD, Maram Alafif MBBS, Jennifer Chang MD
University of California, San Diego, San Diego, CA, USA

Abstract Category

Head and Neck

Summary & Objectives

Eagle syndrome (ES) is a rare clinical diagnosis characterized by symptomatic elongation of the styloid process and/or ossified stylohyoid ligament. Presentation is varied and frequently nonspecific but has historically been subdivided into two subtypes: “classic” ES or “styalgia” and vascular ES or “stylocarotid syndrome.” The former is typically characterized by orofacial pain, globus sensation, odynophagia, otalgia, and tinnitus associated with prior trauma or tonsillectomy. Pathologic contact between the styloid process and local CN V, VII, IX, X, and XII branches is the proposed underlying mechanism. Vascular ES has been associated with complications of compression and injury to the internal carotid artery including dissection and thrombosis. A constellation of consequent neurologic symptoms is reported, including transient ischemic attacks, stroke, syncope, and vertigo. Although ES is increasingly recognized in surgical disciplines, it remains underrepresented in radiologic literature. Our exhibit aims to (1) conduct a comprehensive literature review of ES as it pertains to diagnostic radiology and interventional radiology, as well as surgical approaches; (2) highlight key radiologic features of ES; (3) present imaging findings of ES from our institution.

Purpose

ES is an underrecognized diagnosis in the radiology literature. Our goal is to provide a comprehensive summary of the various clinical presentations, radiographic features, and surgical considerations of ES. We aim to highlight some of the key imaging features through presentation of cases from our institution.

Materials & Methods

For this exhibit, we queried multiple databases to conduct a thorough literature review. We additionally searched our institutional PACS database for radiographic cases of ES. These search results were reviewed alongside clinical documentation and selectively included based on both radiographically evident and clinically diagnosed ES. We also hope to highlight those cases with diagnostic angiography or venography, as well as those with surgical intervention and their clinical outcomes.

Results & Conclusion

Eagle syndrome is a rare clinical entity associated with a broad spectrum of clinical symptoms ranging from paroxysmal orofacial pain to ischemic stroke from carotid artery dissection. In addition to the historically recognized classic and carotid subtypes, a novel “jugular” variation has been proposed. This hypothesized jugular ES has been described to present with persistent headache and to be associated with complications of peri-mesencephalic subarachnoid hemorrhage and idiopathic intracranial hypertension. Treatment of ES includes conservative pharmacologic management, local injections, and operative measures such as styloidectomy. Despite its overall low prevalence, radiologists should draw attention to ES in patients with unilateral or bilateral elongated styloid processes or ossified stylohyoid ligaments with corresponding symptoms as a potential etiology—especially in those with evidence of neurovascular compression or injury.

References

Badhey A, Jategaonkar A, Anglin Kovacs AJ, et al. Eagle syndrome: A comprehensive review. Clin Neurol Neurosurg. 2017 Aug;159:34-38. DOI: 10.1016/j.clineuro.2017.04.021. Epub 2017 May 6. PMID: 28527976.

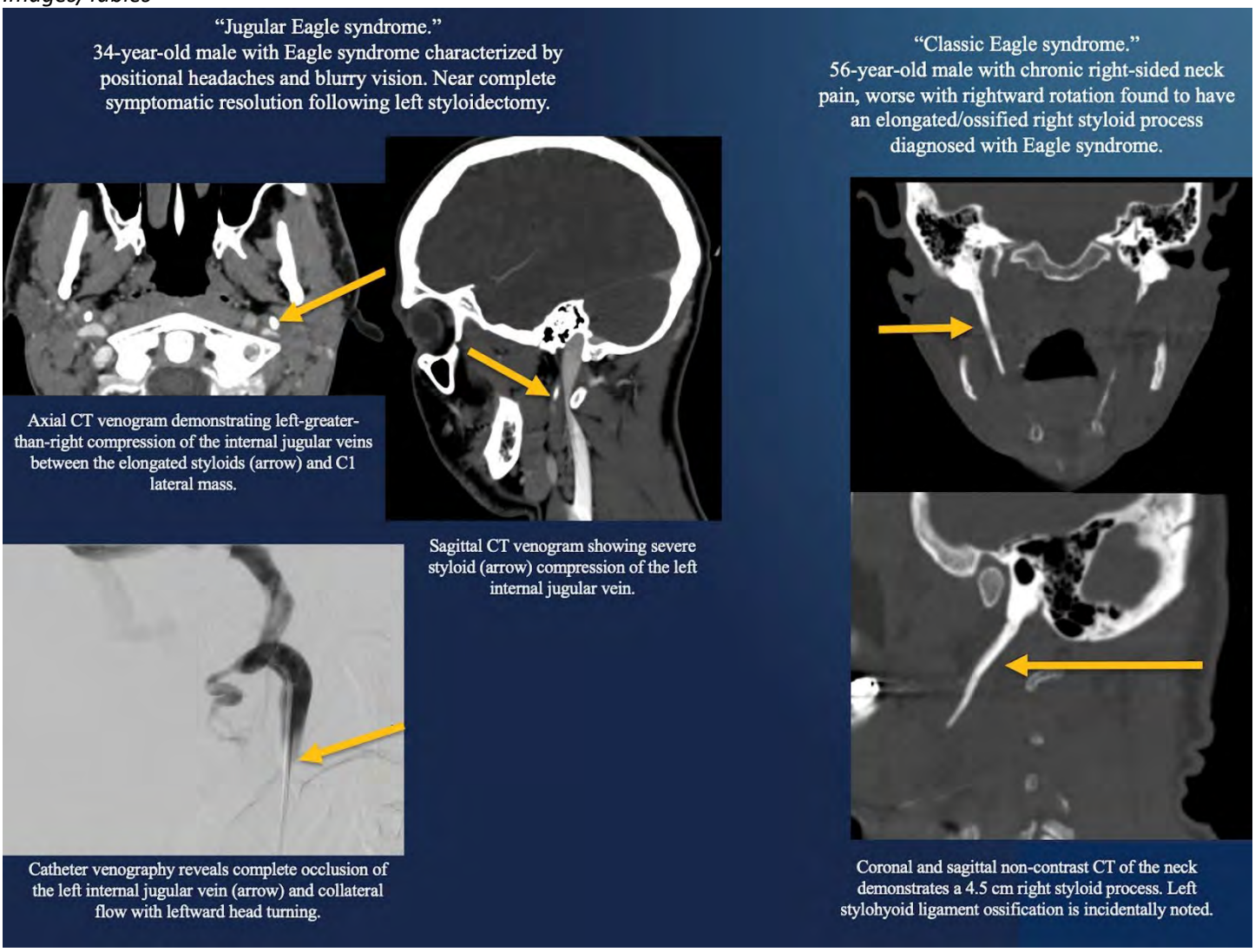
Pagano S, Ricciuti V, Mancini F, et al. Eagle syndrome: An updated review. Surg Neurol Int. 2023 Nov 3;14:389. DOI: 10.25259/SNI_666_2023. PMID: 38053694; PMCID: PMC10695462.

Murtagh RD, Caracciolo JT, Fernandez G. CT findings associated with Eagle syndrome. AJNR Am J Neuroradiol. 2001 Aug;22(7):1401-2. PMID: 11498437; PMCID: PMC7975191.

Zamboni P, Scerrati A, Menegatti E, et al. The eagle jugular syndrome. BMC Neurol. 2019 Dec 21;19(1):333. DOI: 10.1186/s12883-019-1572-3. PMID: 31864313; PMCID: PMC6925502.

Ceylan A, Köybaşioğlu A, Celenk F, et al. Surgical treatment of elongated styloid process: experience of 61 cases. Skull Base. 2008 Sep;18(5):289-95. DOI: 10.1055/s-0028-1086057. PMID: 19240828; PMCID: PMC2637062.

Images/Tables



399

Neuroradiologic Applications of Photon-Counting Computed Tomography

Jamie E. Clarke M.D., M.S.[1], Daphne Zhu B.S[2], Jay Acharya M.D.[1], John Go M.D.[3], Timothy J. Amrhein M.D.[4]

[1]University of California, Los Angeles, Los Angeles, CA, USA. [2]Division of Neuroradiology, Department of Radiology, Duke University, Durham, NC, USA. [3]Division of Neuroradiology, Department of Radiology, University of California Los Angeles (UCLA), Los Angeles, CA, USA. [4]Duke University, Durham, NC, USA

Abstract Category

New Techniques/Advanced Imaging/Informatics/AI/Professional Development/Misc

Summary & Objectives

Photon-counting computed tomography (PCCT) represents a significant advancement for the field of radiology. Photon-counting detectors (PCDs) used in PCCT offer substantial improvements in spatial resolution, contrast-to-noise ratio (CNR), and radiation dose efficiency compared to conventional energy-integrating detectors (EIDs). As such, PCCT can enhance neuroradiologic diagnostic efficacy and accuracy by increasing the resolution of images, and thus the sensitivity of subtle findings across a range of neurological conditions. Entities seen on PCCT that were often previously too spatially blurred to visualize include subtle dural tears, CSF-venous fistulae, small distal vessel occlusions, microaneurysms and other microvascular structures, tiny temporal bone defects and facial fractures, and much more. PCCT may also allow for detection of subtle fractures or defects in shunt catheters, intravascular stents, and orthopedic hardware within the brain and spine. Recent studies have indicated that PCCT can be paired with myelography to identify cerebrospinal fluid (CSF)-venous fistulas (CVFs) that were previously missed on digital subtraction myelography (DSM) or dynamic CT myelography using EIDs. Other CSF leak entities, such as dural ectasia and dural tears, also benefit

from PCCT myelography, enabling precise localization and differentiation of CSF leaks. Additional recent studies comparing the imaging quality of PCCT head CT angiography (CTA) to EID-CT highlighted PCCT's capacity to provide improved visualization of small arteries and enhance diagnostic confidence for intracranial aneurysms. Additionally, the sharper reconstruction kernels of PCCT improve arterial segment evaluation, facilitating more accurate diagnoses small vessel stenosis. In head and neck imaging, PCCT proves advantageous for detailed evaluation of intricate anatomical structures, particularly structures in the temporal bone as well as the cranial nerves. The application of PCCT to spine imaging is also gaining traction, providing detailed images of spinal anatomy and pathology. The higher resolution enhances visualization of critical vascular and nervous tissue structures, improving the ability of neuroradiologists to clearly visualize and quantitatively assess spinal nerve impingement, intervertebral disc herniations, paraspinal vascular abnormalities, bony lesions, and vertebral body compression. PCCT also shows promise in evaluating spinal hardware positioning and adjacent subtle tissue abnormalities. Overall, PCCT is positioned to dramatically advance the field of neuroradiology, with applications across every neuroradiology subdivision.

Purpose

The objectives of this educational exhibit are to (1) provide background information regarding the physics of PCCT, with a specific emphasis on aspects that differentiate it from EID-CT, (2) provide a summary of PCCT applications based on neuroradiology subdivision, including descriptions of head and neck, neurovascular, spine, and interventional neuroradiology entities in which PCCT may aid in assessment and/or diagnosis, and (3) explain the current limitations and future directions of PCCT implementation.

Materials & Methods

N/A

Results & Conclusion

N/A

References

Benson JC, Campeau NG, Diehn FE, et al. Photon-Counting CT in the Head and Neck: Current Applications and Future Prospects. *AJNR Am J Neuroradiol*. 2024;45(8):1000-1005. doi:10.3174/ajnr.A8265

Diehn FE, Zhou Z, Thorne JE, et al. High-Resolution Head CTA: A Prospective Patient Study Comparing Image Quality of Photon-Counting Detector CT and Energy-Integrating Detector CT. *AJNR Am J Neuroradiol*. Published online September 5, 2024:ajnr;ajnr.A8342v1. doi:10.3174/ajnr.A8342

Madhavan AA, Yu L, Brinjikji W, et al. Utility of Photon-Counting Detector CT Myelography for the Detection of CSF-Venous Fistulas. *AJNR Am J Neuroradiol*. 2023;44(6):740-744. doi:10.3174/ajnr.A7887

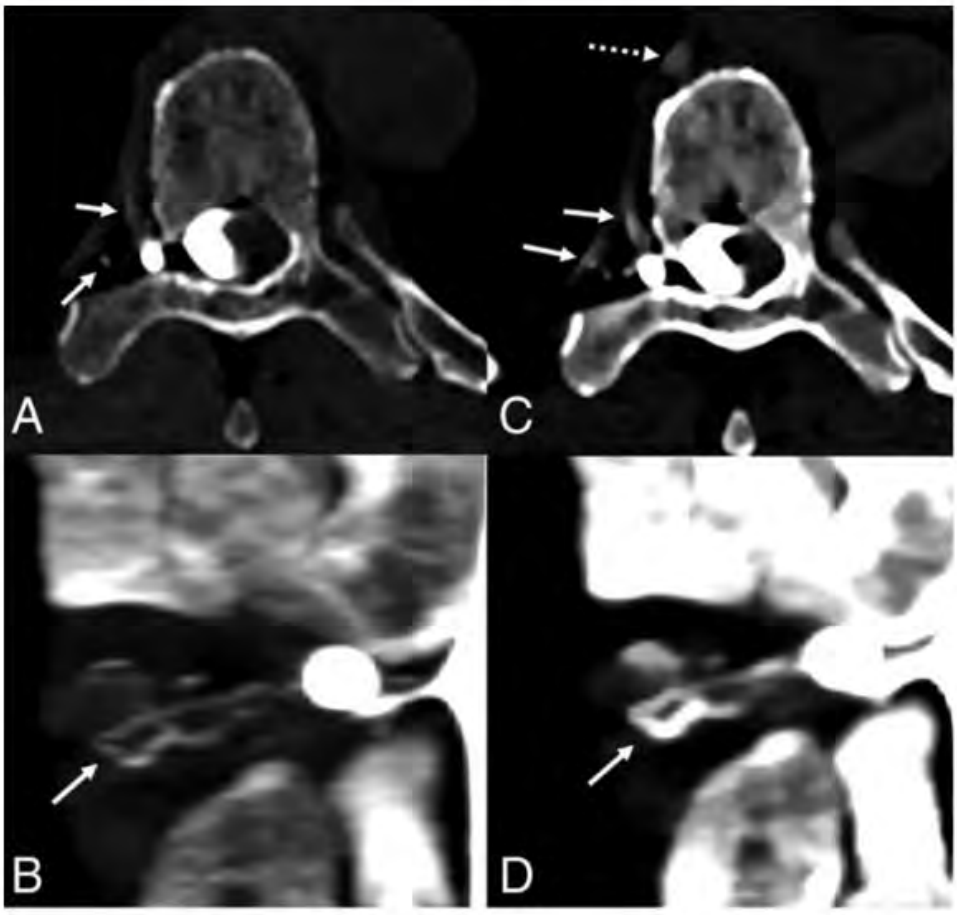
Tóth A, Chetta JA, Yazdani M, et al. Neurovascular Imaging with Ultra-High-Resolution Photon-Counting CT: Preliminary Findings on Image-Quality Evaluation. *AJNR Am J Neuroradiol*. Published online May 17, 2024:ajnr;ajnr.A8350v2. doi:10.3174/ajnr.A8350

Willemink MJ, Persson M, Pourmorteza A, Pelc NJ, Fleischmann D. Photon-counting CT: Technical Principles and Clinical Prospects. *Radiology*. 2018;289(2):293-312. doi:10.1148/radiol.2018172656

Images/Tables

FIGURE

Figure 1. Exemplary case of myelography images (A-D) acquired on a PCCT for identification of tiny veins (solid arrows) and the more distal azygous vein (dotted arrow) draining a right T6 CSF-venous fistula (image courtesy of Dr. Timothy J. Amrhein and colleagues who published this figure in the following AJNR article: doi:10.3174/ajnr.A7887)



400

Providing Insight into Acute Spinal Cord Infarct: Imaging Pearls, Challenges and Differential Diagnosis

Dhruti Maisuri MD, Ryan Sanchez DO, Hasan Zalov MD, Bundhit Tantiwongokosi md, Jason Lally MD, Achint Singh MD, Prabhakar Kesava MD
UTHSCSA, SAN ANTONIO, TEXAS, USA

Abstract Category

Spine

Summary & Objectives

- Acute spinal cord infarction is uncommon finding with diagnostic challenges.
- Imaging pitfall can occur during acute phase of ASCI. For example, acute spinal cord infarct may mimic other spinal cord pathologies like demyelination or mass lesion.
- Key MRI sequences for ASCI are T2W and DWI sequences. Additional STIR images are useful to diagnose possible co-existing bone infarct.

Purpose

1. Present case based review that demonstrates the MRI findings of acute spinal cord ischemia (ASCI) in both adults and children
2. To review the vascular anatomy of the spinal cord as it pertains to imaging findings in ASCI

3. Discuss common and uncommon etiologies of ASCI
4. Discuss radiological differential diagnosis of ASCI

Materials & Methods

The exhibit will review important imaging features of acute spinal cord ischemia in pediatric and adult patients at a tertiary care center and discuss possible differential diagnosis in acute clinical setting. Cases from our institution have been collected and presented with relevant MRI images. Important diagnostic, clinical and demographic features of each case is reviewed.

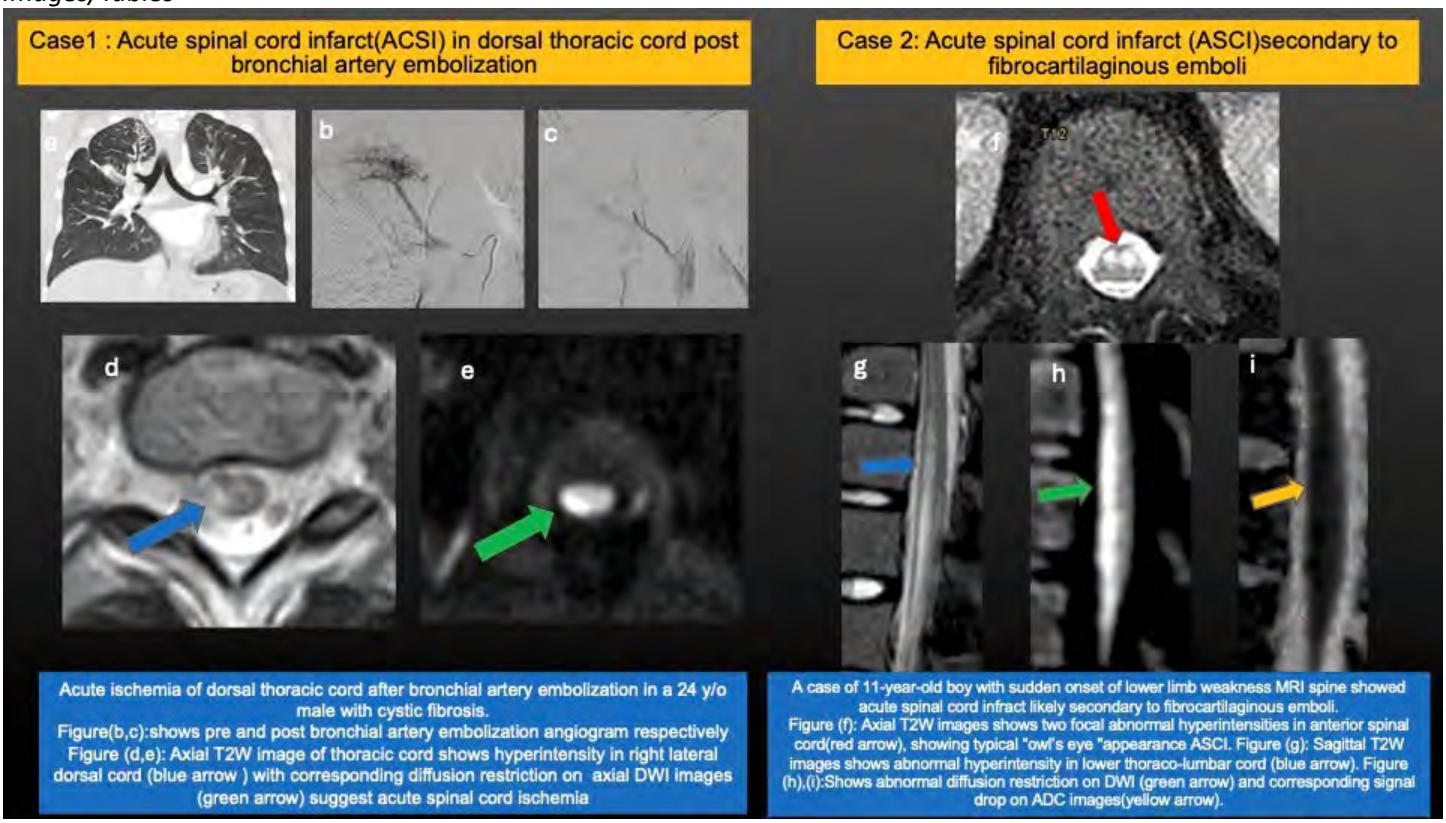
Results & Conclusion

Acute spinal cord ischemia is an uncommon diagnosis that requires a high index of suspicion by both the referring clinician and neuroradiologist interpreting the spinal MRI. Diagnosis can be especially challenging in the pediatric patient. This educational exhibit will present case based review of ASCI in pediatric and adult patients from our tertiary care center with an emphasis on the MRI findings including importance of DWI. For example “Owl ‘s eye " appearance is pathognomic for anterior spinal cord infarct. Based on our experience, diffusion weighted imaging (DWI) is highly recommended in all cases of acute myelopathy when possible. The STIR sequence is essential for detection of associated bone infarcts. The cases will demonstrate and discuss, a variety of etiologies of ASCI including atherosclerotic disease, thoracoabdominal dissection/ aneurysm repair, trauma, bronchial artery embolization for hemoptysis, and sports related injury and fibrocartilaginous emboli. Examples of anterior and posterior spinal artery infarcts will be shown. The exhibit will also review spinal cord vascular anatomy as it pertains to the MRI findings of ASCI. Finally, we will discuss the radiological differential diagnosis(like tumour, infection/inflammation, demyelination).

References

- Nogueira RG, et al, Restricted diffusion in spinal cord infarction demonstrated by magnetic resonance line scan
- Reisner A, et al, Spinal cord infarction following minor trauma in children: fibrocartilaginous embolism as a putative cause*. J Neurosurg Pediatr* 2013;11:445–50
- Thron AK, Vascular anatomy of the spine and spinal cord*, Interventional Neuroradiology.* New York*:* Informa Healthcare*;* 2008*:*39–55

Images/Tables



408

Imaging of Pulsatile Tinnitus

Hunter Carlock MD, Pavan Kottamasu MD, Yu T Zhao MD, Brian Won MD, Thomas Marini MD, Sankarsh Jetty MD, Shehanaz Ellika MBBS
University of Rochester Medical Center, Rochester, NY, USA

Abstract Category

Head and Neck

Summary & Objectives

Learning objectives of this educational exhibit:

- Review the definition and types of tinnitus.
- Summarize the imaging workup of pulsatile tinnitus.
- Review various etiologies of pulsatile tinnitus including arterial causes, arteriovenous causes, venous causes, and vascular tumors.
- Review other causes of tinnitus including bone dysplasias and temporomandibular joint pathology.

Tinnitus is the auditory perception of internal origin in the absence of external sound source and can significantly influence wellbeing and performance of affected individuals. This affects 25% of the western world, predominantly ages 40-70 but more common in elderly, and equally distributed among men and women. Pulsatile tinnitus is defined as auditory perception synchronous to the patient's heartbeat, and non pulsatile tinnitus is defined as continuous sound, often described as ringing, buzzing, or clicking. The most common cause of pulsatile tinnitus is due to atherosclerotic plaque contributing to arterial narrowing with turbulent blood or compensatory increased blood flow in cervical arteries. Craniocervical arterial dissection is another cause of pulsatile tinnitus due to similar mechanism of altered blood flow dynamics. Aberrant internal carotid artery is a congenital vascular anomaly resulting from failure of formation of extracranial internal carotid artery with arterial collateral pathways through the middle ear causing pulsatile tinnitus. Additional causes of pulsatile tinnitus include arteriovenous causes such as arteriovenous malformation and dural arteriovenous fistula. Venous causes of pulsatile tinnitus include dural venous sinus stenosis, jugular bulb dehiscence, sigmoid sinus dehiscence, sigmoid sinus diverticulum, intracranial hypertension, and idiopathic venous tinnitus. Vascular tumors causing pulsatile tinnitus include paragangliomas, meningiomas, hypervascular metastases, and endolymphatic sac tumors.

Purpose

Tinnitus evaluation can be challenging to both referring clinicians and radiologists. The purpose of this educational exhibit is to showcase the various causes of pulsatile tinnitus, along with its imaging workup and imaging features.

Materials & Methods

Teaching examples of pulsatile tinnitus were acquired from imaging archives at the author's institution.

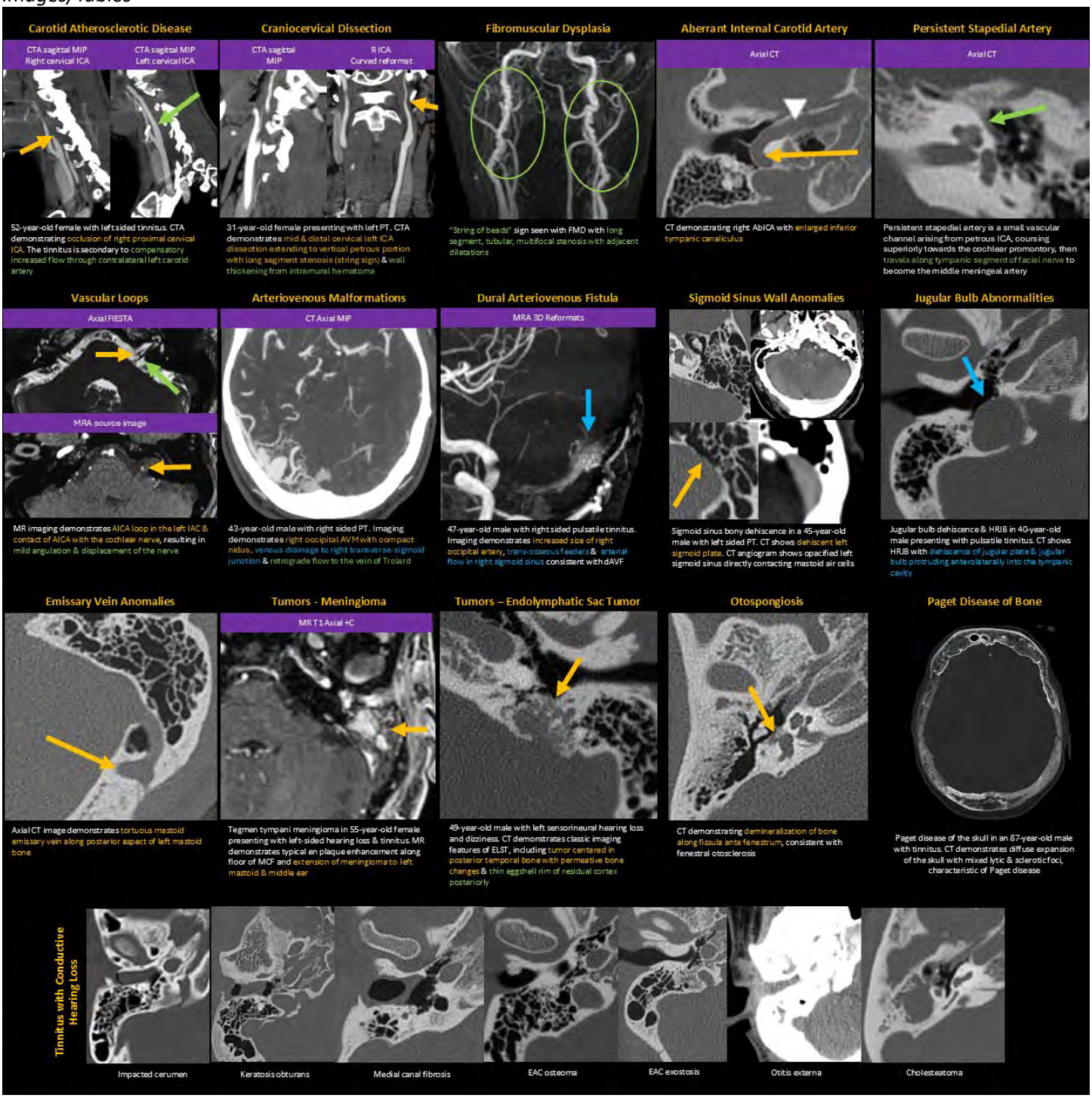
Results & Conclusion

Through this educational exhibit, the authors showcase imaging examples of the various causes of pulsatile tinnitus including arterial causes, arteriovenous causes, venous causes and vascular tumors. The authors will review imaging work up of pulsatile tinnitus along with ACR appropriate criteria.

References

1. Cummins DD, Caton MT, Shan V, et al. MRI and MR Angiography Evaluation of Pulsatile Tinnitus: A Focused, Physiology-Based Protocol. *J Neuroimaging* 2021;32(2):253-263. DOI:https://doi.org/10.1111/jon.12955
2. Shaar BA, Qureshy K, Almalki Y, et al. Ringing in the Ears: Approaches to Imaging and Management of Tinnitus. *Innovations in Surgery and Interventional Medicine*. 2024;4(2024):9-13. DOI: https://doi.org/10.36401/ISIM-23-02
3. Kumar R, Rice S, Lingam RK. Detecting causes of pulsatile tinnitus on CT arteriography-venography: A pictorial review. *Eur J Radiol* 2021;139:109722. DOI: https://doi.org/10.1016/j.ejrad.2021.109722
4. Abdalkader M, Nguyen TN, Norbash AM, et al. State of the Art: Venous Causes of Pulsatile Tinnitus and Diagnostic Considerations Guiding Endovascular Therapy. *Radiology* 2021;300(1):2-16. DOI: https://doi.org/10.1148/radiol.2021202584
5. Narsinh KH, Hui F, Duvvuri M, et al. Management of vascular causes of pulsatile tinnitus. *J Neurointerv Surg* 2021;14(11):1151-1157. DOI: https://doi.org/10.1136/neurointsurg-2021-018015

Images/Tables



412

Decoding Leukodystrophies: The Role of MRI in Diagnosis and Management

Jordan B Hughes MD[1], Anisa Chowdhary MD[1], Anish Neupane MD[1], Ajay Malhotra MD[2]
[1]Bridgeport Hospital, Bridgeport, CT, USA. [2]Yale School of Medicine, New Haven, CT, USA

Abstract Category

Adult Brain Inflammatory/Infectious Disease/Degenerative/Metabolic

Summary & Objectives

Leukodystrophies are a group of CNS white matter disorders that usually present early in childhood. They are caused by inherited enzyme deficiencies that lead to abnormal myelin formation, turnover or breakdown (1). Typical leukodystrophies include Alexander disease, Canavan disease, globoid cell leukodystrophy (Krabbe disease),

megalencephalic leukoencephalopathy with subcortical cysts, metachromatic leukodystrophy, Pelizaeus-Merzbacher disease, vanishing white matter disease and x-linked adrenoleukodystrophy. In addition to these typical leukodystrophies, numerous atypical and less common leukodystrophies have been described. MRI is the imaging modality of choice for evaluation of leukodystrophies. MRI is useful in helping to establish a diagnosis and assessing disease severity. All leukodystrophies tend to have symmetric involvement and there can be significant overlap in MRI findings across many leukodystrophies. However, certain characteristics such as distribution and sparing or involvement of the subcortical U-fibers can suggest a diagnosis of one leukodystrophy over another. An algorithm has been proposed that utilizes multiple MRI findings to assist in the diagnosis of white matter disorders (2). Even with characteristic imaging features on MRI, genetic testing is usually required for definitive diagnosis (3).

Purpose

Our objective is to review and demonstrate key imaging characteristics of several leukodystrophies including some of the distinguishing features that can favor a diagnosis of one type of leukodystrophy over another.

Materials & Methods

In this exhibit, we retrospectively reviewed images from our PACS system to present cases that help illustrate characteristic MRI imaging features of several leukodystrophies.

Results & Conclusion

MRI remains an important tool in evaluation of leukodystrophies. Careful MRI analysis can help narrow diagnosis, assess severity and monitor disease progression resulting in a significant impact on patient care and management.

References

1.Cheon J, Kim I, Hwang Y et al. Leukodystrophy in Children: A Pictorial Review of MR Imaging Features. *Radiographics* 2002;22(3):461-76. doi:10.1148/radiographics.22.3.g02ma01461

2. Schiffmann R, van der Knaap MS. Invited article: an MRI-based approach to the diagnosis of white matter disorders. *Neurology* 2009;72(8):750-59. doi:10.1212/01.wnl.0000343049.00540.c8

3. Kevelam SH, Steenweg ME, Srivastava S, et al. Update on Leukodystrophies: A Historical Perspective and Adapted Definition. *Neuropediatrics* 2016;47(6):349-54. doi:10.1055/s-0036-1588020

Images/Tables

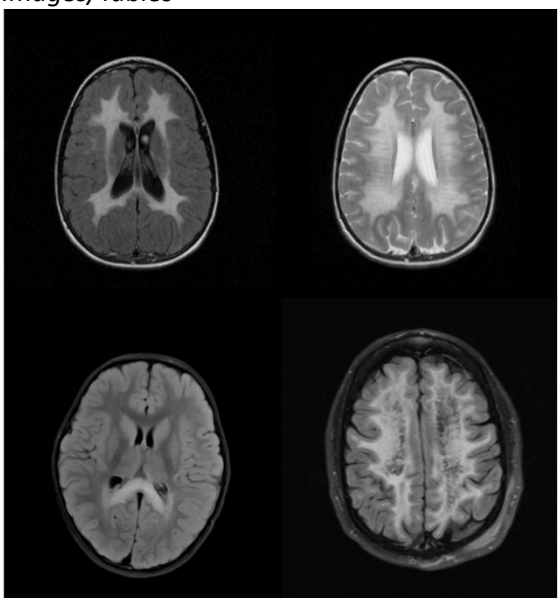


Figure 1. (A) Axial FLAIR images in an 8 year-old with previously diagnosed metachromatic leukodystrophy demonstrate symmetric periventricular white matter hyperintensity with sparing of the subcortical U-fibers . (B) T2 images in the same patient show a “tigrioid stripe” appearance of the periventricular white matter. (C) Axial FLAIR images in a 4 year-old with x-linked adrenoleukodystrophy demonstrate bilateral peritrigonal hyperintensities with involvement of the splenium of the corpus collosum . (D) Axial FLAIR images in a 6 year-old demonstrate periventricular and subcortical hyperintensities with “tigroid stripes” consistent with a known history of vanishing white matter disease.

416

Assessment of Intraventricular Brain Lesions in Children - A Systematic Approach of Typical and Atypical Masses

Otavio Augusto Ferreira Dalla Pria MD[1], Nitesh Shekhrajka MD[1], Joan A Maley MD, FACR[1], Takashi Shawn P Sato MD[1], Sara Reis Teixeira MD, Ph.D.[2], Laiz Laura de Godoy MD, Ph.D.[3]

[1]University of Iowa Health Care, Iowa City, IA, USA. [2]Children's Hospital of Philadelphia, Philadelphia, PA, USA. [3]University of Pennsylvania Health System, Philadelphia, PA, USA

Abstract Category

Pediatrics

Summary & Objectives

Intraventricular brain lesions encompass myriad presentations in both clinical symptomology and radiological findings and frequently represent a challenge for the radiologist since multiple imaging features overlap among these lesions. Nevertheless, they account for a relevant incidence in our daily practice regardless of being an experienced neuroradiologist or a junior resident taking calls. Given their importance, a constant review of these entities is mandatory to succeed in neuroradiology.

Purpose

This exhibit aims: 1. To review the literature concerning children's intraventricular brain lesions, including tumors, cysts, infection, and others; 2. To describe multi-modality imaging findings helpful in narrowing the differentials and relevant clinical presentations based on location, age, sex, etc. 3. To depict cases of supra and infratentorial intraventricular brain lesions in children with a systematic approach by organizing them into two main subgroups: a) Supratentorial – lateral, third ventricles (choroid plexus and ventricle wall), foramen of Monroe, and septum pellucidum b) Infratentorial - fourth ventricle (choroid plexus and ventricle wall). Each subgroup will be split into typical and atypical lesions based on their typical location and imaging appearance.

Materials & Methods

1.Concise exposition delineating the embryology, anatomical configuration, and physiological attributes pertinent to the ventricular system; 2. Illustration of diverse typical cases featuring intraventricular cerebral lesions, including but not limited to cysts, ependymoma, subependymoma, central neurocytoma, subependymal giant cell tumor, choroid plexus neoplasm, medulloblastoma, meningiomas, juxtaposed with a comprehensive examination of atypical intraventricular tumors, such as atypical teratoid/rhabdoid tumors, cavernous malformation, metastasis, lymphoma, chordoma, etc. Furthermore, the incorporation of cases initially presumed to originate intrinsically but ultimately diagnosed within the extraventricular ambit due to radiological manifestations.

Results & Conclusion

This exhibit presents a practical approach to pediatric intraventricular lesions, which is useful for daily neuroradiology/pediatric radiology practice. We expect to contribute with familiarization of neuroimaging features, including pattern of enhancement, presence of calcification, hemorrhage, diffusivity, and location, as well as clinical factors, such as age and gender to narrow differential diagnosis of typical intraventricular masses. In addition, we included challenging atypical intraventricular masses, which may come across in our routine as neuroradiologists.

References

1.Jelinek, J., Smirniotopoulos, J.G., Parisi, J.E. and Kanzer, M., 1990. Lateral ventricular neoplasms of the brain: differential diagnosis based on clinical, CT, and MR findings. *American journal of neuroradiology*, *11*(3), pp.567-574.

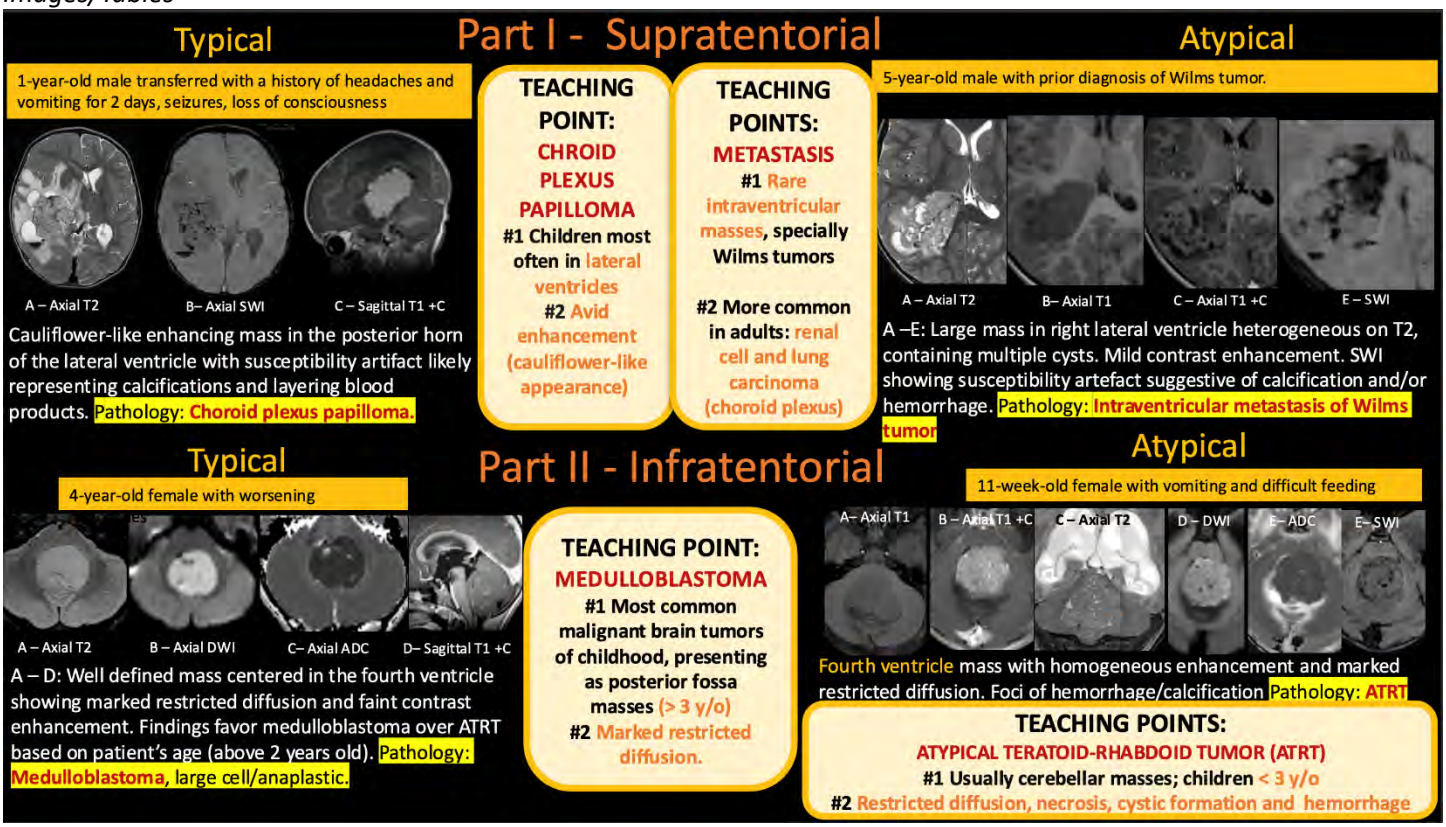
2.Gonçalves, F.G., Mahecha-Carvajal, M.E., Desa, A., Yildiz, H., Talbeya, J.K., Moreno, L.A., Viaene, A.N. and Vossough, A., 2024. Imaging of supratentorial intraventricular masses in children: a pictorial review—part 1. *Neuroradiology*, *66*(5), pp.677-698.

3.Goncalves, F.G., Mahecha-Carvajal, M.E., Desa, A., Yildiz, H., Talbeya, J.K., Moreno, L.A., Viaene, A.N. and Vossough, A., 2024. Imaging of supratentorial intraventricular masses in children: a pictorial review—part 2. *Neuroradiology*, *66*(5), pp.699-716.

4.Suh, D.Y. and Mapstone, T., 2001. Pediatric supratentorial intraventricular tumors. *Neurosurgical focus*, *10*(6), pp.1-14.

5.Osborn, A.G., Louis, D.N., Poussaint, T.Y., Linscott, L.L. and Salzman, K.L., 2022. The 2021 World Health Organization classification of tumors of the central nervous system: what neuroradiologists need to know. *American Journal of Neuroradiology*, *43*(7), pp.928-937.

Images/Tables



417

Characteristics and Risk Factors for Intracranial Subdural Hematomas

Caline Azzi MD[1], Armin Tafazolimoghadam MD[2], Mahla Radmard MD[1], Soyeb Aftab[3], Chi Trinh[1], Tej D. Azad MD[1], Ali Bydon MD[1], Arjun S. Chanmugam MD, MBA[1], David M. Yousem MD, MBA[1]
[1]Johns Hopkins, Baltimore, Maryland, USA. [2]Tehran University of Medical Sciences, Tehran, Iran, Iran, Islamic Republic of. [3]All India Institute of Medical Sciences, New Delhi, India, India

Abstract Category

Head and Neck

Summary & Objectives

Subdural hematomas (SDHs) are common manifestations of head trauma in patients with positive non-contrast head CT scans (NCCT). This study investigates the patient characteristics and risk factors linked to SDHs larger than 5 mm versus those smaller than 5 mm, aiming to provide clarity on outcomes and treatment implications.

Purpose

Subdural hematomas (SDHs) are common manifestations of head trauma in patients with positive non-contrast head CT scans (NCCT). This study investigates the patient characteristics and risk factors linked to SDHs larger than 5 mm versus those smaller than 5 mm, aiming to provide clarity on outcomes and treatment implications.

Materials & Methods

We performed a retrospective analysis of NCCT reports for patients evaluated at two emergency departments within our health system from July 1, 2018, to June 30, 2024 to identify SDH cases. We analyzed electronic medical records to gather data on demographics (age, gender, race), comorbidities (hypertension, chronic kidney disease, diabetes), and relevant NCCT findings, allowing for a comprehensive comparison of outcomes based on hematoma size, specifically focusing on a 5 mm cut-off.

Results & Conclusion

Results: Among 262 patients, 140 had SDHs ≤ 5 mm, while 122 had SDHs > 5 mm. There were 168 males (mean age 56.22 years, SD 17) and 94 females (mean age 61.23 years, SD 15.24). The racial demographics included 160 White patients (mean age 61.91, SD 14.57), 83 Black patients (mean age 52.55, SD 17.63), and 19 patients of other races (mean age 49.16, SD 17.87). Bivariate analysis revealed significant associations between SDH size and several factors, including age over 65 (p=0.01), Glasgow Coma Scale (GCS) score (p=0.045), thrombocytopenia (p=0.03), and bleeding diathesis

(p=0.01). Larger SDHs were more likely to impact multiple extra-axial regions (p<0.001), cause midline shift (p<0.001), and be accompanied by epidural hematomas (p=0.04). Notably, patients with SDHs > 5 mm had a higher likelihood of surgical intervention (p<0.001), complications (p<0.001), prolonged hospital stays, and more follow-up NCCTs (p=0.002), along with reduced chances of being discharged home (p<0.001).
Conclusion: This study highlights the near-even distribution of SDHs based on size, with age and coagulopathy as significant risk factors for larger hematomas, which carry poorer prognoses and higher surgical needs. The findings advocate for tailored follow-up strategies that could enhance resource allocation and improve outcomes in emergency settings for patients with varying SDH sizes.
References
Vande Vyvere T, Pisică D, Wilms G, Claes L, Van Dyck P, Snoeckx A, van den Hauwe L, Pullens P, Verheyden J, Wintermark M, Dekeyzer S, Mac Donald CL, Maas AIR, Parizel PM. Imaging Findings in Acute Traumatic Brain Injury: a National Institute of Neurological Disorders and Stroke Common Data Element-Based Pictorial Review and Analysis of Over 4000 Admission Brain Computed Tomography Scans from the Collaborative European NeuroTrauma Effectiveness Research in Traumatic Brain Injury (CENTER-TBI) Study. J Neurotrauma. 2024 Oct;41(19-20):2248-2297. doi: 10.1089/neu.2023.0553. Epub 2024 Apr 18. PMID: 38482818.
In 2010, the National Institute of Neurological Disorders and Stroke (NINDS) created a set of common data elements (CDEs) to help standardize the assessment and reporting of imaging findings in traumatic brain injury (TBI). However, as opposed to other standardized radiology reporting systems, a visual overview and data to support the proposed standardized lexicon are lacking. We used over 4000 admission computed tomography (CT) scans of patients with TBI from the Collaborative European NeuroTrauma Effectiveness Research in Traumatic Brain Injury (CENTER-TBI) study to develop an extensive pictorial overview of the NINDS TBI CDEs, with visual examples and background information on individual pathoanatomical lesion types, up to the level of supplemental and emerging information (e.g., location and estimated volumes). We documented the frequency of lesion occurrence, aiming to quantify the relative importance of different CDEs for characterizing TBI, and performed a critical appraisal of our experience with the intent to inform updating of the CDEs. In addition, we investigated the co-occurrence and clustering of lesion types and the distribution of six CT classification systems. The median age of the 4087 patients in our dataset was 50 years (interquartile range, 29-66; range, 0-96), including 238 patients under 18 years old (5.8%). Traumatic subarachnoid hemorrhage (45.3%), skull fractures (37.4%), contusions (31.3%), and acute subdural hematoma (28.9%) were the most frequently occurring CT findings in acute TBI. The ranking of these lesions was the same in patients with mild TBI (baseline Glasgow Coma Scale [GCS] score 13-15) compared with those with moderate-severe TBI (baseline GCS score 3-12), but the frequency of occurrence was up to three times higher in moderate-severe TBI. In most TBI patients with CT abnormalities, there was co-occurrence and clustering of different lesion types, with significant differences between mild and moderate-severe TBI patients. More specifically, lesion patterns were more complex in moderate-severe TBI patients, with more co-existing lesions and more frequent signs of mass effect. These patients also had higher and more heterogeneous CT score distributions, associated with worse predicted outcomes. The critical appraisal of the NINDS CDEs was highly positive, but revealed that full assessment can be time consuming, that some CDEs had very low frequencies, and identified a few redundancies and ambiguity in some definitions. Whilst primarily developed for research, implementation of CDE templates for use in clinical practice is advocated, but this will require development of an abbreviated version. In conclusion, with this study, we provide an educational resource for clinicians and researchers to help assess, characterize, and report the vast and complex spectrum of imaging findings in patients with TBI. Our data provides a comprehensive overview of the contemporary landscape of TBI imaging pathology in Europe, and the findings can serve as empirical evidence for updating the current NINDS radiologic CDEs to version 3.0.

Images/Tables

Table 1: Assessing the relation between study variables and the initial size of SDH

		SDH ≤ 5mm N=140	SDH >5mm N=122	P-value
Age group (65+)		73 (52.1%)	82 (67.2%)	0.01
Gender (F)		46 (32.9%)	48 (39.3%)	0.28
Race	White	92 (65.7%)	68 (55.7%)	0.16
	Black	41 (29.3%)	42 (34.4%)	
	others	7 (5.0%)	12 (9.8%)	
Antiplatelet/Anticoagulant use		45 (32.1%)	40 (32.8%)	0.91
Alcohol abuse		34 (24.3%)	27 (22.1%)	0.68
Mechanism	Fall	77 (55.0%)	82 (67.2%)	0.10
	MVA	34 (24.3%0	18 (14.8%)	
	Assault	23 (16.4%)	14 (11.5%)	
	Others	6 (4.3%)	8 (6.6%)	
GCS	13-15	112 (84.2%)	82 (71.3%)	0.045
	9-12	4 (3.0%)	8 (7.0%)	
	3-8	17 (12.8%)	25 (21.7%)	
Thrombocytopenia		15 (10.9%)	25 (20.5%)	0.03
Bleeding Diathesis		3 (2.1%)	12 (9.8%)	0.01
Location	Frontal	48 (34.3%)	21 (17.2%)	<0.001
	Temporal	11 (7.9%)	0	
	Parietal	11 (7.9%)	8 (6.6%)	
	Occipital	5 (3.6%)	2 (1.6%)	
	Multiple	59 (42.1%)	88 (72.1%)	
	Others	6 (4.3%)	3 (2.5%)	
SAH		52 (37.1%)	59 (48.4%)	0.07
EDH		1 (0.7%)	6 (4.9%)	0.04
Midline shift		12 (8.6%)	57 (46.7%)	<0.001
Surgical Treatment		4 (2.9%)	19 (15.6%)	<0.001
Specific surgical treatment	None	132 (94.3%)	103 (84.4%)	0.004
	Craniotomy	4 (2.9%)	15 (12.3%)	
	Burr hole	0	3 (2.5%)	
	others	4 (2.9%)	1 (0.8%)	
Medical Management		127 (90.7%)	116 (95.1%)	0.17
Complication (at least one)		27 (19.3%)	53 (43.4%)	<0.001
Discharge	Home	103 (73.6%)	57 (46.7%)	<0.001
	Rehabilitation	25 (17.9%0	47 (38.5%)	
	Death	12 (8.6%)	18 (14.8%)	
Observation (ICU)		75 (53.6%)	36 (29.5%)	<0.001
Length of hospitalization		2.00 (1.00, 5.00)	4.50 (2.00, 14.00)	<0.001

- Categorical data are presented as numbers (percentages) and analyzed using the Chi-square test.
- Quantitative data are presented as the median (first quartile [Q1], third quartile [Q3]) and analyzed using the Mann-Whitney test.

425

Differential Diagnosis of Demyelinating Spinal Cord Lesions

Afua O Addo[1], Kevin Thomas[2], Shannon Chu[2], Usiwat Abdul[2], Kevin Hu[2], Rowan Melcher[1], Cesar Colasante MD[2], Murtaza Syed MD[2], Mishal Shahab MBBS[3], Markus Lammle MD, PhD[3]

[1]Norton College of Medicine, SUNY Upstate Medical University, Syracuse, 13202, USA. [2]SUNY Upstate Medical University, Syracuse, NY, USA. [3]Department of Radiology, SUNY Upstate Medical University, Syracuse, New York, USA

Abstract Category

Spine

Summary & Objectives

Demyelinating diseases of the central nervous system are caused by damage to the myelin sheath or to the oligodendrocytes which produce and maintain it.[1] The differential diagnoses include but are not limited to primary CNS autoimmune causes, as seen in multiple sclerosis (MS), Acute Disseminated Encephalomyelitis (ADEM), Neuromyelitis Optica (NMO), and Myelin Oligodendrocyte Glycoprotein Antibody-Associated Disease (MOGAD); systemic autoimmune disorders such as Neurosarcoidosis, Sjogren's Syndrome, Systemic Lupus Erythematosus (SLE), Neuro-Behçet Disease, and Paraneoplastic Myelitis; infectious causes such as Herpes Simplex Virus (HSV) Encephalitis and Human T-Lymphotropic Virus Type-1 Associated Myelopathy (HAM); Transverse Myelitis which is associated with idiopathic, infectious, or MS-related causes; metabolic causes as seen in Subacute Combined Degeneration (SCD); vascular disorders with spinal cord ischemia, infarction, sometimes associated with vascular malformations; lymphoproliferative disorders such as Spinal Non-Hodgkin's Lymphoma (NHL); and genetic causes such as X-linked Adrenoleukodystrophy (X-ALD).

Clinical presentations of these conditions may be non-specific. MRI diagnostic imaging can provide valuable information regarding detection, differential diagnosis, clinical management and prognosis. MRI findings typically demonstrate low signal intensity on T1 and high signal intensity on T2 and STIR images. Some lesions on imaging are more focal or multifocal, others longitudinal, or coalescent. The presentation can be acute, remittent, or chronic. Some are reversible and others are persistent. Some occasionally demonstrate contrast enhancement. Conditions such as ADEM can be tumefactive, presenting mass-like, and sometimes mistaken for an intraspinal tumor.[2]

However, there are several classic MRI imaging findings for individual demyelinating disorders, such as "Dawson's fingers", multifocal hyperintensities on T2 and STIR images, with either discrete or diffuse lesions for MS[2]; "open ring sign", diffuse hyperintensity in T2 and STIR images, and involvement of the area postrema for ADEM; involvement of optic pathways in combination with the "bright spotty sign", patchy or diffuse hyperintense lesions on T2 and STIR images, and long segment cord involvement for NMO[2]; bilateral optic neuritis and "H sign" for MOGAD[3]; long segment involvement and post contrast "trident sign" for Neurosarcoidosis[4-5] and HAM[5]; T2 hyperintensity of the dorsal columns for Sjogren's Syndrome[6]; long segment cord hyperintensity on T2 and STIR images for SLE[7], Paraneoplastic Myelitis[8], and Transverse Myelitis[2,6]; short segment posterolateral cord involvement for Neuro-Behçet Disease[9]; T2 hyperintense, punctate lesions for HSV Encephalitis[10]; the "inverted V-sign" spanning multiple cord segments for SCD[11]; intra- or extradural T2 enhancement for vascular malformations[12]; solitary or multiple T2 hyperintense lesions that may compress the spinal cord for NHL[13]; and thoracic spinal cord atrophy for X-ALD.[14]

Imaging findings are always interpreted in the context of patient history, clinical presentation and cause over time, and laboratory findings. Specific imaging findings and common presentations of demyelinating disorders with spinal cord involvement are demonstrated in this educational exhibit.

Purpose

To review the various causes, incidences, clinical presentations, and classic imaging findings in demyelinating disorders with manifestation in the spinal cord.

Materials & Methods

N/A

Results & Conclusion

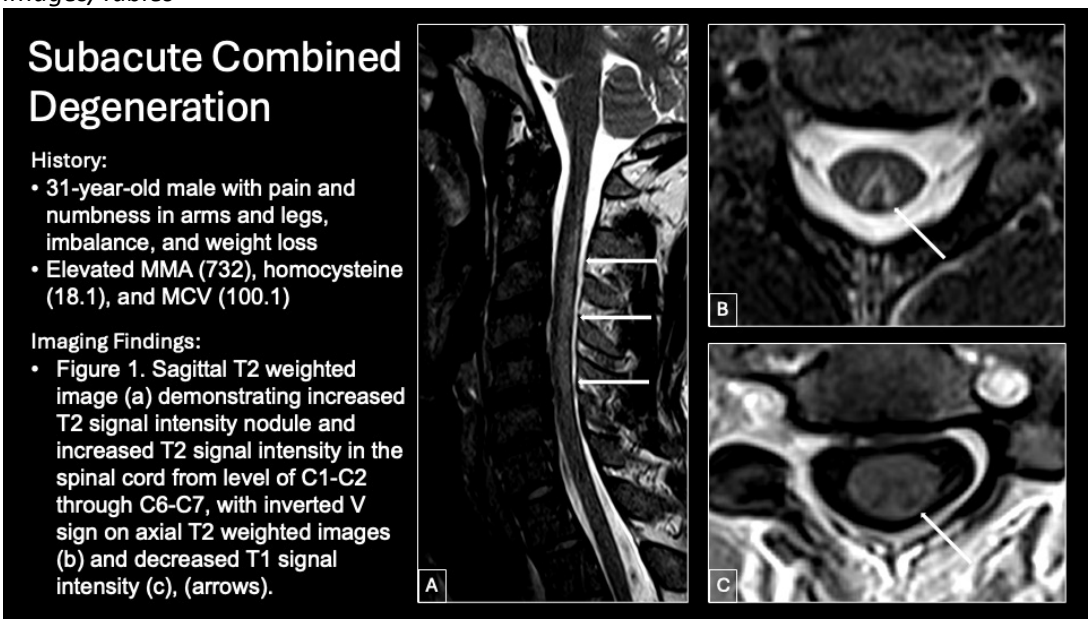
N/A

References

1. Smith AB, Smirniotopoulos JG. Imaging evaluation of demyelinating processes of the central nervous system. Postgrad Med J. 2010 Apr;86(1014):218-29. doi: 10.1136/pgmj.2009.087452.

2. Barkhof F, Koeller KK. (2020). Demyelinating diseases of the CNS (brain and spine). *Diseases of the Brain, Head and Neck, Spine 2020–2023: Diagnostic Imaging*, 165-17

3. Dubey D, Pittock SJ, Krecke KN, et al. Clinical, Radiologic, and Prognostic Features of Myelitis Associated With Myelin Oligodendrocyte Glycoprotein Autoantibody. JAMA Neurol. 2019 Mar 1;76(3):301-309.
4. Zalewski N, Krecke K, Weinshenker B, et al. Central Canal Enhancement and the Trident Sign in Spinal Cord Sarcoidosis. Neurology. 2016;87(7):7434.doi:10.1212/wnl.0000000000002992
5. Dixon L, McNamara C, Dhasmana D, et al. Imaging Spectrum of HTLV-1-Related Neurologic Disease: A Pooled Series and Review. Neurol Clin Pract. 2023 Jun;13(3):e200147.
Images/Tables

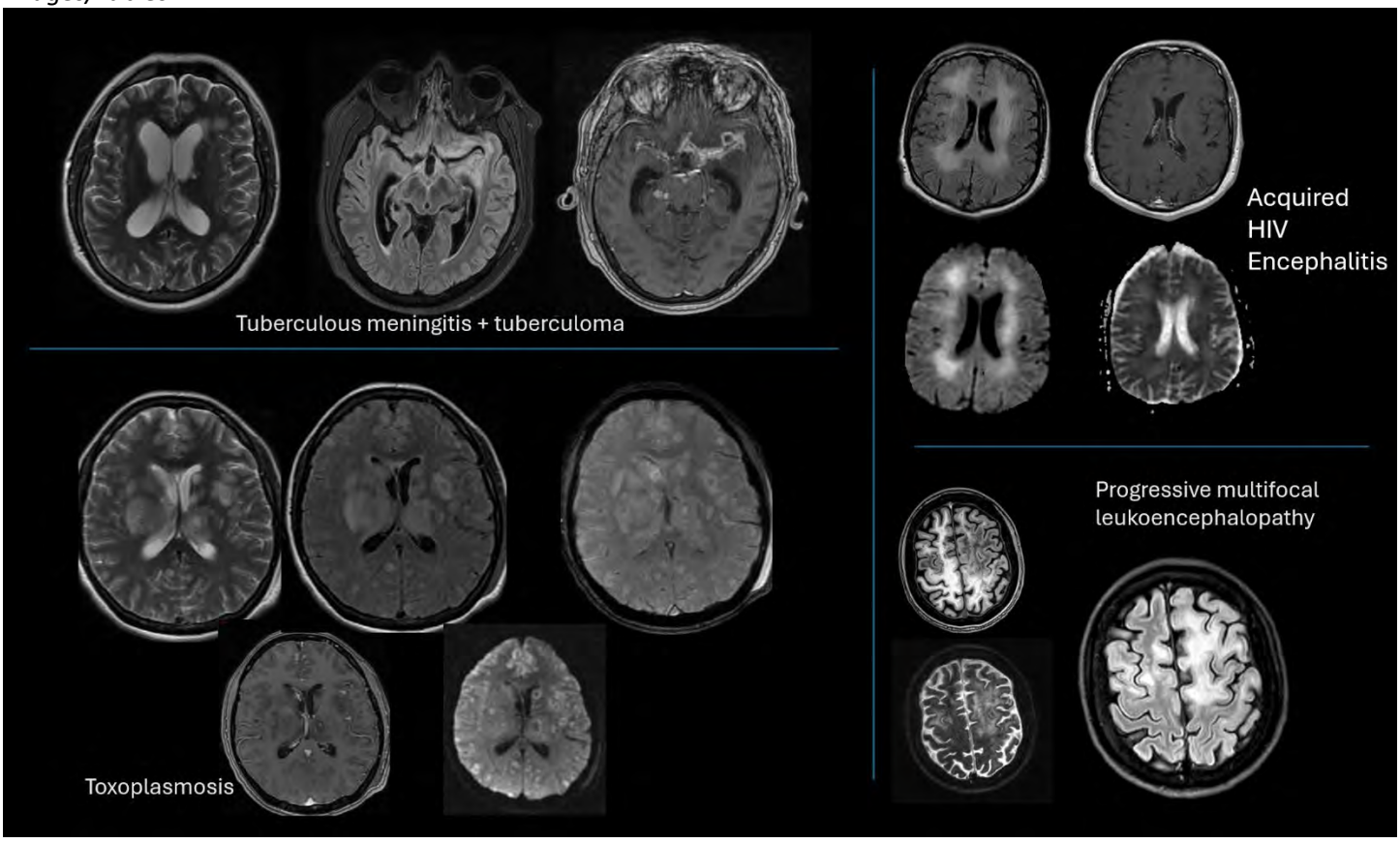


445

Hidden Threats: Neuroradiological Insights into CNS Opportunistic Infections in Immunocompromised Patients

Karla Daniela Fuentes Badillo MD, Arturo Maximiliano Rodriguez Saldivar MD, Haziel Maya Garcia MD, Mariana Mercado Flores MD
Hospital Universitario Dr. Jose Eleuterio Gonzalez, Monterrey, Nuevo Leon, Mexico
Abstract Category
Adult Brain Inflammatory/Infectious Disease/Degenerative/Metabolic
Summary & Objectives
Hidden Threats: Neuroradiological Insights into CNS Opportunistic Infections in Immunocompromised Patients
Purpose
To analyze the neuroradiological characteristics of central nervous system (CNS) opportunistic infections in immunocompromised patients.
Materials & Methods
Neuroradiological insights into central nervous system (CNS) opportunistic infections are critical for accurate diagnosis and management, particularly in immunocompromised patients. The imaging findings vary depending on the causative pathogen and the host's immune status.
In HIV-infected patients, CNS opportunistic infections such as progressive multifocal leukoencephalopathy (PML), toxoplasmosis, and cryptococcosis are common. These infections can present with mass lesions, meningoencephalitis, demyelination, atrophy, and vascular lesions on imaging. The introduction of highly active antiretroviral therapy (HAART) has significantly reduced the incidence of these infections, although immune reconstitution inflammatory syndrome (IRIS) can complicate the imaging appearance post-HAART initiation.
Bacterial infections, including those caused by Streptococcus, Haemophilus, and Neisseria species, typically present with meningitis, cerebritis, and abscess formation. Tuberculosis, a granulomatous infection, often manifests as tuberculomas, which are the most common parenchymal form of the disease. Fungal infections, such as cryptococcal meningitis, are prevalent in immunocompromised hosts and can present with meningeal enhancement, abscesses, and hydrocephalus.

Parasitic infections like toxoplasmosis and neurocysticercosis show characteristic imaging patterns, including ring-enhancing lesions and cystic formations.
MRI is the preferred modality for evaluating CNS infections due to its superior soft tissue contrast and ability to detect early parenchymal changes. Diffusion-weighted imaging (DWI) is particularly useful in differentiating pyogenic abscesses from other ring-enhancing lesions and in early detection of viral encephalitis lesions. Proton magnetic resonance spectroscopy (MRS) can provide specific metabolic patterns, such as the presence of lactate and cytosolic amino acids in abscesses, aiding in diagnosis.
Results & Conclusion
In summary, neuroradiological evaluation of CNS opportunistic infections involves recognizing specific imaging patterns associated with different pathogens. MRI, including advanced techniques like DWI and MRS, plays a crucial role in the early and accurate diagnosis of these infections.
References
Bowen LN, Smith B, Reich D, Quezado M, et al. HIV-associated opportunistic CNS infections: pathophysiology, diagnosis and treatment. Nat Rev Neurol. 2016;12(11):662-674. doi:10.1038/nrneurol.2016.149
Smith AB, Smirniotopoulos JG, Rushing EJ. Central Nervous System Infections Associated with Human Immunodeficiency Virus Infection: Radiologic-Pathologic Correlation. RadioGraphics. 2008;28(7):2033-2058. doi:10.1148/rg.287085135
Shih RY, Koeller KK. Bacterial, Fungal, and Parasitic Infections of the Central Nervous System: Radiologic-Pathologic Correlation and Historical Perspectives: From the Radiologic Pathology Archives. RadioGraphics. 2015;35(4):1141-1169. doi:10.1148/rg.2015140317b
Images/Tables



447

Manifestations of HIV/AIDS in the Central Nervous System

Eric Lopez MD, Shin Mei Chan MD, Shankarapryan Sivanushanthan MD, MS, Allen Ye MD, PhD, Weiya Mu MD
UCSF, San Francisco, CA, USA
Abstract Category
Adult Brain Inflammatory/Infectious Disease/Degenerative/Metabolic

Summary & Objectives

HIV/AIDS causes a wide range of pathology in the central nervous system (CNS), including direct sequelae of the viral infection, opportunistic infections and characteristic neoplasms in the immunocompromised host, and treatment-related effects. Although the incidence of opportunistic infection has decreased with the advent of highly active antiretroviral therapy (HAART), familiarity with the CNS manifestations of HIV/AIDS, or neuroAIDS, remains critical for timely diagnosis and treatment of these patients, particularly among populations without consistent access to antiretrovirals. In this presentation, we provide a pictorial review of manifestations of HIV/AIDS in the brain and spine.

Purpose

We review the imaging findings, differential diagnosis and treatment of CNS manifestations of HIV/AIDS, including neurodegenerative, infectious, and neoplastic pathology, as well as treatment-related effects.

Materials & Methods

First, we discuss the direct consequences of HIV on the central nervous system, including HIV encephalopathy in the context of HIV-associated neurocognitive disorders and HIV-related vacuolar myelopathy in the spinal cord. We also explore HIV-mediated cerebrovascular disease, which can cause infarcts, hemorrhages and aneurysms. These findings are nonspecific, particularly in older patient populations in which radiographic overlap with atherosclerosis can present a diagnostic challenge. Next, we discuss the opportunistic CNS infections commonly associated with AIDS, with toxoplasmosis being the most common, as well as cytomegalovirus and progressive multifocal leukoencephalopathy (PML). We also discuss imaging findings of CNS fungal infection, including cryptococcosis and coccidiomycosis. We then explore the immune reconstitution inflammatory syndrome, a treatment-related, paradoxical worsening of existing disease after the initiation of HAART, which is most commonly associated with PML and cryptococcal infection. Then, we discuss primary CNS lymphoma, which is an EBV-related large B-cell lymphoma seen in this population. Finally, we review CD8+ encephalitis, a more recently described and likely underdiagnosed entity, associated with higher levels of HIV RNA found in the cerebral spinal fluid relative to the serum (HIV escape).

Results & Conclusion

We review imaging findings of pathologies caused by HIV/AIDS in the brain and spine. Understanding the typical imaging presentations of and differential diagnoses for these pathologies is critical to accurate and timely diagnosis and treatment.

References

Chong J, Di Rocco, A, Tagliati M, et. al. MR findings in AIDS-associated myelopathy. *American Journal of Neuroradiology* 1999;20(8)1412-1416. https://pmc.ncbi.nlm.nih.gov/articles/PMC7657747/

Corr PD. Imaging of cerebrovascular and cardiovascular disease in AIDS patients. *American Journal of Roentgenology* 2006;187,7:236-242. DOI: https://doi.org/10.2214/AJR.05.0190

Narvid J, Callen A, Talbott J, et al. Brain MRI features of CSF human immunodeficiency virus escape. *Journal of Neuroimaging* 2018;28,6:601-607. DOI: https://doi.org/10.1111/jon.12552

Smith A, Smirniotopoulous JG, Rushing EJ. Central nervous system infections associated with human immunodeficiency virus infection: radiologic-pathologic correlation. *RadioGraphics* 2018;28,7. DOI: https://doi.org/10.1148/rg.287085135

454

Pearls and Pitfalls of Cerebral Perfusion Computed Tomography - Beyond Stroke Causes

Otavio Augusto Ferreira Dalla Pria MD[1], Laiz Laura de Godoy MD, Ph.D.[2], Daniel Gewolb MD[2], Thomas Reith MD[1], Daniella Karassawa Zanoni MD[3], Nitesh Shekhrajka MD[1], Robert M Kurtz MD[2], Joan A Maley MD, FACR[1], Minako Hayakawa MD, Ph.D.[1]

[1]University of Iowa Health Care, Iowa City, IA, USA. [2]University of Pennsylvania Health System, Philadelphia, PA, USA. [3]University of Iowa Health Care, Iowa, IA, USA

Abstract Category

Interventional/Vascular/Stroke

Summary & Objectives

Stroke affects hundreds of thousands of Americans every year and is considered a medical emergency due to its time-sensitive therapeutic plan. In this setting, proper imaging evaluation is crucial to determine the appropriateness of interventional treatment. Radiologists play a pivotal role in this scenario by analyzing cerebral hemodynamics and helping neurologists/neuro-interventionists select patients at-risk but still viable brain parenchyma through advanced

imaging techniques. In this context, Perfusion computed tomography (CTP) of the brain is a reliable method for evaluating acute stroke. Sometimes, CTP is the first brain imaging in the patient's workup, and considering that time is vital for decision-making, it's essential to be aware of potential pitfalls and differentials for CTP findings. Knowledge of imaging patterns and potential pitfalls of this technique is essential to the radiologist since not all perfusion abnormalities happen due to stroke.

Purpose

This presentation aims to review fundamentals of CTP and its applicability in setting of acute stroke, by showing areas of core infarct and penumbra. However, it will also show potential pitfalls due to inappropriate imaging acquisition, cardiovascular hemodynamics, and differential diagnosis that may affect the CTP findings, such as, seizures/post ictal phase, infection/inflammatory diseases, demyelinating diseases, tumors, etc.

Materials & Methods

1. Concise exposition delineating the imaging acquisition technique and CTP functionality. 2. Potential problems with imaging acquisition and patient underlying conditions that may affect the results. 3. Illustration of diverse cases featuring the use of CTP in acute stroke evaluation. 4. Incorporation of cases other than stroke that caused abnormal findings on CTP, and 5. Conclusion and take-home messages.

Results & Conclusion

This exhibit presented a practical approach to CTP in a stroke setting and enhanced the radiologists' knowledge about the broad spectrum of underlying conditions that can affect CTP interpretation. Hopefully, this presentation will increase the appropriate differential diagnosis when interpreting these exams.

References

1. Siegler, J.E., Rosenberg, J., Cristancho, D., Olsen, A., Pulst-Korenberg, J., Raab, L., Cucchiara, B. and Messe, S.R., 2020. Computed tomography perfusion in stroke mimics. *International Journal of Stroke*, *15*(3), pp.299-307.

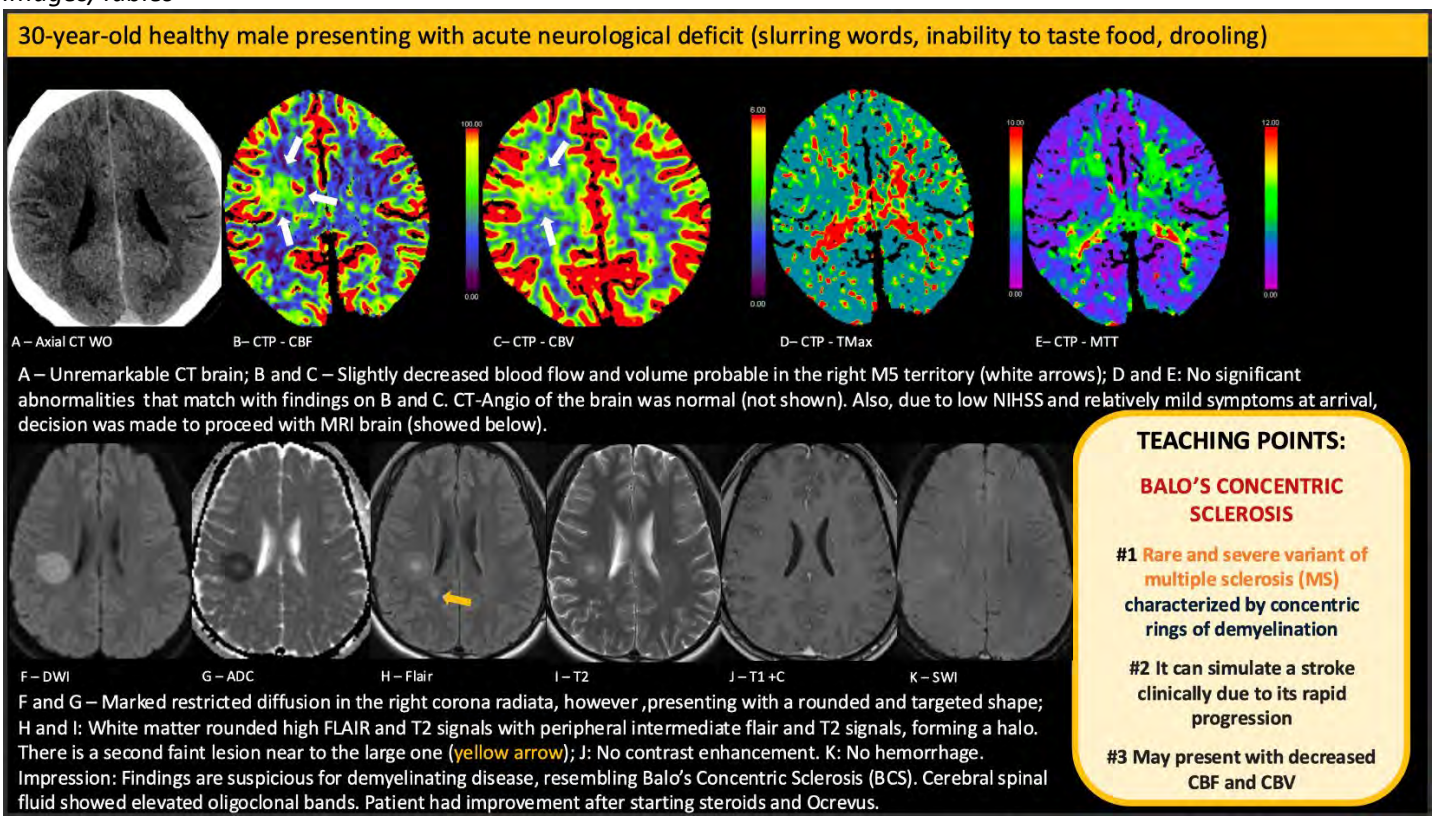
2. Mangla, R., Ekhom, S., Jahromi, B.S., Almast, J., Mangla, M. and Westesson, P.L., 2014. CT perfusion in acute stroke: know the mimics, potential pitfalls, artifacts, and technical errors. *Emergency radiology*, *21*, pp.49-65.

3. Donahue, J. and Wintermark, M., 2015. Perfusion CT and acute stroke imaging: foundations, applications, and literature review. *Journal of Neuroradiology*, *42*(1), pp.21-29.

4. Heit, J.J. and Wintermark, M., 2016. Perfusion computed tomography for the evaluation of acute ischemic stroke: strengths and pitfalls. *Stroke*, *47*(4), pp.1153-1158.

5. Bivard, A., Levi, C., Spratt, N. and Parsons, M., 2013. Perfusion CT in acute stroke: a comprehensive analysis of infarct and penumbra. *Radiology*, *267*(2), pp.543-550.

Images/Tables



455

Posterior Fossa: Embryology and Congenital/Developmental Abnormalities

Hunter Carlock MD, Brian Won MD, Sankarsh Jetty MD, Shehanaz Ellika MBBS
University of Rochester Medical Center, Rochester, NY, USA

Abstract Category

Pediatrics

Summary & Objectives

Learning objectives for this study:

- Review embryology of brainstem and cerebellum.
- Review the congenital and developmental abnormalities that may occur including their clinical presentation, genetics, and imaging appearances.

The posterior fossa of the skull includes the cerebellum and brainstem. A key point of embryogenesis of the posterior fossa structures occurs at 5-10 weeks gestation during ventral induction and closure of the neural tube, where the prosencephalon, mesencephalon, and rhombencephalon begin to differentiate. At 10 weeks, the rhombencephalon further differentiates by indentation at the pontine flexure, with the more superior portion (metencephalon) eventually differentiating into the pons and medulla and inferior portion (myelencephalon) differentiating into the spinal cord. This separation at the pontine flexure gives rise to the fourth ventricle, with the anterior membrane developing into choroid plexus and posterior aspect forming Blake's pouch. Blake's pouch eventually regresses to form the foramen of Magendie. The cerebellum is formed by the rhombencephalon predominantly around 4-10 weeks from lateral rhombic lips eventually forming the cerebellar hemispheres, and the vermis formed by the mesencephalon at 9 weeks, fusing with the developing cerebellum craniocaudally.

Given the complexity of posterior fossa embryogenesis, a variety of developmental abnormalities may occur. Abnormalities to these pathways include cerebellar or vermian agenesis, dysplasia, or hypoplasia.

Rhombencephalosynapsis occurs when aplastic vermis is present with varying degrees of fusion of the cerebellar hemispheres.

Cerebellar dysplasias occur due to disruption of the development of the cerebellar lobules or folia. A variety of genetic causes have been discovered including mutations to *LAMA1*, *CXCR4, GPSM2, RAC3,* and *VLDLR* along with alpha-dystroglycanopathies and tubulinopathies.

Dandy-Walker malformations occur due to failure in developmental the anterior membrane of the rhombencephalon, which leads to posterior fossa cyst formation resembling the fourth ventricle. Dandy-Walker malformations are often associated with hydrocephalus, dysgenesis of the corpus callosum, schizencephaly, and meningoceles. Prognosis is variable but may be associated with degree of hydrocephalus.

Other cystic malformations of the posterior fossa include arachnoid cyst and Blake's pouch cyst. Mega cisterna magna may mimic posterior fossa cyst and should be differentiated from these other developmental abnormalities.

Chiari malformations are abnormalities of the hindbrain where the cerebellar tonsils are inferior displaced through the foramen magnum.

Cerebellar hypoplasia, cerebellar hyperplasia or macrocerebellum, combined cerebellar and brainstem malformations, predominantly brainstem malformations and cerebellar disruptions will also be discussed.

Purpose

The purpose of this study is to review the embryogenesis of the posterior fossa structures along with its associated congenital and development abnormalities.

Materials & Methods

A review of the embryology of the posterior fossa will be showcased along with multiple teaching examples of congenital and developmental abnormalities of the posterior fossa provided by the authors' institutional imaging archives.

Results & Conclusion

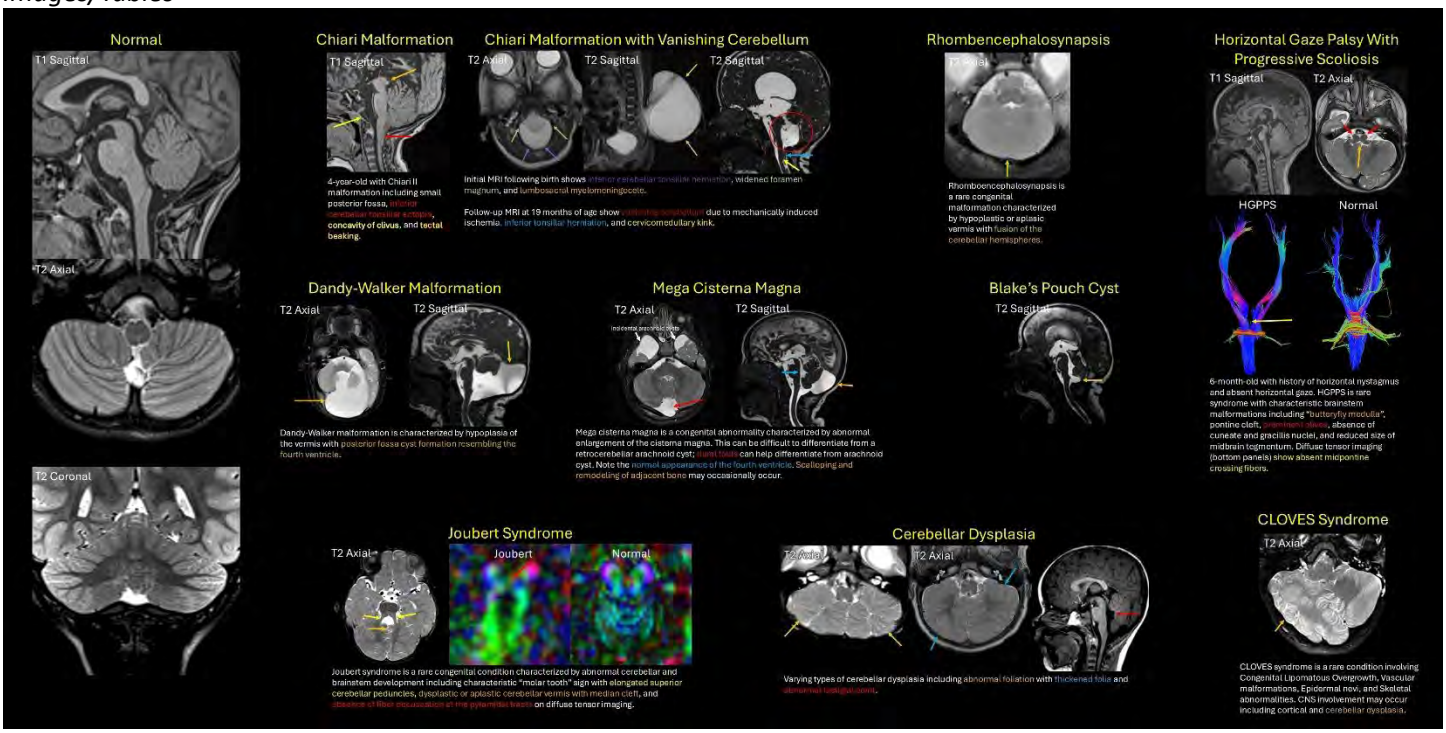
An educational exhibit was shown to review the embryological development of the posterior fossa along with associated congenital and developmental abnormalities.

References

1. Cotes C, Bonfante E, Lazor J, et al. Congenital basis of posterior fossa anomalies. *Neuroradiol J* 2015;28(3):238-253. DOI: https://doi.org/10.1177.1971400915576665
2. Bosemani T, Orman G, Boltshauser E, et al. Congenital Abnormalities of the Posterior Fossa. *Radiographics* 2015;35. DOI: https://doi.org/10.1148/rg.351140038

3. Niesen CE. Malformations of the posterior fossa: Current perspectives. *Semin Pediatr Neruol* 2002;9(4):320-334. DOI: https://doi.org/10.1053/spen.2002.32508
4. Shoja MM, Ra,mdjam, Kemsem CJ, et al. Embryology of the craniocervical junction and posterior cranial fossa, part II: Embryogenesis of the hindbrain. *Clin Anat* 2018;31(4):488-500. DOI: https://doi.org/10.1002/ca.23048
5. Whitehead MT, Barkovich MJ, Sidpra J, et al. Refining the Neuroimaging Definition of the Dandy-Walker Phenotype. *Am J Neuroradiol* 2022;43(10):1488-1493. DOI: https://doi.org/10.3174/ajnr.A7659

Images/Tables



465

Assessment of Intraventricular Brain Lesions in Adults - A Systematic Approach of Typical and Atypical Masses

Otavio Augusto Ferreira Dalla Pria MD[1], Nitesh Shekhrajka MD[1], Daniel Gewolb MD[2], Joan A Maley MD, FACR[1], Laiz Laura de Godoy MD, Ph.D.[2], Robert M Kurtz MD[2]

[1]University of Iowa Health Care, Iowa City, IA, USA. [2]University of Pennsylvania Health System, Philadelphia, PA, USA

Abstract Category

Adult Neoplasms/Epilepsy/Trauma

Summary & Objectives

Intraventricular brain lesions encompass myriad presentations in both clinical symptomology and radiological findings and frequently represent a challenge for the radiologist since multiple imaging features overlap among these lesions. Nevertheless, they account for a relevant incidence in our daily practice regardless of being an experienced neuroradiologist or a junior resident taking calls. Given their importance, a constant review of these entities is mandatory to succeed in neuroradiology.

Purpose

This exhibit aims: 1. To review the literature concerning adults' intraventricular brain lesions, including tumors, cysts, infection, and others; 2. To describe multi-modality imaging findings helpful in narrowing the differentials and relevant clinical presentations based on location, age, sex, etc. 3. To depict cases of supra and infratentorial intraventricular brain lesions in adults with a systematic approach by organizing them into two main subgroups: a) Supratentorial – lateral, third ventricles (choroid plexus and ventricle wall), foramen of Monroe, and septum pellucidum b) Infratentorial - fourth ventricle (choroid plexus and ventricle wall). Each subgroup will be split into typical and atypical lesions based on their typical location and imaging appearance.

Materials & Methods

1.Concise exposition delineating the embryology, anatomical configuration, and physiological attributes pertinent to the ventricular system; 2. Illustration of diverse typical cases featuring intraventricular cerebral lesions, including but not limited to cysts, ependymoma, subependymoma, central neurocytoma, choroid plexus neoplasm, meningiomas, juxtaposed with a comprehensive examination of atypical intraventricular tumors, such as, cavernous malformation, metastasis, lymphoma, chordoma, etc. Furthermore, the incorporation of cases initially presumed to originate intrinsically but ultimately diagnosed within the extraventricular ambit due to radiological manifestations.

Results & Conclusion

This exhibit presents a practical approach to adults intraventricular lesions, which is useful for daily neuroradiology practice. We expect to contribute with familiarization of neuroimaging features, including pattern of enhancement, presence of calcification, hemorrhage, diffusivity, and location, as well as clinical factors, such as age and gender to narrow differential diagnosis of typical intraventricular masses. In addition, we included challenging atypical intraventricular masses, which may come across in our routine as neuroradiologists.

References

1. Stratchko, L., Filatova, I., Agarwal, A. and Kanekar, S., 2016, April. The ventricular system of the brain: anatomy and normal variations. In *Seminars in Ultrasound, CT and MRI* (Vol. 37, No. 2, pp. 72-83). WB Saunders.

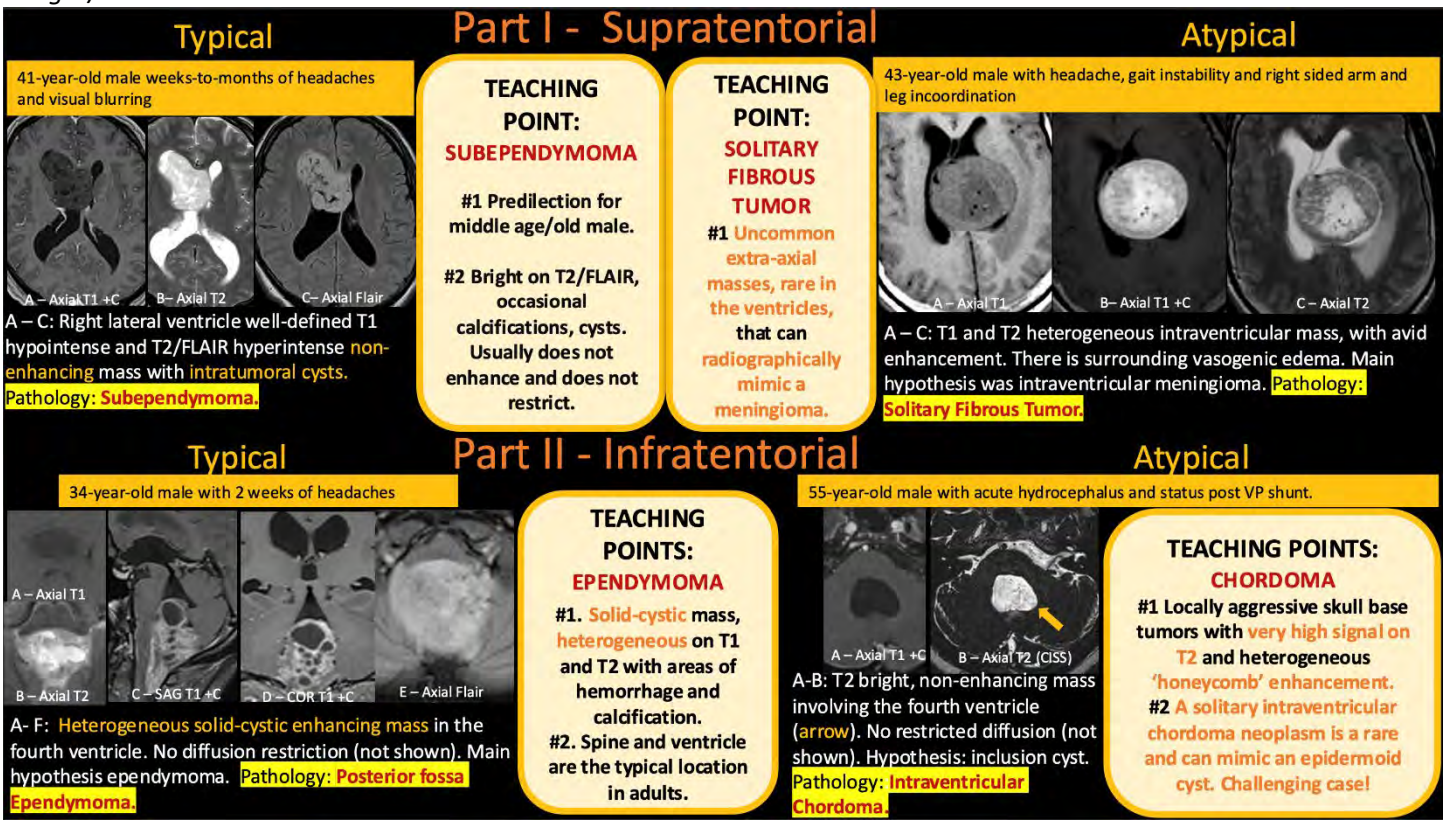
2. Vandesteen, L., Drier, A., Galanaud, D., Clarençon, F., Leclercq, D., Karachi, C. and Dormont, D., 2013. Imaging findings of intraventricular and ependymal lesions. *Journal of Neuroradiology*, *40*(4), pp.229-244.

3. Castro, F.D.D., Reis, F. and Guerra, J.G.G., 2014. Intraventricular mass lesions at magnetic resonance imaging: iconographic essay-part 1. *Radiologia brasileira*, *47*, pp.176-181.

4. Castro, F.D.D., Reis, F. and Guerra, J.G.G., 2014. Intraventricular mass lesions at magnetic resonance imaging: iconographic essay-part 2. *Radiologia brasileira*, *47*, pp.245-250.

5. Fenchel, M., Beschorner, R., Naegele, T., Korn, A., Ernemann, U. and Horger, M., 2012. Primarily solid intraventricular brain tumors. *European Journal of Radiology*, *81*(4), pp.e688-e696.

Images/Tables



467

The Anchor of Swallowing and Speech: Hyoid Bone Abnormalities

Maram Alafif[1], Liza Blumenfeld MA, CCC-SLP, BCS-S[2], Julie Bykowski[1]
[1]University of California San Diego, San Diego, California, USA. [2]Department of Otolaryngology Head and Neck Surgery, UC San Diego Health, San Diego, CA, USA

Abstract Category

Head and Neck

Summary & Objectives

- Understand hyoid bone anatomy and muscular attachments.
- Review hyoid bone function in speech and swallowing.
- Describe imaging features of injuries and pathology involving the hyoid bone.
- Appreciate imaging findings that assist in treatment decision-making for head and neck cancer.
- Recognize the importance of a multidisciplinary approach to treating head and neck cancer and functional rehabilitation before, during, and after treatment in correlation with imaging findings.

Purpose

The hyoid bone occupies a strategic position and participates in critical vital functions. Knowledge of the anatomy and function of the hyoid-larynx complex is necessary for radiologists to provide optimal patient care. This exhibit will review the imaging anatomy of the hyoid bone and its muscular attachments, its role in swallowing and phonation, and summarize the contributing pathologies through cases.

Materials & Methods

A review of the Radiology and EMR databases identified patients with hyoid fracture, tumor invasion, necrosis, and partial and total resection. This exhibit uses cross-sectional imaging, speech pathology, and swallow evaluations to reinforce the inclusion of the hyoid bone in search patterns of disease and identification of pathologic processes that impact surgical management and rehabilitation.

Results & Conclusion

- The hyoid bone is the only bone in our bodies with no direct attachment to other bones. It is a horseshoe-shaped bone located in the front of the neck below the mandible that supports the tongue and plays a vital role in speech and swallowing.
- High-resolution CT and MRI complement each other as the modalities of choice for characterizing the bony structures and the extent of hyoid bone pathology.
- The interpretation of imaging studies should consider the patient's history, physical findings, comorbidities, and previous treatments or procedures that may influence the visualized structures.
- Accurate evaluation of hyoid bone involvement in head and neck cancer and subsequent complications of treatment is crucial for early intervention to improve the functional outcome and quality of life for these patients.
- Radiologists should familiarize themselves with the anatomical considerations and contraindications for minimally invasive surgical procedures in head and neck cancer to provide optimal treatment.
- Partial or complete resection of the hyoid bone can result in decreased tongue strength. However, swallowing can be maintained, and tongue strength can be regained with rehabilitation and patient adaptation. Vocal restoration can be achieved by creating a fistula between the tracheostoma and the esophagus and placing a silastic prosthesis for speech rehabilitation.

References

- Auvenshine RC DDS, PhD, Pettit NJ DMD, MSD. The hyoid bone: an overview. Cranio. 2020;38(1):6-14. doi:10.1080/08869634.2018.1487501
- Sanguanchom M, Keskool P, Sureepong P, et al. Assessing Tongue Strength and Swallowing Function Following Hyoid Bone Resection Surgery. Ear Nose Throat J. 2023 August 22. doi:10.1177/01455613231191019 [Epub ahead of print]

Images/Tables

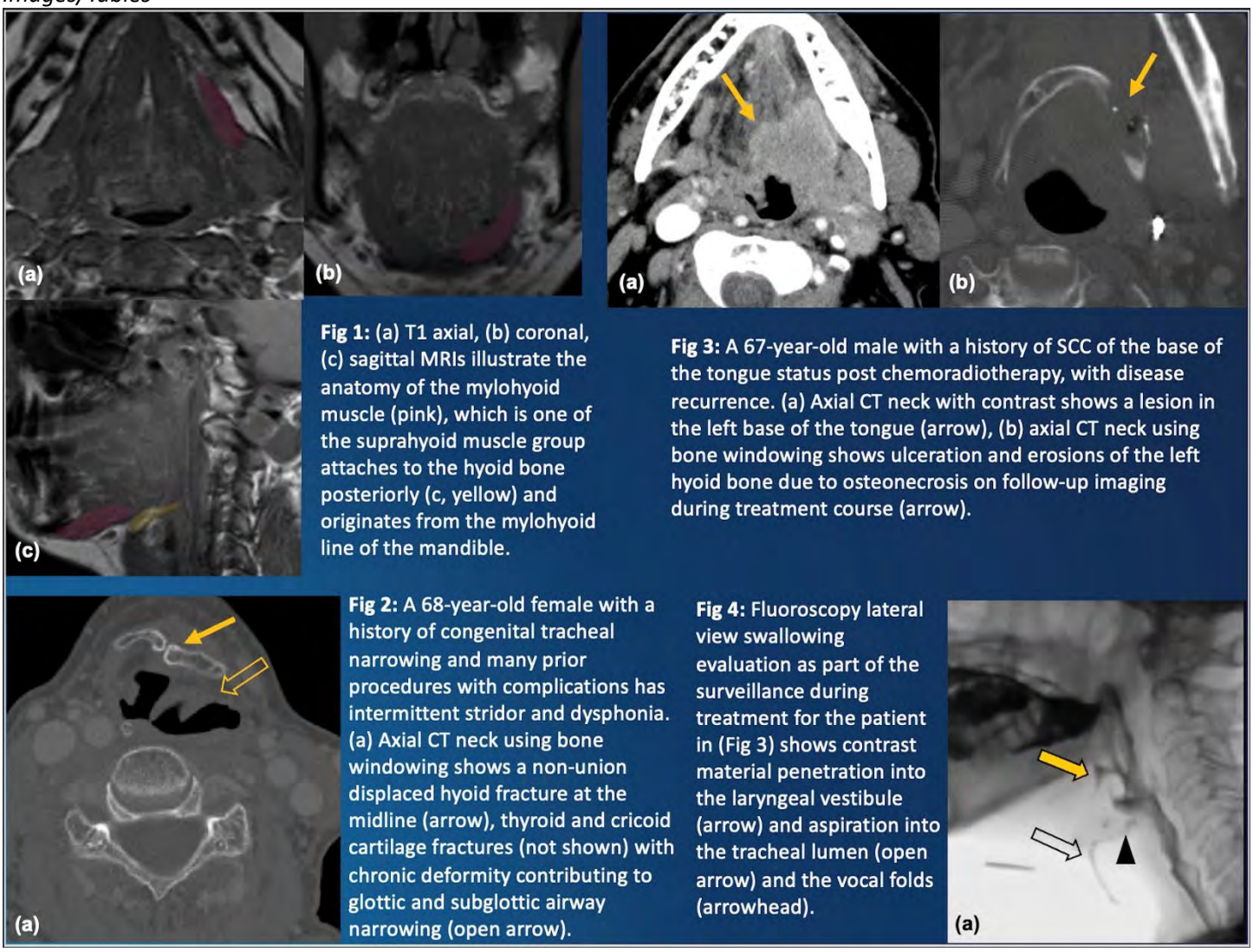


Fig 1: (a) T1 axial, (b) coronal, (c) sagittal MRIs illustrate the anatomy of the mylohyoid muscle (pink), which is one of the suprahyoid muscle group attaches to the hyoid bone posteriorly (c, yellow) and originates from the mylohyoid line of the mandible.

Fig 3: A 67-year-old male with a history of SCC of the base of the tongue status post chemoradiotherapy, with disease recurrence. (a) Axial CT neck with contrast shows a lesion in the left base of the tongue (arrow), (b) axial CT neck using bone windowing shows ulceration and erosions of the left hyoid bone due to osteonecrosis on follow-up imaging during treatment course (arrow).

Fig 2: A 68-year-old female with a history of congenital tracheal narrowing and many prior procedures with complications has intermittent stridor and dysphonia. (a) Axial CT neck using bone windowing shows a non-union displaced hyoid fracture at the midline (arrow), thyroid and cricoid cartilage fractures (not shown) with chronic deformity contributing to glottic and subglottic airway narrowing (open arrow).

Fig 4: Fluoroscopy lateral view swallowing evaluation as part of the surveillance during treatment for the patient in (Fig 3) shows contrast material penetration into the laryngeal vestibule (arrow) and aspiration into the tracheal lumen (open arrow) and the vocal folds (arrowhead).

473

Comprehensive Cranial Abnormalities in Patients with Bronchopulmonary Dysplasia: A Novel Cranial Morphology Not Previously Described

Marianne Nabbout MD, Amit Agarwal, Sania Razzaq, Giridhar Dasegowda, Charles Glasier, Fnu Abhilasha, Janice Murphy, Sateesh Jayappa, Eylem Ocal, Raghu Ramakrishnaiah
University of Arkansas for Medical Sciences, Little Rock, Arkansas, USA

Abstract Category

Pediatrics

Summary & Objectives

Bronchopulmonary dysplasia (BPD) is among the most common and serious sequelae of preterm birth. Severe BPD (sBPD) is defined as the need for positive pressure at 36 weeks postmenstrual age (PMA). An estimated 16% of infants born under 32 weeks PMA have sBPD, translating to 13,000 babies diagnosed with sBPD annually in the US alone. The clinical presentation of sBPD is diverse and complex. While extensive research has been conducted on pulmonary manifestations of sBPD, little attention has been given to neurological, calvarial, skull base, and maxillofacial abnormalities that occur in these patients, especially in pediatric neuroradiology literature [1].

Purpose

The aim of this educational exhibit is to present initial observations from a retrospective review of head CT scans from infants with sBPD patients at a tertiary care hospital.

Materials & Methods

We included patients who underwent CT scans with bone window imaging and three-dimensional reconstructions at our tertiary care facility. These findings are frequently seen in sBPD patients and may be related to the underlying lung disease and management.

Results & Conclusion

• Diffuse Calvarial Thickening: All the calvarial bones showed distinct thickening with a preponderance of frontal bone (Fig B, arrow). The individual calvarial bones displayed a distinctive pinched appearance near the cranial sutures (Fig A, arrow), resembling a "string of sausages"

• Craniosynostosis: Primarily affected the coronal suture (Fig A, arrow), followed by the sagittal suture. Lambdoid suture fusion was never detected.

• Brachycephaly (Fig B, double side arrow)

• J shaped Sella turcica (Fig B, asterisk)

• Widely Patent Anterior Fontanelle: The anterior fontanelle displayed distinctive characteristics, wider than normal, everted, and tapered bony margins with bulging fontanelle as opposed to the premature closure or narrowing seen in syndromic craniosynostosis (Fig. B curved arrows).

• Malar Eminence Prominence: Prominence of the malar eminence was seen, along with absent pneumatization of the maxillary sinuses (Fig C, arrows).

• Poorly pneumatized middle ear cavity (Fig. D, curved arrows).

• Amorphous Skull Base: The skull base showed an overall amorphous appearance, with an etched-out otic capsule in the temporal bones (Fig D, arrows).

• Oval Window Atresia.

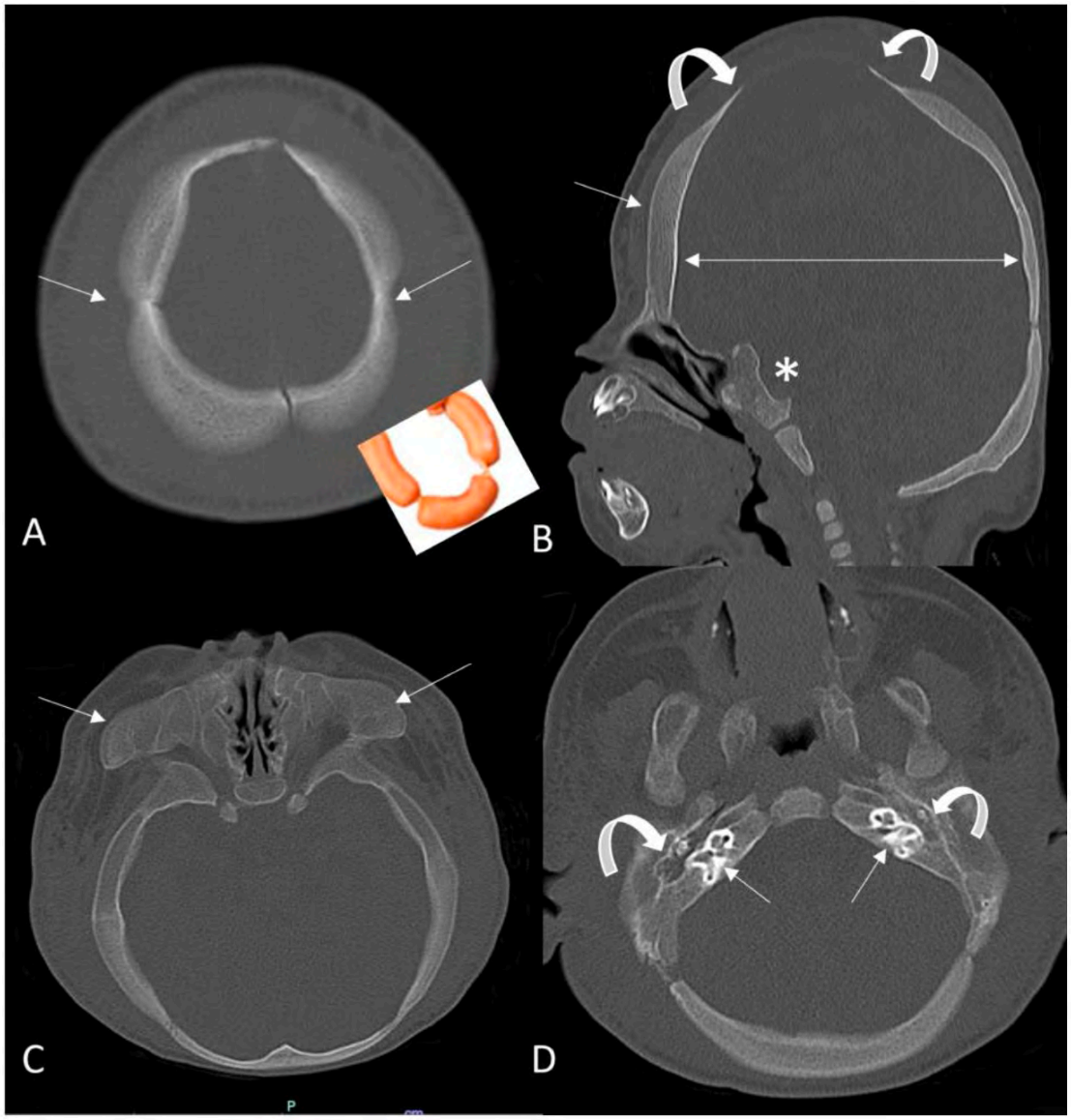
• Cerebral Parenchymal Volume Loss: Moderate to severe cerebral parenchymal volume loss was observed, often accompanied by ventricular enlargement, unrelated to bronchopulmonary dysplasia.

• **Conclusion**: Our preliminary observation suggests that bronchopulmonary dysplasia and its management may have a broader impact on the cranial structures. Further systematic investigations are warranted to validate these findings and gain insights into the underlying mechanisms, potentially leading to improved patient outcomes.

References

[1] Zapatero ZD, Zhang H, Zandifar A, et al. A Novel Phenotype of Calvarial Thickening and Increased Rates of Premature Calvarial Suture Closure in Children With Chronic Lung Disease. *J Craniofac Surg* 2023 Sep 1;34(6):1845-1850. DOI: 10.1097/SCS.0000000000009528. Epub 2023 Jul 11. PMID: 37431930.

Images/Tables



479

Not in Vein? Anatomical Variants of the Dural Venous Sinus and Their Clinical Implications.

Garrett H Yoon MD, Mohamed Aburadi BS, Esther A Nimchinsky MD/PHD
Rutgers New Jersey Medical School, Newark, NJ, USA

Abstract Category

Interventional/Vascular/Stroke

Summary & Objectives

The dural venous sinuses (DVS), venous channels between layers of dura mater, allow for blood and CSF drainage from intracranial parenchyma, meninges, and other cranial structures[1]. Recognizing variations in DVS anatomy using CT venography (CTV) or magnetic resonance venography (MRV) is important for surgical planning and avoiding potential complications[2]. Anatomical variations in the dural venous sinuses are common, with studies reporting an incidence rate of up to 51% in the general population[3,4]. Common variations include transverse sinus hypoplasia, sigmoid sinus hypoplasia, and remnant occipital and falcine sinuses. In some cases, variants may be clinically relevant due to altered dynamics, and in others, they may be recruited to compensate for stenoses elsewhere in the system, as in cases of thrombotic occlusion or idiopathic intracranial hypertension. This case-based visual presentation will highlight different dural venous sinus variants and their clinical significance.

Learning Objectives:

- Review normal intracranial dural venous sinus anatomy and discuss relevant imaging techniques including CT and MR venography.
- Discuss common dural venous sinus variants including superior sagittal sinus atresia, persistent falcine sinus, and persistent occipital sinus. More uncommon variants will also be featured.
- Discuss the clinical implications and management of venous sinus variants.
- Discuss the clinical presentation and imaging findings associated with chronic cerebrospinal venous insufficiency.

Purpose

N/A

Materials & Methods

N/A

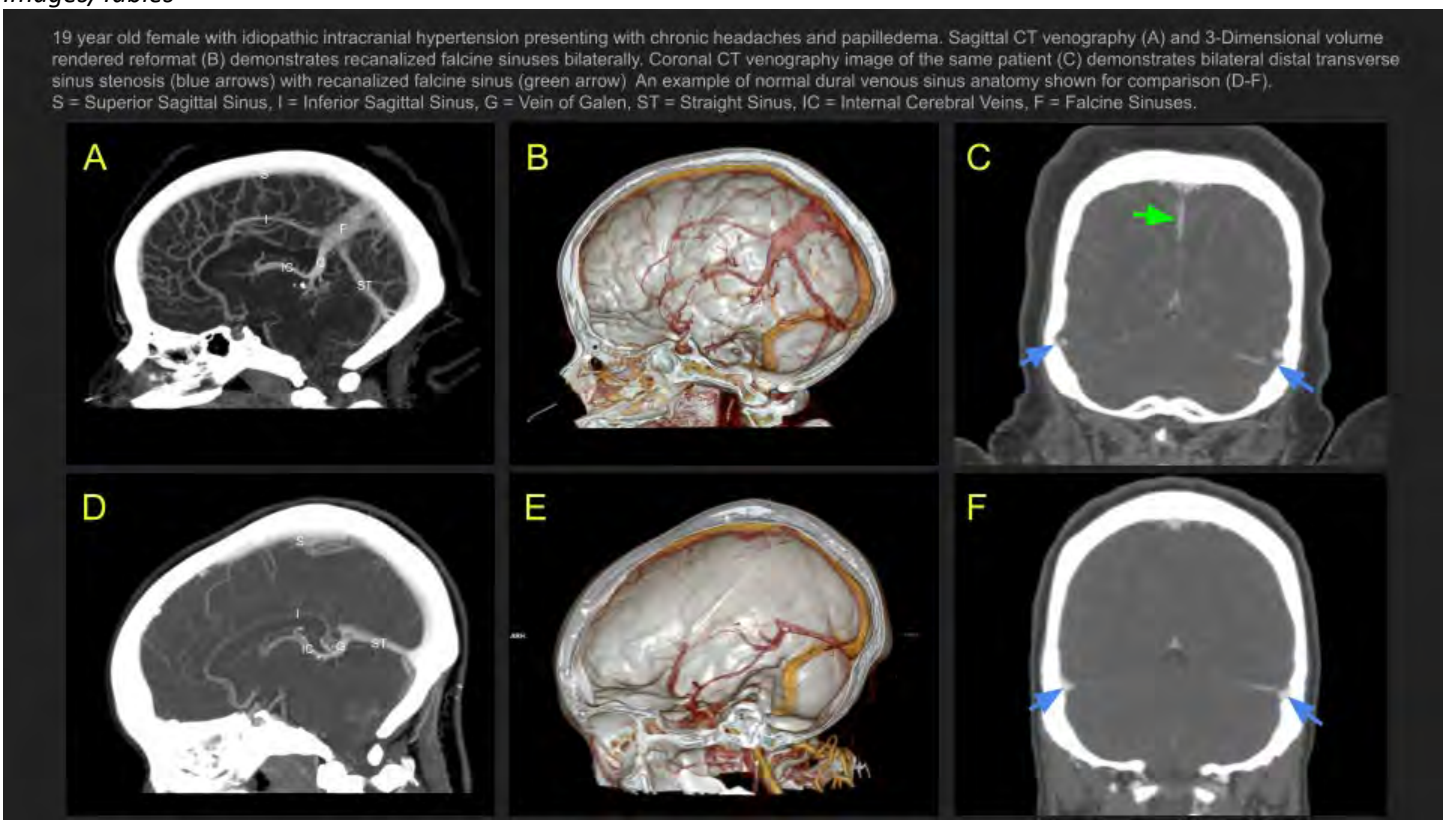
Results & Conclusion

N/A

References

1. Curé JK, Van Tassel P, Smith MT. Normal and variant anatomy of the dural venous sinuses. Semin Ultrasound CT MR. 1994;15(6):499-519.
2. Khandelwal N, Agarwal A, Kochhar R, et al. Comparison of CT venography with MR venography in cerebral sinovenous thrombosis. *AJR Am J Roentgenol*. 2006;187(6):1637-1643.
3. Bayaroğulları H, Burakgazi G, Duman T. Evaluation of dural venous sinuses and confluence of sinuses via MRI venography: anatomy, anatomic variations, and the classification of variations. *Childs Nerv Syst*. 2018;34(6):1183-1188.
4. Ozkacmaz S, Dadali Y, Alpaslan M, Uçar I. The morphological variants of dural venous sinuses. *J Anat Soc India*. 2020;69(4):207.

Images/Tables



481

Role of Hypoperfusion Intensity Ratio in Vessel Occlusions: Insights on Safety and Clinical Outcomes

Sana Rehman MD[1], Arsalan Nadeem MBBS[2], Arbab B. U. Kasi MD[3], Ali Husnain MD[4], Summaiyya Waseem MBBS[5], Sohail Kumar MD[6], Syed M Owais MD[7], Nasreen Banu MBBS[8], Dhairya A Lakhani MD[9], Hamza A Salim MD[1], Risheng Xu MD[1], Vaibhav S Vagal MD[10], Yasmin N Aziz MD[11], Argye E Hillis MD[1], Richard Leigh MD[12], Adam A Dmytriw MD[13], Adrien Guenego MD[14], Gregory W Albers MD[15], Jeremy J Heit MD[15], Tobias D Faizy MD[16], Vivek S Yedavalli MD, MS[1]

[1]Russell H. Morgan Department of Radiology and Radiological Science, Johns Hopkins School of Medicine, Baltimore, Maryland, USA. [2]Allama Iqbal Medical College, Lahore, Punjab, Pakistan. [3]Mass General Brigham, Boston, Massachusetts, USA. [4]Department of Radiology, Section of Interventional Radiology, Northwestern University, Chicago, Illinois, USA. [5]Dow University of Health Sciences, Karachi, Sindh, Pakistan. [6]HMH JFK University Medical Center, Edison, New Jersey, USA. [7]University of Toledo, Toledo, Ohio, USA. [8]Shadan Institute of Medical Sciences, Hyderabad, Telangana, India. [9]Department of Neuroradiology, Rockefeller Neuroscience Institute, West Virginia University, Morgantown, West Virginia, USA. [10]Stony Brook University Renaissance School of Medicine, New York, New York, USA. [11]Department of Neurology and Rehabilitation Medicine, University of Cincinnati, Cincinnati, Ohio, USA. [12]Department of Neurology, Johns Hopkins Medicine, Baltimore, Maryland, USA. [13]Neuroendovascular Program, Massachusetts General Hospital, Boston, Massachusetts, USA. [14]Department of Diagnostic and Interventional Neuroradiology, Erasme University Hospital, Anderlecht, Brussels, Belgium. [15]Department of Neurology, Stanford University, Stanford, California, USA. [16]Department of Radiology, Neuroendovascular Program, University Medical Center Münster, Münster, Münster, Germany

Abstract Category

Interventional/Vascular/Stroke

Summary & Objectives

The hypoperfusion intensity ratio (HIR) has emerged as a valuable metric in the imaging and management of acute ischemic stroke (AIS) due to large vessel occlusion (LVO). By quantifying the ratio of brain tissue volume with delayed blood flow (time-to-maximum [Tmax] >10 seconds versus Tmax >6 seconds),[1] HIR helps identify areas of hypoperfusion, distinguishing between the potentially salvageable penumbra and irreversibly injured core.[2] This exhibit explores the role of HIR with the following objectives:

- To explain how HIR identifies salvageable brain tissue and differentiates between the ischemic penumbra and core infarct.
- To highlight HIR's predictive value in evaluating infarct growth, collateral circulation, and post-treatment outcomes.
- To compare HIR with traditional metrics like the computed tomography angiography (CTA)-based collateral scoring and other advanced imaging modalities such as DWI MRI, and DSA.
- To address the implications of HIR in minimizing hemorrhagic complications and optimizing therapeutic decision-making in AIS care.

Purpose

To discuss the role of HIR as a predictive and stratifying metric in the management of AIS with LVO. This exhibit seeks to highlight HIR's potential to improve patient selection for thrombolytic and mechanical thrombectomy procedures by evaluating its accuracy in estimating tissue viability and clinical outcomes.[3] Through a better understanding of HIR, clinicians can make more informed therapeutic decisions, reduce the risk of hemorrhagic complications, and improve functional outcomes.

Materials & Methods

This exhibit will draw from a comprehensive review of clinical studies and recent literature on HIR's application in ischemic stroke management. Studies examining HIR's correlation with key metrics (e.g. Tmax thresholds, ASPECTS, and CTA collateral scores) were reviewed to determine its predictive power in assessing infarct progression and treatment response. HIR's calculation is based on computed tomography perfusion (CTP) imaging,[4] where the hypoperfused brain regions with Tmax >6 seconds and >10 seconds are used to derive the ratio (**Figure 1**).

Results & Conclusion

This exhibit will demonstrate that HIR values offer predictive insight into clinical outcomes and tissue response to reperfusion therapies. Key findings from the literature indicate the following:

- Higher HIR values, indicating more extensive hypoperfused regions, correlate with rapid infarct growth, poor collateral status, and unfavorable clinical outcomes, as well as a lower likelihood of successful recanalization in LVO.[4]
- Lower HIR values are linked to robust collateral circulation, delayed infarct progression, and more favorable recovery profiles. These patients benefit more from reperfusion therapies, showing improved functional outcomes and reduced risk of post-treatment hemorrhagic transformation.
- Compared to CTA-based scoring, HIR provides a more objective measure of tissue at risk and potential for infarct progression, enhancing its value as a biomarker for identifying candidates for thrombectomy and thrombolysis.[3-5]

References

[1] Bang OY, Saver JL, Alger JR, et al. Determinants of the distribution and severity of hypoperfusion in patients with ischemic stroke. *Neurology*. 2008;71(22):1804-1811. DOI: https://doi.org/10.1212/01.wnl.0000335929.06390.d3
[2] Rehman S, Nadeem A, Kasi ABU, et al. Role of Hypoperfusion Intensity Ratio in Vessel Occlusions: A Review on Safety and Clinical Outcomes. *AJNR Am J Neuroradiol*. 2024 Oct 30:ajnr.A8557. DOI: https://doi.org/10.3174/ajnr.A8557
[3] Guenego A, Marcellus DG, Martin BW, et al. Hypoperfusion Intensity Ratio Is Correlated With Patient Eligibility for Thrombectomy. *Stroke*. 2019;50(4):917-922. DOI: https://doi.org/10.1161/STROKEAHA.118.024134
[4] Olivot JM, Mlynash M, Inoue M, et al. Hypoperfusion intensity ratio predicts infarct progression and functional outcome in the DEFUSE 2 Cohort. *Stroke*. 2014;45(4):1018-1023. DOI: https://doi.org/10.1161/STROKEAHA.113.003857
[5] Guenego A, Fahed R, Albers GW, et al. Hypoperfusion intensity ratio correlates with angiographic collaterals in acute ischaemic stroke with M1 occlusion. *Eur J Neurol*. 2020;27(5):864-870. DOI: https://doi.org/10.1111/ene.14181

Images/Tables

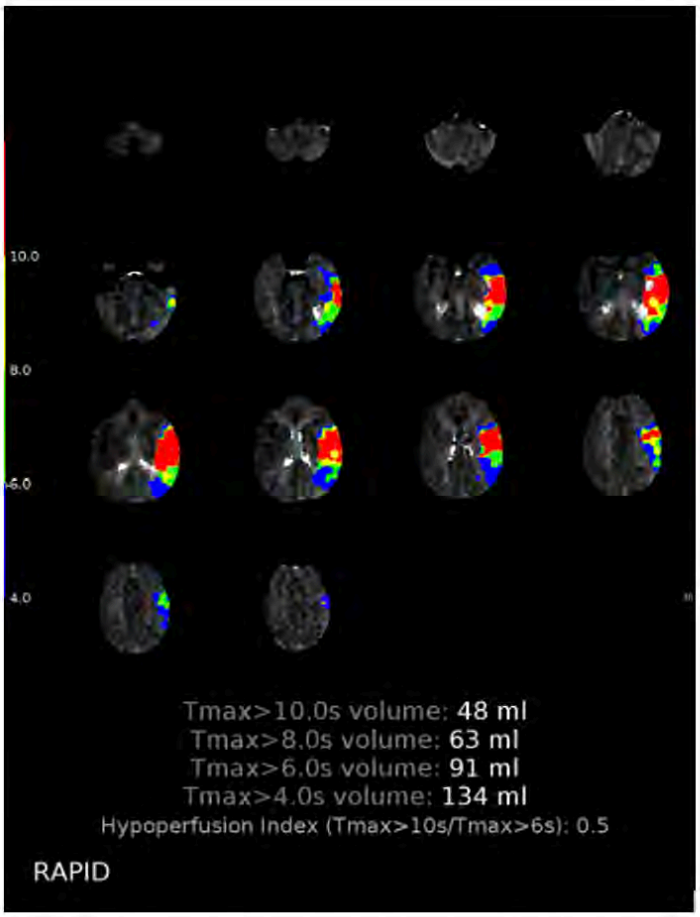


FIG 1. This figure illustrates the calculation of HIR in a patient with left MCA stroke. It is derived by taking the ratio of the volume of brain tissue with a time-to-maximum (Tmax) delay greater than 10 seconds (coded in red, 48 ml in this example) to the volume of brain tissue with a Tmax delay greater than 6 seconds (coded in green, 91 ml in this example), yielding an HIR of 0.5. This calculation is generally conducted using automated software.

493

Beyond the Usual Suspects: Uncommon Cerebellopontine Angle Masses

Mohamed Tantawi MBBCh, Abel Abebe MD, Azin Aein MD, Alaha Al Taweel MD
UTMB, Galveston, TX, USA

Abstract Category

Adult Brain Inflammatory/Infectious Disease/Degenerative/Metabolic

Summary & Objectives

The cerebellopontine angle (CPA) is an intricate space between the brainstem, cerebellum and the petrous temporal bone, where a variety of benign and malignant pathologies can be encountered. Vestibular schwannomas and meningiomas constitute the majority of the typical masses reported in the CPA. However, familiarity with other types of CPA pathologies is crucial for making an accurate diagnosis and guiding clinical management. This educational exhibit aims at providing radiology trainees with a detailed imaging review of a wide spectrum of uncommon CPA masses.

Purpose

The purpose of this educational exhibit is to describe the imaging features of uncommon CPA masses on CT and MRI, outlining the distinguishing features from the typical CPA masses.

Materials & Methods

A retrospective review of all the CPA masses detected on head CT and brain MRI studies in the past 5 years at our institution was performed for the purposes of this exhibit. The standard MRI protocols for brain masses at our institution comprised T1-weighted, T2-weighted, Fluid-attenuated inversion recovery (FLAIR), diffusion-weighted imaging (DWI), susceptibility-weighted imaging (SWI) and contrast-enhanced sequences. Specific sequences for the internal auditory canal were available for select cases. Pathology reports for all the patients who underwent CPA mass resection or biopsy were reviewed to confirm the final diagnosis.

Results & Conclusion

A variety of different pathologies can be encountered in the CPA due to the complex anatomy of this region. Different CPA pathologies can have a similar clinical presentation, depending on the structures involved or compressed by the lesion. Hence, imaging plays a pivotal role in making the accurate diagnosis and deciding the next steps in management. The imaging features of CPA masses primarily rely on the tissue of origin and the pathology of the lesion. We detail in this exhibit the distinguishing CT and MRI features of several uncommon CPA lesions including chondrosarcoma (Case 1), enlarged suprameatal tubercle (Case 2), venous cavernoma (Case 3), tuberculous granuloma (Case 4), hemangioblastoma, and metastatic squamous cell carcinoma, among other lesions.

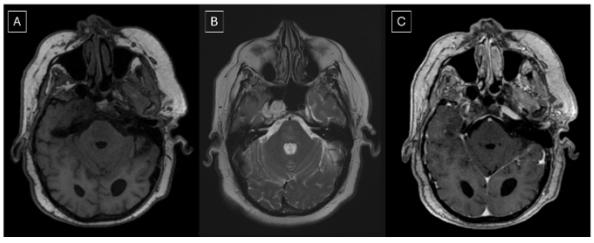
References

Bonneville F, Sarrazin JL, Marsot-Dupuch K, et al. Unusual lesions of the cerebellopontine angle: a segmental approach. Radiographics 2001;21(2):419-38. DOI: https://doi.org/10.1148/radiographics.21.2.g01mr13419

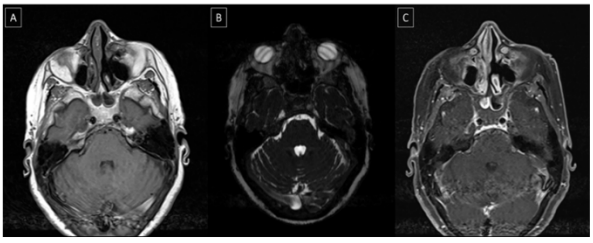
Bonneville F, Savatovsky J, Chiras J. Imaging of cerebellopontine angle lesions: an update. Part 1: enhancing extra-axial lesions. Eur Radiol 2007;17(10):2472-82. DOI: https://doi.org/10.1007/s00330-007-0679-x

Images/Tables

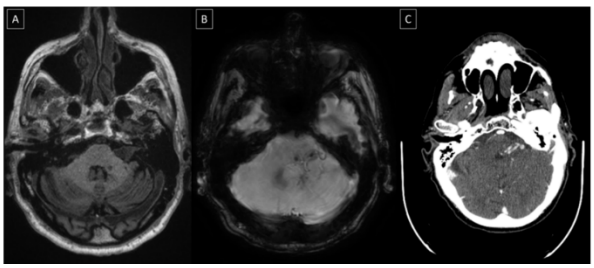
Case 1



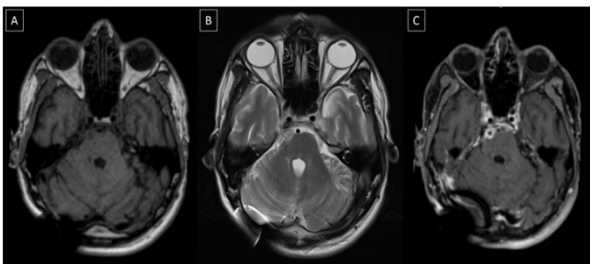
Case 3



Case 2



Case 4



495

Understanding Hypothalamic Hamartoma: A Radiological Educational Exhibit

Markus Lammle MD[1], shirin Habibi Arvanagh MD[2], Nassim Said[3]
[1]SUNY Upstate Medical University, Syracuse, New York, USA. [2]Department of Radiology, Iran University of Medical Sciences, Tehran, Tehran, Iran, Islamic Republic of. [3]School of Health Sciences, University of Georgia, Tbilisi, Georgia, USA

Abstract Category

Adult Neoplasms/Epilepsy/Trauma

Summary & Objectives

Hypothalamic hamartomas, also known as cinereum gland hamartomas, usually arise from the cinereum gland in the hypothalamus region. They are rare, benign brain lesions often associated with gelastic seizures, cognitive impairments, and behavioral disturbances. Early and accurate diagnosis through imaging is crucial for effective management.

Purpose

This study aims to provide a comprehensive educational overview of hypothalamic hamartoma (HH), focusing on its radiological characteristics, differential diagnosis, clinical implications, and management.

Materials & Methods

1. Anatomy, Pathophysiology, and Clinical Manifestations: This section provides an overview of hypothalamic anatomy, pathophysiological mechanisms, and clinical presentations of HH.
2. Imaging Techniques and Findings: Detailed discussion of MRI characteristics, the role of CT imaging, and advanced imaging techniques in diagnosing HH.
3. Differential Diagnosis: Distinguishing HH from other hypothalamic and suprasellar lesions.
4. Clinical Correlation: The correlation between imaging findings and clinical symptoms, their impact on endocrine function, and neurological outcomes.
5. Treatment and prognosis: We will provide an overview of surgical and non-surgical treatment options, medical treatment indications, stereotactic radiosurgery's role, and case studies. We will also discuss the prognosis of HH.
6. Case Studies: Illustrative cases are presented, including imaging findings, clinical presentation, treatment, and follow-up.

Results & Conclusion

This article summarizes the critical educational points about the radiological features, clinical implications, and management of hypothalamic hamartoma, emphasizing the importance of understanding HH for radiologists in accurately diagnosing and aiding in patient management.

References

1. Cohen NT, Cross JH, Arzimanoglou A, Berkovic SF, Kerrigan JF, Miller IP, Webster E, Soeby L, Cukiert A, Hesdorffer DK, Kroner BL, Saper CB, Schulze-Bonhage A, Gaillard WD; Hypothalamic Hamartoma Writing Group. Hypothalamic Hamartomas: Evolving Understanding and Management. Neurology. 2021 Nov 2;97(18):864-873. doi: 10.1212/WNL.0000000000012773. Epub 2021 Oct 4. PMID: 34607926; PMCID: PMC8610628.
2. Mittal S, Mittal M, Montes JL, Farmer JP, Andermann F. Hypothalamic hamartomas. Part 1. Clinical, neuroimaging, and neurophysiological characteristics. Neurosurg Focus. 2013 Jun;34(6):E6. doi: 10.3171/2013.3.FOCUS1355. PMID: 23724840.
3. Consales, A., Ardemani, G., Cinnante, C.M. et al. Neuroimaging appearance of hypothalamic hamartomas in monozygotic twins with Pallister-Hall syndrome: case report and review of the literature. BMC Neurol 22, 118 (2022). https://doi.org/10.1186/s12883-022-02618-0

499

Vascular Complications of Head and Neck Trauma: A Case Review

Gilberto J Aquino MD, Rajiv Mangla MD
SUNY Upstate Medical University, Syracuse, NY, USA

Abstract Category

Interventional/Vascular/Stroke

Summary & Objectives

- To explain the various vascular abnormalities that can occur after blunt or penetrating head and neck trauma.

- To use a case-based approach to describe the imaging findings characteristic of head and neck post-traumatic vascular complications

Purpose

The aim is to provide trainees with a comprehensive guide of sample cases to learn the imaging findings concerning for vascular complications after head and neck trauma.

Materials & Methods

We will collect approximately 3-4 cases of each possible complication after head and neck trauma, including minimal intimal injury, dissection, intraluminal thrombus, intramural hematoma, pseudoaneurysm, arterial transection, arteriovenous fistula, and dural venous sinus injury. On each individual case, we will show different imaging modalities (CT, MRI, DSA) and the imaging findings that characterize each potential vascular complication. We will also educate on particularly important findings to include in radiology reports.

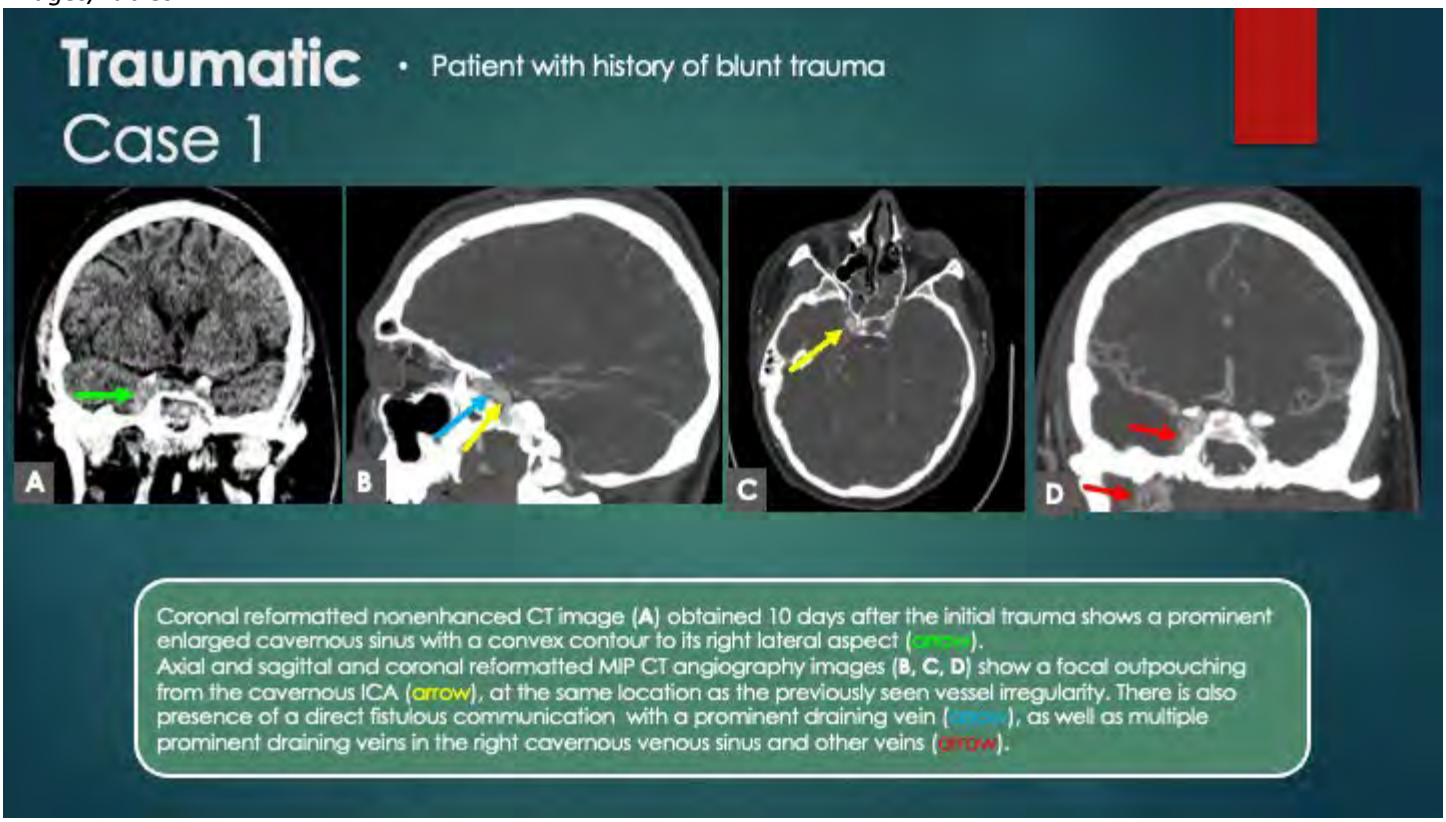
Results & Conclusion

A wide range of cases will be used to educate readers on imaging findings to look for when reading CT, MRI, or DSA after head and neck trauma.

References

Anne G. Osborn, Luke L. Linscott, Karen L. Salzman. Osborn's Brain. Elsevier. 2023.
Rohini Nadgir, David M. Yousem. Neuroradiology: The Requisites. Elsevier. 2016.
Nagpal P., Policeni B.A., Bathla G., et al. Blunt Cerebrovascular Injuries: Advances in Screening, Imaging, and Management Trends. Am J of Neuroradiol. 2017.

Images/Tables



502

Grab the FUEL, Light the FUSE, Stoke the FLAMES: Imaging of MOGAD and Its Clinico-radiologic Variants

Rouzbeh Mashayekhi MD, Michael Covington MD, Jefferson Chen MD, Katharina Eikermann-Haerter MD, James Ryan Loftus MD
NYU Langone Medical Center, New York, NY, USA

Abstract Category

Adult Brain Inflammatory/Infectious Disease/Degenerative/Metabolic

Summary & Objectives

Myelin oligodendrocyte glycoprotein antibody-associated disease (MOGAD) is an increasingly recognized demyelinating condition affecting both pediatric and adult populations. MOGAD presents with a range of heterogeneous clinical phenotypes, with commonly encountered manifestations including optic neuritis, transverse myelitis, and acute disseminated encephalomyelitis (ADEM). Both monophasic and relapsing disease courses have been described. In addition to these typical presentations, specific clinico-radiologic syndromes have been attributed to underlying MOGAD. These include MOG-antibody-associated cerebral cortical encephalitis (MOG antibody-associated CCE) with described variants: FLAIR hyperintense lesions in anti-MOG-associated encephalitis with seizures (FLAMES) and FLAIR hyperintense lesions with U-fiber and subcortical enhancement (FUSE), and MOGAD-associated aseptic meningitis (MOGAM) with a specific subtype, FLAIR-variable unilateral enhancement of the leptomeninges (FUEL).
Key Learning Objectives of this Exhibit are:
1) Review the epidemiology, pathophysiology, and imaging features of MOGAD.
2) Discuss the clinical and radiologic differences between MOGAD and other demyelinating conditions such as multiple sclerosis (MS) and neuromyelitis optica spectrum disorders (NMOSD).
3) Recognize the imaging features of less common variants of MOGAD, including FLAMES, FUEL, and FUSE.

Purpose

This educational exhibit will review the clinical and imaging manifestations of MOGAD and its variants with the aim of improving familiarity among neuroradiologists and, in turn, leading to earlier diagnosis and better patient outcomes.

Materials & Methods

This exhibit highlights the most up-to-date, relevant clinical and epidemiologic information regarding MOGAD and how it differs from other demyelinating conditions such as MS and NMOSD. Next, individual cases from a tertiary academic institution will be reviewed to illustrate the imaging findings of MOGAD, its clinico-radiologic variants, and their differences from other demyelinating conditions, using MRI studies of the orbits, brain, and spine.

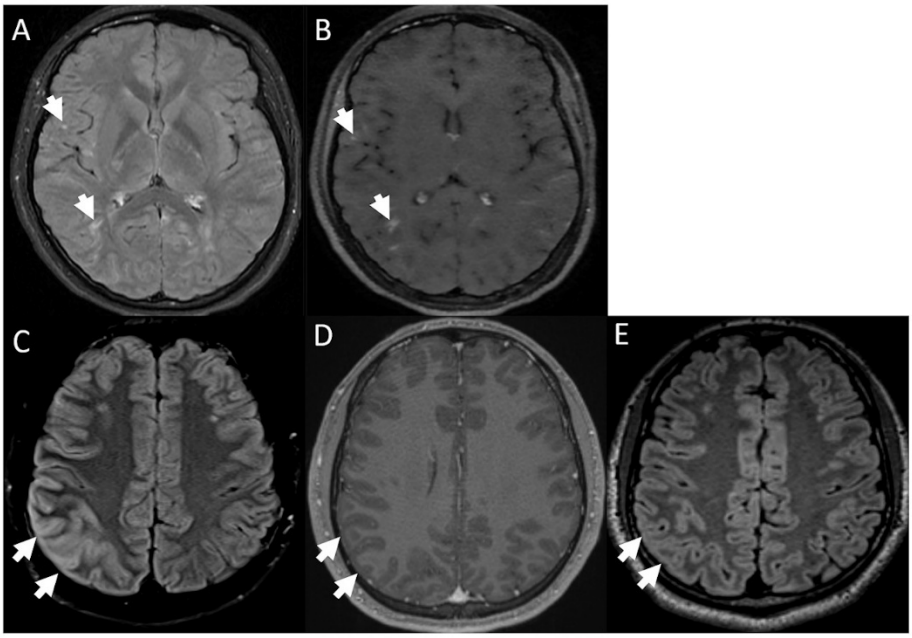
Results & Conclusion

This educational exhibit will thoroughly explore MOGAD, an increasingly recognized demyelinating disorder, and its multiple variants, each with unique imaging features, through real-life cases.

References

1. Banwell B, Bennett JL, Marignier R, Kim HJ, Brilot F, Flanagan EP, Ramanathan S, Waters P, Tenembaum S, Graves JS, Chitnis T, Brandt AU, Hemingway C, Neuteboom R, Pandit L, Reindl M, Saiz A, Sato DK, Rostasy K, Paul F, Pittock SJ, Fujihara K, Palace J. Diagnosis of myelin oligodendrocyte glycoprotein antibody-associated disease: International MOGAD Panel proposed criteria. Lancet Neurol. 2023 Mar;22(3):268-282. doi: 10.1016/S1474-4422(22)00431-8. Epub 2023 Jan 24. PMID: 36706773.
2. Budhram A, Mirian A, Le C, Hosseini-Moghaddam SM, Sharma M, Nicolle MW. Unilateral cortical FLAIR-hyperintense Lesions in Anti-MOG-associated Encephalitis with Seizures (FLAMES): characterization of a distinct clinico-radiographic syndrome. J Neurol. 2019 Oct;266(10):2481-2487. doi: 10.1007/s00415-019-09440-8. Epub 2019 Jun 26. PMID: 31243540.
3. Lim GZ, Chan VEY, Yu WY, Tan NCK, Yeo T. FLAIR hyperintense lesions with U-fiber and subcortical enhancement (FUSE) in MOG antibody-associated cerebral cortical encephalitis. Neurol Sci. 2024 Feb;45(2):809-812. doi: 10.1007/s10072-023-07092-1. Epub 2023 Oct 4. PMID: 37792111.
4. Budhram A, Kunchok AC, Flanagan EP. Unilateral Leptomeningeal Enhancement in Myelin Oligodendrocyte Glycoprotein Immunoglobulin G-Associated Disease. JAMA Neurol. 2020 May 1;77(5):648-649. doi: 10.1001/jamaneurol.2020.0001. PMID: 32119057.

Images/Tables



14-year-old female with headaches, paresthesias and vision loss found to have positive anti-MOG antibody with titer of 1:1,000. Axial T2 FLAIR-weighted image (A) demonstrates multiple subcortical T2 FLAIR hyperintense lesions including in the right operculum and parietal lobe involving the U-fibers (arrows). 3D T1-weighted post-contrast image (B) shows concordant enhancement in these regions consistent with the radiologic pattern of FUSE (arrows).
21-year-old male with seizures found to have positive anti-MOG antibody with titer of 1:160. Axial T2 FLAIR-weighted image (C) demonstrates right parietal cortical T2 FLAIR hyperintensity and sulcal effacement (arrows) without enhancement on T1-weighted post contrast images (arrows, D). The T2 FLAIR hyperintensity and sulcal effacement resolved on follow up (arrows, E) consistent with the clinico-radiologic presentation of FLAMES.

509

Post Neurointerventional Vessel Wall Imaging Finding, Etiology, Outcomes, and potential Pitfalls

Khaled H Al Tawil MD[1], Mona Kharaji MD[1], Ahmed A Safwat MD[1], Maoxue Wang MD[1], Cristina Sanchez-Vizcaino MD[1], Mahmud Mossa-Basha MD[2]
[1]University of Washington Medical Center, Seattle, WA, USA. [2]University of Washington Medical Center, Seattle, washington, USA

Abstract Category

Interventional/Vascular/Stroke

Summary & Objectives

- Post interventional vessel wall MRI (VWI) is routinely completed at our institution for acute ischemic stroke. Interventions are performed to reconstitute blood flow in the setting of large vessel occlusion, however, arterial wall injury within the selected arterial segments resultant from stent retriever deployment is common. We will discuss the common post-interventional VWI findings, potential subsequent complications related to the VWI features and provide image examples for each.
- There are common pitfalls in VWI which can have significant impact on the diagnostic interpretation. These pitfalls include Slow flow, venous flow, and vasa vasorum. Their etiology will be discussed as well.

Purpose

- To educate fellow Neuroradiologists and Neuro-Interventionalists on the common post neurointerventional VWI findings, pitfalls, and their etiology. This will help current and future colleagues better understand VWI and hopefully have a positive impact on the patient's clinical course.

Materials & Methods

- We will review stroke post-interventional VWI cases using PACS cases from the University of Washington database to give visual examples of various findings on post-interventional VWI.
- We will use a selected list of published papers as a reference to better describe and outline these findings and their pathophysiology.

-We will discuss each finding we believe is valuable and provide an appropriate imaging example. We will give a list of pearls to utilize when interpreting post-interventional VWI.
-We will discuss and provide examples of outcomes related to the imaging findings on post-intervention VWI, including imaging features that increase the likelihood of hemorrhagic conversion and worsened outcomes.

Results & Conclusion
- Post-neurointerventional VWI findings which can affect the patient's clinical course. These findings include patterns of vessel wall enhancement among others. Each finding was presented with a real patient case from our hospital. Neuroradiologists and neuro-interventionalists viewing and reporting these studies benefit from reviewing these findings seen on stroke post-interventional VWI.
- Some post-interventional VWI pitfalls and mimics can negatively affect the read quality. Hence, the interpreting radiologist should have a good understanding of what these pitfalls are and their causes as well.

References

- 1-Bhagya Sannananja, Chengcheng Zhu, Niranjan Balu, Laura Eisenmenger, Hediyeh Baradaran, Myriam Edjlali, Javier M Romero, Prabakhar Shantha Rajiah, Rui Li, Mahmud Mossa-Basha, Report from the society of magnetic resonance angiography: clinical applications of 7T neurovascular MR in the assessment of intracranial vascular disease, Journal of NeuroInterventional Surgery, 16, 8, (846-851), (2023)
-
- 2-Goyal M, Menon BK, van Zwam WH, Dippel DW, Mitchell PJ, Demchuk AM, et al.; HERMES Collaborators. Endovascular thrombectomy after large-vessel ischaemic stroke: a meta-analysis of individual patient data from five randomised trials. Lancet. 2016;387:1723–1731. doi: 10.1016/S0140-6736(16)00163-X.
  3-A. Lindenholz, I.C. van der Schaaf, A.G. van der Kolk, H.B. van der Worp, A.A. Harteveld, L.J. Kappelle, J. Hendrikse, MRI Vessel Wall Imaging after Intra-Arterial Treatment for Acute Ischemic Stroke, American Journal of Neuroradiology, 41, 4, (624-631), (2020).

530

Empowering Radiologists with AI: A Clear and Concise Tutorial of Generative AI for Radiologists

Jeremy B Nguyen MD[1], Gautam Dua MD[1], Haley Gould MD[1], Janis Park MD[1], Matthew Parker MD[2]
[1]Tulane University School of Medicine, New Orleans, LA, USA. [2]Tulane Radiology, New Orleans, LA, USA

Abstract Category

New Techniques/Advanced Imaging/Informatics/AI/Professional Development/Misc

Summary & Objectives

Generative AI is a branch of artificial intelligence that focuses on creating models that can generate new content. Unlike traditional AI, which primarily deals with classification and decision-making, generative AI models learn patterns from vast amounts of existing data and use this knowledge to generate original outputs, such as text, images, audio, and video. By understanding the underlying distribution of the input data, these models can generate novel content that resembles the original data while remaining unique. Among the various types of generative models, **Transformer networks** have been particularly revolutionary, driving advancements in **natural language processing (NLP)** and other generative tasks.

Purpose

- To describe the general principle artificial intelligence
- To discuss the concept of machine learning and deep learning
- To explain the architecture of a neural network and its elements, including the “artificial neurons”, and network layers.
- To describe the core concepts of Generative AI with the eemphasis on the model's ability to create new data (e.g., text, images, music) by learning from existing datasets.
- To describe the general architecture and operations of Transformer networks and mathematical Attention Theory
- To explain the importance and impact of Generative AI
- To discuss some practical application of Generative AI

Materials & Methods

This exhibit will provide a concise tutorial of Generative AI without delving into complex programming and mathematics. The radiologist will gain a foundational understanding of **deep learning** within machine learning, along with the core concepts and techniques of generative AI. The radiologist will also learn the general features of Transformer networks and the conceptual Attention Theory. Practical applications of generative AI, relevant to the field of radiology, will also be discussed to provide a comprehensive overview.

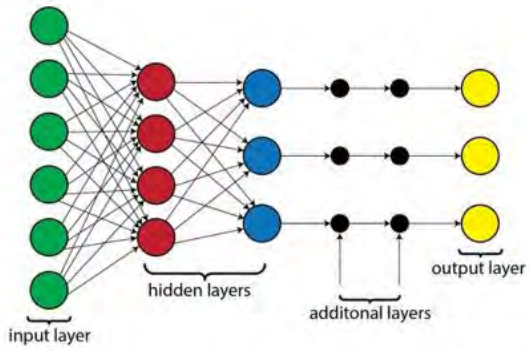
Results & Conclusion

Generative AI represents a powerful technology with the potential to create new, valuable content across many domains, but it also requires careful handling to ensure it benefits society responsibly. Generative AI is expected to continue transforming fields such as entertainment, education, healthcare, and creative industries. Future research aims to improve the controllability of these models, allowing users to have more precise control over the generated outputs. After the completion of this tutorial, the radiologist will have a firm conceptual knowledge of the operation of Transformer networks and Generative AI and along with its applications giving the radiologist a firm foundation to further explore of Generative AI in more depth.

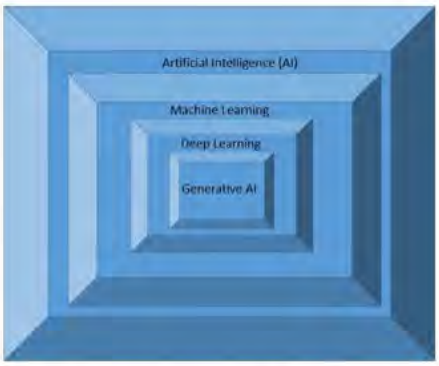
References

- Vaswani, A., Shazeer, N., Parmar, N., Uszkoreit, J., Jones, L., Gomez, A. N., Kaiser, Ł., & Polosukhin, I. (2017). Attention is all you need. *Advances in Neural Information Processing Systems*, 30, 5998–6008. https://doi.org/10.48550/arXiv.1706.03762
- Chartrand G, Cheng P, Vorontsov E et al. Deep Learning: **A Primer for Radiologists.** *Radiographics***.** 2017;37(7):2113-2131.

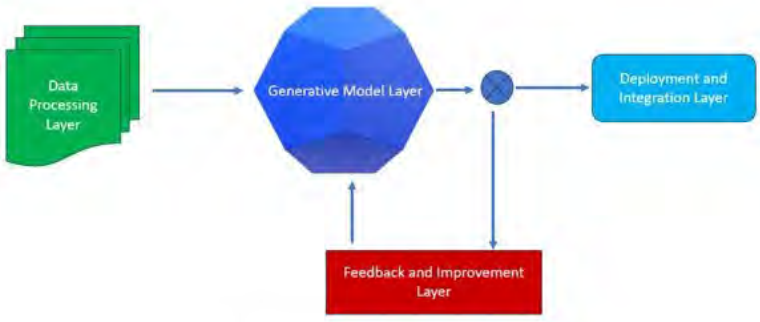
Images/Tables



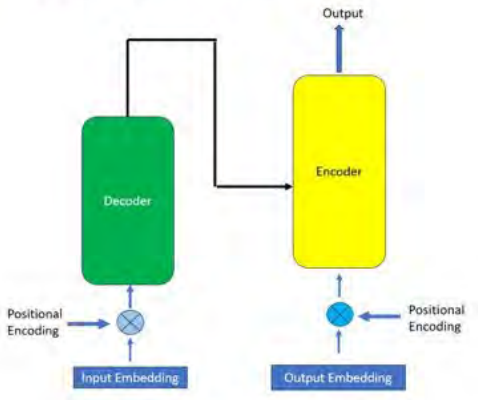
General architecture of a deep learning neural network



Generative AI is s subset of deep learning



General architecture of Generative AI system



Basic architecture of a Transformer Network

532

Chronic Subdural Hematoma Inflammatory Changes: the Role of Contrast-Enhanced MRI

Devan W. Vidrine M.D., M.A.[1], Jamie E. Clarke M.D., M.S.[1], Milan H. Samarage M.D.[2], Aryan Gajjar[3], Kambiz Nael M.D.[4], Jeremiah N. Johnson M.D.[2], Ameera F. Ismail M.D.[1]

[1]Division of Neuroradiology, Department of Diagnostic Radiology, University of California Los Angeles, Los Angeles, CA, USA. [2]Department of Neurosurgery, University of California Los Angeles, Los Angeles, CA, USA. [3]University of California Los Angeles, Los Angeles, CA, USA. [4]Division of Neuroradiology, Department of Radiology and Biomedical Imaging, University of California San Francisco, San Francisco, CA, USA

Abstract Category

Interventional/Vascular/Stroke

Summary & Objectives

Chronic subdural hematomas (cSDH) are increasingly common in the aging population. The literature now emphasizes inflamed and leaky dural capillaries as a driver of cSDH expansion. Middle meningeal artery (MMA) embolization addresses recurrent bleeds from inflamed capillaries within the membranes of cSDH by halting their arterial supply. cSDH are typically imaged with non-contrasted computed tomography (NC-CT). However, contrast-enhanced magnetic resonance imaging (CE-MRI) is a superior tool for visualizing cSDH inflammatory changes.

Purpose

This educational exhibit discusses the role of CE-MRI in evaluating cSDH. It presents cases of cSDH imaged on CE-MRI and angiographically during MMA embolization, showcasing specific neuroradiologic findings that correlate with the inflammatory changes driving cSDH. In doing so, the authors (1) highlight the most updated research on the etiology and natural history of cSDH; (2) emphasize the limits of NC-CT in capturing the complexity of cSDH; (3) describe the CE-MRI findings that reflect cSDH inflammatory changes; and (4) ultimately pose the question of whether certain CE-MRI features can predict cSDH response to MMA embolization.

Materials & Methods

We provide NC-CT, CE-MRI, and angiographic images obtained from cases of cSDH, which were diagnosed and treated at UCLA/Ronald Reagan Hospital.

Results & Conclusion

Our understanding of cSDH is evolving – changes in the cellular, molecular model for cSDH have led to changes in clinical management. CE-MRI is an important tool for capturing inflammatory processes related to cSDH formation, progression, and persistence. Specifically, CE-MRI is an effective tool for demonstrating cSDH chronicity, structural complexity including internal septations, and enhancement patterns that reflect evolving inflammatory changes.

References

1. Feghali J, Yang W, Huang J, et al. Updates in Chronic Subdural Hematoma: Epidemiology, Etiology, Pathogenesis, Treatment, and Outcome. *World Neurosurg*. 2020 Sep;141:339-345. DOI: https://doi.org/10.1016/j.wneu.2020.06.140.
2. Kan P, Maragkos GA, Srivatsan A, et al. Middle Meningeal Artery Embolization for Chronic Subdural Hematoma: A Multi-Center Experience of 154 Consecutive Embolizations. *Neurosurgery*. 2021 Jan 13;88(2):268-277. DOI: https://doi.org/10.1093/neuros/nyaa379.
3. Hasan D, Nikoubashman O, Pjontek R, et al. MRI appearance of chronic subdural hematoma. *Front Neurol*. 2022 Aug 8;13:872664. DOI: https://doi.org/10.3389/fneur.2022.872664.
4. Edlmann E, Giorgi-Coll S, Whitfield PC, et al. Pathophysiology of chronic subdural haematoma: inflammation, angiogenesis and implications for pharmacotherapy. *J Neuroinflammation*. 2017 May 30;14(1):108. DOI: https://doi.org/10.1186/s12974-017-0881-y.

Images/Tables

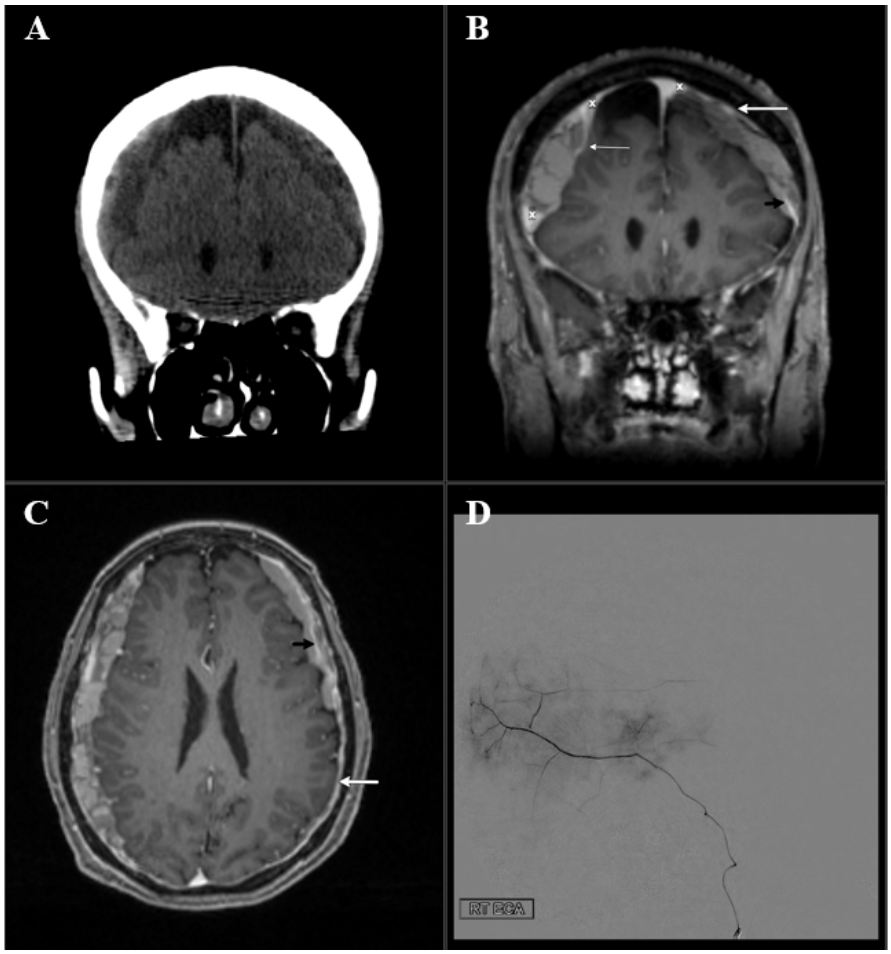


Figure 1: A 73-year-old female presenting for severe headache without a history of trauma, imaging obtained at presentation **A**: Coronal NC-CT of the brain demonstrates bilateral subdural fluid collections with mixed density consistent with cSDH with subacute components. **B**: Coronal post-contrast T1W image demonstrating pachymeningeal enhancement (thick arrow) and enhancement of an internal septation (black arrow) within the left cSDH. Three "spandrel-like" areas of enhancement (x) are seen adjacent to the superior sagittal sinus and at the superior and inferior aspects of the right-sided cSDH. An enhancing inner membrane of the right cSDH is also seen (thin arrow) **C**: Axial slice of the post-contrast T1W image from panel B showing pachymeningeal enhancement (thick arrow) and enhancement of an internal septation of the left-sided cSDH (black arrow). **D**: Lateral view of a superselective microcatheter contrast injection in the parietal occipital branch of the right middle meningeal artery demonstrating a diffuse vascular "blush" in the cSDH inflammatory tissues immediately subdural, as noted on the CE-MRI.

535

When AI starts to inspire you: Decision making with artificial intelligence

Sevcan Turk MD[1], Sevtap Turk MS[2]

[1]University of Pennsylvania, Philadelphia, PA, USA. [2]Istanbul University-Cerrahpasa, Istanbul, Istanbul, Turkey

Abstract Category

New Techniques/Advanced Imaging/Informatics/AI/Professional Development/Misc

Summary & Objectives

Encouraging radiologists to enhance their understanding about the nature of artificial intelligence decision-making.

Purpose

- Highlight the role of artificial intelligence applications in healthcare decision-making; quality, accuracy, efficiency, and personalization.
- Discuss the role of artificial intelligence to improve diagnostic accuracy in current clinical use.
- Discuss the patient safety concerns; trust, reproducibility, explainability, and accountability.
- Discuss the impact of artificial intelligence tools in radiologic diagnosis for underserved areas.
- Discuss the potential bias in machine learning with the potential impact.
- Discuss the regulatory considerations from FDA to the reading room.
- Discuss radiology training in the era of ChatGPT.

Materials & Methods

Overview of potential benefits and limitations of artificial intelligence applications in radiology and healthcare decision-making including quality, accuracy, efficiency, and personalization. Highlight the potential impact of artificial intelligence tools including patient safety concerns, trust, explainability, accountability, and bias. Discuss the potential impact on underserved areas and radiology training. Brief discussion of regulatory consideration and implementation.

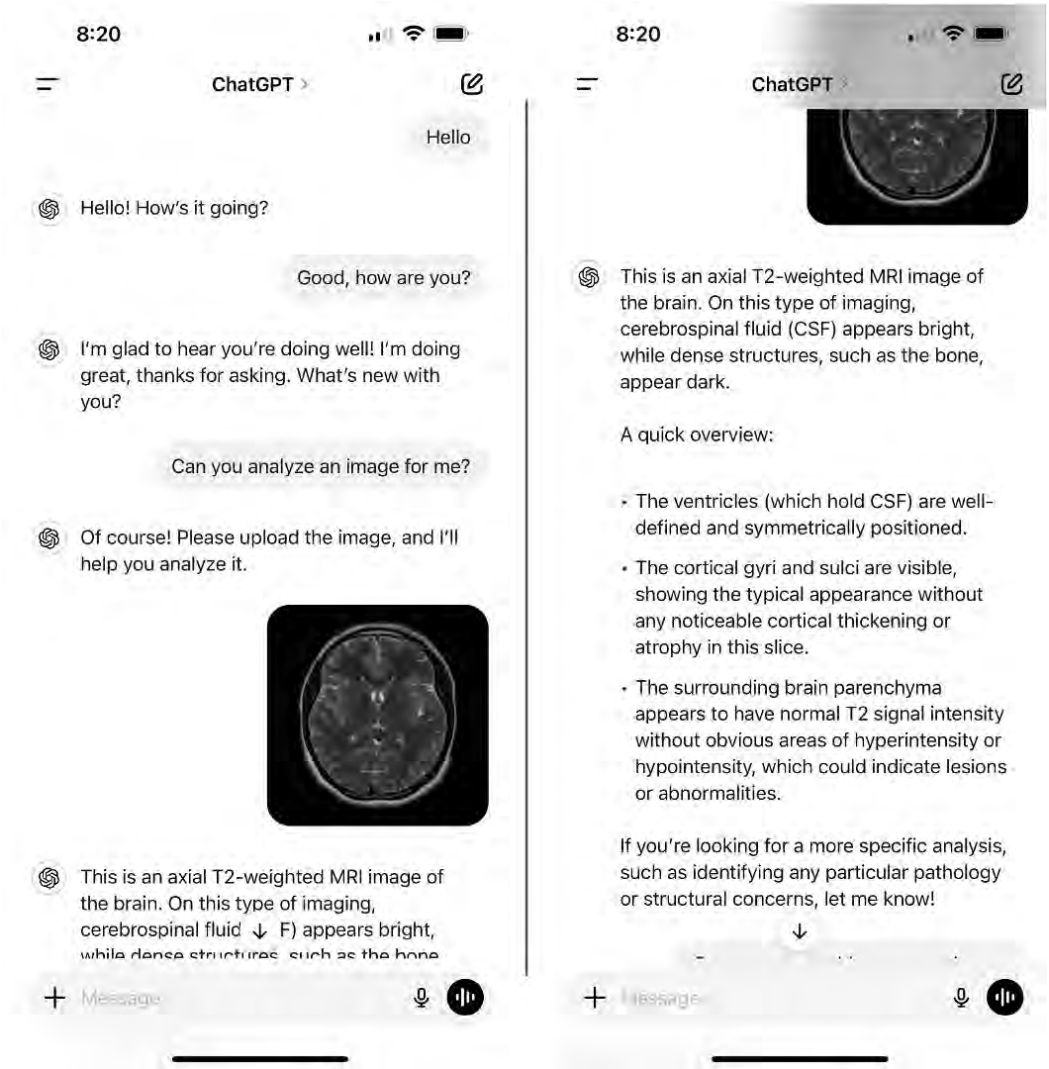
Results & Conclusion

Radiologists will be able to recognize potential benefits and limitations of artificial intelligence augmented decision-making as well as the impact on radiology training, healthcare in underserved areas and be aware of the legal considerations.

References

1. Clinical, Cultural, Computational, and Regulatory Considerations to Deploy AI in Radiology: Perspectives of RSNA and MICCAI Experts, Marius George Linguraru, Spyridon Bakas, Mariam Aboian, Peter D. Chang, Adam E. Flanders, Jayashree Kalpathy-Cramer, Felipe C. Kitamura, Matthew P. Lungren, John Mongan, Luciano M. Prevedello, Ronald M. Summers, Carol C. Wu, Maruf Adewole, and Charles E. Kahn, Jr, Radiology: Artificial Intelligence 2024 6:4
2. Ethics of Artificial Intelligence in Radiology: Summary of the Joint European and North American Multisociety Statement, J. Raymond Geis, Adrian P. Brady, Carol C. Wu, Jack Spencer, Erik Ranschaert, Jacob L. Jaremko, Steve G. Langer, Andrea Borondy Kitts, Judy Birch, William F. Shields, Robert van den Hoven van Genderen, Elmar Kotter, Judy Wawira Gichoya, Tessa S. Cook, Matthew B. Morgan, An Tang, Nabile M. Safdar, and Marc Kohli, Radiology 2019 293:2, 436-440
3. Rouzrokh P, Khosravi B, Faghani S, Moassefi M, Vera Garcia DV, Singh Y, Zhang K, Conte GM, Erickson BJ. Mitigating Bias in Radiology Machine Learning: 1. Data Handling. Radiol Artif Intell. 2022 Aug 24;4(5):e210290. doi: 10.1148/ryai.210290. PMID: 36204544; PMCID: PMC9533091.
4. Rodman A, Buckley TA, Manrai AK, Morgan DJ. Artificial Intelligence vs Clinician Performance in Estimating Probabilities of Diagnoses Before and After Testing. *JAMA Netw Open.* 2023;6(12):e2347075. doi:10.1001/jamanetworkopen.2023.47075

Images/Tables



542

Differential diagnosis of sinonasal lesions utilizing CT, MRI and PET/CT

Jiaqiong Wang M.D., Ph.D.[1], Russ Kuker M.D.[2], Robert Quencer MD[2]

[1]Temple University Hospital, Fox Chase Cancer Center, Philadelphia, PA, USA. [2]University of Miami Miller School of Medicine, University of Miami Hospital/Jackson Memorial Hospital, Miami, FL, USA

Abstract Category

Head and Neck

Summary & Objectives

Sinonasal lesions often present with nonspecific symptoms, but commonly include rhinorrhea, sinus congestion, epistaxis, postnasal drip. If there is expansion into orbital cavities, patients may present with proptosis and facial swelling. The differential diagnosis of sinonasal lesions includes benign and malignant disease. The objective of this educational exhibition is to facilitate the accurate diagnosis of sinonasal disease utilizing CT, MRI and PET/CT.

Purpose

The purpose of this study is to promote the accurate diagnosis of sinonasal lesions by combining CT, MRI and PET/CT.

Materials & Methods

Patients with sinonasal symptoms were evaluated with CT and MRI. If imaging findings revealed tumor, the patient was further evaluated with PET/CT utilizing the radiotracers F-18 FDG or Ga-68 Dotatate. Some patients with history of other primary tumors were evaluated by PET/CT, and those who had incidental abnormal findings in the sinonasal region were further evaluated by CT and MRI. The final diagnosis was made by pathology.

Results & Conclusion

This study characterizes various types of sinonasal disease on CT, MRI and PET/CT, including mucocele, mucus retention cyst, chronic noninvasive fungal sinusitis, sinonasal squamous cell carcinoma (SCC), lymphoma, inverted sinonasal papilloma, esthesioneuroblastoma and sinus meningoencephalocele. Mucus retention cyst and fungal mycetoma do not demonstrate bone erosion on CT, and are not hypermetabolic on F-18 FDG PET/CT. Lymphoma, squamous cell carcinoma and some inverted papillomas demonstrate bone destruction, and are hypermetabolic on F-18 FDG PET. Esthesioneuroblastoma presents with a “dumbbell-shaped” soft tissue mass passing through the cribriform plate, associated with bone remodeling or resorption, without aggressive bone destruction, and is positive on Ga-68 Dotatate PET/CT. Figure 1 shows a case of right sinonasal SCC. F-18 FDG PET/ CT scan showed a hypermetabolic soft tissue mass centered in the right nasal cavity extending to bilateral maxillary sinuses and left posterior ethmoid sinus. There was destruction of the posterolateral wall of the left maxillary sinus with tumor extension into the pterygopalatine foramen and sphenopalatine foramen. There was destruction of the osseous posterior nasal septum, posterior medial maxillary sinus, floor of the right ethmoid sinus and posterior lamina papyracea and nasal turbinate. MRI showed a lobulated T1 isointense, T2 isointense, enhancing soft tissue mass in the right nasal cavity and right ethmoid sinus. There was also mucosal thickening in the paranasal sinus, and fluid collection in the maxillary sinuses and complete obliteration of the right sphenoid sinus. Figure 2 shows a case of left maxillary palatal high-grade lymphoma, FDG PET/CT revealed a large, hypermetabolic lesion centered in the left hard palate and extending anterior-superiorly with erosive changes of the left maxilla sinus. Figure 3 shows a case of hypermetabolic inverted sinonasal papilloma in the right lateral nasal cavity and right medial maxillary sinus associated with bone erosion. Figure 4 shows a case of a sphenoid meningoencephalocele with hypometabolism in the herniated brain tissue in the left sphenoid sinus and hypometabolism in the adjacent abnormal left anterior temporal lobe. Table 1 summarizes the features of different sinonasal lesions and how imaging can facilitate the differential diagnoses.

References

1. Tzelnick S, Bernstine H, Domachevsky L, Soudry E. Clinical Implications of Incidental Sinonasal Positive FDG Uptake on PET-CT. Otolaryngol Head Neck Surg. 2019; 160(4):729-733. doi: 10.1177/0194599818821862.
2. Dondi F, Pasinetti N, Guerini A, et al. Prognostic role of baseline ^{18} F-FDG pet/CT in squamous cell carcinoma of the paranasal sinuses. Head Neck. 2022;44(11):2395-2406. doi: 10.1002/hed.27145.
3. Sato T, Hiraishi T, Tada M, et al. Meningoencephalocele in the Lateral Sphenoid Sinus Showing Malformation of Cortical Development: A Case Report. NMC Case Rep J. 2022; 9: 281-287. doi: 10.2176/jns-nmc.2022-0152.

Images/Tables

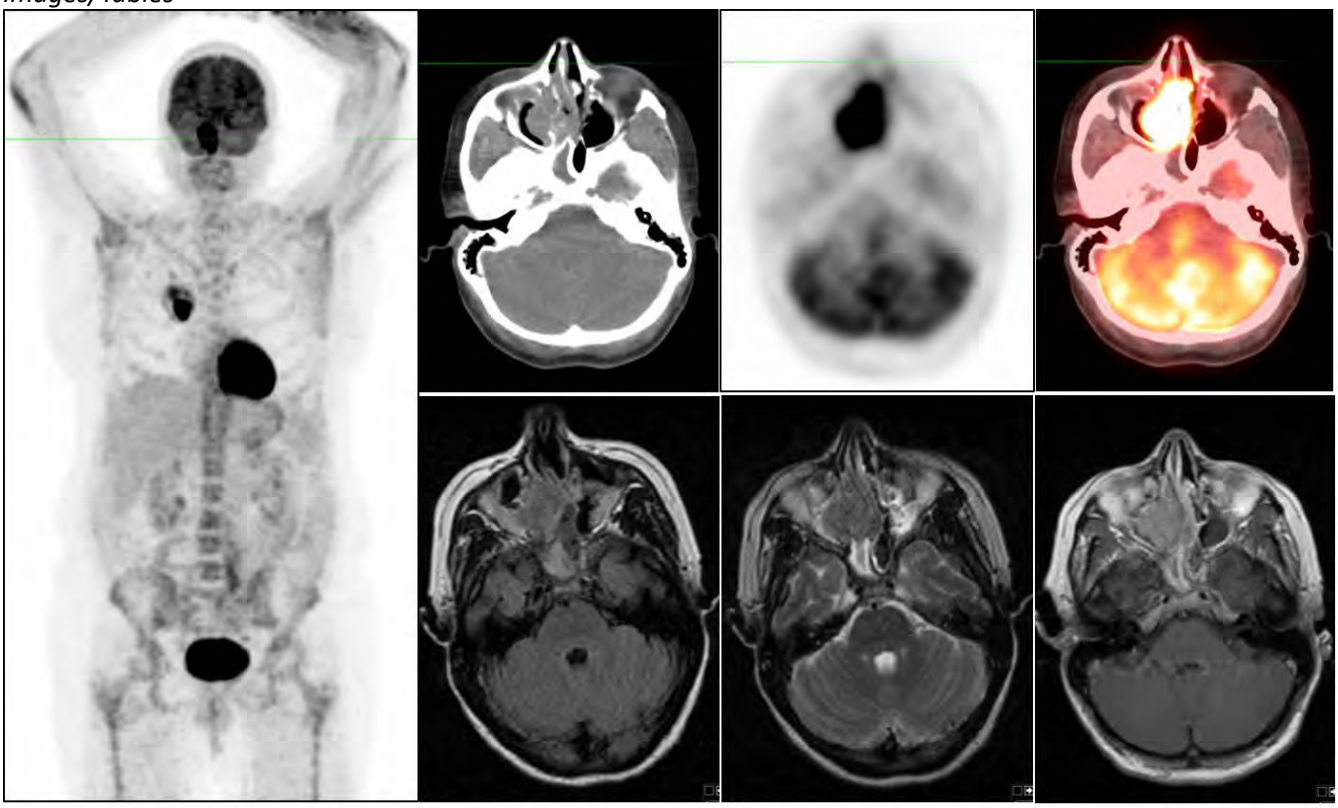


Figure 1. Right sinonasal squamous cell carcinoma. A 44 y.o. female with history of right upper lobe mass was referred for F-18 FDG PET CT scan. There was a hypermetabolic right upper lobe mass, which was pathologically proven high-grade spindle and giant cell carcinoma. Synchronously, there was a hypermetabolic soft tissue mass (SUV max 13.2) centered in the right nasal cavity extending to the medial aspect of the right maxillary sinus. The lesion extended from the floor of the right nasal cavity potentially into the left posterior ethmoid sinus. There was opacification of right sphenoethmoidal recess, right posterior ethmoid and sphenoid sinuses. There was destruction of the posterolateral wall of the right maxillary sinus with extension of tumor into the pterygopalatine foramen with involvement of the sphenopalatine foramen. There was destruction of the osseous posterior nasal septum, posterior medial maxillary sinus, floor of the right ethmoid sinus and posterior lamina papyracea and nasal turbinates. Periosteal thickening of the right sphenoid sinus is seen and to a lesser extent involving the maxillary sinus consistent with an element of chronic sinusitis. MRI showed a lobulated T1 isointense, T2 isointense, enhancing soft tissue mass in the right nasal cavity and right ethmoid sinus. There was also mucosal thickening in the right maxillary sinus, left sphenoid sinus, with fluid collection in the maxillary sinuses and complete obliteration of the right sphenoid sinus. The patient underwent nasal endoscopy and maxillary anterostomy, the pathology revealed squamous cell carcinoma.

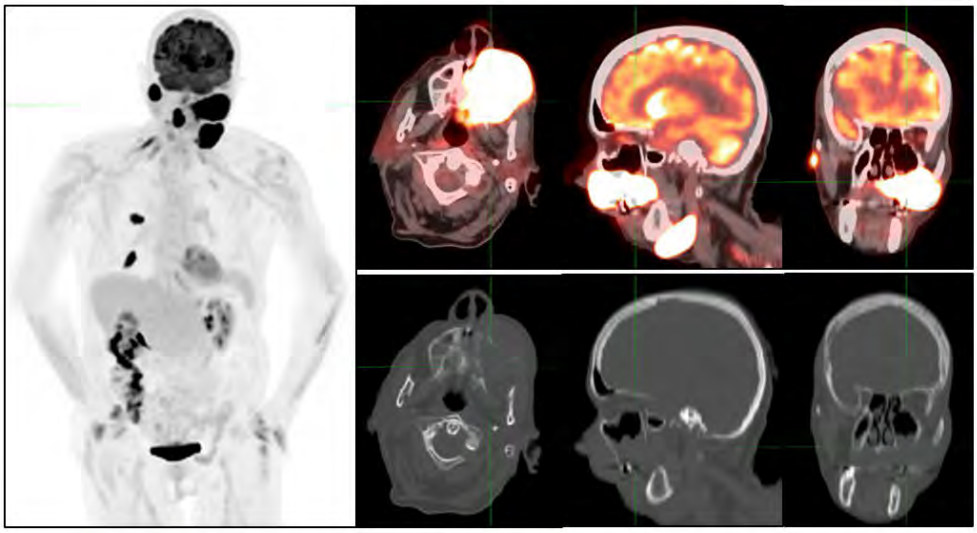


Figure 2. Left maxillary palatal high-grade lymphoma. Pre-treatment PET/CT revealed a large, hypermetabolic maxillary palatal lesion centered in the left hard palate, this lesion extended anterior-superiorly with erosive changes of the left maxilla sinus, with SUV max 24.0. Additionally, there was a hypermetabolic lesion at the right palatine tonsil with SUV max 24.0. There was an enlarged, hypermetabolic right intraparotid lymph node with SUV max 24.1, as well as a left level 1B conglomerate lymph node with SUV max 24.7. There were hypermetabolic lesions in the right lung, concerning for pulmonary involvement of lymphoma. Biopsy of left maxillary palatal mass showed high-grade lymphoma.

543

Acute Cerebral Venous Thrombosis: Combination of Susceptibility-weighted Imaging and Gd-MR Venography to e away is the Best Protocol for Earlier Diagnosis before Hemorrhagic Complications Occur.

Masahiro Ida MD
Mito Medical Center, Ibaraki, Ibaraki, Japan

Abstract Category

Interventional/Vascular/Stroke

Summary & Objectives

Cerebral venous thrombosis (CVT) is a rare but potentially critical cerebrovascular disorder. Severe vasogenic edema and multiple parenchymal hemorrhages are serious neurologic complications following acute CVT, which can lead to significant morbidity and mortality. It is important to identify acute CVT earlier than severe complications occur. Combination of FLAIR, SWI and Gd-MRV demonstrates the best sensitivity and accuracy among standard MR sequences to diagnose acute CVT and to predict impending hemorrhage.

Purpose

The learning objectives of this article are

- To describe the utilities of Diffusion-weighted imaging **(DWI)** ,T2-weighted fluid-attenuated inversion-recovery **(FLAIR)** and susceptibility-weighted imaging **(SWI)** for the diagnosis of **acute cerebral venous thrombosis (CVT)** and,
- To present the accuracy of Gd-enhanced MR venography **(Gd-MRV)** for definitive diagnosis of acute CVT in an early stage before hemorrhagic complications

Materials & Methods

In Mito Medical Center, MR protocol for diagnosis of acute CVT on an emergency is as follows. MR is the modality of the first choice.

1. DWI to detect acute ischemic cytotoxic edema.
2. T2-weighted imaging (T2-WI) to identify vasogenic edema and acute hemorrhage.
3. FLAIR to detect acute CVT as high-signal.
4. Time-of-flight MR angiography (MRA) to see dural arteriovenous fistula.
5. SWI to estimate increased concentration of intravenous deoxyhemoglobin
6. Gd-MR venography (Gd-enhanced 3D gradient-echo T1-weighted imaging) to detect acute CVT.

Results & Conclusion

- MRI is more sensitive than nonenhanced CT for detecting CVT. The empty delta sign on contrast-enhanced CT is visible in acute CVT, however, the sensitivity is insufficient (approximately 30% of acute CVT).
- **DWI** can be useful to identify cytotoxic edema caused by decreased cerebral perfusion. Acute CVT causes to increased venous congestion and pressure, which leads to elevated capillary pressure and a decrease in cerebral perfusion.
- **¨FLAIR** intraarterial signal¨ is a useful finding for detecting acute arterial occlusion. FLAIR also can depict acute CVT as high signal **(¨FLAIR intravenous signal¨)**. The signal of deoxyhemoglobin in acute CVT is very hypointense on T2-WI and may be mistakenly thought to indicate a flow void.
- The magnetic susceptibility of elevated deoxyhemoglobin makes medullary veins more hypointense on **SWI (¨SWI congestion sign¨)**. If acute clots do not resolve and collateral pathways of venous drainage are insufficient, intravenous pressure continue to increase, which leads to congestion of deoxyhemoglobin in the cortical and medullary veins. SWI sequence offers high sensitivity to identify elevated retrograde intravenous pressure and increased deoxyhemoglobin concentration in the medullary and capillary veins, which predict an increased risk of vasogenic edema and hemorrhagic complications.
- **Gd-MRV** provides positive intravascular blood-pool contrast enhancement without signal void caused by physiological turbulent flow. Especially, source images of Gd-MRV can display not only dural sinuses but also cortical and medullary veins precisely. GD-MRV can image acute CVT securely as filling defects in the dural sinus and cortical veins. Gd-MRV is clinically available and accurate technique for definitively diagnosing acute CVT.

We concluded that **combination of FLAIR, SWI and Gd-MRV demonstrates the best sensitivity** and accuracy among standard MR sequences to diagnose acute CVT and to predict impending hemorrhage earlier than hemorrhagic complications occur.

References
1. Canedo-Antelo M, Baleato-González S, Mosqueira AJ, et al. Radiologic Clues to Cerebral Venous Thrombosis. Radiographics. 2019 Oct; 39(6):1611-1628. doi: 10.1148/rg.2019190015
2. Sadik JC, Jianu DC, Sadik R, et al. Imaging of Cerebral Venous Thrombosis. Life (Basel). 2022 Aug 10;12(8):1215. doi: 10.3390/life12081215.
3. Boukerche F, Balakrishnan S, Kalapos P, et al. Detection of cerebral cortical vein thrombosis with high-resolution susceptibility weighted imaging — A comparison with MR venography and standard MR sequences. Neuroradiology. 2023 May;65(5):885-892. doi: 10.1007/s00234-023-03123-y.

550

Trends in Diagnostics, Etiologies, and Treatment Approaches for Pulsatile Tinnitus

Alexander Krawec BS[1], Tereza Vitkovska MS[1], Jamie E Clarke M.D., M.S.[1], Ava Jafarpour B.S.[1], John Go M.D.[2], Jay Acharya M.D.[1]

[1]UCLA David Geffen School of Medicine, Los Angeles, CA, USA. [2]Division of Neuroradiology, Department of Radiology, University of California Los Angeles (UCLA), Los Angeles, CA, USA

Abstract Category

Interventional/Vascular/Stroke

Summary & Objectives

This exhibit summarizes the diagnostics, etiologies, and treatments for pulsatile tinnitus most frequently discussed in the cited literature and quantifies their relative prevalence. The objectives of this educational exhibit are to share the authors' findings from a review of the 100 most-cited articles on pulsatile tinnitus, identify current trends in neuroradiology research, and outline clinical care advancements surrounding pulsatile tinnitus. Additionally, the exhibit aims to present the current state of knowledge on pulsatile diagnostics and treatment approaches.

Purpose

The purpose of this exhibit is to equip medical professionals with insights that can enhance clinical decision-making in pulsatile tinnitus cases. By providing a comprehensive analysis of diagnostic and treatment trends, this exhibit aims to improve patient outcomes, reduce the diagnostic burden, and streamline treatment strategies for pulsatile tinnitus.

Materials & Methods

The authors identified the top 100 most-cited articles on pulsatile tinnitus, highlighting significant research focused on neuroradiologic diagnostic and treatment approaches. This process involved tracing the historical development of diagnostic modalities, identifying key advancements, and recognizing contributions from various authors, specialties, and countries. The analysis categorized discussed etiologies, which included structural, cardiovascular, and mass effect-driven phenomena, as well as the types of interventions and diagnostic studies utilized.

Results & Conclusion

Results indicated that 100% of reviewed papers discussed underlying etiologies of pulsatile tinnitus, with sigmoid sinus diverticulum and/or dehiscence being the most common, followed by dural arteriovenous fistula and other arteriovenous malformations. Tumor-related etiologies appeared in only 11% of articles. A spectrum of treatments was discussed, with 78% of papers mentioning interventions that ranged from observation and lifestyle modification to invasive surgeries. Open head and neck surgeries and endovascular procedures were noted as the most frequently cited interventions. Diagnostic modalities varied, with 71% of studies using CT (56% with angiographical components) and 58% using MRI (69% with angiography). Invasive studies such as digital subtraction angiography (DSA) and lumbar puncture (LP) were also prevalent (25% and 11%, respectively). Surprisingly, temporal bone CT (TBCT) was discussed in only 13% of articles, suggesting an area for potential growth in future studies.

This exhibit underscores a rapidly evolving focus on pulsatile tinnitus in recent research, with significant advancements in diagnostic and treatment approaches, although gaps remain in standardized diagnostics and awareness among clinicians. These insights could guide future research to address underrepresented diagnostic techniques, such as TBCT, and foster improved clinical guidelines to ensure consistent and effective patient care for pulsatile tinnitus.

References
1. Alkhatib SG, Kandregula S, Flesher K, et al. Imaging of pulsatile tinnitus. *Radiographics* 2024;44(10). DOI: https://doi.org/10.1148/rg.240030
2. Schuknecht B, Kleinjung, T. Clinical Neuroimaging in the Evaluation of Tinnitus. In: Schlee, W, Langguth, B, De Ridder, D, et al., eds. *Textbook of Tinnitus* 2nd ed. New York: Springer, Cham; 2024:363-375

3. Lynch P, Mitton T, Killeen DE, Kutz JW, Newcomer M. Diagnosing pulsatile tinnitus: a review of 251 patients. *Otol Neurotol* 2022;43(1):128-136. DOI: https://doi.org/10.1097/MAO.0000000000003370
4. Narsinh KH, Hui F, Saloner D, et al. Diagnostic approach to pulsatile tinnitus: a narrative review. *JAMA Otolaryngol Head Neck Surg* 2022;148(5):476-483. DOI: https://doi.org/10.1001/jamaoto.2021.4470
5. Narvid J, Do HM, Blevins NH, Fischbein NJ. CT angiography as a screening tool for dural arteriovenous fistula in patients with pulsatile tinnitus: feasibility and test characteristics. *AJNR Am J Neuroradiol* 2011;32(3):446-453. DOI: https://doi.org/10.3174/ajnr.A2328

Images/Tables

Studies Described *in top-cited literature*	**CT** *71%*	**Angiographic** *56%*
		Non-angiographic *44%*
		Temporal Bone CT *13%*
	MRI *58%*	**Angiographic** *69%*
		Non-angiographic *31%*
	Invasive *36%*	**DRA** *25%*
		Lumbar Puncture *11%*

554

“From stenosis to synangiosis”. What the neuroradiologist should know about Moyamoya disease.

Gustavo Alejandro Averanga Ticona MD, Ignacio Belisle MD, Diego Miñarro MD, Manuel Perez Akly MD, Cristina Besada MD
Italian Hospital of Buenos Aires, Buenos Aires, Buenos Aires, Argentina

Abstract Category

Interventional/Vascular/Stroke

Summary & Objectives

Moyamoya disease (MMD) is a chronic and progressive cerebrovascular disease characterized by bilateral stenosis or occlusion of the circle of Willis arteries with the subsequent formation of prominent collateral circulation responsible for supplying the brain parenchyma.
When MMD presents in childhood, the initial symptoms are usually ischemic. In adults, approximately half of patients develop intracranial hemorrhage from rupture of the fragile moyamoya collateral vessels.
Computed tomography has a limited role in the diagnostic characterization of this pathology, so its performance should be considered when MRI is not available.
MRI provides a greater amount of information regarding the characterization and pre/post surgical assessment of Moyamoya disease. Some advanced sequences are also useful so they should be included in the protocol.
Moyamoya disease inevitably results in a serious health problem with progressive neurological deterioration.

Purpose

Review the radiological characteristics in the diagnosis, pre and postoperative evaluation of Moyamoya disease through the illustration with own cases, taking into account the evidence and update on the subject.

Materials & Methods

An extensive literature review was conducted to redefine concepts and update the topic. Dozens of pathological cases were retrospectively analyzed with pre- and postoperative images, where conventional and advanced neuroimaging were evaluated in pediatric and adult patients.

Results & Conclusion

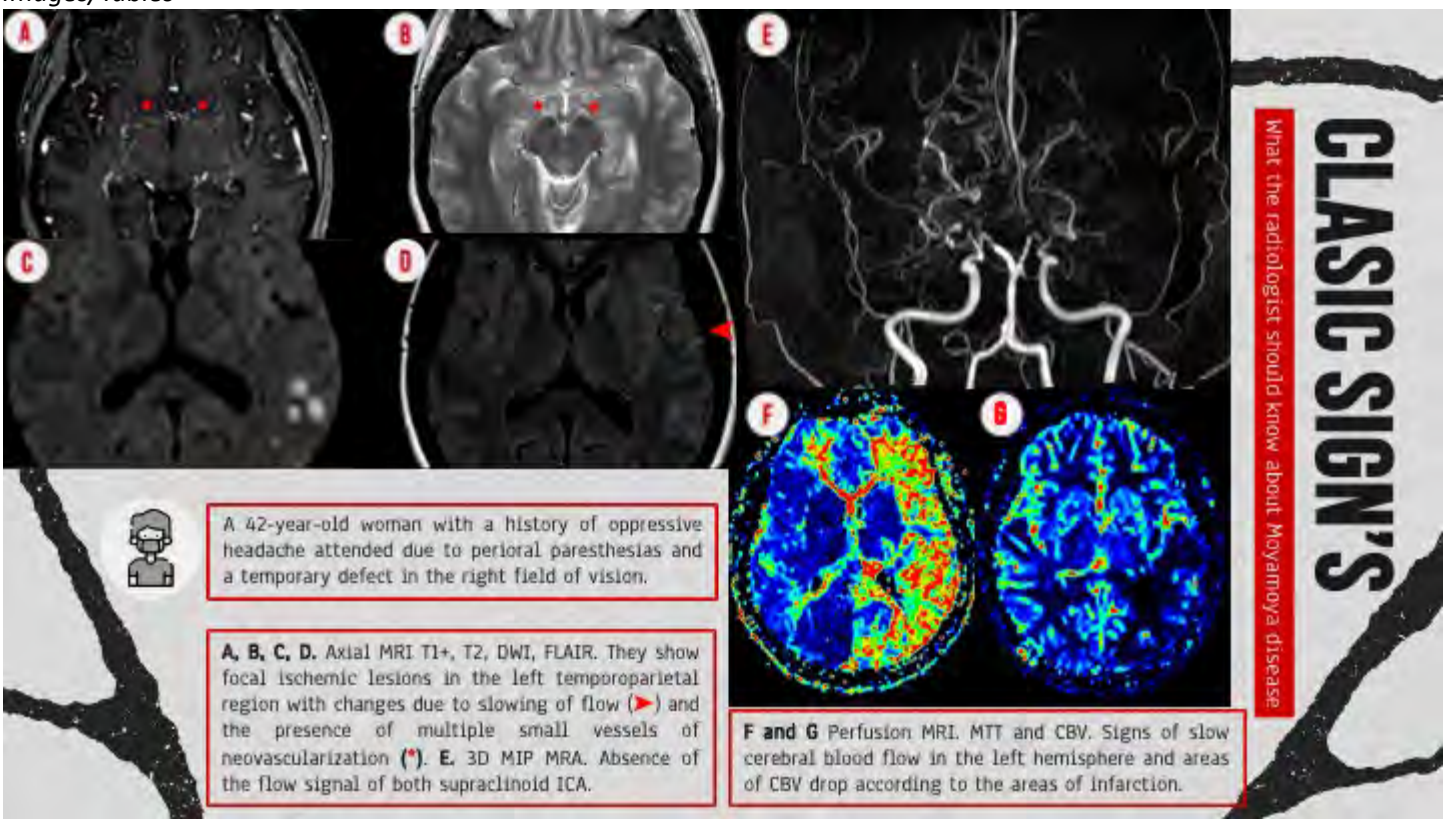
The concepts and differences between the terms Moya Moya disease and syndrome will be redefined, as well as the pathophysiological conditions involved and the differential diagnoses that can generate errors in the diagnosis.

The role of conventional (structural and vascular) and advanced images (perfusion with and without gadolinium, vascular network sequence) in the diagnostic process, perioperative and postoperative follow-up will be reviewed, with the identification of direct and indirect signs that suggest the presence and state of the disease.

References

- Ihara M, Yamamoto Y, Hattori Y et al. Enfermedad de Moyamoya: diagnóstico e intervenciones. Lanceta Neurol. 2022;21(8):747-58. doi:10.1016/S1474-4422(22)00165-X
- Filimonova E, Ovsiannikov K, Rzaev J. Neuroimagen en la angiopatía de Moyamoya: revisión actualizada. Clin Neurol Neurosurg. 2022;222:107471. doi.org/10.1016/j.clineuro.2022.107471

Images/Tables



575

Single-Site Study of Physician BT-RADS Scoring Distribution for MRIs of Brain Tumors

Evan J Bian, Michael Essien MBchB, MPH, Brent D Weinberg MD, PhD
Emory University, Atlanta, GA, USA

Abstract Category

Adult Neoplasms/Epilepsy/Trauma

Summary & Objectives

The radiology report can have vast stylistic variation dependent on radiologist preference, leaving the door open for ambiguity and inconsistency. This is problematic for accurately understanding the efficacy of brain tumor treatment response through MRI, where it can already be challenging to differentiate progression from treatment-related changes. As a result, a Brain Tumor Reporting and Data System (BT-RADS) was introduced to provide neuroradiologists with a structured reporting method to promote uniformity and simplicity in their radiological reports of brain tumors. These scores can be used by neuro-oncologists to determine follow-up after surgical treatment and predict patient clinical outcomes. Current literature has demonstrated the efficacy of BT-RADS - studies have demonstrated strong inter-rater agreement in blinded studies consisting of physicians at different training levels. Others have demonstrated BT-RADS improves physician satisfaction with communication and reduces hedge word usage when compared to free prose reports. However, there has been no study of how score distributions over time vary between readers in a real practice environment.

Purpose
It remains unclear how individual radiologists utilize BT-RADS in comparison to their peers. Individual variation in the same practice can help predict the performance of BT-RADS usage in real practice. This project evaluates the relative distribution of BT-RADS score distributions for individual faculty in a large university practice, comparing score distributions between faculty and to the overall distribution at the institution. We hypothesize that BT-RADS has some variability between individual readers and seek to understand differences in real-world BT-RADS performance between individuals.
Materials & Methods
All MRI reports generated on brain tumor patients at our institution between 2021 and 2024 were studied. Data collected included tumor type, tumor genetics, patient age, surgery and radiation treatment dates, BT-RADS scores, and primary faculty reader. Only readers who had performed > 100 reports during the period were included. Reports which did not clearly assign a score were also excluded. Individual faculty distributions of BT-RADS scores were compared to each other and the overall study site - differences were assessed using a chi square test. A multivariate analysis on diagnosis, genetics, and age/sex of patients was also conducted.
Results & Conclusion
4246 reports of brain MRIs read by board-certified neuroradiologists using the BT-RADS system were obtained. 12 total faculty members read over 100 reports (range 111-676). The rate of BT-RADS score 2 (stable) for the overall site was 49.56%, with a range of 39.78% - 55.79% among the readers. Three readers who varied the most from the overall rate of BT-2 scoring were statistically significant ($p < 0.05$). Overall rate of BT-RADS scores 3c and 4 (suspected progression or highly likely progression) was 15.55%, with a range of 8.31% - 23.64% among the readers. Three different readers who varied the most from the overall rate of BT-3c/4 scoring were statistically significant ($p < 0.05$).
Overall, there was moderate variation within the group, and future analysis will determine causes of variation and strategies to improve agreement. Continuing to validate the use of BT-RADS for multi-institution and radiological society use can be beneficial to patient care through fostering effective communication between neuroradiologists and referring physicians.
References
1. Weinberg, B. D., Gore, A., Shu, H. G., Olson, J. J., Duszak, R., Voloschin, A. D., & Hoch, M. J. (2018). Management-Based Structured Reporting of Posttreatment Glioma Response with the Brain Tumor Reporting and Data System. Journal of the American College of Radiology: JACR, 15(5), 767–771. https://doi.org/10.1016/j.jacr.2018.01.022
2. Schwartz, L. H., Panicek, D. M., Berk, A. R., Li, Y., & Hricak, H. (2011). Improving communication of diagnostic radiology findings through structured reporting. Radiology, 260(1), 174–181. https://doi.org/10.1148/radiol.11101913
3. Kim, S., Hoch, M. J., Peng, L., Somasundaram, A., Chen, Z., & Weinberg, B. D. (2022). A brain tumor reporting and data system to optimize imaging surveillance and prognostication in high-grade gliomas. Journal of neuroimaging: official journal of the American Society of Neuroimaging, 32(6), 1185–1192. https://doi.org/10.1111/jon.13044
4. Gore, A., Hoch, M. J., Shu, H. G., Olson, J. J., Voloschin, A. D., & Weinberg, B. D. (2019). Institutional Implementation of a Structured Reporting System: Our Experience with the Brain Tumor Reporting and Data System. Academic radiology, 26(7), 974–980. https://doi.org/10.1016/j.acra.2018.12.023
5. Essien, M., Cooper, M. E., Gore, A., Min, T. L., Risk, B. B., Sadigh, G., Hu, R., Hoch, M. J., & Weinberg, B. D. (2024). Interrater Agreement of BT-RADS for Evaluation of Follow-up MRI in Patients with Treated Primary Brain Tumor. AJNR. American journal of neuroradiology, 45(9), 1308–1315. https://doi.org/10.3174/ajnr.A8322

607

Recognizing Iatrogenic Cerebral Amyloidosis

Jacob A Alderete BS, Jamie Clarke MD, Antony Alvarado BS, Snehin Rajkumar BS, Jay Acharya MD
UCLA, Los Angeles, CA, USA
Abstract Category
Adult Brain Inflammatory/Infectious Disease/Degenerative/Metabolic
Summary & Objectives
Cerebral Amyloid Angiopathy (CAA), an inflammatory condition primarily affecting older adults, is linked to a range of neurological deficits. Increasingly, however, iatrogenic cerebral amyloid angiopathy (ICAA) is being recognized in younger patients, typically emerging an average of 35 years post-neurosurgery due to potential transmission. ICAA is thought to be caused by iatrogenic transmission of beta-amyloid plaques during neurological surgery, with possible links

to the use of cadaveric graft tissue, but its exact cause is unknown. Given its rarity, delayed onset, and association with older populations, ICAA is likely underdiagnosed, with potential for increased diagnoses as awareness grows.
ICAA, similar to spontaneous CAA (sCAA), most often presents with lobar intracerebral hemorrhage (ICH), transient focal neurologic event (TFNE), or seizures. On imaging, typical findings include lobar or cerebellar cerebral microbleeds (CMBs), cortical superficial siderosis (cSS), and convexity subarachnoid hemorrhage (cSAH), all findings similar to sCAA. Given the similar clinical and radiological symptoms of ICAA to sCAA, knowledge of patient history and demographics is critical. Any history of neurosurgery is most important to know for diagnosis of ICAA, and specifically use of cadaveric dural grafts can help with diagnosis. However, while there seems to be a relationship between cadaveric dural grafts and ICAA, it is unknown if it is neurosurgery in general that can cause the condition, and more research is needed to truly understand the pathophysiology of ICAA. Demographically, younger patients (age less than 50, according to Boston Criteria) are more likely to have ICAA as relative to sCAA. While it is useful to know this and emphasizes the importance of asking for neurosurgical history in younger patients with suspected CAA, this likely leaves out many older patients with ICAA who underwent surgical procedures at an older age. Given this information, it is important to inquire about surgical history for all patients with suspected CAA, even in older individuals.
With increased awareness of historical and imaging factors associated with ICAA, more cases are likely to be discovered, allowing for greater understanding of the condition, both in its pathogenesis and in specific findings that may differentiate it from sCAA, as imaging findings are not currently distinguishable between the two diseases.
Purpose
This exhibit aims to enhance understanding of ICAA and its hallmark imaging features. Better awareness can support earlier detection and expand epidemiological insights into ICAA.
Materials & Methods
We conducted literature searches in Web of Science and PubMed using specific Boolean search terms summarized findings from the most-cited papers focused on disease characteristics.
Results & Conclusion
Although rare, ICAA is likely underdiagnosed and expected to rise in prevalence as recognition of its distinct pathogenesis improves. As populations previously exposed to cadaveric dura reach the average onset period of symptoms, increased detection of ICAA could allow for earlier diagnosis, aiding in treatment and epidemiological tracking.
References
1. Kaushik K, van Etten ES, Siegerink B, Kappelle LJ, Lemstra AW, Schreuder FHBM, Klijn CJM, Peul WC, Terwindt GM, van Walderveen MAA, Wermer MJH. Iatrogenic Cerebral Amyloid Angiopathy Post Neurosurgery: Frequency, Clinical Profile, Radiological Features, and Outcome. Stroke. 2023 May;54(5):1214-1223. doi: 10.1161/STROKEAHA.122.041690. Epub 2023 Apr 10. PMID: 37035916; PMCID: PMC10121246.
2. Banerjee G, Samra K, Adams ME, Jaunmuktane Z, Parry-Jones AR, Grieve J, Toma AK, Farmer SF, Sylvester R, Houlden H, Rudge P, Mead S, Brandner S, Schott JM, Collinge J, Werring DJ. Iatrogenic cerebral amyloid angiopathy: an emerging clinical phenomenon. J Neurol Neurosurg Psychiatry. 2022 May 16:jnnp-2022-328792. doi: 10.1136/jnnp-2022-328792. Epub ahead of print. PMID: 35577510.
3. Charidimou A, Boulouis G, Frosch MP, Baron JC, Pasi M, Albucher JF, Banerjee G, Barbato C, Bonneville F, Brandner S, Calviere L, Caparros F, Casolla B, Cordonnier C, Delisle MB, Deramecourt V, Dichgans M, Gokcal E, Herms J, Hernandez-Guillamon M, Jäger HR, Jaunmuktane Z, Linn J, Martinez-Ramirez S, Martínez-Sáez E, Mawrin C, Montaner J, Moulin S, Olivot JM, Piazza F, Puy L, Raposo N, Rodrigues MA, Roeber S, Romero JR, Samarasekera N, Schneider JA, Schreiber S, Schreiber F, Schwall C, Smith C, Szalardy L, Varlet P, Viguier A, Wardlaw JM, Warren A, Wollenweber FA, Zedde M, van Buchem MA, Gurol ME, Viswanathan A, Al-Shahi Salman R, Smith EE, Werring DJ, Greenberg SM. The Boston criteria version 2.0 for cerebral amyloid angiopathy: a multicentre, retrospective, MRI-neuropathology diagnostic accuracy study. Lancet Neurol. 2022 Aug;21(8):714-725. doi: 10.1016/S1474-4422(22)00208-3. PMID: 35841910; PMCID: PMC9389452.
4. Storti B, Canavero I, Gabriel MM, Capozza A, Rifino N, Stanziano M, Tagliabue L, Bersano A. Iatrogenic cerebral amyloid angiopathy: An illustrative case of a newly introduced disease. Eur J Neurol. 2023 Oct;30(10):3397-3399. doi: 10.1111/ene.15997. Epub 2023 Aug 8. PMID: 37494007.
5. Panteleienko L, Mallon D, Oliver R, Toosy A, Hoshino Y, Murakami A, Kaushik K, Wermer MJH, Hara H, Yakushiji Y, Banerjee G, Werring DJ. Iatrogenic cerebral amyloid angiopathy in older adults. Eur J Neurol. 2024 Jun;31(6):e16278. doi: 10.1111/ene.16278. Epub 2024 Mar 21. PMID: 38511868; PMCID: PMC11235778.

625

Enhanced Detection of Epileptogenic Lesions: The Utility of Ultra-High-Field 7T MRI in Drug-Resistant Focal Epilepsy

James B Burke MD[1], Eman Mahdi MD[2], Taha Ashraf[3], Nada Abdelsattar[3], Matthew Glasser MD PhD[1], Jullie Pan PhD[4], Joseph P Cousins Md PhD[4], Ayman Nada MD[1]

[1]Washington University, St. Louis, MO, USA. [2]Virginia Commonwealth University, Richmond, VA, USA. [3]Fayoum University, Faiyum, Faiyum, Egypt. [4]University of Missouri, Columbia, MO, USA

Abstract Category

Adult Neoplasms/Epilepsy/Trauma

Summary & Objectives

Advances in MRI at 7T allow for increased SNR yielding far superior anatomic detail compared to conventional 1.5T and 3T imaging. A particularly effective application of higher magnet strength is in the evaluation of epilepsy, where up to 20-30% of patients with focal epilepsy demonstrate no imaging findings to explain their disease at 1.5T and 3T imaging. The added tissue resolution afforded at 7T allows radiologists to uncover previously occult epileptogenic foci such as focal cortical dysplasia, anomalies of migration, tumor, and scarring. The increased SNR and anatomic detail with 7T imaging is not without consequence; however, as stronger magnetic fields result in drawbacks such as longer scan times and increased susceptibility signal loss, which engenders new difficulties and accommodations for imaging.

Purpose

This presentation aims to advance the radiology trainee and neuroradiologists' understanding of ultra-high-field 7T imaging, to discuss the utility of UHF 7T in the evaluation and diagnosis of epilepsy, to evaluate the technical challenges of 7T imaging and their solutions, and primarily to showcase several real-world cases where 7T imaging uncovered epileptogenic foci with negative exams at lower magnetic field strength.

Materials & Methods

Multiple patients with drug resistant focal epilepsy underwent scanning with UHF 7T (Terra, Siemens Healthineers, Erlangen, Germany). The MR protocols included important sequences required for detection of epileptogenic foci such as high-resolution 2D T2 coronal imaging of the hippocampus, and 3D T1 MPRAGE. Other advanced sequences were also utilized e.g. 3D T1 MP2RAGE, FGATIR, and EDGE. The detected epileptogenic foci encompassed several categories such as hippocampal sclerosis, various types of focal cortical dysplasias, grey matter heterotopia, meningoceles/encephaloceles, and cerebrovascular disorders.

Results & Conclusion

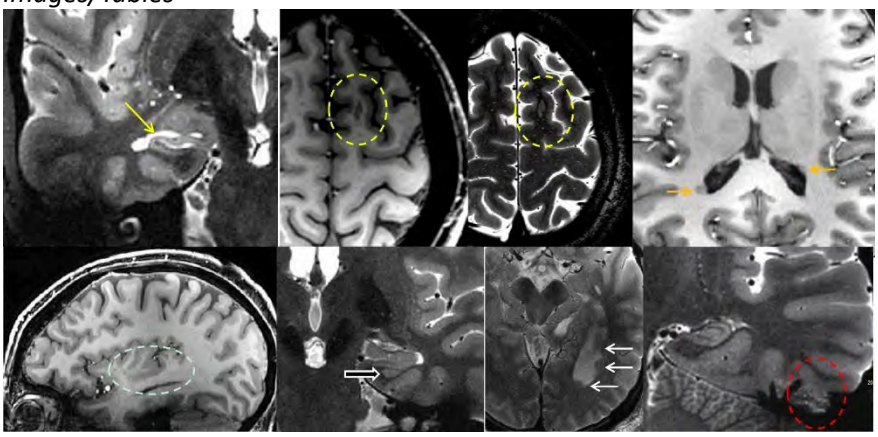
7T imaging was able to help identify epileptogenic foci in a variety of different disease pathologies including hippocampal sclerosis, focal cortical dysplasia, grey matter heterotopia, and meningocele/encephalocele. Imaging with higher magnetic field strengths is a useful diagnostic tool for cases of treatment drug-resistant epilepsy, can help guide more definite treatment options, and can identify previously imaging-occult causes of disease.

References

Park JE, Cheong EN, Jung DE, et al. Utility of 7 tesla magnetic resonance imaging in patients with epilepsy: a systemic review and meta-analysis. Front Neurol 2021;12:621936. doi: 10.3389/fneur.2021.621936

Opheim G, Kolk A, Block KM, et al. 7T epilepsy task force consensus recommendations on the use of 7T MRI in clinical practice. J. Neurol. 2021;96;327-341. doi:10.1212/WNL.0000000000011413

Images/Tables



627

Imaging of autoimmune encephalitis: a pictorial review

Yang Tang MD[1], Unsong Oh MD[2], Syed Mohammad Gharavi MD[3], Melissa Kang MD[1]
[1]Virginia Commonwealth University, Richmond, VA, USA. [2]Virginia Commonwealth University, Department of Neurology, Richmond, VA, USA. [3]Virginia Commonwealth University, Department of Radiology, Richmond, VA, USA

Abstract Category

Adult Brain Inflammatory/Infectious Disease/Degenerative/Metabolic

Summary & Objectives

Autoimmune encephalitis is a heterogenous group of CNS inflammatory disorders caused by immune-mediated response to the neurons. The symptoms are non-specific and frequently include psychiatric disturbances, memory loss, seizure or altered mental status. It can be divided into two groups. Group 1 is caused by autoantibodies against intracellular antigen, frequently paraneoplastic and with poor response to immune therapy. Group 2 is caused by autoantibodies against cell surface antigen, frequently non-paraneoplastic and with better response to immune therapy.

Purpose

The purpose of the case based pictorial review is to illustrate the MRI characteristics of autoimmune encephalitis and discuss the differential diagnoses.

Materials & Methods

Cases were collected by searching the PACS archives of a large academic tertiary institution. The diagnosis was confirmed by either positive autoantibody, or by pertinent clinical history/response to immune therapy when autoantibody was not tested or tested negative (presumed diagnosis).

The representative cases are grouped into the following categories by the dominant brain regions involved:
Limbic encephalitis, striatal encephalitis, cortical encephalitis, brain stem encephalitis, cerebellitis and meningoencephaltis.

Differential diagnoses including viral encephalitis, brain neoplasms (glioma or lymphoma), demyelinating disease (ADEM, NMOSD/MOGAD), vasculitis, MELAS and other CNS inflammatory diseases will be discussed.

Results & Conclusion

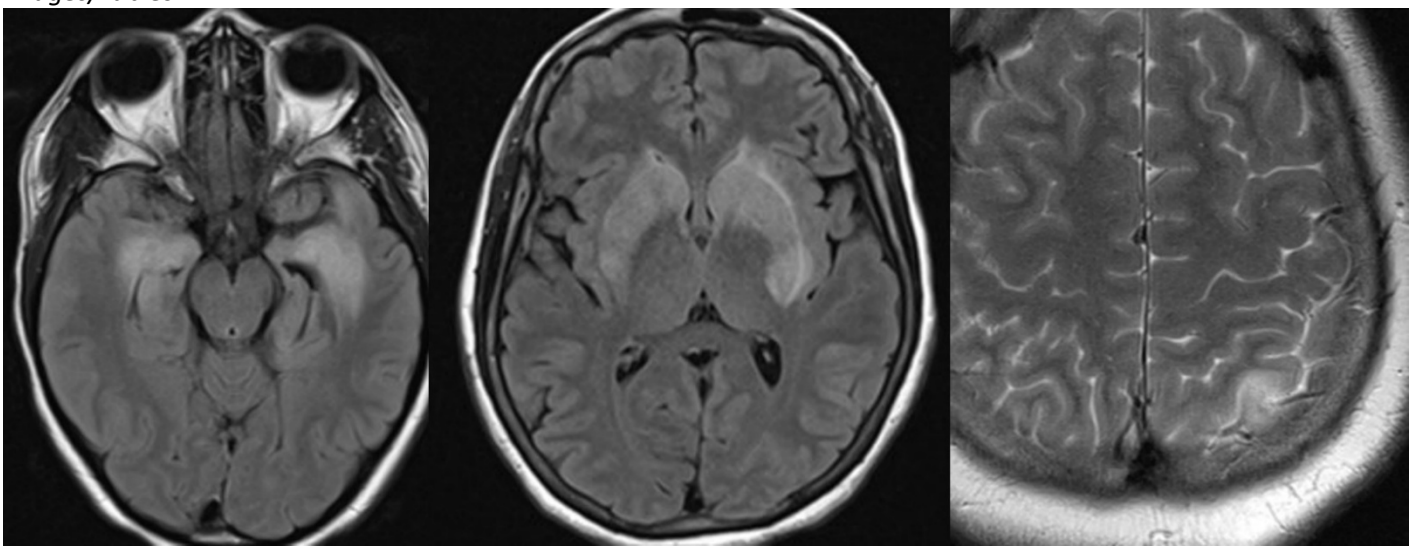
Autoimmune encephalitis is a relatively uncommon and under-diagnosed condition. It is critical for the neuroradiologist to become familiar with the variable imaging appearance of this disease.

References

Sanvito F, Pichiecchio A, Paoletti M, Rebella G, Resaz M, Benedetti L, Massa F, Morbelli S, Caverzasi E, Asteggiano C, Businaro P, Masciocchi S, Castellan L, Franciotta D, Gastaldi M, Roccatagliata L. Autoimmune encephalitis: what the radiologist needs to know. Neuroradiology. 2024 May;66(5):653-675. doi: 10.1007/s00234-024-03318-x. Epub 2024 Mar 20. PMID: 38507081; PMCID: PMC11031487.

Kelley BP, Patel SC, Marin HL, Corrigan JJ, Mitsias PD, Griffith B. Autoimmune Encephalitis: Pathophysiology and Imaging Review of an Overlooked Diagnosis. AJNR Am J Neuroradiol. 2017 Jun;38(6):1070-1078. doi: 10.3174/ajnr.A5086. Epub 2017 Feb 9. PMID: 28183838; PMCID: PMC7960083.

Images/Tables



628

Scanning the Crisis: Neuroimaging Perspectives on Drug Overdose in the Mountain State

Abdul AL halak DO, Erin Butcho MD, Justin McCloskey MD
WVU Medicine, Morgantown, WV, USA

Abstract Category

Adult Brain Inflammatory/Infectious Disease/Degenerative/Metabolic

Summary & Objectives

This study aims to explore the patterns of central nervous system (CNS) injuries associated with drug overdoses, focusing on their major complications and the development of differential diagnoses for toxic-metabolic encephalopathies. With West Virginia experiencing the highest rate of drug overdose deaths in the U.S., understanding these patterns is critical for improving patient outcomes.

Purpose

The purpose of this research is to educate healthcare professionals on the CNS sequelae of drug overdoses, particularly regarding imaging findings and clinical implications. By identifying common imaging patterns and clinical presentations, this work aims to enhance the diagnostic process for patients experiencing toxic-metabolic encephalopathies.

Materials & Methods

A comprehensive review of the literature and case studies was conducted, focusing on imaging findings in patients with acute and chronic drug overdose scenarios. Various imaging modalities, including MRI and CT scans, were utilized to assess CNS injuries resulting from different substances, such as fentanyl, heroin, cocaine, methamphetamine, ethanol, and methanol.

Results & Conclusion

Drug overdoses are important differential diagnoses to consider in the setting of toxic-metabolic encephalopathies. Diffusion restriction in the setting of acute overdose can be reversible or irreversible. Complications which can overlap with drug overdoses include hypoxic-ischemic injury, septic-embolic disease, acute hemorrhage, acute infarcts and rhabdomyolysis.

References

- Spencer M, Garnett M, Miniño A. Drug Overdose Deaths in the United States, 2002-2022 Key Findings Data from the National Vital Statistics System.; 2024. https://www.cdc.gov/nchs/data/databriefs/db491.pdf
- West Virginia Health Statistics Center. West Virginia Fatal Drug Overdoses: Key Drugs and Demographics, 2024

635

Progressive multifocal leukoencephalopathy (PML) Typical and atypical features.

Asif Jamal MD[1], Huda Al Jadiry MD[2], Taneya Shestopalova MD[2], Abel Abebe MD[2], Usama Habib MD[2]
[1]UTMB, Houston, TX, USA. [2]University of Texas Medical Branch (UTMB), Galveston, TX, USA

Abstract Category

Adult Brain Inflammatory/Infectious Disease/Degenerative/Metabolic

Summary & Objectives

•Progressive multifocal leukoencephalopathy (PML) is a rare CNS disease caused by the reactivation of the JC (John Cunningham) virus, which primarily targets glial cells. In the general population, PML is typically asymptomatic or presents as a lifelong persistent or latent infection. However, in immunocompromised individuals, this rare disease can be debilitating and often fatal.

•The clinical symptoms depends on the area of white matter involvement. The symptoms ranges from headache to altered mental status or stroke like symptoms. Spinal cord and optic nerves are usually spared.

•PML has characteristic imaging appearances, though it can sometimes present with atypical features. Recognizing the imaging characteristics that require prompt attention is essential for the effective management of these patients. This essay presents diagnostic features, illustrated through case-based learning.

OBJECTIVES:

We aim to enhance the delivery of care and ultimately reduce mortality and morbidity in patients with progressive multifocal leukoencephalopathy (PML). This goal can be achieved through the early recognition of PML.

We will discuss key MRI features and sequences that play a crucial role in diagnosing PML and predicting outcomes. For instance, the susceptibility sequence can help identify the endpoint stage of the neuroinflammatory process and provide insights into potential prognosis.

This case-based learning essay is primarily designed for trainees, though the detailed imaging findings are equally valuable for Neuro-radiologist.
We anticipate that, after reviewing this essay, both neuroradiology trainees and practicing staff will be better equipped to provide timely and effective care for patients with progressive multifocal leukoencephalopathy (PML).

Purpose

•To recognize typical and atypical imaging findings of Progressive Multifocal Leukoencephalopathy (PML)
• To develop systemic approach to accurately and promptly diagnose Progressive Multifocal Leukoencephalopathy (PML)
•To recognize other associated imaging findings with Progressive Multifocal Leukoencephalopathy (PML)
•To explain different subtypes of Progressive Multifocal Leukoencephalopathy (PML) based on imaging features.
•To explain complications of Progressive Multifocal Leukoencephalopathy (PML) based on imaging findings.

Materials & Methods

Our essay aims to evaluate the available data and identify key findings, with a focus on both classic and uncommon imaging features of progressive multifocal leukoencephalopathy (PML). The following topics will be discussed:
1.Introduction and Salient Features of PML
2.Typical Imaging Features of PML
3.Atypical Locations and Appearances of PML
4.Differentiating PML from Other Neurological Conditions Based on Imaging Findings
5.Key MRI Sequences for Identifying and Predicting Prognosis (Presented in a Case-Based Format)
6.PML-Associated Immune Reconstitution Inflammatory Syndrome (PML-IRIS)
7.Imaging Features of PML Based on Etiology

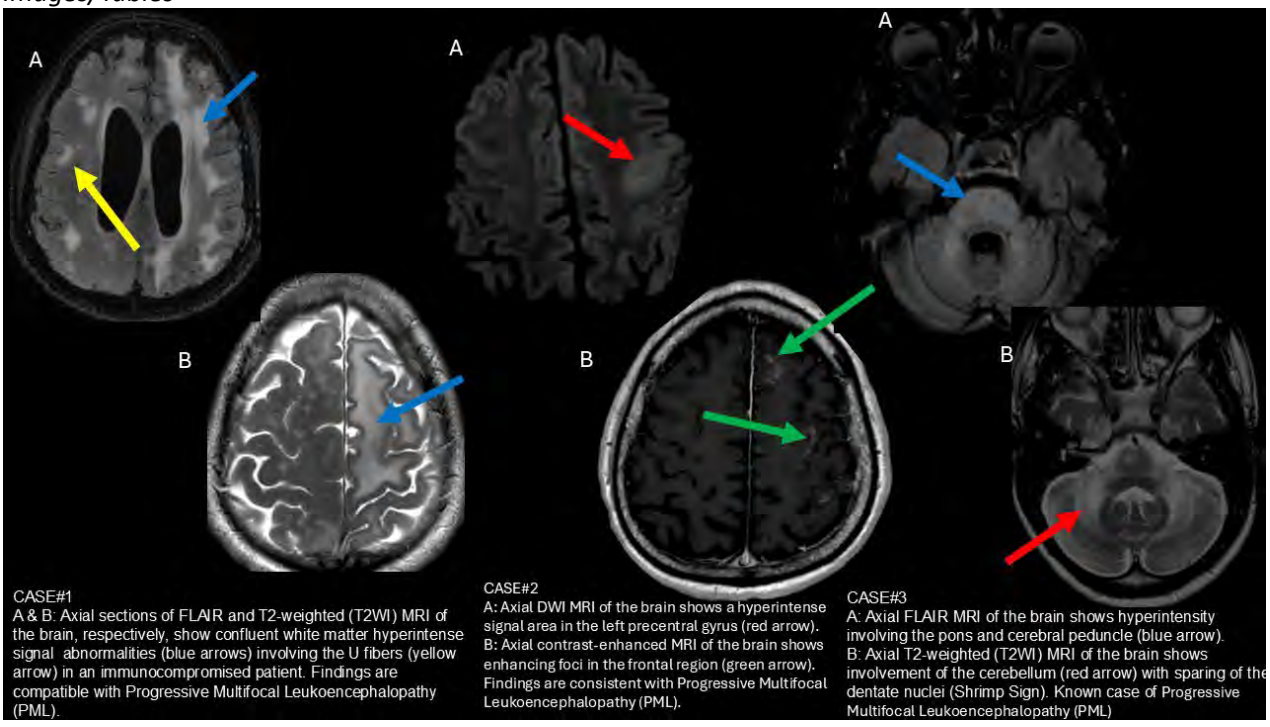
Results & Conclusion

Recognizing the imaging features of progressive multifocal leukoencephalopathy (PML) is crucial for enhancing care coordination among inter-professional teams. For years, PML has posed a serious threat, particularly to immunocompromised patients. Addressing these findings could help refine management strategies by validating accurate imaging diagnostics and improving the monitoring of at-risk patients.

References

Cortese I, Reich DS, Nath A. Progressive multifocal leukoencephalopathy and the spectrum of JC virus-related disease. *Nat Rev Neurol*. 2021;17(1):37-51.
Thurnher MM, Boban J, Rieger A, Gelpi E. Susceptibility-weighted MR imaging hypointense rim in progressive multifocal leukoencephalopathy: The end point of neuroinflammation and a potential outcome predictor. *Am J Neuroradiol*. 2019;40(6):994-1000.

Images/Tables



CASE#1
A & B: Axial sections of FLAIR and T2-weighted (T2WI) MRI of the brain, respectively, show confluent white matter hyperintense signal abnormalities (blue arrows) involving the U fibers (yellow arrow) in an immunocompromised patient. Findings are compatible with Progressive Multifocal Leukoencephalopathy (PML).

CASE#2
A: Axial DWI MRI of the brain shows a hyperintense signal area in the left precentral gyrus (red arrow).
B: Axial contrast-enhanced MRI of the brain shows enhancing foci in the frontal region (green arrow). Findings are consistent with Progressive Multifocal Leukoencephalopathy (PML).

CASE#3
A: Axial FLAIR MRI of the brain shows hyperintensity involving the pons and cerebral peduncle (blue arrow).
B: Axial T2-weighted (T2WI) MRI of the brain shows involvement of the cerebellum (red arrow) with sparing of the dentate nuclei (Shrimp Sign). Known case of Progressive Multifocal Leukoencephalopathy (PML)

639

The Cerebral Blood Volume Index in the Era of Large and Medium Vessel Ischemic Stroke Thrombectomy

Manisha Koneru[1], Dhairya Lakhani[2], Hamza Salim[3], Aneri Balar[3], Adam A Dmytriw[4], Adrien Guenego[5], Benjamin Pulli[6], Dylan Wolman[7], Jeremy Heit[6], Gregory Albers[6], Tobias Faizy[8], Kambiz Nael[9], Max Wintermark[10], Vivek Yedavalli[3]
[1]Cooper University Health Care, Camden, NJ, USA. [2]West Virginia University, Morgantown, WV, USA. [3]Johns Hopkins, Baltimore, MD, USA. [4]Mass Gen Brigham, Boston, MA, USA. [5]Centre Hospitalier Universitaire de Toulouse, Toulouse, Toulouse, France. [6]Stanford, Stanford, CA, USA. [7]Brown University, Providence, RI, USA. [8]Munster Hospital, Munster, Munster, Germany. [9]UCSF, San Francisco, CA, USA. [10]UT Houston, Houston, TX, USA

Abstract Category

Interventional/Vascular/Stroke

Summary & Objectives

The cerebral blood volume index (CBV index) is a perfusion-based marker of collateral status. Several real-world data analyses from observational ischemic stroke cohorts have established relationships between this parameter and a range of favorable and unfavorable stroke outcomes. With the rise of thrombectomy for treating large and medium vessel occlusions, the CBV index may be an informative measure for prognosticating post-treatment outcomes.

Purpose

The objective is to provide an overview of the CBV index, within the context of thrombectomy-treated large vessel and medium vessel occlusion ischemic strokes.

Materials & Methods

In thrombectomy-treated strokes, the CBV index is associated with a variety of efficacy, safety, and clinical outcome measures during the intraprocedural and post-treatment recovery time frames. Higher CBV index values indicate more favorable collateral status. In large vessel occlusion strokes, CBV index thresholds ranging from 0.7 and 0.9 are correlated with slow progressors of core infarct volumes, more favorable 90-day functional recovery, excellent reperfusion with thrombectomy, and stroke etiology. In medium vessel occlusion strokes, the CBV index cutoff of 0.7 discriminates between likelihood of hemorrhagic transformation, 90-day functional recovery, and post-treatment mortality.

Results & Conclusion

In summary, the CBV index is a quantitative perfusion imaging marker capturing collateral status, and it is associated with a variety of procedural, safety, and clinical outcomes in thrombectomy-treated large vessel occlusion and medium vessel occlusions. Thus, this measurement may have utility in prognosticating post-interventional response and anticipating the clinical course and care needs of stroke patients.

References

1. Koneru M, Hoseinyazdi M, Wang R, et al. Pretreatment parameters associated with hemorrhagic transformation among successfully recanalized medium vessel occlusions. J Neurol 2024;271:1901–9.
2. Yedavalli V, Koneru M, Hoseinyazdi M, et al. Robust Collaterals Are Independently Associated With Excellent Recanalization in Patients With Large Vessel Occlusion Causing Acute Ischemic Stroke. *Stroke: Vascular and Interventional Neurology* 2024;4:e001141.
3. Yedavalli VS, Koneru M, Hoseinyazdi M, et al. Low Cerebral Blood Volume Index, Thrombectomy, and Prior Stroke Are Independently Associated With Hemorrhagic Transformation in Medium-Vessel Occlusion Ischemic Stroke. *Stroke: Vascular and Interventional Neurology* 2024;4:e001250.

647

Cavitating Mitochondrial Leukoencephalopathies and their Mimics

Bejoy Thomas MD, DNB, PDCC, Smily Sharma MD, DNB, FRCR, Soumya Sundaram MD, DM, Kesavadas Chandrasekharan MD
Sree Chitra Tirunal Institute for Medical Sciences and Technology, Thiruvananthapuram, Kerala, India

Abstract Category

Pediatrics

Summary & Objectives
Nuclear mitochondrial DNA disorders, though rare, can present as cavitating leukoencephalopathies detected on MR Imaging. Cystic or cavitary changes in the involved white matter, areas of restricted diffusion, involvement of middle blade of corpus callosum, and lactate peak on MR spectroscopy are the common features.
Purpose
The purpose of this educational exhibit is to provide a systematic approach to diagnosing cavitating mitochondrial leukoencephalopathies on MR and differentiating them from other genetic and acquired causes of cavitating leukoencephalopathies.
Materials & Methods
Electronic medical records of our institute were searched using the key words “mitochondrial”, “cavitating leukodystrophy” and “cavitating leukoencephalopathy”. Genetically proven cases of mitochondrial disorders and other leukoencephalopathies showing features of cavitation on MR were included in the review. The MRI scans were performed on 3T or 1.5 T MR scanner. The sequences used for analysis included T2 weighted, T1 weighted, FLAIR, DWI, SWI, and/or MR Spectroscopy, contrast enhanced T1W of brain and T2and contrast T1 weighted images of spine whenever available. MRI scans were reviewed for features like T1 and T2 signal changes, cavitation, restricted diffusion, calcifications on SWI, contrast enhancement, and spinal cord involvement.
Results & Conclusion
Using illustrative cases, detailed imaging features of a multitude of genetically proven mitochondrial cavitating leukoencephalopathies will be discussed including Mitochondrial complex I, complex III (LYRM7 gene variant, IBA57 gene variant), and Multiple Mitochondrial dysfunction Syndrome-5 (ISCA1 gene variant). Notably, the nuclear mitochondrial disorders are associated with white matter cavitation. The common features seen in cavitating mitochondrial leukoencephalopathies include cystic or cavitary changes in the involved white matter, areas of restricted diffusion, involvement of middle blade of corpus callosum, and lactate peak on MR spectroscopy (non- specific). Spinal cord involvement in the form of atrophy or hyperintensities on T2W sequence can be seen in many cases. The mimics of mitochondrial cavitating leukoencephalopathies will also be presented included vanishing white matter disorders showing diffuse white matter liquefaction; megalencephalic leukoencephalopathy with subcortical cysts showing macrocephaly, white matter hyperintensities, and subcortical cysts primarily in the temporal poles; Labrune syndrome showing white matter hyperintensities with cysts and calcifications; and acquired causes like cystic Tumefactive demyelinating lesions.
To conclude, cavitating mitochondrial leukoencephalopathies are a heterogeneous group of disorders characterized by white matter cavitation and/ or cystic changes. Nuclear mitochondrial DNA disorders are more commonly associated with cavitating leukoencephalopathies. MRI plays a pivotal role in in suggesting the diagnosis. The presented review serves as a visual guide for systematic approach to cavitating mitochondrial leukoencephalopathies on MR and differentiating them from the other common mimics.
References
1. Senthilvelan S, Sekar SS, Kesavadas C, Thomas B. Neuromitochondrial Disorders : Genomic Basis and an Algorithmic Approach to Imaging Diagnostics. *Clin Neuroradiol.* 2021; 31(3):559-574. doi: 10.1007/s00062-021-01030-4.

Images/Tables

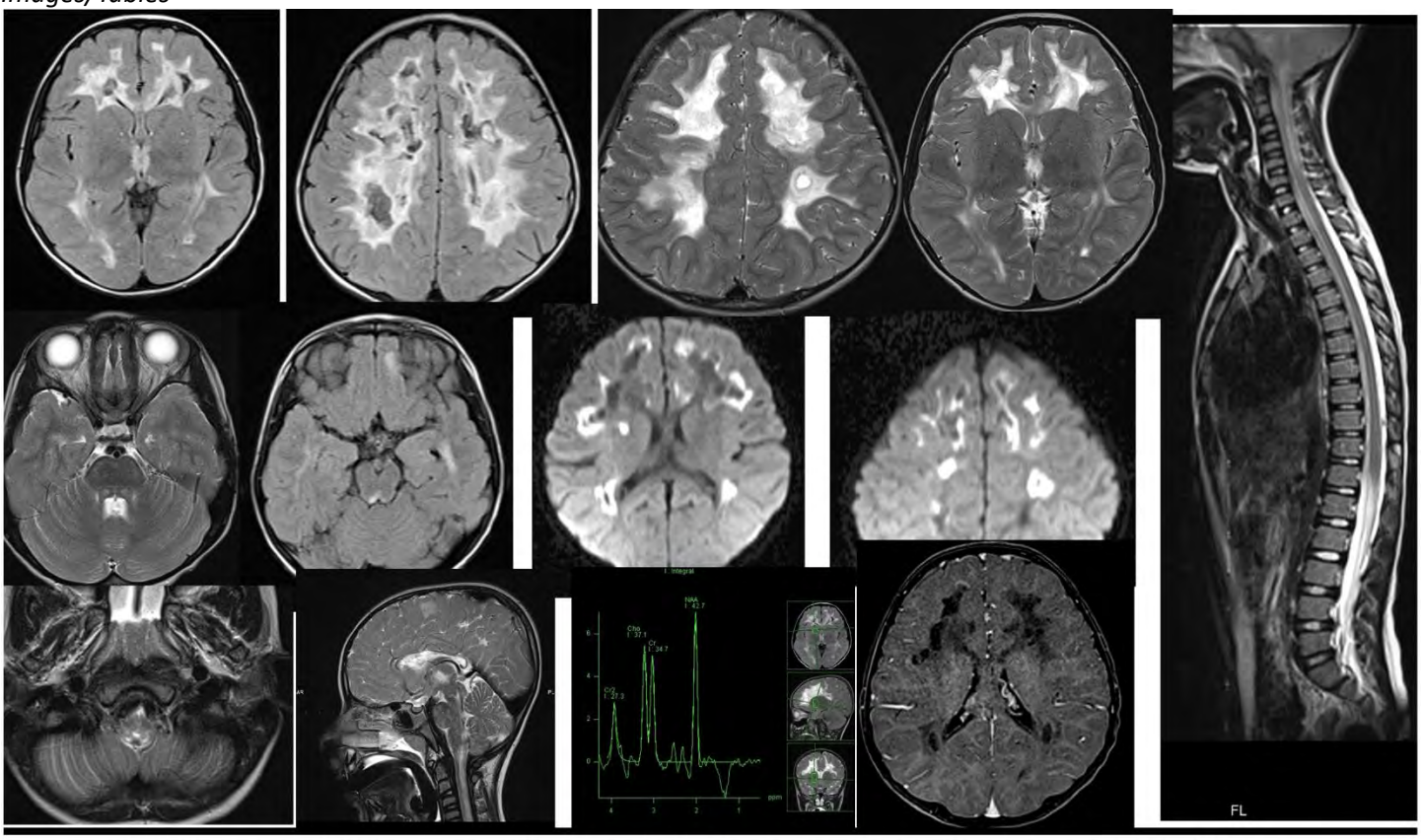


Fig 1: Complex 1 deficiency presenting as cavitating Leukoencephalopathy after a minor viral illness

650

Low-Grade, Epilepsy-Associated Brain Tumors (LEAT): What do neurosurgeons need from neuroradiologist. (Genetics, Neuropathology, and Imaging Insights)

Sangam Kanekar[1], Scott Hwang[2], Jonathan Maffie MD[1]
[1]Penn State Health, Hershey, PA, USA. [2]Hershey, pa, USA

Abstract Category

Pediatrics

Summary & Objectives

Low-grade, epilepsy-associated brain tumors (LEATs) represent a unique subset of brain neoplasms commonly implicated in drug-resistant epilepsy. LEATs are typically slow-growing and include a range of tumor types such as gangliogliomas, dysembryoplastic neuroepithelial tumors (DNETs), pleomorphic xanthoastrocytomas (PXAs), and low-grade gliomas, angiocentric glioma, and papillary glioneuronal tumor (PGNT).

Purpose

1. To discuss the current insights into the genetics, neuropathology, and imaging characteristics of LEATs, shedding light on their clinical relevance and implications for patient management.

Materials & Methods

We conducted a retrospective study of 53 patients identified from our Picture Archiving and Communication System (PACS), all of whom had pathology-proven low-grade, epilepsy-associated brain tumors (LEATs) with imaging findings consistent with these diagnoses. Each patient underwent routine brain MRI using a dedicated epilepsy protocol, including 3D volumetric mapping. Surgical resection was performed on 41 patients, allowing for histologic and genetic confirmation of the tumor diagnosis. Imaging findings were systematically correlated with clinical presentations, histopathological characteristics, and genetic markers.

Results & Conclusion

Neuropathologically, LEATs are distinguished by unique cellular compositions and architectural features, which often contribute to their epileptogenicity. Genetic analyses revealed a spectrum of molecular abnormalities associated with

distinct LEAT subtypes. Gangliogliomas, for instance, comprise dysplastic neurons intermixed with neoplastic glial cells, frequently carrying the BRAF V600E mutation—a genetic alteration associated with increased epileptogenic potential. In contrast, dysembryoplastic neuroepithelial tumors (DNETs) display a columnar architecture with oligodendroglia-like cells in a mucinous matrix. DNETs generally lack BRAF mutations but, in a subset of cases, demonstrate structural rearrangements in the FGFR1 gene. Pleomorphic xanthoastrocytomas (PXAs) are characterized by pleomorphic cellularity and perivascular lymphocytic infiltration and exhibit BRAF mutations alongside CDKN2A deletions.
Imaging, primarily MRI, serves as a crucial tool in diagnosing and planning the surgical management of LEATs. Imaging appearance of LEATs will be discussed in this exhibit. Surgical resection remains the primary treatment, often achieving seizure control, with histopathological examination confirming tumor type and guiding additional therapeutic decisions.
In conclusion, LEATs represent a clinically significant group of brain tumors with distinct genetic, neuropathological, and imaging profiles. Advances in genetics are enhancing our understanding of the molecular mechanisms underlying these tumors, while innovations in imaging continue to refine diagnostic and surgical approaches. Tailoring treatment based on imaging, genetic and pathological insights hold promise for improving outcomes in patients with LEAT-related epilepsy, ultimately aiming to achieve seizure freedom and enhance quality of life.

References

1. Stone, T. J., Rowell, R., Jayasekera, B. A. P., Cunningham, M. O., and Jacques, T. S. (2018b). Review: Molecular characteristics of long-term epilepsyassociated tumours (LEATs) and mechanisms for tumour-related epilepsy (TRE). Neuropathol. Appl. Neurobiol. 44, 56–69.
2. Vogt, V. L., Witt, J. A., Delev, D., Grote, A., von Lehe, M., Becker, A. J., et al. (2018). Cognitive features and surgical outcome of patients with long-term epilepsy-associated tumors (LEATs) within the temporal lobe. Epilepsy Behav. 88, 25–32.
3. Qaddoumi, I., Orisme, W., Wen, J., Santiago, T., Gupta, K., Dalton, J. D., et al. (2016). Genetic alterations in uncommon low-grade neuroepithelial tumors: BRAF, FGFR1, and MYB mutations occur at high frequency and align with morphology. Acta Neuropathol. 131, 833–845

657

Fluid Dynamics in Neurological and Neurodegenerative Disorders: Mechanisms, Imaging and Clinical Implications

Sangam Kanekar[1], Scott Hwang[1], Prasanna Karunanayaka PhD[2]
[1]Hershey, PA, USA. [2]Penn State Health, Hershey, PA, USA

Abstract Category

Adult Brain Inflammatory/Infectious Disease/Degenerative/Metabolic

Summary & Objectives

Fluid dynamics within the brain—encompassing cerebrospinal fluid (CSF) flow, blood circulation, and interstitial fluid exchange—are vital for sustaining neural health and cognitive function. Altered fluid dynamics within the brain and surrounding CSF compartments have emerged as critical factors in the pathogenesis and progression of various neurological disorders, including dementia.
Cerebral fluid dynamics require a delicate balance of blood flow, interstitial fluid movement, and CSF circulation. This balance is essential for maintaining metabolic homeostasis, efficient waste clearance, and normal neuronal function. Disruptions in these systems are increasingly recognized as key contributors to the onset and progression of neurological disorders and dementia, including Alzheimer's disease (AD), Parkinson's disease (PD), vascular dementia, and normal-pressure hydrocephalus (NPH). Impaired CSF clearance, diminished glymphatic function, and reduced cerebral blood flow can lead to neurotoxic accumulation, neuroinflammation, and oxidative stress, ultimately driving neurodegeneration and cognitive impairment.

Purpose

1. To explore the insights into the role of fluid dynamics in AD, PD, NPH and vascular dementia.
2. To discuss the role of fluid dynamics imaging in the common neurological and neurodegenerative disorders.

Materials & Methods

Advanced imaging techniques, such as phase-contrast MRI, arterial spin labeling, diffusion tensor imaging, and CSF flow studies, offer unprecedented insights into cerebral fluid dynamics. These technologies enable precise measurements of CSF circulation, brain perfusion, and glymphatic function, aiding in the diagnosis and staging of dementia and other

neurological conditions. In Alzheimer's disease, reduced CSF clearance through the glymphatic system is linked to amyloid-beta and tau buildup, hallmark proteins of the disease. The glymphatic system, which relies on astroglial water channels for CSF flow and waste removal, declines with age, contributing to protein aggregation and neurodegeneration. Vascular dementia, associated with cerebral hypoperfusion and endothelial dysfunction, impairs blood flow and interstitial fluid exchange, worsening ischemic injury and neuroinflammation. Similarly, Parkinson's disease shows disrupted CSF and interstitial fluid dynamics, likely contributing to alpha-synuclein aggregation and neurodegeneration.

Reduced glymphatic function has also been observed in type 2 diabetes, subarachnoid hemorrhage, ischemic stroke, traumatic brain injury (TBI), and demyelination. Dysfunctional perivascular flow may further impair interstitial fluid drainage, hinder metabolite clearance (such as β-amyloid and other proteins), and is implicated in conditions like cerebral amyloid angiopathy, and small vessel diseases. These disorders, sometimes described as protein-elimination-failure angiopathies, underscore the importance of evaluating fluid dynamics and glymphatic function.

Results & Conclusion

This scientific exhibit explores the integration of advanced imaging techniques in the evaluation of the fluid dynamics in AD, PD, NPH, TBI, MS and vascular dementia. Imaging offers valuable insight into the mechanisms driving neurological and neurodegenerative disorders and dementia. By identifying fluid-related biomarkers and refining diagnostic criteria, imaging not only aids early diagnosis but also opens avenues for targeted interventions, potentially delaying or mitigating cognitive decline in affected populations.

References

1. Albayram, M.S., et al., 2022. Non-invasive MR imaging of human brain lymphatic networks with connections to cervical lymph nodes. Nat. Commun. 13 (1), 203.
2. Agarwal N, Contarino C, Toro EF. Neurofluids: A holistic approach to their physiology, interactive dynamics and clinical implications for neurological diseases. Veins Lymphat 2019;8:49-58.
3. Perosa V, Oltmer J, Munting LP, et al. Perivascular space dilation is associated with vascular amyloid-β accumulation in the overlying cortex. Acta Neuropathol 2022;143:331-348.
4. Lohela TJ, Lilius TO, Nedergaard M. The glymphatic system: Implications for drugs for central nervous system diseases. Nat Rev Drug Discov 2022;21:763-779.

660

MRI-Visible Anatomy of the Brainstem through Mitochondrial and Metabolic Diseases

Sedat Kandemirli MD[1], Bulent Aslan MD[2], Khalid Al-Dasuqi MD[3], Cesar Alves[4]

[1]Duke University, Durham, NC, USA. [2]Beth Israel Deaconess Medical Center, Boston, MA, USA. [3]Sidra Medical Center, Doha, NA, Qatar. [4]Boston Children's Hospital, Boston, MA, USA

Abstract Category

Pediatrics

Summary & Objectives

Primary mitochondrial disorders (PMD) and neurometabolic diseases are a diverse and complex group of genetic conditions, some of which have a propensity for brainstem abnormalities on imaging. Accurate assessment and description of the brainstem involvement is important for differential diagnosis as certain disorders have a more characteristic involvement however, apparent overlap of imaging patterns limits such an approach. A major limitation is relatively vague description of the brainstem involvement of PMD/neurometabolic diseases in the literature, which have started to change in recent years with expert panel curations.

Purpose

The aim of this exhibit is to familiarize neuroradiologists with brainstem anatomy through selected mitochondrial and metabolic diseases for a more precise description of the involvement patterns.

Materials & Methods

Some of the selected cases will include:

Leigh syndrome: Substantia nigra, periaqueductal gray matter, oculomotor nuclei, central tegmental tracts and inferior olivary nuclei. Onset sparing basal ganglia and inferior olivary nuclei involvement: *SURF1*, no inferior olivary nuclei involvement: *MT-ND5*

LBSL: Trigeminal mesencephalic tract, medial lemniscus pyramidal tracts. Involvement of the inferior and superior cerebellar peduncles with relative sparing of middle cerebellar peduncle.

Complex I assembly factor deficiencies like NDUFAF6

Complex IV assembly factor deficiencies like SURF1

X-ALD: To illustrate lateral lemniscus and brachium of inferior colliculus as part of the Loes scoring

Results & Conclusion

This exhibit will overview brainstem anatomy through mitochondrial and neurometabolic diseases.

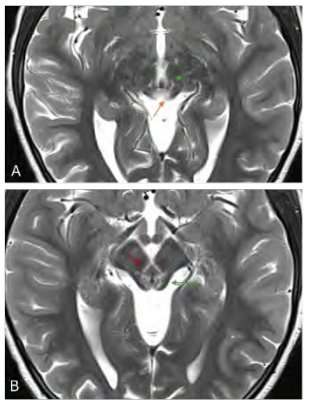
References

Alves C, Whitehead MT (2024) Advancing the neuroimaging diagnosis and understanding of mitochondrial disorders. Neurotherapeutics 21:e00324.

Gonçalves FG, Alves C, Heuer B, Peterson J, Viaene AN, Reis Teixeira S, Martín-Saavedra JS, Andronikou S, Goldstein A, Vossough A (2020) Primary Mitochondrial Disorders of the Pediatric Central Nervous System: Neuroimaging Findings. Radiographics 40:2042-2067.

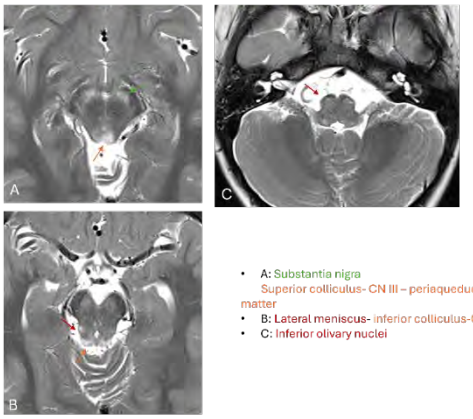
Images/Tables

NDUFAF6 (Complex I assembly factor)



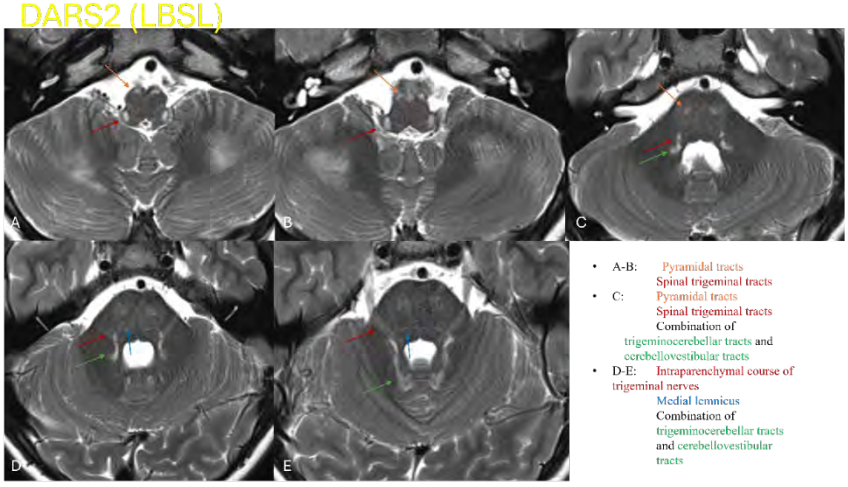
- A: Bilateral superior colliculi
  Trigeminothalmic/spinothalamic tracts- periaqueductal gray matter
- B: Bilateral superior cerebellar peduncle decussation
  CN IV nucleus – periaqueductal gray matter
- C: Laterodorsal tegmental nucleus- MLF-raphe nuclei
- D: ambiguous nuclei
- E: inferior olivary nuclei

SURF1 (Complex I assembly factor)



- A: Substantia nigra
  Superior colliculus- CN III – periaqueductal gray matter
- B: Lateral meniscus- inferior colliculus-CN IV
- C: Inferior olivary nuclei

DARS2 (LBSL)



- A-B: Pyramidal tracts
  Spinal trigeminal tracts
- C: Pyramidal tracts
  Spinal trigeminal tracts
  Combination of trigeminocerebellar tracts and cerebellovestibular tracts
- D-E: Intraparenchymal course of trigeminal nerves
  Medial lemnicus
  Combination of trigeminocerebellar tracts and cerebellovestibular tracts

663

Photon-Counting CT for Aneurysm and Vessel Analysis After Embolization and Stenting.

John Crow MD[1], Marwa Abdelrasoul MD[2], Eric Bass DO[2], Maria Vittoria Spampinato MD[2], Adrienn Toth[2], Maria Gisele Matheus MD[2]
[1]MUSC, Charleston, SC, USA. [2]Charleston, SC, USA

Abstract Category

Interventional/Vascular/Stroke

Summary & Objectives

Evaluation of aneurysms and adjacent vessels post-treatment with embolization or stenting is challenging on conventional CT due to significant beam-hardening artifacts, which obscure the aneurysm and surrounding structures. Photon-Counting CT (PCCT) offers a promising alternative. Unlike traditional CT, which converts X-rays to light and then to electrical signals, PCCT directly converts incident X-ray photons into electrical signals. This direct conversion enables individual measurements of incident photons, including their number and energy, leading to improved resolution and reduced artifacts while potentially decreasing radiation dose. This technology may ultimately provide higher-quality imaging to enhance our ability to evaluate treated vessels and aneurysms.

Purpose

To demonstrate the added value in using PCCT provides in assessing vasculature in cases where traditional CT is severely limited.

Materials & Methods

Explanatory cases from our institution, along with a review of current literature, will illustrate the ability of PCCT to reduce artifacts and improve visualization and assessment of vasculature following aneurysm treatment.

Results & Conclusion

Vessel assessment following embolization treatment remains difficult with traditional CT due to artifacts. Photon-Counting CT significantly enhances visualization and evaluation of post-embolization aneurysms and surrounding vasculature. The improved resolution and artifact reduction may decrease the need for invasive angiography by allowing non-invasive assessment of potential leaks or residual aneurysmal filling. This underscores the potential of PCCT to enhance imaging not only for aneurysms but for other cases where artifact presents a diagnostic challenge.

References

1.Adrienn Tóth, Chetta JA, Yazdani M, et al. Neurovascular Imaging with Ultra-High-Resolution Photon-Counting CT: Preliminary Findings on Image-Quality Evaluation. *American Journal of Neuroradiology*. Published online May 17, 2024. doi:https://doi.org/10.3174/ajnr.a8350
2.Madhavan AA, Girish Bathla, Benson JC, Diehn FE, Nagelschneider AA, Lehman VT. High Yield Clinical Applications for Photon Counting CT in Neurovascular Imaging. *British Journal of Radiology*. 2024;97(1157):894-901. doi:https://doi.org/10.1093/bjr/tqae058

664

Metabolite Clearance: Dementia's Chicken or the Egg?

Kelly Capel MD[1], Anthony Peret MD[1], Leonardo Rivera-Rivera PhD[1], Warren Chang MD[2], Kevin Johnson[1], Laura Eisenmenger MD[1]
[1]University of Wisconsin, Madison, WI, USA. [2]Alleghany Health Network, Pittsburgh, PA, USA

Abstract Category

Adult Brain Inflammatory/Infectious Disease/Degenerative/Metabolic

Summary & Objectives

Present the theorized mechanisms of metabolite clearance and how this could be impacting the development and progression of dementia.
Present the studies supporting these mechanisms and theories.
Present the imaging methods that might be used to study these systems in vivo.

Purpose

The central nervous system is unique in lacking a traditional lymphatic system. Thereby it must use alternative pathways for the clearance of metabolite waste products. Dysfunction in the metabolite clearance is closely related to neurodegenerative diseases, although the exact mechanisms are still unknown. The purpose of this exhibit is to present

the theorized mechanisms of metabolite clearance, studies supporting these mechanisms, and imaging methods that might be used to study these systems in vivo.

Materials & Methods

We will present the theories and studies supporting the existence of two main drainage routes: the glymphatic system and the intra-mural periarterial (IPAD) pathway. They both follow the vascular channels and are sometimes regrouped under the term "paravascular clearance." We will also present innovative MRI sequences that can be used to directly study the potential vascular mechanisms that may be involved including 4D flow MRI, Blood Oxygenation Level Dependent (BOLD), Arterial Spin Labelling (ASL), Displacement Encoding with Stimulated Echoes (DENSE), and Diffusion Tensor Imaging (DTI).

Results & Conclusion

The glymphatic system represents a brain-wide network involving the circulation of cerebrospinal fluid (CSF) in the perivascular space, depending on astroglial aquaporin-4 (AQP4) water transport, whereas the IPAD pathway refers to a drainage route occurring along the basement membrane in the cerebral blood vessels' walls. The driving force responsible for the paravascular clearance pathway remains unidentified. The cardiac cycle-related blood flow is considered by some a major driving force of paravascular clearance; however, recent data claim arterial pulsations are too weak to drive clearance of waste products. Another important mechanism is vasomotion, a low-frequency oscillation in vasodilation of arterioles, relatively independent of the cardiac cycle and likely regulated by vascular smooth muscle cells. Advanced magnetic resonance imaging (MRI) techniques are of paramount interest in assessing metabolite clearance. As this area of research progresses, it will be essential for the neuroradiologist to understand the concept of brain metabolite clearance and the potential implications.

References

Taoka T, Naganawa S. Glymphatic imaging using MRI. J Magn Reson Imaging. Jan 2020;51(1):11-24. doi:10.1002/jmri.26892

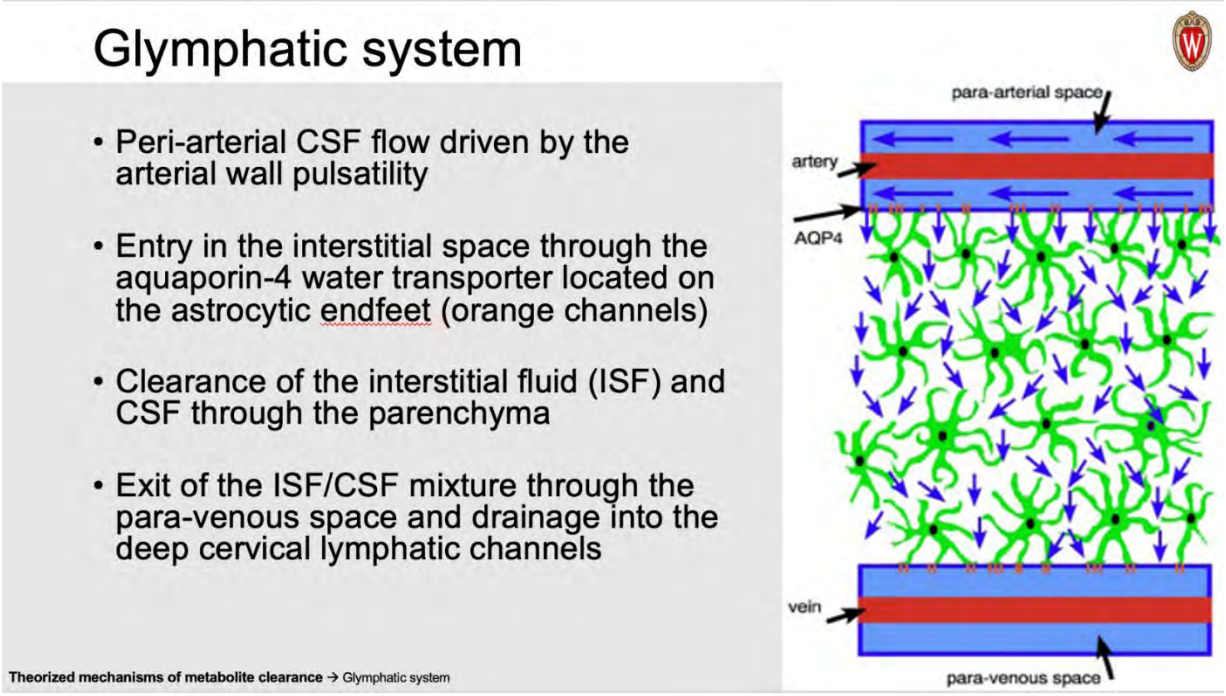
Rivera-Rivera LA, Cody KA, Rutkowski D, et al. Intracranial vascular flow oscillations in Alzheimer's disease from 4D flow MRI. Neuroimage Clin. Aug 12 2020;28:102379. doi:10.1016/j.nicl.2020.102379

Aldea R, Weller RO, Wilcock DM, Carare RO, Richardson G. Cerebrovascular Smooth Muscle Cells as the Drivers of Intramural Periarterial Drainage of the Brain. Front Aging Neurosci. 2019;11:1. doi:10.3389/fnagi.2019.00001

Diem AK, MacGregor Sharp M, Gatherer M, Bressloff NW, Carare RO, Richardson G. Arterial Pulsations cannot Drive Intramural Periarterial Drainage: Significance for Aβ Drainage. Front Neurosci. 2017;11:475. doi:10.3389/fnins.2017.00475

Iliff JJ, Wang M, Liao Y, et al. A paravascular pathway facilitates CSF flow through the brain parenchyma and the clearance of interstitial solutes, including amyloid β. Sci Transl Med. Aug 15 2012;4(147):147ra111. doi:10.1126/scitranslmed.3003748

Images/Tables



665

Don't Forget About the Vessels: Alzheimer's Disease and Neurovascular Dysfunction

Anthony Peret MD[1], Kelly Capel MD[1], Warren Chang MD[2], Jackie Junn MD[3], Leonardo Rivera-Rivera PhD[1], Kevin Johnson PhD[1], Laura Eisenmenger MD[1]

[1]University of Wisconsin, Madison, WI, USA. [2]Alleghany Health Network, Pittsburgh, PA, USA. [3]Emory University, Atlanta, GA, USA

Abstract Category

Adult Brain Inflammatory/Infectious Disease/Degenerative/Metabolic

Summary & Objectives

- Review the relationship of AD to vascular disease
- Present the current standard of care when performing and evaluating MRIs in AD
- Discuss advanced vascular MRI/MRA sequences and research supporting more direct imaging of vascular dysfunction

Purpose

Alzheimer's disease (AD), a chronic neurodegenerative disorder characterized by insoluble beta-amyloid deposition in extracellular senile plaques and abnormal accumulation of hyperphosphorylated tau proteins in neurofibrillary tangles, is the leading cause of dementia. In the last two decades, numerous sources supported the hypothesis that AD and neurovascular dysfunction are intricately related. This exhibit will highlight the relevant studies highlighting this relationship, the imaging techniques commonly employed and innovative AD imaging approaches, as well as the future directions for this area of research.

Materials & Methods

We will present the relationship of AD to systemic vascular disease, cerebrovascular disease, and specific cerebrovascular disease metrics, focusing on current clinically available MRI sequences as well as highlight more advanced MRI sequences currently under investigation.

Results & Conclusion

The so-called "vascular hypothesis" suggests that several neurovascular anomalies play a role in the development and progression of AD, contributing to neuronal loss and cognitive impairment. Indirect signs of vascular pathology are the most commonly described both clinically and in research such as white matter hyperintensities, microhemorrhages, and decreased cerebral blood flow (CBF); however, direct measures of vascular disease such as increased blood flow pulsatility, decreased vessel wall compliance, and increased blood brain barrier permeability may be more sensitive markers of vascular disease. In preclinical AD, vascular biomarkers occur before cognitive impairment and before detectable increases in standard AD biomarkers. Advanced magnetic resonance imaging (MRI) techniques like dynamic contrast-enhanced MRI (DCE-MRI), 4D-flow MRI, functional MRI (fMRI), and arterial spin labeling (ASL) MRI can provide a more comprehensive analysis of hemodynamic variables. The use of these imaging techniques to evaluate vascular biomarkers could provide a non-invasive tool in managing patients at risk of AD, allowing early detection of the disease and stratification of selected patients according to risk for dementia.

References

Sweeney MD, Kisler K, Montagne A, Toga AW, Zlokovic BV. The role of brain vasculature in neurodegenerative disorders. *Nat Neurosci*. Oct 2018;21(10):1318-1331. doi:10.1038/s41593-018-0234-x

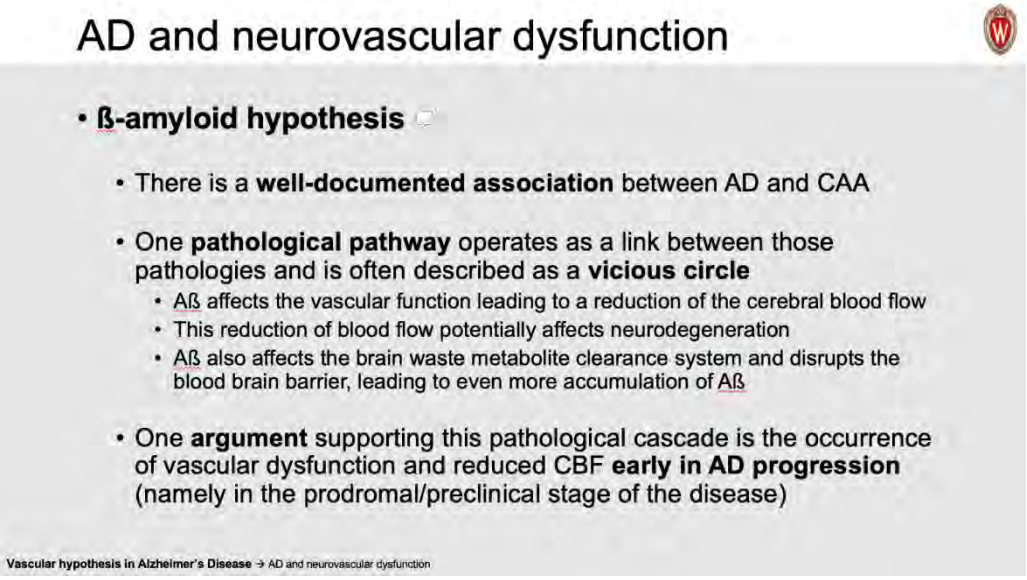
Rivera-Rivera LA, Turski P, Johnson KM, et al. 4D flow MRI for intracranial hemodynamics assessment in Alzheimer's disease. *Journal of Cerebral Blood Flow and Metabolism: Official Journal of the International Society of Cerebral Blood Flow and Metabolism*. 2016//10/ 2016;36(10):1718-1730. doi:10.1177/0271678X15617171

Govindpani K, McNamara LG, Smith NR, et al. Vascular Dysfunction in Alzheimer's Disease: A Prelude to the Pathological Process or a Consequence of It? *J Clin Med*. May 10 2019;8(5)doi:10.3390/jcm8050651

Di Marco LY, Farkas E, Martin C, Venneri A, Frangi AF. Is Vasomotion in Cerebral Arteries Impaired in Alzheimer's Disease? *Journal of Alzheimer's disease: JAD*. 2015 2015;46(1):35-53. doi:10.3233/JAD-142976

Berman SE, Rivera-Rivera LA, Clark LR, et al. Intracranial Arterial 4D-Flow is Associated with Metrics of Brain Health and Alzheimer's Disease. *Alzheimers Dement (Amst)*. Dec 1 2015;1(4):420-428. doi:10.1016/j.dadm.2015.09.005

Images/Tables



667

Advancing Pediatric Neuro-Oncology: The Power of PET/MRI

Nazanin Maleki M.D[1], Basimah Albalooshy M.D[1], Raisa Amiruddin M.D[1], Peter Madsen M.D[2], Karuna Shekdar M.D[1], Erin Schwartz M.D[1], Lisa States M.D[1], Mariam Aboian MD, PhD[1]

[1]Department of Radiology, Children's Hospital of Philadelphia, Philadelphia, PA, USA. [2]Department of Neurosurgery, Children's Hospital of Philadelphia, Philadelphia, PA, USA

Abstract Category

Pediatrics

Summary & Objectives

PET/MRI benefits pediatric neuro-oncology by reducing radiation and sedation while aiding diagnosis, staging, and treatment. We present successful PET/MRI cases and explore future applications like amino acid PET for improved outcomes.

Purpose

PET/MRI plays a significant role in Pediatric Oncology, but its implementation in Pediatric Neuro-Oncology has not been well established. PET/MRI addresses a major challenge in pediatrics by providing a capability for serial imaging to track disease response to therapy while minimizing radiation exposure and sedation events. PET/MRI has become a critical imaging modality in the management of pediatric brain neoplasms and metastases, aiding in diagnosis, staging, treatment planning, and follow-up, all while reducing radiation burden, minimizing time spent in the hospital, and reducing the number of sedation events.

Materials & Methods

At Children's Hospital of Philadelphia, we have gained extensive experience in utilizing hybrid PET/MRI to manage complex cases referred from multiple institutions. We present a series of cases where hybrid PET/MRI provided critical information for patient management including nasopharyngeal rhabdomyosarcoma, refractory metastatic germ cell tumor, and neuroblastoma. We offer a forward-looking perspective on the current role of FDG PET/MRI and future applications of amino acid PET in improving patient outcomes and its role in distinguishing tumor progression from post-treatment changes. Amino acid PET/MRI use cases were compiled from the literature review. They demonstrated the definitive roles of amino acid PET/MRI in decision making in brain tumor diagnosis, immediate post-surgical assessment, and delayed treatment response assessment.

Results & Conclusion

18F-FDG PET/MRI representative cases from clinical practice will include:

Case 1: Refractory Metastatic Germ Cell Tumor

Clinical Presentation: 18 year old male with refractory metastatic germ cell tumor with anterior mediastinal mass and intracranial metastasis

Clinical Problem: Whole body evaluation in addition to detailed analysis of brain metastases in time efficient manner.

Imaging Solution: PET/MRI allowed detailed evaluation of hypermetabolic metastatic disease to the mediastinum and lungs and further detailed delineation of hemorrhagic brain metastases. Companion CT of the chest allowed detailed anatomic analysis of pulmonary metastases.

Case2. Nasopharyngeal rhabdomyosarcoma

Clinical Presentation: A 4-year-old boy with a history of nasopharyngeal rhabdomyosarcoma with cerebellar metastasis. The patient underwent proton therapy, chemotherapy, and resection.

Clinical Problem: How to monitor nasopharyngeal mass after treatment in the setting of extensive postsurgical changes on MRI.

Imaging Solution: PET/MRI provides an excellent imaging method for monitoring disease recurrence in the setting of post-treatment changes in the nasopharyngeal location. The recurrent tumor was identified as a hypermetabolic lesion, while MRI was not definitive.

Case 3: Neuroblastoma

Clinical Presentation: A 7-year-old male with high-risk relapsed progressive neuroblastoma was treated with resection, chemotherapy, and proton radiation.

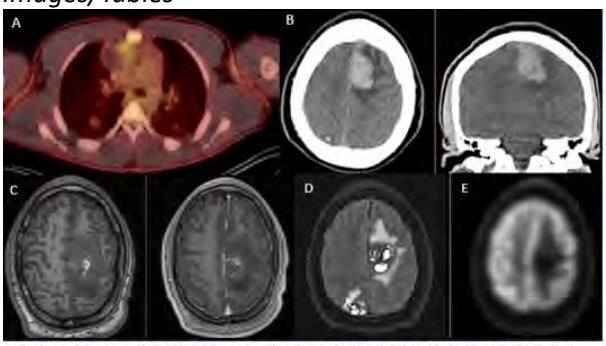
Clinical Problem: How to monitor nasopharyngeal mass within the sphenoid sinus in the setting of extensive postsurgical changes.

Imaging Solution: PET/MRI provides an excellent imaging method for monitoring disease recurrence in the sphenoid sinus, while MRI was not definitive.

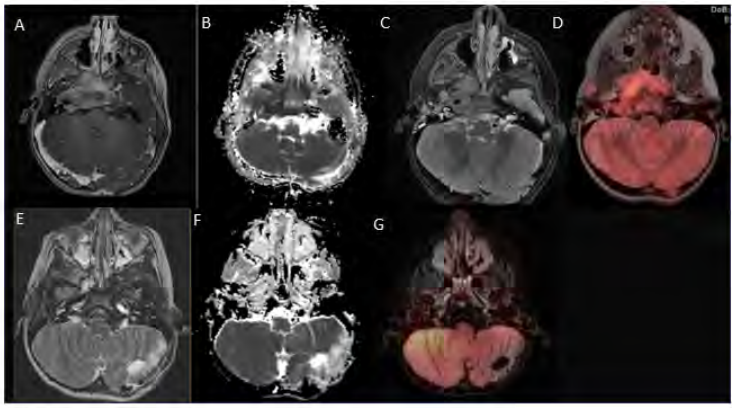
References

Pedersen C, Messina S, Daldrup-Link H, et al. Pediatric PET/MRI neuroimaging: overview. In: Stattaus J, Juergens K, eds. PET/MRI in Oncology: Current Clinical Applications and Future Directions. Springer, Cham; 2021. DOI: 10.1007/978-3-030-82367-2_62.

Images/Tables

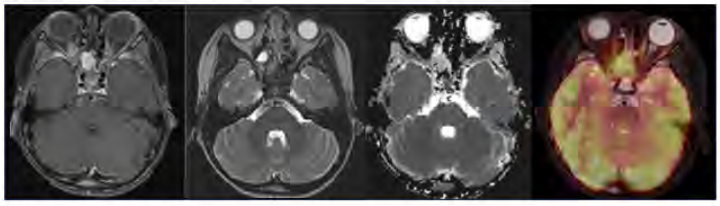


Case1. Image A (PET/CT) demonstrates a hypermetabolic large right anterior mediastinal mass. Image B (CT) axial and coronal CT shows hyperdense hemorrhagic metastasis in the left medial frontal lobe and right parietal lobe. Image C depicts T1 pre and post contrast with peripheral T1 hyperintense hemorrhagic component as well as peripheral enhancement. In image D this shows peripheral T2 hypointensity/hemosiderin and surrounding T2 hyperintense vasogenic edema. Image E demonstrates a photopenic hemorrhagic metastases in (PET/MRI).



Case2.
Pretreatment images:
Image A shows an ill-defined infiltrative mass lesion involving the right nasopharynx, with heterogenous enhancement. Image B demonstrates low ADC signal indicative of hypercellularity. Image C this mass depicts iso to hypointense abnormal T2 signal. Image D (PET/MRI) the mass shoes diffuse increased radiotracer uptake.

Posttreatment images:
Image E shows residual abnormal T2 iso to hypointense infiltrative signal with variable ADC signal in image F. Image G (PET/MRI) depicts no radiotracer uptake in keeping with interval resolution of the tumor.



Case3. Image A post contrast T1 shows an oval enhancing mass lesion in right sphenoid sinus. Image B the mass demonstrates T2 hyperintense signal. Variable ADC signal is seen in image C. Image D PET/MRI shows increased radiotracer uptake confirming metastatic deposit in right sphenoid sinus.

671

Dementia: How Should We Think About It?

Kelly Capel MD[1], Anthony Peret MD[1], Warren Chang MD[2], Jackie Junn MD[3], Robert Cadman PhD[1], Kevin Johnson PhD[1], Laura Eisenmenger MD[1]

[1]University of Wisconsin, Madison, WI, USA. [2]Alleghany Health Network, Pittsburgh, PA, USA. [3]Emory University, Atlanta, GA, USA

Abstract Category

Adult Brain Inflammatory/Infectious Disease/Degenerative/Metabolic

Summary & Objectives

- Review the different types of dementia.
- Familiarize the learner with the available modalities and typical imaging features of dementia.
- To facilitate early and accurate diagnosis.

Purpose

The goal of this presentation is to demonstrate the full range of complementary structural and molecular imaging techniques available to the radiologist in the evaluation of cognitive impairment. Imaging of dementia disorders including Alzheimer's disease, cerebral amyloid angiopathy, frontotemporal dementia, Lewy body dementia, and vascular dementia will be reviewed. Imaging of alternative diagnoses will also be included, such as normal pressure hydrocephalus, Creutzfeldt-Jakob disease, and chronic traumatic encephalopathy.

Materials & Methods

Dementia refers to a group of heterogeneous, debilitating syndromes characterized by memory loss and cognitive dysfunction, usually caused by neurodegenerative disease. The most common cause is Alzheimer's disease, with more than six million people currently affected in the United States. Traditionally, Alzheimer's disease was suspected clinically and confirmed on postmortem analysis, while the role of imaging was limited to excluding alternative diagnoses. However, new neuroimaging techniques are enabling early and accurate diagnosis of neurodegenerative disease. While the prognosis of Alzheimer's disease remains poor, a new targeted therapies have been shown to slow the disease progression, making early diagnosis vitally important. With advanced neuroimaging techniques now able to objectively diagnose neurodegenerative disorders, radiologists should be familiar with the evaluation for dementia and the imaging findings.

Results & Conclusion

An understanding of the structures involved in neurodegenerative diseases combined with the high spatial resolution of modern MRI, has made it possible to suggest several types of dementia based on imaging. For example, regional volume loss involving the entorhinal cortex, the hippocampus, the precuneus, and cingulate gyrus can all support a diagnosis of Alzheimer's disease. In contrast, involvement of the frontotemporal regions suggests FTD, and abnormality of the occipital lobe is typical for Lewy body dementia. Quantification software can aid in assessing brain volumes.

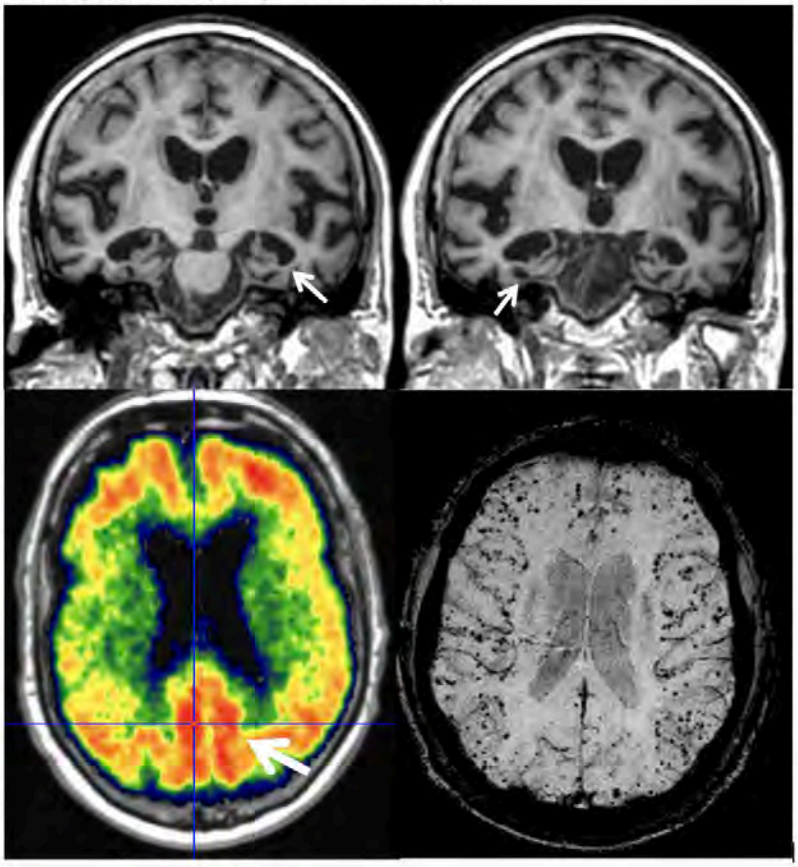
In addition to anatomic findings, molecular imaging can demonstrate functional abnormalities in patients with dementia. FDG PET is the most commonly used radiotracer in dementia imaging, and can identify hypometabolism in key regions, often before structural changes. Newer molecular imaging biomarkers for *B*-amyloid aggregates and tau protein may help differentiate neurodegenerative disorders, identify patients at risk for developing dementia, and monitor treatment of newer drugs that directly target amyloid aggregates. Functional MRI and DTI are other options for functional assessment. Imaging of neurodegenerative disorders has made antemortem diagnosis possible.

References

1. Cummings J, Aisen P, Apostolova LG, Atri A, Salloway S, Weiner M. Aducanumab: Appropriate Use Recommendations. J Prev Alzheimers Dis. 2021;8(4):398-410.
2. Oldan JD, Jewells VL, Pieper B, Wong TZ. Complete Evaluation of Dementia: PET and MRI Correlation and Diagnosis for the Neuroradiologist. AJNR Am J Neuroradiol. 2021 Jun;42(6):998-1007.
3. Patel KP, Wymer DT, Bhatia VK, Duara R, Rajadhyaksha CD. Multimodality Imaging of Dementia: Clinical Importance and Role of Integrated Anatomic and Molecular Imaging. Radiographics. 2020 Jan-Feb;40(1):200-222.
4. Zukotynski K, Kuo PH, Mikulis D, Rosa-Neto P, Strafella AP, Subramaniam RM, Black SE. PET/CT of Dementia. AJR Am J Roentgenol. 2018 Aug;211(2):246-259

Images/Tables

Figure 1 (A-D). Dementia Imaging in Multiple Patients. A and B. 85-year-old female with Alzheimer's disease. Coronal T1-weighted MR image, obliquely oriented through the perpendicular axis of the hippocampus shows marked medial temporal lobe and hippocampal atrophy (arrows). C. Florbetapir F-18 PET/MR in a second patient with Alzheimer's disease shows increased cortical uptake corresponding to abnormal amyloid deposition, particularly in the posterior cingulate gyrus (arrow). D. Cerebral amyloid angiopathy. Susceptibility weighted imaging demonstrates numerous punctate microhemorrhages, particularly along the subarachnoid space.



672

MR Imaging of Peripheral Nerve Sheath Tumors

Mona Dabiri MD, Rodrigo Luna MD, Shivani Ahlawat MD, Laura Fayad MD
Johns Hopkins University, Baltimore, Maryland, USA

Abstract Category

Adult Neoplasms/Epilepsy/Trauma

Summary & Objectives

The combination of conventional MRI and DWI with ADC mapping is an excellent tool for evaluating PNSTs for malignancy, offering a variety of features for distinguishing benign and malignant disease. Similarly, in patients with a predisposition to PNSTs throughout the body, the evaluation of disease burden and potential malignant degeneration can be made with WB-MRI including WB-DWI and ADC mapping. Radiologists should be aware of non-neurogenic malignancies such as lymphoma and metastatic disease that can affect peripheral nerves, and non-neoplastic conditions such as traumatic neuromas and intraneural ganglions.

Clinics care points

- MPNSTs, which exhibit restricted diffusion, are indicated by low ADC values (<1.0–1.1×10^ (-3) mm^2/s) on DWI, a differentiating feature from benign PNSTs [10].
- Other differentiating features of benign PNST and MPNST include that larger size, irregular shape, rapid growth, increased heterogeneity and perilesional edema and enhancement of MPNSTs.
- For patients with NF syndromes, WB-MRI with WB-DWI avoids radiation exposure (particularly useful in children) and is utilized to determine disease burden as well as characterization of detected tumors.

- Patients with NF1 must be closely monitored for MPNSTs, with a 10% lifetime risk of malignant degeneration of benign neurofibromas [3].
- Radiologists should be aware of the appearance of non-neurogenic tumors and non-neoplastic conditions that can mimic PNSTs.

Purpose

- **Evaluating PNSTs for malignancy:** To explore the effectiveness of combining conventional MRI with Diffusion-Weighted Imaging (DWI) and Apparent Diffusion Coefficient (ADC) mapping in differentiating between benign and malignant Peripheral Nerve Sheath Tumors (PNSTs).
- **Assess Disease Burden in Patients with Predisposition**: To discuss the use of Whole-Body MRI (WB-MRI) with Whole-Body Diffusion-Weighted Imaging (WB-DWI) and ADC mapping in assessing disease burden and potential malignant transformation in patients with a predisposition to PNSTs.
- **Identify Non-Neurogenic Malignancies and Non-Neoplastic Conditions**: To highlight the importance for radiologists of recognizing non-neurogenic malignancies, like lymphoma and metastatic disease, and non-neoplastic conditions, such as traumatic neuromas and intraneural ganglions, which can affect peripheral nerves.
- **Differentiate Between Similar Tumor Types**: To address the challenges in differentiating between certain types of tumors, specifically schwannomas from neurofibromas, schwannomas from Malignant Peripheral Nerve Sheath Tumors (MPNSTs), and traumatic neuromas from PNSTs.

Materials & Methods

We have reviewed english language papers for material and methods.

Results & Conclusion

The combination of conventional MRI and DWI with ADC mapping is an excellent tool for evaluating PNSTs for malignancy, offering a variety of features for distinguishing benign and malignant disease. Similarly, in patients with a predisposition to PNSTs throughout the body, the evaluation of disease burden and potential malignant degeneration can be made with WB-MRI including WB-DWI and ADC mapping. Radiologists should be aware of non-neurogenic malignancies such as lymphoma and metastatic disease that can affect peripheral nerves, and non-neoplastic conditions such as traumatic neuromas and intraneural ganglions. Despite a variety of sensitive features that enable the detection of malignancy, it can be challenging to accurately differentiate some tumors, especially schwannomas from neurofibromas, schwannomas from MPNSTs and occasionally, traumatic neuromas from PNSTs.

References

1.Ahlawat, S., Blakeley, J. O., Langmead, S., Belzberg, A. J., & Fayad, L. M. (2020). Current status and recommendations for imaging in neurofibromatosis type 1, neurofibromatosis type 2, and schwannomatosis. Skeletal Radiology, 49, 199-219. https://doi.org/10.1007/s00256-019-03290-1

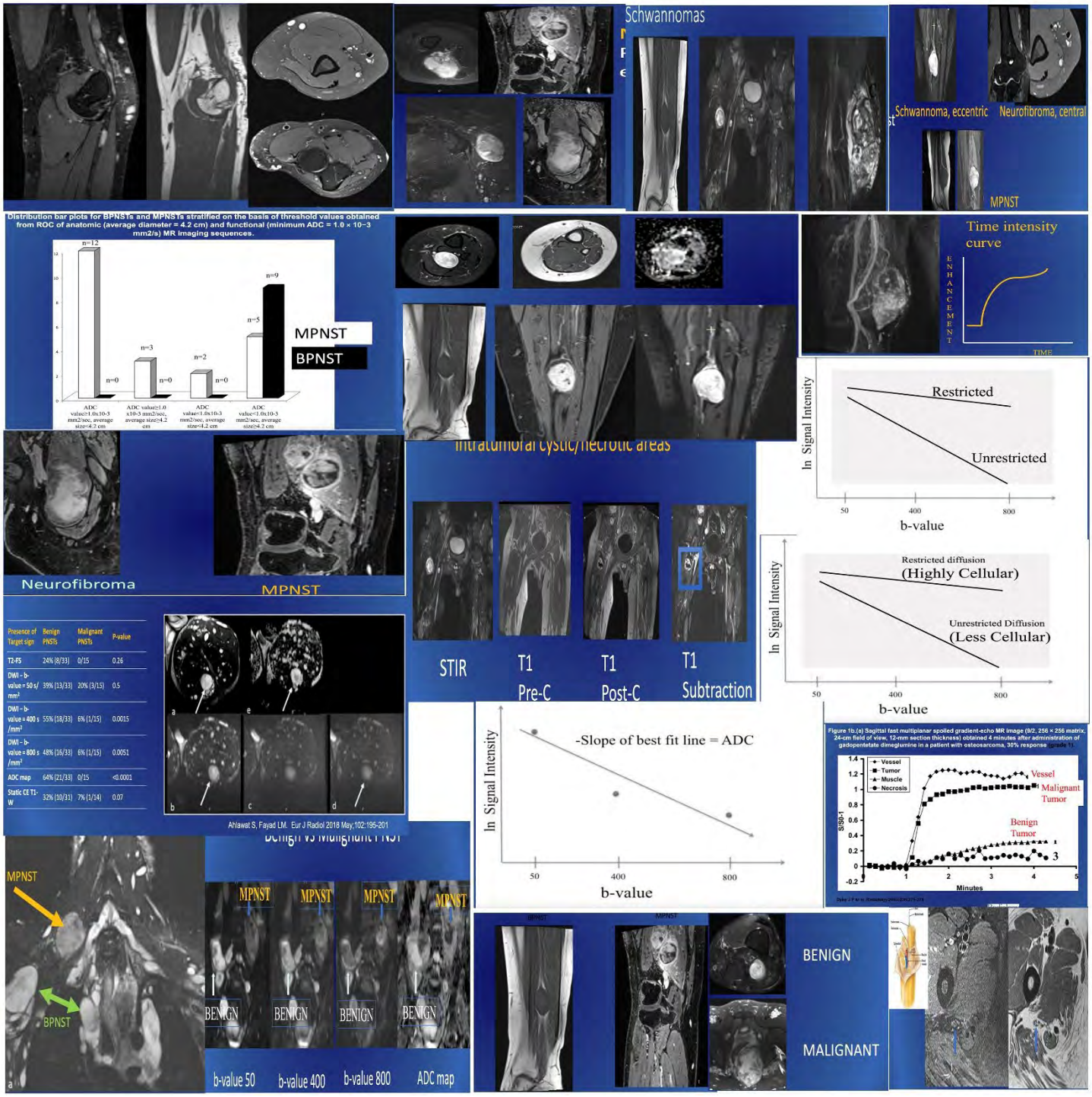
2.Wei C-J, Yan C, Tang Y, Wang W, Gu Y-H, Ren J-Y, Cui X-W, Lian X, Liu J, Wang H-J, Gu B, Zan T, Li Q-F and Wang Z-C (2020) Computed Tomography-Based Differentiation of Benign and Malignant Craniofacial Lesions in Neurofibromatosis Type I Patients: A Machine Learning Approach. Front. Oncol. 10:1192. doi:10.3389/fonc.2020.01192.

3.Yuan, Y., Gao, J., Xiong, G., & Guo, L. (2023). Diagnostic accuracy of multiparametric ultrasound for peripheral nerve schwannoma. Acta Radiologica, 64(4), 1608–1614. DOI: 10.1177/02841851221125109.

4.Choi, Y. J., Lee, I. S., Song, Y. S., Kim, J. I., Choi, K.-U., & Song, J. W. (2019). Diagnostic Performance of Diffusion-Weighted (DWI) and Dynamic Contrast-Enhanced (DCE) MRI for the Differentiation of Benign From Malignant Soft-Tissue Tumors. Journal of Magnetic Resonance Imaging, 50, 798–809. DOI: 10.1002/jmri.26607.

5.Jack, Andrew S., Charlotte J. Huie, and Line G. Jacques. "Epidemiology of Peripheral Nerve Sheath Tumors." Diagnostic Assessment and Treatment of Peripheral Nerve Tumors (2021): 3-16.

Images/Tables



680

Common and Uncommon Patterns of Diffusion Restriction in the Acute Setting: Beyond Acute Ischemic Stroke

Huy Tram N Nguyen MD, Vanessa Peters MD, Irfan Hussain MD, Momin Muzaffar MD
University of Chicago, Chicago, IL, USA

Abstract Category

Adult Brain Inflammatory/Infectious Disease/Degenerative/Metabolic

Summary & Objectives

Diffusion restriction observed on diffusion-weighted imaging (DWI) remains an invaluable marker in neuroradiology, primarily recognized for its high sensitivity in detecting cytotoxic edema in acute ischemic stroke, but also for detection

of pyogenic abscesses and assessment of cellularity in intracranial neoplasms. However, the utility of DWI beyond ischemic stroke is often underappreciated in routine clinical practice. Various neurological conditions, including atypical infections, trauma, toxin exposure, metabolic derangement, and acute demyelinating processes, can also exhibit patterns of restricted diffusion. Recognizing these patterns across diverse pathologies is essential for accurate timely diagnosis, guiding treatment, and improving patient outcomes.

This educational exhibit aims to broaden the understanding and application of diffusion restriction as an imaging marker in conditions beyond acute ischemic infarcts and neoplasia, with a focus on non-ischemic, non-neoplastic, and non-pyogenic neurological pathologies. This exhibit will highlight how diffusion restriction in these conditions can be divided into several recognizable patterns: symmetric or asymmetric cortical involvement (with potential extension into the subcortical white matter); symmetric or asymmetric subcortical white matter involvement; deep gray matter and infratentorial involvement; and isolated deep gray matter involvement. Additionally, the pathophysiological mechanisms underpinning diffusion restriction will be briefly reviewed.

Purpose

The purpose of this exhibit is to showcase the spectrum of neurological diseases that can present with restricted diffusion in the acute clinical setting. A diverse array of traumatic, toxic/metabolic, inflammatory, and demyelinating processes can mimic acute stroke and potentially confound interpretation in a busy emergency radiology service. By contrasting the common and uncommon manifestations of diffusion restriction typically associated with each of these processes, this exhibit will distill the differential diagnosis based on certain signature patterns.

Materials & Methods

This exhibit will illustrate certain recognizable patterns of diffusion restriction in the following entities:

- Traumatic and iatrogenic processes: typical and atypical patterns of diffuse axonal injury and fat emboli
- Toxic or metabolic processes: mitochondrial encephalomyopathy with lactic acidosis and stroke-like episodes (MELAS), Wernicke encephalopathy, osmotic demyelination syndrome, hypoxic ischemic encephalopathy, delayed anoxic leukoencephalopathy, hypoglycemic encephalopathy, drug toxicity (including opioid, methotrexate, and metronidazole), cytotoxic lesions of the corpus callosum (CLOCCs), hyperammonemic encephalopathy, and transient seizure activity
- Encephalitides: Creutzfeldt-Jakob disease (CJD), herpes encephalitis, anti-MOG (myelin oligodendrocyte glycoprotein) encephalitis, limbic encephalitis
- Demyelinating processes: acute disseminated encephalomyelitis (ADEM) and metachromatic leukodystrophy

Results & Conclusion

Acute ischemic stroke is not the only condition to consider in the acutely ill patient presenting with diffusion abnormalities on MRI. For neuroradiologists, recognizing the diverse range of neurological pathologies and their characteristic patterns of diffusion restriction is essential for refining differential diagnoses and achieving accurate diagnostic outcomes.

References

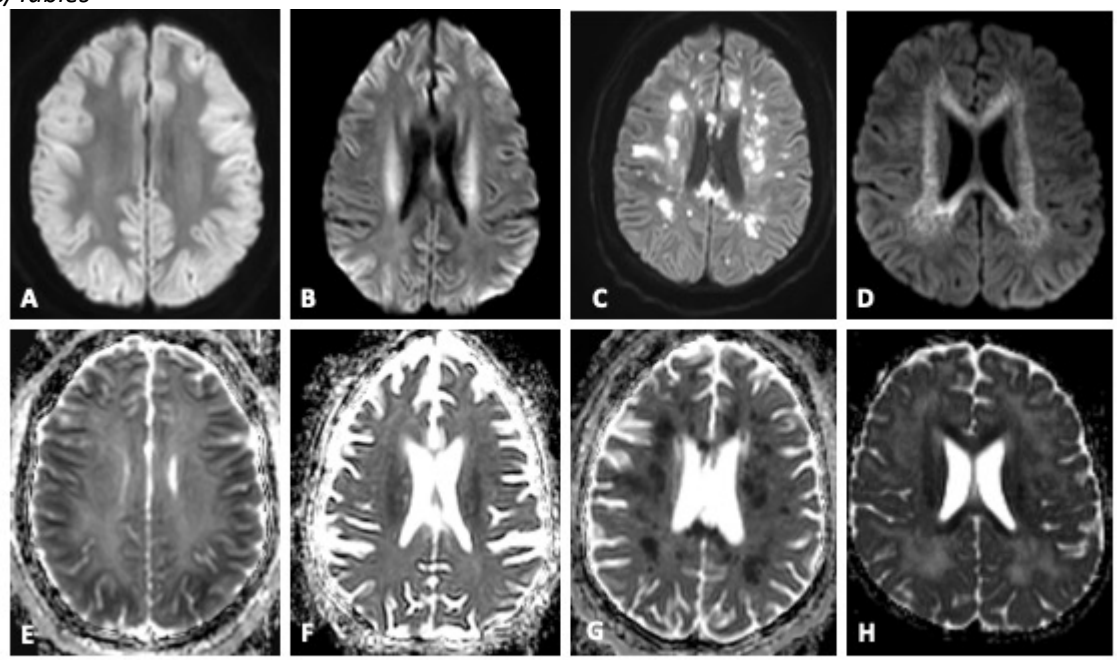
Adam GP, Burns J, Deva DP, et al. Magnetic resonance imaging of arterial stroke mimics: a pictorial review. Insights Imaging 2018;9:815–31. DOI: 10.1007/s13244-018-0637-y.

De Oliveira AM, Paulino MV, Vieira APF, et al. Imaging Patterns of Toxic and Metabolic Brain Disorders. Radiographics. 2019 Oct;39(6):1672-1695. DOI: 10.1148/rg.2019190016.

Gaddamanugu S, Shafaat O, Sotoudeh H, et al. Clinical applications of diffusion-weighted sequence in brain imaging: beyond stroke. Neuroradiol J 2020;33:219–32. DOI: 10.1007/s00234-021-02819-3.

Vilela P. Acute stroke differential diagnosis: Stroke mimics. Eur J Radiol. 2017 Nov;96:133-144. DOI: 10.1016/j.ejrad.2017.05.008.

Images/Tables



DWI and respective ADC maps illustrating:
(A, E) Hypoxic Ischemic Encephalopathy
(B, F) Hypoglycemic Encephalopathy
(C, G) Fat Emboli
(D, H) Metachromatic Leukodystrophy

686

CADASIL: A Model for Vascular Dementia?

Laura Eisenmenger MD[1], Kevin Johnson PhD[1], Jeremy Bockholt PhD[2], Jane Paulsen PhD[1]
[1]University of Wisconsin, Madison, WI, USA. [2]Georgia State University, Atlanta, GA, USA

Abstract Category

Adult Brain Inflammatory/Infectious Disease/Degenerative/Metabolic

Summary & Objectives

- Review the cause of Cerebral Autosomal Dominant Arteriopathy with Subcortical Infarcts and Leukoencephalopathy (CADASIL)
- Discuss the pathophysiology and common imaging findings of CADASIL
- Discuss the impact of CADASIL in patients with this disease as well as how this disease can be studied to further our understanding of vascular dementia

Purpose

CADASIL is caused by a mutation in the gene *Notch3*, which encodes a receptor protein expressed in vascular smooth muscle cells and pericytes. When mutated, expression of the gene leads to generalized degeneration of vascular smooth muscle cells affecting small and medium sized arteries. The purpose of this exhibit is to review the cause, clinical presentations, and imaging evaluation of CADASIL itself as well as how the study of CADASIL can be applied to the broader understanding of vascular dementia.

Materials & Methods

CADASIL is marked by progressive small vessel disease (SVD), white matter hyperintensities (WMH), white matter hypointensities (WMhypo), lacunar infarcts, enlarged perivascular spaces (PVS), cerebral microbleeds, atrophy, and cognitive decline. Clinical dementia is often multi-factorial with concomitant and entangled contributions from proteinopathies (e.g. Alzheimer's disease (AD)), synucleinopathies (e.g. Lewy bodies), and vascular disease. Recent multi-center consortium studies have begun to evaluate participants with a gene mutation for CADASIL to characterize the onset and progression of small vessel disease using CADASIL as a monogenic model of vascular contributions to cognitive impairment and dementia (VCID). Many researchers consider CADASIL a ready monogenetic model for studying VCID from which comparisons can be made to elucidate VCID.

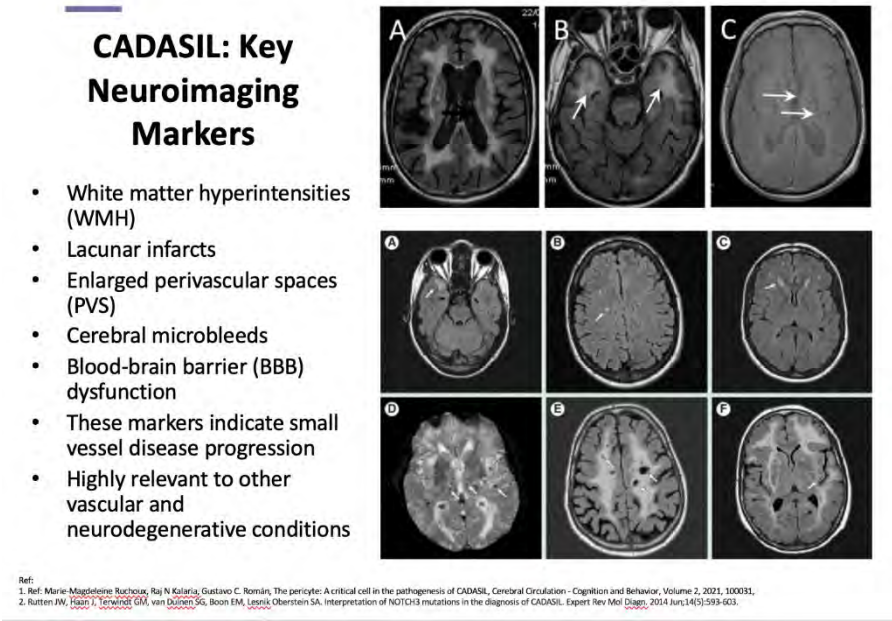
Results & Conclusion

Vascular impairments are the 2nd leading cause of dementia and represent a common contributing factor to mixed and AD. Biomarkers for AD have been developing over the past decade leading to a current classification system based on the presence of biomarkers for amyloid, tau, and neurodegeneration (ATN). However, data suggests that over half of the participants clinically diagnosed with AD dementia have vascular disease at autopsy and subsequently may have vascular contributions to cognitive impairment and dementia (VCID). Yet, the mediation of AD dementia by vascular disease is poorly understood. Evaluating a vascular phenotype of AD with a monogenic form of small vessel disease (SVD), Cerebral Autosomal Dominant Arteriopathy with Subcortical Infarcts and Leukoencephalopathy (CADASIL), using a suite of unique and advanced imaging biomarkers including 4D flow MRI, diffusion tenser imaging (DTI), displacement encoding with stimulated echoes, would provide key insights into potential vascular influences on AD dementia and is supported by the National Plan to Address Alzheimer's Disease.

References

1. Quick, S., Moss, J., Rajani, R.M., & Williams, A. (2021). A Vessel for Change: Endothelial Dysfunction in Cerebral Small Vessel Disease. *Trends in Neurosciences*, 44(4), 289–302. Link to Article
2. Alzheimer's Disease Neuroimaging Initiative (ADNI). ADNI Website
3. MarkVCID Consortium (Markers for Vascular Contributions to Cognitive Impairment and Dementia). MarkVCID Website
4. Dominantly Inherited Alzheimer Network (DIAN). DIAN Website
5. Wardlaw, J.M., Smith, E.E., Biessels, G.J., et al. (2013). Neuroimaging standards for research into small vessel disease and its contribution to ageing and neurodegeneration. *The Lancet Neurology*, 12(8), 822–838. Link to Article
6. Di Donato, I., Bianchi, S., De Stefano, N., et al. (2017). Cerebral Autosomal Dominant Arteriopathy with Subcortical Infarcts and Leukoencephalopathy (CADASIL) as a model of small vessel disease: Update on clinical, diagnostic, and management aspects. *BMC Medicine*, 15(1), 41. Link to Article
7. Joutel, A., & Chabriat, H. (2017). Pathogenesis of white matter changes in CADASIL: Beyond vessel-intrinsic mechanisms. *Clinical Science*, 131(8), 635–651. Link to Article
8. Pantoni, L. (2010). Cerebral small vessel disease: From pathogenesis and clinical characteristics to therapeutic challenges. *The Lancet Neurology*, 9(7), 689–701. Link to Article
9. Rajani, R.M., & Williams, A. (2017). Endothelial cell-oligodendrocyte interactions in small vessel disease and aging. *Clinical Science*, 131(5), 369–379. Link to Article
10. International Society for Vascular Behavioural and Cognitive Disorders (VASCOG). VASCOG Website

Images/Tables



704

Neuroimaging Characteristics of Melanocytic Lesions and Immune-mediated Hypophysitis in Melanoma Patients

Mehdy M Haidar MD[1], Carol Lima MD[1], Kamil Abu-Shaban MD[1], Derya Turk BS[2], Mahdi Daklallah BS[3], Anant Krishnan MD[1]

[1]Corewell Health William Beaumont University Hospital, Royal Oak, MI, USA. [2]Wayne State University, Detroit, MI, USA. [3]Oakland University William Beaumont school of medicine, Auburn Hills, MI, USA

Abstract Category

Adult Neoplasms/Epilepsy/Trauma

Summary & Objectives

This presentation introduces the spectrum of melanocytic CNS lesions, covering their embryology and imaging characteristics, including neurocutaneous melanosis, primary melanocytic schwannoma, primary meningeal melanocytic tumors, malignant melanocytic nerve sheath tumors, malignant melanoma, and immune-mediated hypophysitis linked to melanoma treatment.

Purpose

Melanocytic lesions of the central nervous system (CNS) are rare but can present significant diagnostic challenges. This review aims to:

- Highlight the neuroimaging features of melanocytic CNS lesions, including but not limited to neurocutaneous melanosis, melanotic schwannoma, primary meningeal melanocytic tumors, choroidal and nasal melanoma, and malignant melanocytic nerve sheath tumors, and contrast these with metastatic cutaneous melanoma.
- Briefly discuss the embryology/origin of these conditions, their biological markers that distinguish them from secondary melanomas, and also examine immune-mediated hypophysitis related to melanoma immunotherapy, focusing on its unique MRI findings.
- Discuss the role of MRI in differentiating these lesions from other CNS neoplasms.
- Illustrate the clinical progression and management strategies for patients with these rare conditions.
- Emphasize the importance of early diagnosis and a multidisciplinary approach in managing these complex cases.

Materials & Methods

A retrospective review was conducted on melanocytic CNS lesions in our imaging database, emphasizing cases with pathology confirmation. MRI and CT imaging data, clinical presentations, and pathology were reviewed. Cases included a 13-year-old and a younger child with neurocutaneous melanosis, a 52-year-old with melanotic schwannoma of the internal auditory canal (IAC), a 74-year-old with widespread intracranial primary meningeal melanocytic tumor, a 71-

year-old with a circumscribed spinal primary meningeal melanocytic tumor with later diffuse leptomeningeal recurrence, a 40-year-old with malignant melanocytic nerve sheath tumor, an 82-year-old with choroidal melanoma, multiple patients with immune-mediated hypophysitis during melanoma treatment, nasopharyngeal melanoma and patients with metastatic melanoma. Tumor location, appearance, progression, and treatment outcomes were evaluated.

Results & Conclusion

Results:

Neuroimaging revealed distinctive findings for each condition. Neurocutaneous melanosis presented with symmetric T1 hyperintensity in the amygdala and temporal lobes. Melanotic schwannoma of the internal auditory canal and cerebellopontine angle presented with T1 shortening and hemorrhage. Primary meningeal melanocytic tumor presented with bilateral leptomeningeal enhancement and later disease progression despite immunotherapy. In all spinal cases, the initial diagnosis was of a nerve sheath tumor; however, precontrast T1 shortening was later recognized. In one such patient, a large mass with subsequent multiple recurrences was discovered. Malignant melanocytic nerve sheath tumor demonstrated foraminal extension and aggressive growth. Immune-mediated hypophysitis was identified by pituitary enlargement during treatment, sometimes mistaken for a sellar metastasis, with resolution of the pituitary 'mass' following corticosteroid therapy. Metastatic systemic melanoma with multiple intracranial lesions, many hemorrhagic and/or with T1 shortening, was observed.

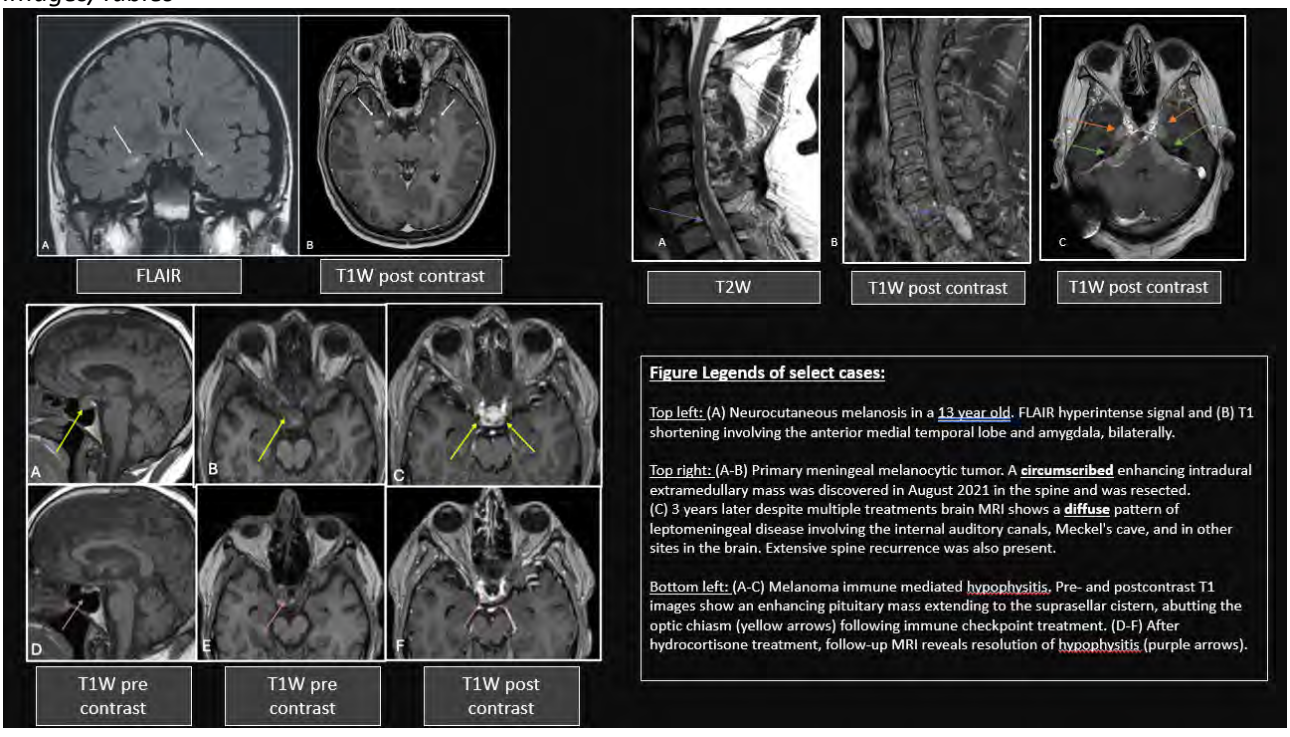
Conclusion:

Neuroimaging is essential for the early diagnosis and management of melanocytic CNS lesions, enabling differentiation from other CNS neoplasms. MRI plays a pivotal role in identifying immune-mediated hypophysitis as a complication of melanoma treatment and distinguishing it from metastatic disease. Multidisciplinary care, including neuroradiology, neuro-oncology, and endocrinology, is crucial for optimizing outcomes in these rare conditions. Early detection and tailored treatment plans significantly influence patient prognosis.

References

1. Mitre V, Heym K, Clark GD, Venkatramani R. Neurocutaneous melanosis and leptomeningeal melanoma. *J Pediatr Hematol Oncol* 2021;**43**(8):e195-e197.
2. Flores-Sarnat L. Neurocutaneous melanocytosis. In: *Handbook of Clinical Neurology*. Vol. 111. Elsevier; 2013:369–385.
3. Koirala M, Sharma MR, Adhikari S, et al. Melanocytic nerve sheath tumors: a comprehensive review. *AJNR Am J Neuroradiol* 2022;**43**(5):635–642.
4. Küsters-Vandevelde HVN, Küsters B, van Engen-van Grunsven ACH, et al. Primary melanocytic tumors of the central nervous system: a review with focus on molecular aspects. *Brain Pathol* 2015;**25**(2):209–226.

Images/Tables



711

MYCN-Amplified Spinal Ependymomas, a Rare Aggressive Subtype: Illustrative Cases

Paran Davari MD, Minerva Zhou MD, Soonmee Cha MD
Department of Radiology and Biomedical Imaging, University of California, San Francisco, CA, USA

Abstract Category

Spine

Summary & Objectives

Spinal ependymomas are typically slow-growing tumors with a favorable prognosis. Recently, a new aggressive subtype characterized by MYCN amplification has been identified, displaying distinct histopathological and molecular features. This subtype is rare, and studies describing its radiologic characteristics are limited. In this case series, we present the imaging findings and clinical outcomes of three patients with MYCN-amplified spinal ependymomas from our institution, aiming to expand the understanding of this rare tumor entity.

Purpose

The purpose of this study is to highlight the imaging features and clinical behavior of MYCN-amplified spinal ependymomas, a rare aggressive subtype. Given the limited research on this entity, even a small case series can be valuable in informing differential diagnoses and guiding follow-up protocols. We aim to present detailed imaging and clinical findings that may aid in future management and prognosis discussions. As awareness of this subtype grows, our observations can serve as a basis for further exploration of MYCN-amplified spinal ependymomas and their unique characteristics.

Materials & Methods

This case series includes three patients with MYCN-amplified spinal ependymomas from our institution. Clinical histories, imaging studies, and histopathological evaluations were retrospectively analyzed. Imaging features, including tumor location, signal characteristics, peritumoral edema, cord compression, and metastatic spread, were evaluated on MRI. Histopathological examination confirmed MYCN amplification and assessed tumor differentiation features, including the presence of perivascular pseudo-rosettes, GFAP expression, and dot-like EMA positivity.

Results & Conclusion

The lesions were intradural extramedullary, characterized by T1 isointensity, T2 hyperintensity, and avid enhancement on MRI. The tumors spanned multiple vertebral body levels, adhered closely to the spinal cord, and showed areas lacking a clear plane, suggesting infiltration. Associated peritumoral edema and cord compression were noted. Complete resection was challenging, and residual or recurrent disease was observed. Leptomeningeal spread and intracranial involvement affecting cranial nerves and the brainstem were also noted. Histopathology confirmed MYCN amplification and ependymal differentiation.

MYCN-amplified spinal ependymomas are a rare aggressive subtype with early CNS dissemination and challenging surgical management. The lack of a clear tissue plane and close association with the cord contribute to high local recurrence, emphasizing the need for vigilant imaging follow-up, particularly of the resection bed. Given the limited research, our observations can provide valuable insights for developing differential diagnoses, follow-up protocols, and management strategies for this aggressive subtype.

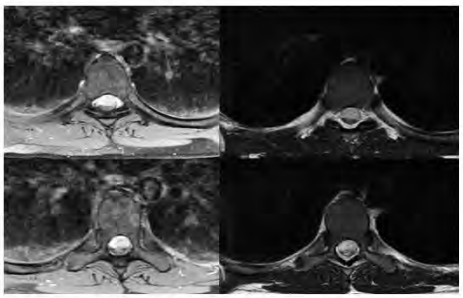
References

1. Ghasemi DR, Sill M, Okonechnikov K, et al. MYCN amplification drives an aggressive form of spinal ependymoma. Acta Neuropathol. 2019;138(6):1075. doi:10.1007/s00401-019-02056-2
2. Rao S, Sugur H, Konar S, Arivazhagan A, Santosh V. MYCN amplification in spinal ependymoma: A five-year retrospective study. Neuropathology. 2023;43(6):457-462. doi:10.1111/neup.12912
3. Raffeld M, Abdullaev Z, Pack SD, et al. High level MYCN amplification and distinct methylation signature define an aggressive subtype of spinal cord ependymoma. Acta Neuropathol Commun. 2020;8(1):1-11. doi:10.1186/s40478-020-00973-y
4. Swanson AA, Raghunathan A, Jenkins RB, et al. Spinal cord ependymomas with MYCN amplification show aggressive clinical behavior. J Neuropathol Exp Neurol. 2019;78(9):791-797. doi:10.1093/jnen/nlz064
5. Louis DN, Perry A, Wesseling P, et al. The 2021 WHO Classification of Tumors of the Central Nervous System: a summary. Neuro Oncol. 2021;23(8):1231. doi:10.1093/neuonc/noab106

Images/Tables



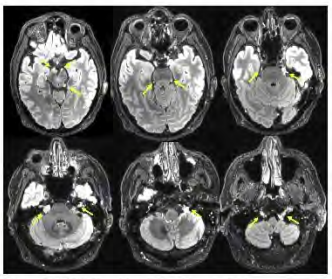
1. Sagittal T2 weighted and T1 weighted postcontrast with fat saturation images (left, right) demonstrating slight T2 hyperintensity relative to the cord and avid enhancement of the lesion. Caudal to the mass there is cord expansion and extensive T2 hyperintense signal abnormality. Patient C.



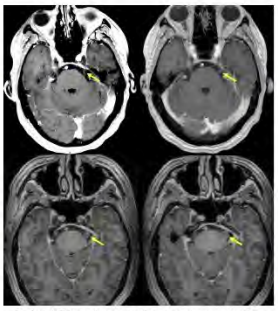
2. Axial T1 postcontrast with fat saturation (left) and T2-weighted images (right) demonstrating the mass filling the canal and resulting cord compression. At another axial level (bottom), there is a focal area without clear plane between the cord and mass with associated cord signal abnormality suspicious for infiltration.



3. Sagittal T1 postcontrast images with fat saturation of the cervical, lower thoracic, and lumbar spine demonstrating diffuse extent of metastatic enhancing nodules in patient C.



4. Axial FLAIR images demonstrating extensive metastatic nodules involving the cranial nerves and along the brainstem in patient B.



5. Axial T1 postcontrast images demonstrating subtle asymmetric enhancement of the left trigeminal nerve (top left), which becomes more prominent on three months follow-up imaging (top right) and continues to progresses to a discrete, minimally to non-enhancing nodule on six (bottom left) and nine months (bottom right) follow-up.

712

Pulsatile Tinnitus: Venous Etiologies and Endovascular Treatment Options

Sudhakar R Satti MD, Alberto Iaia MD
CHRISTIANACARE HEALTH SYSTEM, NEWARK, DE, USA

Abstract Category

Interventional/Vascular/Stroke

Summary & Objectives

Pulsatile tinnitus (PT) secondary to arterial vascular etiologies is well described and recognized by neuroradiologists. PT secondary to venous etiologies is under recognized and etiologies frequently missed by interpreting radiologists. Beyond deep venous sinus thrombosis many neuroradiologist do not report additional findings because “there is nothing to do”. Due to deeper understanding of venous pathology in the setting of PT and venous hypertension (IIH and cognitive effects), endovascular treatment options are rapidly evolving.

The main objective of this educational exhibit is to highlight importance of careful analysis of cerebrovascular venous anatomy for sources of tinnitus. Identification of venous will minimize rates of false negative interpretations of cross-sectional imaging (CTV and MRV) and help guide treatment options.

Purpose

Highlight common causes of venous pulsatile tinnitus including:

1. Venous stenosis (Transverse sinus)
2. Venous Diverticulum
3. Venous emissary veins (transmastoid and suboccipital)
4. Venous varix

Ultimately, this educational exhibit will improve the understanding the audience of the importance recognition of common venous etiologies of PT and educate them about treatment options.

Materials & Methods

Electronic review of all venograms performed at our institution between 2010-2024. Cases of PT secondary to venous etiologies will be reviewed and key cases highlighting the spectrum of disease will be presented.

1. Present case examples of PT secondary to venous etiologies (cross sectional imaging and angiographic correlation)
2. Demonstrate endovascular treatment options for PT of venous origin
3. Ultimately, this educational exhibit will improve the understanding the audience of the importance recognition of common venous etiologies of PT

Results & Conclusion

The audience of this education exhibit on venous etiologies for pulsatile tinnitus will leave having a deeper understanding of the importance of recognizing common venous causes, will be able to recognize and describe the finding on cross-sectional imaging, and appropriately refer patients for cerebral angiography/venography and pressure measurements when appropriate. Ultimately, this exhibit will improve patient care and reduce the rate of false negative interpretation.

References

A proposed framework for cerebral venous congestion.
Arun A, Amans MR, Higgins N, Brinjikji W, Sattur M, Satti SR, Nakaji P, Luciano M, Huisman TA, Moghekar A, Pereira VM, Meng R, Fargen K, Hui FK. Neuroradiol J. 2022 Feb;35(1):94-111. doi: 10.1177/19714009211029261. Epub 2021 Jul 5. PMID: 34224274; PMCID: PMC8826290.

State of the Art: Venous Causes of Pulsatile Tinnitus and Diagnostic Considerations Guiding Endovascular Therapy
Mohamad Abdalkader, Thanh N. Nguyen, Alexander M. Norbash, Eytan Raz, Maksim Shapiro, Stéphanie Lenck, Waleed Brinjikji, Peter Weber, and Osamu Sakai
Radiology 2021 300:1, 2-16

713

Discovering the Hidden Leak: Advanced Detection and Management of Spontaneous Intracranial Hypotension Secondary to Cerebrospinal Fluid-Venous Fistulas

Donna Parizadeh MD MPH
Trinity Health Midatlantic/Mercy Catholic Medical Center, Darby, PA, USA

Abstract Category

Spine

Summary & Objectives

Cerebrospinal fluid-venous fistulas are increasingly recognized as a cause of spontaneous intracranial hypotension. Patients typically present with positional headaches, often exacerbated by Valsalva maneuvers, and may experience symptoms such as tinnitus and cognitive dysfunction. Diagnosing CSFVFs is challenging due to the need for advanced imaging that can accurately differentiate these fistulas from other CSF leaks and localize them for targeted treatment. Understand the clinical presentation and diagnostic challenges of cerebrospinal fluid-venous fistulas (CSFVFs).

Purpose

- Understand the clinical presentation and diagnostic challenges of cerebrospinal fluid-venous fistulas (CSFVFs).
- Recognize the advanced imaging techniques required for accurate detection.
- Explore the efficacy and limitations of various treatment options for managing spontaneous intracranial hypotension (SIH).

Materials & Methods

Not applicable.

Results & Conclusion

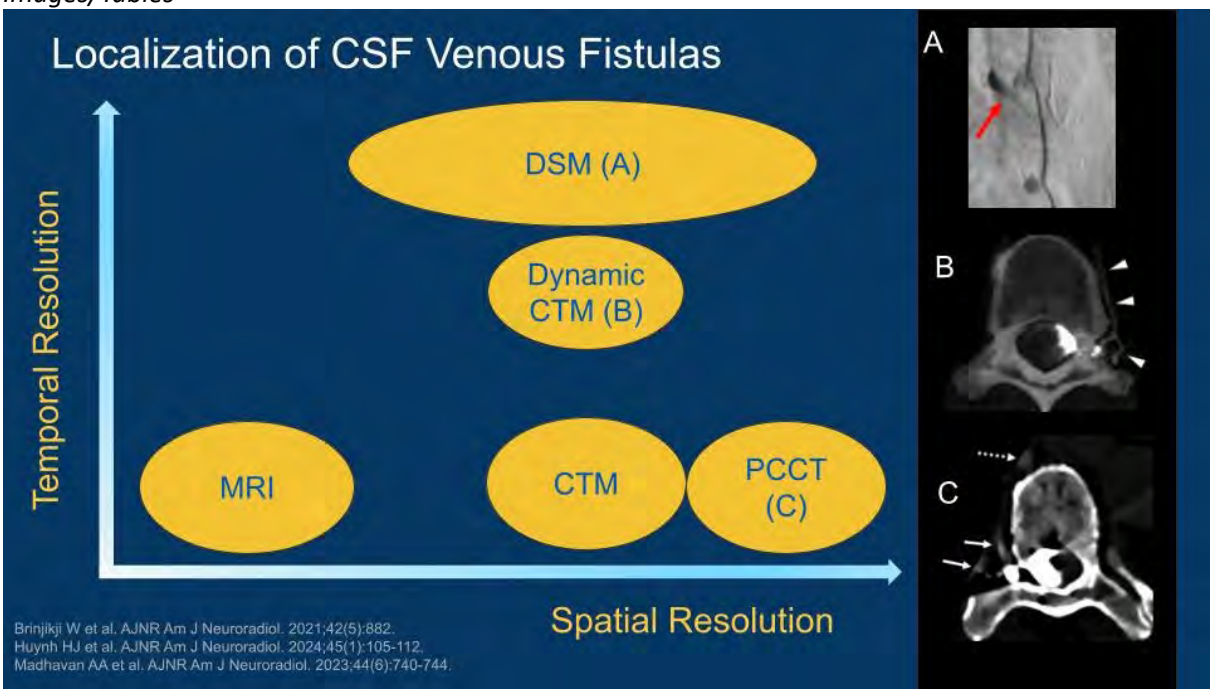
Digital subtraction myelography, particularly in the lateral decubitus position, and dynamic CT myelography have been the most effective and commonly used modalities for detecting CSFVFs since their initial description a decade ago. Recent advancements in imaging technology have significantly improved the detection and management of CSFVFs. Photon-counting detector (PCD) CT myelography offers superior spatial and temporal resolution, enhancing the detection of CSFVFs, particularly in patients with intermediate- and high-probability Bern scores. The use of a denoising high-resolution deep convolutional neural network further improves the conspicuity of CSFVFs on PCD CT myelography. Dynamic CT myelography with real-time bolus tracking (dCTM-BT) standardizes the timing of CTM acquisitions, showing excellent diagnostic performance. Additionally, cone beam CT myelography performed after digital subtraction myelography (DSM) increases diagnostic yield, identifying fistulas that may be missed on DSM alone.

Treatment options for CSFVFs include epidural blood patches, surgical ligation, and endovascular embolization. While epidural blood patches often provide only transient relief, surgical ligation is considered a definitive treatment, with approximately 70% of patients achieving complete symptom resolution. Endovascular embolization, particularly transvenous embolization has emerged as a reliable and effective treatment, demonstrating a 95% treatment response rate with significant improvement in clinical outcomes.
In conclusion, a state-of-the-art approach to CSFVFs involves advanced imaging for precise diagnosis and a combination of surgical and endovascular treatments for effective management. Mastery of these techniques and treatment options is essential for improving patient outcomes in spontaneous intracranial hypotension cases

References

Schievink WI, Moser FG, Maya MM. CSF-venous fistula in spontaneous intracranial hypotension. Neurology 2014;83:472–3. doi:10.1212/WNL.0000000000000639.
Madhavan AA, Brinjikji W, Cutsforth-Gregory JK, et al. Myelographic Techniques for the Localization of CSF-Venous Fistulas: Updates in 2024. AJNR Am J Neuroradiol 2024;45(10):1403-1412. doi:10.3174/ajnr.A8299.
Huynh TJ, Parizadeh D, Ahmed AK, et al. Lateral Decubitus Dynamic CT Myelography With Real-Time Bolus Tracking (dCTM-BT) for Evaluation of CSF-Venous Fistulas: Diagnostic Yield Stratified by Brain Imaging Findings. AJNR Am J Neuroradiol 2023;45(1):105-112. doi:10.3174/ajnr.A8082.
Konovalov A, Gadzhiagaev V, Vinogradov E, Nikitin N, Eliava S, Konovalov N. Surgical Treatment Efficacy of CSF-Venous Fistulas: Systematic Review. World Neurosurgery 2022;161:91-96. doi:10.1016/j.wneu.2022.02.036.
Brinjikji W, Garza I, Whealy M, Kissoon N, Atkinson JLD, Savastano L, Madhavan A, Cutsforth-Gregory J. Clinical and imaging outcomes of cerebrospinal fluid-venous fistula embolization. J Neurointerv Surg 2022;14:953-956. doi:10.1136/neurintsurg-2021-018466.

Images/Tables



720

Brain Sagging Dementia: A Primer for Neuroradiologists

Jakob von Morgenland B.S.[1], Jamie E Clarke M.D., M.S.[1], Wouter Schievink MD[2], Marcel Maya MD[3], Jay Acharya M.D.[1]
[1]Division of Neuroradiology, Department of Diagnostic Radiology, University of California Los Angeles (UCLA), Los Angeles, CA, USA. [2]Department of Neurosurgery, Cedars Sinai Medical Center, Los Angeles, CA, USA. [3]Division of Neuroradiology, Department of Radiology, Cedars Sinai Medical Center, Los Angeles, CA, USA

Abstract Category

Adult Brain Inflammatory/Infectious Disease/Degenerative/Metabolic

Summary & Objectives

Brain sagging dementia presents with neuropsychological features corresponding to frontotemporal dementia as a result of spontaneous intracranial hypotension (Hong et al, 2002). Despite this being a relatively rare abnormality,

cognitive deficits generally show high rate of reversal with early treatment of CSF leakage that causes downward displacement of the brain, or 'brain sag' (Schievink, 2006).

Purpose

This bibliometric analysis aims to bring awareness of this underdiagnosed reversible form of dementia to reform early diagnostic strategies and treatment approaches.

Materials & Methods

The top 40 most-cited articles were collected from Web of Science. Multiple search queries were used due to the heterogeneity in terminology to describe brain sagging dementia, including: "brain sag dementia," "CSF leak dementia," "spontaneous intracranial hypotension dementia," "CSF fistula dementia," "intracranial hypotension dementia," "intracranial hypotension syndrome," "frontotemporal brain sagging syndrome," and "brain sagging syndrome." Web of Science was used to analyze the author, institution, title, keywords, abstract, subject category, citation and usage count, in addition to diagnostic approaches and treatment strategies for brain sagging dementia.

Results & Conclusion

Patients with brain sagging dementia typically present with orthostatic headaches and cognitive deficits mimicking frontotemporal dementia. Diagnosis through MRI is used to identify characteristic findings such as downward displacement likely with meningeal enhancement, narrowed mamillopontine distance, lateral ventricular angle, and pontomesenphalic angle and low CSF pressure with lumbar puncture (Wicklund et al, 2011; Shah et al, 2013). Patients may also be evaluated through the Bern score, which predicts the likelihood of CSF leakage based on MRI, lumbar puncture opening pressure, suprasellar and prepontine cisterns. Early conservative treatments including bedrest, hydration, and caffeine intake prove beneficial in some patients, though more invasive treatments, such as epidural blood patch repair of dural defects causing CSF leaks, have a higher rate of repair and reversal of the brain sagging and associated cognitive deficits (Walker et al, 2008). Despite the positive clinical outcomes of treatment for patients with brain sagging dementia, misdiagnosis and delay in effective care often precludes these patients from partial or full recovery of cognitive deficits incurred from the condition (Schievink, 2006). Further research is needed to better define the long-term effects of CSF leakage and associated spontaneous intracranial hypotension on behavioral health and cognitive decline, the mechanisms linking brain sagging to modulations in cognitive function, and the effectiveness of early treatment modalities through standardized patient studies.

Brain sagging dementia remains a widely unrecognized and misdiagnosed condition despite decades of research. Early recognition, prompt diagnosis, and expedient treatment is essential for targeting the cognitive and behavioral deficits that may be reversible early on in the disease course but are likely to progress to chronic impairment later on in the disease course for the patient. This educational exhibit serves to share the authors' finding through a comprehensive literature review bibliometric analysis to bring awareness and attention to brain sagging dementia, the associated cognitive and behavioral manifestations that arise, and the collective consensus on appropriate diagnostic and treatment approaches with an effort to improve patient outcomes.

References

1. Hong, M., Shah, G. V., Adams, K. M., et al. Spontaneous intracranial hypotension causing reversible frontotemporal dementia. *Neurology*, 2002; 58(8), 1285-1287. DOI: doi.org/10.1212/WNL.58.8.1285.
2. Schievink, W. I. Spontaneous spinal cerebrospinal fluid leaks and intracranial hypotension. *Jama*, 2006; 295(19), 2286-2296. DOI: doi.org/10.1001/jama.295.19.2286.
3. Shah, L. M., McLean, L. A., Heilbrun, M. E., et al. Intracranial hypotension: improved MRI detection with diagnostic intracranial angles. *American Journal of Roentgenology*, 2013; 200(2), 400-407. DOI: doi.org/10.2214/AJR.12.8611.
4. Walker, L., & DeMeulemeester, C. Spontaneous intracranial hypotension masquerading as frontotemporal dementia. *The Clinical neuropsychologist*, 2008; 22(6), 1035-1053. DOI: doi.org/10.1080/13854040701874386.
5. Wicklund, M. R., Mokri, B., Drubach, D. A., et al. Frontotemporal brain sagging syndrome: an SIH-like presentation mimicking FTD. *Neurology*, 2011; 76(16), 1377-1382. DOI: doi.org/10.1212/WNL.0b013e3182166e42.

729

Delta T1 (dT1) Maps to Quantitatively Assess Extent of Ablation After Laser Interstitial Thermal Therapy (LITT) Treatment of Contrast Enhancing Brain Tumors

Kathleen M Schmainda PhD, Melissa A Prah, Max Krucoff MD
Medical College of Wisconsin, Milwaukee, WI, USA

Abstract Category

Adult Neoplasms/Epilepsy/Trauma

Summary & Objectives

LITT is quickly becoming standard of care for treatment of many radiographically progressive primary and metastatic brain tumors, whether due to recurrent disease or radiation necrosis,[1] as it has demonstrated clinical benefit for both conditions.[1] It also has the added advantage of being minimally invasive with short recovery times and lower complication rates than open surgical resections. While extent of ablation (EOA) with LITT is generally considered oncologically equivalent to extent of resection (EOR) in open surgeries, there is no standard method to assessing EOA. Importantly, visual interpretation of the pre and post-contrast images (T1, T1+C) are routinely confounded by post-ablative coagulation necrosis and inflammation after LITT, making interpretation challenging. These treatment related changes result in bright precontrast signal on T1 that is difficult to distinguish from post-contrast enhancement on T1+C. Because the use of LITT is rapidly expanding, it is imperative to develop a modality to accurately and quantitatively assess EOA that can be broadly applied. As a solution we propose the use of delta T1 (dT1) maps created from the difference between calibrated T1 and T1+C images, which are describe here with examples provided.

Purpose

To demonstrate the utility of delta T1 (dT1) maps to provide an objective and accurate determination of ablation extent in response to Laser Interstitial Thermal Therapy (LITT) for Brain Tumor.

Materials & Methods

Delta T1 maps are created from the difference between calibrated T1 and T1+C image. The calibration file, which was previously determined for T1 and T1+C datasets,[2] transforms each input image to a standardized scale resulting in quantitative images. The standardized T1 is then registered to and subtracted from the standardized T1+C, resulting in a quantitative dT1 map. The dT1 enables an easy and consistent way to determine contrast enhancing (CE) volumes, free of confounding pre-contrast bright signal.

Results & Conclusion

Shown in **Figure 1** are the processing steps used to create dT1 maps from routinely collected T1 and T1+C images. This stepwise process has been incorporated into an automated workflow within IB RadTech™ (Imaging Biometrics LLC, Elm Grove, WI). **Figure 2** shows results for a patient with recurrent glioblastoma. The dT1 maps were obtained 6 days before and 1 day after LITT ablation. Immediately post-ablation, coagulation necrosis and inflammation cause a hazy increased signal on both T1 and T1+C making it difficult to discern the spatial extent of the LITT treatment field. Alternatively, dT1 maps clearly show the EOA by eliminating the confounding pre-contrast factors. To date we have obtained post-ablation dT1 maps for over 50 patients. Quantitative analysis of EOA is underway to assess the ability of dT1 to predict outcomes as compared to conventional methods of assessment. While a similar study was performed for the determination of extent of surgical resection[3], this is the first study to evaluate the use of dT1 for the evaluation of surgical ablation.
In conclusion, dT1 maps provide better alternative to conventional methods for the assessment of extent of surgical resection and ablation. Routine incorporation of the dT1 maps into the radiologists' workflow for post-surgical evaluation is encouraged.

References

1. Srinivasan ES, Grabowski MM, Nahed B V., et al. Laser interstitial thermal therapy for brain metastases. *Neurooncol Adv* 2021;3:V16–25.
2. Schmainda KM, Prah MA, Zhang Z, et al. Quantitative Delta T1 (dT1) as a replacement for adjudicated central reader analysis of contrast-enhancing tumor burden: A subanalysis of the American college of radiology imaging network 6677/radiation therapy oncology group 0625 multicenter brain tumor trial. *American Journal of Neuroradiology* 2019;40:1132–9.
3. Laing B, Prah MA, Best BJ, et al. Application of Delta T1 Maps for Quantitative and Objective Assessment of Extent of Resection and Survival Prediction in Glioblastoma. *Neurosurgery Practice* 2024;5:1–7.

Images/Tables

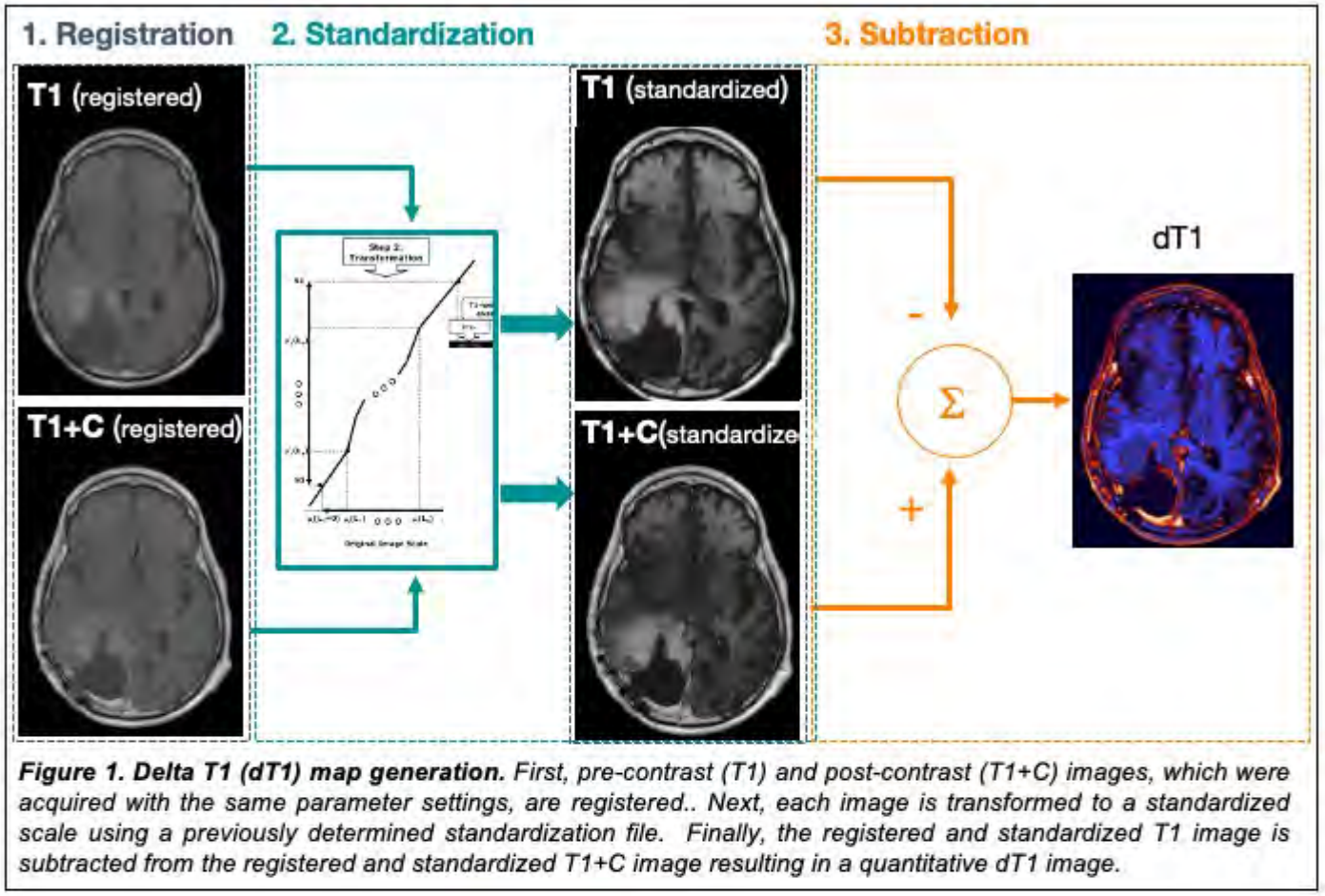


Figure 1. Delta T1 (dT1) map generation. *First, pre-contrast (T1) and post-contrast (T1+C) images, which were acquired with the same parameter settings, are registered.. Next, each image is transformed to a standardized scale using a previously determined standardization file. Finally, the registered and standardized T1 image is subtracted from the registered and standardized T1+C image resulting in a quantitative dT1 image.*

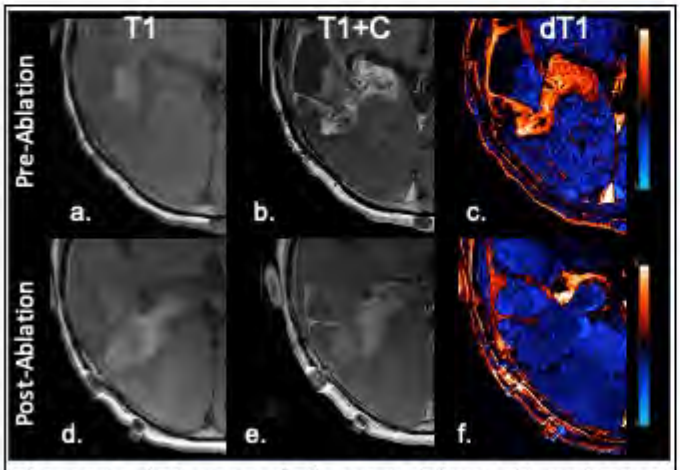


Figure 2. dT1 maps *(c,f) created from T1 and T1+C obtained 6d before (a,b) and 1d after (d,e) LITT ablation for a patient with recurrent GBM. The treatment field, difficult to discern on T1, T1+C (d,e), is clear on dT1 (f).*

734

Malformations of Cortical Development: Classification, Pattern Recognition and Genotype-Phenotype Correlation

Rayan Alowaisheq[1], Salman Aldeheshi[1], Zahra AL Zadjali[1], Zainab Al Buraiki[1], Nasser Al Qahtani[2], Dalia Jadkarim[1], Manal Nicolas-Jilwan[3]

[1]King Faisal Specialist Hospital & Research Centre, Riyadh, Riyadh, Saudi Arabia. [2]King Saud Medical City, Riyadh, Riyadh, Saudi Arabia. [3]Beirut, Lebanon, Lebanon

Abstract Category

Pediatrics

Summary & Objectives

The classification of malformations of cortical development is constantly changing with increasing knowledge of their molecular and genetic basis, rendering the interpretation of imaging challenging. The objectives of our presentation are:

1. To understand the main stages of embryologic brain development and recently standardized classification of malformations of cortical development.
2. To provide illustrative MRI cases of the full spectrum of these disorders with phenotype-genotype correlation when available.

Purpose

Malformations of cortical development are a heterogenous group of disorders characterized by abnormal formation of the cerebral cortex. While imaging plays a pivotal role in their diagnosis, its interpretation is challenging as the classification of these disorders is constantly changing with increasing knowledge of their molecular and genetic basis. The first part of our presentation is a concise overview of embryologic brain development and recently standardized classification of malformations of cortical development. This is followed by illustrative cases which highlight the key imaging features of the full spectrum of these conditions.

Materials & Methods

We conducted a retrospective search of the reports of brain MRI exams obtained at our institution using the following keywords: microcephaly, megalencephaly, simplified gyral pattern, polymicrogyria, pachygyria, lissencephaly, cobblestone, heterotopia, schizencephaly, dysgyria, stenogyria, cortical dysplasia, tuberous sclerosis, congenital muscular dystrophy and walker-warburg. We included the following cases:

1. A spectrum of cortical abnormalities seen in microcephalic patients: normal gyral pattern, simplified gyral pattern, extensive right hemispheric polymicrogyria in a child with microcephalic osteodysplastic primordial dwarfism type I, bilateral perisylvian polymicrogyria, lissencephaly and extensive band heterotopia in a child with TUBA1A mutation.
2. A patient with Cowden syndrome and hemimegalencephaly.
3. Cases that illustrate the pachygyria-lissencephaly spectrum. These encompass a patient with DCX mutation and bilateral anterior pachygyria and band heterotopia, a patient with DCX mutation and diffuse anterior predominant lissencephaly, a 3-year old girl with extensive band heterotopia and a heterozygeous variant of unknown significance of the DCX gene, as well as a 10 year-old boy with posterior lissencephaly.
4. Two cases of cobblestone cortical malformation in a 4 year-old with LAMA-2 congenital muscular dystrophy and a 2 year-old with homozygeous LAMB1 mutation.
5. Walker-Warburg syndrome and diffuse polymicrogyria (this case highlights the overlapping spectrum of polymicrogyria/cobblestone malformation in cortical overmigration).
6. Pathology proven type 1b focal cortical dysplasia with transmantle heterotopia and type 2b focal cortical dysplasia in two patients.
7. Tuberous sclerosis.
8. Subependymal nodular and laminar heterotopia.
9. Two cases of schizencephaly, closed lip and open lip.
10. Chiari II malformation with stenogyria.

Results & Conclusion

The overlapping imaging features of malformations of cortical development, their variable appearance through the different stages of myelination, and their inconsistent classification in the literature, render their diagnosis difficult. Knowledge of key neuroimaging patterns is crucial for adequate interpretation.

References
Severino M, Geraldo AF, Utz N, et al. Definitions and classification of malformations of cortical development: practical guidelines. Brain. 2020 Oct 1;143(10):2874- 2894.
Najm I, Lal D, Alonso Vanegas M, et al. The ILAE consensus classification of focal cortical dysplasia: An update proposed by an ad hoc task force of the ILAE diagnostic methods commission. Epilepsia. 2022 Aug;63(8):1899-1919.

741

Imaging characteristics of myelin oligodendrocyte glycoprotein associated disease (MOGAD) that can differentiate from other CNS autoimmune diseases

Priyanka Garigipati MD, Soonmee Cha MD
University of California San Francisco, San Francisco, CA, USA

Abstract Category
Adult Brain Inflammatory/Infectious Disease/Degenerative/Metabolic

Summary & Objectives
Autoimmune CNS diseases involve the immune system mistakenly targeting components within the brain and spinal cord, leading to inflammation, demyelination, and various neurological symptoms and deficits. Myelin oligodendrocyte glycoprotein antiboy-associated disease (MOGAD) is one such autoimmune disease [1, 2] but there are others, including neuromyelitis optica spectrum disorder (NMOSD), multiple sclerosis (MS), and acute disseminated encephalomyelitis (ADEM) [3,4]. Despite overlap of clinical and imaging features with other demyelinating disorders, studies have highlighted unique imaging features to help distinguish MOGAD including pattern of optic neuritis, longitudinal extensive transverse myelitis, supratentorial deep grey matter, and brainstem lesions. This education exhibit will fulfill the following objectives:

1. Overview of diagnostic criteria of MOGAD
2. Distinguishing imaging features of MOGAD on MRI
3. Present exemplary imaging features from MOG-antibody positive patients at UCSF that highlight
    1. Optic neuritis involving the anterior, retrobulbar region lesions
    2. Cerebellar peduncle involvement
    3. Brainstem, particularly pontine, lesions
    4. Subcortical, deep grey matter lesions involving the thalamus
    5. Thoracic spinal cord and conus medullaris involvement
    6. Ill-defined, large supratentorial lesions
4. Discuss key differences and overlaps of clinical and MRI features among MOGAD, NMOSD, MS, and ADEM

Purpose
MOGAD is an autoimmune demyelinating disease of the central nervous system that shares several overlapping clinical and imaging features with other demyelinating disorders such as NMOSD, MS, and ADEM. However, several studies have illustrated imaging features unique to MOGAD that can differentiate it from other autoimmune diseases that can lead to prompt appropriate clinical management.

Materials & Methods
A retrospective review of 27 cases of patients with serum positive MOG-antibody titers were reviewed from our institutional database. The imaging and reported findings were reviewed for presence of optic nerve, spinal cord, brainstem, and supratentorial lesions.

Results & Conclusion
Our findings are consistent with published literature on MOGAD imaging. Of the 27 patients reviewed, 14 patients (52%) exhibited pre-chiasmatic optic nerve lesions, 11 patients (41%) showed brainstem lesions, and 8 patients (30%) showed cerebellar peduncle involvement. Majority of the patients presented with ill-defined supratentorial subcortical white matter lesions that do not resemble classic lesions expected in NMOSD or MS. Exemplary case findings were compiled to concisely demonstrate the salient imaging features that distinguish MOGAD from other CNS autoimmune diseases to improve diagnostic accuracy and facilitate prompt targeted therapeutic management.

References
1. Ambrosius W, Michalak S, Kozubski W, et al. Myelin Oligodendrocyte Glycoprotein Antibody-Associated Disease: Current Insights into the Disease Pathophysiology, Diagnosis and Management. *Int J Mol Sci* 2020;22
2. Sechi E. NMOSD and MOGAD. *Continuum (Minneap Minn)* 2024;30:1052-1087

3. Li Y, Liu X, Wang J, et al. Clinical Features and Imaging Findings of Myelin Oligodendrocyte Glycoprotein-IgG-Associated Disorder (MOGAD). *Front Aging Neurosci* 2022;14:850743
4. Shahriari M, Sotirchos ES, Newsome SD, et al. MOGAD: How It Differs From and Resembles Other Neuroinflammatory Disorders. *AJR Am J Roentgenol* 2021;216:1031-1039

746

Pediatric pituitary MRI: From congenital to tumoral lesions

Diego Guerrero MD, Diego Herrera MD, Valentina Munera MD, Duban Zuluaga MD
Universidad de Antioquia, Medellín, Antioquia, Colombia

Abstract Category

Pediatrics

Summary & Objectives

Children can suffer from a variety of pathologies related to the sella turca and the pituitary gland. The following will be highlighted:

- Congenital lesions such as interruption of the pituitary stalk or pituitary duplication.
- Hormonal disorders associated with precocious puberty or short stature.
- Tumor lesions such as adenomas, craniopharyngiomas and germinomas.

The objective of this educational exhibition is to highlight the imaging findings that allow the diagnosis of the most important lesions affecting the pituitary gland in pediatrics.

Purpose

- Highlight the most important anatomical elements of pituitary MRI.
- Based on the understanding of the hypothalamic-pituitary axis, understand congenital pituitary lesions and their clinical implications.
- Present the imaging findings of the most common pituitary tumors in the pediatric population.
- Present guidelines for optimizing MRI technique according to pathology.

Materials & Methods

- A review of the literature.
- Analysis of own cases based on 25 years of experience in the Neuroradiology department of the Universidad de Antioquia.

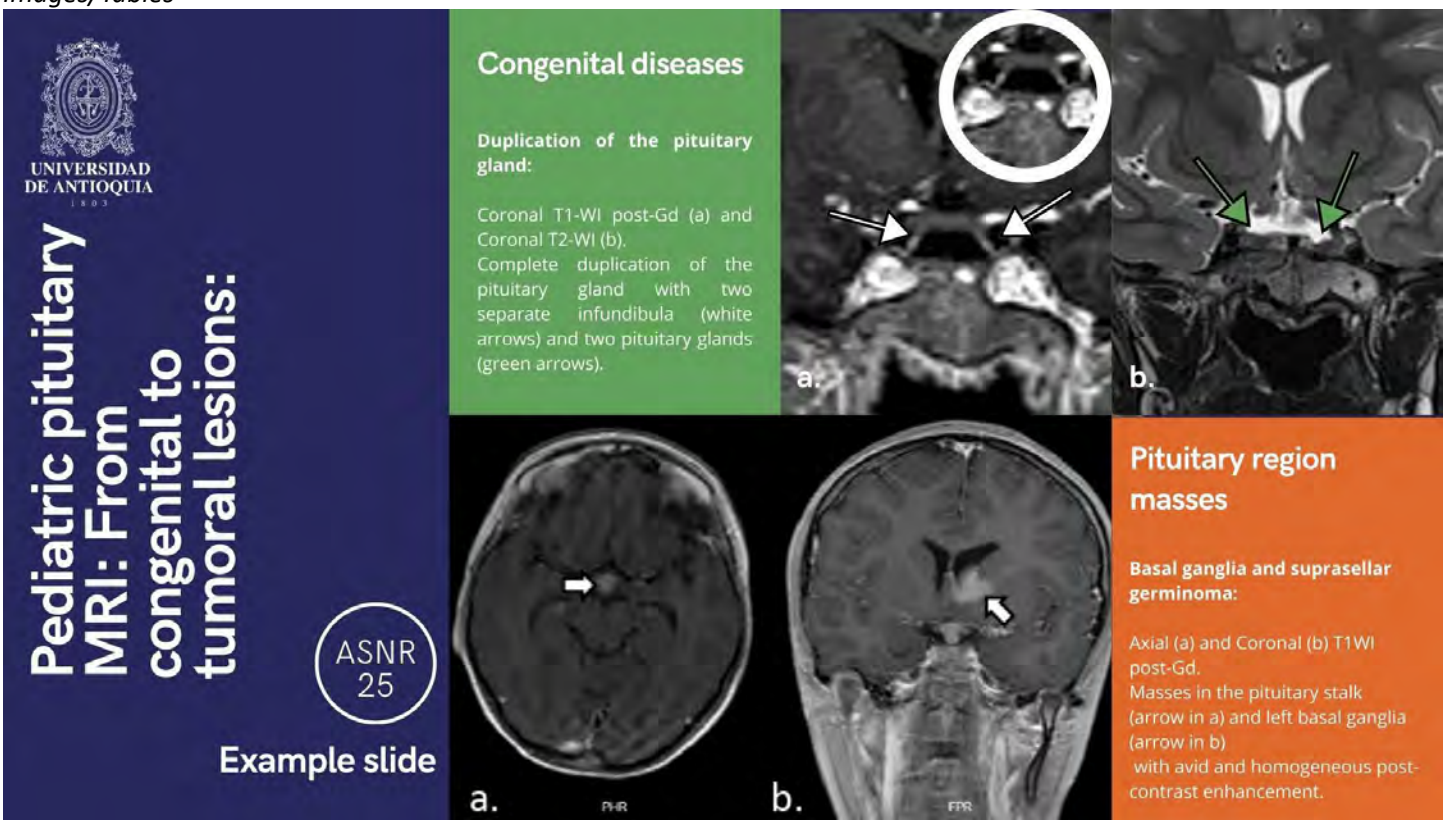
Results & Conclusion

Understanding the embryology, anatomy and physiopathology of the pituitary gland allows for an adequate diagnostic approach to congenital and tumoral lesions that may affect the pituitary gland in children. The imaging characteristics of the major entities affecting the pituitary gland in the pediatric population are presented schematically.

References

- Delman BN, Fatterpekar GM, Law M, Naidich TP. Neuroimaging for the pediatric endocrinologist. Pediatr Endocrinol Rev. 2008;5:708–19.
- Argyropoulou, M.I., Kiortsis, D.N. MRI of the hypothalamic-pituitary axis in children. Pediatr Radiol 35, 1045–1055 (2005). https://doi.org/10.1007/s00247-005-1512-9
- Chaudhary V, Bano S. Imaging of pediatric pituitary endocrinopathies. Indian J Endocrinol Metab 2012;16:682–91 doi:10.4103/2230-8210.100635 pmid:23087850

Images/Tables



773

Muddying the Waters: Addition of Imaging ENE (iENE) to American Joint Committee on Cancer 9th edition (AJCC9) and Potential Pitfalls for HPV- mediated Oropharyngeal SCC (OPSCC) Management Decisions.

Jacqueline Junn[1], Bhagya Sannananja[1], Jennifer Becker[1], Kristen Baugnon[2], Ashley Aiken[1]
[1]Atlanta, GA, USA. [2]A, GA, USA

Abstract Category

Head and Neck

Summary & Objectives

This educational exhibit aims to illustrate imaging features that radiologists use to determine iENE and how that correlates with pathologic confirmation of ENE (pENE). The purpose of this exhibit is to present cases where imaging suggested Grade 1 iENE, defined as a node with “ill-defined nodal border” infiltrating into the surrounding fat but did not have pENE.

Purpose

Current AJCC 8 does not include iENE for HPV-mediated OPSCC based on lack of specificity as shown on earlier studies (1). However, iENE will be added back to AJCC 9th update as grades 1 through 3, based on a new study showing iENE correlates with prognosis for OPSCC (2).

While AJCC staging is important to predict prognosis, it is also crucial for management decisions. This update particularly affects HPV-mediated OPSCC patients as it may affect eligibility for clinical trials and pathways for de-escalation therapy. Therefore, potential problems with interobserver variability and accuracy, specifically for grade 1 iENE, may inappropriately preclude the patient's treatment options.

Materials & Methods

We will illustrate a series cases with HPV-mediated OPSCC with staging CT exams demonstrating Grade 1 iENE. All these patients underwent transoral robotic operation and neck dissection as well as de-descalation therap. The final pathology on all of these patients was without pENE.

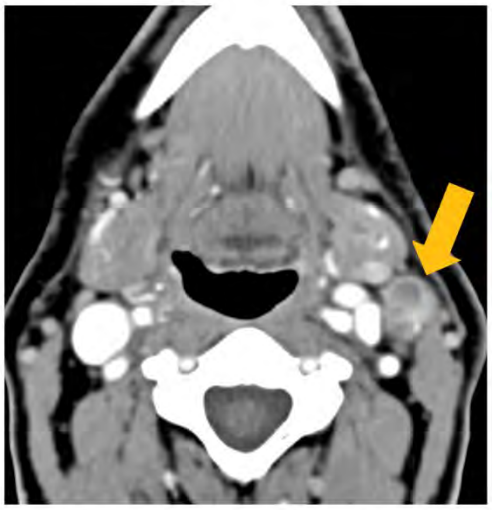
Results & Conclusion

Our educational exhibit is critical, especially when the American Joint Committee on Cancer (AJCC) update is occurring to the 9th edition of the staging manual soon. Currently, iENE is not part of the staging system for HPV-mediated OPSCC in the 8th edition of the AJCC staging guide although it is for HPV-negative OPSCC. However, the 9th edition will likely include all three categories of ENE in staging due to Billfalk-Kelly et al.'s study that showed poor outcomes only on iENE (3- Billfalk-Kelly). Unfortunately, Billfalk-Kelly's study did not have pathologic confirmation on their patients. Our exhibit emphasizes the importance of confirming iENE with pathology to predict patient outcomes accurately. In this HPV-mediated OPSCC population, Grade 1 iENE on imaging alone may not be sufficient for upstaging HPV-mediated OPSCC nodal disease and altering patients' treatment plans.

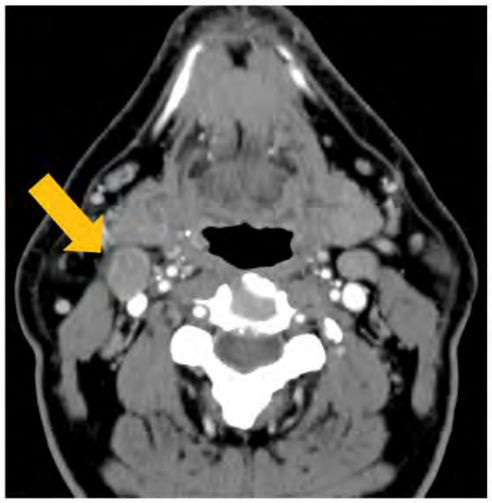
References

1. Aiken AH, Poliashenko S, Beitler JJ, et al. Accuracy of Preoperative Imaging in Detecting Nodal Extracapsular Spread in Oral Cavity Squamous Cell Carcinoma. *AJNR Am J Neuroradiol*. 2015 Sep;36(9):1776-81. doi: 10.3174/ajnr.A4372. Epub 2015 Jul 30. PMID: 26228885; PMCID: PMC7968765.
2. Henson C, Abou-Foul AK, Yu E, et al. Criteria for the diagnosis of extranodal extension detected on radiological imaging in head and neck cancer: Head and Neck Cancer International Group consensus recommendations. *Lancet Oncol*. 2024 Jul;25(7):e297-e307. doi: 10.1016/S1470-2045(24)00066-4. PMID: 38936388.
3. Billfalk-Kelly A, Yu E, Su J, et al. Radiologic Extranodal Extension Portends Worse Outcome in cN+ TNM-8 Stage I Human Papillomavirus-Mediated Oropharyngeal Cancer. *Int J Radiat Oncol Biol Phys*. 2019 Aug 1;104(5):1017-1027. doi: 10.1016/j.ijrobp.2019.03.047. Epub 2019 Apr 4. PMID: 30953712.

Images/Tables



Patient 1: Left level 2A nodes with fat infiltration, which would equate to published guideline of iENE Grade 1. The final pathology was negative for ENE



Patient 2: Right level 2A node shows adjacent fat infiltration. This would also equate to published guideline of iENE Grade 1. The final pathology was negative for ENE

781

Pictorial Review of a Surprising Tumor Mimic of the Central Nervous System: Extranodal Rosai-Dorfman Disease

Ceylan Altintas Taslicay MD, Heba Al Qudah MD, Samir A Dagher MD, Richard Dagher MD, Ahmed Msherghi MD, Sahar Alizada MD, Alexander Khalaf Assistant Professor, Max Wintermark Professor, Maria Gule-Monroe Associate Professor
The University of Texas, MD Anderson Cancer Center, Houston, TEXAS, USA

Abstract Category

Adult Brain Inflammatory/Infectious Disease/Degenerative/Metabolic

Summary & Objectives

To review and illustrate the imaging characteristics of extranodal Rosai-Dorfman Disease (RDD) of the central nervous system (CNS).

To demonstrate various extranodal RDD masses of the CNS by specific anatomic location in a case-based approach.

To discuss the differential diagnoses and emphasize the key imaging findings leading to correct diagnosis.

Purpose

RDD is a rare, idiopathic, and non-neoplastic histioproliferative disease. It can affect many organ systems, including nodal (70%) or extranodal (30%) sites. Extranodal involvement can occur anywhere in the body, including CNS, which is rare. It can exhibit imaging features that mimic neoplasms, creating a diagnostic challenge. Here, we do an image-rich review to present the imaging characteristics of extranodal RDD of the CNS and comprehensively discuss differential diagnoses and key teaching points.

Materials & Methods

We retrospectively reviewed pathologically confirmed RDD cases seen at our institution from 2006 to 2024. Only extra nodal RDD cases of the CNS were analyzed for anatomical locations and radiologic appearance. Also, the mimickers were recorded.

Results & Conclusion

7 cases of extranodal RDD of the CNS (4 male and 3 female, mean age 47.3 years [range 15-69]) were included. Specific sites of involvement included the following: dural-based intracranial, n = 4; dural-based spinal, n = 1; and cerebellar parenchymal, n = 2. Only one patient had organ involvement outside the CNS, and all the others had isolated disease. The most common CNS manifestation was dural-based lesions. There were only two parenchymal lesions, both with cerebellar involvement.

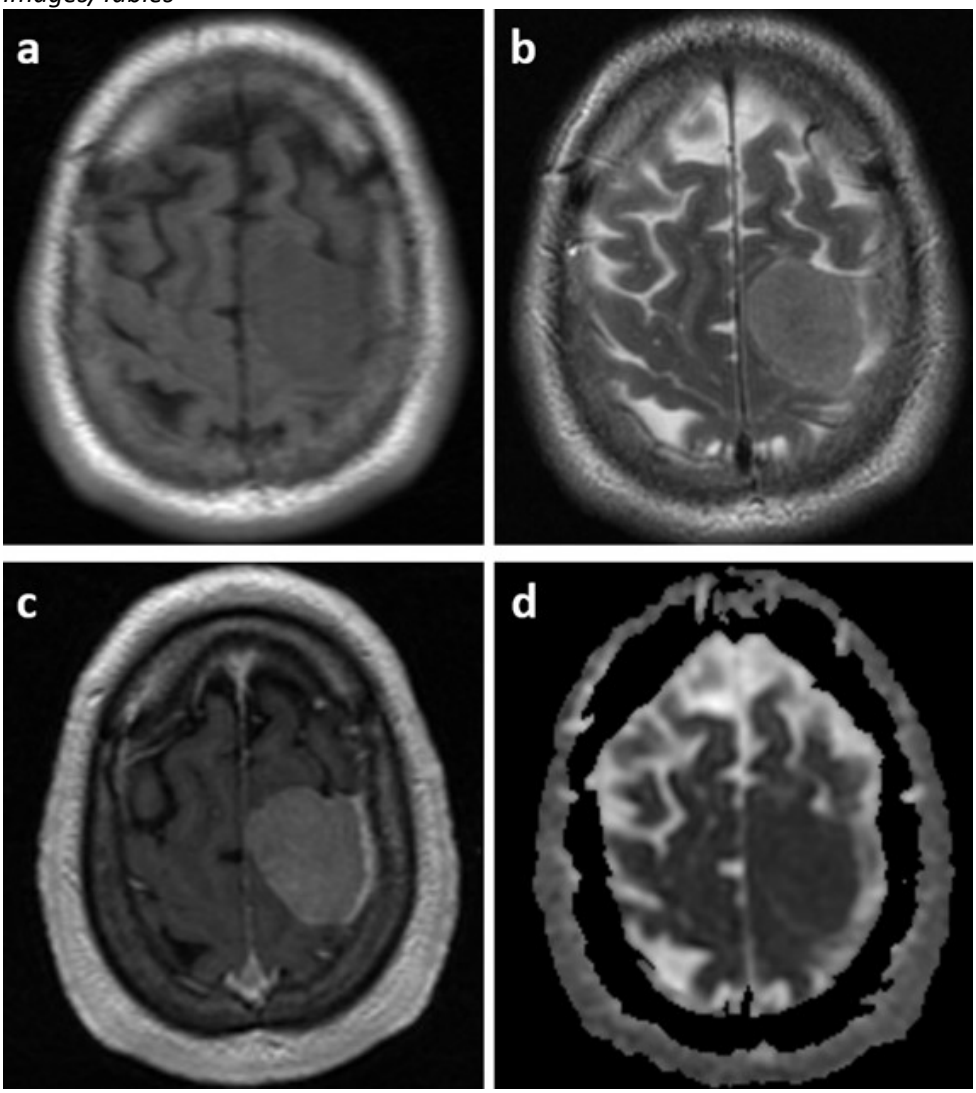
Here, we present one of the largest series of extranodal RDD of the CNS. The diagnosis of extranodal RDD of the CNS remains challenging, and the condition is often misdiagnosed as other dural-based neoplasms, such as meningioma, preoperatively. Extranodal RDD of the CNS often presents as an isolated disease of the CNS, compounding an already challenging diagnosis.

Figure: Axial T1-W (a), T2-W (b), and post-contrast T1-W (c) images demonstrate a T1 and T2 isointense, left frontal dural-based lesion with homogenous contrast enhancement mimicking meningioma. There is no obvious diffusion restriction on ADC map (d).

References

1. Luo Z, Zhang Y, Zhao P, Lu H, Yang K, Zhang Y, Zeng Y. Characteristics of Rosai-Dorfman Disease Primarily Involved in the Central Nervous System: 3 Case Reports and Review of Literature. World Neurosurg. 2017 Jan;97:58-63. doi: 10.1016/j.wneu.2016.09.084. Epub 2016 Sep 28. PMID: 27693766.
2. Raslan OA, Schellingerhout D, Fuller GN, Ketonen LM. Rosai-Dorfman disease in neuroradiology: imaging findings in a series of 10 patients. AJR Am J Roentgenol. 2011 Feb;196(2):W187-93. doi: 10.2214/AJR.10.4778. PMID: 21257861.
3. Elshikh M, Schellingerhout D, Rayan J, Taher A, Elsayes AK, Mujtaba B, Garg N. Disease Characteristics, Radiologic Patterns, Comorbid Diseases, and Ethnic Differences in 32 Patients With Rosai-Dorfman Disease. J Comput Assist Tomogr. 2020 May/Jun;44(3):450-461. doi: 10.1097/RCT.0000000000000983. PMID: 31972751.

Images/Tables



782

Unmasking Stroke Mimics: When Neoplasms Simulate Stroke

Yilmarie Mercado-Vargas M.D., Keerthi Arani M.D., Joseph Mettenburg M.D., Ph.D.
UPMC, Pittsburgh, PA, USA

Abstract Category

Interventional/Vascular/Stroke

Summary & Objectives

Strokes are medical emergencies characterized by sudden onset of focal neurological deficits caused by ischemic or hemorrhagic infarcts. If not recognized and treated promptly, it can lead to severe disability or even death. The typical imaging features of a stroke can vary depending on the type of imaging modality (CT vs MRI) and specific MRI sequences. Tumors may mimic strokes and have similar imaging features such as edema, mass effect, diffusion restriction, and contrast enhancement.

Purpose

The purpose of this educational exhibit is to highlight imaging features that can help differentiate strokes from stroke mimics, particularly neoplasms such as oligodendroglioma, other glial tumors, atypical lymphoma, metastatic disease, and plasma cell infiltration.

Materials & Methods

Case based reviews of stroke will show the expected maturation of infarcts on CT and MRI including features on DWI/ADC, T2, T2-FLAIR, T1, susceptibility weighted, and contrast enhanced T1 weighted imaging. The role of perfusion

weighted MRI and MR spectroscopy will be reviewed. We will discuss common pitfalls in diagnosing subacute infarcts versus neoplasm, especially when prior imaging is unavailable.

Results & Conclusion

A solid understanding of the imaging characteristics of both strokes and their neoplastic mimics is essential for making accurate and timely diagnoses.

References

Adam G, Ferrier M, Patsoura S, et al. Magnetic resonance imaging of arterial stroke mimics: a pictorial review. Insights into imaging 2018; 9:815-31. DOI: https://doi.org/10.1007/s13244-018-0637-y

784

Callosal Catastrophes: The Breakdown of the Corpus Callosum

Erik Balians[1], Humza Haque MD[2], Mariam Thomas MD[3], Jimmy Huang MD[3], Mariet Asadoorian[3], Michael Nguyen MD[3], Ryan Beck MB,BCh[3], Omid Jafari MD[3], Catherine Yim MD[3], Gasser Hathout MD[3]

[1]UCLA, Los Angeles, CA, USA. [2]Cedars Sinai Medical Center, Los Angeles, CA, USA. [3]Olive View-UCLA Medical Center, Sylmar, CA, USA

Abstract Category

Adult Brain Inflammatory/Infectious Disease/Degenerative/Metabolic

Summary & Objectives

The corpus callosum is a vital structure in the human brain, comprising a dense bundle of myelinated nerve fibers that bridge the left and right cerebral hemispheres. This connection facilitates interhemispheric communication, enabling the integration of sensory, motor, and cognitive functions. Remarkably, the corpus callosum contains approximately 200–300 million axonal projections, making it the largest white matter structure in the brain.

Its development begins in utero and continues into the third decade of life, underscoring its importance in neural maturation. Various pathologies can affect the corpus callosum, including congenital disorders, infections, demyelinating diseases, tumors, and infarcts. The clinical manifestations of these conditions often depend on the specific regions of the corpus callosum involved.

Objective:

• To provide a concise overview of the embryology and histology of the corpus callosum.
• To elucidate the blood supply and its variations pertinent to the corpus callosum.
• To examine the imaging characteristics of various pathologies that affect the corpus callosum.
• To review the functional anatomy of the corpus callosum, focusing on the neural tracts and symptoms associated with specific pathological processes

Purpose

The purpose of the exhibit is to provide a comprehensive review of the embryology, anatomy, blood supply (including variants), and diseases affecting the corpus callosum, along with the associated symptoms.

Materials & Methods

This exhibit will feature detailed illustrations depicting the embryology, histology, anatomy, and blood supply of the corpus callosum. A case-based format will be employed to explore various pathologies, their imaging appearances, and the clinical manifestations associated with diseases affecting the corpus callosum

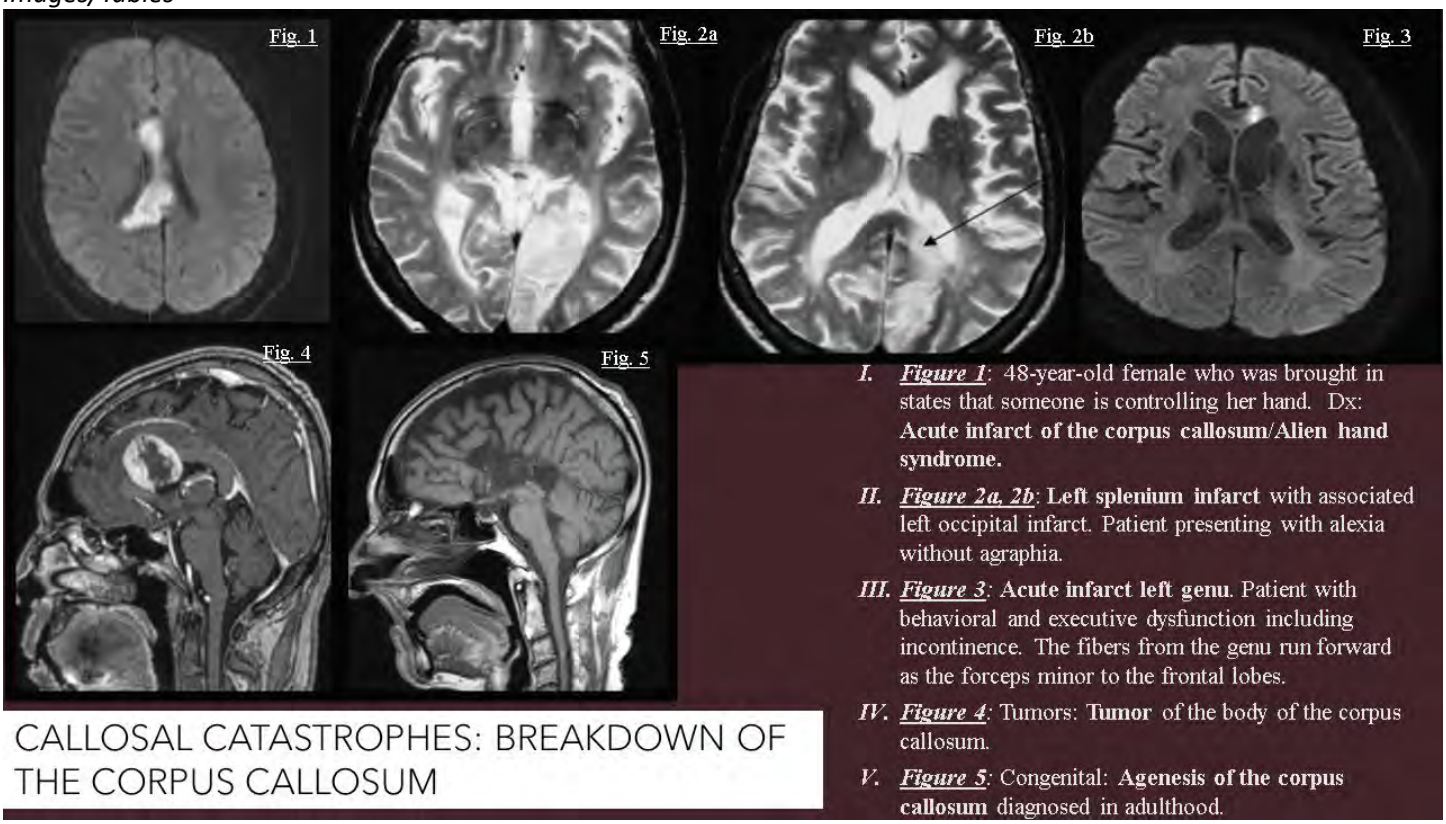
Results & Conclusion

Understanding the corpus callosum's intricate anatomy and its role in interhemispheric communication is crucial for diagnosing and managing conditions that disrupt its function. By comprehensively reviewing its development, vascular supply, and associated pathologies, this exhibit aims to enhance clinical awareness and improve patient outcomes related to corpus callosum disorders.

References

1. Hathout, G. M. *Clinical Neuroradiology: A case based approach*. Cambridge University Press; 2009.
2. Goldstein, A. . *Neuroanatomy, corpus callosum*. StatPearls [Internet]. https://www.ncbi.nlm.nih.gov/books/NBK448209/ Accessed November 5, 2024.
3. Reinarz SJ, Coffman CE, Smoker WR, Godersky JC. MR imaging of the corpus callosum: normal and pathologic findings and correlation with CT. *AJR Am J Roentgenol*. 1988;151(4):791-798. doi:10.2214/ajr.151.4.791

Images/Tables



785

The Radiological Spectrum of the Postoperative Spine: Pitfalls and Prognosis

David Plitt MD[1], Mohammed Qureshi[2], Isaac Botchey MPH MS[3], Dipesh Bhatt[2], Himanshu Katta MD[1], Steven Lev MD[1]
[1]NUMC, East Meadow, NY, USA. [2]AUC, Cupecoy, Cupecoy, Sint Maarten (Dutch part). [3]New York Institute of Technology, Old Westbury, NY, USA

Abstract Category

Spine

Summary & Objectives

1. To review the basic goals and principles of spine surgery for the neuroradiologist.
2. To recognize common and unusual postoperative complications in spine surgery
3. To identify radiologic signs of early and delayed complications to help guide timely intervention and prevent progression.

Purpose

To review and categorize imaging findings and complications encountered of the postoperative spine with an emphasis on the radiological workup and diagnostic challenges.

Materials & Methods

We retrospectively reviewed the imaging studies (CT and MR) for spine surgery patients presenting to the emergency department at our Level I Trauma Center during the past ten years. The relative advantages of different imaging modalities—radiographs, CT, MRI, and nuclear medicine scans—in evaluating the postoperative spine are discussed. Cases were selected based on documented postoperative complications, including neurological deficits, mechanical instability, infection, and construct failure. We organized our cases by complication etiology, highlighting patterns of injury.

Results & Conclusion

Results:

Postoperative spine complications were classified into four primary etiologies: mechanical, infectious, neurological, and alignment-related. Mechanical complications included hardware malposition, construct fractures, and pseudarthrosis. We illustrate examples of pedicle screws, rods and plates showing subtle shifts, loosening or failure. Early detection of pseudarthrosis and minor hardware displacement was essential to prevent further instability or deformity. Various

surgical procedures and their indications were examined, including vertebroplasty and the associated risk of cement leaks. Infectious complications were characterized by fluid collections, abscess formation, and delayed healing around hardware sites. MRI with contrast was effective in identifying abscesses and discitis-ostetomyelitis, while nuclear medicine scans helped confirm infection in equivocal cases. Neurological sequelae ranged from nerve root compressions to spinal cord injury, often associated with hardware malpositioning or postoperative alignment changes. Contrast MR was crucial in distinguishing epidural fibrosis from recurrent disk herniation. Alignment-related conditions included progressive kyphotic deformities and scoliosis, often exacerbated by pseudarthrosis or hardware failure. We also demonstrate bone graft malposition and cage migration (subsidence) as complications impacting long-term stability of the postsurgical construct.

Conclusion:

Recognizing postoperative spine complications is essential to prevent recurrent or worsening symptoms and progressive deformity. Radiologists must be adept in distinguishing normal from abnormal postoperative findings to help avert long-term complications.

References

1. Ghodasara N, Yi PH, Clark K, Fishman EK, Farshad M, Fritz J. Postoperative Spinal CT: What the Radiologist Needs to Know. RadioGraphics 2019 39:6, 1840-1861

Images/Tables



787

Extranodal Rosai-Dorfman Disease of the Head and Neck: A Pictorial Review of Your Friendly Tumor Mimic

Ceylan Altintas Taslicay MD, Heba Al Qudah MD, Samir Dagher MD, Richard Dagher MD, Ahmed Msherghi MD, Sahar Alizada MD, Alexander Khalaf Assistant Professor, Max Wintermark Professor, Maria Gule-Monroe Associate Professor
The University of Texas, MD Anderson Cancer Center, Houston, TEXAS, USA

Abstract Category

Head and Neck

Summary & Objectives

To review and illustrate the imaging characteristics of extranodal Rosai Dorfman Disease (RDD) in the head and neck (H&N), which can present with features mimicking aggressive neoplasms.

To demonstrate various extranodal RDD masses of the H&N by specific anatomic location in a case-based approach.
To discuss the differential diagnoses and emphasize the key imaging findings leading to correct diagnosis.

Purpose

RDD is a rare, idiopathic, and non-neoplastic histioproliferative disease. It can affect many organ systems, including nodal (70%) or extranodal (30%) sites. Extranodal involvement can occur anywhere in the body, including the H&N. It can exhibit imaging features that mimic aggressive neoplasms, creating a diagnostic challenge. Here, we do an image-rich review to present the CT, MRI, and 18F-FDG PET/CT imaging characteristics of extranodal RDD in the H&N, and comprehensively discuss differential diagnoses and key teaching points.

Materials & Methods

We retrospectively reviewed pathologically confirmed RDD cases seen at our institution from 2006 to 2024. Only extra nodal RDD cases were analyzed for anatomical locations and radiologic appearance. Also, the mimickers were recorded.

Results & Conclusion

23 cases of extranodal RDD in the H&N (15 female and 8 male, mean age 50.8 years [range 4-81]) were included. Specific sites of involvement included the following: pituitary, n = 1; lacrimal gland, n = 2; paranasal sinus, n = 4; salivary gland, n = 2; vocal cord, n=1; skin, n = 2; nasal cavity, n = 9; nasal septum, n=4; skull-base, n=3; nasopharynx, n=2, Meckel cave, n=1; hard palate, n=1; and clavicle, n = 1. Seven patients had isolated extranodal RDD disease, and the others also had lymph nodes and other organ involvements outside the H&N. The most affected site was the nasal cavity in extranodal RDD of the H&N.

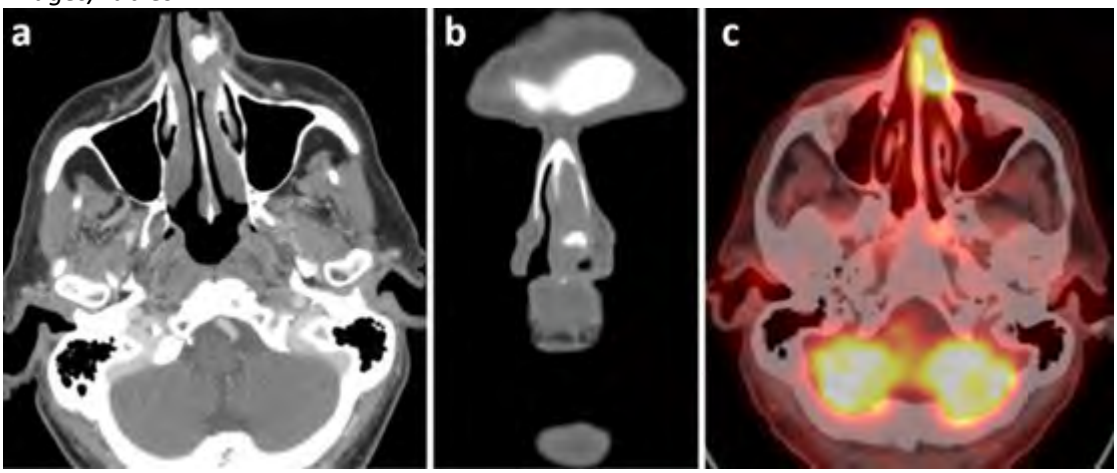
The clinical presentation and radiological imaging findings of extranodal RDD of the H&N overlap significantly with other neoplastic processes of the H&N. Although the diagnosis is challenging to make prospectively, including RDD in the differential when appropriate may help guide workup. PET/CT, in particular, is very helpful in evaluating the extent of the disease, and when there is involvement of multiple subsites, it can help increase the specificity of diagnosis.

Figure: Axial (a) and coronal (b) CT images of the sinuses demonstrate a soft tissue mass that occupies much of the lower left nasal cavity and nasal aperture, with more inferiorly, a calcific tumor component. PET-CT (c) reveals the hypermetabolic activity of this mass.

References

1. Raslan OA, Schellingerhout D, Fuller GN, Ketonen LM. Rosai-Dorfman disease in neuroradiology: imaging findings in a series of 10 patients. AJR Am J Roentgenol. 2011 Feb;196(2):W187-93. doi: 10.2214/AJR.10.4778. PMID: 21257861.
2. Xu Q, Fu L, Liu C. Multimodality imaging-based evaluation of Rosai-Dorfman disease in the head and neck: A retrospective observational study. Medicine (Baltimore). 2017 Dec;96(51):e9372. doi: 10.1097/MD.0000000000009372. PMID: 29390533; PMCID: PMC5758235.
3. Cao X, Yao B, Ma J, Li D, Wang L, Zhang J, Wu Z. Rosai-Dorfman Disease in the Skull Base: A Case Series Study. World Neurosurg. 2023 May;173:e351-e358. doi: 10.1016/j.wneu.2023.02.051. Epub 2023 Feb 14. PMID: 36796628.

Images/Tables



788

Artificial Intelligence: A Blessing or a Curse. Discussing Security Concerns of Diagnostic Models in Radiological Assessment

Ryan Marinelli PhD Fellow[1], Markus Lammle MD[2]
[1]University of Oslo, Oslo, Oslo, Norway. [2]SUNY, Syracuse, NY, USA

Abstract Category

New Techniques/Advanced Imaging/Informatics/AI/Professional Development/Misc

Summary & Objectives

Radiology is a field that drives off of innovation, thus it is readily adopting AI powered tools into workflows. Since radiologists are specialized in their own field, they may not understand the risks involved with using AI tools and possible vulnerabilities.

Due to the iterative nature of software, models are often retrained to stay relevant to various contexts. This additional input leaves models vulnerable as it provides an attack vector into sensitive systems. By crafting malicious input, it is possible to derail the performance of models. This issue has been investigated by applying adversarial attacks to a variety of data sources. One notable paper is [1] , where an adversarial patch was used to attack models classifying pneumonia and COVID-19. Likewise, in [2], a more subtle attack using single pixel manipulations is evaluated.

The concern with the literature is that analysis tends to evaluate an adversarial method across datasets, but not applying various methods to the same dataset. Given there are many imaging datasets, it is difficult to make a comparison on the effectiveness of the methods. For instance, comparing various flavors of MRI scans might not be so informative. By comparing multiple methods on the same dataset, the goal is to get a better understanding of the methodology within a more focused scope.

Purpose

To familiarize the reader with potential security concerns related to the use of artificial intelligence, and possible defenses.

Materials & Methods

The dataset evaluated is from the 2017 Pediatric Bone Age Challenge. This data was selected because the images differences in classes represent an ordinal variable. For instance, one could evaluate if the model is overestimating or underestimating bone age. Additionally, the data is more sparse and represents particular challenges for the model to learn.

The data is used to train a YOLO(You Only Look Once) model to perform the classification. The Fast Gradient Sign Method and Carlini Wagner methods are used to attack the data to determine how significantly performance is diminished is determined by Mean Average Precision on a validation dataset.

Results & Conclusion

Results

The model saw a drop in mAP when applying FGSM and Carlini Wagner. After FGSM, mAP dropped from 64% to 17%. With C&W, performance dropped to 12%. Less examples were needed using C&W to cause greater impact.

Conclusion

Carlini Wagner is more suited for attacks for a particular class of images. As it is more intensive, it may be more suitable for targeted attacks. FGSM may be more suitable for more broadly attacks within this domain as it is lighter but is less performant.

References

[1] Matsuo, Y., and Takemoto, K. (2021) "Backdoor Attacks to Deep Neural Network-Based System for COVID-19 Detection from Chest X-ray Images." *Applied Sciences* 11(20): 9556.

[2] Tsai, M.J., Lin, P.Y., and Lee, M.E. (2023) "Adversarial Attacks on Medical Image Classification." *Cancers* 15(17): 4228.

Images/Tables

Summary of Attacks

Type of Attack	Description	Impact on Model
Data Poisoning	Training data manipulation	Weakens performance
Model Inversion	Inferring information on meta-data from predictions	HIPPA concerns
Evasion Attacks	Misclassifying input	Could trick into wrong scan reads
Model Stealing	Reverse-Engineering the model	Stealing model
Backdoor	Embedding behavior in model	Weakens performance under specific conditions

790

The Corpus Callosum Through the Lifespan: A Comprehensive Imaging Review from Development to Disease.

Betoul G I Mukhayer MD[1], Rand Kaller[2], Jay Starkey MD[1]
[1]OHSU, Portland, Oregon, USA. [2]OHSU, Portland, OR, USA

Abstract Category

Adult Brain Inflammatory/Infectious Disease/Degenerative/Metabolic

Summary & Objectives

This educational exhibit aims to comprehensively review the embryology, anatomy and function of the corpus callosum and offer a comprehensive insight into its imaging findings, ranging from developmental anomalies like agenesis and lipomas to structural changes related to hydrocephalus and post shunting changes in corpus callosum impingement syndrome, and everything in between.

Purpose

To create a comprehensive and engaging educational tool that enhances the learner's repertoire, our exhibit spans an extensive range of corpus callosum topics, including embryological development, normal and abnormal anatomy, diverse disease processes, and post-procedural and post-surgical changes. This exhibit goes beyond standard reviews by delving into the imaging findings of pathologies with characteristic corpus callosum changes—from cytotoxic lesions to malignancies—and examining their potential prognostic significance across a wide array of intracranial conditions, from trauma (e.g., DAI) to multiple sclerosis. Unique features such as detailed exploration of enlarged perivascular spaces, insights into conditions like NPH and its diagnostic relevance through callosal angle measurement, DTI and it's relation, commissurotomy, and post-shunting changes will be included to provide added clinical value. We will also introduce

techniques for differentiating these pathologies, offering a memorable and engaging approach to understanding the differential diagnosis of corpus callosum lesions while emphasizing the central (pun intended) importance of this structure in neuroradiology.

Materials & Methods

Searching our departmental PACS using a custom AI search tool and personal case collections, we have found excellent images representative of each entity. We present information in an unknown case format to increase learning and engagement.

Outline: Corpus Callosum Imaging and Related Pathologies

I. Embryology and Anatomy

- Embryology
- Anatomy

II. Congenital or Hereditary Anomalies

- Callosal agenesis/partial agenesis, related entities. Radiology signs: colpocephaly, Probst bundles, Texas long horn /moose head/ viking helmet/ racing car
- Septo-Optic Dysplasia / Optic Nerve Hypoplasia
- Interhemispheric cysts with callosal agenesis
- Callosal lipomas
- Leukodystrophies (adrenoleukodystrophy, metachromatic leukodystrophy)

III. Acquired Variations, Abnormalities and Pathologies

- Enlarged Virchow-Robin spaces
- Infarction
- Diffuse Axonal Injury
- Cytotoxic Lesions of the Corpus Callosum
- Demyelination/multiple sclerosis
- Glioblastoma
- Lymphoma
- Wallerian degeneration
- Alterations in DTI in various pathologies

IV. Procedural Considerations

- Commissurotomy
- Callosal signal changes or cysts in shunting
- Callosal angle in NPH (and practical measurement)

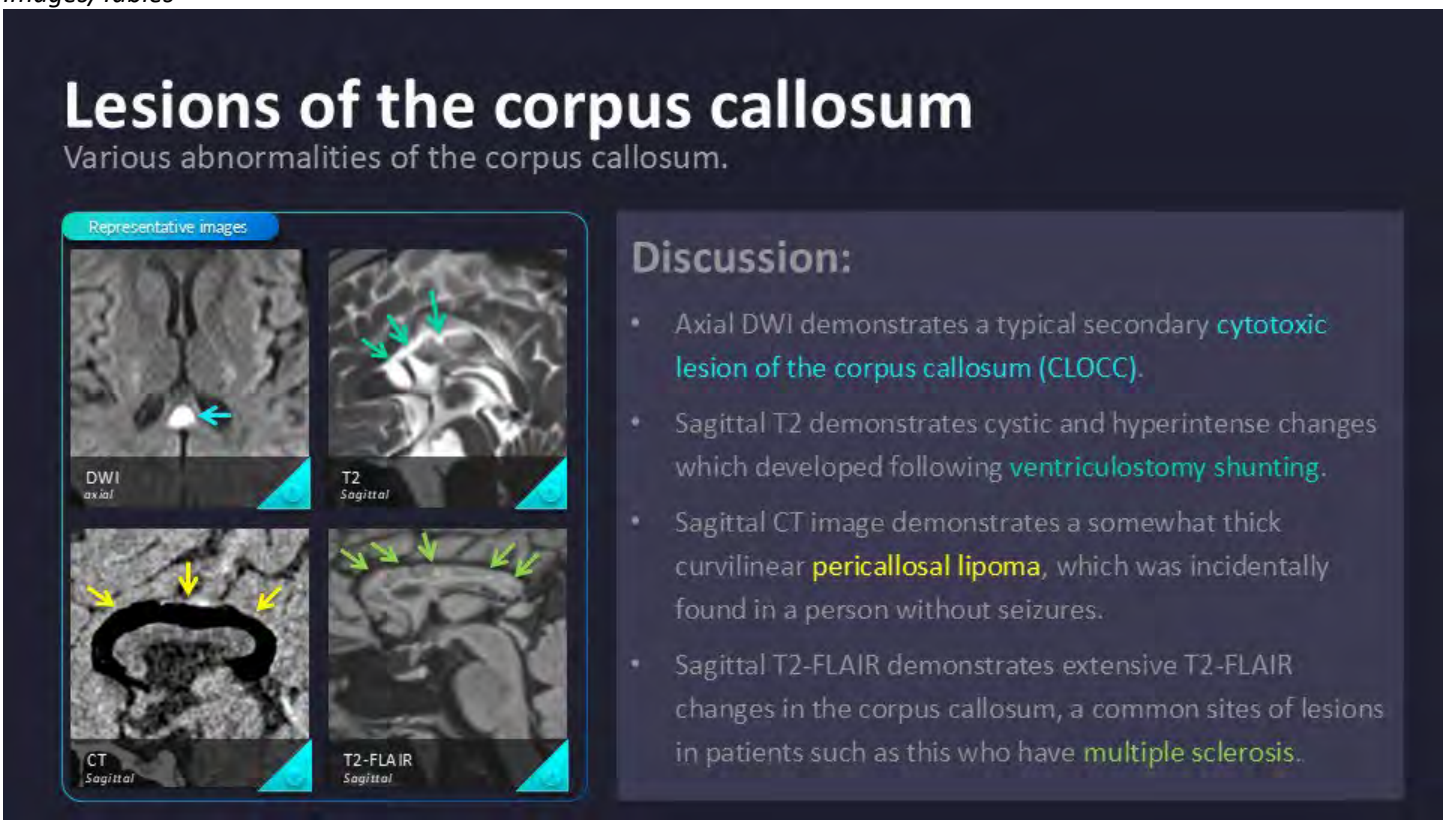
Results & Conclusion

Many intracranial conditions, whether congenital or acquired from trauma, inflammation, or malignancy, can involve the corpus callosum. Recognizing and understanding the imaging of the normal and abnormal corpus callosum is important for guiding clinical teams to accurate diagnosis and effective patient management.

References

1. Cho NS, Jenabi M, Arevalo-Perez J, et al. Diffusion Tensor Imaging Shows Corpus Callosum Differences between High-Grade Gliomas and Metastases. J Neuroimaging. 2018;28(2):199-205. doi:10.1111/jon.12478
2. Hetts SW, Sherr EH, Chao S, Gobuty S, Barkovich AJ. Anomalies of the Corpus Callosum: An MR Analysis of the Phenotypic Spectrum of Associated Malformations. American Journal of Roentgenology. 2006;187(5):1343-1348. doi:10.2214/AJR.05.0146
3. Ho ML, Moonis G, Ginat DT, Eisenberg RL. Lesions of the Corpus Callosum. American Journal of Roentgenology. 2013;200(1):W1-W16. doi:10.2214/AJR.11.8080
4. Starkey J, Kobayashi N, Numaguchi Y, Moritani T. Cytotoxic Lesions of the Corpus Callosum That Show Restricted Diffusion: Mechanisms, Causes, and Manifestations. RadioGraphics. 2017;(In Publication).
5. Yang Y, Fischbein N, Chukus A. Differential Diagnosis of Corpus Callosum Lesions: Beyond the Typical Butterfly Pattern. RadioGraphics. 2021;41(3):E79-E80. doi:10.1148/rg.2021200146

Images/Tables



794

Post Treatment Complications in Patients with Head and Neck Cancers: A Primer for Radiologists.

Seyed Mohammad Gharavi MD[1], Melissa kang MD[1], Yang Tang MD[1], Lazar Jankovic MD[2]
[1]Virginia Commonwealth Univerisity, Richmond, VA, USA. [2]Virginia Commonwealth University, Richmond, VA, USA

Abstract Category

Head and Neck

Summary & Objectives

Malignancies of the head and neck are often treated with surgery, radiation therapy, chemotherapy or immunotherapy. In addition to expected post treatment changes, different less frequent complications can occur depending on the methods of treatment. Familiarity with these complications can help the radiologists more accurately interpret follow up scans.

Purpose

To briefly review some of the most common complications of surgery and radiation in patients with head and neck cancer.

Materials & Methods

Example of the cases which will be shown are:
Mandible osteoradionecrosis, thyroid and arytenoid chondronecrosis, necrosis of the reconstruction graft, necrosis of the neopharynx and pre-vertebral abscess.

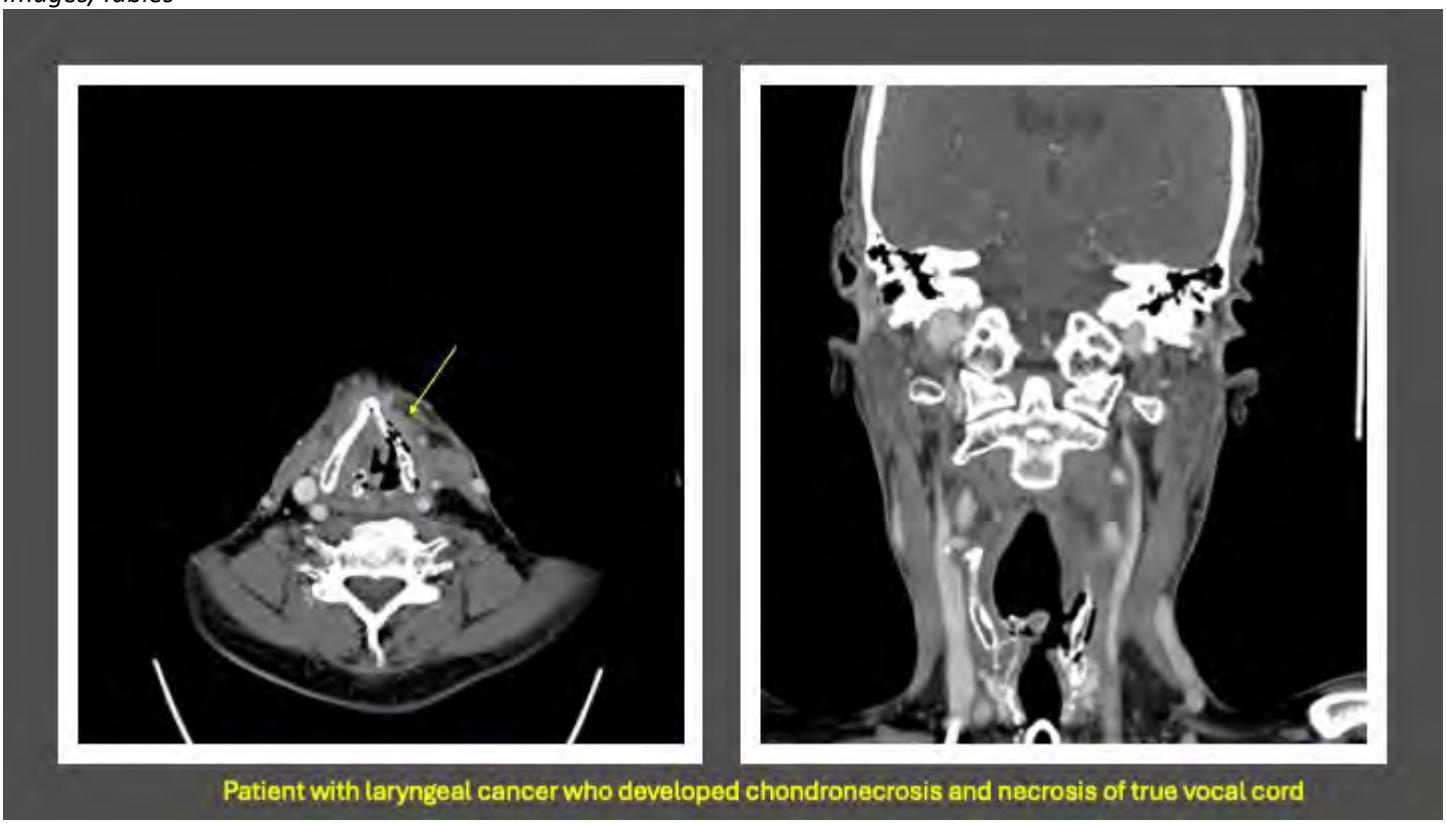
Results & Conclusion

This review highlights the complexities in distinguishing between expected treatment effects and less frequent but more serious complications.

References

Brahmbhatt S, Overfield CJ, Rhyner PA, Bhatt AA. Imaging of the Posttreatment Head and Neck: Expected Findings and Potential Complications. Radiol Imaging Cancer. 2024 Jan;6(1):e230155. doi: 10.1148/rycan.230155.

Images/Tables



797

Imaging of Orbital Emergencies

Mohammed Usman Syed BS[1], Tausif Siddiqui BS[1], Steve J Stephen MBA[1], Zahin Alam BS[2], Hunter R Carlock MD[3], Zissan Sarwardhi MBBS[4], Akm A Rahman MD;DO[3]

[1]University of Rochester School of Medicine and Dentistry, Rochester, NY, USA. [2]Hackensack Meridian School of Medicine, Nutley, NJ, USA. [3]University of Rochester Medical Center, Imaging Sciences, Rochester, NY, USA. [4]Dhaka Medical College and Hospital, Dhaka, Bangladesh, Bangladesh

Abstract Category

Head and Neck

Summary & Objectives

There are 2.5 million eye injuries annually accounting for 3% of all ED visits in the US. Clinical examination of orbital emergencies may be limited by edema and accompanying injuries. Therefore, imaging is essential to assess for signs of orbital fractures, foreign bodies, or occult globe rupture. The first-line imaging modality is CT with contrast of the facial bones and orbits, which is highly sensitive for orbital fracture detection, while providing a rapid assessment of orbital soft tissues, the ocular globe, and the intra-orbital space. MRI is limited in emergent orbital evaluation due to longer acquisition times and the potential for the presence of metallic foreign bodies, but remains useful for assessment of optic neuritis, non-radiopaque foreign bodies as well as retinal and choroidal detachments. The orbit, formed by seven bones, houses the eye and associated structures including the optic nerve, extraocular muscles, lacrimal gland, and orbital fat. Without urgent diagnosis and treatment, orbital emergencies involving these structures may lead to loss of vision.

Educational Objectives

1. Review the normal orbital anatomy and associated structures.
2. Present a case collection of orbital emergencies including endophthalmitis, ruptured globe, foreign body, retrobulbar hemorrhage, optic nerve injury, and orbital fracture.
3. For each case presented, provide a discussion of the epidemiology, presentation, anatomic involvement, imaging modalities, unique imaging features, and management.

Purpose

In this educational exhibit, we will present a case collection of orbital lesions with a discussion of the aforementioned features and an emphasis on the imaging features associated with worrisome lesions requiring urgent attention to prevent loss of vision.

Materials & Methods

Images of presented cases will be drawn from our institutional server and de-identified prior to presentation.

Results & Conclusion

Key Clinical and Imaging Features

Orbital compartment syndrome (OCS) due to trauma or hemorrhage may lead to ischemia of the optic nerve and retina. OCS may present with eye pain, reduced vision, and swelling. Diagnosis involves tonometry, fundoscopy, and CT imaging. Treatment includes cantholysis.

Endophthalmitis is a rare inflammation of the vitreous humor, caused by bacterial or fungal infection or noninfectious factors. Symptoms include corneal haziness and decreased vision. Treatment may include antibiotics, antifungals, and vitrectomy.

Orbital fractures may lead to ocular muscle entrapment, globe rupture, or retrobulbar hematoma. Symptoms include pain, swelling, and restricted ocular movement. Treatment may involve surgery, decongestants, and corticosteroids to reduce swelling.

Orbital foreign bodies may cause damage, infection, and vision loss. Diagnosis involves CT imaging to assess ferromagnetic objects and possible MRI for non-radio-opaque objects. Surgical removal is often required to prevent damage to surrounding structures.

Symptoms of optic nerve injury include headache, nausea, and unilateral vision impairment. Diagnosis involves fundoscopy and CT imaging. Treatment includes observation, corticosteroids, or surgery.

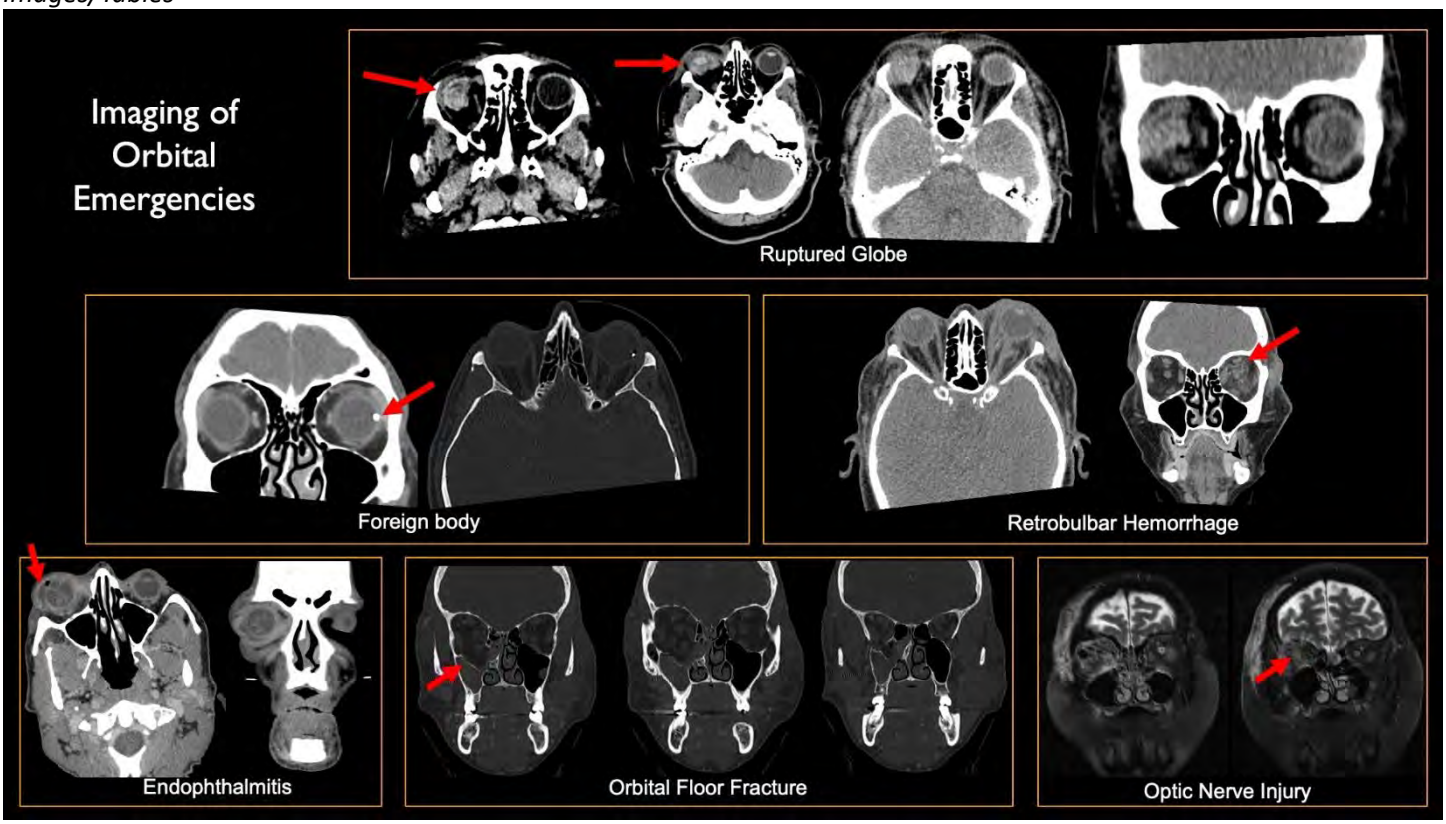
Conclusion

The orbit is a small pyramidal space with complex anatomy and critical structures that may be impacted by traumatic and nontraumatic orbital emergencies. Therefore, urgent imaging to evaluate the extent of orbital structure involvement is crucial for early detection of underlying injuries or pathological processes to prevent significant morbidity and potential loss of vision.

References

1. Cellina M, Cè M, Marziali S, Irmici G, Gibelli D, Oliva G, Carrafiello G. Computed tomography in traumatic orbital emergencies: a pictorial essay-imaging findings, tips, and report flowchart. Insights Imaging. 2022 Jan 12;13(1):4. doi: 10.1186/s13244-021-01142-y. PMID: 35022818; PMCID: PMC8755868.
2. Chazen JL, Lantos J, Gupta A, Lelli GJ Jr, Phillips CD. Orbital soft-tissue trauma. Neuroimaging Clin N Am. 2014 Aug;24(3):425-37, vii. doi: 10.1016/j.nic.2014.03.005. PMID: 25086805.
3. Perez FA. Imaging of Nontraumatic Orbital and Neuro-ophthalmological Emergencies. Semin Roentgenol. 2020 Apr;55(2):132-149. doi: 10.1053/j.ro.2019.11.004. Epub 2019 Nov 16. PMID: 32438976.
4. McCallum E, Keren S, Lapira M, Norris JH. Orbital Compartment Syndrome: An Update With Review Of The Literature. Clin Ophthalmol. 2019 Nov 7;13:2189-2194. doi: 10.2147/OPTH.S180058. PMID: 31806931; PMCID: PMC6844234.

Images/Tables



801

Jugular foramen lesions: what an unusual case can teach us

Matheus Carlota, Barbara Pfluck, Fernanda V Pereira, Bianca Franca, Vitor Lima, Marcos Marins
Campinas, SP, Brazil

Abstract Category

Adult Neoplasms/Epilepsy/Trauma

Summary & Objectives

Summary:

This study focuses on the radiological evaluation of lesions involving the jugular foramen, a critical anatomical region located at the base of the skull. These lesions may arise from various etiologies, including tumors, infections, and vascular anomalies, often presenting diagnostic challenges due to their complex anatomy and proximity to vital structures such as cranial nerves and blood vessels. Using advanced imaging techniques, including contrast-enhanced CT and MRI, we conducted a comprehensive analysis of the clinical and radiological features of these lesions. Our findings highlight the role of radiologic imaging in the accurate diagnosis and preoperative planning for surgical interventions.

Objectives:

1. To identify the different types of lesions affecting the jugular foramen, their radiological characteristics, and associated clinical features.
2. To assess the role of multimodal imaging techniques, particularly CT and MRI, in evaluating jugular foramen lesions.
3. To discuss the diagnostic challenges and surgical implications of these lesions, emphasizing their impact on treatment planning and patient outcomes.

Purpose

To enhance the understanding of lesions involving the jugular foramen and to underscore the importance of advanced neuroimaging techniques in their diagnosis. These lesions, though rare, can have significant clinical implications due to their anatomical location and potential to affect critical neural and vascular structures. By systematically reviewing a series of cases, this research aims to contribute to improving diagnostic accuracy and providing valuable insights for clinicians and neuroradiologists. Ultimately, our goal is to refine diagnostic strategies and guide more effective, tailored treatment plans for patients with jugular foramen lesions.

Materials & Methods

A case of neurofibromatosis type 1 (NF1) with meningocele encroaching upon the jugular foramen was used as the primary reference for this study. This case provided a framework for analyzing and comparing other lesions affecting the jugular foramen. We performed a retrospective review of imaging studies (CT and MRI) with lesions involving the jugular foramen. The imaging features of these lesions were systematically compared, focusing on distinguishing characteristics such as tumor margins, internal structure, contrast enhancement, and relationship to adjacent vascular and bony structures. The cases reviewed include jugular glomus tumors, metastatic lesions, high jugular bulb anomalies, jugular diverticula, endolymphatic sac tumors, schwannomas, and meningiomas. Special attention was given to the differential imaging features that allow for the accurate diagnosis of these conditions and to highlight distinguishing factors between benign and malignant lesions in this region.

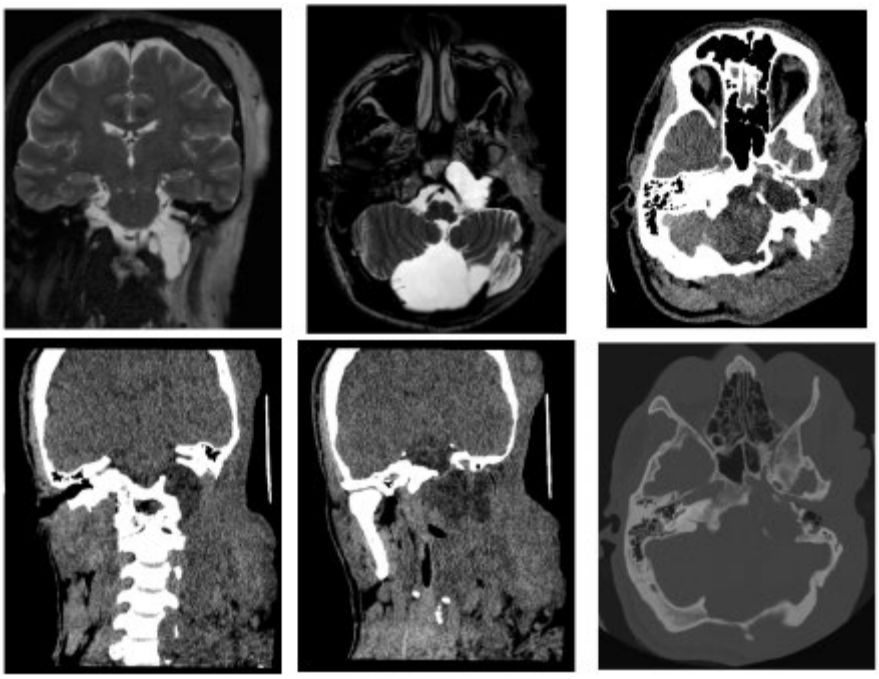
Results & Conclusion

Recognizing the differing patterns of bone destruction linked to these lesions is crucial for accurate differential diagnosis. This exhibit aims to enhance knowledge in neuroradiology by providing a systematic approach to evaluating jugular foramen lesions, highlighting the importance of radiological features that assist in distinguishing between various pathological conditions.

References

Vogl TJ, Bisdas S. Differential diagnosis of jugular foramen lesions. Skull Base. 2009 Jan;19(1):3-16. doi: 10.1055/s-0028-1103121. PMID: 19568338; PMCID: PMC2637573.

Images/Tables



803

Visualizing the Unseen: A Simplified Approach to MRI for Retinoblastoma

Pavan K. Kottamasu MD, MBA[1], Hunter Carlock MD[1], Priya R. Gupta MD[2], Sankarsh Jetty MD[1], Jeevak Almast MD[1], Ashwani K. Sharma MD[1], Steven P. Meyers MD, PhD[1], Shehanaz Ellika MD[1]

[1]The University of Rochester Medical Center, Rochester, NY, USA. [2]Cornerstone Eye Associates, Rochester, NY, USA

Abstract Category

Pediatrics

Summary & Objectives

Retinoblastoma (RB) is the most common intraocular malignancy of young children, with most cases diagnosed prior to age 2. The most common presentation of RB is leukocoria (abnormal whitening of the retinal red reflex). Other signs and symptoms of RB include behavior concerning for reduced vision, strabismus, eye redness, and eye pain. On fundus examination, RB classically presents as one or multiple nodular, white/cream-colored masses often associated with increased vascularity. Although ophthalmology can assess whether RB is endophytic or exophytic, whether it involves

the anterior chamber, or has associated vitreous seeding and retinal detachment, cross-sectional imaging is imperative to assess the extent of tumor invasion, presence of additional synchronous or metachronous intracranial tumors, and leptomeningeal seeding.

Although computed tomography (CT) can help identify calcifications in RB, it is contraindicated when RB is suspected, as it exposes patients with germline mutations to radiation, increasing the risk of secondary malignancies. Magnetic resonance imaging (MRI) is the ideal imaging modality to evaluate for optic nerve involvement, extraocular extension, presence of additional synchronous or metachronous intracranial tumors in the pineal and suprasellar regions, and leptomeningeal seeding. Once the patient is adequately staged, ophthalmology can select from a variety of therapies with or without adjuvant chemotherapy, depending on the extent of tumor invasion.

Our educational exhibit aims to tackle the following objectives:

1. Review the key points in imaging diagnosis and management of RB.
2. Discuss MR imaging protocols and sequences to include in an exam to adequately assess RB, including the role of diffusion weighted imaging and heavily T2 weighted sequences.
3. Present examples of common findings seen with RB, including pre- and post-laminar optic nerve invasion; choroidal, scleral, and/or extra-scleral invasion; iris neovascularization; vitreous seeding; and presence of trilateral or quadrilateral retinoblastoma.
4. Define and grade the severity and extent of RB using MR findings.
5. Review the role of intra-arterial chemotherapy in RB.
6. Discuss common findings in postoperative imaging of the orbit following enucleation.

Purpose

Retinoblastoma can be challenging to evaluate on MRI. The purpose of our educational exhibit is to provide a simplified approach for neuroradiologists to protocol and interpret RB studies.

Materials & Methods

Teaching examples were created utilizing MR images of various RB patients along with their post operative imaging from our home institution's picture archiving and communication system (PACS).

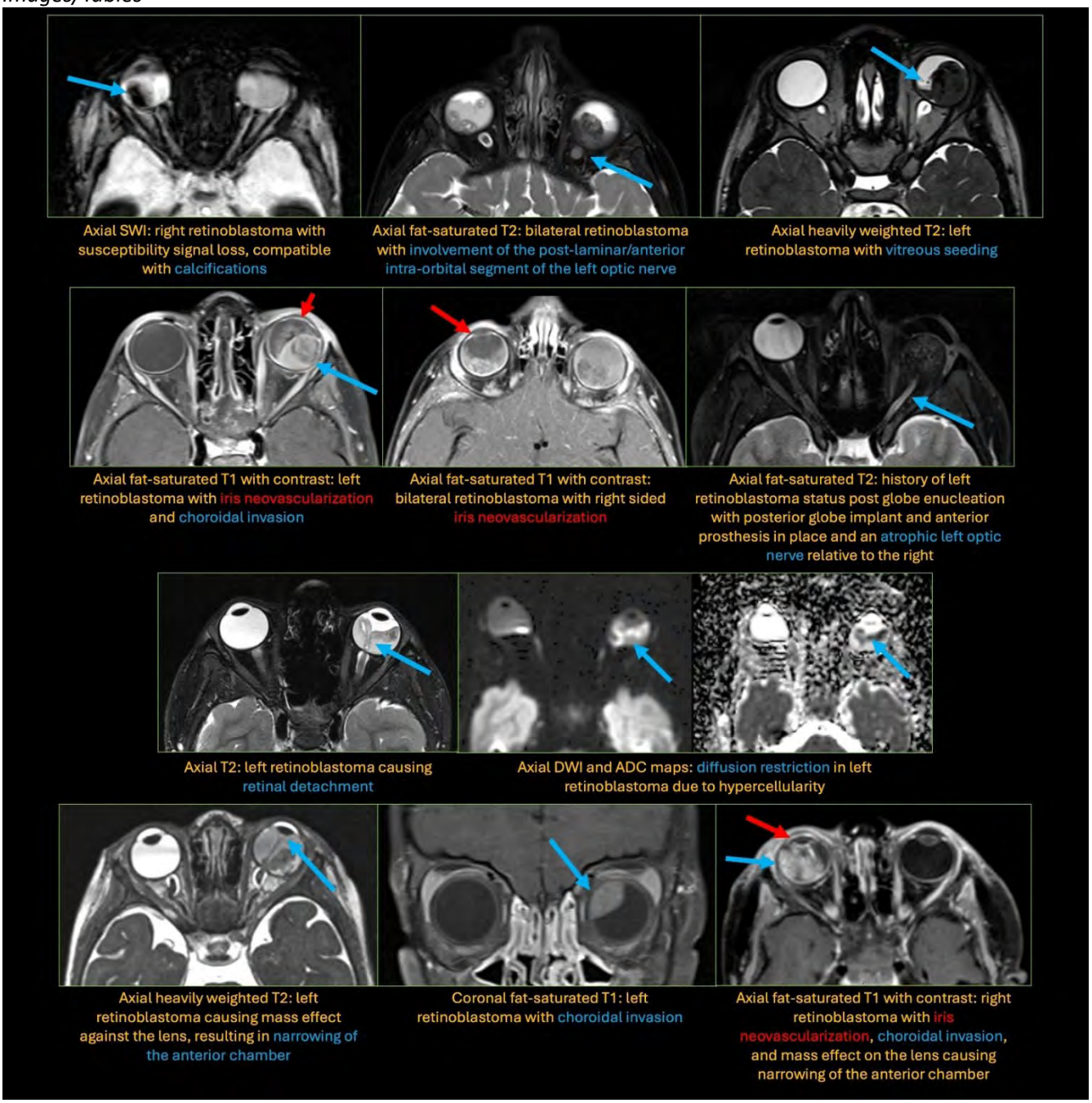
Results & Conclusion

Through this educational exhibit, we will showcase the imaging appearances of RB, imaging protocols to adequately image the globe and brain with additional MR imaging sequences, discuss the role of intra-arterial chemotherapy, and the imaging appearances following globe enucleation.

References

1. Razek AA, Elkhamary S. MRI of retinoblastoma. *Br J Radiol*. 2011 Sep;84(1005):775-84. DOI: 10.1259/bjr/32022497.
2. de Graaf P, Göricke S, Rodjan F, et al; European Retinoblastoma Imaging Collaboration (ERIC). Guidelines for imaging retinoblastoma: imaging principles and MRI standardization. *Pediatr Radiol*. 2012 Jan;42(1):2-14. DOI: 10.1007/s00247-011-2201-5.
3. Pai V, Muthusami P, Ertl-Wagner B, et al. Diagnostic Imaging for Retinoblastoma Cancer Staging: Guide for Providing Essential Insights for Ophthalmologists and Oncologists. *Radiographics*. 2024 Apr;44(4):e230125. DOI: 10.1148/rg.230125. Erratum in: *Radiographics*. 2024 Apr;44(4):e249003. DOI: 10.1148/rg.249003. PMID: 38451848.
4. Abramson DH, Marr BP, Dunkel IJ, et al. Intra-arterial chemotherapy for retinoblastoma in eyes with vitreous and/or subretinal seeding: 2-year results. *Br J Ophthalmol*. 2012 Apr;96(4):499-502. DOI: 10.1136/bjophthalmol-2011-300498.
5. Gobin YP, Dunkel IJ, Marr BP, et al. Intra-arterial chemotherapy for the management of retinoblastoma: four-year experience. *Arch Ophthalmol*. 2011 Jun;129(6):732-7. DOI: 10.1001/archophthalmol.2011.5.

Images/Tables



814

Neuroimaging in Lyme Disease: Characterizing Subtle and Atypical Signs of Neuroborreliosis

Aditya Duhan MD[1], FNU Vaibhav MBBS[2], Hirohiko Ito MD[1], Simran Singh Cheema MD[3], Rajiv Mangla MD[1], Vipul Kaliraman MBBS[4], Amar Swarnkar MD[1]

[1]State University of New York Upstate Medical University, Syracuse, NY, USA. [2]Pt. B.D. Sharma PGIMS, Rohtak, Haryana, India. [3]University of alabama, Birmingham, Alabama, USA. [4]Maulana Azad Medical College, New Delhi, New Delhi, India

Abstract Category

Adult Brain Inflammatory/Infectious Disease/Degenerative/Metabolic

Summary & Objectives

Lyme disease, a tick-borne infection caused by Borrelia burgdorferi, can manifest as neuroborreliosis, with rare cerebral vasculitis presentations. This type of vasculitis can affect various cranial nerves, nerve roots, and cerebral vessels, leading to diverse imaging findings. Identifying these patterns is crucial to differentiate Lyme-related vasculitis from other CNS pathologies, and guiding appropriate management. We present a series of cases illustrating the imaging

features of Lyme disease-induced vasculitis in the brain, with emphasis on manifestations such as cranial nerve enhancement, vascular involvement, and parenchymal changes on MRI.

Purpose

This pictorial essay aims to provide a comprehensive overview of the neuroimaging spectrum associated with Lyme disease-related cerebral vasculitis. By illustrating the variable presentation and specific imaging characteristics, we aim to facilitate early and accurate diagnosis, allowing for effective differentiation from other causes of CNS vasculitis and demyelinating diseases.

Materials & Methods

A retrospective review of MRI findings from confirmed cases of neuroborreliosis with vasculitis was performed. Imaging modalities included T1-weighted and T2-weighted MRI, FLAIR, gadolinium-enhanced sequences, diffusion-weighted imaging (DWI), and MR angiography. Key features were evaluated in each case, focusing on nerve enhancement, parenchymal involvement, and vessel wall changes.

Results & Conclusion

Imaging findings demonstrated a range of presentations in Lyme disease-associated vasculitis:

Cranial Nerve Enhancement: Bilateral trigeminal, facial, and oculomotor nerve enhancements were identified.

Vascular Involvement: Vessel wall enhancement indicative of inflammation and vascular changes, with focal stenosis or vessel narrowing, was observed.

Parenchymal Changes: Hyperintensities in the white matter, brainstem involvement, and cerebellar changes were noted, highlighting the variable presentation.

Spinal Involvement: In cases with Lyme-associated Guillain-Barré syndrome, enhancement of ventral nerve roots was observed in the thoracic spine.

Conclusion: This pictorial essay provides an necessary visual guide to recognizing the neuroimaging patterns associated with Lyme disease-related vasculitis. Early diagnosis and differentiation from other CNS inflammatory conditions are critical for timely intervention and management, potentially preventing long-term neurological complications.

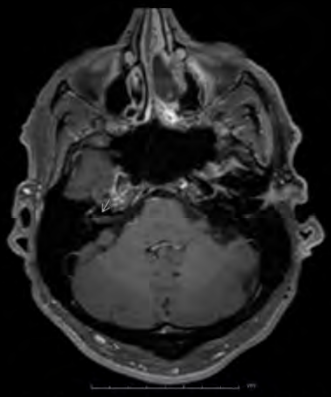
References

1. Lindland ES, Solheim AM, Andreassen S, et al. Imaging in Lyme neuroborreliosis. Insights Imaging 2018;9:833–44
2. Agarwal R, Sze G. Neuro-Lyme Disease: MR Imaging Findings. Radiology 2009;253:167–73

Images/Tables

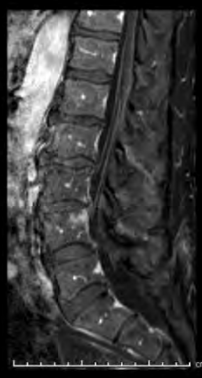


Case of Lyme disease showing enhancement of bilateral trigeminal nerves.



Enhancement in the region of the right geniculate ganglion without obvious thickening of the facial nerve. Findings concerning for infection or inflammation, later proven case of lyme disease.

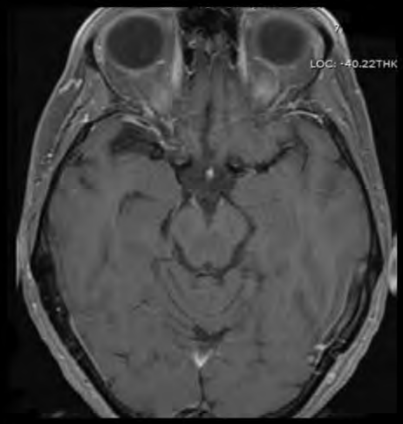
A



B



A & B: Lyme Guillain-Barre syndrome showing enhancement of the ventral nerve roots throughout multiple levels of the thoracic spine.



Lyme disease showing enhancement of bilateral oculomotor nerves.

816

MR Neurography of the Trigeminal Nerve: How We Do It.

Armaghan Faghihimehr MD[1], Seyed Mohammad Gharavi MD[1], Josephina Vossen MD[1], Yujie Qiao MD[1], Fatima Kadiri MD[2]
[1]Virginia Commonwealth University, Richmond, VA, USA. [2]Virginia commonwealth university, Richmond, VA, USA

Abstract Category

Head and Neck

Summary & Objectives

MR neurography is an imaging method to visualize and asses peripheral nerves. it can be used to evaluate nerve entrapment, tumors, traumatic injury or neuralgia. Unlike electro diagnostic studies , MR neurography can determine the exact site of pathology. A few studies have shown usefulness of MR neurogrphy in evaluation of inferior alveolar and lingual nerves.

Purpose

To discuss the sequences and specifications of MR neurography of the Trigeminal nerves.

To show some examples of Trigeminal nerve pathologies which can be detected by this technique.

Materials & Methods

Different sequences and specifications of trigemminal nerve MR neurogrphy will be discussed. Several pathologies of trigeminal nerve decide by this imaging method will be shown.

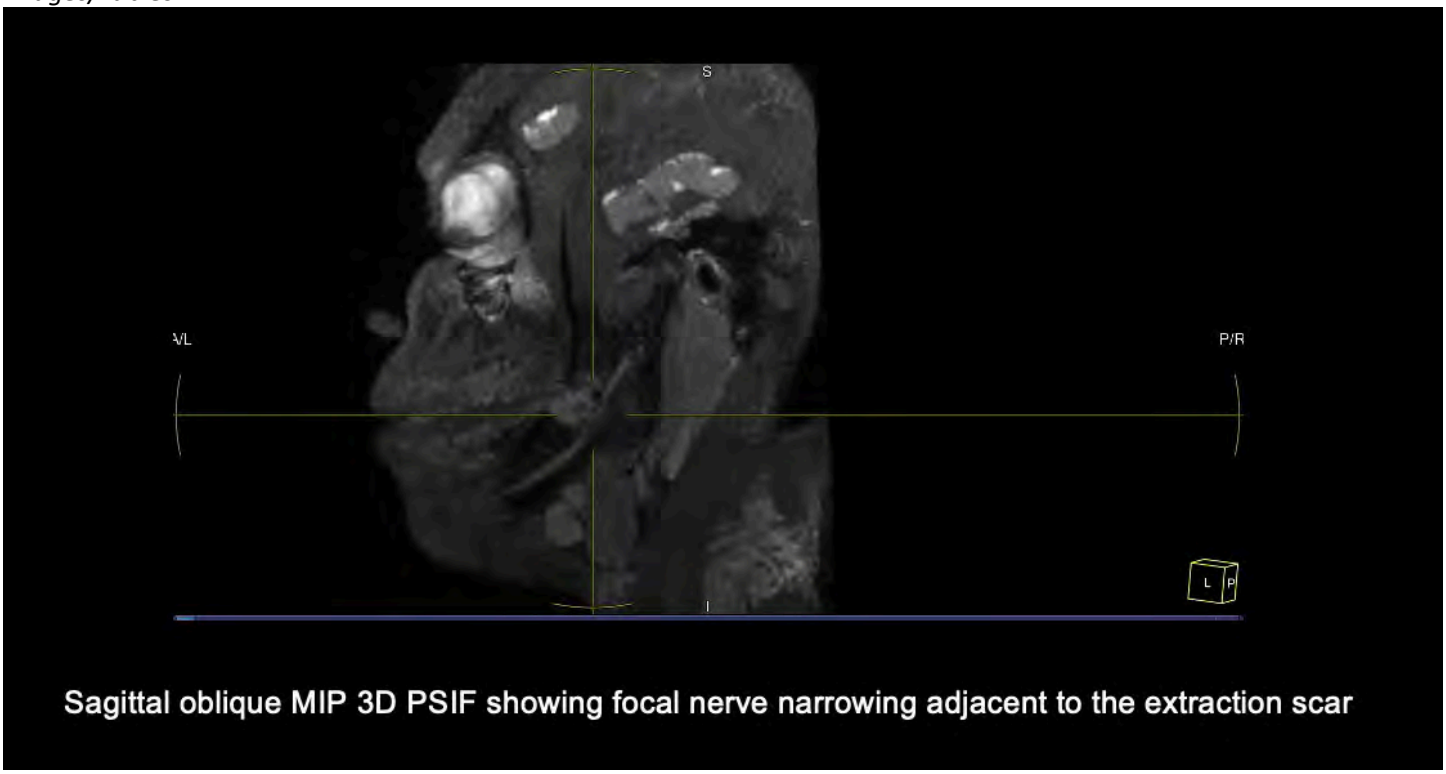
Results & Conclusion

MR neurography is a useful method in detecting trigeminal nerve pathologies.

References

Van der Cruyssen F, Croonenborghs TM, Renton T, Hermans R, Politis C, Jacobs R, Casselman J. Magnetic resonance neurography of the head and neck: state of the art, anatomy, pathology and future perspectives. Br J Radiol. 2021 Mar 1;94(1119):20200798. doi: 10.1259/bjr.20200798.

Images/Tables



Sagittal oblique MIP 3D PSIF showing focal nerve narrowing adjacent to the extraction scar

820

CAR T-Cell Related Neurotoxicity: What the Neuroradiologist Needs to Know

Simon Doran MB BCh BAO[1], Michael Courtney MB BCh BAO[2], Hannah Cherniawsky MD MSc[3], Farahna Sabiq MD[1]
[1]Division of Neuroradiology, Department of Radiology, University of British Columbia, Vancouver, BC, Canada. [2]Department of Radiology, St James's Hospital, Dublin, Dublin, Ireland. [3]Leukemia/BMT Program of British Columbia, Vancouver General Hospital, Vancouver, British Columbia, Canada

Abstract Category

Adult Brain Inflammatory/Infectious Disease/Degenerative/Metabolic

Summary & Objectives

Chimeric antigen receptor (CAR) T-Cell systemic immunotherapy is a novel treatment increasingly used to treat hematologic malignancies. Neurotoxicity is a common complication of the therapy and in a small number of cases can be fatal[1]. Neuroradiologists play a critical role in detecting CAR-T related neurotoxicity, in excluding other causes of neurological deterioration and in guiding clinical management decisions. In this educational review, we will explore CAR-T Cell therapy neurotoxicity and focus on what the neuroradiologist needs to know in current clinical practice.

Purpose

This review will educate Neuroradiologists on the basic pathophysiology of CAR T-Cell neurotoxicity. We will outline optimal imaging modalities and protocols for detecting neurotoxicity in patients post CAR T-cell therapy, emphasizing the role of MRI. We will improve recognition of CAR T-Cell neurotoxicity by highlighting the imaging features and clinical manifestations of neurotoxicity associated with CAR T-cell. Finally, we will familiarize neuroradiologists with the clinical grading system used, facilitating effective communication with hematologists-oncologists and intensivists.

Materials & Methods

This educational exhibit draws on a literature review of current up-to-date practice in CAR T-Cell immunotherapy, as well as our own clinical experience in a CAR T-Cell immunotherapy centre. We will present imaging from cases at our institutions to highlight the radiological features.

Results & Conclusion

The most common CAR T-Cell immunotherapy neurotoxicity complication is immune effector cell-associated neurotoxicity syndrome (ICANS). ICANS is a neuropsychiatric syndrome occurring in 23-67% of patients in the days to weeks following CAR T-Cell therapy[1,2]. It typically occurs concurrently or just after the other major CAR T-Cell related complication of cytokine release syndrome (CRS)[3] which is an immune activation pro-inflammatory condition resulting in vascular endothelial damage and which in severe cases can lead to disseminated intravascular coagulation (DIC)[2]. The exact pathophysiology of ICANS is uncertain but it is thought to be driven by pro-inflammatory cytokines (Interleukin-6) disrupting the crucial BBB with subsequent leakage of inflammatory cytokines into CSF and cerebral oedema[3].

CT is useful in the acute setting as a first-line assessment for stroke, hemorrhage, or cerebral oedema, although in low-grade ICANS it will frequently be normal. MRI will more accurately detect the findings of ICANS which include symmetric bilateral high T2/FLAIR signal in the periventricular and subcortical white matter, thalami [Figure A] and brainstem which can expand to include basal ganglia, cingulate gyrus, hippocampus [Figure B] and splenium of the corpus callosum. Uncommon findings include hemorrhage, cortical stroke [Figure C], diffuse cerebral oedema and myelitis [Figure D]. MRI brain with and without contrast protocol should be utilised[2]. While contrast enhancement is not a common finding in CAR T-Cell neurotoxicity[1], contrast aids in the evaluation for CNS tumour which is a potential mimic.

A standard clinical grading system is used for assessing ICANS and this will be described in detail in the educational exhibit[4].

In summary this educational exhibit provides an overview of CAR T-Cell Neurotoxicity and details several imaging examples to ensure as Neuroradiologists we can recognise the features of ICANS and contribute effectively to patient care.

References

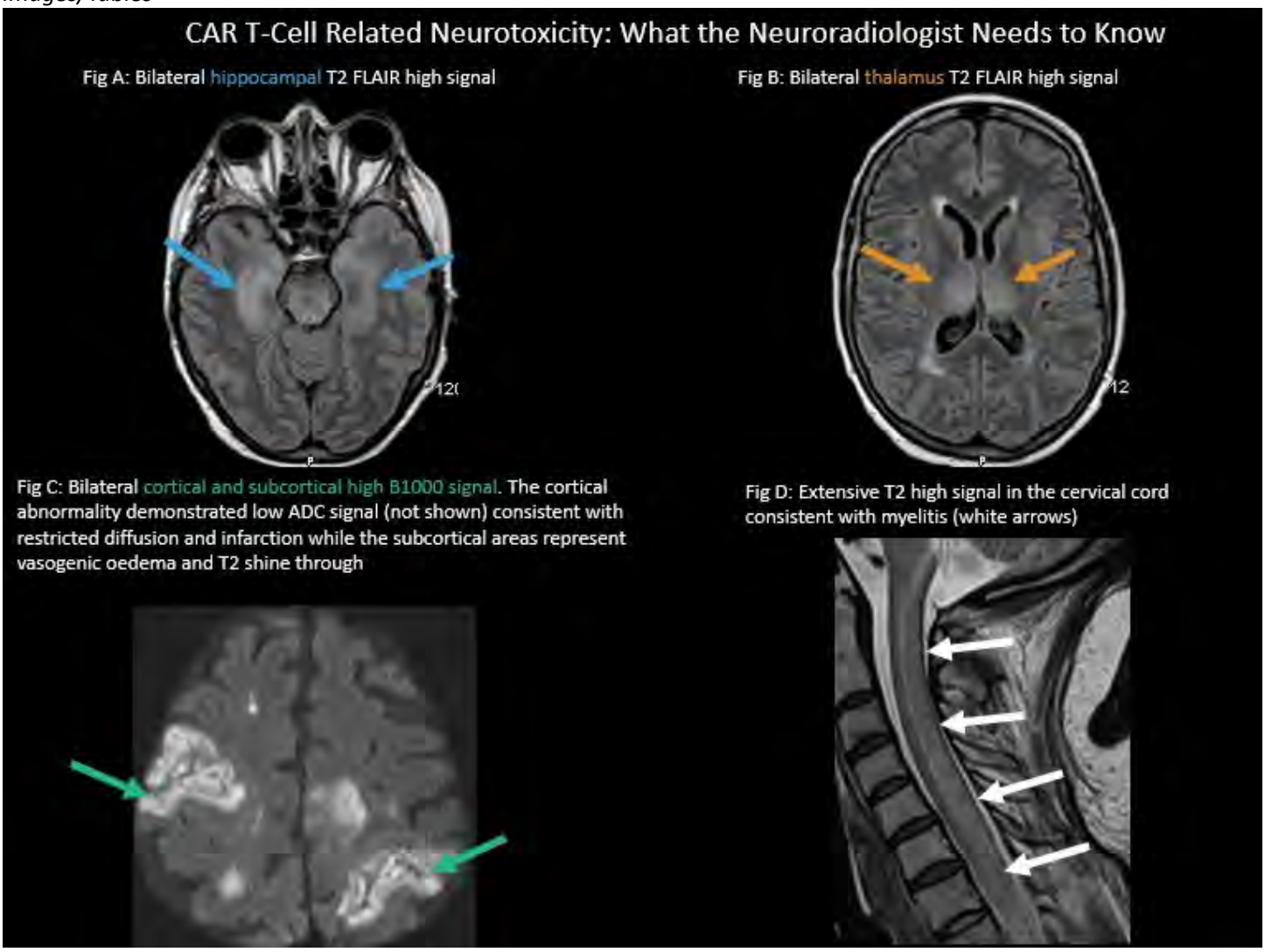
1. de Groot PM, Arevalo O, Shah K, et al. Imaging Primer on Chimeric Antigen Receptor T-Cell Therapy for Radiologists. *RadioGraphics*. 2022;*42*(1):176–194. https://doi.org/10.1148/rg.210065

2. Santomasso BD, Nastoupil L J, Adkins S, et al. Management of Immune-Related Adverse Events in Patients Treated With Chimeric Antigen Receptor T-Cell Therapy: ASCO Guideline. *Journal of Clinical Oncology*. 2021;*39*(35):3978–3992. https://doi.org/10.1200/JCO.21.01992

3. Morris EC, Neelapu SS, Giavridis T, et al. Cytokine release syndrome and associated neurotoxicity in cancer immunotherapy. *Nature Reviews Immunology.* 2022;*22*(2):85–96. https://doi.org/10.1038/s41577-021-00547-6

4. Lee DW, Santomasso BD, Locke FL, et al. ASTCT Consensus Grading for Cytokine Release Syndrome and Neurologic Toxicity Associated with Immune Effector Cells. *Biology of Blood and Marrow Transplantation*. (2019);*25*(4):625–638. https://doi.org/10.1016/j.bbmt.2018.12.758

Images/Tables



834

Imaging Spectrum of CNS Multiple Myeloma in the New Treatment Era

Ryan S Hirschi MD, Daniel Murphy MD, Karen L Salzman MD, Blair Winegar MD
University of Utah School of Medicine, Salt Lake City, Utah, USA

Abstract Category

Adult Neoplasms/Epilepsy/Trauma

Summary & Objectives

Summary:

Multiple myeloma is a monoclonal proliferation of plasma cells with various clinical and imaging presentations throughout the body. In addition to osseous involvement, we outline the less-common central nervous system (CNS) manifestations of disease. CNS myeloma (CNS-MM) is a form of extramedullary disease characterized by plasma cell infiltration of the CNS, meninges or cerebrospinal fluid. It is much rarer and carries a poor prognosis, with an average survival of two months. It can be problematic to diagnose due to heterogeneous clinical symptoms which are often confounded by neurological symptoms caused by the typical features of myeloma and/or treatment side-effects. Specifically, we review the imaging features of cranial, dural, and leptomeningeal myelomatosis.

Lytic osseous lesions are the main finding of multiple myeloma, occurring in up to 90% of patients during illness and commonly affect the skull. However, the reported incidence of extramedullary disease has increased in recent times,

which may be in part due to improved survival through the use of enhanced treatment modalities. Dural involvement of multiple myeloma rarely occurs in isolation, and has few studied treatment options. Plasmacytomas are discrete, solitary tumors of neoplastic monoclonal plasma cells which can occur in bone, soft tissue, and less commonly, as extra-axial intracranial masses. In contrast to other CNS manifestations of disease, intracranial plasmacytomas can often be treated successfully with radiation. Leptomeningeal involvement of myeloma can present with similar signs, symptoms, and imaging findings of leptomeningeal metastases from other hematologic malignancies. Treatment of leptomeningeal myelomatosis includes intrathecal chemotherapy and radiotherapy. Thus, in myeloma patients presenting with heterogeneous neurologic symptoms, a multifactorial approach is needed to confirm diagnosis.

Educational Objectives:

1. Review the range of disorders referred to as monoclonal gammopathies, and the evolution of associated treatment options.
2. Review the role of imaging in meeting diagnostic criteria for monoclonal gammopathies.
3. Review CNS manifestations of multiple myeloma including cranial, dural, and leptomeningeal disease and the associated imaging findings.

Purpose

.

Materials & Methods

.

Results & Conclusion

.

References

1. Ormond Filho AG, Carneiro BC, Pastore D, et al. Whole-body imaging of multiple myeloma: diagnostic criteria. *RadioGraphics* 2019; 39 (4): 1077-1097. DOI: https://doi.org/10.1148/rg.2019180096

2. Fernandez LG, Oyon DE, Gondi V, et al. Secondary CNS myeloma with remission after systemic CNS-penetrating agents. *Neuro-Oncology Advances* 2022; 4(1):1-8. DOI: https://doi.org/10.1093/noajnl/vdac106

3. Egan PA, Elder PT, Deighan WI, et al. Multiple myeloma with central nervous system relapse. *Haematologica* 2020; 105 (7): 1780-1790. DOI: 10.3324/haemotol.2020.248518

4. Parillo M, Vaccarino F, Quattrocchi CC. Imaging findings in a case of leptomeningeal myelomatosis, a rare but critical central nervous system complication of multiple myeloma. *The Neuroradiology Journal* 2023; 36(5):616-620. doi:10.1177/19714009221150849

5. Gangatharan SA, Carney DA, Prince HM, et al. Emergence of central nervous system myeloma in the era of novel agents. *Hematol Oncol* 2012; 30: 170-174. DOI: https://doi.org/10.1002/hon.1021

Images/Tables

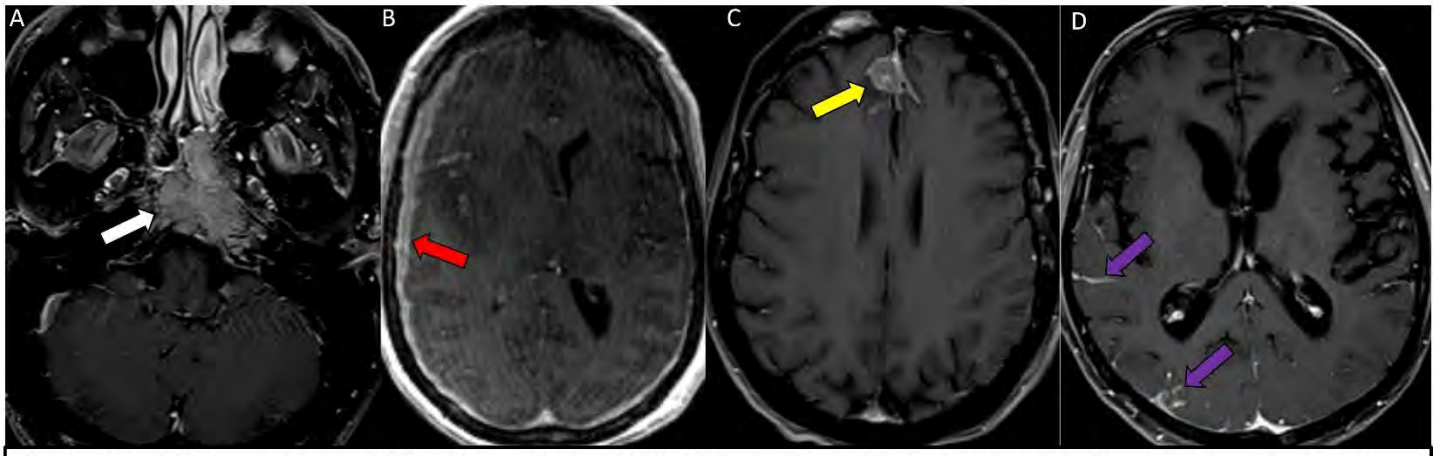


Figure 1: Axial T1 post contrast MRI of four patients with multiple myeloma. (A) depicts an enhancing mass along the central skull base with involvement of the clivus (white arrow). (B) depicts irregular dural enhancement along the right cerebral hemisphere (red arrow) with myeloma involvement demonstrated on biopsy. (C) depicts an enhancing, dural based mass arising along the right anterior falx (yellow arrow) consistent with a plasmacytoma. (D) depicts leptomeningeal disease in the right temporoparietal region (purple arrows) in a patient with CSF positive for multiple myeloma.

838

Imaging Insights and Considerations for Spine Metastasis Patients Undergoing SBRT

Javid Azadbakht[1], David Haynor[1], Simon S. Lo[2], Mahmud Mossa-Basha[1]

[1]Department of Radiology, University of Washington School of Medicine, Seattle, Washington, USA. [2]Department of Radiation Oncology, University of Washington School of Medicine, Seattle, Washington, USA

Abstract Category

Spine

Summary & Objectives

The spine is the most frequently affected site for bone metastases, occurring in nearly two-thirds of cases involving common cancers in both men and women (1, 2). Advancements in diagnosing and treating spinal metastases have resulted in better survival outcomes and improved quality of life for patients. There is a growing focus on tailored imaging to refine treatment planning for tumor ablation and reduce complications. Over the last decade, stereotactic body radiotherapy (SBRT) has been integrated into clinical treatment protocols (3). It has shown promising rates of local control for oligometastatic lesions in the spine, all while administering minimal radiation exposure to nearby vital organs, particularly the spinal cord (4). This study aims to explore the role of imaging in optimizing SBRT, focusing on its contributions to treatment planning, procedural precision, and post-treatment monitoring.

Purpose

The aim of this work is to highlight the role of both conventional and advanced imaging techniques in the management of spinal metastases treated with SBRT. Specific focus is given to how imaging facilitates treatment planning, navigational precision during procedures, and the monitoring of treatment response. The goal is to assess how various imaging modalities can improve patient outcomes by refining treatment approaches and minimizing complications.

Materials & Methods

This review examines current imaging modalities used in spinal metastases patients undergoing SBRT. Conventional imaging techniques are discussed in conjunction with advanced MR imaging methods, including Diffusion and Perfusion imaging of the spine. The role of CT myelography is also explored. Imaging findings are examined to identify potential pitfalls in interpretation, and attention is given to distinguishing between expected post-treatment changes and signs of local failure.

Results & Conclusion

Imaging is an indispensable component in the management of spinal metastases undergoing SBRT. Tailored imaging strategies enhance treatment planning, help navigate the complexities of tumor ablation, and ensure minimal radiation exposure to critical structures (5). Advanced imaging techniques contribute to distinguishing between normal post-treatment changes and early signs of local failure, improving patient outcomes and minimizing complications.

References

1. Aaron AD. The Management of Cancer Metastatic to Bone. JAMA 1994, 272, 1206–1209.

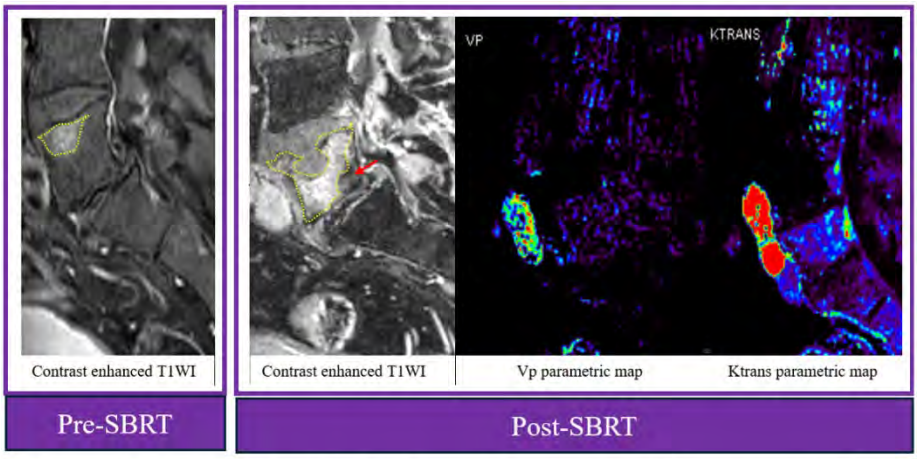
2. McLinton A, Hutchison C. Malignant Spinal Cord Compression: A Retrospective Audit of Clinical Practice at a UK Regional Cancer Centre. Br. J. Cancer 2006, 94, 486–491.

3. Pan H, Simpson DR, Mell LK, et al. A Survey of Stereotactic Body Radiotherapy Use in the United States. Cancer 2011, 117, 4566–4572.

4. Sahgal A, Roberge D, Schellenberg D, et al. The Canadian Association of Radiation Oncology Scope of Practice Guidelines for Lung, Liver and Spine Stereotactic Body Radiotherapy. Clin. Oncol. 2012, 24, 629–639.

5. Spratt DE, Beeler WH, de Moraes FY, et al. An Integrated Multidisciplinary Algorithm for the Management of Spinal Metastases: An International Spine Oncology Consortium Report. Lancet Oncol. 2017, 18, e720–e730.

Images/Tables



Salivary gland metastasis to the lumbar vertebra. In pre-SBRT image, a well-defined area of marrow enhancement (dashed yellow line) is noted in the anterosuperior corner of the vertebral body, involving the anterior aspect of the superior endplate. Post-SBRT image reveals expansion of this hyperenhanced area (dashed yellow line) with depression of the superior endplate. A new irregularly shaped lesion (arrow) has also emerged in the posterior inferior aspect of the same vertebral body. MR perfusion parametric maps show no increased perfusion in either lesion, suggesting the benign nature of the marrow hyperenhancement and highlighting MR perfusion's limitations in evaluating perfusion in bone lesions, and differentiating capability between tumor recurrence/progression and pseudoprogression.

850

Brown-Séquard Syndrome: Traumatic and Nontraumatic Causes

Willem Calderon[1], Paulo Puac[2], Carlos Zamora[3], Alex Rovira[1]
[1]Hospital Universitari Vall d´Hebron, Barcelona, Catalonia, Spain. [2]University of Ottawa, Ottawa, Ontario, Canada. [3]University of North Carolina, Chapel Hill, North Carolina, USA

Abstract Category

Spine

Summary & Objectives

Summary:

• Background.
• Etiologic classification of Brown-Sequard Syndrome.
• Imaging findings.

Objectives:

- Identify the various causes of Brown-Séquard syndrome.
- Recognize the key imaging features of different pathologies associated with Brown-Séquard syndrome.
- Understand the role of MRI in the differential diagnosis of Brown-Séquard syndrome.

Purpose

Brown-Séquard syndrome is a rare type of incomplete spinal cord syndrome caused by lesions affecting one side of the spinal cord. Clinically, it is characterized by an ipsilateral upper motor neuron deficit due to partial or complete interruption (hemisection) of the corticospinal tract, with symptoms varying based on the site and mechanism of injury. Although several etiologies can lead to Brown-Séquard syndrome, trauma remains the most common cause. MRI is crucial for the diagnostic evaluation of patients with suspected spinal cord injury, providing detailed insights into lesion location and extent.

Materials & Methods

We will review the key imaging findings associated with Brown-Séquard syndrome, covering both traumatic and non-traumatic etiologies.

- Traumatic: stab wound, blunt trauma, cervical vertebral fractures, cervical vertebral dislocation, and unilateral or bilateral cervical facet locking.

- Non-traumatic: idiopathic spinal cord herniation, cord ischemia, disc herniation, tumors, epidural hematoma, intramedullary hemorrhage, multiple sclerosis, infectious diseases, and arteriovenous malformations.

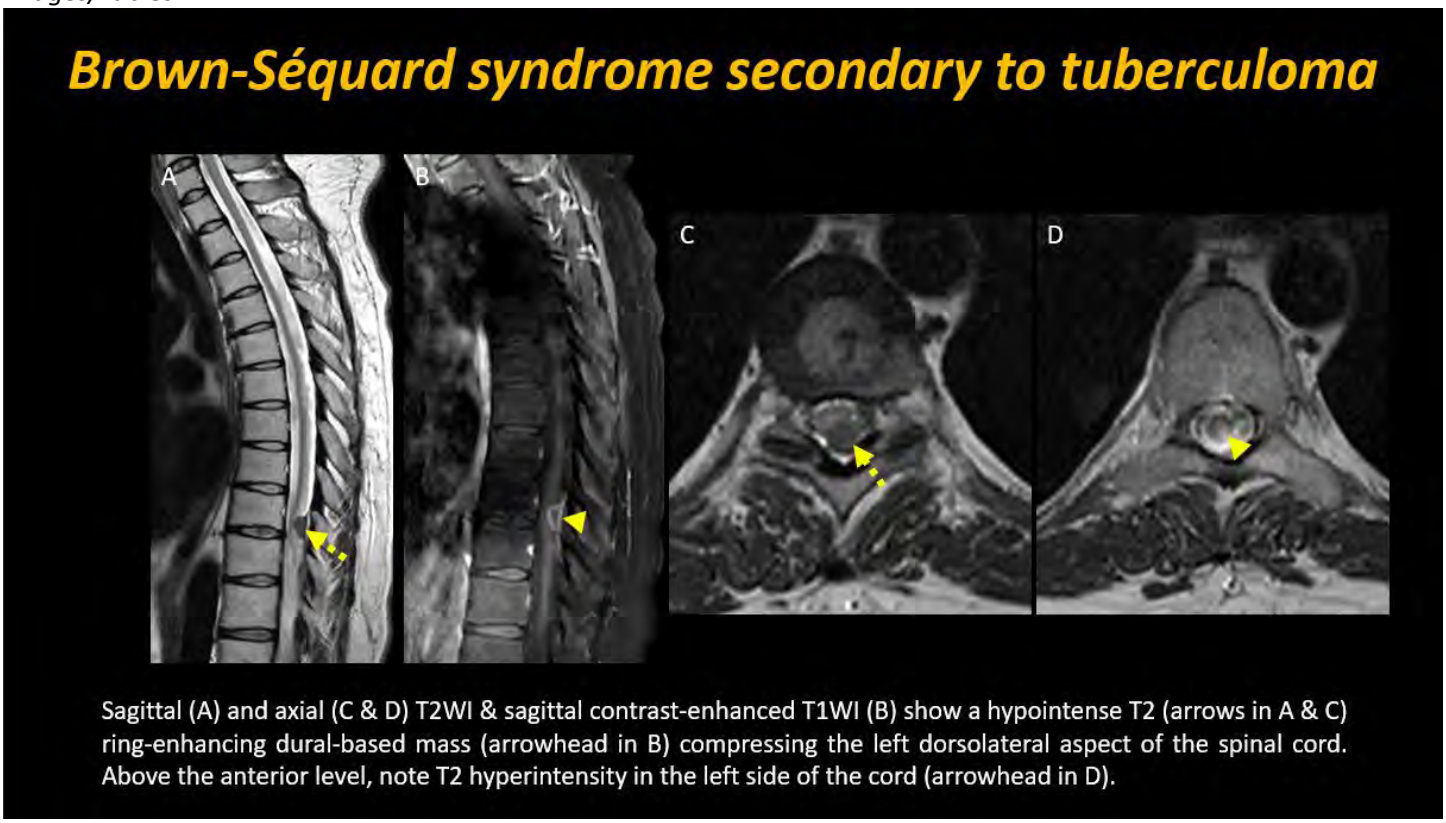
Results & Conclusion

Brown-Séquard syndrome can arise from various unilateral spinal cord pathologies, necessitating prompt analysis via spine MRI for accurate diagnosis and effective management.

References

- Mathews MS, Peck WW, Brant-Zawadzki M. Brown-Séquard syndrome secondary to spontaneous bleed from postradiation cavernous angiomas. *AJNR Am J Neuroradiol*. 2008;29(10):1989-1990.
- Dubey D, Modur PN. Teaching NeuroImages: partial brown-Séquard syndrome: a rare presentation of CMV myelitis. *Neurology*. 2014;83(6):e80.
- de Andrada Pereira B, Meyer BM, Alvarez Reyes A, Orenday-Barraza JM, Brasiliense LB, Hurlbert RJ. Traumatic cervical spine subarachnoid hemorrhage with hematoma and cord compression presenting as Brown-Séqüard syndrome: illustrative case. *J Neurosurg Case Lessons*. 2022;4(23):CASE22431.

Images/Tables



851

Imaging Insights and Clinico-Pathological Features of Rosette-Forming Glioneuronal Tumors: A Comprehensive Review from an Academic Medical Center.

Shahodat Voreis MD, Suyash Mohan MD, Ling-Lin Pai MD PhD, MacLean Nasrallah MD PhD, Alvand Hassankhani MD

Hospital of the University of Pennsylvania, Philadelphia, PA, USA

Abstract Category

Adult Neoplasms/Epilepsy/Trauma

Summary & Objectives

Rosette-forming glioneuronal tumors (RGNT) are rare WHO grade 1 primary CNS neoplasms. While predominantly a posterior fossa tumor, there are several case reports of RGNT occurring in the supratentorial brain and even spinal cord. There is association with mutations in FGFR1, NF1 and PIK3CA. Here we discuss characteristic imaging features of RGNT, as well as histopathology based on 6 pathology proven cases at our institution. This clinical report will include brief review of existing literature for comprehensive discussion of other encountered tumor locations, presentation and management of RGNT.

Purpose
We will discuss imaging features of rosette-forming glioneuronal tumors based on our institutional experience with a brief discussion of concordance/discordance with existing literature.
Materials & Methods
Cases were identified by pathologic diagnosis and confirmed by molecular study results. Patients with RGNT tumors harboring defining PIK3CA and FGFR1 by targeted next generation sequencing were included in the study. A detailed histopathologic assessment of all tumors was conducted by a group of neuropathologists. The imaging of these cases was initially read by sub-specialty trained neuroradiologists and re-reviewed by a neuroradiologist specializing in neuro-oncologic imaging. Further, PubMed search for term "RGNT" was conducted from year 2002 - 2024 to include existing case reports and case series for a comprehensive review.
Results & Conclusion
RGNT are low grade CNS neoplasms with a somewhat distinct imaging characteristic. On MRI these tumors are hypointese on T1, hyperintense on T2 and FLAIR with variable enhancement and facilitated diffusion. At our institution, 6 patients with RGNT underwent treatment and/or surveillance. Among the 6 patients, 3 were in the posterior fossa and 3 were supratentorial. Surgical intervention varied, with 4 undergoing partial or complete resection, while 2 underwent biopsy only. On follow up, minimal tumor progression was noted in 2 patients and frank recurrence in one. This case series highlights that RGNT is not confined to the posterior fossa and, despite its low-grade nature, may demonstrate a propensity for slow progression or recurrence.
Our findings reinforce the need for heightened awareness of RGNT's variable anatomic locations and potential for progression. MRI characteristics, when combined with molecular markers, facilitate diagnosis and help guide management, though long-term follow-up maybe warranted.
References
Louis DN, Perry A, Wesseling P, et al. The 2021 WHO Classification of Tumors of the Central Nervous System: a summary. *Neuro Oncol* 2021;23(8):1231-1251. DOI: 10.1093/ neuonc/noab106.
Yang C, Fang J, Li G, et al. Histopathological, molecular, clinical and radiological characterization of rosette-forming glioneuronal tumor in the central nervous system. *Oncotarget* 2017;8(65):109175-109190. DOI: 10.18632/oncotarget.22646.
Wilson CP, Chakraborty AR, Pelargos PE, et al. Rosette-forming glioneuronal tumor: an illustrative case and a systematic review. *Neurooncol Adv* 2020;2(1):vdaa116. DOI: 10.1093/noajnl/vdaa116.

874

Enhancing Diagnostic Precision in Craniospinal Injuries through Diffusion-Weighted Imaging

FAHAD FAROOQ MD[1], aditya duhan MD[1], FNU Vaibhav MBBS[2], Vipul Kaliraman MBBS[3], RAJIV MANGLA MD[1], Amar Swarnkar MD[4]
[1]SUNY UPSTATE MEDICAL UNIVERSITY, SYRACUSE, NEWYORK, USA. [2]Pt. B.D. SHARMA PGIMS, Rohtak, Haryana, India. [3]Maulana Azad Medical College, New Delhi, New Delhi, India. [4]State University of New York Upstate Medical University, SYRACUSE, NY, USA
Abstract Category
Spine
Summary & Objectives
Diffusion-weighted imaging (DWI) has emerged as a critical modality for assessing traumatic craniocervical and spine injuries, providing unique insights into tissue integrity and injury severity. This educational exhibit highlights a range of craniocervical and spinal trauma cases where DWI revealed critical findings not apparent on standard MRI sequences. The cases demonstrate DWI's ability to detect subtle yet clinically significant abnormalities, such as diffuse axonal injury, cord edema, and ischemic changes, thus underscoring its indispensable role in trauma imaging.
Purpose
This exhibit aims to educate neuroradiologists on the application of DWI in the assessment of craniocervical and spine injuries, with a focus on its advantages over traditional imaging modalities. Through a collection of varied case presentations, we aim to demonstrate how DWI enables early detection and improved characterization of trauma-induced abnormalities, which are critical for accurate diagnosis and optimal patient care.
Materials & Methods
A retrospective analysis was conducted of craniocervical and spine trauma cases evaluated at our institution over the past two years. Cases were selected based on the presence of specific DWI findings, including diffusion restriction

indicative of ischemia, trauma-induced edema, and diffuse axonal injury. DWI findings were compared with standard MRI sequences to assess their additional diagnostic value. Literature from relevant radiology journals, including *Radiology* and *RadioGraphics*, was reviewed to support the findings and underscore the importance of DWI in trauma imaging.

Results & Conclusion

Results

In the case series, DWI demonstrated superior sensitivity for detecting acute trauma-related abnormalities that were not apparent on T1- and T2-weighted MRI. In craniocervical injuries, DWI successfully identified areas of restricted diffusion within the brainstem and spinal cord, corresponding to axonal injury and ischemic damage. In spinal cord trauma cases, DWI differentiated acute traumatic changes from chronic myelopathy, aiding in the prediction of neurological outcomes. Findings are consistent with prior studies highlighting DWI's role in identifying microstructural changes that are often missed by conventional MRI.

Conclusions

This exhibit confirms DWI as an essential tool in the evaluation of craniocervical and spine trauma, enhancing diagnostic accuracy and informing patient management. DWI provides critical insights into the severity and extent of injury, making it particularly valuable for cases where conventional MRI may yield inconclusive findings. The sensitivity of DWI in detecting trauma-induced microstructural abnormalities supports its expanded use in routine trauma assessment, with implications for better prognostic evaluations and improved patient care.

References

1. Shabani S, Meyer BP, Budde MD, et al. Diagnostic Imaging in Spinal Cord Injury. Neurosurgery Clinics 2021;32:323–31
2. Thurnher MM, Law M. Diffusion-Weighted Imaging, Diffusion-Tensor Imaging, and Fiber Tractography of the Spinal Cord. Magnetic Resonance Imaging Clinics 2009;17:225–44
3. Zhang JS, Huan Y. Multishot diffusion-weighted MR imaging features in acute trauma of spinal cord. Eur Radiol 2014;24:685–92

Images/Tables

Parameter	Description	Role of DWI
Craniocervical Junction Injuries	Injuries affecting the craniocervical junction (C0-C2), often challenging to detect on CT or conventional MRI.	DWI helps identify microstructural changes and detect edema or ischemia, improving sensitivity.
Spinal Cord Injuries	Traumatic or non-traumatic injuries affecting spinal cord integrity and function.	DWI can reveal areas of acute infarction, ischemia, or demyelination, aiding in early diagnosis.
Ligamentous Injuries	Involvement of ligaments such as the anterior/ posterior longitudinal ligaments, often missed on standard imaging.	DWI highlights ligamentous injury with edema patterns, especially in subtle injuries.
Disc Pathologies	Includes herniation, bulging, or degenerative changes.	DWI aids in distinguishing acute disc pathology from chronic changes by evaluating water content.
Vertebral Marrow Lesions	Lesions within vertebral marrow that can indicate trauma, infarction, or tumors.	DWI can differentiate benign from malignant marrow lesions by assessing diffusion restriction.
Fractures	Complex fractures, including occult or small fractures missed on initial imaging.	DWI is useful for detecting edema in fractures that are not obvious on CT or standard MRI.
Spinal Abscesses and Infections	Spinal infections such as abscesses or osteomyelitis.	DWI can help identify abscesses by demonstrating restricted diffusion, aiding in diagnosis.
Clinical Applications	Enhanced precision in diagnosing various craniocervical and spinal injuries.	DWI contributes to early detection, improved management, and targeted treatment plans.
Limitations of DWI	Susceptible to artifacts, especially in areas close to bone or air-tissue interfaces.	Awareness of limitations improves diagnostic accuracy and minimizes false positives.

882

MRI Defacing Algorithms: Balancing Privacy and Data Integrity in Neuroimaging

Arsalan Nadeem MBBS[1], Umar Akram[1], Sana Rehman MD[2], Vivek S Yedavalli MD, MS[2]
[1]Allama Iqbal Medical College, Lahore, Punjab, Pakistan. [2]Russell H. Morgan Department of Radiology and Radiological Science, Johns Hopkins School of Medicine, Baltimore, Maryland, USA

Abstract Category

New Techniques/Advanced Imaging/Informatics/AI/Professional Development/Misc

Summary & Objectives

This exhibit discusses defacing algorithms used in magnetic resonance imaging (MRI) to protect patient privacy by anonymizing facial features while preserving essential brain data.[1] The objectives are to:

- Summarize the primary techniques and mechanisms behind defacing algorithms in MRI.
- Discuss their impact on neuroimaging measurements and data usability.
- Examine how defacing affects subsequent automated processing and segmentation.
- Evaluate the strengths and limitations of each algorithm to guide researchers in selecting the most suitable tool based on their study requirements.

Purpose

Neuroimaging datasets are increasingly shared in open repositories for research purposes.[2] Consequently, the risk of re-identification through facial features has become a major privacy concern. Defacing algorithms aim to reduce this risk by obscuring identifiable facial structures in MRI scans. This exhibit aims to review and compare various defacing methods, illustrating their impact on privacy, data integrity, and usability in neuroimaging studies.

Materials & Methods

This exhibit will present findings from a literature review of popular defacing algorithms, including Defacer, QuickShear, MRI Deface, PyDeface, FSL Deface, and MRI Reface.[1] It will cover the evaluation criteria used in these studies, such as anonymization effectiveness, accuracy in brain volume preservation, and computational efficiency. Each algorithm's approach to facial feature masking, as well as its impact on MRI segmentation, brain volume measurements, and compatibility across different imaging modalities and age groups, will be discussed (**Table 1**).

Results & Conclusion

Variability exists in the efficacy and performance of defacing algorithms including aspects such as privacy protection, impact on neuroimaging, and trade-offs:

- Most algorithms mitigate re-identification risks by altering facial features, but methods like MRI Reface achieve the highest anonymization accuracy with minimal impact on brain structure.[1]
- MRI Reface and AnonyMI have the least impact on brain measurements and are highly compatible with downstream analyses, while QuickShear and Face Masking may introduce variability in brain volume estimates.[3]
- Faster algorithms such as PyDeface and FSL Deface offer practical, rapid anonymization, though they may occasionally compromise data quality.[4] MRI Reface, though more time-intensive, provides a balanced solution between privacy and data integrity.

This exhibit will reinforce that the choice of defacing algorithm should be tailored to the specific needs of the study, considering the trade-off between data privacy and integrity. Further improvements in defacing methods are essential to ensure reliable, high-quality data for neuroimaging research.

References

[1] Schwarz CG, Kremers WK, Wiste HJ, et al. Changing the face of neuroimaging research: Comparing a new MRI de-facing technique with popular alternatives. *Neuroimage*. 2021;231:117845. DOI: https://doi.org/10.1016/j.neuroimage.2021.117845

[2] Jack CR, Bernstein MA, Fox NC, et al. The Alzheimer's Disease Neuroimaging Initiative (ADNI): MRI methods. *J Magn Reson Imaging*. 2008;27(4):685-691. DOI: https://doi.org/10.1002/jmri.21049

[3] Gao C, Landman BA, Prince JL, et al. A reproducibility evaluation of the effects of MRI defacing on brain segmentation. *medRxiv*. Published online May 21, 2023:2023.05.15.23289995. DOI: https://doi.org/10.1101/2023.05.15.23289995

[4] Bhalerao GV, Parekh P, Saini J, et al. Systematic evaluation of the impact of defacing on quality and volumetric assessments on T1-weighted MR-images. *Journal of Neuroradiology*. 2022;49(3):250-257. DOI: https://doi.org/10.1016/j.neurad.2021.03.001

Images/Tables

Table 1: Merits and Demerits of Defacing Algorithms

Defacing Algorithm	Merits	Demerits
AFNI-based Defacing	Successful anonymization of both CT and MRI data.	Limited effectiveness in handling the structural differences in CT data.
FSL-based Defacing	Effective anonymization of both CT and MRI data.	Similar limitations as AFNI-based defacing in handling CT data structure.
SPM-based Defacing	Commonly used in medical imaging studies.	May lead to changes in volumetric estimates post-defacing, potentially compromising data integrity.
Freesurfer-based Defacing	Frequently used method in medical imaging research.	Similar to SPM-based defacing, may introduce changes in volumetric estimates, affecting data fidelity.
pydeface	Offers flexibility and customization options.	May not consistently preserve data integrity.
QuickShear	Prioritizes privacy protection.	May compromise data fidelity and subsequent automated analysis outcomes.
FaceMasking	Focuses on privacy protection by removing facial features.	Similar to QuickShear, may introduce errors in subsequent analysis outcomes.
MRI Reface	Balances privacy and processing speed.	Requires further validation across different datasets to ensure effectiveness and compatibility.
AnonyMI	Balances identity protection and geometrical preservation effectively.	Requires further validation across different datasets to ensure effectiveness and compatibility.

902

Pediatric hypomyelinating leukodystrophies: a review of imaging findings

Saumya Gurbani MD, PhD[1], Laura Hayes MD[1], Manish Bajaj MD[2], Tushar Chandra MD[2], Stephanie Keller MD[1], Susan Palasis MD[1]

[1]Emory University, Atlanta, GA, USA. [2]Nemours Children's Hospital, Orlando, FL, USA

Abstract Category

Pediatrics

Summary & Objectives

Hypomyelinating leukodystrophies (HLDs) represent a group of genetic disorders resulting in abnormal myelination of neuronal axons and can have a wide range of imaging features. In this work, we present a review of these disorders and their imaging findings.

Learning Objectives:

1. Describe the neurobiology of myelination and genes implicated in hypomyelinating leukodystrophies.
2. Describe the normal evolution of myelination in children, and the imaging techniques for evaluating these changes.
3. Review the spectrum of findings seen in hypomyelinating leukodystrophies.

Purpose

Hypomyelinating leukodystrophies (HLDs) represent a broad range of genetic disorders characterized by reduced myelin content, often presenting from infancy to early childhood. As opposed to demyelinating leukodystrophies, which result in destruction of normal myelin, or a delay in normal myelination, HLDs refer to the abnormal production and maintenance of myelin. Signs of abnormal hypomyelination can be recognized on MRI, which plays a key role in the

diagnostic workup of these patients prior to confirmatory genetic testing. In this work, we review normal myelin development and then present the spectrum of abnormal myelination patterns seen in various HLDs along with important clinical findings.

Materials & Methods

This exhibit will review the expected MRI findings of normal myelination through infancy and early childhood. This will be followed by a review of the approach to identifying imaging signs suggestive of hypomyelination, including correlation with pertinent clinical findings that are essential for diagnosis. The difference in the imaging appearance of demyelinating leukodystrophies and delayed myelination will be emphasized.

Cases of children with HLD were retrospectively identified using a search of the medical records. Imaging was correlated with genetic analysis, metabolic testing, and pathology when available. Examples of various HLDs including Pelizaeus-Merzbacher disease (PMD), Pelizaeus-Merzbacher-like disease, POLR3-related leukodystrophy/4H syndrome, TUBB4A-related leukodystrophy/hypomyelination with atrophy of the basal ganglia and cerebellum (H-ABC), Fucosidosis, Cockayne syndrome, and DEGS1-related leukodystrophy will be presented. For imaging findings reported in the literature that were not identified in our retrospective search, examples from the literature are presented with appropriate citation.

Results & Conclusion

MRI plays a key role in the diagnosis and differentiation of patients with abnormal myelination. Demyelinating leukodystrophies, delayed myelination and HLD have distinct imaging features that can allow their differentiation. Neuroimaging may be the first to suggest the early diagnosis of HLD, which in turn may provide the opportunity for novel therapeutic interventions to be applied.

References

1. Cheon JE, Kim IO, Hwang YS, Kim KJ, Wang KC, Cho BK, Chi JG, Kim CJ, Kim WS, Yeon KM. Leukodystrophy in children: a pictorial review of MR imaging features. Radiographics. 2002 May-Jun;22(3):461-76. doi: 10.1148/radiographics.22.3.g02ma01461. PMID: 12006681.
2. Vanderver A, Prust M, Tonduti D, Mochel F, Hussey HM, Helman G, Garbern J, Eichler F, Labauge P, Aubourg P, Rodriguez D, Patterson MC, Van Hove JL, Schmidt J, Wolf NI, Boespflug-Tanguy O, Schiffmann R, van der Knaap MS; GLIA Consortium. Case definition and classification of leukodystrophies and leukoencephalopathies. Mol Genet Metab. 2015 Apr;114(4):494-500. doi: 10.1016/j.ymgme.2015.01.006. Epub 2015 Jan 29. PMID: 25649058; PMCID: PMC4390457.

Images/Tables

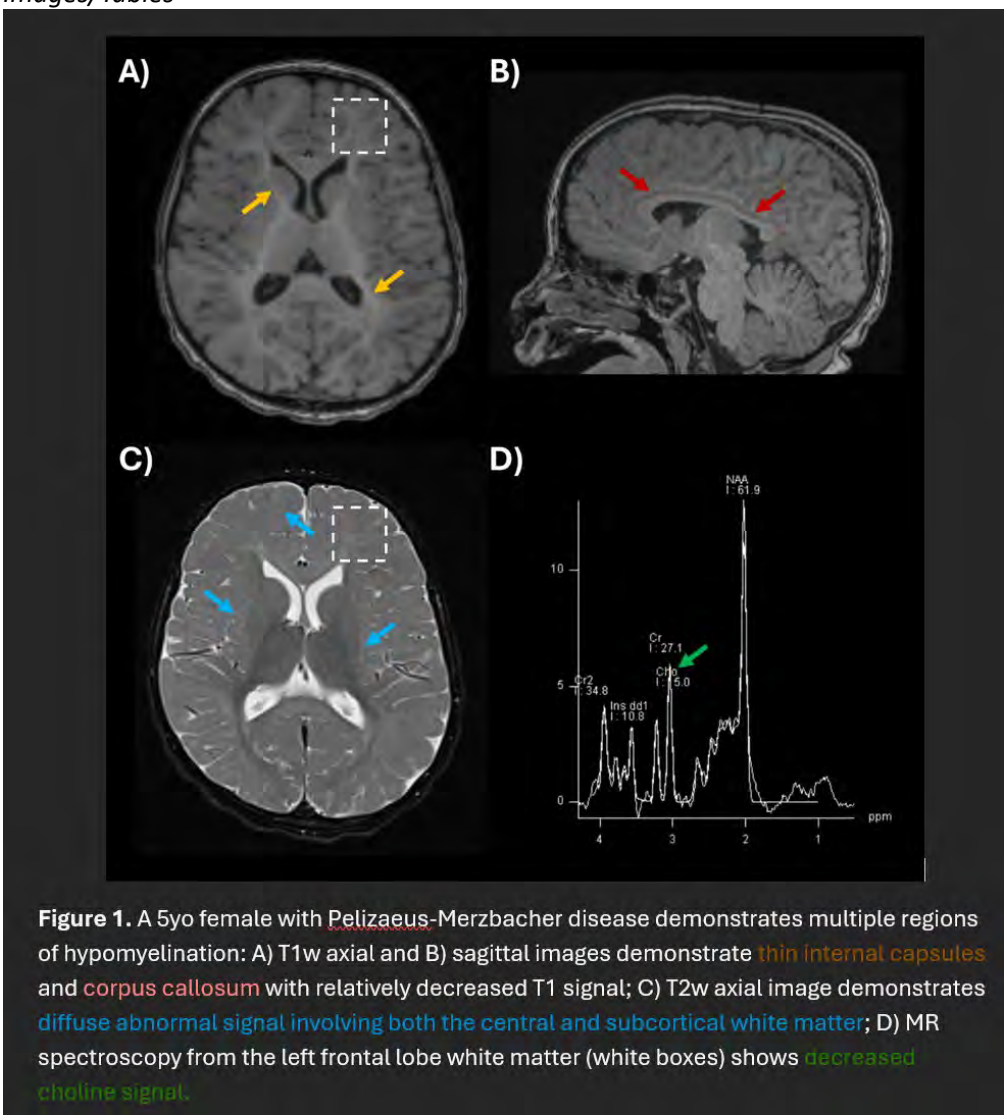


Figure 1. A 5yo female with Pelizaeus-Merzbacher disease demonstrates multiple regions of hypomyelination: A) T1w axial and B) sagittal images demonstrate thin internal capsules and corpus callosum with relatively decreased T1 signal; C) T2w axial image demonstrates diffuse abnormal signal involving both the central and subcortical white matter; D) MR spectroscopy from the left frontal lobe white matter (white boxes) shows decreased choline signal.

906

Delayed Complications of Radiotherapy for Nasopharyngeal Carcinoma

zahra AL Zadjali[1], Rayan Alowaisheq[1], Zainab Al Buraiki[1], Salman Aldeheshi[1], Nasser Al Qahtani[2], Dalia Jadkarim[1], Manal Nicolas-Jilwan MD[3]

[1]King Faisal Specialist Hospital & Research Centre, Riyadh, Saudi Arabia, Saudi Arabia. [2]King Saud Medical City, Riyadh, Saudi Arabia, Saudi Arabia. [3]Beirut, Lebanon, Lebanon

Abstract Category

Head and Neck

Summary & Objectives

Radiotherapy is the mainstay of treatment for nasopharyngeal carcinoma. It carries a risk of various complications, several of which are frequently encountered on imaging studies. The objectives of the presentation are:

1. To present a concise overview of the pattern of spread of nasopharyngeal carcinoma and the standard target volumes of irradiation.
2. To provide a pictorial overview of the full spectrum of radiotherapy complications encountered on CT and MRI imaging.

Purpose

Radiotherapy is the mainstay of treatment for nasopharyngeal carcinoma but carries a risk of multiple complications. We present a brief overview of the pattern of spread of this tumor and the standard target volumes of irradiation which dictate the resultant complications. We subsequently provide a pictorial overview of the full spectrum of radiotherapy complications encountered on CT and MRI imaging.

Materials & Methods

We conducted a retrospective review of our database of CT and MRI of the head and neck in patients with treated nasopharyngeal carcinoma. We selected exams of patients aged 26-74 years which illustrate the entire range of delayed complications of radiation treatment. These include:

1. Chronic rhinosinusitis and chronic otomastoiditis. The CT of one patient is included and shows both complications.
2. Glandular injury (fatty replacement of the salivary glands, decreased size of the thyroid gland, pituitary insufficiency).
3. Vascular injury: A case of internal carotid artery occlusion and another patient with internal carotid pseudoaneurysm are included.
4. Injury of the brain parenchyma, most commonly involving the temporal lobes. We present 4 cases. The first case illustrates the most common pattern of bilateral anterior temporal gliosis. The second case demonstrates anterior temporal injury with associated calcifications. We also include a case of radiation necrosis of the temporal lobe. Finally, the MRI of a patient with cystic necrosis of the temporal lobe is shown.
5. Osteoradionecrosis: We present two cases of osteoradionecrosis of the central skull base and upper cervical spine respectively.
6. Choanal stenosis and synechiae. These are seen on the CT of a 70 year-old male who was subsequently operated for release of synechiae.
7. Radiation induced tumors. We encountered an anterior temporal meningioma as well as a neuroendocrine tumor of the sinonasal cavities occurring several years after irradiation.

Results & Conclusion

Knowledge of the full range of potential complications of nasopharyngeal carcinoma irradiation is crucial for an adequate diagnosis to be made. A systematic evaluation of all structures at risk should always be performed.

References

Lee CC, Ho CY. Post-treatment late complications of nasopharyngeal carcinoma. Eur Arch Otorhinolaryngol. 2012;269(11):2401-9.

King AD, Ahuja AT, Yeung DK, et al. Delayed complications of radiotherapy treatment for nasopharyngeal carcinoma: imaging findings. Clin Radiol. 2007;62(3):195-203.

Hou J, He Y, Li H, et al. Evolution of radiation-induced temporal lobe injury after intensity-modulated radiation therapy in nasopharyngeal carcinoma: a large cohort retrospective study. Radiat Oncol. 2024;19(1):9.

914

A Familiar Threat in a Changing World: North American Flavivirus Encephalitides, their MRI Characteristics, and Implications for Public Health

Vrushab Gowda MD[1], Mark Munir BS[2], Brooks Applewhite MD[1]

[1]Massachusetts General Hospital/Harvard Medical School, Boston, MA, USA. [2]Oakland University William Beaumont School of Medicine, Rochester, MI, USA

Abstract Category

Adult Brain Inflammatory/Infectious Disease/Degenerative/Metabolic

Summary & Objectives

Orthoflaviviruses have long been recognized agents of viral encephalitis transmitted through an arthropod vector, primarily mosquitoes of the genera *Aedes* and *Culex* and ticks of the genus *Ixodes*. In temperate North America, domestically acquired flaviviruses—such as West Nile virus (WNV), Eastern Equine Encephalitis virus (EEEV), St. Louis encephalitis virus (SLEV), and Powassan virus—typically exhibit seasonal patterns of variation correlating to vector activity, punctuated by periodic outbreaks. This differs from tropical and subtropical climes with transmission occurring throughout the year. Concerningly, data suggest that flavivirus infections will become increasingly common as rising global temperatures translate to new epidemiological trends, with broader geographic ranges of disease-carrying organisms, longer vector reproduction periods, and greater human contact during extended warm-weather months(1). Flavivirus encephalitides often present with nonspecific symptoms that are frequently serologically occult. MRI is critical in guiding additional testing, including CSF-based immunologic assays that are necessary for diagnostic certainty. Rapid diagnosis aids in providing early supportive care, cessation of unnecessary treatment of flavivirus mimics (e.g. other viral encephalitides, toxic-metabolic encephalopathies, autoimmune encephalitis, etc.), and timely reporting for

epidemiological monitoring. To these aims, this educational exhibit seeks to improve recognition of key imaging features of flavivirus encephalitides, anticipating an increase in domestic and global flavivirus prevalence due to climate change.

Purpose

Demonstrate key imaging features common to the flavivirus encephalitides, as well as distinguishing characteristics unique to several.

Materials & Methods

Images drawn from institutional case archive.

Results & Conclusion

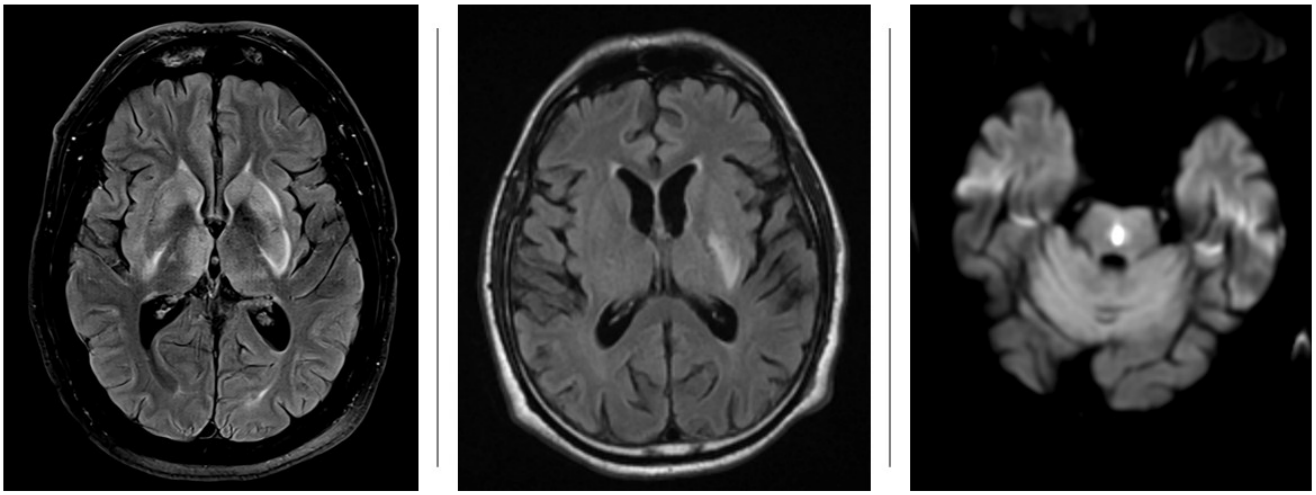
Flavivirus encephalitides share MRI characteristics that can aid in distinguishing them from other pathologies—such as other viral encephalitides, toxic-metabolic encephalopathies, and autoimmune encephalitis. Commonly, T2/FLAIR hyperintense cerebral edema is present in the bilateral deep gray nuclei and brainstem, with relative sparing of the cortex(2). This distribution, for example, is distinct from patterns of HSV encephalitis, which predominantly involve the temporal lobes and spares the deep gray matter. T2/FLAIR hyperintensity may be accompanied by restricted diffusion and microhemorrhage, while contrast enhancement and meningeal involvement are less frequent. Additionally, some imaging characteristics may confer specificity. For example, the “parenthesis sign” has been described with EEE(3)—symmetric T2/FLAIR hyperintensity in the internal and external capsules—while a particular tropism for the substantia nigra and red nuclei have been attributed to WNV and SLEV(4-5).

With rising global temperatures driving an increased incidence of flavivirus infections worldwide, early identification of flavivirus encephalitis is essential to tailored intervention and prompt epidemiologic reporting. Given high mortality rates and common pathologic mimics requiring entirely different management paradigms, radiologists can play an integral role in both timely diagnosis and appropriate treatment.

References

1. Harrigan RJ, Thomassen HA, Buermann W, Smith TB. A continental risk assessment of West Nile virus under climate change. Glob Chang Biol. 2014 Aug;20(8):2417-25.
2. Deresiewicz RL, Thaler SJ, Hsu L, Zamani AA. Clinical and neuroradiographic manifestations of eastern equine encephalitis. N Engl J Med. 1997;336(26):1867-1874.
3. Nickerson JP, Kannabiran S, Burbank HN. MRI findings in eastern equine encephalitis: the “parenthesis” sign. Clinical Imaging. 2016;40(2):222-223.
4. Bosanko CM, Gilroy J, Wang AM, et al. West Nile Virus Encephalitis Involving the Substantia Nigra. Archives of Neurology. 2003;60(10):1448.
5. Cerna F, Borna Mehrad, Luby JP, Burns D, Fleckenstein JL. St. Louis Encephalitis and the Substantia Nigra: MR Imaging Evaluation. American Journal of Neuroradiology. 1999;20(7):1281-1283.

Images/Tables



Eastern Equine Encephalitis | Powassan Encephalitis | West Nile Virus Encephalitis

917

Iron Deposition: Neuroimaging Relevance and Correlation with Abdominal Findings

Andrés Miranda Merchak MD[1], Felipe Alarcón Garrido MD, MSc[2], Santiago Ferdman Jorquera MD[2], Mauricio Rivera Parra MD[2], María Valentina Quijada Viso MD[1]

[1]Hospital Barros Luco Trudeau, Santiago, ,, Chile. [2]Clínica Santa María, Santiago, ,, Chile

Abstract Category

Adult Brain Inflammatory/Infectious Disease/Degenerative/Metabolic

Summary & Objectives

Imaging findings related to abdominal iron deposition are well-documented in the literature, whereas neuroimaging findings are less commonly recognized. The main objective is to present cases involving iron deposits in the choroid plexus and pituitary gland, correlated with abdominal MRI findings and laboratory studies.

Purpose

To highlight the diagnostic utility of specific MRI sequences, such as susceptibility-weighted and T2-weighted imaging, in detecting iron deposits.

Materials & Methods

This study presents a retrospective analysis of clinical cases where iron deposition was identified through MRI in both central nervous and abdominal regions.

- **Imaging Protocols:**
  - **Brain MRI:** Patients underwent brain MRI with susceptibility-weighted imaging (SWI) and T2-weighted sequences to assess iron deposits.
  - **Abdominal MRI:** Abdominal MRI was performed for each patient using T1-weighted in-phase and out-of-phase sequences, as well as T2-weighted imaging, focusing on signal characteristics in the liver, pancreas, spleen, myocardium, and bone marrow.
  - **CT Scans:** Non-contrast CT scans of the brain were used to differentiate between calcific and non-calcific deposits in areas of low signal intensity on MRI.
- **Laboratory Assessments:**
  - Serum ferritin and other iron studies were conducted to quantify systemic iron levels, with specific attention to ferritin levels as an indicator of iron overload.
  - Hormonal evaluations were performed to assess pituitary function, particularly in the second case, where neuroimaging suggested possible hypopituitarism.

Results & Conclusion

Case 1: Patient with a history of multiple blood transfusions. Brain MRI demonstrated marked hypointensity in the choroid plexus on susceptibility-weighted imaging (SWI) and decreased signal in the pituitary gland on T2-weighted sequences. Cerebral CT ruled out calcific components. Abdominal MRI revealed low liver signal intensity on T2-weighted imaging and significantly increased signal on out-of-phase T1-weighted imaging, indicating iron deposition.

Case 2: Patient with no relevant history. Brain MRI showed findings similar to those of the first case. Abdominal MRI evidenced low T2 signal in the liver, pancreas, and spleen, with increased signal on out-of-phase T1-weighted imaging. Susceptibility sequences displayed signal voids, especially with increased echo time, observed in the myocardium and bone marrow as well. Estimated iron content was 3.8 mg/g, with ferritin levels of 1,627 ng/ml. Laboratory studies confirmed hypopituitarism.

Conclusions

Both cases underscore the utility of susceptibility and T2-weighted to detect iron overload. In the second case, neuroimaging findings led to a diagnosis of hemochromatosis and pituitary dysfunction.

MRI has potential as a biomarker for diagnosis, monitoring, and treatment response in patients with iron deposition syndromes.

References

1. Loughnan R, Ahern J, Tompkins C, et al. Association of Genetic Variant Linked to Hemochromatosis With Brain Magnetic Resonance Imaging Measures of Iron and Movement Disorders. *JAMA Neurol*. 2022;79(9):919-928. doi:10.1001/jamaneurol.2022.2030
2. Stankiewicz J, Panter SS, Neema M, Arora A, Batt CE, Bakshi R. Iron in chronic brain disorders: imaging and neurotherapeutic implications. *Neurotherapeutics*. 2007;4(3):371-386. doi:10.1016/j.nurt.2007.05.006
3. Schenck JF. Magnetic resonance imaging of brain iron. *J Neurol Sci*. 2003;207(1-2):99-102. doi:10.1016/s0022-510x(02)00431-8

4. Kira R, Ohga S, Takada H, Gondo K, Mihara F, Hara T. MR choroid plexus sign of iron overload. *Neurology*. 2000;55(9):1340. doi:10.1212/wnl.55.9.1340
5. Nielsen JE, Jensen LN, Krabbe K. Hereditary haemochromatosis: a case of iron accumulation in the basal ganglia associated with a parkinsonian syndrome. *J Neurol Neurosurg Psychiatry*. 1995;59(3):318-321. doi:10.1136/jnnp.59.3.318

Images/Tables

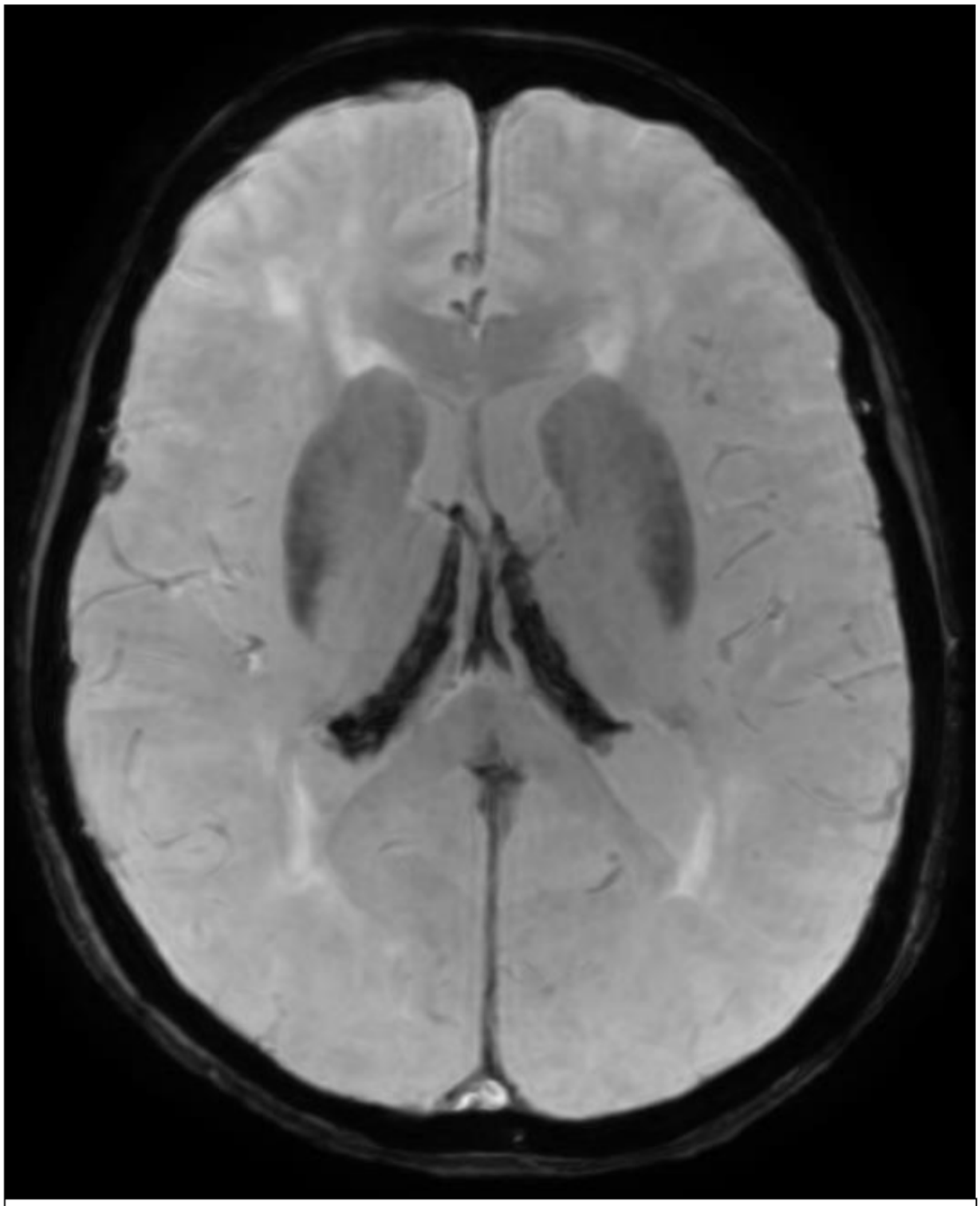


Image 1. SWI shows marked magnetic susceptibility artifact in both choroid plexuses.

936

Clinically Significant Incidentals on Computed Tomography Angiography of The Head and Neck

Nima Hamidi DO, Roman Finocchiaro MD, Michael Bates DO, Micheal Markovic MD, Kyle J Hunter MD, Jeffrey W Prescott MDPHD, Vikas Jain MD
Metrohealth, Cleveland, OH, USA

Abstract Category

Head and Neck

Summary & Objectives

Computed tomography angiography of the head and neck (CTA H&N) is a non-invasive technique that allows for detailed cross-sectional imaging of the head and neck vasculature. Additionally, the exam covers critical anatomical structures from the aortic arch to the vertex. In the MetroHealth system alone, utilization of this exam has increased from 843 exams in 2018 to 3,110 exams in 2023. Previous literature reports that 40% of exams have one or more incidental findings. Considering the exam's increasing utilization, familiarity with critical and frequently encountered incidentals on CTA H&A is vital to readers.

Purpose

1. Identify common and clinically significant incidentals on CTA H&N through a literature review.
2. Showcase a representative sample of incidentals encountered on CTA H&N.

Materials & Methods

A Medline via PubMed literature review was completed for retrospective studies reporting incidental findings on CTA H&N. Reported incidentals were reviewed, and those with clinical significance affecting management or highest frequency were identified. A subsequent search of MetroHealth's Picture Archiving and Communication System (PACS) was completed from 11/05/2019 to 11/05/2024 for CTA H&N for the incidentals above. A sample of clinically relevant incidentals were selected to be presented in this educational exhibit.

Results & Conclusion

The Medline search returned 37 studies, 3 of which met our inclusion criteria. Lung cancer, pulmonary embolism, and carotid aneurysm were the most clinically significant incidentals. Thyroid nodules, lung nodules, and sinus disease were the most frequently encountered incidentals. Of the 1,707 CTA H&N with incidentals completed at the MetroHealth system between 2019 and 2024, few representative cases were selected for this educational exhibit.

References

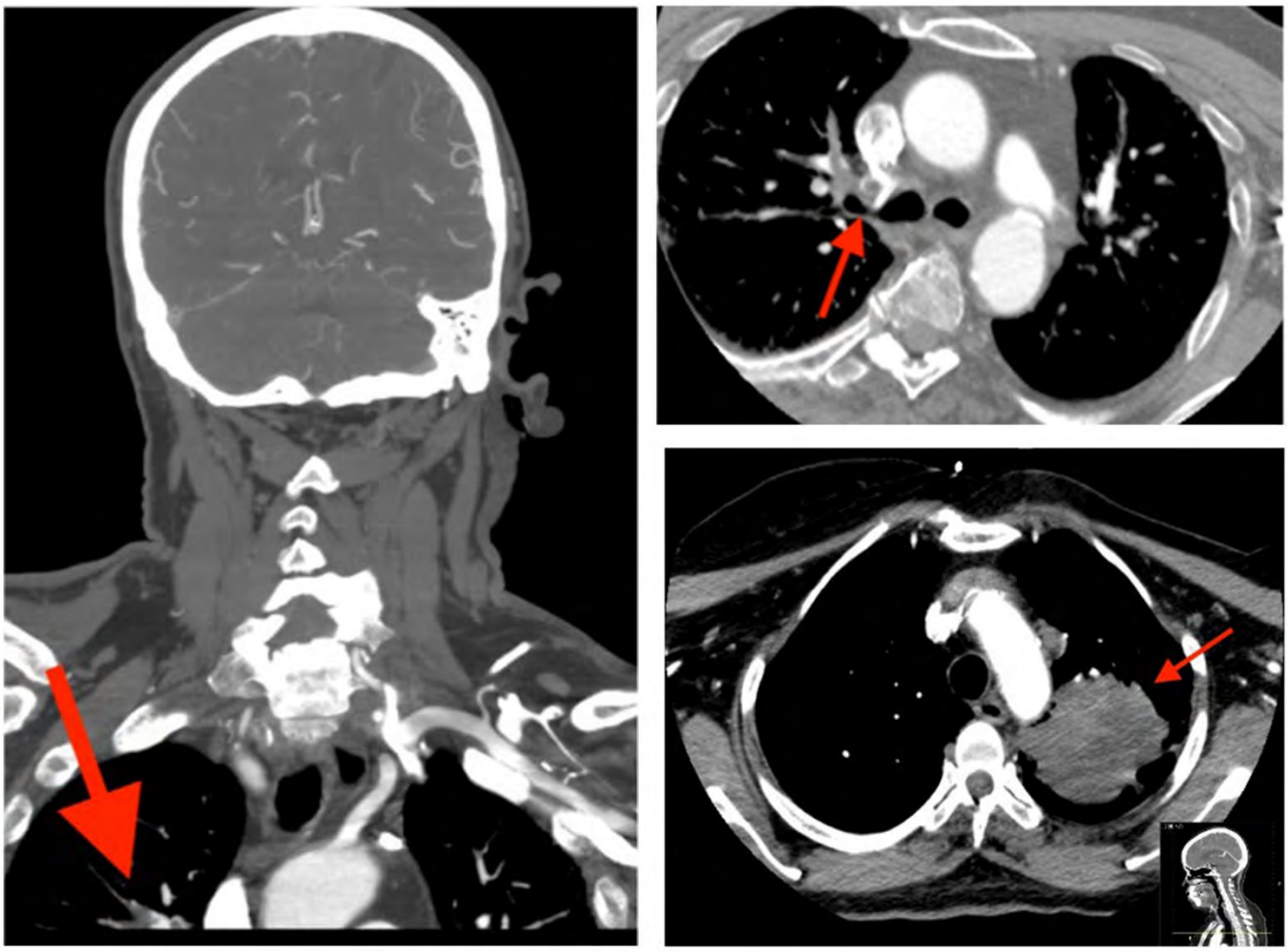
Chen G, Guangliang Y, Xue J, et al. The undiagnosed potential clinically significant incidental findings of neck CTA: A large retrospective single-center study. Medicine 99(43):p e22440, October 23, 2020. | DOI: 10.1097/MD.0000000000022440

Rositzka M, Hoffmann KT, Meyer HJ, et al. Incidental findings on CT angiography of the head and neck in stroke patients. Evaluation of frequency and detection rate. Clin Neurol Neurosurg. 2020 Jun;193:105783. doi: 10.1016/j.clineuro.2020.105783.

Scariano GN, Kim AH, King AH, et al. The Clinical Impact of Incidental Findings in Neck Computed Tomography Angiography. J Vasc Surg. September 6, 2020 72:3e310. DOI: 10.1016/j.jvs.2020.06.090

Tu LH, Malhotra A, Venkatesh AK, et al. Head and Neck CTA Utilization: Analysis of Ordering Frequency and Nonroutine Results Communication, With Focus on the 50 Most Common Emergency Department Clinical Presentations. AJR Am J Roentgenol. 2022 Mar;218(3):544-551. doi: 10.2214/AJR.21.26543.

Images/Tables



941

Imaging and Clinical Features of Progressive Multifocal Leukoencephalopathy

Yoshiaki Ota MD, Bhaumik Debayan MD
University of Colorado, Aurora, CO, USA

Abstract Category

Adult Brain Inflammatory/Infectious Disease/Degenerative/Metabolic

Summary & Objectives

Progressive multifocal leukoencephalopathy (PML) is an infectious disease of the white matter, which is caused by polyomavirus JC that affects myelin. PML usually occurs in patients with chronic corticosteroids and under immunosuppressive conditions such as HIV infection, but patients with other conditions such as multiple sclerosis, rheumatoid arthritis, and systemic lupus erythematosus can also be involved. We overview the pathogenesis, various conditions, typical and atypical imaging features, and mimics.

Purpose

The purpose of this exhibit is:
1. To review the pathogenesis of PML
2. To demonstrate typical and atypical imaging features
3. To illustrate imaging mimics.

Materials & Methods

1. Pathogenesis
- Non-inflammatory demyelination
2. Background
- HIV infection

- Multiple sclerosis under natalizumab treatment
- Hematologic and oncologic conditions under immunosuppressant treatment
- Rheumatologic diseases under immunosuppressant treatment
- Organ transplantation

3. Imaging features of PML
- Conventional MRI: typically T1 hypointense and T2 hyperintense lesions in the subcortical U-fiber rather than in periventricular white matter
- Enhancement: typically not associated with enhancement, but commonly seen in the setting of natalizumab-associated PML, which may depend on patients' immunological status
- DWI: DWI hyperintensity at the lesion margin.
- SWI: hypointensity along cortical-subcortical junction adjacent to PML demyelinating lesions
- PET-CT: different FDG uptakes varying based on immunological status

4. Mimics
- Posterior reversible encephalopathy syndrome (PRES)
- PML-IRIS
- CNS lymphoma

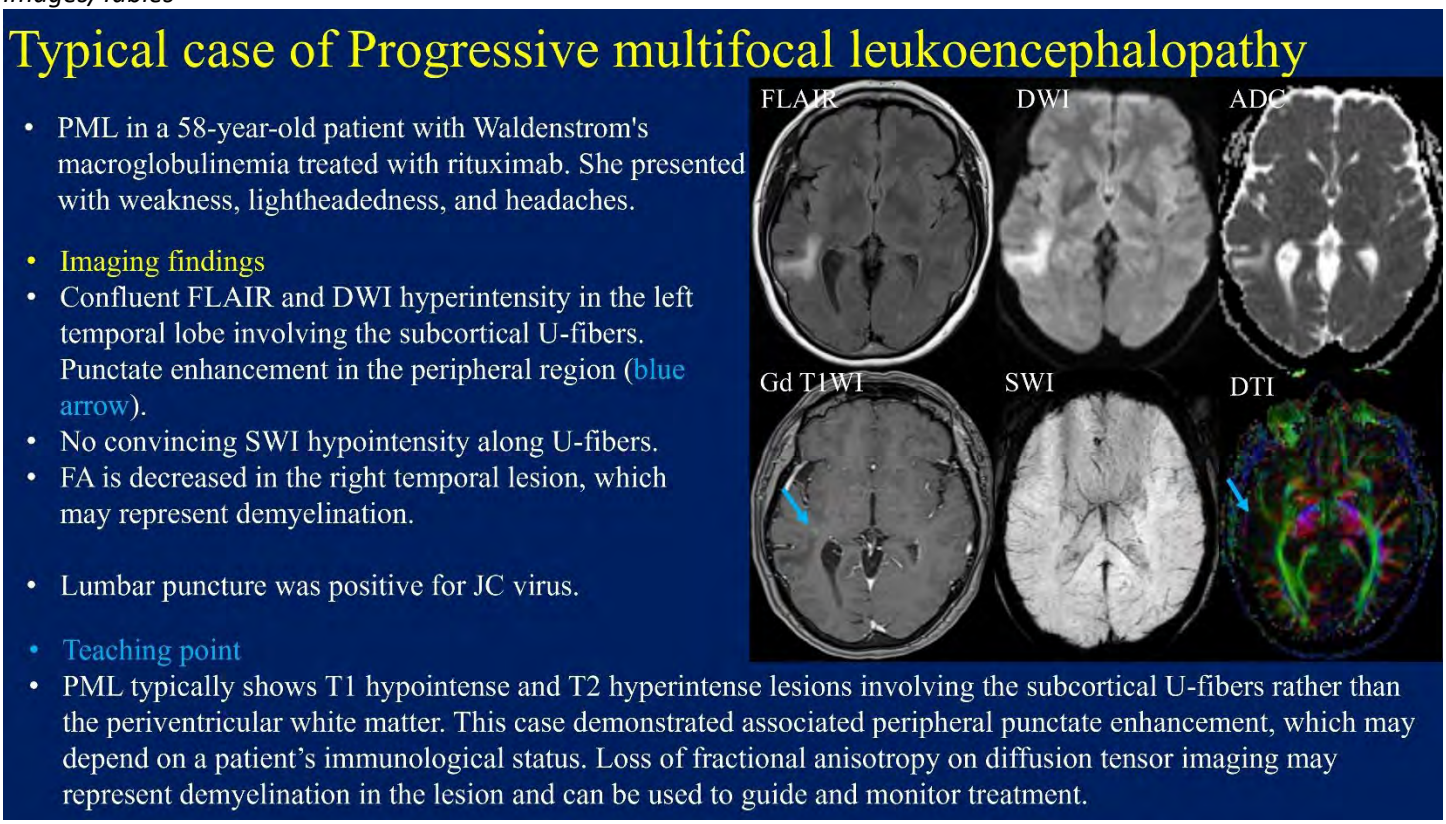
Results & Conclusion

1. JC virus-infected lymphocytes can cross BBB and pass infection to astrocytes and oligodendrocytes, which can result in demyelination.
2. Typical MRI imaging findings of PML include non-edematous T2WI/FLAR hyperintensity associated with rim DWI hyperintensity. Enhancement depends on the patient's immune status. Rim SWI hypointensity can be seen in the case of poor prognosis.
3. PML-IRIS is seen in the HIV-infected cases and natalizumab-associated PML cases. Unlike PML, PML-IRIS usually shows mass effect and enhancement, which is included in diagnostic criteria. Enhancement is known as an early sign of natalizumab-associated PML-IRIS.
4. Mimics include DLBCL, PRES, and other demyelinating diseases, which can be differentiated from PML by imaging.

References

1. Bartsch T, Rempe T, Leypoldt F, et al. The spectrum of progressive multifocal leukoencephalopathy: a practical approach. Eur J Neurol. 2019;26:566-e41. doi: 10.1111/ene.13906.
2. Clifford DB, De Luca A, Simpson DM, et al. Natalizumab-associated progressive multifocal leukoencephalopathy in patients with multiple sclerosis: lessons from 28 cases. Lancet Neurol. 2010;9:438-46. doi: 10.1016/S1474-4422(10)70028-4.
3. Maas RP, Muller-Hansma AH, Esselink RA, et al. Drug-associated progressive multifocal leukoencephalopathy: a clinical, radiological, and cerebrospinal fluid analysis of 326 cases. J Neurol. 2016;263:2004-21. doi: 10.1007/s00415-016-8217-x
4. Sahraian MA, Radue EW, Eshaghi A, et al. Progressive multifocal leukoencephalopathy: a review of the neuroimaging features and differential diagnosis. Eur J Neurol. 2012;19:1060-9. doi: 10.1111/j.1468-1331.2011.03597.x.
5. Küker W, Mader I, Nägele T, et al. Progressive multifocal leukoencephalopathy: value of diffusion-weighted and contrast-enhanced magnetic resonance imaging for diagnosis and treatment control. Eur J Neurol. 2006;13:819-26. doi: 10.1111/j.1468-1331.2006.01362.x.

Images/Tables



946

Diagnosis and Treatment of Degenerative Spinal Cysts

Khoi M Nguyen MD, Linda Lu MD
UCLA, Los Angeles, CA, USA

Abstract Category

Spine

Summary & Objectives

Low back pain (LBP) is the leading cause of disability worldwide, affecting 619 million individuals worldwide in 2020 and is estimated to increase to 843 million causes by 2050. Symptomatic degenerative spinal cysts are an uncommon cause of severe back pain and radiculopathy that may be definitively managed with image-guided interventions, obviating the need for invasive treatments.

Purpose

The purpose of this education exhibit is to provide a case-based review of the pathophysiology and imaging appearance of different degenerative cystic spinal lesions and their respective treatment strategies, with special emphasis on image-guided interventions.

Materials & Methods

N/A

Results & Conclusion

Intraspinal synovial cysts arise from degenerative or post-traumatic disruption of the facet joints. On MRI, these lesions appear as an extradural T2W hyperintense cyst with possible spinal stenosis and compression of the cauda equina nerve roots. Conventional surgical management includes cyst resection with laminotomy or laminectomy. However, image-guided cyst rupture is a minimally invasive option shown to result in significant improvement in symptoms and disability years after injection. Through CT guidance, a spinal needle is placed into the facet joint and contrast is injected to confirm placement. A steroid and anesthetic mixture is forcefully injected to rupture the cyst. Alternatively, the cyst may be aspirated or fenestrated, which has resulted in a 86% complete or partial symptomatic response. However, cysts featuring calcifications or a T2W hypointense rim are associated with persistent symptoms and higher likelihood of requiring surgery.

Discal cysts are typically seen in young adults and thought to arise from annular fissures and subsequent epidural venous plexus rupture. Conventional surgical management includes microdiscectomy but case series report CT-guided aspiration or fenestration may lead to complete symptom resolution.

Ligamentous cysts arise from the ligamentum flavum or posterior longitudinal ligament and appear on MRI as a midline extradural T2W hyperintense cyst that can also result in spinal stenosis and mass effect on cauda equina nerve roots. However, the midline location of these cysts are not percutaneously accessible and are instead managed with minimally invasive surgical cystectomy. Transforaminal epidural injections can be used for symptomatic pain management.

Finally, degenerative changes of interspinous pseudarthroses can lead to interspinous bursitis and extension of the bursa between the ligamentum flavum, resulting in an extradural cyst. Imaging shows communication between the extradural cyst and interspinous bursa. Surgical management of these cysts includes surgical decompression or interspinous fusion to address degenerative changes. Alternatively, patients may undergo image-guided steroid injections for symptomatic management or aspiration/fenestration.

Overall, image-guided interventions can provide symptomatic relief for a variety of degenerative spinal cysts and should be considered prior to surgical management.

References

1. Ferreira ML, de Luca K, Haile LM, Steinmetz JD, Culbreth GT, Cross M, Kopec JA, Ferreira PH, Blyth FM, Buchbinder R et al: Global, regional, and national burden of low back pain, 1990–2020, its attributable risk factors, and projections to 2050: a systematic analysis of the Global Burden of Disease Study 2021. The Lancet Rheumatology 2023, 5(6):e316-e329.

2. Shah, V. N., et al. "Long-Term Effectiveness of Direct CT-Guided Aspiration and Fenestration of Symptomatic Lumbar Facet Synovial Cysts." American Journal of Neuroradiology(2017).

3. Dasenbrock, Hormuzdiyar H., et al. "Successful treatment of a symptomatic L5/S1 discal cyst by percutaneous CT-guided aspiration." Surgical neurology international 1 (2010).

4. DiMaio, Salvatore, et al. "Ligamentum flavum cysts causing incapacitating lumbar spinal stenosis." Canadian journal of neurological sciences 32.2 (2005): 237-242.

5. Baba S, Hayashida M, Kitade K, Kinoshita E, Urata K, Matsushita Y, Oka W, Komiya N, Tsukamoto N, Mae T, Nakashima Y. A Case of Central Posterior Epidural Cyst Associated with Baastrup's Disease Punctured Percutaneously Using Fluoroscopy with a Good Outcome. Spine Surg Relat Res. 2020 Apr 20;4(4):365-368. doi: 10.22603/ssrr.2020-0023. PMID: 33195863; PMCID: PMC7661034.

FIGURE LEGEND

Fig 1 (top left). Cystic lesion arises from the superior L4-L5 disc margin, with right lateral recess stenosis and nerve compression.

Fig 2 (top right). Facet joint after injection with contrast, steroid, and anesthetic under CT guidance. The cyst is no longer visualized and trace contrast is seen in the epidural space, suggesting cyst rupture.

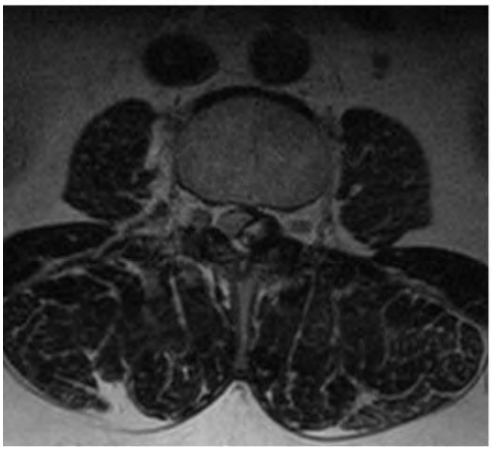
Fig 3 (bottom left). Extradural T2 hyperinstense mass with low signal rim arises from the left L3-4 facet.

Fig 4 (bottom right). Example of CT-guided aspiration/fenestration of a discal cyst.

Images/Tables









947

Mind Over Matter, Going With the Flow: Identifying Reversible Causes of Dementia From White Matter Changes and Glymphatic Flow on Diffusion Tensor Imaging

Manisha Koneru, Hamza Shaikh
Cooper University Health Care, Camden, NJ, USA

Abstract Category

New Techniques/Advanced Imaging/Informatics/AI/Professional Development/Misc

Summary & Objectives

Normal pressure hydrocephalus presents (NPH) with a triad of cognitive decline, urinary incontinence, and gait ataxia. As a result, it is frequently regarded as a potential differential diagnosis in relation to other similar neurodegenerative diseases, such as Alzheimer's. Typical treatment for NPH is cerebrospinal fluid (CSF) diversion procedures, including ventriculoperitoneal shunting or serial lumbar punctures. Notably, NPH symptoms may be reversible in a majority of patients with timely treatment. Consequently, early identification and treatment is crucial for optimal odds of recovery. Newer advanced imaging techniques demonstrate promise to augment the current diagnostic imaging workflow.

Purpose

The purpose is to review clinical presentation, radiographic features of NPH on conventional MRI, and DTI-based features on DTI that have been shown to aid NPH diagnosis.

Materials & Methods
Diagnosis is made typically by identifying magnetic resonance imaging (MRI) features, including enlarged third ventricles, Evan's index value, enlarging subarachnoid space, periventricular or deep white matter hyperintensities, widened Sylvaian fissures, and narrowed callosal angle. However, several of these features overlap with other neurodegenerative diseases. DTI is an advanced MRI technique that relies on analyzing diffusion of water molecules to visualize white matter tracts and glymphatic function. Fractional anisotropy (FA), apparent diffusion coefficient (ADC), and DTI-Analysis Along the Perivascular Space (DTI-ALPS) index are quantitative metrics on DTI that have demonstrated promise to help diagnose NPH patients and prognosticate likelihood of response to CSF diversion.
Results & Conclusion
Thus, DTI has potential as a useful adjunct to the current imaging workup of potential NPH patients.
References
1. Georgiopoulos C, Tisell A, Holmgren RT, et al. Noninvasive assessment of glymphatic dysfunction in idiopathic normal pressure hydrocephalus with diffusion tensor imaging. J Neurosurg 2024;140:612–20.
2. Sedlák V, Bubeníková A, Skalický P, et al. Diffusion tensor imaging helps identify shunt-responsive normal pressure hydrocephalus patients among probable iNPH cohort. *Neurosurg Rev* 2023;46:173.

954

Brachial Plexus MRI In Health and Disease – From Fundamentals to Finer Details

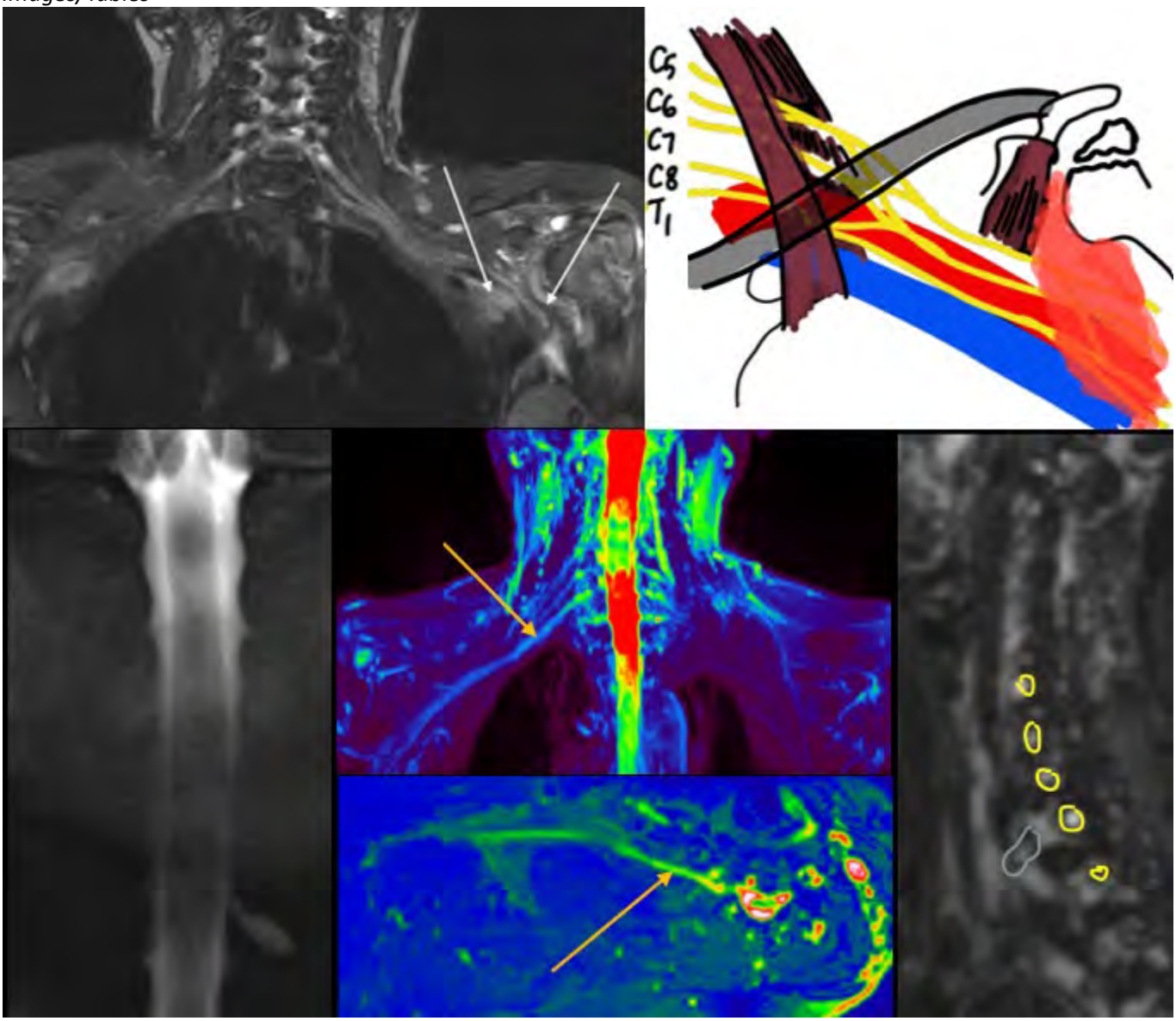
Dr Mridhula Venkatakrishnamurali Maheswari MBBS, Prof.Dr.Babu Peter Sathyanathan MD, DNB, FICR
Barnard Institute of Radiology, Madras Medical College, Chennai, Tamilnadu, India
Abstract Category
Head and Neck
Summary & Objectives
Magnetic Resonance Imaging of the brachial plexus is being increasingly used to identify and characterize brachial plexus pathologies, due to its superior soft tissue resolution and multiplanar imaging capabilities. The complexity of the plexus as well as the surrounding structural anatomy poses a challenge in localising lesions involving the plexus and characterizing them.
In our exhibit, we aim to provide a concise overview of the normal brachial plexus anatomy with landmarks and sequences used in imaging the plexus with their significance, followed by an illustrative review of MRI features of various brachial plexus lesions in a series of cases.
Purpose
The purpose of our exhibit is to illustratively provide a deep insight into the fundamental concepts of brachial plexus MRI along with normal and abnormal features.
We also aim to highlight the usefulness of applications like 3D multiplanar reconstructions (MPR) and Maximum Intensity Projection (MIP) in precise localisation of lesions and detecting subtle abnormalities.
Finally, we also provide an idea of the scope of advanced techniques like Diffusion Tensor Imaging (DTI) and Whole-body MRI (WB-MRI) in diagnosing and guiding management in select cases.
Materials & Methods
Patients presenting with complaints suggestive of brachial plexus involvement, such as upper limb weakness, pain, and/or sensory loss were subjected to MRI of brachial plexus (Siemens – 3T), after history taking and a clinical neurological examination. The findings obtained were analysed. Select patients were additionally subjected to DTI and/or Whole Body MRI, based on clinical and initial imaging features.
Results & Conclusion
MRI of patients with history of trauma revealed features of nerve root avulsion (including pseudomeningoceles), stretch injury, electrocution injury and compression by hematoma and/or fracture fragments involving different components of the brachial plexus. Non traumatic lesions such as chemotherapy induced brachial plexopathy, radiation induced brachial plexopathy, plexiform neurofibroma, schwannoma, invasion by breast carcinoma and Pancoast's tumour were also encountered. Signal intensity alterations, thickening/thinning and non-visualization of specific components of the plexus have been highlighted.
MRI thus plays a pivotal role in the evaluation of brachial plexus pathologies. Familiarity with the MR anatomy, pathological findings and finer techniques in imaging assessment of the brachial plexus aids in accurate diagnosis and also facilitates timely and appropriate therapeutic intervention.

References

Gilcrease-Garcia, B.M., Deshmukh, S.D. and Parsons, M.S. (2020) 'Anatomy, imaging, and pathologic conditions of the brachial plexus', RadioGraphics, 40(6), pp. 1686–1714. doi:10.1148/rg.2020200012.

Szaro P, Geijer M, Ciszek B, McGrath A. Magnetic resonance imaging of the brachial plexus. Part 2: Traumatic injuries. Eur J Radiol Open. 2022 Jan 22;9:100397. doi: 10.1016/j.ejro.2022.100397. PMID: 35111891; PMCID: PMC8789590.

Images/Tables



957

Gridlocks to Blood Clots: Applying Traffic Flow Dynamics to Stroke Neuroradiology

Steven Lev MD[1], Himanshu Katta MD[2], Allen Luk MD[1]

[1]NUMC, East Meadow, NY, USA. [2]NUMC, East Meadow, NJ=Y, USA

Abstract Category

Interventional/Vascular/Stroke

Summary & Objectives

We present a novel approach to stroke risk assessment by integrating CTA, ultrasound, and MR perfusion data, using traffic flow principles to model blood dynamics in the brain and neck. In this model, blood cells navigate arterial "roadways," where narrowing, bifurcations, and tortuous segments create congestion-like disruptions, and "roadblocks" may trigger opening of collateral pathways. Combining structural and hemodynamic data, a personalized ischemic risk profile can be created.

Objectives

1. Develop a computational model combining CTA, MR perfusion, and ultrasound data to calculate ischemic risk using traffic flow analogies.
2. Identify key ischemic risk factors, including vessel elasticity, tortuosity, pressure gradients, shear stress, vessel diameter, and flow velocity.
3. Create tailored risk profiles to improve stroke risk assessment and clinical decision-making.

Purpose

To create a novel ischemic risk model using a traffic dynamics analogy, integrating CTA, MR perfusion, and ultrasound flow data to provide a personalized assessment of stroke risk based on anatomical and flow disruptions.

Materials & Methods

We developed an ischemic risk model by integrating CTA-derived vessel anatomy with flow data from carotid duplex ultrasound and MR perfusion. CTA provides vessel diameter and structural details, identifying areas like bifurcations, tortuous segments, and stenoses. Ultrasound enables direct pressure gradient and estimates of shear stress, while MR perfusion indirectly assesses intracranial pressure gradients through CBF, CBV, and MTT, highlighting regions with compromised perfusion. Rheological factors, including vessel elasticity and blood viscosity, simulate flow resistance. This multi-modality approach can help create a personalized ischemic risk profile, capturing each patient's unique vascular dynamics to identify thrombus-prone zones and overall ischemic risk.

Results & Conclusion

Results

Our ischemic risk model integrates CTA-derived anatomical data with flow measurements from ultrasound and MR perfusion, applying traffic flow principles to simulate cerebral hemodynamics. This model combines both intracranial and extracranial pressure gradients to provide a more comprehensive view of stroke risk, as higher pressure gradients are associated with greater ischemic susceptibility. An estimate of ischemic risk can be obtained with the equation:

$$\mathbf{R \propto (P \times V \times A \times r) / D.}$$

The pressure gradient **P** is derived from a combination of weighted intracranial measurements from MR perfusion and extracranial measurements from ultrasound. Flow velocity **V,** contributing to shear stress, can be measured in real time by ultrasound. The anatomical variation factor **A**, derived from CTA, reflects structural elements such as vessel tortuosity and curvature that can increase thrombogenic potential. Rheology **r** accounts for vessel elasticity and blood viscosity, factors influenced by patient-specific conditions such as age and chronic disease, impacting flow resistance. Finally, vessel diameter **D**, measured from CTA, reflects vessel width, with smaller diameters influencing ischemic risk by restricting flow. By combining data from both extracranial and intracranial sources, the model provides a more detailed risk assessment.

Conclusion

This traffic flow-inspired model provides a framework for stroke risk assessment, integrating intracranial and extracranial data to better reflect ischemic vulnerability. We believe that integrating data from multiple imaging modalities can provide valuable insights, complementing other clinical stroke assessment scales. Future work will focus on clinical validation and refining model parameters.

References

1. Gutti, B., & Fasanmade, O. (2012). Mathematical Modeling and Software Application of Blood Flow for Therapeutic Management of Stroke. *Engineering, 4*(4), 228–233.
2. Samavaki, M., Söderholm, S., Zarrin, A., & Pursiainen, S. (2024). Modeling of blood flow in cerebral arterial circulation and its dynamic impact on electrical conductivity in a realistic multi-compartment head model. *Computer Methods and Programs in Biomedicine, 244*.
3. Kerner, B. S. (2009). *Introduction to Modern Traffic Flow Theory and Control: The Long Road to Three-Phase Traffic Theory*. Springer, New York.

959

Middle Cranial Fossa CSF Leaks: Imaging Can Appear Innocent

Gabrielle Willhelm MD, Mina Gad Elsayed MD, Siddhartha Gaddamanugu MD
University of Alabama at Birmingham, Birmingham, AL, USA

Abstract Category

Head and Neck

Summary & Objectives

Cranial cerebrospinal fluid (CSF) leaks result from an acquired osteodural defect leading to an abnormal communication of the subarachnoid space and pneumatized bone of the cranial fossa. These osteodural defects can result broadly from three categories; traumatic, iatrogenic, and spontaneous. Prompt identification and localization of these defects is important, as untreated cranial CSF leaks result in high rates of morbidity and mortality (1).

Purpose

CSF leaks occur most commonly in the anterior cranial fossa (2), with defects in the middle and posterior cranial fossa being less common. Because of this, current literature primarily focuses on the anterior cranial fossa with a relative paucity of information on middle cranial fossa (MCF) leaks. With this educational excerpt, we aim to address this gap.

Materials & Methods

LEARNING OBJECTIVES:

1. Review middle cranial fossa anatomy and highlight associated predisposing anatomical variants that may increase the risk of developing MCF leaks, such as arachnoid pits and variable pneumatization of the sphenoid bone.
2. Discuss the different etiologies of MCF leaks including traumatic, iatrogenic, and spontaneous. (3). While traumatic CSF leaks are the most common etiology, spontaneous CSF leaks are becoming increasingly more common. While all etiologies will be covered, this presentation will place particular emphasis on spontaneous CSF leaks as these are less likely to close spontaneously and thus are particularly important to recognize and intervene on (4, 5).
3. Delineate clinical presentation and demographics associated with each of the different etiologies, and highlight how clinical presentation may differ between patients presenting with anterior CSF leak and middle CSF leak.
4. Outline imaging protocols for detection and localization of MCF leaks.
5. Highlight current surgical management techniques and how surgical approach may differ from anterior cranial fossa CSF leak repairs.
6. Reinforce the above learning objectives with the illustration of a diverse spectrum of MCF leaks encountered at our institution.

Results & Conclusion

Case 1 consisted of a 40-year-old woman who presented with clear rhinorrhea which worsened with leaning forward. Imaging revealed a defect of the left sphenoid sinus roof with an inferiorly herniated encephalocele and opacification of the sphenoid sinus (Figure 1B). The likely underlying etiology for this leak was an arachnoid granulation and lateral recess pneumatization of the sphenoid sinus. The patient ultimately underwent definitive surgical management with a transpterygoid approach.

Case 2 consisted of a 44-year-old woman with a history of a right middle ear cholesteatoma and three prior right tympanomastoidectomy procedures who presented with new onset hearing loss and vertigo. Imaging revealed a large right tegmen mastoideum defect with a right temporal encephalocele in the external ear (Figure 1D).

Patient is being closely monitored for meningitis while awaiting definitive operative repair.

References

1. Scoffings DJ. Imaging of Acquired Skull Base Cerebrospinal Fluid Leaks. Neuroimaging Clin N Am. 2021 Nov;31(4):509-522.
2. Eljazzar R, Loewenstern J, Dai JB, Shrivastava RK, Iloreta AM Jr. Detection of Cerebrospinal Fluid Leaks: Is There a Radiologic Standard of Care? A Systematic Review. World Neurosurg. 2019 Jul;127:307-315.
3. McNulty B, Schutt CA, Bojrab D, Babu S. Middle Cranial Fossa Encephalocele and Cerebrospinal Fluid Leakage: Etiology, Approach, Outcomes. J Neurol Surg B Skull Base. 2020 Jun;81(3):268-274.
4. Lobo BC, Baumanis MM, Nelson RF. Surgical repair of spontaneous cerebrospinal fluid (CSF) leaks: A systematic review. Laryngoscope Investig Otolaryngol. 2017 Apr 7;2(5):215-224.
5. Mark IT, Cutsforth-Gregory J, Luetmer P, Madhavan AA, Oien M, Farnsworth P, Bathla G, Messina S, Link M, Van Gompel J. Skull Base CSF Leaks: Potential Underlying Pathophysiology and Evaluation of Brain MR Imaging Findings Associated with Spontaneous Intracranial Hypotension. AJNR Am J Neuroradiol. 2024 Oct 3;45(10):1593-1596.

Images/Tables

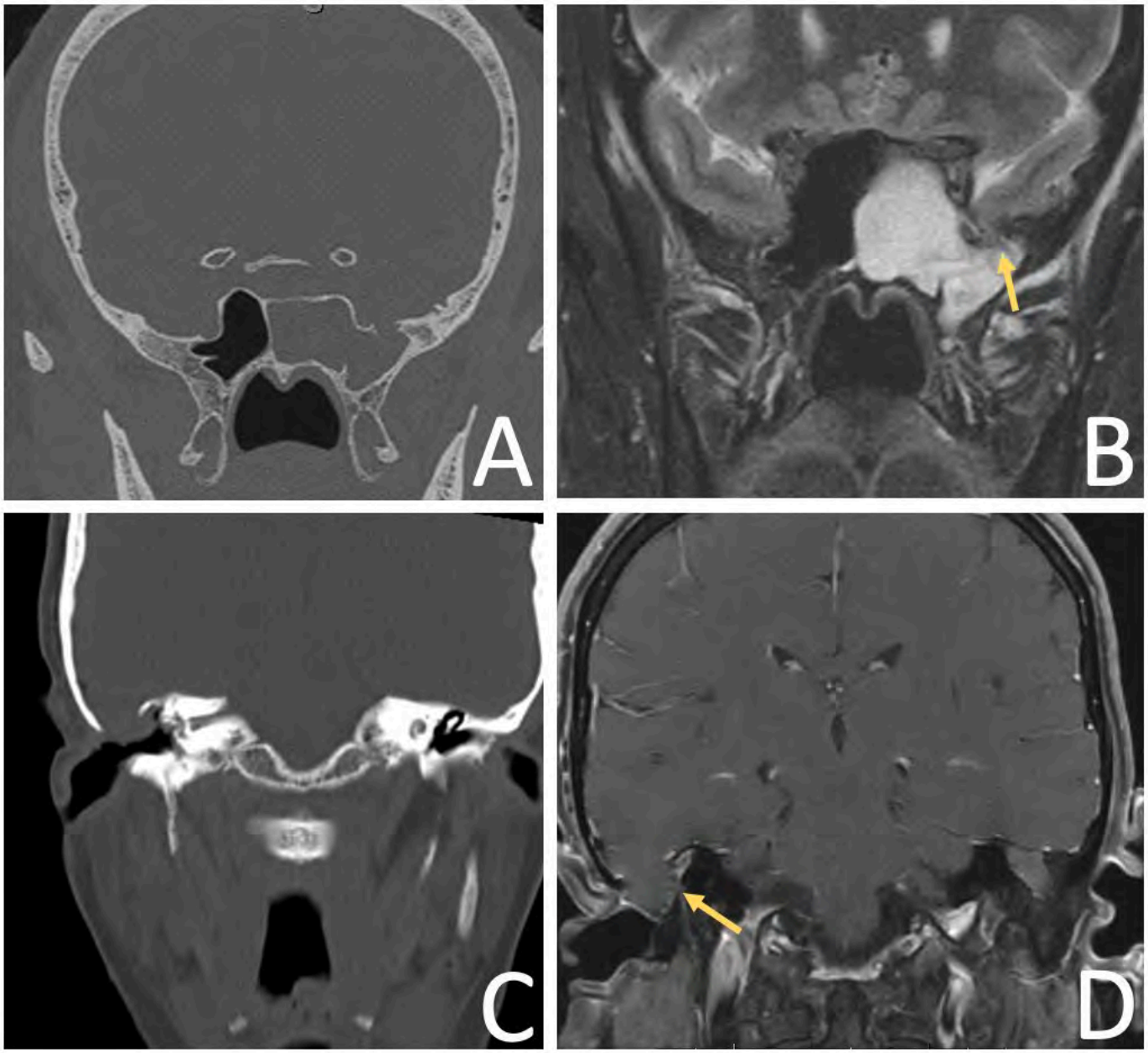


Figure 1: For Case 1, CT sinus without contrast (A) demonstrates opacification of the left sphenoid sinus and a small defect in the sphenoid roof. Same day MR stir sequence of the facial bones (B) demonstrates a 6mm defect in the sphenoid roof with an inferiorly herniated encephalocele (arrow) with hyperintense fluid opacifying the left sphenoid sinus. In Case 2, CT Temporal bone without contrast (C) shows a large anterior tegmen mastoideum defect. An MR brain T1 sequence (D) of the same patient demonstrates a right inferior temporal gyrus encephalocele herniating through the defect (arrow).

971

Pediatric Mitochondrial Disorders: Neuroimaging and Genetic Correlations

Neetika Gupta MBBS,MD[1], Shivaprakash B Hiremath MBBS,MD,FRCR[2], Elka Miller MD,FRCPC[1]
[1]The Hospital for Sick Children, Toronto, ON, Canada. [2]Toronto Western Hospital, Toronto, ON, Canada

Abstract Category

Pediatrics

Summary & Objectives

1. Recognize characteristic neuroimaging patterns associated with specific mitochondrial disorders.

2. Understand the correlation between specific genetic mutations with distinct neuroimaging phenotypes, aiding in accurate diagnosis and tailored treatment approaches.
3. Differentiate mitochondrial disorders from other neurometabolic diseases with overlapping imaging features, ensuring precise diagnosis.
4. Explore the utility of advanced imaging modalities in detecting early and subtle changes of mitochondrial disorders, which can influence prognosis and management.

Purpose

Paediatric mitochondrial disorders frequently exhibit characteristic brain MRI findings that can aid in early diagnosis and inform treatment. This review focuses on the neuroimaging and genetic correlations in pediatric mitochondrial disorders, offering a structured approach to identifying key imaging patterns that could link them to specific genotypes. Correlating specific imaging features with genotypes, can enhance diagnostic accuracy and guide management. Advanced imaging techniques, including MR spectroscopy, offer additional insights into disease progression and prognosis.

Materials & Methods

N/A

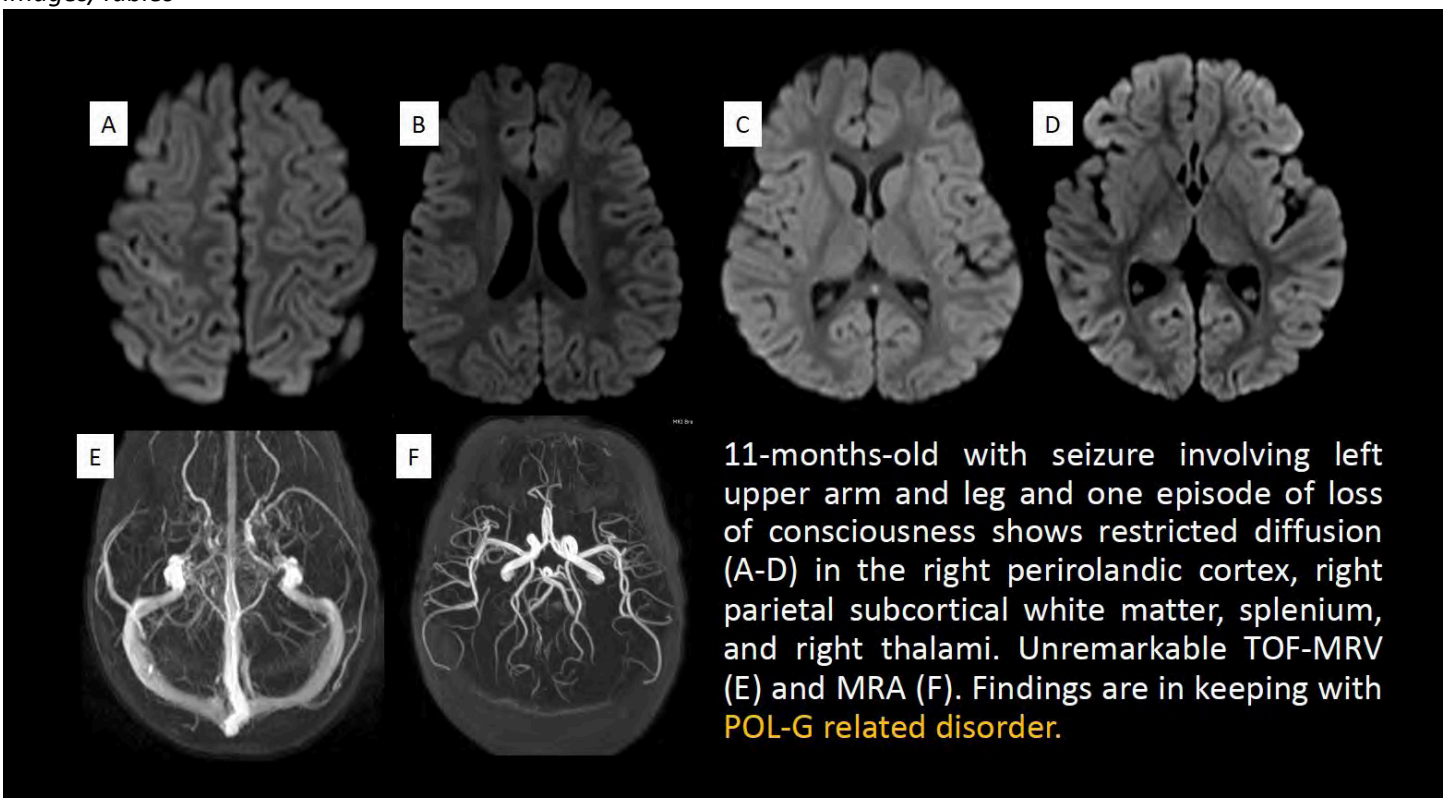
Results & Conclusion

N/A

References

1. Alves CAPF, Whitehead MT. Advancing the neuroimaging diagnosis and understanding of mitochondrial disorders. Neurotherapeutics. 2024 Jan;21(1):e00324. doi: 10.1016/j.neurot.2024.e00324. Epub 2024 Feb 1. PMID: 38306952; PMCID: PMC10903090.
2. Alves, César Augusto Pinheiro Ferreira MD[*]; Gonçalves, Fabrício Guimarães MD, EDiNR, EDiPNR[†]; Grieb, Dominik MD[‡]; Lucato, Leandro Tavares MD, PhD[*]; Goldstein, Amy C. MD[§]; Zuccoli, Giulio MD[||]. Neuroimaging of Mitochondrial Cytopathies. Topics in Magnetic Resonance Imaging 27(4):p 219-240, August 2018. | DOI: 10.1097/RMR.0000000000000173
3. Haas R, Dietrich R. Neuroimaging of mitochondrial disorders. Mitochondrion. 2004 Sep;4(5-6):471-90. doi: 10.1016/j.mito.2004.07.008. Epub 2004 Nov 30. PMID: 16120407.
4. Fabrício Guimarães Gonçalves, César Augusto Pinheiro Ferreira Alves, Beth Heuer, James Peterson, Angela N. Viaene, Sara Reis Teixeira

Images/Tables



973

Neuroimaging in Lysosomal storage disorders

Neetika Gupta MBBS, MD[1], Shivaprakash B Hiremath MBBS,MD,FRCR[2], Elka Miller MD,FRCPC[1]
[1]The Hospital for Sick Children, Toronto, ON, Canada. [2]Toronto Western Hospital, Toronto, ON, Canada

Abstract Category

Pediatrics

Summary & Objectives

1. Review the basic concepts of lysosomal storage disorders in childhood
2. Mention the clinical manifestations and developments in the therapeutic management of lysosomal storage disorders
3. Illustrate imaging manifestations in various lysosomal storage disorders highlighting usual findings and differential diagnosis

Purpose

- Review the basis of lysosomal storage disorders in children.
- Describe the clinical manifestations and developments in therapeutic management of lysosomal storage disorders.
- Illustrate the common and uncommon imaging manifestations in lysosomal storage disorders including

GM1 Gangliosidosis

GM2 Gangliosidosis

1. Tay-Sachs disease – GM2
2. Sandhoff disease

Mucopolysaccharidoses:

1. Hunter syndrome.
2. Hurler's disease

Sphingolipidoses:

1. Gaucher's disease
2. Fabry disease
3. Metachromatic leukodystrophy
4. Krabbe's disease (Globoid-cell Leukodystrophy)
5. Niemann Pick disease

Free Sialic Acid Storage Disorder (Salla disease)

Canavan's disease

Neuronal Ceroid Lipofuscinosis

Materials & Methods

N/A

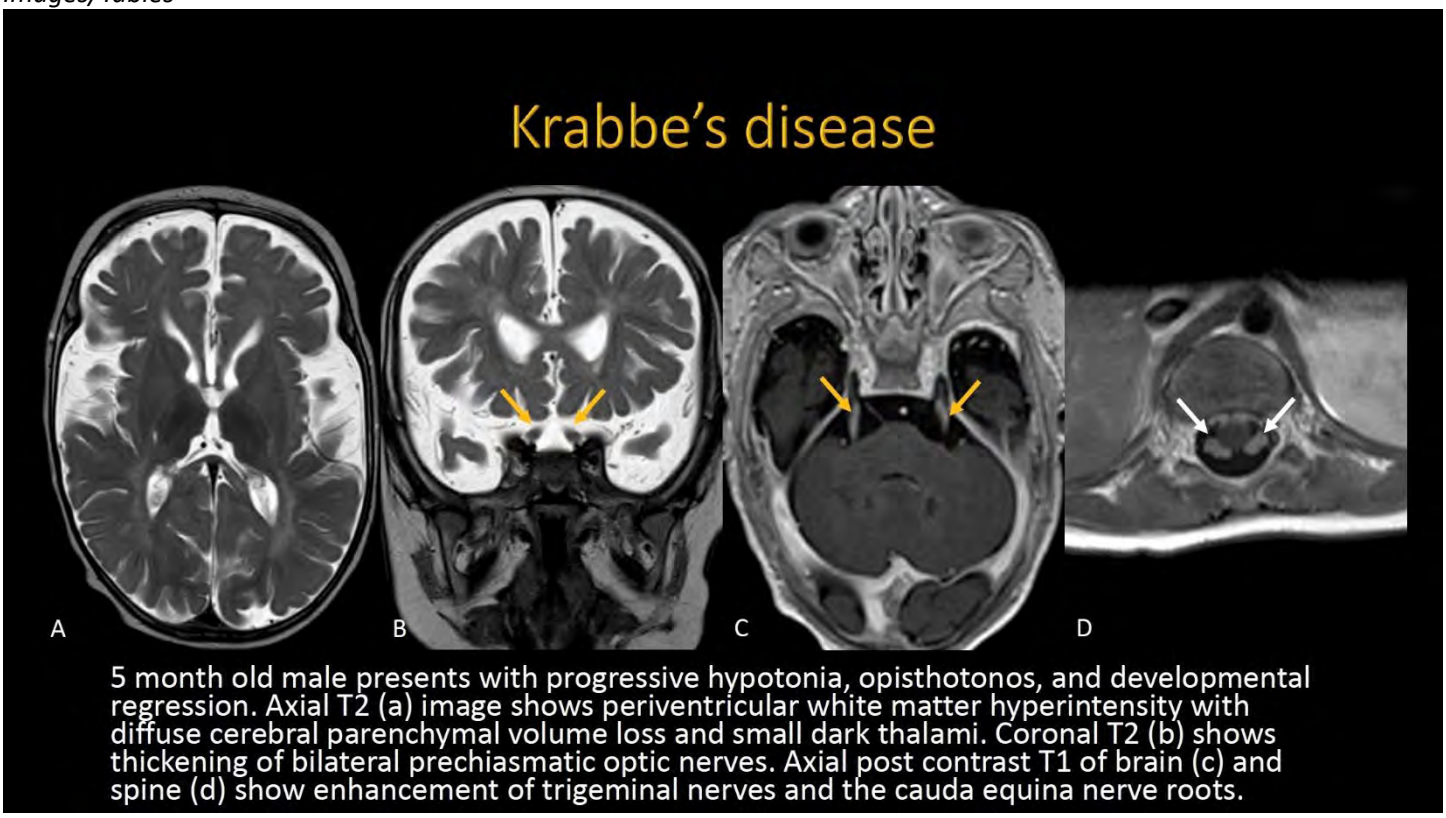
Results & Conclusion

N/A

References

1. D'Arco F, Hanagandi P, Ganau M, Krishnan P, Taranath A. Neuroimaging Findings in Lysosomal Disorders: 2018 Update. Top Magn Reson Imaging. 2018 Aug;27(4):259-274. doi: 10.1097/RMR.0000000000000174. PMID: 30086111.
2. Fagan, N., Alexander, A., Irani, N., Saade, C. and Naffaa, L. (2017), Magnetic resonance imaging findings of central nervous system in lysosomal storage diseases: A pictorial review. J Med Imaging Radiat Oncol, 61: 344-352. https://doi.org/10.1111/1754-9485.12569
3. K. Aydin, A. Serdaroglu, A. Kartal, C. Dilber, S. Haspolat, T. Hirfanoglu, G. Biberoglu, P73 – 2405: Brain MRI findings in children with lysosomal storage disorders, European Journal of Paediatric Neurology, Volume 19, Supplement 1, 2015, Page S114, ISSN 1090-3798,

Images/Tables



975

Cranial Nerve Enhancement: A Pattern-Based Diagnostic Approach

Seyed Amir Ebrahimzadeh MD-MPH, Nasrin Rahimian MD, Erik Pedersen MD
Creighton University, Omaha, Nebraska, USA

Abstract Category

Adult Brain Inflammatory/Infectious Disease/Degenerative/Metabolic

Summary & Objectives

Summary and Objectives:

Cranial nerve enhancement (CNE) on MRI is an important, yet diagnostically challenging finding that spans a wide range of underlying conditions. This exhibit aims to introduce a practical, pattern-based diagnostic framework for evaluating CNE, enabling radiologists to differentiate between key etiologies—such as infectious, inflammatory, and neoplastic causes—through the identification of specific enhancement patterns. By applying this systematic approach, radiologists can enhance diagnostic accuracy and clinical efficiency in managing patients with suspected cranial nerve pathology. The objectives of this exhibit are to (1) categorize the primary patterns of CNE and correlate each with potential underlying diseases, (2) review optimal MRI protocols that maximize detection and specificity in CNE evaluation, and (3) provide a reference guide for the differential diagnosis of CNE to improve clinical outcomes and guide early intervention

Purpose

Purpose:

Cranial nerve enhancement (CNE) is a frequently encountered yet diagnostically complex finding on MRI, associated with a diverse range of pathologies, including neoplastic, infectious, and inflammatory conditions. The purpose of this educational exhibit is to present a structured, pattern-based diagnostic approach for interpreting CNE on MRI, with a focus on recognizing enhancement patterns and correlating them with underlying disease processes. By consolidating a systematic framework, we aim to provide radiologists with practical insights to enhance differential diagnosis and improve clinical outcomes in patients with suspected cranial nerve pathology.

Materials & Methods

Materials and Methods:

This exhibit integrates an extensive literature review and selected cases from our institution, exploring four primary enhancement patterns identified in CNE: unilateral linear, bilateral linear, unilateral thickened, and bilateral thickened

(1). Optimal MRI protocols for evaluating cranial nerves and their advantages and limitations are also discussed. Each CNE pattern is mapped to probable etiologies, categorized by infectious/inflammatory (e.g., multiple sclerosis, viral neuritis), neoplastic (e.g., metastatic spread, primary nerve tumors), and other more rare causes (2).

Results & Conclusion

Results:

This educational exhibit highlights the efficacy of post-contrast 3D-T1-weighted, 3D FLAIR, and high-resolution black-blood sequences for their sensitivity to subtle enhancement. It discusses how linear enhancement patterns are typically associated with infectious or inflammatory etiologies, in contrast to the thickened enhancement patterns, which are often indicative of neoplastic processes. Unilateral linear CNE often corresponds with localized inflammatory or infectious conditions, while bilateral presentations may suggest systemic or multifocal inflammatory diseases. Thickened patterns, particularly bilateral, are strongly suggestive of metastatic involvement, such as leptomeningeal carcinomatosis or neurolymphomatosis. This exhibit underscores the diagnostic advantage of a pattern-based method, which, when applied to targeted imaging sequences, allows for a streamlined approach to evaluating CNE with high specificity for underlying pathology.

Conclusions:

This educational exhibit reviews differential diagnosis of CNE and provides a practical, pattern-based framework for interpreting cranial nerve enhancement on MRI. Implementing this systematic approach, radiologists can improve diagnostic precision and contribute to more timely and targeted patient care, particularly in cases where CNE represents an early manifestation of systemic or neoplastic disease.

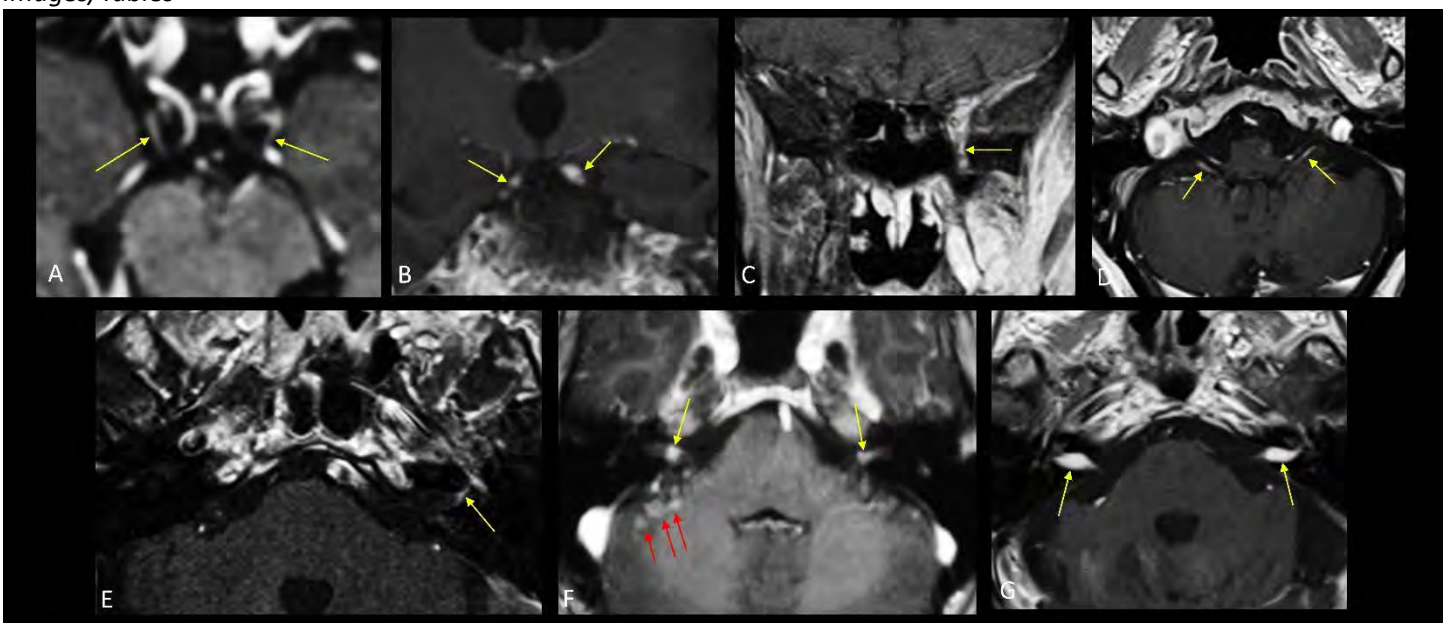
References

References

1. Moltoni G, Romano A, Blandino A, Palizzi S, Romano A, D'Arrigo B, et al. Extra-axial cranial nerve enhancement: a pattern-based approach. La Radiologia medica. 2024;129(1):118-32.

2. Saremi F, Helmy M, Farzin S, Zee CS, Go JL. MRI of cranial nerve enhancement. AJR American journal of roentgenology. 2005;185(6):1487-97.

Images/Tables



A. Linear enhancement of bilateral cranial nerve III in a patient with AIDS.
B. Enhancing nodular thickening with enhancement of bilateral cranial nerve III in a patient with neurolymphomatosis.
C. Enhancing nodular thickening of the left maxillary nerve (V2) due to perineural tumoral spread in a patient with squamous cell carcinoma.
D. Linear enhancement of bilateral cranial nerve IX and X in a patient with Miller-Fischer syndrome.
E. Linear enhancement of the left cranial nerve VII in a patient with Bell's palsy.
F. Enhancing nodular thickening of bilateral cranial nerve VII, in addition to multiple leptomeningeal metastatic foci, in a patient with metastatic lung cancer.
G. Enhancing smooth thickening of bilateral cranial nerve VII in a patient with adverse reaction to checkpoint inhibitor medication.

979

Everyone bites: An Anatomical and Pathological Review of the Mandible

Dylan Tan MD, Mohammad Chaudary MD, Alex Lin MD, Sean O'Rourke MD, YiLi Zhao MD, Gagandeep Singh MD
Columbia University, New York, NY, USA

Abstract Category

Head and Neck

Summary & Objectives

This presentation will review the anatomy and common pathologic lesions of the mandible through use of pictorials, diagrams, and labeled imaging examples. Anatomy of the mandible will be discussed in relation to the adjacent neurovascular and soft tissue structures. Common odontogenic and non-odontogenic lesions found in the mandible will be reviewed with CT and MRI examples.

Purpose

To provide radiology residents, fellows and attendings with an overview of mandibular anatomy, critical structures and common benign and malignant pathologies.

Materials & Methods

N/a

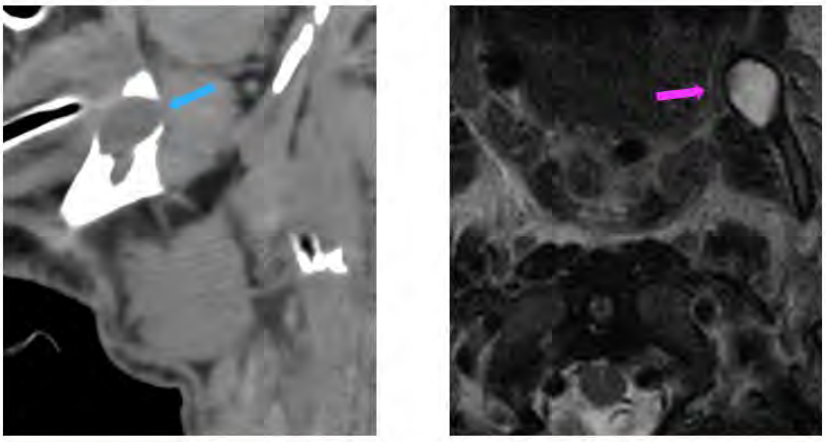
Results & Conclusion

Mandibular lesions are often found incidentally and can be challenging to diagnose. Understanding the anatomy of the mandible and imaging characteristics of common odontogenic and non-odontogenic pathologies helps guide the differential diagnosis and management.

References

1. Holmes KR, Holmes RD, Martin M, et al. Practical Approach to Radiopaque Jaw Lesions. Radiographics 2021;41(4):1164-1185. DOI:10.1148/rg.2021200187
2. Dunfee BL, Sakai O, Pistey R, et al. Radiologic and pathologic characteristics of benign and malignant lesions of the mandible. Radiographics 2006;26(6):1751-1768. DOI:10.1148/rg.266055189

Images/Tables



Sagittal CT of the cervical spine shows an incidental expansile cystic structure arising from the left mandible condylar process. Axial T2-weighted MRI shows a well-circumscribed unilocular cyst. Of note, this patient has complete edentulism. Given the location, dental history and lack of internal soft tissue component, this lesion is most consistent with a solitary bone cyst of the mandible.

982

Pediatric CNS tumors and tumor predisposition syndromes: What you need to know

Raisa Amiruddin MBBS, Austin Moats MD, Aashim Bhatia MD PhD, Mariam Aboian MD PhD, Karuna Shekdar MD
Children's Hospital of Philadelphia, Philadelphia, Pennsylvania, USA

Abstract Category

Pediatrics

Summary & Objectives

Several tumor predisposition tumor syndromes (TPS) have been described in association with common childhood CNS tumors such as medulloblastoma, ATRT, retinoblastoma, choroid plexus carcinoma etc. It is important to recognize TPS as it has a direct impact on treatment and outcome in affected patients, and in surveillance, early detection in unaffected patients. We aim to illustrate neuroimaging findings in common TPS presenting in childhood and in some newly described TPSs and the common gene/genetic pathway affected. The educational exhibit will provide trainees and practicing radiologists, information on CNS tumors and TPS needed to participate in brain tumor board discussions.

Table of Contents

The vast array of TPS can be an intimidating topic. Although there is some overlap with TPS of CNS tumors in adults, we will describe neuroimaging of TPS entities associated with common pediatric CNS tumors.

A: Common TPS:

Neurofibromatosis 1-NF1, Neurofibromatosis 2-NF2, Tuberous sclerosis TSC

Li Fraumeni, Gorlin syndrome, Rhabdoid Tumor predisposition syndrome SMARCB1/A4, Von Hippel Lindau disease VH, Ataxia Telangiectasia

Cowden/PTEN Hamartoma tumor syndrome, DICER1 syndrome 14q32.13

Brain Tumor-polyposis syndrome 2, Retinoblastoma RB1, Lynch syndrome

Noonan syndrome, Constitutional Mismatch Repair Deficiency (CMMRD)

Hereditary paraganglioma-pheochromocytoma (PGL/PCC) syndromes

B: Other TPS:

Shelterin complex gene POT1, MEN1, Familial melanoma-astrocytoma syndrome

BAP1 tumor predisposition syndrome, SMARCE1

Purpose

N/A

Materials & Methods

N/A

Results & Conclusion

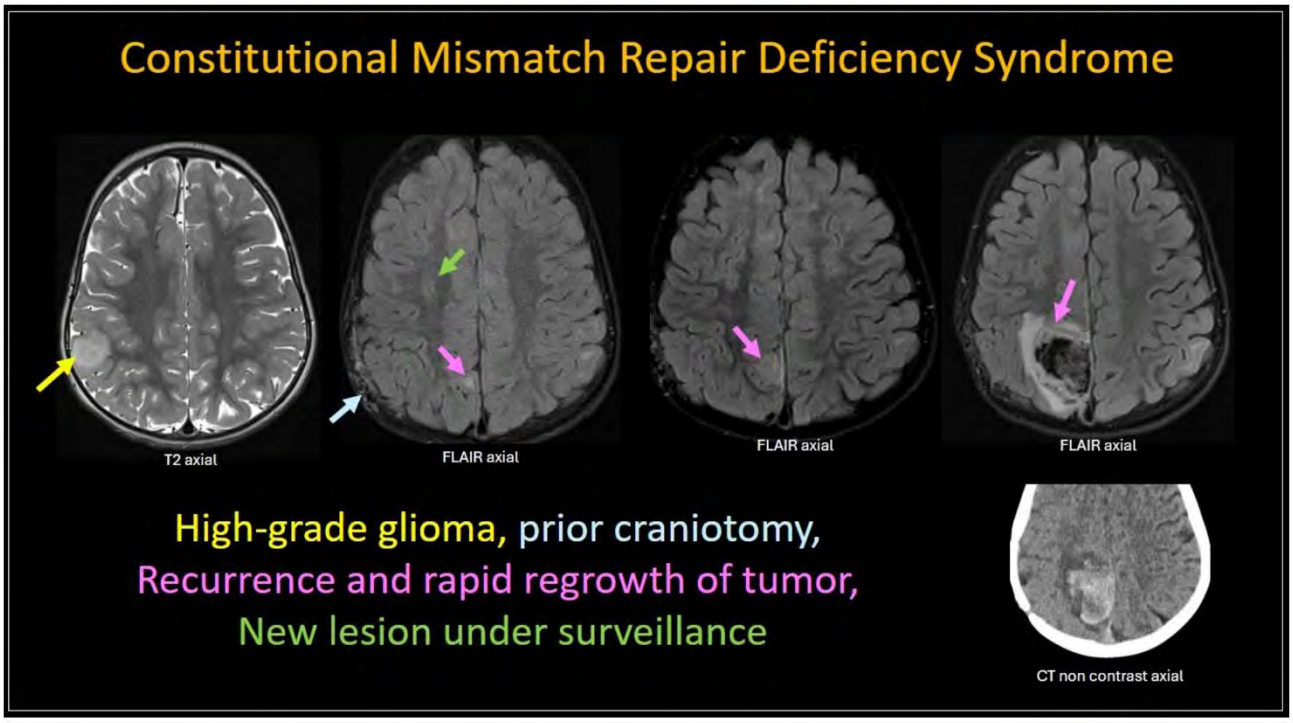
N/A

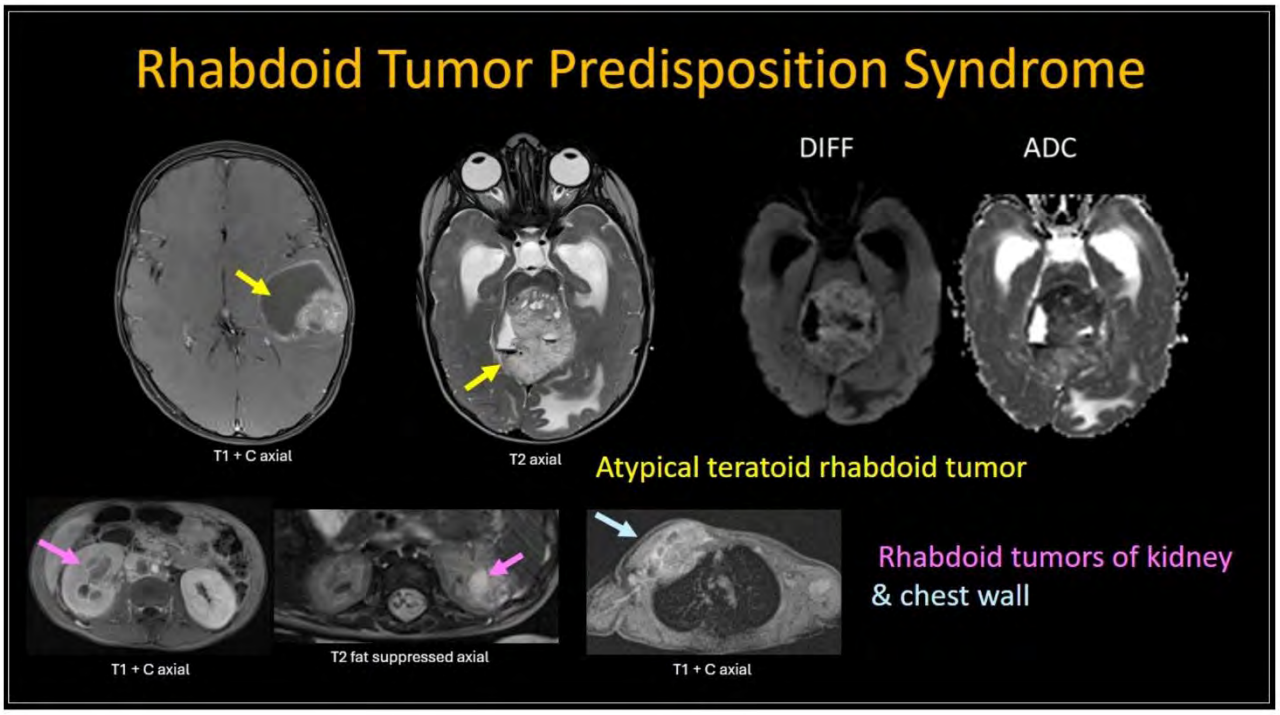
References

1. Genetic syndromes predisposing to pediatric brain tumors, Sameer Farouk Sait , Michael F. Walsh , and Matthias A. Karajannis, Neuro-Oncology Practice 8(4), 375–390, 2021 | doi:10.1093/nop/npab012 | Advance Access date 13 February 2021

2. An update on the central nervous system manifestations of familial tumor predisposition syndromes : David A. Solomon Acta Neuropathologica (2020) 139:609–612

Images/Tables





983

Pediatric Brain MR Elastography: Innovations and Clinical Applications

Adam E. Goldman-Yassen MD, MS[1], Grace McIlvain PhD[2]

[1]Children's Healthcare of Atlanta, Atlanta, GA, USA. [2]Columbia University, New York, NY, USA

Abstract Category

New Techniques/Advanced Imaging/Informatics/AI/Professional Development/Misc

Summary & Objectives

Magnetic Resonance Elastography (MRE) is an emerging non-invasive imaging technique that evaluates the mechanical properties of tissues. The objective of this exhibit is to familiarize neuroradiologists with the principles, techniques, and clinical applications of pediatric brain MRE. We will highlight applications of MRE in pediatric brain imaging, providing insights into its role in assessing brain stiffness changes in developing children and with pediatric-specific disorders.

Purpose

Pediatric brain MR Elastography is a promising modality that can quantitatively assess brain tissue stiffness, which may reflect underlying pathology not easily detected on conventional MRI. Understanding the physiological and pathological variations in brain stiffness across different pediatric age groups could help us better understand brain development and disease pathophysiology, as well as serve as a neuroimaging biomarker. This exhibit aims to enhance the neuroradiologist's understanding of brain MRE, including the theoretical basis, technical considerations, interpretation, and troubleshooting.

Materials & Methods

The exhibit draws on our experience in pediatric brain MRE and includes data from a retrospective cohort of pediatric patients. The methodology section will detail MRE acquisition techniques, parameter settings, and post-processing steps. The exhibit will also demonstrate examples of MRE findings in various pediatric age groups and clinical conditions, including a review of the literature.

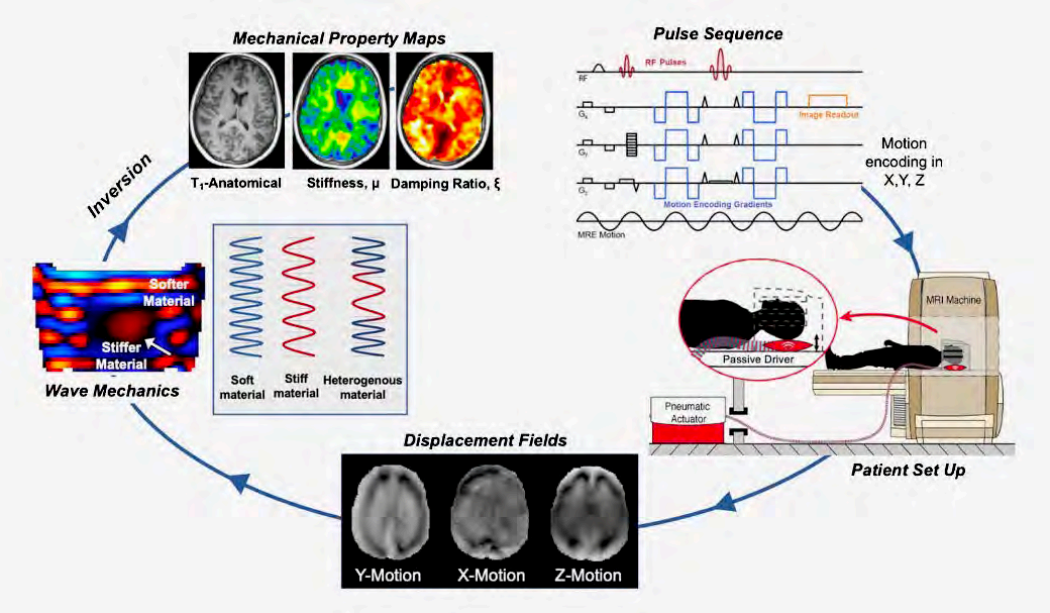
Results & Conclusion

Brain MRE demonstrates significant variations in brain stiffness across different age groups and disease states in pediatric patients. These findings suggest that pediatric brain MRE provides unique and clinically valuable information on brain pathology that complements traditional MRI. In conclusion, pediatric brain MRE is a valuable adjunct in the neuroradiologist's toolkit for evaluating brain structure and function in pediatric patients, with potential implications for earlier and more precise diagnosis of various neurologic conditions. It is therefore essential to understand how to implement, interpret, and trouble shoot brain MRE in children.

References

Khair AM, McIlvain G, McGarry MDJ, Kandula V, Yue X, Kaur G, Averill LW, Choudhary AK, Johnson CL, Nikam RM. Clinical application of magnetic resonance elastography in pediatric neurological disorders. Pediatr Radiol. 2023 Dec;53(13):2712-2722. doi: 10.1007/s00247-023-05779-3. Epub 2023 Oct 5. PMID: 37794174; PMCID: PMC11086054.

Images/Tables



993

Dynamic Imaging Diagnosis of CSF-Venous Fistulas: A Neuroradiologist's Guide to Detection and Treatment

George K Vilanilam MD, David Michaels MD, Edward Stehel MD, Heather M Early MD, Bharat Srivastava MD, Kwan Chen, John D Barr MD, Elvira Allakhverdieva MD, Justin Costello DO, Lee Pride Jr MD
University of Texas Southwestern Medical Center, Dallas, Texas, USA

Abstract Category

Interventional/Vascular/Stroke

Summary & Objectives

Cerebrospinal fluid (CSF)-venous fistula is a cause of clinical spontaneous intracranial hypotension (SIH) that requires specialized radiologic diagnostic techniques for accurate identification and is amenable to minimally invasive image-guided treatment. The primary objective of this exhibit is to discuss, in detail, the neuroradiological techniques involved in diagnosing CSF venous fistulas, drawing on our experience at a large academic medical center to highlight diagnostic strategies and lessons learned.

Purpose

To provide a comprehensive educational guide for neuroradiology-based diagnosis and management of CSF-venous fistulas, drawing on our institutional experience.

Materials & Methods

Five patients with SIH due to CSF-venous fistulas were evaluated and treated at our institution between October 2021 and October 2024. This cohort included three women and two men, aged 53 to 65 years. All patients met clinical and imaging criteria for SIH, underwent evaluation using dynamic digital subtraction myelography, and were subsequently treated with transvenous embolization of their CSF-venous fistula. Clinical histories, cross-sectional and dynamic imaging, treatment techniques, and outcomes were reviewed to compile the educational content for this exhibit.

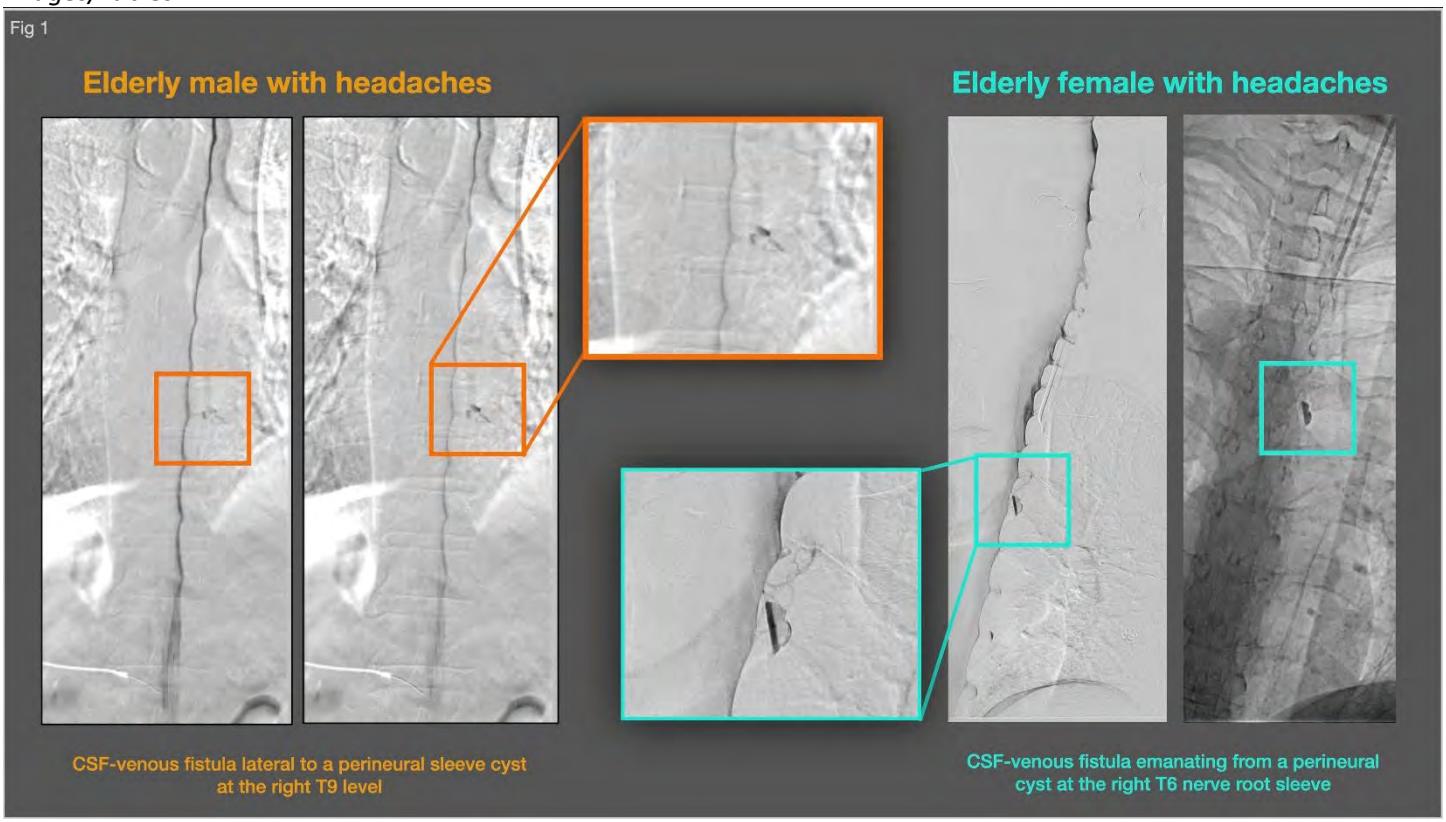
Results & Conclusion

In all cases, the CSF-venous fistula was successfully identified in the mid-thoracic spine, with locations varying from T6 to T9, using our dynamic digital subtraction myelography technique (Fig 1). Each patient experienced a positive clinical response to the transvenous embolization treatment of the fistula, performed using Onyx injection with balloon catheter protection of the transit segmental vein.

References

1. Lützen N, Demerath T, Würtemberger U, et al. Direct comparison of digital subtraction myelography versus CT myelography in lateral decubitus position: evaluation of diagnostic yield for cerebrospinal fluid-venous fistulas. J Neurointerventional Surg. Published online November 2, 2023:jnis2023-020789. doi:10.1136/jnis-2023-020789
2. Madhavan AA, Brinjikji W, Cutsforth-Gregory JK, et al. Myelographic Techniques for the Localization of CSF-Venous Fistulas: Updates in 2024. *AJNR Am J Neuroradiol*. 2024;45(10):1403-1412. Published 2024 Oct 3. doi:10.3174/ajnr.A8299
3. Galvan J, Maya M, Prasad RS, Wadhwa VS, Schievink W. Spinal Cerebrospinal Fluid Leak Localization with Digital Subtraction Myelography: Tips, Tricks, and Pitfalls. *Radiol Clin North Am*. 2024;62(2):321-332. doi:10.1016/j.rcl.2023.10.004
4. Luetzen N, Dovi-Akue P, Fung C, Beck J, Urbach H. Spontaneous intracranial hypotension: diagnostic and therapeutic workup. *Neuroradiology*. 2021;63(11):1765-1772. doi:10.1007/s00234-021-02766-z
5. Kranz PG, Gray L, Malinzak MD, Houk JL, Kim DK, Amrhein TJ. CSF-Venous Fistulas: Anatomy and Diagnostic Imaging. *AJR Am J Roentgenol*. 2021;217(6):1418-1429. doi:10.2214/AJR.21.26182

Images/Tables



999

Basivertebral Nerve Ablation: What Neuroradiologists Should Know

Thomas R Geisbush MD[1], Arzu Ozturk MD[2], Connor Gemmell MD[1], Muhammad T Raj MD[1], Kader K Oguz MD[1], Osama R Raslan MD[1], Arthur B Dublin MD[1], Lotfi Hacein-Bey MD[1]

[1]UC Davis Medical Center, Sacramento, CA, USA. [2]UC Davis Medical Center, Sacramento, CA, USA

Abstract Category

Spine

Summary & Objectives

The management of chronic low back pain (CLBP) is continually evolving with a trend toward further utilization of minimally invasive procedures. Basivertebral nerve ablation (BVNA) has shown promise in alleviating vertebrogenic pain in appropriately selected patients. It is important for neuroradiologists to become familiar with the pre- and post-treatment imaging findings pertaining to this procedure.

Purpose

CLBP is a complex multifactorial condition that is globally the leading cause of years lived with disability, morbidity and a major cause of healthcare spending.[1] First-line management involves conservative approaches such as physical therapy, exercise programs, and non-steroidal anti-inflammatory medications. However, many individuals with CLBP fail to respond to conservative treatment and necessitate more personalized therapeutic strategies. Selective facet joint or epidural steroid injection, rhizotomy, and surgical intervention have all demonstrated varying degrees of effectiveness. Recognizing vertebral endplate inflammation's role as a source of vertebrogenic pain has led to the integration of intraosseous ablation of the basivertebral nerve into low back pain management guidelines since 2019.[2] This exhibit aims to guide neuroradiologists in evaluating diagnostic imaging findings related to patient selection and assessing normal and abnormal imaging post-BVNA.

Materials & Methods

Imaging findings of patients with CLBP unresponsive to conservative therapy were reviewed for eligibility for BVNA. Major eligibility criteria, such as Modic Type 1 or 2 changes observed on lumbar spine MRI, as well as imaging findings that would contraindicate BVNA, such as a procedural target zone less than 10 mm from the spinal canal, were reviewed.[3] Post-BVNA MRI findings including positive clinical response, lack of response, and post procedural complications were then analyzed.

Results & Conclusion

BVNA has proven effective in managing a subset of chronic vertebrogenic pain, as evidenced by two prospective trials, INTRACEPT and SMART.[4,5] Consequently, BVNA is expected to gain broader acceptance and application. Neuroradiologists should become adept at interpreting these imaging results to better understand the efficacy and potential complications associated with BVNA, thereby enhancing patient care and management strategies in treating chronic low back pain.

References

1. Wu A, March L, Zheng X, et al. Global low back pain prevalence and years lived with disability from 1990 to 2017: estimates from the Global Burden of Disease Study 2017. *Ann Transl Med* 2020;8:299–299.
2. Huang J, Delijani K, Jones J, et al. Basivertebral Nerve Ablation. *Semin Intervent Radiol* 2022;39:162–6.
3. Smirniotopoulos JB, Osuala U, Restrepo CR, et al. Basivertebral nerve ablation technique. *Tech Vasc Interv Radiol* https://doi.org/10.1016/j.tvir.2024.100987.
4. Fischgrund JS, Rhyne A, Franke J, et al. Intraosseous basivertebral nerve ablation for the treatment of chronic low back pain: a prospective randomized double-blind sham-controlled multi-center study. *European Spine Journal* 2018;27:1146–56.
5. Smuck M, Khalil J, Barrette K, et al. Prospective, randomized, multicenter study of intraosseous basivertebral nerve ablation for the treatment of chronic low back pain: 12-month results. *Reg Anesth Pain Med* 2021;46:683–93.

Images/Tables

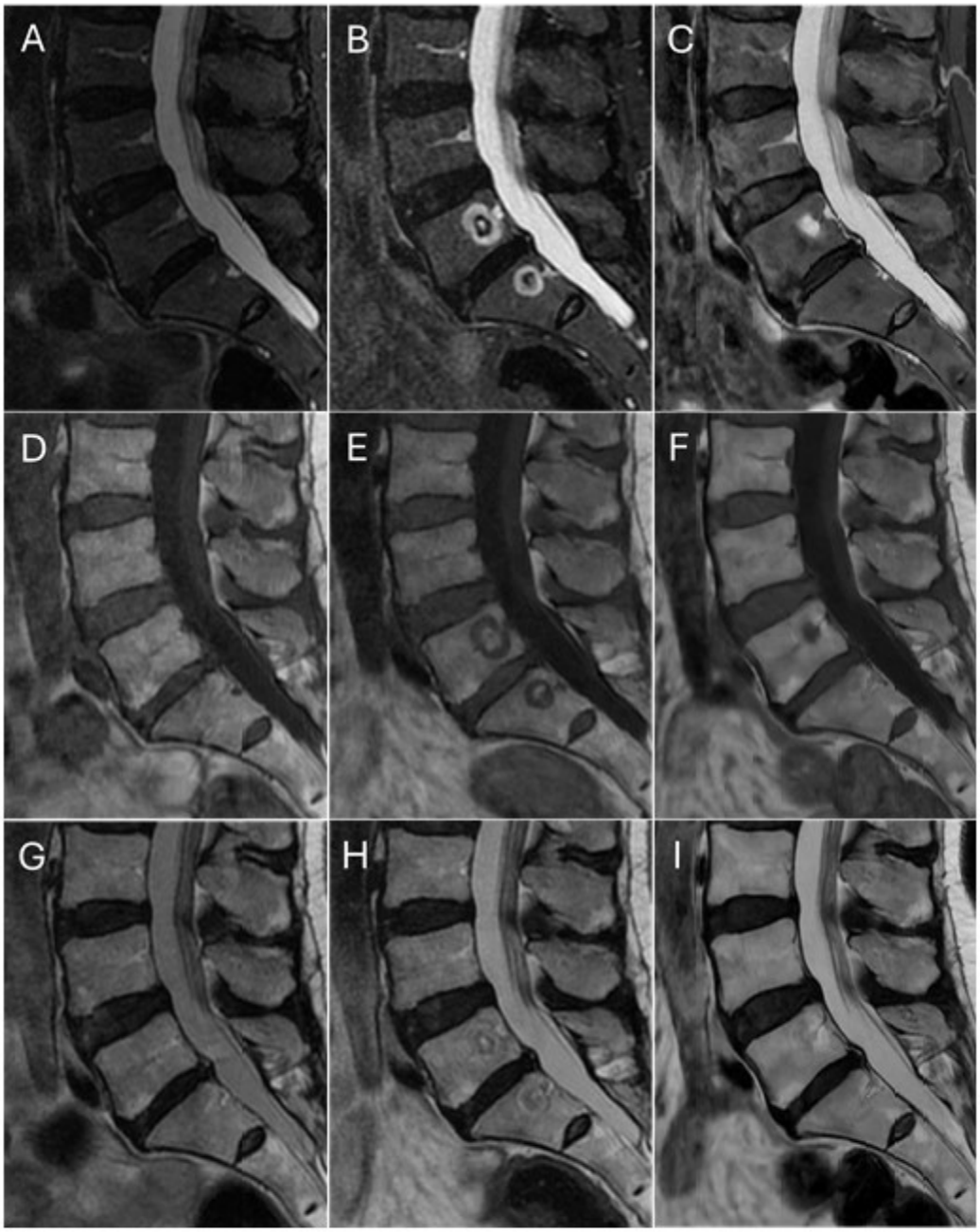


Fig. 1

A, D, and G, Respective sagittal STIR, T1-weighted, and T2-weighted images of the lower lumbar spine in a 64-year-old women with low back pain refractory to conservative management. *B, E, and H,* Respective sagittal STIR, T1-weighted, and T2-weighted images of the lower lumbar spine 2 months after basivertebral nerve ablation to the L5 and S1 vertebral bodies demonstrating targetoid signal alterations through each sequence. *C, F, and I,* Respective sagittal STIR, T1-weighted, and T2-weighted images of the lower lumbar spine 11 months after basivertebral nerve ablation demonstrating persistent but decreased signal alterations in the L5 and S1 vertebral bodies.

1007

To Embolize or Excise?: Key Imaging Features for Cerebrovascular Arteriovenous Malformation Treatment Planning

Manisha Koneru
Cooper University Health Care, Camden, NJ, USA

Abstract Category

Interventional/Vascular/Stroke

Summary & Objectives

Cerebrovascular arteriovenous malformations (AVMs) can be treated via surgical excision or endovascular embolization. Success and appropriateness of each approach is dependent on the characteristics and presentation of the AVM. Treatment planning for open versus endovascular approaches is dependent on certain imaging characteristics of AVMs on pre-procedural imaging.

Purpose

The purpose is to review the clinically-relevant radiographic features of cerebrovascular AVMs and their implications and significance in guiding treatment.

Materials & Methods

Evaluation of features of AVMs appreciated on preprocedural imaging include consideration of three major factors: size, location, and structure of the vasculature. AVMs that are smaller in size, typically less than 3cm in diameter, are more likely to be successful with endovascular embolization than larger AVMs. Location of the AVM dictates feasibility of endovascular intervention and risk of neurological deficits from aberrant embolic agent migration. AVMs located in areas not readily accessible by major arterial branches of the cerebrovasculature may not be appropriate for endovascular embolization. Similarly, AVMs in eloquent brain regions have high risk of inducing ischemic injury due to migration of embolic agents, thus carrying risk for neurological deficits with endovascular approaches. Additionally, characteristics of the feeding arteries and draining veins drive the treatment approach. AVMs with multiple arterial feeding vessels may not be as easily treated with embolization due to a large number of target vessels to occlude. Moreover, highly tortuous arterial vasculature may impede catheter navigation to the target site for embolization. In addition to feeding arterial supply, careful evaluation of the venous drainage is needed. Highly complex, tortuous venous drainage with altered hemodynamics and confluence with multiple venous structures may increase likelihood of aberrant venous occlusion during endovascular embolization, thus elevating the risk of venous infarction and venous hypertension.

Results & Conclusion

Identifying the key structural characteristics of AVMs is essential for guiding treatment decisions, including whether to proceed with endovascular embolization or favor surgical excision.

References

1. Raymond J, Gentric J-C, Magro E, et al. Endovascular treatment of brain arteriovenous malformations: clinical outcomes of patients included in the registry of a pragmatic randomized trial. *J Neurosurg* 2023;138:1393–402.
2. Mohr JP, Parides MK, Stapf C, et al. Medical management with or without interventional therapy for unruptured brain arteriovenous malformations (ARUBA): a multicentre, non-blinded, randomised trial. *Lancet* 2014;383:614–21.

1029

Synthetic MR: Clinical Applications in Pediatric Neuroimaging

SMILY SHARMA MD, DNB, FRCR, Abhishek Nayak DNB, Rakesh Vashishta MD, Bejoy Thomas MD, DNB, PDCC, Chandrasekharan Kesavadas MD, DMRD
Sree Chitra Tirunal Institute for Medical Sciences and Technology, Trivandrum, Kerala, India

Abstract Category

Pediatrics

Summary & Objectives

Synthetic MR is a potentially useful quantitative MR technique in clinical pediatric neuroimaging practice owing to its ability to generate desirable contrast-weighted images, carry out myelin quantification, automated segmentation of brain volumes, and provide quantitative relaxometry data in an abbreviated overall scan time.

The objectives of the presented exhibit are to provide an in-depth discussion of the clinical applications of synthetic MR in pediatric Neuroradiology, using a case-based approach.

Purpose

This educational exhibit aims to comprehensively discuss the clinical applications, advantages, and limitations of synthetic MR [Multiple Dynamic Multiple Echo (MDME) sequence] in pediatric neuroimaging. MDME sequence is US-FDA-approved synthetic MR technique that acquires multi-slice 2D multi-contrast images to rapidly quantify tissue relaxation times in a sequence duration of 5-7 minutes for full brain coverage. A vendor-independent software is then used for fast post processing of the acquired data, lasting less than 1 minute.[1,2]

Materials & Methods

A multitude of clinical applications of synthetic MR are discussed, including those based on quantitative assessment of parametric (T1, T2, PD, R1, and R2) maps and generation of desirable contrast weighted images, including Double Inversion Recovery (DIR) and Phase Sensitive Inversion Recovery (PSIR), which are not routinely acquired due to time constraints.[3] Applications based on myelin quantification and automated segmentation techniques are elaborated.

Results & Conclusion

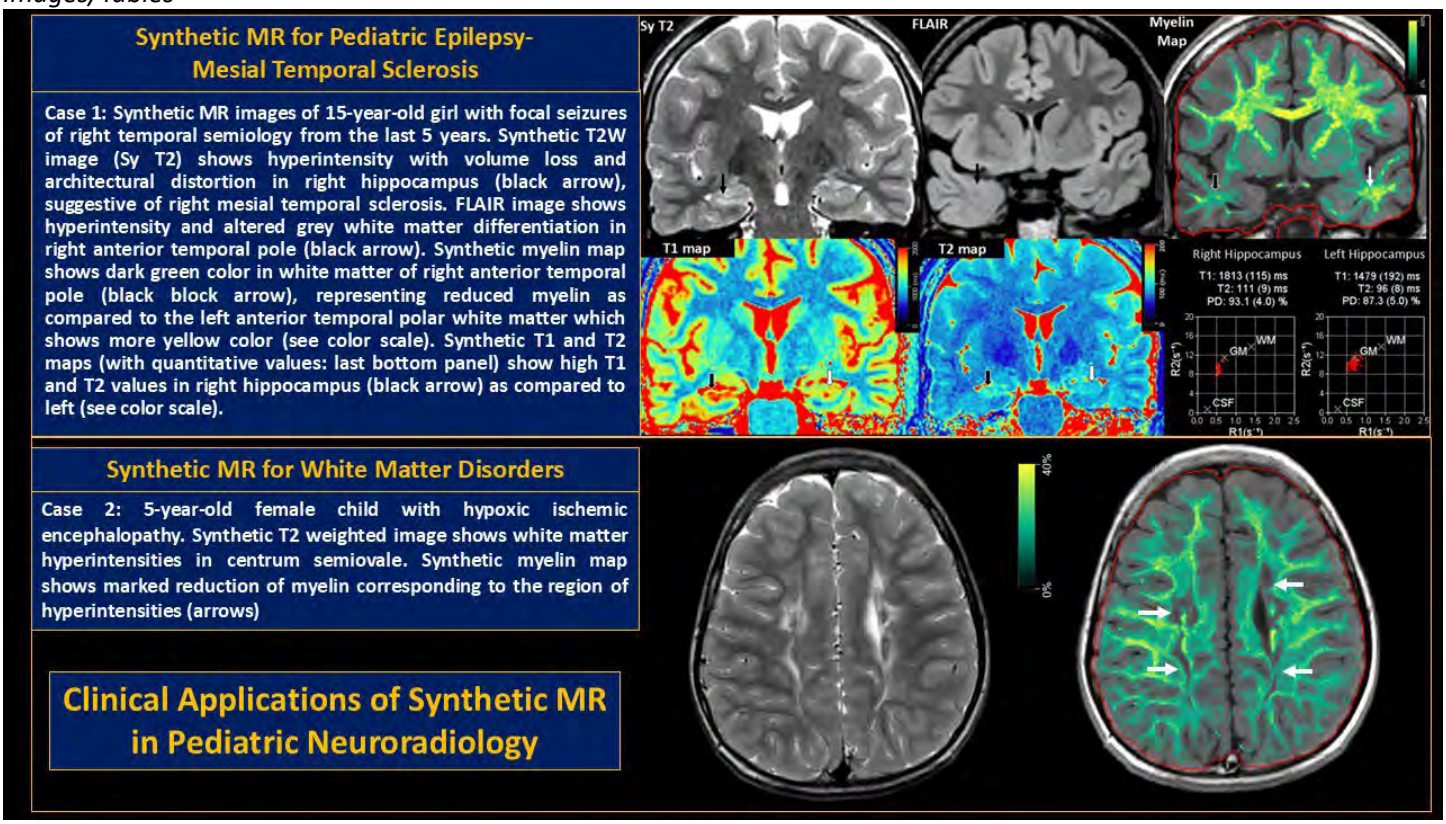
Using illustrative cases, the ability to provide both qualitative and quantitative data through a single sequence by synthetic MR in pediatric neuroimaging is demonstrated, which helps save scan time significantly. The advantages of synthesized PSIR and DIR in pediatric epilepsy cases are discussed, where these allow enhanced detection of subtle focal cortical dysplasias (FCDs) and allow improved detection of the extent of malformations of cortical development owing to improved grey-white matter differentiation. Other potential uses in pediatric epilepsy include detection of myelin loss in anterior temporal neocortical changes associated with mesial temporal sclerosis and in transmantle sign associated with FCDs, as has been demonstrated on histopathology studies.[4] Myelin quantification by synthetic MR is discussed with its potential applications in evaluation of brain development and assessing myelin loss in hypomyelinating and demyelinating leukodystrophies. The advantages of automatic segmentation of brain volumes are elaborated, including objective follow-up of CSF volumes in hydrocephalus and white matter and brain parenchymal volumes and fractions in various white matter disorders. Applications of automated volumetry by synthetic MR in Tuberous Sclerosis are shown where objective comparison of NON [Non-white matter-grey matter-CSF] volumes, indicating the burden of subependymal nodules and tubers, is possible in follow up scans. Potential future applications, including the differentiation of various neoplastic and non-neoplastic brain tumors via quantitative relaxation values, are discussed. Limitations of synthetic MR, including cost, limited availability in resource-poor settings, and synthetic FLAIR artifacts, are also elaborated.

To conclude, synthetic MR has multiple clinical applications in routine neuroradiology practice and is especially useful in pediatric populations as it allows the acquisition of a patient-tailored scan with the additional advantage of providing quantitative information. This can enhance diagnostic precision and improve long-term patient outcomes.

References

1. Ji S, Yang D, Lee J, Choi SH, Kim H, Kang KM. Synthetic MRI: technologies and applications in neuroradiology. *JMRI* 2022;55:1013-25. https://doi.org/10.1002/jmri.27440
2. Tanenbaum LN, Tsiouris AJ, Johnson AN, et al. Synthetic MRI for clinical neuroimaging: results of the magnetic resonance image compilation (MAGiC) prospective, multicenter, multireader trial. *AJNR Am J Neuroradiol* 2017;38:1103-10. https://doi.org/10.3174/ajnr.a5227
3. West H, Leach JL, Jones BV, Care M, Radhakrishnan R, Merrow AC, Alvarado E, Serai SD. Clinical validation of synthetic brain MRI in children: initial experience. *Neuroradiology* 2017;59:43-50. https://doi.org/10.1007/s00234-016-1765-z
4. Li J, Bai YC, Wu LH, Zhang P, Wei XC, Ma CH, et al. Synthetic relaxometry combined with MUSE DWI and 3D-pCASL improves detection of hippocampal sclerosis. *Eur J Radiol* 2022;157:110571. https://doi.org/10.1016/j.ejrad.2022.110571

Images/Tables



1030

High-Riding Jugular Bulb: Imaging Characteristics, Variants, and Clinical Implications in Radiologic Practice

FNU Vabhav MBBS[1], Aditya Duhan MD[2], Rajiv Mangla MD[2], Vipul Kaliraman MBBS[2], Amar Swarnkar MD[2]
[1]Pt. B.D. Sharma PGIMS, Rohtak, Haryana, India. [2]State University of New York Upstate Medical University, Syracuse, NY, USA

Abstract Category

Interventional/Vascular/Stroke

Summary & Objectives

Summary:

The high-riding jugular bulb (HRJB) is a vascular variant where the jugular bulb extends higher than usual within the petrous bone, usually into the middle ear cavity or near the vestibular aqueduct. Although typically asymptomatic, it may present with hearing loss, tinnitus, or dizziness. This exhibit demonstrates HRJB's characteristic imaging findings, explores its variations, and discusses implications for clinical management, highlighting the importance of differentiating HRJB from pathological processes.

Educational Objectives:

- To identify the radiologic characteristics of a high-riding jugular bulb across CT and MRI.
- To differentiate HRJB from pathological lesions that may mimic its appearance.
- To understand the clinical significance of HRJB, especially in surgical and diagnostic contexts.

Purpose

This educational exhibit aims to provide radiologists and clinicians with a comprehensive understanding of HRJB, including its imaging features, common variants, and differential diagnoses, thus enabling accurate identification and management in clinical practice.

Materials & Methods

This exhibit illustrates a series of HRJB cases, each documented with high-resolution CT or MRI imaging. Imaging techniques include:

- **CT**: Bone window views are used to assess bony remodeling and dehiscence in the petrous bone adjacent to HRJB.
- **MRI**: T1, T2, and post-contrast sequences are used to distinguish HRJB from other structures and assess vascular flow.

Results & Conclusion

Key Imaging Findings of High-Riding Jugular Bulb:

- **CT Characteristics**:
  - Smooth remodeling of the petrous bone adjacent to the HRJB, often without signs of mass effect.
  - Occasional bone dehiscence, where HRJB borders the middle ear or vestibular aqueduct without an intervening bony barrier, potentially causing clinical symptoms.
  - Incidental findings of HRJB can include communication with adjacent structures like the internal auditory canal or vestibular aqueduct.
- **MRI Characteristics**:
  - Vascular flow signal is observed within the HRJB, which helps differentiate it from soft-tissue masses.
  - In cases with dehiscence, flow-related signal voids or turbulence may be visualized near the middle ear structures.
  - No post-contrast enhancement is typically seen, differentiating it from pathologies like paragangliomas or other neoplastic masses.

Common Variants of High-Riding Jugular Bulb:

1. HRJB with Dehiscence into the Middle Ear: May appear as a bulging vascular structure on CT with potential bone erosion in the petrous region causing pulsatile tinnitus or conductive hearing loss.
2. **HRJB Proximity to the Vestibular Aqueduct**: High-riding jugular bulbs can extend to the vestibular aqueduct, sometimes causing vestibular symptoms such as dizziness or vertigo.

Conclusion:

A high-riding jugular bulb is a significant anatomical variant that may mimic pathology but is distinguishable through careful imaging analysis. Familiarity with HRJB imaging characteristics and variants is critical for radiologists, as it can prevent misdiagnosis and unnecessary interventions. Recognizing HRJB's specific imaging features facilitates accurate differential diagnosis, guiding treatment planning, and improving patient outcomes.

References

1. Manjila S, Bazil T, Kay M, et al. Jugular bulb and skull base pathologies: proposal for a novel classification system for jugular bulb positions and microsurgical implications. https://doi.org/10.3171/2018.5.FOCUS18106
2. Rauch SD, Xv W-Z, Nadol JB. High Jugular Bulb: Implications for Posterior Fossa Neurotologic and Cranial Base Surgery. Ann Otol Rhinol Laryngol 1993;102:100–7
3. Friedmann DR, Eubig J, Winata LS, et al. Prevalence of Jugular Bulb Abnormalities and Resultant Inner Ear Dehiscence: A Histopathologic and Radiologic Study. Otolaryngol Head Neck Surg 2012;147:750–6

Images/Tables

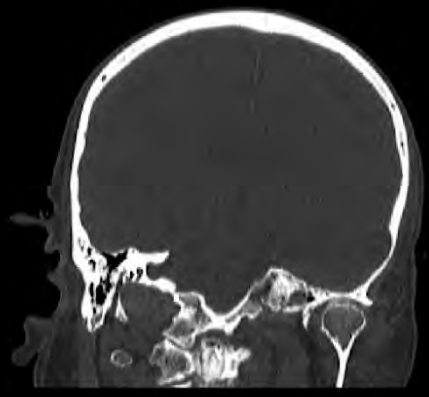


Figure: Coronal CT images highlighting the dehiscence of the mastoid segment of the facial nerve. The area of dehiscence can be seen with a disruption in the bony covering of the facial nerve canal, which is a critical structure within the temporal bone.



Figure: Axial high-resolution CT images of the temporal bone in a 45-year-old patient with pulsatile tinnitus. The image on the left shows a high-riding jugular bulb (indicated by arrow) reaching up to the level of the internal auditory canal (IAC) on the left side, compared to a normal jugular bulb on the right side. This anatomical variation is significant as it may be associated with the patient's symptoms of pulsatile tinnitus.



Figure: Coronal CT image showing a high-riding jugular bulb protruding into the floor of the middle ear cavity. The bony plate overlying the vestibular aqueduct is thinned, indicating potential vulnerability in this area. This anatomical variation can be clinically significant in terms of middle ear and inner ear structures.

1031

Susceptibility-Weighted Imaging: Applications in the Evaluation of Microangiopathies, Hemorrhages, and Cerebral Pathologies

FNU Vaibhav MBBS[1], Aditya Duhan MD[2], Vipul Kaliraman MBBS[3], Rajiv Mangla MD[2], Amar Swarnkar MD[2]
[1]Pt. B.D. Sharma PGIMS, Rohtak, Haryana, India. [2]State University of New York Upstate Medical University, Syracuse, NY, USA. [3]Maulana Azad Medical College, New Delhi, New Delhi, India

Abstract Category

New Techniques/Advanced Imaging/Informatics/AI/Professional Development/Misc

Summary & Objectives

Summary:

Susceptibility-weighted imaging (SWI) is an advanced MRI technique that utilizes the magnetic properties of blood, iron, and calcium, allowing detailed visualization of cerebral microvasculature and microhemorrhages. This exhibit aims to provide insights into the diverse applications of SWI, highlighting its value in diagnosing cerebral microangiopathies, amyloid angiopathy, brain abscess, diffuse axonal injury, and other related pathologies.

Objectives:

1. To demonstrate the diagnostic utility of SWI across various cerebral pathologies.
2. To describe SWI's distinctive imaging patterns in conditions like amyloid angiopathy, hypertensive microangiopathy, and diffuse axonal injury.
3. To guide clinicians in using SWI to improve diagnostic accuracy and patient care.

Purpose

The purpose of this exhibit is to provide an overview of SWI's clinical applications in neuroradiology. By highlighting specific cases, this presentation will illustrate how SWI assists in identifying and differentiating complex cerebral pathologies, offering clinicians enhanced diagnostic tools for more accurate treatment planning.

Materials & Methods

A retrospective review of cases from a tertiary medical center where SWI was used for cerebral imaging was conducted. Imaging sequences included high-resolution SWI and supporting T1- and T2-weighted MRI, with additional CT scans for anatomical and density-based correlation. The cases in this exhibit represent conditions in which SWI has proven diagnostic value, including amyloid angiopathy, hypertensive microangiopathy, brain abscess, diffuse axonal injury, and others. SWI findings were analyzed to identify unique imaging characteristics pertinent to each pathology.

Results & Conclusion

Results:

- Amyloid Angiopathy: SWI is critical in identifying lobar hemorrhages and cortical-subcortical microbleeds, typically located in cortical sulci and accompanied by superficial siderosis.
- Hypertensive Microangiopathy: SWI highlights microbleeds in the basal ganglia, thalamus, pons, and cerebellum, favoring deep brain structures typical of hypertensive hemorrhage.
- Brain Abscess: The "double rim sign" on SWI — a hypointense outer and hyperintense inner rim — distinguishes abscesses from tumors like glioblastoma. Adjacent vessel asymmetry due to congestion is also noted.
- Diffuse Axonal Injury (DAI): SWI is sensitive to small hemorrhagic lesions at the gray-white matter junction, useful as a prognostic marker in trauma cases.
- Septic Emboli: SWI shows scattered microbleeds across cortical and subcortical areas, common in endocarditis or septic emboli cases.
- Anoxic Injury: SWI underscores venous congestion in severe hypoxic injury, with prominent intramedullary and sulcal veins indicating extensive edema and poor prognosis.
- ECMO/Cardiac Surgery: SWI detects subcortical microbleeds in patients post-ECMO or cardiac surgery, reflecting vascular injury from prolonged extracorporeal support.
- Etching in DIC: SWI reveals multiple tiny foci of susceptibility at the cortical-subcortical junction and corpus callosum, related to coagulopathies.
- Pediatric Head Injury: SWI is highly sensitive to abusive head trauma, particularly retinal hemorrhages and the "tadpole sign" (a hyperintense vein clot with an intravascular clot).

Conclusion:

SWI is an integral tool in neuroradiology, offering enhanced sensitivity for microbleeds, vascular abnormalities, and structural changes in diverse cerebral pathologies. By outlining susceptibility variations, SWI facilitates accurate

diagnosis, crucial for effective management in conditions ranging from traumatic injuries to vascular and infectious diseases. This exhibit demonstrates SWI's unique capacity to highlight pathology-specific imaging patterns and guide clinicians in diagnostic accuracy.

References

1. Magnetic resonance susceptibility weighted imaging in neurosurgery: current applications and future perspectives in: Journal of Neurosurgery Volume 123 Issue 6 (2015) Journals
2. Blitstein MK, Tung GA, Blitstein MK, et al. MRI of Cerebral Microhemorrhages. American Journal of Roentgenology https://doi.org/10.2214/AJR.07.2249
3. Chang J, Arani K, Chew S, et al. Susceptibility Etching on MRI in Patients with Microangiopathy. J Neuroimaging 2017;27:43–9
4. Verschuuren S, Poretti A, Buerki S, et al. Susceptibility-Weighted Imaging of the Pediatric Brain. American Journal of Roentgenology https://doi.org/10.2214/AJR.11.8049

Images/Tables

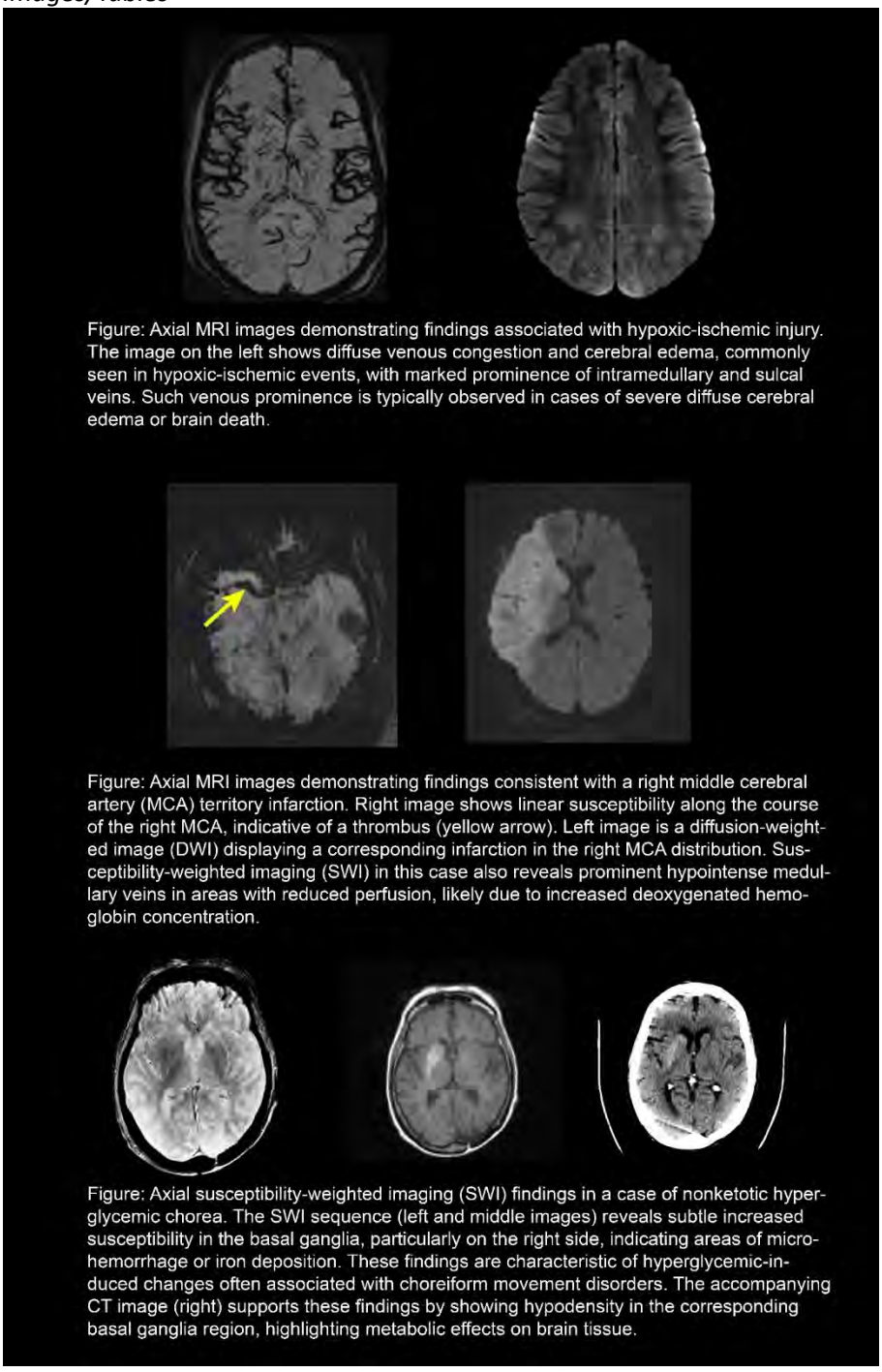


Figure: Axial MRI images demonstrating findings associated with hypoxic-ischemic injury. The image on the left shows diffuse venous congestion and cerebral edema, commonly seen in hypoxic-ischemic events, with marked prominence of intramedullary and sulcal veins. Such venous prominence is typically observed in cases of severe diffuse cerebral edema or brain death.

Figure: Axial MRI images demonstrating findings consistent with a right middle cerebral artery (MCA) territory infarction. Right image shows linear susceptibility along the course of the right MCA, indicative of a thrombus (yellow arrow). Left image is a diffusion-weighted image (DWI) displaying a corresponding infarction in the right MCA distribution. Susceptibility-weighted imaging (SWI) in this case also reveals prominent hypointense medullary veins in areas with reduced perfusion, likely due to increased deoxygenated hemoglobin concentration.

Figure: Axial susceptibility-weighted imaging (SWI) findings in a case of nonketotic hyperglycemic chorea. The SWI sequence (left and middle images) reveals subtle increased susceptibility in the basal ganglia, particularly on the right side, indicating areas of microhemorrhage or iron deposition. These findings are characteristic of hyperglycemic-induced changes often associated with choreiform movement disorders. The accompanying CT image (right) supports these findings by showing hypodensity in the corresponding basal ganglia region, highlighting metabolic effects on brain tissue.

1032

Caught in the Web: Imaging Techniques in Identifying Ischemic Stroke Due to Carotid Web

Ismail Mohamed HALFI M.D, Firdaous TOUARSA M.D, Mohamed JIDDANE Ph.D
Specialities Hospital, Rabat, Rabat-Salé-Kénitra, Morocco

Abstract Category

Head and Neck

Summary & Objectives

- Define the carotid web, its clinical relevance, and its potential to cause ischemic stroke, particularly in younger patients.
- Examine the epidemiology, clinical presentation, and potential etiology of carotid webs.
- Describe CT angiography (CTA) as the gold standard imaging modality for identifying carotid webs, emphasizing its key features and diagnostic capability.
- Discuss the differential diagnosis of carotid webs to improve diagnostic accuracy and subsequent management.
- Review the complications associated with carotid webs and current management strategies.
- Highlight the importance of an interdisciplinary approach to ensure optimal patient outcomes.

Purpose

The purpose of this educational review is to improve understanding of carotid webs—a rare vascular anomaly linked to ischemic stroke—by detailing its presentation, pathophysiology, imaging characteristics, complications, and treatment strategies. By emphasizing the interdisciplinary collaboration among neurologists, radiologists, and vascular surgeons, this review aims to enhance patient care and reduce stroke risk in affected individuals.

Materials & Methods

- **Literature Review**: A comprehensive review of existing studies on carotid webs was conducted, focusing on their pathophysiology, prevalence, risk factors, and clinical presentation.
- **Imaging Analysis**: CT angiography (CTA) cases were reviewed to identify hallmark imaging features of carotid webs, such as the thin, shelf-like intraluminal projection in the carotid bulb.
- **Case Study**: An example of a 42-year-old female patient with sudden-onset hemiparesis, confirmed to have a carotid web via CTA, was included to illustrate clinical and imaging findings.
- **Differential Diagnosis and Management**: Guidelines for distinguishing carotid webs from other vascular anomalies (e.g., atherosclerotic plaque or carotid artery dissection) were reviewed, as were medical and surgical management strategies.

Results & Conclusion

Carotid web is a rare vascular anomaly with significant clinical implications due to its association with ischemic stroke, particularly in young patients. Early detection through CTA, accurate diagnosis, and tailored management strategies, including antiplatelet therapy, anticoagulation, or surgical interventions, are essential for reducing stroke risk. A collaborative, interdisciplinary approach among neurologists, radiologists, and vascular surgeons is critical to optimizing diagnostic accuracy, treatment planning, and patient outcomes.

References

1. Choi, P. M., et al. (2018). Carotid Web and Ischemic Stroke: A Review of Imaging Features and Clinical Management. Stroke.
2. Zhang, A. J., et al. (2019). Carotid Web: Radiologic-Pathologic Correlation and Clinical Implications. Journal of Vascular Surgery.

1033

Emergency Neuroradiology Misses: Case Examples and Lessons Learned

Ismail Mohamed HALFI M.D, Firdaous TOUARSA M.D, Mohamed JIDDANE Ph.D
Specialties Hospital, Rabat, Rabat-Salé-Kénitra, Morocco

Abstract Category

Adult Neoplasms/Epilepsy/Trauma

Summary & Objectives

- Analyze the impact and prevalence of diagnostic errors in emergency neuroradiology.
- Examine the cognitive processes in radiologic decision-making, particularly Type 1 and Type 2 decision-making approaches.

- Identify common types of diagnostic errors in image interpretation and the cognitive biases contributing to these errors.
- Present case examples to illustrate how diagnostic errors occur in practice and highlight lessons for error prevention.
- Review strategies for minimizing diagnostic errors to enhance patient outcomes.

Purpose

This review aims to increase awareness of diagnostic errors in emergency neuroradiology and offer practical strategies to mitigate them. By examining cognitive biases, decision-making processes, and real-life case examples, the review seeks to equip radiologists with tools and insights to reduce misdiagnoses, ultimately improving patient outcomes in high-stakes settings.

Materials & Methods

- **Literature Review**: A comprehensive review of studies on diagnostic error rates in neuroradiology, emphasizing emergency settings, was conducted. This included identifying common diagnostic errors, such as missed strokes and intracranial hemorrhages.
- **Analysis of Decision-Making**: Two types of clinical decision-making, Type 1 (heuristic) and Type 2 (analytical), were analyzed to understand their impact on diagnostic accuracy in emergency neuroradiology.
- **Case Studies**: Real-life cases were reviewed to illustrate errors in emergency neuroradiology. These included cases of cognitive bias (e.g., premature closure) and perceptual errors, providing practical lessons for radiologists.
- **Review of Error-Reduction Strategies**: Various strategies for minimizing diagnostic errors were assessed, including peer reviews, double readings, interdisciplinary discussions, and decision-support systems.

Results & Conclusion

Diagnostic errors in emergency neuroradiology are a significant patient safety concern, often resulting from cognitive biases and perceptual errors under high-pressure conditions. By understanding these types of errors and adopting targeted strategies such as double reading, interdisciplinary collaboration, and cognitive awareness training, radiologists can improve diagnostic accuracy and enhance patient outcomes in emergency settings. This review offers a framework for recognizing and reducing errors, contributing to safer, more effective care in neuroradiology.

References

1. Newman-Toker DE, Makary MA. Measuring diagnostic errors in emergency care. Ann Emerg Med. 2018;72(1):11-13.
2. Graber ML, Trowbridge RL. Cognitive interventions to reduce diagnostic error: A narrative review. BMJ Qual Saf. 2019;28(10):761-768.
3. Croskerry P. The importance of cognitive errors in diagnosis and strategies to minimize them. Acad Med. 2017;92(1):23-30.
4. Patel VL, Cohen T, Murawski M, Patel P. Cognitive approaches to understanding diagnostic errors in radiology. Radiol Clin N Am. 2018;56(1):18-30.

1035

Big Vents: Causes of Hydrocephalus

Ismail Mohamed HALFI M.D, Firdaous TOUARSA M.D, Mohamed JIDDANE Ph.D

Specialties Hôpital, Rabat, Rabat-Salé-Kénitra, Morocco

Abstract Category

Adult Brain Inflammatory/Infectious Disease/Degenerative/Metabolic

Summary & Objectives

- Review the anatomy and structure of the ventricular system and its anatomic variants.
- Explain the classification schemes of hydrocephalus, including intraventricular, extraventricular, normal pressure, and overproduction subtypes.
- Describe imaging findings associated with different types of hydrocephalus.
- Discuss strategies for accurately differentiating hydrocephalus subtypes and avoiding misdiagnosis.

Purpose

This educational exhibit aims to clarify the complex classification and imaging characteristics of hydrocephalus, a condition marked by abnormal cerebrospinal fluid (CSF) accumulation in the brain. By providing a comprehensive

overview of ventricular anatomy and hydrocephalus subtypes, this review seeks to enable healthcare professionals to approach the diagnosis and management of hydrocephalus with increased precision and confidence.

Materials & Methods

- **Anatomic Review**: A detailed review of the ventricular system, including its four interconnected cavities and two canals, was conducted to outline normal anatomy and anatomic variants. This foundational knowledge assists clinicians in distinguishing normal variations from pathological presentations.
- **Classification and Pathophysiology**: Hydrocephalus classification was examined, categorizing the condition based on the site and nature of CSF flow disruption. Classifications include intraventricular obstructive hydrocephalus (IVOH), extraventricular obstructive hydrocephalus (EVOH), normal pressure hydrocephalus (NPH), and overproduction hydrocephalus.
- **Diagnostic Imaging Review**: Imaging findings for each hydrocephalus subtype were analyzed:
    - **IVOH**: Ventricular dilation proximal to obstruction with a normal or reduced fourth ventricle.
    - **EVOH**: Dilation of all ventricles, often due to conditions such as subarachnoid hemorrhage.
    - **NPH**: Ventriculomegaly with normal or slightly elevated CSF pressure, identified through clinical examination and imaging.
    - **SILPAH**: A rare condition resembling severe obstructive hydrocephalus with low intracranial pressure.
- **Differentiation Strategies**: Methods for differentiating hydrocephalus subtypes were reviewed to aid accurate diagnosis and avoid misdiagnosis, focusing on recognizing specific imaging patterns and understanding the underlying pathophysiology.

Results & Conclusion

A comprehensive understanding of ventricular anatomy, hydrocephalus classification, and associated imaging characteristics is essential for accurate diagnosis and effective management of hydrocephalus. By identifying distinct imaging patterns and considering the clinical context, radiologists and clinicians can better differentiate between hydrocephalus subtypes, guiding appropriate therapeutic decisions and improving patient outcomes.

References

1. Bateman GA, Levi CR. Ventricular system and hydrocephalus. Neuroimaging Clin N Am. 2020;30(1):1-18.
2. Kim JH, Lee HK. Obstructive hydrocephalus: Review of pathophysiology and imaging findings. J Neuroradiol. 2022;49(3):229-242.
3. Hashimoto M, Ishikawa M, Mori E. Guidelines for management of hydrocephalus in adults. Neurology. 2021;96(2):121-130.

1036

Cerebellar Ataxia: Differential Diagnosis Based on Common Imaging Patterns

Ismail Mohamed HALFI M.D, Firdaous TOUARSA M.D, Mohamed JIDDANE

Specialties Hôpital, Rabat, Rabat-Salé-Kénitra, Morocco

Abstract Category

Adult Brain Inflammatory/Infectious Disease/Degenerative/Metabolic

Summary & Objectives

- Define ataxia and discuss its origins in either cerebellar or vestibular system dysfunction.
- Describe the role of MRI in assessing cerebellar morphology and identifying potential causes of ataxia.
- Highlight the importance of integrating clinical presentation with MRI findings for accurate diagnosis.
- Review specific MRI findings associated with different types of cerebellar abnormalities and their diagnostic implications.

Purpose

This educational exhibit aims to provide a structured approach for using MRI to evaluate ataxia, a condition characterized by impaired coordination. By focusing on cerebellar morphology and correlating clinical findings, the exhibit seeks to enhance clinicians' ability to differentiate the many potential causes of ataxia and thereby improve diagnostic accuracy.

Materials & Methods

- **Definition and Clinical Presentation**: Ataxia is defined as impaired coordination, often resulting in balance and movement issues, stemming from cerebellar or vestibular dysfunction. Clinical presentations vary widely and may include vertigo, disequilibrium, and gait instability, affecting diagnostic pathways.

- **MRI Evaluation of Cerebellar Morphology**: MRI is examined as the primary modality for assessing cerebellar structure, helping to distinguish between normal cerebellar structure, hypoplasia, and atrophy.
    - **Example**: A patient presenting with vertigo and cerebellar atrophy on MRI may have a chronic degenerative condition, while cerebellar hypoplasia may suggest a developmental anomaly.
- **Clinical and Imaging Correlation**: Ataxia classifications (acute, subacute, or chronic) and their possible etiologies (e.g., traumatic, autoimmune, paraneoplastic, or genetic) were analyzed. MRI findings are combined with clinical information to improve diagnostic precision.
    - **Example**: MRI findings of cerebellar hemorrhage in a case of acute ataxia may suggest trauma, whereas chronic ataxia with cerebellar atrophy may indicate a neurodegenerative process.
- **Specific MRI Findings**: Distinct MRI features, such as cerebellar atrophy and hypoplasia, are reviewed:
    - **Atrophic Cerebellum**: MRI findings, such as associated superficial siderosis or basal ganglia abnormalities, may point toward conditions like hereditary ataxias or neurodegenerative diseases.
    - **Hypoplastic Cerebellum**: Posterior fossa malformations or unilateral hypoplasia on MRI may be indicative of congenital abnormalities.

Results & Conclusion

Integrating MRI findings with clinical data is essential for diagnosing and managing ataxia. Differentiating cerebellar morphologies—normal, hypoplastic, or atrophic—and identifying specific imaging patterns provides valuable insights into the underlying causes of ataxia. This approach supports more targeted diagnostic and therapeutic decisions, ultimately enhancing patient care.

References

1. Gilman, S., et al. (2016). The Cerebellum and Disorders of Ataxia. *Journal of Neurology*.
2. Koht, J., et al. (2020). Neuroimaging in Hereditary Ataxias. *Neuroimaging Clinics of North America*.

1039

Don't Take the Long Way: A Diagnostic Shortcut to Longitudinally Extensive Myelopathies

Ismail Mohamed HALFI M.D, Firdaous TOUARSA M.D, Mohamed JIDDANE Ph.D

Specialties Hôpital, Rabat, Rabat-Salé-Kénitra, Morocco

Abstract Category

Spine

Summary & Objectives

To provide an overview of the different types of myelopathy, explain the pathology of each type, and introduce a diagnostic flowchart to assist radiologists and clinicians in identifying key imaging features and distinguishing among mechanical and non-mechanical causes of myelopathy.

Purpose

This exhibit is designed to clarify the complex spectrum of myelopathies, categorized into mechanical and non-mechanical subtypes. It aims to enhance the understanding of spinal cord anatomy and pathology to aid in the diagnostic process and support clinicians in making more precise and effective diagnostic decisions, especially through a structured decision-making flowchart.

Materials & Methods

- **Review of Spinal Cord Anatomy and Function**
  A brief anatomical review covers the structure of the spinal cord, focusing on the organization of ascending sensory and descending motor tracts, which form the basis for understanding myelopathy symptoms and imaging findings.
- **Classification of Myelopathy Types**
    - **Mechanical Myelopathy**: Discusses physical compression-related spinal cord dysfunction, typically due to degenerative disc disease or trauma, with a focus on spondylotic myelopathy as the most common subtype.
    - **Non-Mechanical Myelopathy**: Covers non-compressive causes such as inflammatory, infectious, neoplastic, and vascular myelopathies. Longitudinally extensive spinal cord lesions associated with conditions like neuromyelitis optica or spinal cord infarction are highlighted as key differentiators.

- **Pathophysiology of Spondylotic Myelopathy**
  Chronic compression from degenerative changes in the cervical spine leads to ischemia and demyelination within the spinal cord. Histologic findings include neuronal loss, myelin degeneration, and gliosis, providing insight into how spondylotic changes lead to spinal cord dysfunction.
- **Clinical and Imaging Findings**
  - **Mechanical Myelopathy**: Characterized by symptoms of chronic spinal cord compression (motor/sensory deficits) and MRI findings of spinal cord compression with high T2 signal, indicating edema or myelomalacia.
  - **Non-Mechanical Myelopathy**: This group presents a range of intrinsic spinal cord lesions without external compression, as seen in multiple sclerosis, transverse myelitis, and neoplastic processes.
- **Specific Imaging Characteristics**
  T2-weighted MRI findings for mechanical myelopathies often show high signal intensity at the compressed area. In non-mechanical cases, inflammatory causes like neuromyelitis optica present with longitudinally extensive lesions, while vascular causes such as infarction display distinct, well-defined areas of spinal cord damage.
- **Decision-Making Diagnostic Flowchart**
  A flowchart is introduced to assist clinicians in differentiating mechanical from non-mechanical myelopathies, guiding evaluation based on cord compression, lesion length, and enhancement patterns to refine the differential diagnosis.

Results & Conclusion

Myelopathy encompasses a wide array of spinal cord dysfunctions, divided into mechanical and non-mechanical origins. A detailed understanding of spinal cord anatomy and pathology, combined with specific MRI findings, is essential for accurate diagnosis. The diagnostic flowchart provided offers a practical approach to improving diagnostic accuracy by emphasizing critical imaging features, ultimately enhancing patient care.

References

1. Smith, J., et al. (2021). Cervical Spondylotic Myelopathy: Diagnosis and Management. Journal of Neurology.
2. Bagnato, F., et al. (2020). MRI of Non-Mechanical Myelopathies: Diagnostic Challenges. Radiology Clinics of North America.

1051

Sacral Dural Arteriovenous Fistula: A Rare but Treatable Etiology of Myelopathy

Andrew J Bush MD, Layla Nachar MD, Maximilian Morvant MD, Paul Gulotta MD, James M Milburn MD
Ochsner Medical Center, New Orleans, LA, USA

Abstract Category

Interventional/Vascular/Stroke

Summary & Objectives

Spinal dural arteriovenous fistulas (sDAVF) are rare vascular lesions that often present with myelopathy-related symptoms. Arteriovenous fistula (AVF) formation leads to arterialization of low-pressure draining veins, thus disrupting the normal physiologic pressure gradient and causing congestive ischemia of the spinal cord. We present a case involving a female in her 80s exhibiting progressive bilateral lower extremity weakness and bowel and bladder incontinence over a 6-month period, with one week of rapid decline requiring hospitalization. In our presentation, we will discuss the pathophysiology, clinical presentation, imaging findings, and treatment options associated with sDAVF, as well as our patient's clinical outcome after treatment.

Purpose

The purpose of our presentation will be to review the angiographic workup for sDAVF and highlight the more rare and often elusive dural fistulas arising from the sacrum. We will also discuss the importance of considering sDAVF once more common etiologies of myelopathy have been ruled out.

Materials & Methods

Our patient's evaluation included spinal magnetic resonance (MR) imaging and catheter-directed angiography, including a retrograde femoral sheath pelvic angiogram, which revealed an sDAVF supplied by the sacral arterial system. The lesion was subsequently treated with transarterial endovascular embolization using Onyx 18.

Results & Conclusion

Our patient's symptoms began to improve within 24 hours of sDAVF embolization. At her two-month follow up appointment, spine MR imaging showed improvement in cord edema, and her symptoms were further improved. To conclude, spinal dural arteriovenous fistula is an important myelopathy etiology to consider once more common etiologies have been ruled out, especially because it can be effectively treated. Angiographic evaluation should include the sacral arterial system as an origin for fistula formation.

References

Ryu B, Sato S, Mochizuki T, et al. Spinal arteriovenous fistula located in the filum terminale externa: A case report and review of the literature. *Interventional Neuroradiology*. 2021 Jun;27(3):451-455. DOI: 10.1177/1591019920968363

1063

Imaging Pediatric Neck Emergencies: Key Radiologic Approaches and Findings

Suryansh Bajaj MD[1], Ajay Malhotra MBBS, MD, MMM, FACR[2]

[1]University of Arkansas for Medical Sciences, Little Rock, Arkansas, USA. [2]Yale School of Medicine, New Haven, Connecticut, USA

Abstract Category

Pediatrics

Summary & Objectives

Accurate imaging is crucial for diagnosing and managing non-traumatic pediatric head and neck emergencies. The appropriate imaging modality, such as ultrasound, CT, or MRI, varies depending on the particular condition. These conditions include orbital and sinus emergencies, deep neck emergencies, ear emergencies, or airway emergencies. Choosing the proper imaging is critical for determining the most suitable treatment approach and distinguishing between cases requiring immediate intervention and those that can be addressed with medical therapy. Familiarity with the clinical features of pediatric emergencies and collaboration with clinicians can ultimately improve diagnostic precision and treatment effectiveness.

Purpose

The purpose of this exhibit is to understand the importance of imaging in pediatric emergencies and to study an overview of common head and neck emergencies.

Materials & Methods

A spectrum of pediatric emergencies will be discussed from a quaternary care dedicated pediatric hospital.

Results & Conclusion

At the end of the exhibit, the reader will have understand:

1. The importance of imaging in pediatric emergencies
2. Common head and neck emergencies
3. Choosing the Appropriate Imaging Modality

- Ultrasound: Safe, cost-effective, but limited depth and operator dependent.
- CT: Rapid, detailed bone imaging, but radiation exposure and contrast risks.
- MRI: Radiation-free, superior soft tissue contrast, but longer scan times.

4. Specific Conditions and Imaging Guidelines

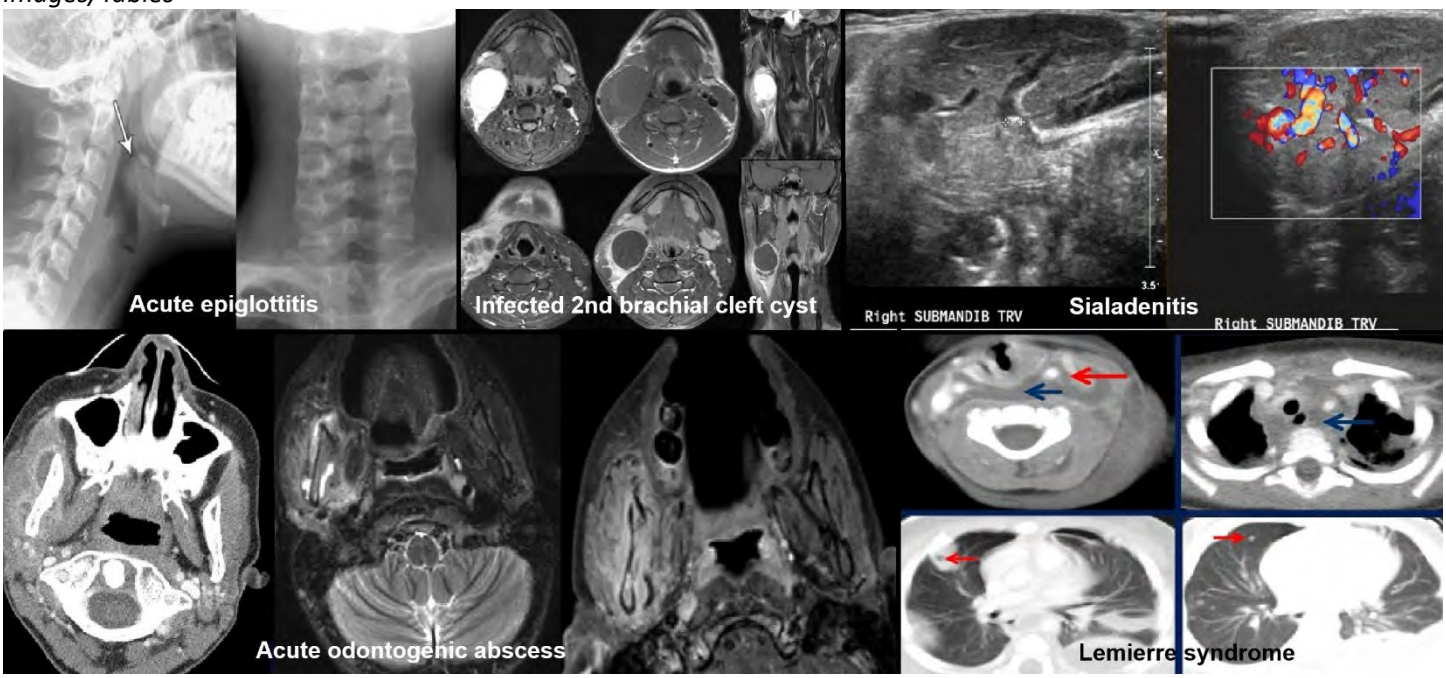
- Orbital Emergencies: Identifying cellulitis and abscesses
- Sinus / Nasal Emergencies: Complications of sinusitis
- Ear Emergencies: Diagnosing otitis and mastoiditis
- Airway Emergencies: Recognizing epiglottitis and croup
- Neck Emergencies: Recognizing infection, foreign body, vascular emergencies, congenital anomalies.

References

LaPlante JK, Pierson NS, Hedlund GL. Common pediatric head and neck congenital/developmental anomalies. *Radiol Clin North Am*. 2015;53(1):181-196. doi:10.1016/j.rcl.2014.09.006

Singh S, Booth TN, Clarke RL. Pediatric head and neck emergencies. *Neuroradiology*. 2024;66(11):2053-2070. doi:10.1007/s00234-024-03466-0

Images/Tables



1066

Imaging in Parotid Pathology: A Diagnostic Challenge and Solution

Suryansh Bajaj MD[1], Ajay Malhotra MBBS, MD, MMM, FACR[2]

[1]University of Arkansas for Medical Sciences, Little Rock, Arkansas, USA. [2]Yale School of Medicine, New Haven, Connecticut, USA

Abstract Category

Head and Neck

Summary & Objectives

Parotid lesions can be classified as inflammatory/infectious, congenital/developmental, autoimmune, adenopathy, mesenchymal neoplasia, benign parenchymal neoplasia, and malignant parenchymal neoplasia.

- Inflammatory/infectious etiologies are far more common than neoplastic changes in children compared to adults. Diffuse bilateral gland enlargement can be seen in acute bacterial and viral inflammation, however lymphoma may rarely have a similar appearance. Juvenile recurrent parotitis, presenting in mid-childhood and frequently resolving by puberty, has characteristic ultrasound and MR imaging appearances of multifocal punctate sialectasis, partially overlapping with HIV sialopathy, which can be distinguished with serologic testing.
- Congenital/developmental lesions are most commonly hemangiomas and venolymphatic malformations. Hemangioma, the most common neonatal lesion, is characterized by a trans-spatial enhancing mass with phleboliths and frequently spontaneously resolves. First branchial cleft cysts are congenital lesions that present during childhood, most commonly with parotidits, and may demonstrate a fistuolous tract to the external auditory canal on imaging.
- Autoimmune disease is most commonly Sjogren's syndrome, with children demonstrating early tooth decay from xerostomia.
- Adenopathy is the most common lesion as the parotid gland is not encapsulated and contains intra-parotid lymph nodes.
- Mesenchymal neoplasia includes neurofibroma and rhabdomyosarcoma.
- Benign and malignant parenchymal neoplasia pathologic entities with pleomorphic adenoma being the most common benign neoplasia and mucoepidermoid carcinoma being the most common malignant neoplasia.

Purpose

Parotid lesions in the pediatric and adult population may arise from a variety of pathologies, many with non-specific imaging appearances. Many of these entities are mistaken for only occurring in either the pediatric or the adult population. We present a review of the various pathologic entities affecting the parotid gland with imaging examples, emphasizing characteristic imaging appearances of certain pathologic entities.

Materials & Methods

Parotid lesions are presented by pathologic category: inflammatory/infectious, congenital/developmental, autoimmune, adenopathy, mesenchymal neoplasia, benign parenchymal neoplasia, and malignant parenchymal neoplasia. Otolaryngologic epidemiological data is reviewed to show relative incidences of lesions in pediatric and adult populations. Role of specialized imaging, including ultrasound, conventional and MR sialography is highlighted.

Results & Conclusion

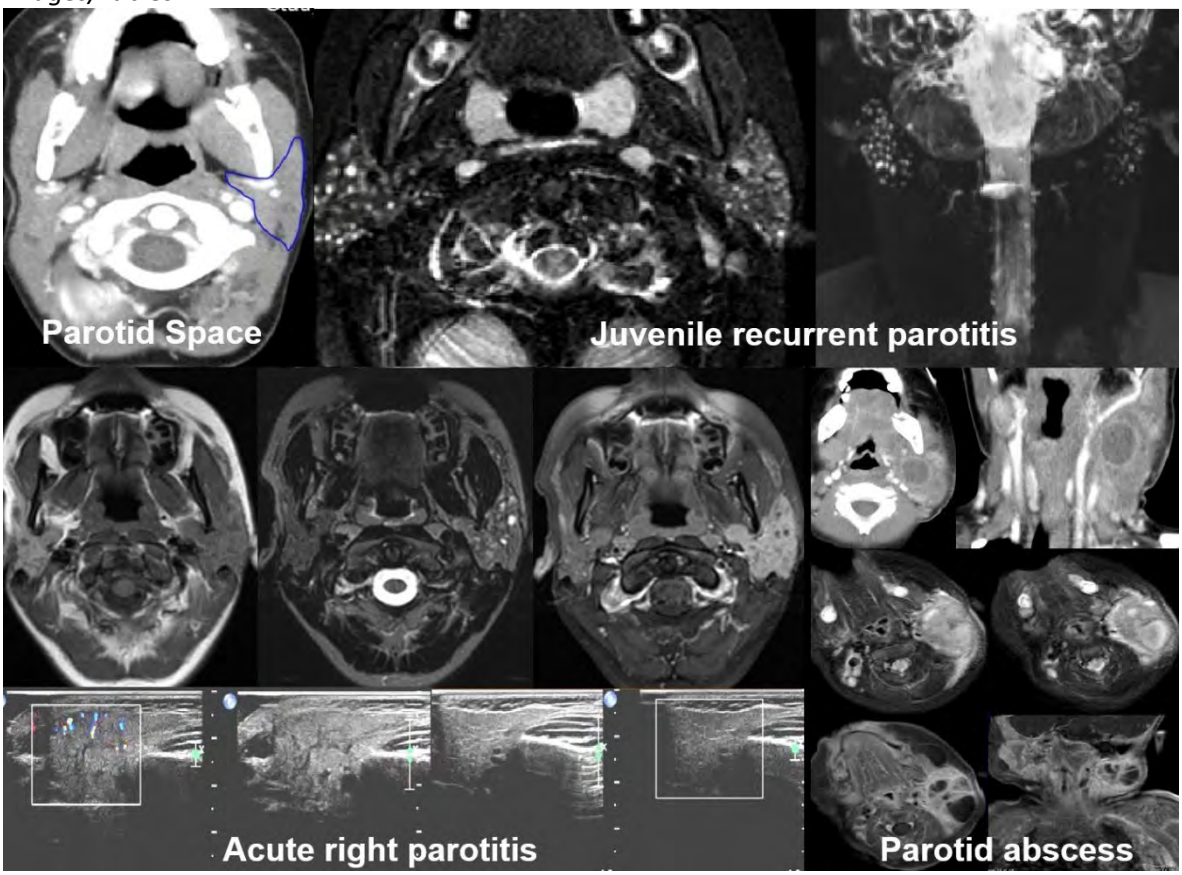
The presentation will review the normal anatomy of parotid space, imaging assessment of parotid lesions in children and the different pathologies involving the pediatric parotid gland. Specific imaging pearls would be provided.

References

Prasad RS. Parotid Gland Imaging. *Otolaryngol Clin North Am*. 2016;49(2):285-312. doi:10.1016/j.otc.2015.10.003

Kuan EC, Mallen-St Clair J, St John MA. Evaluation of Parotid Lesions. *Otolaryngol Clin North Am*. 2016;49(2):313-325. doi:10.1016/j.otc.2015.10.004

Images/Tables



1074

Advancing CNS Tumor Diagnosis and Treatment: A Neuroradiologist's Perspective on Evoloving Molecular Neuropathology"

Neetu soni[1], Manish Ora[2], Girish Bathla[3], Amit Agarwal[1], vivek Gupta[1], Prasanna Vibhute[1], Sheo Kumar MD[4]

[1]Mayo Clinic, Jacksonville, FL, USA. [2]SGPGIMS, Lucknow, UP, India. [3]Mayo Clinic, Rochester, MN, USA. [4]Sanjay Gandhi Institute of Medical Sciences, Lucknow, UP, India

Abstract Category

Adult Neoplasms/Epilepsy/Trauma

Summary & Objectives

Molecular profiling has transformed CNS tumor diagnosis, especially with its incorporation into the 2021 WHO CNS tumor classification. Integrated histopathological and molecular diagnosis is now fundamental in oncology neuropathology, enhancing tumor classification, prognosis, and treatment decisions. Techniques like DNA methylation analysis have led to the discovery of novel tumor types. This exhibit provides an overview of key molecular tools,

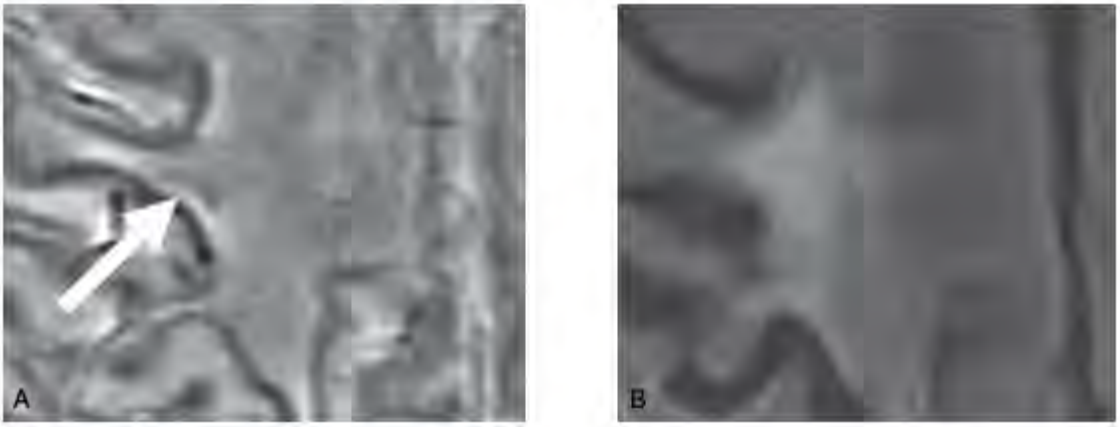
including immunohistochemistry, FISH, DNA methylation profiling, and DNA/RNA next-generation sequencing (NGS), used in CNS tumor diagnosis and management.
Neuroradiologists play a key role in the multidisciplinary team, providing imaging insights that complement the molecular data. Neuroradiologists can collaborate with neuropathologists to integrate these molecular insights with imaging findings, helping to refine the tumor classification, especially in complex or rare cases.
Purpose
1. To provide an overview of key molecular techniques (Immunohistochemistry, FISH, DNA methylation profiling, and NGS).
2. To highlight the role of molecular markers in tumor classification, prognosis, and targeted therapies.
3. To explore the challenges and opportunities in integrating molecular data into clinical practice.
Materials & Methods
This exhibit covers the latest molecular diagnostic techniques, including DNA methylation profiling and DNA/RNA NGS, essential for tumor classification and detecting genetic alterations. It also discusses their use in complex cases, identifying novel tumor types, and subgrouping heterogeneous tumors like medulloblastomas and ependymomas.
Results & Conclusion
Molecular testing is essential for the thorough evaluation of brain tumors. DNA methylation profiling is crucial for accurate tumor classification, especially in complex cases. DNA/RNA NGS allows the detection of genetic alterations, such as ingle nucleotide variants, insertions/deletions, and gene fusions, which inform diagnosis and guide therapy. The integration of molecular profiling into CNS tumor diagnostics has significantly improved both accuracy and treatment strategies. This exhibit emphasizes the importance of these tools in advancing CNS tumor classification and clinical practice.
References
Sahm F, et al. Molecular diagnostic tools for the World Health Organization (WHO) 2021 classification of gliomas, glioneuronal and neuronal tumors; an EANO guideline. Neuro-oncology. 2023 Oct 1;25(10):1731-49.

1082

2024 Revisions to McDonald Diagnostic Criteria for Multiple Sclerosis

MAURO HANAOKA MD
UNIVERSITY OF PENNSYLVANIA, PHILADELPHIA, PA, USA
Abstract Category
Adult Brain Inflammatory/Infectious Disease/Degenerative/Metabolic
Summary & Objectives
The 2024 revisions to the McDonald criteria for multiple sclerosis (MS) diagnosis introduce significant updates aimed at enhancing diagnostic accuracy and facilitating earlier intervention. This review outlines the key changes, including the incorporation of advanced imaging biomarkers and the redefinition of diagnostic parameters, to provide clinicians with a comprehensive understanding of the updated criteria.
Purpose
To inform healthcare professionals about the 2024 McDonald criteria revisions, emphasizing their implications for clinical practice in diagnosing MS. The updated criteria aim to reduce diagnostic delays and improve patient outcomes through the integration of novel biomarkers and refined diagnostic guidelines.
Materials & Methods
An analysis of the 2024 McDonald criteria revisions was conducted, focusing on the inclusion of new imaging biomarkers such as the central vein sign (CVS) and paramagnetic rim lesions (PRLs), as well as the expanded anatomical considerations for lesion dissemination. The review also examines the criteria's application to radiologically isolated syndrome (RIS) and the role of cerebrospinal fluid (CSF) biomarkers in the diagnostic process.
Results & Conclusion
The 2024 McDonald criteria revisions represent a pivotal advancement in MS diagnostics. The inclusion of imaging biomarkers like CVS and PRLs enhances specificity, while the recognition of the optic nerve as a fifth anatomical location for lesion dissemination broadens diagnostic capabilities. These updates are expected to enable earlier and more accurate MS diagnoses, thereby facilitating timely treatment initiation and potentially improving long-term patient outcomes. Clinicians are encouraged to integrate these revised criteria into practice to optimize diagnostic precision and patient care.

References
Montalban X, et al. 2024 Revisions of the McDonald Criteria. Presented at: ECTRIMS Congress; September 18-20, 2024; Copenhagen, Denmark.
Ontaneda D, Cohen J. Revised McDonald Diagnostic Criteria Signals New Era in Multiple Sclerosis Treatment. *NeurologyLive*. October 22, 2024.
Brownlee W, et al. Towards a unified set of diagnostic criteria for multiple sclerosis. Presented at: ECTRIMS Congress; September 18-20, 2024; Copenhagen, Denmark.
Calabresi PA. 2024 Revisions to McDonald Diagnostic Criteria for Multiple Sclerosis. *NeurologyLive*. September 2024.
National Multiple Sclerosis Society. Transforming How We Diagnose MS. *Momentum Magazine*. 2024.
Images/Tables



Paramagnetic Rim Lesion on SWI and FLAIR Imaging.
Paramagnetic rim lesions, indicative of chronic active inflammation in multiple sclerosis, are characterized by a distinct dark rim surrounding the lesion, reflecting iron deposition from ongoing inflammation. This feature helps in differentiating MS lesions from other white matter pathologies. The paramagnetic rim sign provides crucial diagnostic information for assessing lesion activity in multiple sclerosis.
A: SWI shows the lesion with an incomplete rim, blending into surrounding areas, which limits classification as a paramagnetic rim lesion.
B: FLAIR reveals a well-defined, complete rim around the lesion, allowing confident identification as a paramagnetic rim lesion.

1083

Role of Neuroradiology in Pain Management of Back Pain

Brian Barnacle MD, Graham Tooker MD, Jennifer Norris APRN, Leah Palifka MD, David Pastel MD
Dartmouth Health, Lebanon, NH, USA
Abstract Category
Interventional/Vascular/Stroke
Summary & Objectives

- Appreciate that low back pain is a highly prevalent and expensive health problem resulting in over $100 billion in total costs each year in the United States.
- Understand that low back pain is a challenging problem for clinicians to manage.
- Know the types of image guided procedures neuroradiologists can perform to provide both therapeutic benefit to patients and diagnostic information to clinicians.
- Recognize that minimally invasive image guided procedures performed by neuroradiologists can reduce opioid use, manage pain for patients, obviate the need for surgery, and provide diagnostic information to clinicians as to the source of pain.

Purpose
In 2019 approximately 39% of adults in the United States had back pain according to the CDC. Back pain is an expensive problem resulting in over $100 billion in total costs each year in the United States. Low back pain is challenging for clinicians to manage because the common degenerative changes on imaging such as disc bulge, facet arthropathy, and

spinal canal stenosis are also seen in patients without low back pain. Neuroradiologists, with expertise in imaging and anatomy, can perform minimally invasive image guided procedures that provides pain relief to patients, obviates the need for surgery, and provides diagnostic information to clinicians.

Materials & Methods

This educational exhibit reviews some of the common image guided procedures neuroradiologists at our institution offer to patients and clinicians. Vertebral augmentation such as vertebroplasty can provide pain relief to patients with severe activity limiting pain due to vertebral body compression fractures. Image guided epidural steroid injections and transforaminal nerve blocks are procedures we commonly perform for treating spinal stenosis and radiculopathy. Additionally, Bertolloti syndrome can be managed with image guided L5-S1 pseudoarticulation injections. Low back pain can also be managed with image guided sacroiliac joint injections. Image guided injections can provide pain relief to patients and obviate the need for surgery. Moreover, the patient's pain response to these procedures provides useful diagnostic information to clinicians. For instance, short term symptom relief after a nerve block can provide valuable information to a clinician and patient contemplating surgical management. Whereas the failure of a nerve block to treat radiculopathy can help a clinician in their search for another cause of the patient's symptoms.

Results & Conclusion

Low back pain is a significant and costly problem in the United States. Management can be challenging for clinicians. Neuroradiologists can offer a number of minimally invasive image guided procedures that can provide pain relief to patients and diagnostic information to clinicians.

References

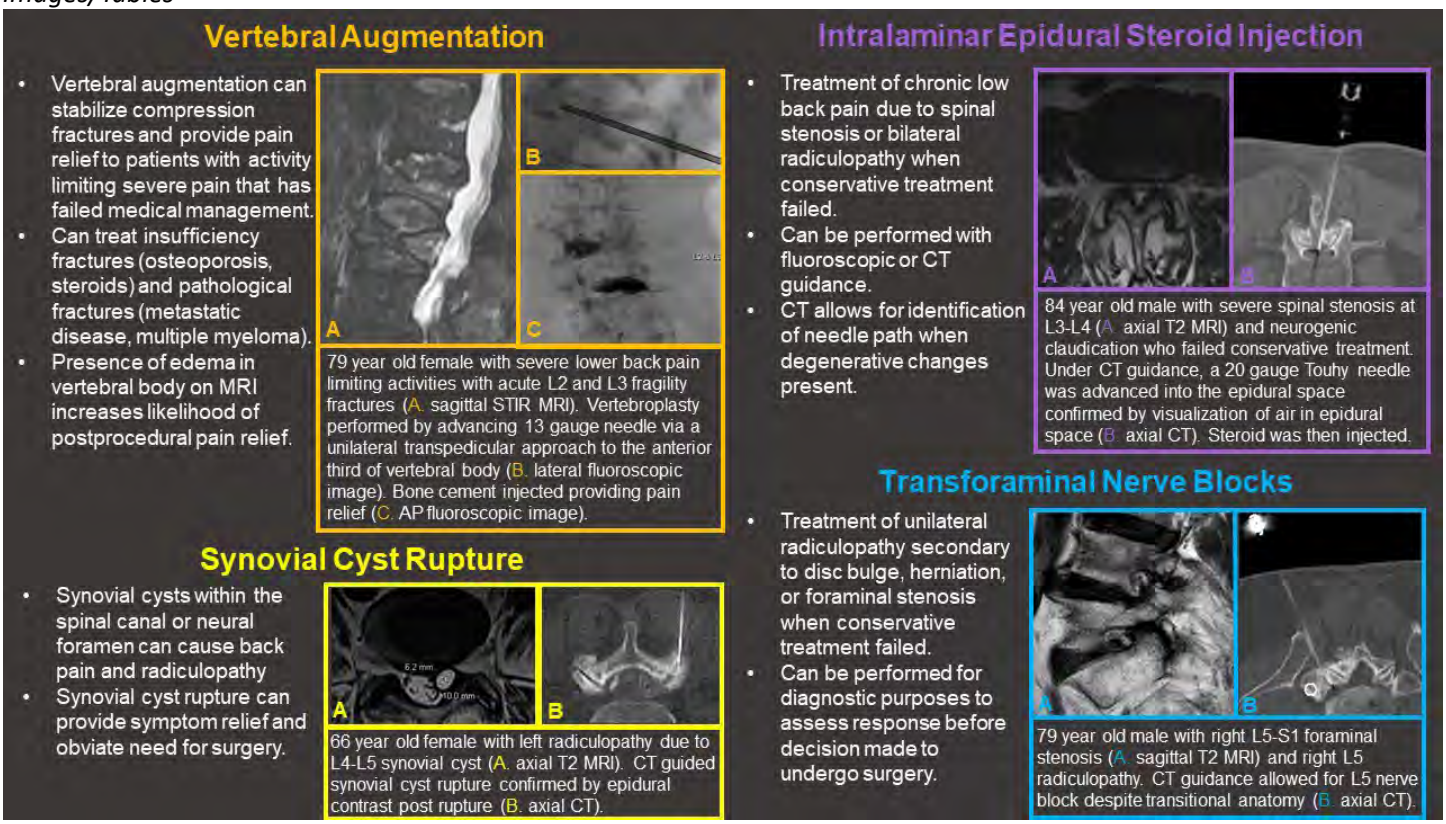
Fletcher A, Moore KJ, Stensby JD, et al. The pain crisis: interventional radiology's role in pain management. *AJR Am J Roentgenol*. 2021;217(3):676-690. doi:10.2214/AJR.20.24265

Lou S, Shi X, Zhang X, et al. Percutaneous vertebroplasty versus non-operative treatment for osteoporotic vertebral compression fractures: a meta-analysis of randomized controlled trials. *Osteoporos Int*. 2019;30(12):2369-2380. doi:10.1007/s00198-019-05101-8

Shah VN, von Fischer ND, Chin CT, et al. Long-term effectiveness of direct CT-guided aspiration and fenestration of symptomatic lumbar facet synovial cysts. *AJNR Am J Neuroradiol*. 2018;39(1):193-198. doi:10.3174/ajnr.A5428

Wagner AL. CT fluoroscopy-guided epidural injections: technique and results [published correction appears in AJNR Am J Neuroradiol. 2005 Jan;26(1):204]. *AJNR Am J Neuroradiol*. 2004;25(10):1821-1823.

Images/Tables



1084

Beyond the Tensor: Expanding the Horizons of Diffusion MRI after 40 years

Mauro Hanaoka MD
University of Pennsylvania, Philadelphia, PA, USA

Abstract Category

New Techniques/Advanced Imaging/Informatics/AI/Professional Development/Misc

Summary & Objectives

Marking the 40th anniversary of diffusion tensor imaging (DTI), this review explores advances that extend beyond the traditional tensor model, emphasizing the need to distinguish diffusion MRI as a modality from DTI as a model. As DTI remains widely integrated into clinical practice, recognizing emerging techniques is critical for expanding its applications and enhancing diagnostic accuracy.

Purpose

To provide an overview of advanced diffusion MRI techniques and models that surpass conventional DTI approaches, aiming to improve clinical and research capabilities in brain imaging.

Materials & Methods

This review covers advanced diffusion acquisition techniques, including high angular resolution diffusion imaging (HARDI) and diffusion spectrum imaging (DSI), which allow for more detailed characterization of neural pathways. It also examines novel tractography approaches, such as constrained spherical deconvolution (CSD), that move beyond principal eigenvector-based tractography to capture complex fiber arrangements. Additionally, it evaluates new diffusion models, such as neurite orientation dispersion and density imaging (NODDI) and the standard model (SM), that provide insights beyond tensor-derived measures like fractional anisotropy (FA) and mean diffusivity (MD). Expanding diffusion MRI's application to gray matter is also discussed through emerging contrasts, such as neurite density exchange imaging (NEXI).

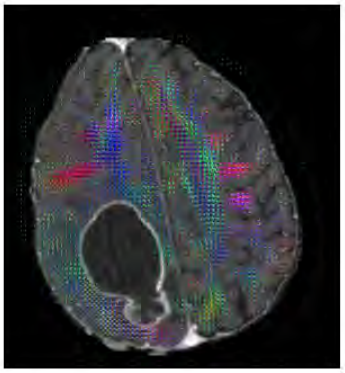
Results & Conclusion

Advanced diffusion MRI techniques demonstrate considerable potential to provide a more comprehensive view of brain microstructure. HARDI and DSI enhance fiber tracking accuracy, CSD offers improved depiction of complex fiber configurations, and models like NODDI and SM yield specific information about cellular architecture that surpasses traditional DTI metrics. Expanding diffusion imaging beyond white matter allows for the exploration of gray matter microstructural properties. Together, these advancements promise a richer understanding of brain architecture, highlighting the value of moving beyond the limitations of the diffusion tensor model and integrating these techniques into clinical and research settings.

References

1. **Tournier JD, Mori S, Leemans A.** Diffusion tensor imaging and beyond. *Magn Reson Med*. 2011;65(6):1532-1556. doi:10.1002/mrm.22924.
2. **Jeurissen B, Leemans A, Tournier JD, et al.** Investigating the prevalence of complex fiber configurations in white matter tissue with diffusion magnetic resonance imaging. *Hum Brain Mapp*. 2013;34(11):2747-2766. doi:10.1002/hbm.22099.
3. **Zhang H, Schneider T, Wheeler-Kingshott CA, Alexander DC.** NODDI: practical in vivo neurite orientation dispersion and density imaging of the human brain. *Neuroimage*. 2012;61(4):1000-1016. doi:10.1016/j.neuroimage.2012.03.072.
4. **Assaf Y, Basser PJ.** Composite hindered and restricted model of diffusion (CHARMED) MR imaging of the human brain. *Neuroimage*. 2005;27(1):48-58. doi:10.1016/j.neuroimage.2005.03.042.
5. **Jensen JH, Helpern JA, Ramani A, et al.** Diffusional kurtosis imaging: the quantification of non-Gaussian water diffusion by means of magnetic resonance imaging. *Magn Reson Med*. 2005;53(6):1432-1440. doi:10.1002/mrm.20508.

Images/Tables



Glioblastoma with associated white matter tract displacement and Fiber Orientation Distributions (FODs) overlaid on T1-Weighted Post-contrast Imaging (T1PC).
A. Axial T1-weighted post-contrast image showing the **glioblastoma** (GBM) in the right frontoparietal region, with peripheral enhancement. The FODs, reconstructed from **single-shell diffusion data (b-value 1000 s/mm²)** with **30 diffusion directions**, are overlaid on the same T1PC image. The **Corticospinal Tract (CST)** is **displaced** laterally by the tumor, as indicated by the change in tract orientation.

1091

Pattern Based Approach in Detecting Chronic Hypoxic Ischemic Brain Injury on MRI: Can it Predict the Time of Insult?

Charu Paruthi DM Neuroradiology, MD Radiodiagnosis, EBIR, Reeta Kanaujiya MD Radiodiagnosis
VMMC and Safdarjung Hospital, New Delhi, Delhi, India

Abstract Category

Pediatrics

Summary & Objectives

Hypoxic Ischemic Brain Injury (HIBI) is a leading cause of cerebral palsy.
Many patients present late in the chronic phase, where it is important to ascertain HIBI as the cause of encephalopathy, and determine the time of the past hypoxic insult.
MRI can be helpful in establishing HIBI as the cause of encephalopathy and also predict the timing of the past hypoxic insult, as it shows different typical patterns in preterm and term HIBI.
The objective of this presentation is to describe the imaging patterns of HIBI in the chronic phase on the basis of underlying pathophysiology, thereby facilitating better understanding.

Purpose

- To describe the pathophysiological basis of hypoxic ischemic brain injury (HIBI) patterns in term and preterm period and its evolution over time
- To illustrate MRI patterns of HIBI in the chronic phase.
- To highlight the key MRI features to differentiate chronic HIBI from other causes of encephalopathy; and correctly predict the time and severity of the past hypoxic ischemic insult

Materials & Methods

Brain involvement and imaging features in HIBI depend on:

- Brain maturity: Term vs pre-term (36 weeks of gestation is usually the cut-off)
- Severity of hypoxic injury: severe vs partial prolonged hypoxia

Two types of brain regions are affected:

- Those with high metabolic activity- Affected in severe hypoxic injury
    - Deep gray matter
    - Areas undergoing active myelination

- Those with relatively low perfusion- Affected in partial hypoxic injury
    - White matter
    - Watershed areas: Periventricular areas in preterm, more lateral parasagittal areas in term

MRI patterns in prenatal/preterm insults:

- Severe HIBI: Thalamus>basal ganglia, hippocampi, brainstem, cerebellum.
- Partial (mild to moderate) HIBI:
    - Periventricular leucomalacia
    - Haemorrhage: Germinal matrix, intraventricular, periventricular-parenchymal
- Mixed patterns
- Sequelae: Prenatal insults heal with cyst formation followed by cyst collapse and resorption, no gliosis

MRI patterns in perinatal insults:

- Severe HIBI: Putamina, ventrolateral thalami, PLIC, perirolandic cortex, dorsal brainstem, hippocampi
- Partial HIBI: Cortical and subcortical white matter of parasagittal regions
- Mixed patterns, cystic encephalomalacia
- Sequelae: Perinatal insults heal with gliosis forming chronic infarcts

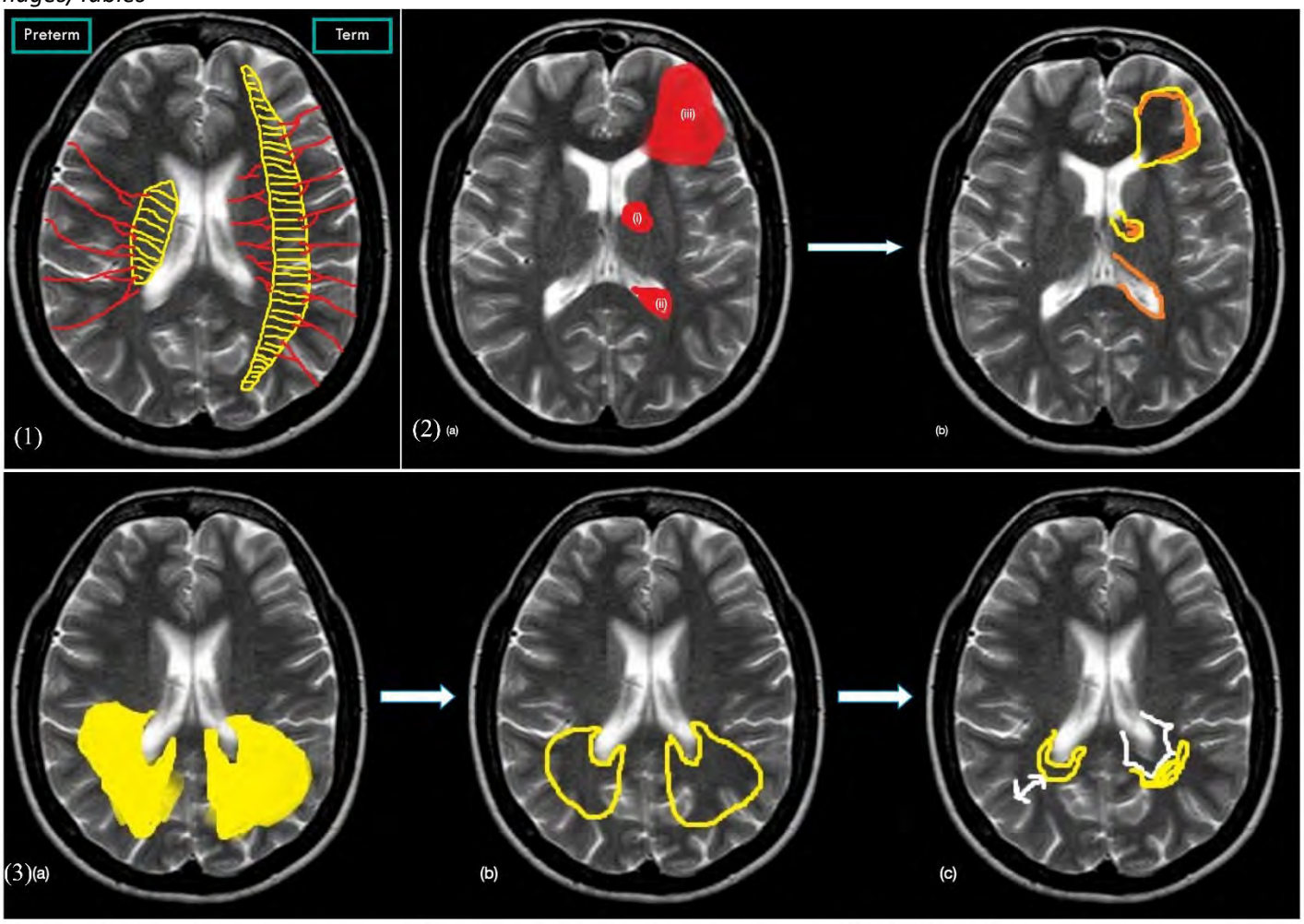
Results & Conclusion

A thorough understanding of pathophysiology can help in understanding the different imaging patterns of HIBI on MRI. Identification of these imaging patterns in patients can thus help to diagnose HIBI as the cause of encephalopathy and reliably predict the timing of the hypoxic injury, which may have medicolegal implications.

References

1. Huang BY, Castillo M. Hypoxic-ischemic brain injury: imaging findings from birth to adulthood. Radiographics. Mar-Apr 2008;28(2):417-39; quiz 617. doi: 10.1148/rg.282075066
2. Ghei SK, Zan E, Nathan JE, et al. MR imaging of hypoxic-ischemic injury in term neonates: pearls and pitfalls. Radiographics. Jul-Aug 2014;34(4):1047-61. doi: 10.1148/rg.344130080
3. Misser SK, Barkovich AJ, Lotz JW, Archary M. A pictorial review of the pathophysiology and classification of the magnetic resonance imaging patterns of perinatal term hypoxic ischemic brain injury - What the radiologist needs to know… SA J Radiol. 2020 Oct 30;24(1):1915. doi: 10.4102/sajr.v24i1.1915
4. Bano S, Chaudhary V, Garga UC. Neonatal Hypoxic-ischemic Encephalopathy: A Radiological Review. Pediatr Neurosci. Jan-Mar 2017;12(1):1-6. doi: 10.4103/1817-1745.205646
5. Fineschi V, Viola RV, La Russa R, Santurro A, Frati P. A Controversial Medicolegal Issue: Timing the Onset of Perinatal Hypoxic-Ischemic Brain Injury. Mediators Inflamm. 2017;2017:6024959. doi: 10.1155/2017/6024959

Images/Tables



(1) Watershed areas in brain at preterm and term gestational period, involved in partial HIBI. (2) Evolution of haemorrhage pattern of partial HIBI at preterm: Hematoma undergoes resorption with cyst formation, leading to porencephalic cyst with hemosiderin lined cyst/ ventricular walls. (3) Evolution of periventricular leukomalacia (PVL) pattern of partial HIBI at preterm: Cystic changes in involved regions, followed by cyst collapse, decreased white matter thickness/volume, passive ventriculomegaly and irregular ventricular walls.

1092

Unmasking a Multifaceted Demon: Spectrum of CNS Imaging Abnormalities in Patients with Acute Lymphocytic Leukemia

Charu Paruthi DM Neuroradiology, MD Radiodiagnosis, EBIR, Rohini Gupta Ghasi MD Radiodiagnosis, M Sarthak Swarup MD Radiodiagnosis
VMMC and Safdarjung Hospital, New Delhi, Delhi, India

Abstract Category

Pediatrics

Summary & Objectives

Acute Lymphocytic Leukemia (ALL) is the commonest pediatric malignancy.

Although ALL is multi-systemic, central nervous system (CNS) is one of the most common sites of involvement and relapse.

Brain and spine is imaged before treatment initiation and during follow-up to detect CNS involvement; which if present, requires treatment modification/amplification.

Various CNS imaging abnormalities can occur in ALL due to numerous causes, not all due to disease metastasis/relapse.

Knowledge of underlying mechanisms and imaging appearances of these is important to reliably diagnose and differentiate them from each other.

Purpose

- Illustrate the radiological findings of various CNS abnormalities in ALL and understand their pathophysiology
- Highlight the key imaging features of each abnormality, to reliably diagnose and differentiate them.
- Formulate a reporting template for evaluating scans of ALL patients.

Materials & Methods

ALL patients with suspected CNS involvement usually undergo CT or MRI. Contrast-enhanced MRI is the investigation of choice.

CNS abnormalities in ALL patients can be due to:

- ⊙ **CNS infiltration/metastasis**- Seen as:
  - **Bony metastasis**
  - **Dural metastasis**

Dural-based or lytic bony masses, usually cellular, showing diffusion restriction and post-contrast enhancement.

  - **Leptomeningeal metastasis:**

Diffuse or focal, smooth or nodular (more common) leptomeningeal enhancement along the brain surface and cranial nerves (usually cisternal portion).

Pachymeningeal enhancement may occur.

  - **Parenchymal involvement:** May be:
    1. Variable sized intra-axial masses with surrounding edema, diffusion restriction and uniform enhancement.
    2. Multiple small enhancing parenchymal nodules with/without surrounding edema
    3. Ill-defined parenchymal involvement showing T2/FLAIR-hyperintensity or CT-hypodensity, with variable enhancement.

Presence of enhancement may differentiate metastasis from other benign causes.

Spine imaging is mandatory to detect leptomeningeal drop metastasis (sometimes the only sign of CNS involvement).

  - **Chloromas**- Cellular soft-tissue deposits (usually in AML)

- ⊙ **Abnormalities due to treatment effect:**
  - **Methotrexate toxicity**

Due to intrathecal methotrexate given during treatment.

Symmetrical areas of T2/FLAIR hyperintensity in bilateral centrum semiovale and periventricular white matter, showing diffusion restriction and no enhancement.

  - **Posterior reversible Encephalopathy syndrome (PRES)**

Due to drugs like L- asparaginase, blood-pressure fluctuations or renal involvement by disease. May be:

    - ‣ **Typical PRES**: Symmetrical involvement of bilateral occipitoparietal cortical and subcortical areas, without enhancement or diffusion restriction.
    - ‣**Atypical PRES**: May present with involvement of basal ganglia, thalami or brainstem. Presence of diffusion restriction or enhancement.
  - **CNS infections**

Due to chemotherapy induced immuno-suppression.

Typical features of common endemic infections seen, as tuberculosis in our setting.

In neutropenic patients, fungal infections as aspergillosis present as fungal brain abscesses.

Bacterial abscess or uncommon infections may occur.

  - **Radiotherapy induced changes**

Usually occur in radiation field (RF). In the spine, additional involvement of vertebrae in RF may give a clue.

Delayed radiation necrosis, though uncommon, may also occur.

Metastasis/relapse usually show increased cerebral blood volume (CBV) on perfusion studies and increased choline on spectroscopy, not seen in other benign abnormalities.

Results & Conclusion

CNS involvement in ALL can be seen due to various causes.

It is important to know their imaging appearances and reliably differentiate metastasis/relapse from other treatment related causes as this dictates the course of further treatment.

Advanced imaging techniques such as MR perfusion and spectroscopy may be helpful.

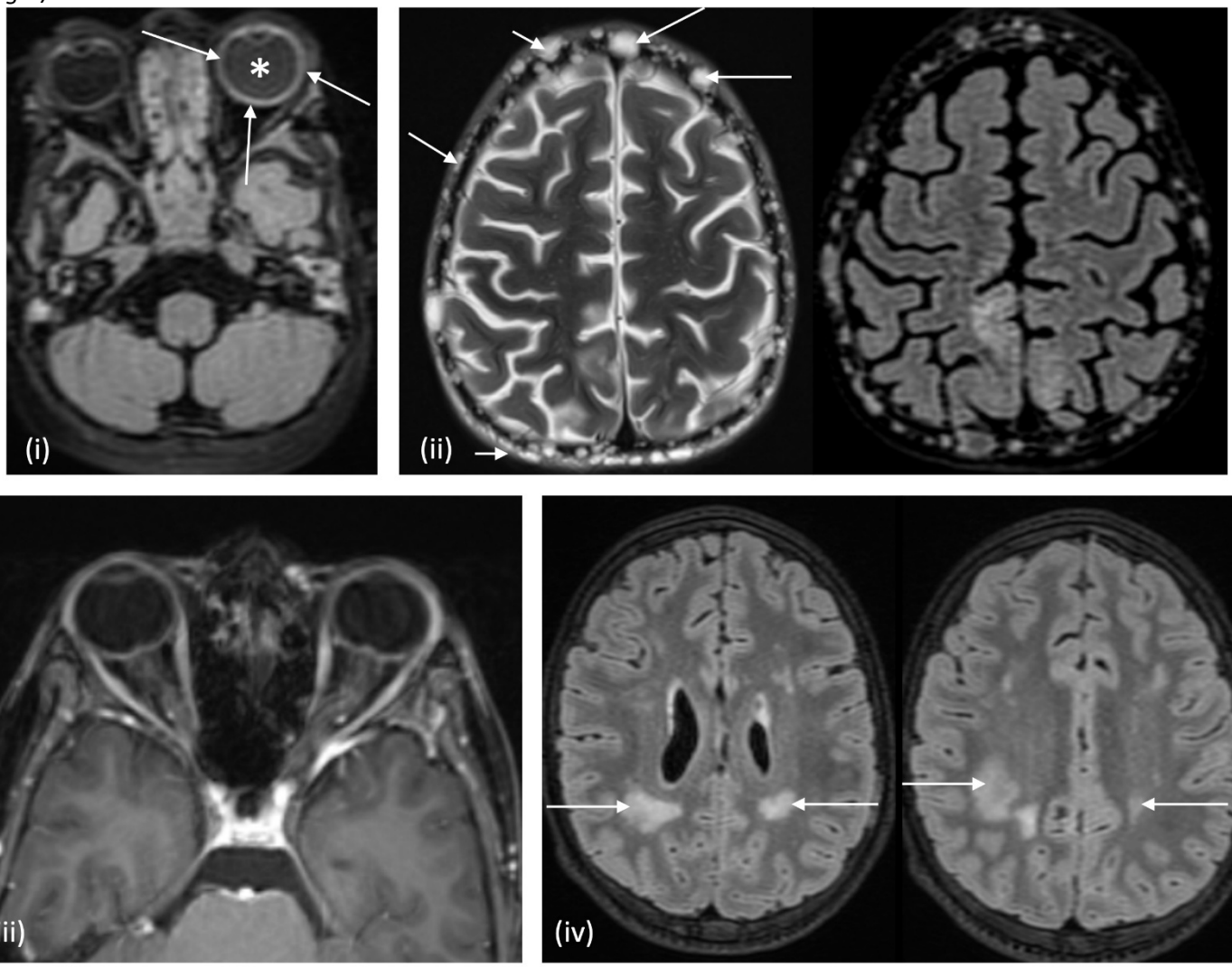
References

Deak D, Gorcea-Andronic N, Sas V, et al. A narrative review of central nervous system involvement in acute leukemias. Ann Transl Med. 2021 Jan;9(1):68. doi: 10.21037/atm-20-3140. PMID: 33553361; PMCID: PMC7859772.

Keraliya AR, Krajewski KM, Giardino AA, et al. Imaging of Nervous System Involvement in Hematologic Malignancies: What Radiologists Need to Know. AJR Am J Roentgenol. 2015 Sep;205(3):604-17. doi: 10.2214/AJR.14.14092. PMID: 26295649.

Lauer M, Kernen E, Schwabe D, Lehrnbecher T, Porto L. The role of magnetic resonance imaging in the diagnosis of central nervous system involvement in children with acute lymphoblastic leukemia. Pediatr Blood Cancer. 2020 Oct;67(10):e28294. doi: 10.1002/pbc.28294. Epub 2020 Aug 2. PMID: 32743972.

Images/Tables



CNS involvement in ALL. i) Atypical metastasis in left eye: FLAIR axial image showing diffuse uveo-scleral hperintensity and thickening in left globe (arrow) with turbid vitreous (asterisk). ii) Another patient of ALL on chemotherapy with raised BP showing multiple lytic calvarial metastasis (arrows) and non-enhancing, non-diffusion restricting, cortical and subcortical T2/FLAIR hyperintensities, which resolved with BP control, suggesting PRES. iii) ALL patient on treatment showing bilateral papilledema with no other abnormality on MRI brain, tested positive for lymphoblasts on CSF examination, indicating CNS relapse. iv) An ALL patient on chemotherapy who received intrathecal methotrexate showing typical MRI findings of methotrexate toxicity.

1093

Common Medical Devices and Prosthesis in the Head and Neck

Abdulrahman Batwa, Kalen Riley
Indiana University, Indianapolis, IN, USA

Abstract Category

Head and Neck

Summary & Objectives

- Identify the medical devices used in the head and neck, along with their roles and functions.

Purpose

- Correlate imaging appearance of these devices with their in-vivo appearance.
- Identify any imaging abnormalities associated with these devices (e.g., misplacement, fracture, etc.).

Materials & Methods

- Instructional materials were acquired from the institutional imaging database.

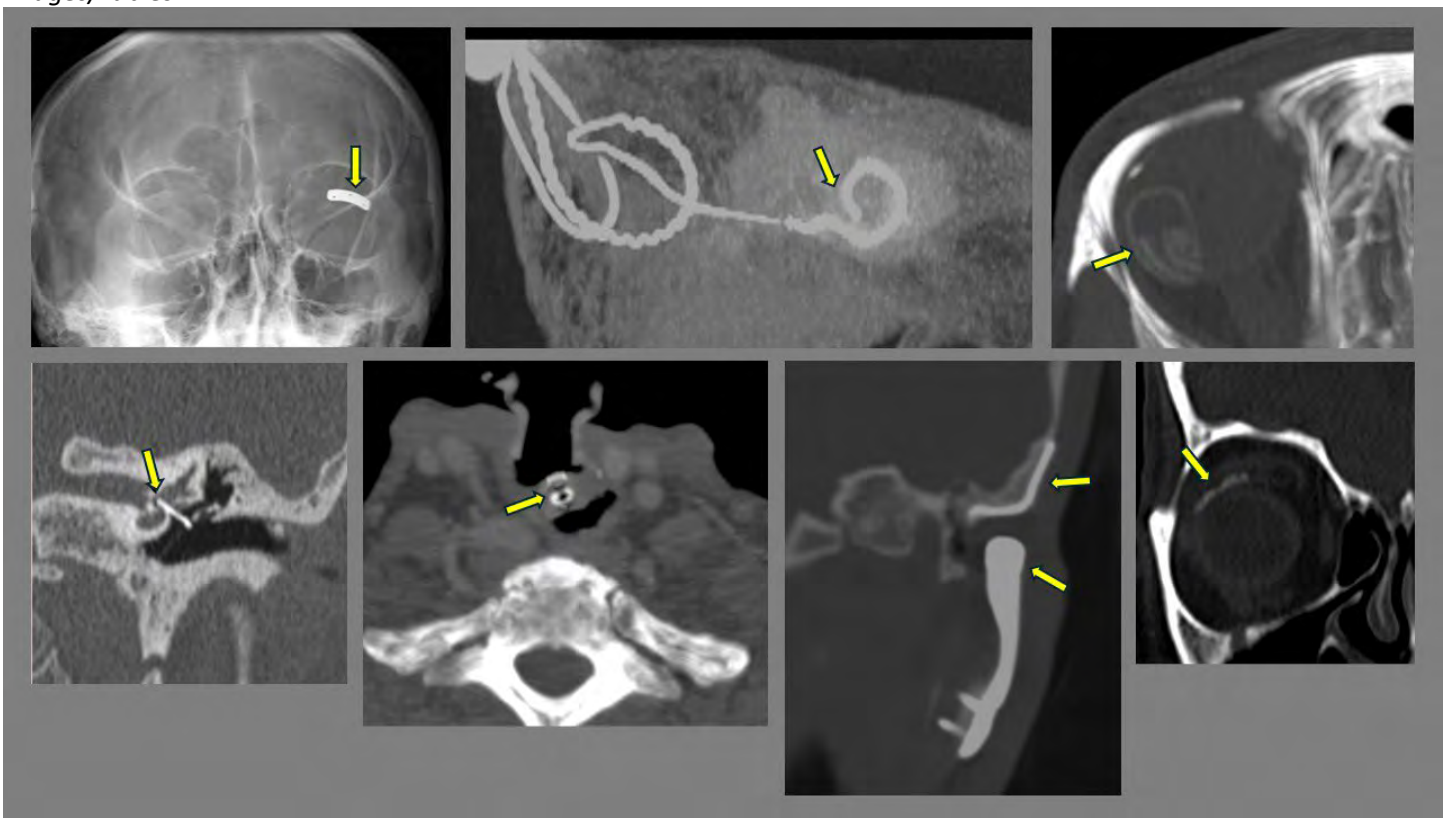
Results & Conclusion

- It is important to identify the imaging characteristics of the various medical devices used in the head and neck. Any imaging abnormalities associated with these devices should correlate with the patient's symptoms.

References

https://doi.org/10.3174/ajnr.A1571

Images/Tables



1094

Going with the Flow: Imaging Patterns and Endovascular Management of Vascular Anomalies of Head and Neck

Charu Paruthi DM Neuroradiology, MD Radiodiagnosis, EBIR
VMMC and Safdarjung Hospital, New Delhi, Delhi, India

Abstract Category

Head and Neck

Summary & Objectives

Vascular anomalies are abnormalities of the vasculature, which may be congenital or acquired. Head and neck is one of the most common sites of involvement.

Due to their complex nature and variable presentation, their diagnosis and treatment is challenging.

These are often dynamic lesions, which evolve over time.

Treatment is aimed to control/halt lesion progress in most of the benign cases. Endovascular treatment is the mainstay treatment and maybe supplemented by surgery.

Management requires proper diagnosis, delineating lesion angioarchitecture and planning. Radiology plays a major role at each step, which we will describe herein.

Purpose

- Classify vascular anomalies and describe the radiological features which help to diagnose these lesions
- Illustrate the salient features of each entity to help differentiate mimickers
- Formulate a reporting template, emphasising key features to be reported which help plan treatment
- Discuss endovascular techniques to treat each abnormality with case examples

Materials & Methods

Ultrasound (US) Doppler, CT and MRI are the most common modalities used for evaluating vascular anomalies.

These can be broadly divided into (ISSVA classification):

- Vascular tumours: Mass present.

Spectrum of pathologies from benign to malignant.

Hemangiomas most common- Well-defined masses with variable vascularity (US-Doppler) and intense progressive enhancement (CECT/CEMRI).

- Vascular malformations: Mass absent.

Classified into:

  - **High flow lesions:** Arterial flow present:
    - Arteriovenous fistulas (AVF)- without nidus
    - Arteriovenous malformations (AVM)- with nidus

US-Doppler- enlarged or entangled vessels with arterial flow.

Dynamic CT/MR angiography (CTA/MRA)- prominent feeding arteries and **early draining veins** (hallmark).

DSA-gold standard.

Salient features to be reported:

Arterial feeders- location, number, stenosis/dilatation/aneurysms

Draining veins- location, number, stenosis/ectasias/pouches

Nidus- size, location, intranidal aneurysms

Treatment goal is to occlude abnormal vessels and exclude them from circulation, maintaining patency of normal branches. This is done by embolising agents- mostly liquid agents (nBCA or EVOH-based agents). Route can be arterial, percutaneous, venous or combined.

  - **Slow flow lesions**:

Without arterial high-flow component. These are variable-sized, multi-compartmental endothelium-lined pouches filled with venous or capillary blood, or lymph.

  - Slow flow capillary malformations [**SFCM]** (clinically detected, no imaging required)
  - Slow flow venous malformations [**SFVM]**
  - Slow flow lymphatic malformations [**SFLM]**
  - Mixed malformations

US-Doppler shows fluid-filled compressible sacs with no detectable arterial flow; slow venous flow, associated phleboliths (SFVM); larger and fewer cysts with no detectable flow (SFLM)

CT/MRI show large fluid channels, typically bright on T2W-MRI, progressive contrast fill-in on delayed images (SFVM); no internal enhancement, internal fluid-fluid levels (SFLM); both enhancing and non-enhancing components (mixed malformations).
DSA entails percutaneous lesion access and obtaining nidogram to delineate lesion angioarchitecture.
Endovascular treatment- injecting sclerosing agents percutaneously within the vascular/lymphatic sac, causing lesion wall inflammation, sclerosis and shrinkage. Commonly used sclerosants are sodium tetradecylsulphate and bleomycin.

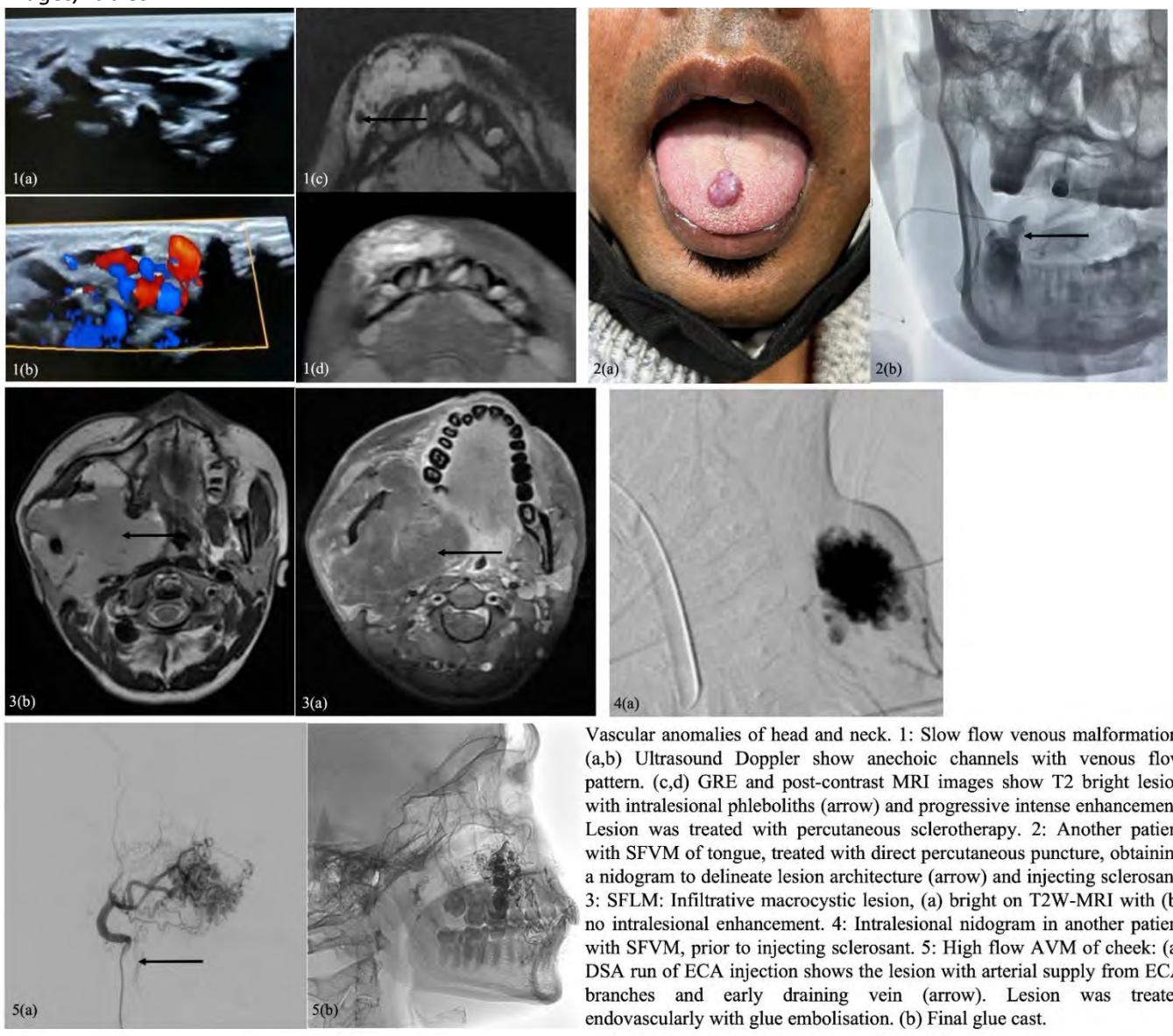
Results & Conclusion

It is important to accurately diagnose and classify vascular anomalies on imaging, to decide further management and endovascular treatment strategies.
Goal of treatment in most cases, especially large SFVM, is lesion control rather than complete cure.
Radiology is the cornerstone in deciding treatment options and planning its execution.
High-flow lesions are usually treated with embolising agents and slow-flow lesions with sclerosants.

References

Ota Y, Lee E, Sella E, Agarwal P. Vascular Malformations and Tumors: A Review of Classification and Imaging Features for Cardiothoracic Radiologists. Radiol Cardiothorac Imaging. 2023 Jul 13;5(4):e220328. doi: 10.1148/ryct.220328. PMID: 37693195; PMCID: PMC10483253.
Nosher JL, Murillo PG, Liszewski M, Gendel V, Gribbin CE. Vascular anomalies: A pictorial review of nomenclature, diagnosis and treatment. World J Radiol. 2014 Sep 28;6(9):677-92. doi: 10.4329/wjr.v6.i9.677. PMID: 25276311; PMCID: PMC4176785.

Images/Tables



Vascular anomalies of head and neck. 1: Slow flow venous malformation. (a,b) Ultrasound Doppler show anechoic channels with venous flow pattern. (c,d) GRE and post-contrast MRI images show T2 bright lesion with intralesional phleboliths (arrow) and progressive intense enhancement. Lesion was treated with percutaneous sclerotherapy. 2: Another patient with SFVM of tongue, treated with direct percutaneous puncture, obtaining a nidogram to delineate lesion architecture (arrow) and injecting sclerosant. 3: SFLM: Infiltrative macrocystic lesion, (a) bright on T2W-MRI with (b) no intralesional enhancement. 4: Intralesional nidogram in another patient with SFVM, prior to injecting sclerosant. 5: High flow AVM of cheek: (a) DSA run of ECA injection shows the lesion with arterial supply from ECA branches and early draining vein (arrow). Lesion was treated endovascularly with glue embolisation. (b) Final glue cast.

1099

Current Neuroimaging Modalities to Distinguish Parkinson's Disease from its Mimics: Imaging Features and Implications for Clinical Practice

Mona Gad[1], Licia P. Luna[2]
[1]Radiology Department, Mansoura University Faculty of Medicine, Mansoura, Dakahlia, Egypt. [2]Department of Radiology, Johns Hopkins University School of Medicine, Baltimore, MD, USA

Abstract Category

Adult Brain Inflammatory/Infectious Disease/Degenerative/Metabolic

Summary & Objectives

Educational Objectives:

1. List common mimickers of Parkinson's disease.
2. Recognize the current state-of-the-art imaging techniques in discriminating Parkinson's disease from its mimics.
3. Identify the specific imaging features for such conditions.
4. Critique limitations of current neuroimaging modalities in clinical practice.

Purpose

The primary goal of this exhibit is to provide a comprehensive and updated overview of the literature on imaging techniques used to differentiate Parkinson's disease from its mimics, aiming at reaching accurate diagnosis and improving the clinical outcomes.

Materials & Methods

In this exhibit, the following points will be discussed and illustrated with diagrams and cases.

A. Neuroanatomy of the brain regions associated with movement.
B. Pathophysiology and clinical presentation of Parkinson's disease.
C. Early imaging features to identify Parkinson's disease.
D. Common Parkinsonian syndromes and specific imaging features for each condition.
E. Qualitative and quantitative MRI measures in the setting of parkinsonism which encompass:

- Significance of the nigrosome-1 (swallow-tail sign) on SWI.
- Midbrain diameter and midbrain-to-pons diameter ratio.
- Proposed brain MRI protocol for patients with clinical suspicion of parkinsonism.

F. Leveraging nuclear neuroimaging techniques in identifying Parkinson's disease and its mimics, with focusing on DaT scan.
G. Shortcomings of current imaging techniques

Results & Conclusion

Results: N/A

Conclusion:

Clinical presentation of Parkinson's disease is not very specific, yet it is imperative to distinguish it from other mimics that may require different management. Advanced MRI sequences and nuclear medicine imaging techniques can provide insights for understanding the characteristic morphological and neurometabolic changes in the setting of parkinsonism, aiming at better therapeutic outcomes.

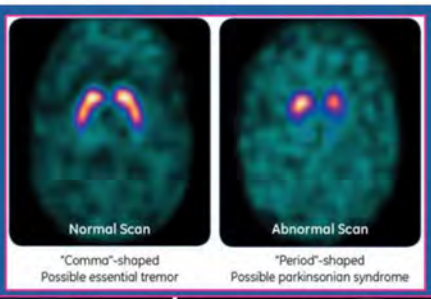
References

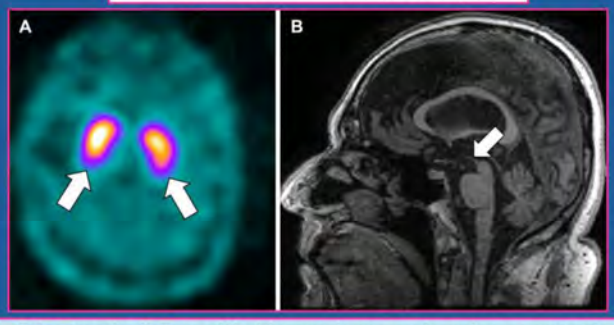
1. Bae YJ, Kim JM, Sohn CH, et al. Imaging the substantia nigra in Parkinson disease and other Parkinsonian syndromes. Radiology. 2021;300(2):260-278. DOI:10.1148/radiol.2021203341
2. Samson E, Noseworthy MD. A review of diagnostic imaging approaches to assessing Parkinson's disease. Brain Disord. 2022;6. DOI:10.1016/j.dscb.2022.100037
3. Quattrone A, Zappia M, Quattrone A. Simple biomarkers to distinguish Parkinson's disease from its mimics in clinical practice: a comprehensive review and future directions. Front Neurol. 2024;15. DOI:10.3389/fneur.2024.1460576

Images/Tables



Sagittal T1WI MRI with illustration of the nigrostriatal dopaminergic pathway

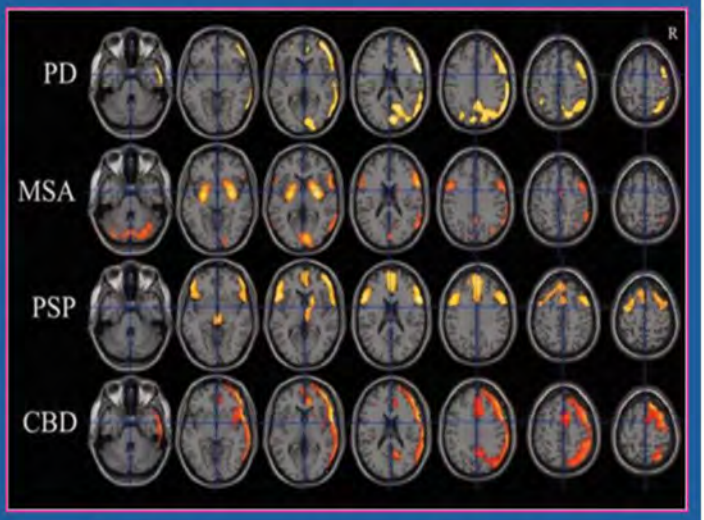




False negative DaT scan (A) with normal comma-shaped appearance of striatum and midbrain atrophy (Hummingbird sign) on sagittal T1WI (B) in a case of PSP



SWI showing normal swallow tail sign in a healthy control (1A) vs absent swallow tail sign in Parkinson's disease (1B)



18 FDG-PET superimposed on normal T1WI-MRI templates showing patterns of regional hypometabolism in the cerebral cortex distinct for each condition

1104

Magnetic Resonance Imaging as a Tool for Recruiting Patients for Organ Donation: Can it Decide When to Proceed

Charu Paruthi DM Neuroradiology, MD Radiodiagnosis, EBIR, Reeta Kanaujiya MD Radiodiagnosis
VMMC and Safdarjung Hospital, New Delhi, Delhi, India

Abstract Category

Adult Brain Inflammatory/Infectious Disease/Degenerative/Metabolic

Summary & Objectives

Recognising brain-death has become increasingly important, especially with increase in rates of organ donation. Absence of blood flow in the brain is the definitive sign of brain-death. MRI, though not widely used for this purpose, holds promise in detecting both vascular and parenchymal features of brain-death. In cases where all criteria are not met, it can help in prognostication and detection of cases which can be withdrawn from life-support system.

Objective: Illustrate the specific features of brain-death on MRI and provide a pathophysiological explanation for these, to help improve their understanding and recognition.

Purpose

To recognize objective MR imaging features for declaring a person brain dead prior to organ donation

To understand the pathophysiology behind appearance of these imaging findings

To devise a MR brain protocol for scanning the patients in a short time for recruiting patients for organ donation

Materials & Methods

Presently organ donation occurs in two settings: Donation after cardiac death; and heartbeating brain dead organ donation. The latter is preferred because retrieval of vital organs like liver, kidney etc is possible, which is not feasible in the former. In this, organs are retrieved after the confirmation of brain death, while cardiac and respiratory functions are still present by artificial means.

Current criteria of brain death include clinical signs of absent brain functions including brain stem reflexes and no electrical activity on EEG. Radioisotope scanning with absent blood flow to the brain is an additional ancillary feature. MRI with MR angiography can serve as an objective means to diagnose brain death. We present the imaging findings of the same, which include

- Gross cerebral edema with loss of gray-white matter differentiation, cortical hyperintensity and bilateral lateral ventricle effacement.
- Diffuse diffusion restriction.
- Transtentorial and tonsillar herniations
- No intracranial vascular flow voids on T2 weighted images
- No flow related signal in intracranial vessels on MR angiography. Flow may be seen in cervical vessels and ECA.
- Prominent transmedullary and cortical veins on susceptibility weighted imaging

When present in combination, these are highly specific for brain death.

Appearance of all these is explained by the underlying pathophysiology of brain death which includes irreversible shutdown of the sodium potassium pump and increased intracranial volume.

Devising preset MRI protocols which include the basic T1 and T2 weighted sequences, diffusion and susceptibility weighted imaging and time of flight MR angiography would take about 10 – 15 minutes on standard MRI scanners and in addition to the other methods, can serve as an objective criteria for declaring patients brain dead prior to organ harvesting.

(Table: Organ donation MRI protocol)

(Table: MRI checklist for diagnosing brain death)

Results & Conclusion

MRI with MR Angiography can serve as a non-invasive and objective method to diagnose brain death timely and recruiting candidates for organ donation, enabling timely initiation of organ harvesting in these.

It is imperative to be aware of the various imaging findings of brain death, which when seen in combination, are highly specific.

It is worthwhile to have a checklist handy when evaluating these cases to allow quick and accurate interpretation.

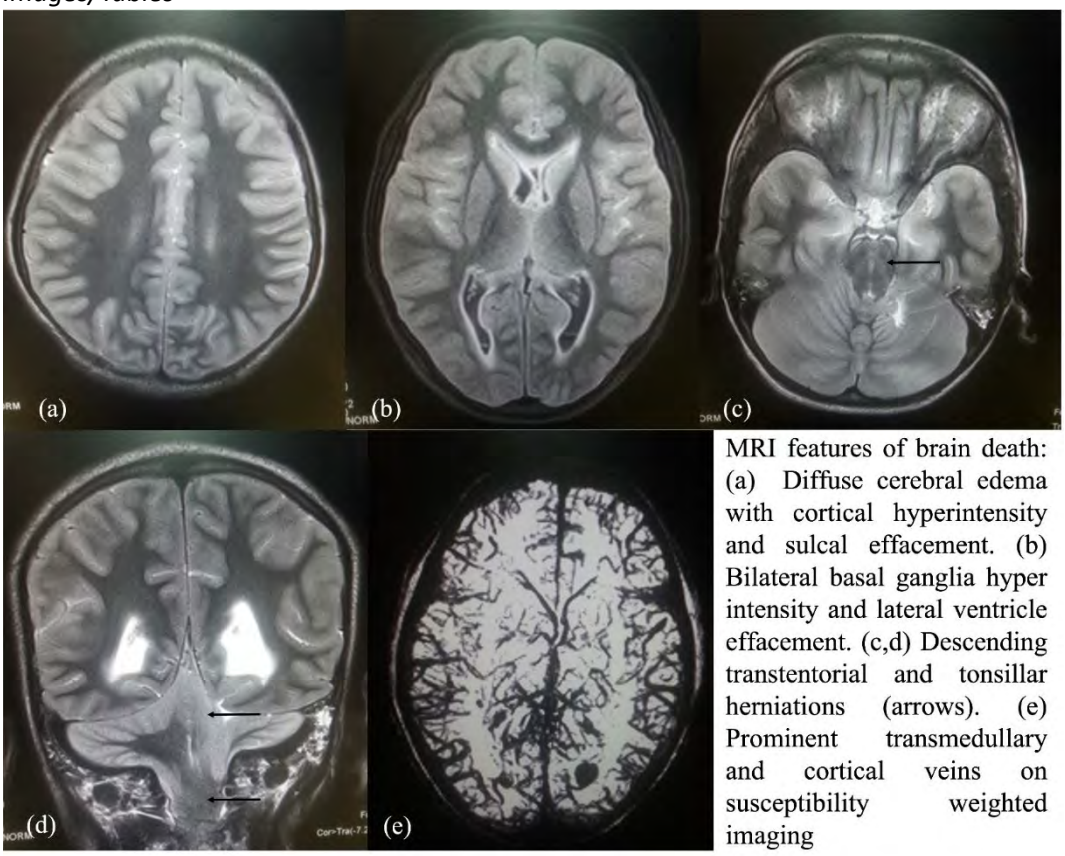
References

Corrêa DG, de Souza SR, Nunes PGC, Coutinho AC Jr, da Cruz LCH Jr. The role of neuroimaging in the determination of brain death. Radiol Bras. 2022 Nov-Dec;55(6):365-372. doi: 10.1590/0100-3984.2022.0016. PMID: 36514681; PMCID: PMC9743262.

Gastala J, Fattal D, Kirby PA, Capizzano AA, Sato Y, Moritani T. Brain death: Radiologic signs of a non-radiologic diagnosis. Clin Neurol Neurosurg. 2019 Oct;185:105465. doi: 10.1016/j.clineuro.2019.105465. Epub 2019 Aug 12. PMID: 31472395.

Sohn CH, Lee HP, Park JB, et al. Imaging findings of brain death on 3-tesla MRI. Korean J Radiol. 2012 Sep-Oct;13(5):541-9. doi: 10.3348/kjr.2012.13.5.541. Epub 2012 Aug 28. PMID: 22977320; PMCID: PMC3435850.

Images/Tables



MRI features of brain death: (a) Diffuse cerebral edema with cortical hyperintensity and sulcal effacement. (b) Bilateral basal ganglia hyper intensity and lateral ventricle effacement. (c,d) Descending transtentorial and tonsillar herniations (arrows). (e) Prominent transmedullary and cortical veins on susceptibility weighted imaging

1111

Revisiting Malformations of Cortical Development: A Pictorial Review of Imaging Correlates of Genetic and Syndromic Causes

SMILY SHARMA MD, DNB, FRCR, Soumya Sundaram MD, DM, Chandrasekharan Kesavadas MD, DMRD, Bejoy Thomas MD, DNB, PDCC

Sree Chitra Tirunal Institute for Medical Sciences and Technology, Trivandrum, Kerala, India

Abstract Category

Pediatrics

Summary & Objectives

MR imaging patterns can provide clues for a few specific genetic and syndromic causes of malformations of cortical development, especially those related to disorders of neuronal migration and the megalencephalic spectrum.

The objectives of this exhibit are to outline a systematic approach for imaging evaluation of cortical malformations and provide an explicit review of the typical genotype-phenotype correlations based on clinical features and MRI patterns.

Purpose

The presented educational exhibit aims to discuss the imaging approach to identify genetic and syndromic causes associated with cortical malformations. The typical imaging patterns, in conjunction with clinical features, can help guide specific genetic analysis and resolve diagnostic dilemmas in variants of uncertain significance.[1,2]

Materials & Methods

Electronic medical records of our institute were searched to identify MRI scans of various malformations of cortical development. Genetically proven and syndromic cases with cortical malformations were included in the review. The MRI scans were performed on a 3T or 1.5T MR scanner. The sequences used for analysis included T2 weighted in multiple planes, 3D isotropic T1 weighted/axial T1 weighted, 3D/ 2D FLAIR (avoided in infants), DWI, SWI, and/or Diffusion Tensor Imaging (DTI) whenever available. Deep phenotyping was done on MRI scans to classify types of cortical malformations and look for the site and extent of malformed cortex, including hemispheric or quadrantic involvement, and associated corpus callosal, basal ganglia, hippocampal, thalamic, posterior fossa, and vascular anomalies.

Results & Conclusion

Using illustrative cases, genetic and syndromic causes of malformations of cortical development with typical imaging patterns are discussed. Associations of megalencephalic syndromes with the PI3K-AKT-mTOR pathway, body overgrowth syndromes, and neurocutaneous syndromes like hypomelanosis of Ito are elaborated. Imaging patterns of various genetic causes of lissencephaly are presented, including classical lissencephaly with posterior-to-anterior gradient in the LIS1 gene variant, and subcortical band heterotopia in females or lissencephaly with anterior-to-posterior gradient in males in the DCX gene variant. Associations of lissencephaly with cerebellar hypoplasia in reelin pathway mutations (RELN, VLDR) and with dysmorphic basal ganglia, hook-shaped frontal horns of lateral ventricles, and dysmorphic brain stem in tubulinopathies are explained. Cobblestone malformations in congenital muscular dystrophies (CMD) are shown with a spectrum ranging from merosin-negative CMD (with no cortical malformations) to Walker Warburg syndrome (with extensive cobblestone malformations, cerebellar polymicrogyria and microcysts, and characteristic brainstem kinking often in the shape of Z). Association of bilateral frontoparietal cobblestone malformations or polymicrogyria with cerebellar cysts in ADGRG1 (previously known as GPR56) gene mutations is also presented. Diffuse periventricular nodular heterotopia with megacisterna magna is often associated with an X-linked FLNA gene mutation, which can also have associated cardiac anomalies. Various patterns of polymicrogyria are presented, and common genetic associations are discussed, like unilateral polymicrogyria with PAX6 gene mutation. Associations with callosal abnormalities and interhemispheric cysts in Aicardi syndrome and with septo-optic dysplasia in Schizencephaly are also shown.

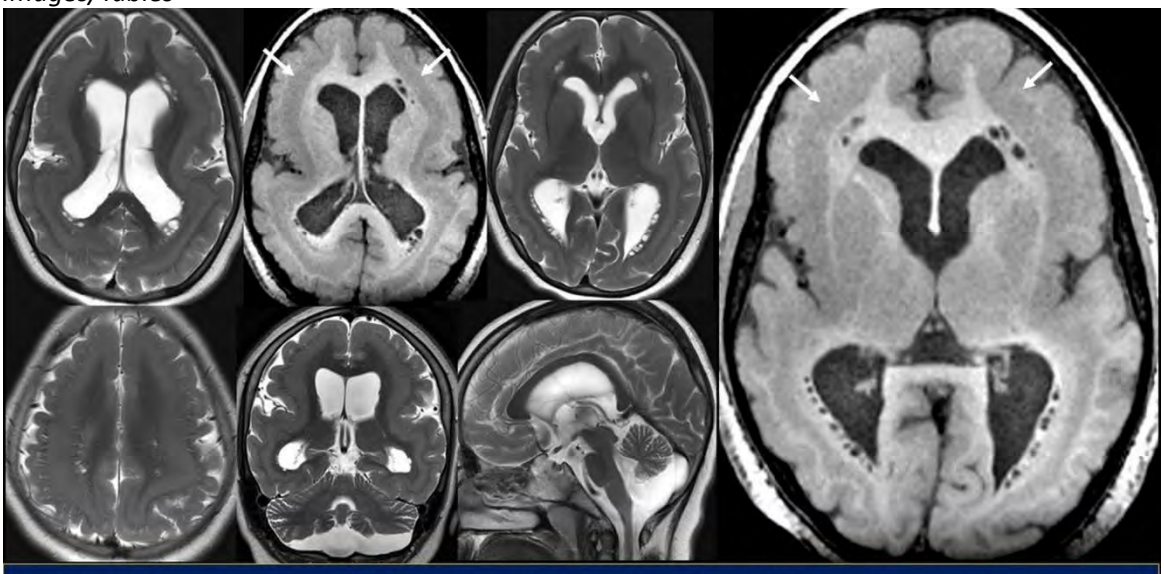
To conclude, neuroradiologists must be aware of at least the typical imaging patterns associated with specific genetic and syndromic causes of cortical malformations in order to guide correct genetic analysis and improve future pregnancy outcomes.

References

1. Brunelli JM, Lopes TJ, Alves IS, et al. Malformations of Cortical Development: Updated Imaging Review. *RadioGraphics* 2024;44:e230239.

2. Mutch CA, Poduri A, Sahin M, Barry B, Walsh CA, Barkovich AJ. Disorders of microtubule function in neurons: imaging correlates. *AJNR Am J Neuroradiol* 2016;37:528-35.

Images/Tables



14-year-old girl with epilepsy and autism. MR brain: T2 and T1 weighted (2nd image in upper row and zoomed image) sequences show subcortical band heterotopia (white arrows) and pachygyria with anterior > posterior gradient. Note the cystic changes in underlying periventricular white matter and down sloping of posterior body and splenium of corpus callosum. Genetic diagnosis confirmed a pathogenic DCX mutation.

1125

Traumatic and Non-Traumatic Spine Emergencies in Geriatric Patients

Nerses Nersesyan Kocharyan[1], Paulo Puac-Polanco[1], Andres Rodriguez[2], Shivaprakash Hiremath[3], Roy Riascos[2], Carlos Torres[1]

[1]The University of Ottawa, Ottawa, Ontario, Canada. [2]The University of Texas Health Science Center at Houston, Houston, Texas, USA. [3]University of Toronto, Toronto, Ontario, Canada

Abstract Category

Spine

Summary & Objectives

1. Elderly patients have a higher risk of fractures and associated complications following low-energy trauma.
2. Aging leads to physiological changes in muscle and bone, making elderly patients more prone to fractures even without osteoporosis.
3. CT is the most effective method for screening elderly patients with a high likelihood of spine injury.
4. In older patients, spine hyperextension may worsen a pre-existing stenosed central canal resulting in cord injury.
5. In patients with pathological vertebral body compression fracture and cord compression, the radiology report should include the spinal instability neoplastic score (SINS), and the epidural spinal cord compression scale (ESCC).

Purpose

The geriatric population (aged 65 and older) is rapidly growing in the world. Elderly patients have distinct causes and treatment considerations for spine injuries, with falls being the most common cause. As the population ages, there is also a greater economic and social burden associated with these injuries.

As this population ages, spine injuries are becoming more common and associated with higher morbidity and mortality rates. This rise can be attributed to several common risk factors among the elderly, including decreased reaction time due to arthritis, poor vision, chronic medication use, degenerative changes in the spine, osteopenia, and the use of anticoagulant medications.

Materials & Methods

Computed tomography (CT) is the most effective method for screening elderly patients who are likely to have sustained injuries. Magnetic resonance imaging (MRI) is recommended for patients who are unable to communicate their injuries or when there is suspicion of spinal cord or ligamentous injury.

This population frequently presents with traumatic injuries, such as central cord syndrome, open book fractures, and odontoid fractures. Additionally, non-traumatic causes such as spondylitic myelopathy, malignant cord compression, and vascular emergencies, including spinal cord infarction and sural fistula, will also be discussed. Lastly, infectious causes such as spinal epidural and subdural abscesses, as well as facet joint arthritis, will be reviewed.

Results & Conclusion

The aging population faces a growing risk of spine injuries, which carry significant health, social, and economic burdens. Optimized diagnostic and treatment strategies are essential to improving outcomes for elderly patients.

References

1. Sadro CT, Sandstrom CK, Verma N, Gunn ML. Geriatric trauma: A radiologist's guide to imaging trauma patients aged 65 years and older. Radiographics . 2015 Jul 1;35(4):1263–85.
2. Joyce MF, Gupta A, Azocar RJ. Acute trauma and multiple injuries in the elderly population . Vol. 28, Current Opinion in Anaesthesiology. Curr Opin Anaesthesiol; 2015. p. 145–50.
3. Ngo B, Hoffman JR, Mower WR. Cervical spine injury in the very elderly. Emerg Radiol. 2000 ;7(5):287–91.
4. Sunder A, Chhabra HS, Aryal A. Geriatric spine fractures – Demography, changing trends, challenges and special considerations: A narrative review. J Clin Orthop Trauma. 2023 Aug 1;43.
5. Reske-Nielsen C, Medzon R. Geriatric Trauma. Vol. 34, Emergency Medicine Clinics of North America. Emerg Med Clin North Am; 2016. p. 483–500.

Images/Tables

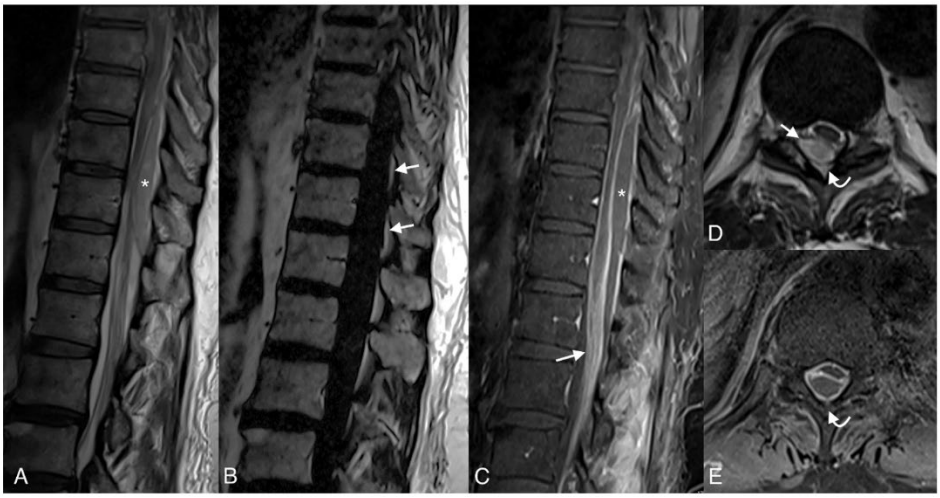


Figure 14. A 68-year-old patient with weakness in the context of CNS listeriosis. MRI demonstrates a high T2WI signal collection (asterisk in A) in the subdural space of the thoracolumbar region (note the preserved high T1WI signal of the fat pad in this region [arrows in B]) associated with ring enhancement on postcontrast T1WI (asterisk in C). There is also diffuse leptomeningeal enhancement of the cauda equina (arrow in C). Axial T2 (D) and postcontrast T1WI (E) confirm the location of the collection (arrow in D) in the subdural space given the preserved epidural fat pad (curved arrows in D &E).

1142

The Value of a Map: ADC Quantification to Guide Sinonasal Malignancy Diagnosis

Prajeet Kaza MD, Blair Winegar MD, Richard Wiggins MD, Yoshimi Anzai MD
University of Utah, Salt Lake City, UT, USA

Abstract Category

Head and Neck

Summary & Objectives

Sinonasal malignancies have high morbidity owing to primary tumor location, proximity to valuable structures, and aggressive behavior. Therefore, a precise radiologic differential diagnosis is essential to our clinical colleagues to guide management of these potentially devastating tumors. For instance, a newly discovered sinonasal mass for which there is a high pre-sampling radiologic suspicion for lymphoma would necessitate non-fixated tissue for flow cytometry and would steer treatment towards a nonsurgical oncology approach[1]. However, a significant overlap in imaging appearances is a barrier to a confident pre-biopsy pathologic diagnosis. One of the most useful tools that can guide imaging-based diagnosis is the Apparent Diffusion Coefficient (ADC) map generated from the Diffusion Weighted Imaging (DWI), which has become a standard sequence in modern magnetic resonance imaging of the head and neck. Various studies have been performed to select an average ADC value to differentiate benign entities from malignancies, with described sensitivities and specificities of the selected cutoffs[2]. It is important to note that average ADC values are influenced by tumor heterogeneity, such as necrosis, hemorrhage, or cystic degeneration. A simple diagnostic approach to differentiate specific sinonasal malignancies would be useful.

Purpose

The purpose of this presentation is to evaluate the minimum ADC values of commonly encountered sinonasal malignancies with ratios with brain parenchyma (cerebellum) ADC as an internal control. We will review any trends that may aid in diagnosis or guide a differential.

Materials & Methods

Only pre-treatment MR imaging was used for data acquisition. Scans without a confirmed histopathologic diagnosis were excluded. Careful attention was made to avoid undue effect of air-related susceptibility artifact by sampling within solid tumor tissue. While circular region of interest (ROI) was typically favored, a combination of circular and free-hand

ROI tool was used to avoid non-tumor tissues, such as mucus, displaced orbital bones, partially eroded ethmoid sinus walls, or macroscopically evident cystic/necrotic tumor components. With each measurement, the minimum and average ADC values were obtained from the PACS (Philips Intellispace) at three consecutive slices. Rarely are two measurements taken in the same slice but geographically separated when three consecutive slices exceed the tumor's craniocaudal tumor length.

Results & Conclusion

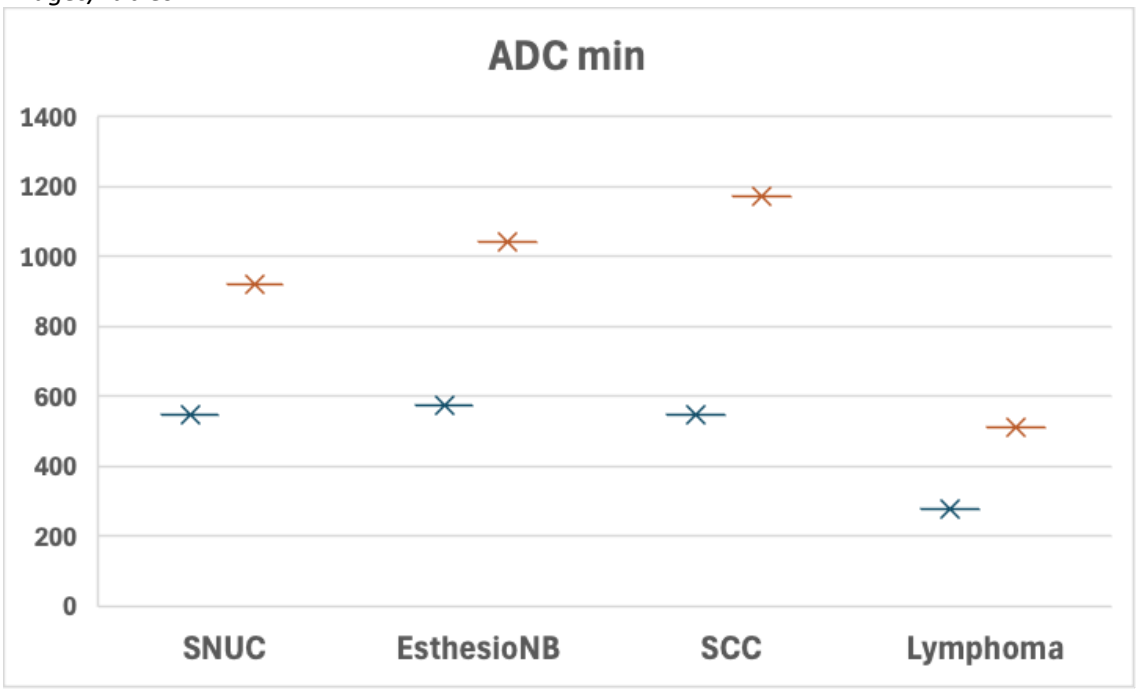
The preliminary results showed the minimum ADC values of lymphoma were significantly lower than the other three malignancies (chart "ADC min") with no observed overlap in this data set. Additionally, sinonasal undifferentiated carcinoma (SNUC) were associated with marginally lower ADC values compared to squamous cell carcinoma (SCC) and esthesioneuroblastoma, although these values overlapped. Going forward, we expect larger data sets to strengthen these findings and uncover further trends that will enhance noninvasive diagnostic capabilities and guide clinical management.

References

Bitner BF, Htun NN, Wang BY, Brem EA, Kuan EC. Sinonasal lymphoma: A primer for otolaryngologists. *Laryngoscope Investig Otolaryngol*. 2022 Oct 4;7(6):1712-1724. DOI: 10.1002/lio2.941.

El-Gerby KM, El-Anwar MW. Differentiating Benign from Malignant Sinonasal Lesions: Feasibility of Diffusion Weighted MRI. *Int Arch Otorhinolaryngol*. 2017 Oct;21(4):358-365. DOI: 10.1055/s-0036-1597323.

Images/Tables



1162

Camurati-Engelmann Disease: A Case Report with Emphasis on Neuroradiological MRI Findings

Renata Miyake Almeida Prado MD, Ana Julia Ferreira Fernandes MD, Camila Sekine Ikeda MD, Otavio Shiguemitsu Valenciano MD, Maíra Gil Caliani MD, Helena Cristina da Silva MD PhD, Mariana Akuri MD, Marina Cristina Akuri MD
HCFAMEMA, Marília, São Paulo, Brazil

Abstract Category

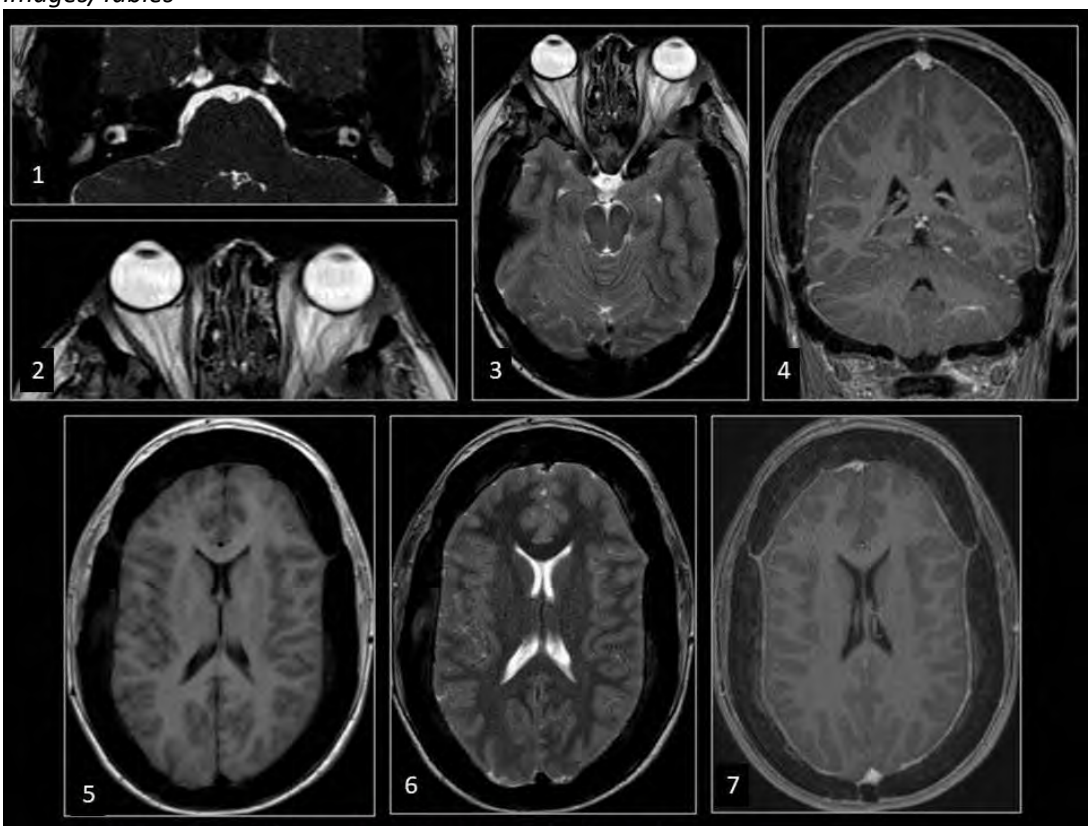
Adult Brain Inflammatory/Infectious Disease/Degenerative/Metabolic

Summary & Objectives

Camurati-Engelmann Disease (CED), also known as progressive diaphyseal dysplasia, is a rare autosomal dominant disorder, with approximately 300 cases reported in the literature to date. The disease is caused by mutations in the gene encoding TGFβ-1 (Transforming Growth Factor β1), located on chromosome 19q13, leading to reduced osteoclastic activity and increased osteoblastic activity. CED is characterized by progressive hyperostosis, particularly affecting the diaphyseal cortex of long bones, though other sites, such as the skull and pelvis, may also be involved. Clinical presentation typically includes limb pain, muscle weakness, gait abnormalities, and, in cases with cranial involvement,

symptoms related to the compression of neurological structures, such as optic neuropathy, hearing loss, tinnitus, and headache.
This study aims to describe the neuroradiological features of Camurati-Engelmann Disease in Magnetic Resonance Imaging (MRI) of a 25-year-old female patient with a typical clinical history of lower limb pain beginning in childhood, with genetic confirmation at age six, who has developed hearing loss, tinnitus, and visual acuity reduction over the past two years.
Purpose
N/A.
Materials & Methods
This case report on CED used a patient's medical records as well as X-rays and brain MRIs available in the institution to assess cortical thickening of the lower limbs long bones as well as cranial involvement, characterized by diffuse skull hyperostosis. This report further explores the impact of the cranial changes on neural structures and ocular globes, with a literature review of the most common findings, correlating them with the patient's symptoms.
Results & Conclusion
A 25-year-old female presents with a history of progressive lower limb pain that began in her first year of life, with a genetic confirmation of CED at age six. She exhibits typical clinical and radiological findings, including pain and fusiform diaphyseal thickening of the long bones in the lower limbs. Over the last two years, she has developed hearing loss, tinnitus, and reduced visual acuity, leading her to seek specialized medical care.
A cranial MRI was then performed, revealing diffuse hyperostosis of the skull, with consequent narrowing of the internal acoustic canals and optic nerve canals, in addition to bilateral proptosis. We also observed sulcal effacement, slight pachymeningeal thickening and enhancement, as well as signs of papilledema and distension of the optic nerve sheaths bilaterally—findings likely associated with intracranial hypertension secondary to the compressive effect of cranial bone expansion in CED.
Camurati-Engelmann Disease has no cure, and treatment generally involves corticosteroids and losartan for pain management, along with decompressive surgery in select cases.
In conclusion, radiology plays an integral role in monitoring disease progression, providing essential information for therapeutic decisions and interventions aimed at symptom relief and improving patients' quality of life.
References
1. Wallace SE. Camurati-Engelmann disease. GeneReviews® [Internet] 2023 Aug 31.
2. Bogas M, Bogas V, Pinto F. Doença de Camurati-Engelmann: manifestações típicas de uma doença rara. Rev Bras Reumatol 2009;49:308–14.
3. Carlson ML;Beatty CW;Neff BA;Link MJ;Driscoll CL; Skull base manifestations of Camurati-Engelmann disease. Archives of otolaryngology--head & neck surgery.
4. Fonte AC da, Gonçalves CM, Catalan J, et al.. Doença de Camurati-Engelmann: relato de caso com acometimento ósseo grave. Radiol Bras 2005;38:471–2.
5. Restrepo JP, Molina M del P. Camurati–Engelmann Disease: Case Report and Review of Literature. Revista Colombiana de Reumatología (English Edition) 2016 Jul 1.

Images/Tables



1. Axial balanced-FFE MRI demonstrates narrowing of the internal auditory canals.
2. Axial T2-weighted MRI showing signs of papilledema and distension of the optic nerve sheaths bilaterally.
3. Axial T2-weighted MRI shows narrowing of the optic nerve canals, distension of the optic nerve sheaths bilaterally and bilateral proptosis.
4. Coronal T2-weighted MRI shows calvarial thickening, as well as incidental finding of developmental venous anomaly in the left cerebellar hemisphere.
5. Axial non-contrast-enhanced T1-weighted MRI shows diffuse calvarial thickening, with low signal intensity, and sulcal effacement.
6. Axial T2-weighted MRI shows diffuse calvarial thickening, with low signal intensity, and sulcal effacement.
7. Axial contrast-enhanced T1-weighted MRI shows diffuse calvarial thickening, with low signal intensity, as well as slight pachymeningeal thickening and enhancement.



X-rays evidencing fusiform diaphyseal thickening of the long bones in the lower limbs, sparing the epiphyses.

1167

Vein and Simple: A Cerebral Guide to Neuroanatomical Vascular Variants

Joshua C Wright MD, Vasant Patwardhan MD, Divya Balchander MD, Katherine Wei MD, Edward Kuoy MD, Charles Li MD
University of California Irvine, Orange, CA, USA

Abstract Category

Interventional/Vascular/Stroke

Summary & Objectives

Our objective is to review the common and uncommon neurovascular variants and their associated clinical and/or surgical significance. We will provide a case-based overview of different neurovascular variants including categories such as intracranial Circle of Willis variants, persistent carotid-vertebrobasilar arterial anastomoses, and skull base neurovascular variants.

Purpose

It is estimated that a complete Circle of Willis, the anastomotic connection between the anterior and posterior circulations of the brain, is only present in about 24% of individuals. Common physiologic variations of the Circle of Willis include duplicated, fenestrated, hypoplastic, or absent vessels, most commonly occurring in the posterior circulation. The clinical implications of Circle of Willis variants are variable, as some variants pose higher risks in surgical or endovascular interventions, for example in the context of aneurysm coiling and pituitary intervention.

Other well-known but less commonly seen neurovascular variants include different variants of persistent carotid-vertebrobasilar arterial anastomoses, which occur due to anomalies in embryological development. Usually persistent carotid-vertebrobasilar anastomoses are incidental findings and do not result in any clinical significance. They are, however, known to be associated with intracranial vascular anomalies such as aneurysms. Examples of skull base neurovascular anomalies include aberrant internal carotid artery, persistent stapedial artery, and hypoplasia or agenesis of the internal carotid artery. These may have a wide range of clinical presentations, such as pulsatile tinnitus, hearing loss, or a vascular retrotympanic mass on otoscopic examination. Knowledge of these anatomic variants is imperative as their presence could drastically alter surgical approach in skull base procedures.

Materials & Methods

Examples for each of the neurovascular variants will be obtained from patients imaged at an academic medical center. Relevant cases will be presented with high quality cross sectional imaging.

Results & Conclusion

Understanding the nuances of neurovascular variants is essential for accurate diagnosis and effective treatment planning. This exhibit will highlight the importance of recognizing these variants to prevent surgical complications and improve patient outcomes. Advanced imaging techniques play a crucial role in identifying these variants, facilitating better clinical decision-making.

References

1. Prince EA, Ahn SH. Basic vascular neuroanatomy of the brain and spine: what the general interventional radiologist needs to know. Semin Intervent Radiol. 2013 Sep;30(3):234-9. doi: 10.1055/s-0033-1353475. PMID: 24436544; PMCID: PMC3773035.
2. Rosner J,Q Reddy V, Lui F. Neuroanatomy, Circle of Willis. [Updated 2023 Jul 24]. In: StatPearls [Internet]. Treasure Island (FL): StatPearls Publishing; 2024 Jan-. Available from: https://www.ncbi.nlm.nih.gov/books/NBK534861/
3. Dimmick SJ, Faulder KC. Normal variants of the cerebral circulation at multidetector CT angiography. Radiographics. 2009 Jul-Aug;29(4):1027-43. doi: 10.1148/rg.294085730. PMID: 19605654.
4. Saltzman G. Patent primitive trigeminal artery stud-ied by cerebral angiography. Acta Radiol 1959;51:329–336
5. Oelerich M, Schuierer G. Primitive hypoglossal artery: demonstration with MR and CT angiography.Eur Radiol 1997;7:1492–1494.

Images/Tables

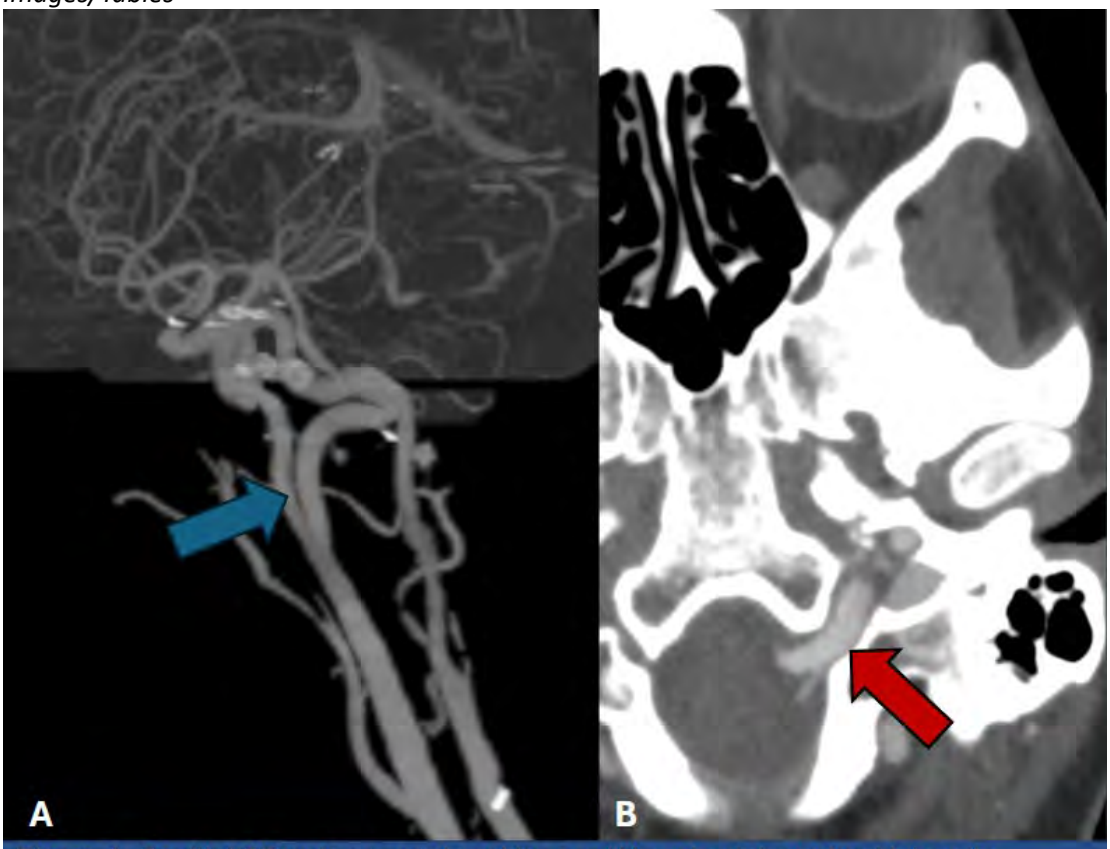


Figure 1. Sagittal 3D volume-rendered image (A) and axial maximal intensity projection image (B) of the patient's CT angiogram of the head demonstrate variant persistent left hypoglossal artery, with connection between the distal cervical internal carotid artery and the basilar artery (blue arrow). There is also expansion of the left hypoglossal canal (red arrow).

1168

Imaging Manifestations of Rhinocerebral Mucormycosis: CaseReport and Literature Review

Ana Júlia F Fernandes MD, Camila S Ikeda MD, Luísa C de Almeida Aguilar MD, Renata M Almeida Prado MD, Otavio S Valenciano MD, Marina C Akuri MD, Helena C da Silva PHD
FAMEMA, Marilia, São Paulo, Brazil

Abstract Category

Adult Brain Inflammatory/Infectious Disease/Degenerative/Metabolic

Summary & Objectives

Mucormycosis is a rare yet serious fungal infection predominantly affecting immunocompromised individuals, such as those with uncontrolled diabetes mellitus. In Brazil, between 2018 and June 14, 2021, medications were distributed for 143 cases of the disease. Imaging plays a critical role in early diagnosis and in determining the extent of disease progression. Techniques like CT and MRI identify hallmark signs of infection, and reveal spread to critical areas.This case describes a 62-year-old male with uncontrolled diabetes who presented with facial swelling, nasal obstruction, and orbital pain, leading to a diagnosis of rhinocerebral mucormycosis.

Purpose

Demonstrate characteristic imaging findings of mucormycosis in rhinocerebral regions, highlighting the role of CT and MRI in diagnosing and assessing the extent of fungal invasion in sinonasal, orbital, and intracranial compartments, with an emphasis on supporting early intervention and improving patient outcomes.

Materials & Methods

N/A

Results & Conclusion

The patient, a 62-year-old male, presented to the emergency department, reporting progressive facial swelling, nasal obstruction, and orbital pain on the right side, with a gradual reduction in visual acuity. He reported a history of uncontrolled diabetes mellitus. Physical examination revealed periorbital swelling and ptosis of the left eye. The possibility of infectious involvement was considered. Initial cranial computed tomography showed opacification of the maxillary, ethmoidal, and sphenoidal sinuses, with evidence of soft tissue density content within the nasal cavity. Subsequent MRI of the brain and orbit demonstrated signal alteration in the left gyrus rectus and adjacent peripheral gadolinium enhancement, in close proximity to the chiasmatic region of the left optic nerve, with ring enhancement involving the gyrus rectus, with extension to the left optic tract. These findings were consistent with an inflammatory / infectious process involving the optic nerve and adjacent cerebral structures. Additionally, the imaging revealed diffuse thickening of the sinonasal mucosa and evidence of orbital fat involvement. A biopsy of the nasopharyngeal mucosa further validated the diagnosis by demonstrating broad, non-septate hyphae. Antifungal treatment was promptly initiated, and surgical debridement of necrotic tissue from the nasal cavity was performed. Despite aggressive medical and surgical interventions, the patient's condition deteriorated, ultimately resulting in death.

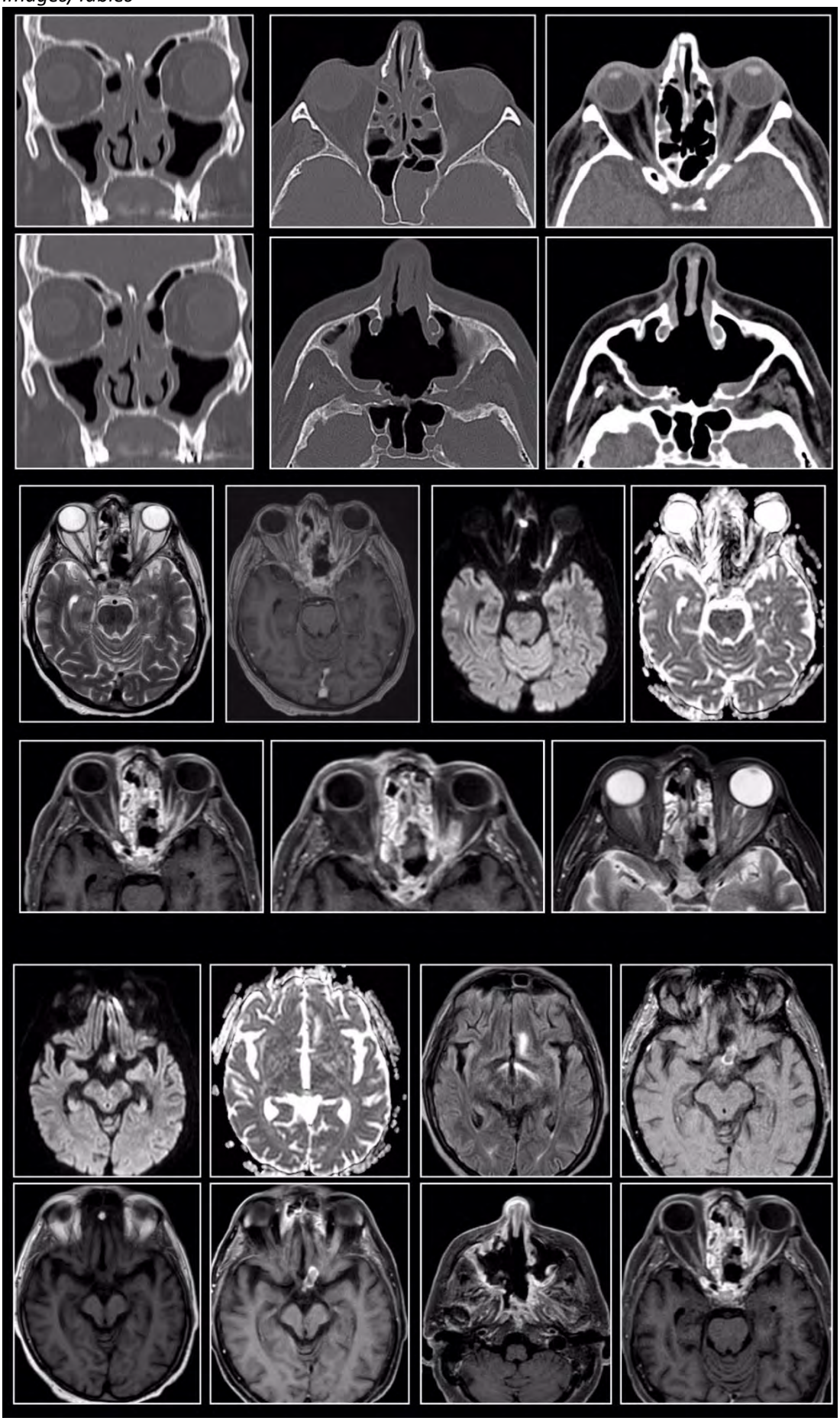
This case illustrates the critical role of advanced imaging modalities in the diagnosis, evaluation, and management of rhinosinusal mucormycosis, an aggressive and often fatal infection, particularly in immunocompromised patients. MRI findings were pivotal in identifying the extent of orbital and intracranial involvement, guiding the therapeutic approach. The optic nerve involvement and the inflammatory changes in the cerebral structures highlighted the severity and progression of the infection, correlating with clinical deterioration. Early recognition of imaging patterns characteristic of invasive fungal sinusitis is crucial, as delayed diagnosis can lead to extensive tissue necrosis and poor outcomes. This underscores the need for a high index of suspicion in diabetic or immunocompromised individuals presenting with atypical sinus or orbital symptoms.In conclusion, it is crucial for radiologists to recognize the imaging findings of mucormycosis, which should be integrated with clinical and laboratory findings to enable timely intervention in cases of invasive fungal infections.

References

STEINBRINK, Julie M.; MICELI, Marisa H. Mucormycosis. **Infectious Disease Clinics**, v. 35, n. 2, p. 435-452, 2021.

AGRAWAL, Rishi et al. Pulmonary mucormycosis: risk factors, radiologic findings, and pathologic correlation. **Radiographics**, v. 40, n. 3, p. 656-666, 2020.

Images/Tables



1174

Before the Mask: From Scan to Sedation – Neuroradiologic Insights for Safer Anesthesia

Chelsea Muennichow DO[1], Isaac Botchey[2], Steven Lev MD[1]
[1]NUMC, East Meadow, NY, USA. [2]NYIT, Old Westbury, NY, USA

Abstract Category

New Techniques/Advanced Imaging/Informatics/AI/Professional Development/Misc

Summary & Objectives

Summary

We review the pivotal importance of providing neuroradiologic insights to the anesthesiologist in regard to planning and patient safety during neuro, spine, and head and neck surgeries. Awareness and understanding of a variety of key neuroimaging findings—such as elevated intracranial pressure, spinal stability issues, and potential airway obstructions can better equip the anesthesiologists with the specific knowledge needed to anticipate and address intraoperative challenges.

Objectives

1. To identify crucial neuroradiologic findings that directly impact anesthesiology planning and patient safety in brain, spine, and head and neck surgeries.
2. To provide anesthesiologists with targeted insights on critical considerations, such as airway management, blood pressure control, and anesthetic agent selection, based on neuroradiologic imaging.
3. To promote effective interdisciplinary collaboration, ensuring that neuroradiologic findings are communicated effectively to anesthesiologists to support safer surgical outcomes in complex neuro cases.

Purpose

To enhance anesthesiology planning and patient safety by communicating essential neuroradiologic insights that anesthesiologists need to know for neuro-related surgical cases.

Materials & Methods

We review neuroradiologic cases from the past 10 years at our Level 1 trauma center, focusing on findings relevant to anesthetic planning in neuro, spine, and head and neck surgeries. Using CT/CTA, with select MRI studies, we compiled cases with findings that can directly influence anesthesiology management.

We organize by location(brain/ head and neck/ spine) and highlight specific imaging findings that impact anesthetic approaches, including airway management, blood pressure control, and anesthetic agent selection. We underscore the importance of neuroradiologic insights in informing anesthesia decisions for safer surgical outcomes.

Results & Conclusion

Results

We illustrate critical imaging insights that are essential for anesthetic planning in neuro, spine, and head and neck surgeries, each with specific considerations that significantly impact anesthesiologist decision-making.

In the brain, imaging findings of elevated intracranial pressure (ICP), midline shift, and herniation risk must be noted, as these impact blood pressure control and the selection of agents like propofol, which minimizes further increases in ICP. In cases with significant midline shift, maintaining stable cerebral perfusion without inducing additional pressure is critical, necessitating strict control over blood pressure and ventilation.

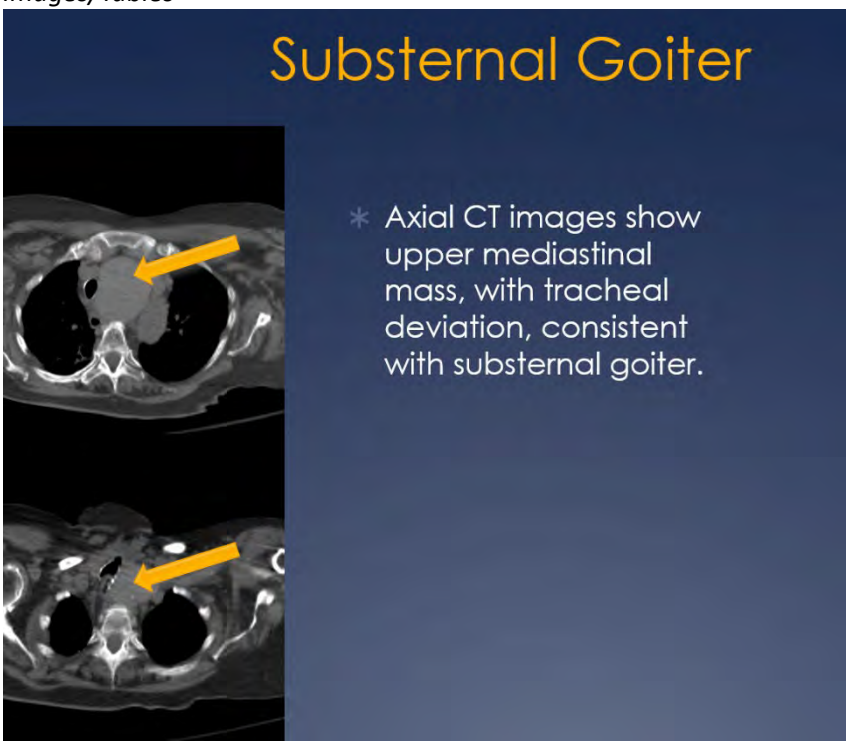
For head and neck cases, imaging findings affecting airway management and vascular stability are important. Large neck masses, pancoast tumors, tracheal deviation, and vascular anomalies like an aberrant right subclavian artery, can present specific challenges for anesthesia. When masses are detected, anesthesiologists may consider fiber-optic intubation to avoid airway obstruction upon muscle relaxation during anesthesia. Carotid artery stenosis or jugular vein compression require careful hemodynamic monitoring, as reduced venous outflow or compromised carotid flow can negatively impact intraoperative cerebral perfusion.

In the spine, particularly cervical, stability and cord compression are prominent concerns. Atlantoaxial instability, severe stenosis, and neoplasms necessitate specialized intubation techniques to prevent movement of unstable vertebrae and reduce neurological risk. The vertebral artery must be protected during neck movement to maintain stable posterior circulation.

Conclusion

Neuroradiology plays a critical role guiding safe and effective anesthetic planning for complex neuro, spine, and head and neck surgeries. Direct communication of imaging findings enables anesthesiologists to anticipate potential intraoperative challenges.

References
1. Crosby, E. T., & Warltier, D. C. (2006). Airway management in adults after cervical spine trauma. *The Journal of the American Society of Anesthesiologists, 104*(6), 1293-1318.
2. Ho, S., Hambidge, O., & John, R. (2020). Anaesthesia for neurosurgery. *Anaesthesia & Intensive Care Medicine, 21*(1), 33-38.
3. Randell, T., Hakala, P., Kyttä, J., & Kinnunen, J. (1998). The relevance of clinical and radiological measurements in predicting difficulties in fibreoptic orotracheal intubation in adults. *Anaesthesia, 53*(12), 1144-1147.
4. Wintermark, M., & Rizvi, T. (2025). Modern Neuroradiology Relevant to Anesthetic and Perioperative Management. In *Cottrell & Patel's Neuroanesthesia* (pp. 96-121): Elsevier.
Images/Tables



1186

Practical Neurovascular Embryology: Relevance in Accurate Interpretation of Code Stroke CTAs

Charlotte Y Chung MD PhD
NYU Langone Health, New York, NY, USA

Abstract Category
Interventional/Vascular/Stroke

Summary & Objectives

Anatomic variants in the cerebral arterial circulation are well recognized. Our classical understanding of these variants evolved from classifying commonly seen variants as distinct entities according to their location and morphology. While helpful from a descriptive standpoint, this perspective suggests the existence of only a finite number of variants – a concept that is flawed from both a developmental and functional standpoint. Familiarity with the overarching processes of neurovascular development allows one to view cerebrovascular territories as systems fed by multiple vessels in balance with one another, and appreciate that anatomical variants in fact exist on a spectrum with respect to branching pattern and location; relative vessel size and dominance; territory supplied; and fusion pattern. In the face of the vast spectrum of cerebrovascular variants, abnormal findings on head and neck CT angiogram for acute stroke evaluation can easily be misinterpreted: benign congenitally hypoplastic or absent vessels may be overcalled as occlusions, while occlusions of normal or variant vessels may be missed or misinterpreted as benign variants. Understanding key concepts of neurovascular development, the resultant spectrum of cerebral arterial variants, and accompanying imaging clues can aid accurate interpretation of code stroke CTAs and minimize potentially clinical devastating diagnostic errors.

Educational Objective

- Outline key concepts and processes of neurovascular embryologic development

- Highlight the nature of cerebral arterial variants as a spectrum
- Illustrate occlusions that can be missed or misinterpreted as congenitally hypoplastic/absent vessels
- Illustrate congenitally hypoplastic/absent vessels and other variants that mimic occlusions

Outline:

- Key Neurovascular Development Concepts:
    1. Fusion and regression of longitudinal and transverse vasculature in the embryonic carotid (anterior) and vertebrobasilar (posterior) circulation
    2. Fusion and annexation of embryonic vascular supply from carotid to vertebrobasilar circulation
    3. Evolution in balance between and relative dominance of arterial suppliers of each cerebrovascular territory
- Imaging clues distinguishing congenital hypoplasia/absence from pathologic occlusions
- Case-based illustrations highlighting missed/misinterpreted or mimics of occlusions:
    1. Related to variants in branching pattern and location (ex. MCA bifurcation versus trifurcation, early MCA branching)
    2. Related to variants in vessel size/relative dominance (ex. hypoplastic vertebral artery, AICA-PICA complex vs PICA occlusion, fetal-type PCA versus P1 occlusion)
    3. Related to variants in fusion pattern (ex. basilar nonfusion, azygous or bi-hemispheric ACA, fenestration)

Purpose

NA

Materials & Methods

NA

Results & Conclusion

NA

References

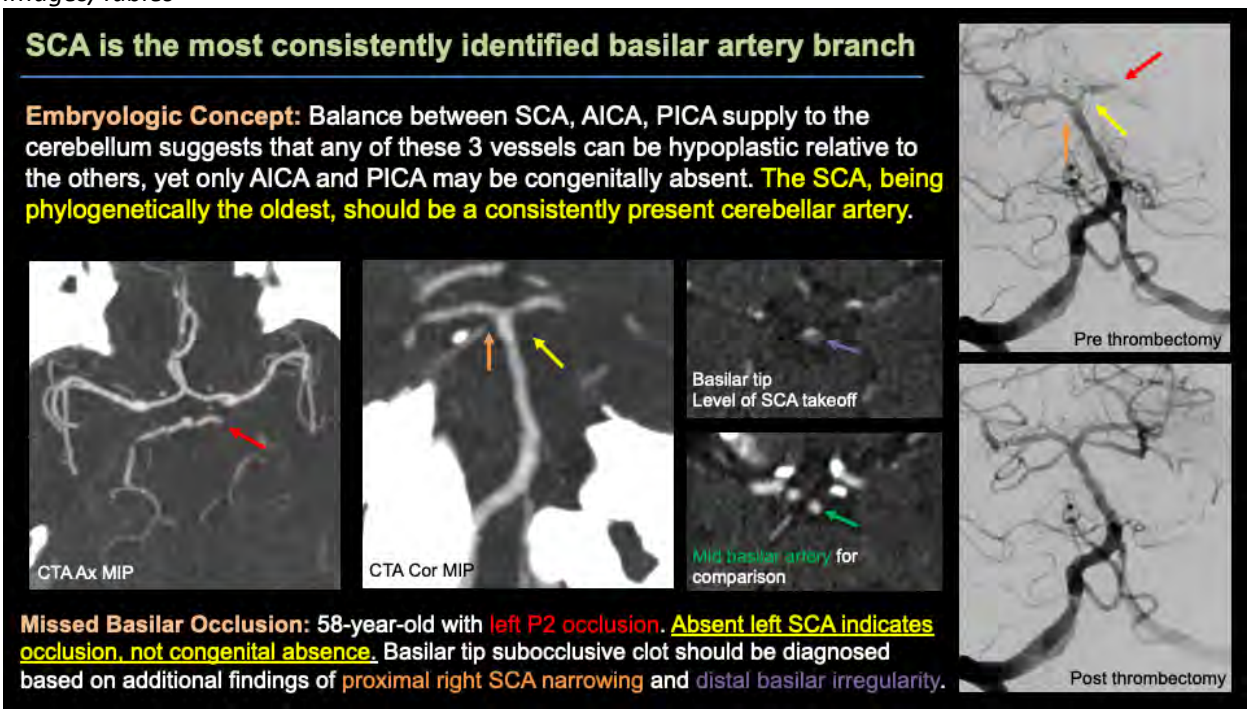
1. Shapiro M, Raz E, Nossek E, et al. Neuroanatomy of the middle cerebral artery: implications for thrombectomy. *J NeuroIntervent Surg* 2020;12:768–73.

2. Klostranec JM, Krings T. Cerebral neurovascular embryology, anatomic variations, and congenital brain arteriovenous lesions. *Journal of NeuroInterventional Surgery* 2022;14:910–9.

3. Shapiro M. neuroangio.org | Your neurovascular education and information source.http://neuroangio.org/. Accessed November 11, 2024.

4. Dimmick SJ, Faulder KC. Normal Variants of the Cerebral Circulation at Multidetector CT Angiography. *RadioGraphics* 2009;29:1027–43.

Images/Tables



1187

Building Bridges: Radiological Perspectives on Commissural Plaque

Erica A Naves[1], Eduardo J A Valadares[2], Aline S Ayres[2], Mika S Setuguti[2], Saymon D B Oliveira[2], Rita C M Pincerato[2]
[1]Hospital Samaritano, São Paulo, SP, Brazil. [2]São Paulo, SP, Brazil

Abstract Category

Pediatrics

Summary & Objectives

1. Anatomy and Embryology
2. Clinical implications of commissural anomalies
3. MRI protocol to access commissural anomalies
4. Spectrum of commissural abnormalities
    1. Anterior commissure developmental anomaly *and related cortex (olfactory cortex (paleocortex) and the lateral and inferior temporo-occipital neocortex)*
    2. Corpus callosum developmental anomaly *and related cortex (most of the hemispheric neocortex)*
    3. Hypocampal developmental anomaly*, besides fornices and hippocampal cortex (archicortex)*
    4. Development of other important related structures: septum pellucidum
5. Associated intracranial anomalies in corpus callosum agenesis
    1. Interhemispheric cyst
    2. Neuronal migration disorders
    3. Agenesis of inferior vermis
    4. Encephalocele
    5. Lipoma of interhemispheric fissure
6. Syndromes Commonly Associated With Commissural Anomalies
    1. Aicardi syndrome
    2. Chiari II malformation
    3. Dandy Walker Continuum
    4. Shapiro Syndrome
    5. Walker-Warburg syndrome
    6. Septo-optic syndrome
    7. Turner syndrome
    8. Moebius syndrome
    9. Joubert syndrome
    10. Holoprosencephaly
7. Fetal MRI
8. Diagnostic workflow of commissural anomalies

Purpose

1. Understand the Anatomy and Embryology of Commissural Plaque
2. Review the Malformations and Syndromes related to Commissural Plaque
3. Tips for evaluating fetal MRI in cases of Commissural Malformations

Materials & Methods

The presentation includes brain MRI scans and graphic representations of brain maturation to document and visually illustrate the stages of brain development, specific neurological patterns, and developmental abnormalities.

Results & Conclusion

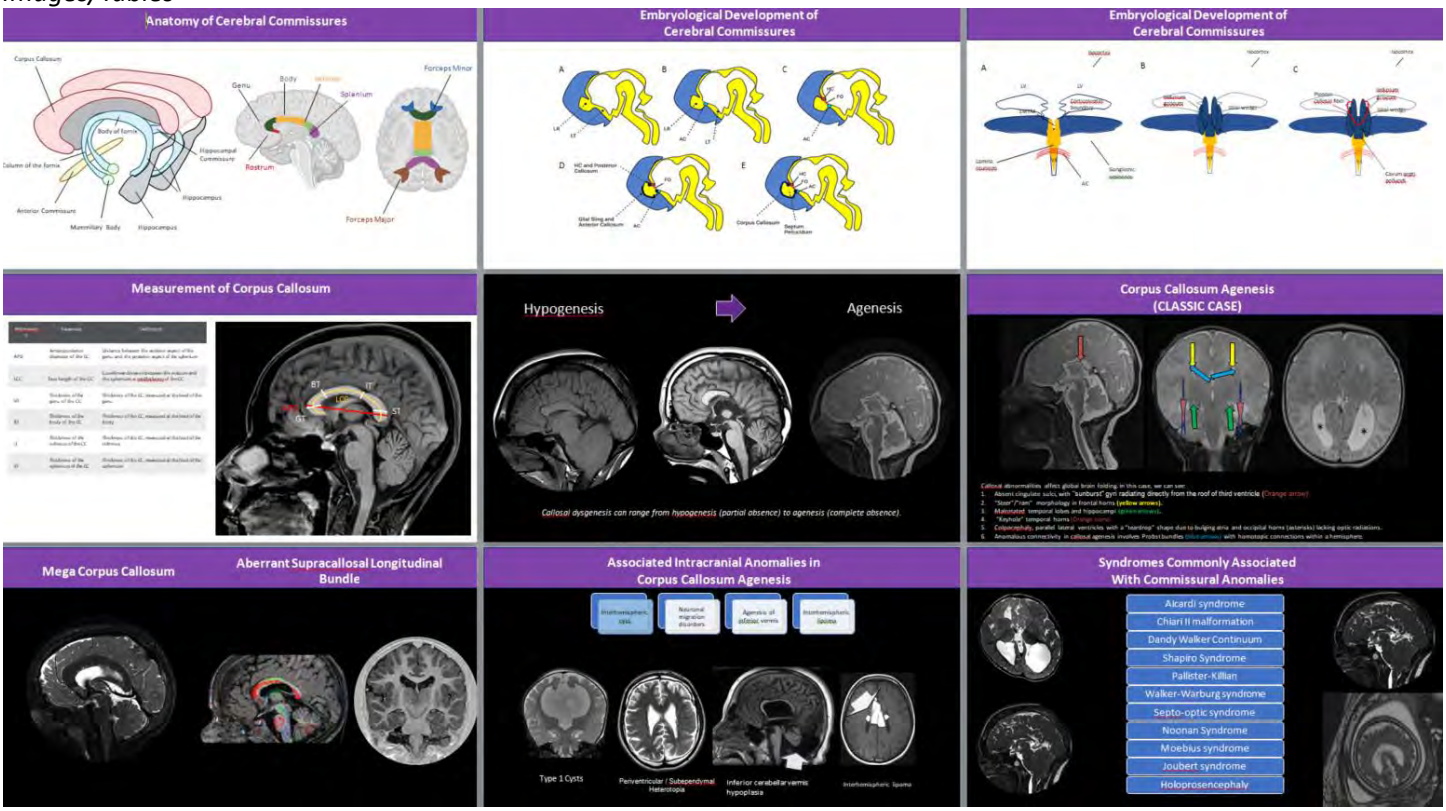
The aim of this presentation is to review patterns of commissural anomalies and provide a diagnostic workflow to assist radiologists while reporting those challenging scans.

References

- Oh KY, Kennedy AM, Selden NR, et al. Asymmetric ventriculomegaly, interhemispheric cyst, and dysgenesis of the corpus callosum (AVID): an imaging triad. J Ultrasound Med. 2012;31:1811-1820. doi: 10.7863/jum.2012.31.11.1811. PMID: 23091253.
- Limoges N, Ostrander B, Kennedy A, et al. Neurological and clinical outcomes in infants and children with a fetal diagnosis of asymmetric ventriculomegaly, interhemispheric cyst, and dysgenesis of the corpus callosum. J Neurosurg Pediatr. 2021;1-5. doi: 10.3171/2021.9.PEDS21252. Epub ahead of print. PMID: 34798596.

- Wahl M, Strominger Z, Jeremy RJ, et al. Variability of homotopic and heterotopic callosal connectivity in partial agenesis of the corpus callosum: a 3T diffusion tensor imaging and Q-ball tractography study. AJNR Am J Neuroradiol. 2009;30:282-289. doi: 10.3174/ajnr.A1361. Epub 2008 Nov 11. PMID: 19001538; PMCID: PMC7051413.
- Chaudhari BP, Ho ML. Congenital Brain Malformations: An Integrated Diagnostic Approach. Semin Pediatr Neurol. 2022;42:100973.

Images/Tables



1190

Pre-surgical Planning Task-Based and Resting State Functional Brain MRI: Current Standards and Future Directions.

Mahmoud Shalaby M.D.

Mercy Catholic Medical Center, Darby, PA, USA

Abstract Category

New Techniques/Advanced Imaging/Informatics/AI/Professional Development/Misc

Summary & Objectives

Functional MRI (fMRI) provides a noninvasive preoperative mapping of the widely distributed brain networks that can help in addressing the challenging balance between brain tumor resection and preserving the vital brain areas and functions.

Purpose

In this educational exhibit, we will provide pictorial review of functional brain anatomy, illustrate the concepts of task-based fMRI maps blood oxygen level-dependent (BOLD) and resting-state fMRI (rs-FMRI), explain the technical and physiological challenges in acquisition such as neurovascular uncoupling (NVU), and provide tips for optimal image acquisition and mitigation of challenges.

Materials & Methods

N/A

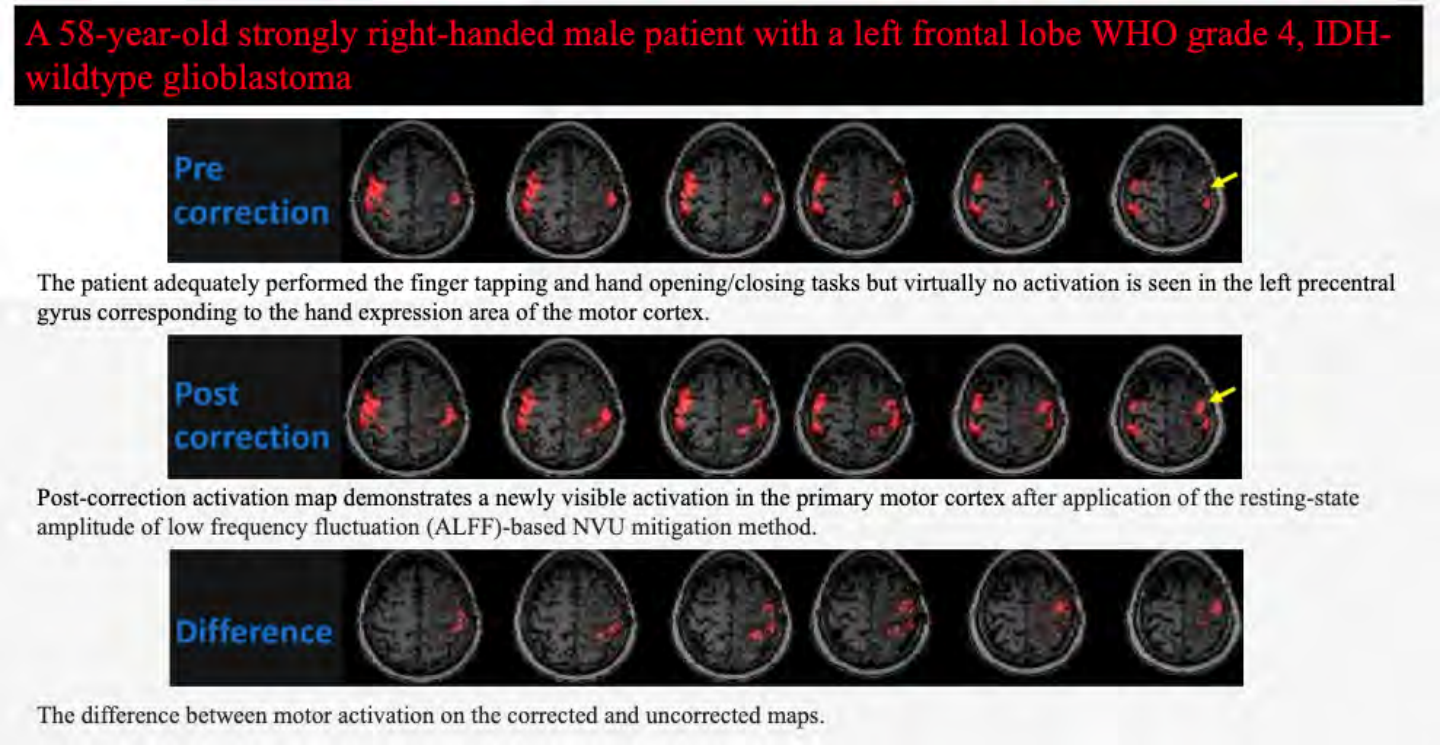
Results & Conclusion

N/A

References

1. Lakhani, D. A., Sabsevitz, D. S., Chaichana, K. L., Quiñones-Hinojosa, A., & Middlebrooks, E. H. (2023). Current state of functional MRI in the presurgical planning of brain tumors. *Radiology: Imaging Cancer*, *5*(6). https://doi.org/10.1148/rycan.230078
2. Luna LP, Sherbaf FG, Sair HI, Mukherjee D, Oliveira IB, Köhler CA. Can preoperative mapping with functional MRI reduce morbidity in brain tumor resection? a systematic review and meta-analysis of 68 observational studies. **Radiology** 2021;300(2):338–349
3. Elliott ML, Knodt AR, Cooke M, et al. General functional connectivity: Shared features of resting-state and task fMRI drive reliable and heritable individual differences in functional brain networks. **Neuroimage** 2019;189:516–532.
4. Pasquini, L., Peck, K. K., Jenabi, M., & Holodny, A. (2023). Functional MRI in neuro-oncology: State of the art and future directions. *Radiology*, *308*(3). https://doi.org/10.1148/radiol.222028
5. Agarwal, S., Welker, K. M., Black, D. F., Little, J. T., DeLone, D. R., Messina, S. A., Passe, T. J., Bettegowda, C., & Pillai, J. J. (2023). Detection and mitigation of neurovascular uncoupling in brain gliomas. *Cancers*, *15*(18), 4473. https://doi.org/10.3390/cancers15184473

Images/Tables



1192

External Carotid Artery Vascular Pathologies: A Comprehensive Overview of Imaging Findings and Interventions

Alyssa Ionno MD[1], Amr Wardeh MD[2], Rajiv Mangla MD[2]

[1]Cleveland Clinic, Cleveland, OH, USA. [2]SUNY Upstate Medical University, Syracuse, NY, USA

Abstract Category

Head and Neck

Summary & Objectives

1. To describe the anatomy of the external carotid artery and its branches.
2. To illustrate various imaging modalities used for the evaluation of ECA pathologies, with emphasis on their specific strengths.
3. To discuss the spectrum of ECA-related pathologies, including trauma, vascular malformations, hypervascular tumors, radiation-induced changes, and Moyamoya disease.

4. To outline the role of interventional techniques, including embolization and surgical revascularization, in managing ECA-related conditions.

Purpose

The external carotid artery (ECA) plays a crucial role in supplying blood to the face, scalp, and neck. This educational exhibit aims to enhance understanding of the complex anatomy of the ECA, its diverse pathologies, and the imaging modalities and interventional techniques used in its diagnosis and treatment. The exhibit is designed for radiologists and clinicians, particularly those involved in neuroradiology, to facilitate better diagnosis and treatment of ECA-related conditions.

Materials & Methods

A comprehensive review of the ECA was performed, focusing on its anatomy, imaging techniques, and pathological conditions. Relevant imaging modalities include computed tomography angiography (CTA), magnetic resonance angiography (MRA), digital subtraction angiography (DSA), and ultrasound. Key pathologies discussed include traumatic injuries, epistaxis, carotid blowout syndrome, hemangiomas, hypervascular tumors, radiation-induced changes, arteriovenous malformations (AVMs), and Moyamoya disease. Various interventional and surgical techniques, including embolization and revascularization procedures, are also reviewed.

Results & Conclusion

Understanding the anatomy of the ECA is crucial for accurate diagnosis and treatment of vascular pathologies. DSA remains the gold standard for vascular assessment and interventions. Trauma, hypervascular tumors, radiation-induced changes, and Moyamoya disease emphasize the importance of the ECA for both collateral circulation and therapeutic procedures. Advances in imaging and interventional techniques have improved outcomes for ECA-related conditions, highlighting the need for specialized expertise in clinical practice.

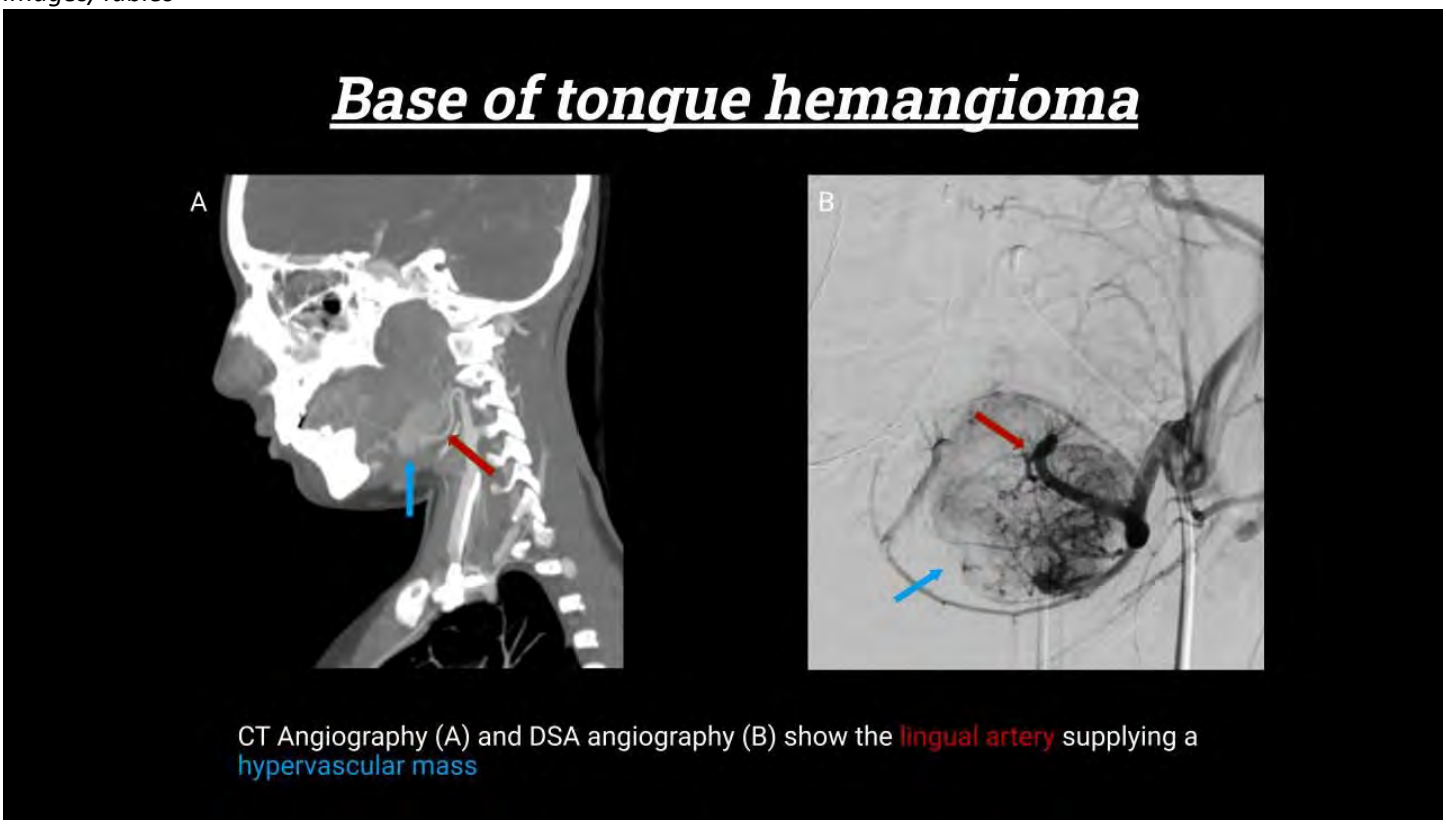
References

1. Culleton S, Wiggins R, McNally JS. Imaging spectrum of extracranial arterial vascular pathology: pearls for the radiologist. Clin Radiol 2022;77(3):167-178. doi: 10.1016/j.crad.2021.10.011. Epub 2021 Nov 17.

2. Mangla S, Sclafani SJ. External carotid arterial injury. Injury 2008;39(11):1249-56. doi: 10.1016/j.injury.2008.06.012. Epub 2008 Oct 5.

3. Li W, Zhao M, Liu X, et al. Understanding external carotid artery collateralisation after cerebral revascularisation in moyamoya disease: insights from quantitative analysis. Stroke Vasc Neurol 2024 Oct 17. [Epub ahead of print]. doi: 10.1136/svn-2024-003336.

Images/Tables



1194

A Deep Dive into Craniotomies: Their Radiographic Appearance and Complications

Linda Lu MD, Khoi Nguyen MD
UCLA, Los Angeles, California, USA

Abstract Category

Head and Neck

Summary & Objectives

Craniotomies are common neurosurgical procedures that involve removal of a portion of the skull to directly access intracranial structures, followed by replacement of the bone flap. This procedure may be utilized to treatment of a range of pathologies including tumors, hemorrhage, vascular malformations, and infection. However, the specific type of craniotomy and surgical approach depends on the location and nature of the pathology.

Purpose

The purpose of this educational exhibit is to provide a review of the many different types of craniotomies, their indications, imaging findings, and post-operative complications. Understanding the various imaging appearances of different post-craniotomy changes and evaluating post-operative complications allows the radiologist to readily interpret complex post-surgical cases and effectively communicate their findings to clinicians.

Materials & Methods

The educational exhibit systematically reviews the indication, variant approaches, accessible anatomy, and associated imaging findings for the different types of craniotomies as well as their respective post-surgical complications. Similar procedures for intracranial access including Burr holes, craniectomy, and cranioplasty are also reviewed.

Results & Conclusion

Anterior approach craniotomies include subfrontal, transsphenoidal, and transmaxillary/transfacial craniotomies. These allow access to the anterior cranial fossa structures such as the sella and clivus. Indications for these craniotomies include cavernous sinus pathology, intra/supra-sellar lesions, or clival masses.

Anterolateral approach craniotomies include cranio-orbtial zygomatic and subtemporal craniotomies. These allow for access and treatment of various structures within the middle cranial fossa such as paranasal sinus or basilar artery pathologies.

Pterional craniotomy is a versatile approach allowing access into the anterior, middle, or posterior fossa to place aneurysm clips or manage sphenoid wing pathologies such as meningioma resection.

Transpetrosal craniotomies are a posterolateral approach to access the middle cranial fossa and treat intradural tumors such as petroclival meningiomas. Suboccipital craniotomies are another posterior approach to access the posterior cranial fossa and may be used to manage vestibular schwannomas or repair Chiari malformations.

Additional procedures that provide access to intracranial structures include Burr holes, cranioplasty, and craniectomy. Burr holes are small holes drilled into the skull and may be used for ventricular drain or shunt catheter placement. A hemicraniectomy involve removal of a portion of the skull to reduce intracranial pressure. A cranioplasty involves removal of a portion of the skull with replacement with either an autologous bone graft, or a bone graft made of titanium or acrylic.

Despite their potential benefits, craniotomies are associated with various complications.

A small scalp and extra-dural hematoma beneath the bone flap is an expected post-craniotomy finding but intracranial hemorrhage is a serious complication. Extra-axial CSF collections are common with the suboccipital approach and resolve over time. An extra-dural abscess appears as a lentiform collection subjacent to the craniotomy flap with associated enhancing dura while a subdural empyema appears as a crescentic collection along the cerebral convexity or falx cerebri.

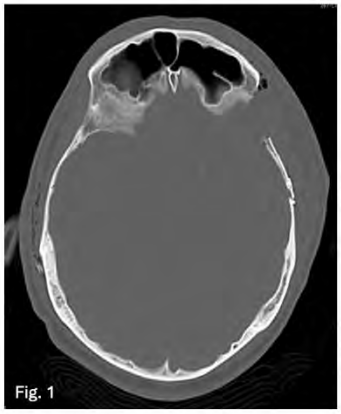
In conclusion, craniotomies are common procedures with complex post-operative imaging findings. An understanding of the various craniotomies and their complications will result improved reporting accuracy and communication with clinicians.

References

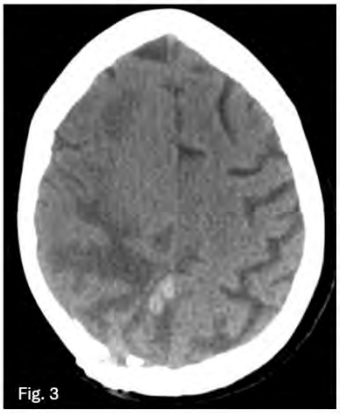
1. “Practical Handbook of Neurosurgery From Leading Neurosurgeons”, Sindou, Marc. Springer Vienna, 2009.
2. Tandon P, Ramamurthi R.Textbook of Neurosurgery, Volume 1. JP Medical Ltd, 2012.
3. Sinclair. AG. Imaging of the post-operative cranium. Radiographics. Vol. 30, No.2.
4. Fukamachi A, Koizumi H, Nukui H Postoperative intracerebral hemorrhages: a survey of computed tomographic findings after 1074 intracranial operations. Surg Neurol 1985;23(6):575–580.

5. Yang XF, Wen L, Shen F et al. Surgical complications secondary to decompressive craniectomy in patients with a head injury: a series of 108 consecutive cases. Acta Neurochir (Wien) 2008;150(12): 1241–1247; discussion 1248.

Images/Tables







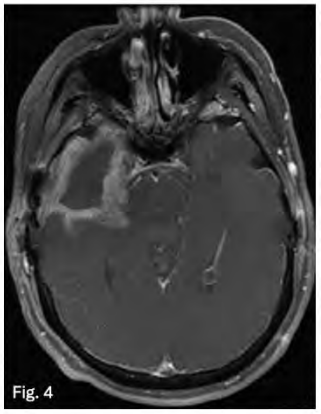


Fig. 1: Axial CT shows an example of a left pterional craniotomy.
Fig. 2: Coronal CT shows an example of a left subfrontal craniotomy.
Fig. 3: Axial CT shows an example of a post-operative intra-axial hemorrhage status post right parietal craniotomy for tumor resection.
Fig. 4: Axial post-contrast T1W image shows an example of a resection bed abscess in the right anterior middle cranial fossa.

1205

Neuro-Oncologic PET MRI-Guided Differentiation of Viable Neoplasm from Radiotherapy Sequelae in the Post-Treatment-Setting: Illuminating the Darkness

Marcus Konner DO[1], Aliah McCalla BEng[2], Ali Nabavizadeh MD[3], Ramon Barajas MD[4], Jana Ivanidze MD, PHD[1]
[1]Weill Cornell Medical Center, New York, NY, USA. [2]Central Michigan University College of Medicine, Saginaw, MI, USA. [3]Hospital of the University of Pennsylvania, Philadelphia, PA, USA. [4]Oregon Health & Science University, Portland, OR, USA

Abstract Category

Adult Neoplasms/Epilepsy/Trauma

Summary & Objectives

We present a case based pictorial and educational review of the role of neuro-oncologic PET imaging in differentiating viable neoplasm from radiotherapy (RT) sequelae in primary and secondary brain tumors in the post-treatment-setting. Based on our extensive clinical experience as a large academic medical center with high PET/MRI volume and integration of neuroradiology and nuclear medicine expertise, we present illustrative cases demonstrating utility of somatostatin-receptor-targeted, amino-acid-analog, and estrogen-receptor-targeted PET, illustrating effects of PET on change in management. We will include patients with primary and secondary CNS malignancies including meningioma and other somatostatin-receptor-positive brain tumors, pituitary neuroendocrine tumor (pitNET), esthesioneuroblastoma, glioblastoma, and metastatic estrogen-receptor-positive (ER+) and triple-negative breast cancer.

Purpose

Contrast-enhanced MRI is critical in the diagnosis and management of patients with primary and metastatic brain neoplasms, enabling accurate lesion localization and providing important information about lesion features allowing for a robust differential diagnosis particularly at initial presentation (1). There are, however, important limitations especially in the post-operative and post-RT setting, when differentiating between recurrent viable tumor and post-treatment/ post-RT changes is critical to optimal management. Perfusion MRI including both dynamic contrast-enhanced (DCE) and dynamic susceptibility contrast (DSC) MRI has shown utility in this clinical context, however, these lack specificity and reproducibility across institutions (2). Recent considerable advances in targeted neuro-oncologic PET, including increased clinical availability of a number of tumor-specific radiotracers, advances in PET/MRI hardware, acquisition protocols, and analysis / interpretation, have resulted in the incorporation of PET in clinical management guidelines in patients with primary and metastatic brain tumors (3,4) It is thus critical for neuroradiologists to become familiar with current targeted PET imaging approaches in this clinical context. We present an overview of clinically available neuro-oncologic PET radiotracers that allow for delineation of neoplasm and post treatment change, with illustrative cases.

Materials & Methods

We present a case-based review of patients with primary and secondary CNS tumors presenting to our academic medical center, who underwent targeted neuro-oncologic PET with subsequent surgery and/or RT and longitudinal follow-up. We will discuss acquisition protocols, interpretation criteria, effects on management, and reimbursement considerations. We will incorporate clinical chart review data including initial presenting symptoms, diagnosis, pathologic diagnosis, clinical course and interventions. We will include brain PET/MRI and PET/CT imaging examples with a variety of radiotracers and diagnoses, including [Ga68] DOTATATE for meningioma, pitNET, PPTID, and metastatic enthesioneuroblastoma, [F18] Fluoroestradiol for ER+ breast cancer brain metastases (BCBM), and [F18] Fluciclovine for triple negative BCBM and glioblastoma.

Results & Conclusion

Our review highlights the clinical utility of neuro-oncologic PET in the post-treatment setting, particularly in differentiating primary and secondary viable neoplasm from RT sequelae, derived from our extensive institutional experience in hybrid neuro-oncologic imaging. Key applications as well as imaging pitfalls are illustrated. Limitations of post-treatment-setting neuro-oncologic MRI in reliably differentiating tumor recurrence from treatment sequelae are highlighted.

In summary, this educational exhibit aims to demonstrate the advantages of neuro-oncologic PET as a promising adjunct in the management of patients with primary and secondary brain neoplasms.

References

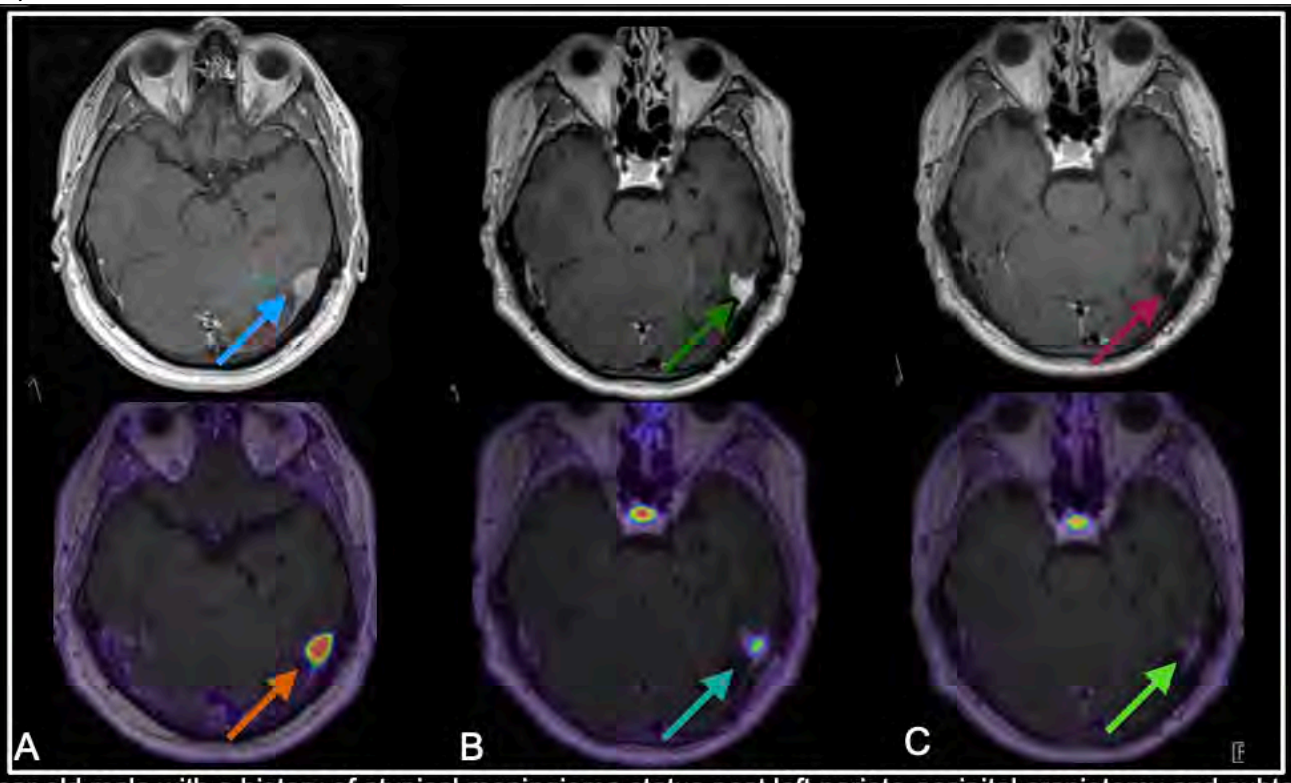
1. Marner, L., Henriksen, O.M., Lundemann, M. et al. Clinical PET/MRI in neurooncology: opportunities and challenges from a single-institution perspective. *Clinical and Translational Imaging* 2017;5: 135–149. DOI: https://doi.org/10.1007/s40336-016-0213-8

2. van Dijken, B. R. J., van Laar, P. J., Smits, M. et al. Perfusion MRI in treatment evaluation of glioblastomas: Clinical relevance of current and future techniques. *Journal of magnetic resonance imaging* 2019; *49*(1), 11–22. DOI: https://doi.org/10.1002/jmri.26306

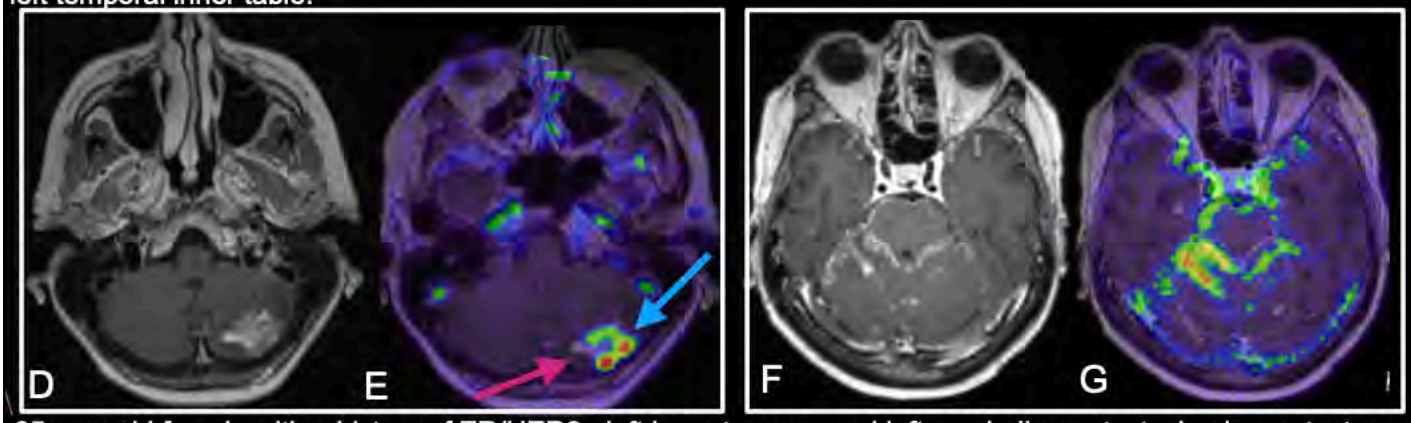
3. Albert NL, Galldiks N, Ellingson BM, et al. PET-based response assessment criteria for diffuse gliomas (PET RANO 1.0): a report of the RANO group. *The Lancet Oncology* 2024;25(1):e29-e41. DOI: https://doi.org/10.1016/S1470-2045(23)00525-9

4. Ivanidze J, Roytman M, Skafida M, et al. Dynamic (68) Ga-DOTATATE PET/MRI in the Diagnosis and Management of Intracranial Meningiomas. *Radiology: Imaging Cancer* 2022;4:e210067. DOI: https://doi.org/10.1148/rycan.210067

Images/Tables



45 year old male with a history of atypical meningioma status post left parieto-occipital craniotomy and subtotal resection.
A: Initial post-operative post-contrast T1-weighted MRI (top panel) and corresponding [Ga68]DOTATATE PET/MRI fused image (bottom panel) demonstrates an enhancing dural based lesion with intense [Ga68]DOTATATE avidity (SUV max 17.6) along the left temporal inner table.
B: Subsequent post-contrast T1-weighted MRI (top panel) and corresponding [Ga68]DOTATATE PET/MRI fused image (bottom panel) obtained 10 months following stereotactic body radiation therapy, showing mildly decreased extent of enhancement with markedly decreased extent of [Ga68]DOTATATE avidity (SUV max 9.6), compatible with treatment response.
C: Resolution of [Ga68]DOTATATE avidity (bottom panel) in region of heterogenous enhancement (top panel) at left temporal inner table.



65 year old female with a history of ER/HER2+ left breast cancer and left cerebellar metastasis s/p mastectomy adjuvant chemotherapy and SBRT two years ago. Now with enlarging enhancing lesion at the site of treated disease. Axial post contrast T1W image (D) and fused F-18-FES- PET axial image (E) demonstrating enhancing lesion with foci of intense FES avidity along the lateral aspect of the lesion, compatible with viable neoplasm; the medial aspect of the enhancing lesion demonstrates no associated FES avidity, compatible with radiotherapy sequelae (in conjunction with lack of avidity on FDG PET (not shown). Patient underwent surgical resection with pathology confirming FES PET findings.
Axial post contrast T1W image (F) and fused F-18-FES- PET axial image (G) obtained one year later demonstrating mild to moderate FES avidity correlating to regions of heterogenous leptomeningeal thickening and enhancement, compatible with viable estrogen receptor positive neoplasm.

1229

Navigating the Diagnostic Challenge: Optimizing CTA for Accurate Detection of Medium Vessel Occlusions in Acute Ischemic Stroke

Aditya Duhan MD[1], FNU Vaibhav MBBS[2], Simran Singh Cheema MD[3], Vipul Kaliraman MBBS[4], Rajiv Mangla MD[5], Amar Swarnkar MD[5]

[1]State University of New York Upstate Medical University, Syracuse, NY, India. [2]Pt. B.D. Sharma PGIMS, Rohtak, Haryana, India. [3]University of alabama at Birmingham, Birmingham, Alabama, USA. [4]Maulana Azad Medical College, New Delhi, New Delhi, India. [5]State University of New York Upstate Medical University, Syracuse, NY, USA

Abstract Category

Interventional/Vascular/Stroke

Summary & Objectives

CT angiography (CTA) is a primary imaging modality for evaluating AIS, offering rapid and reliable visualization of vascular occlusions. Identification of intracranial medium vessel occlusions (MVOs) on CTA is critical for guiding treatment in patients with acute ischemic stroke. MVOs, such as the M2 and M3 segments of the middle cerebral artery and other medium-sized intracranial arteries, pose substantial diagnostic challenges compared to large vessel occlusions, often leading to underdetection and subsequent clinical impact.

Purpose

This exhibit aims to enhance understanding of medium vessel occlusions by reviewing their diagnostic features on CTA, examining challenges in detection, and presenting protocol optimization techniques. Improved recognition of MVOs on CTA can facilitate timely intervention, improving patient outcomes in stroke management.

Materials & Methods

This exhibit explores MVO detection challenges and optimization strategies through a comprehensive review of medium-sized cerebral arteries, typical and variant anatomies, and their appearance on CTA. Key diagnostic pitfalls, including rare anatomical variants, calcified thrombi, and stump occlusions, are discussed. Current protocol recommendations, including image resolution enhancement and optimized scanning parameters, are presented to support accurate MVO detection. Relevant case examples illustrate common findings, diagnostic techniques, and interpretation challenges.

Results & Conclusion

Results:

Diagnostic Challenges: MVO detection is frequently hindered by anatomical complexity, variability, and limitations in conventional CTA resolution. Key challenges include distinguishing MVOs from small vessel artifacts and identifying calcified thrombi and partial occlusions.

Anatomy and Appearance: Common MVO locations, such as the M2 and M3 segments of the middle cerebral artery, often appear as subtle filling defects or faint opacities. Familiarity with normal and variant anatomy aids in differentiating true occlusions from anatomical variations.

Protocol Optimization: Using thinner slice thicknesses, increasing image resolution, and employing advanced CTA protocols improve MVO detection. Newer algorithms and post-processing techniques also assist in enhancing contrast and reducing noise, critical for detecting small vessel occlusions.

Clinical Impact: Early MVO detection has substantial implications for treatment options, reducing morbidity and mortality associated with delayed or missed diagnoses. Rapid identification supports eligibility assessments for targeted interventions, particularly in hyperacute stroke settings.

Conclusion:

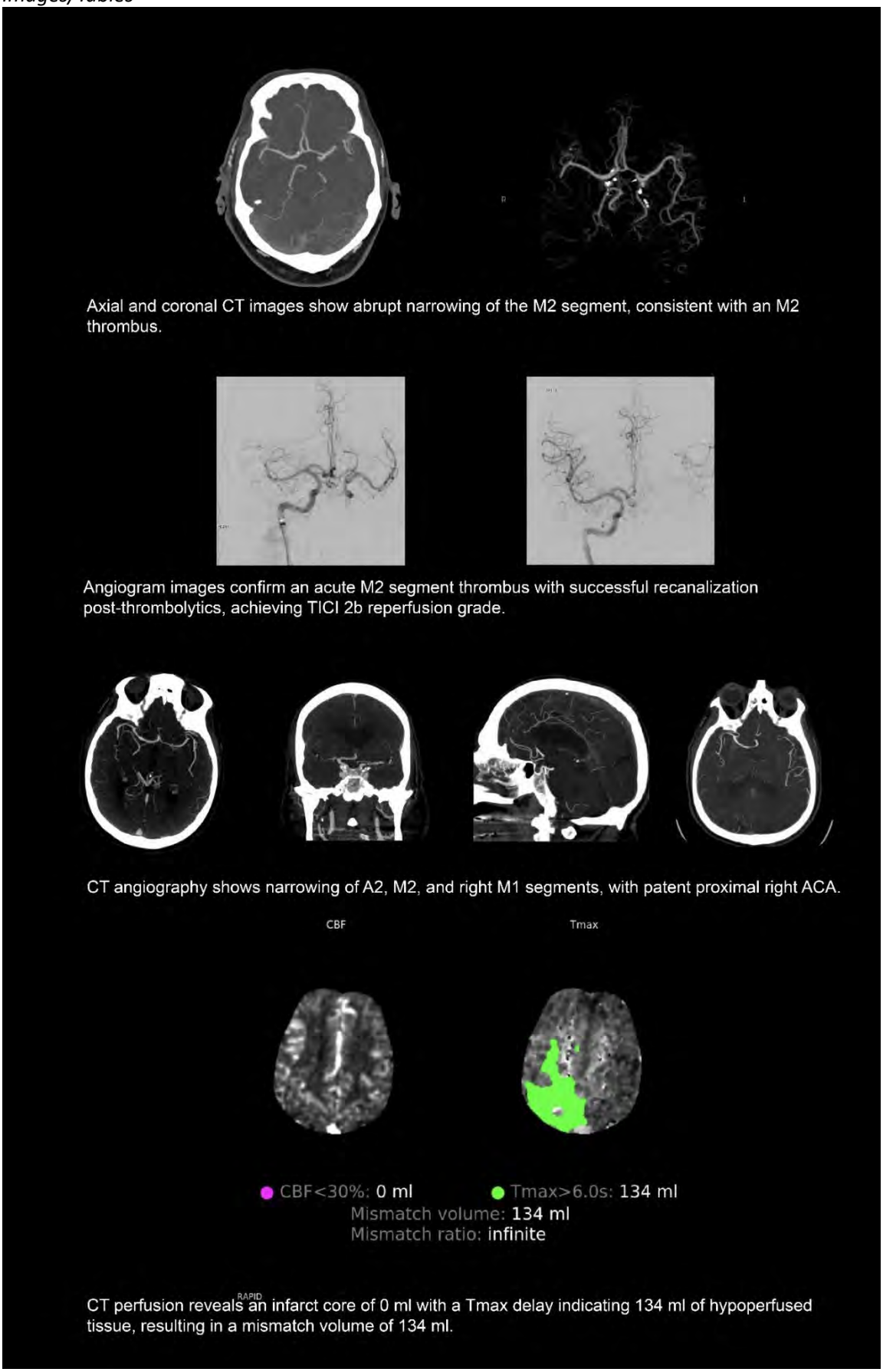
Understanding the relevant anatomy and the variable appearances of MVOs enhances radiologists' and clinicians' ability to identify these occlusions swiftly, especially in emergency scenarios. This exhibit underscores the importance of optimizing CTA protocols and refining imaging interpretation skills for accurate MVO detection. By equipping radiologists with practical insights into MVO characteristics, anatomy, and detection strategies, this review aims to support improved diagnostic accuracy, better clinical outcomes, and consistency in interpretation, ultimately benefiting patient management in acute ischemic stroke.

References

1. Finding MeVO: Identifying Intracranial Medium-Vessel Occlusions at CT Angiography | RadioGraphics
2. Amukotuwa SA, Wu A, Zhou K, et al. Distal Medium Vessel Occlusions Can Be Accurately and Rapidly Detected Using Tmax Maps. Stroke 2021;52:3308–17

3. Mistry EA, Dumont AS. Medium Vessel Occlusion and Acute Ischemic Stroke: A Call for Treatment Paradigm Reappraisal. Stroke 2020;51:3200–2

Images/Tables



Axial and coronal CT images show abrupt narrowing of the M2 segment, consistent with an M2 thrombus.

Angiogram images confirm an acute M2 segment thrombus with successful recanalization post-thrombolytics, achieving TICI 2b reperfusion grade.

CT angiography shows narrowing of A2, M2, and right M1 segments, with patent proximal right ACA.

CT perfusion reveals an infarct core of 0 ml with a Tmax delay indicating 134 ml of hypoperfused tissue, resulting in a mismatch volume of 134 ml.

1231

Imaging Cranial Dural AV Fistulas: Diagnosis, Treatment, and Post-treatment Follow Up

Charlotte Y Chung MD PhD
NYU Langone Health, New York, NY, USA

Abstract Category

Interventional/Vascular/Stroke

Summary & Objectives

Distinct from other vascular malformations, cranial dural arteriovenous fistulae (dAVFs) are abnormal fistulous connections between dural arteries and veins that comprise 10-15% of cranial vascular malformations. Despite advances in imaging techniques, accurate diagnosis based on non-invasive imaging remains challenging. This is in part due to the heterogeneity of dAVFs in terms of location of the shunt, feeding arteries, venous drainage into cortical veins versus dural venous sinuses, and behavior of the lesion. Improved visualization and understanding of dAVF angioarchitecture and pathophysiology have allowed development of novel treatment strategies, particularly endovascular approaches. Understanding the treatment strategy employed is paramount for appropriate evaluation of dAVFs status post treatment.

Educational objectives:

- Discuss up-to-date understanding of cranial dAVF angioarchitecture, pathophysiology, and relevant anatomy.
- Illustrate multimodal radiographic appearance of cranial dAVFs
- Review current treatment, particularly endovascular, strategies of cranial dAVFs
- Illustrate expected and unexpected radiographic appearance of cranial dAVFs status post endovascular embolization, open surgery, and radiosurgery treatment.

Table of Contents/Outline

1. Cranial dural vascular anatomy
2. Classifying dAVFs based on location, angioarchitecture, and pathophysiology
3. Imaging techniques (CT/MRI, CTA, MRA, DSA) for diagnosing cranial dAVFs
4. Diagnosing cranial dAVFs on non-invasive imaging
5. Treatment strategies of cranial dAVFs
6. Expected appearance of cranial dAVFs status post treatment
7. Pictorial review of unexpected findings in the post-treatment follow up of cranial dAVFs

Purpose

NA

Materials & Methods

NA

Results & Conclusion

NA

References

1. Bhatia KD, Lee H, Kortman H, et al. Endovascular Management of Intracranial Dural AVFs: Principles. *AJNR Am J Neuroradiol* 2022;43:160–6.

2. Bhatia KD, Lee H, Kortman H, et al. Endovascular Management of Intracranial Dural Arteriovenous Fistulas: Transarterial Approach. *AJNR Am J Neuroradiol* 2022;43:324–31.

3. Bhatia KD, Lee H, Kortman H, et al. Endovascular Management of Intracranial Dural AVFs: Transvenous Approach. *AJNR Am J Neuroradiol* https://doi.org/10.3174/ajnr.A7300.

4. Tanaka M. Embryological Consideration of Dural AVFs in Relation to the Neural Crest and the Mesoderm. *Neurointervention* 2019;14:9–16.

5. Shapiro M, Raz E, Litao M, et al. Toward a Better Understanding of Dural Arteriovenous Fistula Angioarchitecture: Superselective Transvenous Embolization of a Sigmoid Common Arterial Collector. *AJNR Am J Neuroradiol* 2018;39:1682–8.

Images/Tables

